ICORES 2017

6th International Conference on Operations Research and Enterprise Systems

PROCEEDINGS

Porto, Portugal

23-25 February, 2017

EDITORS

Federico Liberatore, Greg H. Parlier and Marc Demange

http://www.icores.org

SPONSORED BY

INSTICC

PAPERS AVAILABLE AT

SCITEPRESS DIGITAL LIBRARY

ICORES 2017

Proceedings of the
6th International Conference on
Operations Research and Enterprise Systems

Porto - Portugal

February 23 - 25, 2017

Sponsored by
INSTICC - Institute for Systems and Technologies of Information, Control and Communication

In Cooperation with
AFPC - Association Française pour la Programmation par Contraintes
EurAgEng - European Society of Agricultural Engineers

Edited by Federico Liberatore, Greg H. Parlier and Marc Demange

Printed in Portugal
ISBN: 978-989-758-218-9
Depósito Legal: 421068/17

http://www.icores.org
icores.secretariat@insticc.org

Brief Contents

INVITED SPEAKERS

Dries Goossens
Ghent University
Belgium

Olivier Hudry
Télécom ParisTech
France

José Oliveira
Universidade do Minho
Portugal

ORGANIZING COMMITTEES

CONFERENCE CHAIR

Marc Demange, RMIT University, School of Science - Mathematical Sciences, Australia

PROGRAM CO-CHAIRS

Federico Liberatore, Universidad Carlos III de Madrid, Spain
Greg H. Parlier, INFORMS, United States

LOCAL CHAIR

Pedro Nuno Ferreira Pinto Oliveira, Universidade do Porto, Portugal

SECRETARIAT

Vera Coelho, INSTICC, Portugal

GRAPHICS PRODUCTION AND WEBDESIGNER

André Poeira, INSTICC, Portugal
Sara Santiago, INSTICC, Portugal

WEBMASTER

João Francisco, INSTICC, Portugal
Carolina Ribeiro, INSTICC, Portugal

PROGRAM COMMITTEE

El-Houssaine Aghezzaf, Ghent University, Faculty of Engineering and Architecture, Belgium

Maria Teresa Almeida, ISEG, Universidade de Lisboa, Portugal

Cláudio Alves, Universidade do Minho, Portugal

Annalisa Appice, Università degli Studi di Bari Aldo Moro, Italy

Necati Aras, Bogazici Universitiy, Turkey

Claudia Archetti, University of Brescia, Italy

Roberto Aringhieri, Università degli Studi di Torino, Italy

Ronald Askin, Arizona State University, United States

Patrizia Beraldi, University of Calabria, Italy

David Bergman, University of Connecticut, United States

Renato Bruni, University of Roma "La Sapienza", Italy

Ahmed Bufardi, None, Switzerland

Sujin Bureerat, KhonKaen University, Thailand

Alfonso Mateos Caballero, Universidad Politécnica de Madrid, Spain

Valentina Cacchiani, University of Bologna, Italy

Olivier Caelen, Atos Worldline, Belgium

Paola Cappanera, University of Firenze, Italy

Massimiliano Caramia, University of Roma "Tor Vergata", Italy

José Manuel Vasconcelos Valério de Carvalho, Universidade do Minho, Portugal

Lorenzo Castelli, University of Trieste, Italy

Bo Chen, University of Warwick, United Kingdom

Weifeng Chen, California University of Pennsylvania, United States

Ta-Tao Chuang, Gonzaga University, United States

Andre Augusto Cire, University of Toronto, Canada

Roberto Cordone, University of Milan, Italy

Florbela Maria Cruz Domingues Correia, Instituto Politécnico de Viana do Castelo, Portugal

Alysson Costa, University of Melbourne, Australia

Lino Costa, Universidade do Minho, Portugal

Patrizia Daniele, University of Catania, Italy

Mirela Danubianu, "Stefan cel Mare" University of Suceava, Romania

Andrea D'Ariano, University of Roma TRE, Italy

Bernardo D'Auria, Universidad Carlos III de Madrid, Spain

Xavier Delorme, Ecole Nationale Supérieure des Mines de Saint-Etienne, France

Marc Demange, RMIT University, School of Science - Mathematical Sciences, Australia

Paolo Detti, University of Siena, Italy

Clarisse Dhaenens, French National Institute for Research in Computer Science and Control, France

Nikolai Dokuchaev, Curtin University, Australia

Christophe Duhamel, Université Blaise Pascal, Clermont-Ferrand, France, France

Khaled Elbassioni, Masdar Institute, United Arab Emirates

Ali Emrouznejad, Aston University, United Kingdom

Nesim Erkip, Bilkent University, Turkey

Giovanni Fasano, University of Venezia "Ca' Foscari", Italy

Paola Festa, University of Napoli, Italy

Carlo Filippi, University of Brescia, Italy

Ingrid Fischer, Universität Konstanz, Germany

Muhammad Marwan Muhammad Fuad, Aarhus University, Denmark

Antonio Fuduli, University of Calabria, Italy

Heng-Soon Gan, The University of Melbourne, Australia

Claudio Gentile, CNR, Italy

Ron Giachetti, Naval Postgraduate School, United States

Ilias Gialampoukidis, Information Technologies Institute, Greece

Stefano Giordani, University of Roma "Tor Vergata", Italy

Alessandro Giuliani, University of Cagliari, Italy

Giorgio Gnecco, IMT - School for Advanced Studies - Lucca, Italy

Marc Goerigk, Lancaster University, United Kingdom

Boris Goldengorin, Ohio University, United States

Marta Castilho Gomes, CERIS-CESUR, Instituto Superior Técnico, Universidade de Lisboa, Portugal

Dries Goossens, Ghent University, Belgium

Stefano Gualandi, AntOptima, SA, Switzerland

Christelle Guéret, University of Angers, France

Francesca Guerriero, University of Calabria, Italy

Nalan Gulpinar, The University of Warwick, United Kingdom

Tias Guns, KU Leuven, Belgium

Gregory Z. Gutin, Royal Holloway University of London, United Kingdom

Jin-Kao Hao, University of Angers, France

Kenji Hatano, Doshisha University, Japan

Emmanuel Hebrard, LAAS-CNRS, France

Hanno Hildmann, Universidad Carlos III de Madrid, Spain

Chenyi Hu, The University of Central Arkansas, United States

Johann Hurink, University of Twente, Netherlands

Josef Jablonsky, University of Economics, Czech Republic

Angel A. Juan, Open University of Catalonia, Spain

Itir Karaesmen, American University, United States

Daniel Karapetyan, University of Essex, United Kingdom

George Katsirelos, INRA, France

Ahmed Kheiri, Cardiff University, United Kingdom

Philip Kilby, NICTA and the Australian National University, Australia

Jesuk Ko, Gwangju University, Korea, Republic of

Leszek Koszalka, Wroclaw University of Technology, Poland

Sotiria Lampoudi, Liquid Robotics Inc, United States

Giuseppe Lancia, University of Udine, Italy

Dario Landa-Silva, University of Nottingham, United Kingdom

Pierre L'Ecuyer, Universite de Montreal, Canada

Janny Leung, The Chinese University of Hong Kong (Shenzhen), China

Federico Liberatore, Universidad Carlos III de Madrid, Spain

Michele Lombardi, DISI, University of Bologna, Italy

Pierre Lopez, LAAS-CNRS, Université de Toulouse, France

Helena Ramalhinho Lourenço, Universitat Pompeu Fabra, Spain

Guglielmo Lulli, Lancaster University, United Kingdom

Qiang Ma, Kyoto University, Japan

Viliam Makis, University of Toronto, Canada

Enrico Malaguti, University of Bologna, Italy

Arnaud Malapert, Université Nice Sophia-Antipolis CNRS, France

Federico Malucelli, Politecnico di Milano, Italy

Emanuele Manni, University of Salento, Italy

Patrice Marcotte, Université de Montréal, Canada

Concepción Maroto, Universidad Politécnica de Valencia, Spain

Pedro Coimbra Martins, Polytechnic Institute of Coimbra, Portugal

Nimrod Megiddo, IBM Almaden Research Center, United States

Carlo Meloni, Politecnico di Bari, Italy

Marta Mesquita, Universidade de Lisboa, Portugal

Rym MHallah, Kuwait University, Kuwait

Michele Monaci, Università degli Studi di Bologna, Italy

Jairo R. Montoya-Torres, Universidad de los Andes, Colombia

Young Moon, Syracuse University, United States

Gaia Nicosia, Università degli Studi Roma Tre, Italy

Inneke Van Nieuwenhuyse, KU Leuven, Belgium

José Oliveira, Universidade do Minho, Portugal

Pedro Nuno Ferreira Pinto Oliveira, Universidade do Porto, Portugal

Mohammad Oskoorouchi, California State University-San Marcos, United States

Selin Özpeynirci, Izmir University of Economics, Turkey

Massimo Paolucci, University of Genova, Italy

Greg H. Parlier, INFORMS, United States

Gabrielle Peko, The University of Auckland, New Zealand

Ana Isabel Pereira, Instituto Politécnico de Bragança, Portugal

Ulrich Pferschy, University of Graz, Austria

Diogo Pinheiro, Brooklyn College of the City University of New York, United States

Marco Pranzo, University of Siena, Italy

Steven Prestwich, University College Cork, Ireland

Caroline Prodhon, Charles Delaunay Institute, France

Luca Quadrifoglio, Texas A&M University, United States

Arash Rafiey, Indiana State University, United States

Günther Raidl, Vienna University of Technology, Austria

Celso Ribeiro, Universidade Federal Fluminense, Brazil

Michela Robba, University of Genova, Italy

Ana Maria Alves Coutinho Rocha, Universidade do Minho, Portugal

Guzmán Santafé Rodrigo, Universidad Pública de Navarra, Spain

Helena Sofia Rodrigues, Instituto Politécnico de Viana do Castelo, Portugal

Andre Rossi, Université d'Angers, France

Lukas Ruf, Consecom AG, Switzerland

Stefan Ruzika, University of Koblenz-Landau, Germany

Alessia Saggese, University of Salerno, Italy

Mohamed Saleh, Cairo University, Egypt

Flavio Sartoretto, Università Ca' Foscari di Venezia, Italy

Cem Saydam, University of North Carolina Charlotte, United States

Abdelkader Sbihi, EM Normandie, France

Pierre Schaus, UCLouvain, Belgium

Andrea Scozzari, Universita' degli Studi "Niccolo' Cusano", Italy

Laura Scrimali, University of Catania, Italy

Rene Seguin, Defence Research and Development Canada, Canada

Meinolf Sellmann, IBM, United States

Antonio Sforza, University of Napoli "Federico II", Italy

Fabio Stella, University of Milano-Bicocca, Italy

Claudio Sterle, University of Napoli "Federico II", Italy

Thomas Stützle, Université Libre de Bruxelles, Belgium

Wai Yuen Szeto, The University of Hong Kong, Hong Kong

Vadim Timkovski, South University, United States

Norbert Trautmann, University of Bern, Switzerland

Chefi Triki, University of Salento, Italy

Michael Tschuggnall, University of Innsbruck, Austria

Begoña Vitoriano, Complutense University, Spain

Maria Vlasiou, Eindhoven University of Technology, Netherlands

Cameron Walker, University of Auckland, New Zealand

Qi Wang, Northwestern Polytechnical University, China

Dominique de Werra, École Polytechnique Fédérale de Lausanne (EPFL), Switzerland

Gerhard Woeginger, Eindhoven University of Technology, Netherlands

Neil Yorke-Smith, American University of Beirut, Lebanon

Hongzhong Zhang, Columbia University, United States

Yiqiang Zhao, Carleton University, Canada

Sanming Zhou, University of Melbourne, Australia

Jan Zizka, Mendel University in Brno, Czech Republic, Czech Republic

Paola zuddas, university of cagliari, Italy

AUXILIARY REVIEWERS

Mikael Capelle, Thales Alenia Space, France

Yun He, CNRS, LAAS, Université de Toulouse, France

Markus Sinnl, University of Vienna, Austria

Dimitri Thomopulos, University of Bologna, Italy

SELECTED PAPERS BOOK

A number of selected papers presented at ICORES 2017 will be published by Springer in a CCIS Series book. This selection will be done by the Conference Chair and Program Co-chairs, among the papers actually presented at the conference, based on a rigorous review by the ICORES 2017 Program Committee members.

FOREWORD

This book contains the proceedings of the 6th International Conference on Operations Research and Enterprise Systems (ICORES 2017). This conference is sponsored by the Institute for Systems and Technologies of Information, Control and Communication (INSTICC) in cooperation with the Association Française pur la Programmation par Contraintes (AFPC) and the European Society of Agricultural Engineers (EurAgEng).

The purpose of the International Conference on Operations Research and Enterprise Systems is to bring together researchers, engineers and practitioners interested in advances and applications in the field of operations research. Two simultaneous tracks will be held, one on domain independent methodologies and technologies, and the second on practical work developed in specific application areas.

This year ICORES received 90 paper submissions from 36 countries, of which 20% were accepted as full papers. The high quality of the papers received imposed difficult choices during the review process. To evaluate each submission, a double blind paper review was performed by the Program Committee, whose members are highly qualified independent researchers in the two ICORES topic areas.

To recognize the best overall and student contributions, awards based on both the best reviews, as assessed by the Program Committee, and presentation quality, as assessed by session chairs at the conference venue, will be conferred during the closing session of the conference. Based on reviewer evaluations and presentation quality, a short list of authors will be invited to submit extended revised versions of their papers for a book to be published by Springer containing the best ICORES 2017 papers.

The conference program includes a panel and three invited talks delivered by internationally distinguished speakers, namely: Dries Goossens (Ghent University, Belgium), Olivier Hudry, Télécom ParisTech, France) and José Oliveira (Universidade do Minho, Portugal) The ICORES program also includes a Doctoral Consortium on Operations Research and Enterprise Systems that brought together Ph.D. students within the operations research field to discuss their research in an international forum. We would like to thank the Doctoral Consortium Chair, Jorge Pinho de Sousa (Universidade do Porto, Portugal) and the Local Chair, Pedro Nuno Ferreira Pinto Oliveira (Universidade do Porto, Portugal) for their value-added collaboration to ICORES.

We express our thanks to all participants. First to all the authors, whose quality work is the essence of this conference; secondly to all members of the Program Committee and auxiliary reviewers, who helped us with their expertise and valuable time. We also deeply thank the invited speakers for excellent contributions in sharing their knowledge and vision. Finally, special thanks to all the members of the INSTICC team whose collaboration and coordination were fundamental to the success of this conference.

We wish you all an inspiring conference and an unforgettable stay in Porto, Portugal. We hope to meet you again next year for the 7th edition of ICORES, details of which will soon be available at http://www.icores.org.

Federico Liberatore
Universidad Carlos III de Madrid, Spain

Greg H. Parlier
INFORMS, United States

Marc Demange
RMIT University, School of Science - Mathematical Sciences, Australia

CONTENTS

INVITED SPEAKERS

KEYNOTE SPEAKERS

Optimization in Sports League Scheduling

Dries Goossens
Ghent University, Belgium

Abstract: Millions of people, all over the world, are enthralled by sports, be it actively participating or as a fan or spectator. At the same time, almost every sports competition needs a schedule of play, stating who will play whom, when, and where. Not much more than a decade ago, most professional sports competitions were scheduled by unskilled personnel, equipped with little more than pen and paper. A good schedule is important though, because it has an effect on the fairness and outcome of the competition, public attendance, commercial interests, as well as security and the cost of policing. As league owners managed to close astonishing broadcasting deals and the financial interests in the sports industry continued to grow, the importance of a good schedule became more and more apparent.

Sports scheduling is a young academic discipline: although the first substantial contributions were published in the early 80's (e.g. De Werra, 1981), a considerable increase in sports scheduling articles appeared only in recent years, including publications in top journals in operations research. Simultaneously, several academics reached out to the sport scheduling practitioners, offering new methods to deal with the increasingly more complex problem of scheduling a league. In this talk, we attempt to illustrate the many ways in which the sports industry can benefit from operations research, particularly in sports scheduling.

We discuss practical applications involving the scheduling of the Belgian Pro League football (soccer), for which we develop the official schedule since 2006. Our contract with the Belgian Pro League now involves 2 professional and 1 amateur division with interdependencies (e.g. teams from different divisions sharing a stadium or a police force) and play-offs. We present methods that have proven their value in real-life sport scheduling. We discuss fairness issues, such as the carry-over effect, as well as a discrete choice experiment we carried out in order to estimate the impact of the schedule on TV viewership and stadium attendance.

BRIEF BIOGRAPHY

Dries Goossens is assistant professor at the Faculty of Economics and Business Administration of Ghent University. His research interests are mainly in tournament scheduling and related fairness issues (e.g. the carry-over effect); favorite sports are cycling and football (soccer). Together with prof. Frits Spieksma (KU Leuven), he has been computing the official schedule for the Belgian Pro League since 2006. Apart from sports, Dries Goossens has also done research on various combinatorial optimization problems, such as combinatorial auctions, the transportation problem, and the assignment problem.

Research Areas:

Sport scheduling
Combinatorial auctions
Combinatorial optimization

Goossens, D.
Optimization in Sports League Scheduling.
In *Proceedings of the 6th International Conference on Operations Research and Enterprise Systems (ICORES 2017)*, page 5
ISBN: 978-989-758-218-9

Operations Research and Voting Theory

Olivier Hudry
Télécom ParisTech, France

Abstract: One main concern of voting theory is to determine a procedure for choosing a winner from among a set of candidates, based on the preferences of the voters or, more ambitiously, for ranking all the candidates or a part of them. Such a situation occurs, obviously, in the field of social choice and welfare and especially of elections, but also in many other fields: games, sports, artificial intelligence, spam detection, Internet applications, statistics, and so on. It is customarily agreed that the search for a "good" voting procedure goes back at least to the end of the eighteenth century, with the works of the chevalier Jean-Charles de Borda (1733-1799) and of Marie Jean Antoine Nicolas Caritat, marquis de Condorcet (1743-1794). Kenneth Arrow's theorem (1951) ruined the hope of designing a "good" procedure by showing that there does not exist a "good" voting method, with respect to some "reasonable" axiomatic properties; this is known as the famous "Arrow's impossibility theorem".

In this presentation, we will pay attention to some contributions of operations research to the design and the study of some voting procedure.

First, we show through an easy example that the voting procedure plays an important role in the determination of the winner. More precisely, we show how, for an election with 5 candidates, the choice of the voting procedure allows electing anyone of the 5 candidates with the same individual preferences of the voters. This example provides also the opportunity to recall some main procedures, including the ones advocated by Borda or by Condorcet, and leads to the statement of Arrow's theorem.

In a second step, more devoted to a mathematical approach, we define the so-called median procedure, extending Condorcet's method. In this procedure, the aim is to compute a ranking of the candidates which minimizes the number of disagreements with respect to the voters' preferences. Thus we obtain a combinatorial optimization problem. We show how to state it as a linear programming problem with binary variables or as a graph theoretic problem. This allows also studying the complexity of this median procedure.

Last, we show, once again through easy examples, that the lack of some desirable properties for the considered voting procedure may lead some "paradoxes" like the following ones:

- Abstention can lead to a more desirable result for me than if I vote for my favourite candidate!
- If I vote for my favourite candidate, he or she loses the election but if I vote for the candidate that I most dislike, my favourite candidate wins!
- Even if every voter prefers candidate A to candidate B (unanimity), B may beat A in the election!
- and so on...

BRIEF BIOGRAPHY

Olivier Hudry is a professor in theoretical computer science and discrete mathematics at the Computer Science and Networks department of Telecom ParisTech, one of the main French graduate engineering schools. In his PhD thesis (1989), he studied mathematical aspects of elections, especially the complexity of the aggregation of individual preferences into a collective one which summarizes the opinions of the voters as well as possible. He obtained his "habilitation à diriger des recherches" of the University Paris 6 in 1998, devoted to discrete mathematics and combinatorial optimization in graphs. He was the elected president of the French association of operations research (ROADEF) from 2008 to 2010 and has been the head of the team "Mathematics of Information, Communication and Computation" of Telecom ParisTech since 2011. He is also the editor-in-chief of the journal "Mathematics and Social Sciences". His current research topics are discrete mathematics, graph theory, combinatorics, combinatorial optimization, operations research.

Hudry, O.
Operations Research and Voting Theory.
In *Proceedings of the 6th International Conference on Operations Research and Enterprise Systems (ICORES 2017)*, page 7
ISBN: 978-989-758-218-9

The Role of Operations Research to Support Portuguese SMEs
Challenges and Opportunities

José Oliveira
Universidade do Minho, Portugal

Abstract: Since Portugal joined the European Economic Community in 1986, significant structural changes have occurred in the Portuguese economy in response to the growing challenges and opportunities that are result of globalisation and European integration. Portuguese companies, especially small and medium-sized enterprises (SMEs), had to adjust their business and their production processes to meet the requirements of their new European customers. Traditionally SMEs in northern Portugal belonged to activity sectors with intensive but low-skilled and low-productivity labour with an emphasis on footwear, textiles and clothing. For some time, companies remained in a competitive position through a strategy of low wages.

Twenty years later (2005), the opening up of the European market promoted strong competition and overcapacities due to new market entrants from south-east Asia and the eastern European countries. Consequently, many Portuguese SME companies have ended their manufacturing operations in Europe; other companies have chosen to move to countries where the cost of labour is lower. Several companies that survived the opening of the European market selected the production of higher added value products based on innovation and the incorporation of technology. Other companies have chosen to outsource the production of their products to companies located in very low-wage countries, so that their products remain competitive. All these strategies have resulted in more complex manufacturing processes.

Over the past 30 years, Portuguese SMEs achieved important improvements (innovations) in their businesses, in their productivity by incorporating information and communications technologies, using quality management system for the institution of a continuous improvement process, and other practices that allowed them to control and minimize the cost of production and/or improve the level of service provided. In the last decade there has been a very interesting evolution of lean management projects in Portuguese SMEs that seek for excellence in security, quality, cost and delivery, improving their processes, eliminating loss and reducing variability.

We are currently surfing the "technological wave" in direction to the "Industry 4.0", and Portuguese SME companies will face new challenges. Lean practices are no longer enough to ensure that SMEs can increase their level of competitiveness, since the manufacturing process no longer has visible (or easy to identify) waste. There is now an awareness among managers of SMEs that it is necessary to include other optimization measures in their (production) processes. The change in the production paradigm in mass to the mass customization, leading to the emergence of increasingly smaller orders, involves the manufacture of small series with delivery dates ever shorter, and supply with increasingly competitive prices. Satisfying these demands requires increasingly detailed studies of the real problems, and the development of solution methods increasingly sophisticated.

It is in this context that Operational Research will be increasingly used as a methodology to promote the increase of competitiveness of enterprises. However, in the case of the Portuguese SMEs the resources for scientific research investment in partnerships with universities are very limited, or even non-existent. In order to change this situation incentive programs have been provided for modernization and innovation of SMEs and their production processes. The establishment partnerships enterprise-university is still embryonic, and it is for the universities (in this case of Operational Research) demonstrate that they can produce better solutions than those that companies succeed by their own means. This lecture will present some case studies of operational research methodology implementation in the context of SMEs in the north of Portugal.

Oliveira, J.
The Role of Operations Research to Support Portuguese SMEs: Challenges and Opportunities.
In *Proceedings of the 6th International Conference on Operations Research and Enterprise Systems (ICORES 2017)*, pages 9-10
ISBN: 978-989-758-218-9

BRIEF BIOGRAPHY

José A. Oliveira studied Mechanical Engineering at the University of Porto, Portugal (1991). He was Process Engineer at Texas Instruments Portugal (1991-1992) and Blaupunkt - Auto Rádio Portugal (1992). He graduated with a Ph.D. in Production and Systems Engineering at University of Minho, Portugal (2001). His main research interests are Optimization with Heuristic Methods in Industrial and Systems Engineering, with main focus in the Supply Chain, Logistics, Routing and Scheduling.

PAPERS

FULL PAPERS

Search-and-Fetch with 2 Robots on a Disk
Wireless and Face-to-Face Communication Models

Konstantinos Georgiou[1,*], George Karakostas[2,*] and Evangelos Kranakis[3,*]
[1]*Department of Mathematics, Ryerson University, 350 Victoria St., Toronto, ON, M5B 2K3, Canada*
[2]*Dept. of Computing & Software, McMaster University, 1280 Main St. West, Hamilton, Ontario L8S 4K1, Canada*
[3]*School of Computer Science, Carleton University, 1125 Col. By Dr., Ottawa, ON K1S 5B6, Canada*
konstantinos@ryerson.ca, karakos@mcmaster.ca, kranakis@scs.carleton.ca

Keywords: Search & Fetch, Distributed Algorithm, Rendevouz, Exploration, Face-to-Face Model, Wireless Model.

Abstract: We introduce and study *treasure-evacuation* with 2 robots, a new problem on distributed *searching and fetching* related to well studied problems in searching, rendezvous and exploration. The problem is motivated by real-life search-and-rescue operations in areas of a disaster, where unmanned vehicles (robots) search for a victim (treasure) and subsequently bring (fetch) her to safety (the exit). One of the critical components in such operations is the communication protocol between the robots. We provide search algorithms and contrast two standard models, the face-to-face and the wireless model. Our main technical contribution pertains to the face-to-face model. More specifically, we demonstrate how robots can take advantage of some minimal information of the topology (i.e., the disk) in order to allow for information exchange without meeting. The result is a highly efficient distributed treasure-evacuation protocol which is minimally affected by the lack of distant communication.

1 INTRODUCTION

We introduce the study of a new distributed problem on *searching and fetching* called *treasure evacuation*. Two robots are placed at the center of a unit disk, while an exit and a treasure lie at unknown positions on the perimeter of the disk. Robots search with maximum speed 1, and they detect an interesting point (either the treasure or the exit) only if they pass over it. The exit is immobile, while the treasure can be carried by any of the robots. The goal of the search is for at least one of the robots to bring (fetch) the treasure to the exit, i.e. evacuate the treasure, in the minimum possible completion time. The robots do not have to evacuate, rather they only need to co-operate, possibly by sharing information, so as to learn the locations of the interesting points and bring the treasure to the exit. Contrary to previous work, this is the first time an explicit ordering on the tasks to be performed is imposed (first the treasure, then the exit). This makes the problem inherently different in nature and more difficult than similarly looking results.

Finding an optimal algorithm turns out to be a challenging task even when the robots have some knowledge, e.g., the arc-distance α between the exit and the treasure. We propose treasure-evacuation protocols in two communication models. In the *wireless* model robots exchange information instantaneously and at will, while in the *face-to-face* model information can be exchanged only if the robots meet. We aim at incorporating this knowledge into our algorithm designs. We offer algorithmic techniques such as planning ahead, timing according to the explicit task ordering, and retrieval of unknown information through inference and not communication.

Part of our contribution is that we demonstrate how robots can utilize the knowledge of the arc-distance α between the interesting points. We propose protocols that induce worst case evacuation time $1+\pi-\alpha/2+3\sin(\alpha/2)$ for the wireless model and $1+\pi-\alpha+4\sin(\alpha/2)$ for the face-to-face model. The upper bound in the face-to-face model, which is our main contribution, is the result of a non-intuitive evacuation protocol that allows robots to exchange information about the topology without meeting, effectively bypassing their inability to communicate from distance. Finally, we complement our results above by showing that any algorithm in the face-to-face model needs time at least $1+\pi/3+4\sin(\alpha/2)$, if $\alpha \in [0,2\pi/3]$ and at least $1+\pi/3+2\sin(\alpha)+2\sin(\alpha/2)$, if $\alpha \in [2\pi/3,\pi]$.

*Research supported in part by NSERC.

Georgiou, K., Karakostas, G. and Kranakis, E.
Search-and-Fetch with 2 Robots on a Disk - Wireless and Face-to-Face Communication Models.
In *Proceedings of the 6th International Conference on Operations Research and Enterprise Systems (ICORES 2017)*, pages 15-26
ISBN: 978-989-758-218-9

1.1 Contributions

Rendezvous, treasure hunting and exploration have been subjects of extensive research in the broad area of distributed and online computing (see related work below). Challenges in each of these fundamental tasks arise from different computation, communication or knowledge limitations, with admittedly numerous variations. The novel distributed problem of treasure-evacuation that we introduce and study in this work combines in a complex way challenges from all these fundamental tasks. As such, progress towards solving generic treasure-evacuation-like problems will unavoidably touch on state-of-the-art techniques of achieving these tasks.

In treasure-evacuation, two stationary targets (a treasure and an exit that we call *interesting points*) are hidden on a specific domain. At first, robots need to (a) perform treasure hunting in this online environment. Interestingly, the knowledge of the location of one of these targets may or may not reveal the location of the other. In particular, the task of the robots does not end when both interesting points are located, rather, only when the treasure-holder learns (and finds) the location of the exit as well. Given communication limitations, the latter can be accomplished *efficiently* only if (b) a sufficient portion of the environment is explored before both interesting points are found, or (c) if information can be exchanged between robots. In case (b), robots "invest" in domain exploration in an attempt to expedite treasure evacuation once the interesting points are found. In case (c), robots may need to attempt to rendezvous (not very late in the time horizon) so that the distributed system becomes cognitive of the environment and consequently completes the given task. Clearly, in order for a distributed system to accomplish treasure evacuation efficiently, robots need to perform and balance all tasks (a),(b),(c) above, i.e to perform treasure hunting, while learning the environment either by exploration or by rendezvous. A unique feature of treasure-evacuation is that only the treasure has to be brought to the exit.

The last observation gives some first evidence of the difficulty of solving treasure-evacuation, even when the domain is a disk. Can a robot choose a trajectory (maybe staying far from the exit) to help the treasure-holder expedite evacuation? If a robot discovers the treasure, is it a good strategy to become the treasure holder and greedily search for the exit? Should robots learn the environment by investing on exploration or on rendezvous and hence on message exchange? Finally, is it possible in a non-wireless environment for robots to exchange information without meeting? An efficient algorithm should somehow address all these questions.

From the discussion above, it is not a surprise that plain vanilla algorithms cannot be efficient. Indeed, our algorithms (for both the wireless and face-to-face models) adapt their strategies, among others, with respect to the distance of the interesting points. On one hand, there are configurations where the evacuation protocols are simple and greedy-like. However, the reader can verify from our analyses that, had we followed such simplistic approach for all configurations, the evacuation time would have been much worse than our upper bounds. The simplest example of this kind will be transparent even in the analysis of the wireless model, in which robots can exchange information at will. To achieve our upper bound, robots choose different trajectories (still greedy-like) for various distances of the interesting points. Nevertheless, the analysis in this case is relatively simple.

Our main technical contribution pertains to the face-to-face model where robots can exchange information only if they meet. In particular, we explicitly exhibit distributed strategies that allow robots to exchange information even from distance. At a high level, and given that interesting points are located by robots at some (carefully defined) critical intervals in the time horizon, robots choose (occasionally) highly non-intuitive trajectories, not in order to locate the remaining interesting points, rather to potentially meet their fellow robots. The trajectories are carefully chosen so that a robot may deduce information, using an involved protocol, as to what the other robot has found, and hence learn the environment regardless of whether the rendezvous is realized or not. For the treasure-holder, this would result in learning the location of the exit. For the other robot(s), this would be an altruistic attempt to help the fellow treasure-holder. In particular, that could result in that the non treasure-holder never finds the exit, still expediting the treasure evacuation time. We note that once the trajectories are determined (which is the heart of our contribution) correctness and performance analysis is a matter of an exhaustive and technical case analysis. Interestingly, the efficiency of our algorithm for the face-to-face model is only slightly worse than the solution for the wireless case (but significantly better than the naive solution for the face-to-face model), indicating that lack of communication can be compensated by clever algorithms.

Finally, we complement our results by proving some lower bounds for treasure evacuation with 2 robots for the face-to-face model. That concludes the first attempt to study distributed problems of this kind, i.e. optimization treasure hunting problems where the distributed systems learn the online environment by a

combination of exploration and rendezvous, a feature which, to the best of our knowledge, is also novel.

1.2 Related Work

Traditional search is concerned with finding an object with specified properties within a search space. Searching in the context of computational problems is usually more challenging especially when the environment is unknown to the searcher(s) (see (Ahlswede and Wegener, 1987; Alpern and Gal, 2003; Stone, 1975)). This is particularly evident in the context of robotics whereby exploration is taking place within a given geometric domain by a group of autonomous but communicating robots. The ultimate goal is to design an algorithm so as to accomplish the requirements of the search (usually locating a target of unknown a priori position) while at the same time obeying the computational and geographical constraints. The input robot configuration must also accomplish the task in the minimum possible amount of time (Berman, 1998).

Search has a long history. There is extensive and varied research and several models have been proposed and investigated in the mathematical and theoretical computer science literature with particular emphasis on probabilistic search (Stone, 1975), game theoretic applications (Alpern and Gal, 2003), cops and robbers (Bonato and Nowakowski, 2011), classical pursuit and evasion (Nahin, 2012), search problems as related to group testing (Ahlswede and Wegener, 1987), searching a graph (Koutsoupias et al., 1996), and many more. A survey of related search and pursuit evasion problems can be found in (Chung et al., 2011). In pursuit-evasion, pursuers want to capture evaders who try to avoid capture. Examples include *Cops and Robbers* (whereby the cops try to capture the robbers by moving along the vertices of a graph), *Lion and Man* (a geometric version of cops and robbers where a lion is to capture a man in either continuous or discrete time), etc. Searching for a motionless point target has some similarities with the lost at sea problem, (Gluss, 1961; Isbell, 1967), the cow-path problem (Beck, 1964; Bellman, 1963), and with the plane searching problem (Baeza-Yates and Schott, 1995). This last paper also introduced the "instantaneous contact model", which is referred to as wireless model in our paper. When the mobile robots do not know the geometric environment in advance then researchers are concerned with exploring (Albers and Henzinger, 2000; Albers et al., 2002; Deng et al., 1991; Hoffmann et al., 2001). Coordinating the exploration of a team of robots is a main theme in the robotics community (Burgard et al., 2005; Thrun, 2001; Yamauchi, 1998) and often this is combined with the mapping of the terrain and the position of the robots within it (Kleinberg, 1994; Papadimitriou and Yannakakis, 1989).

Evacuation for grid polygons has been studied in (Fekete et al., 2010) from the perspective of constructing centralized evacuation plans, resulting in the fastest possible evacuation from the rectilinear environment. There are certain similarities of our problem to the well-known evacuation problem on an infinite line (see (Baeza Yates et al., 1993) and the recent (Chrobak et al., 2015)) in that the search is for an unknown target. However, in this work the adversary has limited possibilities since search is on a line. Additional research and variants on this problem can be found in (Demaine et al., 2006) (on searching with turn costs), (Kao et al., 1996) (randomized algorithm for the cow-path problem), (Kao et al., 1998) (hybrid algorithms), and many more.

A setting similar to ours is presented in the recent works (Czyzowicz et al., 2014; Czyzowicz et al., 2016; Czyzowicz et al., 2015a; Czyzowicz et al., 2015b) where algorithms are presented in the wireless and non-wireless (or face-to-face) communication models for the evacuation of a team of robots. The "search domain" in (Czyzowicz et al., 2014; Czyzowicz et al., 2016; Czyzowicz et al., 2015a) is a unit circle (while in (Czyzowicz et al., 2015b) the search domain is a triangle or square), however, unlike our search problem, in these papers all the robots are required to evacuate from an unknown exit on the perimeter. Moreover, in none of these papers is there a treasure to be fetched to the exit.

Our work is also an attempt to analyze theoretically search-and-fetch problems that have been studied by the robotics community since the 90's, e.g. see (Jennings et al., 1997). A scenario similar to ours (but only for 1 robot) has been introduced by Alpern in (Alpern, 2011), where the domain was discrete (a tree) and the approach/analysis resembled that of standard search-type problems (Alpern and Gal, 2003). In contrast, our problem is of distributed nature, and our focus is to demonstrate how robots' communication affects efficiency.

1.3 Problem and Model Motivation

Our problem is motivated by real-life surveillance and search-and-rescue operations where unmanned vehicles, e.g. drones, search for victims in areas of a disaster. Indeed, consider a group of rescuer-mobile-agents (robots), initially located strategically in a central position of a domain. When alarm is triggered and a distress signal is received, robots need to locate a vic-

tim (the treasure) and bring her to safety (the exit). Our problem shares similarities also with classic and well-studied cops-and-robbers games; robots rest at a central position of a domain (say, in the centre of a disk as in our setup) till an alarm is triggered by some "robber" (the treasure in our case). Then, robots need to locate the stationary robber and subsequently bring him to jail (the exit). Interestingly, search-and-fetch type problems resemble also situations that abound in fauna, where animals hunt for prey which is then brought to some designated area, e.g. back to the lair. As such, further investigation of similar problems will have applications to real-life rescue operations, as well as to the understanding of animal behavior, as it is common in all search problems.

From a technical perspective, our communication models are inspired by the recent works on evacuation problems (Czyzowicz et al., 2014; Czyzowicz et al., 2015a; Czyzowicz et al., 2015b). Notably, the associated search problems are inherently different than our problem which is closer in nature to search-type, treasure-hunt, and exploration problems. Also, our mathematical model features (a) a distributed setting (b) with objective to minimize time, and (c) where different communication models are contrasted. None among (a),(b),(c) are well understood for search games, and, to the best of our knowledge, they have not been studied before in this combination.

Specific to the problem we study are the number of robots (2 and not arbitrarily many - though our results easily extend to swarms of robots), the domain (disk), and the fact the robots have some knowledge about the interesting points. Although extending our results to more generic situations is interesting in its own right, the nature of the resulting problems would require a significantly different algorithmic approach. Indeed, our main goal is to study how limitations in communication affect efficiency, which is best demonstrated when the available number of robots, and hence computation power, is as small as possible, i.e. for two robots. In fact, it is easy to extend our algorithms for the n-robot case.

Notably, search-and-fetch problems are challenging even for 1 robot as demonstrated in (Georgiou et al., 2016b). In particular, the work of (Georgiou et al., 2016b) implies that establishing provably optimal evacuation protocols for 2-robots is a difficult task, even when the domain is the disk. Nevertheless, we view the domain that we study as natural. Indeed, a basic setup in search-and-rescue operations is that rescuer-robots inhabit in a base-station, and they stay inactive till they receive a distress signal. As it is common in real-life situations, the signal may only reveal partial information about the location of a victim, e.g. its distance from the base-station, along with the distance between the points. When there are more than one interesting points to be located, this kind of information suggests that the points lie anywhere on cocentric circles. When the points are equidistant from the base-station, robots need only consider a disk, as it is the case in our problem. We believe that with enough technical and tedious work, our results can also extend to non-equidistant points, however the algorithmic significance of the proposed distributed solutions may be lost in the technicalities.

In order to demonstrate that robots with primitive communication capabilities are in fact not much less powerful than in the wireless model, it is essential to assume that robots have some knowledge of the distance between the interesting points. The reader may also view this piece of advice as an algorithmic challenge in order to bypass the uncertainty regarding the locations of the interesting points. Notably, our algorithms adapt strategies as a function of the distance of the interesting points, trying to follow protocols that would allow them to detect the actual positions of the points without necessarily visiting them. As an easy example, note that if a robot has explored already a contiguous arc of length $\alpha+\varepsilon$, the discovery of an interesting point reveals the location of the other α-arc distant away interesting point (our algorithm makes use of distance α in a much more sophisticated way). As a result, had we assumed that distances are unknown, robots may not be able to deduce such important information about the topology using partial exploration, and the problem would require an inherently different algorithmic approach. Apart from that, partial knowledge of the input is also interesting due to the efficiency-information tradeoffs that are naturally induced by the problem, which is also a standard theme in competitive analysis, e.g. see (Hipke et al., 1999) and (Georgiou et al., 2016b).

Admittedly, the model we introduce is simple but natural, general, and complex enough to require non-standard algorithmic solutions. Most importantly, our model allows us to demonstrate in a relatively clean way a couple of novel algorithmic techniques for attacking challenging and newly introduced types of distributed problems. We anticipate that the ideas introduced in this work will initiate new research directions towards solving a family of problems that are not yet understood from a theoretical perspective.

1.4 Notation & Organization

A treasure and an exit are located at unknown positions on the perimeter of a unit-disk and at arc dis-

tance α (in what follows all distances will be arc-distances, unless specified otherwise). Robots start from the center of the disk, and can move anywhere on the disk at constant speed 1. Each of the robots detects the treasure or the exit only if its trajectory passes over that point on the disk. Once detected, the treasure can be carried by a robot at the same speed. We refer to the task of bringing the treasure to the exit as *treasure-evacuation*. We use the abbreviations T, E for the treasure and the exit, respectively. For convenience, in the sequel we will refer to the locations of the exit and the treasure as *interesting* points. For an interesting point I on the perimeter of the disk, we also write $I = E$ ($I = T$) to indicate that the exit (treasure) lies in point I. For a point B, we also write $B = null$ to denote the event that neither the treasure nor the exit is placed on B.

We focus on the following online variations of treasure-evacuation with 2 robots, where the exact distance α between T, E is known, but not their positions. In **2-TE**$_w$ (Section 2), information between robots is shared continuously in the time horizon, i.e. messages between them are exchanged instantaneously and at will with no restrictions and no additional cost or delays. In **2-TE**$_{f2f}$ (Section 3), the communication protocol between the robots is face-to-face (non-wireless)—abbreviated F2F (or f2f), where information can be exchanged only if the robots meet at the same point anywhere. We give two algorithms: in the former case we prove a $1+\pi-\alpha+4\sin(\alpha/2)$ and in the latter case a $1+\pi-\alpha/2+3\sin(\alpha/2)$ upper bound, resp., on the treasure evacuation time, where α is the arc distance between treasure and exit. Finally in Section 4 we provide a lower bound for treasure-evacuation with 2 robots in the F2F model.

Any omitted proofs, due to space limitations, can be found in the full version of the paper (Georgiou et al., 2016a).

2 WIRELESS MODEL

As a warm-up we present in this section an upper bound for the wireless model, which will also serve as a reference for the more challenging face-to-face model. The algorithmic solution we propose is simple and it is meant to help the reader familiarize with basic evacuation trajectories that will be used in our main contribution pertaining to the face-to-face model.

Theorem 2.1. *For every $\alpha \in [0,\pi]$, problem 2-TE$_w$ can be solved in time $1+\pi-\alpha+4\sin(\alpha/2)$.*

To prove Theorem 2.1, we propose Algorithm 1 that achieves the promised bound. Intuitively, our algorithm follows a greedy like approach, adapting its strategy as a function of the distance α of the interesting points. If α is small enough, then the two robots move together to an arbitrary point on the disk and start exploring in opposing directions. Otherwise the two robots move to two antipodal points and start exploring in the same direction. Exploration continues till an interesting point is found. When that happens, the robot that can pick up the treasure and fetch it to the exit in the fastest time (if all locations have been revealed) does so, otherwise remaining locations are tried exhaustively. Detailed descriptions of the evacuation protocol can be seen in Algorithm 1, complemented by Figure 1.

Noticeably, the performance analysis we give is tight, meaning that for every $\alpha \geq 0$, there are configurations (placements of the interesting points) for which the performance of the algorithm is exactly $1+\pi-\alpha+4\sin(\alpha/2)$. Most importantly, the performance analysis makes explicit that naive algorithms that do not adapt strategies together with α are bound to perform strictly worse than our upper bound. Also, the achieved upper bound should be contrasted to the upper bound for the face-to-face model (which is achieved by a much more involved algorithm), which at the same time is only $\alpha/2-\sin(\alpha/2)$ more costly than the bound we show in the wireless model.

Algorithm 1 takes advantage of the fact that robots can communicate to each other wirelessly. This also implies that lack of message transmission is effectively another method of information exchange. In what follows point A will always be the starting point of R_2, and A' denotes its antipodal point. For the sake of the analysis and w.l.o.g. we will assume that R_2 is the one that first finds an interesting point $I = \{E, T\}$, say at time $x := \widehat{\mathrm{AI}}$. We call B, C the points that are at clockwise and counter-clockwise arc-distance α from I respectively. Figure 1 depicts the interesting points encountered.

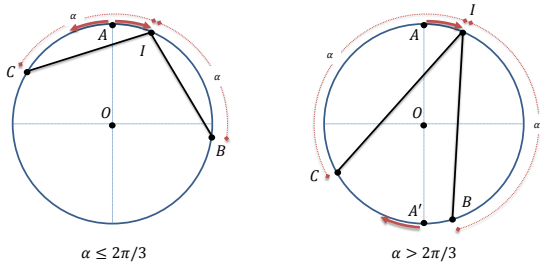

Figure 1: The points of interest for our Algorithm 1.

The description of Algorithm 1 is from the perspective of the robot that finds first an interesting point, that we always assume is R_2. Next we assume that the finding of any interesting point is instanta-

neously transmitted and received by the two robots. Also, if at any moment, the positions of the interesting points are learned by the two robots, then the robots attempt a "confident evacuation" using the shortest possible trajectory. This means for example that if the treasure is not picked up by any robot, then the two robots will compete in order to pick it up and return it to the exit, moving in the interior of the disk.

Algorithm 1: Wireless Algorithm.

Step 1. If $\alpha \leq 2\pi/3$, then the two robots move together to an arbitrary point on the ring and start moving in opposing directions, else they move to arbitrary antipodal points A, A' on the cycle and start moving in the same direction.

Step 2. Let I be the first interesting point discovered by R_2, at time $x := \widehat{\mathrm{AI}}$. Let B, C be the points that are at clockwise and counter-clockwise arc-distance α from I respectively.

Step 3. If $x \geq \alpha/2$ then robots learn that the other interesting point is in B, else R_2 moves to B, R_1 moves to C.

Step 4. Evacuate

Correctness of Algorithm 1 is straightforward, since the two robots follow a "greedy-like evacuation protocol" (still, they use different starting points depending on the value of α). Also, the performance analysis of the algorithm, effectively proving Theorem 2.1, is a matter of a straightforward case-analysis. We note that our worst-case analysis is tight, in that for every $\alpha \geq 0$ there exist configurations in which the performance is exactly as promised by Theorem 2.1. Moreover, we may assume that $\alpha > 0$ as otherwise the problem is solved when one interesting point is found.

Note that our algorithm performs differently when $\alpha \leq 2\pi/3$ and when $\alpha > 2\pi/3$. Let $x := \widehat{\mathrm{AI}}$ be the time that R_2 first discovers interesting point I. Then it must be that $x \leq \alpha/2$ and $x \leq \pi - \alpha$ for the cases $\alpha \leq 2\pi/3$ and $\alpha > 2\pi/3$ respectively (see also Figure 1). This will be used explicitly in the proof of the next two lemmata. We also assume that R_2 always moves clockwise starting from point A. R_1 either moves counter-clockwise starting from A, if $\alpha \leq 2\pi/3$, or it moves clockwise starting from the antipodal point A' of A, if $\alpha > 2\pi/3$. In every case, the two robots move along the perimeter of the disk till time x when R_2 transmits the message that it found an interesting point.

The performance of Algorithm 1 is described in the next two lemmata which admit proofs by case analyses. Each of them examines the relative position of the starting point of robot R_2 (which finds an interesting point first) and the two interesting points.

Lemma 2.2. *Let A be the starting point of R_2 which is the first to discover an interesting point I. Let also the other interesting point be at C, where $\widehat{CI} = \alpha$. If A lies in the arc $\widehat{CI}$, then the performance of Algorithm 1 is $1 + \pi - \alpha + 4\sin(\alpha/2)$, for all $\alpha \in [0, \pi]$.*

Lemma 2.3. *Let A be the starting point of R_2 which is the first to discover an interesting point I. Let also the other interesting point be at B, where $\widehat{IB} = \alpha$. If A lies outside the arc $\widehat{IB}$, then the performance of Algorithm 1 is $1 + \pi - \alpha + 4\sin(\alpha/2)$, for all $\alpha \in [0, \pi]$.*

It is clear now that Lemmata 2.2, 2.3 imply that for all $\alpha \in [0, \pi]$, the overall performance of Algorithm 1 is no more than $1 + \pi - \alpha + 4\sin(\alpha/2)$ concluding Theorem 2.1.

3 F2F MODEL

The main contribution of our work pertains to the face-to-face model and is summarized in the following theorem.

Theorem 3.1. *For every $\alpha \in [0, \pi]$, problem 2-TE$_{f2f}$ can be solved in time $1 + \pi - \alpha/2 + 3\sin(\alpha/2)$.*

Next we give the high-level intuition of the proposed evacuation-protocol, i.e. Algorithm 2, that proves the above theorem (more low level intuition, along with the formal description of the protocol appears in Section 3.1).

Denote by β the upper bound promised by the theorem above. It should be intuitive that when the distance of the interesting points α tends to 0, there is no significant disadvantage due to lack of communication. And although the wireless evacuation-time might not be achievable, a protocol similar to the wireless case should be able to give efficient solutions. Indeed, our face-to-face protocol is a greedy algorithm when α is not too big, i.e. the two robots try independently to explore, locate the interesting points and fetch the treasure to the exit without coordination (which is hindered anyways due to lack of communication). Following a worst case analysis, it is easy to see that as long as α does not exceed a special threshold, call it α_0, the evacuation time is β, and the analysis is tight.

When α exceeds the special threshold α_0, the lack of communication has a more significant impact on the evacuation time. To work around it, robots need to exchange information which is possible only if they meet. For this reason (and under some technical conditions), robots agree in advance to meet back in the center of the disk to exchange information about their findings, and then proceed with fetching the treasure

to the exit. Practically, if the rendezvous is never realized, e.g. only one robot reaches the center up to some time threshold, that should deduce that interesting points are not located in certain parts of the disk, potentially revealing their actual location. In fact, this recipe works well, and achieves evacuation time β, as long as α does not exceed a second threshold, which happens to be $2\pi/3$.

The hardest case is when the two interesting points are further than $2\pi/3$ apart. Intuitively, in such a case there is always uncertainty as to where the interesting points are located, even when one of them is discovered. At the same time, the interesting points, hence the robots, might be already far apart when some or both interesting points are discovered. As such, meeting at the center of the disk to exchange information would be time consuming and induces evacuation time exceeding β. Our technical contribution pertains exactly to this case. Under some technical conditions, the treasure-finder might need to decide which of the two possible exit-locations to consider next. In this case, the treasure-holder follows a trajectory not towards one of the possible locations of the exit, rather a trajectory closer to that of its peer robot aiming for a rendezvous. The two trajectories are designed carefully so that the location of the exit is revealed no matter whether the rendezvous is realized or not.

3.1 Algorithm & Correctness

In our main Algorithm 2, robots R_1, R_2 that start from the centre of the circle, move together to an arbitrary point A on the circle (which takes time 1). Then they start moving in opposing directions, say, counterclockwise and clockwise respectively till the locate some interesting point.

In what follows we describe only the trajectory of R_2 which is meant to be moving clock-wise (R_1 performs the completely symmetric trajectory, and will start moving counter clock-wise). In particular all point references in the description of our algorithm, and its analysis, will be from the perspective of R_2's trajectory which is assumed to be the robot that first visits either the exit or the treasure at position I. By B, C, D we denote the points on the circle with $\widehat{DC} = \widehat{CI} = \widehat{IB} = \alpha$ (see Figure 2). As before, and in what follows, $I \in \{E, T\}$ represents the position on the circle that is first discovered in the time horizon by any robot (in particular by R_2), and that holds either the treasure or the exit. Finally, O represents the centre of the circle, which is also the starting point of the robots.

According to our algorithm, R_2 starts moving from point A till it reaches an interesting point I at time $x := \widehat{AI}$. At this moment, our algorithm will decide to run one of the following subroutines with input x. These subroutines describe evacuation protocols, in which the treasure must be brought to the exit. Occasionally, the subroutines claim that robots evacuate (with the treasure) from points that is not clear that hold an exit. As we will prove correctness later, we comment on these cases by writing that "correctness is pending".

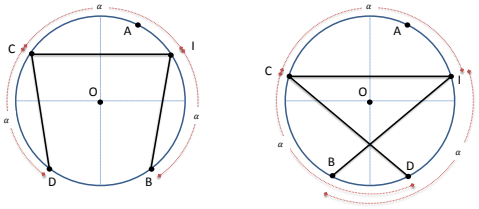

Figure 2: The points of interest from the perspective of R_2, when $\alpha \leq 2\pi/3$ on the left, and when $\alpha \geq 2\pi/3$ on the right.

$\mathcal{A}_1(\mathbf{x})$ (Figure 3 i): If $I = T$, pick up the treasure and move to B along the chord IB. If $B = E$ evacuate, else go to C along the chord BC and evacuate.
(Figure 3 ii): If $I = E$ move to B along the chord IB. If $B = T$, pick up the treasure, and return to I along the chord BI and evacuate. If $B = null$, then go to C along the chord BC. If the treasure is found at C, pick it up, and move to I along the chord CI and evacuate (else abandon the process).

$\mathcal{A}_2(\mathbf{x})$ (Figure 3 iii): At the moment robots leave point A, set the timer to 0.
If $I = T$, pick up the treasure and go to the centre O of the circle. Wait there till the time $t_0 := \max\{x, \alpha - x + 2\sin(\alpha/2)\} + 1$. If R_1 arrives at O by time t_0, then go to C and evacuate (correctness is pending). Else (if R_1 does not arrive at O by time t_0) go to B and evacuate (correctness is pending).
(Figure 3 iv): If $I = E$, move to B along the chord IB. If $B = T$, pick up the treasure, and return to I along the chord BI and evacuate. If $B = null$, then go to the centre O and halt.

$\mathcal{A}_3(\mathbf{x})$ (Figure 3 v): If $I = T$ pick up the treasure. If R_1 is already at point I go to C and evacuate (correctness pending). If R_1 is not at point I, then move along chord ID for additional time $y := \alpha/2 - x + \sin(\alpha/2) + \sin(\alpha)$, and let K be such that $\overline{IK} = y$. If R_1 is at point K, then go to B and evacuate (correctness is pending), else (if R_1 is not at point K) go to C and evacuate (correctness pending).
(Figure 3 vi): If $I = E$, move to B along the chord IB. If $B = T$, pick up the treasure, and return to I along the chord BI and evacuate. If $B = null$, then

move along chord BC until you hit C (or you meet the other robot- whatever happens first) and halt at the current point, call it K.

It is worthwhile discussing the intuition behind the subroutines above. First note that if a robot ever finds a treasure, it picks it up. The second important property is that each robot simulates $\mathcal{A}_1$ either till it finds the treasure or till it fails to find the treasure after finding the exit. At a high level, $\mathcal{A}_1$ greedily tries to evacuate the treasure. This means that if the treasure is found first, then the robot tries successively the possible locations of the exit (using the shortest possible paths) and evacuates. If instead the exit is found, then it successively tries the (at most) two possibilities of the treasure location, and if the treasure is found, it returns it to the exit.

$\mathcal{A}_2$ and $\mathcal{A}_3$ constitute our main technical contribution. Both algorithms are designed so that in some special cases, in which the exact locations of the interesting points are not known, the two robots schedule some meeting points so that if the meeting (rendezvous) is realized or even if it is not, the treasure-holder can deduce the actual location of the exit. In other words, we make possible for the two robots to exchange information without meeting. Indeed after finding the treasure, in $\mathcal{A}_2$, R_2 goes to the centre of the ring and waits some finite time till it makes some decision of where to move the treasure, while in $\mathcal{A}_3$, R_2 moves along a carefully chosen (and non-intuitive) chord, and again for some finite time, till it makes a decision to move to a point on the ring. If instead the exit is found early, then the trajectories in $\mathcal{A}_2$, $\mathcal{A}_3$ are designed to support the other robot which might have found the treasure in case the latter does not follow $\mathcal{A}_1$.

The next non-trivial and technical step would be to decide when to trigger the subroutines above. Of course, once this is determined, i.e. once the trajectories are fixed, correctness and performance analysis is a matter of exhaustive analysis.

We are ready to define our main non-wireless algorithm. We remind the reader that the description is for R_2 that starts moving clockwise. R_1 performs the symmetric trajectory by moving counter-clockwise.

Our main algorithm uses parameter $\bar{x}(\alpha) := 3\alpha/2 - \pi - \sin(\alpha/2) + 2\sin(\alpha)$, which we abbreviate by $\bar{x}$ whenever α is clear from the context. By Lemma Aa, $\alpha_0 \approx 1.22353$ is the unique root of $\bar{x}(\alpha) = 0$, while $\bar{x}$ is positive for all $\alpha \in (\alpha_0, \pi)$ and negative for all $\alpha \in [0, \alpha_0)$.

Lemma 3.2. *For every $\alpha \in [0,\pi]$, Algorithm 2 is correct, i.e. a robot brings the treasure to the exit.*

Algorithm 2: Non-Wireless Algorithm.

Step 1. Starting from A, move clockwise until an interesting point I is found at time $x := \widehat{AI}$.

Step 2. Proceed according to the following cases:

- If $\alpha > 2\pi/3$ and $I = T$ and $\alpha > x \geq \alpha - \bar{x}$, then run $\mathcal{A}_3$(x).
- If $\alpha > 2\pi/3$ and $I = E$ and $x \leq \bar{x}$, then run $\mathcal{A}_3$(x).
- If $\alpha_0 \leq \alpha \leq 2\pi/3$ and $I = T$ and $\alpha > x \geq \alpha - \bar{x}$, then run $\mathcal{A}_2$(x).
- If $\alpha_0 \leq \alpha \leq 2\pi/3$ and $I = E$ and $x \leq \bar{x}$, then run $\mathcal{A}_2$(x).
- In all other cases, run $\mathcal{A}_1$(x).

Proof. First, it is easy to see that the treasure is always picked up. Indeed, if the first interesting point I that is discovered (by any robot) is the treasure, then the claim is trivially true. If the first interesting point I found, say, by R_2 is an exit, then R_2 (in all subroutines) first tries the possible location B for the treasure, and if it fails it tries location C (in other words it always simulates $\mathcal{A}_1$ till it fails to find the treasure after finding the exit). Meanwhile R_1 moves counter-clockwise on the ring, and sooner or later will reach C or B. So at least one of the robots will reach the treasure first. In what follows, let R_2 be the one who found first the treasure (and picks it up). We examine three cases.

If R_2 is following subroutine $\mathcal{A}_1$, then the treasure is brought to the exit. Indeed, in that case R_2 expects no interaction from R_1 and greedily tries to evacuate (see subcases i,ii in Figure 3).

If R_2 is following subroutine $\mathcal{A}_2$, then it must be that $\alpha_0 \leq \alpha \leq 2\pi/3$, that $\alpha - \bar{x} \leq x < \alpha$, and that it has not found any other interesting point before (by Lemma Aa we have $\alpha - \bar{x} < \alpha$ and $\bar{x} > 0$ for all $\alpha > \alpha_0$). Figure 3 subcase iii depicts exactly this scenario, where $I = T$. Note that from R_2's perspective, the exit can be either in B or in C, and R_2 chooses to go to the center. This takes total time $x+1$. If the exit was at point C, then R_1 would have found it in time $\alpha - x \leq \bar{x}$ and that would make it to follow $\mathcal{A}_2$. So, R_1 would first check point D (where the treasure is not present), and that would make it to go to the centre arriving at time $\alpha - x + 2\sin(\alpha/2) + 1$ (an illustration of this trajectory is shown in Figure 3 subcase iv, if R_1 was moving clockwise). R_2 is guaranteed to wait at the center till time t_0 (which is the maximum required time that takes each robot to reach the centre). In that case, R_2 meets R_1 at the center (because R_1 did find the exit in C), and R_2 correctly chooses C as the evacuation point. Finally, if instead the exit was not in C, then R_1 would not make it to the centre by time t_0.

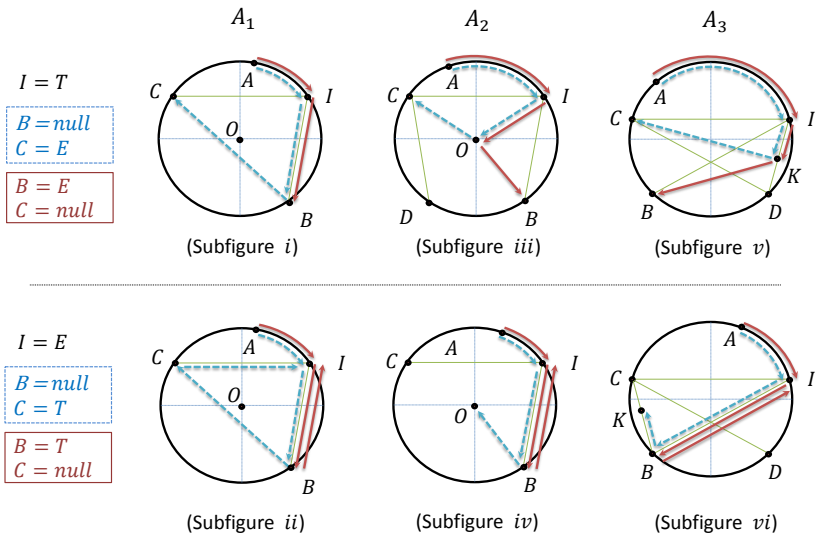

Figure 3: The non-wireless algorithm for two robots with performance $\pi - \alpha/2 + 3\sin(\alpha/2)$.

That can happen only if the exit is at point B, and once again R_2 makes the right decision to evacuate from B.

In the last case, R_2 is following subroutine $\mathcal{A}_3$, and so it must be that $\alpha > 2\pi/3$, that $\alpha - \bar{x} \le x < \alpha$, and that it has not found any other interesting point before. Figure 3 subcase v depicts this scenario. Note that the exit could be either in C or in D.

If the exit is in C, then $\alpha - x \le \bar{x}$, and R_1 would follow $\mathcal{A}_3$ too. This means, R_1 would go to point D (where there is no treasure), and that would make it travel along the chord DI (an illustration of this trajectory is shown in Figure 3 subcase vi, if R_1 was moving clockwise). If R_1 reaches I, it waits there, and when R_2 arrives in I, R_2 makes the right decision to evacuate from C. Otherwise R_1 does not reach I, and it moves up to a certain point in the chord ID similarly to R_2. Note that the meeting condition on a point K on the chord, with $y = \overline{IK}$, would be that $\widehat{\mathrm{AI}} + \overline{IK} = \widehat{\mathrm{CA}} + \overline{CD} + (\overline{DI} - \overline{IK})$, which translates into $y = x + \sin(\alpha/2) + \sin(\alpha) - \alpha/2$, i.e. the exact segment of ID that R_2 traverses before it changes trajectory. The longest R_2 could have traveled on the chord ID would be when $x = \alpha - \bar{x}$, but then $\overline{IK}$ would be equal to $\alpha - \pi + 3\sin(\alpha) \le 2\sin(\alpha) = \overline{ID}$ for all $\alpha > 2\pi/3$. Therefore, the two robots meet indeed in somewhere in the chord ID. Note also that in this case, R_2 makes the right decision and goes to point C in order to evacuate.

If instead the exit is in B, then again R_2 travels till point K (which is in the interior of the chord ID). But in this case, R_1 will not meet R_2 in point K as it will not follow $\mathcal{A}_3$. Once again, R_2 makes the right decision, and after arriving at K it moves to point B and evacuates. ■

3.2 Algorithm Analysis

In this section we prove that for all $\alpha \in [0,\pi]$, the evacuation time of Algorithm 2 is no more than $1 + \pi - \alpha/2 + 3\sin(\alpha/2)$, concluding Theorem 3.1. In the analysis below we provide, whenever possible, supporting illustrations, which for convenience may depict special configurations. In the mathematical analysis we are careful not to make any assumptions for the configurations we are to analyze.

It is immediate that when a robot finds the first interesting point at time $x \ge \alpha$ after moving on the perimeter of the disk, then that robot can also deduce where the other interesting point is located. In that sense, it is not surprising that, in this case, the trajectory of the robots and the associated cost analysis are simpler.

Lemma 3.3. *Let x be the time some robot is the first to reach an interesting point $I \in \{E,T\}$ from the moment robots start moving in opposing directions. If $x \ge \alpha$, then the performance of the algorithm is at most $1 + \pi - \alpha/2 + 3\sin(\alpha/2)$. Also, $x \ge \alpha$ is impossible, if $\alpha > 2\pi/3$.*

Proof. Note that 1 is the time it takes both robots to reach a point, say A, on the ring. So we will tailor our analysis to the evacuation time from the moment robots start moving (in opposing directions) from point A.

Let x be the time after which R_2 (without loss of generality) is the first to find an interesting point $I \in \{E,T\}$. Let also B be the other interesting point $\{E,T\} \setminus I$. For R_2 to reach first I, it must be the case that R_1 does not have enough time to reach B, and

hence $x \leq 2\pi - \alpha - x$, that is $x \leq \pi - \alpha/2$. Since also $x \geq \alpha$, we conclude that $\alpha \leq 2\pi/3$.

Next we examine the following cases. For our analysis, the reader can use Figure 2 as reference (although A is depicted in the interior of the arc CI, we will not use that $\widehat{\mathrm{AI}} \leq \alpha$).

Case 1 ($I = T$): R_2 picks up the treasure and moves along the chord $\overline{IB} = 2\sin(\alpha/2)$. The worst case treasure-evacuation time then is $\max_{\alpha \leq x \leq \pi - \alpha/2} \{x + 2\sin(\alpha/2)\} = \pi - \alpha/2 + 2\sin(\alpha/2)$.

Case 2 ($I = E$): According to the algorithm, R_2 moves towards the treasure point B along the chord IB, and reaches it in time $x + 2\sin(\alpha/2)$. R_1 moves counter-clock wise and will reach the position of the treasure in time $2\pi - \alpha - x$. Whoever finds the treasure first will evacuate from the exit, paying additional time $2\sin(\alpha/2)$. Hence, the total cost can never exceed

$$\begin{aligned} &\min\{x + 2\sin(\alpha/2), 2\pi - \alpha - x\} + 2\sin(\alpha/2) \\ \leq &\pi - \alpha/2 + 3\sin(\alpha/2) \qquad \text{(by Lemma Ab)} \end{aligned}$$

It is easy to see that in both cases, the cost of the algorithm is as promised. ■

By Lemma 3.3 we can focus on the (much more interesting) case that R_2, which is the first robot that finds an interesting point, arrives at I at time $x := \widehat{\mathrm{AI}} < \alpha$. A reference for the analysis below is Figure 3 which is accurately depicting point A at most α arc-distance away from I. For the sake of better exposition, we examine next the cases $\alpha \leq 2\pi/3$ and $\alpha \geq 2\pi/3$ separately. Note that in the former case robots may run subroutines $\mathcal{A}_1$ or $\mathcal{A}_2$, while in the latter case robots may run subroutines $\mathcal{A}_1$ or $\mathcal{A}_3$. For both lemmata below, the reader may consult Figures 2 and 3.

Lemma 3.4. *Let x be the time some robot is the first to reach an interesting point $I \in \{E, T\}$ from the moment robots start moving in opposing directions. If $x < \alpha$, then the performance of the algorithm is at most $1 + \pi - \alpha/2 + 3\sin(\alpha/2)$, for all $\alpha \in [0, \pi]$.*

Proof. As before, we omit in the analysis below the time cost 1, i.e. the time robots need to reach the periphery of the disk. We examine the following cases for R_2, which is the robot that finds I.

($I = T, B = E, C = null$): If R_2 runs $\mathcal{A}_1$, then it must be that $x \leq \alpha - \bar{x}$, so the cost is $x + 2\sin(\alpha/2) \leq \alpha - \bar{x} + 2\sin(\alpha/2) \leq \pi - \alpha/2 + 3\sin(\alpha/2)$ (see Figure 3 i).

If R_2 runs $\mathcal{A}_2$, then it must be that $\alpha - \bar{x} \leq x < \alpha$ and $\alpha \leq 2\pi/3$, and the robot goes to the centre in order to learn where the exit is (see Figure 3 iii). Independently of where the exit is, and by Lemma 3.2, R_2 makes the right decision and evacuates in time $1 + \max_{\alpha - \bar{x} \leq x < \alpha}\{x, \alpha - x + 2\sin(\alpha/2)\} + 1 \leq \max\{\alpha, \bar{x} + 2\sin(\alpha/2)\} + 2$ which, by Lemma Ac, is at most $\pi - \alpha/2 + 3\sin(\alpha/2)$ for all $\alpha \leq 2\pi/3$. Note that the analysis of this case is valid, even if $I = T$ is not the first interesting point that is discovered, and it is from the perspective of the robot that finds the treasure.
If R_2 runs $\mathcal{A}_3$, then it must be that $\alpha - \bar{x} \leq x < \alpha$ and $\alpha > 2\pi/3$. Then the trajectory of R_2 is as in Figure 3 v, and the exit is found correctly due to Lemma 3.2. For the sake of the exposition, we will do the worst case analysis for both cases $B = E$ and $C = E$ now (i.e. we only insist in that $I = T$ and that R_2 runs $\mathcal{A}_3$).
The total time for the combined cases is $\widehat{\mathrm{AI}} + \overline{IK} + \max\{\overline{KB}, \overline{KC}\}$, where $\overline{IK} = y$ (see definition of $\mathcal{A}_3$). Since as we have proved, K lies always in chord ID, and since $\widehat{\mathrm{DB}} = 3\alpha - 2\pi$ we have that

$$\begin{aligned} \overline{BK} \leq &\max\{\overline{BI}, \overline{BD}\} \\ \leq &\max\{2\sin(\alpha/2), 2\sin(3\alpha/2 - \pi)\} \\ \leq &2\sin(\alpha/2) \end{aligned}$$

We also have that $\overline{KC} \leq \overline{CI} = 2\sin(\alpha/2)$. So the cost becomes no more than

$$\begin{aligned} &x + y + 2\sin(\alpha/2) = \alpha/2 + 3\sin(\alpha/2) + \sin(\alpha) \\ \leq &\pi - \alpha/2 + 3\sin(\alpha/2) \qquad \text{(by Lemma Ad)} \end{aligned}$$

for all $\alpha \in [0, \pi]$.

($I = T, B = null, C = E$): Since I is found first, we must have $x \leq \alpha/2$, hence both robots run $\mathcal{A}_1$, see Figure 3 i. Robot R_2 that finds the treasure will evacuate in time no more than $x + 2\sin(\alpha/2) + 2\sin(\alpha) \leq \alpha/2 + 2\sin(\alpha/2) + 2\sin(\alpha) < \pi - \alpha/2 + 3\sin(\alpha/2)$ for all $\alpha \in [0, \pi]$.

($I = E, B = T, C = null$): If R_2 is the first to find the treasure, then this case is depicted in Figure 3 i. This happens exactly when $x + 2\sin(\alpha/2) \leq 2\pi - x - \alpha$, so that the total evacuation time is $x + 4\sin(\alpha/2) \leq \pi - \alpha/2 + 3\sin(\alpha/2)$ for all $\alpha \in [0, \pi]$.
Otherwise $x > \pi - \alpha/2 - \sin(\alpha/2)$, and R_1 is the robot that reaches the treasure first. If R_1 decides to run $\mathcal{A}_1$, then the cost would be $2\pi - x - \alpha + 2\sin(\alpha/2) < \pi - \alpha/2 + 3\sin(\alpha/2)$ for all $\alpha \in [0, \pi]$. Finally, if R_1 decides to run $\mathcal{A}_2$ or $\mathcal{A}_3$, then we have already made the analysis in case $I = T, B = E, C = null$ above.

($I = E, B = null, C = T$): Note that in all cases, both robots will run the same subroutine. In particular, if robots run either $\mathcal{A}_2$ or $\mathcal{A}_3$, then we have already done the analysis in case $I = T, B = E, C = null$ above.

Finally, if both robots run $\mathcal{A}_1$, it must be either because $\alpha \leq \alpha_0$, or because $x \geq \bar{x}$, while the cost is always $\alpha - x + 2\sin(\alpha/2) + 2\sin(\alpha)$ (the case is depicted in Figure 3 ii, with reverse direction). If $\alpha \leq \alpha_0$, then the evacuation cost would be at most $\alpha + 2\sin(\alpha/2) + 2\sin(\alpha)$ which by Lemma Ah is at most $\pi - \alpha/2 + 3\sin(\alpha/2)$, for all $\alpha \in [0, \alpha_0]$. If $x \geq \bar{x}$, then the cost would be at most $\alpha - \bar{x} + 2\sin(\alpha/2) + 2\sin(\alpha) = \pi - \alpha/2 + 3\sin(\alpha/2)$.

■

Note that Lemmata 3.3, 3.4 imply that the performance of Algorithm 2 is, in the worst case, no more than $1 + \pi - \alpha/2 + 3\sin(\alpha/2)$, concluding also Theorem 3.1.

3.3 Extension to n Robots

We can easily extend our 2-robot algorithms to the n-robot case (when n is even, otherwise we ignore one robot) by splitting the robots into pairs, defining points in intervals of length $4\pi/n$ on the cycle, assigning each pair of robots to each such point, and letting them run the corresponding 2-robot algorithm.

4 LOWER BOUNDS

We conclude the study of treasure evacuation with 2 robots by providing the following lower bound pertaining to distributed systems under the face-to-face communication model.

Theorem 4.1. *For problem 2-TE_{f2f}, any algorithm needs at least time* $1 + \pi/3 + 4\sin(\alpha/2)$ *if* $0 \leq \alpha \leq 2\pi/3$, *or* $1 + \pi/3 + 2\sin(\alpha) + 2\sin(\alpha/2)$ *if* $2\pi/3 \leq \alpha \leq \pi$.

For the proof, we invoke an adversary (not necessarily the most potent one), who waits for as long as there are three points A, B, C with $AB = BC = \alpha$ on the periphery such that at most one of them has been visited by a robot. Then depending on the moves of the robots decides where to place the interesting points.

5 CONCLUSION

In this paper we introduced a new problem on *searching and fetching* which we called *treasure-evacuation* from a unit disk. We studied two online variants of treasure-evacuation with two robots, based on different communication models. The main point of our approach was to propose distributed algorithms by a collaborative team of robots. Our main results demonstrate how robot communication capabilities affect the treasure evacuation time by contrasting face-to-face (information can be shared only if robots meet) and wireless (information is shared at any time) communication.

There are several open problems in addition to sharpening our bounds. These include problems on 1) the number of robots, 2) other geometric domains (discrete or continuous), 3) differing robot starting positions, 4) multiple treasures and exits, 5) limited range wireless communication, 6) robots with different speeds, 6) different a priori knowledge of the topology or partial information about the targets, etc. In particular, we anticipate that nearly optimal algorithms for small number of robots, e.g. for $n = 3, 4$, or any other variation of problem we consider will require new and significantly different algorithmic ideas than those we propose here, still in the same spirit.

REFERENCES

Ahlswede, R. and Wegener, I. (1987). *Search problems*. Wiley-Interscience.

Albers, S. and Henzinger, M. R. (2000). Exploring unknown environments. *SIAM Journal on Computing*, 29(4):1164–1188.

Albers, S., Kursawe, K., and Schuierer, S. (2002). Exploring unknown environments with obstacles. *Algorithmica*, 32(1):123–143.

Alpern, S. (2011). Find-and-fetch search on a tree. *Operations Research*, 59(5):1258–1268.

Alpern, S. and Gal, S. (2003). *The theory of search games and rendezvous*. Springer.

Baeza Yates, R., Culberson, J., and Rawlins, G. (1993). Searching in the plane. *Information and Computation*, 106(2):234–252.

Baeza-Yates, R. and Schott, R. (1995). Parallel searching in the plane. *Computational Geometry*, 5(3):143–154.

Beck, A. (1964). On the linear search problem. *Israel Journal of Mathematics*, 2(4):221–228.

Bellman, R. (1963). An optimal search. *SIAM Review*, 5(3):274–274.

Berman, P. (1998). On-line searching and navigation. In Fiat, A. and Woeginger, G. J., editors, *Online Algorithms: The State of the Art*, pages 232–241. Springer.

Bonato, A. and Nowakowski, R. (2011). *The game of cops and robbers on graphs*. AMS.

Burgard, W., Moors, M., Stachniss, C., and Schneider, F. E. (2005). Coordinated multi-robot exploration. *Robotics, IEEE Transactions on*, 21(3):376–386.

Chrobak, M., Gasieniec, L., T., G., and Martin, R. (2015). Group search on the line. In *SOFSEM 2015*. Springer.

Chung, T. H., Hollinger, G. A., and Isler, V. (2011). Search and pursuit-evasion in mobile robotics. *Autonomous robots*, 31(4):299–316.

Czyzowicz, J., Gasieniec, L., Gorry, T., Kranakis, E., Martin, R., and Pajak, D. (2014). Evacuating robots from an unknown exit located on the perimeter of a disc. In *DISC 2014*, pages 122–136. Springer, Austin, Texas.

Czyzowicz, J., Georgiou, K., Dobrev, S., Kranakis, E., and MacQuarrie, F. (2016). Evacuating two robots from multiple unknown exits in a circle. In *ICDCN 2016*.

Czyzowicz, J., Georgiou, K., Kranakis, E., Narayanan, L., Opatrny, J., and Vogtenhuber, B. (2015a). Evacuating robots from a disc using face to face communication. In *CIAC 2015*, pages 140–152. Springer, Paris, France.

Czyzowicz, J., Kranakis, E., Krizanc, D., Narayanan, L., Opatrny, J., and Shende, S. (2015b). Wireless autonomous robot evacuation from equilateral triangles and squares. In *ADHOC-NOW 2015, Athens, Greece, June 29 - July 1, 2015, Proceedings*, pages 181–194.

Demaine, E. D., Fekete, S. P., and Gal, S. (2006). Online searching with turn cost. *Theoretical Computer Science*, 361(2):342–355.

Deng, X., Kameda, T., and Papadimitriou, C. (1991). How to learn an unknown environment. In *FOCS*, pages 298–303. IEEE.

Fekete, S., Gray, C., and Kröller, A. (2010). Evacuation of rectilinear polygons. In *Combinatorial Optimization and Applications*, pages 21–30. Springer.

Georgiou, K., Karakostas, G., and Kranakis, E. (2016a). Search-and-fetch with 2 robots on a disk: Wireless and face-to-face communication models. *CoRR*, abs/1611.10208.

Georgiou, K., Karakostas, G., and Kranakis, E. (2016b). Search-and-fetch with one robot on a disk. In *12th International Symposium on Algorithms and Experiments for Wireless Sensor Networks*.

Gluss, B. (1961). An alternative solution to the lost at sea problem. *Naval Research Logistics Quarterly*, 8(1):117–122.

Hipke, C., Icking, C., Klein, R., and Langetepe, E. (1999). How to find a point on a line within a fixed distance. *Discrete Appl. Math.*, 93(1):67–73.

Hoffmann, F., Icking, C., Klein, R., and Kriegel, K. (2001). The polygon exploration problem. *SIAM Journal on Computing*, 31(2):577–600.

Isbell, J. R. (1967). Pursuit around a hole. *Naval Research Logistics Quarterly*, 14(4):569–571.

Jennings, J. S., Whelan, G., and Evans, W. F. (1997). Cooperative search and rescue with a team of mobile robots. In *ICAR*, pages 193–200. IEEE.

Kao, M.-Y., Ma, Y., Sipser, M., and Yin, Y. (1998). Optimal constructions of hybrid algorithms. *J. Algorithms*, 29(1):142–164.

Kao, M.-Y., Reif, J. H., and Tate, S. R. (1996). Searching in an unknown environment: An optimal randomized algorithm for the cow-path problem. *Information and Computation*, 131(1):63–79.

Kleinberg, J. (1994). On-line search in a simple polygon. In *SODA*, page 8. SIAM.

Koutsoupias, E., Papadimitriou, C., and Yannakakis, M. (1996). Searching a fixed graph. In *ICALP 96*, pages 280–289. Springer.

Nahin, P. (2012). *Chases and Escapes: The Mathematics of Pursuit and Evasion*. Princeton University Press.

Papadimitriou, C. H. and Yannakakis, M. (1989). Shortest paths without a map. In *ICALP*, pages 610–620. Springer.

Stone, L. (1975). *Theory of optimal search*. Academic Press New York.

Thrun, S. (2001). A probabilistic on-line mapping algorithm for teams of mobile robots. *The International Journal of Robotics Research*, 20(5):335–363.

Yamauchi, B. (1998). Frontier-based exploration using multiple robots. In *Proceedings of the second international conference on Autonomous agents*, pages 47–53. ACM.

APPENDIX

Lemma A. *a) There exists some* $\alpha_0 \in (0,\pi)$ *such that* $3\alpha/2-\pi-\sin(\alpha/2)+2\sin(\alpha)$ *is positive for all* $\alpha \in (\alpha_0,\pi)$ *and negative for all* $\alpha \in [0,\alpha_0)$. *In particular,* $\alpha_0 \approx 1.22353$.

b) $\min\{x+2\sin(\alpha/2), 2\pi-\alpha-x\} + 2\sin(\alpha/2) \leq \pi-\alpha/2+3\sin(\alpha/2)$, $\forall\alpha\in[0,\pi]$.

c) $\max\{\alpha,\bar{x} + 2\sin(\alpha/2)\} + 2 \leq \pi - \alpha/2 + 3\sin(\alpha/2)$ *for all* $\alpha \in [0,2\pi/3]$.

d) $\alpha+\sin(\alpha)\leq\pi$ *for all* $\alpha\in[0,\pi]$.

e) $\alpha-\sin(\alpha/2)+2\sin(\alpha)\leq\pi$ *for all* $\alpha\in[0,\pi]$.

f) $\alpha/2 + 2\sin(\alpha) \leq \pi - \alpha + 2\sin(\alpha/2)$, $\forall\alpha \in [0,2\pi/3]$. .

g) $\max_{0\leq x\leq\pi-\alpha}\{\sin(\pi/2-\alpha/2-x)\} \leq \sin(\alpha/2)$, $\forall\alpha\in[2\pi/3,\pi]$

h) $\max_{0\leq x\leq\alpha/2}\{x+2\sin(\alpha/2-x)\}+2\sin(\alpha)\leq\pi-\alpha+4\sin(\alpha/2)$, $\forall\alpha\in[0,2\pi/3]$.

i) $\max_{0\leq x\leq\pi-\alpha}\{x+2\sin(\pi/2-\alpha/2-x)\}\leq\pi-\alpha+2\sin(\alpha/2)$, $\forall\alpha\in[2\pi/3,\pi]$

j) $\sin(\alpha)\leq\sin(\alpha/2)$, $\forall\alpha\in[0,2\pi/3]$, *and* $\sin(\alpha)\geq\sin(\alpha/2)$, $\forall\alpha\in[2\pi/3,\pi]$.

Process Optimization for Cutting Steel-Plates

Markus Rothe, Michael Reyer and Rudolf Mathar
Institute for Theoretical Information Technology, RWTH Aachen University, Kopernikusstraße 16, 52074 Aachen, Germany
{rothe, reyer, mathar}@ti.rwth-aachen.de

Keywords: Two-Stage Three-Dimensional Guillotine Cutting, Residual Bin-Packing Problem, Mixed Integer Programming Model, Reuseable Leftovers.

Abstract: In this paper, we consider the two-stage three-dimensional guillotine cutting stock problem with usable leftover. There are two properties that distinguish our problem formulation from others. First, we allow the items to be rotated. Second, we consider the case in which leftover material is to be reused in subsequent production cycles. Third, we solve the problem in three dimensions. The optimization problem is formulated as a mixed integer linear program. To verify the approach, several examples show that our formulation performs well.

1 INTRODUCTION

In many areas of industrial production large or long pieces of material need to be cut into smaller ones. E.g., it needs to be decided from which reel of raw material a cable of a specific length will be produced. This is an example for a one-dimensional problem. An example for a two-dimensional problem is to cut patterns from pieces of large leather. In our case, we want to cut items out of slabs of steel. This is a three-dimensional problem.

The cutting stock problem is similar to the bin packing problem and the knapsack problem. In the bin packing problem objects of different sizes must be packed into a finite number of bins. The classical bin packing problem minimizes the number of bins that are used. For the knapsack problem, there is only one bin of a certain volume and the objects to pack have a value and a volume. Then, the objective is to maximize the value of the packed objects. Both problems are, in general, NP-hard problems.

In this paper, we formulate a problem that is similar to the above mentioned problems and solves the cutting stock problem. The problem is formulated such that the optimization program becomes linear and we can find an optimal solution according to our objective function.

The general problem of cutting stock is explored widely in the literature. The earliest work we found, that minimizes scrap material, is (Kantorovich, 1960). We cite the English translation, which is, to the best of our knowledge, a translation from the original Russian publication from 1939. (Kurt Eisemann, 1957), and (Gilmore and Gomory, 1961), utilize linear programming to solve cutting stock problems. P. Gilmore and Gomory investigate the one dimensional problem of cutting items from stock of several standard lengths. They devise the method of column generation in their work. P. Gilmore and Gomory continued their work in (Gilmore and Gomory, 1965). Here, they extend their formulation to multistage cutting stock problems of two and more dimensions.

(Farley, 1988), adapt the approach of (Gilmore and Gomory, 1961), with some practical adaptations. In particular, they introduce guillotine cuts, which will be explained in detail in the following section.

Solutions not utilizing linear programming have also been published, e.g., tree-search algorithms, (Christofides and Whitlock, 1977). The survey (Hinxman, 1980), summarizes many more publications. (Dyckhoff et al., 1985), give a detailed catalog of criteria for characterization of real-world cutting stock problems (Dyckhoff et al., 1985). (Yanasse et al., 1991), describe heuristics for the cutting stock problem. (Carnieri et al., 1994), formulate the cutting stock problem as a Knapsack algorithm and also give heuristics to enhance computational efficiency.

(Kalagnanam et al., 2000), formulate the problem for the steel industry, without considering the depth of the slabs. (Martello et al., 2000), present a three-dimensional bin packing problem, while allowing arbitrary, i.e., non-guillotine, cuts. (Morabito and Arenales, 2000), focus on a simplified cutting pattern. In their book *Operations Research: Applications and Algorithms*, (Wayne L Winston and Jeffrey B Goldberg, 2004), summarize and extend some of the aforemen-

Rothe, M., Reyer, M. and Mathar, R.
Process Optimization for Cutting Steel-Plates.
In *Proceedings of the 6th International Conference on Operations Research and Enterprise Systems (ICORES 2017)*, pages 27-37
ISBN: 978-989-758-218-9

tioned as well as many more methods.

(Silva et al., 2010), consider waste, but lack the third dimension in their problem formulation. They also mention the value of the surplus material on a conceptual level, but do not show it in their problem formulation. (Burke et al., 2011), present an iterative packing methodology based on squeaky wheel optimization. (Furini and Malaguti, 2013), make similar formulations as previously found in the literature, but focus on the run-time of the solution.

The recent results from (Andrade et al., 2013), lay the foundation for our problem formulation. (Andrade et al., 2013), investigate two-stage two-dimensional guillotine cutting stock problems with usable leftover. We will extend their formulation for two-stage three-dimensional guillotine cutting stock problems with usable leftover. The term "stage" will be explained when we describe the constrains that are imposed by our production machinery.

There are three properties that distinguish our problem formulation from others. First, we allow the items to be rotated.

Second, we consider the case in which leftover material is to be reused in subsequent production cycles. I.e., after one production cycle, leftover material is added to the set of slabs.

Third, we solve the problem in three dimensions. On the one hand, this is needed to calculate the weight, which is required in our objective function. On the other hand, this opens up for the possibility to cut an item from a slab that is thicker than necessary, if the value of the leftover material permits or even dictates this decision.

The remainder of the present paper is organized as follows. In Section 2, we present the problem we want to solve and the model we use. In Section 3, we propose an optimization program to solve the problem. In Section 4, we discuss some examples and their solutions. Finally, we summarize our results in Section 5.

2 PROBLEM FORMULATION AND MODEL DESCRIPTION

The overall goal is to fulfill customer orders of blocks of steel. We call the ordered blocks of steel *items*. These items are cut from larger *slabs* of steel. As the size of an item is defined by the customer, the size is, in general, different and arbitrary from item to item.

The problem we solve in this work is the decision which item is cut from which slab and how items are geometrically placed on each slab. Due to the production process, or technical and economic restrictions,

(a) (b) (c)

Figure 1: Guillotine cutting in (b) and (c).

these problems can have an abundance of constraints. It is not important that the material we are working with is steel. However, the machines that are used for cutting the slabs create certain constraints in our problem formulation.

In general, when items are cut from slabs, the original slab is cut up into items and surplus material. The surplus material can either be useful in the future or it is so small that it is thrown away. If it is kept we call it *leftover material* and it will be placed in the set of slabs for future usage. If it is thrown away we call it *scrap material*.

One of our goals is to use surplus material more frequently than new slabs. Otherwise, the slabs in stock could increase over time. Our solution for this problem is to attach a value per kilogram to all the slabs. The less a slab weights in total, the smaller its value per kilogram.

The machines cutting the slabs can only do full straight cuts, parallel to the edges of the slab and not stop halfway through the material. This is called guillotine cutting.

Figure 1a shows how the blue item can *not* be cut from the gray slab if it is placed in the bottom left corner. The item has either to be cut as seen in Fig. 1b or Fig. 1c. Leftover material will have different shapes, not only depending on the exact geometrical placement of the item on the slab, but also depending on the exact cuts being made. Currently, in order to calculate the dimensions of the surplus material, the problem formulation assumes a strict cutting order, which will be explained shortly.

Our model follows (Lodi and Monaci, 2003), in using the notion of shelves, as does (Andrade et al., 2013). Shelves are a way to connect the restriction on guillotine cutting and geometric placement of items. Figure 2 shows the general layout of items and shelves on a slab.

In this figure, item 1 and item 2 are on the same shelf, while item 3 is on a separate shelf. To make this clear, a shelf is just a notion to group and place items on a slab. Further, shelf ν is opened by item ν. The height of all items, that are placed in this shelf after item ν must be less than or equal to the height of item ν. I.e., the height of shelf ν is equivalent to the height

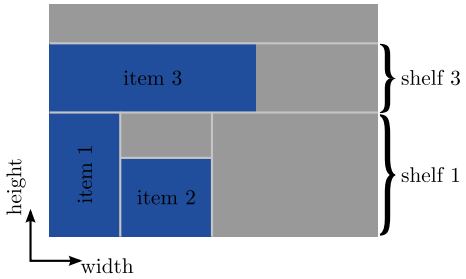

Figure 2: Shelves.

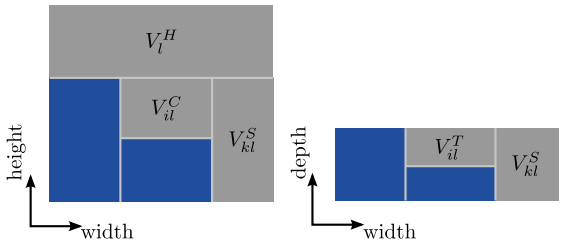

(a) (b)

Figure 3: Positions of leftover material.

of item ν. An item is either placed in an existing shelf or opens a new shelf. As a result, if item $\hat{\nu}$ was placed in an existing shelf, then shelf $\hat{\nu}$ does not exist.

As was mentioned earlier, the size and form of the surplus material depends on the order in which cuts are made. Therefore, our problem formulation assumes a specific order of the cuts. This is necessary to calculate the precise dimensions, and hence the value, of the surplus material. The result of the cuts is depicted in Fig. 3.

The figure is ambiguous about the depth of V_{il}^C, which is the leftover material filling the height above item i on slab l. It has the same depth as the slab, which is clear from the following cutting order.

1. Slabs are cut in the direction of "width" such that shelves are cut out.
2. Each shelf is cut in the direction of "height" such that the widths of items are correct.
3. V_{il}^C are trimmed from the items.
4. V_{il}^T are trimmed from the items.

Trimming in this context means to cut unwanted pieces from the items, e.g., separating V_{il}^T from the item.

(Andrade et al., 2013), describe their model as having "two stages".

> In the first stage, parallel longitudinal (horizontal) guillotine cuts are produced on a plate, without moving it, to produce a set of strips. In the second stage, these strips are pushed, one by one, and the remaining parallel transversal (vertical) guillotine cuts are made on each strip. ((Andrade et al., 2013, p. 2))

(a) Exact case. (b) Non-exact case.

Figure 4: Two-stage cutting patterns.

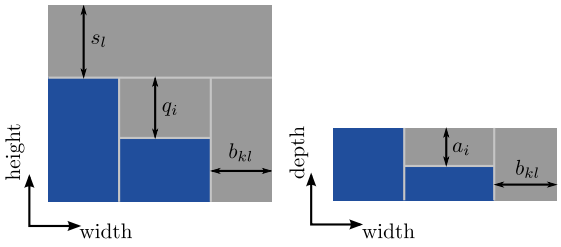

(a) (b)

Figure 5: Measuring the leftover material.

Further, (Andrade et al., 2013), distinguish between the exact and non-exact cases of matching items to shelves. Figure 4a shows the exact case. Here, all items in the same shelf have the same height. On the other hand, Fig. 4b shows the non-exact case. Here, trimming is necessary, because items in the same shelf might have a different height. Recall that (Andrade et al., 2013), only account for two dimensions. They do not treat trimming as a separate stage.

Our formulation matches items to slabs in three dimensions considering the non-exact case. Items are trimmed at most two times, but items are not stacked in the third dimension. So we call our problem a two-stage three-dimensional non-exact guillotine cutting stock problem.

The objective function of our optimization problem will maximize the value of the surplus material, accounting for the lost value of cut slabs. A value needs to be attached to the volumes of the pieces of surplus material. In order to calculate the volumes, the measures depicted in Fig. 5 are used.

As we mentioned earlier, the value of each piece of surplus material is a function of its weight. The weight of each piece is calculated by simply multiplying its volume by the weight per volume unit. The constants g_l^e define the boundaries of the weight classes. α_l^e is the value relative to the value of the slab the piece originates from. l denoting the slab, e denoting the weight class. Explicit example values for g_l^e and α_l^e are given in Table 1. E.g., the value per kilogram of a piece of surplus material weighting between 2.1 kg and 5 kg is 0.5 times the value per kilogram of the slab it originates from.

Surplus material is considered waste if one of its sides is too small. See $d_l^{W_{\min}}$, $d_l^{H_{\min}}$, $d_l^{T_{\min}}$ in Table 1.

We allow items to be rotated in the width-height-axis. This is done by copying each item and rotating the copy. We then restrict placement such that only one of these items is produced. More on this in the optimization program itself.

Further, we require items to be sorted by decreasing height, i.e., $h_i \geq h_{i+1}$. This is a result of how the height of shelves is determined in our optimization problem. The first item to be placed in a shelf defines its height. Only items with a larger index are allowed to be put into this shelf. So all items following the first item must have the same or a smaller height, such that they can be placed on any of the existing shelves. Therefore, items are sorted by decreasing height before given an index.

3 THE OPTIMIZATION PROGRAM

Below is the complete optimization program, which will be explained afterwards.

Define $\mathbb{F}_N = \{1,\dots,N\}$ for any $N \in \mathbb{N}$. Unless otherwise mentioned, the constraints apply to $\forall i \in \mathbb{F}_n$, $\forall k \in \mathbb{F}_n$, $\forall l \in \mathbb{F}_p$. n and p are number of items and number of slabs, respectively, see Table 1.

The main variables are x_{ikl}, i.e., it is one if item i is placed in shelf k on slab l.

$$\text{maximize} \quad \sum_{i=1}^{n}\sum_{k=1}^{i}\sum_{l=1}^{p} w_i h_i t_i G_l p_i x_{ikl} \tag{1}$$

$$-\sum_{l=1}^{p} M_l P_l u_l \tag{2}$$

$$-\sum_{l=1}^{p} (P_l^0 - P_l) R_l \tag{3}$$

$$+\sum_{j=1}^{|V|} F_j \tag{4}$$

$$\text{subject to} \quad \text{all conditions in Table 2}\,,$$

$$\sum_{l=1}^{p}\sum_{k=1}^{i}\sum_{i\in c_i} x_{ikl} = 1\,,$$

$$\forall c_i = \{j \mid j = i \text{ or } j \text{ is rotated version of } i\}\,, \tag{5}$$

$$\sum_{k=i+1}^{n}\sum_{l=1}^{p} x_{ikl} = 0\,, \tag{6}$$

$$u_l \geq \frac{1}{n}\sum_{i=1}^{n}\sum_{k=1}^{n} x_{ikl} \tag{7}$$

$$b_{kl} = W_l x_{kkl} - \sum_{i=k}^{n} w_i x_{ikl}\,,$$

$$\forall k \in \mathbb{F}_n\,,\ \ \forall l \in \mathbb{F}_p\,, \tag{8}$$

$$b_k = \sum_{l=1}^{p} b_{kl}\,, \tag{9}$$

$$s_l = H_l u_l - \sum_{k=1}^{n} h_k x_{kkl}\,, \tag{10}$$

$$q_i = \sum_{l=1}^{p}\sum_{k=1}^{i} (h_k - h_i)\, x_{ikl}\,, \tag{11}$$

$$a_i = \sum_{l=1}^{p}\sum_{k=1}^{i} (T_l - t_i)\, x_{ikl}\,, \tag{12}$$

$$s_l \geq d_l^{H_{\min}} - \hat{H}(1 - z_l^H)\,, \tag{13}$$

$$s_l \leq \hat{H} z_l^H + d_l^{H_{\min}}\,, \tag{14}$$

$$V_l^H \leq s_l W_l T_l G_l\,, \tag{15}$$

$$V_l^H \leq H_l W_l T_l G_l z_l^H\,, \tag{16}$$

$$b_k \geq \sum_{l=1}^{p} d_l^{W_{\min}} x_{kkl} - (1 - z_k^S)\hat{W}\,, \tag{17}$$

$$b_k \leq \hat{W} z_k^S + \sum_{l=1}^{p} d_l^{W_{\min}} x_{kkl}\,, \tag{18}$$

$$G_l V_{kl}^S \leq M_l z_k^S\,, \tag{19}$$

$$V_{kl}^S \leq b_k h_k T_l G_l\,, \tag{20}$$

$$V_{kl}^S \leq W_l h_k T_l G_l x_{kkl}\,, \tag{21}$$

$$q_i \geq \sum_{l=1}^{p}\sum_{k=1}^{i} d_l^{H_{\min}} x_{ikl} - (1 - z_i^C)\hat{H}\,, \tag{22}$$

$$q_i \leq \hat{H} z_i^C + \sum_{l=1}^{p}\sum_{k=1}^{i} d_l^{H_{\min}} x_{ikl}\,, \tag{23}$$

$$G_l V_{il}^C \leq M_l z_i^C\,, \tag{24}$$

$$V_{il}^C \leq w_i q_i T_l G_l\,, \tag{25}$$

$$V_{il}^C \leq w_i H_l T_l G_l \sum_{k=1}^{i} x_{ikl}\,, \tag{26}$$

$$a_i \geq \sum_{l=1}^{p}\sum_{k=1}^{i} d_l^{T_{\min}} x_{ikl} - \hat{T}(1 - z_i^T)\,, \tag{27}$$

$$a_i \leq \hat{T} z_i^T + \sum_{l=1}^{p}\sum_{k=1}^{i} d_l^{T_{\min}} x_{ikl}\,, \tag{28}$$

$$G_l V_{il}^T \leq M_l z_i^T\,, \tag{29}$$

$$V_{il}^T \leq w_i h_i a_i G_l\,, \tag{30}$$

$$V_{il}^T \leq w_i h_i T_l G_l \sum_{k=1}^{i} x_{ikl}\,, \tag{31}$$

$$R_l = M_l - \underbrace{\sum_{i=1}^{n}\sum_{k=1}^{i} w_i h_i t_i G_l x_{ikl}}_{\text{assigned items}}$$

Table 1: Inputs and Identifiers.

Input or Identifier	Description
w_i, h_i, t_i	Width, height and depth of item i, with $i = 1, \ldots, n$.
p_i	Value of item i per kilogram.
W_l, H_l, T_l	Width, height and depth of slab l, with $l = 1, \ldots, p$.
G_l	Weight per volume unit of slab l, e.g., $7.85 \cdot 10^{-6} \frac{kg}{mm^3}$.
$M_l = W_l H_l T_l G_l$	Weight of slab l.
$\hat{W} = \max_{l=1,\ldots,p} \{W_l\}$	Greatest width of slabs.
$\hat{T} = \max_{l=1,\ldots,p} \{T_l\}$	Greatest height of slabs.
$\hat{H} = \max_{l=1,\ldots,p} \{H_l\}$	Greatest depth of slabs.
P_l^0	Purchase value of slab l per kilogram.
P_l	Current value of slab l per kilogram.
g_l^e	Boundaries of weight classes, specific to slab l, e.g., $\left(g_1^1 \quad g_1^2 \quad g_1^3 \quad g_1^4 = g_1^m\right) = \left(0 \quad 2.1 \quad 5.1 \quad 10.1\right)$.
α_l^e	Relative value for weight classes, specific to slab l, e.g., $\left(\alpha_1^1 \quad \alpha_1^2 \quad \alpha_1^3 \quad \alpha_1^4 = \alpha_1^m\right) = \left(0.2 \quad 0.5 \quad 0.6 \quad 1\right)$.
$d_l^{W_{\min}}, d_l^{H_{\min}}, d_l^{T_{\min}}$	Minimum width, height, and depth before leftover material is considered waste, e.g., $d_l^{W_{\min}} = d_l^{H_{\min}} = d_l^{T_{\min}} = 10\,cm$

$$
\begin{aligned}
&- \sum_{k=1}^{n} V_{kl}^S - \sum_{i=1}^{n} V_{il}^C \\
&- \sum_{i=1}^{n} V_{il}^T - V_l^H \,, \qquad (32)
\end{aligned}
$$

$$
\begin{aligned}
V := \quad & \left\{ V_l^H > 0 \mid l = 1, \ldots, p \right\} \\
& \cup \left\{ V_k^S > 0 \mid k = 1, \ldots, n \right\} \\
& \cup \left\{ V_i^C > 0 \mid i = 1, \ldots, n \right\} \\
& \cup \left\{ V_i^T > 0 \mid i = 1, \ldots, n \right\} \,, \qquad (33)
\end{aligned}
$$

$$
\begin{aligned}
& z_{je}^R g_{l(j)}^e \leq V_j \,, \\
& \qquad \forall j \in \mathbb{F}_{|V|} \,, \;\; \forall e \in \mathbb{F}_m \,, \qquad (34)
\end{aligned}
$$

$$
\begin{aligned}
& V_j < g_{l(j)}^{e+1} + M_{l(j)} (1 - z_{je}^R) \,, \\
& \qquad \forall j \in \mathbb{F}_{|V|} \,, \;\; \forall e \in \mathbb{F}_{m-1} \,, \qquad (35)
\end{aligned}
$$

$$
\sum_{e=1}^{m} z_{je}^R = 1 \,, \;\; \forall j \in \mathbb{F}_{|V|} \,, \qquad (36)
$$

$$
\begin{aligned}
& F_{je} \leq V_j P_{l(j)}^0 \alpha_{l(j)}^e \,, \\
& \qquad \forall j \in \mathbb{F}_{|V|} \,, \;\; \forall e \in \mathbb{F}_m \,, \qquad (37)
\end{aligned}
$$

$$
\begin{aligned}
& F_{je} \leq M_{l(j)} P_{l(j)}^0 \alpha_{l(j)}^e z_{je}^R \,, \\
& \qquad \forall j \in \mathbb{F}_{|V|} \,, \;\; \forall e \in \mathbb{F}_m \qquad (38)
\end{aligned}
$$

In the following, the objective function and the constraints will be discussed in detail.

The objective is to maximize the profit from the production of one batch of items. In general, the profit is calculated by subtracting the costs from the revenue. The costs, on the one hand, consist of the slabs that are used for production, see Eq. (2), and the scrap material, see Eq. (3). The revenue, on the other hand, consists of the produced items, see Eq. (1), and the reusable leftover material, see Eq. (4). Note that the objective function is linear in the variables x_{ikl}, u_l, R_l, and F_j, c.f., Table 2.

From Eq. (5) and Eq. (6) we see that all items have to be produced. This means Eq. (1) of the objective is constant and does not influence the optimal solution. However, we will simplify that for the solver.

If we use a slab, it decreases the revenue. I.e., its value is subtracted in Eq. (2). The production will result not only in items that we want to produce. There will also be surplus material. As discussed earlier this can either be leftover material or scrap material.

The scrap material originates from a slab with a purchase value P_l^0 and this is the value we lose if we throw it away. As we have already accounted for the current value in Eq. (2), we need to compensate for that in Eq. (3).

The leftover material is a kind of positive revenue. It is not being paid for by a customer at this moment, but it might be in future production cycles. So this value is added to the objective, and thereby to the revenue, in Eq. (4).

The constraints are described in the following. Equation (5) describes that each item should only be produced once. Usage of the set c_i prevents that both, the original and the rotated version of an item, are produced.

Equation (6) means that an item i can only be placed in shelves 1 to i. In other words, an item can open a shelf or be placed in an existing one. As items are sorted by height, this ensures equivalence to the case where the height of a shelf is not determined by

Table 2: (Auxiliary) Variables.

Variable	Description
$x_{ikl} \in \{0,1\}$	Set to 1 if item i is placed in shelf k on slab l.
$u_l \in \{0,1\}$	Set to 1 if slab l is used.
$b_{kl} \geq 0$	Remaining width in shelf k on slab l, see Fig. 5a.
$b_k \geq 0$	Remaining width in shelf k, see Eq. (9).
$s_l \geq 0$	Remaining height above top shelf on slab l, see Fig. 5a, Eq. (10).
$q_i \geq 0$	Remaining height above item i in its assigned shelf, see Fig. 5a, Eq. (11).
$a_i \geq 0$	Remaining depth above item i in its assigned shelf, see Fig. 5b, Eq. (12).
$V_{kl}^S \geq 0$	Weight of leftover material filling the *width* of shelf k on slab l, see Fig. 3. A shelf is located on exactly one slab, so it is $\neq 0$ for exactly one combination of k and l or all are 0 if the leftover material is waste.
$V_k^S = \sum_{l=1}^{p} V_{kl}^S \geq 0$	Weight V^S of shelf k.
$V_{il}^C \geq 0$	Weight of leftover material filling the *height* above item i on slab l, see Fig. 3. It is $\neq 0$ for only one combination of i and l or all equal 0 if waste.
$V_i^C = \sum_{l=1}^{p} V_{il}^C \geq 0$	Weight V^C above item i.
$V_{il}^T \geq 0$	Weight of leftover material filling the *depth* above item i on slab l, see Fig. 3. It is $\neq 0$ for only one combination of i and l or all equal 0 if waste.
$V_i^T = \sum_{l=1}^{p} V_{il}^T \geq 0$	Weight V^T above item i.
$V_l^H \geq 0$	Weight of leftover material on the top of slab l, see Fig. 3.
$z_k^S, z_i^C, z_i^T, z_l^H \in \{0,1\}$	Set to 0 if associated weights are waste.
$V_j \geq 0\,, \quad \forall j \in \mathbb{F}_{\lvert V \rvert}$	An element from the set V, see Eq. (33).
$z_{je}^R \in \{0,1\}\,, \quad \forall j \in \mathbb{F}_{\lvert V \rvert}$	Set to 1 if weight j is in class e.
F_{je}	Value of leftover material j in weight class e. Not equal 0 for one weight class.
$F_j = \sum_{e=0}^{m} F_{je} \geq 0\,, \quad \forall j \in \mathbb{F}_{\lvert V \rvert}$	The value of weight j.
R_l	Weight of leftover material that is waste.

the first, but highest item.

Equation (7) sets u_l to one if slab l is used.

Equation (8) and Eq. (9) set the variable b_k which describes the remaining width in shelf k, see also Fig. 5. Equation (10), Eq. (11), and Eq. (12) set s_l, q_i, and a_i, respectively. See also Fig. 5.

Equation (13) and Eq. (14) set the variable z_l^H to zero if the associated weight V_l^H is waste. V_l^H is considered waste if $s_l < d_l^{H_{\min}}$. In that case, z_l^H in Eq. (14) can either be 0 or 1, but with Eq. (13) it has to be 0. Then again, if $s_l \geq d_l^{H_{\min}}$, z_l^H in Eq. (13) can either be 0 or 1, while Eq. (14) sets it to 1.

The weights, which are calculated to get the value of the leftover material, are best understood by looking at Fig. 3. The weight V_l^H is calculated in Eq. (15) and Eq. (16). The latter one is set to zero if it is considered waste. This is done so that no value is added for it in the objective function.

In Eq. (17) and Eq. (18) z_k^S is set to 0 if V_{kl}^S is scrap material. Otherwise, z_k^S is set to 1. In both equations, the summation over l "picks" the correct slab as x_{kkl} can only be one for one l. Beside of that, it works analogously to Eq. (13) and Eq. (14).

The next three equations, Eq. (19), Eq. (20), and Eq. (21), set the weight V_{kl}^S. It is set to its actual value if it is usable, otherwise it is set to 0. To be more precise, the equations set the upper limit of the weight and the objective indirectly maximizes the weight such that the upper limit will be reached. Equation (19) limits V_{kl}^S to the weight of the slab or sets it to 0 if it is scrap material. Equation (20) and Eq. (21) need to be interpreted in conjunction. Equa-

tion (20) limits V_{kl}^S as if shelf k is on slab l, which is not necessarily true. Equation (21) then limits V_{kl}^S to 0 if x_{kkl} equals 0, i.e., only the correct combination of k and l lead to a value unequal 0.

Equation (22) and Eq. (23) set z_i^C in a similar way as Eq. (17) and Eq. (18) set z_k^S. The sum to find the correct $d_l^{H_{\min}}$ needs to be a sum over x_{ikl}. This is because an item, not being the first item in a shelf, can be located on any shelf.

The next three equations, Eq. (24), Eq. (25), and Eq. (26), set the weight V_{il}^C in the same way as Eq. (19), Eq. (20), and Eq. (21) set V_{kl}^S. Equation (26) has an additional sum, compared to the calculation of V_{kl}^S. The argument here is similar to the one above. Item i can be located on any shelf, so we sum over the shelves k in order to pick the correct x_{ikl}.

Equation (27) and Eq. (28) set z_i^T in the same way as z_i^C is set. Equation (29), Eq. (30), and Eq. (31) define the weight V_{il}^T in the same way as V_{il}^C is defined.

R_l is the sum of the weight of scrap material from slab l. It is calculated in Eq. (32) as the remainder from substracting produced and reusable items from the slab weight. I.e., everything that is not an item or reusable leftover is scrap material.

Equation (4) uses the set V, which is defined in Eq. (33). V is the set of all weights not of size zero. Recall that these weights are only those that are associated to reusable material.

The rest of the constrains are used to finally calculate the value of the reusable material. z_{je}^R denotes if weight j is in the weight class e. Let $l(j)$ denote the slab on which weight j is located. $l(j)$ is linear, because $V_j = V_k^S : l(j) = l \Leftrightarrow V_{kl}^S > 0$, analogously for C, T. Then, z_{je}^R shall equal 1 if $g_{l(j)}^e \leq V_j < g_{l(j)}^{e+1}$. This is accomplished by Eq. (34), Eq. (35), and Eq. (36). Equation (35) will set z_{je}^R to zero if V_j is lighter than the boundary g^e. Equation (34) will set z_{je}^R to zero if V_j is heavier than g^e. Both these equations allow z_{je}^R to be either 0 or 1 if the above inequality holds. In that case Eq. (36) forces z_{je}^R to be 1 and we have our desired behavior.

With this information we can finally calculate F_{je}, which is the value of V_j. As the name suggests, it is non-zero only for one specific value of e. Unfortunately, we cannot multiply V_j by z_{je}^R as we want our problem to stay linear. Therefore, Eq. (37) sets the upper limit of its value regardless of z_{je}^R. Then, Eq. (38) sets an even larger upper limit, but only if z_{je}^R equals 1. Otherwise, it sets it to 0, which is what we want if V_j does not lie in this specific weight class. In our objective function, the sum is above F_j, not F_{je}. This is explained in Table 2.

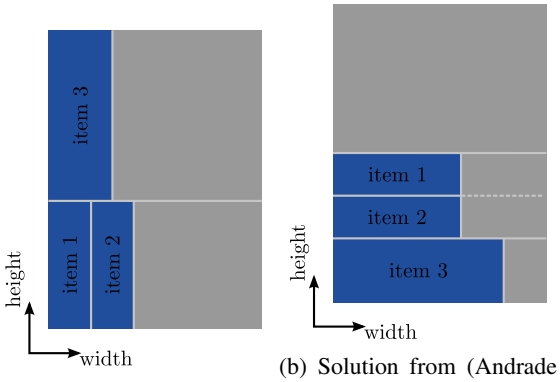

(a) Our solution.

(b) Solution from (Andrade et al., 2013).

Figure 6: Example 1, input data No. 1, Table 3.

Table 3: Input data No. 1.

(a) Slabs in stock

ID	W	H	T
1	500	700	45

(b) Items in order

ID	w	h	t
−3	150	400	45
−1	100	300	45
−2	100	300	45
3	400	150	45
1	300	100	45
2	300	100	45

4 EVALUATION

The optimization program was implemented using CVX, which is an add-on for MATLAB. CVX allows a high level description of the program, which is close to the description in Section 3. CVX can use several solvers. The solver we use is Gurobi ((Gurobi Optimization, Inc., 2016)) as it can solve binary integer linear programs.

In all examples, the boundaries and relative values of the weight classes are the ones from Table 1. Also, the weight per volume is given there.

Please note that some of the slabs had to be drawn incomplete in order to keep the page size down. This was done only in areas where no items are placed and is denoted by a dotted line at the top of the slab.

Example 1

We compare our solution to the one named $\mathcal{M}_1^L$ in (Andrade et al., 2013), which is also implemented in CVX/Gurobi. As mentioned earlier, the solution in (Andrade et al., 2013), solves the problem in two dimensions. Therefore, in our example, the thickness of the ordered items matches the thickness of the slabs in stock.

Later, we will also show an example where the thickness between slab and items is different.

Table 4: Input data No. 2.

(a) Slabs in stock

ID	W	H	T
1	350	650	40
2	300	300	40

(b) Items in order

ID	w	h	t
1	200	330	40
2	150	300	40
3	150	300	40

The data from Table 3 produces the solutions shown in Fig. 6. The table shows the rotated items, where the item with identifier $-i$ denotes the rotated version of the item with itentifier i. We will omit these in later tables. The items in this specific table are also ordered by height as needed for in our problem formulation.

We denote a cut which should not be necessary in the final cutting procedure with a dashed line. Our solution results in two quite large pieces of surplus material. The solution from (Andrade et al., 2013), results in a solution with three smaller pieces of surplus material. We also rotated all items before feeding the input to the algorithm from (Andrade et al., 2013). Still, its solution was to put all three items side by side, i.e., also creating three pieces of surplus material. Subjectively, two larger pieces of surplus material are better than three smaller ones.

Putting the solution from (Andrade et al., 2013) into our objective function, we get a smaller, i.e., worse, objective value. That means, according to our valuation, we have a better overall value of items and slabs, compared to the algorithm from (Andrade et al., 2013). It is also shown that the rotation of items is of importance.

Example 2

This example, see Fig. 7, underlines how our optimization problem finds really good solutions if slabs can be filled. There is no leftover material on slab 2, so slab 1 produces a nice large piece of leftover material in addition to a smaller one. The smaller one is just slightly above the size limitations of scrap material, so it is put back to the set of slabs for the next run, too.

Assume, we rotate item 1 on slab 1. The values of the used slabs, as well as the value of the produced items stays the same. Still, the value of the objective function decreases, because the sum of the values of the surplus material decreases. Note that, the sum of the weights of the surplus material stays also the same. The value of the surplus material decreases, because the function, described by g_l^e and α_l^e, is a concave function. This function is essential for the performance of the optimization program.

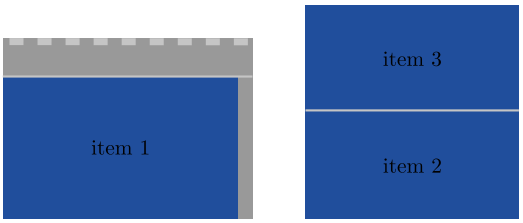

(a) Slab 1 (b) Slab 2

Figure 7: Example 2, input data No. 2, Table 4.

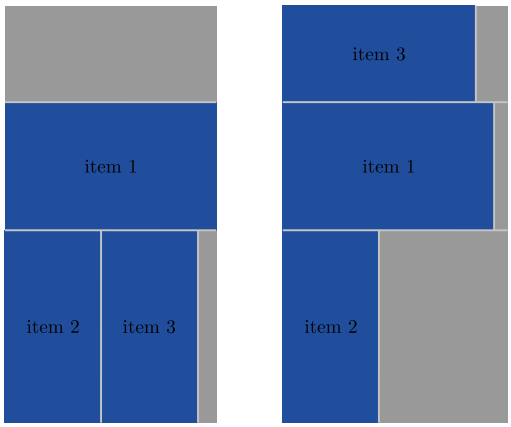

(a) Input data No. 3 (b) Input data No. 4

Figure 8: Ex. 3, data No. 3 and 4, Tables 5 and 6.

Example 3

Two slightly different variations of input data is examined in this example. Table 5 shows input data no. 3, while Table 6 shows input data no. 4. The only difference is the size in the direction of x of the slab.

Figure 8 shows both solutions. Again, it is all about the value of the leftover material. It is clear the solution with the highest value of the leftover material is optimal, because all of the items have to be produced according to the objective function.

With input data No. 4, if the items would be placed as seen in Fig. 8a, then the value of the leftover material would be less than is shown. This directly depends on the weight groups. As a result the weight groups have to be empirically adjusted, according to the slab sizes and items ordered.

Table 5: Input data No. 3.

(a) Slabs in stock

ID	W	H	T
1	330	650	40

(b) Items in order

ID	w	h	t
1	200	330	40
2	150	300	40
3	150	300	40

Table 6: Input data No. 4.

(a) Stock

ID	W	H	T
1	350	650	40

(b) Order

ID	w	h	t
1	200	330	40
2	150	300	40
3	150	300	40

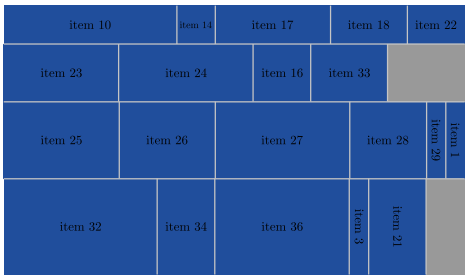

(a) Slab 1

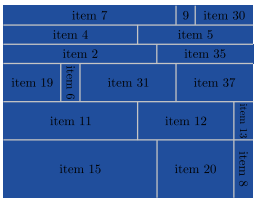

(b) Slab 2

Figure 9: Example 4, input data No. 5, Table 7.

Example 4

In Fig. 9 we show the result of an optimization which barely fits on the slabs and where items have many similar dimensions. This is where the optimization problem really shines and a manual solution would be really time consuming if you would even find one.

Example 5

Compared to the last example, Fig. 10 shows the result of items, which don't have many similar sizes. The result does not look as nice and dense as the previous one, but it still produces many larger pieces of surplus material. Note that slab 1 is not used, i.e., smaller blocks of steel are used first, because they have a smaller value. This is exactly what we want.

Example 6

Figure 11 is a slight variation of the previous example. The sizes of slab 2 and slab 3 are decreased. As a result not all items fit on these two slabs.

As can be seen from the figure, item 7 is put on slab 1, but it would neatly fit into the upper right corner of slab 3. The optimization problem can't find this solution, because it makes strict assumptions about the layout of the items. Further investigation about cutting patterns and their application to the formulation of the optimization problem might be a direction of future research.

Table 7: Input data No. 5.

(a) Stock

ID	W	H	T
1	240	140	10
2	130	100	10

(b) Order

ID	w	h	t	ID	w	h	t
1	40	10	10	20	40	30	10
2	80	10	10	21	50	30	10
3	50	10	10	22	20	30	10
4	70	10	10	23	60	30	10
5	60	10	10	24	70	30	10
6	20	10	10	25	60	40	10
7	90	10	10	26	50	40	10
8	30	10	10	27	70	40	10
9	10	10	10	28	40	40	10
10	90	20	10	29	10	40	10
11	70	20	10	30	10	30	10
12	50	20	10	31	20	50	10
13	10	20	10	32	80	50	10
14	20	20	10	33	30	40	10
15	80	30	10	34	30	50	10
16	30	30	10	35	10	50	10
17	60	20	10	36	70	50	10
18	40	20	10	37	20	40	10
19	30	20	10				

(a) Slab 1

(b) Slab 2 (c) Slab 3

Figure 10: Example 5, input data No. 6, Table 8.

Example 7

In previous examples, the thickness of items matched

Table 8: Input data No. 6.

(a) Stock

ID	W	H	T
1	300	300	45
2	170	250	45
3	150	100	45

(b) Order

ID	w	h	t
1	94	50	45
2	65	37	45
3	51	88	45
4	78	56	45
5	32	66	45
6	54	36	45
7	58	29	45
8	53	72	45
9	95	75	45
10	89	87	45

(a) Slab 1

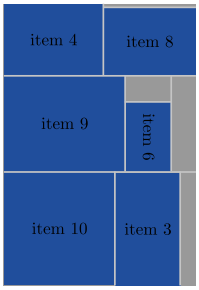

(b) Slab 2

(c) Slab 3

Figure 11: Example 6, input data No. 7, Table 9.

the thickness of the slabs. Now, we show that our formulation can give unexpected results if there are several slabs with different thicknesses to pick from.

In Fig. 12, we show the results of our formulation with input data no. 8, Table 10. One might assume that producing the item on slab 2, which matches its thickness, is the best option. As you can see, our formulation places the item on slab 1, which is considerably thicker than it needs to be. Simply put, the value

Table 9: Input data No. 7.

(a) Stock

ID	W	H	T
1	300	300	45
2	150	220	45
3	120	100	45

(b) Order

ID	w	h	t
1	94	50	45
2	65	37	45
3	51	88	45
4	78	56	45
5	32	66	45
6	54	36	45
7	58	29	45
8	53	72	45
9	95	75	45
10	89	87	45

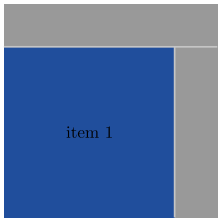

(a) Slab 1

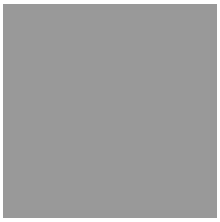

(b) Slab 2

Figure 12: Example 7, input data No. 8, Table 10.

Table 10: Input data No. 8.

(a) Stock

ID	W	H	T
1	500	700	25
2	500	700	15

(b) Order

ID	w	h	t
1	400	400	15

of the leftover material dictates this placement.

Cuts that trim the thickness can take a long time, because the area to cut can be quite large compared to the other cuts. If these trims were not desired, the optimization problem could either be extended by a penalty for these cuts or items and orders could simply be matched in thickness before given to the optimization program.

Runtime and Quality

Besides example 4, the runtime of our examples was always below one minute, which is a reasonable runtime to collect and place orders. Example 4 took about 5000 seconds, which is considerable more than the other solutions. Limiting the time allowed by the solver for Example 4 to 60 seconds, we still got a feasible solution. I.e., while not as dense as the solution shown in Fig. 9, all items were placed on the slabs.

5 SUMMARY

In this paper, we developed an optimization program that solves the problem of cutting steel-plates, where only guillotine cuts are allowed. We consider surplus material as a form of value. Our solution is modeled in three dimensions in order to assign a value to the surplus material. We use the notion of shelves to model the placement of items on slabs and allow items to be rotated.

As has been shown in the examples, our problem formulation gives subjectively good results, i.e., the problem is apparently well solved. We have shown that preferable few, big leftovers are created and small slabs are used first, see Examples 1 and 6 respectively.

Example 4 showed that our formulation allows the tradeoff between runtime and quality. Example 5 showed good performance, even for items of random size.

In some cases, the placement using shelves might not be optimal and a more advanced placement might yield better results in the case of sparser placements. Consider Example 6, item 7 could fit on slab 3 with a proper cutting order. Although, modeling and finding optimal solutions of placements not following the notion of shelves is much more difficult.

Including the third dimension is necessary to achieve optimal solutions, see Example 7. Our results are strongly dependent on the choice of weight classes and their values, see Examples 2 and 3. A proper optimization of these could be the topic of future research. Although, the values from Table 1 produce good results for the sizes we used in our examples.

In the future, the number of cuts or a penalty for using many different slabs could be incorporated easily into the objective function. But these considerations should be justified by concrete requirements of a factory.

REFERENCES

Andrade, R., Birgin, E., and Morabito, R. (2013). Two-stage two-dimensional guillotine cutting stock problems with usable leftover.

Burke, E. K., Hyde, M. R., and Kendall, G. (2011). A squeaky wheel optimisation methodology for two-dimensional strip packing. *Computers & Operations Research*, 38(7):1035–1044.

Carnieri, C., Mendoza, G. A., and Gavinho, L. G. (1994). Solution procedures for cutting lumber into furniture parts. *European Journal of Operational Research*, 73(3):495–501.

Christofides, N. and Whitlock, C. (1977). An Algorithm for Two-Dimensional Cutting Problems. *Operations Research*, 25(1):30–44.

Dyckhoff, H., Kruse, H.-J., Abel, D., and Gal, T. (1985). Trim loss and related problems. *Omega*, 13(1):59–72.

Farley, A. A. (1988). Practical adaptations of the Gilmore-Gomory approach to cutting stock problems. *Operations-Research-Spektrum*, 10(2):113–123.

Furini, F. and Malaguti, E. (2013). Models for the two-dimensional two-stage cutting stock problem with multiple stock size. *Computers & Operations Research*, 40(8):1953–1962.

Gilmore, P. and Gomory, R. (1961). A Linear Programming Approach to the Cutting-Stock Problem. *Operations Research*, 9(6):849–859.

Gilmore, P. C. and Gomory, R. E. (1965). Multistage Cutting Stock Problems of Two and More Dimensions. *Operations Research*, 13(1):94–120.

Gurobi Optimization, Inc. (2016). Gurobi Optimizer Reference Manual. http://www.gurobi.com/.

Hinxman, A. I. (1980). The trim-loss and assortment problems: A survey. *European Journal of Operational Research*, 5(1):8–18.

Kalagnanam, J. R., Dawande, M. W., Trumbo, M., and Ho Soo Lee (2000). The Surplus Inventory Matching Problem in the Process Industry. *Operations Research*, 48(4):505–516.

Kantorovich, L. V. (1960). Mathematical Methods of Organizing and Planning Production. *Management Science*, 6(4):366–422.

Kurt Eisemann (1957). The Trim Problem. *Management Science*, 3(3):279–284.

Lodi, A. and Monaci, M. (2003). Integer linear programming models for 2-staged two-dimensional Knapsack problems. *Mathematical Programming*, 94:257–278.

Martello, S., Pisinger, D., and Vigo, D. (2000). The Three-Dimensional Bin Packing Problem. *Operations Research*, 48(2):256–267.

Morabito, R. and Arenales, M. (2000). Optimizing the cutting of stock plates in a furniture company. *International Journal of Production Research*, 38(12):2725–2742.

Silva, E., Alvelos, F., and Valério de Carvalho, J. M. (2010). An integer programming model for two- and three-stage two-dimensional cutting stock problems. *European Journal of Operational Research*, 205(3):699–708.

Wayne L Winston and Jeffrey B Goldberg (2004). *Operations Research: Applications and Algorithms*. Duxbury press Belmont, CA.

Yanasse, H. H., Zinober, A. S. I., and Harris, R. G. (1991). Two-dimensional Cutting Stock with Multiple Stock Sizes. *Journal of the Operational Research Society*, 42(8):673–683.

Optimizing Spare Battery Allocation in an Electric Vehicle Battery Swapping System

Michael Dreyfuss and Yahel Giat
Department of Industrial Engineering, Jerusalem College of Technology, HaVaad HaLeumi 21, Jerusalem, Israel
{*dreyfuss, yahel*}*@jct.ac.il*

Keywords: Battery Swapping, Electric Vehicle, Exchangeable Item Repair System, Window Fill Rate, Spare Allocation Problem

Abstract: Electric vehicle battery swapping stations are suggested as an alternative to vehicle owners recharging their batteries themselves. To maximize the network's performance spare batteries must be optimally allocated in these stations. In this paper, we consider the battery allocation problem where the criterion for optimality is the window fill rate, i.e., the probability that a customer that enters the swapping station will exit it within a certain time window. This time is set as the customer's tolerable wait in the swapping station. In our derivation of the window fill rate formulae, we differ from previous research in that we assume that the swapping time itself is not negligible. We numerically analyse the battery allocation problem for a hypothetical countrywide application in Israel and demonstrate the importance of estimating correctly customers' tolerable wait, the value of reducing battery swapping time and the unique features of the optimal battery allocation.

1 INTRODUCTION

Electric vehicles' batteries need to be recharged frequently with inconveniently long recharging time. The US-based corporation Better Place suggested to overcome this problem by separating battery ownership from the vehicle's ownership so that customers purchase the vehicle from the auto-maker and lease battery services from a third party ("the firm"). The firm will construct a network of battery swapping stations in which car owners replace their depleted batteries for charged ones from the station's stock. Separately, the depleted batteries are recharged and put back in the stock to be given to future customers. To improve the network's performance, the firm may decide to place spare batteries in each station. Therefore, given a total budget of spare batteries, the firm must decide how to allocate the spare batteries among the battery swapping stations with the goal of optimizing a predetermined service measure.

The service measure that we consider in this paper is a generalization of the fill rate. With the fill rate, the firm will allocate batteries to maximize the fraction of customers who are served upon arrival. In reality, however, the fill rate is rarely an accurate proxy for the firm's costs. For example, if the battery provider is obliged by contractual commitment to provide service within a certain time then it does not need to have a battery ready for the customer immediately when she arrives. From the customers' standpoint, too, there is a certain tolerable or acceptable period of wait, which may depend on their level of patience or expectation. If a customer entering the station expects being served within the ten minutes it would take to fill a tank of a conventional car, then the firm experiences reputation and contractual losses only if the customer waits more than ten minutes. Thus, the firm's objective should be to maximize the *window fill rate*, i.e., the probability that a customer is served *within* the tolerable wait.

To address this problem, we use research in the field of exchangeable-item repair systems. Customers arrive to these systems with a failed item and exchange it for an operable item in a manner similar to the battery swapping scheme. Furthermore, since battery charging docks are relatively inexpensive, one may assume that there are ample servers in each location so that each location can be modelled as an $M/G/\infty$ queue. (Dreyfuss and Giat, 2016) develop an algorithm for finding a near-optimal solution in such multi-location systems assuming that the item's assembly and disassembly times are negligible. This assumption is clearly unrealistic for the battery swapping problem since battery removal and installation times are significant compared to the customer's tolerable wait.

In this paper, we develop the window fill rate for-

Dreyfuss, M. and Giat, Y.
Optimizing Spare Battery Allocation in an Electric Vehicle Battery Swapping System.
In *Proceedings of the 6th International Conference on Operations Research and Enterprise Systems (ICORES 2017)*, pages 38-46
ISBN: 978-989-758-218-9

mula for the case of positive item assembly and disassembly times and show that a Δ *increase* in the assembly and disassembly time is equivalent to a Δ *decrease* in the tolerable wait. Using this finding we apply the (Dreyfuss and Giat, 2016) algorithm to find a solution to the battery swapping problem, i.e., how to allocate spare batteries in the network, and make the following contributions.

We estimate the battery allocation problem of the Better Place corporation if it had succeeded going widespread in Israel and derive the optimal solution for different service criteria. This example provides valuable insight into the critical importance of assessing correctly the tolerable wait time and the significant losses that the firm incurs if it neglects to do so. Second, we estimate the savings attained by reducing battery swapping time. Third, we show how customer arrival rate creates two classes of battery exchange stations and therefore managers should develop two different policies with respect to their service time to customers. Although the Better Place adventure has ended with bankruptcy in 2013, the battery swapping idea is either applied or considered by other companies (e.g. XJ Group Corporation in Qingdao, Tesla in California and Gogoro in Taipei). The model presented in this paper, therefore, may yet be applied in real-life large-scale situations.

2 LITERATURE REVIEW

Electric vehicles are considered an environmentally-friendly alternative to internal combustion engine cars and are projected to eventually replace these fuel-burning cars (Dijk et al., 2013). Drivers, however, are still wary of these vehicles and therefore, many governments provide substantial tax incentives to encourage their widespread adoption. Notable examples are West European countries, the United States, China and Japan (Zhou et al., 2015). Despite these efforts, many drivers are wary of purchasing these cars and most governments adoption goals have not been met (Coffman et al., 2016). The major customer concern is the "range anxiety", namely, the fact that batteries have limited range and their recharging time is very long compared to internal combustion engine cars. An innovative idea to overcome these issues was introduced by the US-based company Better Place who proposed to separate the vehicle ownership from the battery ownership. In lieu of owning the battery, car owners will purchase battery services from a firm that will establish a network of battery swapping stations. Researcher are examining many aspects of this proposition such as the station design, the battery removal and installation times, the required number of spare batteries and the network layout and managing the loads on the power grid (Mak et al., 2013; Yang and Sun, 2015; Sarker et al., 2015). We contribute to this research by solving the spare battery allocation problem and demonstrating a large-scale application of this problem.

The assumption that customers will tolerate a certain wait is at the core of this paper, which lies at the intersection of inventory and customer service models. While the concept of a tolerable wait is hardly ever considered in inventory models, it is quite common in the service industry and is associate with numerous terms such as "expectation" (Durrande-Moreau, 1999), "reasonable duration" (Katz et al., 1991), "maximal tolerable wait" (Smidts and Pruyn, 1999) and "wait acceptability" (Demoulin and Djelassi, 2013). From a service-oriented approach, the customer's attitude to wait is mainly subjective and has cognitive and affective aspects (Demoulin and Djelassi, 2013). From a logistics point of view this wait is more objective and usually stated in the service contract. Indeed, researchers have observed that most inventory models fail "to capture the time-based aspects of service agreements as they are actually written" (Caggiano et al., 2009, p.744). Our paper fills this void by incorporating the tolerable wait into the optimization criterion.

Our battery swapping network may be modelled as an exchangeable-item repair system (Avci et al., 2014). These inventory systems have been investigated by researchers in different contexts (Basten and van Houtum, 2014). A common performance measure for such systems is the fill rate, which measures the fraction of customers who are served upon arrival (Shtub and Simon, 1994; Caggiano et al., 2007). These papers, however, do not develop explicit formulas for the window fill rate but use numerical techniques. In contrast, (Berg and Posner, 1990) develop a formula for the window fill rate in a single location when item assembly and disassembly is zero, and (Dreyfuss and Giat, 2016) find that the window fill rate is generally S-shaped with number spares in the location and exploit this property to develop an efficient near-optimal algorithm for finding the optimal spare allocation. We extend these papers by considering the case of positive assembly and disassembly times.

3 THE MODEL

Customers arrive with a depleted battery to a battery swapping network that comprises L stations. Upon ar-

rival, the battery is removed and placed in a charging dock and once it is fully recharged it is added to the station's stock. To reduce customer waiting time, the network keeps a number of spare batteries, so that if there is a spare battery available on stock it is installed in the client's vehicle in exchange of the depleted battery that she had brought. Customers are served according to a first-come, first-serve policy and leave the swapping station once their battery is replaced.

For each station l, $l = 1,...,L$, we assume that customer arrival rate follows an independent Poisson process with parameter λ_l (see (Avci et al., 2014) for a justification of this assumption). We assume that there are ample charging docks in each station and that charging time at each dock is i.i.d. The combination of these two assumptions is that once the battery is removed from the vehicle, charging commences immediately and that recharging times are independent. Let $R_l(t)$ denote the cumulative probability of a battery to be recharged by time t and let r_l denote the mean recharging time. Battery removal and battery installation times are t_1 and t_2, respectively. The battery swapping time, $t_1 + t_2$, is assumed to be no more than the tolerable wait.

3.1 Single Station

Consider a random customer, Jane, that arrives at time s to station l that was allocated b spares. The non-stationary window fill rate, $F_l^{NS}(s,t,b)$ is the probability that Jane will exit the station by time $s+t$. This happens if and only if by date $s+t-t_2$ Jane is at the head of the queue and there is at least one charged battery available at the station's stock. By "head of the queue" we mean that all the customers who arrived before Jane ("Pre-Jane customers") have either exited the station or are in the process of installing batteries in their vehicles. We can ensure this by verifying a supply and demand equation for recharged batteries. On the supply side, we consider the initial number of spare batteries in the station, b, plus all the batteries whose recharging was completed during the time segment $[0, s+t-t_2]$. On the demand side we consider the number of Pre-Jane customer plus Jane herself. Let:

- N_1 denote the number of batteries brought by Pre-Jane customers who were recharged before $s+t-t_2$.
- N_2 denote the number of batteries brought by Pre-Jane customers who were recharged after $s+t-t_2$.
- N_3 denote the number of batteries brought by customers who arrived after Jane ("Post-Jane customers") and were recharged before $s+t-t_2$.
- Z denote a Binary variable that is equal to one if Jane's battery is recharged by $s+t-t_2$ and zero otherwise.

The probability that Jane will exit the station by $s+t$ is the probability that the supply is greater than the demand as follows

$$\begin{aligned} F_l^{NS}(s,t,b) &= Pr[Supply \geq Demand] \\ &= Pr[b+N_1+Z+N_3 \geq N_1+N_2+1] \\ &= Pr[b+Z+N_3 \geq N_2+1] \end{aligned} \quad (1)$$

Since the battery brought by Jane begins recharging at $s+t_1$, the probability for $Z=1$ is the probability that a battery completes recharging during the interval $[s+t_1, s+t-t_2]$, which is equal to $R_l(t-t_1-t_2)$. Therefore, we can condition on the value of Z and rewrite (1) as

$$\begin{aligned} F_l^{NS}(s,t,b) &= R_l(t-t_1-t_2)Pr[b+1+N_3 \geq N_2+1] \\ &\quad + \big(1-R_l(t-t_1-t_2)\big)Pr[b+N_3 \geq N_2+1] \\ &= Pr[N_2-N_3 \leq b-1] + R_l(\hat{t})Pr[N_2-N_3=b], \end{aligned} \quad (2)$$

where $\hat{t} := t-t_1-t_2$.

Our assumption that batteries arrive according to a Poisson process and the ample server assumption guarantee that N_2 and N_3 are independent Poisson random variables that are also independent of Z. Recall, N_2 is the number of batteries who arrived between $[0,s]$ and were not repaired by $s+t-t_2$. Of these customers, consider a customer that arrives during the time interval $[u, u+du]$ in $[0,s]$. Due to the conditional uniform distribution property of the Poisson process, the probability for this is du/s (Ross, 1981, Chapter 3.5). This customer's battery is removed and begins to be recharged at $u+t_1$. The probability that recharging is completed only after $s+t-t_2$ is $1-R_l\big(s+t-t_2-(u+t_1)\big)$. Thus,

$$\begin{aligned} N_2 &\sim Poisson\Big(\lambda_l s \int_{u=0}^{s} \big(1-R_l(s+t-t_2-u-t_1)\big)\frac{du}{s}\Big) \\ &\sim Poisson\Big(\lambda_l \int_{u=\hat{t}}^{s+\hat{t}} \big(1-R_l(u)\big)du\Big). \end{aligned} \quad (3)$$

To derive the distribution of N_3 we consider the customers who arrived between $[s, s+t-t_2]$ and whose batteries were recharged by $s+t-t_2$. Of these customers, consider a customer that arrives during the time interval $[u, u+du]$. The probability for this is $du/(t-t_2)$. This customer's battery is removed and begins to be recharged at $u+t_1$. The probability that recharging is completed by $s+t-t_2$ is, therefore

$R_l\big(s+t-t_2-(u+t_1)\big)$. Thus,

$$N_3 \sim Poisson\Big(\lambda_l(t-t_2)\int_{u=s}^{s+t-t_2} R_l(s+t-t_2-u-t_1)\frac{du}{t-t_2}$$

$$\sim Poisson\Big(\lambda_l\int_{u=-t_1}^{\hat{t}} R_l(u)du = \lambda_l\int_{u=0}^{\hat{t}} R_l(u)du\Big). \quad (4)$$

The stationary window fill rate is obtained by taking the limit of s in (3) to infinity, which results with the following proposition:

Proposition 1. *The stationary window fill rate for station l with b spares is given by*

$$F_l(t,b) = Pr[N \le b-1] + R_l(\hat{t})Pr[N=b] \quad (5)$$

where $N := N_2 - N_3$ and where N_3 is defined in (4) and $N_2 \sim Poisson\big(\lambda_l \int_{u=\hat{t}}^{\infty}(1-R_l(u))du\big)$.

3.2 The Network

Let $\vec{b} = (b_1,...,b_L)$ be a network battery allocation and let $\lambda := \sum\lambda_l$ denote the (total) arrival rate to the network. The network's window fill rate, $F(t,\vec{b})$, is the weighted average of the local window fill rates. Therefore, given a budget of B spare batteries, the battery allocation problem is:

$$\max_{\vec{b}\ge 0} F(t,\vec{b}) := \sum_{l=1}^{L}\frac{\lambda_l}{\lambda}F_l(t,b_l) \quad s.t. \quad \sum_{l=1}^{L} b_l = B. \quad (6)$$

Since the window fill rate depends only on $\hat{t} = t-t_1-t_2$ we can instead assume that the battery removal and installment times are zero and use the adjusted tolerable wait, $\hat{t}$, in lieu of the true tolerable wait t. The implication of this observation is that we can use the results of (Dreyfuss and Giat, 2016) who assume zero swapping time. In the remainder of this section, we apply the results of (Dreyfuss and Giat, 2016) to our model with positive swapping time. We state only the results that are necessary for understanding the battery allocation application.

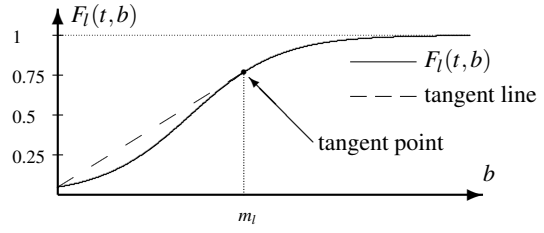

Figure 1: The window fill rate for an S-shaped station.

Result 1: The Shape of the Window Fill Rate

$F_l(t,b)$ is strictly increasing in b. If $t \ge r_l + t_1 + t_2$ then $F_l(t,b)$ is concave in b. Otherwise, $F_l(t,b)$ is either concave in b or initially convex and then concave (S-shaped) in b. The tangent point decreases with t and increases with t_1+t_2.

Result 2: The Optimization Algorithm

By (6), the window fill rate is a separable sum of either concave or S-shaped functions. For each S-shaped station we define the tangent point, m_l, as the first integer such that $\big(F_l(t,m_l) - F_l(t,0)\big)/m_l > \Delta F_l(t,m_l)$, where $\Delta F_l(t,b)$ is the first difference of $F_l(t,b)$ and is given by

$$\Delta F_l(t,b) := F_l(t,b+1) - F_l(t,b)$$
$$= \big(1-R_l(t)\big)Pr[N=b] + R_l(t)Pr[N=b+1]. \quad (7)$$

For concave stations we set the tangent point to zero. For each station, let $H_l(t,b)$ denote the concave covering function of $F_l(t,b)$ in the following manner:

$$H_l(t,b) = \begin{cases} F_l(t,0) + \frac{F_l(t,m_l)-F_l(t,0)}{m_l}b & \text{if } 0 \le b \le m_l - 1 \\ F_l(t,b) & \text{if } b \ge m_l. \end{cases}$$

That is, for any b smaller than the tangent point, we replace $F_l(t,b)$ with the straight line connecting the point $\big(0,F_l(t,0)\big)$ and the point $\big(m_l,F_l(t,m_l)\big)$. By construction, for all $b \ge 0$,$H_l(t,b)$ is concave and $H_l(t,b) \ge F_l(t,b)$. Finally, we define $H(t,\vec{b})$ as the weighted sums of all the stations' functions $H_l(t,b_l)$ similarly to (6).

Since $H(t,\vec{b})$ is a separable sum of concave functions we can use a greedy algorithm to maximize it. This algorithm will choose the "best for the buck" station and since H_l is initially linear, it will stay with stay with this station until it has reached the station's tangent point. It then continues with the next best station and so forth. Before switching to the next linear slope it is possible that stations that have reached their tangent will get additional spares (as long as their current slope is steeper than the next best linear slope). However, once a region begins receiving slopes in its linear region, it will be the only one to receive spares until it has reached its tangent point. Consequently, the algorithms produces an allocation with properties stated in the following result.

Result 3: The Optimal Allocation

$\vec{b}^H$ satisfies one of the following two cases:

1. For every $l = 1 \ldots L$, either $b_l^H \ge m_l$ or $b_l^H = 0$ and the optimal solution to (6), $\vec{b}^F = \vec{b}^H$.

2. There exists a single station, denoted by $\hat{l}$ such that $0 < b^H_{\hat{l}} < m_{\hat{l}}$. For every other station $l \neq \hat{l}$, either $b^H_l \geq m_l$ or $b^H_l = 0$. In this case:
   (a) The optimal value of F is bounded above by $H(t, \vec{b}^H)$.
   (b) The distance from optimum is bounded by $\frac{\lambda_{\hat{l}}}{\lambda}\left(H_{\hat{l}}(t, b^H_{\hat{l}}) - F_{\hat{l}}(t, b^H_{\hat{l}})\right)$.

4 NUMERICAL APPLICATION

The US-based corporation Better Place was founded in 2007 with the ambitious goal of a large-scale adoption of fully electric cars. Since battery-related issues are the greatest obstacle to achieving this goal, Better Place developed a unique business model in which it retained battery ownership. Customers were to purchase the car absent the battery and Better Place was to provide battery swapping and recharging services and to assume all the battery-related risks (Dijk et al., 2013).

Although Better Place has filed for bankruptcy in 2013, its business model is still considered a promising solution to solving the battery problem in the electric car industry (Avci et al., 2014). Most of the cars produced for Better Place's customers were sold in Israel, in which Better Place even completed the construction of fifty battery swapping stations before it filed for bankruptcy. The following section is a hypothetical full scale application of the Better Place model in a country with geographical and demographical characteristics similar to Israel.

Each of the three largest gas companies in Israel operate approximately two hundred fifty gas stations and accordingly we assume that the battery service firm ("the firm") operates a network of two hundred fifty battery swapping stations distributed throughout the country, with a total arrival of approximately 14,000 customers per hour. The population density in Israel is such that the center region is the densest, followed by the northern region. The south of Israel, which constitutes more than half of Israel's land area, is sparsely populated. Therefore, the number of stations per customer in the south is higher than the number of stations in the center, reflecting the large geographical size that must be serviced. To model the differences between the different stations in Israel, as well as differences between small neighborhood stations and busy major stations we assume that the arrival rates to the stations are equally spaced between 6.4 and 106 customers per hour.

An empty battery can be recharged to 50% of capacity within twenty minutes (Bullis, 2013). Since there are many factors that affect recharging time we assume that the recharging time is distributed normally with mean forty minutes and standard deviation ten minutes. Battery swapping time, i.e., the battery removal and battery installation, is considerably shorter than recharging time and with state-of-the-art design, battery swapping can be done in less than two minutes (Mak et al., 2013). Each station is assumed to have ample battery rechargers since recharging docks are relatively inexpensive. Since the electric vehicle cars are poised as an alternative to the traditional gasoline-fueled cars, we assume that the tolerable wait for refueling is similar for both cars. Anecdotal evidence suggests that a ten minute wait for battery swapping is tolerated by customers. Finally, we use a baseline budget of nine thousand spare batteries.

To summarize, the baseline parameters of the example are: $L = 250$ stations; $N = 9000$ spare batteries; $\lambda_l = 6 + 0.4 \cdot l$ customers per hour, $t_1 + t_2 = 2$ minutes, $R_l \sim Normal(40, 10^2)$ minutes and the optimization criterion is the window fill rate for a tolerable wait $t = 10$ minutes($F10$).

4.1 The Baseline Scenario

Figure 2 describes the near-optimal spare allocation for the baseline case, $\vec{b}^H$, and Figure 3 displays the window fill rate for the optimal allocation as a function of t, $F(\vec{b}^H, t)$. Recall, that the optimization algorithm supplies spares to the station with the steepest slope until it reaches its tangent point and only then proceeds to the next station. The tangent line's slope and the tangent point are increasing with the arrival rate and therefore the bigger the station index, the greater the tangent point. The near-optimal allocation dictates that the 50 slowest-moving stations will have no spares, whereas each of the busier stations will receive at least its tangent point. Station 51 is the exception; it has only two spares although its tangent point is 19 (see case 1 of Result 3). This implies that the solution $F(\vec{b}^H, 10) = 88.5\%$ is a lower bound that it not necessarily optimal. However, the distance between the bounds is a mere 0.02% (see notes to Table 1).

The low arrival rate stations are not given any spares and consequently, their window fill rate is almost zero. To compensate customers for the longer wait, the system's managers could offer customers, for example, discounted meals or drinks. Behavioral research about customer waiting experience may be used to incentivize customers to agree to longer than usual waiting times (Maister, 1985).

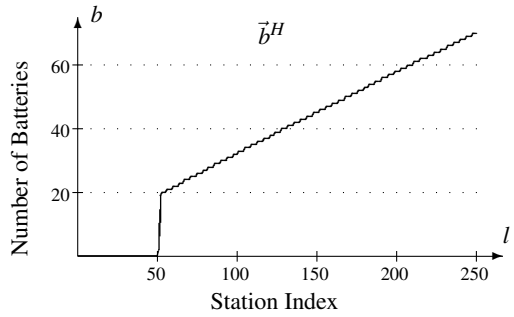

Figure 2: The spare battery allocation for the baseline case.

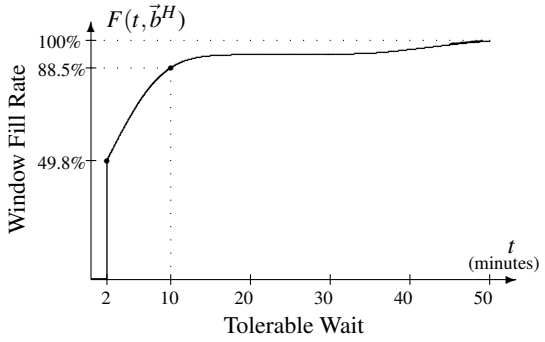

Figure 3: The window fill rate as a function of t for the baseline optimal allocation.

4.2 The Effect of the Tolerable Wait

Table 1 details performance statistics for the baseline criterion, $F10$, and three other optimization criteria; the window fill rate for tolerable waits of two ($F2$), five ($F5$) and fifteen ($F15$) minutes. For the performance statistics, we use the same measures that we use for the optimality criteria, i.e., the window fill rates for two, five, ten and fifteen minutes. We see that different criteria lead to significantly different optimal values of the objective function. As is discussed below, the near-optimal spare allocations also differ dramatically. These observations stress the importance of defining the criterion for optimality correctly. For example, if the firm optimizes $F2$ instead of the "correct" criterion $F10$, then the percentage of satisfied customers (i.e., customers who were serviced within ten minutes) decreases from 88.5% to 77.5%. Similarly, if the firm errs to the other side and optimizes $F15$ then the percent of satisfied customers decreases from 88.5% to 84.9%.

Figure 4 compares the near-optimal allocations for three different criteria, $F2$, $F10$ and $F15$. When $t = 15$, the tangent points are appreciably less than the baseline case and therefore the 9000 batteries are enough to supply all the stations with their tangent points. At this point, all the stations are in their con-

Table 1: The network's performance for different optimization criteria.

		Performance Statistic			
		$F2$	$F5$	$F10$	$F15$
Criterion	$F2$	73.5%[1]	76.5%	77.5%	77.6%
	$F5$	70.6%	78.6%[2]	82.8%	83.2%
	$F10$	49.8%	68.5%	88.5%[3]	93.5%
	$F15$	35.0%	54.2%	84.9%	97.9%[4]

Notes:
[1] Lower bound displayed. The distance between bounds is 0.12%.
[2] Lower bound displayed. The distance between bounds is 0.05%.
[3] Lower bound displayed. The distance between bounds is 0.02%.
[4] Optimal value displayed.

cave region and the residual batteries are distributed among all the stations. Conversely, when $t = 2$ the tangent points are higher than in the baseline case. Now, the busy stations will demand more batteries to reach their tangent point and so the budget is depleted after allocating spares to fewer stations compared to the baseline case.

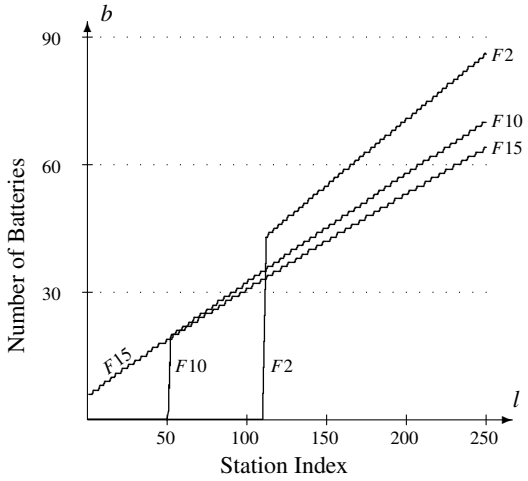

Figure 4: The spare battery allocation for different optimization criteria.

4.3 The Budget Effect

Figure 5 describes the near-optimal spare allocation for the baseline case and for spare budgets of 7000 and 11000 batteries. In the baseline scenario, the number of spare batteries in the network is 9000. If we increase the budget then the lower-rate stations will receive batteries one by one according to their tangent point. Eventually, all the stations will reach their tangent point. Now, any additional batteries will be distributed among all the stations instead of given to only particular stations. In contrast, if the budget is decreased then some slowest-moving stations will forfeit all their batteries. The busiest stations, how-

ever, will lose at most the few (if any) batteries they received beyond their tangent point.

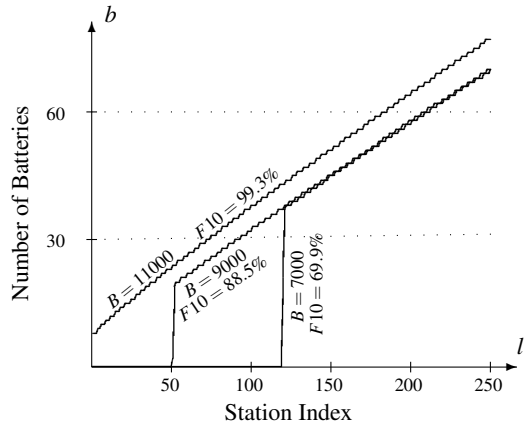

Figure 5: The window fill rate and spare battery allocation for different values of B.

4.4 The Swapping Time Effect

A corollary of Proposition 1 is that a $+\Delta$ change to the swapping time, t_1+t_2 is equivalent to a $-\Delta$ change to the tolerable wait, t. Figure 6 shows how the near-optimal allocation changes with the swapping time. As the swapping time increases, the tangent points increase too and therefore the busiest stations require more spares. As a consequence, more and more slow-moving stations will remain with zero spares.

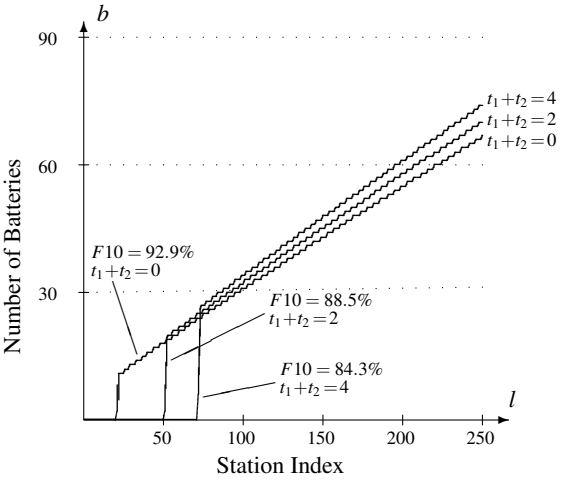

Figure 6: The spare battery allocation for different battery swapping times.

Thus far, we assume that the budget of spares is fixed. Consider, now the dual problem of (6).

$$\min_{\vec{b}\geq 0} \sum_{l=1}^{L} b_l \quad s.t. \quad F(t,\vec{b}) \geq \alpha. \tag{8}$$

where α is the network's required performance.

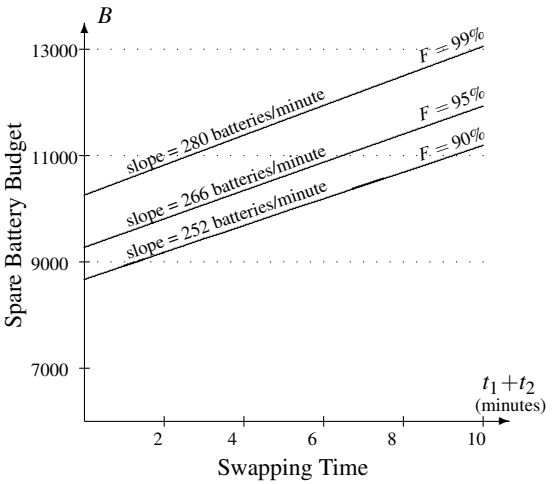

Figure 7: The spares budget for different performance target levels.

We may easily solve (8) using the optimization algorithm. The allocation of spares is done in an identical manner, but now the stopping condition is that we have reached the required level of service. Figure 7 displays the budget required to reach a 90%, 95% and 99% window fill rates for different swapping times. The slope of the graph reveals the savings obtained by reducing swapping time. For the performance levels of 90%, 95% and 99% the graph is almost linear and a minute reduction in the swapping time saves the network approximately 252, 266 and 280 batteries, respectively.

4.5 Optimizing Total Inventory Costs

The problems (6) and (8) assume that either the budget or the service level is predetermined. We now consider the problem of minimizing the total inventory costs. Let c_B denote the cost of a battery and let c_p denote the penalty cost each time a customer is not served within the tolerable wait. Since batteries have a limited lifetime, T, the planning horizon is T and the total number of customers arriving into the network during the planning horizon is λT where, recall, $\lambda = \sum \lambda_l$. The problem is given by

$$\min_{\vec{b}\geq 0} TC(\vec{b}) := c_b \sum_{l=1}^{L} b_l \; + \; c_p \lambda T \left(1 - F(t,\vec{b})\right). \tag{9}$$

We can easily adjust the optimization algorithm to find the optimal solution to (9). Each time we consider adding a battery we measure its contribution to the window fill rate, δ. As long as $\delta c_p \lambda T \geq c_b$ we increase the number of batteries in the network.

Batteries for family sized electric vehicles range between 20kWH and 80kWH with current prices reaching as low as US$200 per-kWh (Sarker et al., 2015). We therefore examine battery prices of up to US$25,000. We conservatively estimate battery life to be four years, and since we assume 12 daily hours of operation $T = 17520$ hours (Arcus, 2016). Finally, the arrival rate to the network is the sum of the arrivals to all the stations, $\lambda = 14,050$ per hour.

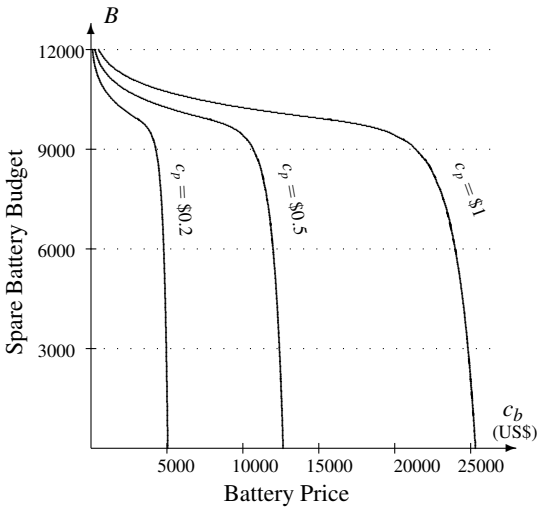

Figure 8: Spares Budget for different penalty costs and battery price.

In Figure 8 we depict the near-optimal spares budget depending on battery prices for different penalty costs. Interestingly, the budget may be very sensitive or very insensitive to battery prices. For example, when the penalty is $1, then in the battery price range of $3261 and $21378 then budget size will only change between 11000 and 9000 batteries. In stark contrast, if the price increases from $21378 to only $25321, then the optimal budget will decrease from 9000 to 0 batteries.

5 CONCLUSIONS

In this paper, we suggest a model to solve the spare battery allocation problem. Since customers will tolerate a certain wait when they enter the station we claim that to minimize its penalty costs the network should maximize the fraction of customers who are served within the tolerable wait, the window fill rate.

We show that the relationship between the window fill rate when item removal and installment times are positive to the window fill rate with zero removal and installment times. Using this relationship, we build on (Dreyfuss and Giat, 2016) to solve our problem. To illustrate the application of the model we estimate a hypothetical application of a full-scale battery swapping network in Israel, similar to the network envisioned by the Better Place corporation. Our numerical analysis of the problem reveals interesting findings such as the value of better battery swapping design, the creation of different classes of stations and the critical importance of estimating the tolerable wait correctly.

The model assumes that battery swapping time is deterministic and that the customer arrival rate is constant over time. While the first assumption is reasonable, the second assumption is clearly unrealistic. We leave addressing these issues to future research.

REFERENCES

Arcus, C. (2016). Plug-in electric vehicle market penetration and incentives: a global review. *CleanTechnica*. [online] Available at: https://cleantechnica.com/2016/05/31/battery-lifetime-long-can-electric-vehicle-batteries-last/ [Accessed 22 Sep. 2016].

Avci, B., Girotra, K., and Netessine, S. (2014). Electric vehicles with a battery switching station: Adoption and environmental impact. *Management Science*, 61(4):772–794.

Basten, R. and van Houtum, G. (2014). System-oriented inventory models for spare parts. *Surveys in Operations Research and Management Science*, 19(1):34–55.

Berg, M. and Posner, M. (1990). Customer delay in M/G/∞ repair systems with spares. *Operations Research*, 38(2):344–348.

Bullis, K. (2013). Forget battery swapping: Tesla aims to charge electric cars in five minutes. *MIT Technology Review*. [online] Available at: http://www.technologyreview.com/news/516876/forget-battery-swapping-tesla-aims-to-charge-electric-cars-in-five-minutes/ [Accessed 22 Sep. 2016].

Caggiano, K., Jackson, L., Muckstadt, A., and Rappold, A. (2007). Optimizing service parts inventory in a multi-echelon, multi-item supply chain with time-based customer service-level agreements. *Operations Research*, 55(2):303–318.

Caggiano, K., Jackson, L., Muckstadt, A., and Rappold, A. (2009). Efficient computation of time-based customer service levels in a multi-item, multi-echelon supply chain: A practical approach for inventory optimization. *European Journal of Operational Research*, 199(3):744–749.

Coffman, M., Bernstein, P., and Wee, S. (2016). Electric vehicles revisited: a review of factors that affect adoption. *Transport Review*, forthcoming.

Demoulin, N. and Djelassi, S. (2013). Customer responses to waits for online banking service delivery. *International Journal of Retail & Distribution Management*, 41(6):442–460.

Dijk, M., Orsato, R., and Kemp, R. (2013). The emergence of an electric mobility trajectory. *Energy Policy*, 52:135–145.

Dreyfuss, M. and Giat, Y. (2016). Optimal spares allocation in an exchangeable-item repair system with tolerable wait. Working Paper, Jerusalem College of Technology.

Durrande-Moreau, A. (1999). Waiting for service: ten years of empirical research. *International Journal of Service Industry Management*, 10(2):171–189.

Katz, K., Larson, B., and Larson, R. (1991). Prescriptions for the waiting in line blues: entertain, enlighten and engage. *Sloan Management Review*, (Winter):44–53.

Maister, D. (1985). The psychology of waiting lines. In Czepiel, J., Solomon, M., and Heath, C. S. D., editors, *The Service Encounter*, pages 113–123. Lexington Books, Lanham, 2nd edition.

Mak, H., Rong, Y., and Shen, Z. (2013). Infrastructure planning for electric vehicles with battery swapping. *Management Science*, 59(7):1557–1575.

Ross, S. (1981). *Introduction to probability models*. Academic Press, NY, 2nd edition.

Sarker, M., Hrvoje, P., and Ortega-Vazquez, M. (2015). Optimal operation and services scheduling for an electric vehicle battery swapping station. *IEEE Transactions on Power Systems*, 30(2):901–910.

Shtub, A. and Simon, M. (1994). Determination of reorder points for spare parts in a two-echelon inventory system: The case of non-identical maintenance facilities. *European journal of operational research*, 73(3):458–464.

Smidts, A. and Pruyn, A. (1999). How waiting affects customer satisfaction with service: the role of subjective variables. In *Proceedings of the 3rd International Research Seminar in Service Management*, pages 678–696. Universite d'Aix-Marseille.

Yang, J. and Sun, H. (2015). Battery swap station location-routing problem with capacitated electric vehicles. *Computers & Operations Research*, 55:217–232.

Zhou, Y., Wang, M., Hao, H., Johnson, L., and Wang, H. (2015). Plug-in electric vehicle market penetration and incentives: a global review. *Mitigation and Adaptation Strategies for Global Change*, 20(5):777–795.

Optimal Price Reaction Strategies in the Presence of Active and Passive Competitors

Rainer Schlosser and Martin Boissier
Hasso Plattner Institute, University of Potsdam, Potsdam, Germany
{*rainer.schlosser, martin.boissier*}*@hpi.de*

Keywords: Dynamic Pricing, Competition, Optimal Control, Response Strategies, Reaction Time, Price Cycles.

Abstract: Many markets are characterized by pricing competition. Typically, competitors are involved that adjust their prices in response to other competitors with different frequencies. We analyze stochastic dynamic pricing models under competition for the sale of durable goods. Given a competitor's pricing strategy, we show how to derive optimal response strategies that take the anticipated competitor's price adjustments into account. We study resulting price cycles and the associated expected long-term profits. We show that reaction frequencies have a major impact on a strategy's performance. In order not to act predictable our model also allows to include randomized reaction times. Additionally, we study to which extent optimal response strategies of active competitors are affected by additional passive competitors that use constant prices. It turns out that optimized feedback strategies effectively avoid a decline in price. They help to gain profits, especially, when aggressive competitors are involved.

1 INTRODUCTION

In many markets, firms have to deal with competition and stochastic demand. Sellers are required to choose appropriate pricing decisions to maximize their expected profits. In E-commerce, it has become easy to observe and to change prices. Hence, dynamic pricing strategies that take the competitors' strategies into account will be used increasingly. However, optimal price reactions are not easy to find. While some market participants use mostly constant prices others use automated price adjustment strategies. Applications can be found in a variety of contexts that involve perishable (e.g., fashion goods, seasonal products, event tickets) as well as durable goods (e.g., books, natural resources, gasoline). In many markets, it can be observed, that the application of response strategies typically leads to cyclic price patterns over time, cf. Edgeworth cycles, see, e.g., Maskin, Tirole (1988), Noel (2007). We want to explain such effects from a theoretical perspective.

In this paper, we study oligopoly pricing models in a stochastic dynamic framework. In our model, the sales probabilities are allowed to be an arbitrary function of time and the competitors' prices. Our aim is to take into account (i) various competitors' strategies, (ii) different (randomized) reaction times, and (iii) additional passive competitors that use constant prices.

Selling products is a classical application of revenue management theory. The problem is closely related to the field of dynamic pricing, which is summarized in the books by Talluri, van Ryzin (2004), Phillips (2005), and Yeoman, McMahon-Beattie (2011). The survey by Chen, Chen (2015) provides an excellent overview of recent pricing models under competition.

In the article by Gallego, Wang (2014) the authors consider a continuous time multi-product oligopoly for differentiated perishable goods. They use optimality conditions to reduce the multi-dimensional dynamic pricing problem to a one-dimensional one. Gallego, Hu (2014) analyze structural properties of equilibrium strategies in more general oligopoly models for the sale of perishable products. The solution of their model is based on a deterministic version of the model. Martinez-de-Albeniz, Talluri (2011) consider duopoly and oligopoly pricing models for identical products. They use a general stochastic counting process to model customer's demand.

Further related models are studied by Yang, Xia (2013) and Wu, Wu (2015). Dynamic pricing models under competition that also include strategic customers are analyzed by Levin et al. (2009) and Liu, Zhang (2013). Dynamic pricing competition models with limited demand information are analyzed by Tsai, Hung (2009), Adida, Perakis (2010) and Chung

Schlosser, R. and Boissier, M.
Optimal Price Reaction Strategies in the Presence of Active and Passive Competitors.
In *Proceedings of the 6th International Conference on Operations Research and Enterprise Systems (ICORES 2017)*, pages 47-56
ISBN: 978-989-758-218-9

et al. (2012) using robust optimization and learning approaches. Many models consider continuous time models with finite horizon and limited inventory. In most existing models, discounting is not included and the demand is assumed to be of a special functional form. We consider infinite horizon models with unlimited inventory (i.e., products can be reproduced or reordered). Demand is allowed to depend generally on time as well as the prices of all market participants.

While many publications concentrate on (the existence of) equilibrium strategies, we do not assume that all market participants act rationally. In many markets it can be observed that automated strategies that are used by firms are relatively simple and aggressive. The most common strategy is to slightly undercut the competitor's price, cf. Kephart et al. (2000). In order to be able to respond to various potentially suboptimal pricing strategies we provide applicable solution algorithms that allow to compute optimal response strategies.

The main contribution of this paper is threefold. We (i) derive optimal price response strategies that anticipate competitors' prices, (ii) we quantify the impact of different (randomized) reaction times on expected long-term profits of all market participants, and (iii) we are able to explain different types of price cycles.

This paper is organized as follows. In Section 2, we describe the stochastic dynamic oligopoly model with infinite time horizon (durable goods). We allow sales probabilities to depend on competitor prices as well as on time (seasonal effects). The state space is characterized by time and the actual competitors' prices. The stochastic dynamic control problem is expressed in discrete time. In Section 3, we consider a duopoly competition. The competitor is assumed to frequently adjust its prices using a predetermined strategy. We assume that the price reactions of competitors as well as their reaction times can be anticipated. We set up a firm's Hamilton-Jacobi-Bellman equation and use recursive methods (value iteration) to approximate the value function. We are able to compute optimal feedback prices as well as expected long-term profits of the two competing firms. Evaluating price paths over time, we are able to explain specific price cycles. Furthermore, the results obtained are generalized to scenarios with randomized reaction times and mixed strategies.

In Section 4, we analyze optimal response strategies in the presence of active and passive competitors. We study how the duopoly game of two active competitors is affected by additional passive competitors. We show how to compute optimal pricing strategies and to evaluate expected profits. We also illustrate how the cyclic price paths of the active competitors are affected by different price levels of passive competitors. Finally, we evaluate the expected profits when different strategies are played against each other. Conclusions and managerial recommendations are offered in final Section 5.

2 MODEL DESCRIPTION

We consider the situation where a firm wants to sell goods (e.g., gasoline, groceries, technical devices) on a digital market platform (e.g., Amazon, eBay). We assume that several sellers compete for the same market, i.e., customers are able to compare prices of different competitors.

We assume that the time horizon is infinite. We assume that firms are able to reproduce or reorder products (promise to deliver), and the ordering is decoupled from pricing decisions. If a sale takes place, shipping costs c have to be paid, $c \geq 0$. A sale of one item at price a, $a \geq 0$, leads to a net profit of $a - c$. Discounting is also included in the model. For the length of one period, we will use the discount factor δ, $0 < \delta < 1$.

Since in many practical applications prices cannot be continuously adjusted, we consider a discrete time model. The sales intensity of our product is denoted by λ. Due to customer choice, the sales intensity will particularly depend on our offer price a and the competitors' prices. We also allow the sales intensity to depend on time, e.g., the time of the day or the week. We assume that the time dependence is periodic and has an integer cycle length of J periods. In our model, the sales intensity λ is a general function of time, our offer price a and the competitors' prices $\vec{p}$. Given the prices a and $\vec{p}$ in period t, the jump intensity λ satisfies, $t = 0, 1, 2, ...$, $a \geq 0$, $\vec{p} \geq \vec{0}$,

$$\lambda_t(a, \vec{p}) = \lambda_{t \bmod J}(a, \vec{p}). \tag{1}$$

In our discrete time model, we assume the sales probabilities (for one period) to be Poisson distributed. I.e., the probability to sell exactly i items within one period of time is given by, $t = 0, 1, 2, ...$, $a \geq 0$, $\vec{p} \geq \vec{0}$, $i = 0, 1, 2, ...$,

$$P_t(i, a, \vec{p}) = \frac{\lambda_t(a, \vec{p})^i}{i!} \cdot e^{-\lambda_t(a, \vec{p})}. \tag{2}$$

For each period t, a price a has to be chosen. We call strategies $(a_t)_t$ admissible if they belong to the class of Markovian feedback policies; i.e., pricing decisions $a_t \geq 0$ may depend on time t and the current

prices of the competitors. By A we denote the set of admissible prices. A list of variables and parameters is given in the Appendix, cf. 3.

By X_t we denote the random number of sales in period t. Depending on the chosen pricing strategy $(a_t)_t$, the random accumulated profit from time/period t on (discounted on time t) amounts to, $t = 0,1,2,...,$

$$G_t := \sum_{s=t}^{\infty} \delta^{s-t} \cdot (a_s - c) \cdot X_s. \tag{3}$$

The objective is to determine a non-anticipating (Markovian) pricing policy that maximizes the expected total profit $E(G_0)$.

In the following sections, we will solve dynamic pricing problems that are related to (1) - (3). In the next section, we study a duopoly situation. We assume that the competitor frequently adjusts his/her prices and show how to derive optimal response strategies. We analyze the impact of different reaction times as well as randomized reaction times. We also consider the case in which the competitor plays mixed strategies. In Section 4, we compute pricing strategies for oligopoly scenarios with active and passive competitors.

3 OPTIMAL REACTION STRATEGIES IN A DUOPOLY

3.1 Fixed Reaction Times

In some applications, sellers are able to anticipate transitions of the market situation. Such information can be used to optimize expected profits. In particular, the price responses of competitors as well as their reaction time can be taken into account. In this case, a change of the market situation $\vec{p}$ can take place within a period. A typical scenario is that a competitor adjusts its price in response to our price with a certain delay. In this section, we assume that the pricing strategy and the reaction time of the competitor is known; i.e., we assume that choosing a price a at time t is followed by a state transition (e.g., a competitor's price reaction) and the current market situation $\vec{p}$ changes to a subsequent state described by a transition function F, which can depend on $\vec{p}$ and a.

In the following, we want to derive optimal price response strategies to a given competitor's strategy. For simplicity, we consider the sale of one type of product in a duopoly situation. We assume that the state of the system (the market situation) is one-dimensional and simply characterized by the competitor's price p, i.e., we let $\vec{p} := p$.

In real-life applications, a firm is not able to adjust its prices immediately after the price reaction of the competing firm. Hence, we assume that in each period the price reaction of the competing firm takes place with a delay of h periods, $h < 1$. I.e., after an interval of size h the competitor adjusts its price from p to $F(a)$, see Figure 1.

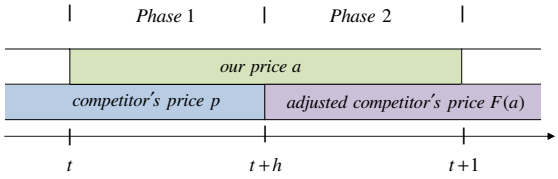

Figure 1: Sequence of price reactions in case of a duopoly.

Thus in period t, the probability to sell exactly i items during the first interval of size h is $P_t^{(h)}(i,a,p) := Pois(h \cdot \lambda_t(a,p))$, while for the rest of the period the sales probability changes to $P_t^{(1-h)}(i,a,F(a)) = Pois((1-h) \cdot \lambda_t(a,F(a)))$.

We will use value iteration to approximate the value function, which represents the present value of future profits. For a given "large" number T, $T \gg J$, we let $V_T(p) = 0$ for all p, and compute, $t = 0,1,2,...,T-1$, $0 < h < 1$, $p \in A$,

$$\begin{aligned} V_t(p) = \max_{a \in A} \Big\{ & \sum_{i_1 \geq 0} P_t^{(h)}(i_1,a,p) \\ & \cdot \sum_{i_2 \geq 0} P_{t+h}^{(1-h)}(i_2,a,F(a)) \\ & \cdot \big((a-c) \cdot (i_1+i_2) + \delta \cdot V_{t+1}(F(a))\big) \Big\}. \end{aligned} \tag{4}$$

The associated pricing strategy $a_t^*(p)$, $t = 0,1,2,...,J-1$, $p \in A$, is determined by the argmax of

$$\begin{aligned} a_t^*(p) = \arg\max_{a \in A} \Big\{ & \sum_{i_1 \geq 0} P_t^{(h)}(i_1,a,p) \\ & \cdot \sum_{i_2 \geq 0} P_{t+h}^{(1-h)}(i_2,a,F(a)) \\ & \cdot \big((a-c) \cdot (i_1+i_2) + \delta \cdot V_{t+1}(F(a))\big) \Big\}. \end{aligned} \tag{5}$$

In case $a_t^*(p)$ is not unique, we choose the largest one.

Remark 3.1. Our recursive solution approach also allows to solve problems with perishable products and finite horizons T. Equations (4)-(5) just have to be evaluated for all $t = 0,1,2,...,T-1$.

To illustrate our approach we will consider a numerical example for durable goods. We assume that the competitor applies one of the most common strategies: the competitor undercuts our current price by ε down to a certain minimum (e.g., the shipping costs c). The sales dynamics of the following example above are based on a large data set from the Amazon market for used books, see Schlosser et al. (2016).

Definition 3.1. We define the sales probabilities $P_t^{(h)}(i,a,p) := Pois\left(h \cdot e^{\vec{x}(a,p)'\vec{\beta}}/(1+e^{\vec{x}(a,p)'\vec{\beta}})\right)$, using linear combinations of the following five regressors $\vec{x} = \vec{x}(a,p)$ given coefficients $\vec{\beta} = (\beta_1,...,\beta_5)$:

(i) constant / intercept

$$x_1(a,p) = 1$$

(ii) rank of price a compared to price p

$$x_2(a,p) = 1 + \left(1_{\{p<a\}} + 1_{\{p\leq a\}}\right)/2$$

(iii) price gap between price a and price p

$$x_3(a,p) = a - p$$

(iv) total number of competitors

$$x_4(a,p) = 1$$

(v) average price level

$$x_5(a,p) = (a+p)/2$$

Example 3.1. We assume a duopoly. Let $c = 3$, $\delta = 0.99$, $0 \leq h \leq 1$, and let $F(a) := \max(a-\varepsilon, c)$, ε=1, $a \in A := \{1,2,...,100\}$. For the computation of the value function, we let $T := 1000$. We assume the sales probabilities $P_t^{(h)}(\cdot,a,p)$, see Definition 3.1, where $\vec{\beta} = (-3.89,-0.56,-0.01,0.07,-0.02)$.

Figure 2a and Figure 3a show optimal response strategies for different reaction times h=0.1 and h=0.9. The case $h = 0.1$ illustrates a fast reaction time of the competitor; $h = 0.9$ represents a slow reaction of the competitor. If $h = 0.5$ both competing firms react equally fast. In all three cases the optimal response strategy are of similar shape. If the competitor's price is either very low or very large, it is optimal to set the price to a certain moderate level. If the competitor's price is somewhere in between (intermediate range), it is best to undercut that price by one price unit ε. If h is larger, the upper price level is increasing and the intermediate range is bigger.

The application of optimal response strategies leads to cyclic price patterns over time, cf. Edgeworth cycles, see, e.g., Maskin, Tirole (1988), Kephart et al.

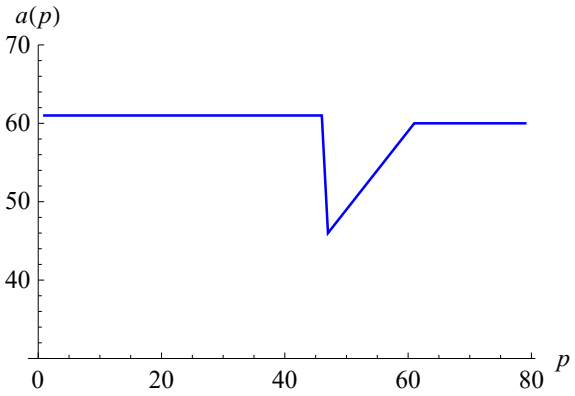

(a) Optimal response policy.

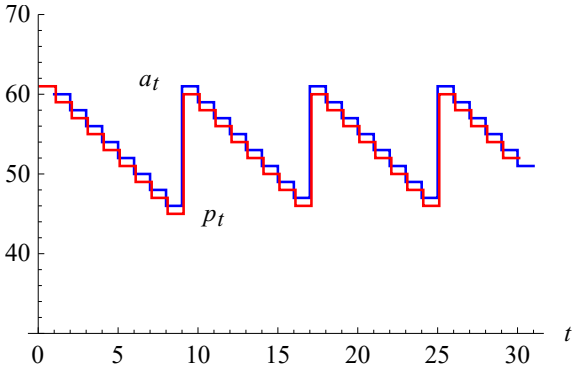

(b) Evaluated price paths over time.

Figure 2: Optimal response policy and price paths for Example 3.1 with $h = 0.1$.

(2000), or Noel (2007). The resulting price paths are shown in Figure 2b and Figure 3b. If the reaction time of the competitor is longer, we observe that the cycle length and the amplitude of the price patterns are increasing. Note, roughly $h \cdot 100\%$ of the time our firm is offering the lowest price; i.e., the parameter h can also be used to model situations in which one firm is able to adjust its prices more often than another firm.

In addition, we are able to analyze the impact of the reaction time on expected long-term profits of our firm as well as the competitor. We assume that the competitor faces the same sales probabilities and shipping costs as we do. The competitor's expected profits can be recursively evaluated by, cf. (4), $t = 0,1,2,...,T-1$, $0 < h < 1$, $a \in A$, $V_{T+h}^{(c)}(a) = 0$,

$$V_{t+h}^{(c)}(a) = \sum_{i_2 \geq 0} P_{t+h}^{(1-h)}(i_2, F(a), a) \cdot \sum_{i_1 \geq 0} P_{t+1}^{(h)}\left(i_1, F(a), a_{t+1 \bmod J}^*(F(a))\right) \cdot \left((F(a)-c)\cdot(i_1+i_2) + \delta \cdot V_{t+h+1}^{(c)}\left(a_{t+1 \bmod J}^*(F(a))\right)\right). \quad (6)$$

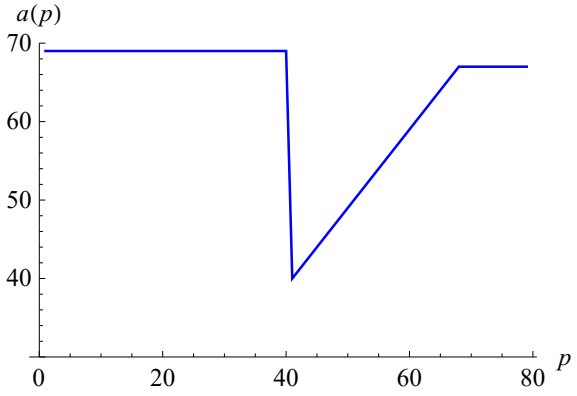

(a) Optimal response policy.

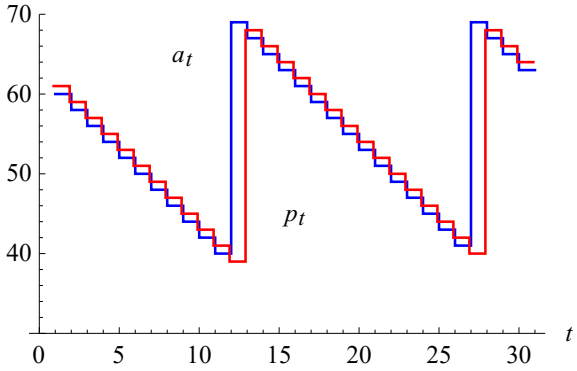

(b) Evaluated price paths over time.

Figure 3: Optimal response policy and price paths for Example 3.1 with $h = 0.9$.

Due to the cyclic price paths, the expected future profits $V_0(p)$ and $V_h^{(c)}(a)$ are (almost) independent of the initial states/prices. Figure 4 depicts V as well as the competitor's expected profits $V^{(c)}$ as a function of h. We observe that the expected profit V is linear increasing in the competitor's reaction time; the competitor's profit $V^{(c)}$ is decreasing in h. Note, the impact of h is substantial. The disadvantage of the player that stops the undercutting phase can already be compensated if our reaction time is smaller than 0.46, i.e., if h exceeds the value 0.54.

3.2 Randomized Reaction Times

Due to the significant impact of reaction times, firms will try to minimize their reaction times by anticipating their competitor's time of adjustment. In order not to act predictable, firms will randomize their reaction times. Moreover, firms will try to gain advantage by updating their prices more frequently.

In case the reaction time is not deterministic, the model can be adjusted. If the distribution of the reaction time of competitors is known, the Hamilton-Jacobi-Bellman (HJB) equation, cf. (4), can be modified. The different reaction scenarios just have to be considered with the corresponding probability. Note, the reaction times of different competitors can be observed in the long run.

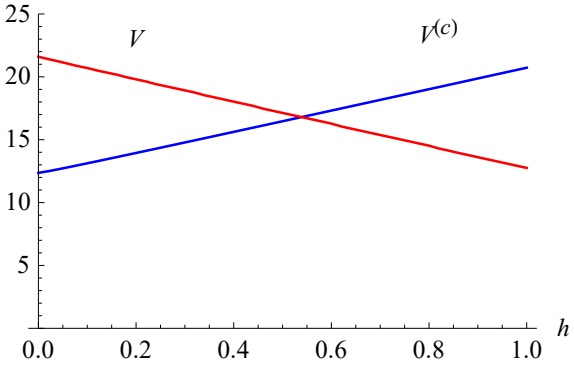

Figure 4: Expected profit for different reaction times of the competitor; Example 3.1.

Strategic firms will try to optimally time their price adjustments. In order not to act predictable, firms might use randomized strategies. In the following, we consider such a scenario. We assume that each firm adjusts its price with a certain intensity (e.g., on average once a period of size 1). We model that approach as follows: we assume that at each point in time d, $d = t+\Delta, t+2\Delta, ..., t+1$, $0 < \Delta \ll 1$, our firm adjusts its price with probability q, $0 < q \ll 1$; i.e., on average we adjust our price q/Δ times a period of size 1. Similarly, the competitor adjusts its price with probability $q^{(c)}$, $0 < q^{(c)} \ll 1$.

The competitor applies a certain strategy $F(a)$. By a^- we denote our current price at time d, the beginning of the sub-period $(d, d+\Delta)$. With probability $q^{(c)}$, the competitor adjusts its price from p to $F(a^-)$. With probability q, we adjust the price a^- to price a. Since q and $q^{(c)}$ are assumed to be "small" we do not consider the case in which both firms adjust their prices at the same time. The related value function is given by, $a^-, p \in A$, $t = 0, \Delta, 2\Delta, ..., T-\Delta$, $\tilde{V}_T(a^-, p) = 0$,

$$\begin{aligned}
\tilde{V}_t(a^-,p) &= (1-q-q^{(c)}) \\
&\cdot \sum_{i\geq 0} P_t^{(\Delta)}(i,a^-,p) \cdot \Big((a^- - c)\cdot i + \delta^\Delta \cdot \tilde{V}_{t+\Delta}(a^-,p)\Big) \\
&+ q^{(c)} \cdot \sum_{i\geq 0} P_t^{(\Delta)}(i,a^-,F(a^-)) \\
&\cdot \Big((a^- - c)\cdot i + \delta^\Delta \cdot \tilde{V}_{t+\Delta}(a^-,F(a^-))\Big) \\
&+ q \cdot \max_{a\in A} \Bigg\{ \sum_{i\geq 0} P_t^{(\Delta)}(i,a,p) \\
&\cdot \Big((a-c)\cdot i + \delta^\Delta \cdot \tilde{V}_{t+\Delta}(a,p)\Big)\Bigg\}. \qquad (7)
\end{aligned}$$

The optimal price $\tilde{a}_t^*(a^-,p)$, $t=0,\Delta,2\Delta,...,J-\Delta$, is determined by the arg max of (7). The competitor's expected profit corresponds to, $t=0,\Delta,2\Delta,...,T-\Delta$, $\tilde{V}_T^{(c)}(a^-,p)=0$,

$$\begin{aligned}\tilde{V}_t^{(c)}(a^-,p) &= (1-q-q^{(c)})\\ &\cdot\sum_{i\geq 0}P_t^{(\Delta)}(i,p,a^-)\cdot\Big((p-c)\cdot i+\delta^{\Delta}\cdot\tilde{V}_{t+\Delta}^{(c)}(a^-,p)\Big)\\ &+q^{(c)}\cdot\sum_{i\geq 0}P_t^{(\Delta)}(i,F(a^-),a^-)\\ &\cdot\Big((F(a^-)-c)\cdot i+\delta^{\Delta}\cdot\tilde{V}_{t+\Delta}^{(c)}(a^-,F(a^-))\Big)\\ &+q\cdot\sum_{i\geq 0}P_t^{(\Delta)}\left(i,p,\tilde{a}^*_{t \bmod J}(a^-,p)\right)\\ &\cdot\Big((p-c)\cdot i+\delta^{\Delta}\cdot\tilde{V}_{t+\Delta}^{(c)}\left(\tilde{a}^*_{t \bmod J}(a^-,p),p\right)\Big). \quad (8)\end{aligned}$$

Example 3.2. We assume the duopoly setting of Example 3.1. We let $c=3$, $F(a):=\max(a-\varepsilon,c)$, $\varepsilon=1$, $a\in A:=\{1,2,...,100\}$, δ=0.99, Δ=0.1. We use $T:=1000$. We consider different reaction probabilities q and $q^{(c)}$.

1 contains the expected profits $(\tilde{V}\ ,\ \tilde{V}^{(c)})$ of the two competing firms for different reaction probabilities. We observe that $\tilde{V}$ is increasing in q and decreasing in $q^{(c)}$. For $\tilde{V}^{(c)}$ it is the other way around. It turns out, that the ratio $q/q^{(c)}$ of the adjustment frequencies is a critical quantity.

Table 1: Expected profits $\tilde{V}$ and $\tilde{V}^{(c)}$ for different reaction probabilities q, $q^{(c)}=0.05,0.1,0.2$, $\delta=0.99$, $\Delta=0.1$; Example 3.2.

$q^{(c)}\backslash q$	0.05	0.1	0.2
0.05	(16.53, 17.07)	(16.80, 16.81)	(17.01, 16.62)
0.1	(16.26, 17.36)	(16.48, 17.09)	(16.75, 16.84)
0.2	(16.03, 17.59)	(16.22, 17.37)	(16.48, 17.12)

The overall adjustment frequency plays a minor role as long as the ratio $q/q^{(c)}$ is the same. Hence, the expected profits of both firms can be approximated by the profits from the model with deterministic reaction time, cf. Section 3.1, where $h=q/q^{(c)}$, i.e., the percentage of time our firm has the most recent price.

Figure 5b illustrates the (simulated) price paths for the parameter setting of Example 3.2. Figure 5a shows the deterministic case of Example 3.1 for $h=0.5$. We observe that overall the price patterns have similar characteristics. However, in the randomized case, the timing of the price reactions is not predictable. While in the deterministic $h=0.5$ case (cf.

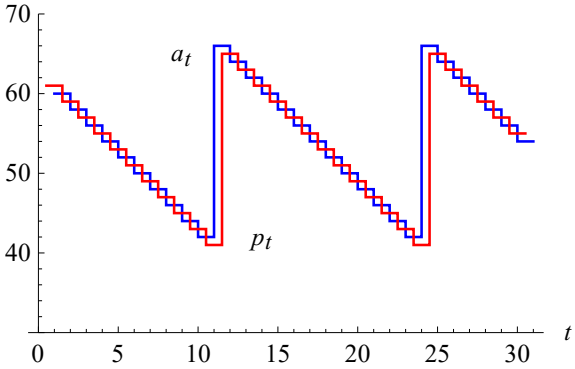

(a) Deterministic reaction times $h=0.5$, Example 3.1.

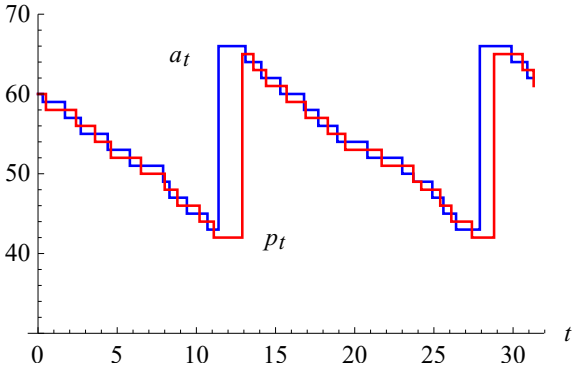

(b) Randomized reaction times for $\Delta=0.1$, $q=q^{(c)}=0.1$; Example 3.2.

Figure 5: Evaluated price paths over time.

Section 3.1) we have $\tilde{V}=16.44$ and $\tilde{V}^{(c)}=17.13$, in the randomized case ($\Delta=0.1$, $q=q^{(c)}=0.1$) the expected profits are $\tilde{V}=16.48$ and $\tilde{V}^{(c)}=17.09$. I.e., in both models the advantage of the aggressive player is basically the same; in the model with randomized reaction times the advantage is slightly smaller.

3.3 Mixed Competitors' Strategies

Our results show that if the competitor's strategy is known, suitable response strategies can be computed. Hence, firms might try to randomize their strategies. In this section, we will analyze scenarios in which competitors play a mixed pricing strategy.

We assume that the competitor plays strategy $F_k(a)$, $a\in A$, with probability π_k, $1\leq k\leq K<\infty$, $\sum_k\pi_k=1$.

We assume deterministic reaction times. We adjust our model, cf. Section 3.1, by using a weighted sum of the potential price reactions. The Hamilton-Jacobi-Bellman (HJB) equation can be written as, $t=0,1,2,...,T-1$, $0<h<1$, $p\in A$,

$$V_t(p) = \max_{a\in A}\Bigg\{\sum_{i_1\geq 0} P_t^{(h)}(i_1,a,p) \cdot\sum_k \pi_k \cdot \sum_{i_2\geq 0} P_{t+h}^{(1-h)}(i_2,a,F_k(a)) \cdot\big((a-c)\cdot(i_1+i_2)+\delta\cdot V_{t+1}(F_k(a))\big)\Big\}, \quad (9)$$

where $V_T(p)=0$ for all p. The associated pricing strategy $a_t^*(p)$, $t=0,1,2,...,J-1$, $0<h<1$, $p\in A$, is determined by the argmax of (9). The resulting competitor's expected profits can be computed by (starting from, e.g., $V_{T+h}^{(c)}(a)=0$), $t=0,1,2,...,T-1$, $0<h<1$, $a\in A$,

$$V_{t+h}^{(c)}(a) = \sum_j \pi_k \cdot \sum_{i_2\geq 0} P_{t+h}^{(1-h)}(i_2,F_k(a),a) \cdot \sum_{i_1\geq 0} P_{t+1}^{(h)}\left(i_1,F_k(a),a_{t+1 \bmod J}^*(F_k(a))\right) \cdot\Big((F_k(a)-c)\cdot(i_1+i_2)+\delta\cdot\tilde{V}_{t+h+1}^{(c)}\left(a_{t+1 \bmod J}^*(F_k(a))\right)\Big). \quad (10)$$

The models described above allow computing suitable pricing strategies in various competitive markets. As long as the number of competing firms is small, the value function and the optimal prices can be computed. Note, due to the coupled state transitions in general the value function has to be computed for all states in advance. When the number of competitors is large this can cause serious problems since the state space can grow exponentially (curse of dimensionality). Hence, the approach is suitable, if the number of competitors is small and their strategies are known. If the number of competitors is large and the firm's strategies are unknown, we recommend using simple but robust strategies, see Schlosser et al. (2016).

4 COMPETITION WITH ACTIVE AND PASSIVE SELLERS

If the pricing strategies and the reaction times of different competitors are known the model can be extended to an oligopoly setting. For each additional competitor the state space of the model has to be extended by one dimension. Note, only active competitors that frequently adjust their prices should be taken into account. Inactive customers will be treated as external fixed effects.

In the following, we assume one active competitor and Z passive competitors. The prices of the passive competitors are denoted by $\vec{z}=(z_1,...,z_Z)$, $z_j\geq 0$, $j=1,...,Z$, and assumed to be constant over time. The active competitor plays a (non-randomized) strategy $F(a)$ that refers to our price a (not the passive one). The Hamilton-Jacobi-Bellman (HJB) equation can be written as, $t=0,1,2,...,T-1$, $0<h<1$, $p\geq 0$, $V_T(p,\vec{z})=0$ for all $p,\vec{z}$,

$$V_t(p,\vec{z}) = \max_{a\in A}\Bigg\{\sum_{i_1\geq 0} P_t^{(h)}(i_1,a,p,\vec{z}) \cdot \sum_{i_2\geq 0} P_{t+h}^{(1-h)}(i_2,a,F(a),\vec{z}) \cdot\big((a-c)\cdot(i_1+i_2)+\delta\cdot V_{t+1}(F(a),\vec{z})\big)\Big\}. \quad (11)$$

The associated pricing strategy amounts to, $t=0,1,2,...,J-1$, $0<h<1$, $p\in A$,

$$a_t^*(p,\vec{z}) = \arg\max_{a\in A}\Bigg\{\sum_{i_1\geq 0} P_t^{(h)}(i_1,a,p,\vec{z}) \cdot \sum_{i_2\geq 0} P_{t+h}^{(1-h)}(i_2,a,F(a),\vec{z}) \cdot\big((a-c)\cdot(i_1+i_2)+\delta\cdot V_{t+1}(F(a),\vec{z})\big)\Big\}. \quad (12)$$

The competitor's profits can be computed by (starting from, e.g., $V_{T+h}(a,\vec{z})=0$ for all $a,\vec{z}$), $t=0,1,2,...,T-1$, $0<h<1$, $a\geq 0$,

$$V_{t+h}^{(c)}(a,\vec{z}) = \sum_{i_2\geq 0} P_{t+h}^{(1-h)}(i_2,F(a),a,\vec{z}) \cdot \sum_{i_1\geq 0} P_{t+1}^{(h)}\left(i_1,F(a),a_{t+1 \bmod J}^*(F(a),\vec{z}),\vec{z}\right) \cdot\Big((F(a)-c)\cdot(i_1+i_2)+\delta\cdot V_{t+h+1}^{(c)}\left(a_{t+1 \bmod J}^*(F(a),\vec{z}),\vec{z}\right)\Big). \quad (13)$$

Note, the value function does not need to be computed for all price combinations of passive competitors in advance. The value function and the associated pricing policy can be computed separately for specific market situations (e.g., just when they occur).

In the following, we consider an example with active and passive competitors.

Example 4.1. We assume the duopoly setting of Example 3.1. We let $F(a):=\max(a-\varepsilon,c)$, $\varepsilon=1$, $c=3$, $h=0.5$, $a\in A:=\{1,2,...,100\}$, $\delta=0.99$, and $T=1000$. Furthermore, we consider an additional passive competitor with the constant price z, $z=15,20,25$.

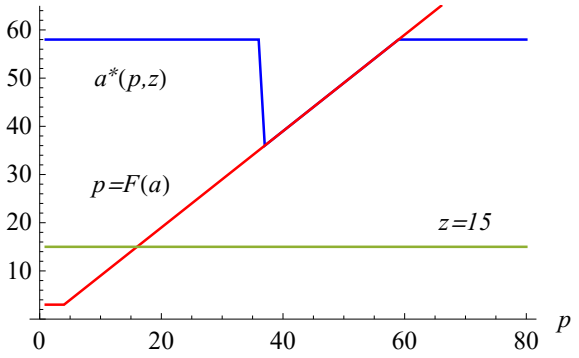

(a) Optimal response strategy.

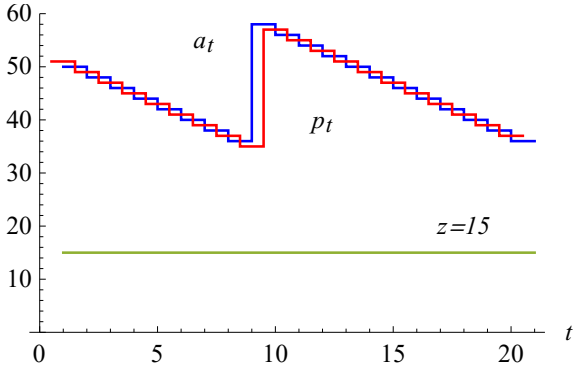

(b) Evaluated price paths over time.

Figure 6: Optimal response strategy and evaluated price paths for Example 4.1; $h = 0.5$, $z = 15$.

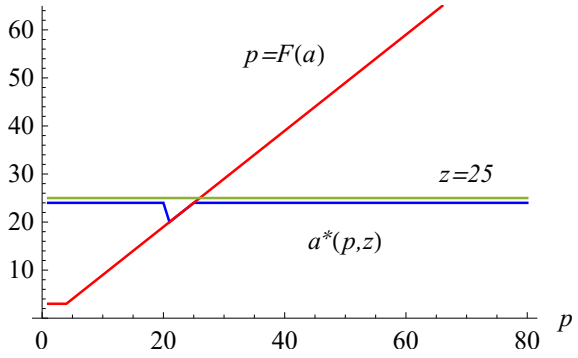

(a) Optimal response strategy.

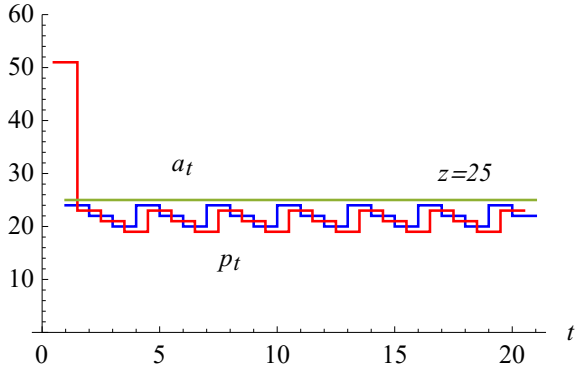

(b) Evaluated price paths over time.

Figure 7: Optimal response strategy and evaluated price paths for Example 4.1; $h = 0.5$, $z = 25$.

The results of the three cases $z = 15$, $z = 20$, and $z = 25$ are illustrated in Figure 6, 7 and 8. We observe three different characteristics. If the passive competitor's price is low ($z = 15$) the cyclic price battle between our firm and the aggressive firm takes place at a higher price level, see Figure 6b. The response strategies of the three firms are displayed in Figure 6a.

If the price of passive firm is sufficiently high ($z = 20$), then the cyclic price paths of the two active firms take place below that level. If the constant price is "moderate" ($z = 20$), then a mixture of the characteristics shown in Figure 6 and 7 is optimal. We also observe that it is not advisable to place price offers that slightly exceed competitors' prices, cf. Figure 8.

At the end of this section, we want to generally evaluate the outcome when different (time homogeneous) strategies are played against each other. We assume time homogeneous demand and $h = 0.5$. If firm 1 plays a pure strategy S_1 and firm 2 plays the pure strategy S_2 then the associated expected profits can be computed by, $t = 0,1,2,...,T-1$, $V_T^{(1)}(a) = V_T^{(2)}(a) = 0$, for all $a \geq 0$,

$$V_t^{(1)}(a) = \sum_{i_1 \geq 0} P^{(0.5)}(i_1, S_1(a), a)$$

$$\cdot \sum_{i_2 \geq 0} P^{(0.5)}(i_2, S_1(a), S_2(S_1(a)))$$

$$\cdot \Big((S_1(a) - c) \cdot (i_1 + i_2) + \delta \cdot V_{t+1}^{(1)}(S_2(S_1(a))) \Big), \tag{14}$$

$$V_t^{(2)}(a) = \sum_{i_1 \geq 0} P^{(0.5)}(i_1, S_2(a), a)$$

$$\cdot \sum_{i_2 \geq 0} P^{(0.5)}(i_2, S_2(a), S_1(S_2(a)))$$

$$\cdot \Big((S_2(a) - c) \cdot (i_1 + i_2) + \delta \cdot V_{t+1}^{(2)}(S_1(S_2(a))) \Big). \tag{15}$$

By S_U we denote the response strategy $F(a) := \max(a - \varepsilon, c)$, which slightly undercuts the competitor's price. By S_{RU} we denote the optimal response strategy to S_U. By S_{RRU} we denote the optimal response strategy to S_{RU}, cf. (11)-(12). Considering Example 4.1 with $z = 20$, the expected profits of the different strategy combinations are summarized in 2.

We observe that the aggressive strategy S_U yields very good results with the exception when the competitor also plays S_U. The strategy S_{RU} yields good results in all three constellations. Strategy S_{RRU} is excellent when played against S_{RU} but yields only mod-

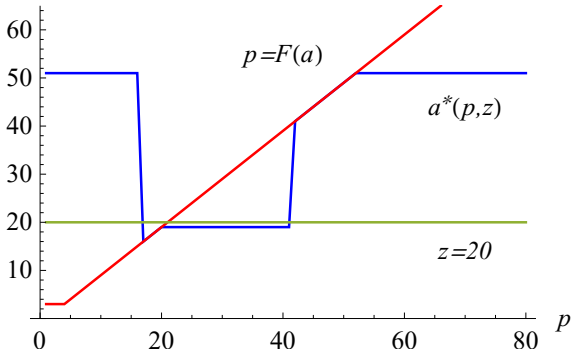

(a) Optimal response strategy.

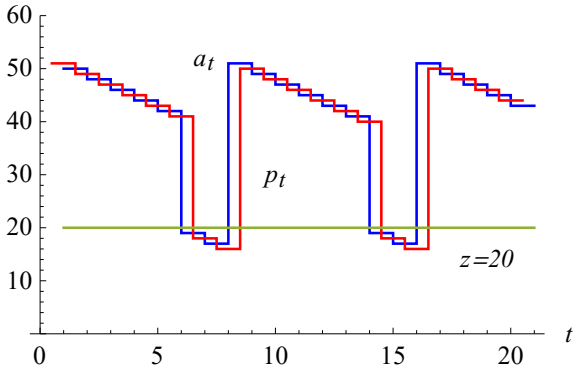

(b) Evaluated price paths over time.

Figure 8: Optimal response strategy and evaluated price paths for Example 4.1; $h = 0.5$, $z = 20$.

Table 2: Expected profits $V_0^{(1)}(50)$ of firm 1 when its strategy $S_1 = \{S_U, S_{RU}, S_{RRU}\}$ is played against a strategy $S_2 = \{S_U, S_{RU}, S_{RRU}\}$, $z = 20$, Example 4.1.

$S_1 \backslash S_2$	S_U	S_{RU}	S_{RRU}
S_U	1.69	9.85	9.91
S_{RU}	9.42	9.66	9.58
S_{RRU}	8.76	10.62	8.76

erate results in the other two cases. For other z values, cf. Example 4.1, the results are similar. Iterating mutual strategy responses further is a way to identify equilibrium strategies.

Finally, our example shows that optimal response strategies have a significant impact on expected profits. They help to gain profits, especially, when aggressive competitors are involved. On the other hand, we learn that it is also important to know the competitors' strategies. In practical applications, the competitors' price reactions can be inferred from market data over time.

5 CONCLUSION

With a rise in E-commerce it has become easier to observe and to adjust prices automatically. As a result, dynamic pricing strategies are applied by an increasing number of firms. This paper analyzes stochastic dynamic infinite horizon oligopoly models characterized by active and passive competitors. We set up a dynamic pricing model including discounting and shipping costs. The sales probabilities are allowed to depend on time and can arbitrarily depend on our price as well as the competitors' prices. Hence, our model is suitable for practical applications. Data-driven estimations of sales intensities under pricing competition can be used to calibrate the model.

Given a competitor's response strategy, we are able to compute optimal reaction strategies that take the anticipated competitors' price adjustments into account. In general, it is optimal to slightly undercut competitor's prices. However, when the price falls below a certain lower bound it is advisable to raise the price to an optimally chosen upper level. Our examples show that the model can be used to explain and to study Edgeworth price cycles.

We also verify that reaction times have a significant impact on long-term profits. Hence, firms will try to strategically time their price adjustments. In order not to act predictable firms might use randomized strategies. Using a generalized version of our model, we show how to derive optimal response strategies when reaction times are randomized. We observe that the ratio of frequencies of the competitors' prices adjustments is crucial for the firm's expected profits, i.e., to be able to adjust prices more often than the competitors do is an important competitive advantage.

In an extension of the model, we have considered additional players with fixed price strategies. We have presented a solution approach that allows deriving optimal response strategies. We have analyzed how the presence of additional passive competitors affects the price battle of active players that frequently adjust their prices. The solution approach is even applicable when the number of passive competitors is large. Our technique to compute prices remains simple and is easy to implement.

Moreover, we have evaluated the outcome when different reaction strategies are played against each other. It turned out that our optimized feedback strategies effectively avoid a decline in price. Especially, when competitors play aggressive strategies it is important to react in a reasonable way in order not to loose potential profits. Our approach allows to derive and to study price response strategies for various real-life applications especially in E-commerce.

Iterating mutual strategy responses, cf. Table 2, may also be the key to identify equilibrium strategies. Note, mutual strategy responses do not necessarily have to converge as pure strategy equilibria might not exist, see Kephart et al. (2000). In such cases, the approach used in Section 3.3 might help to identify equilibria in mixed strategies.

In future research we will use market data to estimate competitors' response strategies. We will also extend the model to study the sale of perishable products with finite initial inventory levels.

REFERENCES

Adida, E., G. Perakis. 2010. Dynamic Pricing and Inventory Control: Uncertainty and Competition. *Operations Research* 58 (2), 289–302.

Chen, M., Z.-L. Chen. 2015. Recent Developments in Dynamic Pricing Research: Multiple Products, Competition, and Limited Demand Information. *Production and Operations Management* 24 (5), 704–731.

Chung, B. D., J. Li, T. Yao, C. Kwon, T. L. Friesz. 2012. Demand Learning and Dynamic Pricing under Competition in a State-Space Framework. *IEEE Transactions on Engineering Management* 59 (2), 240–249.

Gallego, G., M. Hu 2014. Dynamic Pricing of Perishable Assets under Competition. *Management Science* 60 (5), 1241–1259.

Gallego, G., R. Wang. 2014. Multi-Product Optimization and Competition under the Nested Logit Model with Product-Differentiated Price Sensitivities. *Operations Research* 62 (2), 450–461.

Kephart, J. O., J. E. Hanson, A. R. Greenwald. 2000. Dynamic Pricing by Software Agents. *Computer Networks* 32, 731-752.

Levin, Y., J. McGill, M. Nediak. 2009. Dynamic Pricing in the Presence of Strategic Consumers and Oligopolistic Competition. *Operations Research* 55, 32–46.

Liu, Q., D. Zhang. 2013. Dynamic Pricing Competition with Strategic Customers under Vertical Product Differentiation. *Management Science* 59 (1), 84–101.

Martinez-de-Albeniz, V., K. T. Talluri. 2011. Dynamic Price Competition with Fixed Capacities. *Management Science* 57 (6), 1078–1093.

Maskin, E., J. Tirole. 1988. A Theory of Dynamic Oligopoly, II: Price Competition, Kinked Demand Curves and Edgeworth Cycles. *Econometrica* 56 (6), 571–599.

Noel, M. D. 2007. Edgeworth Price Cycles, Cost-Based Pricing, and Sticky Pricing in Retail Gasoline Markets. *The Review of Economics and Statistics* 89 (2), 324–334.

Phillips, R. L. 2005. *Pricing and Revenue Optimization.* Stanford University Press.

Schlosser, R., M. Boissier, A. Schober, M. Uflacker. 2016. How to Survive Dynamic Pricing Competition in E-commerce. *Poster Proceedings of the 10th ACM Conference on Recommender Systems*, RecSys 2016, Boston, MA, USA.

Talluri, K. T., G. van Ryzin. 2004. *The Theory and Practice of Revenue Management.* Kluver Academic Publishers.

Tsai, W.-H., S.-J. Hung. 2009. Dynamic Pricing and Revenue Management Process in Internet Retailing under Uncertainty: An Integrated Real Options Approach. *Omega* 37 (2-37), 471–481.

Wu, L.-L., D. Wu. 2015. Dynamic Pricing and Risk Analytics under Competition and Stochastic Reference Price Effects. *IEEE Transactions on Industrial Informatics* 12 (3), 1282–1293.

Yang, J., Y. Xia. 2013. A Nonatomic-Game Approach to Dynamic Pricing under Competition. *Production and Operations Management* 22 (1), 88–103.

Yeoman, I., U. McMahon-Beattie. 2011. *Revenue Management: A Practical Pricing Perspective*. Palgrave Macmillan.

APPENDIX

Table 3: List of variables and parameters.

t	time / period
X	random number sold items
G	random future profits
c	shipping costs
δ	discount factor
F	competitor's reaction strategy
Z	number of passive competitors
A	set of admissible prices
$V, V^{(c)}$	value functions
a	offer price
$\vec{p}, \vec{z}$	competitors' prices
λ	sales intensity
P	sales probability
J	cycle length
h	reaction time
$q, q^{(c)}$	reaction probabilities

Using the FMEA Method as a Support for Improving the Social Responsibility of a Company

Patrycja Hąbek and Michał Molenda
Faculty of Organization and Management, Silesian University of Technology, Roosevelta 26 str., Zabrze, Poland
{patrycja.habek, michal.molenda}@polsl.pl

Keywords: Corporate Social Responsibility, Failure Mode and Effects Analysis, Sustainability, Risk Assessment, ISO 26000.

Abstract: The concept of Corporate Social Responsibility (CSR) is based on companies voluntarily respecting environmental and social needs while making business decisions and at the same time taking into account the expectations of stakeholders. The notion of CSR is well known nowadays and practised by businesses around the world. However, this concept is sometimes interpreted and implemented differently. It is important to realize that the concept of CSR should be considered from the perspective of manufactured products as well as all processes realized in the company. The focus in this paper is on company processes. Socially responsible processes are those that do not adversely affect the company stakeholders. Therefore, the need arises to assess the risk of potential failures that may occur in company processes, taking into account the subjects of social responsibility. The authors present the possibility of using Failure Mode and Effects Analysis (FMEA) for this purpose. This paper presents an example of using a modified FMEA method which it is hoped can on one hand provide inspiration for further development of tools dedicated to CSR implementation at the operational level, and on the other hand offer help to those companies which want to integrate CSR into company processes.

1 INTRODUCTION

The Corporate Social Responsibility (CSR) concept is receiving increased attention from the business as well as the academic community (Crifo et al. 2016; Dahlsrud 2008; Fifka 2013a; Rok et al. 2007; Du et al. 2010; Lin-Hi & Müller 2013). CSR can be defined as a concept that integrates, on a voluntary basis, social and environmental concerns into a business' operations and interactions with its stakeholders. Unfortunately, not so rarely the concept is considered only as a marketing or public relations tool to improve company image (Mahoney et al. 2013; Wolniak & Hąbek 2015). Whereas in reality it is only possible to achieve long-term benefits from CSR implementation if socially responsible behaviour is integrated into all the processes in an enterprise. However, even a company with deep involvement in the affairs of the local community is not responsible if at the same time it does not respect employee rights, does not care about the environment and does not ensure the safety of its products. The activities of socially responsible manufacturers should be focused on the creation of products and services that are safe for the customer and at the same time do not threaten the environment, in addition the production processes of these products must be conducted in a safe manner and with concern for the environment (Paliwoda-Matiolańska 2014; Bluszcz & Kijewska 2014; Ryszko 2015).

Many companies are currently implementing CSR and even publish reports disclosing CSR data, however, there are still few tools that focus on the implementation of this concept at the operational level and tools which can be applied to all processes functioning in the company. One method that has been modified for this purpose and can be used to make a company's processes socially responsible is the Failure Mode and Effects Analysis (FMEA). The aim of the FMEA method is to consistently and systematically identify potential defects/failures in the product, process or design and then eliminate them or minimize the risks associated with them. Through the subsequent analysis with the FMEA method we can continually improve our products, processes or projects.

The aim of this article is to present the concept of using the FMEA methodology to improve the processes of a socially responsible organization.

Hąbek, P. and Molenda, M.
Using the FMEA Method as a Support for Improving the Social Responsibility of a Company.
In *Proceedings of the 6th International Conference on Operations Research and Enterprise Systems (ICORES 2017)*, pages 57-65
ISBN: 978-989-758-218-9

The remainder of the paper is structured as follows. The next two sections provide an overview of the CSR concept and give a short description of the FMEA method. This is followed by a section dedicated to the modified FMEA method that can be used to implement social responsibility into processes. The paper ends with conclusions and recommendations for further research.

2 CORPORATE SOCIAL RESPONSIBILITY – THE CONCEPT

Changes occurring in the environment, such as globalization and changing societal expectations, have caused companies to become the object of increasing pressure from different groups among its stakeholders to ensure not only profit but also greater social value. Consumers are becoming increasingly interested in how the company whose products they buy treats its employees and suppliers, and if the company has a negative impact on the natural environment or whether it is involved in corrupt practices.

Corporate Social Responsibility (CSR) is a broad term which has been differently defined (Gaweł et al. 2015; Line & Braun 2007; Maignan et al. 2002; Vveinhardt & Andriukaitienė 2014; Elkington 1999). For example, the European Commission understand it as a voluntary inclusion by a business of social and environmental concerns in their commercial (economic) activities and their relations with their stakeholders (COM 2001). Guidance on social responsibility (ISO 26000: 2010) defines the concept as the responsibility of an organization for the impacts of its decision and activities on society and the environment, through transparency and ethical behaviour that: contribute to sustainable development, including the health and welfare of society, take into account the expectations of stakeholders, are in compliance with applicable law and consistent with international norms of behaviour, are integrated throughout the organization and practices in its relationship. Referring to the above definitions, it seems that a key aspect of the CSR concept is running a business based on building lasting and transparent relationships with all stakeholders (Hąbek 2009). Identification of and engagement with stakeholders are crucial in the implementation of social responsibility in a company (Maignan et al. 2002). We can define stakeholders as individual people and groups of people, inside and outside the organization, who are interested in the results of its operations.

In order to systematize the knowledge of CSR and clarify the values which should act as guidance for organizations in its activities, in the ISO 26000:2010 the following areas of social responsibility (which are called the core subjects) have been defined: organizational governance, human rights, labour practices, the environment, fair operating practices, consumer issues, commitment and social development. The core subjects of CSR should be considered holistically in an organization rather than concentrating on a single issue. Therefore, it can be stated that responsibility is managed when, for example, employee policies are developed, when customer relationship strategies are implemented, when supply chains are managed, when leaders are really committed to a quality culture, when firms manage processes to achieve quality improvement, and when firms use measurement systems to improve their activities (Tarí 2011; Cierna & Sujova 2015).

Only comprehensive implementation of this concept enables enterprises to achieve values in the economic, social and environmental dimension. For this reason, the concept of corporate social responsibility should be considered from the perspective of all of company processes (Paliwoda-Matiolańska 2014).

Unfortunately CSR in companies is implemented variously and good practices often show one-dimensional practices concerning, e.g., environment protection or philanthropic activities. In addition, for many managers CSR is seen simply as a tool to improve company image or enhance public relations. To achieve the long-term benefits of its implementation, socially responsible behaviour should be integrated into and refer to all the processes in an enterprise. Therefore, there is a need to develop tools for the operationalization of CSR throughout an organization. In this paper, the authors suggest using for that purpose the methodology of FMEA.

3 FAILURE MODE AND EFFECTS ANALYSIS

Failure Modes and Effects Analysis (FMEA) is a step-by-step approach for identifying all possible failures in a design, manufacturing or assembly process, or a product or service. “Failure modes”

means the ways, or modes, in which something might fail. Failures are any errors or defects, especially ones that affect the customer, and can be potential or actual. "Effects analysis" refers to studying the consequences of those failures. Failures are prioritized according to how serious their consequences are, how frequently they occur and how easily they can be detected. The purpose of the FMEA is to take actions to eliminate or reduce failures, starting with the highest-priority ones. Failure modes and effects analysis also documents current knowledge and actions about the risks of failures, for use in continuous improvement (Tague 2005; Wolniak 2011).

FMEA first emerged in studies conducted by NASA in 1963. It eventually spread to the car manufacturing industry, where it aided in the identification and quantification of possible defects at the product design stage (Puente et al. 2002). FMEA is currently utilized in the automotive, aerospace, and electronic industries to identify, prioritize, and eliminate known potential failures, problems, and errors in systems during the design stage and prior to releasing the product (Stamatis 1995). Several industrial FMEA standards, such as those developed by the Society of Automotive Engineers, the US Military of Defense, and the Automotive Industry Action Group, employ Risk Priority Numbers (RPNs) to measure the risk and severity of failures (Rhee & Ishii 2003). RPN is an index that can represent the degree of risk that a product, process or design possesses. It consists of three indicators, namely, Occurrence (O), Severity (S), and Detection (D).

$$RPN = O \times D \times S \quad (1)$$

Where O is the probability of the failure, S is the severity of the failure, and D is the probability of not detecting the failure. FMEA consists of two stages. Potential failure modes are identified in the first stage, and the values of severity, occurrence, and detection are assigned. The manager makes recommendations for corrective action in the second stage, and RPN must be recalculated after undertaking such corrective action (Su & Chou 2008; Gajdzik & Sitko 2016).

The Risk Priority Number (RPN) can take the maximum value of 1000. In practice, established boundaries of this index are used, which can be defined as the level of acceptability of the risk. It is often assumed that the value of the RPN below 120 for the failure is an acceptable level of risk. In such a case it will not be necessary to make changes in the system. If the value of the RPN is in the range of 120-160, then corrective action should be taken which decreases the RPN value (Molenda et al. 2016).

Chen (2007) pointed out that FMEA provides a structured systematic identification of the potential failure modes in design, manufacturing, or management. FMEA provides a qualitative evaluation of the necessary corrective actions by studying the impact of failure on the system and by focusing on the problems affecting systematic reliability (Zasadzień 2014; Midor 2014). Failure modes and effects analysis also documents current knowledge and actions about the risks of failures, for use in continuous improvement.

The results of the FMEA analysis serve as a basis for the introduction of changes in the product design or production processes, aimed at reducing the risk of occurrence of defects identified as critical. If it is not possible to completely eliminate the causes of defects, action should be taken in order to enhance their capability to detect or reduce the negative effects of their occurrence. Implementation of the recommended corrective action should be continuously monitored and their effects subjected to verification (Wyrębek 2012; Skotnicka-Zasadzień 2012; Wojtaszak & Biały 2015).

4 FMEA FOR CSR – MAKING THE PROCESSES SOCIALLY RESPONSIBLE

In this section of the paper the authors present the procedure for social responsible risk assessment (see Figure 1) using the methodology of FMEA (FMEA for CSR/ FMEA4CSR). This method allows identifying problems and inconsistencies (weak points) that may occur during the process, taking into consideration the core subjects of the CSR concept. The similar concept was presented by Duckworth and Rosemond (2010).

The example presented in the paper applies to the process functioning in a production company. The authors are aware that conducting a risk assessment on one process will not ensure that the whole organization achieves improvements in social responsibility. The intention of the authors was to show an exemplary solution for the selected process.

The first step in the FMEA4CSR is to determine the process in the organization which should be studied. It is good to take a process-oriented approach which allows for the holistic analysis of risk on all aspects of social responsibility for that

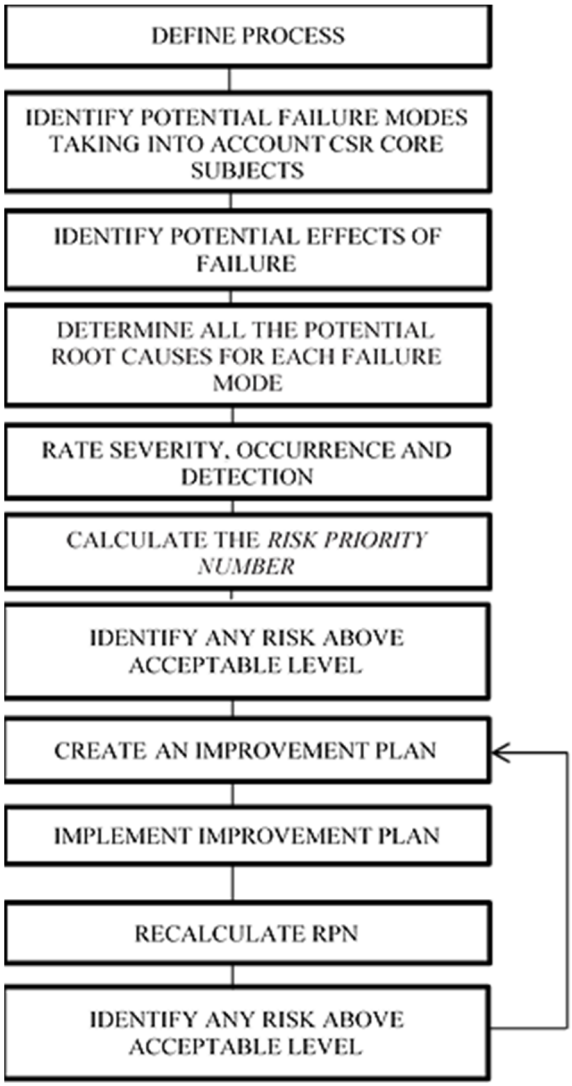

Figure 1: Stages of FMEA4CSR.

process. At this stage, a cross-functional team should be established consisting of the various groups involved in the process (engineering, purchasing, health and safety, human resources, new product development, etc.) which should be encouraged to complete the FMEA form.

The advantage of utilizing a cross-functional team approach is the varied experience and perspectives that each individual brings to the task. Although increased team diversity often leads to intense discussions when rating severity and occurrence, this difficulty in building consensus creates thoughtful debate about the organization's role in improving socially responsible behaviour (Duckworth & Rosemond 2010).

As an example, the maintenance process in a production company has been selected.

When the process for analysis has been selected and the team of experts set up it is necessary to identify the basis data about the process. To properly analyse the process, with accordance to the process approach, it should be determined the scope of the process, its suppliers, inputs as well as outputs. As the process has to be analysed from the perspective of social responsibility it is important to identify in the same time all the stakeholders involved in the process (see Table 1). It is good to present the information about the process in graphic form to enable a better understanding of the subject of the analysis. This phase is also dedicated to identifying the stakeholders (employees, customers, shareholders, community, government, local businesses, etc.) of the process whose needs and expectations will form the basis for further analysis. We have to bear in mind that identification of stakeholders is crucial to proceeding with the implementation of social responsibility in a company.

Table 1: Withdrawal of machines and equipment process identification.

SUPPLIERS	INPUTS	PROCESS	OUTPUT	STAKEHOLDERS
• company owners • maintenance department • machine manufacturer • health and safety department	• worn out, unnecessary machine • withdrawal order • plan for dismantling and removing from the plant • documentation of the machine (dismantling manual, design documentation) • instructions for safe removal and disposal of the machine	**withdrawal of machines and equipment (used, worn out, unnecessary)**	• dismantled and removed machine • records in the register about the machine removal • worn consumables materials (oils, lubricants, etc.) • emission of gases into the environment • registration and inventory of used parts and consumables materials • records of environmental hazardous materials	• company owners • employees working within the process • environmental inspectors • accounting department

The assessment of the severity of identified failure modes in FMEA4CSR should be done from the point of view of all stakeholders of the process, and not just from a customer's point of view as in the classical FMEA methodology.

After determining the stakeholders, all the outputs of the process should be identified, which may have an impact on these stakeholders. The next step is to identify all the process inputs (materials, energy, information, and human resources, etc.) required to conduct the process. The final task will be to identify the suppliers for the pre-defined inputs of the process. The goal of this analysis is to identify the potential social responsibility risks associated with the selected process. When the process is determined, we should focus on the critical function to that process. The functions constituting the maintenance process in an exemplary organization are shown in Table 2.

Table 2: Functions of maintenance process.

1.	Planning of investment for production resources
2.	Execution of the investment, the purchase of machines and equipment
3.	Installation and labelling of machines and equipment. Introduction to the register
4.	First commissioning and validation of machines and equipment
5.	Training for machine operators
6.	Planning of inspections and repairs
7.	Monitoring of the operations and diagnostics of machines and equipment
8.	Implementation of the plan of inspections and repairs
9.	Cost calculation of repair work
10.	Supply for maintenance (parts, consumable materials, etc.)
11.	**Withdrawal of machines and equipment**
12.	Diagnostics. Breakdown removal

For the further analysis we have chosen the process of withdrawal of machines and equipment (Table 5).

For the identified function in the selected process, all potential failure modes should be identified. At this stage we should use the knowledge of the team members as well as the data from the analysis of other processes or benchmarking studies. The next step is the analysis of all potential causes of the failure modes. At this stage we can use other tools such as the Ishikawa diagram. Because often the failures involve a cascade of effects, next we should analyse the impact of those failures. The direct effect or the consequence from the stakeholders' point of view should be taken into account (Kaźmierczak 2016). Another step of FMEA4CSR is to determine the Severity (S), Occurrence (O) and Detection (D) indicators. Each indicator can be a number between <1-10>. The ratios we determined are based on the data in Table 3 and Table 4. It should be noted here that the D indicator is fixed arbitrarily on the basis of knowledge about the possibility of detection of a failure. Number 1 applies when such a possibility is very big and number 10 when the failure is difficult to detect. Subsequently, we can calculate the Risk Priority Number (RPN) index. The RPN values allow us to determine the priority risks that can threaten social responsibility performance.

Table 3: Criteria of severity and occurrence ratings.

Rating	Severity [S]	Rating	Occurrence [O]
1	meaningless	1	negligible
2-3	low	2-3	occasional
4-6	moderate	4-6	moderate
7-8	high	7-8	high
9-10	very high	9-10	very high

Table 4: Criteria of detection ratings.

Rating	Detection [D]
1	very high
2-5	high
6-8	moderate
9	low
10	accidental

Then we can focus on ranking the failure from the most important, from the point of view of the stakeholders, when the number of RPN is the greatest, to the least important. Then we must fix the limit (a number RPN) between critical failures and other failures. For all critical failures we should determine the corrective actions, i.e., actions which enable eliminating the causes of the failures. After completion of these activities the RPN index should be re-calculated and if there are still critical failures, the introduction of corrective actions should be repeated to achieve an acceptable level of risk.

In our example, we established the limit for RPN between the critical and the other failure modes at

Table 5: FMEA4CSR example sheet for the selected process – part A.

PROCESS: WITHDRAWAL OF MACHINES AND EQUIPMENT							
CORE SUBJECT	SOCIAL RESPONSIBILITY FAILURE MODE	CAUSES	FAILURE EFFECTS	S	O	D	RPN
Organizational Governance	No systems for tracking and/or reporting on social and environmental results	Reducing the cost of bureaucracy and reduction of employment	No information on emissions and pollution which occurred during the dismantling and removal of the machines No information regarding the threats to employees during removal of the machines	7	8	3	168
	No organizational policy for the protection of property, which is to prevent the theft of technical resources	Lack of awareness of the top management of the risks of theft of the dismantled machines or their components	Material losses arising from theft of unprotected elements of the machines	7	7	4	196
Human Rights	Lack of clear message about the importance of human rights in the organization	Top management is convinced that at all levels of the organization human rights are respected	Performing activities that threaten health during realization of the process	9	7	4	252
	Lack of processes for resolving grievances	Information about complaints of employees are blocked by direct superiors	Carrying out the process under pressure beyond normal working hours	9	5	2	90
Labour Practices	Conditions of work do not comply with national law	Lack of training of middle-level managers in terms of the law in force concerning the implementation of the process	Working in conditions that threaten the health and lives of workers carrying out the process	9	7	1	63
Environment	Lack of system for tracking waste created by the organization	Adoption by top management policy, oriented only on the financial results. Reducing bureaucracy	No information on emissions and pollution caused by errors during the dismantling and removal of machines	5	5	3	75
	Lack of identification and action associated with protecting the natural environment	Lack of environmental policy	Uncontrolled pollution arising during the dismantling and removal of machines	8	7	4	224
Fair Operating Practices	Lack of identification of risk associated with corruption	Lack of awareness of top management associated with the resale of used machines undervalued	Company financial losses associated with selling the withdrawn machines undervalued	7	3	8	168
Consumer Issues	Unknown impact						
Community Involvement and Development	Unknown impact						

Table 6: FMEA4CSR example sheet for the selected process – part B.

PROCESS: WITHDRAWAL OF MACHINES AND EQUIPMENT						
CORE SUBJECT	SOCIAL RESPONSIBILITY FAILURE MODE	IMPROVEMENT PLAN	S	O	D	RPN
Organizational Governance	No systems for tracking and/or reporting on social and environmental results	The introduction of an emissions control system as well as system to keep track of accidents occurring during the removing of withdrawn machines	7	3	1	21
	No organizational policy for the protection of property, which is to prevent the theft of technical resources	The establishment of a special committee whose task will be to calculate the value of withdrawn machines	7	1	4	28
Human Rights	Lack of clear message about the importance of human rights in the organization	The introduction of documented organizational rules in the company, which include labour standards during the removal of withdrawn machines	9	2	4	72
	Lack of processes for resolving grievances					
Labour Practices	Conditions of work do not comply with national law					
Environment	Lack of system for tracking waste created by the organization					
	Lack of identification and action associated with protecting the natural environment	The adoption of environmental policies and the development of procedures for environment protection while removing machines that will secure the process from uncontrolled emission to the environment	8	4	2	48
Fair Operating Practices	Lack of identification of risk associated with corruption	The adoption of procedures to ensure the valuation and resale of the withdrawn machines and its components for the actual value	7	1	6	42
Consumer Issues	Unknown impact					
Community Involvement and Development	Unknown impact					

120. Thus, the RPN for the failure modes obtained above this limit need corrective action. In the present case we identified five critical social responsibility failure modes. For each we have proposed an improvement plan and re-calculated the RPN index (Table 6). After the implementation of the improvements, an acceptable level of risk was achieved. We can conclude that the FMEA4CSR method enables the identification of potential risks associated with the business processes and allows us to better understand the impact on society, the environment and economics. The added value of this analysis is increased awareness among managers, as well as the employees involved, especially in the analysed process. This raised awareness will influen-ce the development of appropriate organizational culture facilitating the implementation of the CSR concept.

5 CONCLUSIONS

The authors presented in this paper a method called FMEA for CSR (FMEA4CSR) that is used as a tool for risk analysis which identifies and prioritizes

actions for improving socially responsible processes. These prioritized actions allow us to rethink the types and volume of resources needed to minimize the risks associated with the specific failure modes. FMEA4CSR is based on seven core subjects of social responsibility defined in ISO 26000. Because CSR is a concept which is based on the stakeholders theory, identification and analysis of their needs and expectations is crucial for the implementation of this concept. Therefore, FMEA4CSR takes into account in the risk assessment not only the severity of potential failure modes for customers (as in the classical FMEA), but also for the other stakeholders. In the proposed methodology the significance of potential failure modes for all the company's stakeholders involved in the process is considered. Thus, it is reasonable to use the expert knowledge in the analysis as it is in the case of the FMEA method. Therefore, it is recommended to integrate the methodology with one of the participatory methods (e.g. Charrette, Syncon, Delphi, Groupware, etc.) in order to reach consensus between stakeholders or at least the justifications for the different opinions, scores, etc. and to make sure the results are clear to all of them.

The purpose of using this tool is the continuous improvement of socially responsible processes. Identification of the risks associated with each of the core subjects of social responsibility leads not only to determining the priority issues, but also improves awareness among employees. This improved awareness is an added value to this analysis and is invaluable in the implementation of CSR in a company. Summarizing, FMEA4CSR can be used as a practical tool for the continuous improvement of social responsibility within a company at the operational level.

We must bear in mind that we cannot always find the ideal solution. Social responsibility approach may sometimes conflict with the other company's goals (e.g. environmental protection goal and keeping production which pollutes the environment but simultaneously giving an employment for many people). It is not always possible to meet all expectations at the same time and the company must make a choice. Therefore there is a need for further discussion on this multi-criteria aspect of the problem. Future research may be concentrated also on the implementation of the core subjects of CSR in product or design FMEA. It could be also interesting to discuss other tools traditionally used in quality improvement and their potential benefits in social responsibility improvement programmes.

ACKNOWLEDGEMENTS

The paper is the result of the statutory research project No 13/030/BK_16/0024 entitled "Production engineering methods and tools for development of smart specializations".

REFERENCES

Bluszcz, A. & Kijewska, A., 2014. W kierunku społecznej odpowiedzialności przedsiębiorstw górniczych. *Przegląd Górniczy*, 70(4), pp.45–51.

Chen, J.K., 2007. Utility Priority Number Evaluation for FMEA. *Journal of Failure Analysis and Prevention*, 7(5), pp.321–328. Available at: http://link.springer.com/10.1007/s11668-007-9060-2 [Accessed September 16, 2016].

Cierna, H. & Sujova, E., 2015. Parallels Between Corporate Social Responsibility and the EFQM Excellence Model. *MM Science*, October, pp.670–676.

COM, 2001. *GREEN PAPER. Promoting a European Framework for Corporate Social Responsibility*, Available at: http://eur-lex.europa.eu/legal-content/EN/TXT/?uri=URISERV%3An26039.

Crifo, P., Diaye, M.-A. & Pekovic, S., 2016. CSR related management practices and firm performance: An empirical analysis of the quantity–quality trade-off on French data. *International Journal of Production Economics*, 171, pp.405–416. Available at: http://www.sciencedirect.com/science/article/pii/S0925527314004137 [Accessed December 17, 2015].

Dahlsrud, A., 2008. How corporate social responsibility is defined: an analysis of 37 definitions. *Corporate Social Responsibility and Environmental Management*, 15(1), pp.1–13. Available at: http://doi.wiley.com/10.1002/csr.132 [Accessed September 26, 2016].

Du, S., Bhattacharya, C.B. & Sen, S., 2010. Maximizing Business Returns to Corporate Social Responsibility (CSR): The Role of CSR Communication. *International Journal of Management Reviews*, 12(1), pp.8–19. Available at: http://doi.wiley.com/10.1111/j.1468-2370.2009.00276.x [Accessed August 11, 2016].

Duckworth, H.A. & Rosemond, A.M., 2010. *Social Responsibility: Failure Mode Effects and Analysis*, Boca Raton: CRC Press.

Elkington, J., 1999. *Cannibals with Forks: Triple Bottom Line of 21st Century Business*, Capstone Publishing Ltd. Available at: http://www.amazon.com/Cannibals-Forks-Triple-Century-Business/dp/1841120847 [Accessed December 21, 2015].

Fifka, M.S., 2013a. Corporate Responsibility Reporting and its Determinants in Comparative Perspective - a Review of the Empirical Literature and a Meta-analysis. *Business Strategy and the Environment*, 22(1), pp.1–35. Available at: http://doi.wiley.com/10.1002/bse.729 [Accessed August 11, 2016].

Fifka, M.S., 2013b. Corporate Responsibility Reporting and its Determinants in Comparative Perspective - a Review of the Empirical Literature and a Meta-analysis. *Business Strategy and the Environment*, 22(1), pp.1–35.

Gajdzik, B. & Sitko, J., 2016. Steel mill products analysis using qualities methods. *Metalurgija*, 55(4), pp.807–810.

Gaweł, E. et al., 2015. Corporate Social Responsibility as an Instrument of Sustainable Development of Production Enterprises. *Management Systems in Production Engineering*, 3(19), pp.152–155.

Hąbek, P., 2009. Społeczna odpowiedzialność przedsiębiorstw jako koncepcja firmy zorientowanej na interesariuszy. *Organizacja i Zarządzanie*, 2(6), pp.69–86.

Kaźmierczak, J., 2016. Engineering of Needs (EoN): the role of identifying and analyzing needs in Engineering and Engineering Management. In *ESME 2016 International Conference on Economic Science and Management Engineering*. Guilin.

Line, M. & Braun, R., 2007. *Baseline Study on CSR Practices in the New EU Member States and Candidate Countries*, Available at: http://docs.china-europa-forum.net/undpconference_26062007_brochure.pdf.

Lin-Hi, N. & Müller, K., 2013. The CSR bottom line: Preventing corporate social irresponsibility. *Journal of Business Research*, 66(10).

Mahoney, L.S. et al., 2013. A research note on standalone corporate social responsibility reports: Signaling or greenwashing? *Critical Perspectives on Accounting*, 24(4-5).

Maignan, I. et al., 2002. Corporate Social Responsibility in Europe and the U.S.: Insights from Businesses' Self-presentations. *Journal of International Business Studies*, 33(3), pp.497–514.

Midor, K., 2014. An analysis of the causes of product defects using quality management tools. *Management Systems in Production Engineering*, 16(4), pp.162–167.

Molenda, M., Hąbek, P. & Szczęśniak, B., 2016. *Zarządzanie jakością w organizacji. Wybrane zagadnienia*, Gliwice: Wydawnictwo Politechniki Śląskiej.

Paliwoda-Matiolańska, A., 2014. *Odpowiedzialność społeczna w procesie zarządzania przedsiębiorstwem*, Warszawa: CH Beck.

Puente, J. et al., 2002. A decision support system for applying failure mode and effects analysis. *International Journal of Quality & Reliability Management*, 19(2), pp.137–150. Available at: http://www.emeraldinsight.com/doi/abs/10.1108/02656710210413480 [Accessed September 16, 2016].

Rhee, S.J. & Ishii, K., 2003. Using cost based FMEA to enhance reliability and serviceability. *Advanced Engineering Informatics*, 17(3), pp.179–188.

Rok, B. et al., 2007. *Corporate Social Responsibility in Poland. Baseline Study.*, Warsaw.

Ryszko, A., 2015. Environmental Proactivity and its Determinants: Selected Issues Based on the Example of Poland. In *15th International Multidisciplinary Scientific GeoConference SGEM 2015. Environmental Economics*. pp. 259–266. Available at: http://www.sgem.org/sgemlib/spip.php?article6535 [Accessed October 2, 2016].

Skotnicka-Zasadzień, B., 2012. Analiza Efektywności Zastosowania Metody FMEA w Małym Przedsiębiorstwie Przemysłowym. *Systemy Wspomagania w Inżynierii Produkcji*, pp.142–153.

Stamatis, D.H., 1995. *Failure Mode and Effects Analysis*, ASQ Quality Press.

Su, C.-T. & Chou, C.-J., 2008. A systematic methodology for the creation of Six Sigma projects: A case study of semiconductor foundry. *Expert Systems with Applications*, 34(4), pp.2693–2703.

Tague, N.R., 2005. *The Quality Toolbox*, Milwaukee: American Society for Quality, Quality Press. Available at: https://www.amazon.com/Quality-Tool box-Nancy-R-Tague/dp/0873896394.

Tarí, J.J., 2011. Research into Quality Management and Social Responsibility. *Journal of Business Ethics*, 102(4), pp.623–638. Available at: http://link.springer.com/10.1007/s10551-011-0833-x [Accessed September 23, 2016].

Vveinhardt, J. & Andriukaitienė, R., 2014. Social Responsibility Discourse in Empirical and Theoretical Lithuanian Scientific Studies. *Engineering Economics*, 25(5), pp.578–588. Available at: http://www.inzeko.ktu.lt/index.php/EE/article/view/4898 [Accessed September 14, 2016].

Wojtaszak, M. & Biały, W., 2015. Problem solving techniques as a part of implementation of six sigma methodology in tire production. Case study. *Management Systems in Production Engineering*, 19(3), pp.133–137.

Wolniak, R., 2011. Wspomaganie metody FMEA w przedsiębiorstwie produkcyjnym. *Problemy Jakości*, 43(1), pp.15–21.

Wolniak, R. & Hąbek, P., 2016. Quality Assessment of CSR Reports – Factor Analysis. *Procedia - Social and Behavioral Sciences*, 220, pp.541–547. Available at: http://linkinghub.elsevier.com/retrieve/pii/S1877042816306310 [Accessed July 19, 2016].

Wolniak, R. & Hąbek, P., 2015. Reporting Process of Corporate Social Responsibility and Greenwashing. In *15th International Multidisciplinary Scientific GeoConference SGEM 2015. Environmental Economics*. Available at: http://www.sgem.org/sgemlib/spip.php?article6565 [Accessed September 29, 2016].

Wyrębek, H., 2012. Znaczenie metody FMEA w zarządzaniu jakością w przedsiębiorstwach. *Zeszyty Naukowe Uniwersytetu Przyrodniczo-Humanistycznego w Siedlcach. Administracja i Zarządzanie*, 19(nr 92), pp.151–165.

Zasadzień, M., 2014. Using the Pareto Diagram and FMEA (Failure Mode and Effects Analysis) to Identify Key Defects in a Product. *Management Systems in Production Engineering*, 4(16), pp.153–156.

Discontinued Products
An Empirical Study of Service Parts Management

Luís Miguel D. F. Ferreira[1], Amílcar Arantes[2] and Cristóvão Silva[1]
[1]*Department of Mechanical Engineering, University of Coimbra, Polo II Pinhal de Marrocos, 3030 Coimbra, Portugal*
[2]*CERIS, CESUR, Instituto Superior Técnico, Universidade de Lisboa, Av. Rovisco Pais, Lisboa,1049-001, Portugal*
luis.ferreira@dem.uc.pt, amilcar.arantes@tecnico.ulisboa.pt, cristovao.silva@dem.uc.pt

Keywords: Service Parts, Discontinued Products, Empirical Study.

Abstract: The procurement and inventory management of service parts for discontinued products has often been overlooked by companies, resulting in several problems such as stock outs, rush orders or obsolete stocks. Accordingly, the main aim of this work is to develop a methodology to deal with these issues following product discontinuation. To this end, an empirical study – based on action research principles – was carried out in a producer of household appliances, which is bound by law to provide service parts for its products for a period of 15 years after they have been discontinued. The work was developed in three stages: characterization of the company situation; definition of a procedure to eliminate obsolete stocks; and definition of a procedure to manage active service parts. The resulting methodology and respective procedures are presented and the results obtained with the implementation are discussed.

1 INTRODUCTION

Rapid technological innovation and recurrent changes in consumer preferences are decreasing product lifecycles. This places pressure on stock management, with a requirement for suitable stock levels for all service parts. Service parts are used to replace old parts that are no longer operational due to total failure or malfunction. Moreover, after a product has been discontinued, many of the service parts needed in the post product life cycle are often out of production (Inderfurth and Mukherjee, 2006).

Service parts for products like household appliances or automobiles are considered an important element of a company´s business. In some industry sectors the service parts business can represent up to 25% of the revenues and 40% to 50% of the profits of manufacturing firms (Dennis and Kambil, 2003; Cohen et al. 1999). Thus, it is important for industrial companies to guarantee the availability of service parts in order to provide the desired after-sales service level. As a result, companies are forced to stock an enormous amount of service parts.

It is often the case that many service parts for discontinued products are recognized as a major source of inventory stock-out or obsolescence. The inventory costs associated with service parts for discontinued products are much higher than those of service parts for current products. Moreover, the level of competition that exists in the market means that any stock-out of service parts cannot be tolerated, since this has a negative impact on the brand image of the company (Hong et al., 2008).

Therefore, it is important to manage service parts carefully, because production lines used for manufacturing a particular service part are likely to be discontinued, prior to demand falling to zero. Moreover, in some countries, manufacturers are required by law to provide past model service parts for several years after production has ceased. Yet, procurement and inventory management of service parts are complex subjects due to the high number of service parts involved; the intermittent nature of their demand patterns; the high responsiveness needed to minimise the downtime cost for the customer; and the high risk of stock obsolescence (Hong et al., 2008).

Hence, the main aim of this work is to develop a methodology to help manage these service part issues in the period following product discontinuation, namely: eliminating obsolete stock and managing active service parts.

Ferreira, L., Arantes, A. and Silva, C.
Discontinued Products - An Empirical Study of Service Parts Management.
In *Proceedings of the 6th International Conference on Operations Research and Enterprise Systems (ICORES 2017)*, pages 66-74
ISBN: 978-989-758-218-9

2 LITERATURE REVIEW

After-sales service is a period following on from the start of the product lifecycle and before the end of life date. When after-sales service ends, the manufacturer no longer guarantees the supply of replacement parts for the product. This period may be a legal requirement, or it may be set by the company. In some cases, it can go beyond the legal limit, in a bid to increase the service level and improve the company´s image. As it is normal that replacement parts are needed after some period of use, their demand peaks sometime after demand for the product itself. This can be seen in Figure 1 below. While this is normally the case, there may be exceptions to this rule.

The end of after-sales service may also occur unexpectedly, severely complicating the management of service parts. Where a machine is dependent on a part to continue functioning, a stock out of that part will make the machine obsolete. This means that all the other parts of that machine reach the end of the after-sales service period earlier than expected. Another source of uncertainty occurs when one part is substituted by another. An example may be when a firm manufacturing mobile phone batteries brings a new battery to market which is cheaper and lasts longer; when the consumer changes battery, they will likely choose the new model over the old model. This source of uncertainty is difficult to predict (Hong et al., 2005).

There is a considerable body of literature concerning demand forecasting and inventory management of service parts. Several documented approaches exist, ranging from relatively simple models like Croston's method (Croston, 1972) and its refinement (Syntetos and Boylan, 2001; Syntetos and Boylan, 2005) to more complex algorithms like the stochastic forecasting model presented by Hong et al (2008). This last method considers four major factors in their model to forecast service parts: product sales, the discard rate of the product, the failure rate of the service part and the replacement probability of the service part.

Wang and Syntetos (2011) presented an innovative idea to forecast demand for spare parts that relies upon the demand generation process itself, comparing it successfully with a traditional time-series method. Leifker et al. (2014) presented two approaches for dealing with the problem of extending maintenance or supply contracts for spare parts of discontinued products: one includes the use of a continuous-time dynamic program and the other makes use of a two-stage stochastic algorithm. Rego and Mesquita (2015) presented a case study on spare parts inventory management, comparing several methods using different forecasting techniques and inventory management policies by simulating with field data (10 032 spare parts references); results of the simulations allowed the recommendation of best

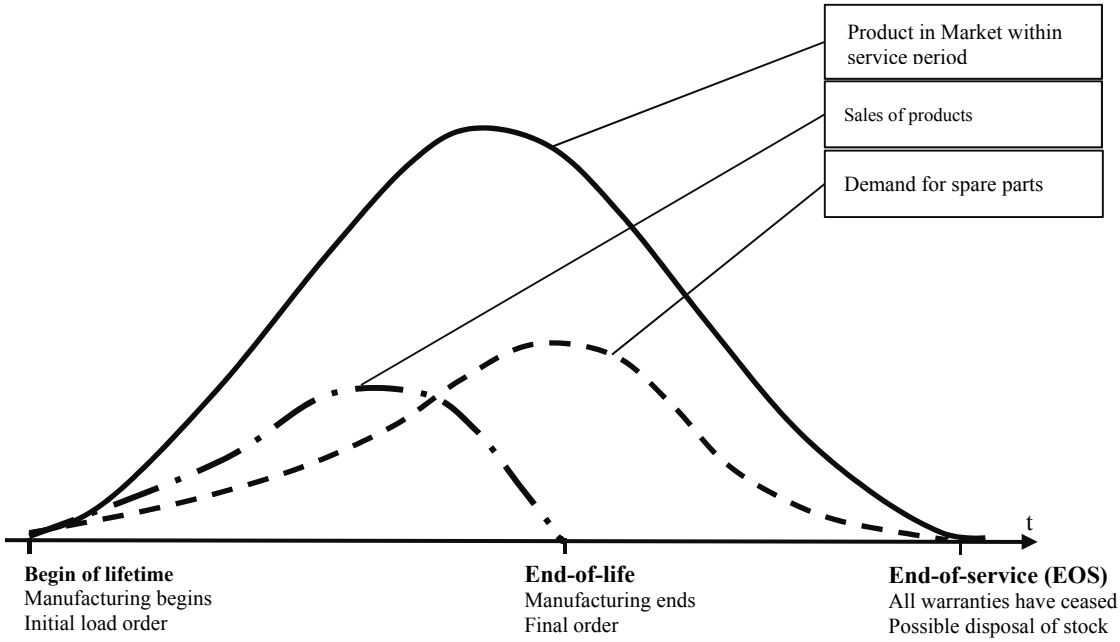

Figure 1: The lifecycle for spare parts. [Adapted from Inderfurth and Mukherjee (2006)].

policies to be followed within each spare part category. Some authors have proposed practical approaches to manage service parts for discontinued products in practice. Teunter and Fortuin (1998) present a model developed to determine the size of a final order for service parts which was implemented in an electronic equipment company, with the objective of covering the demand until all service obligation has ended. Teunter and Haneveld (1998) refer to a case study of a company that produces appliances for which they developed a model for service parts management in its final phase. The model considers an ordering policy which consists of an initial order up-to-level at time 0, the instant when the product is discontinued, and a subsequent series of decreasing order-up-to levels for various intervals of the planning horizon.

However, previous research has focused primarily on the planning and operational aspects (e.g. the determination of optimum spare parts inventory levels) and has neglected the strategic and organisational problems manufacturing companies must solve to manage their spare parts business effectively during post product life cycle. Moreover, a gap between research and practice has been identified by several authors; for a comprehensive literature review on service parts management and on the gap between research and practice we refer to Bacchetti and Saccani (2012). Here, for instance, the authors make the point that "*despite the wealth of literature on the subject, no attention has in practice been paid to proper management and control of service-parts inventory*" or that "*incremental mathematical inventory research is not likely to enhance practice*".

This gap between research and practice is probably due to the mathematical complexity of the proposed methods and their need for data which are often not available. It is also important to mention that the adoption of simple but formalised procedures for the management of service parts during the post product life cycle can help companies achieve substantial benefits, not only by reducing costs but also by improving the company image (Botter and Fortuin, 2000).

3 RESEARCH METHOD

In this paper, the case of a company which produces household appliances is presented. In the past, the procurement and inventory management of service parts during the post product life cycle had been overlooked by the company. This resulted in several problems such as stock outs, rush orders and obsolete stock – stock of service parts for which the service contract has expired. Moreover, sometimes service part production also required components for which the original supplier was no longer operating and this would imply a time-consuming negotiation process with a new supplier.

To solve these problems, the company decided to start a project to define procedures to manage the procurement and inventory management of service parts during the post product life cycle. Moreover, it was the intention of the company managers that the procedures to be implemented should avoid using complex mathematical algorithms that users would find hard to understand as well as models that would require data which would not be easily accessible, or even available, from the company information systems.

Therefore, this study applied the principles of action research, allowing a link to be established between the company and the researchers (Middel et al. 2005). Nevertheless, two conditions need to be respected for the approach taken to fall within the field of action research. Firstly, the research objective and project plan were driven by the researcher's agenda rather than by the participating company representatives. Secondly, the project plan was motivated primarily by the development of procedures for the management of service parts during the post product life cycle and not by the aim of transforming the individual organization's practices. In any case, the focus of the research is to introduce changes in reality (Baker and Jayaraman 2012).

4 THE PROPOSAL

In this section, we present the proposal for the management of service parts during the post product life cycle. The project to define the requested procedures was developed in three stages, which are described in the following subsections: the characterisation of the company service parts; the definition of a procedure to eliminate obsolete stocks and the definition of a procedure to manage service parts.

4.1 Characterisation of the Company

In the case study company, the procurement process for service parts during the post product life cycle was as follows: when the stock for a given service part reaches its reorder level, a production order for this

service part is scheduled by the logistics department. To manufacture the required service part, the necessary components are taken from stock and these can also eventually reach the reorder level. If this happens, an order for the component is placed by the company purchasing department. The size of this order is calculated to satisfy the estimated demand for the next six months, based on a simple average of the demand seen for this component since the time the product became discontinued and adjusted according to the conditions of the contract between the company and the supplier.

This stage of the project was designed to provide a clear understanding of how many spare parts were exclusively used in the post product life cycle. The company information systems held information about all the components used in the service parts of discontinued products. However, accessing the required information was difficult (for example, data about the time remaining until the end of the service contracts). In part, this information was incomplete because each component could be used in several service parts and each service part may be necessary for several products. Moreover, the data was spread over two different information systems (IS 1 and IS 2 in Figure 2).

Therefore, a support database was developed to easily access all relevant data about the components of discontinued products. This database was fed with data from both company information systems (Figure 2), and was used to identify all the necessary information for the required procurement process Using data from the first company information system (IS1), each component (Comp.) was related to the service parts (SP) where it is used. The second information system (IS2) shows how each service part was related to the final products where they are used, and for each final product (FP) the date of the last production run was recorded. Furthermore, the corresponding supplier of each component has also been identified. The result of this operation is presented in Table 1.

The information contained in the database provided a description of the discontinued product service parts and their respective components. Some of these characteristics (namely the "Time remaining to end of service") allow the parts and their components to be divided into three major groups: for

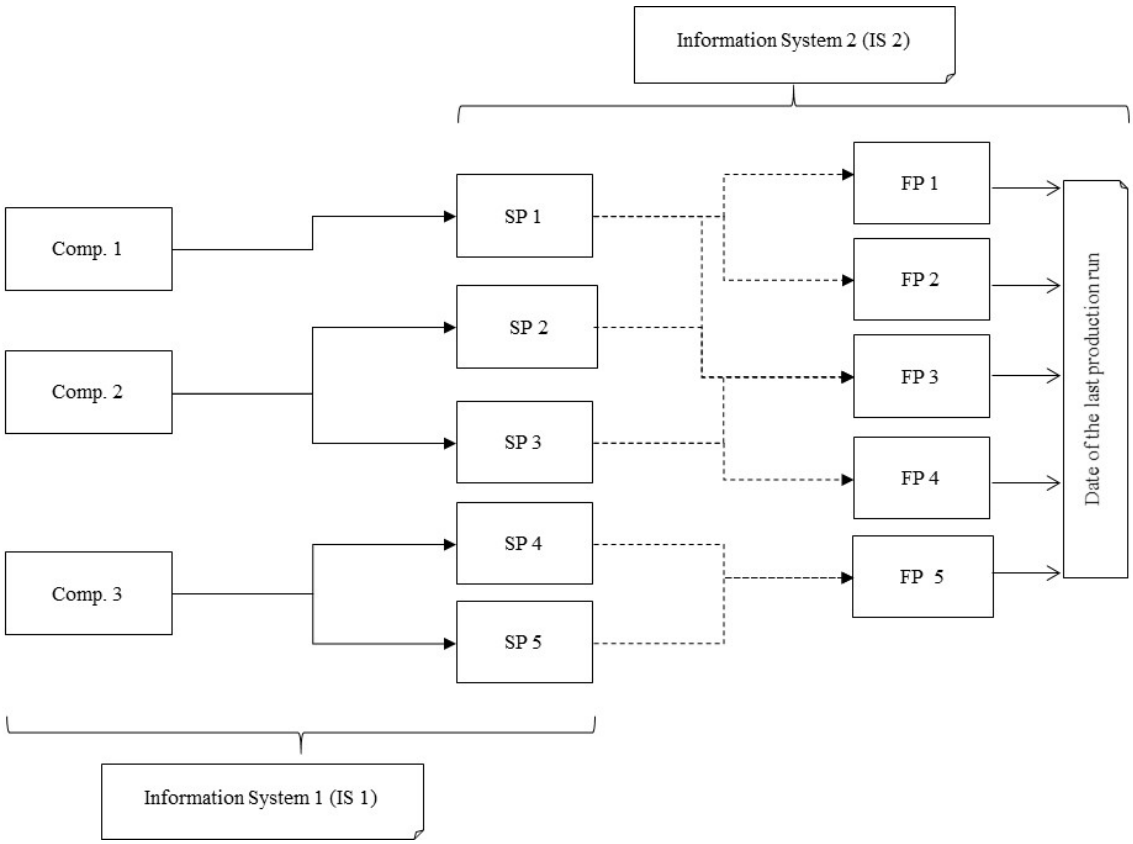

Figure 2: Data collection from the company information systems.

Table 1: Component information.

Compo-nent	Time to end service(years)	Stock (units)	Stock (€)	Supplier
…	…	…	…	…
C10	5	1524	480	XYZ
C11	1	149	30	?
…	…			
Cn	-2	46	202	ABC
…	…	…	…	…

the first group, the company is no longer required to provide support; for the second group, the company is required to provide parts and components within the 15-year limit; and for the third group, no end-of-service date exists (this represents around 50% of the components listed). The complete listing of Table 1 showed that the company manages approximately 1300 components, exclusively used in service parts for discontinued products.

These 1300 components are required in around 1800 service parts for discontinued products (there are more service parts than components as each component can be used in various parts). In turn, these parts are used in 6530 end products (appliances). The 1300 components represent 14% of the total number managed by the company and 9% of the company stock value. Three percent of these components representing obsolete stock. Another conclusion from analysing Table 1 was that approximately 50% of the components had no active supplier assigned.

This represents a major difficulty for the management and procurement of those components, because if a stock-out of one of these components occurred, the company would have to start a negotiation process with a new supplier, meaning long lead times. The lack of an active supplier could be due to two reasons: the usual component supplier has ceased trading or a long time has passed since the company has placed an order with the supplier who, due to production changes, is not able or not willing to supply that component anymore.

4.2 A Procedure to Eliminate Obsolete Component Stocks

The previous project stage identified some obsolete components stocks. A procedure to eliminate these stocks was required. The stock of these components could simply be sold as scrap; nevertheless, they could still be valuable as components for the production of service parts of discontinued products, despite the fact that the company has no obligation to do so.

In the past, if the company received an order for a service part which was no longer active (covered under the post product life cycle period) and for which there was no available stock, the client was informed that the company was no longer required to provide this service part and the stock out was not considered a service-level failure by the company. Nevertheless, it is clear that this situation could reflect badly on the company. To avoid these kinds of problems a procedure to eliminate obsolete stocks was defined, as shown in Figure 3.

In this situation, clients are informed which service parts have reached the end-of-service period. Clients are informed that if they wish they may place a final order for these service parts. If the stock components for the of end of life service parts is sufficient to cover the client's final order, the order is delivered. If the stock of components is not sufficient to cope with the service part production, an order for the required components is placed. After the final client orders, if some service parts or components remain in stock, they are then sold as scrap. This procedure is now scheduled for the beginning of each year for all service parts which have reached their end-of-life date the previous year.

This procedure allows obsolete stock to be removed, including both spare parts and the components which they alone use, given the direct link between the two. In addition, the warehouse space allocated to these parts and components becomes available for other stock. Finally, and most importantly, this approach ensures customer satisfaction (service level), given that the customer is warned in advance of the service part's end-of-life. They are provided with the opportunity to make a last order, guaranteeing a fixed quantity and with a lead time of around one month. It was also decided that this procedure would be carried out at the start of each year, covering the service parts which had reached their end-of-life during the previous year.

4.3 A Procedure to Manage Active Service Parts

This last stage of the project defined a procedure to improve the management process of active service parts. The main objective of managing service parts is to establish a component ordering procedure which ensures an adequate inventory level. The availability of components to produce service parts is vital to the company. Long lead times are associated with component orders and this is not acceptable to the end customer who is waiting for their household appliance to be repaired.

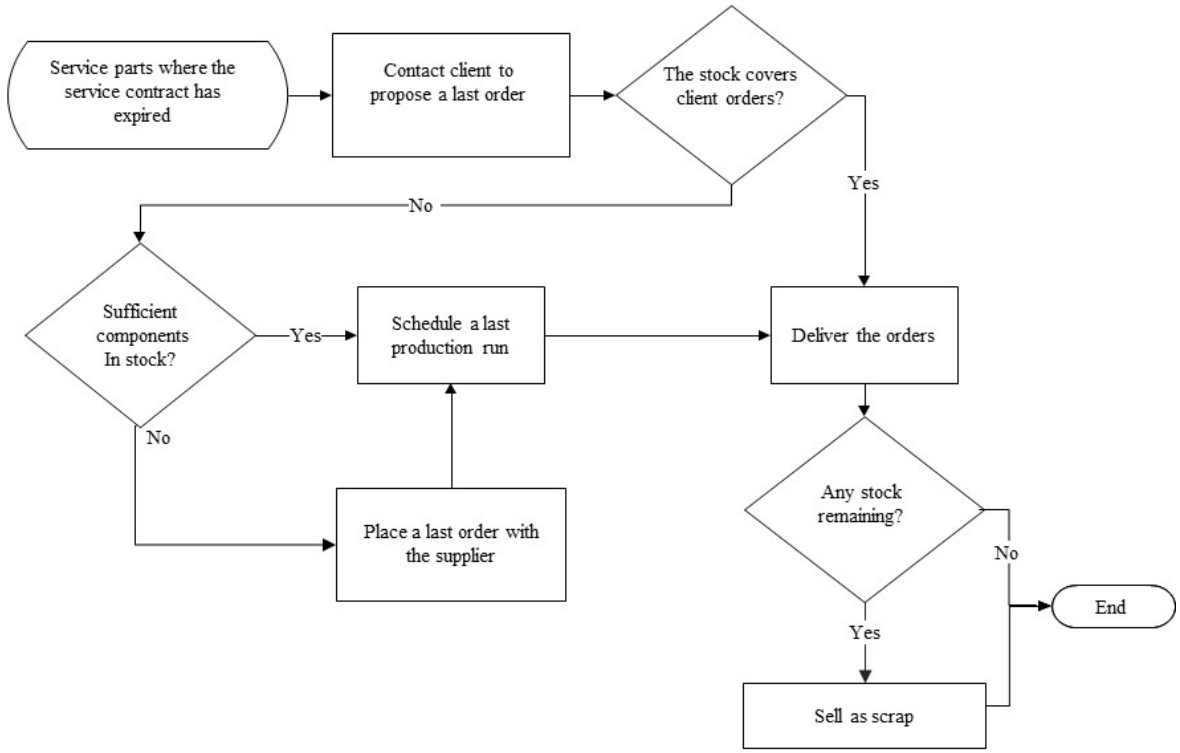

Figure 3: Flowchart showing the procedure to eliminate obsolete stock.

The process for acquiring the components used to manufacture the service parts for end products which are still current is relatively simple as this depends on the demand (for spare parts). However, when there is intermittent demand for service parts, forecasting methods are used so that inventory levels can be properly managed.

In the past, the company used the average service part demand over the previous six months to forecast the demand for the next six months, whenever the component reorder point was reached. The forecast demand for the next six months would help anticipate the component procurement process and the service part production, thus avoiding long lead times for the final client. In this respect, two distinct situations are possible: (1) service parts with components for which there are active suppliers and (2) service parts with components for which there are no active suppliers. In both cases demand forecasting is important to guarantee an effective procurement process and efficient inventory level management. Additionally, in the second case forecasting is also important to help the purchasing department negotiate with potential new suppliers.

At the beginning of the project the company considered that the forecasting method used was not the most effective. Thus, in order to identify which forecasting method to use for managing service parts it was decided to study the demand patterns (using available data from a seven-year period).

The service parts were classified according to their demand patterns as: slow moving, intermittent, erratic and lumpy, as proposed by Syntetos et al. (2005). This classification was made considering the values calculated using: inter-demand interval (IDI) and the squared coefficient of variation of the demand sizes (CV^2).

Considering that the company had asked to avoid complex algorithms that would be difficult for the user to understand and considering the available data, three demand forecasting models were tested: the Croston Model (Croston, 1972), the SBA model (Syntetos and Boylan, 2005) and the simple average in use by the company.

As proposed by the authors, demand for slow moving components should be forecast by the Croston method and the others by the SBA model. Using historical data, the accuracy of these models was compared with the result obtained using the simple average procedure in place in the company. The comparison of the models was made comparing the forecasting errors, considering the mean absolute percentage error (MAPE). Table 2 presents the inter-demand interval (IDI) and the squared coefficient of

variation of the demand sizes (CV^2) for three randomly selected service parts.

The forecasting errors obtained for each component are presented in Table 3. It is clear that there is no forecasting method tested which outperforms the others for all the cases. Thus, it was decided to keep the simple average procedure, already in place in the company. This decision is in accordance with the findings of Sytentos et al. (2015).

Table 2: Demand patterns of three randomly selected service parts.

	SP. 1	SP. 2	SP. 3
IDI	2.35	1.02	1.94
CV^2	1.25	0.37	2.7

Having identified the forecasting model to be used, the support database developed during this project (referred to in the previous section) was used to elaborate a list of all the components with no available supplier. For these components, a single average of the past demand (since time 0) was used to estimate their future demand till the end of their service life. This list was sent to the purchasing department who was responsible for initiating contacts to find potential suppliers for those components.

The demand estimate based on past demand helped the purchasing managers negotiate with the selected suppliers. To avoid the same problem in the future (where components have no supplier available), a simple procedure represented in Figure 4 was implemented in the company.

Table 3: Performance of the forecasting models.

Service Parts	Forecasting model	MAPE
1	SBA ($\alpha = 0.10$)	43%
	Average	42%
2	Croston ($\alpha = 0.17$)	76%
	Average	96%
3	SBA ($\alpha = 0.15$)	202%
	Average	203%

The database developed during this research project allowed an historical record to be created, comprising demand data for the service parts. At the beginning of each year, the list of components is checked to identify all components where demand existed last year. For these components, all suppliers are contacted to verify if they are still able to deliver the required component. If not, the purchasing department will be required to initiate contacts to find a new supplier.

For the components with available suppliers the procurement process in place in the company will be as follows. Whenever the reorder point is attained, an order to satisfy the demand for the next six months will be made, considering the simple average of the past six months' demand.

5 RESULTS

This project allowed the company to make the management of spare parts during the post product life cycle more efficient and reliable, anticipating some of the problems usually felt. To achieve this objective, several procedures were developed to support the procurement decisions for these spare parts, according to the time period remaining that the company has to assure the availability of spare parts.

The comparison of forecasting methods showed that a simple six-month average could produce adequate results to define the order quantity for service parts. The procurement and inventory management procedures for service parts described were implemented in the company and have been used on an ongoing basis.

The implemented procedures led to a 4% reduction in stock outs, raising the service from a level of 95% to 99%. The improvement essentially resulted from a set of formal procedures that guarantee the existence of suppliers for any service parts components in the post product life cycle. This avoided extremely long lead times from a negotiation process which does not meet the expectations of final clients.

Another result of this project was a 10% reduction of the inventory value of service part components in. This was mainly due to eliminating obsolete stock, which also helped increase warehouse efficiency.

6 CONCLUSION

This paper demonstrates how an action research project can provide performance improvements in the management of service parts used in the post product life cycle. Simple, but formal procedures are

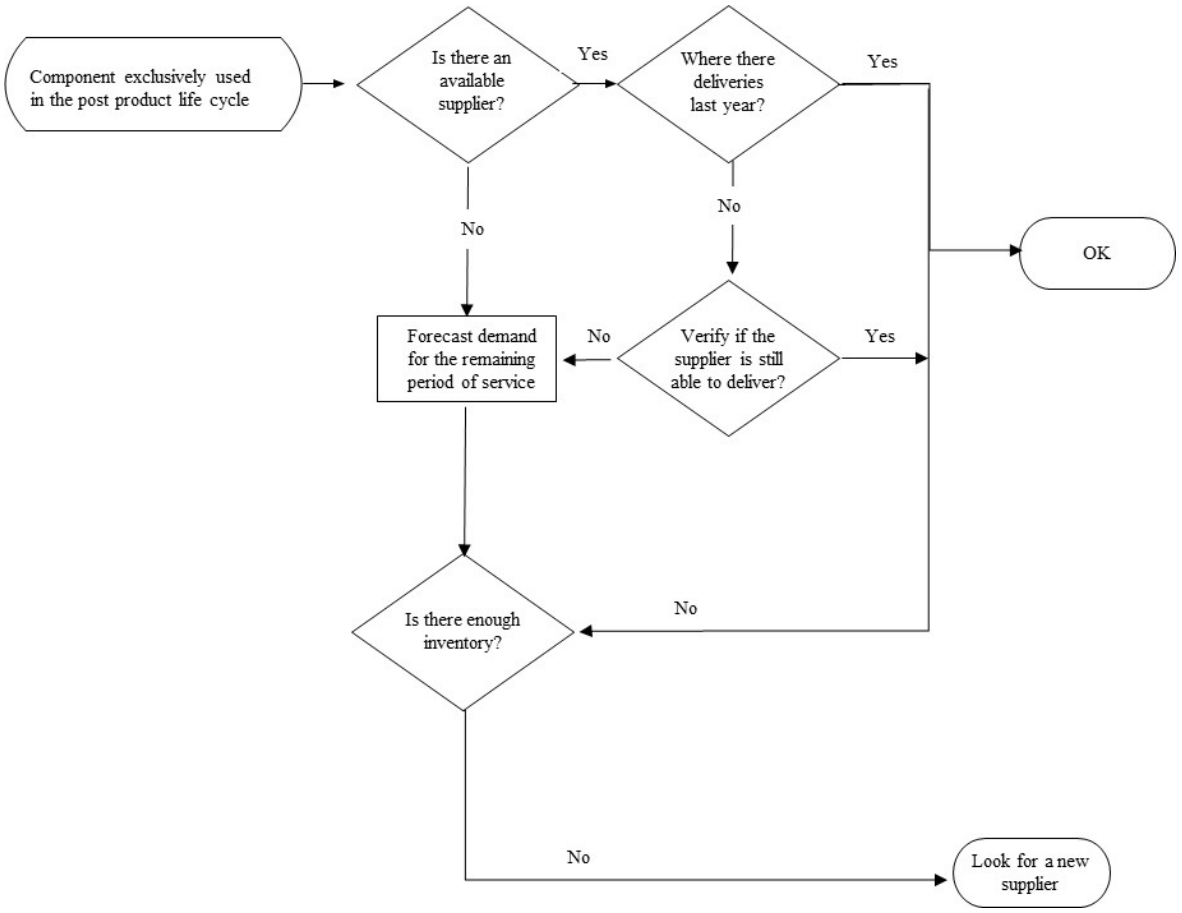

Figure 4: Procedure to guarantee the availability of suppliers.

employed to eliminate obsolete stocks and to manage active service parts. The simplicity of the developed procedures was important for their acceptance in the company, since it is well known that most managers feel uncomfortable if they are unable to understand the models that support the results. Moreover, available methods described in the literature often require data which is not available in most companies.

The procedures implemented during the project make use of a forecasting method. To choose the forecasting method three well known models were tested: the Croston model, the SBA model and a simple six-month average of past demand. It was found that no method outperforms the others, therefore it was decided to maintain the six-month average already in use in the company.

The implementation of the procedures has allowed the company to improve the service levels of service parts for past product life cycle.

The action research model used in the development of the procedures to manage spare parts for the post product life cycle contributed both to achieving practical results in the field and to developing new knowledge. This was achieved through the active participation of both researchers and company employees, which characterises the action research model.

REFERENCES

Bacchetti, A. and Saccani, N., 2012. Spare parts classification and demand forecasting for stock control: Investigating the gap between research and practice. *Omega*, vol. 40, no. 6, pp. 722-737.

Baker, T. and Jayaraman, V., 2012. Managing information and supplies inventory operations in a manufacturing environment. Part 1: An action research study. *International Journal of Production Research*, vol. 50, no. 6, pp. 1666-1681.

Botter, R and Fortuin, L., 2000. Stocking strategy for service parts: a case study. *International Journal of Operation and Production Management*; vol. 20, pp. 656-74.

Croston, J.D., 1972. Forecasting and stock control for intermittent demands. *Operational Research Quarterly*, vol. 23, pp. 289-303.

Cohen, M.A., Zheng, Y.S. and Wang, Y., 1999. Identifying opportunities for improving Teradyne's service-parts logistics system. *Interfaces*, vol. 29, no. 4, pp. 1-18.

Dennis, M.J. and Kambil, A., 2003. Service management: building profits after the sales. *Supply Chain Management Review*, vol. 7, no. 1, pp. 42-48.

Hong, J. S., Koo, H., Lee, C. and Ahn, J., 2008. Forecasting service parts demand for a discontinued product. *IIE Transactions*, vol. 40, No. 7, pp. 640-649.

Inderfurth, K. and Mukherjee, K. 2006. Analysis of spare part acquisition in post product life cycle. Otto von Guericke University. *FEMM* Working Paper 2006/006.

Leifker, N.W., Jones, P.C. and Lowe, T.J., 2014. Determining Optimal Order Amount for End-of-Life Parts Acquisition with Possibility of Contract Extension. *The Engineering Economist*, vol. 59, no. 4, pp.259–281.

Middel, R., Coghlan, D., Brennan, L. and McNichols, T., 2006. Action research in collaborative improvement. *International Journal of Technology Management*, vol. 33, no. 1, pp. 67-91.

Nagarur, N., Hu, T. and Baid, K., 1994. A computer based inventory management system for spare parts. *Industrial Management & Data Systems*, vol. 94, pp. 22-28.

Rego, J.R. and Mesquita, M.A., 2015. Demand forecasting and inventory control: A simulation study on automotive spare parts. *International Journal of Production Economics*, vol. 161, pp.1-16.

Syntetos, A. A. and Boylan, J. E., 2001. On the bias of intermittent demand estimates. *International Journal of Production Economics*, vol. 71, no. 1/3, pp. 457-466.

Syntetos, A. A. and Boylan, J. E., 2005. The Accuracy of Intermittent Demand Estimates. *International Journal of Forecasting*, vol. 21, pp. 303-314.

Syntetos, A. A. and Boylan, J. E. and Croston, J. D., 2005. On the Categorization of Demand Patterns. *Journal of the Operational Research Society*, vol. 56, pp. 495-503.

Teunter, R. H. and Fortuin, L., 1998. End-of-life service: A case study. *European Journal of Operational Research*, vol. 107, no. 1, pp. 19-34.

Teunter, R. H. and Fortuin, L., 1999. End-of-life service. *International Journal of Production Economics*, vol. 59, pp. 487-497.

Teunter, R.H. and Haneveld, W.K. Klein, 1998. The 'final order' problem. *European Journal of Operational Research*, vol. 107, no. 1, pp. 35-44.

Wang, W. and Syntetos, A.A., 2011. Spare parts demand: Linking forecasting to equipment maintenance. *Transportation Research Part E: Logistics and Transportation Review*, vol. 47, no. 6, pp. 1194-1209.

The Possibilistic Reward Method and a Dynamic Extension for the Multi-armed Bandit Problem: A Numerical Study

Miguel Martín, Antonio Jiménez-Martín and Alfonso Mateos
Decision Analysis and Statistics Group, Universidad Politécnica de Madrid,
Campus de Montegancedo S/N, Boadilla del Monte, Spain
miguel.martin@alumnos.upm.es, {antonio.jimenez, alfonso.mateos}@upm.es

Keywords: Multi-armed Bandit Problem, Possibilistic Reward, Numerical Study.

Abstract: Different allocation strategies can be found in the literature to deal with the multi-armed bandit problem under a frequentist view or from a Bayesian perspective. In this paper, we propose a novel allocation strategy, the possibilistic reward method. First, possibilistic reward distributions are used to model the uncertainty about the arm expected rewards, which are then converted into probability distributions using a *pignistic probability transformation*. Finally, a simulation experiment is carried out to find out the one with the highest expected reward, which is then pulled. A parametric probability transformation of the proposed is then introduced together with a dynamic optimization, which implies that neither previous knowledge nor a simulation of the arm distributions is required. A numerical study proves that the proposed method outperforms other policies in the literature in five scenarios: a Bernoulli distribution with very low success probabilities, with success probabilities close to 0.5 and with success probabilities close to 0.5 and Gaussian rewards; and truncated in [0,10] Poisson and exponential distributions.

1 INTRODUCTION

The *multi-armed bandit problem* has been at great depth studied in statistics (Berry and Fristedt, 1985), becoming fundamental in different areas of economics, statistics or artificial intelligence, such as reinforcement learning (Sutton and Barto, 1998) and evolutionary programming (Holland, 1992) .

The name *bandit* comes from imagining a gambler playing with K slot machines. The gambler can pull the arm of any of the machines, which produces a reward payoff. Since the reward distributions are initially unknown, the gambler must use exploratory actions to learn the utility of the individual arms. However, exploration has to be controlled since excessive exploration may lead to unnecessary losses. Thus, the gambler must carefully balance *exploration* and *exploitation*.

In its most basic formulation, a K-armed bandit problem is defined by random variables $X_{i,n}$ for $1 \leq i \leq K$ and $n \geq 1$, where each i is the index of an arm of a bandit. Successive plays of arm i yield rewards $X_{i,1}, X_{i,2}, \ldots$ which are independent and identically distributed according to an unknown law with unknown expectation μ_i. Independence also holds for rewards across arms; i.e., $X_{i,s}$ and $X_{j,t}$ are independent (and usually not identically distributed) for each $1 \leq i < j \leq K$ and each $s,t \geq 1$.

A gambler learning the distributions of the arms' rewards can use all past information to decide about his next action. A *policy*, or *allocation strategy*, A is then an algorithm that chooses the next arm to play based on the sequence of previous plays and obtained rewards. Let n_i be the number of times arm i has been played by A during the first n plays.

The goal is to maximize the sum of the rewards received, or equivalently, to minimize the regret, which is defined as the loss compared to the total reward that can be achieved given full knowledge of the problem, i.e., when the arm giving the highest expected reward is pulled/played all the time. The *regret* of A after n plays can be computed as

$$\mu^* n - \sum_{i=1}^{K} \mu_i E[n_i], \text{ where } \mu^* = \max_{1 \leq i \leq K} \{\mu_i\}, \quad (1)$$

and $E[\cdot]$ denotes expectation.

In this paper, we propose two allocation strategies, the *possibilistic reward* (PR) method and a dynamic extension (DPR), in which the uncertainty about the arm expected rewards are first modelled by means of possibilistic reward distributions. Then, a *pignistic probability transformation* from decision the-

Martin, M., Jiménez-Martín, A. and Mateos, A.
The Possibilistic Reward Method and a Dynamic Extension for the Multi-armed Bandit Problem: A Numerical Study.
In *Proceedings of the 6th International Conference on Operations Research and Enterprise Systems (ICORES 2017)*, pages 75-84
ISBN: 978-989-758-218-9

ory and transferable belief model is used to convert these possibilistic functions into probability distributions following the *insufficient reason principle*. Finally, a simulation experiment is carried out by sampling from each arm according to the corresponding probability distribution to identify the arm with the higher expected reward and play that arm.

The paper is structured as follows. In Section 2 we briefly review the allocation strategies in the literature. In Section 3, we describe the possibilistic reward method and its dynamic extension. A numeric study is carried out in Section 4 to compare the performance of the proposed policies against the best ones in the literature on the basis of five scenarios for reward distributions. Finally, some conclusions are provided in Section 5.

2 ALLOCATION STRATEGY REVIEW

As pointed out in (Garivier and Cappé, 2011), two families of bandit settings can be distinguished. In the first, the distribution of X_{it} is assumed to belong to a family of probability distributions $\{p_\theta, \theta \in \Theta_i\}$, whereas in the second, the rewards are only assumed to be bounded (say, between 0 and 1), and policies rely directly on the estimates of the expected rewards for each arm.

Almost all the policies or allocation strategies in the literature focus on the first family and they can be separated, as cited in (Kaufmann et al., 2012), in two distinct approaches: the frequentist view and the Bayesian approach. In the *frequentist view*, the expected mean rewards corresponding to all arms are considered as unknown deterministic quantities and the aim of the algorithm is to reach the best parameter-dependent performance. In the *Bayesian approach* each arm is characterized by a parameter which is endowed with a prior distribution.

Under the **frequentist view**, Lai and Robbins (Lai and Robbins, 1985) first constructed a theoretical framework for determining optimal policies. For specific families of reward distributions (indexed by a single real parameter), they found that the optimal arm is played exponentially more often than any other arm, at least asymptotically. They also proved that this regret is the best one. Burnetas and Katehakis (Burnetas and Katehakis, 1996) extended their result to multiparameter or non-parametric models.

Later, (Agrawal, 1995) introduced a generic class of index policies termed *upper confidence bounds* (UCB), where the index can be expressed as simple function of the total reward obtained so far from the arm. These policies are thus much easier to compute than Lai and Robbins', yet their regret retains the optimal logarithmic behavior.

From then, different policies based on UCB can be found in the literature. First, Auer et al. (Auer et al., 2002) strengthen previous results by showing simple to implement and computationally efficient policies (UCB1, UCB2 and UCB-Tuned) that achieve logarithmic regret uniformly over time, rather than only asymptotically.

Specifically, policy UCB1 is derived from the index-based policy of (Agrawal, 1995). The index of this policy is the sum of two terms. The first term is simply the current average reward, $\bar{x}_i$, whereas the second is related to the size of the one-sided confidence interval for the average reward within which the true expected reward falls with overwhelming probability. In UCB2, the plays are divided in epochs. In each new epoch an arm i is picked and then played $\tau(r_i+1)-\tau(r_i)$ times, where τ is an exponential function and r_i is the number of epochs played by that arm so far.

In the same paper, UCB1 was extended for the case of normally distributed rewards, which achieves logarithmic regret uniformly over n without knowing means and variances of the reward distributions. Finally, UCB1-Tuned was proposed to more finely tune the expected regret bound for UCB1.

Later, Audibert et al. (Audibert et al., 2009) proposed the UCB-V policy, which is also based on upper confidence bounds but taking into account the variance of the different arms. It uses an empirical version of the Bernstein bound to obtain refined upper confidence bounds. They proved that the regret concentrates only at a polynomial rate in UCB-V and that it outperformed UCB1.

In (Auer and Ortner, 2010) the UCB method of Auer et al. (Auer et al., 2002) was modified, leading to the improved-UCB method. An improved bound on the regret with respect to the optimal reward was also given.

An improved UCB1 algorithm, termed *minimax optimal strategy in the stochastic case* (MOSS), was proposed by Audibert & Bubeck (Audibert and Bubeck, 2010), which achieved the distribution-free optimal rate while still having a distribution-dependent rate logarithmic in the number of plays.

Another class of policies under the frequentist perspective are the Kullback-Leibler (KL)-based algorithms, including DMED, K_{inf}, KL-UCB and kl-UCB.

The *deterministic minimum empirical divergence* (DMED) policy was proposed by Honda & Takemura (Honda and Takemura, 2010) motivated by

a Bayesian viewpoint for the problem (although a Bayesian framework is not used for theoretical analyses). This algorithm, which maintains a list of arms that are close enough to the best one (and which thus must be played), is inspired by large deviations ideas and relies on the availability of the rate function associated to the reward distribution.

In (Maillard et al., 2011), the K_{inf}-based algorithm was analyzed by Maillard et al. It is inspired by the ones studied in (Lai and Robbins, 1985; Burnetas and Katehakis, 1996), taking also into account the full empirical distribution of the observed rewards. The analysis accounted for Bernoulli distributions over the arms and less explicit but finite-time bounds were obtained in the case of finitely supported distributions (whose supports do not need to be known in advance). These results improve on DMED, since finite-time bounds (implying their asymptotic results) are obtained, UCB1, UCB1-Tuned, and UCB-V.

Later, the KL-UCB algorithm and its variant KL-UCB+ were introduced by Garivier & Cappé (Garivier and Cappé, 2011). KL-UCB satisfied a uniformly better regret bound than UCB and its variants for arbitrary bounded rewards, whereas it reached the lower bound of Lai and Robbins when Bernoulli rewards are considered. Besides, simple adaptations of the KL-UCB algorithm were also optimal for rewards generated from exponential families of distributions. Furthermore, a large-scale numerical study comparing KL-UCB with UCB, MOSS, UCB-Tuned, UCB-V, DMED was performed, showing that KL-UCB was remarkably efficient and stable, including for short time horizons.

New algorithms were proposed by Cappé et al. (Cappé et al., 2013) based on upper confidence bounds of the arm rewards computed using different divergence functions. The kl-UCB uses the Kullback-Leibler divergence; whereas the kl-poisson-UCB and the kl-exp-UCB account for families of Poisson and Exponential distributions, respectively. A unified finite-time analysis of the regret of these algorithms shows that they asymptotically match the lower bounds of Lai and Robbins, and Burnetas and Katehakis. Moreover, they provide significant improvements over the state-of-the-art when used with general bounded rewards.

Finally, the *best empirical sampled average* (BESA) algorithm was proposed by Baransi et al. (Baransi et al., 2014). It is not based on the computation of an empirical confidence bounds, nor can it be classified as a KL-based algorithm. BESA is fully non-parametric. As shown in (Baransi et al., 2014), BESA outperforms TS (a Bayesian approach introduced in the next section) and KL-UCB in several scenarios with different types of reward distributions.

Stochastic bandit problems have been analyzed from a **Bayesian perspective**, i.e. the parameter is drawn from a prior distribution instead of considering a deterministic unknown quantity. The Bayesian performance is then defined as the average performance over all possible problem instances weighted by the prior on the parameters.

The origin of this perspective is in the work by Gittins (Gittins, 1979). Gittins' index based policies are a family of Bayesian-optimal policies based on indices that fully characterize each arm given the current history of the game, and at each time step the arm with the highest index will be pulled.

Later, Gittins proposed the Bayes-optimal approach (Gittins, 1989) that directly maximizes expected cumulative rewards with respect to a given prior distribution.

A lesser known family of algorithms to solve bandit problems is the so-called *probability matching* or *Thompson sampling* (TS). The idea of TS is to randomly draw each arm according to its probability of being optimal. In contrast to Gittins' index, TS can often be efficiently implemented (Chapelle and Li, 2001). Despite its simplicity, TS achieved state-of-the-art results, and in some cases significantly outperformed other alternatives, like UCB methods.

Finally, Bayes-UCB was proposed by Kaufmann et al. (Kaufmann et al., 2012) inspired by the Bayesian interpretation of the problem but retaining the simplicity of UCB-like algorithms. It constitutes a unifying framework for several UCB variants addressing different bandit problems.

3 POSSIBILISTIC REWARD METHOD

The allocation strategy we propose accounts for the frequentist view but they cannot be classified as either a UCB method nor a Kullback-Leibler (KL)-based algorithm. The basic idea is as follows: the uncertainty about the arm expected rewards are first modelled by means of possibilistic reward distributions derived from a set of infinite nested confidence intervals around the expected value on the basis of Chernoff-Hoeffding inequality. Then, we follow the *pignistic probability transformation* from decision theory and transferable belief model (Smets, 2000), that establishes that when we have a plausibility function, such as a possibility function, and any further information in order to make a decision, we can convert this function into an probability distribution following the *in-*

sufficient reason principle.

Once we have a probability distribution for the reward in each arm, then a simulation experiment is carried out by sampling from each arm according to their probability distributions to find out the one with the highest expected reward higher. Finally, the picked arm is played and a real reward is output.

We shall first introduce the algorithm for rewards bounded between [0,1] in the real line for simplicity and then, we will extend it for any real interval. The starting point of the method we propose is Chernoff-Hoeffding inequality (Hoeffding, 1963), which provides an upper bound on the probability that the sum of random variables deviates from its expected value, which for [0,1] bounded rewards leads to:

$$P\left(\left|\frac{1}{n}\sum_{t=1}^{n}X_t - E[X]\right| > \varepsilon\right) \leq 2e^{-2n\varepsilon^2} \Rightarrow$$
$$P\left(\left|\frac{1}{n}\sum_{t=1}^{n}X_t - E[X]\right| \leq \varepsilon\right) \geq 1 - 2e^{-2n\varepsilon^2} \Rightarrow$$
$$P\left(E[X] \in \left[\frac{1}{n}\sum_{t=1}^{n}X_t - \varepsilon, \frac{1}{n}\sum_{t=1}^{n}X_t + \varepsilon\right]\right) \geq 1 - 2e^{-2n\varepsilon^2}.$$

It can be used for building an infinite set of nested confidence intervals, where the confidence level of the expected reward ($E[X]$) in the interval $I = [\frac{1}{n}\sum_{t=1}^{n}X_t - \varepsilon, \frac{1}{n}\sum_{t=1}^{n}X_t + \varepsilon]$ is $1 - 2e^{-2n\varepsilon^2}$.

Besides, a fuzzy function representing a possibilistic distribution can be implemented from nested confidence intervals (Dubois et al., 2004):

$$\pi(x) = sup\{1 - P(I), x \in I\}.$$

Consequently, in our approach for confidence intervals based on Hoeffding inequality, the *sup* of each x will be the bound of minimum interval around the mean ($\frac{1}{n}\sum_{t=1}^{n}X_t$) where x is included. That is, the interval with $\varepsilon = \left|\frac{1}{n}\sum_{t=1}^{n}X_t - x\right|$.

If we consider $\hat{\mu}_n = \frac{1}{n}\sum_{t=1}^{n}X_t$, for simplicity, then we have:

$$\pi(x) = \begin{cases} min\{1, 2e^{-2n_i \times (\hat{\mu}_n - x)^2}\}, & \text{if } 0 \leq x \leq 1 \\ 0, & \text{otherwise} \end{cases}.$$

Note that $\pi(x)$ is truncated in $[0,1]$ both in the x axis, due to the bounded rewards, and the y axis, since a possibility measure cannot be greater than 1. Fig. 1 shows several examples of possibilistic rewards distributions.

3.1 A Pignistic Probability Transformation

Once the arm expected rewards are modelled by means of possibilistic functions, next step consists of

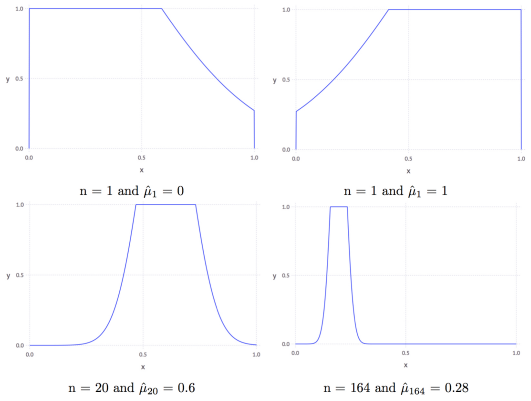

Figure 1: Possibilistic rewards distributions.

picking the arm to pull on the basis of that uncertainty. For this, we follow the *pignistic probability transformation* from decision theory and transferable belief model (Smets, 2000), which, in summary, establishes that when we have a plausibility function, such as a possibility function, and any further information in order to make a decision, we can convert this function into an probability distribution following the *insufficient reason principle* (Dupont, 1978), or consider equipossible the same thing that equiprobable. In our case, it can be performed by dividing $\pi(x)$ function by $\int_0^1 min\{1, 1 - e^{-2n_i \times (\hat{\mu}_n - x)^2}\}dx$.

However, further information is available in form of restrictions that allow us to model a better approximation of the probability functions. Since a probability density function must be continuous and integrable, we have to smooth the gaps that appear between points close to 0 and 1. Besides, we know that the probability distribution should be a unimodal distribution around the sampling average $\hat{\mu}_n$. Thus, the function must be monotonic strictly increasing in $[0, \hat{\mu}_n)$ and monotonic strictly decreasing in $(\hat{\mu}_n, 1]$. We propose the following approximation to incorporate the above restrictions:

1. $\pi(x)$ is transformed into an intermediate function $\pi_r(x)$ as follows:
   (a) Multiply the not truncated original function, $2e^{-2n_i \times (\hat{\mu}_n - x)^2}$, by $\frac{1}{2}$ in order to reach a maximum value 1.
   (b) Fit the resulting function in order to have $\pi_r(0) = 0$ and $\pi_r(1) = 0$:

$$\Delta_{low} = e^{-2n_i \times (\hat{\mu}_n)^2}, \qquad \Delta_{up} = e^{-2n_i \times (\hat{\mu}_n - 1)^2},$$

$$\pi_r(x) = \begin{cases} \frac{e^{-2n_i \times (\hat{\mu}_n - x)^2} - \Delta_{low}}{1 - \Delta_{low}}, & \text{if } x \leq \hat{\mu}_n \\ \frac{e^{-2n_i \times (\hat{\mu}_n - x)^2} - \Delta_{up}}{1 - \Delta_{up}}, & \text{if } x > \hat{\mu}_n \\ 0, & \text{otherwise} \end{cases}.$$

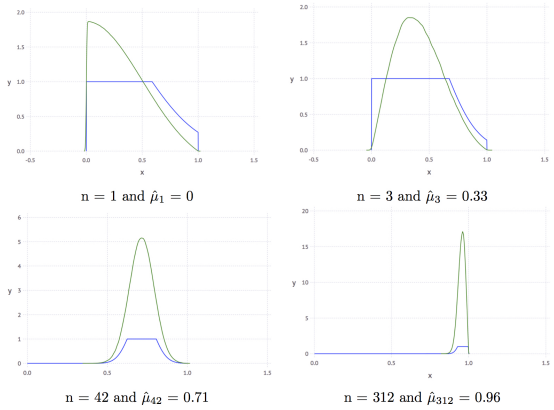

Figure 2: Pignistic probability transformation examples.

Two exceptions have to be considered. When all the rewards of past plays are 0 or 1, then the transformations to reach $\pi_r(0) = 0$ or $\pi_r(1) = 0$ are not applied, respectively.

2. The pignistic transformation is applied to $\pi_r(x)$ by dividing by $\int_0^1 \pi_r(x)dx$, leading to the probability distribution

$$P(x) = \pi_r(x)/C, \quad \text{with } C = \int_0^1 \pi_r(x)dx.$$

Fig. 2 shows the application of the pignistic probability transformation to derive a probability distribution (in green) from the $\pi(x)$ functions (in blue) in Fig. 1.

The next step is similar to Thompson sampling (TS) (Chapelle and Li, 2001). Once we have built the pignistic probabilities for all the arms, we pick the arm with the highest expected reward. For this, we carry out a simulation experiment by sampling from each arm according to their probability distributions. Finally, the picked arm is pulled/played and a real reward is output. Then, the possibilistic function corresponding to the picked arm is updated and started again.

3.2 Parametric Probability Transformation and Dynamic Optimization

In the previous section, rewards were bound to the interval [0,1] and the most used possibility-probability transformation according to pignistic or maximal entropy methods (Smets, 2000) was implemented. Now, we extend rewards to any real interval $[a,b]$ and interpret the possibility distribution $\pi_r(x)$ as a probability distribution set that encloses any distribution $P(x)$ such as $\forall A = [a,b] \rightarrow \pi_r(x \in A) \leq P(x \in A) \leq 1 - \pi_r(x \notin A)$. Consequently, another distribution enclosed by $\pi_r(x)$ that minimizes the expected regret for any particular reward distribution could be used.

In order to trade off performance and computational cost issues, we were able to modify our previous probabilistic-possibilistic transformation to create a family of probabilities just adding an α parameter as follows:

$$P(x) = \pi_\alpha(x)/C \quad \text{with} \quad C = \int_a^b \pi_\alpha(x)dx$$

and

$$\pi_\alpha(x) = \begin{cases} \frac{e^{-2n_i \times \alpha(\frac{\hat{\mu}_n - x}{b-a})^2} - \Delta\alpha_{low}}{1 - \Delta\alpha_{low}}, & \text{if } x \leq \hat{\mu}_n \\ \frac{e^{-2n_i \times \alpha(\frac{\hat{\mu}_n - x}{b-a})^2} - \Delta\alpha_{up}}{1 - \Delta\alpha_{up}}, & \text{if } x > \hat{\mu}_n \\ 0, & \text{otherwise} \end{cases},$$

where

$$\Delta\alpha_{low} = e^{-2n_i \times \alpha(\frac{\hat{\mu}_n}{b-a})^2}, \Delta\alpha_{up} = e^{-2n_i \times \alpha(\frac{\hat{\mu}_n - 1}{b-a})^2}, \text{and } \alpha > 1.$$

By adding parameter α, it is possible to adjust the transformation for any particular reward distribution to minimize the expected regret. For this, an optimization process for parameter α will be required.

Alternatively to manually tuning parameter α, we propose modifying the PR algorithm to dynamically tune it while bearing in mind the minimization of the expected regret. Thus, the advantage of the new *dynamic possibilistic reward* (DPR) is that it requires neither previous knowledge nor a simulation of the arm distributions. In fact, the reward distributions are not known in the majority of the cases. Besides, the performance of the DPR against PR and other policies in terms of expected regrets will be analyzed in the next section.

Several experiments have shown that the scale parameter α is correlated with the inverse of the variance of the reward distribution shown by the experiment. As such, analogously to Auer et al. (Auer et al., 2002), for practical purposes we can fix parameter α as

$$\alpha = 0.5 \times \frac{(b-a)^2}{\tilde{var}}, \tag{2}$$

where $\tilde{var}$ is the sample variance of the rewards seen by the agent and $[a,b]$ the reward interval.

4 NUMERICAL STUDY

In this section, we show the results of a numerical study in which we have compared the performance of

PR and DPR methods against other allocation strategies in the literature. Specifically, we have chosen KL-UCB, DMED+, BESA, TS and Bayes-UCB, since they are the most recent proposals and they outperform other allocation strategies (Chapelle and Li, 2001; Cappé et al., 2013; Baransi et al., 2014). Additionally, we have also considered the UCB1 policy, since it was one of the first proposals in the literature that accounts for the uncertainty about the expected reward.

We have selected five different scenarios for comparison. For this, we have reviewed numerical studies in the literature to find out the most difficult and representative scenarios. An experiment consisting on 50,000 simulations with 20,000 iterations each was carried out in the five scenarios. The Python code available at http://mloss.org/software/view/415 was used for simulations, whereas those policies not implemented in that library have been developed by the authors, including DMED+, BESA, PR and DPR.

4.1 Scenario 1: Bernoulli Distribution and Very Low Expected Rewards

This scenario is a simplification of a real situation in on-line marketing and digital advertising. Specifically, advertising is displayed in banner spaces and in case the customer clicks on the banner then s/he is redirected to the page that offers the product. This is considered a success with a prize of value 1. The success ratios in these campaigns are usually quite low, being about 1%. For this, ten arms will be used with a Bernoulli distribution and the following parameters: [0.1, 0.05, 0.05, 0.05, 0.02, 0.02, 0.02, 0.01, 0.01, 0.01].

First, a simulation is carried out to find out the best value for parameter α to be used in the PR method, see Fig. 3. $\alpha = 8$ is identified as the best value and used for this scenario 1. Note that in DPR, no previous knowledge regarding the scenario is required.

Now, the 50,000 simulations with 20,000 iterations each are carried out. Fig. 4 shows the evolution of the regret for the different allocation strategies under comparison along the 20,000 iterations corresponding to one simulation (using a logarithmic scale), whereas Fig. 5 shows the multiple boxplot corresponding to regrets throughout the 50,000 simulations.

The first two columns in Table 1 show the mean regrets and standard deviations for the policies. The three with lowest mean regrets are highlighted in bold, corresponding to DPR, PR and BESA, respectively. The variance is similar for all the policies under consideration. It is important to note that although PR

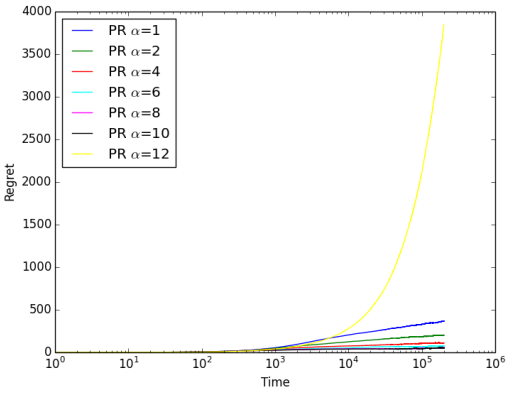

Figure 3: Selecting parameter α for PR in scenario 1.

($\alpha = 8$) slightly outperforms DPR, DPR requires neither previous knowledge nor a simulation regarding the arm distributions, which makes DPR more suitable in a real environment.

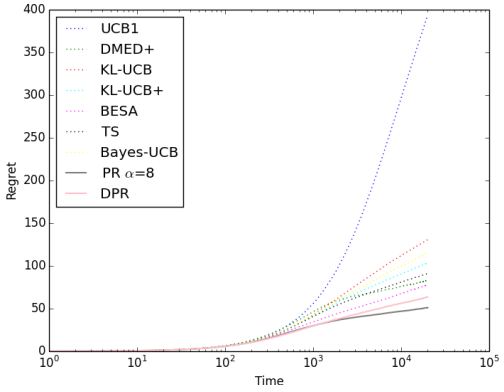

Figure 4: Policies in one simulation for scenario 1,

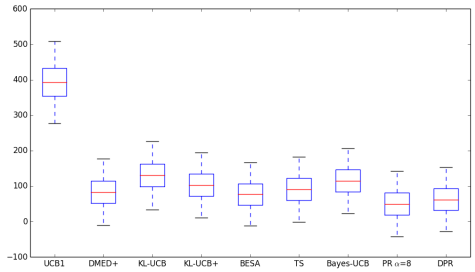

Figure 5: Multiple boxplot for policies in scenario 1.

Note that in the above multiple boxplots negative regret values are displayed. It could be considered an error at first sight. The explanation is as follows: the optimum expected reward μ^* used to compute regrets is the theoretic value from the distribution, see Eq. (1). For instance, in an arm with Bernoulli distribution with parameter 0.1, μ^* after n plays is $0.1 \times n$. However, in the simulation the number of success if the arm is played n times may be higher than this

Table 1: Statistics in scenarios 1, 2 and 3.

	Bernoulli (low)		Bernoulli (med)		Bernoulli (G)	
	Mean	σ	*Mean*	σ	*Mean*	σ
UCB1	393.7	57.6	490.9	104.9	2029.1	125.9
DMED+	83.1	46.1	356.8	151.5	889.8	313.2
KL-UCB	130.7	47.9	491.5	104.3	1169.6	233.2
KL-UCB+	103.3	46.0	349.7	104.7	879.7	254.5
BESA	**78.1**	53.9	**281.6**	260.9	**768.75**	399.2
TS	91.1	45.6	**284.2**	125.1	-	-
Bayes-UCB	115.1	46.6	366.3	104.5	-	-
PR	**51.1***	49.2	380.5	426.2	**431.0***	383.5
DPR	**63.6**	49.1	**214.6***	185.1	**643.0**	387.1

amount, overall in the first iterations, leading to negative regret values.

4.2 Scenario 2: Bernoulli Distribution and Medium Expected Rewards

In this scenario, we still consider a Bernoulli distribution but now parameters are very similar in the 10 arms and close to 0.5. This leads to the greatest variances in the distributions, where in almost all arms in half of the cases they have a value 1 and 0 in the other half. Thus, it becomes harder for algorithms to reach the optimal solution. Moreover, if an intensive search is not carried out along a sufficient number of iterations, we could easily reach sub-optimal solutions. The parameters for the 10 arms under consideration are: [0.5, 0.45, 0.45, 0.45, 0.45, 0.45, 0.45, 0.45, 0.45, 0.45].

First, a simulation was carried out again to find out the best value for parameter α to be used in the PR method in this scenario and $\alpha = 2$ was selected.

In Fig. 6 the regrets throughout the 50,000 simulations corresponding to the different policies are shown by means of a multiple boxplot.

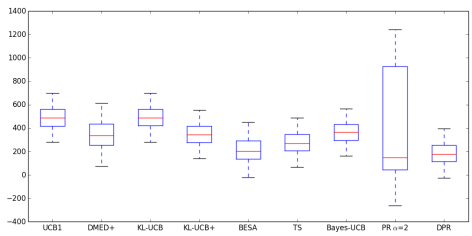

Figure 6: Multiple boxplot for policies in scenario 2.

It draws to attention the high variability on the regret values for the PR method ($\alpha = 2$). Fig. 7 shows the histograms corresponding to PR ($\alpha = 2$) and DPR. As expected, regret values are mainly concentrated close to value 0 and around value 1000. Note that the success probability is 0.45 in 9 out of the 10 arms, whereas it is 0.5 for the other one. The probability difference is then 0.05 and as the reward is 1 (if successful) and 20,000 iterations are carried out, we expect regret values around value 1000.

The dotted vertical lines in the histograms represent the regret value 0 and the mean regret throughout the 50,000 simulations. Note that the mean regret for PR is not representative. The number of regret observations around the value 1000 is considerably higher for PR than DPR, which explains the higher standard deviation in PR and demonstrates that DPR outperforms PR in this scenario.

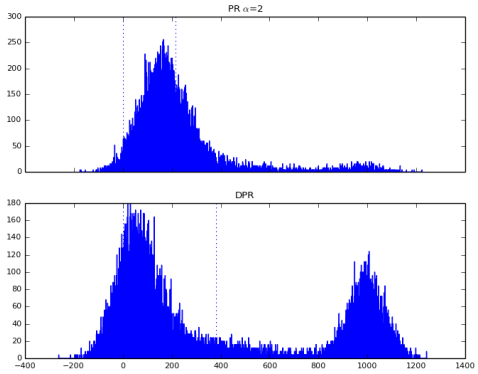

Figure 7: Histograms for PR ($\alpha = 2$) and DPR in scenario 2.

The three allocation strategies with lowest average regrets, highlighted in bold in the third and fourth columns in Table 1, corresponds to DPR, BESA and TS, respectively. However, DPR outperforms BESA and TS, whose performances are very similar but BESA has a higher variability.

4.3 Scenario 3: Bernoulli Distribution and Gaussian Rewards

In this scenario, Bernoulli distributions with very low expected rewards (about 1% success ratios) are again considered but now rewards are not 0 or 1, they are normally distributed. This scenario has never been considered in the literature but we consider it interesting for analysis. We can also face this scenario in on-line marketing and digital advertising. As in scenario 1, advertising is displayed in banner spaces and in case the customer clicks on the banner then s/he is redirected to the page that offers the product. However, in this new scenario the customer may buy more than one product, the number of which is modeled by a normal distribution.

The success ratios in these campaigns are usually quite low, as in scenario 1, being about 1%. For this, the ten arms will be used with a Bernoulli distribution

and the following parameters: [0.1, 0.05, 0.05, 0.05, 0.02, 0.02, 0.02, 0.01, 0.01, 0.01]. Besides, the same $\sigma = 0.5$ is used for the normal distributions, whereas the following means (μ) are considered: [1, 2, 1, 3, 5, 1, 10, 1, 8, 1]. Moreover, all rewards are truncated between 0 and 10. Thus, the expected rewards for the ten arms are [0.1, 0.1, 0.05, 0.15, 0.1, 0.02, 0.2, 0.01, 0.08, 0.01], and the seventh arm is the one with the highest expected reward.

TS and Bayes-UCB policies are not analyzed in this scenario since both cannot be applied. $\alpha = 70$ will be used in the PR method. Fig. 8 shows the multiple boxplot for the regrets throughout the 50,000 simulations, whereas the mean regrets and the standard deviations are shown in last two columns of Table 1.

The three policies with lowest mean regrets, highlighted in bold in Table 1, correspond to PR, DPR and BESA, respectively, the three with a similar variability. However, PR outperforms DPR and BESA in this scenario.

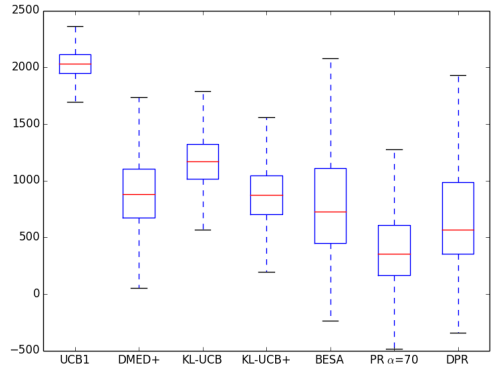

Figure 8: Multiple boxplot for policies in scenario 3.

4.4 Scenario 4: Truncated Poisson Distribution

A truncated in [0,10] Poisson distribution is used in this scenario. It is useful to model real scenarios where the reward depends on the number of times an event happens or is performed in a time unit, for instance, the number of followers that click on the "like" button during two days since it is uploaded. The values for parameter λ in the Poisson distribution for each arm are: [0.75, 1, 1.25, 1.5, 1.75, 2, 2.25].

The variant kl-poisson-UCB was also considered for analysis, whereas TS and Bayes-UCB will no longer be considered since both cannot be applied in this scenario.

First, the selected value for parameter α to be used in the PR method in this scenario is 12. Fig. 9 shows the multiple boxplot for the regrets throughout the 50,000 simulations, whereas the first two columns in

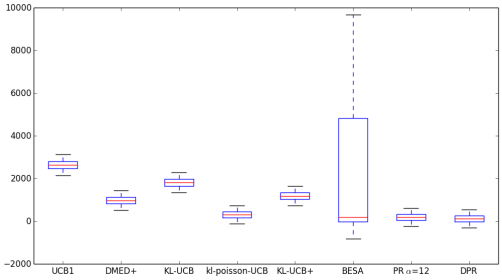

Figure 9: Multiple boxplot in the fourth scenario (Poisson).

Table 2 show the mean regrets and standard deviations.

One should observe the high variability on the regret values in BESA. Fig. 10 shows the histograms corresponding to BESA and DPR. As expected, regret values are mainly concentrated around 7 values (0, 5000, 10,000, 15,000, 20,000, 25,000, 30,000), with the highest number of regret values around 0, followed by 5000 and so on. Note that the different of λ values in the 7 arms is 0.25 and $0.25 \times 20,000$ iterations carried out in each simulation is 5000, which matches up with the amount incremented in the 7 points the regrets are concentrated around.

The number of regret observations around the value 0 regarding the remaining values is considerably higher for DPR than BESA, which explains a higher standard deviation in BESA and demonstrates that BESA is outperformed by the other policies in this scenario.

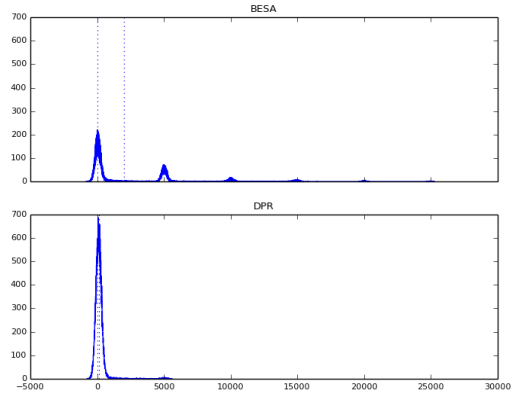

Figure 10: Histograms for BESA and DPR.

DPR again outperforms the other algorithms on the basis of the mean regrets, including PR ($\alpha = 12$), see Table 2. kl-poisson-UCB Poisson is the only policy whose results are close to DPR and PR. However, the variability in DPR is higher than in all the other policies apart from BESA.

Table 2: Statistics in scenarios 4 and 5.

	Truncated Poisson		Truncated Exponential	
	Mean	σ	*Mean*	σ
UCB1	2632.65	246.03	1295.79	514.03
DMED+	978.56	225.24	**645.70**	493.8
KL-UCB	1817.4	236.57	1219.98	510.69
kl-poisson-UCB	**314.99**	201.79	-	-
KL-exp-UCB	-	-	786.30	498.16
KL-UCB+	1190.64	225.82	813.45	494.59
BESA	2015.73	3561.5	755.87	2323.22
PR	**196.24**	212.45	**580.31**	2182.02
DPR	**153.3***	409.17	**282.83***	814.72

4.5 Scenario 5: Truncated Exponential Distribution

A truncated exponential distribution is selected in this scenario, since it is usually used to compare allocation strategies in the literature. It is used to model continuous rewards, and for scales greater than 1 too. Moreover, it is appropriate to model real situations where the reward depends on the time between two consecutive events, for instance, the time between a recommendation is offered on-line until the customer ends up buying. The values for parameter λ in the exponential distribution for each arm are: [1, 1/2, 1/3, 1/4, 1/5, 1/6].

The variant kl-exp-UCB was incorporated into the analysis in this scenario, whereas TS and Bayes-UCB cannot be applied.

The best value for parameter α for the PR method is 6. Fig. 11 shows the multiple boxplot for the regrets throughout the 50,000 simulations. The mean regret and the standard deviations are shown in last two columns of Table 2.

PR and DPR again outperform the other policies, with PDR being very similar to but slightly better than PR in this scenario. Moreover, DPR requires neither previously knowledge nor a simulation of the arm distributions, what makes DPR more suitable in a real environment. The best four policies are the same as in scenario 4, with a truncated Poisson, changing the KL-poisson-UCB with KL-exp-UCB.

5 CONCLUSIONS

In this paper we propose a novel allocation strategy, the possibilistic reward method, and a dynamic extension for the multi-armed bandit problem. In both methods the uncertainty about the arm expected rewards are first modelled by means of possibilistic reward distributions derived from a set of infinite nested confidence intervals around the expected value. Then, a *pignistic probability transformation* is used to convert these possibilistic function into probability distributions. Finally, a simulation experiment is carried out by sampling from each arm to find out the one with the highest expected reward and play that arm.

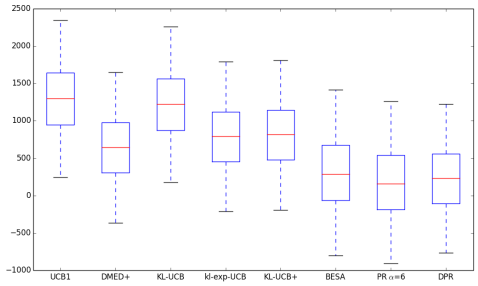

Figure 11: Multiple boxplot for policies in the fifth scenario.

A numerical study suggests that the proposed method outperforms other policies in the literature. For this, five complex and representative scenarios have been selected for analysis: a Bernoulli distribution with very low success probabilities; a Bernoulli distribution with success probabilities close to 0.5, which leads to the greatest variances in the distributions; a Bernoulli distribution with success probabilities close to 0.5 and Gaussian rewards; a truncated in [0,10] Poisson distribution; and a truncated in [0,10] exponential distribution.

In the first three scenarios, in which the Bernoulli distribution is considered, PR or DPR are the policies with the lowest mean regret and with similar variability regarding the other policies. BESA is the only policy with results that are close to DPR and PR, mainly in scenario 1. Besides, DPR and PR clearly outperform the other policies in scenarios 4 and 5, in which a truncated Poisson and exponential are considered, respectively. In both cases, DPR outperforms PR.

ACKNOWLEDGEMENTS

The paper was supported by the Spanish Ministry of Economy and Competitiveness MTM2014-56949-C3-2-R.

REFERENCES

Agrawal, R. (1995). Regret bounds and minimax policies under partial monitoring. *Advances in Applied Probability*, 27(4):1054–1078.

Audibert, J.-Y. and Bubeck, S. (2010). Sample mean based index policies by o(log n) regret for the multi-armed bandit problem. *Journal of Machine Learning Research*, 11:2785–2836.

Audibert, J.-Y., Munos, R., and Szepervári, C. (2009). Exploration-exploitation trade-off using variance estimates in multi-armed bandits. *Theoretical Computer Science*, 410:1876–1902.

Auer, P., Cesa-Bianchi, N., and Fischer, P. (2002). Finite-time analysis of the multiarmed bandit problem. *Machine Learning*, 47:235–256.

Auer, P. and Ortner, R. (2010). UCB revisited: Improved regret bounds for the stochastic multi-armed bandit problem. *Advances in Applied Mathematics*, 61:55–65.

Baransi, A., Maillard, O., and Mannor, S. (2014). Sub-sampling for multi-armed bandits. In *Proceedings of the European Conference on Machine Learning*, page 13.

Berry, D. A. and Fristedt, B. (1985). *Bandit Problems: Sequential Allocation of Experiments*. Chapman and Hall, London.

Burnetas, A. N. and Katehakis, M. N. (1996). Optimal adaptive policies for sequential allocation problems. *Advances in Applied Mathematics*, 17(2):122 – 142.

Cappé, O., Garivier, A., Maillard, O., Munos, R., and Stoltz, G. (2013). Kullbackleibler upper confidence bounds for optimal sequential allocation. *Annals of Statistics*, 41:1516–1541.

Chapelle, O. and Li, L. (2001). An empirical evaluation of thompson sampling. In *Advances in Neural Information Processing Systems*, pages 2249–2257.

Dubois, D., Foulloy, L., Mauris, G., and Prade, H. (2004). Probability-possibility transformations, triangular fuzzy sets, and probabilistic inequalities. *Reliable Computing*, 10:273–297.

Dupont, P. (1978). Laplace and the indifference principle in the 'essai philosophique des probabilits.'. *Rendiconti del Seminario Matematico Universit e Politecnico di Torino*, 36:125–137.

Garivier, A. and Cappé, O. (2011). The kl-ucb algorithm for bounded stochastic bandits and beyond. Technical report, arXiv preprint arXiv:1102.2490.

Gittins, J. (1979). Bandit processes and dynamic allocation indices. *Journal of the Royal Statistical Society*, 41:148–177.

Gittins, J. (1989). *Multi-armed Bandit Allocation Indices. Wiley Interscience Series in Systems and Optimization*. John Wiley and Sons Inc., New York, USA.

Hoeffding, W. (1963). Probability inequalities for sums of bounded random variables. *Advances in Applied Mathematics*, 58:13–30.

Holland, J. (1992). *Adaptation in Natural and Artificial Systems*. MIT Press/Bradford Books, Cambridge, MA, USA.

Honda, J. and Takemura, A. (2010). An asymptotically optimal bandit algorithm for bounded support models. In *Proceedings of the 24th annual Conference on Learning Theory*, pages 67–79.

Kaufmann, E., Cappé, O., and Garivier, A. (2012). On bayesian upper confidence bounds for bandit problems. In *International Conference on Artificial Intelligence and Statistics*, pages 592–600.

Lai, T. and Robbins, H. (1985). Asymptotically efficient adaptive allocation rules. *Advances in Applied Mathematics*, 6:4–22.

Maillard, O., Munos, R., and Stoltz, G. (2011). Finite-time analysis of multi-armed bandits problems with kullback-leibler divergences. In *Proceedings of the 24th Annual Conference on Learning Theory*, pages 497–514.

Smets, P. (2000). Data fusion in the transferable belief model. In *Proceedings of the Third International Conference on Information Fusion*, volume 1, pages 21–33.

Sutton, R. S. and Barto, A. G. (1998). *Introduction to Reinforcement Learning*. MIT Press, Cambridge, MA, USA, 1st edition.

A Dynamic and Collaborative Truck Appointment Management System in Container Terminals

Ahmed Azab[1], Ahmed Karam[2] and Amr Eltawil[1]
[1]*Department of Industrial Engineering and Systems Management, Egypt-Japan University of Science and Technology, POBox 179, New Borg Elrab city, 21934 Alexandria, Egypt*
[2]*Mechanical Engineering Department, Faculty of Engineering at Shoubra, Benha University, Cairo, Egypt*
{ahmed.azab, eltawil}@ejust.edu.eg, ahmed.mustafa@feng.bu.edu.eg

Keywords: Container Terminal, Integrated Simulation Optimization, Dynamic Model, Collaboration, Truck Appointment System.

Abstract: Given the rising growth in containerized trade, Container Terminals (CTs) are facing truck congestion at the gate and yard. Truck congestion problems not only result in long queues of trucks at the terminal gates and yards but also leads to long turn times of trucks and environmentally harmful emissions. As a result, many terminals are seeking to set strategies and develop new approaches to reduce the congestions in various terminal areas. In this paper, we tackle the truck congestion problem with a new dynamic and collaborative truck appointment system. The collaboration provides shared decision making among the trucking companies and the CT management, while the dynamic features of the proposed system enable both stakeholders to cope with the dynamic nature of the truck scheduling problem. The new Dynamic Collaboration Truck Appointment System (DCTAS) is developed using an integrated simulation-optimization approach. The proposed approach integrates an MIP model with a discrete event simulation model. Results show that the proposed DCTAS could reduce the terminal congestions and flatten the workload peaks in the terminal.

1 INTRODUCTION

In maritime logistics, one of the most important performance measures is the delivery time of a container to a customer. The containerized cargos are transported through the global supply chain, and each chain consumes a part of the total delivery time. Due to that, the decision makers in each phase of the transhipment operations are trying to reduce the total transshipment time taking into consideration the financial, economic, environmental, and even political barriers.

Container terminals are essential nodes in the global supply chain due to the tremendous growth of the containerized cargo trade around the world (figure 1). As a result, the research interests are directed to tackle the CTs' problems and develop robust and reliable solutions for the terminal operators. Figure 2 illustrates the various areas in CTs. Most of CTs can be divided into three main areas: Seaside, yard area, and landside. The seaside is the area where the vessels are berthed, loaded and/or unloaded with the desired containers using quay cranes. Containers are transported by internal transport means like manned trucks or automated guided vehicles to be temporarily stored in the yard blocks. At the yard, handling operations are performed using the yard equipment like yard cranes and straddle carriers. The operations in each yard block depend on vessel's operations and hinterland operations. On the other side of the terminal, the landside comprises the gates, which are provided with X-Ray scanners where an import container is allowed to leave the terminal, and an export container is allowed to enter the yard area.

CT problems were classified by (Bierwirth and Meisel 2010) to operational problems and strategic problems. The operational problems are related to the scheduling of operations and assignment of the resources. Operational problems are solved simultaneously in the short term and solutions and schedules are updated daily. Examples include berth allocation and quay crane assignment (Karam and Eltawil 2015; Karam and Eltawil 2016), and container handling problems (Mohamed Gheitha et al. 2014; Gheith et al. 2016). In this paper, more discussion about landside problems will be introduced mainly for managing the external trucks arrival.

Azab, A., Karam, A. and Eltawil, A.
A Dynamic and Collaborative Truck Appointment Management System in Container Terminals.
In *Proceedings of the 6th International Conference on Operations Research and Enterprise Systems (ICORES 2017)*, pages 85-95
ISBN: 978-989-758-218-9

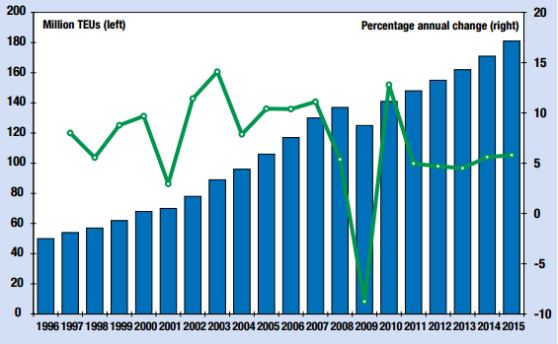

Figure 1: Global containerized trade, 1996–2015 (million TEUs and percentage annual change). (Source: UNCTAD secretariat).

Export/import containers are delivered/picked up from the terminal by external trucks. These trucks are operated by trucking companies to perform the delivery/pick-up operations in minimal time and cost. On the other hand, CTs set the appropriate schedules and rules to reduce the congestion in various terminal areas. To manage the transaction between the terminal and the trucking companies, some CTs adopted a Truck Appointment System (TAS) to control the arrival of external trucks, while some other terminals do not follow an appointment system. The appointment systems can be used to increase the service quality in CTs for all transshipment means; trucks, train, barges and vessels (Zehendner and Feillet 2014). Many terminals have developed Truck Appointment Systems (TAS) to make balance in truck arrivals to alleviate the terminal rush hours. The benefits of the TAS have been reported in literature as will be shown later. In this paper, we propose a dynamic and collaborative appointment management solution to support decision makers in the terminals gain more benefits from applying the appointment systems.

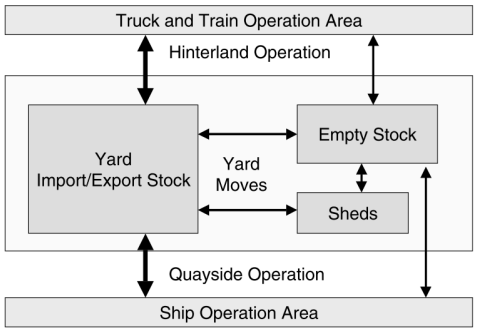

Figure 2: Operation areas of a seaport container terminal and flow of transports (Steenken et al. 2005).

The remaining of the paper is organized as follows. Section 2 discusses related literature. The proposed system is explained in section 3. Section 4 presents the numerical experiment. Section 5 shows the results, and section 6 illustrates the conclusion.

2 PREVIOUS WORK

Landside operations affect the whole terminal performance and therefore, decision problems related to landside operations received an increasing interest in literature. Scheduling the arrival of external trucks is considered one of the most important landside problems addressed in the literature. One of the earliest case studies is conducted by Murty et al. (2005) at HongKong International Terminal (HIT) , which resulted in the reduction of terminal congestion using the truck appointment system. Authors developed a decision support system based on an information system to help in making the terminal operational decisions efficiently. A comprehensive study by Morais and Lord (2006) is developed to review the appointment system implemented in terminals across North America. They adopted various strategies to reduce the idling of truck, congestion at gates and emissions related to CT drayage operations. Namboothiri and Erera, (2008) used a planning strategy for pickup and delivery operations in CTs based on an integer programming heuristic. The sequence of the drayage operations is determined by minimizing the transportation cost. An improvement in productivity and capacity utilization is obtained with some sensitivity to poor selection of the appointment time.

Huynh and Walton (2008) and Huynh (2009) investigated limiting the arrivals and individual appointments versus the block appointments. In addition, they introduced combined mathematical model and DES model. Guan and Liu (2009) stated that the TAS is one of the most viable strategies to avoid the terminal congestion and improve the system efficiency. To achieve that, authors formulated a nonlinear optimization model and applied a multi-server queuing model. Chen and Yang (2010) studied the export container's drayage operations in Chinese CT. They proposed an integer programming model in order to reduce the transportation cost through time window management. They indicated that the peak arrivals are smoothed by solving the problem using a genetic algorithm (GA). Zhao and Goodchild (2010) studied the impact of using the arrival information of external trucks on the yard operations. They concluded that prior knowledge about the arrival time

of external trucks reduces the queue lengths at gates and re-handling frequency at the yard. Chen et al. (2011) introduced a stationary time-dependent queueing model providing a supporting tool to improve demand management at CTs.

Simulation was used in many studies for developing and testing truck appointment systems. Sharif et al., (2011) developed an agent-based simulation model to achieve a steady arrival of external trucks at container terminals. The results showed that the congestion at CTs can be minimized by using gate congestion information and estimating the truck idling times. Karafa (2012) conducted a case study using a dynamic traffic simulation model to investigate the congestions and related emissions. They concluded that extending the gate working hours increases the terminal productivity and reduces the emissions especially at peak hours. Based on a previous work, Van Asperen et al., (2013) used a DES model to investigate the effect of truck announcement system on the yard operations performance, and a significant reduction in yard crane moves is obtained using the proposed algorithms.

Zhang et al., (2013) developed an optimization approach for truck appointments to reduce the heavy truck congestions in CTs. A method based on Genetic Algorithms (GA) and Point Wise Stationary Fluid Flow Approximation (PSFFA) was designed to solve the problem that resulted in reducing truck turn times. In a series of papers, Chen, Govindan, Yang, et al. (2013), Chen, Govindan and Yang (2013) and Chen, Govindan and Golias (2013) studied various strategies and approaches to optimize the appointments of external trucks in the terminal. Various performance measures and objective are examined such as transportation cost, fuel consumption, shifted arrivals, and truck waiting times. A new concept of chassis exchange introduced by Dekker et al., (2013) to reduce the CT congestion using simulation as a calculation tool. Zhao and Goodchild (2013) used a hybrid approach of simulation and queuing models to examine the impact of the TAS on the performance of yard crane operations. The results showed a significant improvement in system performance and efficiency. Zehendner and Feillet (2014) formulated a mixed integer programming model to get the optimum number of appointments considering the CT workload. Results are validated using DES to ensure the improvements of service quality for both the trucks and also for all terminal resources.

Azab and Eltawil (2016) studied the effect various arrival patterns of external trucks on truck turn times in CTs through a simulation-based study. Their results show that arrival patterns have a significant effect on the terminal performance in such a way that makes it important to consider the arrival pattern effects during the design of the truck appointment system. Li et al., (2016) proposed some response strategies that help in solving the problem of truck arrivals' deviation from its appointments. Results showed that the greenness of operations is significantly affected by the use of truck appointments. Chen and Jiang (2016) introduced some strategies to manage the truck arrivals within the time windows based on truck-vessel service relationship to reduce the terminal congestion.

To sum up, an increasing attention is paid to the TAS in literature. However, only two studies (Phan and Kim (2015) and Phan and Kim (2016)) investigated the TAS with considering the collaboration among trucking companies and the container terminal. In these two papers, an iterative approach is used to model the collaboration among trucking companies and the terminal operator. The iterative approach consists of two levels which are interconnected by a feedback loop. The first level is a mathematical model which includes a sub-problem for each trucking company to minimize the total waiting cost of trucks at the yard. On the other hand, the second level is a procedure to estimate the expected times at the yard of trucks based on the solution of first level. This iterative approach enables the collaboration process.

By careful investigation of the approaches proposed in Phan and Kim (2015) and Phan and Kim (2016), we notice three gaps that are needed to be covered to improve the existing approaches. The first gap is related to the second level where a simple procedure is typically used to estimate the truck turn times. This simple procedure lacks real world aspects such as the waiting times of trucks at gate. The second gap is that the existing approach did not consider the randomness of the terminal operations. The third gap is related to the number of times the trucking companies and terminal operator send their decisions to each other. According to Phan and Kim (2016) , their iterative approach needs about nine iterations on average to terminate and produce the final solution. In contrast, the proposed system in this paper requires only 2 iterations between trucking companies and the container terminal. From a practical point of view, large number of iterations may cause some of trucking companies not to submit their appointment applications for some reasons such as not having time to reschedule their truck operation or forgetting to resubmit their applications. In this case, the quality of the solution may be impaired.

Based on the above understandings, we propose a new approach for dynamic and collaborative truck appointment scheduling in container terminals. The proposed approach considers the collaboration among trucking companies and terminal operators by a pre-processing integration of a mixed integer programming model and a discrete event simulation (DES) model. The contributions of the proposed approach are as follows:

1) The turn times of trucks are estimated based on a simulation model which enables capturing several real world aspects as well as the stochastic nature of the terminal operations.
2) By employing the pre-processing integration, the trucking companies send their rescheduled appointments to the terminal two times only. Thus, this improves the applicability of the proposed new appointment system.

3 THE PROPOSED DYNAMIC AND COLLABORATIVE TRUCK APPOINTMENT SYSTEM

In this section, the proposed Dynamic Collaborative Truck Appointment System is introduced (DCTAS) based on the collaboration concepts. The paper introduces an integrated simulation optimization approach to achieve the collaboration goal considering both the dynamic and stochastic nature of the problem. The proposed DCTAS (figure 3) can be illustrated in five operational steps as follows:

Step (1): each trucking company submits an arrival proposal to the terminal. This proposal contains the preferable arrival time of their external trucks based on some factors such as; ship arrival, container dwell time, ship departure, available trucks, etc.

Step (2): once the terminal operators receive the submitted proposal, the terminal working load is updated and the performance measures are determined. To do this, a DES model of the terminal is introduced to help the terminal operator to estimate the total truck turn time for the trucking company and evaluate the terminal congestion at each yard block (YB) during each working hour (time window). It is assumed that the workload of the CT contains the set of confirmed appointments that are already reserved before the terminal appointment application's deadline for each time window (Tw) and the ship tasks assigned to each yard block.

Step (3): The terminal operators publishes the schedule information online with the expected turn times for all submitted requests. Each trucking company is then capable of knowing how much time they are supposed to spend in the terminal (turn time) to achieve their delivery/pick up tasks.

Step (4): To avoid going to the terminal in congestion times, the trucking company will use the mixed integer programming (MIP) model available as a scheduling tool for their trucks. The MIP model is solved to reduce the transportation cost in the CT considering the previous preferable arrival time (step 1) and the terminal performance measures (step 2), and a new arrival request will be issued.

Step (5): the new schedule will be submitted as a confirmed appointment request and the terminal workload will be updated waiting the new requests to be submitted and confirmed.

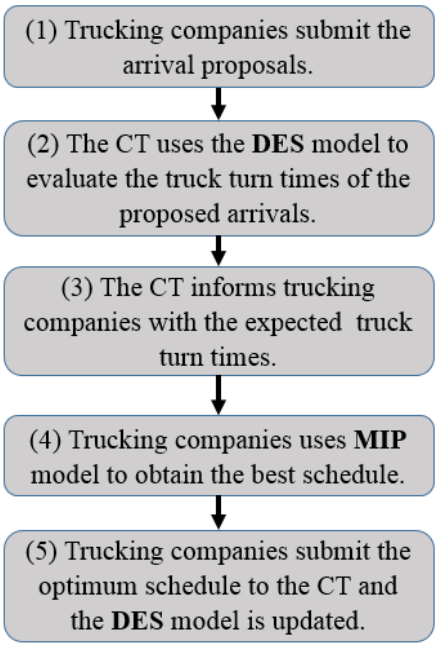

Figure 3: The operational steps of the proposed DCTAS.

As illustrated, the DCTAS provides an interactive management strategy between the stakeholders to cope with the dynamic nature of the appointment process in CTs. Interacting communication among stakeholders can be implemented easily using an online collaboration platform. In a previous work, (Azab et al. 2016) adopted a design thinking strategy to design and synthesize an online information system for transportation logistics. Whenever a trucking company is ready to submit the preferable arrival times, the system receives the appointments and deals with the workload updates and changes hourly.

Moreover, using the DES model is expected to enhance the solution and to accommodate the system's actual variability and randomness. This randomness results from the stochastic operations and events such as the gate service rate, inter-terminal traveling times, yard crane handling rates, quay crane handling rate, and the failure of equipment. The proposed simulation optimization approach integrates the MIP model with the DES model in a pre-processing way (Bierwirth and Meisel 2015) in which the problem under particular circumstances is solved to produce the input data for the other problem. The DES model provide the input to the MIP model. After solving the MIP model, the optimum truck appointment schedule is evaluated using the simulation model to get the turn time of trucks after optimization.

3.1 The DES Model

The DES model is built using "Flexsim CT®" package, which is a special software for simulating container terminal operations. The basic elements of the model are shown in figure 4. The 3D DES model includes five yard blocks, five yard cranes, four gates, and a single shared gate queue. When the external truck arrives at the gate according to the predetermined schedule (Tables 2-3), the truck joins a single queue shared among the four gates. Trucks will leave the gate queue to the first available gate and will be processed according to an Erlang distribution (0.65,4) (Guan and Liu 2009). Once the truck completes processing at the gate, the trucks are directed to the yard block that contains a container to be picked up or to the location of the container where it will be dropped off. Yard cranes are the equipment that handles the container within the blocks to/from the external trucks. The external trucks leave the terminal after finishing the pickup/drop off operation. On the seaside of the terminal, the arriving vessels are berthed, and there is a truck gang that serves each quay crane assigned to the vessel. The internal trucks deliver the containers between the seaside and yard area. At the yard block, the highest priority is given to shipside operations, next to gate side operations and lastly to internal yard operations.

There are some assumptions that are used in this simulation model. At the gates, it is assumed that all arriving trucks will share the same queue before going to the first available gate, and external trucks travel time within the terminal is neglected. As a result, the truck turn time will be the sum of the gate queue waiting time, the gate service time, the yard waiting time, and the yard service time. To obtain more accurate results, each time window is divided into four time intervals, and the average truck turn time is calculated per each time interval. Moreover, the collision of trucks traveling through the internal transportation network of the terminal is not considered. Because the problem is regarded as a design problem for a new appointment system, the input parameters are driven from literature and based on some experience. Berth and yard cranes service rates are represented by the average net moves/hr calculated form the busy time and truck throughput for each crane. Table 1 illustrates the input parameters to the DES model.

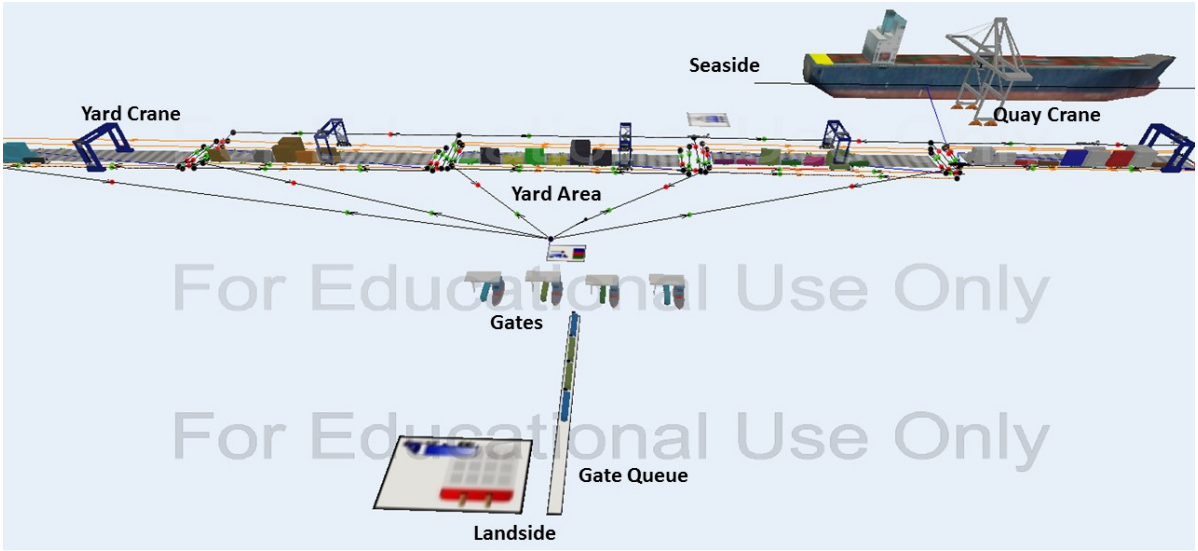

Figure 4: 3D discrete event simulation model.

Table 1: the input parameters to DES model.

General parameters	
Working hours (Tws)	8:00 am- 12 pm
Truck speed (max)	300 m/min (18 km/hour)
Container dwell time	Exponential(0.3) [days]
Gate Parameters	
Process time (min)	Erlang (0.65, 4)
Gate capacity	1 truck/one gate
Yard parameters	
Crane speed (max)	90 m/min (empty/loaded)
Block capacity (max)	24 containers
Crane net moves	27.7 move/hr (average)
Quayside parameters	
crane speed (max)	120 m/min (empty/loaded)
Crane net moves	12.3 move/hr (average)

3.2 The Scheduling Problem: MIP Model

In most container Terminals, the arrival of external trucks from the hinterland is a random process that is affected by the preferable arrival times of trucking companies. These preferable arrival times are not known by the terminal operators to be considered in planning and scheduling operations. As a result, a truck may arrive during a congestion time where the waiting time is costly and the emissions are high. On the other hand, if these trucks are forced to come at certain times that are specified by the terminal operators, it may be inconvenient for some trucking companies due to the trucks availability and other operations outside the terminal. To tackle this problem, the following mathematical model considers both, the convenience of trucking companies to arrive at their preferable times and the total time spent in the terminal which is influenced by the terminal congestion.

Based on the mathematical models formulated by (Phan and Kim 2015), we modified the model to consider the truck turn time (TT_{jt}) of trucks which is derived from the DES model. The proposed DCTAS assumes that each trucking company develops its preferable schedule considering the available number of trucks at each time window ($s_{k\tau}$). The trucking company's operator defines all tasks to be performed, which represents a pick up or a delivery operation for one container using one truck. Tasks that are assigned in the same preferable arrival hour (time window) are grouped together in one task group. For a certain task group, Containers can be delivered or picked up from the same yard block or from several yard blocks (table 2). The used parameters and indices in MIP model are defined as follows:

i index for a task group
j index for a yard block
k index for a trucking company
τ index of a time window
t index of a time interval. Note that multiple time intervals exist in a time window
b_i^l earliest possible (lower) bound of the time window for task group i
b_i^u latest possible (upper) bound of the time window for task group i
d_i number of tasks to be done for task group i
$S_{k\tau}$ number of available trucks of company k during time window τ
p_i most preferable time window at which containers of task group i to be stored or retrieved
σ number of time intervals per each time window
a_{ij} maximum number of containers of task i that can be allocated to yard block j
w_i^+ cost of late arrival by a unit time compared with the preferable time window of task i
w_i^- cost of early arrival by a unit time compared with the preferable time window of task i
w_k truck waiting cost in the terminal of truck company k per time interval
P congestion penalty in $, a strategic parameter determined by the terminal manager.
TT_{jt} average truck turn time for a truck arriving at yard block j at time interval t derived variables from the DES model

Sets
I set of task groups.
K set of trucking companies.
T set of time intervals.
J set of yard blocks j
W set of time windows.

Decision variables:
$X_{ij\tau}$ number of trucks for task group i which are deployed to yard block j at time window τ

Derived variables from the MIP model:
λ_{ijt} average arrival rate of trucks for task group i at yard block j at time interval t

Minimize:

$$\sum_{i\in I}\sum_{j\in J}\left[w_i^+ \sum_{\tau\in W} X_{ij\tau}\,(\tau - p_i)^+ + \; w_i^- \sum_{\tau\in W} X_{ij\tau}\,(p_i - \tau)^+ + \sum_{t\in T}(w_k + p)TT_{jt}\,\lambda_{ijt}\right] \quad (1)$$

Subjected to:

$$\sum_{j\in J}\sum_{\tau\in W} X_{ij\tau} \geq d_i \quad \forall i \in \mathrm{I} \quad (2)$$

$$\sum_{i\in I}\sum_{j\in J} X_{ij\tau} \leq S_{k\tau} \quad \forall k \in \mathrm{K}, \tau \in \mathrm{W} \quad (3)$$

$$\sum_{\tau\in W} X_{ij\tau} \leq a_{ij} \quad \forall i \in \mathrm{I}, j \in \mathrm{J} \quad (4)$$

$$b_i^l \sum_j X_{ij\tau} \leq \tau \sum_j X_{ij\tau} \leq b_i^u \sum_j X_{ij\tau} \quad \forall i \in \mathrm{I}, \tau \in \mathrm{W} \quad (5)$$

$$\lambda_{ijt} = \frac{X_{ij\tau}}{\sigma} \quad \forall i \in \mathrm{I}, j \in \mathrm{J}, \tau \in \mathrm{W} \quad (6)$$

$$\lambda_{ijt} \geq 0\,, X_{ij\tau}\; integer \quad \forall i \in \mathrm{I}, j \in \mathrm{J}, \tau \in \mathrm{W}, t \in T \quad (7)$$

The objective function (1) is to minimize the cost of shifting (delaying or advancing) the appointment and the truck turn time (TT_{jt}) cost within the terminal. The total number of scheduled trucks must satisfy the number of containers to be delivered or picked up (2). Constraint (3) states that the number of trucks to be assigned to task *i* cannot be larger than the resource level of the trucking company. The capacity constraint of each yard block is described in (4) to ensure that the number of containers for each task group have to be smaller than or equal to the available spaces in yard blocks. There is an earliest and latest feasible time window for each container (5). To calculate the arrival rate for each task group, constraint (6) is used. Constraint (7) illustrates the domain of each variable in the problem.

4 NUMERICAL EXPERIMENTS

In this section, a numerical example is solved to illustrate the operational scenario and performance of the proposed DCTAS. Table 2 shows a proposed appointment application for 4 trucking companies. Each trucking company is assumed to have a specific number of containers (d_i) in the terminal. The task group is a set of tasks that will be submitted by the same trucking company at the same preferred arrival time (p_i). It is assumed also that each trucking company knows which yard block (*j*) holds its containers. To create a workload in the terminal, the externally confirmed applications and inter-terminal tasks are developed in order to investigate the response of the proposed system to the heavy-loaded time windows. The proposed system (DCTAS) is expected to shift the proposed arrival appointments to the time windows where the turn time cost will be minimized with consideration of the preferred arrival times. Table 3 illustrates the tasks that are assumed to be already reserved and confirmed.

To start working with the DCTAS, all tasks are loaded to the simulation model input. Each task has a corresponding arrival time, the number of containers, and yard block location. By running the DES model, the external trucks arrive to the terminal model according to the predetermined scheduled times and released out of the system as the task is completed. The average truck turn times at each yard block are recorded for each time window to be used in the MIP model input. Other performance measures can be derived from the simulation model such as the queue length at gates, waiting times at gates and yard, service rate at gates and yard, cranes' utilization, etc.

Table 2: Proposed appointment applications for four trucking companies.

Truck. Company	Task group	*di*	*Pi*	*j*
TC1	1	5	2	1
	2	3	4	2
	3	1	3	1
		2		2
TC2	4	3	4	4
	5	4	3	2
	6	4	1	3
TC3	7	4	2	1
		2		3
	8	2	1	2
		3		4
TC4	9	3	2	4
	10	1	3	3
		5		5

Table 3: the reserved tasks in the CT.

Confirmed tasks	*Di*	*Tw*	*j*
11	30	2	1
12	30	3	2
13	30	2	3
14	30	2	4
15	30	3	5
16	10 (to ship)	3-4	1

To get statistically reliable results, the simulation model is run for 35 replications which are used to determine the 95% confidence intervals of the targeted mean performance measures. After obtaining the results from the simulation model, the derived variables are sent to the MIP model. The MIP model is solved using a personal computer with Intel® Core i7 CPU and 4 GB RAM. IBM Ilog CPLEX Optimization Studio version 12.2 is used to code the problem and get the optimum solution. The cost parameters in the objective function are assumed to be \$1, \$4, \$5, and \$2 per each time for w_i^+, w_i^-, w_k, and P respectively. Table 4 shows the available number of trucks ($s_{k\tau}$) for each trucking company per each time window. In Constraint 3, the number of available trucks is used to guarantee that the new assigned tasks do not exceed the trucking company's available trucks per each time window.

5 RESULTS AND ANALYSIS

Table 5 shows the MIP model optimum solution of the provided instance. In Table 4, *di* represents the number of containers submitted before solving the problem. After solving the DCTAS problem, the X_{ijt} describes the new scheduled tasks proposed for the trucking company to reduce the total cost of delivering a container to the terminal. There are three possibilities noticed from the results to occur after the solution to the input schedule of the DCTAS. The first possibility, there will be no change in the schedule such as task group 8. The second possibility, the task group preferred time window will be advanced or delayed resulting in an advancing and/or delaying cost without any change in the number of containers per task. For example, the arrival time of task group 5 is shifted from Tw3 to Tw2. This seems reasonable because, at yard block 2, the workload in Tw3 was the highest among the other three time windows in the same block before the solution. The third possibility is that the task group will be decomposed to smaller mini-task groups. It is evident that the second and third possibility may occur together like in task groups 1, 2, 7, and 10.

Table 4: the available number ($S_{k\tau}$) of trucks for each trucking company per each time widow.

Truck. Company	Tw1	Tw2	Tw3	Tw4
TC1	3	5	6	4
TC2	7	4	1	5
TC3	6	1	2	4
TC4	3	4	3	4

Table 5: The DCTAS solution.

Truck. Company	Obj. value (\$)	Task group	*di*	*Xijt*	*Tw*	*j*
TC1	137.8	1	5	2	1	1
				3	4	
		2	3	1	1	2
				2	2	
		3	1	1	4	1
			2	2	2	2
TC2	114.7	4	3	3	4	4
		5	4	4	2	2
		6	4	4	1	3
TC3	101.75	7	4	4	4	1
			2	1	2	3
				1	3	
		8	2	2	1	2
			3	3	1	4
TC4	130.31	9	3	3	4	4
		10	1	1	4	3
			5	4	2	5
				1	3	

To investigate the solution performance, the simulation model is used to test the performance of the output schedule from the MIP model and compare it with simulation results before solving the MIP model. In other words, we need to see how the proposed schedule differs from the optimum schedule after applying the DCTAS. The average truck turn times at each block *j* per each time window τ ($TT_{j\tau}$) are recorded for the proposed (preferred) appointments and the optimum appointments. Figures (5-9) show a comparison between the $TT_{j\tau}$ values for the proposed (preferred) appointments by the trucking companies versus the optimum appointments after applying the DCTAS.

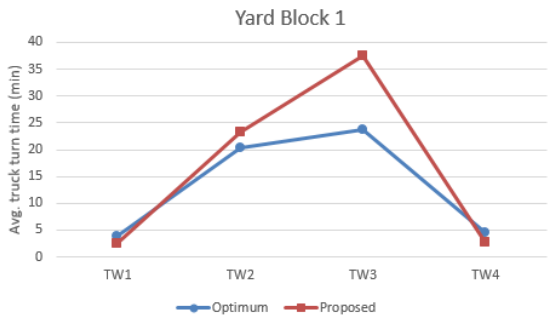

Figure 5: Average $TT_{1\tau}$.

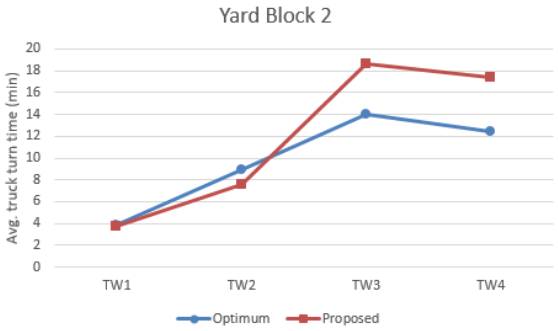

Figure 6: Average $TT_{2\tau}$.

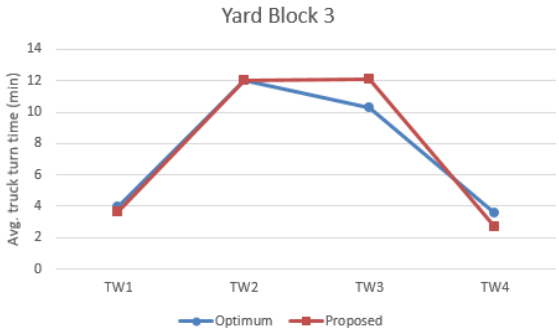

Figure 7: Average $TT_{3\tau}$.

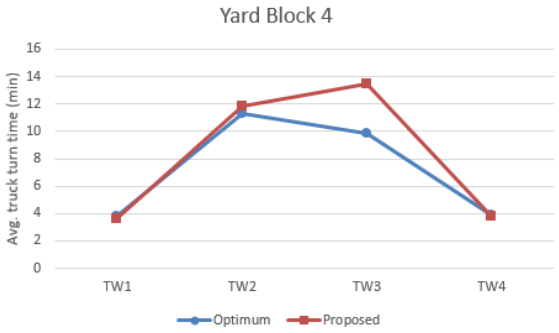

Figure 8: Average $TT_{4\tau}$.

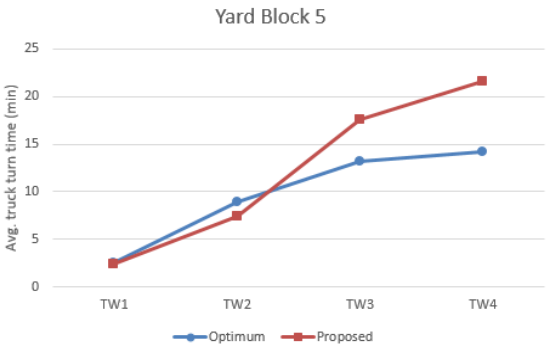

Figure 9: Average $TT_{5\tau}$.

Results show that there is a difference between the $TT_{j\tau}$ values before and after applying the proposed appointment management system. To confirm this difference, a t-test is conducted for $TT_{j\tau}$ values with a 95% confidence interval using Minitab 17 statistical software to test the 35 samples (replications) of $TT_{j\tau}$. The statistical results show that there is a significant difference between the average $TT_{j\tau}$ values before and after solution for most points such as Tw3 at YB1, Tw4 at YB2, Tw4 at YB3, Tw3 at YB4, and Tw4 at YB. While, some points did not depict significant differences in average $TT_{j\tau}$ such as Tw1 at YB2, Tw2 at YB3, Tw2 at YB4, Tw4 at YB4. It is noticed that the number of proposed tasks within some task groups increased after solution because some task groups are decomposed to two or three tasks. However, this reduces the turn time cost for the external trucks, some trucking companies may be inconvenient due to shifting their preferable arrival times. For the CT, distributing the arrival appointments over the terminal working hours is good to avoid congestion in certain times windows. From another side, reducing congestion and decreasing waiting time will result in less emissions and less fuel cost as well increased efficiency for the trucking companies. The results showed also that the average queue length at gates is reduced by 21% and the average truck turn time is reduced by 22.6% after applying the proposed system.

6 CONCLUSIONS

This paper proposed an integrated appointment system by which both the CT and trucking companies collaborate in determining the arrival schedule of external trucks. The proposed Dynamic Collaboration Truck Appointment System (DCTAS) integrates a discrete event simulation model with an MIP model

using pre-processing integration. In the proposed DCTAS, the terminal operator firstly uses the simulation model to evaluate the turn times of the trucks considering their preferred arrival times. Then, the trucking companies solve the MIP model to reduce the total stay cost in the terminal. Finally, the terminal operator uses the rescheduled appointments of the trucking companies as inputs to the simulation model to produce the final appointment times and container schedule.

The results showed that the DCTAS could reduce truck congestion at the time windows where the terminal workloads are high. Moreover, the DCTAS could smooth the terminal workload and balance the arrival processes of external trucks. Thus, both stakeholders can benefit from applying the proposed appointment strategy. In addition, the rescheduling frequency is reduced compared to the existing literature approaches.

For future work, the proposed system will be implemented to a real case study and the effect of applying the proposed DCTAS on landside operations, yard operations and seaside operations will be investigated. Also, it is important to examine the emissions from trucks and terminal equipment after applying the DCTAS. One more issue that is expected to increase the appointment system performance is to consider truck sharing and collaboration between the trucking companies to reduce the empty truck trips. For instance, a trucking company may have a truck with an empty trip during a pickup task, which can be utilized by another trucking company to deliver a container to the terminal. This truck sharing process can be considered also in the appointment process.

REFERENCES

Van Asperen, E., Borgman, B. & Dekker, R., 2013. Evaluating Impact Of Truck Announcements On Container Stacking Efficiency. *Flexible Services And Manufacturing Journal*, 25(4), Pp.543–556.

Azab, Ahmed; Mostafa, Noha; And Park, Jaehyun, "Ontimecargo: A Smart Transportation System Development In Logistics Management By A Design Thinking Approach" (2016). PACIS 2016 Proceedings. Paper 44 Http://Aisel.Aisnet.Org/Pacis2016/44.

Azab, A.E. & Eltawil, A.B., 2016. A Simulation Based Study Of The Effect Of Truck Arrival Patterns On Truck Turn Time In Container Terminals, ECMS 2016 Proceedings Edited By: Thorsten Claus, Frank Herrmann, Michael Manitz, Oliver Rose European Council For Modeling And Simulation. Doi:10.7148/2016-0080.

Bierwirth, C. & Meisel, F., 2010. A Follow-Up Survey Of Berth Allocation And Quay Crane Scheduling Problems In Container Terminals. *European Journal Of Operational Research*, 244(3), Pp.675–689. Available At: Http://Dx.Doi.Org/10.1016/J.Ejor.2009.05.031.

Bierwirth, C. & Meisel, F., 2015. A Follow-Up Survey Of Berth Allocation And Quay Crane Scheduling Problems In Container Terminals. *European Journal Of Operational Research*, 244(3), Pp.675–689. Available At: Http://Dx.Doi.Org/10.1016/J.Ejor.2009.05.031.

Chen, G., Govindan, K., Yang, Z.Z., Et Al., 2013. Terminal Appointment System Design By Non-Stationary M(T)/E K/C(T) Queueing Model And Genetic Algorithm. *International Journal Of Production Economics*, 146(2), Pp.694–703. Available At: Http://Dx.Doi.Org/10.1016/J.Ijpe.2013.09.001.

Chen, G., Govindan, K. & Golias, M.M., 2013. Reducing Truck Emissions At Container Terminals In A Low Carbon Economy: Proposal Of A Queueing-Based Bi-Objective Model For Optimizing Truck Arrival Pattern. *Transportation Research Part E: Logistics And Transportation Review*, 55(X), Pp.3–22. Available At: Http://Dx.Doi.Org/10.1016/J.Tre.2013.03.008.

Chen, G., Govindan, K. & Yang, Z., 2013. Managing Truck Arrivals With Time Windows To Alleviate Gate Congestion At Container Terminals. *International Journal Of Production Economics*, 141(1), Pp.179–188. Available At: Http://Dx.Doi.Org/10.1016/J.Ijpe.2012.03.033.

Chen, G. & Jiang, L., 2016. Managing Customer Arrivals With Time Windows: A Case Of Truck Arrivals At A Congested Container Terminal. *Annals Of Operations Research*, Pp.1–17. Available At: "Http://Dx.Doi.Org/10.1007/S10479-016-2150-3.

Chen, G. & Yang, Z., 2010. Optimizing Time Windows For Managing Export Container Arrivals At Chinese Container Terminals. *Maritime Economics & Logistics*, 12(1), Pp.111–126.

Chen, X., Zhou, X. & List, G.F., 2011. Using Time-Varying Tolls To Optimize Truck Arrivals At Ports. *Transportation Research Part E: Logistics And Transportation Review*, 47(6), Pp.965–982. Available At: Http://Dx.Doi.Org/10.1016/J.Tre.2011.04.001.

Dekker, R. Et Al., 2013. A Chassis Exchange Terminal To Reduce Truck Congestion At Container Terminals. *Flexible Services And Manufacturing Journal*, 25(4), Pp.528–542.

Gheith, M., Eltawil, A.B. & Harraz, N.A., 2016. Solving The Container Pre-Marshalling Problem Using Variable Length Genetic Algorithms. *Engineering Optimization*, 48(4), Pp.687–705. Available At: Http://Www.Tandfonline.Com/Doi/Full/10.1080/0305215X.2015.1031661.

Guan, C. & Liu, R. (Rachel), 2009. Container Terminal Gate Appointment System Optimization. *Maritime Economics & Logistics*, 11(4), Pp.378–398. Available At: Http://Dx.Doi.Org/10.1057/Mel.2009.13.

Huynh, N., 2009. Reducing Truck Turn Times At Marine Terminals With Appointment Scheduling.

Transportation Research Record: Journal Of The Transportation Research Board, 2100, Pp.47–57.

Huynh, N. & Walton, C.M., 2008. Robust Scheduling Of Truck Arrivals At Marine Container Terminals. *Journal Of Transportation Engineering*, 134(8), Pp.347–353.

Karafa, J., 2012. Simulating Gate Strategies At Intermodal Marine Container Terminals. , (May). Available At: Http://Www.Memphis.Edu/Ifti/Pdfs/Student_Reserach_Jeff_Karafa.Pdf.

Karam, A. & Eltawil, A.B., 2015. A New Method For Allocating Berths, Quay Cranes And Internal Trucks In Container Terminals. *2015 International Conference On Logistics, Informatics And Service Science, LISS 2015*.

Karam, A. & Eltawil, A.B., 2016. Functional Integration Approach For The Berth Allocation, Quay Crane Assignment And Specific Quay Crane Assignment Problems. *Computers And Industrial Engineering*, Pp.1–15.

Li, N. Et Al., 2016. Disruption Management For Truck Appointment System At A Container Terminal: A Green Initiative. *Transportation Research Part D: Transport And Environment*.

Mohamed Gheitha, A.B.E.& N.A.H. & Mizuno, 2014. An Integer Programming Formulation And Solution For The Container Pre- Marshalling Problem M. In Pp. 2047–2056.

Morais, P. & Lord, E., 2006. Terminal Appointment System Study. *Transportation Research Board*, 1(March), P.123.

Murty, K.G. Et Al., 2005. Hongkong International Terminals Gains Elastic Capacity Using A Data-Intensive Decision-Support System. *Interfaces*, 35(1), Pp.61–75.

Namboothiri, R. & Erera, A.L., 2008. Planning Local Container Drayage Operations Given A Port Access Appointment System. *Transportation Research Part E: Logistics And Transportation Review*, 44(2), Pp.185–202.

Phan, M.H. & Kim, K.H., 2016. Collaborative Truck Scheduling And Appointments For Trucking Companies And Container Terminals. *Transportation Research Part B: Methodological*, 86, Pp.37–50.

Phan, M.H. & Kim, K.H., 2015. Negotiating Truck Arrival Times Among Trucking Companies And A Container Terminal. *Transportation Research Part E: Logistics And Transportation Review*, 75, Pp.132–144. Available At: Http://Dx.Doi.Org/10.1016/J.Tre.2015.01.004.

Sharif, O., Huynh, N. & Vidal, J.M., 2011. Application Of El Farol Model For Managing Marine Terminal Gate Congestion. *Research In Transportation Economics*, 32(1), Pp.81–89. Available At: Http://Dx.Doi.Org/10.1016/J.Retrec.2011.06.004.

Steenken, D., Vob, S. & Stahlbock, R., 2005. Container Terminal Operation And Operations Research - A Classification And Literature Review. *Container Terminals And Automated Transport Systems: Logistics Control Issues And Quantitative Decision Support*, Pp.3–49.

Zehendner, E. & Feillet, D., 2014. Benefits Of A Truck Appointment System On The Service Quality Of Inland Transport Modes At A Multimodal Container Terminal. *European Journal Of Operational Research*, 235(2), Pp.461–469. Available At: Http://Dx.Doi.Org/10.1016/J.Ejor.2013.07.005.

Zhang, X., Zeng, Q. & Chen, W., 2013. Optimization Model For Truck Appointment In Container Terminals. *Procedia - Social And Behavioral Sciences*, 96(Cictp), Pp.1938–1947. Available At: Http://Www.Sciencedirect.Com/Science/Article/Pii/S1877042813023458.

Zhao, W. & Goodchild, A. V, 2013. Using The Truck Appointment System To Improve Yard Efficiency In Container Terminals. *Maritime Economics & Logistics*, 15, Pp.101–119. Available At: Http://Www.Palgrave-Journals.Com/Mel/Journal/V15/N1/Pdf/Mel201223a.Pdf?WT.Ec_Id=MEL-201303.

Zhao, W. & Goodchild, A. V., 2010. The Impact Of Truck Arrival Information On Container Terminal Rehandling. *Transportation Research Part E: Logistics And Transportation Review*, 46(3), Pp.327–343. Available At: Http://Dx.Doi.Org/10.1016/J.Tre.2009.11.007.

New Scenario-based Stochastic Programming Problem for Long-term Allocation of Renewable Distributed Generations

Ikki Tanaka[1] and Hiromitsu Ohmori[2]
[1]*Graduate School of Science and Technology, Keio University, Kanagawa, Japan*
[2]*Department of System Design Engineering, Keio University, Kanagawa, Japan*
ikki0407@gmail.com, ohm@sd.keio.ac.jp

Keywords: Stochastic Optimization, Power Systems, Renewable Energy Sources, Distributed Generations, Expansion Planning.

Abstract: Large installation of distributed generations (DGs) of renewable energy sources (RESs) on distribution network has been one of the challenging tasks in the last decade. According to the installation strategy of Japan, long-term visions for high penetration of RESs have been announced. However, specific installation plans have not been discussed and determined. In this paper, for supporting the decision-making of the investors, a new scenario-based two-stage stochastic programming problem for long-term allocation of DGs is proposed. This problem minimizes the total system cost under the power system constraints in consideration of incentives to promote DG installation. At the first stage, before realizations (scenarios) of the random variables are known, DGs' investment variables are determined. At the second stage, after scenarios become known, operation and maintenance variables that depend on scenarios are solved. Furthermore, a new scenario generation procedure with clustering algorithm is developed. This method generates many scenarios by using historical data. The uncertainties of demand, wind power, and photovoltaic (PV) are represented as scenarios, which are used in the stochastic problem. The proposed model is tested on a 34 bus radial distribution network. The results provide the optimal long-term investment of DGs and substantiate the effectiveness of DGs.

1 INTRODUCTION

1.1 Background

Large penetration of RESs-based DGs in distribution network implies that distribution companies (DISCOs) need to deal with the intermittent nature of RES such as wind speed and solar radiation in order to maintain the demand-and-supply balance continuously, and accommodate expected demand growth over the planning horizon (Eftekharnejad et al., 2013). DGs refer to small-scale energy generations and are most generally used to guarantee that sufficient energy is available to meet peak demand. Distributed generation planning (DGP), which determines the optimal siting, sizing, and timing, is modeled to tackle above problem. The objective of DGP is to ensure that the reliable power supply to the consumers is achieved at a lowest possible cost. DGP plays an important role as a strategic-level planning in modern power system planning. Commonly used approaches to solve the DGP are: sensitivity analysis-based approaches, mixed-integer linear programming, and nonlinear programming. However, the above methods can not fully handle the uncertainties. Consequently, stochastic programming and metaheuristic-based approaches have been used these days, to consider the uncertainties at the energy planning (Payasi et al., 2011; Jordehi, 2016).

1.2 Related Work

Much attention has been paid to solving several stochastic problems for one-type capacity planning. For multi-resource type, the scenario-based techniques also have been proposed to consider various uncertainties (Huang and Ahmed, 2009; Baringo and Conejo, 2013b; Munoz et al., 2016).

In power system planning on transmission and distribution network, many approaches have been developed considering some RESs, energy conversion and transmission, and the uncertainties that are caused by demand, pricing, and intermittent renewables (Verderame et al., 2010). An energy planning in individual large energy consumers was formulated as a mixed integer linear programming model by using

Tanaka, I. and Ohmori, H.
New Scenario-based Stochastic Programming Problem for Long-term Allocation of Renewable Distributed Generations.
In *Proceedings of the 6th International Conference on Operations Research and Enterprise Systems (ICORES 2017)*, pages 96-107
ISBN: 978-989-758-218-9

fuzzy parameters in (Mavrotas et al., 2003). (Atwa et al., 2010) proposed a probabilistic mixed integer nonlinear problem for distribution system planning.

Several studies related to stochastic optimization of DGP have been proposed. In (Fu et al., 2015), a chance-constrained stochastic programming model was formulated for managing the uncertainty of PV, which was solved by an algorithm combining the multi-objective particle swarm optimization with support vector machines. (Abdelaziz et al., 2015) provided an energy loss minimization problem which determines the optimal location of RES-based DGs and the location and daily schedule of dispatch-able DG. In the problem, the uncertainties between wind power, PV and demand were considered using the diagonal band Copula and sequential Monte Carlo method. In (Saif et al., 2013), the uncertainties of wind energy, PV, and energy storage system were produced as chronological ones for a two-layer simulation-based allocation problem. In (Pereira et al., 2016), the allocation problem of VAR compensator and DG was formulated as a mixed-integer nonlinear problem and solved by using meta-heuristic algorithms.

A two-stage architecture is commonly used in stochastic programming approaches. At the first stage, DGs' investment variables are determined before realizations of random variables are known, i.e., scenarios. At the second stage, after scenarios become known, operation and maintenance variables which depend on scenarios are solved.

(Carvalho et al., 1997) modeled a two-stage scheme problem of distribution network expansion planning under uncertainty in order to minimize an expected cost along the horizon and solved by the proposed hedging algorithm in an evolutionary approach to deal with scenario representation efficiently. In (Krukanont and Tezuka, 2007), a two-stage stochastic programming for capacity expansion planning was provided in a power system of Japan. This model includes the uncertainties of the demand, carbon tax rate, operational availability. In (Wang et al., 2014), a two-stage robust optimization-based model considering uncertainties of DG outputs and demand was provided for the optimal allocation of DGs and microturbine. (Montoya-Bueno et al., 2015) proposed a stochastic two-stage multi period mixed-integer linear programming model of renewable DG allocation problem considering the uncertainties affected by demand and renewable energy production.

As an allocation problem of energy storage system (ESS), (Nick et al., 2014) formulated the optimal allocation problem as a two-stage stochastic mixed-integer second-order cone programming (SOCP) model. In (Nick et al., 2015), SOCP problem of ESS allocation was solved by using alternative direction method of multipliers. In (Asensio et al., 2016a; Asensio et al., 2016b), the allocation problem of DGs and energy storage was formulated as a stochastic programming model for maximizing the net social benefit taking account of demand response. Since the cost of ESS is very expensive and ESS seems not to be efficient at this stage, ESS is excluded from consideration in this paper.

In solving the two-stage stochastic programming, an effective methodology to create proper scenarios must be needed to represent various uncertainties because it is very difficult to realistically obtain all of the information about the uncertainty and computationally incorporate it into the model. In case some probability distributions are analytically estimated and used instead, the problem commonly becomes very complexed, even if the problem is small. Hence, when the partial information of the uncertainty is available, the stochastic programing model normally needs to be solved using scenarios. There exist many techniques of scenario generation (Dupačová et al., 2000). The uncertainty modeling such as demand and wind speed were developed to create scenarios in (Baringo and Conejo, 2011). The proposed method uses duration curves which is approximated by some demand blocks. (Baringo and Conejo, 2013a) performed the scenario reduction by using K-means clustering algorithm to arrange the historical scenarios of demand and wind into clusters according to the similarities. (Sadeghi and Kalantar, 2014) used Monte Carlo simulation and probability generation load matrix for obtaining the uncertainty of fuel and electricity price, DG outputs, and load. In (Mazidi et al., 2014), the Latin hypercube sampling was used to prepare scenarios of RESs. In (Seljom and Tomasgard, 2015), an iterative-random-sampling-based scenario generation algorithm was developed. They evaluated whether the number of scenarios is enough to obtain reliable results. In (Nojavan and allah Aalami, 2015), the normal distribution and the Weibull distribution were used for generating the scenarios of electric price, demand, and meteorological data. The created scenarios were reduced by the fast forward selection based on Kantorovich distance approach. In (Montoya-Bueno et al., 2016), a probability density function-based scenario generation method was proposed for the allocation problem of wind power and PV.

1.3 Contribution

Most of scenario generation have not considered the correlation between the uncertainties (e.g., demand and solar radiation) and usually the uncertainty

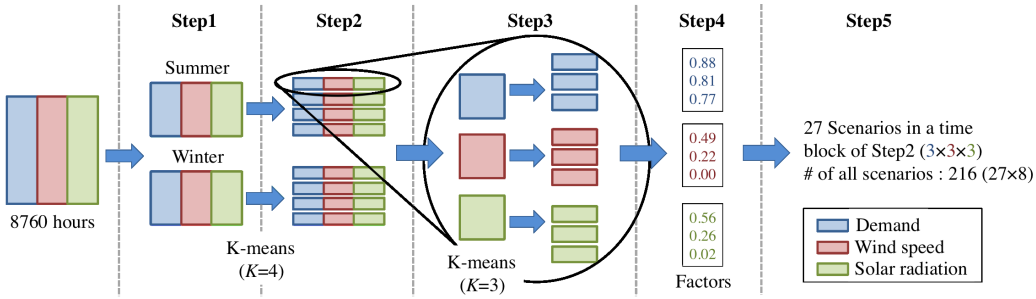

Figure 1: Outline of scenario generation. This figure shows the procedure focused on a block in Step 2.

separations to the levels have been made manually (Baringo and Conejo, 2011; Montoya-Bueno et al., 2016). It is necessary, however, to create scenarios automatically in consideration of the correlations for appropriate scenarios based on data. In optimization problem mentioned above, many researches of optimal DG allocation problem that takes into account the uncertainties have been performed. Most of the studies have considered only one-year's allocation and daily/annual system operation. Realistically, in order to accomplish the optimal system operation in multi-period, obtaining the long-term optimal siting, sizing, and timing is required. Hence, this study provides the two main contributions as follows.

- A new scenario generation method with K-means is proposed to create scenario-levels automatically by using similarity measure. This procedure uses historical data and can be implemented readily. If K-means algorithm is simply applied to the available data, it is not possible to take into account the correlation between demand and meteorological data or seasonal characteristics (e.g., summer and winter). Hence, in the proposed approach K-means clustering is utilized in stages by focusing on demand and seasons. Many scenarios of demand, wind speed, and solar radiation are generated and appropriate probabilities of each scenario are calculated (not equal-probability) by use of divided time blocks.
- A new long-term allocation problem of RES-based DGs is proposed. This model is formulated as a two-stage stochastic programming problem with the objective of minimizing the total system cost. In the proposed model, some devices and constraints are integrated for improving distribution system (i.e., limitation of reverse power flow, generation of DG considering lagging/leading power factor, capacitor bank (CB)). Furthermore, the carbon emission costs and incentives are considered from the point of view of international trends and economics because the problems of carbon emissions are actively discussed at the Conference of the Parties to the UNFCCC to achieve a clean environment and the government generally, in order to reach high renewable penetration levels, subsidizes the DISCOs that invest RES to their distribution system.

1.4 Paper Organization

The reminder of this paper is organized as follows. In Section 2, the details of the proposed scenario generation procedure is described. Section 3 provides the stochastic programming model. The results of the numerical simulations are presented and discussed in Section 4. Finally, the paper is concluded providing some insights and summaries in Section 5.

2 SCENARIO GENERATION

This Section describes the proposed scenario generation method that applies K-means to historical data (i.e. load, wind speed, solar radiation) in stages. The goal is to obtain the scenario levels of demand, electricity price, wind speed, and solar radiation for creating specific scenarios. The role of K-means is to classify a original dataset into a certain number of clusters K. The centroid of each cluster is the mean value of the data allocated to each cluster. The algorithm is based on the iterative fitting process as following steps:

1. Select the number of clusters K according to the specific problem. Randomly place K points, which represent the initial cluster centroids, into the space represented by the clustered dataset.
2. Assign each data to the closest centroid base on the distances.
3. When all data have been assigned, recalculate the new cluster centroids using data allocated to each cluster.
4. Repeat Steps 2 and 3 iteratively until there are no changes in any mean, i.e. the centroids no longer

move. As a result, the clustered dataset is separated into groups minimizing an objective function, in this paper a quadratic distance is used.

Historical data need to be available for scenario creation, i.e. hourly demand, wind speed, solar radiation, and electricity price data for the 8760 hours of the year. Figure 1 shows the overview of the proposed scenario generation. The steps are described below:

Step 1) Normalize data into the [0.0,1.0] interval by dividing by the maximum value of each feature and simultaneously separate into two seasons : summer (April-September) and winter (October-March). Each seasonal group consists of 4380 hours block.

Step 2) Apply K-means (the number of clusters $K = 4$) to only the demand in each seasonal groups created in Step 1 and allocate each data into four groups. Figure 2 shows the clusters of the demand. Moreover, wind speed, solar radiation and price indexed to each demand data are also allocated to the same clusters of the demand. Each divided group is defined as a *time block b*, which is related to the representatives of demand clusters (e.g., peak-load of summer, middle-load of summer, low-load of winter). Total of the number of hours in time block b is represented as N_b^{hours}.

Step 3) Apply K-means ($K = 3$) again into the demand, wind speed, and solar radiation of the data group created in Step 2 respectively and 9 data groups are created per one block. Step 3-5 in Fig. 1 focus on the flow of the one of the data blocks in Step 2.

Step 4) The mean values of each data block in Step 3 are used as a block representative to create the factors of demand, wind speed, and solar radiation. Note that the price levels are determined by the mean values of the price within each demand block. Renewable production models in (Eduardo, 1994) and (Atwa et al., 2010) are used in this paper so that renewable observation data are transformed into power output (i.e., wind generation factor and PV generation factor)

Step 5) Considering the combination of each factor made in Step 4, 27 scenarios are obtained for each time block. Therefore, 216 scenarios are obtained as the total number of scenarios. The probabilities of the factors within each time block, $\text{Pr}_{b,s}^{\text{load}}, \text{Pr}_{b,s}^{\text{WD}}, \text{Pr}_{b,s}^{\text{PV}}$,are defined by the ratio of the number of hours of the blocks divided in Step3 to the corresponding block in Step2, i.e., N_b^{hours}. Hence, the scenario probabilities $\text{Pr}_{b,s}$ are calculated as:

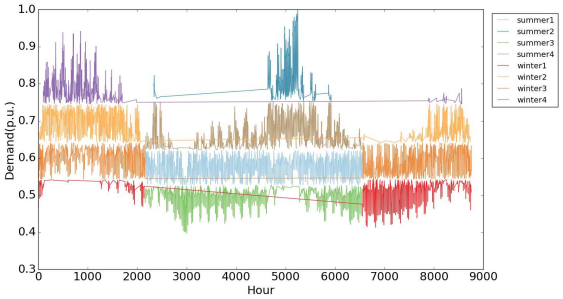

Figure 2: The clusters of demand in Step 2 (time blocks).

$$\text{Pr}_{b,s} = \text{Pr}_{b,s}^{\text{load}} \times \text{Pr}_{b,s}^{\text{WD}} \times \text{Pr}_{b,s}^{\text{PV}}.$$

Note that the time block b represents the demand periods related to season (e.g., high-demand in summer, low-demand in winter) and the index s represents the scenarios in the time block b (e.g., (high demand, large wind, large PV), (low-demand, middle wind, small PV)).

3 OPTIMAL LONG-TERM ALLOCATION PROBLEM OF DISTRIBUTED GENERATION

Two-stage stochastic linear programming is used as a formulation of the long-term allocation problem of DGs. The model uses the scenarios and provides the optimal siting, sizing, and timing of RES-based DGs to be installed (wind power and PV). The nomenclature related to the problem formulation described in Appendix.

3.1 Objective Function

This model minimizes the total system cost consisting of the investment cost π_t^{inv} and operation & maintenance cost in consideration of the incentive μ_t^{inc}. The expected value of the O&M cost in year t is shown as:

$$\sum_{b \in \Omega_{B_t}} N_{t,b}^{\text{hours}} \sum_{s \in \Omega_{S_{t,b}}} \text{Pr}_{t,b,s} \pi_{t,b,s}^{\text{om}} \qquad , t \in \Omega_T \quad (1)$$

where, Ω_{B_t} is the set of time blocks in year t, $N_{t,b}^{\text{hours}}$ is the total hours of time block b in t, $\Omega_{S_{t,b}}$ is the set of the scenarios in t and b, $\text{Pr}_{t,b,s}$ is the probability of the scenario s in t and b, and $\pi_{t,b,s}^{\text{om}}$ is the O&M cost per unit time in t, b, and s. In this paper, it is assumed that the time blocks and scenarios are the same every year,

$$\Omega_{B_t} = \Omega_B, N_{t,b}^{\text{hours}} = N_b^{\text{hours}}, \Omega_{S_{t,b}} = \Omega_{S_b}, \text{Pr}_{t,b,s} = \text{Pr}_{b,s},$$

because, in the same region, the trend of the demand profile and the average of the weather data are considered not to change significantly. It is important to note that the operational environment of the power system is different in each year since the time-dependent parameters exist, such as demand growth factor, discount rate, and price increasing factor, although the scenarios do not change.

Therefore, the aim of the model is minimizing the total system cost over the planning horizon T:

Minimize:

$$\sum_{t\in\Omega_T}\alpha_t\left(\pi_t^{\text{inv}}+\sum_{b\in\Omega_B}N_b^{\text{hours}}\sum_{s\in\Omega_{S_b}}\text{Pr}_{b,s}\pi_{t,b,s}^{\text{om}}\right)-\sum_{t\in\Omega_T}\mu_t^{inc} \tag{2}$$

where $\alpha_t=\frac{1}{(1+d)^t}$ is the present value factor.

3.1.1 Investment Costs

The following equations show the investment costs of the substation, wind turbine, PV, and CB. The costs are, respectively, annualized by using the interest rate and lifetime of the devices. Therefore, the previous year's investment cost is added to the next one except for the first year.

$$\begin{aligned}\pi_t^{\text{inv}}=&\sum_{n\in\Omega_{SS}}\pi_{\text{anu}}^{\text{SS}}X_t^{\text{SS},n}+\sum_{n\in\Omega_L}(\pi_{\text{anu}}^{\text{PV}}X_t^{\text{PV},n}\\&+\pi_{\text{anu}}^{\text{WD}}X_t^{\text{WD},n}+\pi_{\text{anu}}^{\text{CB}}X_t^{\text{CB},n})+\pi_{t-1}^{\text{inv}};t>1,\end{aligned} \tag{3}$$

$$\begin{aligned}\pi_t^{\text{inv}}=&\sum_{n\in\Omega_{SS}}\pi_{\text{anu}}^{\text{SS}}X_t^{\text{SS},n}+\sum_{n\in\Omega_L}(\pi_{\text{anu}}^{\text{PV}}X_t^{\text{PV},n}\\&+\pi_{\text{anu}}^{\text{WD}}X_t^{\text{WD},n}+\pi_{\text{anu}}^{\text{CB}}X_t^{\text{CB},n})\qquad;t=1,\end{aligned} \tag{4}$$

$$\pi_{\text{anu}}^{\text{SS}}=\frac{\pi_{\text{inv}}^{\text{SS}}i(1+i)^{L^{\text{SS}}}}{(1+i)^{L^{\text{SS}}}-1}, \tag{5}$$

$$\pi_{\text{anu}}^{\text{WD}}=\frac{\pi_{\text{inv}}^{\text{WD}}i(1+i)^{L^{\text{WD}}}}{(1+i)^{L^{\text{WD}}}-1}, \tag{6}$$

$$\pi_{\text{anu}}^{\text{PV}}=\frac{\pi_{\text{inv}}^{\text{PV}}i(1+i)^{L^{\text{PV}}}}{(1+i)^{L^{\text{PV}}}-1}, \tag{7}$$

$$\pi_{\text{anu}}^{\text{CB}}=\frac{\pi_{\text{inv}}^{\text{CB}}i(1+i)^{L^{\text{CB}}}}{(1+i)^{L^{\text{CB}}}-1}. \tag{8}$$

3.1.2 Operation and Maintenance Costs

O&M costs are shown in the following equations. Total O&M cost includes the power loss cost, unserved energy cost, purchased energy cost, O&M cost of DGs and CB, and CO_2 emission cost.

$$\pi_{t,b,s}^{\text{om}}=\pi_{t,b,s}^{\text{loss}}+\pi_{t,b,s}^{\text{ENS}}+\pi_{t,b,s}^{\text{SS}}+\pi_{t,b,s}^{\text{new}}+\pi_{t,b,s}^{\text{CB}}+\pi_{t,b,s}^{\text{emi}}, \tag{9}$$

$$\pi_{t,b,s}^{\text{loss}}=\pi^{\text{loss}}\sum_{n,m\in\Omega_N}S^{\text{base}}r^{n,m}I_{t,b,s}^{\text{sqr},n,m}, \tag{10}$$

$$\pi_{t,b,s}^{\text{ENS}}=\pi^{\text{ENS}}\sum_{n\in\Omega_L}S^{\text{base}}P_{t,b,s}^{\text{ENS},n}, \tag{11}$$

$$\pi_{t,b,s}^{\text{SS}}=\pi_{b,s}^{\text{SS}}\eta_t^{\text{SS}}\sum_{n\in\Omega_{SS}}S^{\text{base}}P_{t,b,s}^{\text{SS},n}, \tag{12}$$

$$\pi_{t,b,s}^{\text{new}}=S^{\text{base}}\sum_{n\in\Omega_L}(\pi_{\text{om}}^{\text{PV}}P_{t,b,s}^{\text{PV},n}+\pi_{\text{om}}^{\text{WD}}P_{t,b,s}^{\text{WD},n}), \tag{13}$$

$$\pi_{t,b,s}^{\text{CB}}=S^{\text{base}}\sum_{n\in\Omega_L}\pi_{\text{om}}^{\text{CB}}Q_{t,b,s}^{\text{CB},n}, \tag{14}$$

$$\pi_{t,b,s}^{\text{emi}}=\pi_{t,b,s}^{\text{emi,SS}}+\pi_{t,b,s}^{\text{emi,DG}}, \tag{15}$$

$$\pi_{t,b,s}^{\text{emi,SS}}=\eta_t^{\text{emi}}S^{\text{base}}\sum_{n\in\Omega_{SS}}\pi^{\text{CO}_2}\nu_{\text{emi}}^{\text{SS}}P_{t,b,s}^{\text{SS},n}, \tag{16}$$

$$\begin{aligned}\pi_{t,b,s}^{\text{emi,DG}}=\eta_t^{\text{emi}}S^{\text{base}}\sum_{n\in\Omega_L}\pi^{\text{CO}_2}&\left(\nu_{\text{emi}}^{\text{WD}}P_{t,b,s}^{\text{WD},n}\right.\\&\left.+\nu_{\text{emi}}^{\text{PV}}P_{t,b,s}^{\text{PV},n}\right).\end{aligned} \tag{17}$$

3.1.3 Incentive

Incentive will be paid for the new investment of DGs by using the subsidy rare.

$$\mu_t^{inc}=\alpha_t\sum_{n\in\Omega_L}\left(\gamma_{\text{sub}}^{\text{WD}}\pi_{\text{inv}}^{\text{WD}}X_t^{\text{WD},n}+\gamma_{\text{sub}}^{\text{PV}}\pi_{\text{inv}}^{\text{PV}}X_t^{\text{PV},n}\right). \tag{18}$$

3.2 Constraints

3.2.1 Power Balance Constraints

The following constraints describe the active and reactive power balance of the load and substation buses. It should be mentioned that the scenario of demand, $\eta_{b,s}^{\text{load}}$, is used by multiplying the peak load of each bus.

$$\begin{aligned}&\sum_{n,m\in\Omega_N}\left(P_{t,b,s}^{n,m}-r^{n,m}I_{t,b,s}^{\text{sqr},n,m}\right)-\sum_{m,n\in\Omega_N}\left(P_{t,b,s}^{m,n}\right)\\&+P_{t,b,s}^{\text{ENS},m}+P_{t,b,s}^{\text{WD},m}+P_{t,b,s}^{\text{PV},m}=\eta_t\eta_{b,s}^{\text{load}}P^{\text{load},m},\end{aligned} \tag{19}$$

$$\begin{aligned}&\sum_{n,m\in\Omega_N}\left(P_{t,b,s}^{n,m}-r^{n,m}I_{t,b,s}^{\text{sqr},n,m}\right)-\sum_{m,n\in\Omega_N}\left(P_{t,b,s}^{m,n}\right)\\&+P_{t,b,s}^{\text{SS},m}=\eta_t\eta_{b,s}^{\text{load}}P^{\text{load},m},\end{aligned} \tag{20}$$

$$\begin{aligned}&\sum_{n,m\in\Omega_N}\left(Q_{t,b,s}^{n,m}-x^{n,m}I_{t,b,s}^{\text{sqr},n,m}\right)-\sum_{m,n\in\Omega_N}\left(Q_{t,b,s}^{m,n}\right)\\&+Q_{t,b,s}^{\text{WD},m}+Q_{t,b,s}^{\text{PV},m}+Q_{t,b,s}^{\text{CB},m}=\eta_t\eta_{b,s}^{\text{load}}Q^{\text{load},m},\end{aligned} \tag{21}$$

$$\begin{aligned}&\sum_{n,m\in\Omega_N}\left(Q_{t,b,s}^{n,m}-x^{n,m}I_{t,b,s}^{\text{sqr},n,m}\right)-\sum_{m,n\in\Omega_N}\left(Q_{t,b,s}^{m,n}\right)\\&+Q_{t,b,s}^{\text{SS},m}=\eta_t\eta_{b,s}^{\text{load}}Q^{\text{load},m}.\end{aligned} \tag{22}$$

3.2.2 Voltage and Current Equations

The nodal voltage equation and power flow equation are shown as follows:

$$V^{\mathrm{sqr},m}_{t,b,s} - 2(r^{m,n}P^{m,n}_{t,b,s} + x^{m,n}Q^{m,n}_{t,b,s}) + |z^{m,n}|^2 I^{\mathrm{sqr},m,n}_{t,b,s} - V^{\mathrm{sqr},n}_{t,b,s} = 0, \tag{23}$$

$$V^{\mathrm{sqr},m}_{t,b,s} I^{\mathrm{sqr},m,n}_{t,b,s} = P^{m,n\,2}_{t,b,s} + Q^{m,n\,2}_{t,b,s}. \tag{24}$$

To transform the non-linear equation (24) into the linear equation, the piecewise linear approximation described in (Zou et al., 2010) is used in this paper. The equation is linearized as follows:

$$V^{\mathrm{nom}2} I^{\mathrm{sqr},m,n}_{t,b,s} = \sum_{h\in\Omega_H} \left(k^{m,n,h}_{t,b,s}\Delta P^{m,n,h}_{t,b,s}\right) + \sum_{h\in\Omega_H} \left(k^{m,n,h}_{t,b,s}\Delta Q^{m,n,h}_{t,b,s}\right), \tag{25}$$

$$P^{m,n}_{t,b,s} = P^{+,m,n}_{t,b,s} - P^{-,m,n}_{t,b,s}, \tag{26}$$

$$Q^{m,n}_{t,b,s} = Q^{+,m,n}_{t,b,s} - Q^{-,m,n}_{t,b,s}, \tag{27}$$

$$X^{P+,m,n}_{t,b,s} + X^{P-,m,n}_{t,b,s} \le 1, \tag{28}$$

$$X^{Q+,m,n}_{t,b,s} + X^{Q-,m,n}_{t,b,s} \le 1. \tag{29}$$

$$P^{+,m,n}_{t,b,s} + P^{-,m,n}_{t,b,s} = \sum_{h\in\Omega_H} \Delta P^{m,n,h}_{t,b,s}, \tag{30}$$

$$Q^{+,m,n}_{t,b,s} + Q^{-,m,n}_{t,b,s} = \sum_{h\in\Omega_H} \Delta Q^{m,n,h}_{t,b,s}, \tag{31}$$

$$0 \le \Delta P^{m,n,h}_{t,b,s} \le \Delta S^{m,n,h}_{t,b,s}, \tag{32}$$

$$0 \le \Delta Q^{m,n,h}_{t,b,s} \le \Delta S^{m,n,h}_{t,b,s}, \tag{33}$$

$$k^{m,n,h}_{t,b,s} = (2h-1)\Delta S^{m,n,h}_{t,b,s}, \tag{34}$$

$$\Delta S^{m,n,h}_{t,b,s} = \frac{V^{\mathrm{nom}}\overline{I^{m,n}}}{\overline{H}}. \tag{35}$$

3.2.3 Current, Voltage, and Power Limits

The current on branches, voltage of buses, and power flow on branches should be limited in the allowable range:

$$0 \le V^{\mathrm{nom}2} I^{\mathrm{sqr},m,n}_{t,b,s} \le \overline{S^{m,n}}^2, \tag{36}$$

$$\underline{V}^2 \le V^{\mathrm{sqr},m}_{t,b,s} \le \overline{V}^2, \tag{37}$$

$$0 \le P^{+,m,n}_{t,b,s} \le V^{\mathrm{nom}}\overline{I^{m,n}} X^{P+,m,n}_{t,b,s} \tag{38}$$

$$0 \le P^{-,m,n}_{t,b,s} \le \overline{P^{\mathrm{rev},m,n}} X^{P-,m,n}_{t,b,s}, \tag{39}$$

$$0 \le Q^{+,m,n}_{t,b,s} \le V^{\mathrm{nom}}\overline{I^{m,n}} X^{Q+,m,n}_{t,b,s}, \tag{40}$$

$$0 \le Q^{-,m,n}_{t,b,s} \le V^{\mathrm{nom}}\overline{I^{m,n}} X^{Q-,m,n}_{t,b,s}. \tag{41}$$

3.2.4 Maximum DG Size Limits

The following constraint defines the maximum DG installation capacity of each bus:

$$\sum_{t\in\Omega_T} (\overline{P^{\mathrm{WD}}} X^{\mathrm{WD},n}_t + \overline{P^{\mathrm{PV}}} X^{\mathrm{PV},n}_t) \le \overline{P^{\mathrm{node}}}. \tag{42}$$

3.2.5 DG & CB Generation Limits

$$0 \le P^{\mathrm{WD},n}_{t,b,s} \le \eta^{\mathrm{WD}}_{b,s} P^{\mathrm{avl,WD},n}_t, \tag{43}$$

$$0 \le P^{\mathrm{PV},n}_{t,b,s} \le \eta^{\mathrm{PV}}_{b,s} P^{\mathrm{avl,PV},n}_t, \tag{44}$$

$$0 \le Q^{\mathrm{CB},n}_{t,b,s} \le Q^{\mathrm{avl,CB},n}_t. \tag{45}$$

Constraints (43) – (45) express the minimum and maximum generation of DGs and CB. Note that the scenarios of the wind power and PV, i.e., production factors $\eta^{\mathrm{WD}}_{b,s}$ and $\eta^{\mathrm{PV}}_{b,s}$, are used by multiplying the maximum available output of each installed DG. The following constraints show the maximum available output in each year:

$$P^{\mathrm{avl,WD},n}_t = \overline{P^{\mathrm{WD}}} X^{\mathrm{WD},n}_t C^{\mathrm{WD},n}; t = 1, \tag{46}$$

$$P^{\mathrm{avl,WD},n}_t = \overline{P^{\mathrm{WD}}} X^{\mathrm{WD},n}_t C^{\mathrm{WD},n} + P^{\mathrm{avl,WD},n}_{t-1}; t > 1 \tag{47}$$

$$P^{\mathrm{avl,PV},n}_t = \overline{P^{\mathrm{PV}}} X^{\mathrm{PV},n}_t C^{\mathrm{PV},n}; t = 1, \tag{48}$$

$$P^{\mathrm{avl,PV},n}_t = \overline{P^{\mathrm{PV}}} X^{\mathrm{PV},n}_t C^{\mathrm{PV},n} + P^{\mathrm{avl,PV},n}_{t-1}; t > 1, \tag{49}$$

$$Q^{\mathrm{avl,CB},n}_t = \overline{Q^{\mathrm{CB}}} X^{\mathrm{CB},n}_t C^{\mathrm{CB},n}; t = 1, \tag{50}$$

$$Q^{\mathrm{avl,CB},n}_t = \overline{Q^{\mathrm{CB}}} X^{\mathrm{CB},n}_t C^{\mathrm{CB},n} + Q^{\mathrm{avl,CB},n}_{t-1}; t > 1. \tag{51}$$

The number of installations of DG and CB in each bus is limited as,

$$\sum_{t\in\Omega_T} X^{\mathrm{WD},n}_t \le \overline{X^{\mathrm{WD}}_n}, \tag{52}$$

$$\sum_{t\in\Omega_T} X^{\mathrm{PV},n}_t \le \overline{X^{\mathrm{PV}}_n}, \tag{53}$$

$$\sum_{t\in\Omega_T} X^{\mathrm{CB},n}_t \le \overline{X^{\mathrm{CB}}_n}. \tag{54}$$

The constraints of the reactive power produced by DGs are expressed by using leading/lagging power factor:

$$-\tan(\cos^{-1}(\lambda^{\mathrm{WD}}_{\mathrm{lead}}))P^{\mathrm{WD},n}_{t,b,s} \le Q^{\mathrm{WD},n}_{t,b,s} \le \tan(\cos^{-1}(\lambda^{\mathrm{WD}}_{\mathrm{lag}}))P^{\mathrm{WD},n}_{t,b,s}, \tag{55}$$

$$-\tan(\cos^{-1}(\lambda^{\mathrm{PV}}_{\mathrm{lead}}))P^{\mathrm{PV},n}_{t,b,s} \le Q^{\mathrm{PV},n}_{t,b,s} \le \tan(\cos^{-1}(\lambda^{\mathrm{PV}}_{\mathrm{lag}}))P^{\mathrm{PV},n}_{t,b,s}. \tag{56}$$

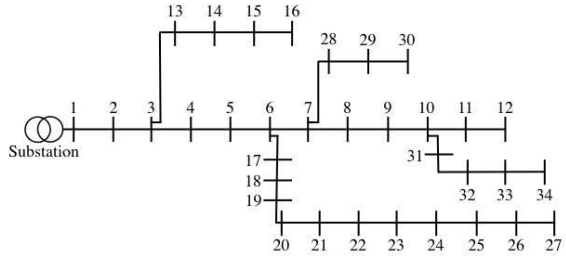

Figure 3: Distribution system configuration.

3.2.6 Investment Limits

The following constraints refer to the annualized and actual investment cost limits considering the lifetime.

$$\pi_t^{\text{inv}} \leq \pi_{\text{inv}}^{\text{bgt}}, \tag{57}$$

$$\sum_{t\in\Omega_T} \alpha_t \Big[\sum_{n\in\Omega_{SS}} \pi_{\text{inv}}^{\text{SS}} X_t^{\text{SS},n} + \sum_{n\in\Omega_L} (\pi_{\text{inv}}^{\text{PV}} X_t^{\text{PV},n} + \pi_{\text{inv}}^{\text{WD}} X_t^{\text{WD},n} + \pi_{\text{inv}}^{\text{CB}} X_t^{\text{CB},n}) \Big] \leq \pi_{\text{LT}}^{\text{bgt}}. \tag{58}$$

3.2.7 Energy Not Supplied Limits

The unserved power must be less than the demand:

$$0 \leq P_{t,b,s}^{\text{ENS},n} \leq \eta_t \eta_{b,s}^{\text{load}} P^{\text{load},n}, \tag{59}$$

$$0 \leq Q_{t,b,s}^{\text{ENS},n} \leq \eta_t \eta_{b,s}^{\text{load}} Q^{\text{load},n}. \tag{60}$$

3.2.8 Substation Limits

The following constraints show the generation limit of the substation.

$$P_{t,b,s}^{\text{SS},n} \leq \frac{S_t^{\text{avl,SS},n}}{\sqrt{1+\tan(\cos^{-1}(\lambda^{\text{SS}}))^2}}, \tag{61}$$

$$0 \leq Q_{t,b,s}^{\text{SS},n} \leq \tan(\cos^{-1}(\lambda^{\text{SS}})) P_{t,b,s}^{\text{SS},n}, \tag{62}$$

$$S_t^{\text{avl,SS},n} = S^{\text{SS},n} + S_t^{\text{new},n}, \tag{63}$$

$$S_t^{\text{new},n} = X_t^{\text{SS},n} \overline{S^{\text{SS}}}; t = 1, \tag{64}$$

$$S_t^{\text{new},n} = X_t^{\text{SS},n} \overline{S^{\text{SS}}} + S_{t-1}^{\text{new},n}; t > 1. \tag{65}$$

The substation expansion is allowed up to the maximum power:

$$S_t^{\text{new},n} \leq \overline{S^{\text{new},n}}. \tag{66}$$

4 NUMERICAL SIMULATION

4.1 Distribution System

The 34-bus three-phase radial feeder, shown in Figure 3, is used to test the proposed scenario generation and allocation problem. The system has 1 substation and 33 buses with/without load. Details of the network are given in (Chis et al., 1997).

Table 1: Simulation parameters.

Total peak load power	5.45 (MVA)	Initial available substation power	5.50 (MVA)
Capacity of wind turbine and PV	100, 2.5 (kW)	Capacity of CB	100 (kVar)
Base power	10 (MVA)	Base voltage	11 (kV)
Maximum power that can be installed at each bus	250 (kW)	Maximum numbers of wind turbine, PV modules, and CB	2, 85, 5
Thermal capacity	6.5 (MVA)	Substation voltage	1.04 (p.u.)
Annual demand growth	2 (%)	Price increasing factor	1 (%)
Minimum/ maximum limits of voltage magnitude	±5% (0.95 and 1.05 p.u.)	Number of segments used in the piecewise linearization	2
Increasing factor of emission cost	2 (%)	Lifetime of devices	20 (years)
Investment cost of transformer, wind turbine, PV module, and CB	20000,125155, 3455,38500(€)	O&M costs of wind turbine, PV, and CB	0.0079,0.0064 (€/kWh) ,0.003(€/kVarh)
Subsidy rate of wind turbine and PV	10, 5 (%)	Power factor at the substation	0.9013
Discount rate	12.5 (%)	Lagging/leading power factor of DGs	0.9013, 0.0
Interest rate	8 (%)	Cost of CO_2 emission	30 (€/tCO_2)
Investment budget per year	350000 (€)	Emission rate of purchased energy	0.55 (tCO_2/MWh)
Investment budget throughout the life cycle of devices	5500000 (€)	Emission rate of wind turbine and PV	0.25 and 0.26 (tCO_2/MWh)
Cost of not supplied energy	15000 (€/MWh)	Maximum expansion of the substation	5 (MVA)
Candidate buses of wind turbines	13-16, 21-27	Candidate buses of PV	11, 12, 24-27, 31-34

Table 2: Model information.

Number of continuous variables	2,810,473
Number of general integer variables	444,960
Number of binary variables	570,240
Number of linear constraints	4,578,985
Number of non zero coefficients	14,070,169

4.2 Data and Parameters

The simulation parameters are shown in Table 1. Actual load data of Tokyo Electric Power Company (TEPCO) are used as demand. The wind speed and solar radiation are the meteorological observation data of Miyakojima Island in Japan from Jan. 1, 2015 to Dec. 31, 2015. A twenty-year period is used as a planning horizon. Demand, wind, PV, and price levels are described in Table 3. The problem is solved using Gurobi 6.5.0 (Gurobi 6.5.0, 2016) on a Linux-based computer with 4-core Intel ®Core i7-4770 at 3.4 GHz and 24 GB of RAM. The information about the overall model is described in Table 2.

4.3 Simulation Cases

The following three cases are consided:

Case A: The investment is only allowed for the expansion of the substation, i.e., the right-hand side of Eq. (42) is zero.

Table 3: Scenario factors of each time block. The values in parentheses represent the factor's probabilities.

Time Blocks	Hours	Price (€/MWh)	Demand factors	Wind factors	PV factors
		97.63	0.61 (0.328)	0.41 (0.370)	0.65 (0.163)
1	1370	98.04	0.58 (0.328)	0.16 (0.207)	0.29 (0.602)
		98.28	0.54 (0.344)	0.00 (0.423)	0.02 (0.235)
		103.08	0.93 (0.433)	0.41 (0.329)	0.68 (0.321)
2	420	103.01	0.84 (0.236)	0.20 (0.443)	0.41 (0.371)
		102.44	0.78 (0.331)	0.00 (0.229)	0.06 (0.307)
		97.84	0.51 (0.212)	1.00 (0.423)	0.62 (0.910)
3	1316	97.68	0.48 (0.444)	0.23 (0.572)	0.28 (0.066)
		97.19	0.44 (0.344)	0.00 (0.005)	0.01 (0.024)
		100.60	0.73 (0.381)	0.92 (0.428)	0.68 (0.451)
4	1286	99.20	0.68 (0.171)	0.28 (0.022)	0.37 (0.271)
		98.26	0.64 (0.448)	0.00 (0.550)	0.05 (0.278)
		94.15	0.52 (0.245)	0.69 (0.109)	0.59 (0.070)
5	960	94.15	0.48 (0.453)	0.33 (0.529)	0.29 (0.060)
		94.15	0.45 (0.302)	0.01 (0.361)	0.01 (0.870)
		94.15	0.73 (0.324)	0.46 (0.236)	0.58 (0.155)
6	1205	94.15	0.69 (0.381)	0.24 (0.441)	0.28 (0.207)
		94.15	0.66 (0.295)	0.00 (0.323)	0.03 (0.638)
		94.15	0.62 (0.370)	0.50 (0.248)	0.57 (0.675)
7	1590	94.15	0.59 (0.304)	0.25 (0.354)	0.27 (0.143)
		94.15	0.56 (0.326)	0.00 (0.397)	0.01 (0.182)
		94.15	0.88 (0.502)	0.49 (0.323)	0.56 (0.726)
8	613	94.15	0.81 (0.168)	0.22 (0.393)	0.26 (0.096)
		94.15	0.77 (0.330)	0.00 (0.284)	0.02 (0.178)

Table 4: O&M costs (€).

Cases	A	B	C
Losses cost	1,163,844	1,012,212	786,011
Not supplied energy cost	45,320	67,221	4,937
Purchased energy cost	24,975,772	22,841,032	16,196,578
DG O&M cost	0	141,731	572,780
Capacitor bank cost	218,980	193,093	134,986
Emission cost	4,567,235	4,196,637	3,043,670
O&M system cost	30,971,152	28,451,927	20,738,962

Table 5: Total system costs (€).

Cases	A	B	C
O&M system cost	30,971,152	28,451,927	20,738,962
Investment costs	413,085	2,228,716	8,369,486
Incentive	0	185,179	697,443
Total costs	31,384,236	30,495,464	28,411,005
Computational time	25262 s	277680 s	34693 s

Case B: All the constraints are considered.

Case C: Case B without investment constraints (57) and (58).

4.4 Results and Discussions

Tables 4 and 5 show the O&M costs and total system costs. Optimal location, sizing, and timing are shown in Tables 6 and 7. The installation of DGs plays an important role to reduce the total system cost despite the fact that the investment costs are increasing. A significant contribution is that it drastically reduces the O&M costs (see Table 4). This is one of the general benefits of DG installment. From Table 4, the greatest cost savings occur in the emission cost because the emission rate of the purchased energy at the substation is two times higher than that of the DGs. Moreover, the losses cost and purchased energy cost are reduced since most DGs are allocated around the terminal buses of radial distribution system. As

Table 6: Optimal location and timing (bus).

Cases	A		B				C			
Years	SUB	CB	SUB	WD	PV	CB	SUB	WD	PV	CB
1		12 21 22 23 25 26 27 33		24 25 26	24 26 27 33 34	11 12 21 22 23 25 26 32		13 14 15 21 22 23 24 25 26 27	11 12 24 25 26 27 31 32 33 34	11 21 22 23 25 26
2		11						14		
3		24				24				
4								16		
5	1							16		
6	1		1							
7							1			23
8						21				
9		21								24
10										
11										
12						27				
13		21 31	1			21 31				21 31
14		14 21 23 25				11 23 24	1			12 21 27
15		11 14 22 26				22 31 33				11 21 25 33
16		11 15 31				21 22 24 31				11 21 22 24
17		13 22				22 25 31				14 15 22 31
18		12 13 24 32				12				11 13 26
19		13 14 21 31								13 24
20		16								15 22 31 32

Table 7: Optimal sizing (kW).

Cases	A		B				C			
Years	SUB	CB	SUB	WD	PV	CB	SUB	WD	PV	CB
1		800		600	262.5	800		1500	1875	600
2		100						100		
3		100				100				
4								100		
5	1000							100		
6	1000		1000							
7							1000			100
8						100				
9		100								100
10										
11										
12						100				
13		200	1000			200				200
14		500				300	1000			300
15		400				400				400
16		400				500				400
17		400				400				500
18		500				100				400
19		500								500
20		100								400
Total	2000	4100	2000	600	262.5	3000	2000	1800	1875	3900

shown in Table 6, the DGs allow the substation expansion to defer. However, the results imply that the expansion is not inevitable due to the intermittent nature of renewable DGs and the demand growth (see Table 7).

The O&M cost of CB decreases even if the number of CB increases (see Tables 4 and 7), implying that CB co-exists well with the large amount of the installed DGs. Without the budget constraints, nearly the same amount of wind turbine and PV are installed. However, in the consideration of the budgets, the wind power to be installed is larger than PV because it is affected by the high subsidy rate of wind.

In the same way, the simulations without the incentive were tested, i.e., the incentives of wind energy and PV are 0. The O&M and total system costs are shown in Tables 8 and 9. Tables 5 and 9 indi-

Table 8: O&M costs (€).

Cases	A	B	C
Losses cost	1,163,844	1,000,584	795,689
Not supplied energy cost	45,320	71,244	359
Purchased energy cost	24,975,772	22,808,383	16,558,486
DG O&M cost	0	133,506	537,774
Capacitor bank cost	218,980	196,581	133,903
Emission cost	4,567,235	4,191,123	3,105,423
O&M system cost	30,971,152	28,401,420	21,131,633

Table 9: Total system costs (€).

Cases	A	B	C
O&M system cost	30,971,152	28,401,420	21,131,633
Investment costs	413,085	2,262,126	7,914,809
Incentive	0	0	0
Total costs	31,384,236	30,663,546	29,046,443

Table 10: Optimal sizing under no incentive (kW).

Cases	A		B				C			
Years	SUB	CB	SUB	WD	PV	CB	SUB	WD	PV	CB
1	0	800	0	300	522.5	800	0	1000	2055	600
2	0	100	0	0	0	0	0	0	7.5	0
3	0	100	0	0	0	100	0	100	0	0
4	0	0	0	0	0	0	0	100	0	0
5	1000	0	1000	0	0	0	0	0	0	0
6	1000	0	0	0	0	0	0	100	0	0
7	0	0	0	0	0	0	1000	0	0	100
8	0	0	0	0	0	100	0	100	0	0
9	0	100	0	0	0	0	0	100	0	0
10	0	0	0	0	0	100	0	0	0	0
11	0	0	0	0	0	0	0	0	0	0
12	0	0	0	0	0	0	0	0	0	0
13	0	200	0	0	0	200	0	0	0	300
14	0	500	0	0	0	300	0	0	0	300
15	0	400	1000	0	0	400	1000	0	0	400
16	0	400	0	0	0	500	0	0	0	400
17	0	400	0	0	0	400	0	0	0	400
18	0	500	0	0	0	0	0	0	0	500
19	0	500	0	0	0	0	0	0	0	400
20	0	100	0	0	0	0	0	0	0	500
Total	2000	4100	2000	300	522.5	2900	2000	1500	2062.5	3900

cate that the incentive is helpful to decrease the total system costs, though the O&M costs of case B is increased slightly. The optimal sizing under no incentive is shown in Table 10. From this result, it is suggested that PV is installed more than wind power in the case that there are no incentives.

It is worth pointing out that the DGs have an important role in terms of system stability as well as cost minimization. The average of the voltage deviations of all scenarios in the first- and final- planning years are illustrated per case in Figure 4. The figure shows that the overall voltage drops as the demand increases for twenty years. Besides, the large installation of DGs makes the amplitude of the voltage more stable than no DGs.

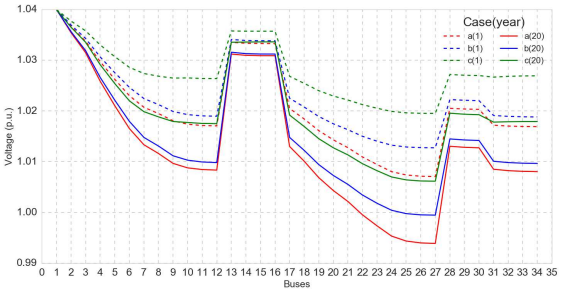

Figure 4: Average of the voltages of all scenarios per case in the first and final year.

5 CONCLUSIONS

The paper has presented a procedure for creating the demand and DG generation scenarios with K-means. Simultaneously, a long-term allocation problem of RES-based DGs has been formulated as a two-stage stochastic programming problem and tested on the 34-bus distribution system. The obtained results and insights are summarized as below:

- The long-term optimal solutions for the decision-making are obtained by solving the stochastic optimization problem with the created scenarios.
- The uncertainties of scenarios are well-represented because the substation expansions are inevitable due to the renewable energy intermittency, while the DG installation reduces the total distribution system cost.
- The proposed method with K-means can be easily implemented, improved to create many scenarios, and expanded to a multi-stage architecture.
- The proposed problem determines the optimal long-term siting, sizing, and timing of DGs, considering the variables and constraints with respect to the practical equipment and economics.
- The results show that an optimal DG allocation is quite important in order to reduce the system cost.

Future research include the following:

- Investigation of the planning results for a large distribution system.
- Comparison with the existing methodologies to analyze whether the results will be much different.
- Improvement of the scenario generation by means of the probability density function and time series model.
- Extension to a multi-stage stochastic programming problem and comparative evaluation of the validity of the solution.

ACKNOWLEDGEMENTS

We gratefully acknowledge the work of members of our laboratory. We are also grateful to the referees for useful comments. This research was supported by JST, CREST.

REFERENCES

Abdelaziz, A., Hegazy, Y., El-Khattam, W., and Othman, M. (2015). Optimal allocation of stochastically dependent renewable energy based distributed generators in unbalanced distribution networks. *Electric Power Systems Research*, 119:34–44.

Asensio, M., de Quevedo, P. M., Munoz-Delgado, G., and Contreras, J. (2016a). Joint distribution network and renewable energy expansion planning considering demand response and energy storage part i: Stochastic programming model. *IEEE Transactions on Smart Grid*, PP(99):1–1.

Asensio, M., de Quevedo, P. M., Munoz-Delgado, G., and Contreras, J. (2016b). Joint distribution network and renewable energy expansion planning considering demand response and energy storage part ii: Numerical results and considered metrics. *IEEE Transactions on Smart Grid*, PP(99):1–1.

Atwa, Y., El-Saadany, E., Salama, M., and Seethapathy, R. (2010). Optimal renewable resources mix for distribution system energy loss minimization. *IEEE Transactions on Power Systems*, 25(1):360–370.

Baringo, L. and Conejo, A. (2011). Wind power investment within a market environment. *Applied Energy*, 88(9):3239–3247.

Baringo, L. and Conejo, A. (2013a). Correlated wind-power production and electric load scenarios for investment decisions. *Applied energy*, 101:475–482.

Baringo, L. and Conejo, A. J. (2013b). Risk-constrained multi-stage wind power investment. *IEEE Transactions on Power Systems*, 28(1):401–411.

Carvalho, P. M., Ferreira, L. A., Lobo, F. G., and Barruncho, L. M. (1997). Distribution network expansion planning under uncertainty: a hedging algorithm in an evolutionary approach. In *Power Industry Computer Applications., 1997. 20th International Conference on*, pages 10–15. IEEE.

Chis, M., Salama, M., and Jayaram, S. (1997). Capacitor placement in distribution systems using heuristic search strategies. *IEE Proceedings-Generation, Transmission and Distribution*, 144(3):225–230.

Dupačová, J., Consigli, G., and Wallace, S. W. (2000). Scenarios for multistage stochastic programs. *Annals of operations research*, 100(1-4):25–53.

Eduardo, L. (1994). Solar electricity: Engineering of photovoltaic systems. *Progensa, Sevilla. ISBN*, pages 84–86505.

Eftekharnejad, S., Vittal, V., Heydt, G. T., Keel, B., and Loehr, J. (2013). Impact of increased penetration of photovoltaic generation on power systems. *IEEE transactions on power systems*, 28(2):893–901.

Fu, X., Chen, H., Cai, R., and Yang, P. (2015). Optimal allocation and adaptive var control of pv-dg in distribution networks. *Applied Energy*, 137:173–182.

Gurobi 6.5.0, Gurobi Optimization, I. (2016). User's manual. http://gams.com/help/topic/gams.doc/solvers/gurobi/index.html.

Huang, K. and Ahmed, S. (2009). The value of multistage stochastic programming in capacity planning under uncertainty. *Operations Research*, 57(4):893–904.

Jordehi, A. R. (2016). Allocation of distributed generation units in electric power systems: A review. *Renewable and Sustainable Energy Reviews*, 56:893–905.

Krukanont, P. and Tezuka, T. (2007). Implications of capacity expansion under uncertainty and value of information: the near-term energy planning of japan. *Energy*, 32(10):1809–1824.

Mavrotas, G., Demertzis, H., Meintani, A., and Diakoulaki, D. (2003). Energy planning in buildings under uncertainty in fuel costs: The case of a hotel unit in greece. *Energy Conversion and management*, 44(8):1303–1321.

Mazidi, M., Zakariazadeh, A., Jadid, S., and Siano, P. (2014). Integrated scheduling of renewable generation and demand response programs in a microgrid. *Energy Conversion and Management*, 86:1118–1127.

Montoya-Bueno, S., Muñoz-Hernández, J., and Contreras, J. (2016). Uncertainty management of renewable distributed generation. *Journal of Cleaner Production*.

Montoya-Bueno, S., Muoz, J. I., and Contreras, J. (2015). A stochastic investment model for renewable generation in distribution systems. *IEEE Transactions on Sustainable Energy*, 6(4):1466–1474.

Munoz, F. D., Hobbs, B. F., and Watson, J.-P. (2016). New bounding and decomposition approaches for milp investment problems: Multi-area transmission and generation planning under policy constraints. *European Journal of Operational Research*, 248(3):888–898.

Nick, M., Cherkaoui, R., and Paolone, M. (2014). Optimal allocation of dispersed energy storage systems in active distribution networks for energy balance and grid support. *IEEE Transactions on Power Systems*, 29(5):2300–2310.

Nick, M., Cherkaoui, R., and Paolone, M. (2015). Optimal siting and sizing of distributed energy storage systems via alternating direction method of multipliers. *International Journal of Electrical Power & Energy Systems*, 72:33–39.

Nojavan, S. and allah Aalami, H. (2015). Stochastic energy procurement of large electricity consumer considering photovoltaic, wind-turbine, micro-turbines, energy storage system in the presence of demand response program. *Energy Conversion and Management*, 103:1008–1018.

Payasi, R. P., Singh, A. K., and Singh, D. (2011). Review of distributed generation planning: objectives, constraints, and algorithms. *International journal of engineering, science and technology*, 3(3).

Pereira, B. R., da Costa, G. R. M., Contreras, J., and Mantovani, J. R. S. (2016). Optimal distributed generation and reactive power allocation in electrical distribution systems. *IEEE Transactions on Sustainable Energy*, 7(3):975–984.

Sadeghi, M. and Kalantar, M. (2014). Multi types dg expansion dynamic planning in distribution system under stochastic conditions using covariance matrix adaptation evolutionary strategy and monte-carlo simulation. *Energy Conversion and Management*, 87:455–471.

Saif, A., Pandi, V. R., Zeineldin, H., and Kennedy, S. (2013). Optimal allocation of distributed energy resources through simulation-based optimization. *Electric Power Systems Research*, 104:1–8.

Seljom, P. and Tomasgard, A. (2015). Short-term uncertainty in long-term energy system modelsa case study of wind power in denmark. *Energy Economics*, 49:157–167.

Verderame, P. M., Elia, J. A., Li, J., and Floudas, C. A. (2010). Planning and scheduling under uncertainty: a review across multiple sectors. *Industrial & engineering chemistry research*, 49(9):3993–4017.

Wang, Z., Chen, B., Wang, J., Kim, J., and Begovic, M. M. (2014). Robust optimization based optimal dg placement in microgrids. *IEEE Transactions on Smart Grid*, 5(5):2173–2182.

Zou, K., Agalgaonkar, A., Muttaqi, K., and Perera, S. (2010). Multi-objective optimisation for distribution system planning with renewable energy resources. In *Energy Conference and Exhibition (EnergyCon), 2010 IEEE International*, pages 670–675. IEEE.

APPENDIX

Nomenclature

Sets:

Ω_B	Set of time blocks
Ω_H	Set of blocks used for the piecewise linearization of quadratic power
Ω_L	Set of load buses
Ω_N	Set of branches
Ω_{SS}	Set of substation buses
Ω_T	Set of years
Ω_{S_b}	Set of scenarios in time block b

Indices:

b	Time block index
h	Index of the segment used for the linearization
n, m	Index of bus numbers
t	Time index
s	Scenario index

Parameters:

$\pi^{\text{SS}}_{\text{anu}}, \pi^{\text{WD}}_{\text{anu}}, \pi^{\text{PV}}_{\text{anu}}, \pi^{\text{CB}}_{\text{anu}}$	Annualized investment costs of transformer, wind turbine, PV module, and capacitor bank
$\pi^{\text{SS}}_{\text{inv}}, \pi^{\text{WD}}_{\text{inv}}, \pi^{\text{PV}}_{\text{inv}}, \pi^{\text{CB}}_{\text{inv}}$	Investment costs of transformer, wind turbine, PV module, and capacitor bank
$\pi^{\text{bgt}}_{\text{inv}}$	Annual investment budget
$\pi^{\text{bgt}}_{\text{LT}}$	Investment budget throughout the lifetime of the devices to be installed
$\pi^{\text{WD}}_{\text{om}}, \pi^{\text{PV}}_{\text{om}}, \pi^{\text{CB}}_{\text{om}}$	Operation and maintenance costs of wind turbine, PV module, capacitor bank
π^{loss}	Cost of power loss
π^{CO_2}	Cost of CO_2 emission
π^{ENS}	Cost of energy not supplied
$\pi^{\text{SS}}_{b,s}$	Cost of energy purchased from upper grid at substation in time block b and scenario s
$C^{\text{WD},n}, C^{\text{PV},n}, C^{\text{CB},n}$	Binary parameters whether bus n is the candidates to install wind turbines, PV modules, and capacitor banks
d	Discount rate
η^{emi}_t	Increasing factor of emission cost
η_t	Increasing factor of load
η^{SS}_t	Increasing factor of energy cost
$\eta^{\text{load}}_{b,s}$	Demand factor in time block b and scenario s
$\eta^{\text{WD}}_{b,s}, \eta^{\text{PV}}_{b,s}$	Production factors of wind turbine and PV module in time block b and scenario s
$\overline{I^{n,m}}$	Maximum current flow of branch n, m
$k^{n,m,h}_{t,b,s}$	Slope of the h-th block of the piecewise linearization for branch n, m in year t, time block b, and scenario s
i	Interest rate
$L^{\text{SS}}, L^{\text{WD}}, L^{\text{PV}}, L^{\text{CB}}$	Lifetimes of transformer, wind turbine, PV module, and capacitor bank
N^{hours}_b	Number of hours in time block b
$P^{\text{load},n}$	Active power of load in bus n
$\overline{P^{\text{WD}}}, \overline{P^{\text{PV}}}$	Maximum active power generations of wind turbine and PV module
$\overline{P^{\text{node}}}$	Maximum active power of RES that can be installed in each bus
$\overline{P^{\text{rev},m,n}}$	Maximum reverse active power flow in branch m, n
λ^{SS}	Power factor at substation
$\lambda^{\text{WD}}_{\text{lead}}, \lambda^{\text{WD}}_{\text{lag}}$	Leading/lagging power factors of wind turbine
$\lambda^{\text{PV}}_{\text{lead}}, \lambda^{\text{PV}}_{\text{lag}}$	Leading/lagging power factors of PV module
$\overline{Q^{\text{CB}}}$	Maximum reactive power generation per capacitor bank
$Q^{\text{load,n}}$	Reactive power of load in bus n
$r^{n,m}$	Resistance of branch n, m
$\nu^{\text{SS}}_{\text{emi}}, \nu^{\text{WD}}_{\text{emi}}, \nu^{\text{PV}}_{\text{emi}}$	Emission rates of purchased energy and distributed generation
$\gamma^{\text{WD}}_{\text{sub}}, \gamma^{\text{PV}}_{\text{sub}}$	Subsidy rates for investment of wind turbines and PV modules
$\overline{H}$	Number of segments used in the piecewise linearization
$\overline{S^{\text{SS}}}$	Maximum power generation of new transformers
$\overline{S^{n,m}}$	Maximum transmission capacity of branch n, m
$\overline{S^{\text{new},n}}$	Maximum new power allowed for investment in the substation n
$S^{\text{SS},n}$	Existing power in the substation n

S^{base} Base power

$\underline{V}, \overline{V}$ Minimum/maximum voltage magnitudes of the distribution network

V^{nom} Nominal voltage of the distribution network

$x^{n,m}$ Reactance of branch n,m

$\overline{X^{\text{WD},n}}, \overline{X^{\text{PV},n}}, \overline{X^{\text{CB},n}}$ Maximum number of wind turbines, PV modules, and capacitor banks to be installed in bus n

$z^{n,m}$ Impedance of branch n,m

$\text{Pr}_{b,s}$ Probability of scenario s in time block b

$\text{Pr}^{\text{load}}_{b,s}, \text{Pr}^{\text{WD}}_{b,s}, \text{Pr}^{\text{PV}}_{b,s}$ Probabilites of demand, wind power production, and PV production in time block b and scenario s

$\Delta S^{n,m,h}_{t,b,s}$ Upper bound of h-th block of the power flow of branch n,m in year t, time block b, and scenario s

α_t Present value factor

Variables:

$\pi^{\text{CB}}_{t,b,s}$ Operation and maintenance cost of capacitor banks in year t, time block b, and scenario s

$\pi^{\text{emi}}_{t,b,s}$ Costs of CO_2 emission in year t, time block b, and scenario s

$\pi^{\text{emi,SS}}_{t,b,s}, \pi^{\text{emi,DG}}_{t,b,s}$ Costs of CO_2 emission from purchased energy and DG in year t, time block b, and scenario s

π^{inv}_{t} Cost of investment in year t

$\pi^{\text{loss}}_{t,b,s}$ Cost of power losses in year t, time block b, and scenario s

$\pi^{\text{ENS}}_{t,b,s}$ Penalty cost for energy not supplied in year t, time block b, and scenario s

$\pi^{\text{new}}_{t,b,s}$ Operation and maintenance costs of distributed generation in year t, time block b, and scenario s

$\pi^{\text{om}}_{t,b,s}$ Operation and maintenance costs of in year t, time block b, and scenario s

$\pi^{\text{SS}}_{t,b,s}$ Cost of energy purchased from upper grid at substation in year t, time block b, and scenario s

μ^{inc}_{t} Incentive for new installation of the distributed generations in year t

$I^{\text{sqr},n,m}_{t,b,s}$ Square of the current flow magnitude of branch n,m in year t, time block b, and scenario s

$P^{\text{avl,WD},n}_{t}, P^{\text{avl,PV},n}_{t}$ Total active power available of wind turbines and PV modules to be installed in bus n and year t

$P^{\text{ENS},n}_{t,b,s}$ Not served active power in bus n, year t, time block b, and scenario s

$P^{\text{WD},n}_{t,b,s}, Q^{\text{WD},n}_{t,b,s}$ Active/reactive power generation of wind turbines in bus n, year t, time block b, and scenario s

$P^{\text{PV},n}_{t,b,s}, Q^{\text{PV},n}_{t,b,s}$ Active/reactive power generation of PV modules in bus n, year t, time block b, and scenario s

$P^{n,m}_{t,b,s}, Q^{n,m}_{t,b,s}$ Active/reactive power flow of branch n,m in year t, time block b, and scenario s

$P^{+,n,m}_{t,b,s}, Q^{+,n,m}_{t,b,s}$ Active/reactive power flow (forward) of branch n,m in year t, time block b, and scenario s

$P^{-,n,m}_{t,b,s}, Q^{-,n,m}_{t,b,s}$ Active/reactive power flow (backward) of branch n,m in year t, time block b, and scenario s

$P^{\text{SS},n}_{t,b,s}, Q^{\text{SS},n}_{t,b,s}$ Active/reactive power purchased from the grid at the substation in bus n, year t, time block b, and scenario s

$\Delta P^{n,m,h}_{t,b,s}, \Delta Q^{n,m,h}_{t,b,s}$ Value of the h-th block of the piecewise linearized active/reactive power of branch n,m in year t, time block b, and scenario s

$Q^{\text{avl,CB},n}_{t}$ Total reactive power available of capacitor banks to be installed in bus n and year t

$Q^{\text{CB},n}_{t,b,s}$ Reactive power compensated by capacitor banks in bus n, year t, time block b, and scenario s

$S^{\text{avl,SS},n}_{t}$ Total power available in the substation n and year t

$S^{\text{new},n}_{t}$ New transformers installed in the substation n and year t

$V^{\text{sqr},n}_{t,b,s}$ Square of voltage magnitude of bus n in year t, time block b, and scenario s

$X^{\text{SS},n}_{t}, X^{\text{WD},n}_{t}, X^{\text{PV},n}_{t}, X^{\text{CB},n}_{t}$ Number of transformers, wind turbines, PV modules, and capacitor banks to be installed in bus n and year t

$X^{P+,n,m}_{t,b,s}, X^{P-,n,m}_{t,b,s}$ Binary variable defined for forward/backward active power flow of branch n,m in year t, time block b, and scenario s

$X^{Q+,n,m}_{t,b,s}, X^{Q-,n,m}_{t,b,s}$ Binary variable defined for forward/backward reactive power flow of branch n,m in year t, time block b, and scenario s

On the Impact of using Mixed Integer Programming Techniques on Real-world Offshore Wind Parks

Martina Fischetti[1,2] and David Pisinger[2]
[1]*Vattenfall BA Wind, Jupitervej 6, 6000 Kolding, Denmark*
[2]*Technical University of Denmark, Operations Research, DTU Management, Produktionstorvet, 424 DK-2800 Kgs. Lyngby, Denmark*
{*martfi, dapi*}*@dtu.dk*

Keywords: Optimization, Mixed Integer Linear Programming, Wind Energy, Routing, Offshore Cables, Green Energy.

Abstract: Wind power is a leading technology in the transition to sustainable energy. Being a new and still more competitive field, it is of major interest to investigate new techniques to solve the design challenges involved. In this paper, we consider optimization of the inter-array cable routing for offshore wind farms, taking power losses into account. Since energy losses in a cable depend on the load (i.e. wind), cable losses are estimated by considering a possibly large number wind scenarios. In order to deal with different wind scenarios efficiently we used a precomputing strategy. The resulting optimization problem considers two objectives: minimizing immediate costs (CAPEX) and minimizing costs due to power losses. This makes it possible to perform various what-if analyses to evaluate the impact of different preferences to CAPEX versus reduction of power losses. Thanks to the close collaboration with a leading energy company, we have been able to report results on a set of real-world instances, based on six existing wind parks, studying the economical impact of considering power losses in the cable routing design phase.

1 INTRODUCTION

With a total global capacity of more than 400 GW by the end of 2015, wind power is a leading technology in the transition away from fossil fuels. Having a yearly market growth of 15-20%, it is however necessary to face new challenges on a market that is always more competitive. According to [Gonzlez et al., 2014] the expenses for electrical infrastructure of a offshore wind farm account for 15-30% of the overall initial costs. Therefore, high-level optimization in this area is a key factor. In this work we focus on the cable routing between offshore wind turbines (the so called inter-array optimization).

The power production of offshore turbines is collected through one or more substations and then conveyed to the coast. The cabling will therefore constitute a tree of cables from each substation to the connected turbines. Different cables with different costs, capacities and resistances are available on the market and the task is therefore not only to connect the turbines in the cheapest possible way, but also to choose appropriate dimensions of the cables to minimize losses.

Thanks to the collaboration with a leading energy company it has been possible to build a detailed model including nearly all the constraints arising in practical applications, and to evaluate the savings of optimized layouts on real cases. The resulting optimization tool has been validated by company experts, and is now routinely used by the planners.

Wind park cable routing optimization has obtained considerable attention in the last years. Due to the large number of constraints and the intrinsic complexity of the problem, many studies (i.e. [Dutta and Overbye, 2011, Gonzlez-Longatt and Wall, 2012, Li et al., 2008, Zhao et al., 2009]) preferred to use ad-hoc heuristics. Only a few papers used Mixed Integer Linear Programming (MILP), notably [Bauer and Lysgaard, 2015, Fagerfjall, 2010, Dutta, 2012, Berzan et al., 2011, Hertz et al., 2012, Cerveira et al., 2016, Pillai et al., 2015]. A MILP approach boosted with heuristics (a so-called mat-heuristic approach) to deal with large-scale wind parks in an acceptable time has been recently proposed in [Fischetti and Pisinger, 2016]. The present work is based on [Fischetti and Pisinger, 2016] but focuses more on real applications of the optimization model and on its economical impact. Several variants of the problem have been proposed in the literature. To the best of our knowledge

Fischetti, M. and Pisinger, D.
On the Impact of using Mixed Integer Programming Techniques on Real-world Offshore Wind Parks.
In *Proceedings of the 6th International Conference on Operations Research and Enterprise Systems (ICORES 2017)*, pages 108-118
ISBN: 978-989-758-218-9

only [Cerveira et al., 2016] has considered power loss in cables. However, [Cerveira et al., 2016] does not take into account variable cable loads due to fluctuating wind. [Bauer and Lysgaard, 2015] proposes an Open Vehicle Routing approach for this problem adding the planarity constraints on the fly. In this Open Vehicle Routing version of the problem, only one cable can enter a turbine, even if this is often not the case in the reality. In [Bauer and Lysgaard, 2015], the possibility of branching cables in the turbines (as we are doing), is mentioned as a future work. However, the substation limits, that could be a major constraint in practical applications, are not considered in [Bauer and Lysgaard, 2015]. Different approaches for the cable network design are provided in [Berzan et al., 2011]. The suggested approach is a divide-and-conquer heuristic based on the idea of dividing the big circuit problem into smaller circuit problems. The proposed MILP model cannot deal with more than 11 turbines. In [Hertz et al., 2012] the cable layout problem for onshore cases is studied. The onshore cable problem is similar to the offshore one with the following differences. First of all, the cable can be of two types: underground cables (connecting turbines to other turbines or to the above-ground level), and above-ground cables. In the first case, the cables need to be dug in the ground. Due to the fact that parallel lines can use the same dug hole, parallel structures are preferred (until a fixed number). The above-ground level cables need to follow existing roads. Such constraints do not exist in the offshore case.

The main contribution of this paper is to analyse how the inter-array cable routing of real-world wind farms can be improved by using modern optimization techniques. A particularly challenging aspect in the cable routing design, is to understand if one could limit power losses by optimizing cable routing. As a general rule, cables with less resistance are also more expensive, therefore we would like here to make a proper trade-off between investments and cable losses. We formulate the optimization problem with immediate costs (CAPEX) and losses-related costs as two separate goals. The two objectives can be merged into a single objective by proper weighing of the two parts. The weighing factor can be considered fixed or can vary: this makes it possible to perform various what-if analyses to evaluate the impact of different preferences (i.e. of different weighing factors). The latter approach is important in cases where a positive pay-back is demanded within a short time horizon, or where liquidity problems hinder choosing the best long-term solution. We report a study of both approaches on a set of real-world instances.

In order to perform the above analysis, we developed a MIP approach to optimize the routing. In the computation of power losses, it is shown that wind scenarios can be handled efficiently as part of data preprocessing, resulting in a MIP model of tractable size. Tests on a library of real-life instances proved that substantial savings can be achieved.

The rest of the paper is organized as follows: Section 2 describes our MILP model, first presenting a basic model and then improving and extending the formulation. In particular, we show how to model power losses, and propose a precomputing strategy that is able to handle this non-linearity efficiently, thus avoiding sophisticated quadratic models that would make our approach impractical. Section 3 compares our optimized solutions with an existing cable layout for a real wind farm (Horns Rev 1), showing that millions of euro can be saved. Section 4 is dedicated to various what-if analyses. Subsection 4.1 describes the real-world wind farms that we considered in our tests while Subsection 4.2 shows the results of our optimization on a testbed of real-world cases, reporting the impact of considering power losses for all the instances. Subsection 4.3 is dedicated to the Pareto optimality study. Some conclusions are finally addressed in Section 5.

2 MATHEMATICAL MODEL FOR CABLE ROUTING OPTIMIZATION

2.1 Basic Model

In the present paper we assume that the location of the turbines has already been defined. We wish to find an optimal cable connection between all turbines and the given substation(s), minimizing the total cable costs. The optimization problem considers that:

- the energy flow leaving a turbine must be supported by a single cable;
- the maximum energy flow (when all the turbines produce their maximum) in each connection cannot exceed the capacity of the installed cable;
- different cables, with different capacities, costs and impedances, can be installed;
- cable crossing should be avoided;
- a given maximum number of cables can be connected to each substation;
- cable losses (dependent on the cable type, the cable length and the current flow through the cable) must be considered in the optimization.

We will first model the problem without cable losses and then discuss in Subsection 2.2 how to efficiently express these constraints. We model turbine positions as nodes of a complete and loop-free directed graph $G = (V,A)$ and all possible connections between them as directed arcs. Some nodes correspond to the substations that are considered as the roots of the trees, being the only nodes that collect energy. Let P_h be the power production at node h. We distinguish between two different types of node:

$$h \in \begin{cases} V_T & \text{if the } h\text{-th node correspond to a turbine} \\ V_0 & \text{if the } h\text{-th node correspond to a substation} \end{cases}$$

Let T denote the set of different cable types that can be used. Each cable type t has a given capacity k_t and unit cost u_t, representing the cost per meter of the cable (CAPEX). Arc costs can therefore be defined as $c^t_{i,j} = dist(i,j)u_t$ for each arc (i,j) and for each type $t \in T$, where $dist(i,j)$ is the distance between turbine i and turbine j. In our model we use the continuous variables $f_{i,j} \geq 0$ for the maximum flow on arc (i,j). The binary variables $x^t_{i,j}$ define cable connections as

$$x^t_{i,j} = \begin{cases} 1 & \text{if arc } (i,j) \text{ with cable type } t \text{ is selected} \\ 0 & \text{otherwise} \end{cases}$$

Finally, variables $y_{i,j}$ indicate whether turbines i and j are connected (with any type of cable). Note that variables $y_{i,j}$ are related to variables $x^t_{i,j}$ as $\sum_{t\in T} x^t_{i,j} = y_{i,j}$. The overall model becomes:

$$\begin{aligned}
\min \quad & \textstyle\sum_{i,j\in V}\sum_{t\in T} c^t_{i,j}x^t_{i,j} && && (1)\\
\text{s.t.} \quad & \textstyle\sum_{t\in T} x^t_{i,j} = y_{i,j} && i,j \in V : j \neq i && (2)\\
& \textstyle\sum_{i:i\neq h}(f_{h,i} - f_{i,h}) = P_h && h \in V_T && (3)\\
& \textstyle\sum_{t\in T} k_t x^t_{i,j} \geq f_{i,j} && i,j \in V : j \neq i, && (4)\\
& \textstyle\sum_{j:j\neq h} y_{h,j} = 1 && h \in V_T && (5)\\
& \textstyle\sum_{j:j\neq h} y_{h,j} = 0 && h \in V_0 && (6)\\
& \textstyle\sum_{i\neq h} y_{i,h} \leq C && h \in V_0 && (7)\\
& x^t_{i,j} \in \{0,1\} && i,j \in V, t \in T && (8)\\
& y_{i,j} \in \{0,1\} && i,j \in V && (9)\\
& f_{i,j} \geq 0 && i,j \in V, j \neq i && (10)
\end{aligned}$$

The objective function (1) minimizes the total cable layout cost. Constraints (2) impose that only one type of cable can be selected for each built arc, and defines the $y_{i,j}$ variables. Constraints (3) are flow conservation constraints: the energy (flow) exiting each node h is equal to the flow entering h plus the power production of that node (except if the node is a substation). Constraints (4) ensure that the flow does not exceed the capacity of the installed cable, while constraints (5) and (6) impose that only one cable can exit a turbine and none can exit the substations (tree structure with root in the substations). Finally, constraints (7) impose the maximum number of cables (C) that can enter each substation.

In order to model no-crossing constraints we need a constraint for each pair of crossings arcs, i.e. a huge number of constraints. We have, therefore, decided to generate them on the fly, as also suggested in [Bauer and Lysgaard, 2015]. In other words, the optimizer considers model (1) - (10) and adds the following new constraints whenever two established connections (i,j) and (h,k) cross

$$y_{i,j} + y_{j,i} + y_{h,k} + y_{k,h} \leq 1. \tag{11}$$

The reader is referred to [Fischetti and Pisinger, 2016] for stronger versions of those constraints. Using this approach, the number of non-crossing constraints actually added to the model decreases dramatically, making the model faster to solve. As presented, the model is able to deal with small size instances only. In order to produce high quality solutions in an acceptable amount of time also for big instances a "matheuristic" framework (as the one proposed in [Fischetti and Pisinger, 2016]) should be used on top of this basic model.

2.2 Cable Losses

In this section we propose an extension of the previous model taking cable losses into account. Let us consider a generic cable (i,j) of type t, supporting a current $g^t_{i,j}$. Power losses increase with the square of the current, according to the formula:

$$3R^t \cdot dist(i,j)(g^t_{i,j})^2 \tag{12}$$

where R^t is the electrical resistance of the 3-phase cable of type t, in Ω/m. The current $g^t_{i,j}$ obviously depends on the considered wind scenario. As a consequence, dealing with equation (12) directly in the model, would imply dealing with non-linearities over multiple scenarios. Nevertheless, (12) can be simplified if we assume that all the turbines in the park have the same power production under the same wind scenario. This is a fair assumptions since typical parks are constructed by using only one turbine model and wake effect is not usually considered in electrical studies. Under this assumption, the current I_s passing through a generic cable (i,j) of type t under scenario s, can be expressed as a function of the number f of turbines supported by the cable as:

$$PLoss^{t,f,s} = (fI^s)^2 R^t dist(i,j). \tag{13}$$

The value $f = 1,...F$ is limited by the capacity of the cables. By introducing the dependency on f in our

main binary variables (now $x_{i,j}^{t,f}$) we can re-write our two objectives as:

$$min \sum_{i,j\in V} \sum_{t\in T} \sum_{f\in F} \sum_{s\in S} \pi_s PLoss^{t,f,s} x_{i,j}^{t,f} \quad (14)$$

and

$$\min \quad \sum_{i,j\in V} \sum_{t\in T} \sum_{f\in F} c_{i,j}^{t} x_{i,j}^{t,f} \quad (15)$$

where π_s is the probability of scenario s. As we have discussed earlier, minimizing losses can imply an increase of the CAPEX cost, therefore the two objective must be properly balanced. In some cases (e.g., when there is no limit on the CAPEX) they can be merged, by using a converting factor for the loss-related term: this is the estimated cost for each MW of production lost over the wind farm lifetime (Net Present Value). This value (denoted as K) is an input value, that the designer can set to the desired project-specific value. The merged objective function, now expressed in €, is then:

$$\min \sum_{i,j\in V} \sum_{t\in T} \sum_{f\in F} c_{i,j}^{t} x_{i,j}^{t,f}$$
$$+K \sum_{i,j\in V} \sum_{t\in T} \sum_{f\in F} \sum_{s\in S} \pi_s PLoss^{t,f,s} x_{i,j}^{t,f} \quad (16)$$

We notice that (16) can be rewritten as:

$$\min \sum_{i,j\in V} \sum_{t\in T} \sum_{f\in F} u_t dist(i,j) x_{i,j}^{t,f}$$
$$+K \sum_{i,j\in V} \sum_{t\in T} \sum_{f\in F} \sum_{s\in S} 3\pi_s (fI^s)^2 R^t dist(i,j) x_{i,j}^{t,f} =$$
$$\min \sum_{i,j\in V} \sum_{t\in T} \sum_{f\in F} (u_t + K \sum_{s\in S} 3\pi_s (fI^s)^2 R^t) dist(i,j) x_{i,j}^{t,f} \quad (17)$$

The non-linear expressions in the objective function (17) can actually be handled implicitly in a pre-processing phase, without changing the original model (1)-(10) at all, according to the following idea. We consider the basic model (1)–(10) without cable losses on a modified instance where each cable type is replaced by a series of "subcables" with discretized capacity and modified cable cost taking both CAPEX and revenue losses due to cable losses into account.

Nearly all wind farms are designed for only one turbine type, hence the maximum power production P_h of each turbine can be assumed to be 1, meaning that we can express the cable capacity as the maximum number of turbines supported. Consider a certain cable type t that can support up to k_t turbines. We replace it by k_t "subcable" types of capacity f = 1, 2, ..., k_t whose unit cost is computed by adding both cable/installation unit costs (u_t) and loss costs (denoted as $loss^{t,f}$) considering the current produced by exactly f turbines. Note that such unit costs increase with f, so the optimal solution will always select the subcable type f supporting exactly the number of turbines connected, hence the approach is correct.

The above approach allows us to easily consider multiple wind scenarios without affecting the model size. This is obtained by precomputing the subcable costs by just considering a weighted average of the loss cost under different wind scenarios (and hence different current productions). To be more specific, if we look again at formula (17), we can now precompute the value

$$loss^{t,f} = K \sum_{s\in S} 3\pi_s (fI^s)^2 R^t \quad (18)$$

where π_s is the probability of scenario s and I^s is the current produced by a single turbine under wind scenario s, assuming negligible wake effect, i.e., all turbines are producing the same amount of energy under a given wind scenario s. We refer to the next subsection for a more detailed example of how cable costs are pre-processed when considering losses. As said, K is a factor to estimate the value (in €) of the MW loss, and can be computed as $K = K_{euro} \cdot 8760$ where K_{euro} is the NPV for a MW/h production over the park lifetime, and 8760 is the number of hours in a year. Notice that K_{euro} acts as a weighting factor between the two objectives: minimize CAPEX costs versus minimize losses.

2.3 Loss Pre-computation

In this section we elaborate on our pre-computing strategy proposed in the previous session, using a concrete example from the real wind park Horns Rev 1. The park consists of 80 2MW turbines and is located about 15 km from the Danish shore. This park will be used as one of our test cases both in Section 3 and 4.

Fixed the turbine layout, one could consider different sets of cables to be used. Different sets can differ in cable cross section or in voltage (33kV or 66kV generally), which reflects in different capacities and resistances. The set of most adequate cables is selected by the electrical specialists in the company. Of course, different cables can lead to different solutions, as we will see in Section 4.

We will now focus on one cable set only, in order to better illustrate how different wind scenarios are handled in the pre-processing phase. Changing the cable data, the process is analogous.

Let us suppose that we are given a set of two cables: the cheapest one can support ten 2MW turbines and the most expensive fourteen turbines. This set of cables will be indicated as cb05 in Section 4. We are provided with the following table, that reports the characteristics of the two cable types.

If we want to optimize on CAPEX costs only, we just need to input to the model the capacity of each

Table 1: Cable information for cb05.

cables	type	n. of 2MW turb.	resistance [Ohm/km]	price [€/m]	install. price [€/m]
cb05	1	10	0.13	180	260
	2	14	0.04	360	260

cable type and its overall cost (cable price plus installation cost). In this case, for example, this would be:

- type 1: supports up to 10 turbines with a unit cost of 440 €/m
- type 2: supports up to 14 turbines with a unit cost of 620 €/m

Table 2 shows how the model will compute the unit price (CAPEX only) depending on the number of turbines connected.

Table 2: CAPEX costs for cb05, depending on the number of turbines connected.

cable type	n. of 2MW turb. supported	price [€/m]
1	1	440
	2	440
	3	440
	4	440
	5	440
	6	440
	7	440
	8	440
	9	440
	10	440
2	11	620
	12	620
	13	620
	14	620

Notice that, considering CAPEX costs only, the cost to use one type of cable is independent of how many turbines it is connected to (up to the capacity limit).

Let us now consider the losses in our optimization using the strategy of Subsection 2.2. As we discussed earlier, the power loss in a cable depends on the current passing through it. Since only a discrete number of turbines can be connected to each cable path, we can express the current as a function of the number f of turbines connected (as shown equation (18)) without any loss of precision in the result.

Still referring to equation (18), the losses depend also on the wind statistics in the site. We can define a wind scenario (s) as a wind speed and its probability to occur (π_s). At a given wind speed, a given turbine will produce a specific current (I_s).

Wind scenarios can be defined in different ways. In this paper we used both real measurements and scenarios derived from Weibull distributions for the specific sites. For the Horns Rev 1 case we are considering, we had real measurements from the site, i.e., a wind speed sample each 10 minutes for 10 years. We grouped all these samples in wind-speed bins of 1m/s, obtaining 25 wind scenarios (from 1 m/s to 25 m/s). The probability of each scenario was obtained looking at the frequency of the specific wind speed over all the samples. In our tests we decided to bin our data every 1 m/s, following the practice in electrical losses computations. However this should not be considered a limit: since the wind scenarios are handled in the pre-processing phase, the number of scenarios does not affect the size of the final optimization model.

Having computed I_s and π_s according to the scenario definition, power losses can now be calculated. Parameter $K_{euro} = 690$ €/MWh was computed by the company experts for a wind park lifetime of 25 years, while resistance R_t is defined according to Table 1. Using equation (18), power loss costs $loss^{t,f}$ can be now precomputed. As shown in (17), the cost considered in the objective for each cable connection will need to include the CAPEX costs (u_t) and the contribution from losses ($loss^{t,f}$). Therefore the final imput to the optimization tool for Horns Rev 1 with cb05, will be as shown in Table 3.

Table 3: Precomputed cable prices for cable cb05 (including installation costs) precomputed considering fixed costs and power losses for Horns Rev 1.

cable type	n. of 2MW turb. supported	price [€/m]
1	1	441.16
	2	442.71
	3	445.27
	4	448.87
	5	453.50
	6	459.15
	7	465.83
	8	473.54
	9	482.28
	10	492.04
2	11	639.77
	12	643.41
	13	647.36
	14	651.63

A comparison between Tables 2 and 3 shows the impact of considering losses on cable prices. While from a installation perspective the cost for each cable type is fixed, it now varies depending on how many turbines are connected. As we will see, this can have an impact on the optimal cable routing.

3 COMPARISON WITH AN EXISTING LAYOUT

We report in this section a comparison between our optimized solutions (considering and not considering losses) and the existing cable routing for Horns Rev 1, a real-world offshore park located in Denmark. Figure 1 shows the actual design for Horns Rev 1 (from [Kristoffersen and Christiansen, 2003]).

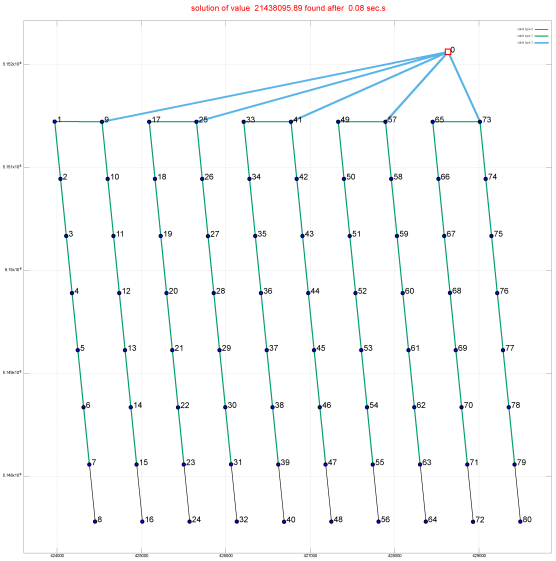

Figure 1: Existing cable routing for Horns Rev 1.

Three different types of cables are used: the thinnest cable supports one turbine only, the medium supports 8 turbines, and the thickest 16. We estimated the costs and resistances of these cables based on the cable cross section. The estimated prices are 85 €/m, 125 €/m and 240 €/m, respectively, plus an estimated 260€/m of installation costs (independent of the cable type). We ran our CAPEX optimization with the above prices obtaining the layout in Figure 2. The optimized layout is significantly different from the existing one. Looking at immediate costs, the optimized layout is over 1.5 M€ less expensive. As already said, this layout is optimized only on immediate costs, nevertheless if we estimate its value in 25 years (considering losses) this layout is still more profitable than the existing one: considering both CAPEX and losses the optimized layout is 1.6 M€ more profitable than the existing one (Net Present Value) .

By optimizing cable losses, one can further increase the value in the long term. Figure 3 shows the optimized solution considering losses (thus optimizing the value of the cable route in its lifetime). Compared with the existing layout (Figure 1), this new layout is about 1.7 M€ (NPV) more profitable in 25years, and still around 1.5 M€ cheaper at construction time.

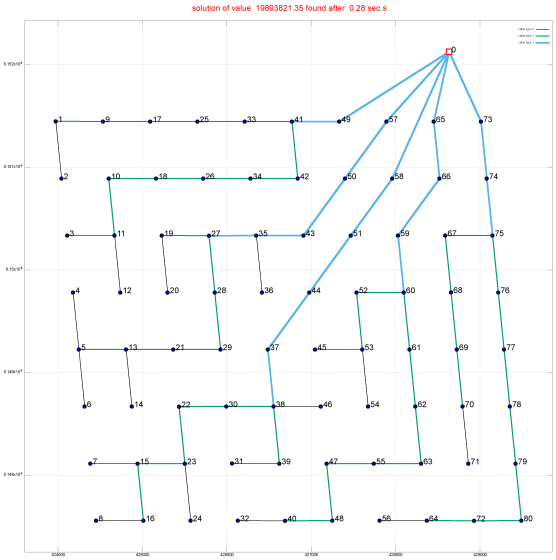

Figure 2: Optimized layout for Horns Rev 1 (CAPEX costs only): this layout results more than 1.5M € more profitable than the existing one.

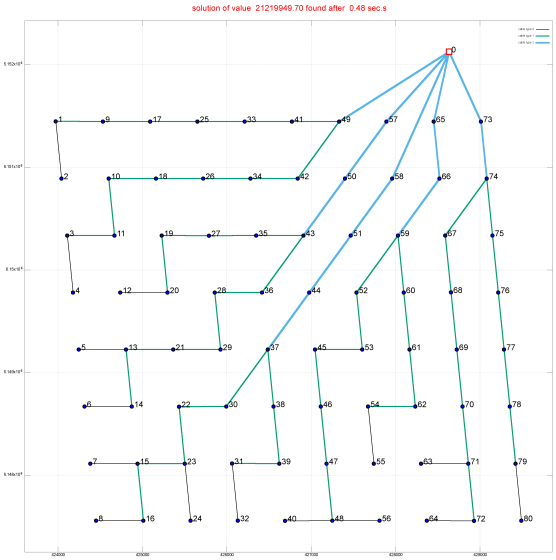

Figure 3: Optimized layout for Horns Rev 1 (considering losses): in the wind park lifetime this layout is estimated to be more than 1.7M€ more profitable than the existing one.

Table 4 summarizes the savings of the two optimized layouts compared with the existing one, both from an immediate cost perspective and from a long-term perspective: values are expressed in K€.

The test shows that millions of euros can be saved using our optimization methods on real parks. In the next section we want to focus on the other great advantage of using automatic optimization tools: the possibility of performing a number of what-if analyses. To the best of our knowledge, this is the first de-

Table 4: Savings of optimized solutions compared with the existing cable routing for Horns Rev 1.

	Savings [K€]	
opt mode	immediate	in 25years
CAPEX	1544	1605
lifetime	1511	1687

tailed study on the impact of different design choices on the cable routing itself and on its impact on immediate costs (CAPEX) and long term costs.

4 WHAT-IF ANALYSIS

We performed a number of what-if analyses on different real-world wind farms. In particular we were interest in understanding the impact of considering power losses in the design phase. We will first compare solutions optimized only for CAPEX costs, with solutions optimized looking at the whole lifetime of the park. We will then study the usage of different types of cable (with different resistances) in both cases, and the long-term savings compared with the possible higher investments costs. We will also perform a multi-criteria analysis where the user can balance between initial costs and long-term savings: this could be of interest, for example, when the company requests that the higher investment must be paid off in a limited number of years.

4.1 Test Instances

We tested our model on the real-world instances proposed in [Fischetti and Pisinger, 2016]. They consider five different real wind farms in operation in United Kingdom and Denmark, and one new wind farm under construction. These parks are Horns Rev 1, Kentish Flats, Ormonde, Dan Tysk, Thanet and Horns Rev 3.

This dataset includes old and new parks, with different power ratings and different number of turbines installed, and therefore represents a good benchmark for our tests. Each park has one substation with its own maximum number of connections (C).

In details:

- Horns Rev 1 has 80 turbines Vestas 80-2MW and $C = 10$
- Kentish Flats has 30 turbines Vestas 90-3MW. It is a near-shore wind farm, so it is connected to the onshore electrical grid without any offshore substation. Nevertheless, only one export cable is connected to the shore, therefore the starting point of the export cable is treated as a substation. We set $C = \infty$ as there is no physical substation limitation in this case.
- Ormonde has 30 Senvion 5MW and $C = 4$
- DanTysk has 80 Siemens 3.6MW and $C = 10$
- Thanet has 100 Vestas 90-3MW and $C = 10$
- Horns Rev 3 has 50 Vestas 164-8MW and $C = 12$

The dataset also includes different sets of cables, indicated as cb01, cb02, cb03, cb04 and cb05.

The cost of the cables considering power losses has been precomputed following the strategy proposed in Subsection 2.2. We computed the cable-loss prices using real measured data (for Horns Rev 1 and 3, Ormonde and DanTysk) and estimations based on Weibull distributions (Kantish Flats and Thanet).

Each combination of site (i.e. wind farm) and feasible cable set represents an instance in the testbed.

4.2 Impact of Considering Power Losses

The aim of this section is to analyse how cable routing changes when cable losses are taken into account. We used the real-world instances presented in the previous section to perform our tests. We ran our optimization tool with a time-limit of 10 hours (Intel Xeon CPU X5550 at 2.67GHz, using Cplex 12.6) in order to have high quality solutions (for the small instances these are the proven optimal solutions).

In all our instances thicker cables are more expensive and have lower resistance. This means that if the designer of the cable routing aims only at minimizing the initial costs (CAPEX), then he/she would go for the cheapest cables satisfying the load, and increase the power losses. On the contrary, focusing only on minimizing the losses, one would prefer to increase the initial costs. Using the methods explained in Section 2.2 we aim at finding the optimal balance between the two objectives, looking at the overall costs in the life time of the park.

As it can be seen from Table 5, the amount of savings varies from instance to instance, depending on the prices, on the restrictions of the specific wind farm and on the structure of the layout.

It should be noticed that the layout optimized on the lifetime always provides some savings in the long term, but the amount highly varies from case to case. In Figure 4 the case of Horns Rev 3 with cable set cb04 is shown.[1] It is seen that both the structure of the cable routing and the usage of thicker cables (green in the figure) increases in the loss-optimized layout.

[1]This is a preliminary layout from Vattenfall, not necessarily reflecting the final layout.

Table 5: Increase in the initial investment and long term savings for our test instances (Net Present Value). The first two columns denote the wind farm and possible cable types. The next column shows how much the investment is increased in the layout taking cable losses into account. In all test cases this amount is paid back in 25 years, and the additional savings by using the lifetime-optimized cable layout are shown in the last column.

wind farm	cable set	increase in initial investment [K€]	savings in 25y [K€]
Horns Rev 1	cb01	1	23
	cb02	24	60
	cb05	103	56
Kentish Flats	cb01	2	3
	cb02	1	4
	cb04	19	8
	cb05	5	1
Ormonde	cb03	9	0
	cb04	19	16
DanTysk	cb01	115	21
Thanet	cb04	15	92
	cb05	1	19
Horns Rev 3	cb04	42	172
	cb05	682	208

In this case the loss-optimized layout is 41 K€ more expensive at construction time (with respect to the CAPEX optimized layout). Nevertheless, in 25 years, this amount is paid back and another 172 K€ are saved (NPV).

We now try to investigate how the optimizer is restructuring the layout in order to have savings in the long run. As already noticed, every wind farm is different, so one cannot define a rule of thumb to design a good cable routing. Nevertheless, observing our layouts, we noticed a different proportion in the usage of the cable types (black and green in the figures). In particular, all the CAPEX solutions minimize the use of the expensive cables: looking only at the immediate costs, it is always preferable to go for the cheapest cable when possible, even creating longer connections. When optimizing considering losses, instead, cables with less resistance become more appealing, even if they are more expensive. In the Horns Rev 1 instance, for example, going from CAPEX optimized to lifetime-optimized the usage of type 1 cables decreases (from 55.5% of the total length to 40.3%) and the usage of type 2 cables increases (from 44.5 to 59.7%).

In Table 6 we report the cable usage (percentage of the total cable length) for all our test-bed solutions.

All in all, it can be observed from our results on real-world instances that in most cases it is convenient to invest in cables with lower resistance. The cable route and the type of cable selection for each connection is not an obvious choice and an optimization tool is necessary to determine it.

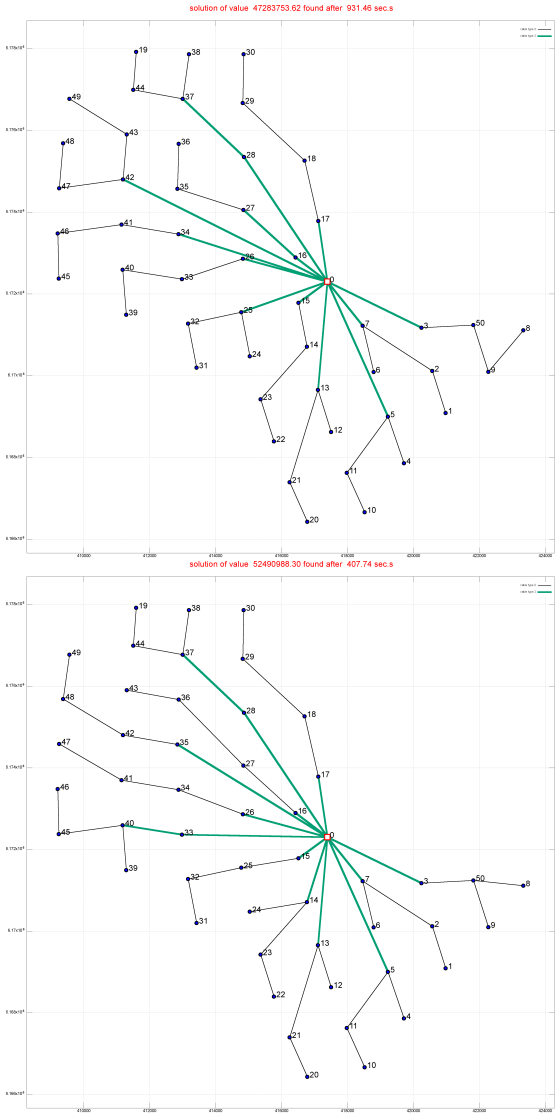

Figure 4: Optimized cable routing for Horns Rev 3, using cable set cb04. We imposed that cable type 2 can support 5 turbines only twice. The top layout is optimized only on CAPEX, the second is also considering power losses.

4.3 Bi-objectivity Tests

As discussed in Subsection 2.2, our problem has to balance between two opposite objectives: minimizing immediate costs and minimizing revenue losses in the long run. As we have seen in the previous tests, these two objectives are not always aligned since the more expensive cables have lower resistances (so less losses). The balancing factor between the two objectives is K_{euro}, that represents the price of energy (Net Present Value). Setting K_{euro} to zero, for example, means that there is no revenue from selling energy, therefore it does not matter to have losses, but it is

Table 6: Analysis on the usage of different types of cables when optimizing considering or not considering losses. The last three columns report the usage of the different cable types as percentage of the total cable length of that layout.

ID	wind farm	cable set	opt mode	length per cable type [%]		
				Type 1	Type 2	Type 3
1	Horns Rev 1	cb01	capex	55.1	40.1	4.8
2			lifetime	53.6	41.7	4.7
3		cb02	capex	57.4	42.6	
4			lifetime	44.1	55.9	
5		cb05	capex	100.0	0.0	
6			lifetime	87.7	12.3	
7	Kentish Flats	cb01	capex	66.4	33.6	0.0
8			lifetime	66.1	33.9	0.0
9		cb02	capex	66.4	33.6	
10			lifetime	60.8	39.2	
12		cb04	capex	90.1	9.9	
13			lifetime	90.1	9.9	
14		cb05	capex	95.6	4.4	
15			lifetime	95.6	4.4	
16	Ormonde	cb03	capex	69.6	30.4	
17			lifetime	76.7	23.3	
18		cb04	capex	66.9	33.1	
19			lifetime	67.4	32.6	
20	DanTysk	cb01	capex	39.0	19.4	41.7
21			lifetime	38.7	22.5	38.8
26	Thanet	cb04	capex	86.3	13.7	
27			lifetime	82.7	17.3	
28		cb05	capex	71.9	28.1	
29			lifetime	71.9	28.1	
30	Horns Rev 3	cb04	capex	57.4	42.6	
31			lifetime	60.7	39.3	
32		cb05	capex	51.8	48.2	
33			lifetime	52.6	47.4	

instead important only to minimize immediate costs. This corresponds to the case that we called "CAPEX optimized" in the previous tests. On the contrary, setting K_{euro} to a high value, implies that big revenue can be earned selling more energy, so it is very important to minimize losses (whatever initial costs this could imply). The balance between the two objectives, in practice, is set by defining the parameter K_{euro} for the specific project of interest. This is a value known by the designer, and varies from project to project. A realistic value for K_{euro} has been used in the tests of the previous subsection (this value considered WACC, subsidies for 10 years of operations and estimated market price). Nevertheless, one could be interested in studying how the balance between immediate costs and long term costs varies when varying K_{euro}. As a practical example, one could be interested in optimizing CAPEX and losses at the same time, but being sure to pay off the extra investment in a short time. We considered, in this test, Horns Rev 3 with cable set cb04. For $K_{euro} = 0$ we have our CAPEX solution of Figure 4 (top), for $K_{euro} = 690$ €/MWh we have our life-time losses optimized solution of Figure 4 (bottom). Company experts estimated 690 €/MWh to be a realistic value for the energy earning over 25 years of operation (expected lifetime of a wind park). We asked them to recompute this value assuming that we want a return of investment in a shorter time. They recomputed it to be $K_{euro} = 176$ for two years, $K_{euro} = 252$ for 3 years, $K_{euro} = 321$ for 4 years, and $K_{euro} = 386$ for 5 years. Setting our balancing factor K_{euro} to these values translates in imposing that extra CAPEX cost will be paid back in 2, 3, 4 or 5 years, respectively. We recomputed the cable costs according to these different values of K_{euro} and re-optimized the layout accordingly. Once the optimized layouts were found, we re-evaluated them with $K_{euro} = 0$ to evaluate their CAPEX costs and $K_{euro} = 690$ to estimate their cost in 25 years. Table 7 shows these figures. For K_{euro} higher than 321 €/MWh the layout is not changing any more. This means that in the lifetime optimized solution ($K_{euro} = 690$) all the additional CAPEX costs were actually paid back in 4 years of operation. In Figure 5 we plot the values from Table 7: the value of the different layouts is decomposed into its CAPEX (x axis) and lifetime-cost part (y axis). The first point (the "+" on the leftmost extreme) represents the value for the CAPEX optimized solution ($K_{euro} = 0$): it has the lowest immediate cost, but the highest cost on the long run. Proceeding from left to right, the next "+"s represent the solutions optimized over 2, 3, 4 and 5 years respectively. From 4 years on, the layout is not changing any more, and equals the solution optimized on the park lifetime ($K_{euro} = 690$), therefore all these layouts are represented at the same coordinates in the plot in Figure 5.

Table 7: Bi-objective analysis for Horns Rev 3 with cable set cb04: changing solutions varying the parameter K_{euro}.

K_{euro}	immediate cost [k€]	total lifetime cost [k€]	revenue loss due to power losses [k€]
0	47283	52663	5379
176	47291	52551	5259
252	47309	52508	5199
321	47325	52490	5165
386	47325	52490	5165
690	47325	52490	5165

5 CONCLUSIONS

In this paper we used a Mixed Integer Linear Programming (MILP) approach to optimize inter-array offshore cable routing considering both the immediate cost of the cables and their power losses during the wind farm lifetime. We proved the importance of using sophisticated optimization tools for this problem. We compared the optimized solution with an existing cable layout, proving that millions of euros can be saved in the given case. We also performed different what-if analyses taking power losses into consideration. Thanks to our optimization methods, we have been able, for the first time, to quantify the impact of considering losses when designing the cable connection of a wind farm. We performed these analyses on

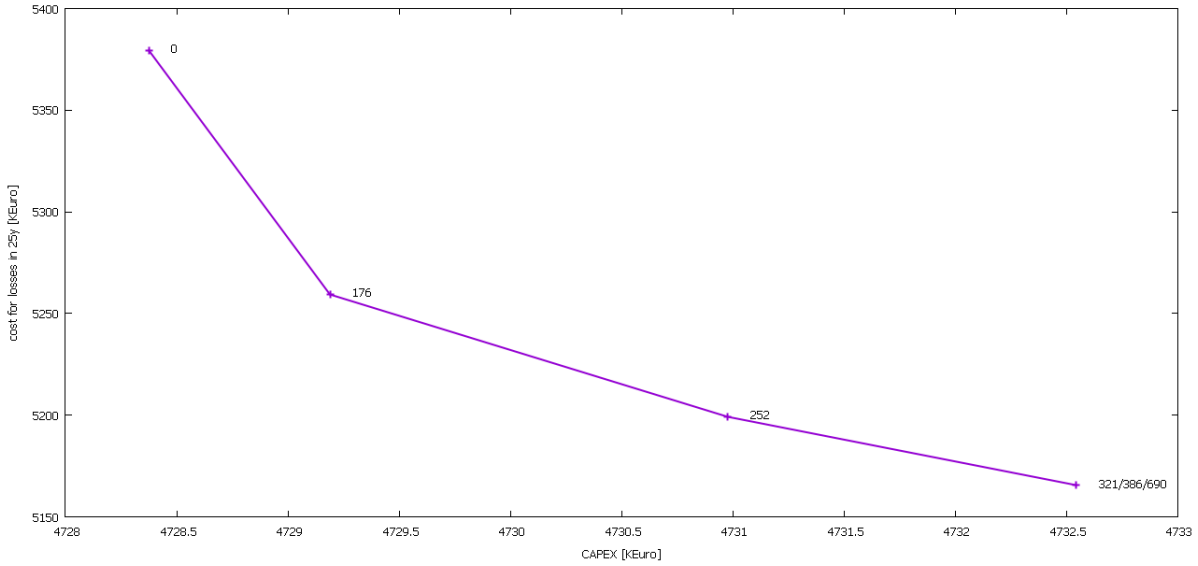

Figure 5: Bi-objective analysis from Table 7. Each "+" corresponds to a layout optimized for a given value of K_{euro} (specified beside each "+") and its coordinates correspond to its immediate cost (x axis) and costs in 25years (y axis). The layouts optimized with $K_{euro} = 321$, 386, and 690 are the same.

a number of real-world instances, analysing the behaviour of the solutions. In general, we observed that it is convenient to invest in cables with less resistance in order to reduce power losses, even if these cables are more expensive at construction time. We used our testbed to evaluate the profitability of the new solutions, both in terms of CAPEX and revenue in the long term. Finally, we performed a Pareto optimality analysis by varying the balancing parameter K_{euro}. This corresponds to giving more or less importance to power losses in the objective function, and is of great importance for designers. In this way, indeed, they can evaluate the return of investment and the impact of their assumptions on the long-term energy price, when designing their cable routing.

ACKNOWLEDGEMENTS

This work was supported by Innovation Fund Denmark. The authors would like to thank Jesper Runge Kristoffersen, Kenneth Skaug, Thomas Hjort and Iulian Vranceanu from Vattenfall BA Wind who helped in defining the cable routing constraints and the cable losses.

REFERENCES

Bauer, J. and Lysgaard, J. (2015). The offshore wind farm array cable layout problem: a planar open vehicle routing problem. *Journal of the Operational Research Society*, (66.3):360–368.

Berzan, C., Veeramachaneni, K., McDermott, J., and Reilly, U. O. (2011). Algorithms for cable network design on large-scale wind farms. Technical report. Massachusetts Institute of Technology.

Cerveira, A., Sousa, A. D., Pires, E. J. S., and Baptista, J. (2016). Optimal cable design of wind farms: The infrastructure and losses cost minimization case. *IEEE Transactions on Power Systems*, (31.6):4319 – 4329.

Dutta, S. (2012). *Data Mining and Graph Theory Focused Solutions to Smart Grid Challenges*. PhD thesis, University of Illinois.

Dutta, S. and Overbye, T. J. (2011). A clustering based wind farm collector system cable layout design. In *Power and Energy Conference at Illinois (PECI)*, pages 1–6.

Fagerfjall, P. (2010). Optimizing wind farm layout: more bang for the buck using mixed integer linear programming.

Fischetti, M. and Pisinger, D. (2016). Optimizing wind farm cable routing considering power losses. Technical report. Danish Technical University.

Gonzlez, J., Payn, M., Santos, J., and Gonzlez-Longatt, F. (2014). A review and recent developments in the optimal wind-turbine micro-siting problem. *Renewable and Sustainable Energy Reviews*, (30):133–144.

Gonzlez-Longatt, F. M. and Wall, P. (2012). Optimal electric network design for a large offshore wind farm based on a modified genetic algorithm approach. *IEEE Systems Journal*, (6.1):164–172.

Hertz, A., Marcotte, O., Mdimagh, A., Carreau, M., and Welt, F. (2012). Optimizing the design of a wind farm collection network. *Information Systems and Operational Research*, (50.2):95–104.

Kristoffersen, J. and Christiansen, P. (2003). Horns rev off-

shore windfarm: Its main controller and remote control system. *Wind Engineering*, (27.5):351–359.

Li, D., He, C., and Fu, Y. (2008). Optimization of internal electric connection system of large offshore wind farm with hybrid genetic and immune algorithm. In *Third International Conference on Electric Utility Deregulation and Restructuring and Power Technologies (DRPT2008)*, pages 2476–2481.

Pillai, A., Chick, J., Johanning, L., and Laleu, M. K. V. D. (2015). Offshore wind farm electrical cable layout optimization. *Engineering Optimization*, (47.12):1689–1708.

Zhao, M., Chen, Z., and Blaabjerg, F. (2009). Optimisation of electrical system for offshore wind farms via genetic algorithm. *IET Renewable Power Generation 3*, (3.2):205–216.

Optimization of Integrated Batch Mixing and Continuous Flow in Glass Tube & Fluorescent Lamp

Mina Faragallah[1] and A. A. Elimam[2]
[1]*Continuous Improvement Engineer, Mondeléz Egypt, 10th Ramadan, Egypt*
[2]*Mechanical Engineering Department, The American University in Cairo, New Cairo, Egypt*
mina@aucegypt.edu, aelimam@aucegypt.edu

Keywords: Production Planning, Continuous Production, Batch Mixing, Linear Programming.

Abstract: This paper deals with production planning of in-series continuous flow, and discrete production plants. The work is applied to glass and fluorescent lamp industry, where raw materials are mixed in batches, charged to a continuous furnace to produce glass tubes, and then assembled into discrete lamps. A non-linear programming model was formulated from the raw material mixing stage till the production of fluorescent lamps. Using the model, the amount of each raw material can be obtained at minimum cost, while satisfying the desired properties of the produced glass. The model also provides the optimum lamp production amounts, inventory levels, and the glass pull rate from the furnace, which determines the production amounts of glass tubes. An important factor in the continuous flow process is the amount of broken glass (cullet) added in the furnace, which has an impact of raw material cost and natural gas consumption. In order to solve the model, separable programming methods and linear approximations were used to transform the non-linear terms. Results are validated versus actual production data from local Glass & Lamp factories, and the model proved to be an efficient tool of integrating the whole process at minimum cost.

1 INTRODUCTION

The sequence of manufacturing a fluorescent lamp starts with the production of light bulb. Glass tube production is considered a continuous process and it is followed by a discrete assembling process. The production of glass bulb starts with mixing of glass basic material. Silica sand, dolomite, limestone, potash feldspar, soda ash, borax, carbon, sodium sulphate, magnesium, and alumina are the major raw materials used to form the glass batch. The batch is then charged to the furnace at 1475^{o}C. In order to shape glass into tubes, the molten glass flow over a rotating hollow cylinder to take the shape and a flow of air is blown inside the hollow cylinder. Then, the formed tubes are pulled using conveyors, cooled down at room temperature, and cut according to the desired length. The edges are modified to facilitate the assembly process. The tubes are then coated with the phosphorous coating, and the tungsten filament are assembled to the coated bulb. After that the bulb goes through exhausting, in which the tubes are vacuumed, the inert gas and the mercury drop are inserted inside the bulb and then, the bulb is sealed. End-Caps are then added to the edges of the sealed bulb and finally the lamp is tested before packaging.

2 PROBLEM DEFINITION

In such an industry, the production processes are dependent to one another. Any stoppages at one of the processes due to breakdowns or material shortages will affect the whole operation. For example, when the assembly process stops, the production of glass tubes should stop as well. However, glass production is a continuous flow operation where the production line runs 24 hours a day over 7 days of the week. The furnace is the crucial component at the whole production line where any change in the production quantity for example should be introduced gradually because of the considerable setup cost. Therefore, furnace shutdown can cause significant loss to the factory. In case of low demand and in order to avoid shutting-down the furnace, the production quantity is reduced to the minimum, leading to lower utilization. In addition, the unit cost of the glass tube increases due

Faragallah, M. and Elimam, A.
Optimization of Integrated Batch Mixing and Continuous Flow in Glass Tube & Fluorescent Lamp.
In *Proceedings of the 6th International Conference on Operations Research and Enterprise Systems (ICORES 2017)*, pages 119-127
ISBN: 978-989-758-218-9

to the reduction in production quantities. Therefore, decisions should be taken with the objective to minimize the total variable cost of the integrated operations. The variable costs are raw material, energy, inventory, and crushing cost. Several factors should be considered in order to achieve such an objective. The variables, representing these factors, are the amount of each raw material inside the glass batch, the Glass Pull Rate (P), the percentage of glass culets added to the batch (MG), the thickness of the glass tube, the inventory level in various stages (straight tube, shaped tube, and fluorescent lamp), and the scheduled scrap quantity. Given these variables, the following variety of actions could be pursued in order to minimize waste

- Given the chemical composition and the cost of each raw material, the factory has to decide upon the weight percentage of each raw material inside the batch to minimize the raw material cost without affecting the basic characteristics of the final product, such as the glass density, and the thermal expansion coefficient.
- Increasing the glass cullet percentage in the batch reduces the raw material, so the raw material cost is reduced. On the other side, the amount of glass cullet required increases, so the amount of glass tubes crushed increases.
- Also, reduction in P cause reduction in the production quantity. However, this will increase the residence time inside the furnace causing changes in the chemical composition of glass inside the furnace. Therefore, change in P should be minimized.
- The factory has to make a decision on the inventory level and on the amount at each stage, straight tube, end-formed tube, fluorescent lamp based on the inventory cost at each level and the storage limits.
- Moreover, the factory might decide upon crashing some of the glass tubes if the inventory level increases.

3 LITERATURE REVIEW

The problem mentioned above have been discussed in the literature under two major research areas, namely: raw material mixing to form the final product and production planning.

Several scholars tackled the raw material glass mixing to reach an efficient batch calculation. Khaimovich and Subbotin (2005) have developed an automated program for this batch calculation. The aim of the program is to decide upon the amount of each raw material to achieve a specified weight percentage of each oxide by developing a system of linear equations. In a follow up paper, Khaimovich (2005) improved on the program to account for the cullet composition.

Changchit and Terrell (1990) developed a linear model to decide upon the amount of each raw material in ceramic batch calculation. The model objective function minimizes the batch cost. Linear constraints were included to ensure satisfying the desired ceramic properties.

Another two models were formulated to model the mixing problem in two different industries. The first is developed by Hayta, Mehmet, and Ünsal Çakmakli (2001) to find the optimum mix of wheat to produce break making flour. The other model, which was developed by Steuer, Ralph E. (1984), modeled the mixing process to form sausage.

In addition to raw material mixing contributions, several articles discussed the production planning of discrete processes. Díaz-Madroñero, Peidro, and Mula (2015) presented a review of mathematical models developed to tackle both production and transportation routing problem. The paper have presented how different models tackled various aspects including production, inventory, and routing. Although many papers tackled the production planning problem in discrete production, small attention is given to the production planning of continuous processes.

Fabian, Tibor (1958) developed an integrated production planning model for the continuous process of iron and steel production. The model was divided into three sections that were integrated at the end of the paper. The first part dealt with the production of iron. The second part of the model was formulated to represent the steel production operation. The final part dealt with the rolling operations. Assumptions were made to facilitate the solution and to guarantee linearity, such as constant batch size and constant size of the output.

In another two scholars, Dutta, Sinha, and Roy developed integrated production steel plant model. In the first (1990), the aim was to optimize the product mix taken into consideration allocation of plant capacities to different products, capacity expansion decisions, and the optimum route of a product across available machines. The second paper (1994) dealt with the allocation of energy in case of shortage. The model developed with the objective of maximizing profit, while considering energy as a

limiting constraint.

Almada-Lobo, Oliveira, and Carravilla (2008) also tackled the production planning and scheduling of continuous process problem in coloured glass containers manufacturing. As a result of changing the product colour, setup time is required to change between colour and it's a sequence dependent process based on the two colours. A multi objective function was formulated to minimize the weighted sum of sequence dependent setup times, average inventory levels, and number of stock-outs.

In addition, Taşkın, and Ünal (2009) developed a MIP model for the production and transportation planning of a float glass manufacturing company called Trakya Cam. The company produces various product sizes in multi facilities. A model was built with the objective of minimizing the total cost including production, inventory, backorder, and transportation cost.

In this paper, a mathematical model is developed to integrate the production processes of fluorescent lamp starting from mixing of raw material till the storing of finished product. The model aimed at minimizing the total operating cost including, raw material, scheduled crushing, inventory at all levels, and energy cost, while. In the developed model, the optimum mix of raw materials is determined not only based on input variation as developed by Changchit and Terrell (1990), but also based on the optimum cullet ratio. Also, the energy cost is considered in the model to take into account the relationship between using glass cullet and energy saving as explained by Vishal, et. Al (2007) as well as Štefanić and Pilipović (2011). In addition to the mixing operation, the model takes into consideration the balance between an in-series continuous-process plant producing glass tubes followed by a discrete plant assembling fluorescent lamps. Integration between in sequence production stages is achieved, so that the demand of the following stage is a requirement from the previous stage. A major distinction between the developed model and the continuous models cited before is that the speed of the continuous process is not constant and it changes from one planning horizon to another depending on demand. Therefore, the amount of raw materials consumed and the output produced is dependent upon that variable.

4 MATHEMATICAL MODELING

4.1 Symbol Definitions

In the following three sections, the model constant parameter, sets, and decision variables are defined.

4.1.1 Constant Parameters

Symbol	Definition
$\%E_m$	Percentage of end-forming waste from the weight of straight tube size m
$\%G_m$	Percentage of cutting waste from the weight of glass tube size m
A_t	Available hours per period t
CB_t	Raw material batch Cost at period t
CC_m	Cost of crushing one glass tube of size m
CI^E_m	Monthly cost to keep one unit of end-formed tube of size m in inventory
CI^G_m	Cost of one glass tube in inventory of size m
CI^L_m	Cost to keep one lamp in inventory of size m
CN	Cost per m^3 of natural gas used in furnace
CP^E_m.	Cost to produce one unit of end-formed tube of size m
CP^L_m	Cost to produce one unit of lamp of size m
CR_i	Cost per Kg of raw material i
D	Outer diameter of glass tube
D_{mt}	Demand of fluorescent lamp of size m in period t
$F(MG\%)$	Relation between cullet ratio percentage, and natural gas consumption
F_{jk}	Chemical influence factor of oxide j on property k
H	Thickness of glass tubes
O_{ij}	Weight percentage of oxide j inside raw material i
P_{ij}	Weight percentage of oxide j inside raw material i
SI^B	Storage capacity of glass cullet
SI^E	Storage capacity of end-formed tubes
SI^G	Storage capacity of glass tubes
SI^L	Storage capacity of fluorescent lamps
SP^E_{mt}	Production capacity of end-formed tube of size m in period t
SP^L_{mt}	Production capacity of fluorescent lamps of size m in period t
SS^E_m	Safety stock of end-formed tubes of size m
SS^G_m	Safety stock of glass tubes of size m
SS^L_m	Safety stock of fluorescent lamps of size m
U^B	Lower limit for percentage of broken glass
U_j	Lower limit for percentage of oxide j
U_k	Lower limit of property k
U^P	Lower Limit of glass pull rate
V^B	Upper limit for percentage of broken glass (glass cullet)
V_j	Upper limit for the percentage of oxide j
V_k	Upper limit of property k
V^P	Upper limit of glass pull rate
W	Raw material batch Weight
X	Standard aggregate tube length
X_m	Standard length of glass tube m
Y_m	Size factor of tube size m
ρ	Density of glass

4.1.2 Sets

Symbol	Definition
I	Set of raw materials used to form the glass batch
J	Set of oxides forming the composition of the output glass
K	Set of required properties of the output glass, such as density and thermal expansion
M	Set of glass tubes sizes produced
T	Set of planning periods

4.1.3 Decision Variables

Symbol	Definition
B_t	Amount of broken glass (cullet) produced in period t
C_{mt}	Amount crushed of glass tubes of size m during period t
E_{mt}	Amount of end formed tubes m produced in period t
G_{mt}	Number of glass tubes of size m produced in period t
$I^B{}_t$	Inventory of broken glass at the end of period t
$I^E{}_{mt}$	Inventory of end formed tubes of size m at the end of period t
$I^G{}_{mt}$	Inventory of glass tubes of size m at the end of period t
$I^L{}_{mt}$	Inventory of fluorescent lamp m at the end of period t
L_{mt}	Amount of fluorescent lamps of size m produced in period t
P	Glass pull rate of glass from the furnace
$Q^E{}_{mt}$	Gross Requirements of end-formed tubes of size m during period t
$Q^G{}_{mt}$	Gross Requirements of glass tubes of size m during period t
R_{it}	Amount raw material i used in the glass batch in period t
$R^B{}_t$	Amount broken glass used in the glass batch in period t

4.2 Integrated Mathematical Model

4.2.1 Objective Function

The objective function is aimed at minimizing the total cost which includes the cost of production, inventory, scheduled crushed glass, raw material, and natural gas.

Min.

$$\begin{aligned}&\sum_{m\in M}\sum_{t\in T}[CP^L.L_{mt}+CP^E.E_{mt}]\\&+\sum_{m\in M}\sum_{t\in T}[CI^L.I^L_{mt}+CI^E.I^E_{mt}+\\&CI^G.I^G_{mt}]+\sum_{m\in M}\sum_{t\in T}CC.C_{mt}+(A_t/W)*\\&\sum_{i\in I}\sum_{t\in T}CR_i.R_{it}*P+CN*f(MG\%)*A_t\end{aligned} \quad (1)$$

4.2.2 Constraints

1. Production Capacity Constraints

A. Mass production processes (fluorescent lamp assembly and end-formed tube production)

$$L_{mt} \le SP^L_{mt}, \forall\, t \in T \,\&\, m \in M \quad (2)$$

$$E_{mt} \le SP^{EF}_{mt}, \forall\, t \in T \,\&\, m \in M \quad (3)$$

B. Continuous flow processes (glass tube production)

$$\sum_{m\in M}(X_m/X)*G_{mt}-(A_t.P)/(\pi.\rho*X*h*(d-h))=0, \forall t\in T \quad (4)$$

Where the amount of glass tube produced in period t is equal to amount of molten glass produced in t (A_t*P) over the mass of one lamp.

The glass pull rate has an operating range as follows

$$U^P \le P \le V^P \quad (5)$$

C. Glass Cullet Production

$$B_t-(\pi.\rho.X_m*h*(d-h)).\sum_{m\in M}[(1-\%G_m).C_{mt}+\%G_m.G_{mt}+\%E_m.E_{mt}]=0, \forall\, t\in T \quad (6)$$

The amount of cullet produced in t is equal to the mass of one lamp multiplied by the cut loss amount

2. Inventory Safety Stock

$$I^L_{mt} \ge SS^L_m, \forall\, t \in T \,\&\, m \in M \quad (7)$$

$$I^E_{mt} \ge SS^E_m, \forall\, t \in T \,\&\, m \in M \quad (8)$$

$$I^G_{mt} \ge SS^G_m, \forall\, t \in T \,\&\, m \in M \quad (9)$$

3. Storage Capacity

$$\sum_{m\in M} Y_m.I^L_{mt} \le SI^L, \forall\, t \in T \quad (10)$$

$$\sum_{m\in M} Y_m.I^E_{mt} \le SI^E, \forall\, t \in T \quad (11)$$

$$\sum_{m\in M} Y_m.I^G_{mt} \le SI^G, \forall\, t \in T \quad (12)$$

$$I^B_t \le SI^B, \forall\, t \in T \quad (13)$$

4. Linkage of In-Sequence Processes

$$Q^E_{mt} - L_{mt} = 0, \forall\, t \in T \,\&\, m \in M \quad (14)$$

$$Q^G_{mt} - E_{mt} = 0, \forall\, t \in T \,\&\, m \in M \quad (15)$$

5. Production & Demand Balance

$$I^L_{mt} - I^L_{m.(t-1)} + D_{mt} - L_{mt} = 0, \quad \forall\, t \in T \,\&\, m \in M \tag{16}$$

$$I^E_{mt} - I^E_{m.(t-1)} + Q^E_{mt} - E_{mt} = 0, \quad \forall\, t \in T \,\&\, m \in M \tag{17}$$

$$I^G_{mt} - I^G_{m.t-1} + Q^G_{mt} + C_{mt} - G_{mt} = 0, \quad \forall\, t \in T \,\&\, m \in M \tag{18}$$

$$I^B_t - I^B_{t-1} - B_t + A/W.P.R^B_t = 0\,, \forall\, t \in T \tag{19}$$

6. Oxide percentages upper limit & Lower Limits

$$U_j \le \frac{\left(\sum_{i\,\epsilon\,I} O_{ij}.\ R_{it}\right)}{\left(\sum_{j\,\epsilon\,J}\sum_{i\,\epsilon\,I} O_{ij}.\ R_{it}\right)} \le V_j, \forall\, t \in T \,\&\, j \in J \tag{20}$$

The numerator is the amount in Kg of oxide j in all raw materials and the broken glass divided by the yielded glass batch weight.
The equations can be written in following linear forms:

$$\sum_{i\,\epsilon\,I} O_{ij}.\ R_{it} - V_j.\left[\sum_{j\,\epsilon\,J}\sum_{i\,\epsilon\,I} O_{ij}.\ R_{it}\right] \le 0\,, \forall\, t \in T \,\&\, j \in J \tag{21}$$

$$\sum_{i\,\epsilon\,I} O_{ij}.\ R_{it} - U_j.\left[\sum_{j\,\epsilon\,J}\sum_{i\,\epsilon\,I} (P_{ij}.\ R_{it})\right] \ge 0\,, \forall\, t \in T \,\&\, j \in J \tag{22}$$

7. Broken glass percentage upper & lower limits

$$R^B_t - V^B.\left[\sum_{j\,\epsilon\,J}\sum_{i\,\epsilon\,I} O_{ij}.\ R_{it}\right] \le 0, \forall\, t \in T \tag{23}$$

$$R^B_t - U^B.\left[\sum_{j\,\epsilon\,J}\sum_{i\,\epsilon\,I} O_{ij}.\ R_{it}\right] \ge 0\,, \forall\, t \in T \tag{24}$$

8. Properties upper & lower control limits
For each oxide, the weight percentage of that oxide from the yielded batch weight is multiplied by a chemical influence factor (F)

$$\sum_{j\in J}\sum_{i\,\epsilon\,I}(F_{jk}.O_{ij}.\ R_{it}) - V_k.\left[\sum_{j\,\epsilon\,J}\sum_{i\,\epsilon\,I} O_{ij}.\ R_{it}\right] \le 0\,, \forall\, k \in K \,\&\, t \in T \tag{25}$$

$$\sum_{j\in J}\sum_{i\,\epsilon\,I}(F_{jk}.O_{ij}.\ R_{it}) - U_k.\left[\sum_{j\,\epsilon\,J}\sum_{i\,\epsilon\,I} O_{ij}.\ R_{it}\right] \ge 0\,, \forall\, k \in K \,\&\, t \in T \tag{26}$$

9. Batch Weight

$$\sum_{i\in I} R_{it} \ge W, \forall\, t \in T \tag{27}$$

10. Non-negativity Constraint

All variables are higher than or equal to zero.

5 COMPUTATIONAL WORK

5.1 Computational Plan

In order to validate the model, it is tested against base case data given by Al-Arabi Lamp and Glass Factory. The model is used to generate the same output variables, such as production and inventory amounts. Input data includes actual demand forecast for six months, cost figures for production, inventory, and crushing, raw material chemical composition, etc. Therefore, the plan goes as below:

- Linear approximation techniques are used for the non-linear terms in the objective function and constraints to transform the integrated model into linear.
- The base case input parameters are fed to the model and the results are compared vs. the actual output variables to prove model validity.
- Then, the integrated model is solved and the optimum solution is compared with Al-Arabi actuals.
- The last step is to test the sensitivity of the integrated model to variability in the raw material, energy, and crushing cost values. Different scenarios are tested and the model response is observed and analyzed.

All computational runs are solved using IBM-ILOG CPLEX V.12.6.2 on an i7 HP ProBook4540s, and the following assumptions are made:

- Raw material chemical compositions are fixed over the planning horizon
- Glass pull rate are fixed over the planning horizon, so once decided by the model, the values are the same from one period to the other.

5.2 Linear Approximations

5.2.1 Separable Programming Techniques

In order to solve the model as linear, the batch cost term in the objective function (1), and the glass cullet inventory balance constraints (19) needs to be linearized. Moreover, a relationship between the glass cullet percentage, and energy cost should be figured out. First, the linearization of constraint (19) and the batch cost term are done using separable programming techniques, where the right hand side of the equation can be expressed as the sum squared of the two variables instead of multiplying both variables. Faragallah (2016)

$$Z_{1.t} = (P + R_t^B)/2 \ , Z_{2.t} = (P - R_t^B)/2 \quad (28)$$

$$Z_{1.t}^2 - Z_{2.t}^2 = P \,.R_t^B \quad (29)$$

It is shown that for the given operating range of glass pull rate (P) and the broken glass (R_t^B), Z_1^2& Z_2^2 can be expressed as linear functions as shown in figure 1.

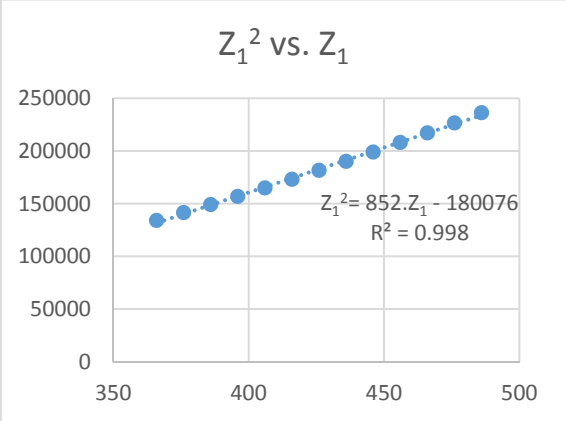

Figure 1: Linear Approximation for the Multiplication of P & R_t^B.

Therefore, (19) can be expressed as

$$B_t - I_t^{BG} + I_{t-1}^{BG} = A/W * (144.\,\mathrm{P} + 708.\,R_t^B - 101952) \quad (30)$$

The same methodology is used for the batch cost term in the objective function, so the term can be transformed into:

$$1.44.\sum_{t\epsilon T}(245.216.\,P - 508.698.\,R_t^B + 73252.5) \quad (31)$$

5.2.2 Natural Gas Cost Formulation

According to Vishal, et. Al (2007) as well as Štefanić and Pilipović (2011), the energy consumption of melting glass is reduced by 2.5 – 3% for every 10% of glass cullet addition to the batch. The average natural gas consumption at 30% glass cullet ratio is 742 m^3/hr. (Abdelrahman 2015) Therefore, a relationship can be derived between the natural gas consumption and the cullet percentage as shown below

$$F(MG\%) = -86*MG\% + 312.18 \quad (32)$$

Therefore, the last term representing the natural gas consumption cost in (Eq. 34) can be expressed as:

$$720.\,C_{NG}.(-86.\,(MG\%) + 312.18) \quad (33)$$

Where $(MG\%) = (R_t^B)/(\sum_{j\,\epsilon\,J}\sum_{i\,\epsilon\,I} PO_{ij}.\ RM_i)$ (34)

The term in (32) is a non-linear term, however, from 2015 batch data from Al-Arabi factory, the denominator for the operational range of cullet percentage has an average value of 442.49 and a standard deviation of 2.03. The model is tested with the average value, and plus and minus 3 standard deviations from the average, and the difference between the three cases was neglected, so the average value of 442.49 is used. Faragallah (2016)

5.3 Validation & Results

The developed model is used to generate the base case data provided by Al-Arabi. Table 1 and table 2 show the demand data for 2014 and cost figures used as an input. Table 3 shows the chemical composition and oxide percentages of raw materials used. All the input data was obtained from Al-Araby Glass Factory. (Abdelrahman 2015)

Besides these data, the glass factory actual plan was to set GPR at 750, cullet ratio of 30%, and to run production for 19 hours a day, and 5 hours per day of crushing. The plant total cost of production, inventory, crushing, raw material, and energy was LE **29,648,991**.

These are the operating parameters fed to the model and it proves efficiency by generate the same production and inventory amounts of glass, end-formed tubes, and lamps

Based on the input data, the number of decisions variables are 188 and the number of constraints are 404 with 96 equalities constraints. The model is solved in almost 240 seconds using CPLEX.

Then the model was solved to provide the optimum solution, which is to run the glass factory at 646 Kg/hr and a cullet ratio of 30%. Table 1, 2 & 3 provides the detailed optimum solution. The total cost of the whole planning horizon, including discrete process production cost, inventory cost, crushing, raw material, and energy cost is equal to

22,488,970 + 739,000 + 1,194,102 + 1,408,674 + 1,634,000 = LE **27,464,746**

With a total savings of LE **2,184,245** over that of Al-Arabi lamp and glass factories actuals.

Table 1: Optimum Result of End-Formed Tubes (EF) & Lamps for 40 Watts.

Month	40 Watts lamp, 1000s units				
	Demand	Units Produced		Inventory Level	
		EF	Lamp	EF	Lamp
July	1,388.8	1,388.8	1,388.8	360	1,386
Aug	1,591.2	1,591.2	1,591.2	360	1,386
Sept	1,586	1,586	1,586	360	1,386
Oct	1,433.9	1,433.9	1,433.9	360	1,386
Nov	1,771.9	1,771.9	1,771.9	360	1,386
Dec	1,739.4	1,739.4	1,739.4	360	1,386

Table 2: Optimum Result of straight tubes for 40 Watts.

Month	40 Watts, 1000s units			
	Required	Produced	Inventory	Crushed
July	1,388.8	1,764.3	1,386	375.47
Aug	1,591.2	1,721.5	1,386	130.3
Sept	1,586	1,721.5	1,386	135.5
Oct	1,433.9	1,878.7	1,386	444.77
Nov	1,771.9	1,814.5	1,386	425.91
Dec	1,739.4	1,752.9	1,386	135.32

Table 3: Optimum Glass Batch Mix.

Parameter	**Output**
silica sand (Kg)	189.80
Soda Ash (Kg)	81.00
Dolomite (Kg)	45.20
Feldspar (Kg)	35.80
Borax (Kg)	4.90
Limestone (Kg)	7.82
Alumina (Kg)	0.00
Sulphate (Kg)	0.91
Carbon (Kg)	0.06
MG (Kg)	132.50
Density (gm/cm^3)	2.488
Thermal Expansion ($10^{-7}*K^{-1}$)	100.60
Batch Cost, LE	271.61

5.4 Sensitivity Analysis

In this section, the impact of various cost figures on the optimum solution is observed and analyzed. The production cost is a major component of the total cost structure, however, the production cost is driven by the demand for lamps. Therefore, the focus is on the effect of crushing, raw material, and energy cost on the model results. A summary of the cost structure for the optimum solution of the integrated model is shown below:
Raw Material Cost = MLE 1.4086
Energy Cost = MLE 1.634
Crushing Cost = MLE 1.194
Inventory Cost = MLE 0.739
Production Cost = MLE 22.489
Total Cost = MLE 27.46

5.4.1 Impact of Raw Material & Natural Gas Cost

Changes in Soda Ash, Silica Sand, and Borax cost per ton are included in the sensitivity because they represent more than 80% of the raw material cost value. Based on historical data, changes in the cost per ton for these materials are forecasted based on the worst case scenario. Faragallah (2016) The same was done for natural gas cost. However, the raw material cost and the energy cost in the total cost function increased without affecting the optimum solution. Therefore, the model is insensitive to changes in Silica Sand, Soda Ash, Borax, and natural gas cost figures given that the remaining cost figures of the objective function do not change.

5.4.2 Impact of Crushing Cost

The crushing cost at Al-Arabi factory is the conversion cost to melt 1 Kg of glass cullet and transform it to glass tubes again. (Elbendary 2015) In order to reduce the crushing cost, the factory can outsource percentage of the glass cullet. With close chemical composition to that of the factory, the outsourced cullet cost is 500 LE/ton. (Abdelrahman 2015)

Therefore, the effect of mixing the outsourced cullet with the current batch mix is tested for different percentages of outsourced cullet (5% - 20%).

Increasing the outsourced cullet percentage up to 5% causes the crushing cost and the glass pull rate to decrease. Figure 2 summarizes the effect of outsourced cullet over the crushing cost.

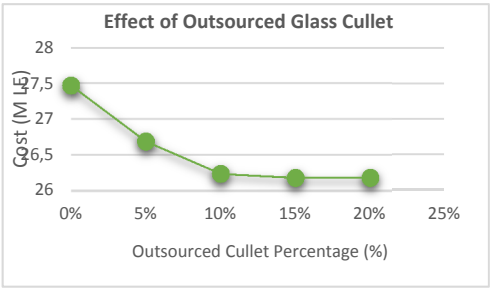

Figure 2: Total cost versus outsourced Cullet Percentage.

From the above figures, increasing the outsourced cullet percentage more than 15% doesn't have an impact on the optimum solution. Therefore, the optimum solution of the integrated model is achieved with 15% outsourced cullet ratio.

At this ratio, no crushing of straight tube is needed. Therefore, the required cullet ratio in the batch mix is achieved through the outsourced cullet and the cut loss from operation. Accordingly, the crushing cost is eliminated, the raw material and energy cost is reduced because the optimum cullet ratio in the batch mix changed from 30% to 35% due to the introduction of outsourced cullet.

6 CONCLUDING REMARKS

Integration of batch, continuous, and discrete manufacturing processes in florescent lamp manufacturing was researched. In literature, glass batch mixing, and continuous production planning for glass furnaces were treated separately in the literature found each by its own. Therefore, a mathematical model was formulated to integrate the optimum mixing of glass batch along with the production planning of discrete glass tubes and florescent lamps. The main factors affecting the manufacturing process were considered. These factors are the glass pull rate of molten glass from the furnace which control the amount of glass tubes produced, the percentage of glass cullet used in the batch which affects the amount of crushed tubes to meet the required cullet ratio, the optimum mix of raw materials, and inventory levels of glass tubes and lamps. The objective function was to reduce the total manufacturing costs including crushing, raw material, inventory, production cost, and energy cost as a function in glass cullet percentage. The objective function and some of the constraints contained non-linear terms. Separable programming methods were used to linearize the model. Then, different Scenarios were tried to test the effect of various parameters on the optimum solution. It was found that changing in raw materials and energy cost values changes the objective function value without affecting the optimum solution. Moreover, trials were made to reduce the crushing cost through using glass cullet from outside sources. It was found that with increasing the amount of outsourced cullet, the glass pull rate along with the crushing cost decreased dramatically till reaching zero. Also, the glass cullet percentage increased causing the raw material and energy costs to decrease. As a result, the total cost decreases with the increase of outsourced cullet ratio till reaching a constant value. Therefore, using outsourced cullet ratio will help reducing the amount of glass crushing, raw material cost, and energy consumption.

The model proved to be a very helpful tool for designing the optimum batch mix based on the raw material chemical composition. In addition, the model will facilitate the planning process of the two factory as an integrated entity and will help improving the total cost.

For future works, the model can be extended to include diversification of customers of the glass factory, which will reduce the unit cost. Deals from other customers, such as other lamp producers, laboratory glass ware companies, etc., should be considered to increase the amount produced of glass tubes. The following issues need to be taken into account in selecting future customers:

- Quantities requested by the customer while staying within the capacity of the glass factory.
- Customization of each order, such as different diameters and lengths which will introduce set-up time to change from one product to another. For example, changing tube diameter may require to change the GPR. This will cause production to stop for some days based on the amount of change and this may delay production to the main customer which is the lamp factory, or to other customers the factory decides to deal with.
- Price discounts given to each customer based on the quantity ordered and the level of customization from the current situation.

REFERENCES

Abdelrahman, Khaed. Personal interview. 27 Sept. 2015

Almada-Lobo, Bernardo, José F. Oliveira, and Maria Antónia Carravilla. "Production planning and scheduling in the glass container industry: A VNS approach." *International Journal of Production Economics* 114.1 (2008): 363-375.

Changchit, Chaweng, and M. Palmer Terrell. "A mathematical model for the calculation of ceramic batch formulas." *Applied Mathematical Modelling* 14.12 (1990): 641-648.

Díaz-Madroñero, Manuel, David Peidro, and Josefa Mula. "A review of tactical optimization models for integrated production and transport routing planning decisions." *Computers & Industrial Engineering* 88 (2015): 518-535.

Dutta, G., G. P. Sinha, and P. N. Roy. "Product-Mix Optimizer for an Integrated Steel Plant." (2000).

Dutta, Goutam, et al. "A linear programming model for distribution of electrical energy in a steel plant." *International Transactions in Operational Research* 1.1 (1994): 17-29.

Elbendary, Farid. Personal interview. 27 Sept. 2015

Fabian, Tibor. "A linear programming model of integrated iron and steel production." *Management Science* 4.4 (1958): 415-449.

Faragallah, Mina W. "Optimization of Integrated Batch Mixing & Continuous Flow in Glass Tube & Fluorescent Lamp." *MS Thesis. The American University in Cairo* (2016).

Hayta, Mehmet, and Ünsal Çakmakli. "Optimization of wheat blending to produce bread making flour." *Journal of food process engineering* 24.3 (2001): 179-192.

Khaimovich, M. M., and K. Yu Subbotin. "Automation of batch formula calculation." *Glass and Ceramics* 62.3-4 (2005): 109-112.

Khaimovich, M. M. "Account of cullet composition in calculation of batch formulas." *Glass and Ceramics* 62.11-12 (2005): 381-382.

Sardeshpande, Vishal, U. N. Gaitonde, and Rangan Banerjee. "Model based energy benchmarking for glass furnace." *Energy Conversion and Management*48.10 (2007): 2718-2738.

Štefanić, Nedeljko, and Ana Pilipović. "Impact of glass cullet on the consumption of energy and environment in the production of glass packaging material." *Proceedings of the 9th WSEAS International Conference on Environment, Ecosystems and Development-EED'11*.

Steuer, Ralph E. "Sausage blending using multiple objective linear programming." *Management Science* 30.11 (1984): 1376-1384.

Taşkın, Z. Caner, and A. Tamer Ünal. "Tactical level planning in float glass manufacturing with co-production, random yields and substitutable products. "*European Journal of Operational Research* 199.1 (2009): 252-26.

A Dwell Time-based Container Positioning Decision Support System at a Port Terminal

Myriam Gaete G.[1], Marcela C. González-Araya[2], Rosa G. González-Ramírez[3] and César Astudillo H.[4]

[1]*Programa de Magíster en Gestión de Operaciones, Facultad de Ingeniería, Universidad de Talca, Camino a Los Niches km 1, Curicó, Chile.*

[2]*Department of Industrial Engineering, Faculty of Engineering, Universidad de Talca, Camino a Los Niches km 1, Curicó, Chile.*

[3]*Facultad de Ingeniería y Ciencias Aplicadas, Universidad de Los Andes, Mons. Álvaro del Portillo 12.455, Las Condes, Santiago, Chile.*

[4]*Departamento de Ciencias de la Computación, Facultad de Ingeniería, Universidad de Talca, Camino a Los Niches km 1, Curicó, Chile*

myriam.gaete@copefrut.cl, mgonzalez@utalca.cl, rgonzalez@uandes.cl, castudillo@utalca.cl

Keywords: Container Terminal, Container Storage Policies, Dwell times, Stacking Strategies.

Abstract: In this article, a methodology as well as a decision support system for the container storage assignment at a yard of a container terminal is proposed. The motivation of the proposed methodology are the cases of container terminals where inland flows present high levels of uncertainty and variability. This situation is typical of ports in developing countries such as is the case in Latin America where due to lack of automation, there are many paper-based procedures and little coordination with the hinterland. The proposed methodology is based on a dwell time segregated storage policy, considering only import containers (due to the difficulty to determine segregation criteria for this type of containers). Dwell times are discretized in order to determine dwell time classes or segregations, so that containers of the same segregation are assigned to close locations at the yard. As a case study, the port of Arica in Chile is considered. A discrete-event simulation model is also proposed to estimate potential benefits of the proposed methodology. Numerical results for the case study show a good performance, with potential reduction of the rehandles incurred.

1 INTRODUCTION

World container port throughput increased by an estimated 5.1% to 651.1 million TEUs (twenty-foot equivalent units) in 2013 and global containerized trade was projected to grow by 5.6% in 2014 (UNCTAD, 2014). Maritime ports are strategic nodes on the international logistic chain whose current role goes beyond the traditional functions of transferring cargo to a more active participation and promotion of value-added services to the port stakeholders. Ports can be conceptualized from a logistics and supply chain management approach and under this vision the traditional port system is extended to an "integrated channel management system" where the port is a key location linking different flows and channels with the port community (Bichou and Gray 2004). In this context, efficient cargo handling operations are essential, as new value-added services, as well as better service levels, agility and predictability are demanded by the users of the port. The productivity of a container terminal is related to an efficient use of labor, equipment and land, and is commonly measured as a function of the ship turnaround time, the transfer rate of containers and the dwell times of the cargo at the port (Dowd and Leschine 1990; Doerr and Sánchez, 2006; Chung, 1993).

At the port, the yard can serve as a buffer between the arrival and departure of temporarily stored cargo which is later loaded on a ship or dispatched to external carriers. The efficiency of the operations at the yard significantly impact ship turnaround times so adequate container storage space assignment policies and yard equipment planning are needed. In addition, minimizing port dwell times is one of the main objectives from the perspective of the shippers in the port supply chain (Lee et al. 2003).

G., M., González-Araya, M., González-Ramírez, R. and H., C.
A Dwell Time-based Container Positioning Decision Support System at a Port Terminal.
In *Proceedings of the 6th International Conference on Operations Research and Enterprise Systems (ICORES 2017)*, pages 128-139
ISBN: 978-989-758-218-9

Coordination of landside operations at a container terminal is not straightforward in ports in developing countries where there are important challenges in terms of infrastructure development, technology implementation and paper-based documental procedures. Latin American and Caribbean (LAC) ports have seen an important increase in their participation in world foreign trade. This growth has put pressure on the freight distribution systems that need to develop better logistics capabilities (Rodrigue, 2012).

In this article, the problem of defining a container storage space allocation policy for import containers is addressed by considering the case of a container terminal that faces a high level of uncertainty in the dispatching process of import containers. This uncertainty is mainly explained by the lack of coordination mechanisms with the hinterland, a situation that can be very common at ports in emerging countries.

The assignment of space at the yard for export containers is not considered in this article. The reason is that yard planners of container terminals have general criteria to group export containers into segregations (e.g., vessel, port of destination, weight, etc.), while for import containers is more difficult to determine. This is explained as the time in which the containers are retrieved depends on the different consignees of the cargo (importers) and the fulfilment of all the procedures, resulting in more uncertainty. In contrast, export containers are loaded to a single vessel at the container terminal.

During the dispatching of an import container, it is possible that other containers may be blocking the container and should be removed to be able to reach the required container. These non-value added movements are refereed as "rehandles" or "reshuffles" of containers. Rehandles represent a high cost with no value for the container terminal, and increase the truck turnaround times of the external trucks at the container terminal, generating congestion and affecting service levels of to the users of the container terminal.

In order to assign a storage space for the import containers in the yard, a dwell time segregated storage policy is proposed. In this case, segregations of import containers are defined based on dwell time intervals, and containers of the same segregation are assigned to close locations. The aim is to reduce potential container rehandles at the moment that they are retrieved from their locations at the yard. Hence, containers with the same interval of dwell time located at close positions in the yard, may incur in less rehandles. In order to estimate dwell times of import containers, classification algorithms are employed. This is justified as the results of the estimations are used to define import container groups based on dwell time ranges so the precise values of the predicted dwell times are not needed. In addition, the design of a decision support system for the assignment of storage space to import containers is proposed. The aim is to assist the yard planner with a tool that may be inter-connected with the Terminal Operator System (TOS) of the container terminal.

As a case study, the container terminal at the port of Arica in Chile is considered. High levels of uncertainty for import container dispatching as well as long dwell times are observed in the container terminal due to the type of cargo handled; around 70% of the cargo is in-transit from Bolivia. The political agreement between Chile and Bolivia establishes special conditions for the in-transit cargo where no storage fee is charged. The current practice of the yard managers is to assign space to containers in a semi-random fashion where containers are located at the yard considering only the space utilization rules that have been set to avoid unutilized space.

In order to validate the methodology proposed in a stochastic environment, a discrete-event simulation model was implemented, to determine the potential impacts in terms of rehandles of containers when are retrieved to be dispatched to external transport carriers.

The article is structured as follows: Section 2 presents a literature review, Section 3 describes the methodology employed and the proposed dwell time segregated storage policy. Section 4 presents the architecture and components of the decision support system for the storage space assignment of import containers. Section 5 presents the case study as well as the simulation model to estimate the benefits of using the proposed support system to assign storage space to import containers. Conclusions and recommendations for further research are provided in Section 6.

2 LITERATURE REVIEW AND BACKGROUND

2.1 Main Contributions Related to Dwell Time Estimations in the Literature

Carlo et al., (2014) presents a review on storage yard operations at container terminals, providing an

overview, trends and research directions. Several contributions have been proposed, both from the perspective of the design of the layout of the yard, storage space policies and stacking algorithms. In this section, we focus the attention on reviewing the main contributions to dwell time estimations in the literature, which is more related to port terminal capacity and the storage space policies of the port terminal.

Port terminal capacity is defined as the amount of cargo that can be handled by a port per time period (Bassan 2007). The first contributions related to capacity analysis at the yard of a Container Terminal are presented by (Dally 1983; Hoffman 1985; Dharmalingam 1987), where storage capacity at the yard is estimated as a function of container dwell times, the number of stacking containers, and the container storage space available expressed in TEUs, among other factors.

Determining the factors that influence port choice and port competitiveness is another research avenue where cargo dwell times are identified as an explanatory variable (De Langen 2007; Nir et al. 2003; Tongzon and Sawant 2007; Veldman and Bückmann 2003). Arvis et al. (2010) identify dwell time as a factor that directly affects operational costs in the ports as it increases inventory levels and uncertainty in the dispatching process. On the other hand, dwell times have also been identified as an element of port competiveness and a factor in port choice related decisions (Magala and Sammons 2008).

From a macro-economic perspective, the impact of port delays at Puerto Limón in Costa Rica, over the regional economy in Central America is estimated in (USAID, 2015). They conclude that reducing port inefficiencies, such as long dwell times of cargo at the ports, may improve the GDP (Gross Domestic Product) of Costa Rica by about 0.5%. Djankov et al. (2006) employed a gravity model to estimate the impact that each additional day required for dispatching cargo may have on the GDP. The unproductive movements undertaken during quay transfer operations are quantified by Chen et al. 2000. They identify storage density as a factor of unproductive movements during ship loading and unloading operations. This refers to the number of containers stacked in the yard and the ground slots used for storage. Furthermore, their results show that housekeeping moves represent the majority of unproductive moves undertaken.

Merckx (2005) estimates dwell time impact on the capacity of a terminal based on a sensitivity analysis, considering five scenarios with different dwell times and container types. The interaction among the terminal operators and the users of the port (e.g. importers/exporters, freight forwarders) is analyzed by Rodrigue and Notteboom (2009) and they conclude that the relationship and collaboration levels could impact container dwell times at the port.

An analysis of dwell times at ports in Sub-Saharan Africa is presented by Raballand et al. (2012). Main findings highlight that dwell times are abnormally long, more than 2 weeks, and also show an abnormal dispersion which increases the inefficiencies of port operations and, in consequence, total logistic costs. Beuran et al. (2012) provide an analysis of the causes of these long dwell times from the shipper perspective, discovering the crucial importance of private sector practices and incentives.

Moini et al. (2012) analyze the factors that determine container dwell times in a port, employing three data mining algorithms: (i) Naive Bayes Algorithm (Kononenko 1990), (ii) Decision Tree C4.5 (Quinlam 1986) and (iii) The Hybrid Bayesian decision tree (Kohavi 1996). Estimation results are compared in terms of four indicators: accuracy, the Kappa coefficient, RSME and execution times. In order to evaluate the results they provide a simulation under different scenarios with the results obtained. An important difference with respect to the work presented herein, is that the authors do not use the results to estimate container storage assignment policies. In addition, the data mining algorithms also differ from those proposed in this article.

Another contribution of the work presented here, is the discretization of a continuous variable (dwell time) for its prediction, justified by the fact that the results are employed as criteria to segregate import containers and assign storage space according to this policy. In contrast, Moini et al. (2012) do not employ classification algorithms in their approach, which is reasonable as their aim is not to determine storage space policies which is an important difference with respect to the work presented here. Finally, another contribution of this work is the simulation proposed model that aims to measure the impact of different storage policies in terms of the number of rehandles incurred when containers are dispatched to external carriers. It is important to point out that in the literature there is no approach proposed in which the input data of a simulation model consists of the results obtained by the classification algorithms for dwell time estimation.

2.2 Determinant Factors of Dwell Times

Table 1: Main Determinant Factors of Dwell Time.

Factor	Reference	Type
Frequency of the sailing schedules of the vessels	Merckkx (2005), Moini *et al.* (2012)	Unique Value
Type of container (e.g., empty/full, dry/reefer, etc.), size (20/40 TEUs) and its contents	Merckkx (2005), Moini *et al.* (2012)	Nominal
Modal split of hinterland connections	Merckkx (2005), Moini *et al.* (2012)	Unique Value
Port Governance and structure	Merckkx (2005), Moini *et al.* (2012)	Unique Value
Location of the Port Terminal and the main products (or logistic chains) that are transferred.	Merckkx (2005), Moini *et al.* (2012)	Unique Value
Terminal working hours and business days	Merckkx (2005), Rodrigue and Notteboom (2009), Moini *et al.* (2012)	Unique Value
Shippers and consignee	Rodrigue and Notteboom (2009), Moini *et al.* (2012)	Nominal
Inspections and regulatory procedures	Moini *et al.* (2012)	Unique Value
Transport corridors	Moini *et al.* (2012)	Nominal
Ocean carriers or Maritime Shipping Company and the demurrage time for the empty containers	Moini *et al.* (2012)	Nominal
Container flow balance (export and import)	Moini *et al.* (2012)	Nominal
Freight Forwarder/Broker and Third Party Logistics Company (3PL)	Moini *et al.* (2012)	Nominal

The main factors considered in the literature as dwell time determinants are presented in Table 1. The factors are divided into two groups: unique value and nominal value. Factors with a unique value are those that may have a unique value at each port and this value does not vary as a function of the cargo transferred at the port (i.e., the frequency on the itineraries, the location of the port terminal, etc.). This type of factor is not considered as the results for predicting dwell time are employed for container space allocation policies and this is influenced by the amount of cargo handled. On the other hand, nominal and numerical factors correspond to factors that vary as a function of the cargo handled, where nominal factors are represented by strings and numerical factors by a number. For instance, a nominal factor is related to the name of the importer or exporter, while the weight of a container is a numerical factor.

3 METHODOLOGY DESCRIPTION

The dwell time segregated storage space policy is based on generating segregations of import containers based on dwell time intervals. In this way, containers of the same segregation are those whose dwell time is predicted to be at the same interval. In order to determine the dwell time classes and estimate the potential impact of the proposed storage space policy, the proposed methodology is described as follows in Table 2.

Table 2: General Methodology.

DWELL TIME BASED STORAGE SPACE POLICY CALIBRATION

INPUT: Data Base with Historical Data on the arrival and departure time of import containers

1. **STAGE 1:** Dwell time prediction by classification algorithms
1.1. Class definition as a function of time intervals in order to discretize the dwell time numerical variable.
1.2. Application and validation of the classification algorithms based on a predictive model.
1.3. Identification of the interrelation among the dwell time measure units based on a multi-classifier generation.
1.4. Performance evaluation of the classification algorithms.

2. **STAGE 2:** Dwell time segregated storage policy implementation and evaluation
2.1. Segregate containers based on the dwell time classes obtained in Stage 1.
2.2. Run the simulation model for a set of instances, testing the performance in terms of the number of rehandles when containers are retrieved. Compare results with alternative storage policies that may resemble the current practice of the container terminal under study.

Output: Policy and impact estimation if dwell-time segregated policy is implemented.

3.1 STAGE 1: Dwell Time Prediction by Classification Algorithms

As observed in Table 2, the first stage consists of applying classification algorithms to predict dwell times. For this, it is necessary to have a data base with historical data about the containers' arrival and departure times at the yard. Step 1.1 is related to the class interval definition. We consider that the classes

may be measured in three time units: hour, day and week. Table 3 presents a more detailed description of Step 1.2.

For the sample size definition, the formula to be used is provided by Cochran (1986), in which the size of the population is assumed to be an input data. For the classification model, different classification algorithms can be evaluated according to the specific characteristics of the container terminal under study. In addition, Step 1.3 consists of the definition of the multi-classifier to determine the inter-relations among different dwell time measure units. Step 1.4 consists of an evaluation of the results obtained by the different classification algorithms. Four performance metrics are considered: (i) the number of instances classified correctly, (ii) the Kappa coefficient, (iii) the computational time and (iv) the mean squared error in time units (Witten et al. 2011).

Table 3: Classification algorithms based on a predictive model.

Step 1.2 Classification algorithm application and validation
INPUT: Data base with historical data on the arrival and departure times of import containers 1. Sample size definition 2. Random sample of instances 3. Definition of the classification model 4. Evaluation of the classification model 5. Estimation of the prediction error
Output: Dwell time predictions.

3.2 STAGE 2: Dwell Time Segregated Storage Policy Implementation and Evaluation

A common practice of terminal operators is to assign space to containers at the yard based on segregations. In order to determine segregations of import containers based on dwell time intervals, the predicted dwell times and intervals found in stage 1 (see Table 2) are employed for an instance of the container terminal under study. Then, a real time stacking heuristic for locating the import containers in each dwell time segregation is defined, so that containers of the same segregation may be assigned to close locations with the aim of reducing rehandles when containers are retrieved.

In order to evaluate the benefits of implementing the policy at the yard, a discrete event simulation model is also proposed, in which the dwell-time storage space policy is implemented to define the location of the import containers at the yard. The dispatching process of the import containers to external carriers is also simulated in order to count the number of rehandles incurred. More details will be provided at section 5 with the case study.

4 DECISION SUPPORT SYSTEM FOR THE ASSIGNMENT OF STORAGE POSITIONS TO IMPORT CONTAINERS

This section details the architecture of a decision support system for the container position assignment at the yard of a container terminal. The aim of the system is two-fold: First, we enhance the capabilities of the TOS with a module that predicts the dwell time based on historical data. Second, we take advantage of that prediction in order to suggest an explicit storage location for the container under scrutiny.

When an import container is unloaded from the vessel and is transported to the yard, the yard planner examines the container and faces the decision of where to store it. The yard planner uses the proposed system to estimate the dwell time based on characteristics associated to the container and historical information of other containers stored in the yard. As opposed to expert intuition, this estimation can be used to make an informed decision. If the yard planner desires, the system can suggest a specific storage location for the container.

When a container is assigned to a particular storage slot at the yard, it is stored until requested by the consignee. There are some cases in which the container may be relocated because it is blocking the access to the yard crane to retrieve another container. These movements are also referred as rehandles. One of the objectives of the yard planner, is to reduce the number of rehandles or relocations of containers, as these are non-value movements that generate additional costs and waiting times.

The storage space at the yard is organized as a three dimensional matrix ordered in bays, columns and rows (see Figure 1 for a pictorial reference). This abstract representation is convenient for maintaining an internal representation of the current state of the storage space. It is possible to define algorithmic operations for assigning a slot to a container, requesting the coordinates of a particular container, and analyzing if there is more containers on top of the requested item (i.e., a container), and so on.

In order to explain the details of our proposed architecture, we will describe a sequence of temporal events and the relationship with each particular

module of the system. Figure 2 depicts the software architecture for the above-mentioned decision support system. This system is constituted by one main module that is connected to the TOS. The TOS corresponds to a software suite designed to manage the resources of the container terminal and it can be an in-house developed software or a generic commercial product (e.g.,Navis N4 TOS).

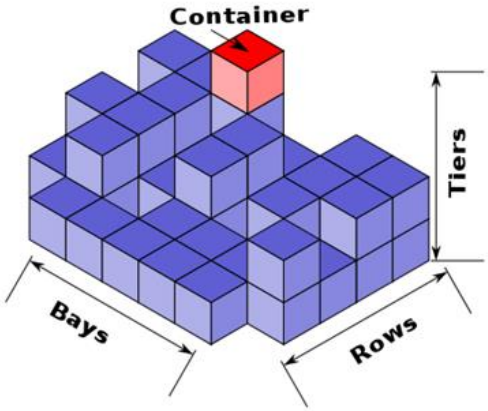

Figure 1: BAROTI System.

The whole process begins when the import container arrives to the port. At that moment, the yard planner accesses the graphical user interface (GUI) to identify the container that must be stored (labelled with the number 1 in the Figure 2). Then, the system connects to the TOS, retrieving statistical information regarding the container such as the name of the consignee, the service or vessel, type of container, weight, etc. This information is fed to the predictor and an estimation for the dwell time is obtained (see number 2 in the Figure 2). This estimation is made based on a mathematical model that use the historical data of containers and dwell time kept in the Container database. The planner use the dwell time estimation to decide where to place the container.

Alternatively, the planner may request to the system a recommendation for the location of the incoming container to the yard. For this matters, the system includes a special module that may suggest to the yard planner, a storage position at the yard (see label 3 in the Figure 2). The module internally ask for a dwell time prediction, which is used as the input for an internal algorithm that outputs a location. This output location is assumed to be the best option for storing the current container. The general assumption is that two containers with a similar dwell time must be located in neighbouring regions. In contrast, two containers with a big difference in their dwell times, are assign to different locations avoiding to interfere to each other.

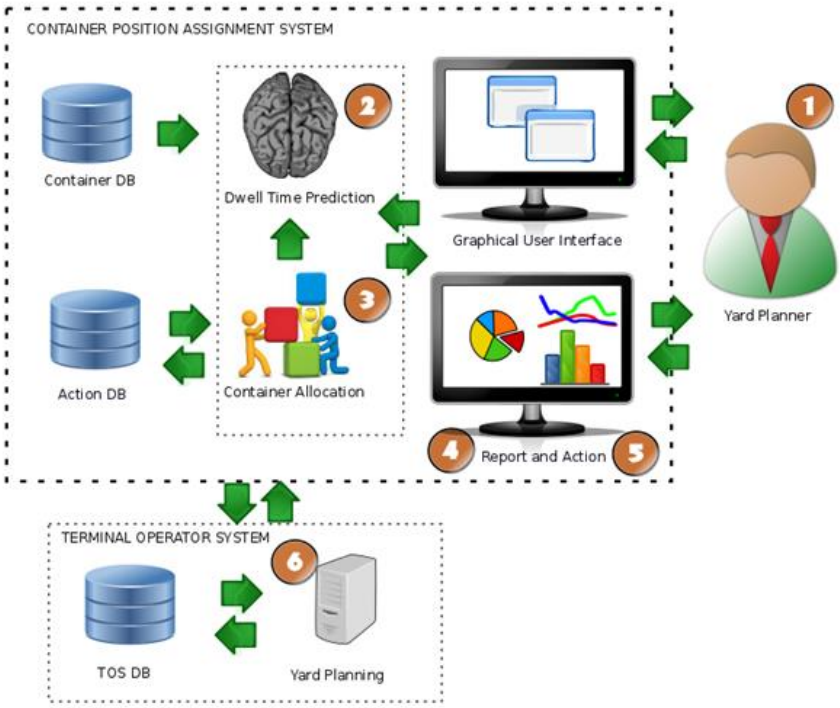

Figure 2: Container Position Assignment System architecture.

Once the dwell time prediction and/ or the storage position of each incoming container at the yard have been determined, the system generated a report with this information. This report may include a graphical representation of the yard. In this report, the location in which the current container must be assigned is specified (label 4 in the Figure 2). Based on this information the yard planner may decide whether to accept to locate the import container in the suggested position. This action (label 5) is recorded in the *Action Database*. Here, our idea is that the learning system is generating solutions for the problem and the human expert can validate them as being correct or wrong, knowledge that can be further exploited to refine the learning method of the system.

Finally (label 6), the decision made by the yard planner is communicated to the TOS, which records the transaction. As a final comment in this matter, we observe that the architecture is not limited for a single user. Rather, more than one yard planner may access the service concurrently, which can be an advantageous feature, as this information for instance, could be provided to the yard crane operators in a mobile device.

5 CASE STUDY: PORT OF ARICA IN CHILE

The port of Arica, Chile is used in this case study because it presents a high level of uncertainty in the import processes and huge container dwell times. The port of Arica occupies the 43rd position in the Latin American containerized movements ranking provided by UN-ECLAC; and the 6th position in the Chilean port system, with a total of 204,174 TEUs transferred in 2013 (Doerr 2013). The port consists of a single multi-purpose terminal whose main characteristic is that about 70% of the cargo corresponds to cargo in transit from Bolivia. The port presents special conditions for cargo handling, due to the political agreements between Chile and Bolivia, a reason for which the cargo has no storage fee (exports for 60 days and imports up to 365 days). Furthermore, the main hinterland (located in Bolivia) is more than 1000 kilometers away, in contrast with the main Chilean ports, Valparaiso and San Antonio, whose main hinterland (Metropolitan Region of Santiago) is located at 120 kilometers from the ports.

The port of Arica lacks coordination of systems with the hinterland such as appointment or booking systems, or electronic data interchange. This fosters the uncertainty and variability in port operations, especially for the import processes. Long service times (truck turnaround times) and container rehandles are commonly observed. Under this situation, the current practice of the yard managers is to assign space to containers in a semi-random fashion, where containers are located at the yard considering only very simple rules that maximize space utilization. A segregation-based policy for storage space assignment of export containers has been an efficient strategy for reducing rehandles incurred when containers are loaded on the vessel. Segregating export containers is commonly done based on the vessel´s characteristics and the corresponding route. These characteristics are considered when the stowage plan is generated and hence, rehandles are potentially minimized. In contrast, the criteria for segregating import containers are not so straightforwardly determined, especially if high levels of uncertainty on the dispatching times are observed.

In this paper a methodology to implement a dwell time segregated policy for assigning space to import containers is proposed. The policy considers segregating containers based on predicted dwell time intervals. In order to evaluate the different classification and multi-classification algorithms employed, the following metrics have been considered: (i) number of instances correctly classified, (ii) accuracy, (iii) Kappa´s coefficient; (iv) the mean squared error; (v) the mean error in time units" and (vi) the mean error for categorized factors.

A data base with container movements for the years 2011, 2012 and August 2013 is included, with a total of 151,640 import containers. Seven factors were considered: (1) size of the container (20/40), (2) type of container (Dry, Reefer, High Cube, etc.), (3) the status of the container (full or empty), (4) weight, (5) ship where the container is unloaded, (6) consignee or customer, and (7) the cargo's port of origin.

The first four factors correspond to characteristics of the container. The factors are numerical (size of container and weight) and nominal (type, status, ship, port of origin, consignee). The only dual attribute is dwell time, and the nominal variable consignee has the largest number of classes (about 5000 to 7000). It is important to mention that the weight and port of origin are factors not previously employed in the literature (see Table 1).

5.1 Results Obtained with the Classification Algorithms

For the classification model, non-supervised classification algorithms were employed as they allow working with known classes. These algorithms follow an opposed strategy than supervised algorithms (Astudillo et al. 2014; Astudillo and Oommen 2014). This is justified by the fact that classes are known, since they are determined in the step 1.1 of the proposed methodology (see Table 1). The applied offline algorithms are Naive Bayes, Lazy Learning, and Rules Induction Learning. Table 4 summarizes the classification algorithms evaluated:

Table 4: Classification Algorithms evaluated.

Algorithms	Reference
K *nearest neighbors* (KNN)	Cover and Hart (1967)
Naive Bayes (NB)	Kononenko (1990)
One Rule (OneR)	R.C. Holte (1993)
Incremental Reduced Error Pruning (IREP) or *Repeated Incremental Pruning to Produce Error Reduction* (RIPPER or JRip)	Fürn Kranz (1994)
K*	Cleary and Trigg (1995)
Decision Table (DT)	Kohavi (1995)
Zero Rule (ZeroR)	Witten and Frank (2000)

Dwell times were measured in days, as this is the commonly used time unit in port Terminals. The year 2011 data was used to generate the model and the 2012 data was used to evaluate it. Data for 2013 was used only for the simulation model described in section 4.2. The algorithms were implemented in JAVA version 1.6.0_25, using the software WEKA (Waikato Environment for Knowledge Analysis) in a personal computer with a processor Intel Core 7, and 8 GB of RAM.

Table 5 summarizes the results found with each algorithm. The classification algorithm that obtained a larger number of correctly classified instances, best accuracy, Kappa´s coefficient values and root mean squared error is the K*. The JRip algorithm obtained the best error values. On the other hand, the K* algorithm had longer computational times (twice as much as JRip).

A multi-classifier algorithm for dwell time predictions was also proposed, and it was trained using the information from the historical data base. Results are presented in Table 6, where it can be observed that the KNN algorithm obtained the larger number of correctly classified instances, accuracy and error values, with a computational time of 40 seconds.

As observed in previous tables, the algorithms without the multi-classifier obtained better results in general. On the other hand, the accuracy values are always lower than 10%, which is explained due to the variability of the ship and consignee factors in the data base. For dwell time predictions, the average error is about 7 days, which is high, but under current operations, managers of the port of Arica are not able to estimate container dwell times, hence in the long run, it is expected that this number can be reduced.

5.2 Impact Assessment of the Proposed Policy via a Discrete Events Simulation Model

A simulation model of the import processes at the port of Arica is proposed in order to evaluate the impact of the storage policies in terms of the number of rehandles incurred. For comparison purposes, a storage policy was implemented considering two variants of the stacking strategy of containers without the dwell time segregation policy. This allows to emulate the current practice of the port managers.

Table 7 outlines the general procedure for the general stacking strategy implemented based on the dwell time segregations policy. Table 8 outlines the procedure for the non-segregation storage policy that employs two stacking strategies: Semi-random and Sequential, which are illustrated respectively in Figure 3 and Figure 4.

The instance implemented considered the movements of containers in the years 2012 and 2013. The yard of the port terminal consists of 19 blocks for import containers with a total of 4820 TEU slots. In order to predict the dwell times, the JRip and multi-classifier algorithms were implemented. The real arrival of containers at the port during each year is taken from the data base. For the random stacking strategies, five replicates were run. For the sequential stacking strategies, no replicates were tested given that the solution obtained is the same since the arrival of containers does not change. For the random stacking strategies standard deviation values were in the range of 140 to 444 rehandles. The simulation model was implemented in the software ExtendSim OR version 9.0 and run in a personal computer with Intel Core 7 and 8Gb RAM. Table 9 presents the results obtained.

Table 5: Results obtained with the classification algorithms.

Algorithms	Number of correctly classified instances	Accuracy	Kappa´s coefficient	Mean squared error	Rootmean squared error	Computational Time (seconds)	Error (days)
Naive Bayes	3,875.8 ± 188.4	6.77%	0.031 ± 0.002	0.058 ± 0.000	0.069 ± 0.000	34.1 ± 2.9	7.88 ± 0.67
OneR	2,365.9 ± 103.3	4.13%	0.019 ± 0.003	0.058 ± 0.000	0.098 ± 0.000	34.1 ± 3.9	8.51 ± 0.20
ZeroR	2,942.3 ± 167.6	5.14%	0.000 ± 0.000	0.058 ± 0.000	0.068 ± 0.000	62.4 ± 4.9	8.21 ± 0.93
Decision table	3,254.6 ± 256.3	5.68%	0.013 ± 0.005	0.058 ± 0.000	0.068 ± 0.000	**27.4 ± 1.6**	7.12 ± 0.44
K*	**4,116.7 ± 88.1**	**7.19%**	**0.038 ± 0.002**	0.058 ± 0.000	**0.067 ± 0.000**	109.0 ± 3.4	7.42 ± 0.10
KNN, K=1	3,966.6 ± 135.2	6.93%	0.035 ± 0.002	0.058 ± 0.000	0.070 ± 0.000	31.1 ± 10.5	8.07 ± 0.17
JRip	2,760.6 ± 164.1	4.82%	0.002 ± 0.001	0.058 ± 0.000	0.068 ± 0.000	36.6 ± 4.1	**6.94 ± 0,88**

As observed in Table 9, the average number of rehandles incurred for both 2012 and 2013 are always lower for the segregated dwell time policies employing any type of stacking strategy. Furthermore, the gap between the average number of rehandles for the non-segregated and segregated policies is around 13%. Comparing the best stacking strategy in each period for the segregated and non-segregated policies, a 6% and a 37% gap were obtained for the 2012 and 2013 periods respectively.

In order to estimate the economic impact of the dwell time segregated storage policy, the period between January and April 2012 is considered. A total of 16,867 rehandles were incurred at present conditions. If the dwell time segregated and sequential stacking strategy is employed, the total number of rehandles incurred is 14,051, with an approximate 17% reduction. If the cost of each rehandle is estimated as 10 dollars, it represents potential savings of about USD $28,000 for the container terminal.

For further implementing the proposed decision support system, the port terminal requires to develop a module that may be interconnected with its TOS. It will be necessary that the port terminal develop a historical data base (Container DB in Figure 2 in section 4) with the characteristics of import containers that have been stored in the yard for at least 2 years and update periodically this database or in real time. The information required considers the characteristics of containers, its cargo, and destination in the hinterland, as well as the dwell times. This information will be the input data for the prediction system. It will be also required to maintain a data base registering the decisions taken by the yard planner in order to analyse the performance of the proposed system.

We estimate that implementing the proposed support system will not alter the current operations of the port terminal, and is not intended to replace the yard planner tasks. The aim of the proposed system is to support yard planner decisions and derive recommendations that will make easier this job and may lead to more efficient operations in the long run.

Table 6: Multi-classifier results.

Algorithms	N° of correctly classified Instances	Accuracy	Computational Time (seconds)	Error (days)
Naive Bayes	3,226.9 ± 122.6	5.63%	79.9 ± 1.5	7.47 ± 0.20
OneR	1,309.6 ± 87.9	2.28%	**19.4 ± 0.9**	8.75 ± 0.25
ZeroR	3,216.4 ± 262.9	5.62%	31.1 ± 9.3	7.29 ± 0.41
Decision table	2,992.7 ± 380.5	5.23%	55.2 ± 4.6	7.18 ± 0.42
K*	3,183.5 ± 98.7	5.56%	114.7 ± 1.6	7.63 ± 0.17
KNN, N=85	**3,608.0 ± 394.8**	**6.30%**	38.7 ± 4.9	**6.92 ± 0.19**
JRip	3,153.1 ± 351.8	5.51%	61.4 ± 8.8	7.27 ± 0.47

Table 7: Segregated stacking strategy.

Dwell time Segregated Stacking Strategy

INPUT: Dwell time predictions for each container and dwell time classes; Yard layout and inventory

1. Define the segregation of containers based on the dwell time class predictions
2. Assign to each block a segregation of containers. One block can contain either a single or several segregations.
3. Once a container arrives, assign it to the corresponding segregation block.
4. Define the location of the container in the block based on the ***Semi-random*** or ***Sequential*** stacking strategies.
5. If a container arrives and there is no available space in the block corresponding to the segregation, then randomly select a block and repeat step 4.

OUTPUT: container location.

Table 8: Non-segregated stacking strategy.

Non-Segregated General Stacking Strategy
INPUT: Yard layout and inventory
1. Randomly select a block with available space. 2. Define the location of the container in the block based on the ***Semi-Random*** or ***Sequential*** stacking strategies. 3. If a container arrives and there is no available space in the predetermined block, then randomly select a block and repeat step 4.
OUTPUT: container location.

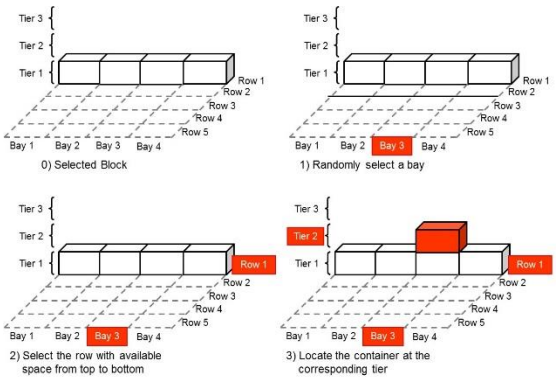

Figure 3: Semi-random stacking strategy illustration.

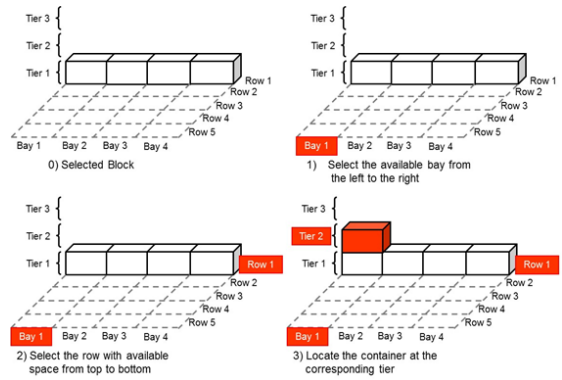

Figure 4: Sequential stacking strategy illustration.

6 CONCLUSIONS AND RECOMMENDATIONS FOR FURTHER RESEARCH

Ship turnaround times are an important productivity indicator for a port terminal. Efficient container handling is needed during the loading and unloading operations. Among several factors that affect the performance of the ship service, the yard operation efficiency is a key element. In addition, for those terminals in which land is very restricted, the planning and scheduling of resources at the yard (space and equipment) are even more critical.

A common practice among yard managers for storage space assignment consists of defining segregations or groups of containers with common characteristics. Export container segregations depend on the vessel´s loading sequence, which is based on the vessel´s route, weight and characteristics of the container, among other factors. On the other hand, segregating import containers is more complex. This is more difficult if the port terminal has no hinterland coordination mechanisms and high levels of uncertainty on the times when import container will be requested.

In this article a dwell time segregated storage space policy for import containers is proposed. In addition, the design of a decision support system for the yard planner based on the proposed storage policy is proposed. The focus of this article was import containers, due to the difficulty to determine the criteria to segregate them. As pointed out before, this relies on the high levels of uncertainty on the dispatching times, and the fact that an important number of rehandles are incurred during this process.

For the proposed policy, dwell times of import containers are predicted by classification algorithms. Then, containers are segregated based on dwell time classes. Import containers of the same dwell time class are assigned to close locations at the yard.

As a case study, we consider the particular case of the port of Arica in Chile. This port presents special conditions for cargo handling. More than 70% of the cargo transferred by the port of Arica corresponds to transit cargo of Bolivia. Due to the political agreements maintained between Chile and Bolivia, there exists a high uncertainty in the dispatching processes of the import containers at the port. In order to evaluate the potential benefits in the daily operations of the yard, a discrete event simulation model is also implemented. Numerical results of the simulation model show that a dwell time segregated storage policy with a sequential stacking strategy provides a significant reduction in the number of rehandles incurred. Considering the real number of containers handled by the port for a specific instance data set, around to 17% reduction in rehandles is obtained by the proposed policy. Finally, it is worthy to mention that the implementation of the decision support system proposed may provide a valuable tool for the yard planner.

Table 9: Numerical Results: Rehandles per time period and stacking strategy.

Storage Policy	Stacking Strategy	Average per policy (DT vs NS)	Rehandles per period	
			2012	2013
Non-segregated policy (NS)	Non-segregated random stacking strategy	45840.6	48611.8	43083.6
	Non-segregated sequential stacking strategy		48756	42911
Dwell time segregation policy (DT)	Dwell time segregated and random stacking strategy (JRip)	39768.76	45785.8	37423.8
	Dwell time segregated and sequential stacking strategy (JRip)		45343	36531
	Dwell time segregated and radom stacking strategy (multi-classifier and KNN, *N*=84)		46377.4	27909
	Dwell time segregated and sequential stacking strategy (multi-classifier and KNN, *N*=84)		**45337**	**26986**
Gap (Avg NS - Avg DT)/Avg DT				13.25%
Gap (Best NS - Best DT) /Best DT [2012]				6.74%
Gap (Best NS - Best DT) /Best DT [2013]				37.11%

Current practices of the managers follow a semi-random assignment of containers at the yard, given the limitations of data and uncertainty in the dispatching times of import containers. Hence, the proposed support system will not change significantly their current operations but in turns, will provide recommendations to the yard planners for the assignment of spaces to containers, without replacing the personnel.

As further research additional factors that may affect dwell time predictions should be analyzed, such as the cargo transported in the container. For instance, we could differentiate containers with cargo of a single or several consignees.

The problem addressed in this article is at the tactical decision level. Hence, another research avenue would be to develop real time stacking strategies based on the dwell time segregated policy. Furthermore, impact assessment for different types of yard equipment could be another research project to be developed (reachstackers vs RTG vs straddle-carriers, etc.). Finally, ship turnaround times can be also considered as a performance metric for the different stacking strategies and a sensitivity analysis to determine the most significant factors determining dwell times for the port of Arica is another research avenue.

REFERENCES

Arvis, J-F, G. Raballand and J-F, Marteau. 2010. "The cost of being landlocked: logistics costs and supply chain reliability". In *Directions in development trade* 55837, Washington DC: The World Bank.

Astudillo, C.A., M. Bardeen, and C. Cerpa, 2014. Editorial: data mining in electronic commerce - support vs. confidence. *Journal of Theoretical and Applied Electronic Commerce Research*, 9(1): I-VIII.

Astudillo, C.A. and B.J., Oommen, 2014. "Topology-oriented self-organizing maps: a survey." *Pattern Analysis and Applications*, 17(2): 1 26.

Bassan, S. 2007. "Evaluating seaport operation and capacity analysis—preliminary methodology", *Maritime Policy & Management*, 34(1): 3 19.

Beuran, M., M.H. Mahihenni, G. Raballand and S. Refas. 2012. "*The impact of demand on cargo dwell time in ports in SSA*." Policy research working paper 6014, Africa Region: The World Bank.

Bichou, K., and R. Gray. 2004. "A logistics and supply chain management approach to port performance measurement", *Maritime Policy & Management*, 31(1): 47 67.

Carlo, H.J., Vis, I.F.A., Roodbergen, K.J. (2014). "Storage yard operations in container terminals: Literature overview, trends, and research directions." *European Journal of Operational Research*, 235: 412-430.

Chen, T., K. Lin and Y-C, Juang. 2000. "Empirical studies on yard operations part 2: quantifying unproductive moves undertaken in quay transfer operations", *Maritime Policy & Management*, 27(2): 191 207.

Chung, K. C. 1993. "Port Performance Indicators". In *Infrastructure Notes: Transportation, water and urban development*. Transport No. PS-6. The World Bank.

Cochran, W.G., 1986. *Sampling techniques*, New York: John Wiley & Sons.

Dally, H.K. 1983. *Container handling and transport: A manual for current practice*, London: CS Publications.

De Langen. 2007. "Port competition and selection in contestable hinterlands: The case of Austria". *European Journal of Transport and Infrastructure Research* 7(1): 1 14.

Dharmalingam, K. 1987. Design of storage facilities for containers- a case study of port Louis Habour, Maritius. *Ports and Harbors*, 32(9): 27 31.

Djankov, S., C., Freund, and C.S., Pham, 2006. "Trading on time". In *Policy research working paper 3909*, Washington DC: The World Bank.

Doerr, O. 2013. "*Latin American and the Caribbean container port throughput, Ranking 2013*". Infrastructure Services Unit, Santiago Chile: UN-ECLAC.

Doerr, O. and R. Sánchez. 2006. "*Indicadores de productividad para la industria portuaria: aplicación en América Latina y el Caribe*". Serie Recursos naturales e infraestructura, 112, Santiago Chile: UN-ECLAC.

Dowd, T.J., and T.M. Leschine. 1990. "Container terminal productivity: a perspective", *Maritime Policy & Management*, 17(2): 107 112.

Hoffman, P. 1985. *Container facility planning: a case description. Port management textbook containerization*, Institute of shipping economics and logistics, 353-364.

Kohavi, R. 1996. "Scaling up the accuracy of Naive-Bayes classifiers: A decision-tree hybrid", In *Proceedings of the second international conference on knowledge discovery and data mining*, 202 207.

Kononenko I., 1990. "Comparison of inductive and Naive Bayesian learning approaches to automatic knowledge acquisition'." In: *Current trends in knowledge acquisition*, edited by B. Wielinga, J. Boose, B. Gaines, G. Schreiber, and M. van Someren. Amsterdam: IOS Press.

Lee, T-W, N.K. Park., and D-W, Lee. 2003. "A. simulation study for the logistics planning of a container terminal in view of SCM", *Maritime Policy & Management*, 30(3): 243 254.

Magala, M., and A. Sammons, A. 2008. "A new approach to port choice modelling". *Maritime Economics and Logistics*, 10(1-2): 9 34.

Merckx, F. 2005. "The issue of dwell time charges to optimize container terminal capacity." In *Proceedings of the International Association of Maritime Economists annual conference 2005*, Limassol, Cyprus.

Moini, N., M. Bolie, M., S. Theofanis, and W. Laventhal. 2012. "Estimating the determinant factors of container dwell times at seaports." *Maritime Economics & Logistics*. 14: 162 177.

Nir, A-S, K., Lin and G-S, Liang. 2003. "Port choice behaviour: from the perspective of the shipper". *Maritime Policy and Management*, 30(2): 165 73.

Quinlam, J.R., 1986. "Induction of decision tree", *Machine learning* 1: 81 106.

Raballand, G., S. Refas, M. Beuran, and G. Isik. 2012. "Why does cargo spend weeks in Sub-Saharan African ports? Lessons from six countries" In *Directions in Development*, Washington DC: The World Bank.

Rodrigue, J.P. 2012. "*The benefits of logistics investments: opportunities for Latin America and the Caribbean*", In: Technical Notes IDB-TN-395, edited by Mary Paden, 1-65, Washington, DC: Inter-American Developing Bank.

Rodrigue, J.P., and T. Notteboom. 2009. "The terminalization of supply chains: reassessing the role of terminals in port/hinterland logistical relationships". *Maritime Policy& Management*. 36(2): 165 183.

Tongzon, J.L. and L. Sawant. 2007. "Port choice in a competitive environment: from the shipping lines' perspective". *Applied Economics*, 39(4): 477 492.

UNCTAD. 2014. "*Review of maritime transport 2014*". United Nations Publications. ISBN 978-92-1-112878-9.

USAID. 2005. "*The broad economic impact of port inefficiency: A comparative study of two ports*". U.S. Agency for International Development, reported by Nathan Associates, Washington, DC. Accessed in: http://pdf.usaid.gov/pdf_docs/PNADC612.pdf.

Veldman, S., and E. Bückmann. 2003. "A model on container port competition: an application for the West European container hub-ports". *Maritime Economics and Logistics*, 5(2): 3 22.

Witten, I., E. Frank, and M.A., Hall. 2011. *Data mining: practical machine learning tools and techniques. Morgan Kaufmann series in data management systems*: Elsevier.

Optimal Policies for Payment of Dividends through a Fixed Barrier at Discrete Time

Raúl Montes-de-Oca[1], Patricia Saavedra[1], Gabriel Zacarías-Espinoza[1] and Daniel Cruz-Suárez[2]
[1]*Departamento de Matemáticas, Universidad Autónoma Metropolitana-Iztapalapa, Av. San Rafael Atlixco 186, Col. Vicentina, Cd. de México 09340, Mexico*
[2]*División Académica de Ciencias Básicas, Universidad Juárez Autónoma de Tabasco, Km 1 Carr. Cunduacán-Jalpa, Cunduacán, Tabasco 86690, Mexico*
{*momr, psb, gzaces*}*@xanum.uam.mx, daniel.cruz@ujat.mx*

Keywords: Reserve Processes, Discounted Markov Decision Processes, Ruin Probability, Optimal Premiums, Dividends.

Abstract: In this paper a discrete-time reserve process with a fixed barrier is presented and modelled as a discounted Markov Decision Process. The non-payment of dividends is penalized. The minimization of this penalty results in an optimal control problem. This work focuses on determining the sequence of premiums that minimize penalty costs, and obtaining a rate for the probability of ruin to ensure a sustainable reserve operation.

1 INTRODUCTION

This work is related to risk theory, which describes the behavior of the reserve process of an insurance company. The classic model was introduced by Filip Lundberg in 1903 (Lundberg, 1909) and developed by Harald Cramér in 1930 (Cramér, 1930). In this model, the premiums are obtained continuously at a constant rate and the total amount of claims over a period of time t is given by a compound Poisson process. The main problem of the classical model was to determine the ruin probability of the reserve process. However, currently, several other interesting problems have been matter of study: minimization of the ruin probability, the distribution of dividends to shareholders, the reinsurance problem, the collection of premiums dependent on the history of each customer, analysis of the reserve process when claims have sub-exponential distributions, just to mention a few (see (Azcue and Muler, 2014), (Dickson, 2005), (Dickson and Waters, 2004), (Gerber, 1981), (Gerber et al., 2006), (Rolski et al., 1999), and (Schmidli, 2009)).

In particular, the problem of interest for the authors of this article is the definition of policies for the distribution of dividends in fixed periods of time when the claims are of light or heavy tails. This issue is relevant because in the classical model, if the intensity of the premiums is higher than the average total amount of claims (the security loading is positive), then with probability 1, the paths of the reserve tend to infinity when the time t increases indefinitely, (see (De-Finetti, 1957)). Therefore, dividends appear as a way to control an unlimited increment of the reserves.

Dividend policies aim to attract shareholders (or investors), in order to address risks. One possible policy is to determine the dividend strategy that maximizes the discounted expected value of a utility function by means of control techniques. This approach has been studied in continuous time such as: (Azcue and Muler, 2014), (Dickson, 2005), (Dickson and Waters, 2004), (Gerber, 1981), (Gerber et al., 2006), and (Schmidli, 2009). On the other hand, discrete-time problems of risk theory have been studied, for instance, in (Bulinskaya and Muromskaya, 2014), (Diasparra and Romera, 2009), (Martínez-Morales, 1991), (Martin-Löf, 1994), (Schäl, 2004), and (Schmidli, 2009) who have applied the optimal control theory in insurance companies. In particular, in (Martin-Löf, 1994) the control techniques were introduced for the first time by means of the theory of discounted Markov Decision Processes.

The discounted Markov Decision Processes (MDPs) (see (Hernández-Lerma and Lasserre, 1996)) at discrete time are those that are periodically observed under uncertainty on transit of their states and with the property that they can be influenced by application of controls (Hernández-Lerma and Lasserre, 1996). A Markov Decision Process (MDP) is generally described as follows: at a particular time n, the system is observed and, depending on its current state, a control is applied; then a cost is paid and, by a prede-

Montes-de-Oca, R., Saavedra, P., Zacarías-Espinoza, G. and Cruz-Suárez, D.
Optimal Policies for Payment of Dividends through a Fixed Barrier at Discrete Time.
In *Proceedings of the 6th International Conference on Operations Research and Enterprise Systems (ICORES 2017)*, pages 140-149
ISBN: 978-989-758-218-9

termined transition law, the system gets to a new state. The sequence of controls is called policy, and a way of assessing their quality is through a performance criterion. The Optimal Control Problem (OCP) consists in determining a policy which optimizes the performance criterion. One way to solve the OCP is using the technique of dynamic programming introduced by Bellman in the middle of the last century.

From this perspective, the problem of dividends is modeled here by using discrete-time MDPs. It is proposed to work within MDPs since similar control problems of dams or inventories, sample storage problems, have been resolved successfully, see (Finch, 1960) and (Ghosal, 1970). On the other hand, discrete-time is used here as it was suggested in (Li et al., 2009). This type of analysis is important in itself as it presents an approximation of the continuous problem and as it is also more realistic from the applications point of view. One approach that will be followed in this work is to study the problem of dividends by fixing an objective capital, (barrier) $Z > 0$. If the reserve exceeds Z, then the dividends are distributed. A model with a fixed barrier reserve of an insurance company is proposed. The reserve process is modelled as an MDP whose admissible control belongs to a compact subset. The bounds of this subset depend on two principles for premium calculation: the expectation principle and the standard deviation principle (see (Dickson, 2005)). The distribution of the total amount of claims, by time interval, represents a compound process which is supposed to be general, in the sense that it only requires for its density to be continuous almost everywhere. The proposed performance criterion is the expected total discounted cost, where the cost penalizes both the failure to pay dividends and the difference between the admissible premiums and a constant which depends on the standard deviation principle to premium calculation. In addition, the dynamic programming technique explicitly determines the optimal solutions, and on the other hand, a rate for the ruin probability is established, which aims to determine long periods of sustainability of the company.

The paper is organized as follows: in the second section the mathematical tools that will be used throughout this work (mainly MDPs and stochastic orders) are presented. The reserve process with a fixed barrier is presented in the third section with an analysis of dividend policies. In the fourth and fifth sections the main results are given: the optimal premium and a rate for the ruin probability with a couple of examples where the theory obtained in this work is applied. Finally, research conclusions are presented.

2 PRELIMINARIES

This section presents some results on the theory that will be used to solve the problem stated in the paper.

2.1 Stochastic Orders

Let X be a Borel space (i.e., a Borel subset of a separable metric space) and suppose that X is complete and partially ordered. The partial order in X is denoted by $\prec$. Moreover a function $g : X \to \mathbb{R}$ is considered to be increasing if $x, y \in X$, $x \prec y$, imply that $g(x) \leq g(y)$, where $\leq$ is the usual order in $\mathbb{R}$. Besides, the Borel σ-algebra of X is denoted by $\mathcal{B}(X)$.

Definition 2.1. *Let X be a complete Borel space and suppose that X is partially ordered. Let P and P' be probability measures on $(X, \mathcal{B}(X))$. It is said that P' **dominates** P **stochastically** if $\int g dP \leq \int g dP'$ for all $g : X \to \mathbb{R}$ measurable, bounded and increasing, so write $P \overset{st}{\leq} P$ when this holds.*

Remark 2.2. *Let P and P' be probability measures on $(\mathbb{R}, \mathcal{B}(\mathbb{R}))$. In this case, $P \overset{st}{\leq} P'$ if $F'(x) \leq F(x)$, for all $x \in R$, where F and F' are the distribution functions of P and P', respectively, (see (Lindvall, 1992) p. 127).*

Lemma 2.3. *((Cruz-Suárez et al., 2004), Lemma 2.6) Let X be a complete Borel space, and suppose also that X is partially ordered. Let P and P' be probability measures on $(X, \mathcal{B}(X))$, such that, $P \overset{st}{\leq} P'$. Then $\int H_* dP \leq \int H_* dP'$, for $H_* : X \to \mathbb{R}$ which is measurable, nonnegative, nondecreasing, and (possibly) unbounded.*

2.2 Discounted Markov Decision Processes

Let X and Y be complete Borel spaces. A **stochastic kernel** on X given Y is a function $P(\cdot|\cdot)$ such that $P(\cdot|y)$ is a probability measure on X for each fixed $y \in Y$, and $P(B|\cdot)$ is a measurable function on Y for each fixed $B \in \mathcal{B}(X)$.

Let $(X, A, \{A(x)|x \in X\}, Q, c)$ be a discrete-time Markov Control Model (see (Bäuerle and Rieder, 2011) or (Hernández-Lerma and Lasserre, 1996) for notation and terminology). This model consists of the state space X, the control set A, the transition law Q, and the cost-per-stage c. For each $x \in X$, there is a nonempty measurable set $A(x) \subset A$ whose elements are the feasible actions when the state of the system is x. Define $\mathbb{K} := \{(x, a) : x \in X, a \in A(x)\}$. c is assumed to be a nonnegative and measurable function on $\mathbb{K}$.

The transition law Q is often induced by an equation of the form

$$x_{n+1} = G(x_n, a_n, \xi_n), \tag{1}$$

$n = 0, 1, \cdots$, with $x_0 \in X$ given, where $\{x_n\}$ and $\{a_n\}$ are the sequences of the states and controls, respectively, and$\{\xi_n\}$ is a sequence of random variables independent and identically distributed (i.i.d.), with values in some space S, common density function Δ, and independent of the initial state x_0; $G : \mathbb{K} \times S \to X$ is a measurable function.

Assumption 2.4. **(a)** *$A(x)$ is compact for all $x \in X$;*

(b) *c is lower semicontinuous and nonnegative;*

(c) *The transition law Q is strongly continuous, that is, the function h', defined on $\mathbb{K}$ by:*

$$h'(x,a) := \int h(y)Q(dy|x,a), \tag{2}$$

is continuous and bounded for every measurable bounded function h on X.

Using the standard notation and definitions in (Hernández-Lerma and Lasserre, 1996), Π denotes the set of all policies and $\mathbb{F}$ is the subset of stationary policies. Each stationary policy $f \in \mathbb{F}$ is identified with the measurable function $f : X \to A$ such that $f(x) \in A(x)$ for every $x \in X$.

Remark 2.5. *Given an initial state $x \in X$ and a stationary policy $f \in \mathbb{F}$, the process determined by (1) is a homogeneous Markov process with transition kernel $Q(\cdot|x, f)$ (see (Hernández-Lerma and Lasserre, 1996) Proposition 2.3.5 p. 19).*

Let $(X, A, \{A(x)|x \in X\}, Q, c)$ be a discrete-time Markov Control Model, in this paper the performance criterion to consider is the **Expected Total Discounted Cost** defined as

$$v(\pi, x) := E_x^{\pi}[\sum_{n=0}^{+\infty} \alpha^n c(x_n, a_n)], \tag{3}$$

when using the policy $\pi \in \Pi$, given the initial state $x_0 = x \in X$. In this case, $\alpha \in (0,1)$ is a given discount factor, and E_x^{π} denotes the expectation with respect to the probability measure P_x^{π} induced by π and x (see (Hernández-Lerma and Lasserre, 1996)).

A policy π^* is said to be **optimal** if

$$v(\pi^*, x) = V^*(x), \tag{4}$$

for each $x \in X$, where

$$V^*(\cdot) := \inf_{\pi \in \Pi} v(\pi, \cdot) \tag{5}$$

is the so-called **optimal value function**.

Remark 2.6. *Assumptions 2.4a) and 2.4b) imply that c is inf-compact on $\mathbb{K}$, that is, for every $x \in X$ and $r \in \mathbb{R}$, the set*

$$A_r(x) := \{a \in A(x) | c(x,a) \leq r\} \tag{6}$$

is compact. Therefore, Assumption 2.4 implies Assumption 1a) and 1b) in (Hernández-Lerma and Lasserre, 1996). Consequently, the validity of the next lemma is guaranteed.

Lemma 2.7. *((Hernández-Lerma and Lasserre, 1996), Theorem 4.2.3 and Lemma 4.2.8) Under Assumption 2.4,*

(a) The optimal value function V^* satisfies the optimality equation

$$V^*(x) = \inf_{a \in A(x)} \{c(x,a) + \alpha \int V^*(y)Q(dy|x,a)\}, \tag{7}$$

for each $x \in X$.

(b) There exists an optimal stationary policy $f^* \in \mathbb{F}$ such that

$$V^*(x) = c(x, f^*(x)) + \alpha \int V^*(y)Q(dy|x, f^*(x)), \tag{8}$$

for each $x \in X$.

(c) $V_n(x) \to V^*(x)$ when $n \to \infty$, where V_n is defined by

$$V_n(x) = \inf_{a \in A(x)} \{c(x,a) + \alpha \int V_{n-1}(y)Q(dy|x,a)\}, \tag{9}$$

for each $x \in X$, with $V_0(\cdot) = 0$.

3 RESERVE PROCESS

A **Risk Process** (see (Asmussen, 2010), (Dickson, 2005), and (Schmidli, 2009)) consists of a pair $(P_t, S_t), t \geq 0$, which describes the premiums earned and the total amount of claims during the period of time $[0,t]$, respectively.

The relationship between P_t and S_t is given as follows:

$$R_t = R_0 + P_t - S_t, \tag{10}$$

$t \geq 0$, where $R_0 = u > 0$ is the initial reserve of the company. In this case, R_t represents the reserve of the company at the time t. The process $\{R_t\}_{t \geq 0}$ is called **Reserve Process.**

The ruin of the company is given at the instant R_t takes a negative value. The main objective then is to determine the probability of this event, which is done in the following definition.

Definition 3.1. *The ruin probability* $\psi(u)$*, with initial reserve* $u > 0$*, is defined by*

$$\psi(u) := Pr[\tau(u) < +\infty] \tag{11}$$

where $\tau(u) := inf\{t > 0 | R_t < 0\}$ *with* $\tau(u) = +\infty$ *if* $R_t > 0$ *for all* $t \geq 0$.

In the classical model of Lundberg and Cramér, the premiums are determined continuously and deterministically, i.e., $P_t = Ct$ where $C > 0$ and $t \geq 0$. In addition, the total amount of claims S_t may depend on two process: a homogeneous Poisson process $\{N(t)\}_{t\geq 0}$, with intensity $\lambda > 0$, and a claims amounts process $\{Y_i : i = 1, 2, \cdots\}$, where Y_i are independent and identically distributed random variables. Thus, the total amount of claims until time t is given by

$$S_t = \sum_{i=1}^{N(t)} Y_i, \tag{12}$$

where $S_t = 0$ if $t = 0$.

Thus, the classical reserve process is described by

$$\begin{aligned} R_t &= u + Ct - \sum_{i=1}^{N(t)} Y_i, \\ &= u + Ct - S_t. \end{aligned}$$

Observe that if $E[S_t]$ denotes the expectation of S_t, and $E[S_t] < +\infty$, then, taking the expectation in the last equation, it is obtained that

$$E[R_t] = u + (C - \lambda E[Y_1])t. \tag{13}$$

Choosing $C > \lambda E[Y_1]$, it is concluded that the average reserves of the company grow indefinitely. In other words, the reserve R_t tends to infinity when t does so with probability $1 - \psi(u)$. The assumption $C > \lambda E[Y_1]$ is known as the **Safety Loading Condition.**

As mentioned above, in the classical model, the safety loading condition allows an insurance company reserves to accumulate indefinitely, which is unrealistic. Although there seems to be a controversy about this point, it has been suggested to establish an upper limit (barrier) Z for the accumulation or earnings in order to sustain the risks (see (Azcue and Muler, 2014), (De-Finetti, 1957), (Dickson, 2005), (Dickson and Waters, 2004), and (Schmidli, 2009)). To reach this end, the reserves of the company must be reduced to Z from time to time, for example, by paying dividends to shareholders.

Remark 3.2. *It is important to mention that in a more general setting, some of the assumptions of the classical model may be relaxed, e.g.,*$\{N(t)\}$ *could be a non-homogeneous Poisson process or a more general renewal process. Hence it is possible to assume that the claim size cumulative distribution function is of a particular parametric form, eg., gamma, Weibull, etc. (see Assumption 3.5 and examples 1 and 2, below).*

Dividends can be understood as payments made by a company to its shareholders, either in cash or in shares. The arguments about the advantages of a dividend refer to the intention of the investors to earn income in the present and to reduce uncertainty. Formally, the dividends, d_t, are defined as $d_t = [R_t - Z]^+$, where $[z]^+ = \max\{0, z\}$.

On the other hand, in the existing literature, different methods are proposed to determine the premium value for the safety loading condition to hold (see (Dickson, 2005) and (Schmidli, 2009)). In this work the expectation principle will be used.

3.1 Discrete-time Reserve Process

Now, a discrete-time reserve model will be developed. The discretization is reasonable because, in practice, decisions of the company about its operations are taken at fixed points of time (see (Bulinskaya and Muromskaya, 2014), (Diasparra and Romera, 2009), (Li et al., 2009), and (Schmidli, 2009)).

Let $\{R_t\}$ be a reserve process with initial reserve $R_0 = u > 0$, and $\{t_n\}$ be an increasing sequence of positive real numbers with $t_0 = 0$. Then, equation (10) implies that

$$R_{t_{n+1}} - R_{t_n} = (P_{t_{n+1}} - P_{t_n}) - (S_{t_{n+1}} - S_{t_n}), \tag{14}$$

for $n = 0, 1, \cdots$, where $(P_{t_{n+1}} - P_{t_n})$ and $(S_{t_{n+1}} - S_{t_n})$ are the premiums earned and the total amount of claims during the period $(t_n, t_{n+1}]$, respectively.

Let $x_{t_n} := R_{t_n}$, $a_{t_n} := (P_{t_{n+1}} - P_{t_n})$ and $\xi_{t_n} := (S_{t_{n+1}} - S_{t_n})$. Then, without loss of generality, it is possible assume that $t_n = n$ for $n > 0$. Then, the discrete-time reserve model is as follows:

$$x_{n+1} = x_n + a_n - \xi_n, \tag{15}$$

with $x_0 = u > 0$.

In this case, x_{n+1} represents the reserve at time $t = n+1$. Moreover, the discrete-time ruin probability is determine by

$$\psi_d(u) := Pr[\tau_d(u) < +\infty] \tag{16}$$

where $\tau_d(u) := \inf\{n \geq 1 | x_n \leq 0\}$ with $\tau_d(u) = +\infty$ if $x_n > 0$ for all $n > 0$.

According to the ruin probability defined above, the ruin of the company is attained when $x_n + a_n - \xi_n \leq 0$ for some $n > 0$.

If the following dynamics is considered:

$$x_{n+1} = [x_n + a_n - \xi_n]^+, \tag{17}$$

for $n = 1, 2, \cdots$, with $x_0 = u > 0$, then dynamics in (17) determines the ruin when $x_n = 0$ for some

$n = 1, 2, \cdots$. However, just as in the continuous case model, if the safety loading condition holds, $E[x_n] \to +\infty$ when $n \to +\infty$.

Remark 3.3. *The dynamics described in (17) is known as the Lindley random walk (see (Asmussen, 2010)) which has various applications, for example, in storage processes, waiting time model, queue size models, to name a few (Asmussen, 2010). (See Remark 3.4, below.)*

3.2 Reserve Process with a Fixed Barrier

This subsection provides a reserve process which is modelled as a discounted Markov Decision Process at discrete time. The motivation is originated from the previous subsection, that is, the possibility of discretizing the reserve process, and the existence of a fixed barrier which defines the payments of dividends (see (Azcue and Muler, 2014), (De-Finetti, 1957), (Dickson, 2005), and (Martínez-Morales, 1991)).

Let Z be a fixed barrier such that, if at time t_n, $x_n > Z$, the surplus $X_n - Z$ is used to pay dividends. Thus, the study of the reserve process focuses on the reserves below barrier Z. Mathematically, this is described by the following dynamics:

$$x_{n+1} = \min\{[x_n + a_n - \xi_n]^+, Z\} \tag{18}$$

with $x_0 = u > 0$.

In this case, x_n, a_n and ξ_n denotes respectively: reserve, premium and the total amount of claims of the company at the beginning of the period $(n, n+1]$.

Remark 3.4. *The dynamics given in equation (18) has been used to describe storage processes with finite capacity such as: dams, inventory, waiting time model and queue sizes, to name a few (see (Finch, 1960) and (Ghosal, 1970)).*

Assumption 3.5. *Suppose that $\{\xi_n\}$ is a sequence of i.i.d. random variables with values on $[0, \infty)$, and a common distribution F whose density Δ is continuous almost everywhere (a.e.), with $E[\xi] < +\infty$ (ξ is a generic element of the sequence $\{\xi_n\}$).*

In the rest of this paper Assumption 3.5 will not be mentioned in each result, but it is supposed to hold.

Remark 3.6. *Observe that Assumption 3.5 considers general distributions which, in practice, permits us to work with distributions with light or heavy tails (see (Azcue and Muler, 2014)).*

Using the expectation principle for premiums calculation, it is ensured that the safety loading condition for the process described in equation (18) holds. Define

$$K := (1 + \varepsilon)E[\xi] \tag{19}$$

and

$$M := (1 + \beta)E[\xi], \tag{20}$$

where $0 < \varepsilon < \beta$. Then, by ((Dickson, 2005) and (Schmidli, 2009)) $K < M$, therefore, the admissible premiums set is the compact subset $[K, M]$. (Note that for all premium $a \in A(x) = [K, M]$, the safety loading condition is satisfied, and β is fixed in order to be competitive in the insurance market.)

Every time that the reserve is below the barrier Z, the non-payments of dividends is penalized. Therefore, the following cost function is proposed:

$$c(x, a) := [Z - x]^+, \tag{21}$$

for each $x \in [0, +\infty)$ and $a \in [K, M]$.

Remark 3.7. *This model defines an MDP: take $X = [0, +\infty)$ as the state space; $A = [K, M]$ as the action space; $A(x) = [K, M]$ as admissible actions for each $x \in X$; the transition law Q is induced by the function $G(x, a, s) := \min\{[x + a - s]^+, Z\}$ for each $(x, a) \in \mathbb{K}$ and $s \in [0, +\infty)$ (see equation (1)). Finally, the cost function is defined in (21).*

According to Remark 3.7, there is a problem (an OCP) to determine the sequence of premiums $\pi = \{a_n\}$ which optimizes

$$v(\pi, x) := E_x^{\pi}\left[\sum_{n=0}^{+\infty} \alpha^n [Z - x_n]^+\right], \tag{22}$$

where $x \geq 0$ is the initial reserve, and α is a given discount factor.

4 OPTIMAL PREMIUMS

In this section the research results are presented using MDPs theory.

By the definition of the cost function in (21) it is concluded that it is nonnegative and continuous. Moreover, for each $x \in X$, $A(x) = [K, M]$ is a compact set. So, now it is only necessary to show Assumption 2.4c) which is presented in the following lemma.

Lemma 4.1. *The transition law Q, induced by (18), is strongly continuous.*

Proof. Let $h : X \to \mathbb{R}$ be a measurable function bounded by the constant γ. Using the Variable Change Theorem ((Ash and Doléans-Dade, 2000) p. 52), it follows that

$$\int h(y)Q(dy|x, a) = \int_0^{\infty} h(min\{[x + a - s]^+, Z\})\Delta(s)ds, \tag{23}$$

$(x, a) \in K$.

Furthermore,

$$\int_0^{\infty} h(min\{[x+a-s]^+,Z\})\Delta(s)ds = \quad (24)$$

$$h(0)(1-F(x+a)) \quad (25)$$

$$+ \quad h(Z)F(x+a-Z) \quad (26)$$

$$+ \quad \int_{x+a-Z}^{x+a} h(x+a-s)\Delta(s)ds, \quad (27)$$

$(x,a) \in \mathbb{K}$, where F is the common distribution function of ξ.

Since density Δ is a continuous function a.e. (see Assumption 3.5), F is also continuous (see (Ash and Doléans-Dade, 2000), p. 175)

Given the above, it suffices to prove that

$$\int_{x+a-Z}^{x+a} h(x+a-s)\Delta(s)ds \quad (28)$$

is a continuous function on $(x,a) \in \mathbb{K}$.

For this purpose, let $\{(x_k,a_k)\}$ be a sequence in $\mathbb{K}$ converging to $(x,a) \in \mathbb{K}$. By the Variable Change Theorem ((Ash and Doléans-Dade, 2000) p. 52),

$$\int_{x+a-Z}^{x+a} h(x+a-s)\Delta(s)ds = \int_0^Z h(y)\Delta(x+a-y)dy. \quad (29)$$

Consider the following functions defined by

$$h_k(y) := h(y)\Delta(x_k+a_k-y)I_{[0,Z]}(y), \quad (30)$$

$$g_k(y) := \gamma\Delta(x_k+a_k-y)I_{[0,Z]}(y), \quad (31)$$

for $k = 1,2,\cdots$, $y \in [0,+\infty)$, where $I_B(\cdot)$ denotes the indicator function on the set B.

Note that $|h_k| \leq g_k$ for all $k \geq 1$. Furthermore, $\{g_k\}$ converges a.e. to the function g which is defined by

$$g(y) := \gamma\Delta(x+a-y)I_{[0,Z]}(y), \quad (32)$$

$y \in [0,+\infty)$.

Furthermore,

$$\begin{aligned} \int g_k(y)dy &= \gamma\int_0^Z \Delta(x_k+a_k-y)dy, \\ &= \gamma Pr[x_k+a_k-Z \leq \xi \leq x_k+a_k], \\ &= \gamma(F(x_k+a_k)-F(x_k+a_k-Z)), \end{aligned}$$

and, as the distribution F is continuous, then

$$\lim_{k\to\infty}\int g_k(y)dy = \int g(y)dy. \quad (33)$$

Finally, by the Dominated Convergence Theorem ((Royden, 1988) p. 92)

$$\begin{aligned} \lim_{k\to\infty} & \int_{x_k+a_k-Z}^{x_k+a_k} h(x_k+a_k-s)\Delta(s)ds \\ &= \lim_{k\to\infty}\int h_k(y)dy \\ &= \int \lim_{k\to\infty} h_k(y)dy \\ &= \int_0^Z h(y)\Delta(x+a-y)dy \\ &= \int_{x+a-Z}^{x+a} h(x+a-s)\Delta(s)ds \end{aligned}$$

and therefore the result holds. □

By Lemma 4.1, Assumption 2.4 holds, and therefore Lemma 2.7 guarantees the existence of the optimal policy, $f^* \in \mathbb{F}$, which, in the context of the reserve process, describes the sequence of optimum premiums that minimizes the performance index given in (22).

Lemma 4.2. *a) The transition law Q, induced by (18), is stochastically ordered, i.e.,*

$$Q(\cdot|x,a) \overset{st}{\leq} Q(\cdot|w,b) \quad (34)$$

for each (x,a), $(w,b) \in \mathbb{K}$ with $x \leq w$ and $a \leq b$.

b) The optimal value function $V^*(\cdot)$, and the value iteration functions $V_n(\cdot)$, defined in (9), are decreasing on X.

Proof. a) Let $(x,a),(w,b) \in \mathbb{K}$ with $x \leq w$ and $a \leq b$. Observe that

$$[x+a-s]^+ \leq [w+b-s]^+, \quad (35)$$

$s \in [0,+\infty)$.

On the other hand, if $\min\{[w+b-s]^+,Z\} = Z$, then $\min\{[x+a-s]^+,Z\} \leq \min\{[w+b-s]^+,Z\}$, and if $\min\{[w+b-s]^+,Z\} = [w+b-s]^+$, by (35) $\min\{[x+a-s]^+,Z\} \leq \min\{[w+b-s]^+,Z\}$. Therefore

$$\min\{[x+a-s]^+,Z\} \leq \min\{[w+b-s]^+,Z\}, \quad (36)$$

$s \in [0,+\infty)$. Thus, by (36) if $\min\{[w+b-\xi]^+,Z\} \leq \varsigma$, then $\min\{[x+a-\xi]^+,Z\} \leq \varsigma$, and therefore

$$\begin{aligned} &Q(\min\{[w+b-\xi]^+,Z\} \leq \varsigma|w,b) \leq \\ &Q(\min\{[x+a-\xi]^+,Z\} \leq \varsigma|x,a). \end{aligned} \quad (37)$$

Finally, by Remark 2.2, the result holds.

b) First it will be shown that V_n is decreasing on X. The proof is made by mathematical induction. Let $x,w \in X$ with $x \leq w$. By definition of V_n, for $n = 1$,

$$V_1(x) = \inf_{a\in A(x)}\{[Z-x]^+\}; \quad (38)$$

this implies that $V_1(x) = [Z-x]^+$, therefore V_1 is decreasing on X.
Now, for $n = 2$,

$$\begin{aligned} V_2(x) &= \inf_{a\in A(x)}\{c(x,a) \\ &+ \alpha\int V_1(\min\{[x+a-s]^+,Z\})\Delta(s)ds\} \\ &= \inf_{a\in A(x)}\{c(x,a) \\ &+ \alpha\int [Z-\min\{[x+a-s]^+,Z\}]^+\Delta(s)ds\} \\ &= \inf_{a\in A(x)}\{c(x,a) \\ &+ \alpha\int (Z-\min\{[x+a-s]^+,Z\})\Delta(s)ds\} \\ &= \inf_{a\in A(x)}\{[Z-x]^+ + \alpha Z \\ &- \alpha\int \min\{[x+a-s]^+,Z\}\Delta(s)ds\} \\ &= \inf_{a\in A(x)}\{[Z-x]^+ + \alpha Z \\ &- \alpha\int yQ(dy|x,a)\}. \end{aligned}$$

Hence, by part (a) of this lemma and using Lemma 2.3 with $H_*(y) = y$, $y \in X$, the function g_*, defined by

$$g_*(a) := -\alpha\int yQ(dy|x,a), \tag{39}$$

$a \in [K,M]$ is decreasing, and so its minimum is M. This implies that

$$V_2(x) = [Z-x]^+ + \alpha Z - \alpha\int yQ(dy|x,a). \tag{40}$$

Since $x \le w$ and after some calculations, it is obtained that $V_2(w) \le V_2(x)$. As x and w are arbitrary, then V_2 is a decreasing function on X. Suppose that V_n is decreasing on X for some $n > 2$. Again, take $x, w \in X$ with $x \le w$. Then

$$\begin{aligned} V_{n+1}(x) &= \inf_{a\in A(x)}\{c(x,a) \\ &+ \alpha\int V_n(\min\{[x+a-s]^+,Z\})\Delta(s)ds\} \\ &= \inf_{a\in A(x)}\{[Z-x]^+ \\ &+ \alpha\int V_n(y)Q(dy|x,a)\}. \end{aligned} \tag{41}$$

Let $a \in [K,M]$. By induction hypothesis and by the stochastic order of Q, it yields that

$$\begin{aligned} &[Z-w]^+ + \alpha\int V_n(y)Q(dy|w,a) \\ &\le [Z-x]^+ + \alpha\int V_n(y)Q(dy|x,a), \end{aligned}$$

then taking minimum on $a \in [K,M]$ on both sides of the inequality, it is obtained that $V_{n+1}(w) \le V_{n+1}(x)$. Therefore, V_{n+1} is decreasing. By Lemma 2.7c), $V_n(x) \to V^*(x)$, $x \in X$, which implies that V^* is a decreasing function on X.

□

Theorem 4.3. *The optimal policy for the reserve process with dividends, induced by (18), is $f^*(\cdot) \equiv M$.*

Proof. Let $x \in X$ be fixed. By Lemma 2.7, V^* satisfies the optimality equation (7), that is,

$$\begin{aligned} V^*(x) &= \inf_{a\in A(x)}\{[Z-x]^+ \\ &+ \alpha\int V^*(y)Q(dy|x,a)\}. \end{aligned}$$

Also, by Lemma 4.2, V^* is decreasing and Q is stochastically ordered. Then, if $a,b \in [K,M]$, with $a \le b$, it is obtained that

$$\begin{aligned} &\alpha\int V^*(y)Q(dy|x,b) \le \\ &\alpha\int V^*(y)Q(dy|x,a). \end{aligned} \tag{42}$$

Adding $[Z-x]^+$ on both sides of the inequality above, it is concluded that, for $a \in [K,M]$,

$$H(a) := [Z-x]^+ + \alpha\int V^*(y)Q(dy|x,a) \tag{43}$$

is a decreasing function and its minimum is reached in M. Since x is arbitrary, the result follows. □

Finally, in this section, by Theorem 4.3 it is obtained that the optimal value function is of the form

$$V^*(x) = v(M,x) = E_x^M\left[\sum_{n=0}^{+\infty}\alpha^n[Z-x_n]^+\right], \tag{44}$$

for each $x \in X$. That is, the expected total discounted cost of the penalties for not reaching the barrier Z, and therefore not paying the dividends to shareholders is brought to present value, given the discount factor α.

5 RATES FOR RUIN PROBABILITY

This section presents a rate for ruin probability which permits to determine a period of sustainability for the company under the optimum reserve process, that is, the process under the optimal policy (premium) $f^*(\cdot) \equiv M$,

$$x_{n+1}^M = \min\{[x_n^M + M - \xi_n]^+, Z\}, \tag{45}$$

with $x_0^M = u > 0$.

To this end,

$$\psi_d^N(u) := Pr[x_0^M = u, x_1^M \neq 0, \cdots, x_{N-1}^M \neq 0, x_N^M = 0] \tag{46}$$

is defined for $u > 0$ and $N > 2$.

Observe that $\psi_d^N(u)$ is the ruin probability when $\tau_d(u) = N$, where τ_d is the stopping time for the state zero (see equation (16)).

Theorem 5.1. *Let $\{x_n^M\}$ be the optimal reserve process generated for the optimal policy $f^* \equiv M$, with $x_0^M = u > 0$ and $N > 2$. Then*

$$\psi_d^N(u) \leq (Pr[\xi < Z + M])^{N-2} \cdot Pr[\xi < u + M]. \tag{47}$$

Proof. The optimal process $\{x_n^M\}$ is a homogeneous Markov process with transition law Q (see Remark 2.5).

Consider the following sets: $B_0 = \{x_0^M = u\}$, $B_N = \{x_N^M = 0\}$ and $B_i = \{x_i^M \neq 0\}$, for $i = 1, 2, \cdots, N-1$, and observe that $B_i \in \mathcal{B}(X)$ for $i = 1, 2, \cdots, N$.

Then, by Proposition 7.3 p. 130 in (Breiman, 1992),

$$\begin{aligned} \psi_d^N(u) = & \\ = & \quad Pr[x_0^M = u, x_1^M \neq 0, \cdots, x_{N-1}^M \neq 0, x_N^M = 0] \\ = & \quad \int_{B_{N-1}} \cdots \int_{B_0} Q(B_N | w_{N-1}, M) \\ & \quad Q(dw_{N-1} | w_{N-2}, M) \cdots \\ & \quad Q(dw_1 | w_0, M) \rho(dw_0), \end{aligned}$$

where the initial distribution ρ is the Dirac measure concentred on u.

On the other hand, observe that

$$Q(B_N | w_{N-1}, M) \leq 1. \tag{48}$$

Therefore

$$\begin{aligned} \psi_d^N(u) & \leq \\ & = \int_{B_{N-1}} \cdots \int_{B_0} Q(dw_{N-1} | w_{N-2}, M) \\ & \cdots \quad Q(dw_1 | w_0, M) \rho(dw_0). \end{aligned}$$

furthermore, for each $i = 1, 2, \cdots, N-1$, $B_i \subseteq \{\xi_{i-1} < x_{i-1}^M + M\} \subseteq \{\xi < Z + M\}$; this implies that

$$Q(B_i | w_{i-1}, M) \leq Pr[\xi_{i-1} < x_{i-1}^M + M] \leq Pr[\xi < Z + M]. \tag{49}$$

So

$$\begin{aligned} \psi_d^N(u) & \leq \\ & = \int_{B_{N-2}} \cdots \int_{B_0} Pr[\xi < Z + M] \\ & \quad Q(dw_{N-2} | w_{N-3}, M) \cdots \\ & \quad Q(dw_1 | w_0, M) \rho(dw_0). \end{aligned}$$

Finally, iterating this way $N-3$ times and since ρ is concentrated in B_0, it is obtained that

$$\psi_d^N(u) \leq (Pr[\xi < Z + M])^{N-2} Q(B_1 | u, M), \tag{50}$$

where $Q(B_1 | u, M) = Q(x_1^M \neq 0 | u, M) = Pr[\xi < u + M]$. □

The examples that follow illustrate the application of Theorem 5.1. To do this, the ruin probability $\psi_d^N(u) = 0.001$ and $\nu := 1 - \psi_d^N(u)$ are considered.

Table 1: Gamma distribution.

u	$\kappa = 1$	years($\approx N$)	$\kappa = 3$	years($\approx N$)
1	Z=4.503	19.07	Z=6.928	18.70
2	M=2	19.11	M=4.732	18.99
3		19.12		19.08
4		19.17		19.09

5.1 Example 1

Suppose that ξ has a Gamma distribution with parameters (λ, κ) whose density is of the form

$$\Delta(s) = \frac{\lambda}{\Gamma(\kappa)} (\frac{s}{\lambda})^{\kappa - 1} e^{-(s/\lambda)}, s > 0, \tag{51}$$

where $\Gamma(k) = \int_0^{+\infty} s^{k-1} e^{-s} ds$ is the Gamma function.

It is known that the Gamma distribution is not analytically integrable, so it is necessary to resort to tables for this distribution given in (Wilks, 2011) Appendix B Table B.2.

In this case, the optimal premium is

$$M = \kappa + \beta\sqrt{\kappa}, \tag{52}$$

where β is the loading factor.

Given $\lambda = \beta = 1$, and different values of u, Z, M, and their respective period of sustainability (in years) are calculated for $\kappa = 1, 3$. These values are shown in Table (1).

5.2 Example 2

Suppose that ξ has a Weibull distribution with parameters (λ, κ). It is known that the distribution function is as follows:

$$F(s) = 1 - e^{-(s/\lambda)^\kappa}, s > 0. \tag{53}$$

Since $F(M+Z)=\nu$, it follows that

$$Z=\lambda(ln(1-\nu)^{-1})^{1/\kappa}-M. \quad (54)$$

In this case, the optimal premium is

$$M=\lambda(\Gamma(1+1/\kappa)+\beta\sqrt{\Gamma(1+2/\kappa)-\Gamma^2(1+1/\kappa)}), \quad (55)$$

where β is the loading factor.

Given $\lambda=\beta=1$, and different values of u, Z, M, and their respective period of sustainability are calculated for $\kappa=0.8,0.6$. These values are shown in Table (2).

Table 2: Weibull distribution.

u	$\kappa=0.8$	years($\approx N$)	$\kappa=0.6$	years($\approx N$)
1	Z=8.64	19.00	Z=20.91	18.98
2	M=2.56	19.08	M=4.14	19.03
3		19.12		19.07
4		19.15		19.10

6 CONCLUSIONS

With the theory presented in this paper, a discrete time reserve process with a fixed barrier was determined, when it was modelled as a discounted Markov Decision Process. The dynamics presented in Equation (18) describes the behavior of the reserves of the company when these are below the barrier. This allows us to set a penalty to take into account non-payments of dividends. By controlling the process generated by premiums, it is found that the optimal policy is M.

On the other hand, the rate presented in Theorem 5.1 permits to determine the periods of sustainability of the company given a ruin probability and an initial reserve. This bound depends on the distribution of the total amount of claims per time interval. It should also be noted that these random variables are only assumed to have continuous density almost everywhere, with finite first and second moments. This condition is satisfied by a wide range of distributions. The examples illustrate how to apply the rate in the case of distribution with light or heavy tails.

ACKNOWLEDGEMENTS

R. Montes-de-Oca, P. Saavedra, and D. Cruz-Suárez dedicate this article to the memory of their co-worker and co-author of the present work, Gabriel Zacarías-Espinoza, whose sensible death occured on November, 10, 2015.

This work was partially supported by CONACYT (México) and ASCR (Czech Republic) under Grant No. 171396.

REFERENCES

Ash, R. B. and Doléans-Dade, C. (2000). *Probability and Measure Theory*. Elsevier, London, 2nd edition.

Asmussen, S. (2010). *Ruin Probability*. World Scientific, Singapore, 2nd edition.

Azcue, P. and Muler, N. (2014). *Stochastic Optimization in Insurance a Dynamic Programming Approach*. Springer, London.

Breiman, L. (1992). *Probability*. SIAM, Berkeley.

Bulinskaya, Y. G. and Muromskaya, A. (2014). Discrete-time insurance model with capital injections and reinsurance. *Methodol. Comput. Appl. Probab.*

Bäuerle, N. and Rieder, U. (2011). *Markov Decision Processes with Applications to Finance*. Springer, Berlin.

Cramér, H. (1930). *On the Mathematical Theory of Risk*. Skandia Jubillee Volume, Stockholm.

Cruz-Suárez, D., de Oca, R. M., and Salem-Silva, F. (2004). Conditions for the uniqueness of optimal policies of discounted markov decision processes. *Math. Methods Oper. Res.*, 60:415–436.

De-Finetti, B. (1957). Su un'impostaziones alternativa della teoria collectiva del rischio. *Trans. XV. Int. Congr. Act.*, 2:433–443.

Diasparra, M. A. and Romera, R. (2009). Bounds for the ruin probability of a discrete-time risk process. *J. Appl. Probab.*, 46:99–112.

Dickson, D. C. M. (2005). *Insurance Risk and Ruin*. Cambridge University Press, Cambridge.

Dickson, D. C. M. and Waters, H. R. (2004). Some optimal dividend problems. *ASTIN Bull.*, 34:49–74.

Finch, P. D. (1960). Deterministic costumer impatience in the queueing system gi/m/1. *Biometrika*, 47:45–52.

Gerber, H. U. (1981). On the probability of ruin in the presence of a linear dividend barrier. *Scand. Acutarial J.*, pages 105–115.

Gerber, H. U., Shiu, E. S. W., and Smith, N. (2006). Maximizing dividends without bankruptcy. *ASTIN Bull.*, 36:5–23.

Ghosal, A. (1970). *Some Aspects od Queueing and Storage System*. Springer Verlag, New York.

Hernández-Lerma, O. and Lasserre, J. B. (1996). *Discrete-time Markov Control Processes: Basic Optimality Criteria*. Springer Verlag, New York.

Li, S., Lu, Y., and Garrido, J. A. (2009). A review of discrete-time risk models. *Rev. R. Acad. Cien. Serie A. Mat.*, 103(2):321–337.

Lindvall, T. (1992). *Lectures on the Coupling Method*. Wiley, New York.

Lundberg, F. (1909). Über die theorie der ruckversicherung. *Transactions of the VIth International Congress of Actuaries*, 1:877–948.

Martin-Löf, A. (1994). Lectures on the use of control theory in insurance. *Scand. Actuarial J.*, pages 1–25.

Martínez-Morales, M. (1991). *Adaptive Premium in an Insurance Risk Process, Doctoral Thesis*. Texas Tech University, Texas.

Rolski, T., Schmidli, H., Schmidt, V., and Teugels, J. L. (1999). *Stochastic Processes for Insurance and Finance*. Wiley, Chichester.

Royden, H. L. (1988). *Real Analysis*. Macmillan, New York.

Schmidli, H. (2009). *Stochastic Control in Insurance*. Springer, London.

Schäl, M. (2004). On discrete-time dynamic programming in insurance: Exponential utility and minimizing the ruin probability. *Scand. Actuarial J.*, pages 189–210.

Wilks, D. S. (2011). *Statistical Methods in the Atmospheric Sciences*. Academic Press, Burlington.

Two-level Approach for Scheduling Multiproduct Oil Distribution Systems

Hossein Mostafaei[1,2] and Pedro M. Castro[1]
[1]*Centro de Matemática Aplicações Fundamentais e Investigação Operacional, Faculdade de Ciências, Universidade de Lisboa, 1749-016 Lisboa, Portugal*
[2]*Department of Applied Mathematics, Azarbaijan Shahid Madani University, Tabriz, Iran*
{hmostafaei, pmcastro}@fc.ul.pt

Keywords: Scheduling, Tree-like Structure, Decomposition Approach, Batch Sequencing.

Abstract: A core component of the oil supply chain is the distribution of products. Of the different types of distribution modes used, transportation by pipeline is one of the safest and most cost-effective ways to connect large supply sources to local distribution centers, where products are loaded into tanker trucks and delivered to customers. This paper presents a two-level optimization approach for detailed scheduling of tree-like pipeline systems with a unique refinery and several distribution centers. A mixed-integer linear programming (MILP) formulation is tackled in each level, with the upper and lower level models providing the aggregate and detailed pipeline schedules, respectively. Both models neither discretize time nor divide a pipeline segment into packs of equal size. Solutions to two case studies, one using real-life industrial data, show significant reductions in both operational cost and the CPU time with regards to previous two level approaches.

1 INTRODUCTION

In today's competitive environment, supply chain management is a major concern for companies and has received growing attention in recent years. The oil supply chain deals with a complex structure and comprises many costly stages such as: oil exploration, refining and product distribution, with transportation costs already surpassing 400 billion dollars in the early eighties (Bodin et al., 1983).

Different types of distribution modes are used in the oil supply chain where the pipeline mode is the most reliable and cost-effective way of transporting high volumes of oil products between refineries (upstream) and distribution centers nearby consumer markets (downstream). Transportation scheduling of petroleum products via pipelines is one of the most challenging management problems with several operational restrictions to be considered.

Pipelines convey a variety of oil derivatives such as heating oil, motor gasoline, jet fuel, and liquefied gas (one after the other). The products usually move through several pipelines before reaching their final destinations. Since there is not a physical barrier in between products, some mixing occurs, producing a contaminated product that is referred to as interface material. An effective sequence of pipeline input and output operations can considerably reduce pipeline operating costs.

In recent years, several authors have applied rigorous optimization tools to pipeline scheduling problems, relying both on discrete- (Rejowski and Pinto, 2003, 2004; Magatao et al., 2004; Herran et al., 2010) and continuous-time MILP formulations (Cafaro and Cerda, 2004; Castro, 2010; Cafaro and Cerda, 2011; Mostafaei and Ghaffari, 2014; Mostafaei et al. 2015a). They have generally considered two operational plans for the pipeline systems: aggregate and detailed, depending on the way pipeline input and output operations are performed. Aggregate plans define the optimal batch sizes and the sequence of batch injections during the time horizon, while detailed plans deal with sequencing and timing of batch removals during a pumping operation.

Mostafaei and co-workers (Ghaffari and Mostafaei, 2015; Mostafaei et al., 2016, 2017) developed continuous time MILP models to tackle the operational planning of straight pipeline networks that permits to achieve both the aggregate and the detailed plans in single step. Compared to a two-level approach developed by Cafaro et al. (Cafaro et al. 2012), they achieved better detailed schedules.

Mostafaei, H. and Castro, P.
Two-level Approach for Scheduling Multiproduct Oil Distribution Systems.
In *Proceedings of the 6th International Conference on Operations Research and Enterprise Systems (ICORES 2017)*, pages 150-159
ISBN: 978-989-758-218-9

Cafaro and Cerda (2010) introduced a continuous time MILP formulation for aggregate scheduling of tree-like pipelines. Castro (2010) and Mostafaei et al. (2015b) developed continuous time MILP formulations to solve the detailed scheduling of the same problem in a single step. However, the single level optimization framework is computationally expensive for large-scale problems. It is the main goal of this paper to propose a computationally more efficient approach relying on hierarchical decomposition to generate the detailed schedule.

In previous two level approaches for straight pipelines (Cafaro et al. 2011, 2012), each product delivery operation in the lower level model should be accomplished in the time interval determined in the upper level model. Such a decision may not avoid unnecessarily flow restarts if a depot is alternatingly active in the aggregate schedule. This limitation is also relaxed in this paper.

The rest of the paper is organized as follows: Section 2 presents a brief description of the problem under study. Section 3 builds a hierarchically decomposition approach for the detailed scheduling of the tree-like pipeline networks. The efficacy of the proposed approach is tested using two case studies, leading to the results in Section 4. The last section puts forward the conclusions and sums up the paper.

2 PROBLEM STATEMENT

We deal with a short-term scheduling problem where a tree-like pipeline must convey oil derivatives from a single refinery to several distribution centers (depots). Such a pipeline system consists of a trunk line known as mainline (pipeline $n0$) and several secondary lines emerging from the mainline at different sites (branch points). Figure 1 shows a tree-like pipeline network with two secondary lines (pipelines $n1, n2$). A pipeline segment ends with a depot and/or a branch point. The secondary line $n2$ in Figure 1 has two segments and two depots.

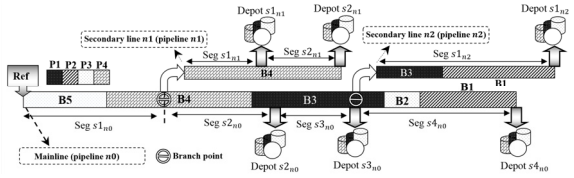

Figure 1: Tree-like pipeline system.

Batches of petroleum products pumped at the refinery are diverted to mainline depots or/and branched into secondary lines. The aim is to determine the optimal batch input and output operations in order to meet depot requirements at minimum total cost subject to the following rules: (1) pipeline segments remain full at any time; (2) each pumping operation involves at most one batch injection at the refinery (3) pipelines work in a single flow direction, from left to right in the diagrams, (4) the refinery should pump product into the mainline in admissible injection rates; (5) in the detailed level, a pumping operation can at most have one batch input in each pipeline and in each depot whereas the aggregate plan relaxes such assumption; (6) pipeline segments should operate in acceptable flowrate ranges, whereas in the aggregate level there are no flowrate segment restrictions; (7) the valves of active depots and segments remain open throughout the pumping operation while they may be turned on/off several times in the aggregate plan.

Given are the following: (i) the number of products to be injected by the refinery (ii) the time horizon length measured in hours (h), (iii) the 0-1 matrix of forbidden sequences between products, (iv) capacity of pipeline segments measured in m^3, (v) volumetric coordinate of depots (m^3), (vi) volumetric coordinate of branch points (m^3), (vii) pump rate at refinery measured in m^3/h, (viii) flowrate range in pipeline segments (m^3/h), (ix) maximum/ minimum volume injected to each pipeline and diverted to depots during each pumping operation (m^3), (x) product inventory at refinery and product demand at depots (m^3).

3 OPTIMIZATION MODEL

In this section, we present a two-level approach for the detailed scheduling of tree-like pipelines. We will sequentially solve the aggregate (upper level) and the detailed (lower level) pipeline scheduling models recently developed by Mostafaei et al. (2015b). The aggregate model (referenced hereafter as the **AP** model) will focus on batch input sequencing problem whereas the detailed schedule (**DP** model) will consider batch output sequencing problem in depots. The approach uses the common sets defined in Mostafaei et al (2015b): (1) $k \in K$; pumping runs (2) $n \in N$; pipelines, (3) $s \in S_n$; depots or segments of pipeline n, (4) $i \in I = \{i_1, i_2, \ldots\}$; batches to move inside the pipeline network, (5) I^{new}; new batches to be pumped into the mainline ($I^{\text{new}} \subseteq I$), (6) $I_n = I_n^{old} \cup I_n^{new}$; batches to move in pipeline n, with I_n^{old} indicating the batches initially inside pipeline n and I_n^{new} denoting the batches to be transferred within the planning horizon; (7) $p \in P$; oil products, (8)

I_n^s ($I_n^s \subseteq I_n$); batches to be diverted into depot s_n, (9) P_i; product contained in old batch i and (10) IN_n; non-empty old batches in secondary line n. Note that pipeline $n0$ is referred to as the *mainline*.

Two alternative objective functions will be explored through the optimization approach. The objective function of the **AP** model will minimize the operational cost of pipeline, including pumping, interface and backorder costs. The **DP** model will reduce the pump operating and maintenance costs subject to fully fulfilling all product deliveries accomplished by the aggregated plan. As stated by Hane and Ratliff (1995), most of the pipeline energy consumption and the pump maintenance costs are linked to flow restarts in idle pipeline segments and consequently it is important to minimize the number of pipeline segments where the flow is resumed or stopped. Restarting the flow in a segment is equivalent to saying that the segment is active through the current pumping run but inactive during the previous one. The opposite condition identifies the stop of the pipeline segment.

Note that minimizing the number of flow stoppages brings another economic benefit to the oil industry since the size of the interface volume between adjacent batches inside a segment tends to increase while it stays inoperative. Future work will involve enforcing pipeline segments to contain a single product when they are inactive.

Here we present the **AP** and **DP** model. The list of model entities can be found in Mostafaei et al. (2015b).

3.1 Aggregate Level (AP)

3.1.1 Pumping Sequence

Let ST_k be the start time of pumping run k and L_k be its duration. Pumping run k can start if the previous run $k-1$ is completed. The length of all runs must not surpass the length of planning horizon.

$$ST_k = ST_{k-1} + L_{k-1}, \quad \forall k \in K(k \geq 2) \tag{1}$$

$$\sum\nolimits_{k \in K} L_k \leq h_{\max} \tag{2}$$

3.1.2 Tracing the Location of Batches

The continuous variable $LPV_{i,n,k}$ is used to track the upper location of batch $i \in I_n$ in pipeline n at the end of pumping run k. This variable is equal to the volume of batches $i'(i' \geq i)$ pursing batch $i \in I_n$ at the end of pumping run k.

$$LPV_{i,k,n} = \sum_{i' \in I_n : i \leq i'} SPV_{i',k,n}, \forall i \in I_n, k \in K, n \in N \tag{3}$$

3.1.3 Injecting Batches from the Refinery

Binary variable $\lambda_{i,k}$ is equal to one if batch $i \in I_{n0}$ is receiving material from the refinery during pumping run k. During run k, batch i can receive material if the lower coordinate of the batch ($LPV_{i,k,n} - SPV_{i,k,n}$) touches the origin of the mainline at the end of pumping run k. If $\lambda_{i,k} = 1$, a positive volume of batch i will be injected into the pipeline at the acceptable pump rate belonging to the interval $[vr_{n0}^{\min}, vr_{n0}^{\max}]$.

$$\sum_{i \in I} \lambda_{i,k} \leq 1, \quad \forall i \in I^{\text{new}} \tag{4}$$

$$LPV_{i+1,k-1,n0} \leq PV_{n0}\left(1 - \lambda_{i,k}\right), \forall i \in I_{n0}, k \tag{5}$$

$$IPV_{n0}^{\min} \lambda_{i,k} \leq IPV_{i,k,n0} \leq IPV_{n0}^{\max} \lambda_{i,k}, \forall i \in I_{n0}, k \tag{6}$$

$$\sum_{i \in I_{n0}} \frac{IPV_{i,k,n0}}{vr_{n0}^{\min}} \leq L_k \leq \sum_{i \in I_{n0}} \frac{IPV_{i,k,n0}}{vr_{n0}^{\min}}, \quad \forall k \tag{7}$$

3.1.4 Product Allocation to Batches

Batch i can at most convey a single product p. Binary variable $y_{i,p}$ is used to allocate products to batches. The volume of batch i containing product p pumped from the refinery ($PPV_{i,p,k}$) should be within a given range. If it conveys a product, new batch $i \in I^{new}$ will be pumped into the mainline in one or more pumping operations. Since each batch can convey a single product, the volume of batch i containing p pumped through run k is equal to $IPV_{i,k,n0}$.

$$\textstyle\sum_{p \in P} y_{i,p} \leq 1, \quad \forall i \in I \tag{8}$$

$$PPV_p^{\min} y_{i,p} \leq \textstyle\sum_k PPV_{i,p,k} \leq PPV_p^{\max} y_{i,p}, \forall i \in I^{new}, k \tag{9}$$

$$\textstyle\sum_{p \in P} y_{i,p} \leq \sum_{k \in K} \lambda_{i,k}, \ \forall i \in I^{new} \tag{10}$$

$$\textstyle\sum_p PPV_{i,p,k} = IPV_{i,k,n0}, \ \forall i \in I_{n0}, k \tag{11}$$

3.1.5 Batch Removal at Depots

Through pumping run k, a batch $i \in I_n^s$ can be discharged to depot s_n only if: (i) its upper coordinate has reached the output facility of depot s_n ($\tau_{s,n}$) at time ST_k and (ii) its lower coordinate has not surpassed $\tau_{s,n}$. If binary variable $x_{i,s,k,n}$ is equal to 1, depot s_n receives a certain volume of batch $i \in I_n^s$ ($DPV_{i,s,k,n}$) that is bounded by ($\tau_{s,n} - LPV_{i+1,k-1,n}$) plus the material injected to batch i from the origin of pipeline n during time interval [ST_k; ST_{k+1}].

$$LPV_{i+1,k-1,n} \le \tau_{s,n} + (PV_n - \tau_{s,n})(1 - x_{i,s,k,n}), \quad \forall i \in I_n^s, s \in S_n, k, n \tag{12}$$

$$LPV_{i,k,n} \ge \tau_{s,n} x_{i,s,k,n}, \quad \forall i \in I_n^s, s \in S_n, k, n \tag{13}$$

$$DPV_{s,n}^{\min} x_{i,s,k,n} \le DPV_{i,s,k,n} \le DPV_{s,n}^{\max} x_{i,s,k,n}, \quad \forall i \in I_n^s, s \in S_n, k, n \tag{14}$$

$$\sum_{s'}^{s} DPV_{i,s',k,n} \le (\tau_{s,n} - LPV_{i+1,k-1,n}) + IPV_{i,k,n} + (PV_n - \tau_{s,n})(1 - x_{i,s,k,n}), \forall i \in I_n^s, s \in S_n, k, n \tag{15}$$

The volume of batch i containing product p discharged to depot $s \in S_n$ will be equal to $DPV_{i,s,k,n}$ if batch i conveys product p, otherwise it will be zero.

$$\sum_{p \in P} PDPV_{i,p,s,k,d} = DPV_{i,s,k,n}, \forall i \in I_n, s \in S_n, k, n \tag{16}$$

$$\sum_{k \in K} PDPV_{i,p,s,k,d} \le |K| DPV_{s,n}^{\max} y_{i,p}, \forall i \in I_n, s \in S_n, n \tag{17}$$

3.1.6 Material Transferred to Secondary Lines

Through pumping run k, a batch i in mainline can be diverted to secondary line n ($u_{i,k,n} = 1$) if its upper and lower coordinates satisfy $LPV_{i,k,n0} - SPV_{i,k-1,n0} \le \sigma_n$ and $LPV_{i,k,n0} \ge \sigma_n$. It means the upper coordinate of batch i has already reached branch point n and its lower coordinate has not surpassed the coordinate of branch point (σ_n). If $u_{i,k,n} = 1$, a portion of batch i has entered secondary line n ($IPV_{i,k,n}$).

$$LPV_{i+1,k-1,n0} \le \sigma_n + (PV_{n0} - \sigma_n)(1 - u_{i,k,n}), \quad \forall i \in I_n, k, n \ne n0 \tag{18}$$

$$LPV_{i,k,n0} \ge \sigma_n u_{i,k,n}, \forall i \in I_n, k, n \ne n0 \tag{19}$$

$$IPV_n^{\min} u_{i,k,n} \le IPV_{i,k,n} \le IPV_n^{\min} u_{i,k,n}, \quad \forall i \in I_n, k, n \ne n0 \tag{20}$$

Let us define binary variable $z_{i,n}$ to identify the existence of batch i in secondary line n. For non-empty old batch $i \in I_n^{old}$ we have $z_{i,n} = 1$ and for new batches $i \in I_n^{new}$:

$$z_{i,n} \le \sum_{k \in K} u_{i,k,n} \le |K| z_{i,n}, \forall i \in I_n^{\text{new}}, n \ne 0 \tag{21}$$

3.1.7 Interface and Forbidden Sequences

Batch $(i+1)_{n0}$ is injected into the mainline right after i_{n0} and consequently there will always be a contamination product at their common boundary which is referred to as interface. The volume of the interface material depends on the specific products p and p' is assumed to be given by parameter $MIX_{p,p'}$. If continuous variable $INTF_{i,p,p',n}$ is the interface volume between batch i and its successor in pipeline n conveying products p and p', we have the following conditions for batches in the mainline and secondary lines, where the domain of Eq. (23) is $i, i' \in I_n(i' < i, first(I_n^{\text{old}}) < i), p, p' \in P, n \ne n0$:

$$INTF_{i,p,p',n0} \ge MIX_{p,p',n0}(y_{i,p} + y_{i-1,p'} - 1), \quad \forall i \in I_{n0}, p, p' \in P. \tag{22}$$

$$INTF_{i,p,p',n} \ge MIX_{p,p',n}(y_{i,p} + y_{i',p'} + z_{i,n} + z_{i',n} - \sum_{i''\ge i'+1}^{i-1} z_{i'',n} - Touch_{p,p'} - 2), \tag{23}$$

For quality reasons, some products should not touch each other inside the pipeline. The next equations prevent forbidden sequences in the mainline and secondary lines.

$$y_{i,p} + y_{i-1,p'} \le 1 + Touch_{p,p'}, \forall i \in I^{\text{new}}, p, p' \in P \tag{24}$$

$$z_{i,n} + z_{i',n} \le \sum_{i''\ge i'+1}^{i-1} z_{i'',n} - y_{i,p} - y_{i',p'} + Touch_{p,p'} + 3, \forall i \in I_n^{\text{new}}, i' < i, p, p' \in P, n \ne n0 \tag{25}$$

3.1.8 Size of Batch i at the End of Run k

At the end of pumping run k, the size of batch i in pipeline n can be obtained from its size at time ST_k ($SPV_{i,k-1,n}$) by adding the material that has entered pipeline n and subtracting the material transferred to its depots and split lines. The next equations compute the size of batch i in the mainline and secondary lines.

$$SPV_{i,k,n0} = SPV_{i,k-1,n0} + IPV_{i,k,n0} - \sum_{s \in S_{n0}} DPV_{i,s,k,n0} - \sum_{n \in N} IPV_{i,k,n}, \forall i \in I_{n0}, k \ge 1 \tag{26}$$

$$SPV_{i,k,n} = SPV_{i,k-1,n} + IPV_{i,k,n} - \sum_{s \in S_n} DPV_{i,s,k,n}, \forall i \in I_n, k \ge 1, n \ne n0. \tag{27}$$

3.1.9 Mass Balance

The total volume entering pipeline n is equal to the volume leaving the pipeline.

$$\sum_{i \in I_{n0}} IPV_{i,k,n0} = \sum_{s \in S_{n0}} \sum_{i \in I_{n0}} DPV_{i,s,k,n0} + \sum_{n \in N} \sum_{i \in I_{n0}} IPV_{i,k,n}, \ \forall k \in K \tag{28}$$

$$\sum_{i \in I_n} IPV_{i,k,n} = \sum_{s \in S_n} \sum_{i \in I_n} DPV_{i,s,k,n}, \forall k \in K, n \ne n0 \tag{29}$$

3.1.10 Material Transferred from Batch i to Mainline' Depots and Secondary Lines

It is possible that during the execution of a pumping run the volume of batch i in the mainline can be taken by multiple active depots and secondary lines. In this case, the volume from batch i to these depots and lines is limited by the following equations.

$$\sum_{s \in S_{n0}: \sigma_n \ge \tau_{s,n0}} DPV_{i,s,k,n0} + \sum_{n' \in N: n' \ge 1}^{n} IPV_{i,k,n} \le \sigma_n - LPV_{i+1,k-1,n0} + IPV_{i,k,n0} + PV_{n0}(1 - u_{i,k,n}), \forall i \in I_{n0}, k \in K, n \in N \tag{30}$$

$$\sum_{s' \in S_{n0}}^{s} DPV_{i,s',k,n0} + \sum_{n \geq 1: \sigma_n \leq \tau_{s,n0}} IPV_{i,k,n} \leq \tau_{s,n0} - LPV_{i+1,k-1,n0} + IPV_{i,k,n0} + PV_{n0}\left(1 - x_{i,s,k,n0}\right), \ \forall i \in I_{n0}, k \in K, s \in S_{n0} \quad (31)$$

3.1.11 Meeting Demand

The total volume of product p unloaded to depot s_n during the planning horizon should be as large as $Demand_{p,s,n}$, the demand of product p at depot s_n. Note that it is possible that some demand is not satisfied within the planning horizon. Slack variable $Back_{p,s,n}$ stands for the unsatisfied demand of product p at depot s_n.

$$\sum_{k \in K} \sum_{i \in I_n} PDPV_{i,p,s,k,d} \geq Demand_{p,s,n} - Back_{p,s,n}, \ \forall p \in P, s \in S_n, n \in N \quad (32)$$

3.1.12 Objective Function of Model AP

$$\min z = \sum_{k \in K} \sum_{i \in I_{n0}} \sum_{p \in P} CP_p . PPV_{i,p,k} + \sum_{n \in N} \sum_{i \in I} \sum_{p \in P} \sum_{p' \in P} CIF_{p,p'} . INTF_{i,p,p',n} + \sum_{n \in N} \sum_{s \in S} \sum_{p \in P} CB_{p,s,n} . Back_{p,s,n}$$

3.2 Detailed Level (DP)

All constraints in model **AP** are part of model **DP** except for the interface and forbidden sequence constraints. The remaining constraints of model **DP** model are listed below.

3.2.1 Feeding Depots and Secondary Lines

In detailed level, active depots must simultaneously receive materials while inserting a new batch from the refinery. Such a condition enforces active depot s_n to receive material from batch i during run k if the upper coordinate of the batch at the end of pumping run $k-1$ ($LPV_{i,k-1,n}$) has reached the volumetric coordinate of the output facility of depot s_n ($\tau_{s,n}$). Moreover, the lower coordinate of the batch i should not surpass ($\tau_{s,n}$) at the end of pumping run k. So Eqs. (12)-(13) need to be changed by the following.

$$LPV_{i+1,k,n} \leq \tau_{s,n} + \left(PV_n - \tau_{s,n}\right)\left(1 - x_{i,s,k,n}\right), \quad \forall i \in I_n^s, s \in S_n, k, n \quad (33)$$

$$LPV_{i,k-1,n} \geq \tau_{s,n} x_{i,s,k,n}, \forall i \in I_n^s, s \in S_n, k, n \quad (34)$$

Note that in detailed plan, the product delivery to an active depot will be accomplished from a single batch. This is not a model restriction but a practical fact since delivery rates may vary with products. Active secondary lines will also receive material from a single batch in detailed level during each pumping operation and therefore Eqs (18)-(19) should be replaced by the following:

$$LPV_{i+1,k,n0} \leq \sigma_n + (PV_{n0} - \sigma_n)\left(1 - u_{i,k,n}\right), \quad \forall i \in I_n, k, n \neq n0 \quad (35)$$

$$LPV_{i,k-1,n0} \geq \sigma_n u_{i,k,n}, \forall i \in I_n, k, n \neq n0 \quad (36)$$

Note that Eqs (33)-(36) increase the number of pumping runs required to find the optimal solution, which is detrimental for computational performance. This is one of the reasons for applying two level approaches for detailed pipeline schedule.

3.2.2 Activated and Stopped Volume

In detailed level, it is important to detect the pipeline segments where the flow is resumed or stopped. To this end, we need to determine the status of pipeline segment in two consecutive runs. Binary variable $v_{s,k,n}$ takes the value of 1 if some material moves in segment s_n through pumping run k. Since the pipeline network features a unique refinery, segment $(s-1)_n$ will be active if segment s_n is active, as imposed by Eq (37). The first segment of mainline is active if the segment is receiving products from the refinery ($\sum_{i \in I_{n0}} \lambda_{i,k} = 1$), and vice versa. The first segment of a secondary line n will be active when some material is transferred to this line from the mainline ($\sum_{i \in I_{n0}} u_{i,k,n} = 1$), and vice versa. On the other hand, depot s_n will be idle if segment s_n is idle, as imposed by Eq (40).

$$v_{s,k,n} \leq v_{s-1,k,n}, \ \forall s \in S_n, k, n \quad (37)$$

$$v_{s,k,n0} = \sum_{i \in I_{n0}} \lambda_{i,k}, \forall k, s = first\ (S_{n0}) \quad (38)$$

$$v_{s,k,n0} = \sum_{i \in I_{n0}} u_{i,k,n}, \forall k, n, s = first\ (S_n) \quad (39)$$

$$\sum_{i \in I_{n0}} x_{i,s,k,n} \leq v_{s,k,n}, \forall s \in S_n, k, n \quad (40)$$

The model also needs to specify the status of the mainline segments branching into secondary lines (segments $s1_{n0}$ and $s3_{n0}$ in Figure 1). Since σ_n is the volumetric coordinated of branch point n and $\tau_{s,n}$ is the volume of segment s_n, we have:

$$v_{s1,k,n} \leq v_{s,k,n0}, \forall k, n, s \in \{S_{n0} | \ \sigma_n = \tau_{s,n0}\} \quad (41)$$

To compute activated and stopped volumes, we first need to determine the active volume of any pipeline n at the end of pumping run k through continuous variable $AV_{k,n}$ (the volume from the

origin of n to the end of furthest active segment s_n). The active volume of a secondary line will be zero if its first segment is idle.

$$AV_{k,n} \geq (v_{s,k,n} - v_{s+1,k,n}).\tau_{s,n}, \forall k,n,s \in S_n \quad (42)$$

$$AV_{k,n} \leq \tau_{s,n} + (PV_n - \tau_{s,n})(1 - v_{s,k,n} + v_{s+1,k,n}), \quad \forall k,n,s \in S_n \quad (43)$$

$$AV_{k,n} \leq PV_n v_{s,k,n}, \forall k, n \neq 0, s = first(S_n) \quad (44)$$

Activated volume of pipeline n during run k ($ACV_{k,n}$) is the idle volume of the pipeline n through run $k-1$, while the stopped volume ($STV_{k,n}$) is the active volume through run $k-1$.

$$ACV_{k,n} \geq AV_{k,n} - AV_{k-1,n}, \quad \forall k \in K, n \in N \quad (45)$$

$$STV_{k,n} \geq AV_{k-1,n} - AV_{k,n}, \quad \forall k \in K, n \in N \quad (46)$$

3.2.3 Flowrate in Pipeline Segment

Aggregate plans usually prevent enforcing flowrate constraints on pipeline segments. These are important since segments typically have different diameters. The detailed plan, as an operational rule, should consider flowrate restrictions, where $vs_{s,n}^{\min}$ and $vs_{s,n}^{\max}$ are minimum and maximum stream flowrates in segment s_n. The flowrate in segment s_n can be computed by the total volume of materials moving along s, divided by the pumping run length L_k. Eq (47) enforces flowrate limitations in mainline segment whereas Eq (48) restrains flowrates in secondary segments.

$$L_k vs_{s,n0}^{\min} - IPV_{n0}^{\max}(1 - v_{s,k,n0}) \leq \sum_{s' \in S_{n0}, s' \geq s} \sum_{i \in I_{n0}} DPV_{i,s',k,n0} + \sum_{\sigma_n \geq \tau_{s,n0}, n \in N} \sum_{i \in I_{n0}} IPV_{i,k,n} \leq L_k vs_{s,n0}^{\max}, \ \forall s \in S_{n0}, k \in K \quad (47)$$

$$L_k vs_{s,n}^{\min} - IPV_n^{\max}(1 - v_{s,k,n}) \leq \sum_{s' \in S_n, s' \geq s} \sum_{i \in I_n} DPV_{i,s',k,n} \leq L_k vs_{s,n}^{\max}, \ \forall s \in S_n, k \in K, n \neq n0 \quad (48)$$

3.2.4 Objective Function of DP Model

$$\min z = \sum_{n \in N} \sum_{k \in K} (CA_n ACV_{k,n} + CS_n STV_{k,n}) + \sum_{i \in I_{n0}} \sum_{k \in K} CF \cdot \lambda_{i,k}$$

4 DECOMPOSITION APPROACH

The detailed scheduling of multi-branched tree structure pipeline networks will become an intractable problem even for short term horizons if all decisions related to the pipeline input and output operations are to be made in a single step. To find the best detailed schedule in reasonable time, we first solve the **AP** model to find the optimal batch sequence in each pipeline at minimum interface, pumping and backorder costs. The resulting solution helps us to identify the exact elements of sets I_n, I^{new}, I_n^s and I_n^{new}, and consequently reduce the constraints domain. Then, after fixing the binary variables $z_{i,n}$ and $y_{i,p}$ and removing the interface and forbidden constraints, we solve the **DP** model to meet demand with minimum number of flow resumes/stoppages and pumping operations. The proposed decomposition procedure will hereafter be called **DSM** and is depicted in Figure 2.

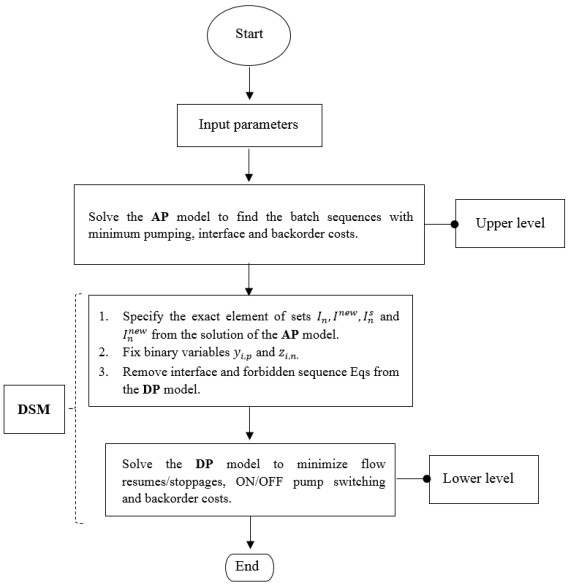

Figure 2: Proposed DSM framework.

4.1 Optimal Number of Pumping Runs

To solve both the upper and the lower models, we should first guess the number of pumping operations for each step. Like previous continuous time approaches, we use an iterative procedure to find the optimal number of pumping operations $|K|$ to be performed. In fact, searching for the optimal solution can be extremely costly, but if the initial guess on the number of pumping runs is accurate, no more than two iterations are usually required. Since all operations may not involve the maximum volume (IPV_{n0}^{max}), a simple expression for the number of pumping operations of model **AP** can be:

$$\left\lceil \frac{\sum_n \sum_s \sum_p Demand_{p,s,n}}{IPV_{n0}^{max}} \right\rceil \leq |K|_{\text{AP}}$$

Moreover, the number of pumping operations in the model **DP** cannot be greater than the number of

product deliveries in model **AP** ($\mathrm{PD}_{\mathrm{AP}}$) and lower than the number of pumping runs in **AP**:

$$|K|_{\mathrm{AP}} \leq |K|_{\mathrm{DP}} \leq \mathrm{PD}_{\mathrm{AP}}$$

4.2 Previous Two Level Approaches

Cafaro and co-workers (2012) were the firsts to develop a two-level approach for the detailed scheduling of straight pipeline systems. In their approach (hereafter **CC**), after finding the product sequence with minimum pumping and interface costs, they fix the aggregate batch sizes, the starting and completion times of each pumping operation in **AP**, and solve the second stage to generate a detailed schedule. In fact, the start and end of pumping operations for a batch injection in the lower level must exactly comply with the start and end times specified for that batch injection in the upper level model. To this end, each product delivery in the lower level model should be accomplished in the same time interval performed in the upper level model. Since the solution quality for the detailed scheduling problem depends on the sequence of product deliveries, the **CC** model does not usually find cost-effective transportation plans.

5 COMPUTATIONAL RESULTS

Two case studies, one of them using industrial data, were solved to validate the efficiency of the proposed two level approach. The implementations were on an Intel® Core(TM) i5-4210U (2.7 GHz) with 6 GB of RAM, running Windows 7, 64-bit operating system using GAMS/CPLEX 12.6 in parallel deterministic mode (using up to 4 threads).

5.1 Example 1

This example deals with a small network and aims to show how we select the elements of sets $I_n, I^{new}, I_n^{\mathrm{new}}$ and I_n^{s} in the lower level model (detailed schedule). We assume that the aggregated transportation plan in Figure 3 is already available. The pipeline topology and its initial status at the start time of planning horizon (time $t = 0.00$ h) is depicted in the first row of Figure 3. The flowrate in pipeline segments can vary between 0.3 and 1.0 m^3/h and the time horizon has a length of 96 h (4 days). The maximum volume input per pumping run is 60 m^3 while the minimum is 10 m^3. The same condition holds for the minimum and maximum batch size diverted to depots. The unit stoppage cost is 0.4 in each segment.

The aggregate pipeline schedule contains two pumping operations. The first operation takes place from time 0.0 h to 30.0 h and involves increasing the amount of product P3 in batch B3 and diverting 20 m^3 of B2 into the secondary line and 10 m^3 of batch B1 into depot N2. The second pumping operation from 30.0 to 90.0 h injects 60 m^3 of new batch B4 into the mainline and the following delivery operations are accomplished at depots: depot N1 receives from batches B3 and B4; batch B2 goes to depots N2 and N3.

To solve **DP** (lower level model) we should first guess the number of pumping operations and specify the exact elements of sets $I_n, I^{new}, I_n^{\mathrm{new}}$ and I_n^{s}. From the aggregated plan, there are a total of 6 product deliveries to depots and so $2 \leq |K|_{\mathrm{DM}} \leq 6$. We will start solving the problem with $|K|_{\mathrm{DM}} = 2$ and keep increasing $|K|_{\mathrm{DM}}$ until no improvement is found in the objective function.

From the solution obtained from the **AP** model, we can now refine the elements of sets $I_n, I^{new}, I_n^{\mathrm{new}}$ and I_n^{s} and reduce the domain of the constraints. It can be observed from Figure 3 that only new batch B4 is injected into the mainline. There are three old batches B1, B2 and B3 and so $I_{n0} = \{\mathrm{B4}, \mathrm{B3}, \mathrm{B2}, \mathrm{B1}\}$. Two new batches B2 and B3 are injected into the secondary line (pipeline $n1$) and so $I_{n1}^{\mathrm{new}} = \{\mathrm{B3}, \mathrm{B2}\}$. There is only one old batch B1 inside the secondary line and so $I_{n1} = \{\mathrm{B1}, \mathrm{B2}, \mathrm{B3}\}$. Depot N1 only receives product from batches B3 and B4 and so $I_{n0}^{\mathrm{N1=s1}} = \{\mathrm{B3}, \mathrm{B4}\}$. Similarly, we have $I_{n0}^{\mathrm{N2=s2}} = I_{n1}^{\mathrm{N3=s1}} = \{\mathrm{B1}, \mathrm{B2}\}$.

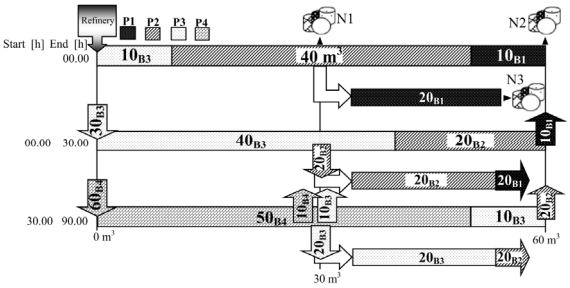

Figure 3: Aggregate pipeline schedule for Example 1.

Figure 4 shows the optimal detailed schedule for Example 1 using **DSM**. It contains 4 batch injections at the refinery and 7 product deliveries to depots. The injection of batch B3 (and batch B4) from the refinery is now accomplished through a sequence of two short pumping runs. There is only one segment stoppage during 4 days that happens in the secondary line during time interval [60.00, 90.00].

Figure 5 shows the optimal pipeline schedule for Example 1 using **CC**. Like **DSM**, 4 batch injections should be accomplished to fully satisfy the given demands. Note that 10 m^3 of batch B1 are being discharged into depot N2 during time interval [0.00, 30.00] of the aggregate plan of Figure 3. This depot should extract the same amount of material during time interval [0.00, 30.00] of the detailed plan. In contrast, it remains inactive in **DSM** (see Figure 4). The aggregate transportation plan enforces depot N2 to be idle during [30.00, 60.00] and to be active during [60.00, 90.00] in **CC**. Such a change in the status of depot N2 leads to a stoppage in the last segment during the third pumping operation. Superfluous flow shutdowns can also be observed in the secondary line that are due to the change in the status of depot N3 that alternatingly becomes active and idle.

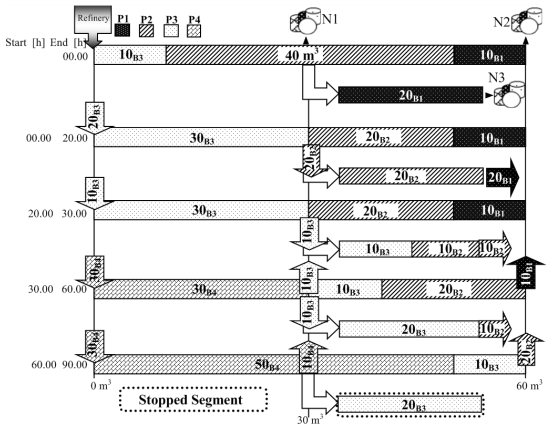

Figure 4: Detailed schedule for Example 1 using DSM.

Table 1: Computational results for Example 1.

	DSM	**CC**
# Pumping runs	4	4
# Constraints	646	646
# Binary vars	90	90
#Continuous vars	285	285
CPUs	0.47	0.42
Stop vol (m^3)	20	70
Obj. Fun[a] ($)	8	28

[a]Both **DSM** and **CC** only minimize pipeline stoppage volumes.

Table 1 gives the computational results of Example 1 for the **CC**, **DSM** approaches. Though the number of pumping operations is the same, the stopped volume of the pipeline in the proposed approach decreases from 70 to 20 m^3. Such a lower shutdown volume in pipeline leads to cost savings of 71.42 %.

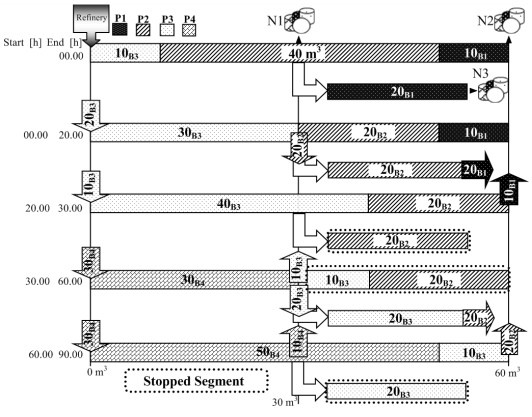

Figure 5: Detailed schedule for Example 1 using CC.

5.2 Example 2 (Real-Life Case Study)

Here we consider a large-scale real-world example from Mostafaei et al. (2015a), involving an Iranian tree-like pipeline with a refinery, a mainline, two secondary lines and six depots (check first row of Figure 6). The first secondary line with two depots starts 3000 m^3 away from the mainline' origin while the other secondary line (single depot) leaves the mainline after 15000 m^3. Batches of four products (P1-P4) should be conveyed and it is forbidden for P1 to touch P4. The product injection rate can vary between 300 and 800 m^3/h, and the time horizon has a total length of 192 h. In both aggregated and detailed levels, at most 13000 m^3 of each product can be injected into the mainline during each operation. Other data for this example, together with the aggregate transportation plan, can be found in Mostafaei et al. (2015b).

Table 2: Computational results for Example 2.

	DSM	**CC**	**Mostafaei et al. (2015b)**
# Pumping runs	13	22	12
# Constraints	5076	9090	5864
# Binary vars	671	1381	782
#Continuous vars	2500	6281	3714
CPUs	64.4	412.60	468.23
Restart vol (m^3)	39200	118400	39200
Obj. Fun[a] ($)	15680	47360	15680

[a]Both DSM and CC only minimize pipeline restart volumes.

Figure 6 shows the optimal detailed schedule for Example 2 using **DSM**. It contains 13 pumping operations and 50 product deliveries to depots. Model size and computational requirements for Example 2 are reported in Table 2.

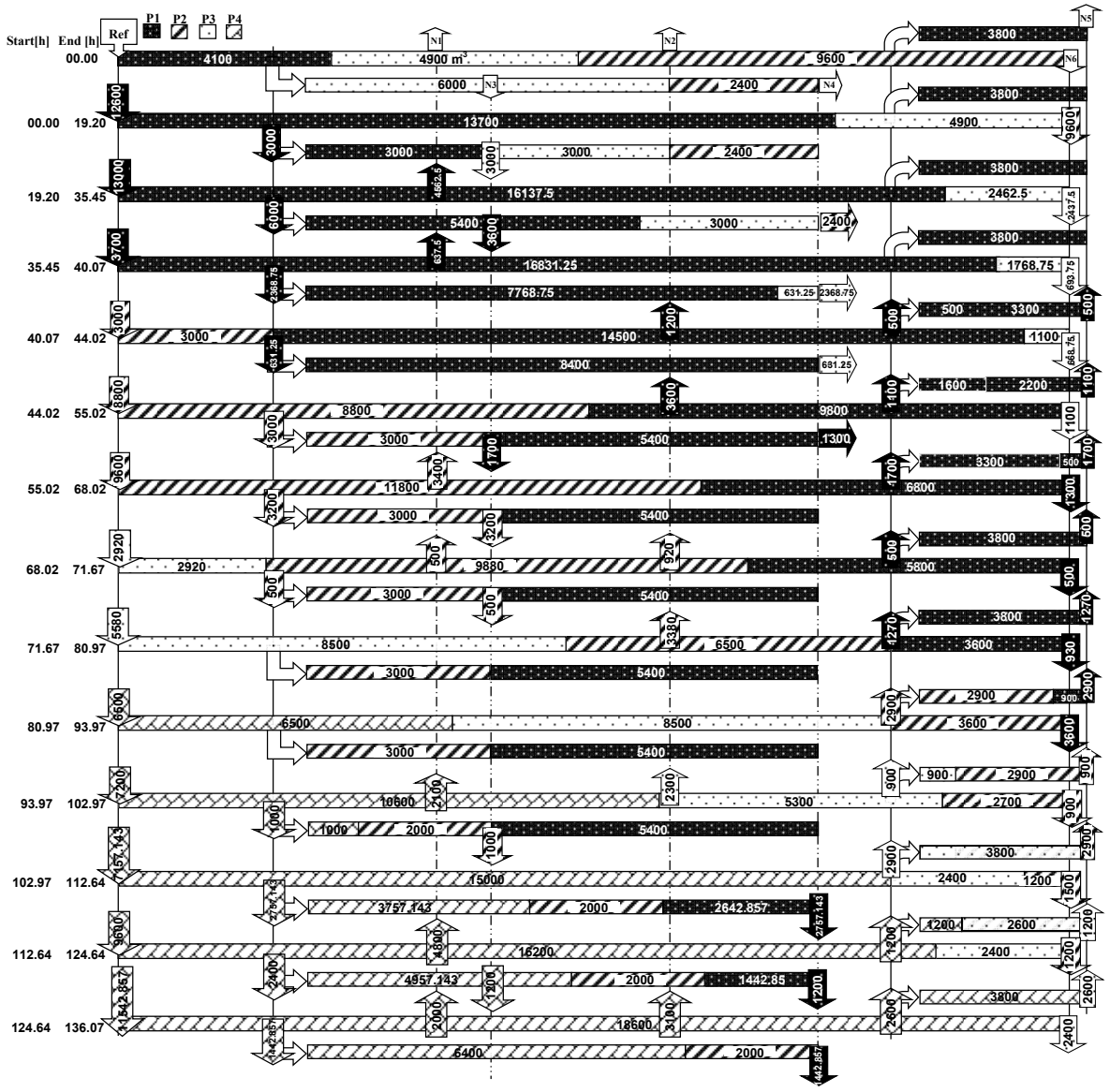

Figure 6: Detailed schedule for Example 2 using DSM.

Three interesting conclusions can be derived from the results. The first, is that the optimal detailed schedule by the **CC** approach involves 22 pump operations against 13 by **DSM**. The second, is that the solution CPU time has been reduced by a factor of 7 with regards to **CC**. The third, is that the objective function value for **DSM** is 66.89 % less expensive than the one for **CC**. This is due to substantial reductions on shutdown volumes. Compared with the single level approach of Mostafaei et al (2015b), the proposed **DSM** approach finds the same solution in a lower CPU time.

6 CONCLUSIONS

This paper presented a novel optimization framework for the detailed scheduling of treelike pipeline networks. The network consists of a refinery, a trunk line, a set of split lines and multiple depots. A computationally efficient two-level approach based on a pair of MILP models has been presented. In the upper level, the optimal sequence of batches in each pipeline is found while the lower level deals with the detailed plan that computes the optimal sequence of batch removals at depots. Through the solution of two

case studies, we showed that the proposed model is more flexible than previous hierarchical approaches and is able to solve large scale problems in reasonable time. Future work will involve applying the proposed method for multi-level tree pipeline networks, with intermediate due dates on demands over long-term horizons.

ACKNOWLEDGMENTS

Financial support from Fundação para a Ciência e Tecnologia through the Investigador FCT 2013 program and project UID/MAT/04561/2013.

REFERENCES

Bodin, L., Golden, B., Assad, A. and Ball, M., 1983. Routing and scheduling of vehicles and crews. The State of the Art. *Computers &Operations Research*, 10 (2), 62.

Cafaro VG., Cafaro DC., Mendéz CA., Cerdá J., 2011. Detailed scheduling of operations in single-source refined products pipelines. *Industrial & Engineering Chemistry Research*, 50: 6240-6259.

Cafaro, D. C., Cerdá, J., 2004. Optimal scheduling of multiproduct pipeline systems using a non-discrete MILP formulation. *Computers & Chemical Engineering*, 28, 2053-2068.

Cafaro, D. C., Cerdá, J., 2011. A rigorous mathematical formulation for the scheduling of tree-structure pipeline networks. *Industrial & Engineering Chemistry Research*, 50, 5064-5085.

Cafaro, V. G., Cafaro, D. C., Mendéz, C. A., Cerdá, J., 2012. Detailed scheduling of single-source pipelines with simultaneous deliveries to multiple offtake stations. *Industrial & Engineering Chemistry Research*, 51, 6145-6165.

Castro, P. M., 2010. Optimal scheduling of pipeline systems with a resource-task network continuous-time formulation. *Industrial & Engineering Chemistry Research*, 49, 11491-11505.

Ghaffari-Hadigheh, A., Mostafaei, H., 2015. On the scheduling of real world multiproduct pipelines with simultaneous delivery. *Optimization and Engineering*, 16, 571-604.

Hane, C. A., Ratliff, H. D., 1995. Sequencing inputs to multi-commodity pipelines. *Annals of Operations Research*, 57, 73-101.

Herran, A., de la Cruz, J. M., de Andres, B., 2010. Mathematical model for planning transportation of multiple petroleum products in a multi-pipeline system. *Computers & Chemical Engineering*, 34, 401-413.

Magatao, L., Arruda, L. V. R., Neves, F. A., 2004. A mixed integer programming approach for scheduling commodities in a pipeline. *Computers & Chemical Engineering*, 28, 171-185.

Mostafaei, H., Alipouri, Y., Shokri, J., 2015. A mixed-integer linear programming for scheduling a multi-product pipeline with dual-purpose terminals. *Computational and Applied Mathematics*, 34, 979-1007.

Mostafaei, H., Castro, P. M., Ghaffari-Hadigheh, A., 2015b. A novel monolithic MILP framework for lot-sizing and scheduling of multiproduct treelike pipeline networks. *Industrial & Engineering Chemistry Research*, 54, 9202–9221.

Mostafaei, H., Castro, P. M., Ghaffari-Hadigheh, A., 2016. Short-term scheduling of multiple source pipelines with simultaneous injections and deliveries. *Computers & Operations Research*, 73, 27-42.

Mostafaei, H., Castro, P.M., 2017. Continuous-time scheduling formulation for straight pipelines. *AIChE J*. doi: 10.1002/aic.15563.

Mostafaei, H., Ghaffari-Hadigheh, A., 2014. A general modeling framework for the long-term scheduling of multiproduct pipelines with delivery constraints. *Industrial & Engineering Chemistry Research*, 53, 7029-7042.

Rejowski, R., Pinto, J. M., 2003. Scheduling of a multiproduct pipeline system. *Computers & Chemical Engineering*, 27, 1229–1246.

Rejowski, R., Pinto, J. M., 2004. Efficient MILP formulations and valid cuts for multiproduct pipeline scheduling. *Computers & Chemical Engineering*, 28, 1511–1528.

Exact Approach to the Scheduling of F-shaped Tasks with Two and Three Criticality Levels

Antonin Novak[1,2], Premysl Sucha[1] and Zdenek Hanzalek[1,2]
[1]*Czech Institute of Informatics, Robotics and Cybernetics, Czech Technical University in Prague, Prague, Czech Republic*
[2]*Department of Control Engineering, Faculty of Electrical Engineering, Czech Technical University in Prague, Prague, Czech Republic*
antonin.novak@cvut.cz, {suchap, hanzalek}@fel.cvut.cz

Keywords: Scheduling, Mixed-criticality, Embedded Systems, Integer Linear Programming.

Abstract: The communication is an essential part of a fault tolerant and dependable system. Safety-critical systems are often implemented as time-triggered environments, where the network nodes are synchronized by clocks and follow a static schedule to ensure determinism and easy certification. The reliability of a communication bus can be further improved when the message retransmission is permitted to deal with lost messages. However, constructing static schedules for non-preemptive messages that account for retransmissions while preserving the efficient use of resources poses a challenging problem. In this paper, we show that the problem can be modeled using so-called F-shaped tasks. We propose efficient exact algorithms solving the non-preemptive message scheduling problem with retransmissions. Furthermore, we show a new complexity result, and we present computational experiments for instances with up to 200 messages.

1 INTRODUCTION

The communication buses in modern vehicles are an essential part of advanced driver assistants. Those systems depend on the data gather by sensors, such as LIDAR, cameras, and radars. The data describing the surrounding environment are communicated through communication buses to ECUs (*Electronic Control Units*) where they are processed, and appropriate actions are taken. For example, if an obstacle is detected in front of the vehicle, the car automatically activates breaks. Not only driver assistant systems rely on the communication. Different ECUs are responsible for running the car as a whole. The fuel is injected accordingly to the current combustion and outside conditions and cars with the drive-by-wire system steer via electronic signals.

The modern vehicle is considered as a fault-tolerant and dependable system. If one part of it breaks down or does not work as expected, the human life is in risk. Since the intra-vehicular communication is the key element of the car, it is subject to a safety certification. The safety certification is a process, where the manufacturer proves that his safety-critical systems such as autonomous driving are working correctly to a high degree of assurance. If manufacturers are not able to demonstrate the correct behavior of the central communication bus, then the whole certification process is not complete. According to *SSR Automotive Warranty & Recall Report 2016*, the number of software-related recalls in 2015 accounted for 15% of all recalls, marking the importance of the certification.

Traditionally, event-triggered communication protocols are commonly used in automotive industry. In the event-triggered environment, the actions are performed *on-demand*, i.e. triggered by some events. Even though, event-triggered protocols are flexible, their usage in modern cars is limited due to certification and verification issues. The response time analysis (i.e. the analysis of the behavior of the system) in real-life event-triggered communication systems including gateways and precedence relations is a very complex problem, therefore the safety certification of systems utilizing the event-triggered environment is a difficult task (Baruah and Fohler, 2011).

An alternative to event-triggered real-time systems is the time-triggered paradigm. Messages in time-triggered communication are transferred through the network at specific times prescribed by a static pre-computed static schedule. The schedule is constructed usually with tools known from *OR/Mathematical Optimization* field (Dvorak and Hanzalek, 2016; Kopetz et al., 2005) such that it re-

Novak, A., Sucha, P. and Hanzalek, Z.
Exact Approach to the Scheduling of F-shaped Tasks with Two and Three Criticality Levels.
In *Proceedings of the 6th International Conference on Operations Research and Enterprise Systems (ICORES 2017)*, pages 160-170
ISBN: 978-989-758-218-9

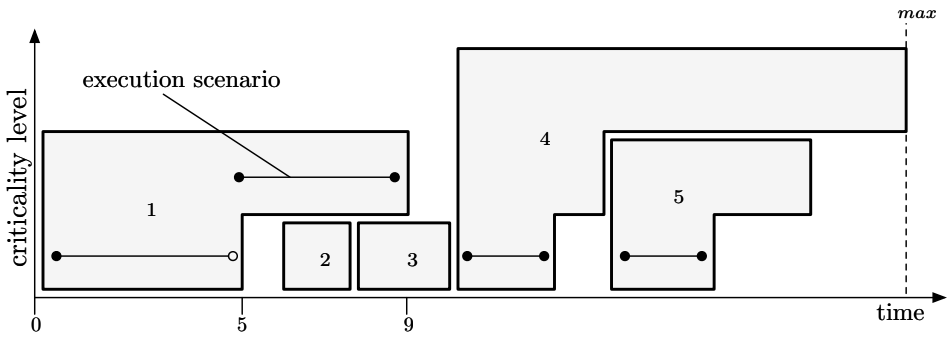

Figure 1: A feasible schedule of F-shaped tasks with a runtime execution scenario denoted by the black line.

spects the problem and safety constraints. Therefore, the certification of the system is achieved via showing feasibility of the produced communication schedule.

The determinism and verifiability of time-triggered communications led to the design of protocols that includes time-triggered communication for safety-critical systems. For example, FlexRay bus is used nowadays in the automotive industry (e.g. Porsche Panamera, Nissan Infinity Q50). One of the disadvantages of time-triggered protocols is their non-flexibility. For example, the static schedule does not take into consideration the message retransmission. The retransmission occurs when a highly critical message is not delivered e.g. due to EM noise. A possible solution how to enable message retransmissions in static time-triggered schedules is to allocate more processing time for each message to account for possible retransmissions. If no retransmission occurs during an actual execution, then the resource is idle until the start time of the next message. However, since retransmissions do not appear as frequently, the average resource utilization would be poor.

In this paper, we introduce a new solution to this problem. We build static schedules that allow retransmission of non-preemptive messages to some degree. An extra time needed for retransmissions is compensated by skipping less critical messages. The trick we use to solve the problem is to include a part of the problem solution to its formulation. Instead of scheduling *rectangles*, denoting the single exact processing time of a message, we schedule so-called *F-shapes*. This leads to an interesting combinatorial problem, where we are given a set of shapes that are aligned on the left side with the right side that is jagged (see an example in Fig. 1). The goal is to pack these shapes as tightly as possible so that they do not overlap.

The use of F-shapes is a very elegant solution that achieves efficient resource utilization. It modifies the traditional scheduling problem into the challenging one where the schedule has to assume alternatives based on the observed runtime scenario. Even though there is an exponential number of possible runtime scenarios, and for each of them, the static schedule is well-defined, we will show, that the introduced formalism makes the problem computationally tractable in practice.

1.1 Application to Automotive

Frequently, in the complex systems, functionalities with different criticality co-exist on a single bus. The adaptation of IEC 61508 safety standard (Bell, 2006), the *ASIL*, defines the application levels with a hazard assessment corresponding to three *Safety Integrity Levels*. Therefore the schedules with three criticality levels arise from the application in the automotive domain:

- messages with high criticality (criticality level 3) are used for safety-related functionalities (their failure may result in death or serious injury to people), such as steering and braking;
- messages with medium criticality (criticality level 2) are used for mission-related functionalities (their failure may prevent a goal-directed activity from being successfully completed), such as combustion engine control;
- messages with low criticality (criticality level 1) are used for infotainment functionalities, such as audio playback.

For the automotive application we assume, the criticality of a message corresponds to its maximum number of possible (re)transmissions and that messages are non-preemptive since the preemption is costly in communications. See an example of a static schedule that accounts for retransmissions in Fig. 1. The individual shapes correspond to messages scheduled on the communication bus. There T_2 and T_3 have low criticality, and no retransmissions are allowed. T_1 and T_5 correspond to messages with medium criticality; thus they can be retransmitted once. The most

critical message is T_4, that can be retransmitted twice. The retransmission of the messages causes a prolongation of the processing time that is depicted in levels on the vertical axis. The top level of each message represents its WCET (*the worst case execution time*), i.e. the time that it takes to transmit the message under the most pessimistic conditions. The prolongations are compensated by skipping less critical messages. With this mechanism, the successful transmission of highly critical messages is guaranteed while in the average case runtime scenario the resource (i.e. communication bus) is efficiently utilized.

Scheduling of safety-critical non-preemptive messages on this time-triggered network can be modeled as the scheduling problem $1|mc = \mathcal{L}, mu|C_{\max}$ (Hanzalek et al., 2016). It represents the scheduling problem with one resource (a communication channel in the network) with non-preemptive mixed-criticality tasks with maximum $\mathcal{L}$ criticality levels, *mu* stands for the match-up of the execution scenario. The criterion is to minimize the maximal completion time $C_{\max}$.

A solution of the scheduling problem is given by a schedule that switches to the higher criticality level when a prolongation of a task occurs. After its successful completion, it matches-up with the original schedule. The trade-off between the safe and efficient schedules is achieved by skipping less critical messages when the prolongation of a more critical one takes place.

1.2 Paper Contribution and Outline

In this paper, we solve the scheduling problem of message retransmission in time-triggered environments. The objective is to find a non-preemptive static schedule that accounts for unforeseen message retransmissions while minimizing the length occupied by time-triggered communication. The uncertainty about the processing time is modeled using an abstraction based on F-shaped tasks. We show the relation between F-shaped tasks and the underlying probability distribution functions. Furthermore, we show a new complexity result that establishes the membership of the considered problem into $\mathcal{APX}$ complexity class, and we provide an approximation algorithm. We study the characterization of the set of optimal solutions for the problem with two criticality levels. Finally, we propose efficient exact algorithms for problems with two and three criticality levels, which solve instances with up to 200 tasks, beating the best-known method by a large margin.

The rest of the paper is organized as follows. In Sec. 2 we survey the related work. In Sec. 3 we show the relation between F-shaped tasks and discretization of cumulative probability distribution functions. In Sec. 5 we prove approximability of the problem. In Sec. 6 and 7 we show properties of the problem with two and three criticality levels and we propose efficient exact algorithms. Finally, in Sec. 8 we present computational results on the sythetic data as well as on the data inspired by a real-life embedded system of our industrial partner.

2 RELATED WORK

The exhaustive survey on mixed-criticality in real-time systems is presented by (Burns and Davis, 2013). This research is traditionally concentrated around event-triggered approach to scheduling. In the seminal paper (Vestal, 2007) proposed a method that assumes different WCETs (*the worst case execution time*) obtained for discrete levels of assurance. Apart from this proposition, the paper presents modified preemptive fixed priority schedulability analysis algorithms. However, the preemptive model is not suitable for communication protocols, and it significantly changes the scheduling problem. (Baruah et al., 2010) formulated the basic model of mixed-criticality systems. They study MC schedulability problem with two criticality levels under special restrictive cases in the event-triggered environment. (Theis et al., 2013) argued that mixed-criticality shall be pursued in time-triggered systems. (Baruah and Fohler, 2011)'s approach in the time-triggered environment assumed preemptive tasks with up to two criticality levels. It makes it unsuitable for communication protocols since the preemption would be costly. (Hanzalek et al., 2016) proposed the problem of non-preemptive mixed-criticality match-up scheduling motivated by scheduling messages on a highly used communication channel. They showed how a schedule with F-shaped tasks can be used to deal with a task disruption by skipping less critical tasks. They provide the relative order MILP model for $1|r_j, \tilde{d}_j, mc = \mathcal{L}, mu|C_{\max}$ scheduling problem, but it can deal with instances with only about 20 messages.

The concept of match-up scheduling was introduced by (Bean et al., 1991). In a case of a disruption, the goal is to construct a new schedule that matches the original one at some point in the future. This concept is mostly studied in the context of manufacturing problems (Qi et al., 2006).

Taking broader perspective, the problem can be viewed as a case of robust and stochastic optimization due to uncertainty about transmission times while satisfying safety requirements. (Bertsimas et al.,

2011) surveys robust versions of various optimization problems, but rather continuous than discrete ones. The field of stochastic optimization is reviewed by (Sahinidis, 2004). They state that integer variables introduced to stochastic programming complicate its solution, yielding suboptimal results even for small-sized problems.

As in our problem, some of the less critical messages are allowed to be skipped, the problem is related to the scheduling with a job rejection. (Shabtay et al., 2013) reviews offline scheduling with a job rejection. These approaches consider two criteria, a measure associated with schedule quality and the cost incurred by rejected jobs. The solution to this problem is a set of accepted jobs and a set of rejected jobs. However, rejected jobs cannot be executed in any execution scenario; thus this model is not suitable for communication protocols mentioned in our motivation.

To the best of our knowledge, the problem of offline non-preemptive mixed-criticality match-up scheduling was addressed by (Hanzalek et al., 2016) only, but it lacks an efficient solution method which is suggested in this paper.

3 NON-PREEMPTIVE MIXED-CRITICALITY SCHEDULING

We assume that a set of communication messages is given to be scheduled on a single communication bus segment. For each message T_i, the criticality $\mathcal{X}_i \in \mathbb{N}$ is specified. It denotes the number of allowed transmissions. Each message (task) is specified by its *criticality levels*. For each *criticality level* $\ell \in \{1,\ldots,\mathcal{X}_i\}$, we define the associated processing time with this level. See an example in Fig. 1. Here, T_1 has criticality $\mathcal{X}_1 = 2$; therefore it can be retransmitted once. The processing time at the first level is given by its BCET (*the best case execution time*) while the processing time at the second level is its WCET (*the worst case execution time*). During the run time execution, exactly one processing time of the message is realized; however, it is not known in advance which it will be.

We can view processing time prolongations as a retransmission of the whole message content. However, this mixed-criticality scheduling model is useful also for scheduling of computational tasks, where the exact computational time is not known in advance, but only a probability distribution is known. Let us consider the processing time of task T_i to be a random variable $\mathcal{T}_i$. Let us assume an arbitrary probability distribution over a discrete set of processing times from $\mathbb{N}$ for a particular task stating $\Pr[\mathcal{T}_i = t]$. The same information given by the probability distribution is captured by the CDF (*cumulative distribution function*) $\mathcal{F}_i$ giving the probability that processing time $\mathcal{T}_i$ is at most t. See Figs. 2a and 2b for such an example. Corresponding processing times $p_i^{(\ell)}$ for each criticality level ℓ are taken from $\mathcal{F}_i$ as $p_i^{(\ell)} = \mathcal{F}_i^{-1}(c_\ell)$, where $\mathcal{F}_i^{-1}$ is the quantile function. The criticality of a task is a user-defined parameter. For example, if we identify criticality levels with a safety standard IEC 61508 SIL (*Safety Integrity Levels*) (Bell, 2006), then the task criticality $\mathcal{X}_i$ is given by the SIL of the functionality carried out by the content and c_ℓ is defined as $1-$*probability of failure* defined by SIL ℓ.

Processing times obtained according to criticality levels then form a single task like the one depicted in Fig. 2d. Since CDFs are non-decreasing functions, a set of processing times $p_i^{(\ell)}$ yields shapes like the F letter rather than ordinary rectangles, hence the name F-shape. See an example in Fig 2. There we see discretization for a task with criticality three at corresponding levels 1, 2 and 3 with the vertical axis on the logarithmic scale.

The solution to the scheduling problem is a feasible static schedule of the given set of F-shaped tasks. Consider a particular example of the schedule with tasks having up to three levels of criticality that is shown in Fig. 1. A feasible schedule with F-shaped tasks describes alternative schedules for any realization of the processing time of messages. Observed prolongations of more critical messages are compensated by skipping execution of less critical messages.

The black line denotes a scenario, where T_1 was disrupted once. The actual processing time of T_1 was 9 instead of 5 due to a disturbance. When the disruption occurred, the execution switched to the next higher criticality level. There, by the assumption, the execution was successful with a probability given by the $\ell = 2$ criticality level. After upon T_1 finished, the execution matched-up back with the lowest criticality level. In general, if a task T_i is prolonged to level ℓ, then all tasks T_j for which $s_i + p_i^{(1)} \leq s_j < s_i + p_i^{(\ell)}$ are not executed. Therefore, in this execution scenario, after T_1 finished, T_4 was up next. Moreover, if we unify the F-shape from Fig. 2d with task T_4 in Fig. 1, then we can say that T_5 will be executed with very high probability of 0.99, but in rare cases, it won't be executed since T_4 is more critical and needs more time to complete. However, here the choice of 0.99 is just for the illustrative purposes only, since the levels of the probability are inputs to the problem and they can be set to any feasible value.

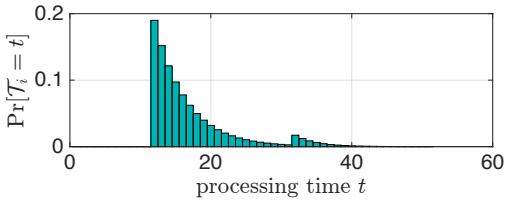

(a) A discrete probability distribution over a set of processing times.

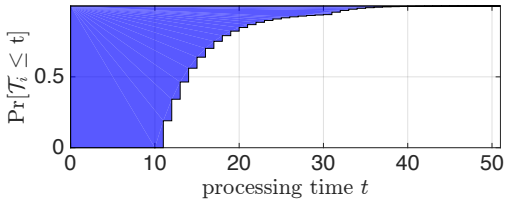

(b) Corresponding cumulative distribution function.

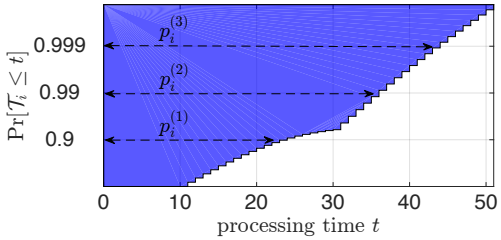

(c) Discretization of a cumulative distribution function

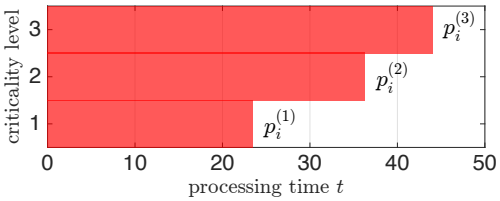

(d) Resulting F-shaped task with $\mathcal{X}_i = 3$

Figure 2: Discretized cumulative distribution function forms an F-shaped task.

4 PROBLEM STATEMENT

We assume a set of non-preemptive F-shaped tasks $I_{\mathcal{MC}} = \{T_1, \ldots, T_n\}$ to be processed on a single machine. We define an F-shaped task and its criticality as follows:

Definition 1 (F-shape)**.** *The F-shape T_i is a pair $(\mathcal{X}_i, \mathbf{P}_i)$ where $\mathcal{X}_i \in \{1, \ldots, \mathcal{L}\}$, $\mathcal{L} \in \mathbb{N}$ is the task criticality and $\mathbf{P}_i \in \mathbb{N}^{\mathcal{X}_i}$, $\mathbf{P}_i = (p_i^{(1)}, p_i^{(2)}, \ldots, p_i^{(\mathcal{X}_i)})$ is the vector of processing times such that*

$$p_i^{(1)} < p_i^{(2)} < \ldots < p_i^{(\mathcal{X}_i)}.$$

The F-shape is an abstraction for non-preemptive tasks with multiple different processing times. See for example T_4 in Fig. 1. It is F-shaped task with criticality $\mathcal{X}_4 = 3$; therefore it has 3 different processing times. Having a set $I_{\mathcal{MC}}$ of F-shaped tasks, we define the feasible schedule as follows:

Definition 2 (Feasible Schedule)**.** *By the schedule for a set of F-shaped tasks $I_{\mathcal{MC}} = \{T_1, T_2, \ldots, T_n\}$ we refer to an assignment $(s_1, s_2, \ldots, s_n) \in \mathbb{N}^n$. We say that schedule $(s_1, s_2, \ldots, s_n)$ for $I_{\mathcal{MC}}$ is feasible if and only if $\forall i, j \in \{1, \ldots, n\}, i \neq j$:*

$$(s_i + p_i^{(\min\{\mathcal{X}_i, \mathcal{X}_j\})} \leq s_j) \vee (s_j + p_j^{(\min\{\mathcal{X}_i, \mathcal{X}_j\})} \leq s_i).$$

Feasibility of a schedule with F-shaped tasks requires that tasks do not overlap on any criticality level. For example in Fig. 1, since T_5 follows after T_4, it cannot start earlier than $s_4 + p_4^{(2)}$, since $\min\{\mathcal{X}_4, \mathcal{X}_5\} = 2$ is the highest common criticality level of T_4 and T_5.

We deal with the problem of finding a feasible schedule for a set of F-shaped tasks with criticality at most $\mathcal{L}$ such that the makespan (i.e. $\max s_i + p_i^{(\mathcal{X}_i)}$) is minimized. In the three-field Graham-Blazewicz notation it is denoted as $1|mc = \mathcal{L}, mu|C_{\max}$, where $mc = \mathcal{L}$ stands for the mixed-criticality aspect of tasks of maximal criticality $\mathcal{L}$ and *mu* stands for the match-up. This problem is known to be $\mathcal{NP}$-hard in the strong sense even for $mc = 2$ (two criticality levels) as shown by reduction from 3-Partition Problem in (Hanzalek et al., 2016).

5 GENERAL PROPERTIES

Since the problem $1|mc = 2, mu|C_{\max}$ is strongly $\mathcal{NP}$-hard, it does not admit FPTAS unless $\mathcal{P} = \mathcal{NP}$. However, we show that the problem is polynomial-time approximable within a constant multiplicative factor.

Proposition 1 (Approximability)**.** *For any given fixed $\mathcal{L}$, the problem $1|mc = \mathcal{L}, mu|C_{max}$ is contained in $\mathcal{APX}$ complexity class.*

Proof. Suppose the algorithm *LCF (Least Criticality First)* that takes an input instance $I_{\mathcal{MC}}$ and schedules tasks in a non-decreasing sequence by their criticalities without waiting. Then the makespan of resulting schedule is

$$LCF(I_{\mathcal{MC}}) = \sum_{i|\mathcal{X}_i=1} p_i^{(1)} + \sum_{i|\mathcal{X}_i=2} p_i^{(2)} + \ldots + \sum_{i|\mathcal{X}_i=\mathcal{L}} p_i^{(\mathcal{L})}$$

A sum of processing times on a given criticality level over a set of tasks is a lower bound on the makespan.

Therefore we have

$$\max\{\sum_{i|\mathcal{X}_i\geq 1} p_i^{(1)}, \sum_{i|\mathcal{X}_i\geq 2} p_i^{(2)}, \ldots, \sum_{i|\mathcal{X}_i\geq \mathcal{L}} p_i^{(\mathcal{L})}\} \leq$$
$$\leq OPT(I_{\mathcal{MC}}) \leq LCF(I_{\mathcal{MC}}) \leq \mathcal{L}\cdot OPT(I_{\mathcal{MC}}).$$

where $OPT(I_{\mathcal{MC}})$ denotes the optimal makespan of $I_{\mathcal{MC}}$ problem instance. □

In fact, this result shows more than that there exists a polynomial-time algorithm producing schedules with a constant bounded quality. For example, for the problem with $\mathcal{L}=2$ criticality levels, actually any left-shifted schedule will be at most twice as worse as the optimal makespan since *LCF* actually produces the worst ordering of tasks in terms of the makespan.

In the following sections, we present exact algorithms for the problem with 2 and 3 criticality levels. Due to the $C_{\max}$ criterion, it can be shown that the search for an optimal solution can be reduced to finding a permutation of tasks. Therefore, any optimal schedule is given by a permutation of tasks π. Hence we denote the makespan of the left-shifted schedule of permutation π by $C_{\max}(\pi)$. In Sec. 6 we give a characterization of the set of optimal permutations for problem $1|mc=2,mu|C_{\max}$ and we introduce a MILP model utilizing it. In Sec. 7, we introduce an operator acting on F-shapes, and we show how the optimal solutions for problems with two and three criticality levels are related.

6 TWO CRITICALITY LEVELS

We showed that optimal solutions to $1|mc=\mathcal{L},mu|C_{\max}$ are given by a permutation π of tasks. For the problem with two criticality levels, the optimal permutations can be characterized more precisely. Let us refer to tasks with criticality $\mathcal{X}_i=2$ as HI-tasks and tasks with criticality $\mathcal{X}_j=1$ as LO-tasks. The key structure of the optimal permutations are *covering blocks*:

Definition 3 (Covering Block)**.** *For any given feasible schedule $(s_1,\ldots,s_n)$, a* HI*-task T_i and a* LO*-task T_j we say that T_j is covered by T_i, denoted as $T_i \in cov(T_j)$, if and only if $s_i+p_i^{(1)} \leq s_j < s_i+p_i^{(2)}$. The covering block B_i is then the* HI*-task T_i and the set of all* LO*-tasks covered by T_i.*

See an example in Fig. 1. There T_1 is covering T_2 and T_3. All these tasks form a covering block. Although the definition of covering block given above is meant for the problem with two criticality levels, the notion of *covering* can be generalized for more criticality levels. We assign a *length* to each covering block. The length is given as the maximum between the processing time $p_i^{(2)}$ of the HI-task T_i and the sum of processing times of tasks covered by T_i plus the processing time of T_i at the first level $p_i^{(1)}$.

Proposition 2 (Covering Block Length)**.** *Given the covering block B_i, its length defined as*

$$\max\{p_i^{(1)} + \sum_{T_j|\,T_i\in cov(T_j)} p_j^{(1)}, \quad p_i^{(2)}\}$$

is invariant with respect to the ordering of LO*-tasks T_j for which $T_i \in cov(T_j)$.*

Clearly, the ordering of LO-tasks T_j for which $T_i \in \mathrm{cov}(T_j)$ does not affect the block length since all LO-tasks are running without waiting. Furthermore, we say that task T_j is *fully covered* by the block B_i, if $B_i = p_i^{(2)}$ and $T_i \in \mathrm{cov}(T_j)$. If exists a task covered by the block B_i that is not fully covered, then we say that B_i is *saturated*. The makespan $C_{\max}$ of the schedule is given by a permutation of covering blocks. However, actually any permutation of covering blocks contributes to the makespan by the same amount; hence it is not subject to optimization.

Proposition 3 (Interchangebility)**.** *For every instance of the problem $1|mc=2,mu|C_{max}$ there exists an optimal solution that is given by an arbitrary permutation of covering blocks.*

A characterization of optimal solutions for $1|mc=2,mu|C_{\max}$ directly follows from Proposition 2 and 3:

Corollary 1. *The optimal solution for $1|mc=2,mu|C_{max}$ is given by an assignment of* LO*-tasks to* HI*-tasks.*

6.1 Covering MILP Model for $1|mc=2,mu|C_{\max}$

The following MILP model relies on Corollary 1. The model assigns LO-tasks to the HI-tasks in order to form covering blocks such that the sum of their lengths is the minimum. The decision variable x_{ij} indicates whether the LO-task T_j is covered by the HI-task T_i; therefore if $T_i \in \mathrm{cov}(T_j)$, then $x_{ij}=1$. The makespan is then given by the sum of lengths of covering blocks and the sum of processing times of all LO-tasks that are not covered.

$$\min \sum_{i|\mathcal{X}_i=2} B_i + \sum_{j|\mathcal{X}_j=1} p_j^{(1)}(1-\sum_{i|\mathcal{X}_i=2} x_{ij}) \quad (6.1)$$

s.t.

$$B_i \geq p_i^{(1)} + \sum_{j|\mathcal{X}_j=1} p_j^{(1)} x_{ij} \; \forall i \in I_{\mathcal{MC}}|_{\mathcal{X}_i=2} \quad (6.2)$$

$$B_i \geq p_i^{(2)} \quad \forall i \in I_{\mathcal{MC}}|_{\mathcal{X}_i=2} \quad (6.3)$$

$$\sum_{i|\mathcal{X}_i=2} x_{ij} \leq 1 \quad \forall j \in I_{\mathcal{MC}}|_{\mathcal{X}_j=1} \tag{6.4}$$

where

$$B_i \in \mathbb{Z}_0^+ \quad \forall i \in I_{\mathcal{MC}}|_{\mathcal{X}_i=2}$$
$$x_{ij} \in \{0,1\} \quad \forall i \in I_{\mathcal{MC}}|_{\mathcal{X}_i=2}, \forall j \in I_{\mathcal{MC}}|_{\mathcal{X}_j=1}$$

The main advantage of this model over the model proposed by (Hanzalek et al., 2016) is that it has much stronger linear relaxation. Further in Sec. 8 we demonstrate its ability to solve an order of magnitude larger instances.

7 THREE CRITICALITY LEVELS

Although two criticality levels are often sufficient for safety-critical application and this case is frequently studied in the field of mixed-critical systems (Burns and Davis, 2013), sometimes the application naturally contains three or more criticality levels. We capture the direct relation between problems with different maximum criticality levels by introducing a transformation given bellow. It is based on the observation that omitting some criticality levels provides an instance of the problem with less criticality level while maintaining a lower bound property. Furthermore, we introduce the *Bottom-up* algorithm that uses this observation. The algorithm is used then together with Covering MILP model for three criticality levels ($\mathcal{L}=3$) shown in Sec. 7.2 to form an efficient solution method.

The transformation is defined as $h^{\pm}$ restrictions:

Definition 4 ($h^{\pm}$ restrictions)**.** *Given the mixed-criticality instance $I_{\mathcal{MC}}$ and a positive integer $h \in \mathbb{N}$, let $I_{\mathcal{MC}}^{h^-}$ and $I_{\mathcal{MC}}^{h^+}$ be sets defined as*

$$I_{\mathcal{MC}}^{h^-} = \{(\min\{h,\mathcal{X}_i\}, (p_i^{(1)},\ldots,p_i^{(\min\{h,\mathcal{X}_i\})})) \mid \forall i \in I_{\mathcal{MC}}\}$$
$$I_{\mathcal{MC}}^{h^+} = \{(\mathcal{X}_i - h + 1, (p_i^{(h)},\ldots,p_i^{(\mathcal{X}_i)})) \mid \forall i \in I_{\mathcal{MC}} : \mathcal{X}_i \geq h\}$$

We refer to $I_{\mathcal{MC}}^{h^-}$ ($I_{\mathcal{MC}}^{h^+}$) as h^- (h^+) restriction of the instance $I_{\mathcal{MC}}$.

The h^- restriction takes an F-shape and cuts off all criticality levels above level h. Similarly, given the set of F-shaped tasks, h^+ restriction drops all tasks with criticality below h, and for the rest, it cuts off criticality levels less than h. Restricting an $I_{\mathcal{MC}}$ instance yields to a mixed-criticality instance since omitting some of the criticality levels for an F-shape gives us an F-shape. The application of the restriction can be viewed as a relaxation the problem.

Proposition 4 (Two Lower Bounds on the Makespan)**.** *For the problem $1|mc=3,mu|C_{max}$ expressions lb^-, lb^+ defined as*

$$lb^{\pm} = \min_{\pi \in \Pi(I_{\mathcal{MC}}^{2^{\pm}})} C_{max}(\pi)$$

are lower bounds on the makespan, where $\Pi(I_{\mathcal{MC}}^{2^+})$ and $\Pi(I_{\mathcal{MC}}^{2^-})$ denote the set of all permutations of elements $I_{\mathcal{MC}}^{2^+}$, $I_{\mathcal{MC}}^{2^-}$ respectively.

Proof. The lb^- is a lower bound on the makespan of $1|mc=3,mu|C_{\max}$ since it relaxes on the overlapping condition at the third criticality level. Similarly, lb^+ is a lower bound on the makespan since it relaxes on the overlapping condition at the first criticality level. □

7.1 Bottom-up Algorithm

We introduce a heuristic algorithm for the problem $1|mc=3,mu|C_{\max}$. Let us refer to tasks with $\mathcal{X}_i=3$ (i.e. criticality 3) as to GREAT-tasks. The *Bottom-up* algorithm is based on the idea of constructing the schedule in two stages. In the first stage, the relaxed problem is solved up to the optimality, which minimizes a lower bound on the optimal makespan of the original problem. The second stage takes the relaxed solution and constructs a locally optimal solution for the original problem.

The first stage of the algorithm solves 2^- restriction of the given problem instance; hence it is an instance of $1|mc=2,mu|C_{\max}$ problem that can be solved with the model described in Section 6. It assigns LO-tasks to HI-tasks and GREAT-tasks; therefore it forms covering blocks. In the second stage, the algorithm defines a new problem instance $I'_{\mathcal{MC}}$ of the problem $1|mc=2,mu|C_{\max}$. The instance is constructed as follows. It contains LO-tasks with processing time equal to the length of covering blocks from the stage one. LO-tasks that are not part of any covering block are assigned to an arbitrary covering block. The assignment of LO-tasks to 2^- restricted GREAT-tasks from the first stage defines HI-tasks in the new instance $I'_{\mathcal{MC}}$. Then, the $I'_{\mathcal{MC}}$ instance is solved once again as an instance of $1|mc=2,mu|C_{\max}$ problem. See the complete description of the *Bottom-up* algorithm in Alg. 1.

In general, the *Bottom-up* algorithm produces suboptimal solutions even though they are provably bounded by a factor of 3 from the optimal solution, as stated by Proposition 1. However, there are cases when we can verify if the produced schedule is optimal. This is achieved by the concept of *critical paths* that captures the cause of achieved makespan.

Algorithm 1: Bottom-up.

1: $\pi \leftarrow$ solve $I^{2^-}_{\mathcal{MC}}$ restriction by Covering MILP 6.1
2: $I'_{\mathcal{MC}} \leftarrow \emptyset$
3: **for each** covering block B_i in the left-shifted solution π **do**
4: **if** $\chi_i = 2$ in $I_{\mathcal{MC}}$ **then**
5: $\mathbf{P}_i \leftarrow (B_i)$
6: $I'_{\mathcal{MC}} \leftarrow I'_{\mathcal{MC}} \cup \{(1, \mathbf{P}_i)\}$
7: **else if** $B_i < p_i^{(3)}$ **then**
8: $\mathbf{P}_i \leftarrow (B_i, p_i^{(3)})$
9: $I'_{\mathcal{MC}} \leftarrow I'_{\mathcal{MC}} \cup \{(2, \mathbf{P}_i)\}$
10: **else**
11: ▷ block B_i is *saturated*, it contributes by a constant term to the makespan of $I'_{\mathcal{MC}}$
12: **end if**
13: **end for**
14: $\pi \leftarrow$ solve $I'_{\mathcal{MC}}$ by Covering MILP 6.1

Definition 5 (Critical Path)**.** *Given the left-shifted schedule $(s_1, \ldots, s_n)$ of the permutation π, the critical path is $\mathcal{CP} \subseteq \{1, \ldots, |\tilde{\pi}|\} \times \{1, \ldots, \mathcal{L}\}$ for some $\tilde{\pi} \subseteq \pi$ such that $\forall (i,\ell) \in \mathcal{CP}, i < |\tilde{\pi}| : s_{\tilde{\pi}(i)} + p^{(\ell)}_{\tilde{\pi}(i)} = s_{\tilde{\pi}(i+1)}$ where $\sum_{(i,\ell)\in\mathcal{CP}} p^{(\ell)}_{\tilde{\pi}(i)} = C_{max}(\pi) = C_{max}(\tilde{\pi})$.*

Essentially, for any given left-shifted schedule, the critical path is a subset of tasks and their criticality levels such that $\forall (i,\ell) \in \mathcal{CP}$ holds that if the processing time $p^{(\ell)}_{\tilde{\pi}(i)}$ is increased by some $\varepsilon > 0$, then the makespan of the same schedule is also increased by ε.

Proposition 5 (Sufficient Optimality Conditions)**.** *If one of following conditions holds, then the schedule produced by the Bottom-up algorithm is optimal for problem $1|mc = 3, mu|C_{max}$.*

1. *There exists a critical path going through the first and the second levels only.*
2. *Every* LO*-task is fully covered by the second criticality level.*

When none of the optimality conditions is satisfied, e.g. a critical path is coming through every criticality level, we get back to the MILP model 7.2 for the problem $1|mc = 3, mu|C_{\max}$ in order to find an optimal solution or for the proof that the current solution is the optimal one. The solver is supplied with the initial solution and a lower bound obtained by the *Bottom-up* algorithm. The computational time of *Bottom-up* algorithm is dominated by lines 1 and 14. The total computational times are reported in Tab. 2.

7.2 Covering MILP Model for $1|mc = 3, mu|C_{\max}$

The Covering MILP model for three criticality levels uses a similar idea as the model for $1|mc = 2, mu|C_{\max}$. It assigns LO-tasks to covering blocks and covering blocks to the GREAT-tasks. The model utilizes the idea that optimal solutions are made of blocks (in this case formed by GREAT-tasks that cover less critical tasks) whose order is interchangeable within a solution. It assigns LO-tasks to the HI-tasks and to 2^- restriction of GREAT-tasks to form covering blocks. Blocks are assigned to the GREAT-tasks in order to create a solution. The big M constant is as large as the number of LO-tasks contained in the problem instance.

$$\min \sum_{i|\chi_i=3} p_i + \sum_{j|\chi_j=2} P_{j,\emptyset} + \sum_{k|\chi_k=1} p_k^{(1)} x_{\emptyset,\emptyset,k} \tag{7.1}$$

s.t.

$$p_i \geq p_i^{(3)} \quad \forall i \in I_{\mathcal{MC}}|_{\chi_i=3} \tag{7.2}$$

$$My_{i,j} \geq \sum_{k|\chi_k=1} x_{i,j,k}$$
$$\forall i \in I_{\mathcal{MC}}|_{\chi_i=3} \cup \emptyset, \forall j \in I_{\mathcal{MC}}|_{\chi_j=2} \tag{7.3}$$

$$P_{j,i} \geq p_j^{(2)} y_{i,j}$$
$$\forall i \in I_{\mathcal{MC}}|_{\chi_i=3} \cup \emptyset, \forall j \in I_{\mathcal{MC}}|_{\chi_j=2} \tag{7.4}$$

$$P_{j,i} \geq p_j^{(1)} y_{i,j} + \sum_{k|\chi_k=1} p_k^{(1)} x_{i,j,k}$$
$$\forall i \in I_{\mathcal{MC}}|_{\chi_i=3} \cup \emptyset, \forall j \in I_{\mathcal{MC}}|_{\chi_j=2} \tag{7.5}$$

$$p_i \geq p_i^{(2)} + \sum_{j|\chi_j=2} P_{j,i} \quad \forall i \in I_{\mathcal{MC}}|_{\chi_i=3} \tag{7.6}$$

$$p_i \geq p_i^{(1)} + \sum_{j|\chi_j=2} P_{j,i} + \sum_{k|\chi_k=1} p_k^{(1)} x_{i,\emptyset,k}$$
$$\forall i \in I_{\mathcal{MC}}|_{\chi_i=3} \tag{7.7}$$
$$\sum_{i|\chi_i=3\cup\emptyset} \sum_{j|\chi_j=2\cup\emptyset} x_{i,j,k} \geq 1$$

$$\forall k \in I_{\mathcal{MC}}|_{\chi_k=1} \tag{7.8}$$

$$\sum_{i|\chi_i=3\cup\emptyset} y_{i,j} \geq 1 \quad \forall j \in I_{\mathcal{MC}}|_{\chi_j=2} \tag{7.9}$$

where

$$y_{i,j} \in \{0,1\} \forall i \in I_{\mathcal{MC}}|_{\chi_i=3} \cup \emptyset, \forall j \in I_{\mathcal{MC}}|_{\chi_j=2}$$
$$x_{i,j,k} \in \{0,1\}$$
$$\forall i \in I_{\mathcal{MC}}|_{\chi_i=3} \cup \emptyset, \forall j \in I_{\mathcal{MC}}|_{\chi_j=2} \cup \emptyset,$$
$$\forall k \in I_{\mathcal{MC}}|_{\chi_k=1} \cup \emptyset : k \neq \emptyset \vee (i = \emptyset \wedge j = \emptyset)$$
$$p_i \in \mathbb{Z}_0^+ \quad \forall i \in I_{\mathcal{MC}}|_{\chi_i=3}$$
$$P_{j,i} \in \mathbb{Z}_0^+ \quad \forall i \in I_{\mathcal{MC}}|_{\chi_i=3} \cup \emptyset, \forall j \in I_{\mathcal{MC}}|_{\chi_j=2}$$

When *Bottom-up* fails to prove optimality, it goes back to this model while supplying the lb^- lower bound and the initial solution. The reason for executing *Bottom-up* ahead solving MILP model 7.2 is two-fold. First, we have observed the solver struggles to prove optimality when the solution is clearly optimal regarding the critical path. The other observation is that if the problem instance contains the majority of tasks with criticality one and two, then solving its 2^- restriction frequently yields optimal solution since the highest criticality levels are not likely to be utilized. The same holds for the instances with a large number of tasks with higher criticality. Furthermore, solving $2^{\pm}$ restrictions of $I_{\mathcal{MC}}$ is cheap compared to the solving the whole MILP model 7.2 as it can be seen in Tab. 1.

8 COMPUTATIONAL EXPERIMENTS

For the problem $1|mc=2,mu|C_{\max}$ we have randomly generated sets of 20 instances with n tasks for each $n \in \{10,\ldots,200\}$. Criticalities of tasks were distributed uniformly. The processing time of a task at level 1 is sampled from the uniform distribution $\mathcal{U}(1,11)$. For tasks with the criticality of 2, the prolongation at level 2 is sampled from uniform distribution $\mathcal{U}(1,10)$.

For the problem $1|mc=3,mu|C_{\max}$ we have randomly generated sets of 20 instances with n tasks for each $n \in \{10,\ldots,80\}$. For each n, the set contains instances with different splits of tasks' criticalities and different distributions for prolongation (e.g. $\mathcal{U}(1,10)$ and $\mathcal{U}(1,7)$ for the second level, $\mathcal{U}(1,10)$ and $\mathcal{U}(1,14)$ for the third level, etc.) in order to generate instances of various properties. We have investigated the impact of different processing time distributions to the overall performance. We have observed that the the proposed approach is not sensitive to the choice of particular distributions, but rather to the difference between combined processing times allocated to each criticality level. Therefore, in our experiments, we have used uniform distributions with parameters that represent challenging instances.

The column *avg t* (*max t*) in Tab. 1 and 2 denotes the average (maximal) computational time for instances that were solved within the time limit of 300 s. The column *unsl* contains the percentage of instances that were not solved within the time limit and *avg gap* denotes average optimality gap proven by the solver for the unsolved instances. Results were obtained with two Intel Xeon E5-2620 v2 @ 2.10 GHz processors using Gurobi Optimizer 6.5 with the algorithms implemented in Python 3.4.

In Tab. 1 it can be seen that our model is able to solve about an order of the magnitude larger problem instances. The *Relative Order* model proposed by (Hanzalek et al., 2016) consistently fails to narrow optimality gap for instances with more than 40 tasks. In Tab. 2 it is shown that the combination of *Bottom-up* heuristic and MILP 7.2 is able to solve reliably instances with 60 tasks up to the optimality and almost all instances with 80 tasks. Moreover, the proven gap is much smaller than for the *Relative Order* model; therefore it shows that our model has stronger linear relaxation.

To put our algorithms into the another test, we tested them on data obtained from our automotive industrial partner. The data comes from a real-life automotive system consisting of a communication messages between 23 ECUs. From this instance, we constructed a probabilistic model that corresponds to the given instance. We are interested in scheduling messages inside the basic period (10 ms); therefore those are messages occurring in every communication cycle. The aim is to minimize $C_{\max}$ to maximize remaining space for other messages with larger periods.

The instance divides messages into three categories. The lowest critical are debug and development messages which do not use any form of a checksum. More critical messages are secured by a parity check. The most critical messages are secured by CRC8 code. The message criticalities are distributed according $\Pr[\mathcal{X}_i = 1] = 0.48$, $\Pr[\mathcal{X}_i = 2] = 0.48$, $\Pr[\mathcal{X}_i = 3] = 0.04$. The length of each message is drawn from distribution $\mathcal{U}(8,12)$. The prolongation on the second and the third criticality level is sampled from $\mathcal{U}(8,16)$ to model the message retransmission and an extra overhead.

The real-life industrial dataset was created by generating 20 instances of the problem $1|mc=3,mu|C_{\max}$ according to distributions mentioned above for each of $n \in \{50,100,150,200\}$, where n is the number of messages. The results are reported in Tab. 3. The computational times were obtained under the same circumstances as described above.

The results for real-life industrial data are quantitatively better compared to those obtained in Tab. 2. The reason is likely that the data contain relatively a few GREAT-tasks and the range of lengths of LO-tasks is relatively narrow. Therefore, many of them are identical, and the solver might be able to exploit this symmetry even though it was not supplied to it. With the Covering MILP model, the solver scales well even for larger instances.

Table 1: Computational results for the problem $1|mc = 2, mu|C_{\max}$.

	Covering MILP 6.1				Relative Order MILP (Hanzalek et al., 2016)			
n tasks	avg t $[s]$	max t $[s]$	unsl $[\%]$	avg gap $[\%]$	avg t $[s]$	max t $[s]$	unsl $[\%]$	avg gap $[\%]$
10	> 0.01	0.03	0	—	13.07 ($\pm$44.93)	200.22	0	—
15	> 0.01	0.03	0	—	49.67 ($\pm$49.38)	127.09	60	27.32 ($\pm$12.54)
20	0.01 ($\pm$0.01)	0.03	0	—	—	—	100	40.09 ($\pm$15.27)
40	0.09 ($\pm$0.17)	0.81	0	—	—	—	100	77.66 ($\pm$6.23)
60	1.37 ($\pm$4.33)	19.71	0	—	—	—	100	84.23 ($\pm$2.90)
80	0.38 ($\pm$0.45)	1.94	0	—	—	—	100	90.72 ($\pm$1.77)
100	1.28 ($\pm$1.38)	5.05	0	—	—	—	100	93.38 ($\pm$0.76)
150	11.77 ($\pm$24.29)	93.01	0	—	—	—	100	96.02 ($\pm$0.24)
200	22.69 ($\pm$61.24)	281.04	0	—	—	—	100	97.33 ($\pm$0.13)

Table 2: Computational results for the problem $1|mc = 3, mu|C_{\max}$.

	Bottom-up w/ Covering MILP 7.2				Relative Order MILP (Hanzalek et al., 2016)			
n tasks	avg t $[s]$	max t $[s]$	unsl $[\%]$	avg gap $[\%]$	avg t $[s]$	max t $[s]$	unsl $[\%]$	avg gap $[\%]$
10	0.02 ($\pm$0.01)	0.04	0	—	0.09 ($\pm$0.07)	0.28	0	—
20	0.16 ($\pm$0.36)	1.66	0	—	—	—	100	28.71 ($\pm$16.62)
30	0.17 ($\pm$0.17)	0.66	0	—	—	—	100	63.28 ($\pm$7.35)
40	0.69 ($\pm$1.02)	3.61	0	—	—	—	100	72.85 ($\pm$6.14)
50	2.40 ($\pm$7.42)	33.56	0	—	—	—	100	80.61 ($\pm$2.96)
60	6.71 ($\pm$11.97)	44.67	0	—	—	—	100	84.30 ($\pm$2.70)
70	11.30 ($\pm$22.31)	79.38	10	0.38 ($\pm$0.19)	—	—	100	89.34 ($\pm$1.43)
80	37.92 ($\pm$68.82)	224.86	20	0.34 ($\pm$0.13)	—	—	100	91.09 ($\pm$1.40)

Table 3: Computational results for the real-life instances.

	Bottom-up w/ Covering MILP 7.2	
n tasks	avg t $[s]$	avg gap $[\%]$
50	0.08 ($\pm$0.14)	—
100	1.17 ($\pm$3.33)	—
150	3.67 ($\pm$7.23)	0.26 ($\pm$0.00)
200	5.34 ($\pm$15.51)	—

9 CONCLUSION

In this paper, we have proposed two exact approaches for the problem of non-preemptive mixed-criticality match-up scheduling for solving the problem of message retransmission in time-triggered communication protocols. We investigated the fundamental properties of F-shapes to obtain efficient models of the problem. Our algorithms outperform recently proposed approach by a large margin. Furthermore, we showed the membership of $1|mc = \mathcal{L}, mu|C_{\max}$ problem in $\mathcal{APX}$ complexity class for an arbitrary fixed $\mathcal{L}$.

ACKNOWLEDGEMENT

This work was supported by the Grant Agency of the Czech Republic under the Project GACR P103-16-23509S. Furthermore, this work was supported by the US Department of the Navy Grant N62909-15-1-N094 SALTT issued by Office Naval Research Global. The United States Government has a royalty-free license throughout the world in all copyrightable material contained herein.

REFERENCES

Baruah, S. and Fohler, G. (2011). Certification-cognizant time-triggered scheduling of mixed-criticality systems. In *Real-Time Systems Symposium (RTSS), 2011 IEEE 32nd*, pages 3–12. IEEE.

Baruah, S., Li, H., and Stougie, L. (2010). Towards the design of certifiable mixed-criticality systems. In *Real-Time and Embedded Technology and Applications Symposium (RTAS), 2010 16th IEEE*, pages 13–22. IEEE.

Bean, J. C., Birge, J. R., Mittenthal, J., and Noon, C. E. (1991). Matchup scheduling with multiple resources, release dates and disruptions. *Operations Research*, 39(3):470–483.

Bell, R. (2006). Introduction to iec 61508. In *Proceedings of the 10th Australian workshop on Safety critical systems and software-Volume 55*, pages 3–12. Australian Computer Society, Inc.

Bertsimas, D., Brown, D. B., and Caramanis, C. (2011). Theory and applications of robust optimization. *SIAM review*, 53(3):464–501.

Burns, A. and Davis, R. (2013). Mixed criticality systems-a review. *Department of Computer Science, University of York, Tech. Rep*.

Dvorak, J. and Hanzalek, Z. (2016). Using two independent channels with gateway for FlexRay static seg-

ment scheduling. *IEEE Transactions on Industrial Informatics*, article in press.

Hanzalek, Z., Tunys, T., and Sucha, P. (2016). Non-preemptive mixed-criticality match-up scheduling problem. *Journal of Scheduling, doi: 10.1007/s10951-016-0468-y*.

Kopetz, H., Ademaj, A., Grillinger, P., and Steinhammer, K. (2005). The time-triggered ethernet (TTE) design. In *Object-Oriented Real-Time Distributed Computing, 2005. ISORC 2005. Eighth IEEE International Symposium on*, pages 22–33. IEEE.

Qi, X., Bard, J. F., and Yu, G. (2006). Disruption management for machine scheduling: the case of spt schedules. *International Journal of Production Economics*, 103(1):166–184.

Sahinidis, N. V. (2004). Optimization under uncertainty: state-of-the-art and opportunities. *Computers & Chemical Engineering*, 28(6):971–983.

Shabtay, D., Gaspar, N., and Kaspi, M. (2013). A survey on offline scheduling with rejection. *Journal of scheduling*, 16(1):3–28.

Theis, J., Fohler, G., and Baruah, S. (2013). Schedule table generation for time-triggered mixed criticality systems. *Proc. WMC, RTSS*, pages 79–84.

Vestal, S. (2007). Preemptive scheduling of multi-criticality systems with varying degrees of execution time assurance. In *Real-Time Systems Symposium, 2007. RTSS 2007. 28th IEEE International*, pages 239–243. IEEE.

Supporting Efficient Global Moves on Sequences in Constraint-based Local Search Engines

Renaud De Landtsheer, Gustavo Ospina, Yoann Guyot, Fabian Germeau and Christophe Ponsard
CETIC Research Centre, Charleroi, Belgium
{*renaud.delandtsheer, gustavo.ospina, yoann.guyot, fabian.germeau, christophe.ponsard*}*@cetic.be*

Keywords: Sequence, Local Search, CBLS, Global Constraints, Global Moves, OscaR.cbls.

Abstract: Constraint-Based Local Search (CBLS) is an approach for quickly building local search solvers based on a declarative modelling framework for specifying input variables, constraints and objective function. An underlying engine can efficiently update the optimization model to reflect any change to the input variables, enabling fast exploration of neighbourhoods as performed by local search procedures. This approach suffers from a weakness when moves involve modifying the value of a large set of input variables in a structured fashion. In routing optimization, if one implements the optimization model by means of integer variables, a two-opt move that flip a portion of route requires modifying the value of many variables. The constraint on this problems are then notified about many updates, but they need to infer that these updates constitute a flip, and waste a lot of time. This paper presents this multi-variable limitation, discusses approaches to mitigate it, and proposes an efficient implementation of a variable type that represents sequences of integers to avoid it. The proposed implementation offers good complexities for updating and querying the value of sequences of integers and some mechanisms to enable the use of state-of-the art incremental global constraints.

1 INTRODUCTION

Constraint-Based Local Search (CBLS) is an approach for representing declarative optimization models for local search optimization where the optimization problem is represented by means of *variables* and *invariants* (Van Hentenryck and Michel, 2009). *Invariants* are directed constraints that have designated input and output variables and that maintain the value of these output variables according to their specification and to the value of the input variables. Decision variables are not the output of any such directed constraints. A local search procedure can explore neighbourhoods by modifying these decision variables and query the value of a variable that is maintained by the model and represents the objective function.

This is the approach implemented by the frameworks Comet, Kangaroo, OscaR.cbls, LocalSolver, and InCELL (Van Hentenryck and Michel, 2009; Newton et al., 2011; De Landtsheer and Ponsard, 2013; Benoist et al., 2011; Pralet and Verfaillie, 2013). In such frameworks, several variable types might be available, such as Boolean, Integer, Float, Set of Integer, and List of Integer. A key aspect that updating invariant should be as efficient as possible in order to provide fast neighbourhood exploration.

An important drawback of the CBLS approach is the potential loss of efficiency of the model compared to a dedicated model to evaluate structured moves involving several variables. We call it the *multi-variable limitation*. The multi-variable limitation occurs when a move requires modifying a large number of input variables altogether, and this move actually implements some structurally consistent modification of the model that could be captured in a more symbolic and global way with a $O(1)$ sized representation. Such more symbolic representation of the move would typically enable efficient global reasoning of the impact of that move onto the constraint of the problem.

For instance, a routing problem, such as a Travelling Salesman Problem (TSP) (Schrijver, 2005), can be represented by a series of integer variables, called "next", each of them being associated with a node of the routing problem, and specifying the node that must be reached when leaving the associated node. Evaluating a 2-opt move, that flips a section of a route, requires modifying each "next" variable associated with nodes included in the flipped section, thus requiring $O(n)$ updates (Croes, 1958). An invariant maintaining the routed distance from a distance matrix is then notified about the change of each modified

Landtsheer, R., Ospina, G., Guyot, Y., Germeau, F. and Ponsard, C.
Supporting Efficient Global Moves on Sequences in Constraint-based Local Search Engines.
In *Proceedings of the 6th International Conference on Operations Research and Enterprise Systems (ICORES 2017)*, pages 171-180
ISBN: 978-989-758-218-9

variable and is therefore updated in $O(n)$ time, simply because it is notified about $O(n)$ updates. The cost of evaluating such move is therefore $O(n)$ time, because of the $O(n)$ updated variables, and the $O(n)$ notifications sent to the listening invariant. A routing optimization engine implemented with a dedicated algorithm could easily reason on the logical meaning of a 2-opt and evaluate the same neighbour in $O(1)$ time, especially if the distance matrix is symmetric (Glover and Kochenberger, 2003).

There are several ways to mitigate the multi-variable limitation, namely, change the order of exploration, transmit more symbolic information beside variables, use symbolic differentiation, or add more structured variable types. Let us review them in order to motivate our approach.

Choosing the Order of Exploration of the Neighbourhood (Glover and Kochenberger, 2003). In the case of the aforementioned 2-opt move, one can gradually widen the flipped route segment, so that each neighbour can be explored in turn, and going from one neighbour to another one requires moving two points. We call this exploration mode the *circle mode*, as opposed to the *star mode*. In star mode, the state of the model is rolled back to the initial state between each explored neighbour. Circle mode exploration is however hard to combine with heuristics such as selecting nodes among the k-nearest ones in vehicle routing, that allows one to suggest a few relevant neighbours among e.g. a 2-opt and explore these moves exclusively.

Transmitting additional symbolic information through the model, e.g. by proposing the notion of "aggregate of variables" such as "array of integer variables" and *transmit the symbolic nature of the move* to the invariants listening to the aggregate, so that they can update their output value efficiently using global algorithms. This approach would not fully solve the issue because the $O(n)$ variables involved in the move would be updated anyway since they exist, and their value might be queried by the invariants listening to the aggregate.

Performing symbolic differentiation of the model to automatically use the best algorithm for evaluating neighbours. This option is complex because it requires reasoning on the structure and global semantic of the model. It also requires to deploy additional reasoning tool, e.g. SMT-solvers like Z3 (De Moura and Bjørner, 2008).

Introducing structured variable types, so that complex moves are performed on the value of the variable and can be described in a more symbolic way as a delta on this value. Those moves can be implemented efficiently and then used as powerful primitives for writing efficient global algorithms.

This paper focuses on this last approach and proposes an implementation of a variable type representing sequences of integers, suitable for a CBLS solver. The goal is to achieve similar algorithmic complexity to the one achievable by a dedicated implementation, while still providing a high degree of declarativity as proposed by the CBLS approach.

We focus on this type of variable for two reasons. First, sequence of integers could be deployed to represent various optimization problems that have a notion of sequencing including car sequencing, routing, flow-shop scheduling, etc. Routing optimization is an area where local search is widely used; it can benefit from our sequence variable. Second, string solving is an active topic of research (Abdulla et al., 2015; Fu et al., 2013; Ganesh et al., 2011; Scott et al., 2015). Providing a variable of type "sequence of integers" supporting efficient global updates within a generic local search engine can constitute an opportunity to make the development inherent to such research easier (Björdal, 2016).

This paper is focusing a lot on the efficiency of the underlying data-structures for representing sequences of integers. It often uses the complexity notation $O(...)$. It implicitly refers to the time complexity, unless otherwise specified.

The paper is structured as follows: Section 2 presents various frameworks for implementing local search and the way they support global constraints on sequences, it also introduces the OscaR.cbls engine with more details; Section 3 presents the requirements over an implementation of such sequence variable in a CBLS framework; Section 4 discusses the data-structure and the API of our implementation and concludes with complexity; Section 5 validates our approach by presenting how global constraints can easily be implemented based on our API (Application Programming Interface); Section 6 presents some benchmarks of our implementation; Finally, Section 7 concludes.

2 BACKGROUND

This section first presents several CBLS frameworks, and then introduces the necessary vocabulary of CBLS for the remaining of the paper, based on the OscaR.cbls engine.

2.1 Local Search Frameworks

Local search frameworks aim at making the development of local search solutions much simpler. To

this end, they provide different degrees of support for the modelling of the problem or the elaboration of the search procedure.

EasyLocal++ is a framework that requires a dedicated model to be developed from scratch using adhoc algorithms. It mainly provides support for declaring the search procedure (Di Gaspero and Schaerf, 2003). As such, it does not suffer from the multi-variable limitation, but it does not provide as much assistance in the development of a model as a CBLS framework would. Notably it does not allow the developer to package efficient global constraints that can be instantiated on demand.

There are a few tools supporting constraint-based local search, namely: Comet (Van Hentenryck and Michel, 2009), Kangaroo (Newton et al., 2011), OscaR.cbls (OscaR Team, 2012), LocalSolver (Benoist et al., 2011), and InCELL (Pralet and Verfaillie, 2013).

Comet, Kangaroo, and OscaR.cbls support Integers and Sets of Integers. InCELL supports a notion of variable that is a sequence of other variables. However, it does not offer a unified data structure for reasoning on the sequence itself, and no information is available about the added value of such sequence of variables (Pralet and Verfaillie, 2013). LocalSolver supports a variable of type list of integers, where each value can occur at most once (Benoist et al., 2011). No detail is given about how these lists of integers are actually implemented and it supports very few invariants and constraints related to this list variable.

Beside CBLS tools, there are many global constraint algorithms that have been developed, notably for routing optimization. The most classical example is the route distance invariants that computes the distance driven by a vehicle, given its route, and that quickly updates this distance when a routing move is performed such as a 2-opt or a 3-opt (Glover and Kochenberger, 2003). Another example is the travelling delivery man problem described in (Mladenović et al., 2013) that relies on pre-computation to update a complex metrics in $O(1)$ for a large proportion of classical routing moves. Such global constraints only require a high-level description of the move to perform their update efficiently. Implementing such algorithm therefore requires something in the vein of our proposed sequence variable. Our contribution is to propose such implementation within a generic framework, under the form of a dedicated variable with the appropriate underlying data structure, so that these global constraints can be implemented easily, and instantiated in a flexible way as done with other constraints in a CBLS engine.

2.2 CBLS, the OscaR Way

Since this contribution has been done in the context of the OscaR.cbls tool, we further introduce the basic concepts of CBLS using the vocabulary of OscaR.cbls. As usual in local search, solving a problem involves specifying a *model* and a *search procedure*.

The *model* is composed of *incremental variables* (integers and set of integers at this point), and *invariants* which are incremental directed constraints maintaining one or more output variables according to the atomic expressions they implement (e.g. Sum: the sum of inputs). *Constraints* are special invariants that maintain their violation as an output variable. They are Lagrangian relaxations of their specification. Beside they also maintain some information about which variable cause the violation.

The *search procedure* is expressed using *neighbourhoods*, which can be queried for a move, given the current state of the model, an acceptance criterion, and an objective function. *Combinators* are a set of operators on neighbourhoods that combine them and incorporate various metaheuristics, so that a complex search strategy is represented by a composite neighbourhood totally expressed in a declarative way (De Landtsheer et al., 2015). A library of combinators is available for specifying standard metaheuristics (e.g. simulated annealing, restart, hill climbing), for managing solution (e.g. when to save the current state, or restore a saved state), and for expressing stop criteria.

In order to set up the floor for the introduction of the new sequence variable, we give details on how the model is represented and it is updated during the search.

The *data structure* behind a model is a graph, called the *propagation graph*, which we can approximate to a directed acyclic graph, where the nodes are *variables* and *invariants*. Variables have an associated type and implement specific algorithms related to their type. Invariants have specific definitions, and implement this definition mostly through incremental algorithms. Edges in the graph represent data flows from variables to listening invariants and from invariants to controlled variables. The directed acyclic graph starts with input (a.k.a. decision) variables, and typically ends at a variable whose value is maintained to be the one of the objective function. Figure 1 illustrates a propagation graph for a simple warehouse location problem.

In such engine, *propagation* is about propagating updates along the propagation graph in such a way that a node is reached at most once by the update wave, and only if one of its inputs has changed and

if needed by the model update. OscaR.cbls manages this wave by sorting the nodes based on the distance from the decision variables. The propagation is coordinated through a dedicated heap that aggregates nodes at the same distance in a list. This offers a slightly better time complexity than the classical approach based on topological sort initially presented in (Van Hentenryck and Michel, 2009).

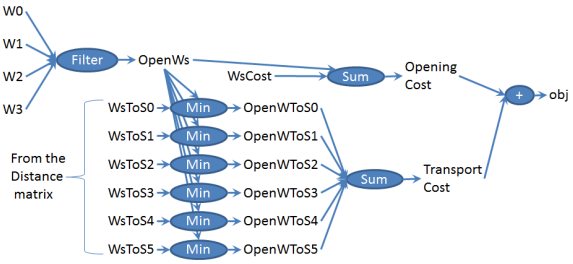

Figure 1: Propagation graph on a warehouse location problem.

The search for a solution starts from an initial solution and explores the specified neighbourhood. Each neighbour solution is examined by modifying the input variables, and querying the objective function of the model which is updated through propagation.

During propagation, variables *notify* each invariant listening to them about their value change. Such notifications carry the necessary information about the value change of the variable. For integer variables, it carries a reference to the variable, and the old and new value of the variable. For set variables, it carries a reference to the variable, the old value of the variable, the new value of the variable, and both the set of values that have been added and removed from the variable. All values transmitted by variables, through notification or through queries to the variables are immutable, to make the implement of algorithms in invariants easier.

3 REQUIREMENTS OVER A SEQUENCE VARIABLE

Our contributed sequence variable implements the following set of requirements, which have been identified from the way such variables are to be used in a CBLS engine, and from opportunities that they could open up, notably for supporting efficient global constraints:

- **speed-exploration** Sequence variables value should be updated very quickly in the context of neighbourhood exploration to reflect moves that are typically explored in routing, such as insert value, remove value, 1-opt, 2-opt, 3-opt.
- **symbolic-large-delta** Sequence variables should transmit the symbolic structure of such move that involve large modification of their value, so that invariants that derive values out of sequences of integer receive the high-level information of the delta that the variable has encountered.
- **pre-computation** There should be some kind of mechanism for invariants to know when they can perform pre-computation on the current value of a sequence variable, so that they can exploit such pre-computation in order to quickly update the neighbour values during neighbourhood exploration.
- **speed-move-taken** Sequence variables should be updated quickly to reflect move that are being taken, considering the same moves as the requirement speed-exploration. This requirement has a lower priority than speed-exploration since there are more neighbours explored than moves taken.
- **immutable-value** The value representing a sequence of integers should be non-mutable, that is: once transmitted to an invariant or saved, it should not be modified. A variable can of course change its value. This requirement is relevant because sequences are represented by complex and non-atomic data structures.

From the set of neighbourhoods mentioned in the speed-exploration and speed-move-taken requirements, we identify the following basic updates that our implementation must support:

- **insert** an integer value at a given position, and shift the tail of the sequence by one position upwards. The parameters of this update are: the position of the insert, and the inserted value.
- **delete** the integer value at a given position, and shift the tail of the sequence by one position downwards. This update has one parameter that is the position of the deleted integer.
- **seq-move** that moves a sub-sequence to another position, and optionally, flip it during the move. This update has four parameters: the start position of the moved segment, the end position of the moved segment, the position after which the segment must be moved to, and a Boolean specifying if the subsequence is flipped during the move.

These updates can be composed together to constitute a composite update, such as a two point move in Pick-up and Delivery Problems (PDP) (Savelsbergh and Sol, 1995), or a value assign in string optimization that is a composition of delete and insert.

4 IMPLEMENTATION

This section presents our implementation of a sequence of integers. It starts by a description of our dedicated data structures for representing immutable sequence values. Then, we introduce how sequence variables interact with sequence values, as well as our check-pointing mechanisms. We wrap up with a table presenting the complexity of all the queries and update operations of our sequence variable.

4.1 Sequences as Mappings

Sequences can be represented using several data structures. Typically, they can be represented using lists, arrays or mappings from positions to values. All these data-structures can be mutable or non-mutable. Mutable data structures are forbidden altogether in our approach because of the immutable-value requirement. Non-mutable lists and array have $O(n)$ complexity for insert, delete and seq-move operations. Besides, lists do not enable accessing their elements by positions efficiently.

Our approach is to represent sequences of integers as a continuous mapping from positions to values, where positions are integer values ranging from zero to the length of the sequence minus one.

Exploring such relations for consecutive values is therefore costly because they are typically implemented through $O(\log(n))$ balanced trees data structures. Our implementation provides a standard mechanism for speeding up sequence explorations. An *explorer* is a temporary non-mutable object representing a certain position in a given sequence. It can be queried for the position in the sequence and the value at its position. Besides, an explorer can be queried for the explorer at the next or at the previous position in the sequence. For instance, an explorer on a red-black tree supports the *value* and *position* queries in $O(1)$ and the *next* and *prev* operation in $O(1)$, amortized.

4.2 Stacked and Concrete Updates

Thanks to the representation as a map, we can implement the *speed-exploration* requirement through stacked updates: when a move is explored, a dedicated non-mutable class is created that offers the same API as a sequence, and behaves according to the value it represents by translating and forwarding queries it receives to the original non-modified sequence. Such dedicated non-mutable class representing modified sequences can be instantiated in $O(1)$ and are called *stacked updates* because they constitute a stack of updates, starting at the *concrete sequence*. For each of the three update classes (insert, remove, seq-move), a dedicated class implementing a sequence modified according to this move class can be implemented.

For instance, considering the *remove* operation, the query that gets the value at a given position is implemented as follows:

```
class RemovedPointSequence(
        originalSequence:IntSequence,
        positionOfRemove:Int)
  extends IntSequence {

 def getValueAtPosition(pos:Int) =
  originalSequence.getValueAtPosition(
     if (pos < positionOfRemove) pos
     else pos+1)
}
```

Each forwarding performed by the stacked updates adds up to the complexity of such queries, generally a $O(1)$ term, which can have a more-less important constant weight. Stacked updates are designed for neighbourhood exploration, provided the exploration is performed in a star mode, and provided each move is performed on the initial value of the sequence. They are however not adapted to exploration performed in circle mode, nor to committing moves when they are actually taken, because they would accumulate and the overhead would make them impractical. Such updates are therefore performed on the concrete representation of sequences.

The concrete representation of a sequence represents the map from positions to values through a double mapping that maps positions to an internal position and then maps the internal position to the actual value.

The first mapping is a piecewise affine bijection, where each affine piece has a slope $+1$ or -1 and an offset. Each of these affine transformations apply within a given interval of value taken from the range of positions in the sequence. A red-black tree maps the starting value of the interval of each affine transformation to the actual transformation. Given a position in the sequence, the corresponding internal position can thus be identified in $O(\log(k))$ where k is the number of affine transformations in this mapping. The reverse transformation is also available with the same representation. This mapping is illustrated in Figure 2.

The second mapping is made of two red black trees, one maps the internal position to the actual value, and the other is the reverse; it maps a value to the set of internal positions where it occurs.

The purpose of the double mapping is that the first mapping can be efficiently updated in $O(k * \log(k))$ to reflect the three update operations considered here. Applying such update can increase or decrease the

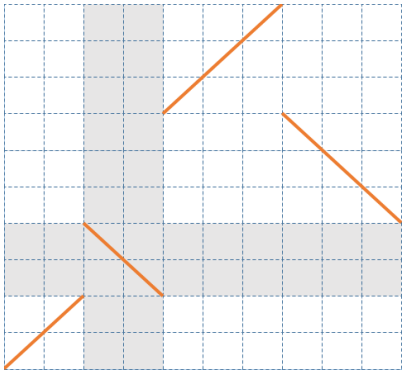

Figure 2: Illustrating the piecewise affine bijection that maps positions to internal positions.

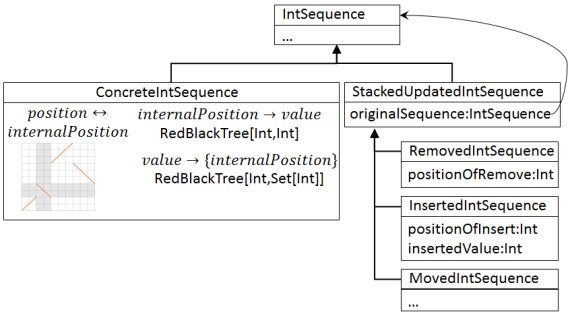

Figure 3: Architecture behind our sequence data structure.

number of affine functions in the first mapping. The update procedure of this mapping ensures that the number of affine functions is minimal, in most cases. This is how the requirement *speed-move-taken* is implemented in our system.

To avoid a significant increase of the number of affine segments in the first mapping, it is bounded at start-up to a maximal value. Whenever this value is reached, a *regularization* operation is performed to simplify the first mapping to the identify function, and correct the two potentially large red black trees of the second mapping accordingly. The choice of this maximal k value is a key choice and will be investigated in more detail later in this paper, both from the theoretical point of view of the resulting complexity and from the practical point of view through some benchmarks.

The concrete representation and the stacked updates are all implemented through non-mutable data structures exclusively to comply with the requirement *immutable-value*.

An illustration of the object actually created in shown in Figure 3 in the case of a sequence with a stacked delete update. It shows the internal structure of the concrete sequence, with its bijection and the two red black trees, and the stacked update representing the sequence where the value at a given position has been deleted. They both implement the API of IntSequence.

4.3 Checkpointing

Sequence variables support a notion of checkpoint that serves the following purposes:

- notify invariants about the possibility to perform pre-computation that they can exploit in order to evaluate neighbour solutions in the context of neighbourhood exploration. Neighbourhoods operating on a sequence variable are therefore required to notify to the variable when they start a star-mode exploration and register the current value as a checkpoint, and must release the checkpoint after the exploration is completed.
- provide an operation "roll back to checkpoint" to neighbourhoods, so that a neighbourhood can simply invoke this update operation, and the variable can reload the previous value in O(1) by reverting to the previous value (which is still stored in the internal structure of the variable)
- provide a notification message that the sequence variable can send to the invariant to notify that the value has been reverted to the latest declared checkpoint. Invariants might be able to update their output and/or internal state efficiently, knowing this high-level information.

The OscaR.cbls framework supports the cross-product of neighbourhoods (De Landtsheer et al., 2015). It is implemented by nesting one neighbourhood into another, with optional, user-specified pruning. The check-pointing mechanism proposed here must therefore support stacked checkpoints, so that the outer and the inner neighbourhoods can both declare their checkpoint and interact with the variable as if they were operating alone.

We can distinguish three strategies for communicating checkpoints between neighbourhoods and invariants. First, a *transparent-checkpoint* approach can be used, where all checkpoint definition and release are communicated to the listening invariant. Second, only the *topmost checkpoint* is communicated, third, only the *latest checkpoint* is communicated; additional release instructions are inserted in this last communication by the sequence variable to ensure a coherent presentation of the checkpoint definition and release. So far, Our system so far incorporates the *latest-checkpoint* strategy.

To use this mechanism, neighbourhoods must first notify that they will explore around the current value of the variable, setting it as a checkpoint, so that invariants are notified that they should perform their pre-computations on this value. Then, the neighbour-

hood can perform its exploration by repeatedly moving to a neighbour solution, evaluating the objective function, and performing a roll-back to the declared checkpoint. When the exploration is completed, the neighbourhood must release its checkpoint through a dedicated method call.

This mechanism of checkpoint is not to be mixed up with the one presented in (Van Hentenryck and Michel, 2005). The checkpoints presented here aim at performing pre-computation, making it possible to reach the efficiency of what Comet calls *differentiation* (Van Hentenryck and Michel, 2009).

4.4 The Sequence Variable and its Delta

To modify a sequence variable, neighbourhoods use the update operations supported by the sequence value. They can also specify a checkpoint to the variable, and call a *rollBackToCheckpoint* to this defined checkpoint. These operations are available through the API of sequence variables.

Upon propagation, a sequence variable notifies its update to all its listening invariants through dedicated data structures representing the succession of updates that have been performed on it since its previous propagation, namely: a succession of insert, delete, seq-move, and checkpoint definitions, starting up with a roll-back to a defined checkpoint, an assignment, or a marker denoting the previously last notified value.

4.5 Complexity of Operations on Sequence Values

The complexity of the main queries implemented on sequence values are summarized in Table 1, where k is the maximal number of affine functions in the first mapping of the concrete sequence, and n is the length of the sequence. It shows the cost on the concrete sequence as well as the additional cost for each stacked update. Computing value at position if logarithmic both in n and k while computing position at value is less efficient. Moving to the next value using an explorer is O(1) in amortized cost.

The complexity of the main update operations are summarized in Table 2. The first column shows the complexity of quick updates. The second column represent the complexities of the concrete updates assuming that no regularization occurs. The third column is the complexity of the concrete updates, considering the amortized complexity of regularization. The regularization operation has a complexity of $O(n * log(k))$, takes place at most every $\Omega(k)$ updates, so it adds $O(n * \log(k)/k)$ amortized complexity. The regularization is not $O(n * \log(n))$ although it requires rebuilding red black trees of size $O(n)$ because the trees are built in a batch mode on already sorted keys, thus in $O(n)$. To compare with, the complexities of these updates on a concrete representation made of a single mapping through red black trees is $O(n)$ for each of these updates.

Concretely, in our implementation, the user can control the value of k through a percentage of the ratio k/n with a default value of 4%

The overall run time of a full-fledged local search solver is dominated by the cost of exploring neighbours, and in a much smaller way, by the cost of performing the moves and performing some pre-computations. Pre-computations being performed by the invariants, they are not considered here. If we exclusively focus on the cost incurred by the data structures, these amount to $O(1)$ per neighbour, and $O(\log(x) + \log(k) * (k + n/k))$ (with x being n or k, depending on the move), respectively.

Table 1: Time complexity of queries on a sequence value.

	value at position	positions of value	explorer	explorer.next
concrete sequence	$O(\log(n) + \log(k))$	$O(\#\text{positions} * \log(k) + \log(n))$	$O(\log(n) + \log(k))$	$O(1)$ amortized
added cost for each stacked update	$O(1)$	$O(\#\text{positions})$	$O(1)$	$O(1)$ amortized

Table 2: Time complexity of updates on a sequence value.

	quick update	concrete update without regularization	concrete update with amortized regularization
insert	$O(1)$	$O(\log(n) + k * \log(k))$	$O(\log(n) + \log(k) * (k + n/k))$
delete	$O(1)$	$O(\log(n) + k * \log(k))$	$O(\log(n) + \log(k) * (k + n/k))$
seq-move	$O(1)$	$O(k * \log(k))$	$O(\log(k) * (k + n/k))$

5 VALIDATING THE CONCEPT OF SEQUENCE VARIABLE

This section validates our concept of sequence variable by explaining how a few representative global constraints or objective functions can be modelled and benefit from our state-of-the-art algorithms. We focus on three examples, two of them are taken from the context of vehicle routing problem: symmetric constant routing distance, and node-vehicle restrictions. The last example is more generic: sequence flipping.

The routes of v vehicles are represented as a single sequence of integers where each integer is present at most once, and represent a node of the routing problem. Their start nodes are 0 to $v-1$ and should always be in the sequence, and in this order. A vehicle implicitly comes back to its start node at the end of its route. Figure 4 shows this encoding for a problem with 3 vehicles and 9 nodes. Also, there is a convention that a subsequence that is moved by a seq-move cannot includes a start node. All our routing neighbourhoods have such behaviour.

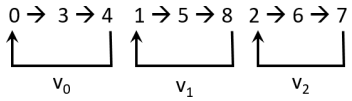

Figure 4: Encoding of a routing problem with three vehicles using a single sequence.

The rationale for this representation is that moves involving two vehicles can be performed efficiently using our efficient data structures since there is no need to transfer data between two sequences.

5.1 Symmetric Constant Routing Distance

Symmetric constant routing distance is an invariant that maintains the total distance driven by all vehicles, based on a distance matrix specifying the distance between each pair of node, knowing that this matrix is symmetric. This metric is very frequent at least in academic literature. It is also a classic example where a global constraint can update its value in $O(1)$ run time against the classical routing neighbourhoods (1-opt, 2-opt, 3-opt) (Glover and Kochenberger, 2003). We illustrate it on the 2-opt only for conciseness and consider a single vehicle.

Upon a two-opt move, the global constraint is notified about a mode update, which is a simple flip. This update specifies a start position and an end position in the sequence that are the start and end of the flipped segment. From these value, it is able to compute the delta on the global distance driven by the considered vehicle since it only is impacted by the changes at the extremities of the flipped segment.

5.2 Node-vehicle Restriction

Given a number of atomic constraints specifying forbidden couples $(node; vehicle)$, a global constraint for node-vehicle restrictions maintains a degree of violation, i.e. the number of such couples that occur in the current routes. A fundamental observation is that the violation degree only changes when nodes are inserted, deleted or when a segment of route is moved from one vehicle to another one. We focus on the last move exclusively as the two others are trivial.

This invariant relies on pre-computation to evaluate such moves efficiently. The pre-computation process examines the routes at the checkpoint, and decorates each step of each route with a map relying each vehicle to number of nodes since the start of the route that cannot be reached by this vehicle, according to given individual constraints. Evaluating a move that moves a segment from one vehicle to another one requires counting the number of nodes within the moved segment that cannot be reached by the vehicle from which the segment is removed, and the number of such nodes that cannot be reached by the vehicle to which the segment is moved. These two values can be obtained in $O(\log(v))$ from the pre-computed values, since we need to identify the vehicles involved by the moves.

5.3 Sequence Flipping

This invariant maintains an output sequence variable to be the flipped value of an input sequence variable. It is not specifically related to routing and clearly demonstrates the flexibility of our framework. This invariant is implemented by translating the moves on the input sequence variable into moves operated on the output sequence variable. It mainly requires translating all indices i appearing in notification messages received from the input sequence variable by transforming them into $\text{length} - i$ when the message are forwarded to the output sequence variable.

6 BENCHMARKING

This section presents a benchmark to illustrate the efficiency of sequence variables and the impact of the k factor of our sequence of integers.

The benchmark exclusively focuses on this variable; run times are to be considered with the greatest

care since they are heavily dependent on the search procedure in use. The latter is under the responsibility of the OR practitioner.

The benchmark is a VRP with 100 vehicles and various numbers of nodes on a symmetric distance matrix and no other constraint. The total distance driven by all vehicles must be minimized. The problem roughly declares as follows, using various bricks of our framework:

```
val routes =
    CBLSSeqVar(m, 0 to v-1, n-1,
               KNFactor)

val totalDistance =
    ConstantRoutingDistance(routes, v,
                            symmetricDistanceMatrix)

val obj = totalDistance
          + 10000*(n - Size(routes))
```

It starts with no node routed, and uses a mix of insert point, one point move, two opt and three opt with various parameters. An important parameter of these neighbourhood is a w factor; when considering neighbour nodes, only the w nearest one are considered by the neighbourhood. For the sake of completeness, the search procedure is given here below. It is instantiated using neighbourhood combinators (De Landtsheer et al., 2015). It combines different classical VRP neighbourhoods using a variant of hill climbing, and ends up with tree opt neighbourhood with a larger w factor.

```
val search =
   BestSlopeFirst(
        InsertPointUnroutedFirst(w=10),
        InsertPointRoutedFirst(w=10),
        onePointMove(w=10),
        twoOpt(w=20),
        threeOpt(w=10))
   exhaust threeOpt(w=20)
```

Figure 5 shows the run time of the optimization engine for various values of the k/n percentage. Each curve reports on a set of benchmark performed with a given value for n, ranging from 1k to 11k by step of 2k. The runs have been performed three times, and the median value is reported. The benchmarks have been executed on a laptop with Intel Core i7 2.3GHz with 16Go of RAM, and 4 Gb allocated to the Java Runtime Environment.

On this diagram, we clearly see the impact of the k/n percentage on the run time. A value of zero is clearly suboptimal; it actually disables the system of piecewise affine bijection presented in Section 4. Above 1, the impact of this factor on the run time reaches a plateau. Efficiency decreases again if the k/n ratio gets too large; a sample value of 20 is illustrated. Another phenomenon to be noted is that the impact of this mechanism grows with the size of the considered problem; this is probably due to the non-linear nature of the complexities, as presented in Section 4.5. A last phenomenon that is clearly visible on the figure is that all curves seem to experience the same behaviour at the same value, although this is possibly due to the coarse steps used in the benchmark. This is an indication that controlling the k via a ratio k/n is an adequate approach.

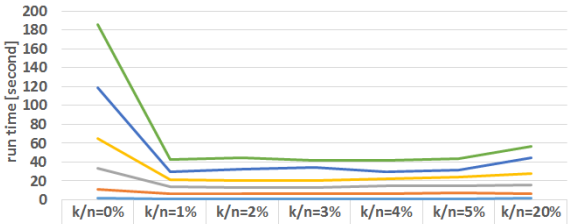

	k/n=0%	k/n=1%	k/n=2%	k/n=3%	k/n=4%	k/n=5%	k/n=20%
11k	186,1	42,4	44,2	41,7	42,2	43,3	56,6
9k	118,5	29,6	32,2	34,5	29,7	31,5	44,8
7k	65	21,4	20,5	20,8	22,1	23,9	27,9
5k	33,1	14,1	13,3	13,4	15,2	14,9	16,2
3k	11,2	6,5	6,8	6,7	6,9	7,3	6,6
1k	2	1,3	1,4	1,3	1,4	1,2	1,5

Figure 5: Run time (in seconds) vs. various values of k/n for various values of n.

7 CONCLUSION

This paper presented an implementation of variables of type "sequence of integers" that is suited for declarative local search frameworks that manipulate concepts such as variable and invariants, also known as Constraint-Based Local Search. The goal is to efficiently represent and apply global moves such as the ones applied in vehicle routing, and to communicate such moves in a concise way to invariants, so that they can apply efficient global algorithms.

A very important open issue to validate our work is to perform comparative benchmark between our approach and other implementations. Such benchmark is however not easy to set up since similar tools mentioned in the background use different models and different search procedure with different trade-offs between seed and optimality. The efficiency of such tool is somehow the product of the efficiency of the model and the efficiency of the search procedure.

Having defined the possible updates to sequence values, and a few global invariants, our next step will be to extend our library of invariants with additional global invariants operating on sequences. The travelling delivery man metrics defined in (Mladenović et al., 2013) is an example of relevant global constraints that can be added to our framework. Such

extension will be of course tailored to our API, which will force us to have quite generic implementations that can operate on any neighbourhoods, since they express their moves through the sequence API. Similarly, an appropriate set of generic neighbourhoods operating on sequences must also be proposed to make this sequence variable fully usable. So far, only routing neighbourhoods have been implemented.

Our sequence variable features a checkpoint mechanism that is useful for global constraints to perform pre-computations. As discussed above, there are several policies on how to manage such checkpoints. Our framework only implements one of these policies, but other policies can be added to the engine. Besides, this mechanism is restricted to sequence variables. It should be made pervasive in the model, so that invariants with other type of variables could also perform such pre-computations.

This new variable type will be included in the CBLS engine of OscaR 4.0 to be released in Spring 2017 (OscaR Team, 2012). With this additional type of variable, we hope that OscaR.cbls will be even more appealing both to users that benefit from highly efficient global constraints in a declarative local search engine, and to researchers who aim at developing new global constraints and will benefit from the whole environment of OscaR.cbls, so they can focus on their own contribution. This implementation will also offer a common benchmarking environment to compare the efficiency of e.g. global constraints within a standard setting.

ACKNOWLEDGEMENTS

This research was conducted under the SAMOBI CWALITY research project from the Walloon Region of Belgium (grant number 1610019).

REFERENCES

Abdulla, P. A., Atig, M. F., Chen, Y.-F., Holík, L., Rezine, A., Rümmer, P., and Stenman, J. (2015). *Norn: An SMT Solver for String Constraints*, pages 462–469. Springer International Publishing, Cham.

Benoist, T., Estellon, B., Gardi, F., Megel, R., and Nouioua, K. (2011). Localsolver 1.x: a black-box local-search solver for 0-1 programming. *4OR*, 9(3):299 – 316.

Björdal, G. (2016). String variables for constraint-based local search. Master's thesis, UPPSALA university.

Croes, G. A. (1958). A method for solving traveling salesman problems. *Operations Research*, 6:791–812.

De Landtsheer, R., Guyot, Y., Ospina, G., and Ponsard, C. (2015). Combining neighborhoods into local search strategies. In *Proceedings of MIC'2015*.

De Landtsheer, R. and Ponsard, C. (2013). Oscar.cbls : an open source framework for constraint-based local search. In *Proceedings of ORBEL'27*.

De Moura, L. and Bjørner, N. (2008). Z3: An efficient SMT solver. In *Proc. of the Theory and Practice of Software, 14th Int. Conf.on Tools and Algorithms for the Construction and Analysis of Systems*, TACAS'08/ETAPS'08.

Di Gaspero, L. and Schaerf, A. (2003). EASYLOCAL++: an object-oriented framework for the flexible design of local-search algorithms. *Software: Practice and Experience*, 33(8):733–765.

Fu, X., Powell, M. C., Bantegui, M., and Li, C.-C. (2013). Simple linear string constraints. *Formal Aspects of Computing*, 25(6):847–891.

Ganesh, V., Kieżun, A., Artzi, S., Guo, P. J., Hooimeijer, P., and Ernst, M. (2011). *HAMPI: A String Solver for Testing, Analysis and Vulnerability Detection*, pages 1–19. Springer Berlin Heidelberg, Berlin, Heidelberg.

Glover, F. and Kochenberger, G. (2003). *Handbook of Metaheuristics*. International Series in Operations Research & Management Science. Springer US.

Mladenović, N., Urošević, D., and Hanafi, S. (2013). Variable neighborhood search for the travelling deliveryman problem. *4OR*, 11(1):57–73.

Newton, M. A. H., Pham, D. N., Sattar, A., and Maher, M. (2011). Kangaroo: an efficient constraint-based local search system using lazy propagation. In *Proceedings of CP'11*, pages 645–659.

OscaR Team (2012). OscaR: Operational research in Scala. Available under the LGPL licence from *https://bitbucket.org/oscarlib/oscar*.

Pralet, C. and Verfaillie, G. (2013). Dynamic online planning and scheduling using a static invariant-based evaluation model. In ICAPS.

Savelsbergh, M. W. P. and Sol, M. (1995). The general pickup and delivery problem. Transportation Science*, 29:17–29.*

Schrijver, A. (2005). On the history of combinatorial optimization (till 1960). In K. Aardal, G. N. and Weismantel, R., editors, Discrete Optimization*, volume 12 of* Handbooks in Operations Research and Management Science*, pages 1 – 68. Elsevier.*

Scott, J., Flener, P., and Pearson, J. (2015). Constraint solving with bounded string variables. In Michel, L., editor, CP-AI-OR 2015*, volume 9075 of* LNCS*, pages 373–390. Springer.*

Van Hentenryck, P. and Michel, L. (2005). Control abstractions for local search. Constraints*, 10(2):137–157.*

Van Hentenryck, P. and Michel, L. (2009). Constraint-based Local Search*. MIT Press.*

Strategic Capacity Expansion of a Multi-item Process with Technology Mixture under Demand Uncertainty: An Aggregate Robust MILP Approach

Jorge Weston, Pablo Escalona, Alejandro Angulo and Raúl Stegmaier
Deparment of Industrial Engineering, Universidad Técnica Federico Santa María, Valparaíso, Chile

Keywords: Capacity Expansion, Machine Requirement Planning, Work Shifts, Robust Optimization.

Abstract: This paper analyzes the optimal capacity expansion strategy in terms of machine requirement, labor force, and work shifts when the demand is deterministic and uncertain in the planning horizon. The use of machines of different technologies are considered in the capacity expansion strategy to satisfy the demand in each period. Previous work that considered the work shift as a decision variable presented an intractable nonlinear mix-integer problem. In this paper we reformulate the problem as a MILP and propose a robust approach when demand is uncertain, arriving at a tractable formulation. Computational results show that our deterministic model can find the optimal solution in reasonable computational times, and for the uncertain model we obtain good quality solutions within a maximum optimal gap of 10^{-4}. For the tested instances, when the robust model is applied with a confidence level of 99%, the upper limit of the total cost is, on average, 1.5 times the total cost of the deterministic model.

1 INTRODUCTION

When a manufacturing industry faces a scenario of increasing demand in the long term and its facilities are close to maximum capacity, the how to expand its production capacity is a key decision. Strategic capacity expansion should determine the level of different production factors over time, such as the number of machines and workers needed to satisfy the production requirement. The objective of this paper is to determine the optimal capacity expansion strategy that minimizes the machinery investment cost, the labor cost, the production cost, and the idle capacity cost over a defined planning horizon, when the future demand is uncertain and there is no knowledge of its distribution. The decision variables are (i) the production requirements needed to satisfy the demand in each period, (ii) the number of machines of each technology needed, (iii) the work shifts necessary to cover the production requirement, and (iv) the workers needed to perform the number of shifts. This considers simultaneously the *machine requirement planning* (MRP) and the *strategic capacity planning* under uncertainty.

In this paper, we developed a multi-item, and multi-period model with technology mixture that determines the optimal expansion strategy considering the machine numbers of each technology, labor, and work shifts needed to satisfy the demand. We considered two different cases: when the demand is deterministic and when it is uncertain. For the first case, we formulated a mixed integer linear program (MILP), which can be solved efficiently with a mixed-integer solver. Then, we incorporated the demand uncertainty into the deterministic model, following a robust approach that considers the best worst case and a non-anticipativity constraint. In this formulation, flexibility is provided to the model via a box-type uncertainty set obtaining a robust model with adjustable robustness; the non-anticipativity constraints, to make the problem tractable, are represented by affine decision rules. The model with demand uncertainty is also an MILP and can be solved with a mixed-integer solver. We used both models to evaluate the impact of a technology mixture in the capacity expansion strategy. We considered three types of technology that differ in terms of production rate, worker requirements, investment cost and production cost.

The main contributions of this work are: (i) An efficient formulation of a strategic capacity expansion model that considers the work shifts as a decision variable; and (ii) the inclusion of the uncertain nature of the demand in the model under a robust approach.

The rest of this paper is structured as follows. In Section 2, a brief literature review is presented, and then, in Section 3 we present the model formulation for the two cases, when the demand is deterministic and when the demand is uncertain. In Section 4, we

Weston, J., Escalona, P., Angulo, A. and Stegmaier, R.
Strategic Capacity Expansion of a Multi-item Process with Technology Mixture under Demand Uncertainty: An Aggregate Robust MILP Approach.
In *Proceedings of the 6th International Conference on Operations Research and Enterprise Systems (ICORES 2017)*, pages 181-191
ISBN: 978-989-758-218-9

report our computational results, and finally, in Section 5 we conclude and present future extensions to this work.

2 RELATED WORK

A *strategic capacity expansion* problem consists of defining the expansion sizes and expansion timing in order to meet the incremental demands within a long-term planning horizon. The objective is to minimize the total costs with respect to the expansion process (Luss, 1982). On the other hand, *machine requirement planning* (MRP) can be defined as the specification of the number of each type of machine needed in each period for a productive process (Miller and Davis, 1977).

A comprehensive review of the strategic capacity expansion problem can be found in Luss (1982), Van Mieghem (2003), Wu et al. (2005), Julka et al. (2007), and Geng et al. (2009) and a more recent review in Martínez-Costa et al. (2014). In particular, Martínez-Costa et al. (2014) described the major decisions and conditioning factors involved in strategic capacity planning. They classified the strategic capacity expansion models according to the *number of sites* involved in the expansion process (a single or multiple sites), the *type of the capacity expansion* considered (expansion by investing/purchasing, outsourcing/subcontracting, reduction and replacement), whether the *uncertainty of the parameters* is considered in the problem formulation, and finally, the *type of mathematical programming model* and its solution procedure.

Our model corresponds to a single-site and multi-item capacity expansion problem under uncertain demand. We consider that capacity expansion can be achieved through machine acquisition and / or by using a flexible workforce in terms of increasing or decreasing the number of shifts. In this sense, the traditional structure of the strategic capacity expansion problem does not consider the relationship between the workforce planning and capacity acquisition decisions. This is related to the natural separation between strategic and tactical decision making. However, when these decisions are addressed separately, sub-optimal solutions are frequently the result. Since workforce flexibility and capacity acquisition can represent substitutable magnitudes, flexible workforce options could be also considered as a means of increasing capacity. In particular, for capital intensive companies, the implementation of one or more shift is an additional tool that managers can use to increment capacity continuously, avoiding the huge investment cost related to equipment acquisition.

To the best of our knowledge, only Fleischmann et al. (2006), Bihlmaier et al. (2009), and Escalona and Ramírez (2012) considered the workforce in their strategic capacity planning. Fleischmann et al. (2006) studied a multi-site and multi-item strategic capacity model with machine replacement and overtime as a means to meeting demand. They considered the same average cost for any overtime, such as prolongation of a shift, weekend shifts, night shifts, or regular third shifts. The model is formulated as an MILP and solved directly using CPLEX. Bihlmaier et al. (2009) analyzed a multi-site and multi-item strategic capacity model without machine replacement that integrates tactical workforce planning via shift work implementation. They consider a detailed set of shifts, such as a late shift, night shift, Saturday shift, and Saturday late shift. They presented a two-stage stochastic MILP for strategic capacity planning under uncertain demand that is solved by Benders decomposition. Escalona and Ramírez (2012) studied the optimal expansion strategy of a process, in terms of machinery, labor, and work shifts, through an aggregated model without machine replacement. They considered that in the process one, two, or three shifts can be worked per time period. The main difficulty related to their model is that shifts are not linear with the number of machines and workers needed to meet the demand. The model is formulated as a mixed integer nonlinear problem and solved by complete enumeration by fixing the shifts during the planning horizon.

Our strategic capacity model also considers uncertain demand. Four primary approaches to considering uncertainty exist (Sahinidis, 2004), which basically comprise (i) stochastic programming, where the uncertain parameters are considered random variables with known probability distributions; (ii) fuzzy programming, where some variables are considered as fuzzy numbers; (iii) stochastic dynamic programming, where random variables are combined with dynamic programming; and (iv) robust optimization, where the uncertainty of the parameters do not follow a known probability distribution, and the solutions are robust, i.e., they perform best in the worst case.

In the literature, two-stage stochastic programming is a dominant approach to handling stochastic capacity planning under various uncertainties (Swaminathan, 2000), (Hood et al., 2003), (Barahona et al., 2005), (Christie and Wu, 2002), (Karabuk and Wu, 2003), (Geng et al., 2009), (Rastogi et al., 2011), (Levis and Papageorgiou, 2004), and (Bihlmaier et al., 2009). A major shortcoming of two-stage stochastic programming is that it generates only a static capacity expansion plan and neglects the dynamic adjust-

ments based on new information when the demand is revealed in each period. Several studies have adapted stochastic dynamic programming to overcome this issue (Rajagopalan et al., 1998), (Asl and Ulsoy, 2003), (Cheng et al., 2004), (Li et al., 2009), (Stephan et al., 2010), (Wu and Chuang, 2010), (Pratikakis et al., 2010), (Chien et al., 2012), (Pimentel et al., 2013), and (Lin et al., 2014).

In summary, few previous research studies on strategic capacity planning considered the workforce as a tool for increasing or decreasing capacity, and to the best of our knowledge, no robust optimization approach exists for dealing with demand uncertainty in strategic capacity planning.

3 MODEL FORMULATION

Consider a capacity expansion problem of a process over a planning horizon of T $(t = 1,...,\tau)$ periods. In this process, I $(i = 1,...,n)$ items are produced, and J $(j = 1,...,m)$ technologies are available for their production. The demand for item i in the period t is d_{it}. Without loss of generality, we assume that the aggregate demand $(\sum_{i\in I} d_{it})$ will increase on the long term, i.e., the aggregate demand follows a positive trend.

Let r_{ij} be the production rate of item i produced with technology type j, and let $\bar{\mu}_j$ be the maximum utilization for each machine of type j that will be considered by the design requirement. In each period it is possible to work K shifts $(k = 1,2,3)$; in each shift the available working time is limited by H_1. The number of shifts that will be worked in the period t is determined by the binary variable W_{kt}, which will be 1 if k shifts are used in period t, else it will be 0. The number of machines of type j needed in each shift to satisfy the demand in period t working k turns is denoted by Y_{jkt}; the number of machines of type j that will be acquired in period t is denoted by V_{jt}; and the number of machines available at the beginning of the planning horizon $(t = 0)$ is B_j.

To meet the demand in each period of the planning horizon, the capacity expansion could happen by: (i) acquiring new machines (expansion by investment) or (ii) modifying the number of shifts (expansion by operational cost). Therefore, in each period it is possible to hire or fire workers. Let Uh_{jt} be the number of workers hired at the beginning of the period t to operate machines of type j, and let Uf_{jt} be the number of workers fired at the beginning of the period t that operated machines of type j. The workers available to operate machines of type j in the period t is denoted by O_{jt}, with $O_{j0} = A_j$ representing the workers available at $t = 0$. The number of workers needed to operate one machine of technology type j is represented by $\bar{O}_j$. Finally, the quantity of item i produced with technology type j in each period t is represented by the variable X_{ijt}.

For this problem the costs that will be considered are: (i) the investment cost of acquiring a machine of type j in the period t (CI_{jt}); (ii) the unitary labor cost in period t (CL_t); (iii) the production cost for one item i produced in a machine of type j in the period t (Cp_{ijt}); (iv) the opportunity cost incurred by idle capacity of technology type j (Cop_{jt}); and, finally, (v) the unitary cost of hiring and firing, denoted by C_h and C_f respectively. It will be assumed that all the mentioned costs are properly brought to present value. A glossary of the terms used in the following sections can be found in appendix A. For this work we are going to consider the cost of opening or closing a shift as negligible, even if in reality they are not cost-free.

3.1 Deterministic Formulation

When demand is deterministic we propose the following capacity expansion problem, denoted by (**P0**).

Problem (**P0**):

$$\min_{\mathbf{X},\mathbf{V},\mathbf{Y},\mathbf{Uh},\mathbf{Uf},\mathbf{W}} \quad TC = \left\{ \sum_{ijt} X_{ijt}\, Cp_{ijt} + \sum_{jt} Cop_{jt} \left(B_j + \sum_{l=1..t} V_{jl} - \sum_{k} Y_{jkt} \right) + \sum_{jt} V_{jt} CI_{jt} + \left(\bar{O}_j \sum_{k} k\, Y_{jkt} \right) CL_t + \sum_{jt} Uh_{jt}\, C_h + \sum_{jt} Uf_{jt}\, C_f \right\} \tag{1}$$

s.t:

$$\sum_{j\in J} X_{ijt} \geq d_{it} \qquad \forall i,t \tag{2}$$

$$\sum_{i\in I} \frac{X_{ijt}}{r_{ijt}} \leq \bar{\mu}_j\, H_1 \sum_{k\in K} k\, Y_{jkt} \qquad \forall j,t \tag{3}$$

$$\sum_{k\in K} Y_{jkt} \leq B_j + \sum_{l=1..t} V_{jl} \qquad \forall j,t \tag{4}$$

$$\sum_{k\in K} W_{kt} = 1 \qquad \forall t \tag{5}$$

$$Y_{jtk} \leq M\, W_{kt} \qquad \forall j,t,k \tag{6}$$

$$\sum_{k\in K} k \left(Y_{jkt} - Y_{j,k,t-1} \right) = \frac{Uh_{jt} - Uf_{jt}}{\bar{O}_j} \qquad \forall j,t \tag{7}$$

$$\sum_{k\in K} k \left(Y_{jk0} \right) = \frac{A_j}{\bar{O}_j} \qquad \forall j \tag{8}$$

$$\mathbf{X} \geq 0 \tag{9}$$

$$\mathbf{Y}, \mathbf{Uh}, \mathbf{Uf}, \mathbf{V} \in \mathbb{Z}^{+} \tag{10}$$

$$\mathbf{W} \in \{0,1\} \tag{11}$$

The objective is to minimize the total cost (TC), considering the production cost, opportunity cost, investment cost, labor cost, and the cost of firing or hiring workers. The satisfaction of demand is ensured by (2). Constraint (3) restricts the total demanded time by the total available time; (4) ensures that the number of machines of technology j available in the period t is greater than the number of machines needed to satisfy the demand assigned in that period to the technology j. Constraints (5) and (6) ensure that the number of work shifts used in period t are of only one type, i.e., $k = 1$ or $k = 2$ or $k = 3$. Constraint (7) represents the continuity and requirement for workers in each period t, and constraint (8) represents an initial condition.

It is easy to show that the problem (**P0**) is equivalent to the problem presented by Escalona and Ramírez (2012) by incorporating the constraints (4) and (5) and considering the following equivalences of variables:

$$w_t NN_{jt} = \sum_{k \in K} k Y_{jkt} \tag{12}$$

$$V_{jt} = ND_{jt} - ND_{j,t-1} \tag{13}$$

$$ND_{jt} = B_j + \sum_{l=1..t} V_{jl} \tag{14}$$

$$NN_{jt} = \sum_{k \in K} Y_{jkt} \tag{15}$$

where w_t is the decision variable that determines the number of shifts needed in period t, NN_{jt} is the number of machines of type j needed in the period t to satisfy the demand, and ND_{jt} is the number of machines of type j available in the period t.

3.2 Uncertain Formulation

In this paper we use a robust approach, where the uncertainty set is defined as a box, which is a particular case of the polyhedral set (Bertsimas and Sim, 2004),(Bertsimas and Thiele, 2006), (Guigues, 2009), and the problem is formulated as an affine multi-stage robust model with a simplified affine policy (Lorca et al., 2016).

Given the uncertain nature of the demand, it cannot be predicted with exactitude. In the best scenario, the estimate of the demand will be close to the actual value, but this will not happen frequently. The most frequent outcome is to have a variation (delta) between the estimate and actual demand. This delta tends to increase as the period analyzed is further in the future. When the variation is positive, the company over-produces, incurring a cost for not selling the excessive units produced; this cost can be estimated using the production cost or an opportunity cost. On the other hand, if this delta is negative, the demand cannot be completely satisfied; in this case the cost incurred by the company is one of lost sales. The lost-sale cost is often discussed since it can result in a loss of profit, a loss of future clients, or the loss of clients whose demand could not be satisfied, causing a bad reputation and loss of confidence in the company. Taking this into consideration, a negative delta is highly undesirable, and therefore it is fundamental to determine how to address the uncertain nature of the demand such that this delta is non-negative (or even 0) most of the time.

Let $D_{it} = \left\{ d_{it} \mid d_{it} \in \left[\bar{d}_{it} - \Gamma \hat{d}_{it} \, , \, \bar{d}_{it} + \Gamma \hat{d}_{it} \right] \right\}$ be the uncertainty set of d_{it}, where $\bar{d}_{it}$ is the nominal value of the demand, and let Γ represent the conservativeness of the model that can be associated with the risk factor of the companies. Denote by D the aggregate uncertainty set, i.e., $D = \underset{it}{\cup} D_{it}$.

Since we sought a robust model that can avoid a negative delta, our worst case will be the one that consider the maximum value that d_{it} can take under the uncertainty set D_{it}; in this case this corresponds to $\bar{d}_{it} + \Gamma \hat{d}_{it}$. Therefore, the demand satisfaction constraint for the robust model can be written as

$$\sum_{j \in J} X_{ijt} \geq \bar{d}_{it} + \Gamma \hat{d}_{it} \quad \forall i,t \tag{16}$$

Replacing (2) in the problem (**P0**) by (16), we obtain a robust model denoted by (**P1**). It is easily noticed that the deterministic problem has two different types of decision variables: (i) strategic decisions, i.e., decisions that affect the productivity in the long term and cannot be modified at the moment of demand realization; and (ii) operational decisions that are made in each period and which therefore depend on the realization of the demand. In the second type we have the production quantity decision variable (**X**). This variable has a clear dependence on the demand realization, dependence that will be addressed via an affine decision rule of the form

$$X(\mathbf{d})_{ijt} = \bar{\chi}_{ijt} + \lambda_{ij} \sum_{\tau=1}^{t} \left(d_{i\tau} - \bar{d}_{i\tau} \right), \tag{17}$$

where the first term ($\bar{\chi}_{ijt}$) represents the nominal value of the quantity of item i to be produced in period t with machines of type j, and λ_{ij} is the percentage of the accumulated over-demand assigned to the item i and machines of technology j. Taking the definition of the uncertain set (D) and the affine decision rules defined by (17) and incorporating them in problem (**P0**), we obtain our affine multi-stage robust model denoted by (**P2**).

Problem (**P2**):

$$\min_{\bar{\chi},\mathbf{V},\mathbf{Y},\mathbf{Uh},\mathbf{Uf},\mathbf{W},\lambda,Z} \left\{ Z + \sum_{jt} V_{jt} CI_{jt} + \sum_{jt} Cop_{jt} \left(B_j + \sum_{l=1..t} V_{jl} - \sum_{k} Y_{jkt} \right) + \sum_{jt} \left(\bar{O}_j \sum_{k} k\, Y_{jkt} \right) CL_t + \sum_{jt} Uh_{jt}\, C_h + \sum_{jt} Uf_{jt}\, C_f \right\} \quad (18)$$

s.t: (4), (5), (6), (7), (8), (9), (10), (11)

$$\sum_{j\in J} \left(\bar{\chi}_{ijt} + \lambda_{ij} \sum_{\tau=1}^{t} \left(d_{i\tau} - \bar{d}_{i\tau} \right) \right) \geq d_{it} \qquad \forall i,t,d \quad (19)$$

$$\sum_{i\in I} \frac{\bar{\chi}_{ijt} + \lambda_{ij} \sum_{\tau=1}^{t} \left(d_{i\tau} - \bar{d}_{i\tau} \right)}{\bar{\mu}_j H_1 r_{ijt}} \leq \sum_{k\in K} k\, Y_{jkt} \qquad \forall j,t,d \quad (20)$$

$$\sum_{ijt} \left(\bar{\chi}_{ijt} + \lambda_{ij} \sum_{k=1}^{t} \left(d_{ik} - \bar{d}_{ik} \right) \right) Cp_{ijt} \leq Z \qquad \forall d \quad (21)$$

$$\sum_{ij} \lambda_{ij} = 1 \quad (22)$$

$$Z \in \Re^{+}, \lambda \in [0,1] \quad (23)$$

We created the auxiliary variable Z in constraint (21) to denote the worst-case production cost. Constraints (19) and (20) are obtained by replacing the variable $\mathbf{X}$ in constraints (2) and (3) by the affine decision rule (17).

Making some straightforward arrangements, and taking into consideration that constraints (19)-(21) are robust constraints that should hold for all $\mathbf{d} \in D$, which is equivalent to maximizing each constraint over the uncertainty set D, it is possible to replace constraints (19)–(21) with the following set of constraints:

$$\sum_{j} \bar{\chi}_{ijt} \geq \Gamma_t \hat{d}_{it} \left(1 - \sum_{j} \lambda_{ij} \right) + \sum_{j} \lambda_{ij} \sum_{\tau=1}^{t-1} \Gamma_\tau \hat{d}_{i\tau} + \bar{d}_{it} \qquad \forall i,t \quad (24)$$

$$\sum_{i} \frac{\bar{\chi}_{ijt}}{r_{ijt}} + \sum_{i} \left(\frac{\lambda_{ij}}{r_{ijt}} \sum_{\tau=1}^{t} \Gamma_\tau \hat{d}_{i\tau} \right) \leq \bar{\mu}_j H_1 \sum_{k\in K} k\, Y_{jkt} \qquad \forall j,t \quad (25)$$

$$\sum_{ijt} \bar{\chi}_{ijt} Cp_{ijt} + \sum_{it} \left(\Gamma_t \hat{d}_{it} \sum_{k=t}^{T} \sum_{j} C_{ijk} \lambda_{ij} \right) \leq Z \quad (26)$$

With these replacements, we obtained a MILP that considers the uncertain nature of the demand and that can be solved by a MIP solver in reasonable computational time. Note that if $\Gamma_t = 0$, the solution is equal to the problem (**P0**) (the nominal problem).

4 COMPUTATIONAL STUDY

The computational study was developed with the following objectives: (*i*) evaluate the computational performance (in terms of CPU time) of the proposed model compared with that presented in the literature; (*ii*) analyze the behavior of the total cost to changes of Γ, i.e., analyze how the total cost grows as more demand (over its expected value) is considered; and (*iii*) test the applicability of our model in an industrial-size example. Since problems (**P0**) and (**P1**) are particular cases of (**P2**), we will only analyze (**P2**).

All experiments were performed with an AMD A6 2.0 GHz processor with 6 GB RAM memory, and the models were solved using CPLEX 12.6.

4.1 Industrial Size Example

We implemented our model using the information presented by a cosmetic company about a packaging process, in particular a sachet filling one, of four items that have high growth potential in the long term. For this process, three types of technology were evaluated. These technologies differ in (*i*) investment cost, (*ii*) unitary production cost, and (*iii*) workers required to operated one machine. For this implementation, we considered a time horizon of ten periods with each period being one year.

The cosmetic company provided the demand forecast for each item, i.e., the nominal value of the demand and the standard deviation of the forecast error. For each item and each period, the company treated the uncertainty through reliability intervals of the form $\hat{F}_{it} \pm \sigma_{it} Z_{1-\frac{\alpha}{2}}$, where $\hat{F}_{it}$ is the demand forecast for the item i at period t, $Z_{1-\frac{\alpha}{2}}$ is the quantile associated with a confidence level of $1-\alpha$, and σ_{it} corresponds to the standard deviation of the forecast error for item i at period t. Note that for this reliability interval, the company assumed that the forecast errors are Gaussian white noise.

Treating the demand uncertainty via reliability intervals can be easily related to the demand uncertainty set defined in Section 3.2 through the following relationships $\bar{d}_{it} = \hat{F}_{it}$, $\Gamma = Z_{1-\frac{\alpha}{2}}$, and $\hat{d}_{it} = \sigma_{it}$, $\forall i \in I$, $t \in T$. Therefore, the demand uncertainty set to be used in this illustrative example is of the form $D_{it} = \left\{ d_{it} \mid d_{it} \in \left[\hat{F}_{it} - Z_{1-\frac{\alpha}{2}} \sigma_{it} \,,\, \hat{F}_{it} + Z_{1-\frac{\alpha}{2}} \sigma_{it} \right] \right\}$, where $Z_{1-\frac{\alpha}{2}} \in \{0,\ 0.25, 0.52,\ 0.84,\ 1.28,\ 1.64,\ 1.96,\ 2.33,\ 2.58,\ 3.29\}$, which corresponds to confidence levels of 0%, 20%, 40%, 60%, 80%, 90%, 95%, 98%, 99%, and 99.9%, respectively. Each problem has 343 variables (133 continuous,

180 integer, and 30 binary variables) and 235 linear constraints.

For this computational study we considered the following set of parameters:

- Demand: The nominal value of demand and the standard deviation of the forecast error are presented in Table 2 and Table 3 in B.
- Production rate (r_{ij}): The production rate is the same for each type of technology, i.e., $r_{ij} = r_i,\ \forall j \in J,\ r_1 = 120,\ r_2 = 170,\ r_3 = 400$, and $r_4 = 600$.
- Maximum utilization (μ_j): $\mu_1 = 0.8,\ \mu_2 = 0.9,\ \mu_3 = 0.98$.
- Available time per shift (H_1): 2080[hours].
- Number of workers needed per machine of technology j ($\bar{O}_j$): $\bar{O}_1 = 3$, $\bar{O}_2 = 2$, and $\bar{O}_3 = 1$.
- Investment cost (CI_{jt}): $CI_{jt} = CI_{j1}(1.15)^{1-t}, \forall t = \{2,...,T\}$, with $CI_{1,1} = \$25000$, $CI_{2,1} = \$50000$, and $CI_{3,1} = \$75000$.
- Opportunity cost (Cop_{jt}): $Cop_{jt} = CI_{jt} f,\ \forall j \in J, \forall t \in T$, where f represents the relation between the useful life and the depreciation time of the machine, and corresponds to 0.10.
- Annual labor cost per worker (CL_t): $CL_t = CL_1(1.15)^{1-t}, \forall t = \{2,...,T\}$, with $CL_1 = \$16032$.
- Unitary production cost (Cp_{ijt}): The production cost will depend only on the type of technology, i.e., $Cp_{ijt} = Cp_{jt},\ \forall i \in I,\ Cp_{jt} = Cp_{j1}(1.15)^{1-t},\ \forall j \in J, \forall t = \{2,...,T\}$, with $Cp_{1,1} = \$1$, $Cp_{2,1} = \$0.75$, and $Cp_{3,1} = \$0.5$.
- Unitary firing and hiring cost: $C_h = \$500$ and $C_f = \$4500$.
- Initial conditions: The number of workers and machines available at the beginning of the planning horizon, for each technology, are 0, i.e., $B_j = A_j = 0,\ \forall j \in J$.

4.2 Results of the Industrial Size Example

The expansion route for this problem involves different shifts and the use of only one type of technology. According to the results, the technology type selected is, regardless of the value of α, the one with the highest investment cost but with the lowest production cost and fewest required workers (type 3). The nominal total cost for the expansion under deterministic demand ($1-\alpha = 0$) is \$8152716. In Figure 1 we show the proportion of the total cost over the nominal cost for each value of $1-\alpha$.

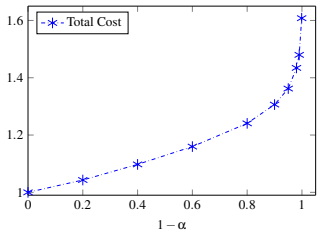

Figure 1: Total cost behavior.

From Figure 1 we observe that the total cost increases exponentially when more variable demand is considered, and therefore each percentage increase is more expensive than the previous one; for example, if a reliability level ($1-\alpha$) of 0.9 is selected, i.e., the demand can be satisfied 95% of the time, the total cost increases to 1.3 times the nominal cost, but if the reliability level selected is 0.99 ,the total cost increases to 1.48 times the nominal cost. Figure 2 presents the expansion route in terms of shifts, total number of machines, and total number of workers needed in each period for four different instances. In all instances, we observed that the shifts changed along the planning horizon, and that an operational expansion (increasing the number of shifts) is always preferred before realizing an investment; with this is possible to determine that is more advisable to expand via shifts before purchasing more machines. Therefore, if the shifts are considered fixed, it is possible to arrive at sub-optimal solutions.

4.3 Sensitivity Analysis

To analyze the impact of the parameters in the expansion strategy, we developed a sensitivity analysis, where the following parameters were varied: (*i*) investment cost, (*ii*) operational cost, and (*iii*) number of workers. For each one the technology mixture and the shifts structure will be analyzed considering a confidence level of 0.9, i.e., $\Gamma = Z_{0.95} = 1.64$. The shifts structure will be considered as the aggregate number of shifts along the planning horizon (*ANS*), i.e., $ANS = \sum_{t,k} kW_{kt}$.

Investment Cost. The investment cost of the actual selected technology type ($j = 3$) was increased until it is not selected anymore. This increase was measured with respect to technology type 1. Figure 3 shows the technology mixture versus the investment cost of technology type 3, (a) when the operational costs are different for each type of technology and (b) when they are the same.

From Figure 3 is possible to observe a gradual transference from machines of technology type 3 to

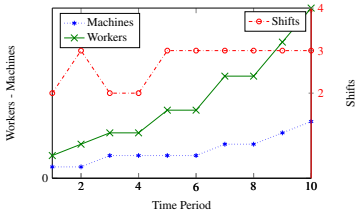

(a) $1-\alpha=0$ ($\Gamma=0$)

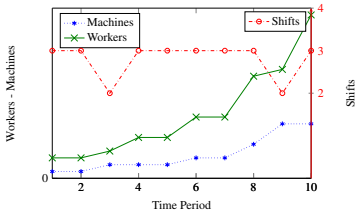

(b) $1-\alpha=0.8$ ($\Gamma=1.28$)

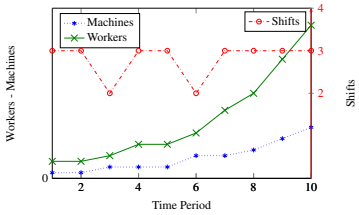

(c) $1-\alpha=0.95$ ($\Gamma=1.96$)

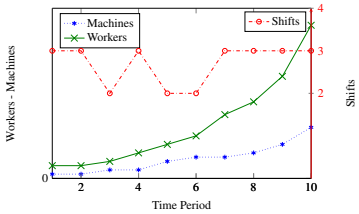

(d) $1-\alpha=0.999$ ($\Gamma=3.29$)

Figure 2: Expansion route by Γ.

machines of technology type 2. Note that this transference happens sooner when the operational costs are the same for all the technologies. In particular, from Figure 3(a), total transference is achieved when the investment cost of technology type 3 is at least 131 times CI_1, and from Figure 3(b), total transference is achieved when the investment cost of the machines of type 3 is 14 times the investment cost of machines of type 1.

We observe that the *ANS* increases when the investment cost increases. This behavior can be explained for two cases, when the rise of the investment cost (i) does not induce technology mixture, and (ii) when it does induce technology mixture. Figure 4 shows the behavior of the cost equilibrium under varying investment cost for both cases.

When the increase in the investment cost does not induce technology mixture (Figure 4(a)), the aggregate investment cost curve moves upwards and the aggregate labor cost stays unchanged. This implies

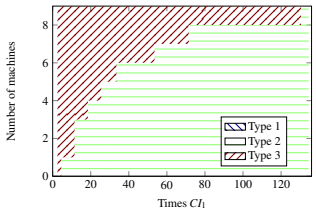

(a) Different operational cost ($Cp_{i1t} > Cp_{i2t} > Cp_{i3t}$)

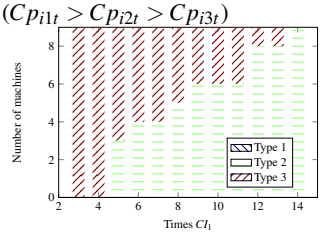

(b) Same operational cost ($Cp_{ijt} = Cp_{it} \forall j \in J$)

Figure 3: Sensitivity to investment cost.

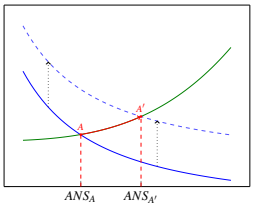

(a) Without technology mixture

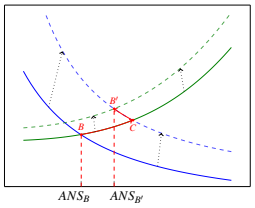

(b) Under technology mixture

Figure 4: Equilibrium dynamic under investment cost variation.

that the equilibrium moves from point A to point A', resulting in a higher cost and a higher *ANS*. In the second case, when the increase in the investment cost induces technology mixture (Figure 4(b)), the curve dynamic can be explained in two stages: (i) the aggregate investment cost increases and (ii) the aggregate labor cost also simultaneously increases; with this the equilibrium moves from point B to point C and finally to point B'. Note that, since in this case the aggregate investment cost increases significantly more than the labor cost, the new equilibrium achieved at point B' implies a higher cost and a higher *ANS*.

Operational Cost. The operational cost of the actual selected technology ($j=3$) was increased until the model stopped selecting it. This increase was measured with respect to technology type 1. Figure 5 shows the technology mixture under varying production cost.

From Figure 5, it is possible to observe a gradual transference from machines of technology type 3 to machines of technology type 2. When the operational cost of the machines of type 3 is 1.19 times that of machines of type 2, the technology transference is total.

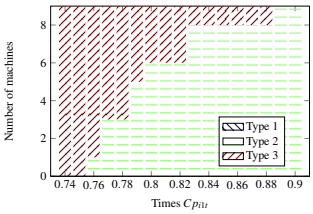

Figure 5: Sensitivity to operational cost.

We also observed that without technology mixture the *ANS* does not change.

Number of Workers. Similar to the previous analysis the number of workers required for technology type 3 was increased until the technology transference was total. The resulting technology mixture is presented in Figure 6, (a) when the operational costs are different for each type of technology and (b) when they are the same.

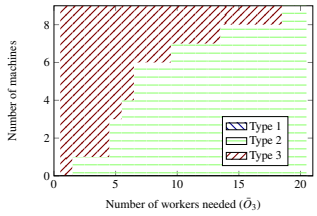

(a) Different operational cost ($Cp_{i1t} > Cp_{i2t} > Cp_{i3t}$)

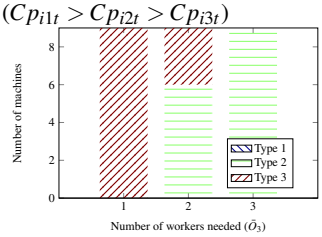

(b) Same operational cost ($Cp_{ijt} = Cp_{it} \forall j \in J$)

Figure 6: Sensitivity to required number of workers.

From Figure 6 it is possible to observe a gradual transference from machines of technology type 3 to machines of technology type 2. Note that this transference starts when both technologies require the same number of workers, and is more drastic when the operational cost is the same for all the technologies (Figure 6(b)).

In this analysis is also possible to note a relationship between the number of workers and the *ANS*. An increase in the number of workers implies a decrease in the *ANS*. Two cases can be recognized: when the rise in the number of workers (i) does not induce technology mixture, and (ii) when it does induce technology mixture. Figure 4 shows the behavior of the cost equilibrium under a variation of the workers requirement for both cases.

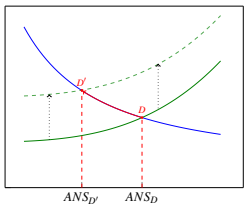

(a) Without technology mixture

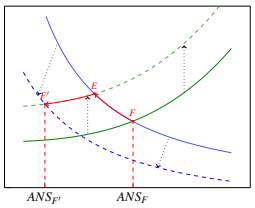

(b) Under technology mixture

Figure 7: Equilibrium dynamic under variation in the required number of workers.

When the increase in the number of workers does not induce technology mixture (Figure 7(a)), the aggregate labor cost curve moves upwards and the aggregate investment cost stays unchanged. This implies that the equilibrium moves from point D to point D', resulting in a higher cost with a lower *ANS*. In the second case, when the increase in the number of workers induces technology mixture (Figure 7(b)), the curve dynamic can be explained in two stages: (i) the aggregate labor cost increases and (ii) the aggregate investment cost simultaneously decreases; with this the equilibrium moves from point E to point F and finally to point E'. Note that the aggregate labor cost varies significantly more than the investment cost and the new equilibrium is achieved at point E', implying a higher cost and a lower *ANS*.

For this industrial-size example, on average, 90% of the cost can be explained as operational. Therefore, when the operational costs are the same for all types of technology, the technology mixture is more sensitive under variation of the investment cost or number of workers. From the sensitivity analysis, we observed that (i) the optimal capacity expansion strategy is more sensitive to the cost that has more influence over the total cost, (ii) the required number of workers is always an important decision factor even when the labor cost represents less than 10% of the total cost, and (iii) the *ANS* has a direct relationship with the investment cost and an inverse one with the labor cost.

4.4 Computational Performance

To evaluate the computational performance of our model and to cover a wide range of data, we generated a set of 180 problems, each one randomly generated around a base case with 10 different items, 5 types of technologies, and a planning horizon of 10 periods, with each problem having 881 variables (551 continuous, 300 integer, and 30 binary variables) and 412 linear constraints. Figure 8 shows the computation times in $\log_2(sec)$ for all instances. In the abscissa the cumulative percentage of instances is presented.

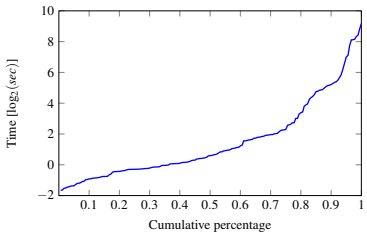

Figure 8: Computation Times.

Figure 8 shows that we observed reasonable computation times; 80% of the instances were solved in less than 10 seconds and 94% of the instances were solved in less than 100 seconds, with a geometric mean of 2.8 seconds. The nominal problem of this instances where solved with the formulation and algorithm presented in Escalona and Ramírez (2012) obtaining an average computational of 584585 seconds to arrive at the optimal solution, therefore our formulation has an average speedup of 25175x.

5 CONCLUSION

In this paper, we develop a capacity expansion model for multi-product, multi-machine manufacturing systems with uncertain demand. At first, a linear deterministic model is presented and later the demand uncertainty is incorporated using a robust approach formulating an affine multi-stage robust model. In contrast with most of the works presented in the literature, our model considers the shifts as a decision variable, allowing more flexibility in the type of expansion that can be used.

For instances that consider a planning horizon of 10 periods, 10 items, and with 5 types of technologies available, the computation times prove to be reasonable ones with times below 100 seconds for most of them (94%), and therefore our model performs better than the one presented in the literature, having an average speedup of 25175x.

From the instances that we tested, we observed the following managerial insights:

- *Fixing beforehand the number of shifts to work along the planning horizon can take us to suboptimal solutions.*
- *The technology mixture is most sensitive to the required number of workers and to the most important cost.*
- *There exists an inverse relationship between labor cost (number of workers) and the aggregate available time and a direct relationship between investment cost and the aggregate available time.*
- *The operational cost by itself does not change the aggregate available time; in fact, if there is no change in the investment cost and number of workers, then the aggregate available time does not change, i.e. the available time, and therefore the work shifts routed along that planning horizon, depend only on the investment and labor costs.*

An interesting discussion that escaped the scope of this work is the analysis of some costs, such as the cost incurred when opening or closing a shift and the opportunity cost which can be determined following business logic instead of the accounting logic used in this work.

Possible extensions of this problem that can be considered are (*i*) the use of a scenario approach with multi-stage programming (Ben-Tal et al., 2009), (Shapiro, 2009), (*ii*) the use of $CVaR^{\Delta}$ to minimize the variability of the solution (Rockafellar and Uryasev, 2000), (Pflug, 2000), (Rockafellar et al., 2006) instead of cost minimization, and (*iii*) considering uncertainty of other parameters such as the maintenance times, production rates, costs, and/or available times.

REFERENCES

Asl, F. M. and Ulsoy, A. G. (2003). Stochastic optimal capacity management in reconfigurable manufacturing systems. *CIRP Annals-Manufacturing Technology*, 52(1):371–374.

Barahona, F., Bermon, S., Gunluk, O., and Hood, S. (2005). Robust capacity planning in semiconductor manufacturing. *Naval Research Logistics*, 52(5):459–468.

Ben-Tal, A., El Ghaoui, L., and Nemirovski, A. (2009). *Robust optimization*. Princeton University Press.

Bertsimas, D. and Sim, M. (2004). The price of robustness. *Operations research*, 52(1):35–53.

Bertsimas, D. and Thiele, A. (2006). Robust and data-driven optimization: Modern decision-making under uncertainty. *INFORMS Tutorials in Operations Research: Models, Methods, and Applications for Innovative Decision Making*.

Bihlmaier, R., Koberstein, A., and Obst, R. (2009). Modeling and optimizing of strategic and tactical production planning in the automotive industry under uncertainty. *OR spectrum*, 31(2):311–336.

Cheng, L., Subrahmanian, E., and Westerberg, A. W. (2004). Multi-objective decisions on capacity planning and production-inventory control under uncertainty. *Industrial & engineering chemistry research*, 43(9):2192–2208.

Chien, C.-F., Wu, C.-H., and Chiang, Y.-S. (2012). Coordinated capacity migration and expansion planning for semiconductor manufacturing under demand uncertainties. *International Journal of Production Economics*, 135(2):860–869.

Christie, R. M. and Wu, S. D. (2002). Semiconductor capacity planning: stochastic modelingand computational studies. *IIE Transactions*, 34(2):131–143.

Escalona, P. and Ramírez, D. (2012). Expansión de capacidad para un proceso, múltiples ítems y mezcla de tecnologías. In *41 Jornadas Argentinas de Informatica*.

Fleischmann, B., Ferber, S., and Henrich, P. (2006). Strategic planning of bmw's global production network. *Interfaces*, 36(3):194–208.

Geng, N., Jiang, Z., and Chen, F. (2009). Stochastic programming based capacity planning for semiconductor wafer fab with uncertain demand and capacity. *European Journal of Operational Research*, 198(3):899–908.

Guigues, V. (2009). Robust production management. *Optimization and Engineering*, 10(4):505–532.

Hood, S. J., Bermon, S., and Barahona, F. (2003). Capacity planning under demand uncertainty for semiconductor manufacturing. *Semiconductor Manufacturing, IEEE Transactions on*, 16(2):273–280.

Julka, N., Baines, T., Tjahjono, B., Lendermann, P., and Vitanov, V. (2007). A review of multi-factor capacity expansion models for manufacturing plants: Searching for a holistic decision aid. *International Journal of Production Economics*, 106(2):607–621.

Karabuk, S. and Wu, S. D. (2003). Coordinating strategic capacity planning in the semiconductor industry. *Operations Research*, 51(6):839–849.

Levis, A. A. and Papageorgiou, L. G. (2004). A hierarchical solution approach for multi-site capacity planning under uncertainty in the pharmaceutical industry. *Computers & Chemical Engineering*, 28(5):707–725.

Li, C., Liu, F., Cao, H., and Wang, Q. (2009). A stochastic dynamic programming based model for uncertain production planning of re-manufacturing system. *International Journal of Production Research*, 47(13):3657–3668.

Lin, J. T., Chen, T.-L., and Chu, H.-C. (2014). A stochastic dynamic programming approach for multi-site capacity planning in tft-lcd manufacturing under demand uncertainty. *International Journal of Production Economics*, 148:21–36.

Lorca, A., Sun, X. A., Litvinov, E., and Zheng, T. (2016). Multistage adaptive robust optimization for the unit commitment problem. *Operations Research*, 64(1):32–51.

Luss, H. (1982). Operations research and capacity expansion problems: A survey. *Operations research*, 30(5):907–947.

Martínez-Costa, C., Mas-Machuca, M., Benedito, E., and Corominas, A. (2014). A review of mathematical programming models for strategic capacity planning in manufacturing. *International Journal of Production Economics*, 153:66–85.

Miller, D. M. and Davis, R. P. (1977). The machine requirements problem. *The International Journal of Production Research*, 15(2):219–231.

Pflug, G. C. (2000). Some remarks on the value-at-risk and the conditional value-at-risk. In *Probabilistic constrained optimization*, pages 272–281. Springer.

Pimentel, B. S., Mateus, G. R., and Almeida, F. A. (2013). Stochastic capacity planning and dynamic network design. *International Journal of Production Economics*, 145(1):139–149.

Pratikakis, N. E., Realff, M. J., and Lee, J. H. (2010). Strategic capacity decision-making in a stochastic manufacturing environment using real-time approximate dynamic programming. *Naval Research Logistics (NRL)*, 57(3):211–224.

Rajagopalan, S., Singh, M. R., and Morton, T. E. (1998). Capacity expansion and replacement in growing markets with uncertain technological breakthroughs. *Management Science*, 44(1):12–30.

Rastogi, A. P., Fowler, J. W., Carlyle, W. M., Araz, O. M., Maltz, A., and Büke, B. (2011). Supply network capacity planning for semiconductor manufacturing with uncertain demand and correlation in demand considerations. *International Journal of Production Economics*, 134(2):322–332.

Rockafellar, R. T. and Uryasev, S. (2000). Optimization of conditional value-at-risk. *Journal of risk*, 2:21–42.

Rockafellar, R. T., Uryasev, S., and Zabarankin, M. (2006). Optimality conditions in portfolio analysis with general deviation measures. *Mathematical Programming*, 108(2-3):515–540.

Sahinidis, N. V. (2004). Optimization under uncertainty: state-of-the-art and opportunities. *Computers & Chemical Engineering*, 28(6):971–983.

Shapiro, A. (2009). On a time consistency concept in risk averse multistage stochastic programming. *Operations Research Letters*, 37(3):143–147.

Stephan, H. A., Gschwind, T., and Minner, S. (2010). Manufacturing capacity planning and the value of multistage stochastic programming under markovian demand. *Flexible services and manufacturing journal*, 22(3-4):143–162.

Swaminathan, J. M. (2000). Tool capacity planning for semiconductor fabrication facilities under demand uncertainty. *European Journal of Operational Research*, 120(3):545–558.

Van Mieghem, J. A. (2003). Commissioned paper: Capacity management, investment, and hedging: Review and recent developments. *Manufacturing & Service Operations Management*, 5(4):269–302.

Wu, C.-H. and Chuang, Y.-T. (2010). An innovative approach for strategic capacity portfolio planning under uncertainties. *European Journal of Operational Research*, 207(2):1002–1013.

Wu, S. D., Erkoc, M., and Karabuk, S. (2005). Managing capacity in the high-tech industry: A review of literature. *The Engineering Economist*, 50(2):125–158.

APPENDIX

A Glossary of Terms

Table 1: Glossary of terms.

Sets	Definition
I	Set of items indexed by i
J	Set of type of machines indexed by j
T	Set of periods indexed by t
K	Set of number of shifts indexed by k, with $k = 1,2,3$
Parameters	
Cp_{ijt}	Unitary production cost for item i produced with a machine of type j in period t
CI_{jt}	Investment cost of a machine of type j in period t
Cop_{jt}	Opportunity cost for a machine of type j in period t
CL_t	Unitary labor cost in period t
C_h	Hiring cost
C_f	Firing cost
B_j	Number of machines of type j available at the beginning of the planning horizon
A_j	Number of workers available to operate the machines of type j at the beginning of the planning horizon
d_{it}	Demand realization of item i in period t
$\bar{d}_{it}$	Nominal demand of item i in period t
$\hat{d}_{it}$	Maximum perturbation for the demand of item i in period t
r_{ijt}	Production rate of items i with machine of type j in period t
$\bar{\mu}_j$	Maximum utilization of machines type j
H_1	Available working time for each work shift
M	A big enough number
$\bar{O}_j$	Number of workers needed to operate one machine of type j
Γ	Level of conservativeness of the model
$\hat{F}_{it}$	Demand forecast of the item i at period t
σ_{it}	Standard deviation of the forecast error for item i at period t
Variables	
X_{ijt}	Number of items i produced with machines of type j in period t
V_{jt}	Number of machines of type j bought in period t
Y_{jkt}	Number of machines of type j needed in each shift to satisfy the demand in period t, working k shifts
W_{kt}	1 if k shifts are worked in period t, 0 otherwise
Uh_{jt}	Number of workers hired in period t to work machines of type j
Uf_{jt}	Number of workers fired in period t that worked machines of type j
w_t	Number of shifts to work in the period t
NN_{jt}	Number of machines of type j needed at period t to satisfy the demand
ND_{jt}	Number of machines of type j available at period t
λ_{ij}	Percentage of the accumulated over-demand assigned to the item i and machine j
$\bar{\chi}_{ijt}$	Nominal quantity of item i to be produced in period t with machines of type j
Z	Worst case production cost.

B Data for Illustrative Example

Table 2: Demand forecast of the item i at period t.

	$\hat{X}_{it}$ $[*10^3 units]$									
i \ t	1	2	3	4	5	6	7	8	9	10
1	100	111	122	138	177	236	330	411	483	605
2	328	420	549	662	788	950	1091	1479	1651	1830
3	367	470	650	762	1021	1140	1293	1736	2227	3111
4	180	226	308	391	523	686	942	1089	1452	1815

Table 3: Standard deviation of the forecast error for item i at period t.

	σ_{it} $[*10^2]$									
i \ t	1	2	3	4	5	6	7	8	9	10
1	30	44	53	70	99	179	292	416	515	858
2	83	130	210	343	532	823	1051	1771	2740	3823
3	142	243	468	747	1126	1335	1829	2590	4040	7805
4	67	96	155	236	423	742	1232	1685	3088	5054

Data Clustering Method based on Mixed Similarity Measures

Doaa S. Ali, Ayman Ghoneim and Mohamed Saleh
Department of Operations Research and Decision Support,
Faculty of Computers and Information, Cairo University
5 Dr. Ahmed Zewail Street, Orman, 12613 Giza, Egypt
{d.saleh, a.ghoneim, m.saleh}@fci-cu.edu.eg

Keywords: Mixed Datasets, Similarity Measures, Data Clustering Algorithms, Differential Evolution.

Abstract: Data clustering aims to organize data and concisely summarize it according to cluster prototypes. There are different types of data (e.g., ordinal, nominal, binary, continuous), and each has an appropriate similarity measure. However when dealing with mixed data set (i.e., a dataset that contains at least two types of data.), clustering methods use a unified similarity measure. In this study, we propose a novel clustering method for mixed datasets. The proposed mixed similarity measure (MSM) method uses a specific similarity measure for each type of data attribute. When computing distances and updating clusters' centers, the MSM method merges between the advantages of k-modes and K-means algorithms. The proposed MSM method is tested using benchmark real life datasets obtained from the UCI Machine Learning Repository. The MSM method performance is compared against other similarity methods whether in a non-evolutionary clustering setting or an evolutionary clustering setting (using differential evolution). Based on the experimental results, the MSM method proved its efficiency in dealing with mixed datasets, and achieved significant improvement in the clustering performance in 80% of the tested datasets in the non-evolutionary clustering setting and in 90% of the tested datasets in the evolutionary clustering setting. The time and space complexity of our proposed method is analyzed, and the comparison with the other methods demonstrates the effectiveness of our method.

1 INTRODUCTION

Unsupervised clustering aims to extract the natural partitions in a dataset without a priori class information. It groups the dataset observations into clusters where observations within a cluster are more similar to each other than observations in other clusters (Bhagat et al., 2013; Tiwari and Jha, 2012). The K-means clustering algorithm is efficiently used when processing numerical datasets, where means serve as centers/centroids of the data clusters. In the K-means algorithm, observations are partitioned into K clusters where an observation belongs to the cluster with the closest mean (i.e., centroid) (Serapião et al., 2016). When dealing with categorical data (Bai et al., 2013; Kim, 2008), K-modes (Ammar and Lingras, 2012) and K-medoids (Mukhopadhyay and Maulik, 2007) clustering algorithms are used instead of K-means. In the K-modes algorithm, modes replace means as the dissimilarity measure and it uses a frequency based method to update modes during the clustering process. On the other hand, K-medoids algorithm computes a cluster medoid instead of computing the mean of cluster. A medoid is a representative observation in a cluster, where the sum of distances to other observations in the cluster is minimal (Mukhopadhyay and Maulik, 2007).

There are four main types of data attributes, which are nominal, ordinal, binary, and numerical. Ordinal and nominal attributes are used to describe categorical data. Nominal attributes are used for labeling variables without any quantitative value. Nominal attributes are mutually exclusive (no overlap) and none of them have any numerical significance such as name, gender, and colors. Ordinal data attributes have ordered values to capture importance and significance, but the differences are not quantified such as (excellent, very good, good and bad) and (very happy, happy, and unhappy). Numerical data attributes can be either discrete or continuous (e.g., temperature, height and weight). Distance or similarity measures are used to solve many pattern recognition problems such as classification, clustering, and retrieval

Ali, D., Ghoneim, A. and Saleh, M.
Data Clustering Method based on Mixed Similarity Measures.
In *Proceedings of the 6th International Conference on Operations Research and Enterprise Systems (ICORES 2017)*, pages 192-199
ISBN: 978-989-758-218-9

problems (Cha, 2007). A distance is mathematically defined as a quantitative degree of how far apart two data points are. The choice of distance/similarity measures depends on the type of data attributes in the processed dataset.

Most of the traditional clustering models are built to deal with either numerical data or categorical data. However in the real world, the collected data often have both numeric and categorical attributes (i.e., a mixed dataset). Thus it's hard to apply traditional clustering algorithm directly to such mixed datasets. When it comes to dealing with mixed datasets, previous work adopted two approaches. The first approach unified the used similarity measure when dealing with mixed datasets (e.g., Parameswari et al., 2015; Shih et al., 2010 and Soundaryadevi and Jayashree, 2015). It converts the mixed dataset either to pure numerical data or to pure categorical data using a pre-processing step before applying the clustering algorithm. Unfortunately, this approach is not practical because there are data instances where the conversion does not give meaningful numerical data. Furthermore, this conversion may lead to loss of information. The second approach divides the original dataset into pure numerical and categorical dataset (e.g. Asadi et al., 2012; Ahmad, 2007; Shih et al., 2010; Mutazinda et al., 2015; and Pinisetty et al., 2012). The appropriate clustering algorithms are used to produce corresponding clusters for these pure datasets. The clustering results on the categorical and numerical datasets are then combined as a categorical dataset on which a categorical data clustering algorithm is employed to get the final output. This approach suffers from excessive complexity through the implementation, especially in the case of dealing huge/large dataset.

Recently, researchers have given much attention to distance learning metric for semi-supervised clustering algorithms (e.g. Relevant Component Analysis, Discriminative Component Analysis) at handling mixed/or complicated datasets (Kumar and Kummamuru, 2008; Baghshah and Shouraki, 2009). Semi-supervised learning clustering algorithms partition a given dataset using additional supervisory information (Kumar and Lingras, 2008). The most popular form of supervision used in this category of clustering algorithms is in terms of pairwise constraints. Learning in a distance metric is equivalent to finding a rescaling of a given dataset by applying the standard Euclidean metric (Xing, 2003). Distance learning metric is mainly processed for semi-supervised clustering algorithms and also suffers from exaggerated complexity through the implementation.

To overcome the previous limitations, we introduce a novel clustering method for the mixed datasets. The proposed mixed similarity measure (MSM) method uses the appropriate similarity measure for each type of data attribute. It combines the capabilities of the K-modes and K-means algorithms when computing distances and updating centers for the clusters. The proposed MSM method is tested using six benchmark real life datasets obtained from the UCI Machine Learning Repository (Blake and Merz, 1998), and it achieved a significant improvement in the clustering performance in a non-evolutionary clustering setting and in an evolutionary clustering setting. The time and space complexity of our proposed method is analyzed, and the comparison with the other methods proves the effectiveness of our method.

The rest of the paper is organized as follows. Section 2 introduces some related works and a background to K-means, K-modes algorithms, and differential evolution. Section 3 presents the proposed MSM method. Section 4 illustrates the differential evolution MSM setting. Section shows the experimental results and analyses. Section 6 concludes the work and discusses future works.

2 BACKGROUND

In this section, we cover preliminary concepts needed in our work. These preliminary concepts are the clustering problem, K-means and K-modes clustering algorithms, and differential evolution algorithm.

2.1 Clustering Problem

Formally, a clustering problem is represented as an optimization problem as follows:

$$Min_{\mu,Z} \quad F(\mu, Z) = \sum_{i=1}^{n} \sum_{j=1}^{k} \mu_{ij}\, d(z_j, x_i) \qquad 1 \le i \le n, \qquad 1 \le j \le k \qquad (1)$$

where n is the number of data points, k is the number of data clusters, and μ_{ij} is a membership of i^{th} data observation to cluster j (i.e. μ_{ij} takes binary values in crisp case). $d(z_j, x_i)$ is the matching distance measure between data point x_i and data cluster center z_j .

2.2 K-Means Clustering Algorithm

The K-means algorithm is a widely used clustering algorithm for numerical data sets because of its simplicity (Bai et al., 2013). K-means algorithm searches for nearly optimal partitions with a fixed number of clusters. The algorithm aims to minimize total distances between data points and centers (Wu et al., 2008) where

$$d(z_j, x_i) = \|\boldsymbol{x_i} - \boldsymbol{z_j}\|^2 \quad (2)$$

is the distance measure between data point x_i and data cluster center z_j. The steps of K-means clustering algorithm are as follows (Kim and Hyunchul, 2008):

1: *Randomly initialize centers for the k clusters*
2: *Each data point is assigned to the cluster with the nearest center (Eq. 2).*
3: *Update the center of each cluster.*
4: *Repeat steps 2 and 3 until the clusters' centers stop changing or other stopping criteria are met.*

Procedure 1: Steps of K-Means algorithm.

In step 3, the j^{th} cluster center is updated by taking the mean of data observations which are grouped in cluster *j* in step 2.

2.3 K-Modes Clustering Algorithm

K-modes clustering algorithm extends the K-means algorithm to cluster categorical data (Gibson et al., 1998), by replacing means of clusters by modes. K-modes algorithm uses a simple matching distance (Aranganayagi and Thangavel, 2009), or a hamming distance when measuring distances between data observations. To understand the matching distance measure, let x and y be two data observations in D dataset and L be the number of attributes in a data observation. The simple matching distance measure between x and y in D is defined as:

$$d_C(x, y) = \sum_{l=1}^{L} \delta(x_l, y_l) \quad (3)$$

where $\delta(x_l, y_l) = \begin{cases} 0 & if\ x_l = y_l \\ 1 & if\ otherwise \end{cases}$.

The steps of the k-modes clustering algorithm is similar to the k-means algorithm (Procedure 1), except that the center of cluster is updated according to the following equation:

$$z_{jl} = a_{rl} \in DOM(A_l), \quad r \in n_j \quad (4)$$

where z_{jl} represents the new updated value of cluster j in the l^{th} attribute, and a_{rl} is the value of the data observation r which has the most frequent value in the l^{th} attribute for the data observations within cluster *j*. With respect to A_l, it expresses all the possible values which can be taken by the attribute l and *DOM* is a domain of this attribute. n_j is the total number of data observations in cluster *j*.

2.4 Differential Evolution

Differential evolution (DE) is a population-based global optimization algorithm that uses a real-coded representation (Saha et al., 2010). DE belongs to the class of genetic algorithms since it uses selection, crossover, and mutation operators to optimize an objective function over the course of successive generations (Suresh et al., 2009). The DE operators are as follow:

1. Mutation operator: In generation t, let $X_{i,t}$ be the i^{th} solution vector in the population of size NP (i.e., $i \in [1, 2, \dots, NP]$). For each solution vector $X_{i,t}$, a mutant vector $V_{i,t+1}$ is generated using three randomly picked solutions from the population using the following equation:

$$V_{i,t+1} = X_{r1,t} + F(X_{r2,t} - X_{r3,t}) \quad (5)$$

where $r_1, r_2, r_3 \in [1, 2, \dots, NP]$ are three mutually distinct random numbers and $r_1, r_2, r_3 \neq i$, and $F \in [0, 2]$ is a real number representing the differential weight.

2. Crossover operator: Let L be the dimension of a solution vector and $j = 1, 2, \dots, L$ be the index for the dimension. The mutant vector $V_{i,t+1}$ and the target solution vector $X_{i,t}$ are crossed to generate a trial solution vector

$$U_{i,t+1} = (u_{1i,t+1}, u_{2i,t+1}, \dots, u_{Di,t+1}) \quad (6)$$

where $u_{ji,t+1} = \begin{cases} v_{ji,t+1}, & if\ r_j \leq CR\ or\ j = rn(i), \\ x_{ji,t}, & if\ r_j \leq CR\ and\ j \neq rn(i). \end{cases}$

where $r_j \in [0, 1]$ is a uniformly generated random number, $CR \in [0, 1]$ is the crossover probability, and $rn(i) \in [1, 2, \dots, L]$ is a randomly chosen dimension index.

3. Selection operator: The trail vector $U_{i,t+1}$ is compared against $X_{i,t}$ and will replace it in the population if the following condition is met where $f(.)$ is the fitness function:

$$X_{i,t+1} = \begin{cases} U_{i,t+1}, & if\ f(U_{i,t+1}) < f(X_{i,t}) \\ X_{i,t}, & otherwise. \end{cases} \quad (7)$$

3 MSM METHOD

The proposed MSM method is a novel clustering model based on using different similarity measures when dealing with mixed datasets. The MSM method has a pool of different similarity measures and uses them according to the type of data attribute under consideration. When computing distances and updating centroids, the MSM method merges between the capabilities of k-modes and K-means algorithms. Thus, we modify some steps in the traditional clustering model. Procedure 2 shows the steps of the MSM method. These modified steps are explained in details in the next sub-sections.

1: *All data elements are assigned a cluster number between 1 and k randomly, where k is the number of clusters desired.*
2: *Find the cluster center of each cluster.*
3: *For each data element, find the cluster center that is closest to the element. Assign the element to the cluster whose center is closest to it.*
4: *Re-compute the cluster centers with the new assignment of elements.*
5: *Repeat steps 3 and 4 till clusters do not change or for a fixed number of times.*

Procedure 2: Steps of the MSM method.

3.1 Computing Distances

In the proposed MSM method, let A and B be two mixed data points with m attributes. When computing the distance between A and B, the MSM method calls the similarity measure according to the attribute type, and compute a sub-distance between the attribute in A and the same attribute in B. The total distance between A and B is the sum of the sub-distances for the m attributes. The used similarity measures are normalized to be in the [0, 1] interval as follows:

- For ordinal data attribute

$$z_{i,n} = \frac{r_{i,n}}{M_n - 1} \quad (8)$$

where $z_{i,n}$ is the standarized value of attribute a_n of the data object i, $r_{i,n}$ is the difference value before standardization, M_n is the upper limit of the domain of attribute a_n.

- For binary and nominal data attribute, we use the matching distance (Equation 3).
- For numerical data attribute, we use the following equation

$$\text{zij(n)} = \frac{|x_{i,n} - x_{j,n}|}{\max x_n - \min x_n} \quad (9)$$

where $z_{i,j}$ is the standardized difference value of attribute a_n between two data objects i and j, $x_{i,n}$ and $x_{j,n}$ are the values of attribute a_n of object i and j before standardization, max x_n and min x_n are the upper and lower limit of the domain of attribute a_n, respectively.

Figure 1 shows an example of two mixed data points A and B. The first two attributes are binary and nominal, so the matching distance is used in measuring the distance between them. The third attribute is ordinal, so the sub-distance is calculated using equation 4, where the domain of this attribute is from 1 to 4. The last attribute is numerical and has the range [150, 175], so the sub-distance is calculated by equation 6. Finally, the total distance between A and B is the sum of these sub-distances, which will be 1.73.

	Binary	Nominal	Ordinal	Numerical	Total
A	0	1	3	170	
B	0	2	4	160	
Distance	0	1	0.33	0.4	1.73

$\frac{1}{4-1} = 0.33$

$\frac{|170-160|}{175-150} = 0.4$

Figure 1: An example of calculating the distances in the MSM method.

3.2 Updating Centers

Generally speaking, the step of updating centers differs according to the type of data (e.g., categorical or numerical). Thus when updating centers, the proposed MSM method updates each value of attribute according also to the data type (see Figure 2). If the value of attribute is numerical, then we use the updating rule of the k-means algorithm. However if the value of attribute is categorical, then we use the updating rule of the k-modes algorithm.

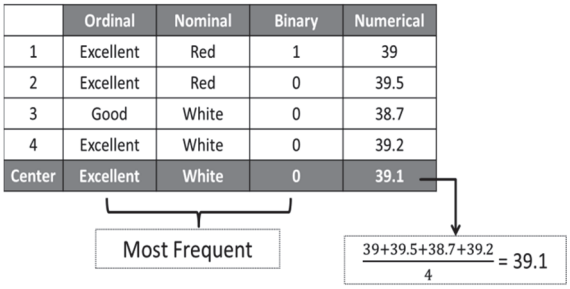

Figure 2: Example for updating centers in the MSM method.

4 EXPERIMENTAL DESIGN

Measuring similarity between data points is a corner stone in the clustering process, whether it is a non-evolutionary clustering setting (e.g., Procedures 1 and 2) or in an evolutionary clustering setting. Thus to evaluate the performance of the MSM method, we compared it against other existing similarity measures in (Boriah et al., 2008) (i.e., matching distance, IOF, and Eskin similarity measures) in addition to the scaling method in (Parameswari et al., 2015) assuming both the non-evolutionary and evolutionary settings. Evolutionary computation techniques play a vital role in improving the data clustering performance because of its ability to avoid falling in local optimal solutions.

We use differential evolution (DE) as an evolutionary technique, where a similarity measure becomes a sub-routine used within the evolutionary setting. For DE with the MSM method (denoted by DE-MSM), procedure 3 illustrates the steps of the algorithm. In step 3, the initialized centers of clusters are randomly determined. The next steps represent the main part of the proposed method, where it starts with updating centers, then updating distances. The mutation and crossover operators then have to be applied using Equations 5 and 6, respectively. The resulting new individual is a candidate which is evaluated against its parent using Equation 7 to select the one with the better fitness. When reaching the maximum number of iterations, we use the accuracy measure performance (Arbelaitz et al., 2013) to select the best individual of the final population.

For the DE, we use a population size of 100 individuals (i.e., 100 different sets of centers), maximum number of iterations of 100, and crossover rate CR of 0.2. These parameters are chosen based on preliminary experiments.

5 EXPERIMENTAL RESULTS AND DISCUSSIONS

The proposed method is tested on six real-life mixed datasets obtained from the UCI Machine Learning Repository (Blake and Merz, 1998). The obtained results of 100 independent runs are summarized in table 1 for the non-evolutionary setting. Table 1 contains the mean and standard deviation of best result of accuracy. We compare the MSM method against three similarity measures(i.e., matching distance, IOF, Eskin, and Scaling) already existing in the literature. We performed T-test with

1: *Input: D = the used dataset, K = number of data clusters, NP = population size*
2: *Output: clusters assignment*
3: *Add randomly initialized clusters'' centers (i.e., individuals of population).*
4: *Evaluate the fitness of all individuals.*
5: *While Stopping Criterion (i.e., maximum number of iterations) is not met; do:*
6: *For each Individual Pi (i = 1 ... NP) in the population, do:*
7: *a) Update centers of the k clusters.*
8: *b) Update distance between data objects and the updated centers of clusters.*
9: *c) Apply the mutation operator using Eq. 5.*
10: *d) Apply the crossover using Eq. 6.*
11: *e) Evaluate the fitness of the offspring C from parent Pi.*
12: *f) Apply selection operator to create new-population by comparing the offspring C against its parent Pi using Eq. 7.*
13: *End For*
14: *End While*
15: *Calculate the accuracy measure performance for every individual in the final population.*
16: *Select the best solution (i.e., set of centers) which has the highest accuracy.*

Procedure 3: The DE-MSM method.

Table 1: Mean ± standard deviation of best solution of 100 independent runs for the simple matching, IOF, Eskin, Scaling and the proposed MSM method.

	Simple Matching	IOF	Eskin	Scaling	MSM	T-test
Breast Cancer	0.8128434 ± 2.69461E-06	0.771992 ± 0.001752535	0.782972 ± 0.001451745	0.814782 ± 0.0027383	0.839089 ± 6.0179E-06	Significant
Zoo	0.8787367 ± 0.000736404	0.861041 ± 0.000184208	0.880504 ± 0.00144237	0.885224 ± 0.0056389	0.913004 ± 0.000432323	Significant
Hepatitis	0.766462 ± 0.000562314	0.710596 ± 0.003786261	0.669242 ± 0.00143719	0.769892 ± 0.0056282	0.8187971 ± 2.72221E-05	Significant
Heart Diseases	0.7520178 ± 9.35633E-06	0.778464 ± 0.001182946	0.6315967 ± 0.000205821	0.761143 ± 0.00088239	0.7953947 ± 1.06071E-05	Significant
Dermatology	0.8476637 ± 0.00152124	0.699989 ± 0.00055469	0.6957118 ± 0.000270416	0.856321 ± 0.0003345	0.8424427 ± 3.90709E-05	Significant
Credit	0.9043666 ± 4.05246E-06	0.864447 ± 0.003066162	0.6360959 ± 0.001083251	0.91882 ± 0.0004267	0.8960072 ± 1.21558E-05	Significant

confidence level 0.05 to illustrate the statistical significant of the results obtained by the MSM method and the second best similarity measure. As shown in Table 1, the MSM method obtained statistically significant better results for four datasets, while simple matching obtained better results for two datasets (where one is not statistically significant). Based on the results, the proposed MSM methods performed better when compared with the other similarity methods, and it improved in about 80% of the tested datasets. Moreover, Table 2 lists the run time of the five clustering similarity methods on different datasets. From Table 2, we can see that the MSM method needs more time than the simple matching method. However, the MSM method consumes time less than IOF, Eskin, and Scaling methods.

Table 2: The running time of the five clustering models on the used datasets.

	Average Running Time (Minutes)				
	Simple Matching	IOF	Eskin	Scaling	MSM
Breast Cancer	4.82	5.33	5.47	4.97	4.94
Zoo	2.11	2.26	2.34	2.17	2.10
Hepatitis	2.69	3.24	3.32	2.87	2.63
Heart Diseases	3.17	3.38	3.41	3.27	3.22
Dermatology	3.68	3.87	3.96	3.71	3.72
Credit	5.19	5.42	5.49	5.34	5.21

We now move to the evolutionary clustering setting, where each similarity measure is used as a sub-routine to compute distances and update centers in the DE algorithm. For the same six real-life mixed datasets, the obtained results of the 100 independent runs are reported in Table 3. Table 3 contains the mean and standard deviation of best result of the accuracy measure performance. To compare our results, we compared the DE with different similarity measures (i.e., DE-MSM, DE-Simple matching, DE-IOF, DE-Eskin, DE-Scaling). Based on the experimental results, the DE setting (Table 3) yields higher accuracy compared to the non-evolutionary setting (Table 1). In addition as shown in Table 3, the DE-MSM obtained statistically significant better results for five datasets, while simple matching obtained better results for one dataset.

6 CONCLUSION AND FUTURE WORK

In this study, we proposed a novel clustering MSM method for the mixed datasets (i.e., datasets with at least two types of data attributes). In contrast to existing approaches in literature dealing with mixed datasets, the MSM method assigns a unique similarity measure for each type of data attribute (e.g., ordinal, nominal, binary, continuous). When dealing with a pure dataset (i.e., with only one type of data attributes), the MSM method will reduce to the K-means or the K-modes algorithms. Using six benchmark real life mixed datasets from the UCI Machine Learning Repository, we first compared the performance of the MSM method against other similarity measures (i.e., simple matching, IOF, Eskin, and Scaling) in a non-evolutionary setting.

Table 3: Mean ± standard deviation of best solution of 100 independent runs for the DE-simple matching, DE-IOF, DE-Eskin, DE-Scaling, and DE-MSM.

	DE-Simple Matching	DE-IOF	DE-Eskin	DE-Scaling	DE-MSM	T-test
Breast Cancer	0.823201 ± 00013254	0.7901874 ± 0.000231	0.805437 ± 0.006119	0.82289 ± 000245	0.8472614 ± 0.07811E-05	Significant
Zoo	0.90132 ± 0.0002621	0.884791± 0.6119E-04	0.899645 ± 0.00332	0.908892 ± 0.002583	0.9435833 ± 2.52812 E-06	Significant
Hepatitis	0.798517± 0.003213	0.769026 ± 0.00371	0.734618 ± 1.842E-04	0.797582± 0.0007739	0.83306326 ± 7.2235E-05	Significant
Heart Diseases	0.762825 ± 0.000765	0.7356806 ± 2.5723E-05	0.6571352 ± 0.00422	0.774329 ± 0.000113	0.82840165 ± 3.77392E-05	Significant
Dermatology	0.85060403 ± 0.000113	0.7285605 ± 0.00117	0.705437 ± 0.0005632	0.8505721 ± 0.00017	0.86351823 ± 1.4426 E-04	Significant
Credit	0.9392598 ± 0.0006234	0.88369739 ± 0.000921	0.7401278 ± 3.48192E-04	0.940456 ± 0.000253	0.91358951 ± 0.000218	Significant

The experimental results showed that the MSM method achieved statistically significant accuracy in 80% of the tested datasets. We then move to evolutionary setting using DE where similarity measures were used to compute distance and update centers during the search process. DE showed its ability to improve the clustering performance compared to the non-evolutionary setting, and DE-MSM achieved statistically significant accuracy in 90% of the tested datasets compared to DE-simple matching, DE-IOF, DE-Eskin and DE-Scaling. The time and space complexity of our proposed method is analyzed, and the comparison with the other methods confirms the effectiveness of our method. For future work, the proposed MSM and/or DE-MSM methods can be used in a multiobjective data clustering framework to deal specifically with mixed datasets. Furthermore, the current work can be extended to data clustering models with uncertainty.

REFERENCES

Ahmad, Dey L., 2007, A k-mean clustering algorithm for mixed numeric and categorical data, Data & Knowledge Engineering, 63, pp. 503–527.

Ammar E. Z., Lingras P., 2012, K-modes clustering using possibilistic membership, IPMU 2012, Part III, CCIS 299, pp. 596–605.

Aranganayagi S., Thangavel K., 2009, Improved K-modes for categorical clustering using weighted dissimilarity measure, International Journal of Computer, Electrical, Automation, Control and Information Engineering, 3 (3), pp. 729–735.

Arbelaitz O., Gurrutxaga I., Muguerza J., Rez J. M., Perona I., 2013, An extensive comparative study of cluster validity indices, Pattern Recognition (46), pp. 243–256.

Asadi S., Rao S., Kishore C., Raju Sh., 2012, Clustering the mixed numerical and categorical datasets using similarity weight and filter method, International Journal of Computer Science, Information Technology and Management, 1 (1-2).

Baghshah M. S., Shouraki S. B., 2009, Semi-supervised metric learning using pairwise constraints, Proceedings of the Twenty-First International Joint Conference on Artificial Intelligence (IJCAI), pp. 1217–1222.

Bai L., Lianga J., Dang Ch., Cao F., 2013, A novel fuzzy clustering algorithm with between-cluster information for categorical data, Fuzzy Sets and Systems, 215, pp. 55–73.

Bai L., Liang J., Sui Ch., Dang Ch., 2013, Fast global k-means clustering based on local geometrical information, Information Sciences, 245, pp. 168-180.

Bhagat P. M., Halgaonkar P. S., Wadhai V. M., 2013, Review of clustering algorithm for categorical data, International Journal of Engineering and Advanced Technology, 3 (2).

Blake, C., Merz, C., 1998. UCI repository machine learning datasets.

Boriah Sh., Chandola V., Kumar V., 2008, Similarity measures for categorical data: A comparative evaluation. The Eighth SIAM International Conference on Data Mining. pp. 243–254.

Cha S., 2007, Comprehensive survey on distance/similarity measures between probability density functions, International journal of mathematical models and methods in applied sciences, 1(4), pp. 300–307.

Gibson D., Kleinberg J., Raghavan P., 1998, Clustering categorical data: An approach based on dynamical systems, In 24th International Conference on Very Large Databases, pp. 311–322.

Kim K.K., Hyunchul A., 2008, A recommender system using GA K-means clustering in an online shopping market, Elsevier Journal, Expert Systems with Applications 34, pp. 1200–1209.

Kumar N., Kummamuru K., 2008, Semi-supervised clustering with metric learning using relative comparisons, IEEE Transactions on Knowledge and Data Engineering, 20 (4), pp. 496–503.

Mukhopadhyay A., Maulik U., 2007, Multiobjective approach to categorical data clustering, IEEE Congress on Evolutionary Computation, pp. 1296 – 1303.

Mutazinda H., Sowjanya M., Mrudula O., 2015, Cluster ensemble approach for clustering mixed data, International Journal of Computer Techniques, 2 (5), pp. 43–51.

Parameswari P., Abdul Samath J., Saranya S., 2015, Scalable clustering using rank based preprocessing technique for mixed data sets using enhanced rock algorithm, African Journal of Basic & Applied Sciences, 7 (3), pp. 129–136.

Pinisetty V.N. P., Valaboju R., Rao N. R., 2012, Hybrid algorithm for clustering mixed data sets, IOSR Journal of Computer Engineering, 6, pp 9–13.

Saha, D. Plewczy´nski, Maulik U., Bandyopadhyay S., 2010, Consensus multiobjective differential crisp clustering for categorical data analysis, RSCTC, LNAI 6086, pp. 30–39.

Serapião B. S., Corrêa G. S. , Gonçalves F. B. , Carvalho V. O., 2016, Combining K-means and K-harmonic with fish school search algorithm for data clustering task on graphics processing units, Applied Soft Computing, 41, pp. 290–304.

Shih M., Jheng J., Lai L., 2010, A two-step method for clustering mixed categroical and numeric data, Tamkang Journal of Science and Engineering, 13 (1), pp. 11–19.

Soundaryadevi M., Jayashree L.S., 2014, Clustering of data with mixed attributes based on unified similarity metric, Proceedings of International Conference On Global Innovations In Computing Technology, pp. 1865–1870.

Suresh K., Kundu D., Ghosh S. , Das S., Han, Y. S., 2009, Multi-Objective Differential Evolution for Automatic Clustering with Application to Micro-Array Data Analysis, Sensors, 9(5), pp. 3981–4004.

Tasdemir K., Merényi E., 2011, A validity index for prototype-based clustering of data sets with complex cluster structures, IEEE transactions on systems, man, and cybernetics—part b, 41(4), pp. 1039–1053.

Tiwari M., Jha M. B., 2012, Enhancing the performance of data mining algorithm in letter image recognition data, International Journal of Computer Applications in Engineering Sciences, II (III), pp. 217–220.

Wu X., Kumar V., Quinlan J. R., Ghosh J., Yang Q. , Motoda H., McLachlan G. J., Ng A., Liu B. , Yu Ph. S., Zhou Zh., Steinbach M., Hand D. J., Steinberg D., 2008, Top 10 algorithms in data mining, Knowledge Information System, 14, pp. 1–37.

Xing E., 2003, Distance metric learning with application to clustering with side-information, in NIPS, pp. 505–512.

SHORT PAPERS

A Heuristic for Optimization of Metaheuristics by Means of Statistical Methods

Eduardo B. M. Barbosa[1] and Edson L. F. Senne[2]
[1]*Brazilian National Institute for Space Research, Rod. Presidente Dutra, Km. 40 - Cachoeira Paulista, SP - 12630-000, São Paulo, Brazil*
[2]*School of Engineering at Guaratinguetá, Univ. Estadual Paulista, Av. Dr. Ariberto Pereira da Cunha, 333 - Guaratinguetá, SP - 12516-410, São Paulo, Brazil*
eduardo.barbosa@inpe.br, edson.senne@unesp.br

Keywords: Metaheuristics, Fine-tuning, Combinatorial Optimization, Nonparametric Statistics.

Abstract: The fine-tuning of the algorithms parameters, specially, in metaheuristics, is not always trivial and often is performed by *ad hoc* methods according to the problem under analysis. Usually, incorrect settings influence both in the algorithms performance, as in the quality of solutions. The tuning of metaheuristics requires the use of innovative methodologies, usually interesting to different research communities. In this context, this paper aims to contribute to the literature by presenting a methodology combining Statistical and Artificial Intelligence methods in the fine-tuning of metaheuristics. The key idea is a heuristic method, called Heuristic Oriented Racing Algorithm (HORA), which explores a search space of parameters, looking for candidate configurations near of a promising alternative, and consistently finds good settings for different metaheuristics. To confirm the validity of this approach, we present a case study for fine-tuning two distinct metaheuristics: Simulated Annealing (SA) and Genetic Algorithm (GA), in order to solve a classical task scheduling problem. The results of the proposed approach are compared with results yielded by the same metaheuristics tuned through different strategies, such as the brute-force and racing. Broadly, the proposed method proved to be effective in terms of the overall time of the tuning process. Our results from experimental studies reveal that metaheuristics tuned by means of HORA reach the same good results than when tuned by the other time-consuming fine-tuning approaches. Therefore, from the results presented in this study it is concluded that HORA is a promising and powerful tool for the fine-tuning of different metaheuristics, mainly when the overall time of tuning process is considered.

1 INTRODUCTION

The tuning of the algorithms parameters, especially, in metaheuristics, is not always trivial and often is performed by *ad hoc* methods according to the problem under analysis. Usually, the choice of incorrect settings can result in an unexpected behaviour of the algorithm, as to converge to a local optimum, or even to present a random behaviour, which does not converges to a good solution within a certain time limit.

In general, there are many challenges related to the tuning of metaheuristics (e.g.: parameters domain, approach strategy, etc.) which require the use of innovative methodologies. These challenges usually interest to different research communities. Therefore, in the contemporary literature there are many researches (e.g.: Dobslaw, 2010; Lessman *et al.*, 2011; Neumüller *et al.*, 2011; Ries *et al.*, 2012; Akbaripour and Masehian, 2013; Amoozegar and Rashedi, 2014; Calvet *et al.*, 2016; and many others) addressed to them. Amongst them, it stands out the using of statistical techniques supported by efficient methods, in order to aid the process understanding and also to reach effective settings.

This paper aims to contribute to the literature by presenting a methodology combining Statistical and Artificial Intelligence methods in the fine-tuning of metaheuristics, such as Design of Experiments (DOE) (Montgomery, 2012) and the concept of Racing (Maron and Moore, 1994; Birattari *et al.*, 2002). The key idea is consider the parameter configurations as a search space and explore it looking for alternatives near of the promising candidate configurations, in order to consistently find the good ones. Broadly, our approach focuses its searches on dynamically created alternatives in an

Barbosa, E. and Senne, E.
A Heuristic for Optimization of Metaheuristics by Means of Statistical Methods.
In *Proceedings of the 6th International Conference on Operations Research and Enterprise Systems (ICORES 2017)*, pages 203-210
ISBN: 978-989-758-218-9

iterative process, and employs a racing method to efficiently evaluate and discard some alternatives, as soon as gather enough statistical evidences against them.

Since the last decades, a variety of strategies for fine-tuning of metaheuristics have emerged in the literature, where it highlight CALIBRA (Adeson-Díaz and Laguna, 2006), which uses DOE to define a parameters search space; F-Race (Birattari *et al*., 2002) and its iterated version I/F-Race (Balaprakash *et al.*, 2007), with an efficient evaluation of candidate configurations; and ParamILS (Hutter *et al*., 2009), whose the alternatives are created from the modifications of a single parameter value.

Inspired by them, our strategy brings these characteristics all together in a single heuristic method, where the exploration of the search space is performed through the candidate configurations in the neighborhood of a promising alternative. The advantage to combine different strategies can be summarized as the hability to define the search space, and the efficiency to focus the search on the candidate configurations inside this search space. Our results confirm the validity of this approach through a case study to fine-tune metaheuristics from distinct natures, such as Simulated Annealing (SA) and Genetic Algorithm (GA), and its effectivity when compared with other tuning approaches, such as brute-force and racing. The quality of the proposed settings for each of them will be evaluated by applying the metaheuristics in a classical optimization problem, such as the task scheduling problem to minimize the total weighted tardiness (TWTP) in a single machine.

The rest of the paper is structured as follows: Section 2 presents the problem of tuning metaheuristics and our approach combining Statistic and Artificial Inteligence methods to address this problem. In Section 3 there is an overview about the scheduling problem, as well as the metaheuristics that will be used in the case study. The proposed approach is applied in a case study (Section 4) to fine-tune the metaheuristics SA and GA. Section 4 also presents the case study results and its analyzes. Our final considerations are in Section 5.

2 THE PROBLEM OF TUNING METAHEURISTICS

Informally, this problem consists of determining the parameter values, such that the algorithms can achieve the best performance to solve a problem within a time limit. This problem is itself an optimization problem, where the goal is to optimize an algorithm (e.g.: better performance, rise the quality of solutions, etc.) to solve different problems (Blum and Roli, 2003; Talbi, 2009).

In general, let M be a metaheuristic with a set of parameters applied on problems $P = \{p_1, p_2, ..., p_n\}$. The parameters (e.g.: α, β, ..., ξ) of M can assume a finite set of values and its cardinality can also vary extensively according to M and P studied. If Θ is a set of candidate configurations, such that θ is any setting of M, then the problem of tuning metaheuristics can be formalized as a state-space:

$$W = (\Theta, P). \quad (1)$$

This problem consists of knowing which is the best setting $\theta \in \Theta$ present in W to solve problems P.

The expected number of experiments for fine-tuning of M on P is the product of $(|\alpha| \times |\beta| \times ... \times |\xi|) \times |P|$. For example, M is a metaheuristic with the following parameters *A, B, C, D*, where $A = \{a_1, a_2, a_3\}$, $B = \{b_1, b_2, b_3, b_4\}$, $C = \{c_1, c_2, c_3\}$, and $D = \{d_1, d_2, d_3, d_4, d_5\}$. Let $|P| = 50$. So, the expected number of experiments for fine-tuning of M on problems P is $(3 \times 4 \times 3 \times 5) \times 50 = 9000$. In short, the best setting of M to solve P is an alternative in (1), such that its determination, in the worst hypothesis, will be given by means of a full search in the state-space W.

2.1 Heuristic Oriented Racing Algorithm

This research proposes an automatic approach to avoid a full search in the state-space (1) and still find a good setting of M to solve P. To do that we combine Statistical and Artificial Intelligence methods (e.g.: DOE and Racing, respectively) to consistently find the good settings based on statistical evaluations of a wide range of problems.

The tuning process begins with an arbitrary selection of n instances ($n > 1$) from a class of optimization problems, and follows by the definitions of ranges for the parameters of metaheuristic. The previously selected instances are treated as a training set, on which are performed experimental studies with the Response Surface Methodology (RSM) to define the best parameters settings for each instance. Therefore, at the end of the experimental phase there will exist n different settings for each parameter, being each one related to an instance.

The settings identified in the training set ensure diversity for the parameters, and they are used to define the bounds of each parameter, that is, a search space of parameters limited by the maximum and minimum values of each parameter in the training set. From there, the goal is to pursue alternatives dynamically created in the neighborhood of some best known candidate configuration, regarding the previously defined bounds of the search space. For each of the alternatives, the target algorithm is ran in an expanded set of instances, bigger than the previous one.

This process (Figure 1) is called Heuristic Oriented Racing Algorithm (HORA), due the way of exploring the alternatives in the search space, that is, using a heuristic method, and by its evaluation process through a racing method.

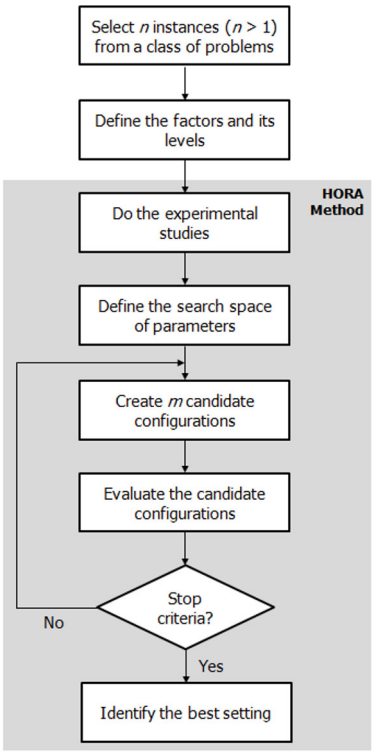

Figure 1: Schema of the proposed approach.

The heuristic method used in the fine-tuning process is illustrated as a pseudo-code in Figure 2. The algorithm receives a promising candidate configuration (S_0), the search space bounds (*B*) and the number of neighbors (*M*). The alternatives (*n*) are created in a main loop and its costs (*C*) are achieved by running the target metaheuristic (Mh) once on different instances (*i*). The solutions are evaluated by the nonparametric Friedman statistic (*T*), and the worst ones are discarded according to the statistical evidences. At each iteration new alternatives are created in the neighborhood of some best known candidate configuration (*S*). The process continues with the surviving ones and the best parameter setting (S^*) is selected as one that has the lowest expected rank.

Just as a racing method, in HORA some candidate configurations, that is, those considered to be good according to the statistical evaluations, are evaluated on more instances. However, it should be highlight that the HORA employs a racing method to evaluate the set of candidate configurations. Besides that, both methods (HORA and racing) differ among them in the way of creation the set of candidate configurations, such that in HORA the alternatives are created on demand in an iterative process, while in racing they are predefined before the fine-tuning process.

```
Input: S0, B, M
Output: S*
S  ← S0;
S' ← {};
n  ← {};
C  ← {};
do while
  i  ← newInstance();
  n  ← newNeighbors(S, B, M);
  S' ← S' ∪ n;
  for each s ∈ S' do
    C ← C ∪ Mh(s, i);
  end
  T  ← statisticalTests(C);
  S' ← collectElite(S', T);
  S  ← identifyBest(S');
until termination criteria is met
S* ← S;
return S*;
```

Figure 2: Pseudo-code of the heuristic method for fine-tuning metaheuristics.

2.2 The Dynamic of the Search Space

The most intuitive way for solving the problem of tuning metaheuristics is the brute-force approach. Broadly, this strategy runs the same number of experiments for all alternatives in the set of candidate configurations. Nevertheless, any alternative with inferior quality in this set must be tested as the good ones.

To avoid this kind of problem, a traditional racing method employs efficient statistics to evaluate the candidate configurations and discard

those considered statistically inferior as soon as gather enough statistics against them.

Even considering the efficiency of a racing method to evaluate the alternatives, both approaches (brute-force and racing) start the tuning process with a large set of candidate configurations. Thus, according to the size of this set, its evaluation must be initially slow.

Different to the traditional approaches, the set of candidate configurations in HORA is dynamically built during the tuning process. The candidate configurations are created on demand in the neighborhood of some best known alternative, as a sequence of sets of candidate configurations:

$$\Theta_0 \subset \Theta_1 \subset \Theta_2 \subset ...$$

From the step k to k+1 the set of candidate configurations is built possibly discarding some alternatives considered statistically inferior. Given that some candidate configurations persist in this set, they are evaluated on more instances. Nevertheless, it is important to note that all the created alternatives must be evaluated on the same instances previously used on evaluating of the persistent alternatives.

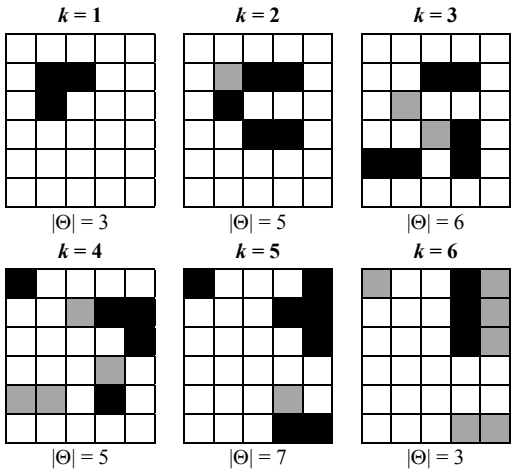

Figure 3: Illustrative process to create (black) and exclude (gray) alternatives from the search space.

To illustrate this process (Figure 3), let us consider any search space, where at each iteration k, m = 3 candidate configurations are created. At the end of an iteration, all alternatives in the set Θ of candidate configurations are evaluated and those with inferior quality are discarded. Therefore, the set Θ is dynamic, that is, its size can increase or decrease. The process continues pursuing the alternatives in the search space until meet a stop criteria (e.g.: number of alternatives in Θ, runtime limit, among others).

The evaluation of the created candidate configurations is done in blocks by instance according to its cost (e.g.: the objective function value). So, the best performance is ranked as 1, the second as 2, and so on. In case of ties between the alternatives, it gives the average ranking to each one. For a detailed description of the evaluation process by means of the racing method using the nonparametric Friedman statistic, we refer to Birattari *et al*. (2002 and 2009).

3 CONSIDERED PROBLEM AND METAHEURISTICS

Scheduling problems are related with the limited resources distribution aiming the achievement of efficient work. It is classical optimization problem involving tasks that must be arranged in m machines ($m \geq 1$) subject to some constraints, in order to optimize an objective function. The key idea is to find the tasks processing order and decide when and on which machine each task should be processed.

A typical scheduling problem is one on which the objective is minimize the total weighted tardiness in a single machine (TWTP). These problems formally expressed as $1|1,d_j|w_jT_j$ (Schmidt, 2000), involve a set of tasks $J = \{1, 2, ..., n\}$ to be processed in a single machine continuously available to process at most one task at a time. Each task ($j \in J$) spends a positive and continuous processing time p_j (time units), has a weight w_j of one task over the others, a start time r_j, and a due date d_j. In general, tardiness may be understood as the difference between the effective completion time and the due date of the tasks, such that the tardiness (T_j) can be computed as $\max(0, C_j - d_j)$, where C_j is the effective completion time of task j.

Metaheuristics are one of the best-known approaches to solving problems for which there is no specific efficient algorithm. Usually, these algorithms differ from each other in terms of searching pattern, but offer accurate and balanced methods for diversification (search space exploration) and intensification (exploitation of a promising region) and share features, such as the use of stochastic components (involving randomness of variables) and have a variety of parameters that must be set according to the problem under study.

The Simulated Annealing (SA) is a probabilistic method proposed in Kirkpatrick *et al*. (1983) and

Cerny (1985) in order to find the global minimum of an objective function with numerous local minima. Widely applied to solve optimization problems, SA simulates a physical process from which a solid is cooled slowly, so that the final product becomes a homogeneous mass to achieve a minimum energy configuration (Bertsimas and Tsitsiklis, 1993).

The SA performance is strongly influenced by a number of parameters. For example, the high temperature in the early stages increases the likelihood of acceptance a low quality solution. Beyond the initial temperature, it is important to set the number of iterations performed on a same temperature, and their cooling rate. Usually, the cooling temperature occurs steadily at a predefined rate α, so that slower, greater the holding of the search space (Roli e Blum, 2003; Talbi, 2009).

By the other hand, the Genetic Algorithm (GA) is a population-based method invented by Holland (1975) inspired in the principles of survival from Darwin's evolution theory. GA simulates an evolution process in which the fitness of individuals (parents) is crucial to generate new individuals (children). The basic operating principle of a GA is to apply the operators (selection, crossover and mutation) on individuals of the population at every generation. Its performance is strongly influenced by a set of parameters, such as the number of generations, crossover and mutation rates.

In a typical GA, the individuals are crossed at a rate between 0.4 and 0.9. For example, if the rate is fixed at 0.5, then half of the population will be formed from the selection and crossover operations. However, if there is no crossover, the population mean fitness must increases to match the best individual fitness rate. From that point, it can only be improved through the mutation. In general, the mutation rate is about 0.001, but may vary according to the problem under analysis.

4 EXPERIMENTAL STUDIES

In our study were selected a set of parameters of each metaheuristic. Those parameters are the most frequently used in the literature and seems to influence the performance of the SA and GA, regardless the studied problem. The considered parameters for SA are: value of the initial temperature (T_0), number of iterations on one temperature stage (SA_{max}) and temperature cooling rate (α); while the chosen parameters for GA are: mutation rate (p_m), crossover rate (p_c), population size (μ) and number of generations (n). The parameters levels (Table 1) were chosen within the real limits of parameters, in order to promote diversity in the search space, as well as differences between each particular parameter setting.

For this study, we define a training set with $n = 4$ instances arbitrarily selected from the benchmark wt40, a TWTP with 40 tasks from the OR-Library (Beasley, 1990). The experimental studies were conducted with a circumscribed Central Composite Design (CCD), whose the axial points establish new limits for an interest region (e.g.: the search space of parameters). A circumscribed design can be used to enlarge the search space exploration if its bounds are in the region of operability, that is, within the real limits of parameters. On the other hand, if the region of interest matches with the parameter limits, another kind of CCD must be chosen (e.g.: face-centred or inscribed) to avoid the parameters infeasibility.

Table 1: Metaheuristics parameters and its levels for the experimental studies.

SA	Low	High
T_0	1.00e4	1.50e6
SA_{max}	500	1500
α	0.900	0.980

GA	Low	High
p_m	0.001	0.025
p_c	0.400	0.900
μ	10	100
n	100	1000

After the experimental studies we have four different results for each parameter, being each one related to an instance. Through those results, we defined the search space of parameters, whose the bounds are the maximum and minimum values of the parameters in the training set. Accordingly, the SA search space is:

- T_0: [1.16e5, 1.65e5];
- SA_{max}: [1316, 1596]; and
- α: [0.945, 0.948].

Whereas, we have the following search space for GA:

- p_m: [0.014, 0.057];
- p_c: [0.684, 0.725];
- μ: [69, 101]; and
- n: [775, 1267].

It is noteworthy in the results, that some parameter values are outside of the limits initially defined (Table 1). However, as pointed before, this occurs due the experimental studies, where the axial points of the CCD overcome the previously set limits in order to ensure an appropriate estimation of parameters.

From there, the exploration of the search space of parameters is done by creating the alternatives in the neighborhood of some best known candidate configuration. For each of the alternatives we ran the target metaheuristics (e.g.: SA and GA) during 15*s* on an expanded set of instances (e.g.: for this study, the expanded set matches all 125 instances from the benchmark wt40). This process was repeated 10 times and the results of fine-tuning of the metaheuristics by means of HORA are presented in terms of mean and standard deviation ($\mu \pm \sigma$) in Table 2. This table also presents the total time (in seconds) of the tuning process.

Table 2: Fine-tuning of metaheuristics (HORA).

SA	Settings	GA	Settings
T_0	1.29e5 ± 4.22e4	p_m	0.040 ± 0.012
SA_{max}	1391 ± 87	p_c	0.699 ± 0.211
α	0.946 ± 0.001	μ	80 ± 11
--	--	n	983 ± 115
t	698*s*	***t***	875*s*

For comparisons, we considered the previously defined search space of parameters, and two fine-tuning approaches, as the *Deceive*, a brute-force approach, and a racing algorithm based in the F-Race method, called *Racing*. The settings used for both approaches are the same, such that, for SA we define: T_0 = {1.16e5, 1.26e5, 1.35e5, 1.45e5, 1.55e5, 1.65e5}, SA_{max} = {1316, 1409, 1502, 1596}, and α = {0.945, 0.946, 0.948}; and for GA we consider: p_m = {0.014, 0.028, 0.043, 0.057}, p_c = {0.684, 0.698, 0.711, 0.725}, μ = {69, 85, 101}, and n = {775, 939, 1103, 1267}.

Each possible combination leads to one different metaheuristic setting, such that, the search spaces have 72 and 192 different candidate configurations for the SA and GA, respectively. The idea is use *Deceive* and *Racing* to select the good as possible candidate configuration out a lot of options. To do that, for the considered approaches, we run the target algorithms during 15*s* on the same extended set of instances previously used (e.g.: 125 instances from the benchmark wt40). This process was repeated 10 times and the results of fine-tuning of the studied metaheuristics by means of brute force and racing method are presented in terms of mean and standard deviation ($\mu \pm \sigma$) in Tables 3 and 4. These tables also present the total time (in seconds) of the tuning process.

It is noted on results that HORA method is the most effective in the fine-tuning of the metaheuristics, in terms of the overall time process. Since it demands a little portion of the time required by the brute-force and racing algorithm, respectively. The pointed divergence can be justified by the size of the set of alternatives, fairly large for *Deceive* and *Racing*, as well as the way of creating the set of candidate configurations in the search space. Given that in HORA it is dynamically done during the tuning process, whereas the others (*Deceive* and *Racing*) use predefined sets of alternatives.

Table 3: Fine-tuning of metaheuristics (Brute-force).

SA	Settings	GA	Settings
T_0	1.34e5 ± 4.39e4	p_m	0.053 ± 0.007
SA_{max}	1419 ± 112	p_c	0.710 ± 0.214
α	0.946 ± 0.001	μ	90 ± 11
--	--	n	988 ± 190
t	5460*s*	***t***	15274*s*

Table 4: Fine-tuning of metaheuristics (Racing).

SA	Settings	GA	Settings
T_0	1.20e5 ± 3.67e4	p_m	0.051 ± 0.010
SA_{max}	1316 ± 0	p_c	0.695 ± 0.210
α	0.946 ± 0.001	μ	90 ± 13
--	--	n	1087 ± 144
t	3213*s*	***t***	11700*s*

The results also show the similarity between the settings, by means of HORA and *Racing*. It is emphasised that both approaches employ the same evaluation method for the candidate configurations.

4.1 Experimental Results

In general, the metaheuristics employ some degree of randomness to diversify its searches and avoid confinement in the search space. Thus, a single run of these algorithms can result in different solutions from the next run. So, to test the quality of our settings, our experimental results were collected after 5 run of the metaheuristics SA and GA on the TWTP.

To generalize our results and compare them among themselves, we use:

$$gap = \frac{f(s) - f(s^*)}{f(s^*)} \times 100, \quad (2)$$

where $f(s)$ is our computed solution and $f(s^*)$ is the best known solution of the problem. Thus, the lower the value of *gap* for the metaheuristics, the better the performance of the algorithms.

We compare the HORA results with *Deceive* and *Racing*. The settings of the metaheuristics through of each approach were presented in Tables 2, 3 and 4, for HORA, *Deceive* and *Racing*, respectively.

The set of results in Tables 5 and 6 are best found value of (2) and its corresponding runtime (t), in 5 run of the studied metaheuristics, in the first 10 instances of the benchmark wt40, from the OR-Library (Beasley, 1990). In these tables, the results of the approaches are underlined by the capital letters D, H and R for *Deceive*, HORA and *Racing*, respectively.

Table 5: SA statistics for the first 10 instances of wt40.

Inst.	gap_D	t_D	gap_H	t_H	gap_R	t_R
1	0.00	56	0.00	36	0.00	42
2	4.65	96	0.00	35	0.00	29
3	6.70	89	0.00	54	0.00	28
4	0.00	45	0.00	33	0.00	29
5	0.00	44	0.00	27	0.00	21
6	0.00	51	0.00	41	0.00	30
7	0.00	87	3.91	81	3.91	68
8	0.00	53	0.00	47	0.00	39
9	0.00	58	0.52	85	1.36	82
10	0.00	62	0.00	56	0.00	38
μ	1.14	64	0.44	50	0.53	41
σ	2.32	18	1.17	19	1.20	18

The SA statistics (Table 5) reveal an increasing of the quality of solutions, when the tuning approach HORA is chosen. It is also noted the similarity between results of HORA and *Racing* in the most instances. According to the statistics, when considering the *gap*, the metaheuristics tuned with HORA is better (closely followed by *Racing*). When considering the execution time, the metaheuristics tuned by *Racing* is faster (closely followed by HORA).

The GA statistics (Table 6) reveal a decreasing of the quality of solutions (e.g.: arithmetic mean) for HORA and *Racing* approaches, when comparing its results with SA. In both cases the results are about the double of the results above (Table 5). Over again, it is noted the similarity between the results of HORA and *Racing* in almost all the selected instances, but for GA, HORA is little faster than *Racing*. However, as observed the runtime is also increased.

In summary, the tuning of metaheuristics by means of the HORA method are competitive and showed the better results for both algorithms. The presented results were statistically analyzed by means of *t*-test at the significance level of 5%, and the comparisons between HORA × *Deceive*, as well as HORA × *Racing*, were not significant. Therefore, considering the time required to the tuning process, HORA is more effective, since it demand less time than the brute-force and racing approaches for achieving the statistically same results.

Table 6: GA statistics for the first 10 instances of wt40.

Inst.	gap_D	t_D	gap_H	t_H	gap_R	t_R
1	0.00	57	0.00	36	0.00	62
2	0.00	100	0.00	65	3.10	51
3	6.70	53	6.70	55	6.70	57
4	0.00	38	1.29	43	1.29	56
5	0.00	30	0.00	5	0.00	7
6	1.34	85	0.00	105	0.00	112
7	0.00	83	0.00	54	0.00	32
8	0.00	50	0.00	89	0.00	94
9	0.34	68	0.00	79	0.00	50
10	0.00	127	0.04	95	0.04	121
μ	0.84	69	0.80	63	1.11	64
σ	1.99	28	2.00	29	2.09	33

5 CONCLUSIONS

This paper presented a method addressed to the problem of tuning metaheuristics. The problem was formalized as a state-space, whose the exploration is done effectively by a heuristic method combining Statistical and Artificial Intelligence methods (e.g.: DOE and racing, respectively).

The proposed method, called HORA, applies robust statistics on a limited number of instances from a class of problems, in order to define a search space of parameters. Thus, from the alternatives dynamically created in the neighborhood of some best known candidate configuration, it employs a racing method to consistently find the good settings. However, it should be highlight that HORA differs from the racing method in the way how the alternatives are created, that is, while racing uses a predefined set of candidate configurations, in HORA the alternatives are created on demand in an iterative process. This feature ensures the dynamic of the search space, such that in some situations it increases and others, it decreases, as well as it makes the evaluation process more efficient.

From a case study, HORA was applied for fine-tuning two distinct metaheuristics. Its results were compared with the same metaheuristics tuned by means of different approaches, such as the brute-force and racing. The HORA method proved to be effective in terms of overall time of the tuning process, since it demands a little portion of the time

required by the other studied approaches. Through the experimental studies it is noted that the metaheuristics SA and GA tuned by means of HORA can reach the same results (eventually better) than the other studied fine-tuning approaches, but the tuning process is much more faster with HORA. This better performance can be explained by the way of exploring the alternatives in the search space, that is, pursuing the good ones in the neighborhood of some best known candidate configuration, and by the efficiency of its evaluation process with a racing method.

In the scope of this study, the metaheuristics SA and GA, as well as the problem TWTP, were used only to demonstrate the HORA approach addressed to the problem of tuning metaheuristics. The results achieved show that the proposed approach may be a promising and powerful tool mainly when it is considered the overall time of tuning process. Additional studies must be conducted in order to verify the effectiveness of the proposed methodology considering other metaheuristics and problems.

REFERENCES

Adeson-Diaz, B., Laguna, M., 2006. Fine-tuning of algorithms using fractional experimental designs and local search. Operations Research, Baltimore, v. 54, n. 1, p. 99-114.

Amoozegar, M.; Rashedi, E., 2014. Parameter tuning of GSA using DOE. In: *4th International Conference on Computer and Knowledge Engineering (ICCKE),* 4., 2014, p. 431-436.

Akbaripour, H.; Masehian, E., 2013. Efficient and Robust Parameter Tuning for Heuristic Algorithms. International Journal of Industrial Engineering & Production Research, Tehran, v. 24, n. 2, p. 143-150.

Balaprakash, P., Birattari, M., Stützle, T., Dorigo, M., 2007. Improvement strategies for the F-Race algorithm: sampling design and iterative refinement. In: *4th International Workshop On Hybrid Metaheuristics*, 4., 2007, p. 108-122.

Beasley, J. E., 1990. OR-Library: Distributing test problems by electronic mail. Journal of the Operational Research Society, Oxford, v. 41, n. 11, p. 1069-1072.

Bertsimas, D., Tsitsiklis, J., 1993. Simulated annealing. Statistical Science, Hayward, v. 8, n. 1, p. 10-15.

Birattari, M., Stützle, T., Paquete, L., Varrentrapp, K., 2002. A racing algorithm for configuring metaheuristics. In: *Genetic apnd Evolutionary Computation Conference*, 2002, New York. p. 11-18.

Birattari, M., Yuan, Z., Balaprakash, P., Stützle, T., 2009. F-Race and iterated F-Race: an overview. Bruxelles: Iridia Technical Report Series. 21 p.

Blum, C., Roli, A., 2003. Metaheuristics in combinatorial optimization: overview and conceptual comparison. ACM Computing Surveys, v. 35, n. 3, p. 268-308.

Calvet, L.; Juan, A. A.; Serrat, C.; Ries, J. 2016. A statistical learning based approach for parameter fine-tuning of metaheuristics. SORT (Statistics and Operations Research Transactions), v. 40, n. 1, p. 201-224.

Cerny, V., 1985. Thermodynamical approach to the traveling salesman problem: an efficient simulation algorithm. Journal of Optimization Theory and Applications, v. 45, p. 41-51.

Dobslaw, F., 2010. A parameter tuning framework for metaheuristics based on design of experiments and artificial neural networks. In: *Sixth International Conference On Natural Computation*, 6., 2010, Cairo, p. 1-4.

Holland, J. H., 1975. *Adaptation in natural and artificial systems*. Boston: University of Michigan Press, 211 p.

Hutter, F., Hoos, H., Leyton-Brown, K., Stützle, T., 2009. ParamILS: an automatic algorithm configuration framework. Journal of Artificial Intelligence Research, v. 36, p. 267-306.

Kirkpatrick, S., Gelatt, C. D., Vecchi, M. P., 1983. Optimization by simulated annealing. Science, London, v. 220, n. 4598, p. 671-680.

Lessmann, S.; Caserta, M.; Arango, I. M., 2011. Tuning metaheuristics: A data mining based approach for particle swarm optimization. Expert Systems with Applications, v. 38, n. 10, New York: Pergamon Press, p. 12826-12838.

Maron, O., Moore, A. W., 1994. Hoeffding races: accelerating model selection search for classification and function approximation. Advances in Neural Information Processing Systems, San Mateo, p. 59-66.

Montgomery, D. C., 2012. *Design and analysis of experiments*. 8th ed. New Jersey: John Wiley & Sons Inc.. 699 p.

Neumüller, C.; Wagner, S.; Kronberger, G.; Affenzeller, M., 2011. Parameter Meta-optimization of Metaheuristic Optimization Algorithms. In: *13th International Conference on Computer Aided Systems Theory (EUROCAST 2011)*, 13., 2011, Las Palmas de Gran Canaria, p. 367-374.

Ries, J.; Beullens, P.; Salt, D., 2012. Instance-specific multi-objective parameter tuning based on fuzzy logic. European Journal of Operational Research, v. 218, p. 305-315.

Schmidt, G., 2000. Scheduling with limited machine availability. European Journal of Operational Research, Amsterdam, v. 121, p. 1-15.

Talbi, E.G., 2003. *Metaheuristics*: from design to implementation. New Jersey: John Wiley & Sons Inc., 593 p.

A Surveillance Application of Satellite AIS
Utilizing a Parametric Model for Probability of Detection

Cheryl Eisler[1], Peter Dobias[1] and Kenzie MacNeil[2]
[1]*Defence Research and Development Canada – Centre for Operational Research and Analysis, 101 Colonel By Drive, Ottawa, ON, Canada*
[2]*CAE Inc., 1135 Innovation Drive, Ottawa, ON, Canada*
{cheryl.eisler, peter.dobias}@drdc-rddc.gc.ca, kenzie.macneil@cae.com

Keywords: Satellite Automatic Identification System (S-AIS), Surveillance, Probability of Detection, Parametric, Performance, Model, Signal Collision.

Abstract: The question of having sufficient surveillance capability to detect illicit behaviour in order to inform decision makers in a timely fashion is of the ultimate importance to defence, security, law enforcement, and regulatory agencies. Quantifying such capability provides a means of informing asset allocation, as well as establishing the link to risk of mission failure. Individual sensor models can be built and integrated into a larger model that layers sensor performance using a set of metrics that can take into account area coverage, coverage times, revisit rates, detection probabilities, and error rates. This paper describes an implementation of a parametric model for Satellite Automated Identification System (S-AIS) sensor performance. Utilizing data from a real data feed, the model was able to determine the percentage of uncorrupted S-AIS messages and the probability of detection of at least one correct S-AIS message received during an observation interval. It is important to note that the model implementation was not actively calculating the effect of message overlap based on satellite altitude and footprint width, or reductions in collisions due to signal de-collision algorithms.

1 INTRODUCTION

The awareness and associated tracking of maritime vessels approaching and within a country's territorial waters (TTW) and its exclusive economic zone (EEZ) are necessities for the enforcement of environmental and commercial laws and regulations, as well as national security and the protection of public safety. This makes maritime domain awareness (MDA) a national priority. There are two aspects to MDA: the quality and quantity of data to collect and fuse, and the reporting/prediction metrics that are used to gather the information into a quantifiable, comparable fashion for decision support. The former is well recognized as an issue for data analytics, data fusion, and big data research topics. The latter falls under the more traditional operational research umbrella, and will be discussed in this paper. The data analytics problem is beyond the scope of this discussion; for a more detailed treatment of data collection requirements for MDA, see Horn *et al.* (2016) and references therein.

Metrics that can be used for historical reporting and forecasting of upcoming activities are of particular interest at the operational level because they provide critical information to military decision makers about the use of surveillance capabilities, such as:

- Will the surveillance capabilities provide sufficient means to detect illicit behaviour?
- What is the likelihood that illicit behaviour would go undetected?
- Will the surveillance capabilities provide sufficient temporal and spatial coverage of the area of responsibility (AOR) to be able to inform decisions in a timely fashion?

The answers to these questions are of the ultimate importance to defence, security, law enforcement, and regulatory agencies, as they provide means of informing asset allocation, as well as establishing a link to the risk of mission failure for given capability sets.

The purpose of this research is to select one surveillance sensor – in this case, the Automatic Identification System (AIS) – to model the performance of, and use it as a test case towards

Eisler, C., Dobias, P. and MacNeil, K.
A Surveillance Application of Satellite AIS - Utilizing a Parametric Model for Probability of Detection.
In *Proceedings of the 6th International Conference on Operations Research and Enterprise Systems (ICORES 2017)*, pages 211-218
ISBN: 978-989-758-218-9

building a more complex, layered model of surveillance capabilities. This will enable reporting and planning for the given capability sets.

This paper is organized as follows. Section 2 provides a brief description of how AIS functions, the utility of the selected sensor, and the inherent complications when trying to model such a sensor. Section 3 describes the simplified performance model chosen and the associated advantages of using such a sub-model within a larger model. Section 4 illustrates how the sensor and performance model were implemented, and provides a test case using real world data from an AIS feed to compute performance parameters. Section 5 discusses some of the limitations of the current model and implementation, and presents proposals for future work. Section 6 concludes the paper.

2 THE AUTOMATIC IDENTIFICATION SYSTEM

One sensor that is now commonly exploited for MDA is AIS, which is a self-reporting system that was designed for enhancing the safety of navigation at sea. AIS transponders are mandated by the International Convention for the Safety of Life at Sea (SOLAS) Convention, 1974 (International Maritime Organization, 2015) for all ships over 300 gross tonnage, all passenger-carrying vessels, and can be used by other vessels on a voluntary basis.

Vessel-mounted AIS transponders are broken into two types. Class A transponders are required on the mandated vessels described previously. Class B transponders are a lower power, less expensive technology which transmit less frequently than their Class A counterparts, and are often used on smaller vessels. It can be estimated that AIS is utilized on anywhere from approximately 400,000 to over 550,000 ships, navigational aids, base stations, and other sources (including active and decommissioned vessels), depending on the data provider (myShipTracking, 2016; MarineTraffic.com, 2016). While the fraction of active Class A versus Class B sources are not directly reported, this does provide a sense of the volume of information received by tracking networks when ships are reporting anywhere from 2 seconds to 6 minutes apart (International Telecommunications Union, 2014).

2.1 Sensor Utility

Terrestrial-based tracking networks provide a means of continuously monitoring so equipped ship traffic within the detection range of the shore-based stations. However, AIS signals were found to be detectable from satellite-based receivers as well. Some of the main limitations with satellite AIS (S-AIS) are the amount of sensor coverage and the revisit rates of the satellite, which can be mitigated in part by monitoring from multiple satellites. So, while coastal AIS systems are advantageous for monitoring of the TTW and a fraction of the EEZ – with distances depending on very high frequency (VHF) ducting properties (Tunaley, 2011a), S-AIS has moved to the forefront of technologies for wide-area surveillance at high refresh rates for reach over almost any AOR.

S-AIS is usually employed in conjunction with other sensors, such as coastal radar (Canadian Coast Guard, 2016), high-frequency surface wave radar (Vesecky *et al.*, 2009), satellite-based synthetic aperture radar (Guerriero *et al.*, 2008), or visual identification (or other onboard sensors) using maritime or aerial assets (Busler *et al.*, 2015). This helps to mitigate some of the known issues with data quality (such as signal errors, technical installation or input errors, or spoofing (Bošnjak *et al.*, 2012)).

2.2 Modelling Complications

Technically, however, S-AIS also suffers from further complications due to the simultaneous reception of a high number of messages within the large reception footprint in conjunction with the AIS communication standard (International Telecommunications Union, 2014). The design of the AIS message system into discrete, fixed width slots limits the reception of messages at the receiver, and the sheer volume of the AIS message traffic produces a high probability of message collision (i.e., message arrivals within the same time slot). On-board processing (OBP) of messages cannot fully resolve such collisions, and as a result, the first pass detection is low (exactEarth, 2012) when ship traffic is dense. While much can be done in terms of antenna design and signal processing (Yang *et al.*, 2014; Yang *et al.*, 2012; Picard *et al.*, 2012) to reduce these effects, there still exists a significant impact on the sensor's overall detection performance.

Some providers have chosen to downlink all messages to ground stations for more efficient spectrum de-collision processing (SDP) (Macikunas and Randhawa, 2012). Algorithms have been proposed and/or implemented (e.g., Cowles *et al.*, 2014; Cherrack *et al.*, 2014) to increase the detection

performance; however, the time latency of the data is dramatically increased (Meger, 2013).

3 SIMPLIFIED S-AIS MODEL

For the purposes of historical reporting and forecasting of upcoming activities at the operational level for defence primarily (but also including security, law enforcement, and regulatory agencies), the following considerations and assumptions are made:

- Any model must run in a practical amount of time so as to be able to provide timely and meaningful decision support (typically viewed as 1-2 days for short turn-around analyses). Thus, simpler is better;
- When representing the capabilities of a system that link to the risk of mission failure, often the "worst case scenario" is chosen to represent the ultimate limit of the system's capabilities. So, for example, if ground stations were unable to perform SDP for some reason, then OBP would be considered the minimum capability provided. It also provides a consistent model and assumption set across all S-AIS providers, since some perform SDP and some perform OBP;
- From a reporting/forecasting standpoint, the timeslots of individual messages are unknown (data not provided), and so the de-collision process cannot be reproduced and modelled directly. While the signal de-collision process can be simulated, it is easier to implement a direct relationship between the number of ships and the probability of detection; and
- Since not all AIS providers utilize SDP, it is assumed that a generic model that can be applied across any provider would provide more utility. It could later potentially be scaled to account for SDP.

3.1 Single Sensor Model

In order to be able to quantify the ability of a collection of disparate sensors, each with their own area coverages, coverage times, revisit rates, detection probabilities, and error rates (false positives, false negatives, bit rate errors, etc.), a set of metrics that can take all of these factors into account is required. Individual sensor models can be built and integrated into a larger model that layers sensor performance over an AOR for a comprehensive capability to report on historical coverages and test out future surveillance plans. High fidelity tools, such as the Systems Tool Kit (STK), can be used to build such a model. The satellite selected for the application here was exactView-1, one of the exactEarth™ constellation of satellites.

Modelling of the coverage of active or non-cooperative passive sensors (i.e., independent of the cooperation of a vessel) in a software package such as STK is generally straightforward; however, modelling of cooperative sensors such as AIS can be more challenging. While all vessels must be represented as objects in a modelled scenario in STK, this does not mean that they can or should be detected by sensors at all times. Different vessels transmit AIS messages at different times and at different rates; therefore, the sensor cannot automatically assume it can "see" the vessel all of the time.

3.2 Sensor Detection Performance

Høye (2004) quantified the parametric relationship between the number of ships in the S-AIS sensor's field of view (FOV) and the probability of detecting a single ship; however, it was assumed that message collisions could not be de-conflicted. Tunaley (2011b) later showed that the probability of extracting an uncorrupted message, γ, from the simultaneous arrival of another singleton message can be derived in the presence of thermal noise, interference from neighbouring channels or even interference in the same channel from terrestrial transmitters (Eq. 1).

$$\gamma = \gamma_o e^{-\lambda \tau_o (1-q)(1+s)} \quad (1)$$

The explanations for, and the values of the parameters in Eq. (1) from (Tunaley, 2011b) for a satellite at 800 km altitude are provided in Table 1. Høye (2004) reports the difference in the s values between 600 km and 800 km altitude as 0.0382, while the difference in the s value between 800 km and 1,000 km altitude as 0.0248. Therefore, the average difference between each 1 km of altitude is ~0.0002. This means the 5 km to 40 km offset in the STK exactView-1 satellite object's altitude has a negligible effect on the 0.6744 value of s for a satellite with 800 km altitude. As a result, a fixed s value was used for the initial model (MacNeil, 2015).

Table 1: Equation parameter definitions.

Parameter	Name	Value
γ_o	Probability of receiving an uncorrupted message at the input system regardless of collisions	0.2683
λ	Mean rate of random messages arriving	Eq. (2)
τ_o	Length of slot (s)	0.0267
q	Probability that an additional signal does not corrupt the message	0.904
s	Effect of range overlap	0.674
M	Number of ships inside the ships cell	Assumed negligible
n_{ch}	Number of VHF channels	2
ΔT	Mean time between message transmissions (s)	Calculated

The mean rate of message arrival (λ) as a function of number of ships (N) in the FOV is given in Eq. (2), with parameter values also provided in Table 1.

$$\lambda = \frac{N - M}{n_{ch}\,\Delta T} \tag{2}$$

Substituting λ from Eq. (2) and all parameter values from Table 1 in Eq. (1) yields Eq. (3).

$$\gamma = \gamma_o e^{-\frac{N}{2\,\Delta T}\tau_o(1-q)(1+s)} \tag{3}$$

$$\gamma = 0.2683 e^{(-0.002145)\frac{N}{\Delta T}}$$

The probability that at least one correct AIS message will be observed during a given interval (T_{obs}) (Tunaley, 2011b) is provided in Eq. (4) after substituting in Eq. (2).

$$p = 1 - \left(1 - \gamma_o e^{-\frac{N}{2\Delta T}\tau_o(1-q)(1+s)}\right)^{T_{obs}/\Delta T} \tag{4}$$

3.3 Model Implementation

The parametric model was implemented using STK to perform its satellite modelling and line-of-sight (LOS) calculations (MacNeil, 2015). The MATLAB scripting language was also selected for use, as it integrates directly with STK and automates the execution of STK commands. The model implementation was driven by a series of MATLAB scripts to perform LOS analysis in STK between a satellite sensor, representing exactView-1 AIS, and three predefined AORs (shown in white in Figure 1). These line-of-sight analyses are referred to in STK as access calculations.

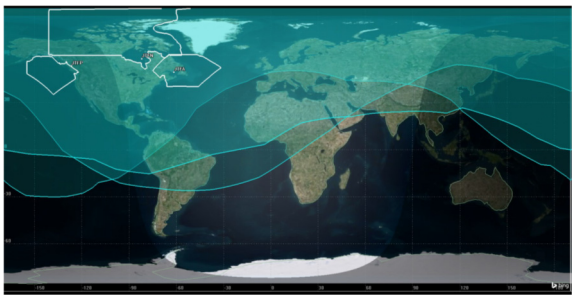

Figure 1: Three Canadian AORs (white outlines) and the exactView-1 AIS sensor FOV (cyan overlay) over time when access is available to each AOR.

The parametric model was designed to take geographically-tagged JavaScript Object Notation (GeoJSON) S-AIS messages from the exactEarth™ satellite feed and calculate the probability of extracting an uncorrupted message when the exactView-1 AIS sensor FOV has access to an AOR. One day's worth of S-AIS position reports (approximately 4.5 million messages) were filtered for Class A messages only. To reduce the problem set, the target areas were selected by the union of all areas covered by the exactView-1 AIS sensor footprint when the sensor had access, or LOS, to each of the AORs separately during the defined scenario period. This left approximately 2.2 million position reports to process. The execution of the model was then broken down into three sequential operations (MacNeil, 2015):

1. Partitioning and reformatting S-AIS position reports into separate ship files based on unique Maritime Mobile Service Identity (MMSI) numbers;
2. Creating the relative STK ephemeris and interval constraint files for each ship; and
3. Analyzing the STK satellite-to-ship access data for each AOR, and collating the data to determine the probability of extracting an uncorrupted message for each observation period.

Additional algorithm implementation details are provided in the paper's appendix.

4 RESULTS

The partitioning and reformatting of the S-AIS position reports took 14.3 hours to complete on a 3.20 GHz Intel® Core i5-4570 with 8 GB (3.18 GB usable) RAM and an Intel® HD Graphics 4600 processor graphics card. The script produced over 61,000 partitioned S-AIS ship data files. The script

excluded, or dropped, message rows that were not Class A position report messages.

The execution of the script to create the STK ephemeris and interval constraint files for each ship took 7.5 hours to complete. The script produced over 43,000 files of each type. The script excluded, or dropped, partitioned ship files that existed outside of all three AOAs.

The creation of the STK scenario and analysis of the satellite-to-ship access took 7.7 hours to complete. Each sensor FOV included approximately 29-39,000 individual ship objects. During the scenario, there were 11-14 access intervals for the AORs. Each access interval was treated as a separate observation period for the purposes of the following results.

For the scenario considered, the execution time was relatively reasonable. However, it may prove challenging to remain within practical time limits when integrating further sensors into the mix, depending on the amount of computations that can be leveraged between sensors. One way to speed up the computations would be to take advantage of MATLAB and STK's parallel processing features; however, both require specialized licensing.

4.1 Uncorrupted Messages

For each access interval, the probability of receipt of an uncorrupted message was calculated using Eq. (3). Given that the duration of each access interval varies, as does the number of messages received, the mean time (ΔT) between messages could not be considered to be constant. ΔT was calculated using the total access duration divided by the number of messages received for the given interval, Figure 2 results, where the data points for the access intervals are shown individually (diamonds) on plots of the function from Eq. (3). The function plots match the access interval ΔT values, while varying the number of ships in the FOV. As the number of ships in the FOV increases or the time between messages decreases the probability of receipt of an uncorrupted message decreases. Thus, as more ships that exist within the FOV and transmit messages more often, the more likely the signal collisions are to cause corruption in the messages.

Previous implementations (such as Tunaley, 2011b; Parsons *et al.*, 2013) assume that the mean time between messages and the observation time are fixed. Here, a single pass of the satellite is utilized over a variable observation time frame, as determined by the sensor's access time to each

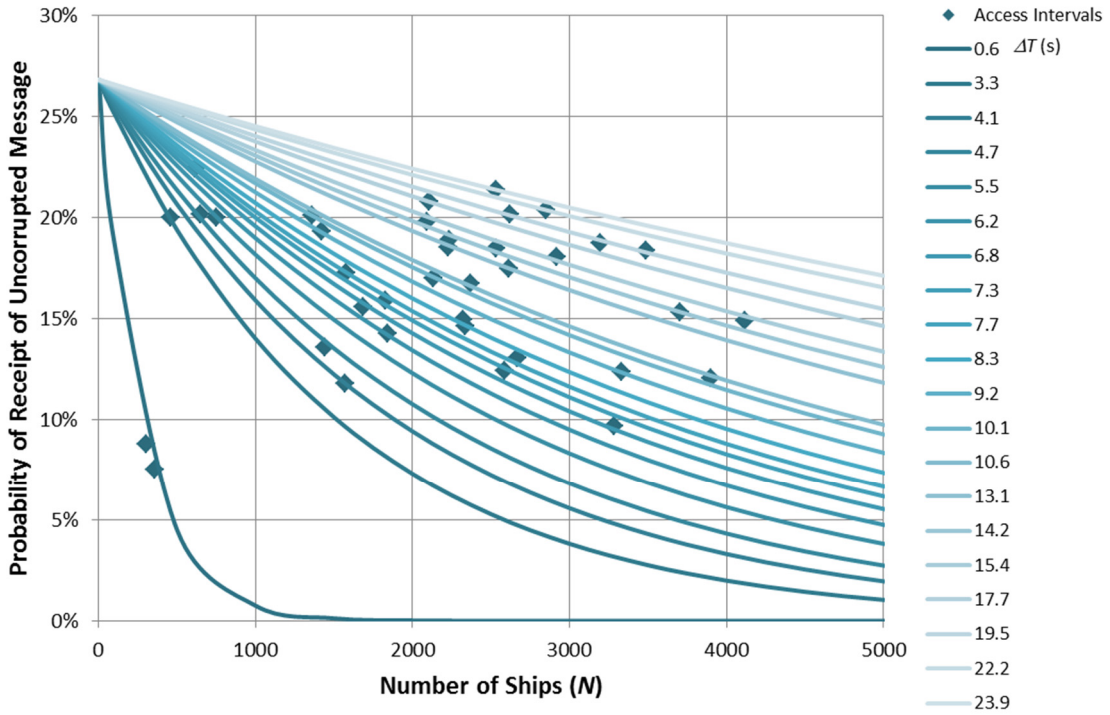

Figure 2: The fraction of messages that are uncorrupted as a function of number of ships in the sensor FOV and the mean time between messages.

AOR. This time frame is significantly longer than the average time a ship is visible within the sensor footprint. The mean time between messages is then calculated based on the received data within that time frame. This cross validates the equation parameters from Table 1, as well as the basic model for on-board processing system performance.

4.2 Probability of Detection

From Eq. (4), $T_{obs}/\Delta T$ is essentially the count of the number of detections in the FOV over the duration of the access interval. Because the FOV is large and the access duration is long, the number of detections observed is in the thousands or tens of thousands. As a result, this term tends to zero, resulting in a near 100% probability of detection of at least one uncorrupted AIS message from any given ship in the FOV.

While edge effects from the shape of the footprint (which is a circular beam projected at an angle over a spherical surface) will reduce the amount of time some ships will remain observed, the observed time would have to be reduced by more than 92% to see any less than 99% probability of detection of at least one correct AIS message.

5 DISCUSSION

Since the purpose of this work was to create a simple preliminary model that could be used as the basis for further integrated model development, there were some noted issues that are planned to be addressed in future work.

5.1 Message Quantity and Quality

The GeoJSON data is contained in a large text file that is organized according to a contact identification column and not by date/time stamp, which makes it difficult to perform read search and sort operations in MATLAB. Initial file parsing would likely be better suited to database operations either through a performed with Structured Query Language (SQL) commands through either a Python or C++/C# application (MacNeil, 2015). An application written in Python would be easier to update and modify since it is a dynamically typed scripting language, and could be integrated with technologies such as ArcGIS for geo-filtering of data points. Programs written in C++/C# are compiled to native machine code, and can be very computationally quick. An application written in C# would also easily integrate with the STK Integration plugin.

Naturally, since the topic deals with corrupted AIS messages, the quality of the data from the AIS feed can be an issue to parse. From the data, it was noted that there were objects that travel semi-erratically across the globe, ship MMSIs which consistently reported the same, or very similar, invalid positions, and objects which contain a single invalid, potentially corrupt message. The first step in helping to resolve some of these issues would be to filter the AIS messages based on Tunaley (2013). This would restrict the MMSIs to valid ship codes of interest. By extending the model to more satellites and to global coverage, location-specific issues should also be resolved.

It is also important to note that the precision of the GeoJSON formatted S-AIS data's report and received date/time is to the second. The time length of a single AIS transmission time slot is 0.0267 seconds. Thus, a small amount of error is introduced when parsing the data.

5.2 Model Refinement

At the moment, the values for the parameters in the governing equations are primarily taken from Tunaley (2011b). The next level of refinement to the model would be to determine the current values for s and q based on the scenario satellite data instead of using a constant value. While a brief analysis of the s value revealed that the difference between a fixed and dynamic value is small; it represents an increase in fidelity of the model and supports extensibility to other satellites. This would require implementing Høye's (2004) model to determine the value based on STK's exactView-1 satellite object's altitude and the partition of the satellite's sensor detection area.

As mentioned in Section 4.1, the model and scripts should be modified to support the entire exactEarth™ satellite constellation. This would enable the computation of the performance of the sensor system as a whole.

As well, the model and scripts could also support global coverage analysis. This would require the removal of the dependency on the AOR access times from the current model and the addition of another time analysis metric (MacNeil, 2015).

5.3 Model Integration

It is intended that, once the entire satellite constellation is modelled, this becomes a sub-model in a larger, layered approach to surveillance

capability planning and reporting. Thus, rather than trying to compare apples to oranges with active/passive versus co-operative sensors, the overall performance of the S-AIS sensor system can be utilized in a simplified fashion to compute the probability of detecting ships. Other sensors and platforms can be integrated over various time frames to determine what combination of capabilities provides sufficient temporal and spatial coverage of the AOR to meet the decision-makers' requirements.

6 CONCLUSIONS

A parametric model (Tunaley, 2011b) for S-AIS senor performance was successfully implemented in STK. Utilizing data from the real S-AIS feed, the model was able to determine the percentage of uncorrupted AIS messages and the probability of detection of at least one correct AIS message received during an observation interval for a one-day scenario period. This model provided a reasonable start towards building a more complex, layered model of surveillance capabilities for reporting and forecasting for defence security, law enforcement, and regulatory applications.

The implementation utilized real-world data to cross-validate the model assumptions and application over a wide variety of inputs. It is important to note that the model implementation was not actively calculating the effect of message overlap based on S-AIS sensor altitude and footprint width for the different satellite altitudes during its orbit. Although an analysis of the effect of message overlap revealed that the difference between the static and calculated values would be minor; further model refinements should still take such details into account. The model and scripts serve as a foundation for future improvements and extensions in both the scope of the model and the performance of the implementation.

COPYRIGHT

REFERENCES

Bošnjak, R., Šimunovića, L., and Kavran, Z., 2012. Automatic Identification System in Maritime Traffic and Error Analysis, *Transactions on Maritime Science*, 02, 77-84.

Busler, J., Wehn, H., and Woodhouse, L., 2015. Tracking Vessels to Illegal Pollutant Discharges Using Multisource Vessel Information, In *36th International Symposium on Remote Sensing of Environment*, The International Archives of the Photogrammetry, Remote Sensing and Spatial Information Sciences, XL-7/W3, 927-932.

Canadian Coast Guard, 2016. Marine Communications and Traffic Services MCTS, Government of Canada. Retrieved from: http://www.ccg-gcc.gc.ca/Marine-Communications/Home (Access Date; 13 September 2016).

Cherrak, O., Ghenniou, H., Thirion-Moreau, N., and Abarkan, E., 2014. Successive Interference Cancellation technique for decollision of AIS signals in maritime surveillance context by a LEO satellite, In *La première édition du Workshop International sur les nouvelles Technologies sans fil et Systèmes répartis*, WITS.

Cowles, P.R., D'Souza, I.A., and Peach, R.C., 2014. Satellite detection of automatic identification system signals, Patent CA 2691120 C, viewed 10 Dec 2016, http://www.google.com/patents/CA2691120C?cl=en.

exactEarth, 2012. Satellite AIS and First Pass Detection: An exactEarth White Paper, viewed 10 Dec 2016, http://cdn2.hubspot.net/hub/183611/file-30951507-pdf/Collateral_for_Download/First_Pass_Detection_White_Paper.pdf.

Guerriero, M., Willett, P., Coraluppi, S., and Carthel, C., 2008. Radar/AIS Data Fusion and SAR tasking for Maritime Surveillance, In *11th International Conference on Information Fusion*, IEEE, 1650-1654.

Horn, S., Collins, Lt(N) J., Eisler, C., and Dobias, P., 2016. Data requirements for anomaly detection, In *2016 Workshop on Maritime Knowledge Discovery and Anomaly Detection*.

Høye, G., 2004. Observation Modelling and Detection Probability for Space-Based AIS Reception – Extended Observation Area, *FFI Report*, FFI/RAPPORT-2004/04390.

International Telecommunications Union, 2014. Technical characteristics for an automatic identification system using time division multiple access in the VHF maritime mobile band (Recommendation ITU-R M.1371-4), viewed 8 Dec 2016, https://www.itu.int/dms_pubrec/itu-r/rec/m/R-REC-M.1371-5-201402-I!!PDF-E.pdf.

Macikunas, A. and Randhawa, B., 2012. Space-based Automated Identification System (AIS) Detection Performance and Application to World-wide Maritime

Safety", In *30th AIAA International Communications Satellite Systems Conference*, ICSSC.

MacNeil, K., 2015. DRDC CORA Task #194: Coastal Surveillance Model Development, Defence Research and Development Canada – Centre for Operational Research and Analysis, DRDC-RDDC-2015-C283.

MarineTraffic.com, 2016. Ships List – Vessel Search | AIS Marine Traffic, viewed 10 Dec 2016, http://www.marinetraffic.com/en/ais/index/ships/all/status:all.

Meger, E., 2013. Limitations of Satellite AIS: Time Machine Wanted!, viewed 10 Dec 2016, http://d284f45nftegze.cloudfront.net/emeger/White%20Paper%20-%20Limitations%20of%20Satellite%20AIS%20-%20Time%20Machine%20Wanted.pdf.

myShipTracking, 2016. My Ship Tracking Free Realtime AIS Vessel Tracking Finder Map, viewed 10 Dec 2016, http://www.myshiptracking.com/search/vessels.

Parsons, G., Youden, J., Yue, B., and Fowler, C, 2013. Satellite Automatic Identification System (SAIS) Performance Modelling and Simulation: Final Findings Report, Defence Research and Development Canada – Ottawa, DRDC Ottawa CR 2013-096.

Picard, M., Ourlarbi, M.R., Flandin, G., and Houcke, S., 2012. An Adaptive Multi-User Multi-Antenna Receiver for Satellite-Based AIS Detection, 6th Advanced Satellite Multimedia Systems Conference and 12th Signal Processing for Space Communications Workshop, IEEE, 273-280.

International Maritime Organization, 2015. SOLAS 1974, Chapter V, Regulation 19. Retrieved from http://www.imo.org/en/About/Conventions/ListOfConventions/Pages/International-Convention-for-the-Safety-of-Life-at-Sea-(SOLAS),-1974.aspx (Access Date: 13 September 2016).

Tunaley, J.K.E., 2011a. Space-Based AIS Performance, *London Research and Development Corporation Technical Report*, LRDC 2011-05-23-001.

Tunaley, J.K.E., 2011b. The Performance of Space-Based AIS System, *London Research and Development Corporation Technical Report*, LRDC 2011-06-20-001.

Tunaley, J.K.E, 2013. Utility of Various AIS Messages for Maritime Awareness, *London Research and Development Corporation Technical Report*, LRDC 2013-10-001.

Vesecky J.F., Laws, K., and Paduan, J.D., 2009. Using HF surface wave radar and the ship Automatic Identification System (AIS) to monitor coastal vessels, In *Geoscience and Remote Sensing Symposium*, IEEE, Volume 3.

Yang, J, Cheng, Y., and Chen, L., 2014. The Detection Probability Modeling and Application Study of Satellite-Based AIS System, In *7th Joint International Information Technology and Artificial Intelligence Conference*, IEEE.

Yang, M., Zou, Y, and Fang, L., 2012. Collision and Detection Performance with Three Overlap Signal Collisions in Spaced-Based AIS Reception, In *11th International Conference on Trust, Security and Privacy in Computing and Communications*, IEEE, 1641-1648.

APPENDIX

The parametric model is written in MATLAB as a series of steps (Figure 3) that process the selected user input data, perform all necessary conversions, and control the execution of STK to compute the LOS calculations necessary to support computation of the probability of reception of an uncorrupted message given the number of ships in the sensor's FOV over a given period of time.

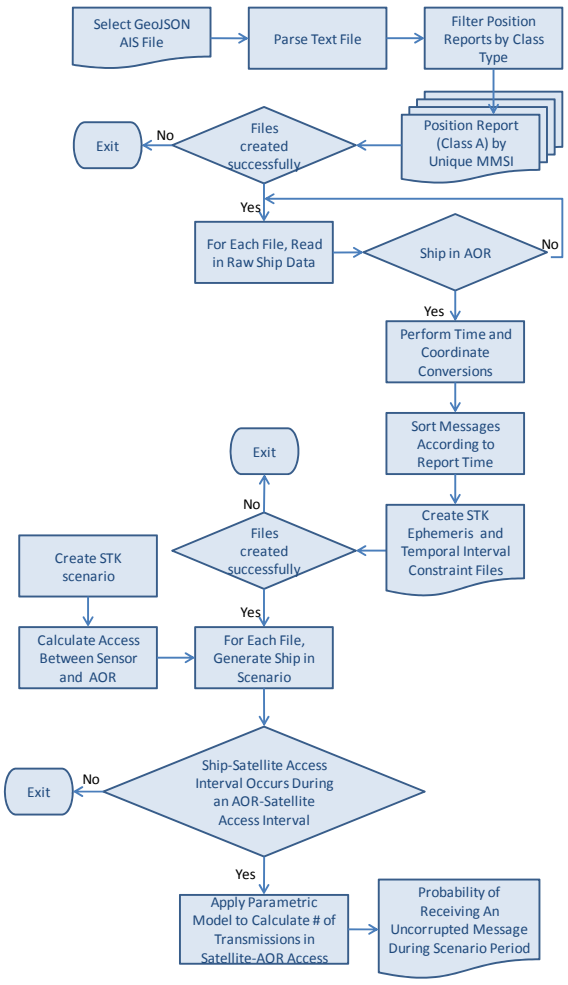

Figure 3: Parametric model implementation in MATLAB.

Design a Study for Determining Labour Productivity Standard in Canadian Armed Forces Food Services

Manchun Fang
Centre of Operational Research and Analysis, Defence Research Development Canada, National Defence Canada, 101 Colonel By Drive, Ottawa, Canada
manchun.fang@forces.gc.ca

Keywords: CAF Food Services, Performance Measure, Labour Productivity, Study Design.

Abstract: Canadian Armed Forces (CAF) Food Services recently implemented a standardized menu at all static service locations. Within this new regime, CAF Food Services requires a standard against which they can measure labour performance and use to inform future rationalization of staffing. To start, a pilot study was conducted in February and March 2015 to collect labour performance data. In this paper, we review the results from the pilot study. Due to issues identified with the pilot study, this paper also proposes a revised design and analytical approach for a follow-on study.

1 INTRODUCTION

Canadian Armed Forces (CAF) Food Services is a decentralized function with an estimated value exceeding $150 Million in cost per year for fresh feeding. As functional authority for CAF Food Services, Strategic Joint Staff (SJS) Directorate Food Services recently implemented a three-week National Standardized Cycle Menu (NSCM) on all static feeding facilities, which has been rolled out across all CAF static feeding facilities since the beginning of November 2014. However, currently CAF Food Services does not have a labour performance standard that can be used to measure and compare the labour performance in CAF Food Services (Mat J4 2014).

Unlike most of other food industry, the CAF Food Services is not profit driven and fulfilling the operational needs is its first priority. Determining a CAF specific labour performance standard for CAF Food Services is significant. As a start, SJS Directorate Food Services planned a pilot study and collected labour performance data in February and March 2015. Directorate Materiel Group Operational Research (DMGOR) was later tasked to provide analytical support. The objective of this work is to review the results from the pilot study. Furthermore, due to the issues identified with the pilot study, the work is also used to provide SJS Directorate Food Services a more rigorous study design and analytical approach for a future follow-on study.

2 RESULTS FROM THE PILOT STUDY

2.1 Data Collection

It is noted here that Operational Research and Analysis was not significantly consulted to set up of the pilot study including the aspects, e.g., the target determination, sample selection, and the sample size determination. In addition, the grouping of facilities and the order of visits were determined by financial consideration, i.e., minimizing the travel cost, not by statistical consideration. Furthermore, the choices of the dates were not randomly selected and the facilities were aware of the dates of visits prior to the data collection.

An existing Excel-based Labour Performance Data Collection Tool (Whiting 2015) was used in the data collection process. Annex A Tables A1 provides a summary of data obtained from the pilot study.

2.2 Data Exploration

This section will summarize the results from the pilot study. Although the design of the pilot study is

Fang, M.
Design a Study for Determining Labour Productivity Standard in Canadian Armed Forces Food Services.
In *Proceedings of the 6th International Conference on Operations Research and Enterprise Systems (ICORES 2017)*, pages 219-227
ISBN: 978-989-758-218-9

not ideal, it provides useful prior information needed for designing a more rigorous future follow-on study.

Volume of Activity

In CAF Food Services, Volume of Activity is used to record the number of meals (including breakfast, lunch and dinner) served in a facility during a fix time period (e.g., daily, monthly or yearly). For the pilot study, Volume of Activity records the total number of meals served during the pilot study period, i.e., a five day period. The Volume of Activity for five days ranges from 2,161, 2,335, 3,037, 4,514, 10,613 and 17,883 for Halifax, Esquimalt, Trenton, Wainwright, Gagetown and Saint-Jean respectively.

Number of Meals per Labour Hour

The number of meals per labour hour is calculated by dividing the total number of meals served by the total number of labour hours spent including labour hours spent by both military and civilian employees see eqn. (1):

$$Number\ of\ meals\ per\ labour\ hour = \frac{Number\ of\ meals\ served}{Total\ labour\ hours\ spent} \quad (1)$$

There is a large variation on the number of meals per labour hour across facilities calculated, which are 1.8, 1.9, 3.6, 3.9, 4.3 and 5.3 for Esquimalt, Halifax, Wainwright, Gagetown, Trenton and Saint-Jean respectively (data from Table A.1).

The Volume of Activity is reported as the most important factor that has impact on the labour productivity (Tremblay 2004). The data from the pilot study also suggests that except for Trenton (Different from the other facilities, Trenton also provides flight feeding which requires less time on serving the food than the in person serving.), there is a relationship between the Volume of Activity and the Number of Meals Per Labour Hour: i.e., the greater the Volume of Activity, the greater the Number of Meals Per Labour Hour (which is consistent with the finding in Tremblay 2004) (See Figure 1).

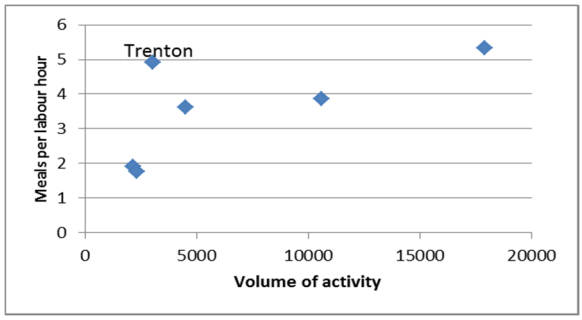

Figure 1: Volume of activity vs. number of meals per labour hour.

Labour Cost per Meal

Table 1 shows that labour cost per meal varies significantly across facilities, which is $3.85, $4.83, $6.22, $6.89, $13.35 and $13.57 for Saint-Jean, Trenton, Gagetown, Wainwright, Halifax and Esquimalt respectively. Some facilities have much higher labour costs per meal than the others, e.g., Halifax and Esquimalt. It needs to be noted that the food material costs and non-food costs (e.g., cost for paper plates) are not included in these figures. Therefore the total cost per meal (including all labour, food material and non-food costs) should be even higher. As such, the total cost per meal in some facilities apparently will not be recoupable by the payments from the diners.

Table 1: Labour cost per meal by facility.

Facility	# of	Total	Labour
Saint-Jean	17,883	$68,775	$3.85
Trenton	3,037	$14,678	$4.83
Gagetown	10,613	$65,972	$6.22
Wainwright	4,514	$31,117	$6.89
Halifax	2,161	$28,855	$13.35
Esquimalt	2,335	$31,686	$13.57

SJS Directorate Food Services reported that the labour rate per hour is the same across CAF Food Services facilities. Therefore, the labour cost per meal is mainly influenced by the labour productivity, i.e., the number of meals per labour hour. It is intuitive that the more meals per labour hour produced the less labour cost per meal. Figure 2 shows this negative correlation between the number of meals per labour hour and labour cost per meal.

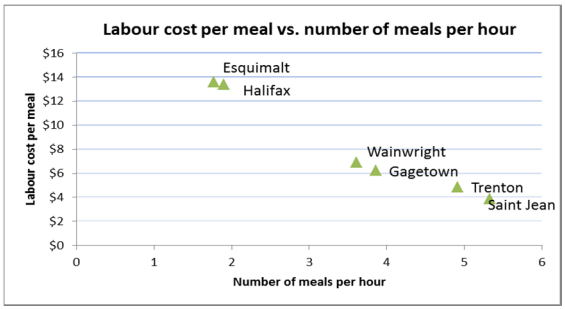

Figure 2: Labour cost per labour hour and number of meals per labour hour.

Additionally, since salary difference exists among different ranks of military cooks and between military and civilian cooks, the labour cost per meal will also be influenced by rank composition of military cooks and civilian and military labour ratio in the facility (see Figure 3).

Figure 3 shows the percentage of civilian hours versus military hours in preparing the meals across facilities. The multiple proportion test shows there is a significant difference (p-value<0.01) on civilian military hours ratios among facilities. The figures for Halifax and Saint-Jean facilities are significantly different; Halifax uses the least civilian labour (52%) and Saint-Jean uses the most civilian labour (90%) among all six facilities.

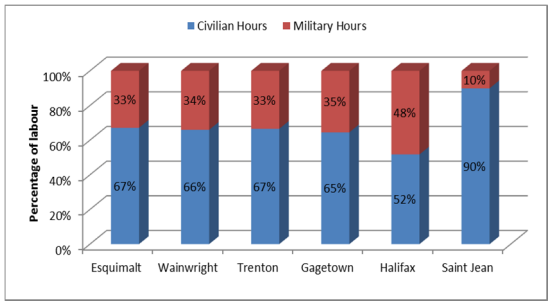

Figure 3: Percentage of civilian vs. military hours spent on preparing meals in the six facilities.

All these data have been incorporated in the calculation of the labour cost per meal in the pilot study.

3 STUDY DESIGN

Due to the issues identified about the approach taken to conduct the pilot study, a new study and its alternative details in study design and method of analysis are proposed.

3.1 Objective of the Study

The study design is driven and determined by the objective of the study. Ultimately, CAF Food Services would like to establish a labour performance standard that can be used to measure and compare the measure performance and inform food services staffing. For this study, as requested, it will only focus on the quantitative side of the labour performance, i.e., the labour productivity.

3.2 Two Labour Performance Standards Should Be Established

With regard to the labour productivity, the first question is: can we set up a uniform labour productivity standard for all facilities in CAF Food Services?

Due to the big variation currently existing on the labour productivity across facilities (as shown in Figure 1), we believe it does not make sense to establish just one labour productivity standard at this time. Based on the data from the pilot study, it is recommended two labour performance standards be established at first:

- one labour performance standard for small facilities (in terms of facilities with small Volumes of Activity); and
- one for large facilities (in terms of facilities with large Volumes of Activity)

3.3 Choice of Target Population

The target population is the population about which information is wanted (Cochran 1977). The choice of the target population should be determined by the objective of the study. The choice of target population will profoundly affect the statistics that result (Lohr & Stratton 2010). Should the target population be composed of all feeding facilities in CAF Food Services? The answer is "No". The reason is because the objective of this study is to develop a labour performance standard for the CAF Food Services not just to get an overall labour performance measure for CAF Food Services. Rogers 2014 provides a clear definition of "standard": "Standard can refer to an aspect of performance, or to the level of performance, or to a combination of both. These standards can be considered minimum levels required, or levels required to be considered best practice." In our context, the labour performance standard here refer to the aspect of labour productivity and the level of the labour productivity; and the standard is

considered as the best practice in CAF Food Services. Therefore, to determine the labour productivity standard for the CAF Food Services, we do not recommend using the entire CAF feeding facilities as the target population; instead we recommend the target population consist of facilities which represent the best practice in CAF Food Services in terms of labour performance, i.e., labour productivity in this study.

Therefore, based on military knowledge about CAF Food Services, SJS Food Service provided the following seven facilities to form the target population, i.e., Saint-Jean, Gagetown, Trenton, Wainwright, Shilo, Cold Lake and Bagotville. These facilities were chosen based on the following considerations:

- examples of CAF feeding facilities with good labour performance, from which the labour performance standard can be drawn from;
- regional consideration (i.e., west, central and east); and
- choice of both operational and training facilities.

3.4 Suggested Grouping of Facilities

According to the annual Volume of Activity for FY14/15 obtained from (Whiting and St-Cyr 2015 & Whiting 2015), these seven facilities have been classified into two groups (Table 2), i.e., small and large facility groups. The facility is classified as a small facility if its annual Volume of Activity is less than 100,000 meal day (Meal day is another way to measure the Volume of Activity. One meal day is equal to three meals.); while the facility is classified as a large facility if its annual Volume of Activity is equal to or greater than 100,000 meal days (Record of Discussion May 2015). Based on these criteria, Saint-Jean, Gagetown, Trenton and Wainwright are classified as large facilities while Shilo, Cold Lake and Bagotville are classified as small facilities.

As described in Section 3.2, two labour performance standards should be established for these two groups respectively.

Table 2: Grouping of seven facilities.

Facility	Meal days	Grouping
Gagetown	267,514	Large
Trenton	127,044	Large
Wainwright	136,269	Large
Saint-Jean	347,940	Large
Shilo	57,590	Small
Cold Lake	69,180	Small
Bagotville	37,260	Small

3.5 Choice of Measure

We agree with (Tremblay 2014) that labour productivity can be used as a quantitative measure of food service performance, and the number of meals per labour hour can be used to measure labour productivity. In addition to quantitative measures, qualitative measurer should also be included in developing the labour performance standard for CAF Food Services, e.g., customer satisfaction (mentioned in CAF Food Services Menu 2013 as well). Both quantitative and qualitative measures together should form a holistic view of labour performance in CAF Food Services. However due to the scope of this study, it was agreed that only the quantitative side of the labour performance is investigated in this study.

According to (River 2000), productivity is defined as a relationship between the total amount of goods or services being produced (outputs) and the organizational resources needed to produce them (inputs). The labour productivity here, i.e., the number of meals per labour hour, is calculated (see eqn. (1)) by dividing the total number of meals by the total number of labour hours spent.

3.6 Suggested Method for Considering NSCM and How to Define the Sampling Frame

CAF Food Services cannot easily change the number of staff in facility solely when the menu changes. NSCM is a three-week cycle menu; hence each cycle is composed of 21 days. Over the span of one year, this cycle will be repeated just a bit more than 17 times. To simplify the study and to take budget constraints into consideration, it should be assumed that the 17 cycles are the same. Therefore, we should be able to focus the future labour study within one cycle. Hence, a random sample should be drawn from 21 days, just a full cycle of NSCM; and the order and dates of on-site visits should be randomly selected.

The sampling frame for this study should be a list of consecutive dates between the study starting date and the 21st date that follows the starting date. Once SJS Directorate Food Services determines the start date of the data collection for the future labour study, the sampling frame can be determined immediately.

3.7 Suggested Sampling Method

In order to reflect real operations, randomization of the dates for on-site visits is necessary and important. The dates should be randomly selected and should not be revealed to the facility in advance.

Further exploration shows the variation within each individual facility on labour productivity is smaller relatively to the variation between facilities. One-way analysis of variance (ANOVA) was used to test the between and within facility variation on labour productivity (See Table 3), i.e., number of meals per labour hour (data from Table A).

Therefore, instead of a simple random sampling, a stratified random sampling method can be used. Each facility should be treated as a stratum in both small and large facility groups. The stratified random sampling should be conducted in the following steps:

- First, clearly specify the strata (each facility is treated as a stratum);
- Then, within each stratum (i.e., each facility), use a simple random sampling method to select a random sample of days from the established sampling frame for the on-site visit;
- Collect data from each visit and calculate the labour productivity for each facility; and
- Pool the results from all facilities (i.e., all strata) within the group (large or small) to get an overall labour productivity measure for the group.

The advantages of this stratified random sampling method are:

- separate estimates can be obtained for each stratum (i.e., each individual facility) without additional sampling; and
- since the data are more homogeneous within each stratum, the stratified sampling estimator usually has smaller variance than the corresponding simple random sampling estimators from the same sample size, i.e., a stratified sample can provide greater precision than a simple random sample of the same size.

3.8 Sample Size and Sample Allocation

In order to do sampling, the sample size and sample allocation should be determined first. The following definitions are used in this determination. Noted here, as mentioned in Section 3.7, each facility is treated as a stratum in the following calculation.

T	*total number of facilities in large or small facility group*
N_i	*total number of units in the* i^{th} *facility,* $i = 1, 2, \dots, T$
N	*total number of units in all facilities*
n_i	*number of samples for the* i^{th} *facility,* $i = 1, 2, \dots, s$
n	*the total sample size for all facilities*
w_i	*the proportion of the sample which will be allocated to the* i^{th} *facility*
C_i	*cost of obtaining a sample from the* i^{th} *facility*
σ_i	*standard deviation for the* i^{th} *facility*
$\hat{y}$	*mean for large or small facility group*
$Var(\hat{y})$	*Variance for the mean of the large or small facility group*
$\hat{y_i}$	*mean for* i^{th} *facility in large or small facility group*
z	*the upper 0.025 (i.e., 0.05/2) critical point of the standard normal distribution*

What is the sample size for estimating mean labour productivity for the large or small facility group to within some margin of error (noted as *b*) with 95% probability? This question can be translated into eqn. (2):

Table 3: Between and within group variation.

	Sum of Square	f	Mean Square	F	Significance
Between Groups	54.228	5	10.846	35.992	.000
Within Groups	7.232	24	0.301		
Total	61.460	29			

$$z[Var(\hat{y})]^{1/2} = b \tag{2}$$

Since the Stratified Random Sampling method is used and the samples are drawn independently from the strata, an unbiased estimator of the sample variance ($Var(\hat{y})$) for the large or small facility group can be calculated using eqn. (3) (Cochran 1977):

$$\begin{aligned} Var(\hat{y}) &= \sum_{i=1}^{T} \left(\frac{N_i}{N}\right)^2 \left(\frac{N_i - n_i}{N_i}\right) \frac{\sigma_i^2}{n_i} \\ &= \frac{1}{n} \sum_{i=1}^{T} \left(\frac{N_i}{N}\right)^2 \left(\frac{N_i - nw_i}{N_i}\right) \frac{\sigma_i^2}{w_i} \end{aligned} \tag{3}$$

where $n_i = nw_i$.

Replacing $Var(\hat{y})$) in eqn. (2), eqn. (2) is changed to

$$z^2 \left(\frac{1}{n} \sum_{i=1}^{T} \left(\frac{N_i}{N}\right)^2 \left(\frac{N_i - nw_i}{N_i}\right) \frac{\sigma_i^2}{w_i} \right) = b^2 \tag{4}$$

Solving this margin of error equation for n leads to:

$$n = \frac{\sum_{i=1}^{T} \left(\frac{N_i}{N}\right)^2 \frac{\sigma_i^2}{w_i}}{\frac{b^2}{z^2} + \frac{1}{N} \sum_{i=1}^{T} \left(\frac{N_i}{N}\right) \sigma_i^2} \tag{5}$$

Using this equation and based on data obtained from the large or small facility group from the pilot study, the total sample size n, required for estimating mean labour productivity to within some margin of error b with 95% probability can be calculated for the large and small facility groups respectively (see Annex B).

However, there is still one parameter w_i which needs to be determined. The variable w_i represents how the sample is allocated to the i^{th} stratum. There are several ways to allocate the sample (Cochran 1977, Lohr & Stratton 2010, Montgomery & Stratton 2010); the following allocation scheme is recommended:

$$w_i = \frac{N_i \sigma_i / \sqrt{C_i}}{\sum_{i=1}^{T} N_i \sigma_i / \sqrt{C_i}} \tag{6}$$

$$n_i = n \frac{N_i \sigma_i / \sqrt{C_i}}{\sum_{i=1}^{T} N_i \sigma_i / \sqrt{C_i}} \tag{7}$$

This allocation scheme was chosen based on the following considerations:

- larger sample size should be assigned to strata containing larger number of elements (i.e., larger N_i);
- larger sample on less homogeneous strata (i.e., larger σ_i); and
- smaller samples from strata with higher cost (i.e., higher C_i).

In summary, the equations above provide not only the calculation of total sample size but also the sample size allocation.

To be conservative and to consider the data obtained from a less ideally designed pilot study, the sample sizes determined based on the pilot data have been inflated to the next integer (see Annex B).

It needs to be noted in the pilot study, the small facility group was formed by two small facilities, i.e., Halifax and Esquimalt. Unfortunately, Cold Lake, Shilo and Bagotville were not included in the pilot study. Due to insufficient data for Shilo, Cold Lake and Bagotville from the pilot data and to get a more robust estimation, the pooled σ_i from the small facility group in pilot study (i.e., Halifax and Esquimalt) was used for Cold Lake, Shilo and Bagotville. The detailed sample size calculation and sample allocation can be found in Annex B. In summary, for large facility group, 16 random samples are needed in total. The number of samples allocated for Wainwright, Trenton, Saint-Jean and Gagetown are 4, 5, 3 and 4 respectively. For small facility group, 13 random samples are needed in total. The sample size for Bagotville, Shilo and Cold Lake are 5, 4 and 4 respectively.

3.9 Suggested Method to Determine the Labour Productivity

Once the data for the selected facilities are collected, the labour performance measurer (i.e., labour productivity) and its variance can be determined.

Two sets of labour productivity will be determined: one for large facility group and one for small facility group. The pooled labour productivity for the large/small facility group can be calculated using a weighted average of the labour productivities (i.e., number of meals per labour hour) across selected facilities within the large/small facility group (see eqn.(8)). The weights individual facility (i.e., individual stratum) receiving is N_i/N. As (Cochran 1977) pointed out this self-weighting scheme is time-saving. The same weighting scheme is used for calculating the variance for the estimated pooled labour productivity (see eqn. (9)).

$$\hat{y} = \frac{1}{N} (N_1 \hat{y}_1 + N_2 \hat{y}_2 + \cdots + N_T \hat{y}_T) \tag{8}$$

$$\begin{aligned} \hat{V}(\hat{y}) &= \frac{1}{N^2} ({N_1}^2 \hat{V}(\widehat{y_1}) + {N_2}^2 \hat{V}(\widehat{y_2}) + \cdots \\ &\quad + {N_T}^2 \hat{V}(\widehat{y_T})) \\ &= \frac{1}{N^2} \sum_{i=1}^{T} {N_i}^2 \left(\frac{N_i - n_i}{N_i}\right) \frac{{S_i}^2}{n_i} \end{aligned} \tag{9}$$

As discussed earlier in Section 3.3, specifically in our context, the labour performance standard refers to the aspect and the level of labour productivity; and the standard is considered as the best practice in CAF Food Services. As these labour productivity measures are generated from the selected CAF Food Service facilities of best practice, the labour productivity generated from the next labour study can be considered as the initial standard. It needs to be noted that establishing the labour performance standard will be an evolving process. Although the current study does not produce a labour performance standard directly, it is significant since it is one of the building blocks in the early stage which will support the establishment of the first labour performance standard for CAF Food Services.

4 CONCLUSIONS

4.1 Summary

This paper first reviews the results from the pilot study conducted in February and March 2015 for CAF Food Services. Due to the issues identified with the pilot study, this report also proposes a revised design and analytical approach for a follow-on study.

In summary, the target population is composed of two groups, i.e., the large facility and small facility groups. The large facility group consists of Wainwright, Trenton, Saint-Jean and Gagetown; and the small facility group consists of Bagotville, Shilo and Cold Lake. These are chosen as facilities of best practice on labour performance based on military knowledge and judgement. A stratified random sampling method is suggested being used to get the random samples for the target population. With the same sample size, a study with a stratified random sampling scheme will be able to produce a more precise estimator compared to that with a simple random sampling scheme. The sample size and sample allocation have been determined based on the data obtained from the pilot study. In summary, for the large facility group, 16 random samples are needed in total. The number of samples allocated for Wainwright, Trenton, Saint-Jean and Gagetown are four, five, three and four respectively. For the small facility group, 13 random samples are needed in total. The sample size for Bagotville, Shilo and Cold Lake are five, four and four respectively. The approach for calculating weighted stratified random sample estimates and their corresponding variances are also determined for the future study.

Although according to the client's request, this study focuses only on the quantitative side of the labour performance, we believe in order to provide the labour performance standard for CAF Foods Services, not only the quantitative measure, but also qualitative measure of labour performance should be considered. Therefore, if it is financially permitted, we recommend that a social study (using techniques, e.g., customer surveys, interviews, or focus groups) be conducted to measure the qualitative aspects of the labour performance. Only focusing on the labour productivity may drive the facilities to pursue fast but not high quality food services.

4.2 Significance of the Study

Unlike most of the other food industries, CAF Food Services is not profit driven and fulfilling the operational needs is its first priority. Given that the CAF Food Services does not have a labour performance standard, establishing one is significant.

It is beneficial to provide a labour performance standard (i.e., level of labour performance of best practice here) against which a performance of a CAF Food Services facility can be measured and compared. Once developed, this labour performance standard could then be used to ensure food service facilities to provide efficient and effective food service support to the CAF and may inform future rationalization of staffing within CAF Food Services. Routine measurement of labour performance could also provide a way for CAF Food Services managers to monitor and track operational improvements over time. This study focuses on the quantitative side of the labour performance, i.e., labour productivity. As summarized in (River 2000), productivity measures can play a key role in business process redesign and optimization, assessing maximum sustainable outputs, lowering products or service unit cost, and exploring the feasibility of out sourcing.

Developing a labour performance standard will be an evolving process. Although the current study does not produce a labour performance standard for CAF Food Services directly, it outlines the requisite study design for data collection and an analytical approach for a future study, which will underpin future development of a labour performance standard for CAF Food Services.

REFERENCES

Request for Operational Research and Analysis: Performance Measure in CAF Food Services, Mat J4 / D Food Services, December 2014.

Definition related to the CAF Food Services, Maj Mike Whiting, Communication on 8 December 2015.

Meeting on Request for Operational Research and.

Analysis, Maj Mike Whiting and Manchun Fang, on 18 December 2014.

Collection Tool-Labour Study, Maj Mike Whiting, Communication on 19 January 2015.

Using Labour Productivity as a Food Services Performance Measurement and Human Resources Management Tool, ADM (Mat) Food Services, Roland Tremblay, 2004.

Sampling Techniques, William G. Cochran, John Wiley & Sons, Inc. 1977.

Sampling: Design and Analysis, Sharon L. Lohr and Richard Stratton, ISBN 10:0-495-10527-9, 2010.

Standards, evaluative criteria and benchmarks, Better Evaluation, Patricia Rogers, Professor of Public Sector Evaluation, RMIT University. Melbourne. March 2014.

Annual Meal Day, Provided by Mark Whiting and Guy St-Cyr, SJS Food Service, Communication on 24 July 2015.

Meal days for FY 13/14 and FY 15/16, Provided by Maj Mark Whiting, Communication on 10 June 2015.

Record of Discussions for meeting between DMGOR and SJS D Food Services, 28 May 2015.

Financial Management, Accounting Standard and Procedures, CAF Food Service Manual, A-85-269-001/FP-001, Nov 2013.

Modern Management. 8th ed. Upper Saddle River, NJ: Prentice Hall Publishing, Certo SC. 2000.

Design and Analysis of Experiments, D.C. Montgomery, Richard Stratton, 2010.

Costing Sheet for Travel for Future Labour Study, Maj Mark Whiting, Communication on 8 June 2015.

ANNEX A: SUMMARY OF DATA FROM PILOT STUDY

Table A: Summary statistics for Halifax obtained from the pilot study.

Facility	Day	Civilian Hours	Military Hours	Civilian Wages	Military Wages	Total Hours	Labour Costs	# of Meals	Meals/Hour
Halifax	D1	24	143	$615	$4086	167	$4701	483	2.9
	D2	120	90	$2502	$2688	210	$5191	496	2.4
	D3	152	143	$3216	$4157	295	$7373	444	1.5
	D4	144	90	$3084	$2688	234	$5773	398	1.7
	D5	136	98	$2901	$2917	234	$5818	340	1.5
Gagetown	D1	334	158	$6875	$4778	492	$11653	2180	4.4
	D2	342	203	$7058	$5977	545	$13034	2272	4.2
	D3	396	225	$8276	$6618	621	$14894	2224	3.6
	D4	348	218	$7215	$6404	566	$13619	2266	4.0
	D5	326	203	$6810	$5962	529	$12773	1671	3.2
Saint-Jean	D1	614	83	$12,122	$2,534	697	$14,656	3816	5.5
	D2	630	68	$12,130	$2,106	698	$14,236	3556	5.1
	D3	606	68	$11,640	$2,106	674	$13,747	3606	5.4
	D4	556	53	$10,523	$1,664	609	$12,187	3523	5.8
	D5	620	60	$12,057	$1,892	680	$13,950	3382	5.0
Wainwright	D1	168	90	$3,738	$2,745	258	$6,484	992	3.8
	D2	168	83	$3,738	$2,517	251	$6,255	1051	4.2
	D3	192	83	$4,269	$2,517	275	$6,786	704	2.6
	D4	136	90	$2,992	$2,617	226	$5,610	963	4.3
	D5	152	90	$3,365	$2,617	242	$5,983	804	3.3
Trenton	D1	104	30	$2,217	$799	134	$3,016	558	4.2
	D2	80	45	$1,825	$1,170	125	$2,995	715	5.7
	D3	80	53	$1,825	$1,384	133	$3,209	650	4.9
	D4	72	45	$1,610	$1,226	117	$2,836	603	5.2
	D5	72	38	$1,610	$1,013	110	$2,622	511	4.7

Table A: Summary statistics for Halifax obtained from the pilot study (Cont.).

Facility	Day	Civilian Hours	Military Hours	Civilian Wages	Military Wages	Total Hours	Labour Costs	# of Meals	Meals/Hour
Esquimalt	D1	200	60	$4,400	$1,658	260	$6,058	435	1.7
	D2	176	83	$3,870	$2,271	259	$6,141	408	1.6
	D3	176	120	$3,870	$3,267	296	$7,137	426	1.4
	D4	152	98	$3,457	$2,668	250	$6,124	365	1.5
	D5	168	90	$3,830	$2,397	258	$6,227	701	2.7

ANNEX B: SAMPLING

As we discussed in Section 3.8, the sample size and sample allocation will be determined using eqns. (5), (6) and (7).

The following sample size calculation and sample allocation are based on the information from the pilot study or provided by (Whiting June 8 2015). The number of the total observation units is 21 (a three-week full cycle of NSCM). For the large facility group:

- Wainwright ($\mathrm{i.e.}, \mathrm{i} = 1$)
  - $\mathrm{N}_1 = 21, \sigma_1 = 0.71, \mathrm{c}_1 = 2.4\mathrm{c}$
  - Using eqn. (6), the weight for Wainwright is calculated: $\mathrm{w}_1 = 0.33$
- Trenton ($\mathrm{i.e.}, \mathrm{i} = 2$)
  - $\mathrm{N}_2 = 21, \sigma_2 = 0.58, \mathrm{c}_2 = \mathrm{c}$
  - Using eqn. (6), the weight for Trenton is calculated: $\mathrm{w}_2 = 0.27$
- Saint-Jean ($\mathrm{i.e.}, \mathrm{i} = 3$)
  - $\mathrm{N}_3 = 21, \sigma_3 = 0.32, \mathrm{c}_3 = \mathrm{c}$
  - Using eqn. (6), the weight for Saint-Jean is calculated: $\mathrm{w}_3 = 0.15$
- Gagetown ($\mathrm{i.e.}, \mathrm{i} = 4$)
  - $\mathrm{N}_4 = 21, \sigma_4 = 0.50, \mathrm{c}_4 = 1.9\mathrm{c}$
  - Using eqn. (6), the weight for Gagetown is calculated: $\mathrm{w}_4 = 0.24$

In the pilot study, the small facility group was formed by two small facilities, i.e., Halifax and Esquimalt. However it was determined later that these three facilities, i.e., Cold Lake, Shilo and Bagotville would be good examples of small feeding facilities in terms of labour performance.

Although there was no data collected for these three small facilities, there is no problem to figure out the N_i and c_i for Cold Lake, Shilo and Bagotville. To get a more robust estimation, the pooled standard deviation from Halifax and Esquimalt was used for Cold Lake, Shilo and Bagotville; therefore, the standard deviation for all three small facilities are computed to be, and assumed to be identical.

For the small facility group:

- Cold Lake (i.e.,i=1)
  - $\mathrm{N}_1 = 21, \sigma_1 = 0.58, \mathrm{c}_1 = 1.5\mathrm{c}$
  - Using eqn. (6), the weight for Trenton is calculated: $\mathrm{w}_1 = 0.34$
- Shilo ($\mathrm{i.e.}, \mathrm{i} = 2$)
  - $\mathrm{N}_2 = 21, \sigma_2 = 0.58, \mathrm{c}_2 = 1.7\mathrm{c}$
  - Using eqn. (6), the weight for Trenton is calculated: $\mathrm{w}_2 = 0.32$
- Bagtoville ($\mathrm{i.e.}, \mathrm{i} = 3$)
  - $\mathrm{N}_3 = 21, \sigma_3 = 0.58, \mathrm{c}_3 = 1.5\mathrm{c}$
  - Using eqn. (6), the weight for Trenton is calculated: $\mathrm{w}_3 = 0.34$

Let $b = 0.25$ (initial determined, can be justified as required) and $z = 1.96$ (is the 97.5% percentile of the standard norm distributions, the critical value for 95%), and according to eqn. (5), the sample size required is approximate 14.59 for estimating the mean of labour performance productivity for the large facility group with 95% probability with marginal error 0.25. Applying the corresponding weights, the sample allocation is calculated for each individual facility as follows:

- Wainwright: $\mathrm{n} \times \mathrm{w}_1 = 3.86 \approx 4$
- Trenton: $\mathrm{n} \times \mathrm{w}_2 = 4.90 \approx 5$
- Saint-Jean: $\mathrm{n} \times \mathrm{w}_3 = 2.74 \approx 3$
- Gagetown: $\mathrm{n} \times \mathrm{w}_4 = 3.09 \approx 4$

It needs to be noted that to be conservative and to consider the less ideal design of the pilot study, the sample sizes determined based on the pilot data have been inflated to the next integer. Therefore, the number of samples allocated for Wainwright, Trenton, Saint-Jean and Gagetown are 4, 5, 3 and 4 respectively.

The same procedure is used for calculating the sample sizes for the small facility group. Calculating based on eqn. (5), the total sample size of 12.44 will be required. Again, for the same reason, the sample size determined based on the pilot data via optimal allocation scheme have been inflated to the next integer. Therefore, the sample size for Bagotville, Shilo and Cold Lake are 5, 4 and 5 respectively:

- Bagotville: $\mathrm{n} \times \mathrm{w}_1 = 4.27 \approx 5$
- Shilo: $\mathrm{n} \times \mathrm{w}_2 = 3.99 \approx 4$
- Cold Lake: $\mathrm{n} \times \mathrm{w}_3 = 4.17 \approx 5$

A New Procedure to Calculate the Owen Value

José Miguel Giménez and María Albina Puente
Department of Mathematics and Engineering School of Manresa, Technical University of Catalonia, Manresa, Spain
{*jose.miguel.gimenez, m.albina.puente*}*@upc.edu*

Keywords: Cooperative Game, Shapley Value, Banzhaf Value, Coalition Structure, Multilinear Extension.

Abstract: In this paper we focus on games with a coalition structure. Particularly, we deal with the Owen value, the coalitional value of the Shapley value, and we provide a computational procedure to calculate this coalitional value in terms of the multilinear extension of the original game.

1 INTRODUCTION

Shapley (Shapley, 1953) (see also (Roth, 1988) and (Owen, 1995)) initiated the value theory for cooperative games. The *Shapley value* applies without restrictions and provides, for every game, a single payoff vector to the players. The restriction of the value to simple games gives rise to the *Shapley–Shubik power index* (Shapley and Shubik, 1954), that was axiomatized in (Dubey, 1975) introducing the transfer property. As a sort of reaction, Banzhaf (Banzhaf, 1965) proposed a different power index that Owen (Owen, 1975) extended to a dummy–independent and somehow "normalized" *Banzhaf value* for all cooperative games. A nice almost common characterization of the Shapley and Banzhaf values would be given in (Feltkamp, 1995).

Games with a *coalition structure* were introduced in (Aumann and Drèze, 1974), who extended the Shapley value to this new framework in such a manner that the game really splits into subgames played by the unions isolatedly from each other, and every player receives the payoff allocated by the restriction of the Shapley value to the subgame he is playing within his union. A second approach was used in (Owen, 1977), when introducing and axiomatically characterizing his coalitional value (*Owen value*). The Owen value is the result of a *two–step procedure*: first, the unions play a *quotient game* among themselves, and each one receives a payoff which, in turn, is shared among its players in an internal game. Both payoffs, in the quotient game for unions and within each union for its players, are given by applying the Shapley value. Further axiomatizations of the Owen value have been given in *e.g.* (Hart and Kurz, 1983), (Peleg, 1989), (Winter, 1992), (Amer and Carreras, 1995) and (Amer and Carreras, 2001), (Vázquez et al., 1997), (Vázquez, 1998), (Hamiache, 1999), (Hamiache, 2001) and (Albizuri, 2002).

Owen applied the same procedure to the Banzhaf value and obtained the *modified Banzhaf value* or *Owen–Banzhaf value* (Owen, 1982). In this case the payoffs at both levels (unions in the quotient game and players within each union) are given by the Banzhaf value.

Alonso and Fiestras suggested to modify the two–step allocation scheme and use the Banzhaf value for sharing in the quotient game and the Shapley value within unions. This gave rise to the *symmetric coalitional Banzhaf value* or *Alonso–Fiestras value* (Alonso and Fiestras, 2002). That same year, Carreras et al. considered a sort of "counterpart" of the Alonso–Fiestras value where the Shapley value is used in the quotient game and the Banzhaf value within unions (Amer et al., 2002). Thus, the possibilities to define a coalitional value by combining the Shapley and Banzhaf values were complete at that moment.

In 1972 Owen introduced the *multilinear extension* (Owen, 1972) and applied it to the calculus of the Shapley value. The computing technique based on the multilinear extension has been applied to many values: in 1975 to the Banzhaf value (Owen, 1975); in 1992 to the Owen value (Owen and Winter, 1992); in 1994 to the Owen–Banzhaf value (Carreras and Magaña, 1994); in 1997 to the quotient game (Carreras and Magaña, 1997); in 2000 to *binomial semivalues* and to *multinomial probabilistic indices* (Puente, 2000); in 2004 to the α*–decisiveness and Banzhaf* α*–indices* (Carreras, 2004); in 2005 to the *Alonso–Fiestras value* (Alonso et al., 2005); in 2011 to *symmetric coalitional binomial semivalues*

Giménez, J. and Puente, M.
A New Procedure to Calculate the Owen Value.
In *Proceedings of the 6th International Conference on Operations Research and Enterprise Systems (ICORES 2017)*, pages 228-233
ISBN: 978-989-758-218-9

(Carreras and Puente, 2011); in 2011 to semivalues (Carreras and Giménez, 2011); in 2015 to *coalitional multinomial probabilistic values* (Carreras and Puente, 2015).

The present paper focus on giving a new computational procedure for the Owen value by means of the multilinear extension of the game.

The organization of the paper is as follows. In Section 2, a minimum of preliminaries is provided. Section 3 is devoted to give a procedure to compute the Owen value.

2 PRELIMINARIES

2.1 Cooperative Games

Let N be a finite set of *players* and 2^N be the set of its *coalitions* (subsets of N). A *cooperative game* on N is a function $v : 2^N \to \mathbb{R}$, that assigns a real number $v(S)$ to each coalition $S \subseteq N$, with $v(\emptyset) = 0$. A game v is *monotonic* if $v(S) \leq v(T)$ whenever $S \subseteq T \subseteq N$ and *simple* if, moreover, $v(S) = 0$ or 1 for every $S \subseteq N$. A player $i \in N$ is a *dummy* in v if $v(S \cup \{i\}) = v(S) + v(\{i\})$ for all $S \subseteq N \backslash \{i\}$, and *null* in v if, moreover, $v(\{i\}) = 0$. Two players $i, j \in N$ are *symmetric* in v if $v(S \cup \{i\}) = v(S \cup \{j\})$ for all $S \subseteq N \backslash \{i, j\}$. Given a nonempty coalition $T \subseteq N$, the restriction to T of a given game v on N is the game $v_{|T}$ on T that we will call a *subgame* of v and is defined by $v_{|T}(S) = v(S)$ for all $S \subseteq T$.

Endowed with the natural operations for real–valued functions, *i.e.* $v + v'$ and λv for all $\lambda \in \mathbb{R}$, the set of all cooperative games on N is a vector space $\mathcal{G}_N$. For every nonempty coalition $T \subseteq N$, the *unanimity game* u_T is defined by $u_T(S) = 1$ if $T \subseteq S$ and $u_T(S) = 0$ otherwise, and it is easily checked that the set of all unanimity games is a basis for $\mathcal{G}_N$, so that $\dim(\mathcal{G}_N) = 2^n - 1$ if $n = |N|$.

By a *value* on $\mathcal{G}_N$ we will mean a map $f : \mathcal{G}_N \to \mathbb{R}^N$, that assigns to every game v a vector $f[v]$ with components $f_i[v]$ for all $i \in N$.

Well known example of value is the *Shapley value* φ (Shapley (Shapley, 1953)), defined as

$$\varphi_i[v] = \sum_{S \subseteq N \backslash \{i\}} p_s [v(S \cup \{i\}) - v(S)$$

for all $i \in N$, $v \in \mathcal{G}_N$, where $s = |S|$ and $p_s = 1/n\binom{n-1}{s}$.

Notice that this value is defined for each N. In fact, it is defined on cardinalities rather than on specific player sets: this means the weighting vector $\{p_s\}_{s=0}^{n-1}$ defines the Shapley value on all N such that $n = |N|$. When necessary, we shall write $\varphi^{(n)}$ for the Shapley value on cardinality n and p_s^n for its weighting coefficients. $\varphi^{(n)}$ induces values $\varphi^{(t)}$ for all cardinalities $t < n$, recurrently defined by the Pascal triangle (inverse) formula given by Dragan (Dragan, 1997). That is

$$p_s^t = p_s^{t+1} + p_{s+1}^{t+1} \quad \text{for} \quad 0 \leq s < t, \tag{1}$$

The *multilinear extension* (Owen, 1972) of a game $v \in \mathcal{G}_N$ is the real–valued function defined on $\mathbb{R}^N$ by

$$f_v(X_N) = \sum_{S \subseteq N} \prod_{i \in S} x_i \prod_{j \in N \backslash S} (1 - x_j) v(S). \tag{2}$$

where X_N denotes the set of variables x_i for $i \in N$.

As is well known, both the Shapley and Banzhaf values of any game v can be easily obtained from its multilinear extension. Indeed, $\varphi[v]$ can be calculated by integrating the partial derivatives of the multilinear extension of the game along the main diagonal $x_1 = x_2 = \cdots = x_n$ of the cube $[0,1]^N$ (Owen, 1972)), while the partial derivatives of that multilinear extension evaluated at point $(1/2, 1/2, \ldots, 1/2)$ give $\beta[v]$ (Owen, 1975).

2.2 Games with Coalition Structure

Given $N = \{1, 2, \ldots, n\}$, we will denote by $B(N)$ the set of all partitions of N. Each $B \in B(N)$ is called a *coalition structure* in N, and a *union* each member of B. The so–called *trivial coalition structures* are $B^n = \{\{1\}, \{2\}, \ldots, \{n\}\}$ (individual coalitions) and $B^N = \{N\}$ (grand coalition). A *cooperative game with a coalition structure* is a pair $[v; B]$, where $v \in \mathcal{G}_N$ and $B \in B(N)$ for a given N. Each partition B gives a pattern of cooperation among players. We denote by $\mathcal{G}_N^{cs} = \mathcal{G}_N \times B(N)$ the set of all cooperative games with a coalition structure and player set N.

If $[v; B] \in \mathcal{G}_N^{cs}$ and $B = \{B_1, B_2, \ldots, B_m\}$, the *quotient game* v^B is the cooperative game played by the unions or, rather, by the *quotient set* $M = \{1, 2, \ldots, m\}$ of their representatives, as follows:

$$v^B(R) = v(\bigcup_{r \in R} B_r) \quad \text{for all } R \subseteq M.$$

By a *coalitional value* on $\mathcal{G}_N^{cs}$ we will mean a map $g : \mathcal{G}_N^{cs} \to \mathbb{R}^N$, which assigns to every pair $[v; B]$ a vector $g[v; B]$ with components $g_i[v; B]$ for each $i \in N$.

If f is a value on $\mathcal{G}_N$ and g is a coalitional value on $\mathcal{G}_N^{cs}$, it is said that g is a *coalitional value of* f iff $g[v; B^n] = f[v]$ for all $v \in \mathcal{G}_N$.

2.2.1 The Owen Value

The *Owen value* (Owen (Owen, 1977)) is the coalitional value Φ defined by

$$\Phi_i[v;P] = \sum_{R\subseteq M\setminus\{k\}} \sum_{T\subseteq B_k\setminus\{i\}} p_r^{m-1} p_t^{b_k-1} \left[v(Q\cup T\cup\{i\}) - v(Q\cup T)\right]$$

for all $i\in N$ and $[v;B]\in\mathcal{G}_N^{cs}$, where $B_k\in B$ is the union such that $i\in B_k$, $Q=\bigcup_{r\in R} B_r$ and

$$p_r^{m-1} = \frac{1}{m}\frac{1}{\binom{m-1}{r}}, p_t^{b_k-1} = \frac{1}{b_k}\frac{1}{\binom{b_k-1}{t}}.$$

This coalitional value was axiomatically characterized by Owen (Owen, 1977) as the only coalitional value that satisfies the following properties: the natural extensions to this framework of

- *efficiency*
- *additivity*
- *the dummy player property*

and also

- *symmetry within unions*: if $i,j\in B_k$ are symmetric in v then

$$\Phi_i[v;B] = \Phi_j[v;B]$$

- *symmetry in the quotient game*: if $B_r,B_s\in P$ are symmetric in $[v;B]$ then

$$\sum_{i\in B_r}\Phi_i[v;B] = \sum_{j\in B_s}\Phi_j[v;B].$$

Finally, as Φ is defined for any N, the following property makes sense and is also satisfied:

- *quotient game property*: for all $[v;B]\in\mathcal{G}_N^{cs}$,

$$\sum_{i\in B_k}\Phi_i[v;B] = \Phi_k[v^B;B^m] \quad \text{for all } B_k\in B.$$

The Owen value can be viewed as a two–step allocation rule. First, each union B_k receives its payoff in the quotient game according to the Shapley value; then, each B_k splits this amount among its players by applying the Shapley value to a game played in B_k as follows: the worth of each subcoalition T of B_k is the Shapley value that T would get in a "pseudoquotient game" played by T and the remaining unions on the assumption that $B_k\setminus T$ leaves the game, *i.e.* the quotient game after replacing B_k with T. This is the way to bargain within the union: each subcoalition T claims the payoff it would obtain when dealing with the other unions in absence of its partners in B_k.

The Owen value is a *coalitional value of the Shapley value* φ in the sense that $\Phi[v;B^n]=\varphi[v]$ for all $v\in\mathcal{G}_N$. Besides, $\Phi[v;B^N]=\varphi[v]$.

3 A COMPUTATIONAL PROCEDURE TO CALCULATE THE OWEN VALUE

In this section we present a new computational procedure to calculate this coalitional value. Before that, we need two previous results that will be given in Lemma 3.1 and Proposition 3.2.

Lemma 3.1. *Let $[v;B]\in\mathcal{G}_N^{cs}$, $B=\{B_1,B_2,\ldots,B_m\}$ a coalition structure in N. The allocations given by Φ to players belonging to a union B_j can be obtained as a linear combination of the allocations to unanimity games u_T, where $T=V\cup W$, $V\subseteq B_j$ and $W\in 2^{B\setminus B_j}$.*

.

Proof Each game $v\in\mathcal{G}_N$ can be uniquely written as linear combination of unanimity games

$$v=\sum_{T\subseteq N:\,T\neq\emptyset}\alpha_T u_T,$$

where $\alpha_T=\alpha_T(v)=\sum_{S\subseteq T}(-1)^{t-s}v(S)$.

By linearity, for all $i\in B_j$,

$$\Phi_i[v;B]=\sum_{T\subseteq N:\,T\neq\emptyset}\alpha_T\Phi_i[u_T]$$

and it suffices consider unanimity games u_T with

$$T=V\cup A_{i_1}\cup A_{i_2}\cup\ldots\cup A_{i_p}$$
$$V\subseteq B_j,\ \{i_1,i_2,\ldots,i_p\}\subseteq M\setminus\{j\}$$
$$\emptyset\neq A_{i_q}\subseteq B_{i_q},\ q=1,\ldots,p.$$

According to the definition of the Owen value it is easy to check that the allocations to players in B_j only depend on the allocations in the unanimity games defined on inside coalitions in B_j and entire unions outside B_j. That is,

$$\Phi_i[u_T;B] = \Phi_i[u_{V\cup A_{i_1}\cup A_{i_2}\cup\ldots\cup A_{i_p}};B] = \Phi_i[u_{V\cup B_{i_1}\cup B_{i_2}\cup\ldots\cup B_{i_p}};B]. \qquad \square$$

Notice that the number of unanimity games of this form is $(2^{b_j}-1)2^m$ with $b_j=|B_j|$ and $m=|M|$.

Proposition 3.2. *Let $B=\{B_1,B_2,\ldots,B_m\}$ be a coalition structure in N. Fixed a union B_j, the allocation to a player i belonging to B_j in a unanimity game u_T, $T=V\cup B_{i_1}\cup\cdots\cup B_{i_h}$, $V\subseteq B_j$ and $\{i_1,\ldots,i_h\}\subseteq M\setminus\{j\}$ is given by*

$$\Phi_i[u_T;B]=\left(\psi/\varphi_j\right)_i[u_T;B]=\begin{cases} p_h^{h+1}p_{v-1}^{v} & i\in T\\ 0 & i\notin T\end{cases}$$

where $(p_s^{h+1})_{s=0}^{h}$ and $(p_s^{v})_{s=0}^{v-1}$ are the weighting coefficients of the induced Shapley value and $p_h^{h+1}=\frac{1}{h+1}$ and $p_{v-1}^{v}=\frac{1}{v}$.

Proof For $i \in T$ we have

$$\Phi_i[u_T;B] = \sum_{R\subseteq M\setminus\{j\}} p_r^m \sum_{S\subseteq B_j\setminus\{i\}} p_s^{b_j}[u_T(Q\cup S\cup\{i\}) - u_T(Q\cup S)]$$

where $Q = \bigcup_{r\in R} B_r$, $b_j = |B_j|$, and $s = |S|$.

Only $u_T(Q\cup S\cup\{i\}) - u_T(Q\cup S)$ does not vanish for coalitions R such that $\{i_1,...,i_h\} \subseteq R \subseteq M\setminus\{j\}$ and for coalitions S such that $V\setminus\{i\} \subseteq S \subseteq B_j\setminus\{i\}$. Then,

$$\Phi_i[u_T;B] = p_h^{h+1} p_{v-1}^v$$

In case of $i \notin T$, all marginal contributions $u_T(Q\cup S\cup\{i\}) - u_T(Q\cup S)$ vanish. □

Example 3.1 On the players set $N = \{1,2,3,4,5,6\}$, let $B = \{\{1,2,3\},\{4,5\},\{6\}\}$ be a coalition structure on N. We will obtain the allocations to players $i \in B_1$ according to Φ for the unanimity games $u_{\{1,2,4,6\}}$ and $u_{\{1,2,4,5,6\}}$. They are

$$\Phi_i[u_{\{1,2,4,6\}};B] = p_2^3 p_1^2 = \frac{1}{3}\frac{1}{2} = \frac{1}{6}, \text{ for } i = 1,2 \text{ and}$$

$$\Phi_3[u_{\{1,2,4,6\}};B] = 0,$$

where $p_2^3 = \frac{1}{3}$ and $p_1^2 = \frac{1}{2}$ are the corresponding weighting coefficient of the induced Shapley value.

In a similar way and according to Lemma 3.1, for $u_{\{1,2,4,5,6\}}$ we obtain

$$\Phi_i[u_{\{1,2,4,5,6\}};B] = p_2^3 p_1^2 = \frac{1}{3}\frac{1}{2} = \frac{1}{6}, \text{ for } i = 1,2 \text{ and}$$

$$\Phi_3[u_{\{1,2,4,5,6\}};B] = 0,$$

Notice that the allocations in both games are the same because coalitions $\{1,2,4,6\}$ and $\{1,2,4,5,6\}$ intersect the same unions B_2 and B_3.

In next theorem we present a new method to compute the Owen value by means of the multilinear extension of the game.

Theorem 3.3. *Let $[v;B] \in \mathcal{G}_N^{cs}$, $B = \{B_1,B_2,\ldots,B_m\}$ a coalition structure in N.*

Then the following steps lead to the Owen value of any player $i \in B_j$ in $[v;B]$.

1. *Obtain the multilinear extension $f(x_1,x_2,\ldots,x_n)$ of game v.*
2. *For every $r \neq j$ and all $h \in B_r$, replace the variable x_h with y_r. This yields a new function of x_k for $k \in B_j$ and y_r for $r \in M\setminus\{j\}$.*
3. *In this new function, reduce to 1 all higher exponents, i.e. replace with y_r each y_r^q such that $q > 1$. This gives a new multilinear function denoted as $g_j((x_k)_{k\in B_j},(y_r)_{r\in M\setminus\{j\}})$ (The modified multilinear extension of union B_j).*
4. *After some calculus, the obtained modified multilinear extension reduces to*
$$g_j((x_k)_{k\in B_j},(y_r)_{r\in M\setminus\{j\}}) = \sum_{V\subseteq B_j}\sum_{W\subseteq M\setminus\{j\}} \lambda_{V\cup W}\prod_{k\in V} x_k \prod_{r\in W} y_r$$
5. *Multiply each product $\prod_{k\in V} x_k$ by $p_{v-1}^{j,v}$ and each product $\prod_{r\in W} y_r$ by p_w^{w+1} obtaining a new multilinear function called $\overline{g}_j$.*
6. *Obtain the partial derivative of $\overline{g}_j$ with respect to x_i evaluated at point $(1,\ldots,1)$ and*
$$\Phi_i[v;B] = \frac{\partial \overline{g}_j}{\partial x_i}(1_{B_j},1_{M\setminus\{j\}}).$$

Proof Steps 1–3 have been already used in many well known works to obtain the modified multilinear extension of union B_j. Step 4 shows the modified multilinear extension as a linear combination of multilinear extensions of unanimity games. Step 5 weights each unanimity game according to Proposition 3.2 so that step 6 gives as usual the marginal contribution of player i and his allocation $\Phi_i[v;B]$ is obtained. □

Example 3.2 Let $v \equiv [68;50,21,20,19,13,9,3]$ be the 7–person weighted majority game and the coalition structure $B = \{\{1\},\{2,3,5\},\{4\},\{6\},\{7\}\}$. We will compute $\Phi[v;B]$.

The set of minimal winning coalitions of the game is

$$W^m(v) = \{\{1,2\},\{1,3\},\{1,4\},\{1,5,6\}\},$$

so that players 2, 3 and 4 on one hand, and 5 and 6 on the other, are symmetric in v. Moreover, player 7 is null and the multilinear extension of v is

$$\begin{aligned} f(X_N) =& x_1x_2 + x_1x_3 + x_1x_4 - x_1x_2x_3 - x_1x_2x_4 - x_1x_3x_4 \\ &+ x_1x_5x_6 + x_1x_2x_3x_4 - x_1x_2x_5x_6 - x_1x_3x_5x_6 \\ &- x_1x_4x_5x_6 + x_2x_3x_4x_5 + x_2x_3x_4x_6 - x_1x_2x_3x_4x_5 \\ &- x_1x_2x_3x_4x_6 + x_1x_2x_3x_5x_6 + x_1x_2x_4x_5x_6 \\ &+ x_1x_3x_4x_5x_6 - x_2x_3x_4x_5x_6. \end{aligned}$$

The coalition structure is

$$B = \{\{1\},\{2,3,5\},\{4\},\{6\},\{7\}\}$$

and steps 1–4 in Theorem 3.3 give the modified multilinear extension of each union B_j, for $j = 1,2,3,4$ (notice that player 7 is null in v and it is not necessary to compute g_5).

$$g_1(x_1,y_2,y_3,y_4,y_5) = x_1y_2 + x_1y_3 - 2x_1y_2y_3 + y_2y_3,$$

$$g_2(x_2,x_3,x_5,y_1,y_3,y_4,y_5) = x_2y_1 + x_3y_1 + y_1y_3 - x_2x_3y_1 - x_2y_1y_3 - x_3y_1y_3 + x_5y_1y_4 + x_2x_3y_1y_3 - x_2x_5y_1y_4 - x_3x_5y_1y_4 - x_5y_1y_3y_4 + x_2x_3x_5y_3 + x_2x_3y_3y_4 - x_2x_3x_5y_1y_3 - x_2x_3y_1y_3y_4 + x_2x_3x_5y_1y_4 + x_2x_5y_1y_3y_4 + x_3x_5y_1y_3y_4 - x_2x_3x_5y_3y_4,$$

$$g_3(x_4,y_1,y_2,y_4,y_5) = y_1y_2 + x_4y_1 + x_4y_2 - 2x_4y_1y_2,$$

$$g_4(x_6,y_1,y_2,y_3,y_5) = y_1y_2 + y_1y_3 + y_2y_3 - 2y_1y_2y_3.$$

Step 5 leads to $\overline{g}_j$ for each $j = 1,2,3,4$.

$$\overline{g}_1(x_1,y_2,y_3,y_4,y_5) = p_0^{1,1}p_1^2x_1y_2 + p_0^{1,1}p_1^2x_1y_3 - 2p_0^{1,1}p_2^3x_1y_2y_3 + p_2^3y_2y_3,$$

$$\overline{g}_2(x_2,x_3,x_5,y_1,y_3,y_4,y_5) = p_0^1p_1^2x_2y_1 + p_0^1p_1^2x_3y_1 - p_1^2p_1^2x_2x_3y_1 + p_2^3y_1y_3 - p_0^1p_2^3x_2y_1y_3 - p_0^1p_2^3x_3y_1y_3 + p_0^1p_2^3x_5y_1y_4 + p_1^2p_2^3x_2x_3y_1y_3 - p_1^2p_2^3x_2x_5y_1y_4 - p_1^2p_2^3x_3x_5y_1y_4 - p_0^1p_3^4x_5y_1y_3y_4 + p_2^3p_1^2x_2x_3x_5y_3 + p_1^2p_2^3x_2x_3y_3y_4 - p_2^3p_2^3x_2x_3x_5y_1y_3 - p_1^2p_3^4x_2x_3y_1y_3y_4 + p_2^3p_2^3x_2x_3x_5y_1y_4 + p_1^2p_3^4x_2x_5y_1y_3y_4 + p_1^2p_3^4x_3x_5y_1y_3y_4 - p_2^3p_2^3x_2x_3x_5y_3y_4,$$

$$\overline{g}_3(x_4,y_1,y_2,y_4,y_5) = p_2^3y_1y_2 + p_0^1q_1^2x_4y_1 + p_0^1p_1^2x_4y_2 - 2p_0^1p_2^3x_4y_1y_2,$$

$$\overline{g}_4(x_6,y_1,y_2,y_3,y_5) = p_2^3y_1y_2 + p_2^3y_1y_3 + p_2^3y_2y_3 - 2p_3^4y_1y_2y_3.$$

Finally, step 6 yields

$$\Phi_1[v;B] = 2p_0^1p_1^2 - 2p_0^1p_2^3 = \tfrac{1}{3},$$

$$\Phi_i[v;B] = p_0^1p_1^2 - p_1^2p_1^2 - p_0^1p_2^3 + p_1^2p_2^3 + p_2^3p_1^2 - p_2^3p_2^3 = \frac{5}{36}, \quad \text{for } i = 2,3,$$

$$\Phi_4[v;B] = 2p_0^1p_1^2 - 2p_0^1p_2^3 = \tfrac{1}{3},$$

$$\Phi_5[v;B] = p_0^1p_2^3 - 2p_1^2p_2^3 - p_0^1p_3^4 + p_2^3p_1^2 - p_2^3p_2^3 + 2p_1^2p_3^4 = \frac{1}{18},$$

$\Phi_6[v;B] = 0$ and

$\Phi_7[v;B] = 0.$

4 CONCLUSIONS

As we have said before, the present work is focussed on the calculus of the Owen value. More precisely, the computation of players' allocations are obtained from the multilinear extension of the game. In the context of games with a coalition structure, the multilinear extension technique has been also applied to computing the Owen value in (Owen and Winter, 1992); as well as the Owen–Banzhaf value in (Carreras and Magaña, 1994); in 1997 to the quotient game (Carreras and Magaña, 1997); the Alonso–Fiestras value in (Alonso et al., 2005); the symmetric coalitional binomial semivalues in (Carreras and Puente, 2011); and coalitional multinomial probabilistic values in (Carreras and Puente, 2015). In all these cases, the first three steps of the procedure are the same.

Instead, the consideration of the modified MLE g_j for the union B_j obtained from the initial one has changed the procedure: first, we weight the terms of g_j multiplying each product $\prod_{k\in V} x_k$ by p_{v-1}^v and each product $\prod_{r\in W} y_r$ by q_w^{w+1} obtaining a new multilinear function called $\overline{g}_j$. Second, we obtain players' marginal contributions by partial differentiation of $\overline{g}_j$. This new procedure has an advantage with respect to the traditional method: the allocations given by the Owen value are available since the weighting coefficients p_k^{k-1} and q_k^{k+1} can be always easily obtained.

REFERENCES

Albizuri, M. J. (2002). Axiomatizations of Owen value without efficiency. *Discussion Paper 25. Department of Applied Economics IV, Basque Country University*.

Alonso, J. M., Carreras, F., and Fiestras, M. G. (2005). The multilinear extension and the symmetric coalition Banzhaf value. *Theory and Decision*, 59:111–126.

Alonso, J. M. and Fiestras, M. G. (2002). Modification of the Banzhaf value for games with a coalition structure. *Annals of Operations Research*, 109:213–227.

Amer, R. and Carreras, F. (1995). Cooperation indices and coalition value. *TOP*, 3:117–135.

Amer, R. and Carreras, F. (2001). Power, cooperation indices and coalition structures. *Power Indices and Coalition Formation*, pages 153–173.

Amer, R., Carreras, F., and Giménez, J. M. (2002). The modified Banzhaf value for games with a coalition structure. *Mathematical Social Sciences*, 43:45–54.

Aumann, R. and Drèze, J. (1974). Cooperative games with coalition structures. *nternational Journal of Game Theory*, 3:217–237.

Banzhaf, J. (1965). Weigthed voting doesn't work: A mathematical analysis. *Rutgers Law Review*, 19:317–343.

Carreras, F. (2004). α–decisiveness in simple games. *Theory and Decision*, 56:77–91.

Carreras, F. and Giménez, J. (2011). Power and potential maps induced by any semivalue: Some algrebraic properties and computation by multilinear extension. *European Journal of Operational Research*, 211:148–159.

Carreras, F. and Magaña, A. (1994). The multilinear extension and the modified Banzhaf–Coleman index. *Mathematical Social Sciences*, 28:215–222.

Carreras, F. and Magaña, A. (1997). The multilinear extension of the quotient game. *Games and Economic Behavior*, 18:22–31.

Carreras, F. and Puente, M. (2011). Symmetric coalitional binomial semivalues. *Group Decision and Negotiation*, 21:637–662.

Carreras, F. and Puente, M. (2015). Coalitional multinomial probabilistic values. *European Journal of Operational Research*, 245:236–246.

Dragan, I. (1997). Some recursive definitions of the Shapley value and other linear values of cooperative tu games. *Working paper 328. University of Texas at Arlington*.

Dubey, P. (1975). On the uniqueness of the Shapley value. *International Journal of Game Theory*, 4:131–139.

Feltkamp, V. (1995). Alternative axiomatic characterizations of the Shapley and Banzhaf values. *International Journal of Game Theory*, 24:179–186.

Hamiache, G. (1999). A new axiomatization of the owen value for games with coalition structures. *Mathematical Social Sciences*, 37:281–305.

Hamiache, G. (2001). The Owen value friendship. *International Journal of Game Theory*, 29:517–532.

Hart, S. and Kurz, M. (1983). Endogeneous formation of coalitions. *Econometrica*, 51:1047–1064.

Owen, G. (1972). Multilinear extensions of games. *Management Science*, 18:64–79.

Owen, G. (1975). Multilinear extensions and the Banzhaf value. *Naval Research Logistics Quarterly*, 22:741–750.

Owen, G. (1977). Values of games with a priori unions. *Mathematical Economics and Game Theory*, R. Henn and O. Moeschlin, eds.:76–88.

Owen, G. (1982). Modification of the Banzhaf-Coleman index for games with a priori unions. *Power, Voting and Voting Power*, M.J. Holler, ed:232–238.

Owen, G. (1995). *Game Theory*. Academic Press Inc.

Owen, G. and Winter, E. (1992). Multilinear extensions and the coalitional value. *Games and Economic Behavior*, 4:582–587.

Peleg, B. (1989). Introduction to the theory of cooperative games. *Chapter 8: The Shapley value. RM 88, Center for Research in Mathematical Economics and Game Theory, the Hebrew University, Israel.*

Puente, M. A. (2000). Aportaciones a la representabilidad de juegos simples y al cálculo de soluciones de esta clase de juegos. *Ph.D. Thesis. Technical University of Catalonia, Spain.*

Roth, A. (1988). *The Shapley Value: Essays in Honor of Lloyd S. Shapley*. Cambridge University Press, Cambridge.

Shapley, L. and Shubik, M. (1954). A method for evaluating the distribution of power in a committee system. *American Political Science Review*, 48:787–792.

Shapley, L. S. (1953). A value for n-person games. *Contributions to the Theory of Games II (H.W. Kuhn and A.W. Tucker, eds)*.

Vázquez, M. (1998). Contribuciones a la teoría del valor en juegos con utilidad transferible. *Ph.D. Thesis. University of Santiago de Compostela, Spain.*

Vázquez, M., Nouweland, A. v. d., and García Jurado, I. (1997). Owen's coalitional value and aircraft landing fees. *Mathematical Social Sciences*, 4:132–144.

Winter, E. (1992). The consistency and potential for values with coalition structure. *Games and Economic Behavior*, 4:132–144.

Variable Neighbourhood Search Solving Sub-problems of a Lagrangian Flexible Scheduling Problem

Alexander Hämmerle[1] and Georg Weichhart[1,2]
[1]*Profactor GmbH, 4407 Steyr-Gleink, Austria*
[2]*Dep. of Business Informatics - Communications Engineering, Johannes Kepler University, 4040 Linz, Austria*
{*alexander.haemmerle, georg.weichhart*}*@profactor.at*

Keywords: Flexible Job Shop Scheduling, Lagrangian Relaxation, Subgradient Search, Variable Neighbourhood Search.

Abstract: New technologies allow the production of goods to be geographically distributed across multiple job shops. When optimising schedules of production jobs in such networks, transportation times between job shops and machines can not be neglected but must be taken into account. We have researched a mathematical formulation and implementation for flexible job shop scheduling problems, minimising total weighted tardiness, and considering transportation times between machines. Based on a time-indexed problem formulation, we apply Lagrangian relaxation, and the scheduling problem is decomposed into independent job-level sub-problems. This results in multiple single job problems to be solved. For this problem, we describe a variable neighbourhood search algorithm, efficiently solving a single flexible job (sub-)problem with many timeslots. The Lagrangian dual problem is solved with a surrogate subgradient search method aggregating the partial solutions. The performance of surrogate subgradient search with VNS is compared with a combination of dynamic programming solving sub-problems, and a standard subgradient search for the overall problem. The algorithms are benchmarked with published problem instances for flexible job shop scheduling. Based on these instances we present novel problem instances for flexible job shop scheduling with transportation times between machines, and lower and upper bounds on total weighted tardiness are calculated for these instances.

1 INTRODUCTION

Manufacturing processes are executed across geographically distributed job shops. Despite this distribution, a globally optimised production schedule is desirable to stay competitive. For implementation of an optimisation algorithm for distributed production networks, we have formulated a flexible job shop problem with transport times to account for the distribution. The jobs have to be scheduled across multiple machines in the production network. Each job is consisting of a defined sequence of operations. The machines assigned to a specific job may be in different shops, requiring transport of the workpiece(s). We regard flexible scheduling problems, i.e. an operation can be processed on alternative machines, where each operation takes a different timespan to be completed. We do not consider transport resources with limited capacities, hence we are not confronted with the additional problem of routing transport resources. Due dates for jobs are specified, and we consider total weighted tardiness as overall objective function.

As the distribution of the production system is one of the distinguishing features of our approach, *distribution* as a general principle, guided the development of our algorithm solving the outlined problem. The scheduling problem has been divided into multiple sub-problems that can be solved in a distributed manner. In a physical modelling approach, a sub-problem corresponds to a physical entity, e.g. a machine, a job or a job shop. With a proper decomposition into sub-problems, a distributed scheduling algorithm allows dynamic scheduling with localised disturbance handling, confined to a small set of sub-problems, and performance improvements through concurrent computing.

We modelled the problem decomposition based on a sound mathematical foundation, and the distributed scheduling algorithm provides not only high-quality upper bounds on total weighted tardiness, but also guaranteed lower bounds.

Lagrangian relaxation is a method satisfying these requirements, with a substantial scientific track record for job shop scheduling problems. Relevant work can be found in (Hoitomt et al., 1993), (Wang et al., 1997), (Chen and Luh, 2003), (Baptiste et al., 2008),

Hämmerle, A. and Weichhart, G.
Variable Neighbourhood Search Solving Sub-problems of a Lagrangian Flexible Scheduling Problem.
In *Proceedings of the 6th International Conference on Operations Research and Enterprise Systems (ICORES 2017)*, pages 234-241
ISBN: 978-989-758-218-9

(Buil et al., 2012), (Chen et al., 1998) and (Kaskavelis and Caramanis, 1998). An analysis of the relevant work shows that predominantly *machine capacity constraints* are relaxed, based on a time-indexed mathematical formulation. The resulting job-level sub-problems (single job-shop scheduling problems) are not $\mathcal{NP}$-hard and they are solved with dynamic programming, with its complexity depending on the required number of timeslots for the scheduling problem instance. The dual problem. through which the sub-problem solutions are brought together, is solved with variants of subgradient search. The effect that the single job-shop scheduling problems are solved concurrently is, that the generated solution is (likely) infeasible, with multiple job-operations scheduled on a single machine. The favourite method for feasibility repair is list scheduling.

Our work relies on the mainstream results of the relevant work. In our approach we relax machine capacity constraints, we use subgradient search to solve the dual problem and we use list scheduling for feasibility repair.

However, when it comes to solving sub-problems, dynamic programming is not efficient enough for problem instances with many timeslots. Such problem instances can easily occur if we regard manufacturing networks with long transportation times between shops, respectively machines. We therefore implemented a new heuristic for solving the sub-problems in more time-efficient manner. For solving the dual problem, we apply a surrogate subgradient search, which allows the sub-problems to be solved approximately. Thus we define our main research contribution:

- Specification of novel problem instances for flexible job shop scheduling with transportation times between machines (FJSSTT), based on published instances for flexible job shop scheduling. These instances are used for benchmarking our algorithms.
- A Variable Neighbourhood Search (VNS) algorithm, efficiently solving job-level sub-problems with many timeslots.
- Calculation of lower and upper bounds on total weighted tardiness for the novel FJSSTT instances.

The remainder of the paper is structured as follows. In section 2 we discuss the benchmark problem instances and their extension with transportation times. The mathematical model including problem formulation and Lagrangian relaxation is described in section 3. Problem solving algorithms are discussed in section 4, and computational results are provided in section 5. Finally we present our conclusions in section 6.

2 FJSSTT PROBLEM INSTANCES

As benchmark instances for flexible job shop scheduling we use the problem instances WT1-WT5, published in (Brandimarte, 1993). Based on these instances, we generated novel FJSSTT problem instances in the following way: (1) For each WT instance the machines are randomly grouped into three job shops. (2) Short/moderate/long transportation times between the job shops were calculated. A lower bound on the makespan for the respective problem instance serves as reference time R. The transportation times are then randomly generated from the following intervals.

- Short transportation times (network type A): $(0.09\,R, 0.11\,R)$
- Moderate transportation times (network type B): $(0.9\,R, 1.1\,R)$
- Long transportation times (network type C): $(9\,R, 11\,R)$

The transportation times between the job shops satisfy the triangle inequality. Within a shop the transportation times are 0. Figure 1 provides an overview of the original instances WT1-WT5 and the generated FJSSTT instances.

Instance	Timeslots	Machines	Jobs	Transportation Times
WT1	300	5	10	-
WT1A	300	5	10	3,4
WT1B	500	5	10	32,34,37
WT1C	3000	5	10	324,326,350
WT2	300	5	20	-
WT2A	300	5	20	3,4
WT2B	1500	5	20	35,36,39
WT2C	4000	5	20	334,362,387
WT3	1500	10	20	-
WT3A	2000	10	20	24,27,29
WT3B	4000	10	20	244,250,263
WT3C	100000	10	20	2500,2512,2861
WT4	3000	10	20	-
WT4A	4000	10	20	25,27
WT4B	5000	10	20	234,242,259
WT4C	50000	10	20	2329,2616,2705
WT5	2000	15	30	-
WT5A	2500	15	30	22,24
WT5B	5000	15	30	208,219,231
WT5C	50000	15	30	2069,2199,2408

Figure 1: Problem instances.

3 MATHEMATICAL MODEL

In this section we describe a mathematical model for the FJSSTT problem with minimisation of total weighted tardiness as objective. Lagrangian relaxation is applied to the machine capacity constraints, and the resulting Lagrangian problem is decomposed into independent job-level sub-problems.

3.1 Problem Formulation

Our problem formulation is based on (Wang et al., 1997). I jobs with individual due dates have to be scheduled on M available machines. We assume immediate availability of jobs. The set of jobs I is $\{0,1,...,I-1\}$ and the set of machines $\mathcal{M}$ is $\{0,1,...,M-1\}$. Job i consists of J_i non-preemptive operations, with $\mathcal{J}_i = \{0,1,...,J_i-1\}$ denoting the set of operations for job i. The operation j of job i is denoted as (i,j). We regard simple, chain-like precedence constraints amongst operations belonging to the same job. The set of alternative machines for operation (i,j) is denoted as $\mathcal{H}_{ij}$, with machine-specific processing times. The scheduling horizon consists of K discrete timeslots, the set of timeslots $\mathcal{K}$ is $\{0,1,...,K-1\}$. The beginning time of an operation is defined as the beginning of the corresponding timeslot, and the completion time as the end of the timeslot.

In the following we introduce further parameters and decision variables used in the mathematical model. Parameters are given with a specific problem instance as input data, whereas the decision variables span the solution space for the scheduling problem.

Parameters

$D_i, i \in I$: Job due dates.

$P_{ijm}, i \in I, j \in \mathcal{J}_i, m \in \mathcal{H}_{ij}$: Processing time of operation (i,j) on machine m.

$R_{mn}, m \in \mathcal{M}, n \in \mathcal{M}$: Transportation time from machine m to machine n.

$W_i, i \in I$: Job tardiness weight.

Variables

$\delta_{ijmk}, i \in I, j \in \mathcal{J}_i, m \in \mathcal{M}, k \in \mathcal{K}$: The binary variable δ_{ijmk} is 1, if operation (i,j) is processed on machine m at timeslot k, and 0 otherwise.

$b_{ij}, i \in I, j \in \mathcal{J}_i$: Beginning time of operation (i,j).

$c_{ij}, i \in I, j \in \mathcal{J}_i$: Completion time of operation (i,j).

$m_{ij} \in \mathcal{H}_{ij}, i \in I, j \in \mathcal{J}_i$: The machine assigned to operation (i,j).

$\lambda_{mk}, m \in \mathcal{M}, k \in \mathcal{K}$: Lagrange multiplier for timeslot k on machine m.

The decision variables δ_{ijmk}, b_{ij} and c_{ij} are not independent, the following relation holds:

$$\delta_{ijmk} = \begin{cases} 1 & \text{if } b_{ij} \leq k \leq c_{ij} \\ 0 & \text{otherwise.} \end{cases} \quad (1)$$

The optimisation objective is the minimisation of the weighted sum of job tardiness, the optimisation problem is then

$$\mathcal{Z} = \min_{b_{ij}, m_{ij}} \sum_{i \in I} W_i T_i, \quad (2)$$

with

$$T_i = max(0, C_i - D_i), \quad (3)$$

where C_i is the completion time for job i, i.e. $C_i = c_{i,J_i-1}$.

Constraints Equation (2) has to be solved subject to a number of constraints. The machine capacity constraints are expressed as

$$\sum_{i \in I} \sum_{j \in \mathcal{J}_i} \delta_{ijmk} \leq 1, \forall m \in \mathcal{M}, \forall k \in \mathcal{K}. \quad (4)$$

Equation (4) states that at each timeslot a machine cannot process more than one operation. Processing time constraints define the relation between beginning time and completion time of operations:

$$c_{ij} = b_{ij} + P_{ijm_{ij}} - 1, \forall i \in I, \forall j \in \mathcal{J}_i. \quad (5)$$

The precedence constraints between job operations are

$$b_{ij} \geq c_{i,j-1} + 1 + R_{m_{i,j-1} m_{ij}}, \forall i \in I, \forall j \in \mathcal{J}_i. \quad (6)$$

The term "1" in (5) and (6) occurs due to the definition of operation beginning time and completion time, respectively. The precedence constraints consider transportation times R_{mn} between machines. For operations $(i,j-1)$ and (i,j) equation (6) states that the beginning time of (i,j) cannot be earlier than the arrival time at machine m_{ij}. We assume immediate availability of transport resources to move workpieces corresponding to jobs between machines. The transportation time between machines located in different job shops covers transport between the shops as well as shop-internal logistics activities.

The occurrence of the term $R_{m_{i,j-1} m_{ij}}$ in (6) renders the constraint non-linear. This non-linearity can easily be resolved, in fact the mathematical model can be formulated as a linear integer program, which is outside the scope of this paper.

3.2 Lagrangian Relaxation

For the FJSSTT problem there are two candidate constraint sets for relaxation: precedence constraints and machine capacity constraints. The relaxation of precedence constraints and decomposition into independent machine-level sub-problems is hampered by the structure of the precedence constraints (6), as the term $R_{m_{i,j-1}m_{ij}}$ couples the precedence constraints across machines. Lagrangian relaxation of machine capacity constraints results in the relaxed problem

$$\mathcal{Z}_D(\lambda) = \min_{b_{ij},m_{ij}} \sum_{i\in I} W_i T_i + \sum_{m\in\mathcal{M}} \sum_{k\in\mathcal{K}} \lambda_{mk} \left[\sum_{i\in I} \sum_{j\in\mathcal{J}_i} \delta_{ijmk} - 1 \right], \quad (7)$$

where λ is the vector of Lagrange multipliers. (7) has to be solved subject to constraints (5) and (6). For a given pair of indices m,k the term in brackets is positive if the capacity constraint for timeslot k on machine m is violated. $\mathcal{Z}_D(\lambda)$ can be reformulated as

$$\mathcal{Z}_D(\lambda) = \min_{b_{ij},m_{ij}} \sum_{i\in I} W_i T_i + \sum_{i\in I} \sum_{j\in\mathcal{J}_i} \sum_{k=b_{ij}}^{c_{ij}} \lambda_{m_{ij}k} - \sum_{m\in\mathcal{M}} \sum_{k\in\mathcal{K}} \lambda_{mk}. \quad (8)$$

The structure of $\mathcal{Z}_D(\lambda)$ allows the decomposition into independent job-level sub-problems

$$\mathcal{S}_i = \min_{b_{ij},m_{ij}} W_i T_i + \sum_{j\in\mathcal{J}_i} \sum_{k=b_{ij}}^{c_{ij}} \lambda_{m_{ij}k}. \quad (9)$$

$\mathcal{S}_i$ is a one job scheduling problem and can be characterised as follows, cf. (Chen et al., 1998). A job requires the completion of a set of operations, and each operation can be performed on one of several alternative machines. The job operations must satisfy a set of chain-like precedence constraints (6), considering transportation times between machines. Furthermore processing time constraints (5) have to be satisfied. Each machine has a marginal cost for utilisation at each timeslot within the scheduling horizon under consideration. The scheduling problem is to determine the machine and the completion time of each operation of the job to minimise the sum of job tardiness and the total cost of using the machines to complete the job, where the cost of using machine m at time k is given as λ_{mk}.

With the introduction of sub-problems $\mathcal{S}_i$, the relaxed problem can be reformulated,

$$\mathcal{Z}_D(\lambda) = \sum_{i\in I} \mathcal{S}_i - \sum_{m,k} \lambda_{mk}. \quad (10)$$

The Lagrangian dual problem, optimising the Lagrange multiplier values, is

$$\mathcal{Z}_D = \max_{\lambda} \mathcal{Z}_D(\lambda). \quad (11)$$

It can be shown that $\mathcal{Z}_D(\lambda)$ is concave and piece-wise linear, thus hill-climbing methods like sub-gradient search can be applied to solve the dual problem. The one job scheduling problem is not $\mathcal{NP}$-hard, and it can be exactly solved with dynamic programming, with complexity $O\left(K\sum_j \left|\mathcal{H}_{ij}\right|\right)$. However, we will see in section 5 that the efficiency of dynamic programming is not good enough to cope with FJSSTT instances with many timeslots. Thus a fast heuristic has to be developed to solve the one job scheduling problems. In the following section we will describe such a heuristic approach.

4 PROBLEM SOLVING

In this section we first describe the formulation of the dual problem, which is followed by the sub-problem solving heuristic Variable Neighbourhood Search (VNS).

4.1 Dual Problem

In order to solve the Lagrangian dual problem (11) we apply two variants of the subgradient search (SG): standard SG, and surrogate SG. The standard SG method requires the dual problem (and thus the sub-problems (9)) to be fully optimised, otherwise proper subgradient directions can not be calculated. With the dual problem fully optimised, the dual cost $\mathcal{Z}_D$ are a lower bound on total weighted tardiness. In the surrogate SG method it is sufficient to solve the dual problem approximately, and thus we can apply VNS to solve the sub-problems.

In an SG iteration l the Lagrange multipliers are adjusted for the next iteration according to

$$\lambda_{mk}^{l+1} = \lambda_{mk}^{l} + s_l \gamma_{mk}^{l}, \quad (12)$$

with a positive, scalar step-size s_l and γ_{mk}^{l}, an element of the subgradient vector γ^l,

$$\gamma_{mk}^{l} = \sum_{i\in I} \sum_{j\in\mathcal{J}_i} \delta_{ijmk}^{*} - 1. \quad (13)$$

δ_{ijmk}^{*} denotes the optimal value for δ_{ijmk} in iteration l, resulting from solving $\mathcal{Z}_D(\lambda)$ with Lagrange multipliers λ^l. The element γ_{mk}^{l} can be interpreted as violation

of the machine capacity constraint for machine m and timeslot k in SG iteration l.

In the standard SG method we use a common formula for the calculation of step-sizes:

$$s_l = \alpha_l \frac{\mathcal{Z}^* - \mathcal{Z}_D(\lambda^l)}{\|\gamma^l\|^2}, \tag{14}$$

with a scalar $\alpha_l, 0 < \alpha_l < 2$. $\mathcal{Z}^*$ is an upper bound on $\mathcal{Z}_D$ and is updated if feasibility repair improves the upper bound. The search is initialised with a parameter α_0, and α_l is halved after Γ iterations if no improvement in $\mathcal{Z}_D$ has been achieved.

The step-sizes for the surrogate SG method are calculated according to (Bragin et al., 2014):

$$s_l = \beta_l \frac{s_{l-1} \left\|\tilde{\gamma}^{l-1}\right\|}{\|\tilde{\gamma}^l\|}, \tag{15}$$

with the surrogate subgradient vector $\tilde{\gamma}^l$. The parameter β_l is adjusted according to

$$\beta_l = 1 - \frac{1}{\Omega \cdot l^\rho}, \rho = 1 - \frac{1}{l^r}, \tag{16}$$

with configuration parameters Ω and r. The step-size calculation is initialised with configuration parameter s_0. With the step-size formula (15) (Bragin et al., 2014) prove convergence of the surrogate SG method, and they show that upon convergence the lower bound property of dual cost is preserved.

4.2 Variable Neighbourhood Search

To solve a one job scheduling problem approximately we propose a Variable Neighbourhood Search (VNS) heuristics with the following neighbourhood structures. Let J denote the number of operations of the job under consideration.

Neighbourhood Structure $AM1$**:** An operation j is chosen at random, and a random alternative machine is assigned to j. If this move causes the violation of precedence constraints, it is rejected. $AM1$ is configured with a distance parameter $AM1_{Dist}$, denoting the number of operations for whom alternative machines are assigned cascadingly. Assigning an operation j to a different machine implies that the duration is changed.

Neighbourhood Structure $AM2$**:** An operation j is chosen at random, and a random alternative machine is assigned to j. The new beginning time of j and all successive operations $k > j$ is the respective earliest feasible beginning time considering the precedence constraints, plus some small, random slack. $AM2$ uses a distance parameter $AM2_{Dist}$.

Neighbourhood Structure SL**:** Applying SL to the incumbent solution, a neighbour solution results from a cascade of leftward shifts, starting with a random operation j. Let x_{SL} be the neighbour solution after shifting j, and let σ denote the available slack between operations $j-1, j$. The shift distance SL_{Dist} is a random integer from the interval $(1, \sigma)$. If $\sigma = 0$ the move SL is rejected. Otherwise in the next step of the cascade operation $j+1$ is shifted leftward, with distance SL_{Dist}. Successively the operations $j, j+1, ..., J$ are shifted leftward by SL_{Dist}. After each shift the cost of the resulting neighbour solution are evaluated according to (9). The neighbour solution with minimal cost is the result of applying SL.

Neighbourhood Structure SR**:** Analogous to SL the neighbourhood structure SR defines a cascade of rightward shifts, with a shift distance SR_{Dist}. The cascade starts with a random operation and ends with the first operation.

In the shaking phase of the proposed VNS the neighbourhood structure $AM2$ is used, with increasing values for $AM2_{Dist}$. If no improvement is achieved, the last shaking level is the generation of a new random solution "in the neighbourhood" of the incumbent solution. The term "neighbourhood" reflects the fact that the beginning time of the first operation in the random solution is within a maximal distance L to the beginning time of the first operation in the incumbent solution. However, this last level is a massive shaking of the incumbent solution, and allows to bridge broad valleys in the fitness landscape, guiding the local search to new areas in the search space.

In the local search phase the neighbourhood structures $SL \rightarrow AM1 \rightarrow SR$ are used, in the indicated sequence. Figure *Algorithm 1* shows the pseudocode of the proposed VNS algorithm. The algorithm is initialised in lines 2 - 7. An initial solution is generated at random, and configuration parameters are set. The indicated values for parameters A, B, F, L, G are exemplary. For a randomly generated solution, parameter G denotes the maximal distance between two consecutive operations.

5 COMPUTATIONAL RESULTS

In computational experiments with the problem instances outlined in figure 1 we compared the performance of two algorithms:

1. Algorithm ***StDP***: Standard SG solves the dual problem, dynamic programming is used to solve

Algorithm 1: VNS Pseudocode.

```
1: Initialisation
2: x ← random solution
3: A ← 50                                          ▷ Number of VNS iterations
4: B ← 50                                          ▷ Number of local search iterations
5: F ← 3                                           ▷ The maximal value of AM2_Dist
6: L ← 50
7: G ← 5
8: VNS iterations
9: for a ← 1,A do
10:     f ← 1
11:     while f ≤ F + 1 do                         ▷ Shaking loop
12:         if f = F + 1 then
13:             x̂ ← random solution "in the neighbourhood" of x
14:         else
15:             AM2_Dist ← f
16:             x̂ ← AM2neighbour solution with incumbent solutionx
17:         end if
18:         for b ← 1,B do                         ▷ Local search iterations
19:             for l ← 1,3 do
20:                 if l = 1 then
21:                     x' ← SL neighbour solution with incumbent solution x̂
22:                 else if l = 2 then
23:                     AM1_Dist = 1
24:                     x' ← AM1 neighbour solution with incumbent solution x̂
25:                 else if l = 3 then
26:                     x' ← SR neighbour solution with incumbent solution x̂
27:                 end if
28:                 if cost(x') ≤ cost(x̂) then
29:                     x̂ ← x'
30:                 end if
31:             end for
32:         end for
33:         if cost(x̂) < cost(x) then
34:             x ← x̂
35:             f ← 1
36:         else
37:             f ← f + 1
38:         end if
39:     end while
40: end forreturn x
```

the sub-problems. SG configuration: $\alpha_0 = 2, \Gamma = 20$.

2. Algorithm ***SuVNS***: Surrogate SG solves the dual problem, VNS solves the sub-problems. SG configuration: $s_0 = 0.2, \Omega = 25, r = 0.1$.

Both algorithms use a list scheduling algorithm for feasibility repair. Our implementation supports concurrent computing with respect to solving sub-problems. The experiments were performed on the following computer hardware: Intel® Core™ i7-6700 CPU @ 3.40GHz, 4 cores and 8 GB ram. On the software side, the operating system was Microsoft® Windows™ 10 Pro using Java 1.8 as programming and execution environment.

Figure 2 shows the results of computational experiments with 800 SG iterations, and feasibility repair every 2 iterations. The deterministic algorithm *StDP* was executed once per problem instance. To gather statistical results for the non-deterministic algorithm *SuVNS*, 10 runs were performed with *SuVNS* per problem instance. In figure 2 column UB^* refers to

		Algorithm StDP			Algorithm SuVNS					
Instance	UB*	UB	LB	Runtime	Max UB	UB^M	Min UB	Min LB	Max LB	Runtime
WT1	57	66	43.8	13	79	71	57	43.7	44.0	36
WT1A	138	95	58.2	12	97	90	84	57.5	58.0	35
WT1B	757	573	550.0	29	584	581	574	550.2	550.4	28
WT1C	9869	9030	9004.1	1104	9023	9023	9023	9019.0	9019.1	30
WT2	252	321	128.8	23	350	328	296	125.9	126.8	70
WT2A	911	450	215.6	23	463	441	389	212.0	212.8	67
WT2B	2564	1629	1346.7	538	1695	1660	1628	1336.3	1337.0	59
WT2C	21787	17287	17193.6	5013	17288	17278	17267	17210.1	17211.4	55
WT3	128	281	92.2	1427	276	234	184	85.5	87.1	223
WT3A	4580	2244	1319.6	2920	2370	2282	2185	1310.2	1311.7	443
WT3B	40521	37501	36939.2	15494	37564	37481	37429	36938.6	36940.6	330
WT3C	414403	-	-	-	405531	405477	405402	405182.8	405184.5	194
WT4	112	112	102.2	11956	112	112	112	102.9	105.3	371
WT4A	986	529	449.3	24519	521	503	481	459.4	461.6	545
WT4B	22823	17377	16832.8	38897	17369	17305	17229	16839	16841	424
WT4C	479835	-	-	-	422277	422236	422206	421988	421989	372
WT5	166	166	166.0	15466	169	167	166	153.6	156.7	421
WT5A	3128	887	836.4	27886	905	890	875	845.7	849.8	782
WT5B	28732	17347	16205.0	164000	17289	17204	17100	16218.1	16220.1	600
WT5C	536977	-	-	-	339851	339746	339654	338873.2	338874.2	592

Figure 2: Computational results.

Instance	A	B	G	F	L
WT1	50	100	5	3	50
WT1A	50	100	5	3	50
WT1B	50	100	5	3	50
WT1C	50	100	5	3	50
WT2	50	100	5	3	100
WT2A	50	100	5	3	100
WT2B	50	100	5	3	100
WT2C	50	100	5	3	100
WT3	150	200	5	3	50
WT3A	100	150	5	3	50
WT3B	100	150	5	3	50
WT3C	50	100	5	3	50
WT4	100	100	5	3	50
WT4A	100	150	5	3	50
WT4B	100	150	5	3	50
WT4C	100	150	5	3	50
WT5	50	150	5	3	50
WT5A	100	150	5	3	400
WT5B	100	150	5	3	400
WT5C	100	150	5	3	50

Figure 3: VNS configurations.

the best known value for total weighted tardiness for the respective problem instance. For the instances WT1-5 these values are taken from (Sobeyko and Mönch, 2015), for the FJSSTT instances they are calculated with list scheduling. For algorithm *StDP* lower and upper bound on total weighted tardiness are indicated (columns LB, UB) as well as the runtime in seconds. The columns $\mathrm{Max}\,UB, UB^M, \mathrm{Min}\,UB$ indicate maximum, mean value and minimum for total weighted tardiness calculated with algorithm *SuVNS*. Minimium and maximum for lower bounds are given in columns $\mathrm{Min}\,LB, \mathrm{Max}\,LB$. The VNS algorithm is configured according to figure 3. The configurations were determined in computational experiments with sub-problems, benchmarking VNS with exact solutions calculated with dynamic programming.

Analysing the results for problem instances WT1-5, we note that the duality gap for instances indicates if algorithms *StDP* and *SuVNS* work well on the instance. The duality gaps for WT4 and WT5 are small, and the algorithms provide upper bounds very close or equal to the best known values. For WT2 and WT3 the duality gaps are distinct, and the calculated upper bounds significantly deviate from the best known values. A remarkable result is provided by *StDP* for WT5: the duality gap is 0, proving optimality of the upper bound 166.

The results for the FJSSTT instances show a strong dependence of the *StDP* runtime on the number of timeslots specified for the problem instance, cf. figure 1. For WT3C, WT4C and WT5C we were not able to calculate solutions with *StDP* and reasonable runtime. The algorithm *SuVNS* is clearly advantageous in terms of runtime, and the upper bounds are of good quality, comparing them with *StDP* results.

6 CONCLUSIONS

The computational experiments have shown promising results. However, the list scheduling method employed for feasibility repair is rather weak, and we expect a more sophisticated heuristic to improve the results. Furthermore, it is advisable to extend the computational experiments to more problem instances.

So far we have been concerned with static scheduling problems. In a dynamic scheduling problem, a schedule is executed and disturbances like transportation delays or machine failures hamper the scheduled processing of operations. It would be interesting to apply the proposed, distributed algorithm to dynamic scheduling problems, and to explore the possibilities of localised disturbance handling.

As a next step we want to improve the quality of the feasibility repair mechanism. Also more experiments with MK problems will take place. The algorithm will be extended to allow dynamic rescheduling (e.g. in case of a machine break down).

ACKNOWLEDGEMENTS

This research is funded by the Austrian Ministry for Transport, Innovation and Technology www.bmvit.gv.at through the project NgMPPS-DPC.

REFERENCES

Baptiste, P., Flamini, M., and Sourd, F. (2008). Lagrangian bounds for just-in-time job-shop scheduling. *Computers & Operations Research*, 35(3):906–915.

Bragin, M. A., Luh, P. B., Yan, J. H., Yu, N., and Stern, G. A. (2014). Convergence of the Surrogate Lagrangian Relaxation Method. *Journal of Optimization Theory and Applications*, 164(1):173–201.

Brandimarte, P. (1993). Routing and scheduling in a flexible job shop by tabu search. *Annals of Operations research*, 41(3):157–183.

Buil, R., Piera, M. A., and Luh, P. B. (2012). Improvement of lagrangian relaxation convergence for production scheduling. *Automation Science and Engineering, IEEE Transactions on*, 9(1):137–147.

Chen, H., Chu, C., and Proth, J.-M. (1998). An improvement of the Lagrangean relaxation approach for job shop scheduling: a dynamic programming method. *Robotics and Automation, IEEE Transactions on*, 14(5):786–795.

Chen, H. and Luh, P. B. (2003). An alternative framework to Lagrangian relaxation approach for job shop scheduling. *European Journal of Operational Research*, 149(3):499–512.

Hoitomt, D. J., Luh, P. B., and Pattipati, K. R. (1993). A practical approach to job-shop scheduling problems. *Robotics and Automation, IEEE Transactions on*, 9(1):1–13.

Kaskavelis, C. A. and Caramanis, M. C. (1998). Efficient Lagrangian relaxation algorithms for industry size job-shop scheduling problems. *IIE transactions*, 30(11):1085–1097.

Sobeyko, O. and Mönch, L. (2015). Heuristic Approaches for Scheduling Jobs in Large-scale Flexible Job Shops. *Computers & Operations Research*. accepted for publication.

Wang, J., Luh, P. B., Zhao, X., and Wang, J. (1997). An optimization-based algorithm for job shop scheduling. *Sadhana*, 22(2):241–256.

Ability to Separate Situations with a Priori Coalition Structures by Means of Symmetric Solutions

José Miguel Giménez
Department of Mathematics, Technical University of Catalonia, Avda. Bases de Manresa 61, E-08242 Manresa, Spain
jose.miguel.gimenez@upc.edu

Keywords: Cooperative game, Coalition structure, Marginal contribution, Semivalue, Separability.

Abstract: We say that two situations described by cooperative games are inseparable by a family of solutions, when they obtain the same allocation by all solution concept of this family. The situation of separability by a family of linear solutions reduces to separability from the null game. This is the case of the family of solutions based on marginal contributions weighted by coefficients only dependent of the coalition size: the semivalues. It is known that for games with four or more players, the spaces of inseparable games from the null game contain games different to zero-game. We will prove that for five or more players, when a priori coalition blocks are introduced in the situation described by the game, the dimension of the vector spaces of inseparable games from the null game decreases in an important manner.

1 INTRODUCTION

Probabilistic values as a solution concept for cooperative games were introduced in (Weber, 1988). The payoff that a probabilistic value assigns to each player is a weighted sum of its marginal contributions to the coalitions, where the weighting coefficients form a probabilistic distribution over the coalitions to which it belongs. A particular type of probabilistic values is formed by the semivalues that were defined in (Dubey et al., 1981). In this case the weighting coefficients are independent of the players and they only depend on the coalition size. Semivalues represent a natural generalization of both the Shapley value (Shapley, 1953) and the Banzhaf value (Banzhaf, 1965; Owen, 1975). According to this approach, many works deal with the semivalues, with general properties as in (Carreras and Giménez, 2011), or applied to simple games as in (Carreras et al., 2003), and many others.

It is possible to find two cooperative games that obtain the same payoff vector for each semivalue. We say that these games are inseparable by semivalues. By the linearity property of semivalues, we can reduce the problem of separability between games to separability from the null game. The vector subspace of inseparable games from the null game by semivalues is called in (Amer et al., 2003) shared kernel and its dimension is $2^n - n^2 + n - 2$, where n denotes the number of players. For spaces of cooperative games with four or more players, the shared kernel contains games different to zero-game

The semivalues form an important family of solutions. We can evaluate their amplitude according to their faculty to separate games. Two games are separable if their difference does not belong to the shared kernel. The dimension of this subspace would mark the separation impossibility. In this paper we consider coalition structures in the player set. It is not difficult to find in the literature many papers devoted to the modified semivalues by coalition structures, for instance (Albizuri, 2009) or (Giménez and Puente, 2015), among others. Our purpose is to reduce the dimension of the vector subspace of inseparable games from the null game. For cooperative games with five or more players, modified semivalues for games with coalition structure (Amer and Giménez, 2003) are able to reduce in a significant way the dimension of the shared kernel.

In addition, once an a-priori ordering is chosen in the player set, we can see in (Amer et al., 2003) that the shared kernel is spanned by specific $\{-1,0,1\}$-valued games. These games are known as commutation games. Now, we will prove that the vector subspace of inseparable games from the null game by modified semivalues is spanned by games introduced here with the name of expanded commutation games.

The paper is organized as follows. In Section 2 we remember the solution concepts of semivalue and semivalue modified for games with a coalition structure whose allocations can be computed by means of

Giménez, J.
Ability to Separate Situations with a Priori Coalition Structures by Means of Symmetric Solutions.
In *Proceedings of the 6th International Conference on Operations Research and Enterprise Systems (ICORES 2017)*, pages 242-249
ISBN: 978-989-758-218-9

the multilinear extension (Owen, 1972) of each game. Also, nomenclature and main results for inseparable games by semivalues are described. Section 3 shows that commutation games that are the solution for the problem of separability by semivalues does not have in general the same properties with respect to separability by modified semivalues. In section 4 two sufficient conditions for separability by modified semivalues are proposed. Finally, in Section 5 we determine the dimension and a basis of the vector subspace of inseparable games from the null game by modified semivalues.

2 PRELIMINARIES

2.1 Cooperative Games and Semivalues

A *cooperative game* with transferable utility is a pair (N,v), where N is a finite set of *players* and $v : 2^N \to \mathbb{R}$ is the so-called *characteristic function*, which assigns to every *coalition* $S \subseteq N$ a real number $v(S)$, the *worth* of coalition S, and satisfies the natural condition $v(\emptyset) = 0$. With G_N we denote the set of all cooperative games on N. For a given set of players N, we identify each game (N,v) with its characteristic function v.

The *multilinear extension* MLE (Owen, 1972) of cooperative game $v \in G_N$ is a function $f_v : [0,1]^N \to \mathbb{R}$ defined as

$$f_v(x_1,x_2,...,x_n) = \sum_{S\subseteq N} \prod_{i\in S} x_i \prod_{j\notin S} (1-x_j) v(S), \quad (1)$$

so that it provides all information of the game contained in its characteristic function v.

A function $\psi : G_N \to \mathbb{R}^N$ is called a *solution* and it represents a method to measure the negotiation strength of the players in the game. The payoff vector space $\mathbb{R}^N$ is also called the allocation space. The *semivalues* (Dubey et al., 1981) as solution concept were introduced and axiomatically characterized by Dubey, Neyman and Weber in 1981. The payoff to the players for a game $v \in G_N$ by a semivalue ψ is an average of marginal contributions of each player:

$$\psi_i[v] = \sum_{S\ni i} p_s [v(S) - v(S\backslash\{i\})] \quad \forall i \in N, \quad (2)$$

where the weighting coefficients p_s only depend on the coalition size and verify $\sum_{s=1}^{n} \binom{n-1}{s-1} p_s = 1$ and $p_s \geq 0$ for $1 \leq s \leq n$. With $Sem(G_N)$ we denote the set of all semivalues on G_N.

Given a number $\alpha \in \mathbb{R}$, $0 < \alpha < 1$, we call *binomial semivalue* ψ_α to the semivalue whose coefficients are $p_{\alpha,s} = \alpha^{s-1}(1-\alpha)^{n-s}$. The extreme cases correspond to values $\alpha = 0$ and $\alpha = 1$. For $\alpha = 0$ we obtain the dictatorial index ψ_0, with coefficients $(1,0,...,0)$, whereas for $\alpha = 1$ we obtain the marginal index ψ_1, with coefficients $(0,...,0,1)$:

$$(\psi_0)_i[v] = v(\{i\}) \ \ \forall i \in N,$$
$$(\psi_1)_i[v] = v(N) - v(N\setminus\{i\}) \ \ \forall i \in N.$$

It is proven in (Amer and Giménez, 2003) that n different binomial semivalues form a reference system for the set of semivalues on G_N. Given n different numbers α_j in $[0,1]$, for every semivalue $\psi \in Sem(G_N)$ they exist unique coefficients λ_j, $1 \leq j \leq n$, such that $\psi = \sum_{j=1}^{n} \lambda_j \psi_{\alpha_j}$.

The Banzhaf value (Banzhaf, 1965; Owen, 1975) is the binomial semivalue for $\alpha = 1/2$. As it happens for the Banzhaf value, we see in (Amer and Giménez, 2003) that the allocation by every binomial semivalue can calculate replacing in the partial derivatives of MLE the variables by value α:

$$(\psi_\alpha)_i[v] = \frac{\partial f_v}{\partial x_i}(\overline{\alpha}) \quad \forall i \in N, \text{ where } \overline{\alpha} = (\alpha,\ldots,\alpha).$$

In addition, the allocation for every semivalue can be computed by means of a product of two matrices,

$$\psi[v] = B\,\Lambda, \quad (3)$$

where the matrix B depends on each reference system of semivalues $B = (b_{ij})_{1\leq i,j\leq n}$ with $b_{ij} = (\psi_{\alpha_j})_i[v] = \frac{\partial f_v}{\partial x_i}(\overline{\alpha_j})$ and Λ is the column matrix of the coefficients of ψ in this reference system, $\Lambda^t = (\lambda_1\,\lambda_2\cdots\lambda_n)$ if $\psi = \sum_{j=1}^{n} \lambda_j \psi_{\alpha_j}$. Thus, a $(n\times n)$-matrix summarizes the payments by any semivalue to all players of a given game v.

2.2 Cooperative Games and Coalition Structures

The formation of coalition blocks in the player set N gives rise to the construction of modified solutions in attention to this circumstance. It is the case of the Owen coalition value (Owen, 1977) from the Shapley value (Shapley, 1953) or the modified Banzhaf value for games with coalition structure (Owen, 1981) from the Banzhaf value. If we denote by $B = \{B_1,B_2,...,B_m\}$ the coalition structure in N, in both cases, the construction of the modified solutions follows a parallel way. It is considered a modified quotient game for each coalition $S \subseteq B_j$ and it is applied the Shapley or Banzhaf value. This action defines a game in B_j and there it is now applied the same solution obtaining for each $i \in B_j$ the modified allocations.

Given a semivalue $\psi \in Sem(G_N)$ with weighting coefficients p_s^n, the recursively obtained numbers

$$p_s^m = p_s^{m+1} + p_{s+1}^{m+1} \quad 1 \leq s \leq m < n,$$

define a *induced semivalue* ψ^m (Dragan, 1999) on the space of cooperative games with m players. Adding the own semivalue, the family of induced semivalues $\{\psi^m \in Sem(G_M) \,/\, 1 \leq m \leq n\}$ allows us to define the concept of *semivalue modified for games with coalition structure* (Amer and Giménez, 2003) following the same procedure as above. For a player i belongs to coalition block B_j the modified allocation has by expression

$$\psi_i[v;B] = \sum_{S \subseteq B_j \setminus \{i\}} \sum_{T \subseteq M \setminus \{j\}} p^{b_j}_{s+1}\, p^m_{t+1} \Big[v\big(\bigcup_{t \in T} B_t \cup S \cup \{i\}\big) - v\big(\bigcup_{t \in T} B_t \cup S\big) \Big]. \quad (4)$$

For the extreme coalition structures, individual blocks and grand coalition, the modified allocations agree with the allocation by the initial semivalue. Also, the allocations by modified semivalues can be computed by means of a product of matrices, once a reference system of binomial semivalues has been chosen:

$$\psi_i[v;B] = \Lambda^t\, A(i)\, \Lambda. \quad (5)$$

Matrix Λ is like in expression (3). The terms $a_{pq}(i)$, $1 \leq p,q \leq n$, of matrix $A(i)$ can be obtained by means of the following rules:

(i) Obtain the MLE $f_v = f_v(x_1,...,x_n)$ of game v.

(ii) For each $t \in M$, $t \neq j$, and each $m \in B_t$ replace the variable x_m by y_t. Thus, a new function of the variables x_k, y_t for $k \in B_j$ and $t \in M \setminus \{j\}$ is obtained.

(iii) In the above function, reduce all exponents that appear in y_t to 1, that is, replace y_t^r $(r > 1)$ by y_t, obtaining another multilinear function $g_j(x_k, y_t)$ $k \in B_j$ and $t \in M \setminus \{j\}$.

(iv) Calculate the derivative of the function g_j with respect to variable x_i.

(v) Replace each x_k with α_p and each y_t with α_q. Then,

$$a_{pq}(i) = \frac{\partial g_j}{\partial x_i}(\overline{\alpha_p}, \overline{\alpha_q}) \quad \text{for} \quad 1 \leq p,q \leq n. \quad (6)$$

2.3 Separability in Cooperative Games

We say that two cooperative games $v, v' \in G_N$ are *separable* by a solution ψ on G_N if $\psi[v] \neq \psi[v']$ for $v \neq v'$. When we study separability between games according to semivalues, we can only consider separability from the null game, since these solutions verify linearity property.

For each G_N, the linear subspace of all cooperative games inseparable by semivalues from the null game is called in (Amer et al., 2003) *shared kernel* C_N. It is proven that the dimension of C_N is $2^n - n^2 + n - 2$, since games in C_N have to satisfy conditions:

$$\sum_{S \ni i, |S| = s} v(S) = 0 \quad \text{for all } i \in N \text{ and } 1 \leq s \leq n. \quad (7)$$

Grouping these conditions according to coalition sizes, the freedom degrees for each s with $2 \leq s \leq n-2$ are $\binom{n}{s} - n$, whereas $v(S) = 0$ for $|S| = 1, n-1, n$. This way, the dimension of C_N is $2^n - n^2 + n - 2$ for $|N| = n \geq 2$ and $C_N = \{0\}$ if $|N| = 2, 3$.

In game spaces G_N with cardinality $|N| \geq 4$, for a given coalition $S \subseteq N$ and players $i, j \in S$ and $k, l \in N \setminus S$, we define the *commutation game* $v_{S,i,j,k,l}$ as

$$v_{S,i,j,k,l} = 1_S + 1_{S \cup \{k,l\} \setminus \{i,j\}} - 1_{S \cup \{k\} \setminus \{i\}} - 1_{S \cup \{l\} \setminus \{j\}}, \quad (8)$$

where 1_S is the unity game in G_N ($1_S(S) = 1$ and $1_S(T) = 1$ otherwise). If $v \in G_N$ is a commutation game, then $v \in C_N$. In (Amer et al., 2003), it is proven that the shared kernel is spanned by commutation games. Since each commutation game takes non null values uniquely on coalitions of a single size, the number of selected games in the proof of this property is $\binom{n}{s} - n$ for coalitions S with $2 \leq s \leq n-2$ ($|S| = s$).

3 COMMUTATION GAMES AND COALITION STRUCTURES

Let us remember that with C_N we denote the linear subspace of all cooperative games in G_N inseparable from the null game by semivalues.

Proposition 3.1. *Let $f_v = f_v(x_1, x_2, ..., x_n)$ be the MLE of game $v \in G_N$.*

$$v \in C_N \;\Leftrightarrow\; \nabla f_v(\overline{\alpha}) = 0 \;\forall \alpha \in [0,1],\; \overline{\alpha} = (\alpha, \ldots, \alpha).$$

Proof. If $v \in C_N$, then $\psi[v] = 0 \;\forall \psi \in Sem(G_N)$. In particular, for all binomial semivalue ψ_α with $\alpha \in [0,1]$, $\psi_\alpha[v] = \nabla f_v(\overline{\alpha}) = 0$ where $\overline{\alpha} = (\alpha, \alpha, \ldots, \alpha)$.

Conversely, since n binomial semivalues form a reference system in $Sem(G_N)$, every semivalue $\psi \in Sem(G_N)$ can uniquely be written like $\psi = \sum_{j=1}^n \lambda_j \psi_{\alpha_j}$ with $\alpha_j \in [0,1]$ for $1 \leq j \leq n$. Then,

$$\psi[v] = \sum_{j=1}^n \lambda_j \psi_{\alpha_j}[v] = \sum_{j=1}^n \lambda_j \nabla f_v(\overline{\alpha_j}) = 0$$

and game v belongs to the shared kernel C_N. □

Example. Let $N = \{i, j, k, l\}$ be the set of players. For cooperative games with four players the coalition S in the commutation games is only composed by two players. For short, when $S = \{i, j\}$ we write the commutation game $v_{S,i,j,k,l}$ as $v_{i,j,k,l}$, i. e.,

$$v_{i,j,k,l} = 1_{\{i,j\}} + 1_{\{k,l\}} - 1_{\{j,k\}} - 1_{\{i,l\}}.$$

The MLE of this game is $f_{v_{i,j,k,l}} = x_i x_j + x_k x_l - x_j x_k - x_i x_l$. It is easy to see that $\nabla f_{v_{i,j,k,l}}(\overline{\alpha}) = 0 \ \forall \alpha \in [0,1]$, $\overline{\alpha} = (\alpha, \alpha, \alpha, \alpha)$.

Definition 3.2. *We say that a cooperative game $v \in G_N$ is inseparable from the null game by semivalues modified for games with coalition structure if and only if $\psi[v;B] = 0$ for every semivalue ψ on G_N and every coalition structure B in N*

The above definition introduces our central concept of separability between games by modified semivalues; linearity of these solutions allows us to reduce the problem to separability from the null game. Now, the commutation games that give the solution to the problem of separability by semivalues, offer a different answer according to the cardinality of the player set.

Proposition 3.3. *Let G_N be the vector space of cooperative games with four players, $|N| = 4$. Condition of inseparable by semivalues is equivalent to condition of inseparable by semivalues modified for games with coalition structure.*

Proof. For case $|N| = 4$, the shared kernel C_N has dimension 2. According to development in (Amer et al., 2003), a basis for C_N is formed by commutation games $v_{1,4,3,2}$ and $v_{2,4,3,1}$. For the commutation games in a basis of C_N, we will prove that condition of inseparability from the null game by semivalues extends to condition of inseparability from the null game by modified semivalues. For the remaining games in C_N, the property is verified by linearity.

We consider, for example, game $v_{2,4,3,1}$ and simultaneously all possible types of coalition structures in $N = \{1,2,3,4\}$. (a) Four individual blocks. (b) One bipersonal block where game $v_{2,4,3,1}$ takes non-null value and two individual blocks. (c) Like in (b) but taking null value. (d) Two bipersonal blocks where game $v_{2,4,3,1}$ takes non-null values. (e) Like in (d) but taking null values. (f) One coalition block with three players. (g) Only one coalition block with four players.

In cases (a) and (g), both allocations coincide: $\psi[v_{2,4,3,1};B] = \psi[v_{2,4,3,1}] = 0 \ \forall \psi \in Sem(G_N)$, $B = \{\{1\},\{2\},\{3\},\{4\}\}$ or $B = \{\{1,2,3,4\}\}$.

From now, we will use the MLE $f_{v_{2,4,3,1}} = x_2 x_4 + x_1 x_3 - x_3 x_4 - x_1 x_2$.

Case (b). We consider, for instance, coalition structure $B = \{\{1,2\},\{3\},\{4\}\}$. According to rules that lead to coefficients in expression (6) for obtaining value $\psi_1[v_{2,4,3,1};B]$ by means of a product of matrices as in (5), we first determine modified MLE g_1:

$$g_1(x_1,x_2,y_2,y_3) = x_2 y_3 + x_1 y_2 - y_2 y_3 - x_1 x_2\,;$$

$$\frac{\partial g_1}{\partial x_1} = y_2 - x_2 \ \Rightarrow \ a_{pq}(1) = \frac{\partial g_1}{\partial x_1}(\overline{\alpha_p}, \overline{\alpha_q}) = \alpha_q - \alpha_p$$

for $1 \le p, q \le 4$.

Written any semivalue ψ as linear combination of four different binomial semivalues, we can conclude that

$$\psi_1[v_{2,4,3,1};B] = \Lambda^t A(1)\, \Lambda = 0 \quad \forall \psi \in Sem(G_N),$$

since, in this case, matrix $A(1)$ satisfies $a_{pq}(1) = -a_{qp}(1)$ for $1 \le p, q \le 4$. In a similar way, $\psi_2[v_{2,4,3,1};B] = 0 \ \forall \psi \in Sem(G_N)$.

Now, for obtaining value $\psi_3[v_{2,4,3,1};B]$, we determine modified MLE g_2:

$$g_2(y_1,x_3,y_3) = y_1 y_3 + y_1 x_3 - x_3 y_3 - y_1\,;$$

$$\frac{\partial g_2}{\partial x_3} = y_1 - y_3 \ \Rightarrow \ a_{pq}(3) = \frac{\partial g_2}{\partial x_3}(\overline{\alpha_p}, \overline{\alpha_q}) = 0$$

for $1 \le p, q \le 4$.

Then $\psi_3[v_{2,4,3,1};B] = 0$ and, also, $\psi_4[v_{2,4,3,1};B] = 0$.

Case (c). Possible coalition structure $B = \{\{1,4\},\{2\},\{3\}\}$.

$$g_1(x_1,x_4,y_2,y_3) = y_2 x_4 + x_1 y_3 - y_3 x_4 - x_1 y_2\,;$$

$$\frac{\partial g_1}{\partial x_1} = y_3 - y_2 \ \Rightarrow \ a_{pq}(1) = \frac{\partial g_1}{\partial x_1}(\overline{\alpha_p}, \overline{\alpha_q}) = 0$$

for $1 \le p, q \le 4$.

Consequently, $\psi_1[v_{2,4,3,1};B] = 0$. In a similar way, $\psi_4[v_{2,4,3,1};B] = 0$ and $\psi_2[v_{2,4,3,1};B] = \psi_3[v_{2,4,3,1};B] = 0$.

Similar manipulations of MLE $f_{v_{2,4,3,1}}$ in cases (d), (e) and (g) give rise to the same conclusion $\psi[v_{2,4,3,1};B] = 0$.

Conversely, if a game is inseparable from the null game by modified semivalues, in particular, it is inseparable from the null game by semivalues. It suffices to consider the coalition structure formed by individual blocks. □

Proposition 3.4. *For vector spaces of cooperative games G_N with five or more players, every commutation game is separable from the null game by semivalues modified for games with coalition structure.*

Proof. In G_N with $|N| \ge 5$, the commutation game $v_{S,i,j,k,l} = 1_S + 1_{S\cup\{k,l\}\setminus\{i,j\}} - 1_{S\cup\{k\}\setminus\{i\}} - 1_{S\cup\{l\}\setminus\{j\}}$, with $i,j \in S$ and $k,l \in N \setminus S$, has by MLE

$$f_{v_{S,i,j,k,l}} = [x_i x_j + x_k x_l - x_j x_k - x_i x_l] \prod_{p\in S\setminus\{i,j\}} x_p \prod_{q\in N\setminus(S\cup\{k,l\})} (1-x_q).$$

For coalitions S with $2 \le |S| < n-2$, we consider coalition structure $B_S = \{S, N\setminus S\}$. The modified MLE g_1 for players in block S is

$$g_1 = x_i x_j (1-y_2) \prod_{p\in S\setminus\{i,j\}} x_p$$

and

$$\frac{\partial g_1}{\partial x_i} = x_j(1-y_2)\prod_{p\in S\setminus\{i,j\}} x_p\,,$$

where $N\setminus(S\cup\{k,l\})\neq\emptyset$ since $|S|<n-2$.

Then, modified Banzhaf value β separates game $v_{S,i,j,k,l}$, $2\leq|S|<n-2$, from the null game:

$$\beta_i[v_{S,i,j,k,l};B_S] = \frac{\partial g_1}{\partial x_i}(\overline{1/2},\overline{1/2}) = \frac{1}{2^s}\neq 0.$$

For case $|S|=n-2$, $S=N\setminus\{k,l\}$ and the MLE is

$$f_{v_{N\setminus\{k,l\},i,j,k,l}} = [x_ix_j+x_kx_l-x_jx_k-x_ix_l]\prod_{p\in N\setminus\{i,j,k,l\}} x_p.$$

Now, we consider coalition structure $B_{N\setminus\{k,l\}}=\{N\setminus\{k,l\},\{k,l\}\}$ and we obtain the modified MLE g_1 for players in block $N\setminus\{k,l\}$:

$$g_1 = [x_ix_j+y_2-x_jy_2-x_iy_2]\prod_{p\in N\setminus\{i,j,k,l\}} x_p,$$

where $N\setminus\{i,j,k,l\}\neq\emptyset$ since $|N|\geq 5$. Let h be a player in $N\setminus\{i,j,k,l\}$. Again, modified Banzhaf value β separates game $v_{N\setminus\{k,l\},i,j,k,l}$ from the null game:

$$\frac{\partial g_1}{\partial x_h} = [x_ix_j+y_2-x_jy_2-x_iy_2]\prod_{p\in N\setminus\{h,i,j,k,l\}} x_p$$

and

$$\beta_h[v_{N\setminus\{k,l\},i,j,k,l};B_{N\setminus\{k,l\}}] = \frac{\partial g_1}{\partial x_h}(\overline{1/2},\overline{1/2}) = \frac{1}{2^{n-3}}\neq 0.$$

□

4 SUFFICIENT CONDITIONS OF SEPARABILITY

For games with five or more players, the commutation games are not a solution for the problem of inseparability by semivalues modified for games with coalition structure. In this section we provide two sufficient conditions of separability, that is, two necessary conditions of inseparability from the null game by modified semivalues.

Proposition 4.1. *Let us consider vector spaces of cooperative games G_N with $|N|\geq 4$. If there exists a coalition S with $v(S)\neq v(N\setminus S)$, then game v is separable from the null game by semivalues modified for games with coalition structure.*

Proof. Let us suppose S' a coalition with smallest size that verifies $v(S')\neq v(N\setminus S')$. If $|S'|=1$, game v is separable from the null game by semivalues and also by modified semivalues. We can consider that $|S'|=s'\geq 2$ and $s'\leq n/2$. Then, the MLE of game v can be written as

$$f_v = \sum_{S:2\leq|S|\leq s'}\Big[\prod_{i\in S}x_i\prod_{j\in N\setminus S}(1-x_j)v(S)+ \prod_{i\in N\setminus S}x_i\prod_{j\in S}(1-x_j)v(N\setminus S)\Big]+ \sum_{S:s'<|S|<n-s'}\prod_{i\in S}x_i\prod_{j\in N\setminus S}(1-x_j)v(S).$$

Now, we choose the coalition structure $B_{S'}=\{S',N\setminus S'\}$. In such a case, the modified MLE g_1 for players in coalition block S' has by expression

$$g_1 = \sum_{S\subset S',s\geq 2}\Big[(1-y_2)\prod_{i\in S}x_i\prod_{j\in S'\setminus S}(1-x_j)+ y_2\prod_{i\in S'\setminus S}x_i\prod_{j\in S}(1-x_j)\Big]v(S)+ (1-y_2)\prod_{i\in S'}x_i\,v(S')+y_2\prod_{j\in S'}(1-x_j)\,v(N\setminus S'),$$

because terms for coalitions S containing elements as much in S' as in $N\setminus S'$ vanish in MLE g_1. If k is a player in S',

$$\frac{\partial g_1}{\partial x_k} = \sum_{S\subset S',s\geq 2,S\ni k}\Big[(1-y_2)\prod_{i\in S\setminus\{k\}}x_i\prod_{j\in S'\setminus S}(1-x_j)- y_2\prod_{i\in S'\setminus S}x_i\prod_{j\in S\setminus\{k\}}(1-x_j)\Big]v(S)+ \sum_{S\subset S',s\geq 2,S\not\ni k}\Big[-(1-y_2)\prod_{i\in S}x_i\prod_{j\in S'\setminus(S\cup\{k\})}(1-x_j)+ y_2\prod_{i\in S'\setminus(S\cup\{k\})}x_i\prod_{j\in S}(1-x_j)\Big]v(S)+ +(1-y_2)\prod_{i\in S'\setminus\{k\}}x_i\,v(S')-y_2\prod_{j\in S'\setminus\{k\}}(1-x_j)\,v(N\setminus S').$$

Then

$$\frac{\partial g_1}{\partial x_k}(\overline{1/2},\overline{1/2}) = \frac{1}{2^{s'}}\big[v(S')-v(N\setminus S')\big]$$

and the modified Banzhaf value β separates game v from the null game:

$$\beta_k[v;B_{S'}] = \frac{\partial g_1}{\partial x_k}(\overline{1/2},\overline{1/2})\neq 0 \quad \text{for } k\in S'. \quad \square$$

Proposition 4.2. *For spaces of cooperative games G_N with $|N|\geq 6$, let us consider a game v that satisfies $v(S)=v(N\setminus S)\ \forall S\subseteq N$ and $v(\{i\})=0\ \forall i\in N$. If there exists a coalition S with*

$$v(S)\neq\sum_{T\subset S,|T|=2}v(T) \quad \textit{and} \quad 3\leq|S|\leq n/2, \quad (9)$$

then game v is separable from the null game by semivalues modified for games with coalition structure.

Proof. The MLE of game v that satisfies the two first conditions of the statement can be written as

$$f_v = \sum_{S:2\le|S|<n/2} \Big[\prod_{i\in S} x_i \prod_{j\in N\setminus S}(1-x_j) + \prod_{i\in N\setminus S} x_i \prod_{j\in S}(1-x_j)\Big] v(S) + \sum_{S:|S|=n/2} \prod_{i\in S} x_i \prod_{j\in N\setminus S}(1-x_j)\, v(S), \tag{10}$$

where the second sum only appears in case n even number. Let us suppose S' a coalition with smallest size that verifies (9) for $|S'| < n/2$. In such a case, we choose coalition structure $B_{S'} = \{S', N\setminus S'\}$ and write modified MLE g_1 for players in coalition block S':

$$g_1 = \sum_{S\subset S',2\le s<s'} \Big[(1-y_2)\prod_{i\in S} x_i \prod_{j\in S'\setminus S}(1-x_j) + y_2 \prod_{i\in S'\setminus S} x_i \prod_{j\in S}(1-x_j)\Big] v(S) + \Big[(1-y_2)\prod_{i\in S'} x_i + y_2 \prod_{j\in S'}(1-x_j)\Big] v(S').$$

Next, we consider a player j_1 in block S', compute the partial derivative of MLE g_1 with respect to variable x_{j_1} and replace all variables by generic value α grouping the sums as follows:

$$\frac{\partial g_1}{\partial x_{j_1}}(\overline{\alpha},\overline{\alpha}) = \sum_{S\subset S',S\ni j_1,|S|=2} \big[\alpha(1-\alpha)^{s'-1} - \alpha^{s'-1}(1-\alpha)\big] v(S) + \sum_{S\subset S',S\ni j_1,2<s<s'} \big[\alpha^{s-1}(1-\alpha)^{s'-s+1} - \alpha^{s'-s+1}(1-\alpha)^{s-1}\big] v(S) + \sum_{S\subset S',S\not\ni j_1,2\le s<s'-1} \big[\alpha^{s'-s}(1-\alpha)^{s} - \alpha^{s}(1-\alpha)^{s'-s}\big] v(S) + \big[\alpha(1-\alpha)^{s'-1} - \alpha^{s'-1}(1-\alpha)\big]\big[v(S'\setminus\{j_1\}) - v(S')\big].$$

All terms for coalitions S with $S \not\ni j_1$ and $2 \le s < s'-1$ can be written by means of coalitions T with $T \ni j_1$ and $3 \le t < s'$. Then,

$$\frac{\partial g_1}{\partial x_{j_1}}(\overline{\alpha},\overline{\alpha}) = \alpha(1-\alpha)\big[(1-\alpha)^{s'-2} - \alpha^{s'-2}\big] \Big\{\sum_{S\subset S',S\ni j_1,|S|=2} v(S) + v(S'\setminus\{j_1\}) - v(S')\Big\} + \sum_{S\subset S',S\ni j_1,2<s<s'} \big[\alpha^{s-1}(1-\alpha)^{s'-s+1} - \alpha^{s'-s+1}(1-\alpha)^{s-1}\big] v(S) + \sum_{T\subset S',T\ni j_1,2<t<s'} \big[\alpha^{s'-t+1}(1-\alpha)^{t-1} - \alpha^{t-1}(1-\alpha)^{s'-t+1}\big] v(T\setminus\{j_1\}).$$

We shorten polynomial $(1-\alpha)^{s'-2} - \alpha^{s'-2}$ by means of $p_{s'}(\alpha)$ and write $v(S'\setminus\{j_1\})$ as a sum of all values on contained bipersonal coalitions:

$$\frac{\partial g_1}{\partial x_{j_1}}(\overline{\alpha},\overline{\alpha}) = \alpha(1-\alpha)p_{s'}(\alpha)\Big[\sum_{S\subset S',S\ni j_1,|S|=2} v(S) + \sum_{T\subseteq S'\setminus\{j_1\},|T|=2} v(T) - v(S')\Big] + \sum_{S\subset S',S\ni j_1,2<s<s'} \big[\alpha^{s-1}(1-\alpha)^{s'-s+1} - \alpha^{s'-s+1}(1-\alpha)^{s-1}\big] \big[v(S) - v(S\setminus\{j_1\})\big]. \tag{11}$$

It is possible to find coalitions S with $S\subset S'$, $S\ni j_1$ and $2<s<s'$ only in case $s'\ge 4$. Then, the last sum in the above expression can be written as

$$\sum_{S\subset S',S\ni j_1,3\le s<1+s'/2} \big[\alpha^{s-1}(1-\alpha)^{s'-s+1} - \alpha^{s'-s+1}(1-\alpha)^{s-1}\big] \big[v(S) - v(S\setminus\{j_1\})\big] + \sum_{T\subset S',T\ni j_1,1+s'/2<t\le s'-1} \big[\alpha^{t-1}(1-\alpha)^{s'-t+1} - \alpha^{s'-t+1}(1-\alpha)^{t-1}\big] \big[v(T) - v(T\setminus\{j_1\})\big],$$

where case $s = 1+s'/2$ is not considered, since only for s' even number, cardinality of S can take value $s = 1+s'/2$ but, in this case, coefficient $\alpha^{s-1}(1-\alpha)^{s'-s+1} - \alpha^{s'-s+1}(1-\alpha)^{s-1}$ vanish. In the above sums, we can identify coalitions S for $3\le s<1+s'/2$ with coalitions T for $1+s'/2<t\le s'-1$ by means relation $t = s'-s+2$. Then, both sums reduce to

$$\sum_{3\le s<1+s'/2} \big[\alpha^{s-1}(1-\alpha)^{s'-s+1} - \alpha^{s'-s+1}(1-\alpha)^{s-1}\big] \Big\{\sum_{S\subset S',S\ni j_1,|S|=s} \big[v(S) - v(S\setminus\{j_1\})\big] - \sum_{T\subset S',T\ni j_1,|T|=s'-s+2} \big[v(T) - v(T\setminus\{j_1\})\big]\Big\}.$$

Let us suppose that $S' = \{j_1, j_2, \ldots, j_{s'}\}$. For a given cardinality s with $3\le s<1+s'/2$, the last difference of sums vanish, because it can be written as

$$\sum_{S\subset S',S\ni j_1,|S|=s} \Big[\sum_{P\subset S,|P|=2} v(P) - \sum_{Q\subseteq S\setminus\{j_1\},|Q|=2} v(Q)\Big] - \sum_{T\subset S',T\ni j_1,|T|=s'-s+2} \Big[\sum_{P\subset T,|P|=2} v(P) - \sum_{Q\subset T\setminus\{j_1\},|Q|=2} v(Q)\Big] = \sum_{S\subset S',S\ni j_1,|S|=s} \Big[\sum_{P\subset S,P\ni j_1,|P|=2} v(P)\Big] - \sum_{T\subset S',T\ni j_1,|T|=s'-s+2} \Big[\sum_{P\subset T,P\ni j_1,|P|=2} v(P)\Big] =$$

$$\sum_{i=2}^{s'}\left[\binom{s'-2}{s-2}-\binom{s'-2}{s'-s}\right]v(\{j_1,j_i\})=0.$$

Thus, from expression (11), we can write the modified binomial semivalue ψ_α for player $j_1 \in S'$ as

$$(\psi_\alpha)_{j_1}[v;B_{S'}]=\frac{\partial g_1}{\partial x_{j_1}}(\overline{\alpha},\overline{\alpha})=$$

$$\alpha(1-\alpha)p_{s'}(\alpha)\Big[\sum_{T\subset S',|T|=2}v(T)-v(S')\Big].$$

Since $\alpha=1/2$ is the unique real zero of polynomial $p_{s'}$ for values $s'\geq 3$ and game v satisfies inequality (9) for coalition S', we conclude that $(\psi_\alpha)_{j_1}[v;B_{S'}]\neq 0$ for values $\alpha\in(0,1/2)\cup(1/2,1)$ and these modified semivalues separate game v from the null game.

It only lack to see case in which $|S|=n/2$ is the smallest size of coalitions that verify (9). Here, n is a even number and all coalitions in the second sum of expression (10) can be grouped by pairs: S and $N\setminus S$. The selected coalition S' will belong to one or another half of coalitions with size $n/2$; we choose half that contains coalition S' and describe the second sum with S and $N\setminus S$, as the same way that the first sum in (10). Then, by repeating the same procedure as in case $|S|<n/2$, we arrived at the same conclusion. □

5 EXPANDED COMMUTATION GAMES

We denote with D_N the vector subspace of all cooperative games in G_N inseparable from the null game by semivalues modified for games with coalition structure.

Definition 5.1. *In G_N with $|N|\geq 5$, we consider a commutation game with coalition size 2, $v_{i,j,k,l}$, $k,l\in N\setminus\{i,j\}$. The expanded game of commutation game $v_{i,j,k,l}$ is the sum of all commutation games in G_N, $v_{P,i,j,k,l}$, with the same commuted players, i.e.,*

$$v^e_{i,j,k,l}=\sum_{P\ni i,j,P\subseteq N\setminus\{k,l\}}v_{P,i,j,k,l}.$$

Lemma 5.2. *In G_N with $|N|\geq 5$ an expanded commutation game $v^e_{i,j,k,l}$, $k,l\in N\setminus\{i,j\}$, satisfies the following properties:*

(a) $v^e_{i,j,k,l}(S)=v^e_{i,j,k,l}(N\setminus S)\quad\forall S\subseteq N$;

(b) $v^e_{i,j,k,l}(S)=\sum_{T\subset S,|T|=2}v^e_{i,j,k,l}(T)\ \forall S\subseteq N$ *and* $3\leq|S|\leq|N|$;

(c) its MLE is $f_{v^e_{i,j,k,l}}=x_ix_j+x_kx_l-x_jx_k-x_ix_l$.

Proof. It is easy to prove sections (a) and (b); it suffices to check if players i,j,k,l belong or not to coalitions S, since the only bipersonal coalitions that take non-null values in game $v^e_{i,j,k,l}$ are $\{i,j\}$, $\{k,l\}$, $\{j,k\}$ and $\{i,l\}$. In order to verify section (c) we can write MLE of game $v^e_{i,j,k,l}$ as

$$f_{v^e_{i,j,k,l}}=\big[x_ix_j+x_kx_l-x_jx_k-x_ix_l\big]\Big[\prod_{q\in N\setminus\{i,j,k,l\}}(1-x_q)+f_{\sum_{Q\subseteq N\setminus\{i,j,k,l\}}1_Q}\Big],$$

where games 1_Q are considered in $G_{N\setminus\{i,j,k,l\}}$. Since $\sum_{Q\subseteq N\setminus\{i,j,k,l\}}1_Q(T)=1\ \forall T\subseteq N\setminus\{i,j,k,l\}$, $T\neq\emptyset$, $(Q\neq\emptyset)$, its MLE equals the unity in $N\setminus\{i,j,k,l\}$ and section (c) follows. □

Proposition 5.3. *In spaces of cooperative games G_N with $|N|\geq 5$, every expanded commutation game $v^e_{i,j,k,l}$, $k,l\in N\setminus\{i,j\}$ belongs to vector subspace D_N.*

Proof. Section (c) in above Lemma proves that MLE of expanded commutation game $v^e_{i,j,k,l}$, $k,l\in N\setminus\{i,j\}$ in G_N with $|N|\geq 5$ agrees with MLE of commutation game $v_{i,j,k,l}$ in a space of cooperative games with only four players, $\{i,j,k,l\}$.

In order to demonstrate that game $v^e_{i,j,k,l}$, $k,l\in N\setminus\{i,j\}$, is inseparable by modified semivalues, we can consider that players i,j,k,l are distributed in different coalition blocks in the same way that in the proof of Proposition 3.3. The remaining players $N\setminus\{i,j,k,l\}$ will be distributed in the different blocks next to players i,j,k,l or they will form new coalition blocks.

Since variables that correspond to players in $N\setminus\{i,j,k,l\}$ does not appear in the MLE of game $v^e_{i,j,k,l}$, when we compute allocations for players i,j,k,l by means of a product of matrices as in (5), we obtain the same result as in Proposition 3.3, that is, $\psi_p[v^e_{i,j,k,l},B]=0$ for $p=i,j,k,l$, $\forall\psi\in Sem(G_N)$, $\forall B$ coalition structure in N.

For the remaining players, $\psi_q[v^e_{i,j,k,l},B]=0\ \forall q\in N\setminus\{i,j,k,l\}$, since variable x_q does not appear in the MLE. □

Theorem 5.4. *Let us consider vector spaces of cooperative games G_N with five or more players, $|N|\geq 5$. Then,*

(a) $\dim D_N=\binom{n}{2}-n$;

(b) the vector subspace D_N is spanned by expanded of commutation games with coalition size 2.

Proof. We can see in (Amer et al., 2003) that the shared kernel C_N for $|N|\geq 4$ is spanned by 2^n-n^2+n-2 commutation games whose coalitions with non-null value vary from cardinality $s=2$ to $n-2$. We choose the $\binom{n}{2}-n$ commutation games with coalition

size 2. As they are linearly independent in G_N, its expanded games are also linearly independent and, by above Proposition, inseparable from the null game by modified semivalues. The linear subspace spanned by these expanded commutation games is contained in subspace D_N for $|N| \geq 5$.

In addition, as $D_N \subseteq C_N$, the freedom degrees in C_N by a consequence of conditions (7) for coalitions with sizes $s > n/2$ disappear according to necessary condition of inseparability from the null game in D_N: $v(S) = v(N \setminus S)$ (Proposition 4.1). Also, the freedom degrees for coalitions with size from $s = 3$ to $s = n/2$ disappear according to necessary condition $v(S) = \sum_{T \subset S, |T|=2} v(T)\ \forall S \subseteq N$ with $3 \leq |S| \leq n/2$ (Proposition 4.2).

Only the $\binom{n}{2} - n$ freedom degrees for coalition size $s = 2$ in C_N remain in vector subspace D_N. Then, the vector subspace spanned by the $\binom{n}{2} - n$ expanded commutation games agrees with D_N. □

6 CONCLUSION

It is known that every cooperative game with two or three players is separable from the null game by semivalues, so that dimension for the shared kernel C_N is zero in cases $n = 2, 3$. Consequently, vector subspace D_N is only formed by the null game in cases $n = 2, 3$. For games with four players, Proposition 3.3 proves that both separability concepts coincide: $D_N = C_N$ for $n = 4$.

Table 1 compares dimensions of C_N and D_N for cooperative games with few players.

Table 1: Dimensions of kernels according to N.

$\|N\| = n$	2	3	4	5	6	7	8
$\dim G_N$	3	7	15	31	63	127	255
$\dim C_N$	0	0	2	10	32	84	198
$\dim D_N$	0	0	2	5	9	14	20

For games with five or more players, the introduction of modified semivalues for games with coalition structure allows us to reduce in a significant way the dimension of the vector subspace of inseparable games from the null game. According to the linearity property, separability between two games is reduced by both concepts of solution to separability of their difference from the null game. The ability of separation by semivalues has considerably increased by introduction of a priori coalition structures.

ACKNOWLEDGEMENTS

Research supported by grant MTM2015-66818-P from the Spanish Ministry of Economy and FEDER.

REFERENCES

Albizuri, M. J. (2009). Generalized coalitional semivalues. *European Journal of Operational Research*, 196:578–584.

Amer, R., Derks, J., and Giménez, J. M. (2003). On cooperative games, inseparable by semivalues. *International Journal of Game Theory*, 32:181–188.

Amer, R. and Giménez, J. M. (2003). Modification of semivalues for games with coalition structures. *Theory and Decision*, 54:185–205.

Banzhaf, J. F. (1965). Weighted voting doesn't work: A mathematical analysis. *Rutgers Law Review*, 19:317–343.

Carreras, F., Freixas, J., and Puente, M. A. (2003). Semivalues as power indices. *European Journal of Operational Research*, 149:676–687.

Carreras, F. and Giménez, J. M. (2011). Power and potential maps induced by any semivalue: Some algebraic properties and computation by multilinear extensions. *European Journal of Operational Research*, 211:148–159.

Dragan, I. (1999). Potential and consistency for semivalues of finite cooperative TU games. *International Journal of Mathematics, Game Theory and Algebra*, 9:85–97.

Dubey, P., Neyman, A., and Weber, R. J. (1981). Value theory without efficiency. *Mathematics of Operations Research*, 6:122–128.

Giménez, J. M. and Puente, M. A. (2015). A method to calculate generalized mixed modified semivalues: application to the catalan parliament (legislature 2012-2016). *TOP*, 23:669–684.

Owen, G. (1972). Multilinear extensions of games. *Management Science*, 18:64–79.

Owen, G. (1975). Multilinear extensions and the Banzhaf value. *Naval Research Logistics Quarterly*, 22:741–750.

Owen, G. (1977). Values of games with a priori unions. In *Essays in Mathematical Economics and Game Theory*, pages 76–88. R. Henn and O. Moeschelin (Editors), Springer-Verlag.

Owen, G. (1981). Modification of the Banzhaf-Coleman index for games with a priori unions. In *Power, Voting and Voting Power*, pages 232–238. M.J. Holler (Editor), Physica-Verlag.

Shapley, L. S. (1953). A value for n-person games. In *Contributions to the Theory of Games II*, pages 307–317. H.W. Kuhn and A.W. Tucker (Editors), Princeton University Press.

Weber, R. J. (1988). Probabilistic values for games. In *The Shapley value: Essays in honor of L.S. Shapley*, pages 101–119. A.E. Roth (Editor), Cambridge University Press.

Exact Solution of the Multi-trip Inventory Routing Problem using a Pseudo-polynomial Model

Nuno Braga[1], Cláudio Alves[1] and Rita Macedo[2]
[1]*Universidade do Minho, 4710-057, Braga, Portugal*
[2]*Institut de Recherche Technologique Railenium, F-59300, Famars, France*
{*nuno.braga, claudio*}*@dps.uminho.pt, rita.SantosDeMacedo@univ-valenciennes.fr*

Keywords: Inventory Routing Problem, Integer Linear Programing, Network Flow Models, Multi-trip.

Abstract: In this paper, we address an inventory routing problem where a vehicle can perform more than one trip in a working day. This problem was denominated multi-trip vehicle routing problem. In this problem a set of customers with demand for the planning horizon must be satisfied by a supplier. The supplier, with a set of vehicles, delivers the demand using pre-calculated valid routes that define the schedule of the delivery of goods on the planning horizon. The problem is solved with a pseudo-polynomial network flow model that is solved exactly in a set of instances adapted from the literature. An extensive set of computational experiments on these instances were conducted varying a set of parameters of the model. The results obtained with this model show that it is possible to solve instances up to 50 customers and with 15 periods in a reasonable computational time.

1 INTRODUCTION

The vehicle routing problem can be applied in real cases on logistics companies in order to reduce transportation costs, which include, among others, costs associated with drivers, vehicles or fuel. The integration of this problem with the inventory management can reflect in considerable savings, since this provides a more efficient management of the resources than the one achieved through the local optimization of the two problems separately.

In the inventory routing problem the goal is to minimize the total transportation cost from the supplier to the customer, so that the customer maintains an inventory level that will satisfy the demand in each period of a given planning horizon, reducing also possible storage costs.

This problem can incorporate a time horizon information, inventory management policies, routes, fleet type and size (Coelho et al., 2014). Routes are considered to be direct or not, whether a single customer or more are visited, respectively (Coelho et al., 2014). The planning horizon is considered finite if it is defined for a short period, or infinite when the schedule of routes is carried out for a long period of time (Coelho et al., 2014; Bertazzi and Speranza, 2013). Typically, the goal is to minimize the overall transportation costs, reducing penalties associated with inventory level, which typically represent storage costs (Bertazzi and Speranza, 2013).

Several practical applications have been implemented in industry, which enable companies to reduce inventory and transportation costs improving the quality of service. A recent study describes the implementation of this problem in a fuel distribution company (Hanczar, 2012). Another study describes an application of the problem in a company with a fleet of ships that delivers chemicals to warehouses located throughout the world (Miller, 1987). The authors describe an integer programming model that was successfully implemented in this company. The inventary routing problem was also considered in the daily strategy of a company that provides calcium carbonate throughout Europe and it allowed to achieve a reduction in millions of dollars of costs per year (Dauzère-Pérès et al., 2007). In addition, different approaches of this problem have also been applied in the maritime industry (Al-Khayyal and Hwang, 2007; Song and Furman, 2013; Persson and Göthe-Lundgren, 2005; Grnhaug et al., 2010).

The problem explored in this paper is the inventory routing problem that allowed the vehicles to carry out more than one route in each period of the planning horizon and therefore it was denominated multi-trip inventory routing problem. The consideration of multiple routes can provide advantages, in the sense that

Braga, N., Alves, C. and Macedo, R.
Exact Solution of the Multi-trip Inventory Routing Problem using a Pseudo-polynomial Model.
In *Proceedings of the 6th International Conference on Operations Research and Enterprise Systems (ICORES 2017)*, pages 250-257
ISBN: 978-989-758-218-9

the cost of the vehicle is usually fixed for a period of the planning horizon, therefore reducing the costs at this level. On the other hand, the consideration of this variant with multiple routes makes the problem, which is already difficult to solve, even more difficult.

Since there is an increasing interest in applying this problem in practical cases in industry, several heuristics and exact algorithms have been proposed by several authors in the literature. The difficulty of solving the inventory routing problems has been mostly motivated by the development of heuristics, which in many cases show good results (Herer and Levy, 1997; Archetti et al., 2011; Cordeau et al., 2015; Hemmati et al., 2015). In a recent paper, the inventory routing problem with multiple products and vehicles was solved with an exact model (Coelho and Laporte, 2013). The authors describe an integer programming model, to which are also added valid inequalities with the objective of strengthening it. In the model a branch-and-cut is proposed that is able to solve instances with a maximum of 5 vehicles, 5 products, 7 periods and 50 customers. In another problem with a constant customers demand the authors resorted to a Lagrangian relaxation method that derives lower and upper bounds for the model in order to obtain good quality solutions in acceptable times (Zhong and Aghezzaf, 2012). In another paper it is also proposed a method of Lagrangian relaxation combined with a subgradient method, able to solve instances up to 200 customers (Yu et al., 2008). Two integer programming models were proposed to solve the inventory routing problem when the inventory is managed by the supplier and when it is managed by the customer, comparing the two approaches (Archetti and Speranza, 2016).

The multi-trip inventory routing problem is typically more difficult to resolve as compared with the usual vehicle routing problem. This variant was reviewed elsewhere (Şen and Blbl, 2008). Since this is not a trivial problem, several heuristic methods have been proposed. A tabu search algorithm is also described to solve this problem (Taillard et al., 1996). The same problem was addressed with a heuristic algorithm also using tabu search (Brando and Mercer, 1998). The use of constructive heuristic with three phases was also proposed (Petch and Salhi, 2003). An adaptive memory procedure was described (Olivera and Viera, 2007), and the results were compared with those obtained with others from the literature (Taillard et al., 1996; Brando and Mercer, 1998; Petch and Salhi, 2003). A genetic algorithm was also proposed, for the first time, to solve this problem (Salhi and Petch, 2007). A vehicle routing problem with multiple routes and additional accessibility constraints was studied using a tabu search algorithm that involved instances up to 1000 customers (Alonso et al., 2008).

An exact integer programming method was proposed for the problem of routing with a single vehicle with time windows and multiple routes (Azi et al., 2007). The algorithm is divided in two phases: first, all valid routes are generated and in the second phase routes are affected at different periods of the planning horizon. The authors further generalize the algorithm for the case of multiple vehicles (Azi et al., 2010). The authors resorted to a column generation algorithm able to solve instances with a number of customers between 25 and 50.

A pseudo-polynomial network flow model was used to solve the vehicle routing problem with time windows and multiple routes (Macedo et al., 2011). In the model, the underlying graph vertices correspond to instants of time of the planning horizon, and the arcs define valid routes. It is proposed an exact algorithm that considers an iterative disaggregation of the vertices of the graph, which are first aggregated to obtain a smaller model, and thus easier to solve. The model proposed in this article is similar to the one here described (Macedo et al., 2011) in the sense that it uses a pseudo-polynomial network flow model, the arcs define valid routes and the vertices also correspond to instances of time.

In section 2 we present the definition of the problem, showing also an example. On section 3 it is formally presented the pseudo-polynomial network flow model to solve this problem. In section 4 the computational results are shown and finally, some conclusions are presented in section 5.

2 MULTI-TRIP INVENTORY ROUTING PROBLEM

2.1 Definition

The class of inventory routing problems considers a context in which one or more types of products are shipped from a supplier to a set of customers through a fleet of vehicles.

In this problem the customers demand should be satisfied during several periods of a planning horizon. What differentiates this class of problems, from the vehicle routing problem is the fact that the supplier manages the inventory of the customer, i.e., the product amount supplied to each customer in each period is not necessarily equal to their demands. The products deliveries must be carried out in such a way that the customers have available at each period, the re-

quired amount of product.

In this paper, a variant of this problem is addressed that considers the vehicle routing problem with multiple routes, which means that each vehicle can be allocated to more than one route in each period of the planning horizon.

We consider that a fleet of vehicles is located in a warehouse, which supplies a set of customers with a single type of product.

The objective of this problem is to determine the optimal set of routes that minimize the total transportation cost, and any storage costs in the customer. That is, whenever an order is delivered before the set period, incurs in a penalty proportional to the costs of storage of products in the customer. On the other hand, it is considered that customers have an unlimited storage capacity. With regard to anticipated deliveries, they can not be phased. This means that all demand for a period is delivered in a single visit to the corresponding customer, whether made on the same period or in previous periods.

In this problem, the number of available vehicles is limited, as well as the capacity of each vehicle, and the load in each route can not exceed its capacity. It is assumed that each unit of the product transported occupies a unit of volume on the vehicle and the time spent on transportation is equivalent to the distance traveled. Each vehicle can carry out various routes per period, so that, the sum of their lengths does not exceed the duration of a working day.

2.2 Data and Parameters

To clarify the formal presentation of the problem, we provide below an exhaustive list of parameters that characterise it:

- $D = \{0\}$: warehouse;
- $S = \{1, \ldots, N\}$: customers;
- $T = \{1, \ldots, \tau\}$: time periods of the planning horizon.

The warehouse is associated with the index 0. Customers are located within a certain distance from the warehouse, distributed according to their cartesian coordinates. The planning horizon defines the time period for which deliveries to customers will have to be made. This period will subsequently be divided into units of time referred to as work day.

We consider that a customer cannot be visited more than once in each time period and there is a single type of product. Furthermore, we assume that a visit to a customer at a time t requires the delivery of the demand for that period, and eventually the later periods. Stock-outs are not allowed, i.e., all customers must imperatively have at their disposal, in each period, the required quantities of products. Finally, it is considered that there is no initial stock in customers, i.e., at time period 0 of the planning horizon the customers do not have at their disposal any stock.

Below we present the problem data:

- C: vehicle capacity (homogeneous fleet);
- F: number of available vehicles;
- W: duration of a working day;
- d_i^t: demand of customer i on time period t;
- N_{max}: maximum number of customers visited by route.

Some additional settings:

- Ψ_t: set of valid routes in the period t;
- N_r: set of customers visited by route r;
- $\alpha_{irt}^{t'}$: equal to 1 if the route r delivers the demand of the customers i in the period t, or equal to 0 otherwise;
- a route r is characterised by a set of customers (visited by the route) and the periods of demands that are delivered as part of the same route.

The costs considered in this problem are:

- C_v: fixed cost for using a vehicle in a working day;
- C_r: transportation cost associated with the route r;
- C_{h_i}: storage cost of a unit of product on the customers i for a period of time;
- $C_{H_r^t}$: total cost of storage associated with the route r ($C_{H_r^t} = \sum_{i \in N_r} C_{h_i} t_r^i$, being t_r^i the total waiting time until the product is consumed on the customer i delivered through the route r).

2.3 Example of a Problem Instance

Example 1. *Consider the example of an instance for the inventory routing problem.*

The Table 1 indicates all the parameters that define it. Table 1a defines the location of the warehouse, and Table 1b defines the capacity of the vehicles (C), the fleet size (F), the duration of a working day (W), the number os periods of the planning horizon (τ) and the number of customers (N). In Table 1c are represented the customer cartesian coordinates (x, y), as well as the storage costs for each customer (C_{h_i}). Finally, Table 1d defines the demands d_i^t in the period t for the customer i.

The graphical representation of this instance can be observed in Figure 1, showing the warehouse and

Table 1: Example of an instance of the inventory routing problem. (*a*) Warehouse location data, (*b*) general data of the problem, (*c*) customer data and (*d*) customer demands.

A	10	20

(*a*)

C	10
C_v	20
F	5
W	120
T	3
N	5

(*b*)

x	y	C_{h_i}
9	50	24
-9	10	15
-22	22	3
-15	45	9
-3	44	12

(*c*)

t	i	d_i^t
1	1	4
1	2	2
1	3	2
1	4	2
1	5	2
2	1	2
2	2	2
2	3	2
2	4	2
2	5	2
3	1	4
3	2	2
3	3	2
3	4	2
3	5	3

(*d*)

the customers distributed according to their cartesian coordinates. All connections between customers and warehouse (supplier) are also represented, as well as the corresponding distances to be traveled in this route.

Figure 2 represents a valid solution for this instance, which has in the first period a cost of 214, in the second 198 and in the third and last 131, with a total cost of 543. In this case, it is not possible to use a single vehicle in the first period, since the distance that the vehicle would have to travel to deliver all customer demands is greater than 120 (length of a work day). Thus, two vehicles are scheduled for the routes for the first period, and in each of the routes it is delivered the demand for further periods, in particular customers 3 and 4. These deliveries in later periods incur in a penalty for each unit in storage. In the second period, it may resort to a single vehicle that performs two routes. In the third period, a single vehicle performs the remaining deliveries to customers where the demands have not yet been satisfied, making use of a single route. In this latter period there is no storage costs since all demands are satisfied and consumed in this period. In this figure, the information relative to the demand is denoted by d_i^t, and can exist for later periods. The information about the distance (l) traveled and the volume (v) occupied on the vehicle in the route is defined in the arcs as $[l|v]$. Table 2 discriminates the objective function values for the three periods shown in Figure 1.

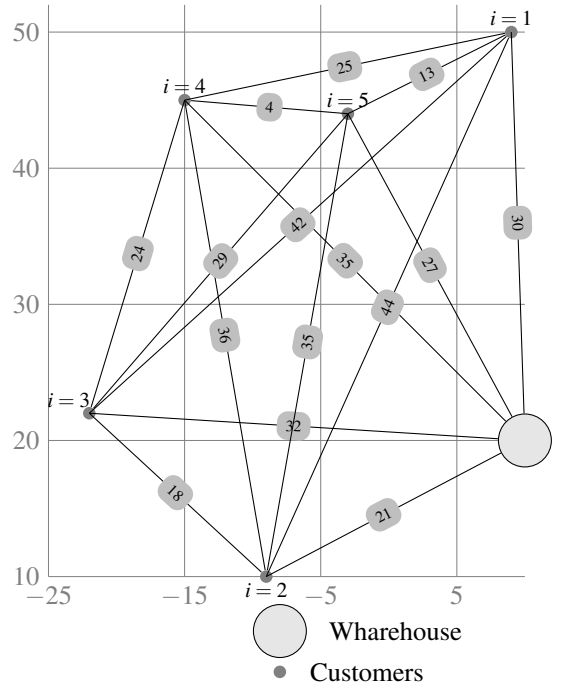

Figure 1: Instance graphical representation with a warehouse, customers and their distances located in midway of the connections.

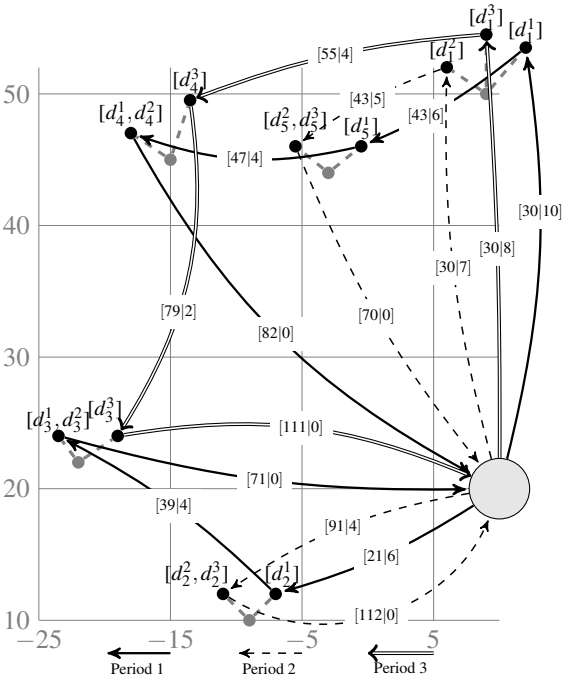

Figure 2: Valid solution to the inventory routing problem instance of Example 1. In the middle of the connection between each customers is shown the distance traveled, as well as the volume of the goods on the vehicle in the route.

Table 2: Objective function values for the three periods.

T	C_r	C_v	C_{h_i}	total
1	82 + 71	20 + 20	$9\times2+3\times2$	214
2	112	20	$12\times3+15\times2$	198
3	111	20	0	131
				543

3 A NETWORK FLOW MODEL FOR THE MULTI-TRIP INVENTORY ROUTING PROBLEM

In this section, we describe a new integer programming model for the multi-trip inventory routing problem.

This network flow model is defined in a set of acyclic and direct graphs, one for each period of the planning horizon, denoted by $G_t = (V, A_t)$, $t \in T$ and V is a set of vertices $V = \{0, \ldots, W+1\}$, and A_t is the set of arcs that represent the set of all valid routes in the period $t \in T$, as well as the waiting time in the warehouse. A flow that runs through the graph represents a working day of a vehicle, i.e., the sequence of routes and waiting times this performs from the moment 0 until time instant w of a given planning horizon. A route is defined by a sequence of customers to visit, as well as the respective product amounts to deliver to each customer. In order for a route to be valid, the sum of the quantities of products to be delivered to each customer must not exceed the capacity of the vehicle, and the necessary travel time cannot exceed a working day (a period of the planning horizon). Note that the same route can start at different instants, keeping it valid. The set of all valid routes is generated in advance, and the variable x^t_{uvr} represents the route r that starts at the instant u and ends at time v of period $t \in T$. Routes are generated through a recursive process that will exclude routes violating the vehicle capacity (C) and/or a maximum duration (W) of the route.

$$\min \sum_{t\in T}\sum_{(u,v)^r\in\Psi_t} C_r x^t_{uvr} + C_v \sum_{t\in T}\sum_{(0,v)^r\in\Psi_t} x^t_{0vr} + \sum_{t\in T}\sum_{(u,v)^r\in\Psi_t} C_{H^t_r} x^t_{uvr} \quad (1)$$

$$\text{s.t.} \sum_{t\in T, t\le t'}\sum_{(u,v)^r\in\Psi_t | i\in N_r} \alpha^{t'}_{irt} x^t_{uvr} = 1, \quad \forall i \in S, t' \in T, \quad (2)$$

$$\sum_{(0,v)^r\in\Psi_t} x^t_{0vr} \le F, \quad \forall t \in T, \quad (3)$$

$$-\sum_{(u,v)^r\in\Psi_t} x^t_{uvr} + \sum_{(v,y)^s\in\Psi_t} x^t_{vys} = \begin{cases} 0, & \text{if } v = 1,\ldots,W-1, \\ -\sum_{(0,v)^r\in\Psi_t} x^t_{0vr}, & \text{if } v = W, \end{cases} \quad \forall t \in T, \quad (4)$$

$$x^t_{uvr} \in \{0,1\}, \forall (u,v)^r \in \Psi_t, \ \forall t \in T. \quad (5)$$

The objective function (1) represents the sum of the transportation costs of the traveled routes C_r, the cost of the vehicles used C_v, and daily storage costs per item C_{H_i}.

Restrictions (2) ensure that deliveries of demands of all periods, for each of the customers are met by one and only one of the traveled routes. This delivery can take place on the same period or in previous periods.

Restrictions (3) impose that more than F vehicles in each period t are not used. Conservation flow is ensured by the restrictions (4).

Example 2. *The graph from Figure 3 represents a valid solution from Figure 2 of Example 1.*

These graphs have a dimension $W = 120$ which represents the duration of a working day, being 0 the beginning and W the end. The set of arcs corresponds to the represented traveled routes. Each vertice defines a time instant and each arch represents a route traveled to visit a series of customers. These flows are the arcs defined for the three periods, in the first one two vehicles perform a route each, in the second period a single vehicle performs two routes and in the third and final period a vehicle performs a single route. This is a valid solution for instance Example 1.

4 COMPUTATIONAL RESULTS

To evaluate the performance of the model, it was used a set of instances adapted from the literature (Moin et al., 2010).

A set of 32 instances was generated, and in all the duration of the planning horizon the working day is $W = 140$. There are two instances for each combination of parameters: number of customers $N \in \{10, 20, 40, 50\}$ and number of periods of the planning horizon $\tau \in \{3, 5, 10, 15\}$.

With this set of instances, different tests were performed varying the capacity of the vehicles. It is considered $C \in \{10, 13, 20\}$, so that, for all instances all the demands are higher than 20%, 15% and 10% of vehicle capacity, respectively. It was also considered an additional constraint on the maximum number of

Table 3: Summary of instances solved to optimality / instances in which the model found a solution / number of instances to solve.

N_{max}	$C = 10$	$C = 13$	$C = 20$
3	12/32/50	12/30/50	12/20/40
4	12/22/50	8/20/20	8/12/20
5	12/18/40	11/12/20	-
10	12/18/40	10/12/20	-

Table 4: Average values of instances solved with different parameters.

C	N_{max}	$\bar{t_r}$	$\bar{t_m}$	$\bar{t_{total}}$	$\bar{n_r}$	$\bar{var}$	$\bar{Lim_{inf}}$	$\bar{Lim_{up}}$	$\bar{gap}$ %	#opt
10	20	6,28	59,64	65,92	13561,08	21970,00	2680,50	2680,50	0	12
13	20	538,65	196,46	735,17	51020,08	62688,58	2499,22	2507,67	0,17	10
10	3	0,51	31,71	32,21	8479,33	16844,25	2738,50	2738,50	0	12
10	4	2,90	90,23	93,13	12961,50	21370,42	2685,00	2685,00	0	12
10	5	6,20	57,88	64,08	13561,08	21970,00	2680,50	2680,50	0	12
13	3	1,25	45,52	46,78	17398,92	28893,67	2672,17	2672,17	0	12
13	4	12,20	390,00	402,22	38345,67	50014,17	2560,10	2576,83	0,61	8
13	5	66,44	151,35	217,80	49527,67	61196,17	2503,21	2507,33	0,09	11
20	3	4,51	36,00	40,53	53169,92	73678,50	2634,42	2634,42	0	12
20	4	95,99	399,87	495,92	209121,33	230754,58	2480,53	2514,42	1,44	8

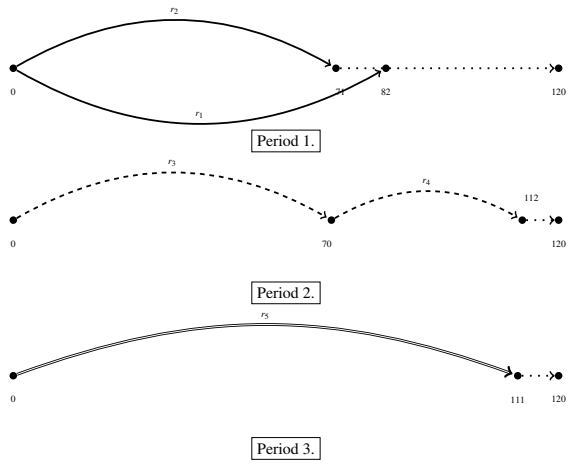

Figure 3: Solution of multi-trip inventory routing problem for three periods.

customers to visit in a route. In Tables 3 and 4, this parameter takes on values that do not restrict, or only limit slightly, the number of customers to consider in a route.

Computational tests were performed using a PC with i7 processor with 3.5 GHz and 32 GB of RAM. The optimization routines resorted to version 12.6.1 of CPLEX. The time limit for resolution of the integer programming model was 900 seconds. For the total time of model generation (including generation of routes) and its resolution it was set a time limit of 9500 seconds.

Tables 3 – 4 report the results obtained and their respective columns have the following meaning:

N_{max}: maximum number of customers to visit on a route;

t_r: generation time of routes;

t_m: execution time of the integer programming model (1) – (4);

t_{total}: total execution time ($t_m + t_m$);

n_r: number of routes generated;

var: number of variables of the integer programming model (1) – (4);

Lim_{inf}: best lower bound;

Lim_{up}: best upper bound;

gap %: gap (percentage);

In tests carried out without limit of customers to visit (N_{max}), where the vehicle capacity is 10 and 13 it was possible to solve, until the optimality, 24 of 18 and 10 of 12 instances, respectively. In this set of tests, where there is no restriction on the maximum number of customers to visit in a route, it was only possible to find a solution for instances with $N \leq 40$.

As expected, increasing the capacity of the vehicles hinders the generation and resolution of the model, since this variation increases the number of valid routes and, consequently, the number of variables. Instances for which it was not possible to find an optimal solution it was however possible to reduce the optimality gap. However, the maximum gap for all the parameters considered was equal to 8.85%.

Table 3 summarises the results obtained for all the instances and aggregates them by the different parameters. Each field in the table reflects the number of in-

stances solved to optimality, the number of instances for which the model found a solution and the number of instances to solve for this combination.

Note that a company that solves this problem will just have to generate all the valid routes once for each set of customers considered, and what will change in practice are the demands.

5 CONCLUSIONS

The multi-trip inventory routing problem has a great practical interest in the industrial field, but on the other hand, it is quite challenging in terms of resolution.

In this paper, we propose a network flow model for multi-trip inventory routing problem, which is solved exactly for a set of adapted instances in the literature. The model was able to solve instances up to 50 customers and 15 time periods in reasonable computational times. Several instances were solved to optimality when set to different parameters. The average gap obtained was relatively low.

ACKNOWLEDGEMENTS

This work was supported by FEDER funding through the Programa Operacional Factores de Competitividade - COMPETE and by national funding through the Portuguese Science and Technology Foundation (FCT) in the scope of the project PTDC/EGE-GES/116676/2010.

REFERENCES

Al-Khayyal, F. and Hwang, S.-J. (2007). Inventory constrained maritime routing and scheduling for multi-commodity liquid bulk, part i: Applications and model. *European Journal of Operational Research*, 176:106–130.

Alonso, F., Alvarez, J. M., and Beasley, E. J. (2008). A tabu search algorithm for the periodic vehicle routing problem with multiple vehicle trips and accessibility restrictions. *Journal of the Operational Research Society*, 59:963–76.

Archetti, C., Bertazzi, L., Hertz, A., and Speranza, M. G. (2011). A hybrid heuristic for an inventory routing problem. *INFORMS Journal on Computing*, 24:101–16.

Archetti, C. and Speranza, M. G. (2016). The inventory routing problem: the value of integration. *International Transactions in Operational Research*, 23:393–407.

Azi, N., Gendreau, M., and Potvin, J.-Y. (2007). An exact algorithm for a single-vehicle routing problem with time windows and multiple routes. *European Journal of Operational Research*, 178:755–66.

Azi, N., Gendreau, M., and Potvin, J.-Y. (2010). An exact algorithm for a vehicle routing problem with time windows and multiple use of vehicles. *European Journal of Operational Research*, 202:756–63.

Bertazzi, L. and Speranza, M. G. (2013). Inventory routing problems with multiple customers. *EURO Journal on Transportation and Logistics*, 2:255–75.

Brando, J. C. S. and Mercer, A. (1998). The multi-trip vehicle routing problem. *Journal of the Operational Research Society*, 49:799–805.

Coelho, L. C., Cordeau, J.-F., and Laporte, G. (2014). Thirty years of inventory routing. *Transportation Science*, 48:1–19.

Coelho, L. C. and Laporte, G. (2013). A branch-and-cut algorithm for the multi-product multi-vehicle inventory-routing problem. *International Journal of Production Research*, 51:7156–69.

Cordeau, J.-F., Lagan, D., Musmanno, R., and Vocaturo, F. (2015). A decomposition-based heuristic for the multiple-product inventory-routing problem. *Computers & Operations Research*, 55:153–66.

Şen, A. and Blbl, K. (Universidade Bilgi, Istambul, Turquia, 2008). A survey on multi trip vehicle routing problem.

Dauzère-Pérès, S., Nordli, A., Olstad, A., Haugen, K., Koester, U., Per Olav, M., Teistklub, G., and Reistad, A. (2007). Omya hustadmarmor optimizes its supply chain for delivering calcium carbonate slurry to european paper manufacturers. *Interfaces*, 37:39–51.

Grnhaug, R., Christiansen, M., Desaulniers, G., and Desrosiers, J. (2010). A branch-and-price method for a liquefied natural gas inventory routing problem. *Transportation Science*, 44:400–415.

Hanczar, P. (2012). A fuel distribution problem application of new multi-item inventory routing formulation. *Procedia - Social and Behavioral Sciences*, 54:726–735.

Hemmati, A., Stlhane, M., Hvattum, L. M., and Andersson, H. (2015). An effective heuristic for solving a combined cargo and inventory routing problem in tramp shipping. *Computers & Operations Research*, 64:274–82.

Herer, Y. T. and Levy, R. (1997). Raising the competitive edge in manufacturingthe metered inventory routing problem, an integrative heuristic algorithm. *International Journal of Production Economics*, 51:69–81.

Macedo, R., Alves, C., Valrio de Carvalho, J., Clautiaux, F., and Hanafi, S. (2011). Solving the vehicle routing problem with time windows and multiple routes exactly using a pseudo-polynomial model. *European Journal of Operational Research*, 214:536–45.

Miller, D. M. (1987). An interactive, computer-aided ship scheduling system. *European Journal of Operational Research*, 32:363–379.

Moin, N., Salhi, S., and Aziz, N. (2010). An efficient hybrid genetic algorithm for the multi-product multi-period inventory routing problem. *International Journal of Production Economics*, 133:334–343.

Olivera, A. and Viera, O. (2007). Adaptive memory programming for the vehicle routing problem with multiple trips. *Computers & Operations Research*, 34:28–47.

Persson, J. A. and Göthe-Lundgren, M. (2005). Shipment planning at oil refineries using column generation and valid inequalities. *European Journal of Operational Research*, 163:631–652.

Petch, R. J. and Salhi, S. (2003). A multi-phase constructive heuristic for the vehicle routing problem with multiple trips. *Discrete Applied Mathematics*, 133:69–92.

Salhi, S. and Petch, R. J. (2007). A ga based heuristic for the vehicle routing problem with multiple trips. *Journal of Mathematical Modelling and Algorithms*, 6:591–613.

Song, J. H. and Furman, K. C. (2013). A maritime inventory routing problem: Practical approach. *Computers & Operations Research*, 40:657–665.

Taillard, xc, ric, D., Laporte, G., and Gendreau, M. (1996). Vehicle routeing with multiple use of vehicles. *The Journal of the Operational Research Society*, 47:1065–70.

Yu, Y. G., Chen, H. X., and Chu, F. (2008). A new model and hybrid approach for large scale inventory routing problems. *European Journal of Operational Research*, 189:1022–40.

Zhong, Y. and Aghezzaf, E.-H. (2012). *Modeling and solving the multi-period inventory routing problem with constant demand rates*. Ghent University, Department of Industrial management.

Variance of Departure Process in Two-Node Tandem Queue with Unreliable Servers and Blocking

Yang Woo Shin[1] and Dug Hee Moon[2]
[1]*Department of Statistics, Changwon National University, Changwon, Gyeongnam 51140, Korea*
[2]*School of Industrial Engineering and Naval Architecture, Changwon National University, Changwon, Gyeongnam 51140, Korea*
{*ywshin, dhmoon*}*@changwon.ac.kr*

Keywords: Variance, Departure Process, Tandem Queue, Finite Buffers, Blocking, Markovian Arrival Process.

Abstract: This paper provides an effective method for evaluating the second moments such as variance and covariance for the number of departures in two-node tandem queue with unreliable servers. The behavior of the system is described by a level dependent quasi-birth-and-death process and the departure process is modeled by a Markovian arrival process. Algorithms for the transient behavior, the variance and covariance structure for the output process and the time to the *n*th departure are developed. We show that the results can be applied to derive approximate formulae for the due-date performance and the distribution of the number of outputs in a time interval.

1 INTRODUCTION

There is an extensive literature for the analysis of manufacturing systems with finite buffers and unreliable servers. Most of the works related to the performance evaluation of manufacturing systems have been focused on analyzing the first order measures such as average production rates and average buffer levels in steady-state e.g. see the monographs (Buzacott and Shanthikumar, 1993; Gershwin, 1994), the survey papers (Dallery and Gershwin, 1992; Papadopoulos and Heavey, 1996; Li et al., 2009) and the references therein. The first order measures can be used to get information about the capabilities of a production system in the long run. However, there may be tremendous variability from a time period to period (Gershwin, 1994, Section 3.2; Tan, 1999a). Thus the second order measures such as the variance of the number of parts produced in a given time period and the inter-departure times and covariance between consecutive inter-departure times are also very useful to design and control production systems in a more effective way. The information about the time dependent second order measures can especially be useful to respond short-term and long-term requirements in an effective and timely way.

Studies on variance of the output process in a serial production line have been presented during the last decades, for a review of recent studies on the variance of the output for production systems, one can refer to the papers (Tan,2000; Tan, 2013; Lagershausena and Tan, 2015). For discrete material flow production systems with finite buffers, Tan (1999b, 2000) use a Markov reward model to calculate the variance of the number of parts produced in a given time period in a two-station production line with finite buffer capacities and deterministic processing times and geometrically distributed failure and repair times. Our approach to be developed in this paper is to model the output process by a Markovian arrival process (MAP) and to use the closed formulae for the transient behavior and the variance and covariance structure for the number of outputs during a period $(0,t]$ and the *n*th departure time in the literature.

This paper is aimed on providing an effective method for evaluating the second moments of the number of outputs and inter-departure times and investigating the effects of the system parameters to the second moments. The results can be applied to the practical problem such as due-time performance in manufacturing system and are basis on analyzing the long line. This paper concerns to the two-station system with finite buffer capacities. A model of a two-node system is simple, but it helps us to understand the behavior of the system and gives some insights of the more complicated system. The approach can also be used as building block for analyzing the more complex system with multiple nodes.

Shin, Y. and Moon, D.
Variance of Departure Process in Two-Node Tandem Queue with Unreliable Servers and Blocking.
In *Proceedings of the 6th International Conference on Operations Research and Enterprise Systems (ICORES 2017)*, pages 258-264
ISBN: 978-989-758-218-9

This paper is organized as follows. In Section 2, the model is described in detail. The moment formulae for MAP are reviewed and algorithms for the performance measures are presented in Sections 3 and 4, respectively. In section 5, numerical results are presented. Concluding remarks are given in Section 6.

2 MODEL

We consider a tandem queueing network that consists of two service stations S_1 and S_2 and one buffer of finite size b between them. Each station S_i has an unreliable server M_i, $i = 1,2$. Assume the following system characteristics.

BAS blocking mechanism : Blocking after service (BAS) rule is adopted, that is, if the buffer is full upon a completion of service at the first station, the server M_1 is blocked and the customer is held at the station where it just completed its service until the station S_2 can accommodate it.

Open and saturated system: In many manufacturing system, it has been assumed that the first station the first station is never starved and the last station is never blocked. For potential applications of the method and results to developing approximation method of more complicated system, we assume that the server M_1 in the first station is never starved and it starts new service immediately after a service completion unless the server is blocked and the server M_2 in the second station is never blocked and the customer at M_2 leaves the system immediately after completing its service.

ODF rule : Each server is either up (operational) or under repair (broken-down) at any time. Operation dependent failure (ODF) is assumed. That is, a server can fail only while the server is working and a server never fails while the server is blocked or starved.

Exponential distributions of service time, failure time and repair time: We define the failure time by the operation time in units between two successive failures (from a repair to a failure). The failure time does not contain the time period while the server is being blocked, starved or repaired. Service time, failure time and repair time of M_i are assumed to be of exponential with rates μ_i, ν_i and η_i, respectively.

Let $X(t)$ be the number of customers in the buffer and at station S_2 and the customer blocked at station S_1. The state space of $X(t)$ is $\{0,1,\cdots,K\}$, where $K = b+2$. Let $J_i(t)$ be service phase of the server M_i at time t denote the states of $J(t)$ by

$$J_i(t) = \begin{cases} w, & M_i \text{ is working} \\ s, & M_i \text{ is starved} \\ b, & M_i \text{ is blocked} \\ f, & M_i \text{ is failed.} \end{cases}$$

The state space of the stochastic process $\boldsymbol{Z} = \{Z(t), t \geq 0\}$ with $Z(t) = (X(t), J_1(t), J_2(t))$ is

$$\mathcal{S} = \cup_{n=0}^{K} \mathcal{S}_n,$$

where

$$\begin{aligned} \mathcal{S}_0 &= \{(0,w,s),(0,f,s)\}, \\ \mathcal{S}_n &= \{(n,j_1,j_2) : j_1, j_2 \in \{w,f\}\}, 1 \leq n \leq K-1, \\ \mathcal{S}_K &= \{(K,b,w),(K,b,f)\}. \end{aligned}$$

The stochastic process $\boldsymbol{Z} = \{Z(t), t \geq 0\}$ forms a Markov chain with generator of the form

$$Q = \begin{pmatrix} B_0 & A_0 & & & \\ C_1 & B_1 & A_1 & & \\ & \ddots & \ddots & \ddots & \\ & & C_{K-1} & B_{K-1} & A_{K-1} \\ & & & C_K & B_K \end{pmatrix}.$$

The matrices B_n, A_n, C_n are as follows:

$$\begin{aligned} B_n &= \begin{pmatrix} * & \nu_2 & \nu_1 & 0 \\ \eta_2 & * & 0 & \nu_1 \\ \eta_1 & 0 & * & \nu_2 \\ 0 & \eta_1 & \eta_2 & * \end{pmatrix}, 1 \leq n \leq K-1, \\ B_0 &= \begin{pmatrix} * & \nu_1 \\ \eta_1 & * \end{pmatrix}, B_K^* = \begin{pmatrix} * & \nu_2 \\ \eta_2 & * \end{pmatrix}, \\ A_n &= \begin{pmatrix} \mu_1 & 0 & 0 & 0 \\ 0 & \mu_1 & 0 & 0 \\ 0 & 0 & 0 & 0 \\ 0 & 0 & 0 & 0 \end{pmatrix}, 1 \leq n \leq K-2, \\ A_0 &= \begin{pmatrix} \mu_1 & 0 & 0 & 0 \\ 0 & 0 & 0 & 0 \end{pmatrix}, \\ A_{K-1} &= \begin{pmatrix} \mu_1 & 0 \\ 0 & \mu_1 \\ 0 & 0 \\ 0 & 0 \end{pmatrix}, \\ C_n &= \begin{pmatrix} \mu_2 & 0 & 0 & 0 \\ 0 & 0 & 0 & 0 \\ 0 & 0 & \mu_2 & 0 \\ 0 & 0 & 0 & 0 \end{pmatrix}, 2 \leq n \leq K-1, \\ C_1 &= \begin{pmatrix} \mu_2 & 0 \\ 0 & 0 \\ 0 & \mu_2 \\ 0 & 0 \end{pmatrix}, C_K = \begin{pmatrix} \mu_2 & 0 & 0 & 0 \\ 0 & 0 & 0 & 0 \end{pmatrix}, \end{aligned}$$

where the diagonal entries of B_n are determined by $Q\mathbf{e} = 0$ and $\mathbf{e}$ is a column vector of appropriate size whose elements are all 1.

3 DEPARTURE PROCESS

Let T be the first time until a customer leaves the system and

$$F_{zz'}(t) = P(Z(T) = z', T \le t \,|\, Z(0) = z),\ z, z' \in \mathcal{S}.$$

Then T is the same as the absorbing time of a Markov chain with rate matrix of the form

$$Q_T = \begin{pmatrix} D_0 & D_1 \\ 0 & 0 \end{pmatrix},$$

where

$$D_0 = \begin{pmatrix} B_0 & A_0 & & & \\ & B_1 & A_1 & & \\ & & \ddots & \ddots & \\ & & & B_{K-1} & A_{K-1} \\ & & & & B_K \end{pmatrix},$$

$$D_1 = \begin{pmatrix} O_0 & & & & \\ C_1 & O_1 & & & \\ & C_2 & O_2 & & \\ & & \ddots & \ddots & \\ & & & C_K & O_K \end{pmatrix}.$$

The matrix $F(t) = (F_{zz'}(t))$ is given by

$$F(t) = \int_0^t \exp(D_0 u)\, du D_1,\ t \ge 0$$

which is the inter arrival time of a Markovian arrival process (MAP) with representation $MAP(D_0, D_0)$, see Lucantoni et al. (1990).

Let $N(t)$ be the number of customers that leave the system during an interval $(0,t]$ and $P(n,t) = (P_{zz'}(n,t))$ be the square matrix of size $|\mathcal{S}|$ whose (z,z')-component is

$$P_{zz'}(n,t) = P(N(t) = n, Z(t) = z' | Z(0) = z).$$

It follows from the Kolomogorov equations that

$$\frac{d}{dt}P(n,t) = P(n,t)D_0 + P(n-1,t)D_1,\ n \ge 1,\ t \ge 0 \tag{1}$$

and $P(0,0) = I$ the identity matrix. The matrix generating function $P^*(w,t) = \sum_{n=0}^{\infty} w^n P(n,t)$ is given by

$$P^*(w,t) = \exp[(D_0 + wD_1)t],\ |w| \le 1,\ t \ge 0.$$

For later use, define the following notation. Let $\boldsymbol{\pi} = (\pi(x), x \in \mathcal{S})$ be the stationary distribution of Q and

$$\begin{array}{lll} \boldsymbol{\Pi} = \mathbf{e}\boldsymbol{\pi}, & \Psi = (\mathbf{e}\boldsymbol{\pi} - Q)^{-1}, & \lambda = \boldsymbol{\pi} D_1 \mathbf{e} \\ \mathbf{c} = \boldsymbol{\pi} D_1 \Psi, & \mathbf{d} = \Psi D_1 \mathbf{e}. & \end{array}$$

It can be easily seen that $\boldsymbol{\pi}\Psi = \boldsymbol{\pi}$, $\Psi\mathbf{e} = \mathbf{e}$ and $\mathbf{ce} = \lambda = \boldsymbol{\pi}\mathbf{d}$.

The following theorem can be found in (Neuts, 1989, Theorems 5.4.1 and 5.4.2; Artalejo et al, 2010).

Theorem 3.1. *In stationary state, that is, $\pi(x) = P(Z(0) = x)$, mean $\mu(t) = E[N(t)]$, variance $\sigma^2(t) = \mathrm{Var}[N(t)]$ and the covariance $\mathrm{Cov}(t,u,v) = Cov[N(t), N(v) - N(u)]$ $(0 < t \le u < v)$ are given as follows:*

$$\begin{aligned} &\mu(t) = \lambda t, \\ &\sigma^2(t) = \tilde{\sigma}^2(t) + 2\mathbf{c}[\exp(Qt) - \boldsymbol{\Pi}]\mathbf{d}, \\ &\mathrm{Cov}(t,u,v) = \boldsymbol{\pi} D_1 [I - \exp(Qt)] \exp[Q(u-t)] \\ &\times [I - \exp(Q(v-u))]\Psi\mathbf{d}. \end{aligned}$$

where

$$\tilde{\sigma}^2(t) = 2(\lambda^2 - \mathbf{cd}) + (\lambda - 2\lambda^2 + 2\mathbf{c}D_1\mathbf{e})t. \tag{2}$$

Remark 1. It is well known that as $t \to \infty$

$$\exp(Qt) = \boldsymbol{\Pi} + O(t^{r-1}e^{-\eta t}), \tag{3}$$

where $-\eta$ is the real part of η^*, the non-zero eigen value of Q with maximum real part, and r is the multiplicity of η^*, see e.g. (Narayana and Neuts, 1992). It can be easily seen from Theorem 3.1 and (3) that $\mathrm{Cov}(t,u,v) \to 0$ as $u - t \to \infty$.

Remark 2. It can be seen from Theorem 3.1 that the variance rate is given by the closed formula

$$\begin{aligned} V &= \lim_{t\to\infty} \frac{\mathrm{Var}[N(t)]}{t} \\ &= (\lambda - 2\lambda^2 + 2\mathbf{c}D_1\mathbf{e}). \end{aligned}$$

Tan (1999b) use numerical result of the asymptotic variance rate V to determine the variance $\sigma^2(t) \approx Vt$ for large t. We can see that $\tilde{\sigma}^2(t)$ provides more accurate approximation of $\sigma^2(t)$ than that of Vt and it is easy to compute $\tilde{\sigma}^2(t)$.

Let ξ_n, $n = 0,1,2,\cdots$ be the nth transition time of $\boldsymbol{N}$ with $\xi_0 = 0$ and set $\tau_n = \xi_n - \xi_{n-1}$ and $Z_n = Z(\xi_n + 0)$, $n = 1,2,\cdots$ with $Z_0 = Z(0)$. The transition probability matrix of $\{Z_n, n = 0,1,2,\cdots\}$ is $P = (-D_0)^{-1}D_1$ and the stationary distribution $\boldsymbol{p}$ of P is given by

$$\boldsymbol{p} = \frac{1}{\lambda}\boldsymbol{\pi} D_1.$$

The following theorem can be found in Artalejo et al. (2010).

Theorem 3.2. *Assume that $Z(0)$ has a distribution $\mathbf{a} = (a(x), x \in \mathcal{S})$ with $a(x) = P(Z(0) = x)$. The mean, variance and covariance of τ_n are given as follows:*

$$\begin{aligned} &\mathbb{E}[\tau_n] = \mathbf{a}P^{n-1}\mathbf{d}_0, \\ &\mathrm{Var}[\tau_n] = 2\mathbf{a}P^{n-1}(-D_0)^{-2}\mathbf{e} - \left(\mathbf{a}P^{n-1}\mathbf{d}_0\right)^2, \\ &\mathrm{Cov}(\tau_k, \tau_n) = \mathbf{a}\mathcal{X}_{k,n}\mathbf{e} - (\mathbb{E}[\tau_k])(\mathbb{E}[\tau_n]),\ 1 \le k < n, \end{aligned}$$

where

$$\begin{aligned} &\mathbf{d}_0 = (-D_0)^{-1}\mathbf{e}, \\ &\mathcal{X}_{k,n} = P^{k-1}(-D_0)^{-1}P^{n-k}(-D_0)^{-1}P,\ 1 \le k < n. \end{aligned}$$

Remark 3. Since $\lim_{n\to\infty} P^n = \mathbf{ep}$, it can be easily seen that for each $k = 1,2,\cdots$,

$$\lim_{n\to\infty} \mathrm{Cov}(\tau_k, \tau_n) = 0.$$

Remark 4. The mean and variance of ξ_n are as follows

$$\mathbb{E}[\xi_n] = \sum_{i=1}^{n} \mathbb{E}[\tau_i],$$

$$\mathrm{Var}[\xi_n] = \sum_{i=1}^{n} \mathrm{Var}[\tau_i] + 2\sum_{i=1}^{n-1}\sum_{j=i+1}^{n} \mathrm{Cov}(\tau_i, \tau_j).$$

Remark 5. Assuming $\mathbf{a} = \boldsymbol{p}$, the mean, variance and covariance of τ_n are as follows:

$$\mathbb{E}[\tau_n] = \frac{1}{\lambda},$$

$$\mathrm{Var}[\tau_n] = \frac{2}{\lambda}\boldsymbol{\pi}\mathbf{d}_0 - \frac{1}{\lambda^2},$$

$$\mathrm{Cov}(\tau_k, \tau_n) = \frac{1}{\lambda}\boldsymbol{\pi}P^n\mathbf{d}_0 - \frac{1}{\lambda^2}, n = 1,2,\cdots.$$

4 ALGORITHMS

It is necessary to $\boldsymbol{\pi}$, $\Psi = (\mathbf{e}\boldsymbol{\pi} - Q)^{-1}$ and $\exp(Qt)$ for the variance, covariance of $N(t)$ and τ_n. In this section, some algorithms for computing $\boldsymbol{\pi}$, $\Psi = (\mathbf{e}\boldsymbol{\pi} - Q)^{-1}$ and $\exp(Qt)$ are presented.

1. Algorithm for stationary distribution $\boldsymbol{\pi}$ of Q. Here, we present an algorithm for stationary distribution $\boldsymbol{\pi}$ of Q. Write $\boldsymbol{\pi} = (\boldsymbol{\pi}_0, \boldsymbol{\pi}_1, \cdots, \boldsymbol{\pi}_K)$, where $\boldsymbol{\pi}_i$ is the vector of size l_i, $0 \le i \le K$. Let $R_1, \cdots, R_K$ be the matrices satisfies the following matrix equations

$$A_{n-1} + R_n B_n + R_n R_{n+1} C_{n+1} = 0,\ 1 \le n \le K-1,$$
$$A_{K-1} + R_K B_K = 0.$$

The solutions of the equation are given as follows:

$$R_K = A_{K-1}(-B_K)^{-1},$$
$$R_n = A_{n-1}[-(B_n + R_{n+1}C_{n+1})]^{-1}, n = K-1, \cdots, 1.$$

Then the stationary distribution $\boldsymbol{\pi}$ of Q is given as follows

$$\boldsymbol{\pi}_n = \boldsymbol{\pi}_0 R_1 \cdots R_n,\ n = 1,2,\cdots,K$$

with

$$\boldsymbol{\pi}_0[B_0 + R_1 C_1] = 0$$

and normalizing condition

$$\boldsymbol{\pi}_0\left(\mathbf{e} + \sum_{n=1}^{K} R_1 \cdots R_n \mathbf{e}\right) = 1.$$

Once $\boldsymbol{\pi}$ is obtained, $\boldsymbol{p} = (\boldsymbol{p}_0, \boldsymbol{p}_1, \cdots, \boldsymbol{p}_K)$ can be calculated by

$$\boldsymbol{p}_k = \begin{cases} \frac{1}{\lambda}\boldsymbol{\pi}_{k+1}C_{k+1}, & k = 0,1,\cdots,K-1, \\ 0, & k = K. \end{cases}$$

2. Algorithm for $(-D_0)^{-1}$. It can be seen from the structure of D_0 that $(-D_0)^{-1}$ is of the form

$$(-D_0)^{-1} = \begin{pmatrix} X(0,0) & X(0,1) & \cdots & X(0,K) \\ & X(1,1) & \cdots & X(1,K) \\ & O & \ddots & \vdots \\ & & & X(K,K) \end{pmatrix}.$$

The block components $X(i,j)$, $0 \le i \le j \le K$ are calculated following the algorithm in (Shin, 2009) as follows :

(1) Compute

$$G_n = A_{n-1}(-B_n)^{-1},\ n = K, K-1, N-2, \cdots, 1$$

and $G_0 = (-B_0)^{-1}$.

(2) Compute $X(n,k)$, $0 \le n \le K$, $k = n, n+1, \cdots, K$ as follows: For $n = 0,1,\cdots,K$, set $X(n,n) = (-B_n)^{-1}$ and

$$X(n,k) = X(n,k-1)G_k,\ k = n+1, n+2, \cdots, K.$$

3. Algorithm for $\Psi = (\mathbf{e}\boldsymbol{\pi} - Q)^{-1}$. Let $E_n = (1,\cdots,1)^T$ $(0 \le n \le K)$ be the l_n-dimensional column vector whose components are all one and $E_1^* = (1,\cdots,1)^T$ be the $(\sum_{i=1}^{K} l_i)$-dimensional column vector, where l_i is the number of elements of $\mathcal{S}_i$. Let $\boldsymbol{\pi}_1^* = (\boldsymbol{\pi}_1, \cdots, \boldsymbol{\pi}_K)$ and $\Pi[i,j] = E_i\boldsymbol{\pi}_j$, $0 \le i,j \le K$. Denote the (i,j) block matrix of a matrix A corresponding to (i,j) block of Q by $A[i,j]$, $0 \le i,j \le K$. Write the matrix Q in the block form

$$Q = \begin{pmatrix} B_0 & Q_{01} \\ Q_{10} & Q_{11} \end{pmatrix},\ \mathbf{e}\boldsymbol{\pi} - Q = \begin{pmatrix} A_{00} & A_{01} \\ A_{10} & A_{11} \end{pmatrix},$$

where

$$A_{00} = E_0\boldsymbol{\pi}_0 - B_0, \quad A_{01} = E_0\boldsymbol{\pi}_1^* - Q_{01},$$
$$A_{10} = E_1^*\boldsymbol{\pi}_0 - Q_{10}, \quad A_{11} = E_1^*\boldsymbol{\pi}_1^* - Q_{11}.$$

Then the block matrix form of Ψ is given by (e.g. (Horn and Johnson, 1985, page 18))

$$\Psi = \begin{pmatrix} A_{00}^{*-1} & -A_{00}^{-1}A_{01}A_{11}^{*-1} \\ -A_{11}^{*-1}A_{10}A_{00}^{-1} & A_{11}^{*-1} \end{pmatrix},$$

where

$$A_{00}^* = A_{00} - A_{01}A_{11}^{-1}A_{10},$$
$$A_{11}^* = A_{11} - A_{10}A_{00}^{-1}A_{01}.$$

The matrix Ψ is calculated by the following step:

(1) Calculate $(-B_0)^{-1}$ using the ordinary algorithm.

(2) Since Q_{11} is block tridiagonal matrix, one can use the algorithm in (Shin, 2009) for $(-Q_{11})^{-1}$.

(3) For A_{11}^{-1} and A_{00}^{-1}, one can use the following formula (see Horn and Johnson(1985, page 19))

$$A_{11}^{-1} = (-Q_{11})^{-1} - \frac{1}{1 + \boldsymbol{\pi}_1^*\mathbf{q}_{11}}\mathbf{q}_{11}\boldsymbol{\pi}_1^*(-Q_{11})^{-1},$$

where $\mathbf{q}_{11} = (-Q_{11})^{-1}E_1^*$. The inverse matrix A_{00}^{-1} is calculated by usual method.

(4) Calculate A_{11}^{*-1} by the formula,

$$\begin{aligned} A_{11}^{*-1} &= (A_{11}+A_{10}(-A_{00}^{-1})A_{01})^{-1} \\ &= A_{11}^{-1}+A_{11}^{-1}A_{10}A_{00}^{*-1}A_{01}A_{11}^{-1}, \end{aligned}$$

where A_{00}^{*-1} is calculated by usual method.

(5) The (i,j) block $\Psi[i,j]$ of Ψ is

$$\Psi[i,j] = \begin{cases} A_{00}^{*-1}, & i=0, j=0, \\ -A_{00}^{-1}(A_{01}A_{11}^{*-1})[j], & i=0, 1\le j\le K, \\ -(A_{11}^{*-1}A_{10})[i]A_{00}^{-1}, & 1\le i\le K, j=0, \\ A_{11}^{*-1}[i,j], & 1\le i,j\le K. \end{cases}$$

4. Calculation of $\exp(Qt)=\sum_{n=0}^{\infty}\frac{t^n}{n!}Q^n$. We use the uniformization technique. Let

$$q=\max_{z\in\mathcal{S}}([-Q]_{zz})$$

and $\Theta = I+\frac{1}{q}Q$. Then

$$\exp(Qt) = Q_M(t)+\mathcal{E}^{(M)}(t),$$

where

$$Q_M(t)=\sum_{n=0}^{M} e^{-qt}\frac{(qt)^n}{n!}\Theta^n,$$

$$\mathcal{E}^{(M)}(t)=\sum_{n=M+1}^{\infty} e^{-qt}\frac{(qt)^n}{n!}\Theta^n.$$

For given $\varepsilon>0$, let $M(\varepsilon)$ be the positive integer such that

$$1-\sum_{n=0}^{M(\varepsilon)} e^{-qt}\frac{(qt)^n}{n!}<\varepsilon.$$

For large t, the following addition formula is useful. First, take an integer n_0 such that $t_0=\frac{qt}{n_0}$ is moderate with $\mathcal{E}^{(M)}(t_0)\mathbf{e}<\varepsilon_0\mathbf{e}$. Note that

$$\begin{aligned} \exp(Qt) &= [\exp(Qt_0)]^{n_0} = \left[Q_M(t_0)+\mathcal{E}^{(M)}(t_0)\right]^{n_0} \\ &= [Q_M(t_0)]^{n_0}+\mathcal{E}^{(M)}(t_0,n_0), \end{aligned}$$

where

$$\mathcal{E}^{(M)}(t_0,n_0)=\sum_{k=1}^{n_0}\binom{n_0}{k}\left[\mathcal{E}^{(M)}(t_0)\right]^{n_0-k}[Q_M(t_0)]^k.$$

Since $Q_M(t_0)\mathbf{e}<(1-\varepsilon_0)\mathbf{e}$ and $\mathcal{E}^{(M)}(t_0)\mathbf{e}<\varepsilon_0\mathbf{e}$, it can be seen that

$$\mathcal{E}^{(M)}(t_0,n_0)\mathbf{e}<(1-(1-\varepsilon_0)^{n_0})\mathbf{e}.$$

5. Calculation of $P(n,t)$. Let $\Theta_0=I+\frac{1}{q}D_0$. Applying the uniformization technique to $P(n,t)$ and using the the Kolmogorov equation (1), it can be seen that

$$P(k,t)=\sum_{n=0}^{\infty} e^{-qt}\frac{(qt)^n}{n!}K_k^{(n)},\ k\ge 1,$$

where $\{K_k^{(n)}\}$ satisfies the followings: for $k=1,2,\cdots$,

$$K_k^{(n+1)}=\frac{1}{q}K_{k-1}^{(n)}D_1+K_k^{(n)}\Theta_0,\ n=0,1,2,\cdots \quad (4)$$

with $K_k^{(0)}=0$, $k\ge 1$ and $K_0^{(0)}=I$ and

$$K_0^{(n+1)}=K_0^{(n)}\Theta_0,\ n\ge 0.$$

The recursive formula (4) is also given in (Lucantoni, 1991). Let

$$\mathcal{E}_k^{(M)}=P(k,t)-\sum_{n=0}^{M} e^{-qt}\frac{(qt)^n}{n!}K_k^{(n)},\ k\ge 0.$$

Note that

$$\exp(Qt)=\sum_{k=0}^{\infty}P(k,t)=\sum_{n=0}^{\infty}e^{-qt}\frac{(qt)^n}{n!}\sum_{k=0}^{\infty}K_k^{(n)}.$$

It can be seen from

$$\Theta^n=\sum_{k=0}^{\infty}K_k^{(n)},\ n\ge 0$$

that $K_k^{(n)}\mathbf{e}<\mathbf{e}$ and hence

$$\mathcal{E}_k^{(M(\varepsilon))}\mathbf{e}<\varepsilon\mathbf{e},\ k\ge 0.$$

5 NUMERICAL RESULTS

We apply the algorithms in section 4 to the system with two-node tandem queue with a finite buffer and server breakdown. We consider the system with service rates $\mu_1=\mu_2=1.0$, failure rates $\nu_1=0.1$, $\nu_2=0.04$ and repair rates $\eta_1=0.5$, $\eta_2=0.2$. The isolated efficiency of each server is the same as $\frac{\eta_i}{\nu_i+\eta_i}=0.833$. In this section, we assume that the system is in stationary state.

1. Speed of convergence to stationary state. We investigate how fast the distribution of the process $\boldsymbol{Z}$ converges to the stationary distribution $\boldsymbol{\pi}$. It can be seen from (3) that $\Delta_Q(t)=\log||\exp(Qt)-\Pi||$ is almost linear for large t. We also have seen that the speed of convergence of $\exp(Qt)$ decreases as buffer size increases. For example, the time $t_s(b):=\min\{t>0:\Delta_Q(t)<-5\}$ are $t_s(3)=74$, $t_s(5)=99$, $t_s(7)=134$.

2. Variance of $N(t)$. Figures 1 and 2 show variance $\sigma^2(t)$ and the difference $\Delta_{\sigma^2}(t)=\sigma^2(t)-\tilde{\sigma}^2(t)$. Figure 1 exhibits that $\sigma^2(t)$ increases almost linearly as t increases as expected in the formula in Theorem 3.1. It can be seen from fig. 2 that $\tilde{\sigma}^2(t)$ can be used instead of $\sigma^2(t)$ for $t\ge t_s$. In fact, it follows from Theorem 3.1 and (3) that for t_s with $\Delta_Q(t_s)<\log_{10}\varepsilon$,

$$|\Delta_{\sigma^2}(t)|<2|\mathbf{cd}|\varepsilon,\ t\ge t_s.$$

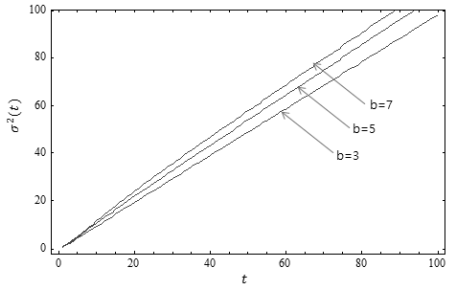

Figure 1: The variance $\sigma^2(t)$.

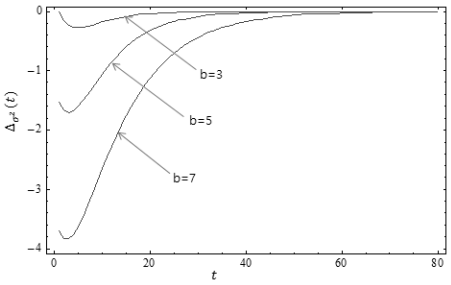

Figure 2: Differences $\Delta_{\sigma^2}(t) = \sigma^2(t) - \tilde{\sigma}^2(t)$.

Indeed, for $b = 5$, $\Delta_{\sigma^2}(64) < 10^{-3}$, $\Delta_{\sigma^2}(81) < 10^{-4}$ and $\Delta_{\sigma^2}(99) < 10^{-5}$.

3. Covariance of $N(t)$. Figure 3 depicts the $\mathrm{Cov}[t] = \mathrm{Cov}[N(t), N(2t) - N(t)]$ and $\lim_{t\to\infty} \mathrm{Cov}[t] = \boldsymbol{\pi}\mathbf{d} - \lambda^2$. Figure 3 shows that $\mathrm{Cov}[t]$ is positive for $b = 3$ and negative for $b = 5$.

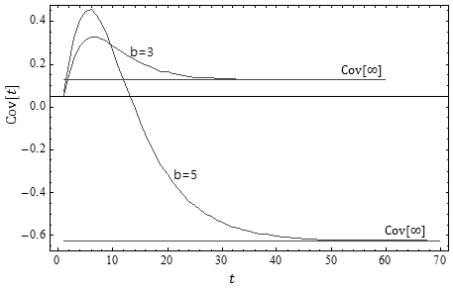

Figure 3: Covariance $\mathrm{Cov}[N(t), N(2t) - N(t)]$ for $b = 3, 5$.

5. Distribution of $N(t)$. The distribution of $N(t)$ is depicted in figure 4 for $t = 30$, $t = 50$, $t = 70$. The figures show that the distribution of $N(t)$ visually resembles the normal distribution. The the pair (skewness, kurtosis) of $N(t)$ are $(-0.2599, 0.5054)$, $(-0.2393, 0.1739)$ and $(-0.2141, 0.1486)$ for $t = 30$, $t = 50$ and $t = 70$, respectively. Here, we approximate the distribution of $N(t)$ in stationary state with the normal distribution $N(\mu(t), \sigma^2(t))$ with mean $\mu(t) = \lambda t$ and variance $\sigma^2(t)$ as Tan (1999b), that is,

$$P(N(t) \geq n) \approx 1 - \Phi\left(\frac{n - 0.5 - \lambda t}{\sqrt{\sigma^2(t)}}\right), \qquad (5)$$

where $\Phi(x) = \int_{-\infty}^{x} \frac{1}{\sqrt{2\pi}} \exp(-y^2/2)\, dy$ is the distribution function of the standard normal distribution and $n - 0.5$ is used for correction of the approximation of discrete random variable using continuous distribution and $\tilde{\sigma}^2(t)$ can be used as an approximation of $\sigma^2(t)$ for large t.

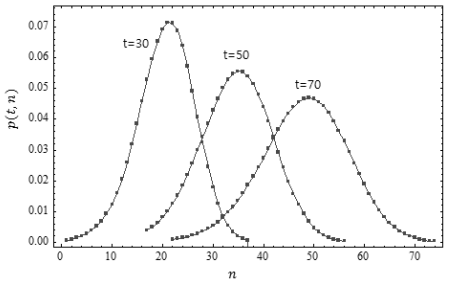

Figure 4: Plot of $p(n,t) = P(N(t) = n)]$ for $b = 5$.

The approximation errors $\Delta_N(t)$ between $P(N(t) \geq n)$ and normal approximation are depicted in figure 5 for $t = 30$, $t = 50$, $t = 70$ and $b = 5$. The maximal error of approximation occurs at the mean λt for each case. Figure shows that the accuracy increases as t increases.

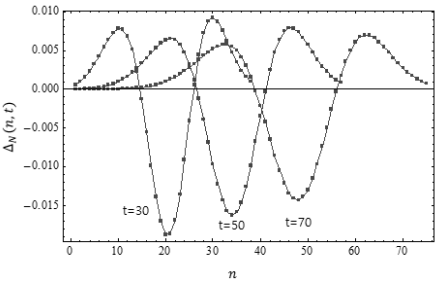

Figure 5: Error of normal approximation for $P(N(t) \geq n)$.

6. Due time performance. The due-time performance of a production line can be measured by a probability

$$p = P(N(t^*) \geq n^*)$$

of meeting a customer's order n^* on time t^*. Some numerical results for t^* for given n^* and p are listed in Table 1.

Table 1: Due time t^*

	p					
n^*	0.5	0.6	0.7	0.8	0.9	0.99
50	72	76	79	84	91	109
70	101	105	110	115	123	143
100	145	150	155	161	170	193

6 CONCLUSIONS

We have provided an algorithm for the transient behavior, the variance and covariance structure for the output process and inter-departure time in two-node tandem queue. Some numerical results are presented. We also showed that the results can be applied to derive approximate formulae for the due-date performance and the distribution of the number of outputs in a time interval.

The algorithm is based on the Markovian arrival process (MAP) which gives closed formula for variance and asymptotic variance. This is a different point from the other methods in the literature for variance of departure process. The algorithm requires only the inversions of the block matrices of size 4 in the computing process. Thus the computational complexity of the algorithm dose not severely depend on the buffer size of the system. The approach using MAP can be easily applied to the system with more general service, failure and repair time than exponential case.

Although the method developed in this paper is quite efficiently, it will be limited to apply the method to the system with multiple nodes due to the rapid increase of the number of states when the number of stations and the buffer capacities increase. Therefore developing approximation methods to estimate the second moment measures in multiple node system are required. There are many approximation methods for throughput in a complicated system, for example, decomposition method and aggregation method (Dallery and Gershwin, 1992; Li et al., 2009) that use the the two-node system. The method of analyzing the two-node system can be used as a building block of analyzing the more complex system.

ACKNOWLEDGEMENTS

The authors are very thankful to three anonymous reviewers for valuable comments and suggestions.

REFERENCES

Artalejo, J. R., Gómez-Corral, A., He, Q. M. (2010). Markovian arrivals in stochastic modelling: a survey and some new results, SORT 34 (2), 101-144.

Buzacott, J. A., Shanthikumar, J. G. (1993). *Stochastic models of manufacturing systems*. Prentice Hall, Englewood Cliffs.

Dallery, Y., Gershwin, B. (1992). Manufacturing flow line systems: a review of models and analytical results, Queueing Systems 12, 3-94.

Gershwin, S. B. (1993). Variance of the output of a tandem production system. In *Queueing Networks with Finite Capacity*. Onvural, R. and Akyildiz, I. (eds), Elsevier Science Publishers, Amsterdam, North-Holland, pp. 291-304.

Gershwin, S. B. (1994). *Manufacturing systems engineering*. Prentice-Hall, Englewood Cliffs.

Horn, R. A., Johnson, C. R. (1985). *Matrix Analysis*. Cambridge University Press.

Lagershausena, S., Tan, B. (2015). On the exact inter-departure and inter-start time distribution of closed queueing networks subject to blocking, IIE Transactions 47, 673-692

Li, J., Blumenfeld, D. E., Huang, N., Alden, J. M. (2009). Throughput analysis of production systems: recent advances and future topics, International Journal of Production Research 47(14), 3823-3851.

Lucantoni, D. M., Meier-Hellstern, K. S., Neuts, M. F. (1990). A single server queue with server vacations and a class of non-renewal arrival processes, Advances in Applied Probability 22, 676-705.

Narayana, S., Neuts, M. F. (1992). The first two moment matrices of the counts for the Markovian arrival process, Stochastic Models 8(3), 459-477.

Neuts, M. F. (1989). *Structured Stochastic Matrices of $M/G/1$ Type and Their Applications*. Marcel Dekker, New York.

Papadopoulos, H. T., Heavey, C. (1996). Queueing theory in manufacturing systems analysis and design: a classification of models for production and transfer lines, European Journal of Operational Research 92, 1-27.

Shin, Y. W. (2009). Fundamental matrix of transition QBD generator with finite states and level dependent transitions, Asia-Pacific Journal of Operational Research 26(5), 1-18.

Tan, B. (1999a). Asymptotic variance rate of the output of a transfer line with no buffer storage and cycle-dependent failures, Mathematical and Computer Modelling 29(7), 97-112.

Tan, B. (1999b). Variance of the output as a function of time: Production line dynamics, European Journal of Operational Research 117(3), 470-484.

Tan, B. (2000). Asymptotic variance rate of the output in production lines with finite buffers, Annals of Operations Research 93, 385-403.

Tan, B. (2013). Modeling and analysis of output variability in discrete material flow production systems. In *Handbook of Stochastic Models and Analysis of Manufacturing System Operations*. Tan,B. and Smith, J. M. (eds), Springer, New York, pp. 287-311.

Development of an Innovative Methodology Supporting Project Risk Management in the Manufacturing Company of the Automotive Industry

Anna Gembalska-Kwiecień
Faculty of Organization and Management, Institute of Production Engineering, Silesian University of Technology, Roosevelta 26 str., Zabrze, Poland
Anna.Gembalska-Kwiecien@polsl.pl

Keywords: Innovations, Project Risk Management, Methodology, Optimization of the Decisions, Management Science.

Abstract: The presented article attempts to develop an innovative methodology for supporting risk management of the implementation of projects. The methodology applies to manufacturing companies of the automotive industry, because it is one of the industries where the projects are comparable to each other. On this basis, it is possible to identify the risks that occurred in the past during the various stages of projects, which can contribute to more effective risk management during the current and future projects. The paper presents selected methods of data analysis: statistical method and method of graphical data visualization. There are also shown recommendations for data collection and processing which will enable the development of the innovation called authorial methodology. This developed methodology describes how to collect data on ongoing projects, as well as how to make their analysis to allow their subsequent use. The presented methodology is to aimed at optimizing decision making for project implementation in management sciences.

1 INTRODUCTION

The basis of production companies of the automotive industry is the completion of projects. Extensive engineering centers, cooperating closely with production facilities, are responsible for the development of existing, and entirely new product concepts. Starting with the implementation of the developed solutions and ending in production. In situation where the project involves cooperation with crucial contractor for the company, or is intended to implement a very important strategic objectives of the company. The success depends on whether the company is competitive on the market.

Regardless of market segment of the company, the completion of projects involves many challenges, which are diverse and complex. However, the common feature for all difficulties is that they carry a risk. It could threaten the planned completion of the project, or lead to a total failure. To avoid failure, people such as project managers, operational managers, or leaders of the various units use methods supporting the management of risks. The aim of these methods is to prepare for the risk (negative risk – called threat »Korczowski, 2010; PMBOK Guide, 2012«) to respond in the incidents of danger, and to eliminate or at least to reduce their undesirable effects. Concept of the risk is also associated with the possibility of incidents which can lead to positive consequences: this risk is called opportunity (Jaafari, 2001). The role of the person responsible for this phase of the project is to make the opportunity happen.

In the case of companies whose functioning is based on the successful completion of projects, it is very important to pay attention to various aspects of the tasks. The aim is to improve efficiency, reduce the amount of unplanned costs and to achieve the intentions according to the plan. In such situations, it is important to draw the appropriate conclusions after, and during the completion of each project.

It should concern issues such as execution management tasks, cooperation with subcontractors, or the quality of the work performed by the individual functional groups. Information about these issues can be useful for risk management in the future, because the knowledge of the past risks or opportunities, combined with the knowledge on how

Gembalska-Kwiecień, A.
Development of an Innovative Methodology Supporting Project Risk Management in the Manufacturing Company of the Automotive Industry.
In *Proceedings of the 6th International Conference on Operations Research and Enterprise Systems (ICORES 2017)*, pages 265-271
ISBN: 978-989-758-218-9

to deal with such situations, can contribute to the fast, and appropriate risk response (Larose, 2006; Pickett and Elliot, 2007).

Sometimes after the completion of the project, there is not enough time to analyze it and draw conclusions, because next project is started very quickly.

In that case it is not possible to share the knowledge gained during the completion of the project with other employees of the company or to catalogue it properly. That is why it would be useful to have a tool to support fast archiving of information and knowledge, and to be able to draw conclusions on the basis of available data.

An obstacle to the practical use of such tool is the fact that each of project is innovative and unique, so their comparative analysis will not always make sense. However if similar projects would be studied, their comparison can provide useful information and lead to conclusions which will be helpful in managing the risk of other similar projects realized by the company in the future.

This situation takes place in companies in automotive industry, which realize many similar projects. This means that the projects are comparable to each other, and on this basis it is possible to formulate a thesis that the identify the risks that have occurred in the past at different stages of projects, it can contribute to more effective risk management during the current and future projects.

To be able to use this approach in practice, it is necessary to know the methodology of data analysis on completed projects in order to identify the risks related with them.

The aim of this paper is to develop the methodology for collecting and analyzing data on completed projects that allow their subsequent analysis, in order to identify key risks of projects, and provide valuable information.

2 METHODS OF DATA ANALYSIS

The development of the methodology of analysis of projects and to implement it as a tool based on a spreadsheet, it is helpful to have knowledge of exploration topics (Dvir, Raz and Shenhar, 2003). The following are methods for the analysis and presentation of data:

- The statistical method, which will be used in creating the spreadsheet, supporting project risk management. This method is based on the analysis of the probability of risks. The possibility of using this method is based on the information gathered from past projects;
- Method of graphical data visualization, which enables to analyze the data through the visual, and thus it gives the chance the data will be noticed in a way that would be difficult to determine through analysis of algorithm by a computer. The method should be used in the process of developing a spreadsheet, because it can provide additional opportunities to draw conclusions by the user through the observation of graphical presentation of the data (Hand, Mannila and Smyth, 2006).

Note, however, that before you can use the selected method, it is necessary to determine the appropriate method of collecting data on developing on developing projects.

3 METHODOLOGY OF DATA COLLECTION AND ANALYSIS

To make valuable data analysis it is necessary to determine the appropriate method of data collection. It was determined that the collection of data may occur as follows:

1) At the beginning of the project and at each of its stages, the following information should be provided:
   a) what budget has been allocated for the completion of the project (planned cost of completion);
   b) time planned for completion;
   c) the identified sources of uncertainty;
   d) the identified risks.
   e) the success factors of the project, which should be provided.
2) After completion of the project and at each of its stages, the following data should be collected:
   a) the amount of money that has been spent on the completion (actual cost);
   b) the duration of completion;
   c) the person responsible for the result of the work performed;
   d) persons/functional group that carried out the work;
   e) other stakeholders involved in the completion and their impact on the project;
   f) sources of uncertainty identified during the implementation;

g) sources of uncertainty, that resulted in materialized risks;
h) risks identified during the completion;
i) materialized risks;
j) financial and timing impact of materialized risks on project/stage;
k) success factors of the project, which should be provided.

In a situation where the above mentioned data was collected, it is possible to analyze it. Based on the literature, its solutions (Atkinson, 1999; Gardiner and Stewart, 2012; Pritchard 2002), and experience, it has been attempted to create a methodology supporting risk management of the completion of projects in the manufacturing company of the automotive industry.

The following is a developed methodology:

1) To conduct a separate analysis of each of the projects/stages:
   a) comparison of the project's budget with actual costs that had to be allocated for its completion;
   b) comparison of the budget of the project's stages with actual costs that had to be allocated for their completion;
   c) comparison of the planned completion time of the project with the actual time that was needed to complete it;
   d) comparison of the planned execution time of subsequent stages with the actual time that was needed to complete them;
   e) comparison of the list of sources of uncertainty identified before the start of project with those that have been identified during the subsequent stages;
   f) specification of the received summary list of uncertainties, which resulted with materialized risk during project's completion;
   g) comparison of the list of risks identified before the start of the project and at each of the stages, with those that have been identified during the completion of the project;
   h) specification of the received summary list of risks that have materialized and note their impact on the project in terms of cost and completion time;
   i) comparing the list of success factors of the project, which should be provided during its completion (and at each of the individual stages) with a list of success factors, which are guaranteed in the completion of tasks;
   j) to determinate which of other stakeholders involved in the project had positive, and which ones had negative impact on its completion;
   k) to determinate which person was responsible for the result of work performed on particular stage, along with details which stage was completed before planned time, which was completed on time and which was delayed;
   l) to determine which person was responsible for the result of work performed on the particular stage, along with details which stage exceeded the budget, which took the assumed costs and which was carried out cheaper than it was expected;
   m) to determine which person/functional group performed work at each stages, along with details which stage was completed before time, which was completed on time and which was delayed;
   n) which person/functional groups performed work at each stage, with details which stage exceeded the budget, which took the assumed costs and which was carried out cheaper than expected.
2) Determination of completion indicators, separately for each of the projects/stages:
   a) The index of the financial viability of the project's completion/stage:

$$W_F = \frac{K_R}{K_P} \cdot 100\% \quad (1)$$

where:
K_R – the actual cost of the phase/project;
K_P – the planned cost of the phase/project.

   b) The index of the time efficiency of the project's completion/stage:

$$W_T = \frac{T_R}{T_P} \cdot 100\% \quad (2)$$

where:
T_R – the actual duration of the project/phase;
T_P – planned duration of the project/phase.

   c) The efficiency indicator of identification sources of uncertainty of the project/stage:

$$W_{N_I} = \frac{N_{P_Z}}{N_{P_Z} + N_{P_{NZ}} + N_{R_{NZ}}} \cdot 100\% \quad (3)$$

where:
N_{P_Z} – the number of types of sources of uncertainty identified before the project/stage started, which have also been identified during its completion;

$N_{P_{NZ}}$ – the number of types of sources of uncertainty identified before the project/stage started, which were not identified during its completion;
$N_{R_{NZ}}$ – the number of types of sources of uncertainty not identified before the project/stage started, which were identified during its completion.

d) The efficiency indicator of identification of sources of uncertainty leading to the materialization of risks:

$$W_{N_M} = \frac{N_{P_{ZM}}}{N_{P_Z} + N_{P_{NZ}} + N_{R_{NZ}}} \cdot 100\% \quad (4)$$

where:
$N_{P_{ZM}}$ – the number of types of sources of uncertainty identified before the project/stage started, which have also been identified during its completion and led to the materialization of risks;
N_{P_Z} – the number of types of sources of uncertainty identified before the project/stage started, which have also been identified during its completion;
$N_{P_{NZ}}$ – the number of types of sources of uncertainty identified before the project/stage started, which were not identified during its completion;
$N_{R_{NZ}}$ – the number of types of sources of uncertainty not identified before the project/stage started, which were identified during its completion.

e) The efficiency indicator of ensuring of the factors' success of the project/stage:

$$W_{CS} = \frac{CS_R}{CS_P} \cdot 100\% \quad (5)$$

where:
CS_R – the number of success' factors of the project/stage provided during its completion;
CS_P – the number of success' factors of the project/stage, which should have been provided during completion.

f) The indicator of financial efficiency of the person responsible for the result of the work carried out within the project/stage:

$$O_{O_F} = \frac{K_P - K_R}{K_P} \cdot 100\% \quad (6)$$

where:
K_P – the planned cost of the project/stage;
K_R – the actual cost of the project/stage.

g) The indicator of time efficiency of the person responsible for the result of the work carried out within the project/stage:

$$O_{O_T} = \frac{T_P - T_R}{T_P} \cdot 100\% \quad (7)$$

where:
T_P – the planned duration of the project/stage;
T_R – the actual duration of the project/stage.

h) The indicator of financial efficiency of the person/functional group responsible for the work carried out within the project/stage:

$$O_{W_F} = \frac{K_P - K_R}{K_P} \cdot 100\% \quad (8)$$

where:
K_P – the planned cost of the project/stage;
K_R – the actual cost of the project/stage.

i) The indicator of time efficiency of the person/functional group responsible for the work carried out within the project/stage:

$$O_{W_T} = \frac{T_P - T_R}{T_P} \cdot 100\% \quad (9)$$

where:
T_P – the planned duration of the project/stage;
T_R – the actual duration of the project/stage.

j) The indicator of efficiency of risk identification of the project/stage:

$$W_{R_I} = \frac{R_{P_Z}}{R_{P_Z} + R_{P_{NZ}} + R_{R_{NZ}}} \cdot 100\% \quad (10)$$

where:
R_{P_Z} – the number of the types of risks identified before the project /stage started, which have also been identified during its completion;
$R_{P_{NZ}}$ – the number of the types of risks identified before the project/stage started, which were not identified during its completion;
$R_{R_{NZ}}$ – the number of types of risks not identified before the project/stage started, that were identified during its completion.

k) The indicator of efficiency of identification of materialized risks in the project/stage:

$$W_{R_M} = \frac{R_{P_{ZM}}}{R_{P_Z} + R_{P_{NZ}} + R_{R_{NZ}}} \cdot 100\% \quad (11)$$

where:
$R_{P_{ZM}}$ – the number of types of risks identified before the project/stage started, which were also identified during its completion, and which were materialized;

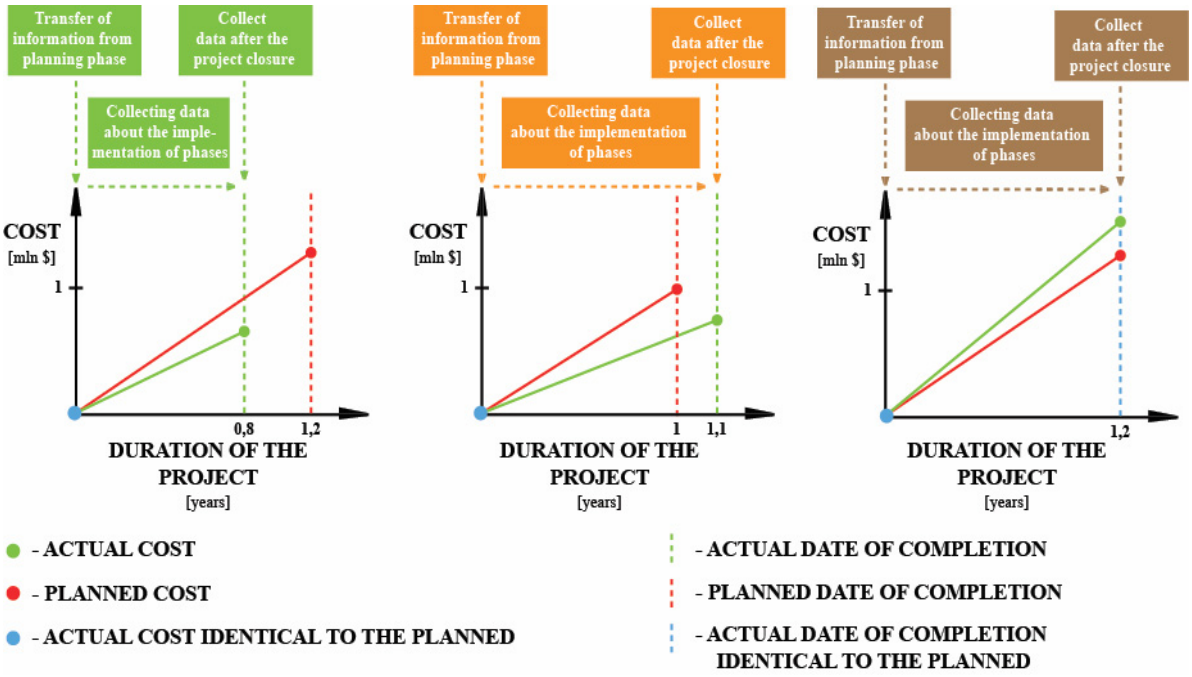

Figure 1: Main stages of the developed methodology (phase of data collection).

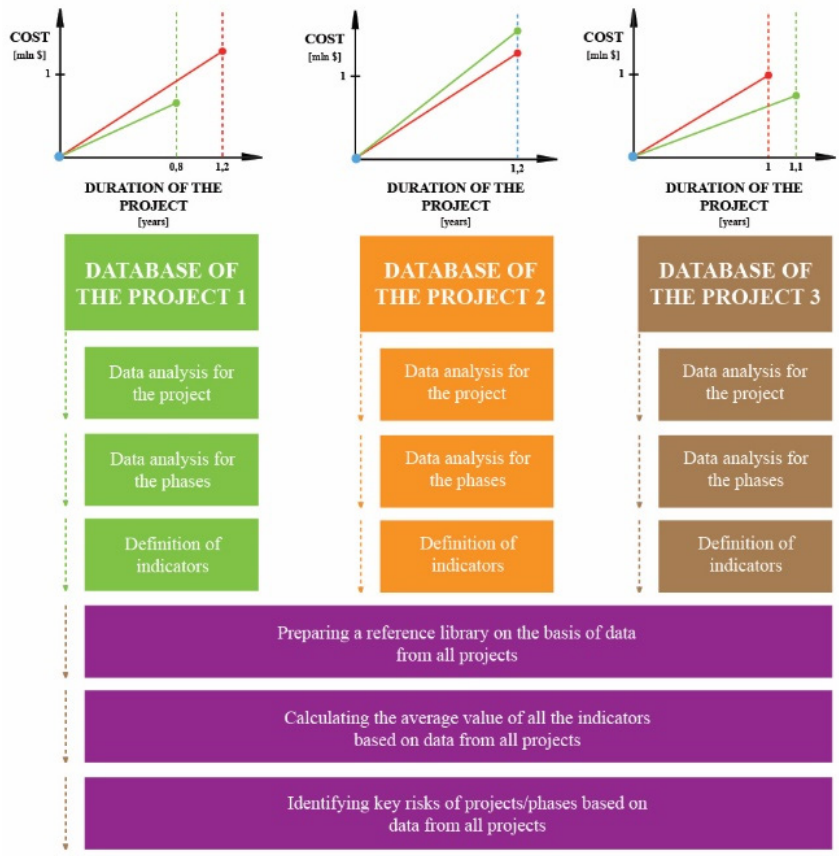

Figure 2: Main stages of the developed methodology (phase of data analysis).

R_{P_Z} – the number of the types of risks identified before the project/stage started, which have also been identified during its completion;
$R_{P_{NZ}}$ – the number of the types of risks identified before the project/stage started, which were not identified during its completion;
$R_{R_{NZ}}$ – the number of types of risks not identified before the project/stage started, which were identified during its completion.

3) Preparation of the reference library by comparing of the corresponding data from all projects, so that in the future it would be possible to further analyze the available data and to have a direct insight into its features.
4) The calculation of the average value of the each of indicators of project/stages of completion based on the values determined through the completion in point 2.
5) Identifying key risks of projects/stages:
   a) calculating the probability of occurrence of each of the risks, based on the data;
   b) determination of the level of severity for each of the risks, keeping the differentiation on the degree of financial risk and the degree of time of the risk, in sequence according to the following formulas:

$$S_{R_F} = |P_R \cdot WR_F| \tag{12}$$

where:
P_R – the probability of risk;
WR_F – the average financial impact (loss/gain caused by the risk);

$$S_{R_T} = |P_R \cdot WR_T| \tag{13}$$

where:
P_R – the probability of risk;
WR_T – medium time impact (shortening the time/delay caused by the risk).

   c) the risk categorization of particular phases – selection of appropriate limit values should be made on the basis of information, experience of the project manager and the nature of the implemented project. For the purposes of this paper categories were determined

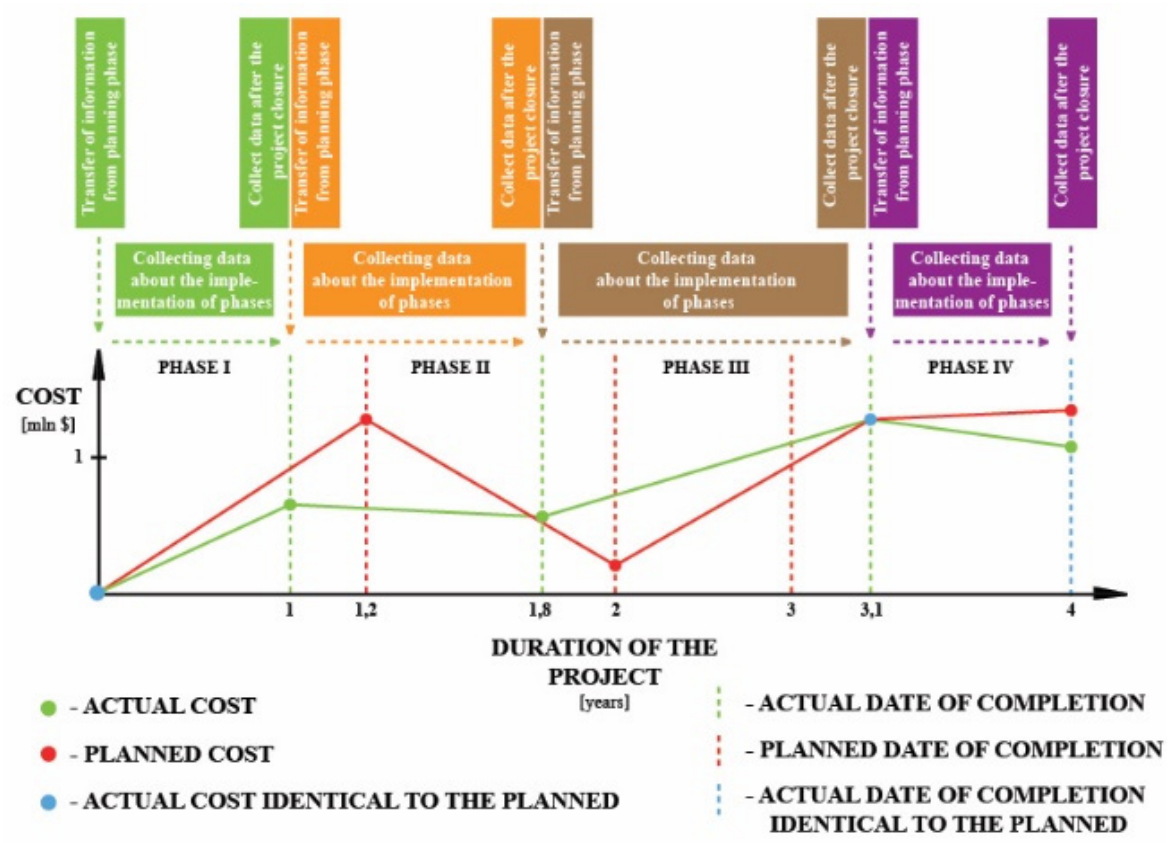

Figure 3: Phase of collect data on the implementation phases of the project.

according to the following criteria:

- low risk – the value of the degree of risk from 0 to 0.15;
- moderate risk – the value of 0.16 to 0.37;
- high risk – the value of 0.38 to 0.75;
- critical risk – the value of 0.76 and above.

Implementation of the described methodology is shown in the example below: Figure 1 (own elaboration based on: Żmuda, 2016). shows the steps of data collection in a situation where the company has completed three projects.

In situation where data were collected for the three projects, the analysis phase can occur, as it is schematically presented below in Figure 2 (own elaboration based on: Żmuda, 2016).

Both the collection and analysis of data for each of particular phases is carried out similarly to carrying out these activities for the project, the idea is presented Figure 3 (own elaboration based on: Żmuda, 2016).

4 CONCLUSIONS

In the presented paper it has been developed a methodology for collecting data on completed projects to allow their subsequent analysis, and also a methodology of data analysis to identify the key risks of projects and to provide a valuable information. Using the developed methodology, in the future it is planned to create a tool to support the completion of projects in the form of a spreadsheet. While continuing work on the field tackled in this paper, it is recommended to implement the developed methodology for the data collection and analysis into a computer application.

While using the developed methodology it should be borne in mind that phenomena such as risk and uncertainty are often very dynamic and they have interdisciplinary nature, thus the degree of repeatability can vary depending on the nature and level of innovation and uniqueness of the delivered project (Gembalska-Kwiecień, 2016). Therefore, using solutions developed from this paper it should be taken into account that it is intended to only assist the decision making process of project manager. It means that in terms of risk management the project manager should in the first place follow the logic, experience gained in the industry and his own assessment of the situation.

ACKNOWLEDGEMENTS

The article is the result of the registered work with symbol 13/030/BK_16/0024 entitled "Production engineering methods and tools for development of smart specializations" carried out in the Institute of the Production Engineering, Department of Organization and Management at Silesian University of Technology.

REFERENCES

Project Management Institute, 2012. *A Guide to the Project Management Body of Knowledge (PMBOK Guide)*. USA, 5th edition.

Atkinson, R., 1999. *Project management: cost, time and quality, two best guesses and a phenomenon, it's time to accept other success criteria*. "International Journal of Project Management", vol. 17, no. 6, pp. 337-342.

Gembalska-Kwiecień, A., 2016. *Innovative forms supporting safe methods of work in safety engineering for the development of intelligent specializations.* "Management Systems in Production Engineering", vol. 24 no. 4, pp. 268-273.

Gardiner, P.D., Stewart, K., 2000. *Revisiting the golden triangle of cost, time and quality: the role of NPV in project control, success and failure*. "International Journal of Project Management", vol. 18, pp. 251-256.

Dvir, D., Raz, T., Shenhar, A., 2003. *An empirical analysis of the relationship between project planning and project success*. "International Journal of Project Management", vol. 21, pp. 89-95.

Hand, D., Mannila, H., Smyth, P., 2006. *Eksploracja danych*, Wydawnictwo Naukowo-Techniczne. Warszawa.

Jaafari, A., 2001. *Management of risks, uncertainties and opportunities on projects: time for a fundamental shift.* "International Journal of Project Management", vol. 19, pp. 89-101.

Korczowski, A., 2010. *Zarządzanie ryzykiem w projektach informatycznych. Teoria i praktyka*, Wydawnictwo Helion. Gliwice.

Office of Government Commerce, 2010. *PRINCE2™ – Skuteczne zarządzanie projektami*, The Stationery Office. London.

Larose, D., 2006. *Odkrywanie wiedzy z danych*, Wydawnictwo Naukowe PWN. Warszawa.

Pickett, T., Elliot, B., 2007. *Transforming Historical Project Data into Useful Information*, AACE International Transactions. Morgantown.

Pritchard, C., 2002. *Zarządzanie ryzykiem w projektach. Teoria i praktyka*, WIG PRESS. Warszawa.

Żmuda, K., 2016. *Opracowanie narzędzia wspomagającego zarządzanie ryzykiem podczas realizacji projektów w przedsiębiorstwie produkcyjnym branży motoryzacyjnej* (unpublished MA thesis), Wydział Organizacji i Zarządzania, Politechnika Śląska. Zabrze.

A Proposed Model for the Students' Perceived Satisfaction in the Computer Architecture Course

An Exploratory Study based on Oliver's Perceived Satisfaction Model

Jorge Fernando Maxnuck Soares, Takato Kurihara and Luís Tadeu Mendes Raunheitte
Universidade Presbiteriana Mackenzie, São Paulo, Brazil
maxnuck.fci@gmail.com, {takato, raunheitte}@mackenzie.br

Keywords: Oliver's Model, Student Satisfaction, Exploratory Factor Analysis (EFA), Computer Architecture and Active Learning Practices.

Abstract: This paper presents a study with the preliminary results of an exploratory research to study the possibility of adapting the Perceived Satisfaction model proposed by Oliver (1997) into a model involving the Student Perceived Satisfaction in the Computer Architecture course, where practical classes were conducted using the Marie CPU simulator as a mechanism of active learning practice. This model seeks to represent the student satisfaction in relation to three latent variables: Equity, Performance and Expectations, where the data processing is performed by applying the correlations technique with the Spearman coefficient. The main goal was to find the correlations regarding the student satisfaction with respect to the use of Marie CPU Simulator as an active learning practice in the Computer Architecture course. The components of these variables, in principle, precede the student satisfaction and allow for the identification of those that are the most relevant to determine this response.

1 INTRODUCTION

This study is divided into the following pillars: 1) The first pillar consists of the satisfaction or disconfirmation model of (Oliver, 1997), widely known in the Marketing and Consumer Satisfaction area. This model is used in this study as a basis to propose another model to be used to assess university students' satisfaction in the Computer Architecture course; 2) The second pillar is the Marie CPU simulator as an active learning practice in the practical classes of the course; 3) The third pillar was the use of Exploratory Factor Analysis as a tool for extracting research data.

The study has as motivation the following points: to understand how the use of active practices relates to the construct satisfaction of the university student and to verify the possibility of (Oliver, 1997) being adapted to the study.

The study and the research are justified by the following reasons: the importance of Oliver's model, for being the most famous and used in relation to consumer satisfaction, the pedagogical importance of understanding the so-called student satisfaction in relation to technical subjects, the ability to evaluate the use of Active Learning Practices (Marie CPU Simulator) in the composition of this satisfaction, the most appropriate use of computing resources in the classroom and the importance of the student satisfaction, the improvement in the perception of which hidden variables, are precursors of this satisfaction.

2 CONSUMER SATISFACTION

In the 60s, the first studies on the subject started to emerge, pioneered by (Cardozo, 1965), showing the relationship between satisfaction and loyalty (repeat purchases). In the 80s, (Czepiel, Rosemberg and Supranat, 1980) introduce one of the first research methodologies on the subject. It is also worth noting the studies conducted by (Kano, 1984) in the same area, a model that correlates customer satisfaction with the customer requirements.

Then, in the 90s, there is a large increase in the number of this type of studies, with several authors addressing the subject of consumer satisfaction,

Soares, J., Kurihara, T. and Raunheitte, L.
A Proposed Model for the Students' Perceived Satisfaction in the Computer Architecture Course - An Exploratory Study based on Oliver's Perceived Satisfaction Model.
In *Proceedings of the 6th International Conference on Operations Research and Enterprise Systems (ICORES 2017)*, pages 272-280
ISBN: 978-989-758-218-9

starting by (Yi, 1991), followed by (Oliver, 1997), in addition to (Fournier and Mick, 1999). The studies conducted by (Fornell, 1992 and 1994) and (Oliver, 1997) stand out because they propose the use of Structural Equation in the mathematical formulation, the same technique used in this study.
On the other hand, (Oliver, 1997) explains Consumer Satisfaction in his model by using the following latent variables: Equity, Performance, Expectations and Emotions, as shown in Figure 1 below:

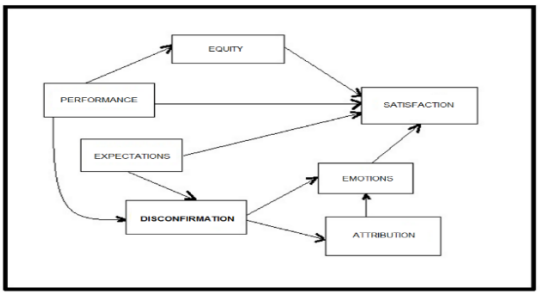

Figure 1: Oliver's Model (Source: Adapted from (Oliver, 1997)).

2.1 Customer Satisfaction Theories

After the pioneering studies conducted by (Cardozo, 1965), others emerged, mainly in the 80s and 90s, when a large number of articles and theories emerged, and among these studies and according to the chronology of these publications, we point out the following highlights in Table 1 follow:

Table 1: Chronology of the main theories on Consumer Satisfaction (Source: Authors).

Author	Characteristics of the study
(Cardozo, 1965)	Repeat Model
(Oliver, 1980)	Disconfirmation Model
(Parasuraman et al., 1985)	Perceived Quality Model.
(Oliver and DeSarbo, 1988)	Performance Model.
(Oliver, 1989)	Stepped Emotions Model
(Westbrook and Oliver, 1991).	Primary Emotions Model
(Yi, 1991)	Options Model
(Fornell, 1994)	Post-purchase usefulness model.
(Fournier and Mick, 1999)	Cognitive and emotional influences Model

Measuring Consumer Satisfaction

There are basically three main aspects for measuring customer satisfaction: 1) Measurement of nonconformity; 2) Measurement by indicators; 3) Measurement by structural equations. Table 2 shows the alternatives, models and authors, which represents a brief literature review and highlights the importance of Oliver, once again justifying the choice of this customer satisfaction model as the basis of the study.

Table 2: (Source: Authors).

Aspect	Models	Some authors
Nonconformity	Expectations vs. Performance	(Weaver and Brickman, 1974); (Westbrook, 1980); (Oliver, 1980, 1981); (Swan and Trawick, 1981); (Oliver, 1988); (Parasuraman, Zeithaml and Berry, 1988); (Haistead, 1989)
	Perceived performance	(Oliver, 1980, 1981); (Churchill and Suprenant,1982); (Cronin and Taylor, 1992, 1994)
	Perceived performance weighted by importance	(Cronin and Taylor, 1992, 1994); (Teas, 1993)
	Minimum acceptable level vs. desired level and performance	(Parasuraman, Zeithaml and Berry, 1994);
Indicators	Multiple indicators of satisfaction	(Folkes, 1984); (Westbrook, 1980, 1987); (Oliver and DeSarbo, 1988); (Tse and Wilton, 1988); (Oliver and Swan, 1989); (Mano and Oliver, 1993); (Oliver, 1989, 1993); (Richins, 1997)
Structural equations	Structural equations	(Churchill and Suprenant, 1982); (Fornell, 1992); Fornell et al. (1994).

3 ACTIVE LEARNING PRACTICES AND COMPUTER SIMULATION

Abstract concepts are essential to the understanding of Computer Architecture and Organization. They are also a source of difficulties for many students, many of whom struggle even with the basic concepts. An interesting approach to help students understand abstract concepts is the use of computational resources. These resources help students and teachers in computer representation, via simulation, to study abstract concepts.

Simulations can be performed in different ways and the success of these simulations is determined by the participant's involvement. The goal is to acquire knowledge and understanding.
Among some of the main advantages of simulation are:

- Pleasant and motivating activity
- It enhances the understanding of more subtle aspects of a concept / principle
- It promotes critical thinking

The purpose of using computers in education is to integrate them in the learning process of the curricular concepts in all modalities and levels of education, being able to act as facilitator between students and the construction of their knowledge, (Valente, 1999).

3.1 Simulations

Simulation environments have the potential to engage students in a deep learning that enables understanding, as opposed to surface learning, which only requires memorization, ensuring that by actively participating and engaging in conversations, student-student or teacher-student are required to perform a simulation.

Simulation is a form of experiential learning. Simulations consist of teaching scenarios, where the student is placed in a world defined by the teacher. It represents a reality within which students interact. The teacher controls the parameters of this world and uses it to achieve the desired teaching results. Simulations serve as laboratory experiments where the students themselves are the test subjects. Simulations can be performed in different ways. The main element is the content of its context. Students must make decisions within their context. Success is often determined by the engagement of the participant. The goal is to acquire knowledge and understanding, developing critical thinking.

3.2 Purposes of CPU Simulation

The study of the main functions of the Central Processing Unit (CPU) in the disciplines of Computer Architecture and Organization, always poses a challenge to the understanding of students to the extent that it gathers new knowledge combined with a data processing dynamics in the machine level.

3.3 Basic Operations and Operation of the Processor

The study of Processors is essential in the disciplines of Computer Architecture and Organization, allowing the understanding of the interrelationship between hardware and software.

One possible strategy for presenting the initial concepts of operation of processors and their programming in machine language is the presentation of a simplified processor as a hypothetical machine (Stallings, 2013) where it is possible to introduce, with reduced complexity, the concepts regarding the use of basic registers such as: accumulator, program counter, instruction register, in addition to addressing memory access, the use of buses and input and output devices. Therefore, by using this idea of simple processor the Computer Architecture and Organization books intend to introduce concepts that are basic to the understanding of any processor, such as CPU (Central Processing Unit), ALU (Arithmetic Logic Unit) and registers.

The strategy applied in the computer courses where the simulator was used consisted of an analytical presentation of a hypothetical machine with 16-bit instructions, divided into 4-bit operation code and 12-bit address to which each instruction refers. This machine was then studied analytically and the CPU simulator was introduced afterwards to strengthen and deepen the students' knowledge.

3.4 Marie CPU Simulator

The simulator MARIE (**M**achine **A**rchitecture that is **R**eally **I**ntuitive and **E**asy) (Null, Lobur, 2010) is a graphical learning environment that didactically presents the operation of the architecture of a hypothetical machine. In this environment the students are able to: create and edit programs in Assembly language; assemble source code in machine code; run the machine-code programs

developed; and observe and debug their programs using various tools provided within the simulator.

The simulator also offers the option of using the path simulator environment that data roam when the instructions are run by the processor of the hypothetical machine under study, in this case, MARIEDataPath. Figure 2 shows this environment.

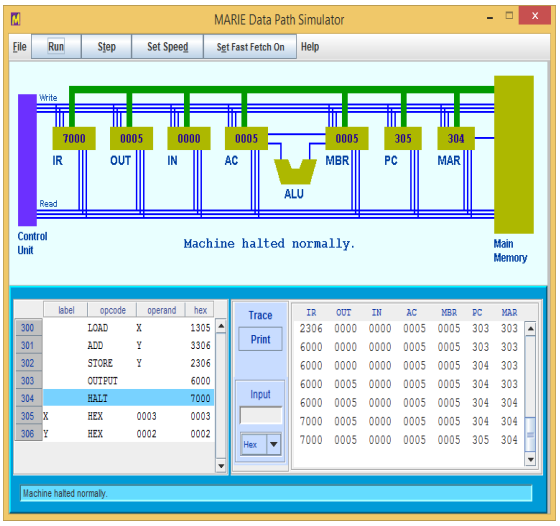

Figure 2: Source: (Null, L.; Lobur, J., 2010).

4 METHODS AND PROCESSES

The research applied to the population, serves to evaluate in a predominantly qualitative way, the student's perception only, as well as the perception of satisfaction of this in the use of the MARIE simulator, not being comparative neither before (without the use of the simulator) nor later. The researched population (140 students) attends an exploratory study for accessibility of this nature (Hair, 205).

The research evaluate the perceived satisfaction at the time of the use of the MARIE simulator during the practical class of Computer Architecture.

A questionnaire was used as the data collection instrument, consisting of three sections, in the first section (variables V1 to V4) the student profile; in the second section, the learning profile (variables V5 to V9); and the third section is divided into three subgroups: equity or opinion on the simulator (variables V10 to V14); performance of the simulator in the learning process (variables V15 to V19); expectations of the simulator in relation to learning (variables V20 to V25). These variables were developed according to the model of Oliver (1997), see Figure 2. The variables included in the questionnaire were distributed as follows:

Table 3: Groups and purpose of the variables included in the questionnaire.

Dimension	Variable	Content in the questionnaire
Student profile	V1 to V4	Gender, Age, Income, Stage of the course in progress (respectively)
Learning profile	V5	I have difficulty with the subject.
	V6	I have failed the same subject.
	V7	I find difficulty in other related subjects
	V8	It is easy to understand the content of the subject.
	V9	I have no difficulty with mathematical logic.
Equity or opinion on the CPU simulator with respect to satisfaction	V10	The use of MARIE® simulator is easy.
	V11	Establishing the relationship with the theory has become easier with the use of MARIE® simulator.
	V12	With MARIE® simulator I can understand what happens internally to the device
	V13	I prefer to study without the use of MARIE simulator
	V14	The use of MARIE® simulator facilitated the understanding of how the registers work
Performance of the CPU simulator with respect to satisfaction	V15	The use of MARIE® simulator increased my interest in the subject.
	V16	The use of MARIE® simulator increased my interest in others correlated subjects
	V17	With the simulator I can study other subjects without teacher assistance.

Table 3: Groups and purpose of the variables included in the questionnaire (Cont.).

Dimension	Variable	Content in the questionnaire
Performance of the CPU simulator with respect to satisfaction	V18	The MARIE® CPU simulator was of great help in the learning process.
	V19	The MARIE® CPU simulator helped better understand the theory with practice.
Expectations regarding the CPU simulator in relation to satisfaction	V20	I expected to understand how registers (REGs) work
	V21	I expected to understand how the main memory works
	V22	I expected to understand how the Arithmetic Logic Unit (ULA) works
	V23	I expected to understand how the main memory and REGs interact
	V24	I expected to understand how the ALU and REGs interact
	V25	I expected to understand how the ALU and the main memory interact

As methodological procedures, this study also comprised the following items:

a) Explanatory classes in the development of the Computer Architecture discipline.
b) Practical classes, approaching the same content, using the Marie® CPU simulator.
c) Data processed with the use of SPSS version 25 (Field, 2009), to establish a correlation between the variables, both qualitative and quantitative. For the correlation, the Spearman's coefficients were used (Cohen, L., Manion, L. and Morrison, K., 2011).
d) To find evidence of validity relating to the scale, we conducted the EFA of the items. Its internal consistency was assessed using the calculation of Cronbach's alpha.
e) The variables from V5 to V25 are qualitative and ordinal, measured using the 5-point Likert scale, as follows: (1) I totally disagree with the statement; (2) I disagree with the statement; (3) I do not agree nor disagree with the statement; (4) I agree with the statement; (5) I completely agree with the statement;
f) For the calculations, we considered the average figures in each dimension and in the total of the Scale, obtained from the scores assigned to each item in relation to the number of component items, generating a response that could range from 1 to 5 points.
g) This study consisted of an exploratory research by accessibility, which led to a population of 120 students, suitable for this preliminary phase of the study.
h) We opted for modeling with the use of exploratory factor analysis (EFA). According to (Pedhazur and Schmelkin, 1991), the exploratory factor analysis (EFA) is a model that seeks to measure the relationship between the indicators (observed variables) and the constructs (factors, latent variables).
i) To measure the reliability, we used the Cronbach's alpha which, according to (Hair et. Al, 2005), considers values higher than 0.7.
j) The factor loadings were determined by the relationships between the observed variables and the construct, generating information on the extent to which a variable is capable of measuring a construct (Schumacker and Lomax, 1996).

5 RESULTS

In order to find evidence of validity related to the internal structure of the scale, we conducted the Exploratory Factor Analysis of the items. Its internal consistency was assessed using the calculation of Cronbach's alpha.

For the calculations, we considered the average numbers in each answer of the variables, generating an answer that could range from 1 to 5 points, with the lowest value being associated with the greatest disagreement with the statement referred to in the variable and the highest value related to the greatest agreement with the statement referred to in the variable.

Table 4a: Matrix of the averages of correlations.

	V10	V11	V12	V13	V14	V15	V16	V17
V10	1							
V11	0.87	1						
V12	0.71	0.67	1					
V13	0.88	0.61	0.77	1				
V14	0.76	0.75	0.83	0.81	1			
V15	0.67	0.65	0.69	0.71	0.72	1		
V16	0.61	0.61	0.68	0.69	0.70	0.69	1	
V17	0.66	0.64	0.61	0.71	0.71	0.69	0.62	1
V18	0.79	0.81	0.82	0.81	0.81	0.79	0.85	0.81
V19	0.89	0.81	0.89	0.86	0.84	0.81	0.87	0.81
V20	0.71	0.86	0.86	0.81	0.83	0.79	0.85	0.89
V21	0.81	0.73	0.79	0.71	0.81	0.70	0.68	0.71
V22	0.87	0.79	0.78	0.76	0.83	0.70	0.64	0.69
V23	0.87	0.79	0.89	0.69	0.86	0.71	0.71	0.65
V24	0.88	0.79	0.87	0.70	0.85	0.71	0.68	0.68
V25	0.81	0.82	0.82	0.68	0.85	0.73	0.69	0.71

Table 4b: Matrix of the averages of correlations.

	V18	V19	V20	V21	V22	V23	V24	V25
V10	0.79	0.89	0.71	0.81	0.87	0.87	0.88	0.81
V11	0.81	0.81	0.86	0.73	0.79	0.79	0.79	0.82
V12	0.82	0.89	0.86	0.79	0.78	0.89	0.87	0.82
V13	0.81	0.86	0.81	0.71	0.76	0.69	0.70	0.68
V14	0.81	0.84	0.83	0.81	0.83	0.86	0.85	0.85
V15	0.79	0,81	0.79	0.70	0.70	0.71	0.71	0.73
V16	0.85	0.87	0.85	0.68	0.64	0.71	0.68	0.69
V17	0.81	0.81	0.89	0.71	0.69	0.65	0.68	0.71
V18	1	0.81	0.79	0.81	0.81	0.81	0.79	0.82
V19		1	0.87	0.82	0.81	0.84	0.85	0.79
V20			1	0.88	0.84	0.81	0.83	0.85
V21				1	0.88	0.86	0.85	0.86
V22					1	0.79	0.76	0.74
V23						1	0.88	0.84
V24							1	0.71
V25								1

Table 5: Highest and lowest correlations between the variables

Var.	Highest correlation	Lowest correlation
V10	0.89 (V19)	0.61 (V16)
V11	0.87 (V10)	0.61 (V13, V16)
V12	0.89 (V19)	0.61 (V17)
V13	0.88 (V10)	0.61 (V14)
V14	0.86 (V23)	0.75 (V11)
V15	0.81 (V19)	0.67 (V10)
V16	0.87 (V19)	0.61 (V11)
V17	0.89 (V20)	0.61 (V12)
V18	0.85 (V16)	0.79 (V10, V 15, V24)
V19	0.87 (V16)	0.79 (V25)
V20	0.89 (V17)	0.71 (V10)
V21	0.88 (V20)	0.68 (V16)
V22	0,88 (V21)	0,64 (V16)
V23	0,89 (V12)	0.65 (V17)
V24	0,88 (V10, V23)	0,68 (V16, V17)
V25	0,86 (V21)	0,68 (V13)

The factor analysis by extracting the key factors with varimax rotation verified the existence of factors with eigenvalues greater than 0.30, the variables with factor loadings below this value were excluded, such as V1, V2 and V3, all related to the student profile and shown in Table 6.

In each of the three dimensions of the model.

Table 6: Factor loading of latent variables.

V1	*0.21*	**V6**	0.73	**V11**	0.78	**V16**	0.55	**V21**	0.74
V2	*0.22*	**V7**	0.61	**V12**	0.61	**V17**	0.68	**V22**	0.72
V3	*0.21*	**V8**	0.41	**V13**	0.72	**V18**	0.72	**V23**	0.83
V4	0.31	**V9**	0.71	**V14**	0.69	**V19**	0.72	**V24**	0.84
V5	0.62	**V10**	0.81	**V15**	0.79	**V20**	0.87	**V25**	0.79

Table 7: Matrix of factor loading of each dimension of the model.

Dimension	Factor loading
Equity (V10 to V14)	0.72
Performance (V15 to V19)	0.69
Expectation (V20 to V25)	0.79

Due to the results shown in Table 7, the following aspects may be highlighted:

1) The lowest factor loading is associated with the dimension performance of the student's perceived satisfaction in relation to the Marie CPU simulator, it means that the performance of the simulator, as an active learning practice, contributes more significantly to reduce the student satisfaction.
2) On the other hand, the highest factor loading is associated with the dimension expectation of the student's perceived satisfaction, it means that this is the dimension that most contributed to the increase of the student satisfaction.

As a result of the latent variables that make up the three dimensions of the student satisfaction construct, that is, V10 to V25, whose factor loadings are indicated in Table 6, the following aspects can be highlighted:

1) V20 has the highest factor loading, which means that the understanding regarding the operation of registers with the Marie CPU simulator is what most contributes to the student satisfaction.

2) V12 has the lowest factor loading, which means that the understanding of the internal operation of the processor, using the Marie CPU simulator, is what least contributes to the student satisfaction.

6 CONCLUSIONS

The student's satisfaction with the use of the simulator as an active practice can be modeled using three dimensions: Expectation with load factor of 0.79, Equity with load factor 0.72 and Performance with load factor of 0.69. The dimension that contributes most to this satisfaction is the expectation, which means that for this population studied, expectations were mostly met, having a greater impact on the perceived satisfaction of the student.

In relation to the expectation dimension variable V20 (expectation of understanding the registers) was the one with a higher load factor (0.87), apparently indicating that understanding the registers is fully met by the MARIE simulator, used as an active practice.

In second place variable V24 (to understand the relation of function between ULA and registers) corresponds to the attendance of greater degree in the student's expectation in its satisfaction, as to the use of the MARIE simulator.

In relation to the equity dimension, the variable V10 (ease of use of the MARIE simulator) is the one that contributed the most to the load factor of this dimension, indicating that the ease of use is perceived by the student as a great contribution to his satisfaction. Second, even in the equity dimension, variable V11 (understanding the theory more easily) is the one that most influences the load factor of this dimension.

In the performance dimension is the variable V15 (interest in the subject) that contributes most to student satisfaction, showing that subjective and qualitative aspects, such as interest, can also be measured.

Secondly, there are the V18 (learning process) and V19 (interrelationship between theory and practice), with a higher load factor in the formation of student satisfaction. These two variables show that less tangible dimensions of learning can be measured and, moreover, have a great impact on student satisfaction.

The use of the satisfaction model (Oliver, 1997), widely used in the Marketing area, is adequate for the modeling of student satisfaction.

Thus, the adaptation of part of the model (Oliver, 1997) has shown to be consistent in evaluating and measuring abstract dimensions of learning and how the use of active practices can contribute to the evaluation of student satisfaction and measurements.

REFERENCES

Cardozo, Richard N. An experimental study of customer effort, expectation, and satisfaction. Journal of Marketing Research, v. II, p.244-249, Aug. 1965.

Churchill, Jr., G.A.; Suprenant, C. An investigation into the customer satisfaction. Journal of Marketing Research. Chicago: AMA, v.19, n.4, p. 491-504, nov., 1982.

Cohen, L., Manion. L e Morrison, K, Research Methods in Education 7th Edition, Routledge, 2011.

Cronin, J.J.; Taylor, S.A Servperf versus servqual: Reconciling performance-based and Perceptionsminus-

expectations measurement of service quality. Journal of Marketing, Chicago: AMA, v.58, n.1, p.125-131, jan., 1994.

Cronin, J.J.; Taylor, S.A. Measuring service quality: A reexamination and extension. Journal of Marketing, Chicago: AMA, v.56, n.3, p.55-68, jul., 1992.

Czepiel, John A.; Rosemberg, Larry e Surprenat, Carol. The development of thought, theory, and research in consumer satisfaction. Theoretical developments in marketing. Chicago, IL : American Marketing Association, 1980. p. 216-219.

Field, Andy, Discovering Statistics Using SPSS, SAGE Publications, 2009.

Fornell, C. A national customer satisfaction barometer: The Sweedish experience. Journal of Marketing, v. 56, n. 1, p. 6-21, Jan. 1992.

Fornell, C. et al. The American customer satisfaction index: nature, purpose and findings. Journal of Marketing, v. 58, n.4, p.7-18, Oct. 1994.

Fournier, Susan e Mick, Davis Glen. Rediscovering satisfaction. Journal of Marketing, v. 63, October 1999.

Hair Jr., J.F. et al. Análise Multivariada de Dados. 5. ed. Porto Alegre: Bookman, 2005.

Haistead, D. Expectations and disconfirmation believes as predictors of consumer satisfaction, repurchase intention, and complaint behavior. Journal of Consumer Satisfaction/ Dissatisfaction and Complaining Behavior. v. 2, p. 17-21, 1989 Available at http: //www.vancouver.wsu.edu/csdcb/ about.htm # journal. Access in: 16Agust2016.

Kano, N. et al. Attractive Quality and Must-be Quality, The Journal of the Japanese Society for Quality Control, Hinshitsu, v.14, n.2, p.147-56, 1984.

Mano, Haim; Oliver, Richard L. Oliver. Assessing the Dimensionality and Structure of the Consumption Experience: Evaluation, Feeling, and Satisfaction, Journal of Consumer Research, 20 Dec, 451-466, 1993.

Null, Linda; Lobur, Julia. "Princípios básicos de arquitetura e organização de computadores". 2.ed. Porto Alegre: Bookman, 2010.

Oliver, Richard L A cognitive model of the antecedents and consequences of satisfaction decisions. Journal of Marketing Research. Chicago: AMA, v. 17, n. 4, p. 460-469, nov., 1980.

Oliver, Richard L. Cognitive, affective, and attribute bases of the satisfaction response. Journal of Consumer Research, Vol.20, December, pp.418-430, 1993.

Oliver, Richard L. Measurement and evaluation of satisfaction processes in retailing settings. Journal of Retailing. Amsterdam: Elsevier, v. 57, n. 3, p. 25-48, 1981.

Oliver, Richard L. Processing of the satisfaction response in consumption: a suggest framework and research propositions. Journal of Consumer Satisfaction/dissatisfaction and Complaining Behavior, Vol.2, pp.1-16, 1989.

Oliver, Richard L.; SWAN, J.E. Equity and disconfirmation perceptions as influences on merchant and product satisfaction. Journal of Consumer Research, Chicago: University of Chicago Press, v. 15, n. 4, p. 374, dec., 1989.

Oliver, Richard L; Desarbo, W.S. Response determinants in satisfaction judgments. Journal of Consumer Reserach, Chicago: University of Chicago Press, v. 14, n. 1, p. 495, mar., 1988.

Parasuraman A, Zheitma, VA e BERRY, LL. SERVQUAL: a conceptual model of service quality and its implications for future research. J Mark. 1985;49(1):41-50 University/McGraw-Hill, 1997.

Parasuraman, A.; Zeithaml, V.; BERRY, L Reassessment of Expectations as a Comparison Standard in Measuring Service Quality: implications for further research. Journal of Marketing, New York: American Marketing Association, Jan. v. 58(1), p. 111-124, 1994.

Folkes, V.S. Consumer reactions to product failure: an attributional approach. Journal of Consumer Research. Chicago: University of Chicago Press, v. 10, n.1, p. 398-409, mar., 1984.

Parasuraman, A.; Zeithaml, V.; Berry, L. SERVQUAL: a multiple-item scale for measuring consumer perceptions of service quality. Journal of Retailing, Amsterdam: Elsevier, v. 64, n. 1, p. 12-40, 1988.

Pedhazur, Elazr J. e Schelkin, Liora Pedhazur. Measurement, Design, and Analysis: An Integrated Approach, Psychology Press, 1991.

Richins, M. Measuring emotions in the consumption experience. Journal of Consumer Research. Chicago: University of Chicago Press, v. 23, n. 3, p. 127, sept., 1997.

Schumacker, Randall E. e Lomax, Richard G. A Beginner's Guide to Structural Equation Modeling. Mahwah, New Jersey, Lawrence Erlbaum Associates, Publishers, 1996.

Stallings, William. Arquitetura e Organização de Computadores. 8.ed. São Paulo: Prentice-Hall Brasil, 2010.

Swan, John E.; Trawick, I. Fredrick. Disconfirmation of Expectations and Satisfaction with a Retail Service, Journal of Retailing, 57, 49-67, 1981.

Teas, R.K. Expectations, performance evaluation, and consumers perceptions of quality. Journal of Marketing, Chicago: AMA, v. 57, n. 3, p. 18-34, oct., 1993.

Tse, G.K.; Wilton, P.C. Models of consumer satisfaction formation: an extension. Journal of Marketing Research. Chicago, AMA, v. 25, n. 2, p. 204-212, may, 1988.

Weaver, D.; Brickman, P. Expectancy, feedback, and disconfirmation as independent factors in outcome satisfaction. Journal of Personality and Social Psychology. Washington: APA, v. 30, n. 3, p. 420-428, mar., 1974.

Valente, J.A. (Org.). O computador na sociedade do conhecimento. Campinas: NiedUnicamp, 1999.

Westbrook, R.A Product/Consumption-based affective responses and postpurchase processes. Journal of Marketing Research, Chicago, AMA, v. 24, n.3, p. 258-270, aug., 1987.

Westbrook, R.A. Intrapersonal affective influences on consumer satisfaction with products. Journal of Consumer Research, Chicago: University of Chicago Press, v. 6, n. 2, p. 49, june, 1980.

Westbrook, R.A. Intrapersonal affective influences on consumer satisfaction with products. Journal of Consumer Research, Chicago: University of Chicago Press, v. 6, n. 2, p. 49, june, 1980.

Westbrook, Robert A., Oliver, The dimensionality of consumption emotion patterns and consumer satisfaction. Journal of Consumer Researchn,, Vol.18, June, pp.84-91, 1991.

Yi, Youjae (1991) A critical review of consumer satisfaction, Review of Marketing 1990, Ed. V.A. Zeithaml, Chicago: AMA, pp. 68-123.

A Near Optimal Approach for Symmetric Traveling Salesman Problem in Euclidean Space

Wenhong Tian[1,2], Chaojie Huang[2] and Xinyang Wang[2]
[1]*Chongqing Institute of Green and Intelligent Technology, Chinese Academy of Sceinces, Chongqing, China*
[2]*School of Information and Software Engineering,*
University of Electronic Science and Technology of China, Chengdu, China
tianwenhong@cigit.ac.cn, tian_wenhong@uestc.edu.cn

Keywords: Symmetric Traveling Salesman Problem (STSP), Triangle Inequality, Random TSP in a Unit Square, TSPLIB Instances, Approximation Ratio, k-opt, Computational Complexity.

Abstract: The traveling salesman problem (TSP) is one of the most challenging NP-hard problems. It has widely applications in various disciplines such as physics, biology, computer science and so forth. The best known absolute (not asymptotic) approximation algorithm for Symmetric TSP (STSP) whose cost matrix satisfies the triangle inequality (called $\triangle$STSP) is Christofides algorithm which was proposed in 1976 and is a $\frac{3}{2}$-approximation. Since then no proved improvement is made and improving upon this bound is a fundamental open question in combinatorial optimization. In this paper, for the first time, we propose Truncated Generalized Beta distribution (TGB) for the probability distribution of optimal tour lengths in a TSP. We then introduce an iterative TGB approach to obtain quality-proved near optimal approximation, i.e., $(1+\frac{1}{2}(\frac{\alpha+1}{\alpha+2})^{K-1})$-approximation where K is the number of iterations in TGB and $\alpha(>>1)$ is the shape parameters of TGB. The result can approach the true optimum as K increases.

1 INTRODUCTION

The TSP is one of most researched problems in combination optimization because of its importance in both academic need and real world applications. For surveys of the TSP and its applications, the reader is referred to (Cook,2012)(An et al., 2012)(Vygen, 2012) and references therein.

After 39 years, Christofides' $\frac{3}{2}$-approximation algorithm (Christofide, 1976) still keeps the best performance guarantee known for the symmetric traveling salesman problem satisfying triangle inequality ($\triangle$STSP), and improving upon this bound is a fundamental open question in combinatorial optimization, see (Cook, 2012)(Gutin and Punnen, 2002) and references therein. (Vygen, 2012) also provides a detailed survey on new approximation algorithms for the TSP. (Johnson et al., 1998) provide a complete comparative study on the local optimization methods for TSP. (Cook, 2012) introduces the TSP from history to the state-of-the art. David (Johnson, 2014) discusses the importance and applications of random TSP.

(Klarreich, 2013) reports that a new progress is a 49.99...96% (totally 46 nines replaced by "...") over the optimum, a tiny margin for "graphical" traveling salesman problems. Notice that a very small percentage improvement may also be of great impact to the total length of large TSP instances.

(Reiter and Rice, 1966) study the cost distribution of local optima under a gradient maximizing search in 39 integer programming problems. Their results suggest that the local optima follow a Beta distribution. (Golden, 1978) examines six problems from the TSPLIB archive (Reinelt,1991). The resulting estimates of optimal solutions are compared to the best solution found by the Lin-Kernighan algorithm (Lin and Kernighan,1973. The authors found that the Beta distribution is "a more appropriate distribution" than the Weibull distribution.

Recently, (Vig and Palekar, 2008), apply sampling techniques similar to Golden, and use the Lin-Kernighan algorithm to find optimal tour costs. The authors estimate raw moments from the one to four of the probability distribution of optimal tour lengths. They use these estimates to fit various candidate distributions including the Beta, Weibull and Normal cases. Vig and Palekar conclude that the Beta distribution yields the best fit.

More recently, (Stuffle, 2009) provide exact solutions to compute the mean, variance, the third

Tian, W., Huang, C. and Wang, X.
A Near Optimal Approach for Symmetric Traveling Salesman Problem in Euclidean Space.
In *Proceedings of the 6th International Conference on Operations Research and Enterprise Systems (ICORES 2017)*, pages 281-287
ISBN: 978-989-758-218-9

and fourth central moment of all tour lengths. The computational complexity of computing variance, the third and fourth central moment is respectively $O(n^2)$,$O(n^4)$ and (n^6) where n is the number of nodes in a TSP.

A typical probability distribution of all tour lengths for a random TSP in a square unit is shown in Fig. 1 where the total node number is 12. An example of TSPLIB Burma14 is shown in Fig.2. Similar results are observed for different total number of cities for which all tour lengths can be obtained.

The organization of remaining parts of this paper is: our major contributions are summarized in Section 2, our methods are introduced in Section 3, and Conclusions and future work are discussed in Section 4.

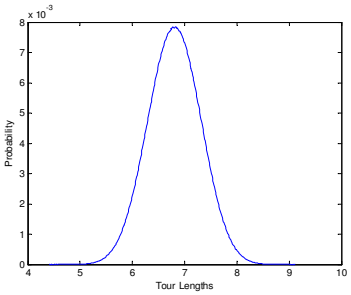

Figure 1: The probability density of random 12-node TSP in a squre unit.

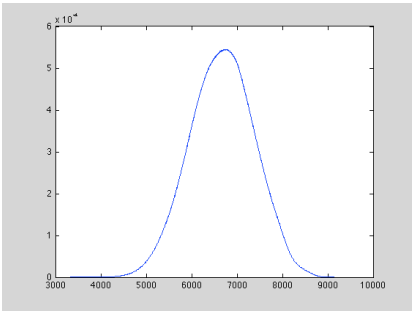

Figure 2: The probability density of all tour lengths in Burma14.tsp with 14 nodes.

2 RESULTS

The main contributions of this work can be summarized as follows:

- We propose Generalized Beta (GB) distribution as the probability density function of all tour lengths distribution in a symmetric TSP in Euclidean space (ESTSP), the four parameters of the GB can be computed from given ESTSP data directly.
- For the first time, we introduce an iterative Truncated GB (TGB) closed-form solution to obtain $(1+\frac{1}{2}(\frac{\alpha+1}{\alpha+2})^{K-1})$-approximation for a STSP where K is the number of total iterations in TGB, and $\alpha(>> 1)$ is the shape parameter of TGB and can be determined once the TSP instance is given. The result can approach the true optimum as K increases.

3 METHODS

Firstly, a problem formulation and some preliminaries are provided in this section.

3.1 Problem Formulation

Consider the n-node TSP defined in Euclidean space. This can be represented on a complete graph G= (V,E) where V is the set of vertices and E is the set of edges. The cost of an edge (u, v) is the Euclidean distance (c_{uv}) between u and v. Let the edge cost matrix be $C[c_{ij}]$ which satisfies the triangle inequality.

Definition 1. Symmetric TSP (STSP) is TSP in Euclidean distance (called ESTSP) and the edge cost matrix C is symmetric.

Definition 2. $\triangle$STSP is a STSP whose edge costs are non-negative and satisfies the triangle inequality, i.e., for any three distinct nodes (not necessary neighboring) (i, j, k), $(c_{ij}+c_{jk}) \geq c_{ik}$.

Definition 3. TSP tour. Given a symmetric graph G in 2-dimensional Euclidean distance and its distance matrix C where c_{ij} denote the distance between node i and j (symmetrically). A tour T has length

$$L = \sum_{k=0}^{N-1} c_{T(k),T(k+1)} \quad (1)$$

where N is the total number of nodes in G and $T(N)$=$T(0)$ so that a feasible tour is formed.

Definition 4. The approximation ratio of an algorithm. The ratio is the result obtained by the algorithm over the optimum (abbreviated as OPT in this paper).

Observation 1. The probability density function of all tour lengths in an ESTSP can be modelled by a Generalized Beta (GB) distribution.

This is observed in Fig. 1 and other ESTSPs for which we can obtain all tour lengths. More results are provided in next section. This is also validated and shown in (Vig and Palekar, 2008), where a scaled Beta distribution is applied with scaled mean and scaled variance. The author validated estimated results by Anderson-Darling (A-D) test and Kolmogorov-Smirnov (K-S) test for random TSP. They use these

estimates to fit various candidate distributions including the Beta, Weibull and Normal cases, and conclude that the (scaled) Beta distribution yields the best fit.

We further propose a Generalized Beta (GB) distribution. The probability density function (pdf) of GB is defined as

$$f(x,\alpha,\beta,A,B) = \frac{(x-A)^{\alpha-1}(B-x)^{\beta-1}}{Beta(\alpha,\beta)} \quad (2)$$

where $Beta(\alpha,\beta)$ is the beta function

$$Beta(\alpha,\beta) = \int_0^1 t^{\alpha-1}(1-t)^{\beta-1}dt, \quad (3)$$

A and B is the lower bound and upper bound respectively, $\alpha > 0$, $\beta > 0$, see (Hahn and Shpiro, page 91-98,126-128,1967). For TSP, A and B represents the minimum and maximum tour length respectively.

The four central moments, mean (μ), variance, skewness and kurtosis of the Generalized Beta distribution with parameters (α, β, A, B) are given by:

$$\mu = A + (B-A)\frac{\alpha}{\alpha+\beta} \quad (4)$$

$$Var = (B-A)^2\frac{\alpha\beta}{(\alpha+\beta)^2(\alpha+\beta+1)} \quad (5)$$

$$Skewness = \frac{2(\beta-\alpha)\sqrt{1+\alpha+\beta}}{\sqrt{\alpha+\beta}(2+\alpha+\beta)} \quad (6)$$

and Kurtosis

$$\frac{6[\alpha^3+\alpha^2(1-2\beta)+\beta^2(1+\beta)-2\alpha\beta(2+\beta)]}{\alpha\beta(\alpha+\beta+2)(\alpha+\beta+3)} \quad (7)$$

The standard deviation is then given by

$$\sigma = \sqrt{Var} \quad (8)$$

Once four central moments are known, or any four parameters of (A, B, μ, Var, skewness, kurtosis) are given, then four parameters of GB, i.e., (α, β, A, B) can be determined easily from the four moments match using Eqns.(4)-(7). When the problem size is not large, the four central moments can be computed exactly using methods proposed in (Stuffle 2009). As the problem size increases, we can find any four parameters of (A, B, μ, Var, skewness) firstly, then find four parameters of GB, i.e., (α, β, A, B).

For medium or large size problem, currently it is not easy to find the fourth central moment. However, the lower bound (A) can be easily computed by LKH code (Helsgaun, 2009). So in the following sections, we find four values (A, mean (μ), variance, skewness) firstly, and then compute other parameters (B, α, β). Firstly we introduce a method to compute maxTSP (B) (Gutin and Punnen, 2002).

Definition 5. maxTSP. The maximum tour length (B) is obtained using LKH where each edge cost (c_{ij}) is replaced by a very large value (M) minus the original edge cost, i.e., (M-c_{ij}). M can be set as the maximum edge cost plus 1.

Since the characteristics of random TSP and TSPLIB instances are different in Euclidean space, we introduce the GB as the probability density function for them separately.

3.2 GB as the Probability Density Function for Random TSP

For medium size random TSP problems with n varying from 20 to 100, we can obtain four central moments easily (Suffle, 2009) and apply four moments match to find four parameters for GB. After obtaining four parameters, we then use linear regression to find closed-form solution to (α, β) of GB for random TSP. For n=20 to n=100, and we find that

$$\alpha(n) = 1.9197n - 32.166, R^2 = 0.9994 \quad (9)$$

$$\beta(n) = 1.1168n - 15.854, R^2 = 0.9982 \quad (10)$$

$$A(n) = 0.6932\sqrt{n} + 0.8029, R^2 = 0.9956 \quad (11)$$

$$B(n) = 0.7649n - 0.6393, R^2 = 0.998 \quad (12)$$

where R^2 is a measure of goodness-of-fit with value between 0 and 1, the larger the better. We observe that Eqns.(9)-(12) are highly accurate by extensive computation results.

Observation 2. The relative errors between estimated results (maxTSPs) by GB and LKH results are within 6.5% for random TSP.

The relative error is defines as (EstimatedValue-OPT)/OPT$\times$100%. We conduct tests for n=100 to n=500. The results are shown in Fig.3 where LKH is used to obtain maxTSP (B) results. We can observe that the relative error between our results and LKH are within 6.5% off the true optimums, with an average below 5%. Table 1 shows four parameters of GB for random TSPs with n varying from 90 to 99.

3.3 GB as the Probability Density Function for TSPLIB Instances in Euclidean Distance

Firstly, we show an example of Burma14.tsp, which we can permute its all tours and find that minimum tour length (A) is 3233 and maximum tour length (B) is 9139, Mean (μ)=6679, Variance=503064, Skewness=-0.0632, Kurtosis=2.7972. Fig. 4 shows exact result (in black color) by permuting all tour

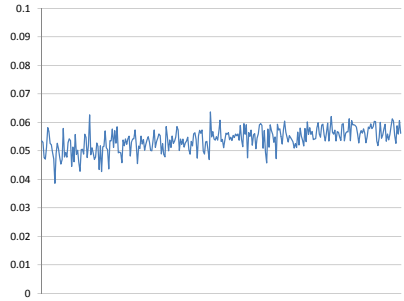

Figure 3: The relative error between estimated results by GB and OPT by LKH for Random TSP n=200 to 500.

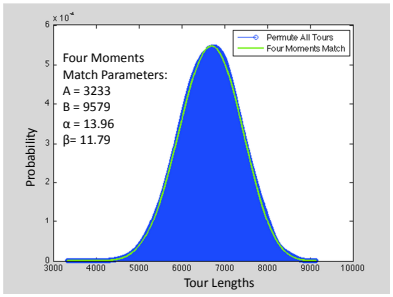

Figure 4: The exact (Permute All Tours) and estimated (Four Moments Match) probability distribution of Burma14.tsp.

lengths and estimated probability density function (in green color) by four central moment match with (A=3233, B=9579, α=13.96,β=11.79). It can be observed that two results match very well.

Observation 3. The relative error between the estimated maximum tour lengths by GB and LKH results is below 7% for medium size TSPLIB instances, with an average below 5%.

We conduct tests by set n=14 to n=52 for which the four central moments can be easily computed and are given in (Stuffle 2009). Fig. 5 shows the relative error between estimated results by GB and OPT by LKH.

In Table 2 we show four parameters of GB for TSPLIB with n varying from 14 to 52.

3.4 Truncated Generalized Beta Distribution based on Christofides Algorithm

Next, we introduce our algorithm, **Truncated Generalized Beta distribution Based on Christofides Algorithm (TGB)**. TGB algorithm performs in seven steps:

- (1). Finding the minimum spanning tree *MST* of the input graph G representation of metric TSP;

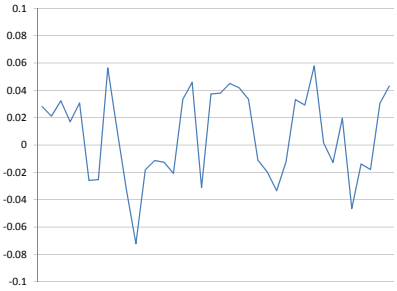

Figure 5: The relative error between estimated results by GB and OPT by LKH for TSPLIB instances for n from 14 to 52.

Table 1: Four parameters of GB for some random TSP instances.

n	A(OPT)	B	α	β
90	7.18	65.75	179.68	96.49
91	7.15	69.49	180.38	96.30
92	7.01	69.18	185.51	108.55
93	8.00	71.24	182.22	100.63
94	7.73	68.58	175.38	94.00
95	7.77	69.53	181.09	105.93
96	7.40	73.10	204.60	115.61
97	8.00	74.01	186.85	107.33
98	7.73	76.44	208.67	123.96
99	7.54	74.95	203.46	109.03

- (2). Taking G restricted to vertices of odd degrees in *MST* as the subgraph G^*; This graph has an even number of nodes and is complete;
- (3). Finding a minimum weight matching M^* on G^*;
- (4). Uniting the edges of M^* with those of the *MST* to create a graph H with all vertices having even degrees;
- (5). Creating a Eulerian tour on H and reduce it to a feasible solution using the triangle inequality, a short cut is a contraction of two edges (i, j) and (j,k) to a single edge (i,k);
- (6). Applying Christofides algorithm to a ESTSP forms a truncated GB (TGB) for the probability density function of optimal tour lengths, with expectation (average) value at most 1.5OPT-ε, where ε is a very small value; Applying k-opt to the result of Christofides algorithm forms another TGB for probability density function of optimal tour lengths;
- (7). Iteratively apply this approach, taking the expectation value of $(K-1)$-th iteration as the upper bound of the K-th iteration, we have the expectation value after K iterations ($K \geq 2$).

Table 2: Four parameters of GB for some TSPLIB instances.

TSPLIB	A(OPT)	B	α	β
burma14	3323	9139	13.97	11.79
ulysses16	73.98	180.52	10.24	6.52
gr17	2085	6160	19.22	10.60
gr21	2707	10680	32.95	19.80
ulysses22	75.3	241.50	17.52	12.79
gr24	1272	4929	51.55	27.21
fri26	937	3681	28.87	16.91
bayg29	1610	6654	42.17	26.42
bays29	2020	8442	45.14	27.52

Lemma 1. Applying Christofides algorithm to a ESTSP forms a truncated GB (TGB) for the probability density function of optimal tour lengths, with expectation (average) value at most 1.5OPT-ε, where ε is a very small value.

Proof. This is because that Christofides algorithm assures that its result is at most 1.5OPT so that those tours with lengths more than 1.5OPT are excluded (truncated), as shown in Fig. 6 where tour lengths larger than 1.5OPT (1.5A) are truncated in black color.

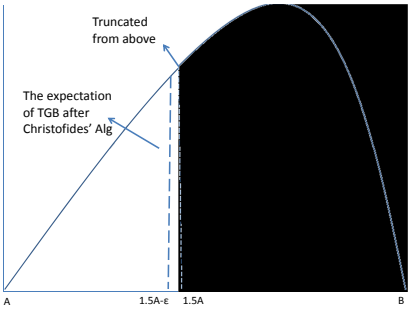

Figure 6: The Truncated GB by applying Christofides algorithm.

The TGB in this case is truncated from above. Set X as the variate of the GB, the probability density function (pdf) of TGB is given by

$$f_t^1(x,\alpha,\beta,A,B,a,b) = \frac{f(x,\alpha,\beta,A,B)}{Pr[a \le X \le b]} = \frac{(x-A)^{\alpha-1}(B-x)^{\beta-1}}{\int_a^b (x-A)^{\alpha-1}(B-x)^{\beta-1}} \tag{13}$$

where a=A and b=1.5A. Therefore 1.5A is the upper bound. We know that the average of Christofides algorithm is at most 1.5OPT-ε (set as μ_t^1) where ε is a very small value, this is also validated in (Blaser et al., 2012).

□

The four parameters of GB for some random TSP and TSPLIB instances are provided in Table 1 and 2 respectively.

Definition 6. k-opt method. Local search with k-exchange neighborhoods, also called k-opt, is the most widely used heuristic method for the TSP. k-opt is a tour improvement algorithm, where in each step k links of the current tour are replaced by k links in such a way that a shorter tour is achieved (see (Helsgaun, 2009) for detailed introduction).

In (Helsgaun, 2009), a method with computational complexity of $O(k^3 + k\sqrt{n})$ is introduced for k-opt.

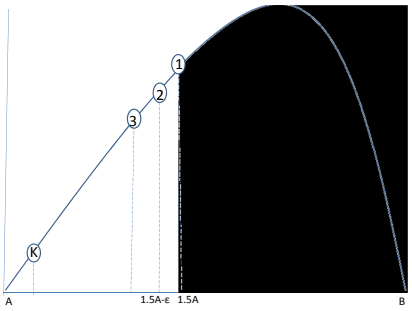

Figure 7: The Iteratively Truncated GB.

Lemma 2. Applying k-opt to the result of Christofides algorithm forms another TGB for probability density function of optimal tour lengths.

Proof. Applying k-opt to the result obtained by Christofide algorithm as shown in Fig.7. The TGB in this case is truncated from above. Denote the first truncation by Christofides' algorithm as the first truncation (K=1). The probability density function of the second TGB is given by

$$f_t^2(x,\alpha,\beta,A,B,a_2,b_2) = \frac{(x-A)^{\alpha-1}(B-x)^{\beta-1}}{\int_{a_2}^{b_2}(x-A)^{\alpha-1}(B-x)^{\beta-1}} \tag{14}$$

In this case, a_2=A, b_2=1.5A because the distribution is based on the result after applying Christofides algorithm which assures the upper bound is at most 1.5A, see Fig.7. Setting $\hat{x}$=$\frac{x-A}{B-A}$, $\hat{a_2}$=$\frac{A-A}{B-A}$=0, $\hat{b_2}$=$\frac{1.5A-A}{B-A}$=$\frac{0.5A}{B-A}$, we have

$$\begin{aligned} C_0 &= \int_{a_2}^{b_2}(x-A)^{\alpha-1}(B-x)^{\beta-1}dx \\ &= \int_0^{\hat{b_2}}((B-A)\hat{x})^{\alpha-1}((B-A)(1-\hat{x})^{\beta-1}dx \\ &= (B-A)^{\alpha+\beta-1}B_2(0,\hat{b_2},\alpha,\beta) \end{aligned} \tag{15}$$

where

$$B_2(0,t,\alpha,\beta) = \int_0^t x^{\alpha-1}(1-x)^{\beta-1}dt \tag{16}$$

By the definition of the expectation (mean) value (denoted as μ_t^2) for $f_t^2(x,\alpha,\beta,A,B,a_2,b_2)$, we have

$$\begin{aligned}\mu_t^2 - A &= \int_{a_2}^{b_2}(x-A)f_t^2(x,\alpha,\beta,A,B,a_2,b_2)\mathrm{d}x \\ &= \frac{\int_{a_2}^{b_2}(x-A)^{\alpha}(B-x)^{\beta-1}\mathrm{d}x}{C_0} \\ &= \frac{(B-A)^{\alpha+\beta}B_2(0,\hat{b_2},\alpha+1,\beta)}{C_0} \\ &= (B-A)\frac{B_2(0,\hat{b_2},\alpha+1,\beta)}{B_2(0,\hat{b_2},\alpha,\beta)} \\ \Rightarrow \mu_t^2 &= A+(B-A)\frac{B_2(0,\hat{b_2},\alpha+1,\beta)}{B_2(0,\hat{b_2},\alpha,\beta)} \quad (17)\end{aligned}$$

Taking the expectation value of $(K-1)$-th iteration as the upper bound ($\hat{b_K} = \frac{\mu_t^{K-1}-A}{B-A}$) of the K-th iteration, we apply this approach Iteratively and have the expectation value after K iterations ($K \geq 2$), denoted as μ_t^K,

$$\begin{aligned}\mu_t^K &= A+(B-A)\frac{B_2(0,\hat{b_K},\alpha+1,\beta)}{B_2(0,\hat{b_K},\alpha,\beta)} \\ &= A+(B-A)g(\hat{b_K})\end{aligned}$$

□

Next we provide the proof for our main theorem.

Theorem 1. Applying TGB iteratively, we can obtain quality-proved approximation, i.e., $(1+\frac{1}{2}(\frac{\alpha+1}{\alpha+2})^{K-1})$-approximation where K is the number of iterations in TGB, α is the shape parameter of TGB and can be determined or estimated once TSP instance is given.

Proof. Notice that the expectation value of the (K-1)-iteration is taken as the upper bound ($\hat{b_K} = \frac{\mu_t^{K-1}-A}{B-A}$ here A is OPT and B is the maxTSP) of the K-iteration, as shown in Fig.7. Setting

$$g(\hat{b_K}) = \frac{B_2(0,\hat{b_K},\alpha+1,\beta)}{B_2(0,\hat{b_K},\alpha,\beta)} \quad (18)$$

The exact expression of $g(\hat{b_K})$ can be stated in a hypergeometric series, and

$$B_2(0,\hat{b_K},\alpha,\beta) = \frac{\hat{b_K}^{\alpha}}{\alpha}F(\alpha,1-\beta,\alpha+1,\hat{b_K}) \quad (19)$$

and $F(a,b,c,x)$

$$\begin{aligned}&= 1+\frac{ab}{c}x+\frac{a(a+1)b(b+1)}{c(c+1)2!}x^2 \\ &+\frac{a(a+1)(a+2)b(b+1)(b+2)}{c(c+1)(c+2)3!}x^3+... \quad (20)\end{aligned}$$

In all cases, we have $\alpha>1$, $\beta>1$, $\hat{b_K} \in (0,1)$, therefore $F(a,b,c,x)$ is an monotonic decreasing function. We have

$$u_t^2 = A+(B-A)g(\hat{b_2}) \leq A+0.5A\frac{\alpha+1}{\alpha+2} \quad (21)$$

continue this for $g(\hat{b_3})$, u_t^3, $g(\hat{b_4})$, u_t^4,..., so forth, we have

$$\hat{b_K} \leq \frac{0.5A}{B-A}(\frac{\alpha+1}{\alpha+2})^{K-1} \quad (22)$$

and

$$\begin{aligned}g(\hat{b_K}) &= \frac{B_2(0,\hat{b_K},\alpha+1,\beta)}{B_2(0,\hat{b_K},\alpha,\beta)} \\ &\leq \frac{\alpha+1}{\alpha+2}\hat{b_K} \\ &= \frac{0.5A(\frac{\alpha+1}{\alpha+2})^{K-1}}{B-A}, \quad (23)\end{aligned}$$

Therefore

$$\begin{aligned}\mu_t^K &= A+(B-A)\frac{B_2(0,\hat{b_K},\alpha+1,\beta)}{B_2(0,\hat{b_K},\alpha,\beta)} \\ &= A+(B-A)g(\hat{b_K}) \\ &\leq (1+\frac{1}{2}(\frac{\alpha+1}{\alpha+2})^{K-1})A, \quad (24)\end{aligned}$$

This means that, after the K-th iterative truncation, we can obtain the expectation value of (μ_t^K) which is close to the optimum (OPT=A) when K increases. Actually, to make the approximation less than C_0, the TGB algorithm needs K to be at least $(1+\frac{log2(C_0-1)}{log(1-1/(\alpha+1))})$. □

Table 3 shows OPT, α, β, iteration numbers and the approximation ratio (Appr) for TSPLIB instances with $n \leq 600$, where (α, β) are obtained (or estimated) from (A, mean, variance, skewness) in Eqns (4)-(7), and K is obtained in by TGB algorithm which modifies LKH code. We observe that the TGB results are consistent with LKH OPT results in most cases, there are only a few cases where TGB results are few percentage difference from OPT, with 0.2% off the true optimum on the average. For instance, the difference is 7.8% for berlin52.tsp and 1.1% for ulysses22.tsp. Our results are consistent with (Applegate et al., 2003). These results validate Theorem 1. Notice that LKH code performs very fast in practice and our results are based on average performance.

4 CONCLUSIONS

In this paper, for the first time, we proposed GB and Truncated Generalized Beta distribution (TGB) for

Table 3: Four parameters for some TSPLIB instances ($n \leq 600$).

	α	K-1	$(1+0.5(\frac{\alpha+1}{\alpha+2})^{K-1})A$	Appr
ulysses22	17.5	91	82.1	1.0042
berlin52	57.4	101	9052.4	1.0900
pr76	115.5	2451	108159.4	1.0000
rat99	128.1	1821	1219.2	1.0000
kroA100	137.3	3366	21285.3	1.0000
pr299	422.2	29117	48194.8	1.0000
lin318	563.1	39112	42042.4	1.0000
rd400	735.1	34936	15275.7	1.0000
d493	695.9	129767	35018.3	1.0000
rat575	892.03	84814	6796.36	1.0000

the probability distribution of optimal tour lengths in a symmetric TSP in Euclidean space. Notice that our TGB results are based on expectation (average) value of probability distribution, which may be overestimated for the number of iterations. In practice, LKH algorithm performs very fast, with estimated computational complexity of $O(n^{2.2})$ [9]. A few possible research directions include:

- Improving the computational complexity. Currently the Christofides algorithm with minimum perfect matching has computational complexity $O(n^3)$. For large instances, this complexity should be reduced.
- Find more efficient ways to compute especially the third and fourth central moments of a given TSP instance.
- Finding more applications. With closed-form probability density function at hand, a lot of things can be done better. For instance, computing more statistical metrics, analyzing the average performance of approximation algorithms and others.

ACKNOWLEDGEMENTS

This research is partially supported by China National Science Foundation (CNSF) with project ID 61672136, 61650110513; and Xi Bu Zhi Guang Project (R51A150Z10). A version of manuscript is posted on http:/arxiv.orgpdf1502.00447.pdf

REFERENCES

D. Applegate, W. Cook, A. Rohe, Chained Lin-Kernighan for large traveling salesman problems, INFORMS Journal on Computing; Winter 2003; 15, 1; ABI/INFORM Global pg. 82.

H. C. An, Robert Kleinberg, David B. Shmoys, Improving Christofides Algorithm for the s-t Path TSP, 2012.

M. Blaser, K. Panagiotou and B. V. R. Rao, A Probabilistic Analysis of Christofides' Algorithm, Algorithm Theory-SWAT 2012, Lecture Notes in Computer Science Volume 7357, 2012, pp 225-236.

N. Christofides, Worst-case analysis of a new heuristic for the travelling salesman problem, Report 388, Graduate School of Industrial Administration, CMU, 1976.

W. Cook, In Pursuit of the Traveling Salesman, Princeton University Press, 2012.

In G. Gutin and A. Punnen, editors, The Traveling Salesman Problem and its Variations, Chapter 1 The Maximum Traveling Salesman Problem, Kluwer Academic Publishers, New York, NY, USA, 2002.

B. L. Golden. Closed-form statistical estimates of optimal solution values to combinatorial problems. In ACM 78: Proceedings of the 1978 annual conference, pages 467-470, New York, NY, USA, 1978. ACM.

G. J. Hahn and S. S. Shpiro, Statistical Models in Engineering, John Wiley & Sons, Inc., New York, 1967.

K. Helsgaun, General k-opt submoves for the Lin-Kernighan TSP heuristic. Mathematical Programming Computation, 2009,doi: 10.1007/s12532-009-0004-6.

D. S. Johnson, L. A. McGeoch, The Traveling Salesman Problem: A Case Study in Local Optimization, Local search in combinatorial optimization 1, 215-310, 1998.

D. S. Johnson, The Traveling Salesman Problem for random points in the unit square: An experimental and statistical study. Technical Report, 2014.

E. Klarreich, Computer Scientists Find New Shortcuts for Infamous Traveling Salesman Problem, SIMONS SCIENCE NEWS, Jan. 29, 2013.

S. Lin, B. W. Kernighan, An effective heuristic algorithm for the traveling-salesman problem. Oper. Res.21, 498-516 (1973).

LKH codes, http://www.akira.ruc.dk/ keld/research/LKH/,last accessed Jan. 15th of 2015.

G. Reinelt. TSPLIB, a traveling salesman problem library. ORSA Journal on Computing, 3(4):376-384, 1991.

S. Reiter and D. B. Rice. Discrete optimizing solution procedures for linear and nonlinear integer programming problems. Management Science, 12(11):829-850, 1966.

P. J. Sutcliffe, Moments over the Solution Space TSP, PhD Thesis, University of Technology, Sydney, 2009.

V. Vig and U. S. Palekar. On estimating the distribution of optimal traveling salesman tour lengths using heuristics. European Journal of Operational Research, 186(1):111-119, April 2008.

J. Vygen, New approximation algorithms for the TSP, OPTIMA 90 (2012), 1-12.

Applying Systems Thinking onto Emergency Response Planning
Using Soft Systems Methodology to Structure a National Act in Sweden

Christine Groβe
Department of Information and Communication Systems, Mid Sweden University, Holmgatan, Sundsvall, Sweden
christine.grosse@miun.se

Keywords: Soft Systems Methodology, Operations Research, Emergency Response Planning, Decision Support, Styrel.

Abstract: This paper outlines a soft systems method approach to model a national preparedness planning procedure for the case of an electrical power shortage. Through the model, we provide a new perspective on enhancing and understanding the joint decision-making environment for the actors involved in the planning procedure, as well as its underlying power structure. By a process of abstraction from the current implementation, a core root definition is presented which provides a generic systems view that can be a useful concept for the study of similar contexts. An action model dedicated to determining meaningful and valid activities is derived, providing insights for the improvement of collaborative emergency response planning in general. The paper, thus, aims to contribute to the communication and cooperation between actors and stakeholders in the development of appropriate decision processes and decision support in the context of emergency preparedness.

1 INTRODUCTION

The constant availability of electricity is, nowadays, a precondition for many parts of infrastructure. It is demanded in almost every part of our day-to-day lives and businesses. Since lacking power affects essential functions of a society's common life, it constitutes a key sector of critical infrastructure (CI). Cascading consequences can harm other sectors of CI and, thereby, affect the industry and population which depends upon them (Rinaldi et al., 2001). These consequences can occur locally, affect a larger community, and also involve global interests. Thus, proper planning of the power supply is necessary. Variations in electricity generation related to consumption can also lead to risk situations in the supply network, which have to be balanced to maintain the reliability of power delivery (Maliszewski and Perrings, 2012).

Due to the dimensions and climate conditions of Sweden, providing electrical power to every inhabited place is challenging for both humans and materials. Maintaining a distributed power grid needs permanent effort. Since infallible protection against all kinds of power shortage seems to be an impossible task, proper continuity management and emergency response planning can help to handle adverse events and alleviate the consequences of them. Sweden's power generation and supply landscape is fragmented due to the privatisation of the electricity market in 1996 (Bergman, 1997). This fragmentation hampers decision paths and complicates communication between the individuals and groups responsible for electrical power in Sweden. In order to manage continuous power delivery, many of the necessary adjustment operations are automated. Nevertheless, in the case of power shortage, a response plan can support reliable decision making. Besides an analysis of the societal consequences, the planning needs to consider responsibilities, a previously defined chain of order, plausible and documented priorities, and a structured approach, enabling an operations team to reach the goals of reconditioning and maintenance while causing as little subsequent problems as possible (Johansson and Hassel, 2014).

Contingency planning – preparing this solid basis for an operational emergency response – depends on information sharing and cooperation between the stakeholders involved (Pramanik at al., 2015), and their perception of a crisis (Nilsson, 2010; Penrose, 2000; van Laere, 2013). The combination of various stakeholders being involved, with their own points of interest and responsibilities, and the sensitivity of the power grid, is expected to cause tensions. The added fact that these tensions can impact interdependent CI impels the following study.

The study investigates the planning process and circumstances with a particular focus on the

Große, C.
Applying Systems Thinking onto Emergency Response Planning - Using Soft Systems Methodology to Structure a National Act in Sweden.
In *Proceedings of the 6th International Conference on Operations Research and Enterprise Systems (ICORES 2017)*, pages 288-297
ISBN: 978-989-758-218-9

stakeholders involved, their interrelations, and the belonging context. The leading research question is:

Which elements of a conceptual system model should be considered during emergency response planning, regarding power supply within the complex context of critical infrastructure?

Since the problem situation appears to be not particularly well-structured, with unclear objectives, a soft system analysis and modelling approach has been chosen to meet the conditions appropriately (Avison and Taylor, 1997). The remainder of the paper reads as follows: after briefly describing the background of systems thinking and the response planning approach, the research process is outlined. After the system analysis, the conceptual system model is presented and discussed, related to the associated context. Final remarks conclude the paper and outline the prospects for further research.

2 BACKGROUND

2.1 Systems Thinking

The term "system" has been discussed for more than half a century. This discussion provoked a number of concepts and opinions. This paper falls short of defining the term in general; rather, the concepts underlying the study and research-leading points of view are marked. Systems can be considered to be '*complexes of elements standing in interaction*' (Bertalanffy, 1968, p. 33). Interactions in this quote suggests that relations between elements are not linear, and by that trivial – rather, they are complex and do not necessarily have correlations by causality or determinism. Searching for a generally valid theory to describe phenomena inside, between and around systems gave rise to the General System Theory, which emphasis its interdisciplinary character by accepting both mathematical and sociological analysis techniques (Bertalanffy, 1968, p. 2). The open system, standing in an exchange relationship to its environment, crosses system borders in useful interaction (Bertalanffy, 1968, p. 141). This illustrates the challenges to set system boundaries, and not only in the context of response planning. The fact that individuals can be seen as elements in one or several systems can result in conflicts in goals and behaviour. The intention to provide a universal approach to all kind of system led to a hierarchical classification of complexity according to corresponding individuals (Boulding, 1956). In this hierarchical order, the social system appeared at the top in terms of complexity. Evidently, influences on power structures and group behaviour, as well as individual target tracking, within and between systems, are all related to this order. It complicates the predictability of interactions and the ensuing decisions within a social system.

Furthermore, modern societies and organisations are characterised by the use of many technical systems. The functionalities of the technical part of a complex system can influence the social environment. In turn, the knowledge and behaviour of an intended user influences the outcome of a technical system. A socio-technical system, as a holistic system, is able to achieve a better outcome than the parts standing alone (Emery and Trist, 1960). Particularly important is the ability of the human, as part of the system, to create improvement and add value to the system (Mumford, 2006). Moreover, their adaptability of behaviour in emergencies is an important aspect for system resilience (Boin and McConnell, 2007).

Besides the technical infrastructure, the power-delivery system relies on the willingness of decision-makers in case of power outages (Maliszewski and Perrings, 2012). This unbalanced power relation requires intervention by the government to preserve societal interests. If conflicts between groups of interests arise, a balancing of risks is required to avoid the damage that could be caused by conflict escalation (Wimelius and Engberg, 2015). In addition, an observer's perspective in his or her role as a system analyst can be biased, which raises further potential for conflicts. An analyst has to respect constitutive characteristics while introducing an observed system to analysis; namely they are: different points of view, events and decisions, interconnectivity and a topic as limitation (Kieser, 2001; Rüegg-Stürm, 2001).

Hence, two dimensions of governance have resulted from the deliberations above, providing a basis for response planning: the *horizontal* – structures for processes, with resources and responsibilities, and the *vertical* – structures for organisation, e.g., power structures within a system. Thus, consequent coordination of the information flow through a system, both horizontal and vertical, provides adequate conditions for communication and cooperation between interrelated elements of a system. A case of particular importance is the response planning system in Sweden regarding the power supply to key consumers in the context of CI.

2.2 Response Planning in the Context of the Power Supply in Sweden

The national planning procedure regarding the power

supply during an event of power shortage, named *STYREL*, was prepared since 2004 and tested by its first iteration in 2010-2011. Purpose of the procedure is to gather data on the infrastructure that depends on electricity. A particular focus lies on the identification of consumers whose activities are essential for national society, with regards to health, safety and interdependent businesses. Consumers are ranked in advance to ensure immediate decision-making during an emergency either caused or accompanied by lacking electricity. Due to the amount of involved departments and companies, the structured approach was developed for an ascertainment of priority lists.

The second iteration (2014-2015) was launched by the following national authorities: (1) the Swedish Civil Contingencies Agency, (2) Energy Department, (3) Swedish Energy Markets Inspectorate, and (4) Swedish national grid provider, Svenska Kraftnät. National agencies identified electricity consumers at a national level, and categorised them depending on their importance to national societal functions. This categorising was conveyed to the county administrative board (CAB) where the respective consumers were located. CABs initiated the operation within their regional area. They provided information to municipalities and called for action. Municipalities identified and ranked key power consumers locally. Local grid operators assisted with details regarding technical feasibility. Lists of categorised consumers were returned to the CAB. Each CAB assessed the data collected from a regional perspective. If power lines cross county borders, adjacent counties had to categorise those lines together. The consumer ranking was finally forwarded to local, regional and national grid providers as a basis for their response planning. (Energy Department 2014)

3 RESEARCH PROCESS

3.1 Soft Systems Methodology

The methodological research concept used in this paper is grounded on the Soft Systems Methodology (SSM) approach developed by Checkland (1972), aligned with the design-oriented research process of *analysis, design, evaluation*, and *diffusion* used in information system research (Österle et al., 2011).

The entire process of SSM in its classical form constitutes seven stages (S) (Checkland, 1989): *S1*: Enter the situation that is considered problematic, *S2*: Express the problem situation, *S3*: Formulate root definitions of the relevant systems, *S4*: Build conceptual models of the systems named in the root definitions, *S5*: Compare the models with real world situations, *S6*: Define possible changes which are both possible and feasible, *S7*: Take action to improve the problem situation.

SSM is arranged in this way to explore different views stakeholders concerned with a situation can have, and to achieve shared understanding about relevant and necessary actions. The object of this approach is to provide structure to a complex problem situation. This structure is used to determine activities that are able to improve the initial situation. SSM is used with similar intentions, exploring complex situations and meeting various stakeholder needs, often in the early stages of systems development (Cundill et al., 2012; Hakami et al., 2013; Mendoza and Prabhu, 2006; Sørensen et al., 2010).

3.2 Data Analysis

S1 is performed within and across documentations and notices about the current planning process. The literature selected is limited to the outlined case and given context in order to gain a holistic understanding of the observed system and its interacting elements. Different interests in the situation and existing correlations are investigated alongside. Discovering significant roles and power structures is part of the argumentative-deductive analysis, as well as exploring the system environment and boundaries. Various criteria are applied to analyse the case. Thereby, individual interpretations by the system observer were kept to the margins for a qualitative text analysis. The epistemological goal of the analysis is to explore what the current situation characterises.

3.3 Conceptual Model Design

Results from the data analysis constitute the systems-thinking foundation for the content of the conceptual system model. Furthermore, the sub-models are based on each other to obtain, step-by-step, a higher level of abstraction. The purpose is to detach the thinking from the current implementation of the planning case in Sweden, and to yield a generic analysis concept for complex response planning situations. For reasons of generality, no explicit modelling language is applied; instead, the model design is based on the figures of SSM used in the literature (e.g. Checkland and Scholes, 1999; Proches and Bodhanya, 2015).

In the course of *S2*, a 'Rich Picture' is created that represents individuals and groups, their conceivable concerns, technical and environmental elements, and interrelations between the components. Researchers' interaction with the case enriches the model. This can

require several iterations to deal with structures (Grochla, 1974; Mingers and Taylor, 1992).

During *S3*, a root definition is formulated that represents a generic system model for planning a power-shortage response. Besides the system definition, the research considers the elements of CATWOE (Smyth and Checkland, 1976), see Table1.

Table 1: Elements of CATWOE, after Checkland and Scholes, 1999, p. 35.

Element	*Description*
Customers	The victim or beneficiaries of T
Actors	Involved persons in / Performer of T
Transformation Process	Conversion of input to output
Weltanschauung	Big picture that makes the T meaningful in the context
Owner	Ruler who could stop T
Environmental constraints	Elements outside which it takes as given

In *S4*, an action model is derived from the root definition, establishing a bridge between concept and practice. The leading question for building this sub-model is: What are the purposeful activities necessary to carry out the specified transformation process, T? Individual interests and goal conflicts are reduced by focusing on the generic root definition.

3.4 Evaluation and Further Steps

During *S5*, the sub-models are compared with a real world situation. Several methods are suggested to perform this step; using formal questioning is the most common (Checkland & Scholes, 1999, p. 43), and is also used in this study. Several stakeholders were confronted with the models during interviews. Eight security coordinators, representing all of the municipalities of one rural, sparsely-inhabited county in northern Sweden, participated in qualitative interviews. In addition, two experts from a local grid provider were questioned. Seven of the people interviewed were involved twice, one of them once, and two had no practical experience in the procedure. The interviews varied in length but generally took about one hour, and are recorded and transcribed.

S6 encourages a debate about the changes that are possible and feasible. Changes to the investigated situation suggested during the performed interviews are presented. Furthermore, conceivable changes regarding the models, in order to adapt them to a broader context, were also debated with the experts.

S7 motivates actors to take action to improve the initial situation. Contributions towards achieving a conceivable improvement of the situation are indicated in the discussion and conclusion section. Attending the implementing process of the possible changes, however, is not part of the current research. SSM promotes a continuous circle using conscious critical reflection and learning (Checkland and Poulter, 2006, p. 61). This circle is supported by the diffusion of the current research results.

4 SOFT SYSTEM MODEL

4.1 Results of the Analysis

Throughout the analysis, documentations regarding the case were examined using the following questions: (A) Which components exist and are relevant to the situation? (B) What are the concerns of the identified components? (C) How do the components relate to each other? (D) Within what context are the components embedded?

Several system components were discovered. On the one side, municipalities, country councils and national authorities are charged with response planning. On the other side, national, regional and local grid providers are responsible for executing the contingency plan in case of a power shortage. In addition, local grid providers are also involved in the planning process, cooperating with the respective municipalities. On top of this, four national responsible authorities, as mentioned in 2.2, initiate the planning procedure. Since the roles of the components within the situation are different, various concerns arise; s like: how shall the practical work be performed? Is the plan feasible, according to technical conditions of the grid? Who will be affected by the decisions made? How can the resulting response plan be used? Moreover, relations between system components can cause the grounds for further concerns. They can be based on power structures as well as on discomfort regarding collaboration or workload. As a result of the separation between planning and execution, without adequate feedback, the commitment of actors may fade away during day-by-day business. This can also affect awareness about the contextual frame. Aside from that, the complexity of the context provides an obstacle to holistic planning, although the holistic view is a necessary requirement for investigating all interdependencies. Since a power shortage can have cascading effects on other infrastructures, national security, the economy, and society can all be affected. Not least, power production and distribution also leads to thoughts about economic and environmental issues for many of involved parties. The system components and their interactions in the context derived from the analysis

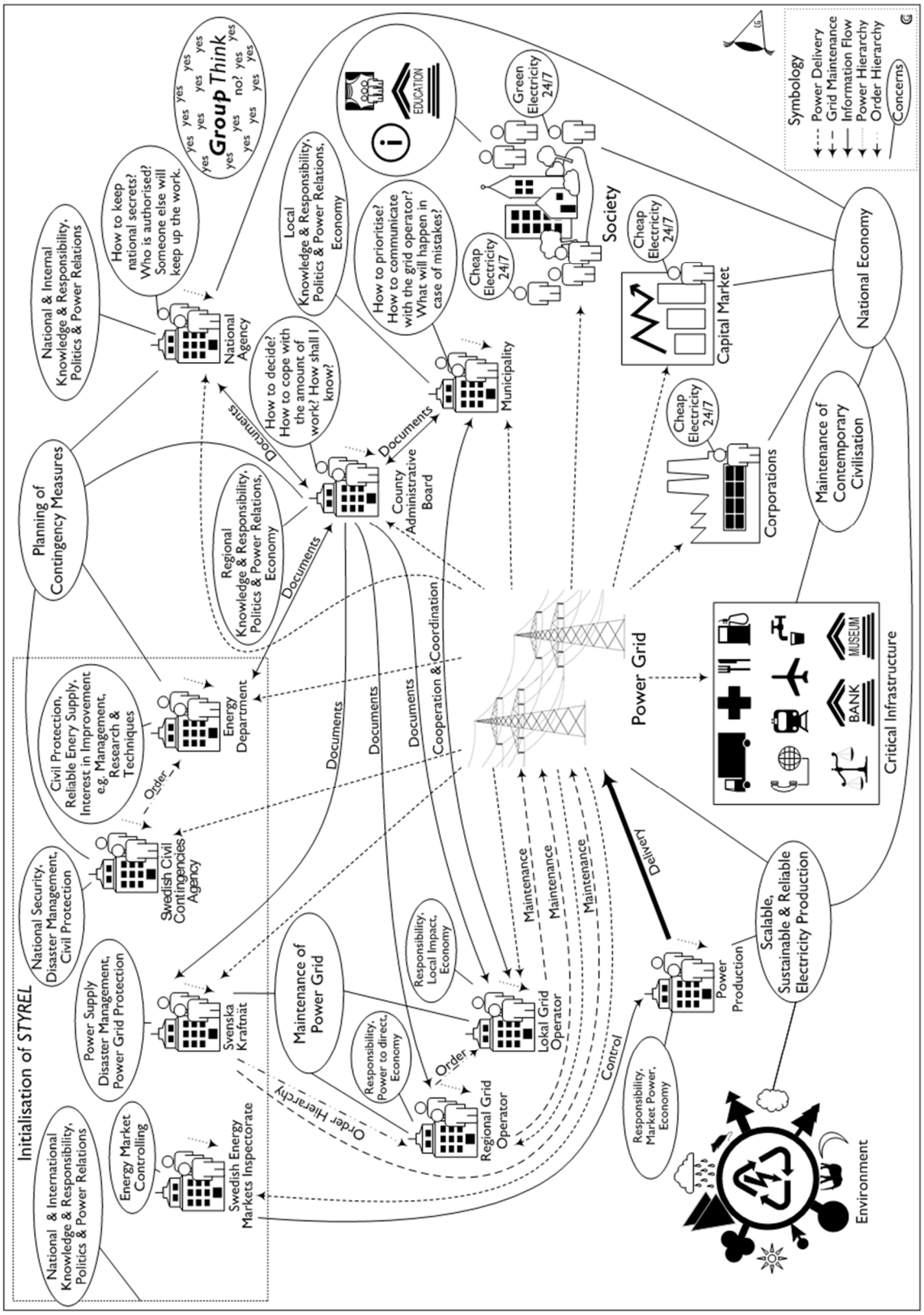

Figure 1: Rich Picture of the Problem Situation.

interactions in the context derived from the analysis above provide the basis for the representations in the next section, which elaborates on the conceptual model performing *S2 - S4*.

4.2 Conceptual System Model (1-3)

4.2.1 Rich Picture of the Problem Situation

The first sub-model of the conceptual system model is the *Rich Picture,* representing the current national constellation, as shown in Figure 1. It contains the elements, their relevant concerns, and relations in the specific situational context discovered during the analysis. Following SSM, the picture includes several different concerns and a certain level of subjectivity. Concerns are exemplary and represent a selection across the conceivable spectrum of matters. Doubts that an individual party has can also be a concern of another party or both parties, exactly as it can be an inappropriate concern.

Besides the national authorities, which initiate the planning process, other decision makers and responsibilities are shown. Their particular concerns and relations between each other are displayed. Moreover, the illustration expresses connections and (inter-) dependencies between society, environment, other CI, and the national economy, as well as the industrial and financial sectors. The fact that all of the actors within the situation also depend on power delivery is represented by dashed arrows between the power grid and the actors. Specific notable aspects appear as labels, figurative expressions, and thoughts. The latter uses straight lines with balloon messages assigned to actors. The dotted arrows indicate a hierarchical order structure within an organisation.

4.2.2 Root Definition of the System

Derived from the case analysis and the Rich Picture, the core root definition of the generic system is prepared and provided in Figure 2 below. This definition represents a generic system to support decision-making on the controlled disconnection and delivery of electricity in the case of a power shortfall.

The owner of the system (O) is the government, because it has the authority to cancel the entire transformation process (T), which constitutes the core concept of the system. Furthermore, the government has a long-term interest at a higher level in the societal and ethical aspects of the process. The grid operators are identified as the intended customers (C) of the system. Their decision-making shall be supported by adequate means produced during the transformation process of the system. Various actors (A) operate inside the conceptual system. These are professionals with different kinds of experience and decision-making power. Between them, various structures of communication and cooperation arise. The Weltanschauung (W) states that decision-making is

Core Root Definition	
A government-owned system, staffed by local, regional and national qualified professionals, which, considering legal regulations and technical limitations, supports planning and preparedness. It provides relevant information for decision-making on power supply in the case of power shortage. The system collects and prioritises power consumers that meet the criterion 'important to society' in order to preserve and maintain critical infrastructure during a crisis situation that makes an impact on local, regional or national society.	
C	grid operators of all kind (local, regional, national)
A	experts and professionals within municipalities, local grid operators, county councils and national authorities
T	need for supported qualified decision-making to enhance resilience – need met by structured information about power consumers
W	planning of decision-making is achievable and enhances emergency management
O	government
E	legal regulations and technical limitations of the grid structure

Figure 2: Core Root Definition of a Generic System to Support Decisions on Power Allocation.

something that can be planned, which enhances emergency management. From the system-owner's perspective, it may also represent another long-term interest to support the resilience of the critical system. Legal regulations as well as technical limitations in the control abilities of power grid components constitute the environmental constraints (E) of the presented generic system.

4.2.3 Action Model

An action model, as Figure 3 demonstrates, is designed following the statements in the core root definition, which help to abstract the thinking from the current implementation. The model presents relevant actions during response planning to obtain support for decisions on power allocation in case of a power shortage. To identify power consumers in need is one of these actions. Classification criteria are needed as well as an understanding about how to use them, observing potential subjectivity. Associated emergencies and their different requirements for decision-making and measurement constitute the crisis scenarios. Moreover, technical limitations to power grid control have to be investigated. Power consumers are classified using criteria. Grid-control abilities affect how consumers can be served.

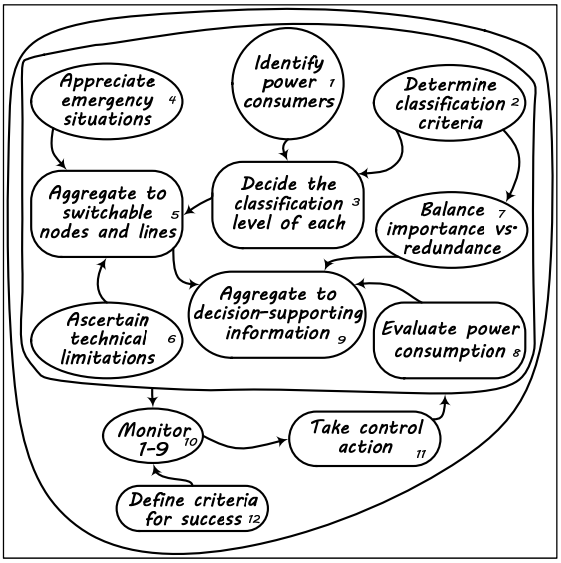

Figure 3: Conceptual Action Model.

Balancing between importance and a reasonable level of redundancy within a region influences information aggregation. Information about power consumption completes the decision.

The monitoring and documentation of the process steps, and results of decisions made, are both necessary to ensure the quality of the process and to provide a basis for improvement. Defined performance criteria assist in the appreciation of the success of the approach and enable the people responsible to take control actions in case of variation. Due to the fact that various actors within the public and private sectors involved in the system, individual goals can differ and the system owner may request an adequate control ability. This control subsystem controls the activities performed during a transformation process by means of a feedback loop.

4.3 Debate and Further Action

The conceptual system model, containing the sub-models, was presented during semi-structured face-to-face interviews. The participants was encouraged to compare the models with the real-world situation. Open-ended questions were asked in order to gain stakeholder perspectives and individual opinions.

Although the Rich Picture was considered to be complex and full of detail by all at the first glance, after a short time and closer inspection, the content and interactions became clear and the participants themselves became interested in further discussion. Many wanted to talk about details that they were particularly interested in. Often, these details were related to their own experiences and concerns. However, aspects concerning the work of others were also noticed with interest. There was a strong consensus that CI and possible cascade effects caused by a power shortfall are central points of their planning work. All of the participants expressed the opinion that the Rich Picture could be used to heighten the general public's awareness regarding the complexity of the situation. In addition, many said they would like to see this picture implemented as a form of interactive training, which would enable the individuals responsible to explore the situation, as well as the planning and response procedure, as a process by themselves, step-by-step.

The root definition and the action model were approached with slight difficulty by some, and were perceived as being less accessible than the Rich Picture. After a short investigation, this opinion changed fast. Participants could see benefits in the generality and experienced the activities as valuable and reasonable. Almost all of the people interviewed could imagine using the action model in other emergency preparedness planning settings too. Some participants mentioned a desire to have a more straightforward process model providing more distinct sequences for the activities. All participants considered a control cycle to be important for their planning work, which is notably absent in the existing

emergency response planning procedure.

The participants felt that more time for detailed consideration, and also further discussion with other actors involved in the procedure, would be desirable. Such collaboration can help people to exchange insights, gain a shared understanding about "expected performance", and, not least, to overcome flaws within the procedure. Further changes and actions was suggested as follows: (A) The usage of the resulting response plan needs clarifying, (B) The expected engagement during the planning activities needs to be communicated, (C) A feedback-loop has to be initiated to improve the procedure and to help actors to stay motivated, (D) Adapted how-to guides for planning activities can be developed in order to lower entry barriers, particularly for new personnel.

5 DISCUSSION AND CONCLUDING REMARKS

One recurring concern in studies within emergency management in Sweden is the need for adequate information paths: both *inside* a system, between actors during planning activities, and *outwardly,* to affected people and groups during emergencies (Enander et al., 2015; Hansén, 2009; Olofsson, 2011; Palm, 2009). Formal and informal practices to reach dedicated stakeholder groups have been presented.

This paper provides an informal basis for establishing communication and encouraging collaboration. First, a Rich Picture was designed, based on the literature analysis. It visualises the structures and (inter-) dependencies between the stakeholders involved, and their communication paths related to the planning process. All known actors are included and their concerns are exemplified. Since the space is limited, just a few issues are specified. However, they do not exclude additional relevant concerns, nor are the formulated thoughts limited to one special group of stakeholders. During the interview, one participant remarked that the secrecy ascribed to the exchanged information was not noted in the picture. Aside from the fact that this can be done easily, the intention during modelling was to keep the complexity manageable for the beholder. Such supplementary information can be valuable and readily interpretable in interactive representations or adapted views concerned with specific aspects, such as information security.

Deduced from the case and problem situation, the core root definition of the generic system was then outlined. The system definition abstracts from the concrete real-world setting, and focuses in on the purpose and circumstances of a generic system, as well as on responsible actors within their different roles. While establishing the core root definition, abstractions are made to obtain a generally valid system definition, with respect to the aim intended by the initial case.

The action model completes the conceptual soft systems analysis model. Meaningful and generally valid activities are developed by an investigation of the core root definition with respect to the research question. The model provides insights for improving collaborative response planning to power shortages. The people interviewed appreciated the value of the generic action model during overarching national response planning. They also perceived its usefulness in other contexts, such as water and fuel emergencies, and even in a more holistic approach for emergency response planning generally. The action model can be adapted to other national or sector-based contexts, e.g., by using modified keywords. It can also be used as a tool to consider conceivable dependencies and local, regional, and national resilience. It makes no claims over the due sequence of activities within an associated transformation process respective process model. Therefore, developing a (reference) process model can be an activity supporting change, according to *S7*. In consequence, the level of flexibility will be reduced for the advantage of lower entry obstacles and a relieved work flow. In the specification of such a model, responsibilities should be formulated and the adequate implementation of a feedback loop considered. In addition, security concerns can be specified, as well as determining authorisation levels regarding access to information.

Furthermore, another control cycle can be modelled in addition to the action model. This second control cycle controls the kind of monitoring, the success criteria, and the control actions needed in order to enable supervision of the controlling activities. Key indicators that facilitate the controlling of the level of success are called the '3 Es' in SSM. Those are *efficacy*, *efficiency* and *effectiveness,* and can be added to the activities and the first control cycle of the action model presented in Section 4.2.3. Thus, it can be assessed whether the measurements work, whether the right activities are performed to meet long-term interests, and whether resource allocation is sparing (Checkland, 1989). The indicator *efficiency* needs careful consideration in the context of power allocation, since efficiency and resilience are slightly contrary concepts. The government should not only put trust in communities' ability to adapt and be resilient (Bulley, 2013); it also has to encourage partnership and communication in order to

reach the favoured collaboration before, during and after a crisis (Powley, 2009; Ödlund, 2010). Such indicators were not detected through the case analysis and interviews. Within the paper, performance indicators are not substantiated due to the generality of the conceptual soft system analysis model.

Since power allocation for power consumers, besides technical constraints, comes with ethical and political concerns, the SSM approach was considered to be informative by the respondents in this paper. As described in Section 4.2, the approach provides a means for structuring the complex situation of collaborative national response planning. The case reported on herein, *STYREL*, shows that emergency response planning is characterised by multiple stakeholders providing different views and perspectives in a distributed environment. Section 4.3 suggests that SSM enabled an open mind-set among the people interviewed, facilitating discussion and suggestions for improvements. As such, increased comprehension of this type can provide a good basis for further improvement of organisational learning and knowledge management. In consequence, these improvements can provide a solid support for achieving reliable decision processes and support for decisions. Thus, applying SSM in the current stage of the emergency preparedness and response planning process resulted in an improved understanding of the complexity of the process and the relationships between the involved parties.

ACKNOWLEDGEMENTS

This research is supported by the Swedish Energy Department alongside the project: "Från myndighet till medborgare och tillbaka: En studie av samverkan och kommunikation inom ramen för Styrel".

REFERENCES

Avison, D. E., and Taylor, V. (1997). Information systems development methodologies: A classification according to problem situation. *Journal of Information Technology, 12*(1), 73–81.

Bergman, L. (1997). Fungera den nya elmarknaden? *Ekonomisk Debatt, 25*(7), 407–413.

Bertalanffy, L. von (1968). *General System Theory: Foundations, Development, Applications.* New York: Braziller.

Boin, A., and McConnell, A. (2007). Preparing for Critical Infrastructure Breakdowns: The Limits of Crisis Management and the Need for Resilience. *Journal of Contingencies and Crisis Management, 15*(1), 50–59.

Boulding, K. E. (1956). General systems theory - The skeleton of science. *Management Science, 2*(3), 197–208.

Bulley, D. (2013). Producing and Governing Community (through) Resilience. *Politics, 33*(4), 265–275.

Checkland, P. B. (1972). Towards a systems-based methodology for real-world problem solving. *Journal of Systems Engineering, 3*(2), 87–116.

Checkland, P., and Poulter, J. (2006). *Learning for action: A short definitive account of soft systems methodology and its use for practitioner, teachers, and students.* Chichester: Wiley.

Checkland, P., and Scholes, J. (1999). *Soft systems methodology in action: A 30-year retrospective* ([New ed.]). Chichester, Eng., New York: Wiley.

Checkland, P. B. (1989). Soft Systems Methodology. *Human Systems Management*. (8), 273–289.

Cundill, G., Cumming, G. S., Biggs, D., and Fabricius, C. (2012). Soft systems thinking and social learning for adaptive management. *Conservation biology : Journal of the Society for Conservation Biology, 26*(1), 13–20.

Energy Department (Ed.) (2014). *Styrel: Handbok för styrels planeringsomgång 2014–2015*. ET2013:23.

Emery, F. E., and Trist, E. L. (1960). Socio-technical systems. In C. W. Churchman & M. Verhulst (Eds.), *Management Science Models and Techniques* (2nd ed., pp. 83–97). Pergamon.

Enander, A., Hede, S., and Lajksjö, Ö. (2015). Why Worry?: Motivation for Crisis Preparedness Work among Municipal Leaders in Sweden. *Journal of Contingencies and Crisis Management, 23*(1), 1–10.

Grochla, E. (1974). Systemtheoretisch-kybernetische Modellbildung betrieblicher Systeme. In E. Grochla, H. Fuchs, & H. Lehmann (Eds.), *Schmalenbachs Zeitschrift für betriebswirtschaftliche Forschung: Vol. 3. Systemtheorie und Betrieb* (pp. 11–22). Opladen: Westdt. Verlag.

Hakami, A., Kumar, A., Shim, S. J., and Nahleh, Y. A. (2013). Application of Soft Systems Methodology in Solving Disaster Emergency Logistics Problems. *International Journal of Mechanical, Aerospace, Industrial, Mechatronic and Manufacturing Engineering, 7*(12), 2470–2477.

Hansén, D. (2009). Effects of Buzzwords on Experiential Learning: The Swedish Case of 'Shared Situation Awareness'. *Journal of Contingencies and Crisis Management, 17*(3), 169–178.

Johansson, J., and Hassel, H. (2014). Impact of Functional Models in a Decision Context of Critical Infrastructure Vulnerability Reduction. In M. Beer, S.-K. Au, & J. W. Hall (Eds.), *2nd International Conference on Vulnerability and Risk Analysis and Management (ICVRAM) and the 6th International Symposium on Uncertainty, Modeling, and Analysis (ISUMA),* 577–586.

Kieser, A. (2001). Konstruktivistische Ansätze. In A. Kieser (Ed.), *Organisationstheorien* (4th ed.). Stuttgart: Kohlhammer.

Maliszewski, P. J., and Perrings, C. (2012). Factors in the resilience of electrical power distribution infrastructures. *Applied Geography, 32*(2), 668–679.

Mendoza, G. A., and Prabhu, R. (2006). Participatory modeling and analysis for sustainable forest management: Overview of soft system dynamics models and applications. *Forest Policy and Economics, 9*(2), 179–196.

Mingers, J., and Taylor, S. (1992). The Use of Soft Systems Methodology in Practice. *Journal of the Operational Research Society, 43*(4), 321–332.

Mumford, E. (2006). The story of socio-technical design: reflections on its successes, failures and potential. *Information Systems Journal*, (16), 317–342.

Nilsson, J. (2010). What's the Problem? Local Officials' Conceptions of Weaknesses in their Municipalities' Crisis Management Capabilities. *Journal of Contingencies and Crisis Management, 18*(2), 83–95.

Olofsson, A. (2011). Organizational Crisis Preparedness in Heterogeneous Societies: The OCPH Model. *Journal of Contingencies and Crisis Management, 19*(4), 215–226.

Palm, J. (2009). Emergency Management in the Swedish Electricity Grid from a Household Perspective. *Journal of Contingencies and Crisis Management, 17*(1), 55–63.

Penrose, J. M. (2000). The role of perception in crisis planning. *Public Relations Review, 26*(2), 155–171.

Powley, E. H. (2009). Reclaiming resilience and safety: Resilience activation in the critical period of crisis. *Human Relations, 62*(9), 1289–1326.

Pramanik, R., Ekman, O., Hassel, H., and Tehler, H. (2015). Organizational Adaptation in Multi-Stakeholder Crisis Response: An Experimental Study. *Journal of Contingencies and Crisis Management, 23*(4), 234–245.

Proches, C. N. G., and Bodhanya, S. (2015). An Application of Soft Systems Methodology in the Sugar Industry. *International Journal of Qualitative Methods, 14*(1), 1–15.

Rinaldi, S. M., Peerenboom, J. P., and Kelly, T. K. (2001). Identifying, understanding, and analyzing critical infrastructure interdependencies. *IEEE Control Systems Magazine, 21*(6), 11–25.

Rüegg-Stürm, J. (2001). *Organisation und organisationaler Wandel: Eine theoretische Erkundung aus konstruktivistischer Sicht. Organisation und Gesellschaft.* Wiesbaden: VS Verlag für Sozialwissenschaften.

Smyth, D. S., and Checkland, P. B. (1976). Using a systems approach: the structure of root definitions. *Journal of Applied Systems Analysis, 5*(1), 75–83.

Sørensen, C. G., Fountas, S., Nash, E., Pesonen, L., Bochtis, D., et al. (2010). Conceptual model of a future farm management information system. *Computers and Electronics in Agriculture, 72*, 37–47.

van Laere, J. (2013). Wandering Through Crisis and Everyday Organizing; Revealing the Subjective Nature of Interpretive, Temporal and Organizational Boundaries. *Journal of Contingencies and Crisis Management, 21*(1), 17–25.

Wimelius, M. E., and Engberg, J. (2015). Crisis Management through Network Coordination: Experiences of Swedish Civil Defence Directors. *Journal of Contingencies and Crisis Management, 23*(3), 129–137.

Ödlund, A. (2010). Pulling the Same Way? A Multi-Perspectivist Study of Crisis Cooperation in Government. *Journal of Contingencies and Crisis Management, 18*(2), 96–107.

Österle, H., Becker, J., Frank, U., Hess, T., Karagiannis, D., et al. (2011). Memorandum on design-oriented information systems research. *European Journal of Information Systems*, (20), 7–10.

Network of $M/M/1$ Cyclic Polling Systems

Carlos Martínez-Rodríguez[1], Raúl Montes-de-Oca[2] and Patricia Saavedra[2]
[1]*Universidad Autónoma de la Ciudad de México, Calzada Ermita Iztapalapa 4163, Col. Lomas de Zaragoza, 09620, Ciudad de México, Mexico*
[2]*Universidad Autónoma Metropolitana-Iztapalapa, Av. San Rafael Atlixco 186, Col. Vicentina, 09340, Ciudad de México, Mexico*
carlos.martinez@uacm.edu.mx, {momr, psb}@xanum.uam.mx

Keywords: Networks of Cyclic Polling System, Exhaustive Policy, Exponential Inter-arrivals Times.

Abstract: This paper presents a Network of Cyclic Polling Systems that consists of two cyclic polling systems with two queues each when transfer of users from one system to the other is imposed. This system is modelled in discrete time. It is assumed that each system has exponential inter-arrival times and the servers apply an exhaustive policy. Closed form expressions are obtained for the first and second moments of the queue's lengths for any time.

1 INTRODUCTION

A Cyclic Polling System (CPS) consists of multiple queues that are attended by a single server in cyclic order. Users arrive at each queue according to independent processes which are independent of the service times. The server attends each queue according to a service policy previously established. When the server finishes, it moves to the next queue incurring in a switchover time. It will be assumed that the switchover times form a sequence of independent and identically distributed random variables. A thorough analysis has been made on this subject. For an overview of the literature on polling systems, their applications and standard results, the authors refer to such surveys as: (Boon et al., 2011; Levy and Sidi, 1990), and (Vishnevskii and Semenova, 2006).

Here a Network of Cyclic Polling System (NCPS) is considered. It consists of two cyclic polling systems, each of them with two queues that are attended, according to an exhaustive policy. The exhaustive policy service consists in attending all users until the queue is emptied. The system is observed at fixed times where the length of the slot is proportional to the time service. The arrivals to each queue are assumed to be Poisson processes with independent identical distributed (i.i.d.) inter-arrival exponential times. When the servers finish, they move to the next queue incurring a switchover time. It will be assumed that the switchover times form a sequence of independent and identically distributed random variables. The novelty in this work is that the two systems are connected in the following way: the users enter the system through one of the queues. After being served instead of leaving the system, they transfer to one of the queues of the other system, see Figure 1. All the users leave the network after being attended by the two servers. This network requires considering two kinds of arrival processes at each queue. One of them corresponds to the arrival process of the users that enter the system for the first time through that queue, and the other one corresponds to the arrival of the transfer users. Specifically, in this article the authors are looking for explicit formulae for the first and second order moments at any time. The buffer occupancy method is applied. It uses the Probability Generating Function (PGF) of the joint distribution function of the queues lengths at the moment the server arrives to the queue to start its service, which is called a *polling instant*. For an overview of this method, see (Takagi, 1986; Cooper and Murray, 1969; Cooper, 1970).

This work was motivated by the subway system, where each line can be considered as a cyclic polling system and the transfer station allows the users to transfer from one line to the other. Networks of polling systems is a rather new topic with few references, and a variety of possible applications, see (Boon et al., 2011; Levy and Sidi, 1990; Vishnevskii and Semenova, 2006; Beekhuizen, 2010). Recent publications about networks of polling stations are: (Beekhuizen et al., 2008b; Beekhuizen et al., 2008a; Aoun et al., 2010; Beekhuizen and Resing, 2009;

Martínez-Rodríguez, C., Montes-de-Oca, R. and Saavedra, P.
Network of $M/M/1$ Cyclic Polling Systems.
In *Proceedings of the 6th International Conference on Operations Research and Enterprise Systems (ICORES 2017)*, pages 298-305
ISBN: 978-989-758-218-9

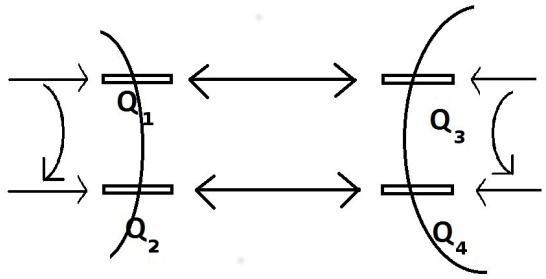

Figure 1: Example of a Network of Cyclic Polling Systems.

van den Bos and Boon, 2013). The problem of interest is to obtain performance measures for the stationary case whenever is possible.

This paper is organized as follows. In section 2 the description of the model and the corresponding notation are presented. In Section 3 the explicit formulae for the queue length processes at polling instants are given. Assuming that stationarity conditions are satisfied, the expected queue lengths processes at any time are provided in Section 4. The concluding remarks are given in section 5. Besides there is Appendix A, which gives the general calculations in order to obtain the joint PGF for the queue lengths of the NCPS.

2 DESCRIPTION OF THE MODEL

Consider an NCPS consisting of two cyclic polling systems, Γ_1 and Γ_2 with two queues each, where Q_1 and Q_2 denote the queues of Γ_1, and Q_3 and Q_4 denote the corresponding queues of Γ_2, all of them with infinite-sized buffer. In each system, a single server visits the queues in a cyclic order, where the exhaustive policy is applied. All the users after being served, transfer to the other system in the following way: users from Q_3 transfer to Q_1, and from Q_4 to Q_2, and viceversa. Users' time of arrival to the other queue is considered as the time of departure from the original queue. All customers are assumed to leave the NCPS after being attended by the two servers, see Figure 1.

Upon completion of a visit to any queue, the servers incur in a random switchover time according to an arbitrary distribution with a finite first moment. A *cycle* is defined as the time interval between two consecutive polling instants. The time period in a cycle during which the server attends a queue is called a *service period*. The intervisit time I_i of queue Q_i is defined as the period beginning at the time the server leaves Q_i in a cycle and ends at the time when queue Q_i is polled in the next cycle; its duration is given by $\tau_i(m+1)-\overline{\tau}_i(m)$. It is important to remark that the case considered in this paper is the one where the server visits the queues in a cyclic order.

At each of the queues in the network, the *total number of users* is the users that arrive for the first time to the system plus the number of transfer users from the other system. For $t \in [t, t+1)$ the arrival processes are denoted by $X_1(t), X_2(t)$, for Q_1 and Q_2 in Γ_1, respectively, and $X_3(t)$, $X_4(t)$, for Q_3 and Q_4 in Γ_2, respectively, with corresponding transfer processes $Y_3(t)$ from Q_1 to Q_3, $Y_4(t)$ from Q_2 to Q_4, $Y_1(t)$ from Q_3 to Q_1, and $Y_2(t)$ from Q_4 to Q_2. It will be supposed that the arrival and the transference processes are independent. The arrival rates at Q_i, for $i = 1,2,3,4$, are denoted by μ_i and $\hat{\mu}_i$ for the output processes, respectively. The process that considers both input-output processes will be denoted by $\tilde{X}_i(t) = X_i(t) + Y_i(t)$ with a rate $\tilde{\mu}_i = \mu_i + \hat{\mu}_i$ that satisfies $\tilde{\mu}_i < 1$, for $i = 1,2,3,4$. Denote the processes $L_i(t)$ for the queue length processes for $i = 1,2,3,4$. In some parts of the article, in order not to complicate the notation, the dependence of t will be omitted.

3 EXPECTED QUEUE LENGTHS PROCESSES AT DISCRETE TIME

In this section it is assumed that the service times are proportional to the length of the slot, so that the arrival rate and the output rates coincide with the mean of the corresponding processes.

As usual, the j-th derivative of a function Ψ is denoted by $\Psi^{(j)}$, $j = 1,2,3,\ldots$. When Ψ is a function of m variables, the notation $D_j\Psi$ will be used for the j-th partial derivative of Ψ, $j = 1,2,\ldots,m$. For $i = 1,2,3,4$, consider $z_i \in \mathbb{C}$ and denote by τ_i the polling instant at queue Q_i and by $\overline{\tau}_i$ the instant when the server leaves the queue and starts a switchover time. In order to obtain the joint PGF for the number or users residing in queue Q_i, when it is polled, for $t \geq 0$ the PGF is considered for each of the arrival processes $X_i(t)$, the transfer process $Y_i(t)$, and the processes $\tilde{X}_i(t)$, for $i = 1,2,3,4$. The corresponding PGFs for each of the processes are:

$$P_i(z_i) = \mathbb{E}\left[z_i^{X_i(t)}\right], \quad \hat{P}_i(z_i) = \mathbb{E}\left[z_i^{Y_i(t)}\right], \tag{1}$$

and

$$\tilde{P}_i(z_i) = \mathbb{E}\left[z_i^{\tilde{X}_i(t)}\right], \tag{2}$$

with

$$\mu_i = \mathbb{E}[X_i(t)] = P_i^{(1)}(1), \tag{3}$$

and $\hat{\mu}_i, \tilde{\mu}_i$ for the mean of the respective processes $\hat{Y}_i(t)$ and $\tilde{X}_i(t)$ for $i = 1,2,3,4$. The PGF for the service period is defined by:

$$\begin{aligned} &S_i(z_i) = \mathbb{E}\left[z_i^{\bar{\tau}_i - \tau_i}\right], \text{ with} \\ &s_i = \mathbb{E}\left[\bar{\tau}_i - \tau_i\right], \text{ for } i = 1,2,3,4. \end{aligned} \tag{4}$$

In a similar manner, the PGF for the switchover time of the server from the moment it stops attending a queue to the time of arrival to the next queue is given by

$$R_i(z_i) = \mathbb{E}\left[z_i^{\tau_{i+1} - \bar{\tau}_i}\right], \tag{5}$$

with the first moment

$$r_i = \mathbb{E}\left[\tau_{i+1} - \bar{\tau}_i\right] \text{ for } i = 1,2,3,4. \tag{6}$$

Observe that the number of users in the queue at times $\bar{\tau}_i$ is zero, i.e., $L_i(\bar{\tau}_i) = 0$ for $i = 1,2,3,4$, and in Γ_1, the number of users at the moment the server stops attending the queue is given by the number of users present at the moment it arrives plus the number of arrivals during the service period plus the users that arrived after being served by the second server. Then the length $L_i(\bar{\tau}_1)$ is given by

$$L_i(\bar{\tau}_1) = L_i(\tau_1) + X_i(\bar{\tau}_1 - \tau_1) + Y_i(\bar{\tau}_1 - \tau_1), \tag{7}$$

for $i = 1,2,3,4$. As it is known, the gambler's ruin problem can be used to model the server's busy period in a cyclic polling system. The result that relates the gambler's ruin problem with the busy period of the server is a generalization of the result given in (Takagi, 1986), Chapter 3. Denote by $\tilde{L}_j$, $j = 0,1,2,\ldots$, the capital equal to j units, and by $g_{n,k}$ the probability of the event no ruin before the n-th period beginning with the initial capital $\tilde{L}_0$, considering a capital equal to k units after $n-1$ events, i.e., given $n \in \{1,2,\ldots\}$, and $k \in \{0,1,2,\ldots\}$, $g_{n,k} := P\left\{\tilde{L}_j > 0, j = 1,\ldots,n, \tilde{L}_n = k\right\}$. This probability can be written as:

$$\begin{aligned} g_{n,k} &= P\left\{\tilde{L}_j > 0, j = 1,\ldots,n, \tilde{L}_n = k\right\} \\ &= \textstyle\sum_{j=1}^{k+1} g_{n-1,j} P\left\{\tilde{X}_n = k - j + 1\right\} \\ &= \textstyle\sum_{j=1}^{k+1} g_{n-1,j} P\left\{X_n + Y_n = k - j + 1\right\} \\ &= \textstyle\sum_{j=1}^{k+1} \sum_{l=1}^{j} g_{n-1,j} P\left\{X_n = k - j - l + 1\right\} \\ &\cdot P\left\{Y_n = l\right\}. \end{aligned} \tag{8}$$

Let $G_n(z)$ and $G(z,w)$ be the polynomials defined by

$$\begin{aligned} &G_n(z) = \textstyle\sum_{k=0}^{\infty} g_{n,k} z^k, \text{ for } n = 0,1,\ldots, \text{ and} \\ &G(z,w) = \textstyle\sum_{n=0}^{\infty} G_n(z) w^n, \end{aligned} \tag{9}$$

for $z, w \in \mathbb{C}$, where it is obtained that

$$g_{0,k} = P\left\{\tilde{L}_0 = k\right\}. \tag{10}$$

In particular for $k = 0$,

$$\begin{aligned} g_{n,0} &= G_n(0) = P\left\{\tilde{L}_j > 0, \tilde{L}_n = 0\right\} \\ &= P\left\{T = n\right\}, \end{aligned} \tag{11}$$

for $j < n$ and the ruin time T. Furthermore,

$$\begin{aligned} G(0,w) &= \textstyle\sum_{n=0}^{\infty} G_n(0) w^n \\ &= \textstyle\sum_{n=0}^{\infty} P\left\{T = n\right\} w^n = \mathbb{E}\left[w^T\right], \end{aligned} \tag{12}$$

is the PGF of T. The gambler's ruin occurs after the n-th game, i.e., the queue becomes empty after n steps, starting with $\tilde{L}_0$ users.

Proposition 1. *For $n \geq 0$, $z, w \in \mathbb{C}$, $z \neq 0$,*

$$G_n(z) = \frac{1}{z}\left[G_{n-1}(z) - G_{n-1}(0)\right]\tilde{P}_i(z).$$

Furthermore,

$$G(z,w) = \frac{zF_i(z) - w\tilde{P}_i(z)\,G(0,w)}{z - wR_i(z)}, \tag{13}$$

$z - wR_i(z) \neq 0$, with a unique pole in the unit circle, which has the form $z = \tilde{\theta}_i(w)$ and satisfies

i) $\tilde{\theta}_i(1) = 1$,

ii) $\tilde{\theta}_i^{(1)}(1) = 1/[1 - \tilde{\mu}_i]$,

iii) $\tilde{\theta}_i^{(2)}(1) = \tilde{\mu}_i/(1 - \tilde{\mu}_i)^2 + \tilde{\sigma}/(1 - \tilde{\mu}_i)^3$,

for $i = 1,2,3,4$.

Proof. Similar to the one given by Takagi (Takagi, 1986) in pp. 45-47. □

In order to model the NCPS it is necessary to consider the users arrival to each queue of Γ_1 at polling instants of system Γ_2. The PGF of the queue length of system Γ_1 at polling instants of Γ_2 is defined as

$$F_{i,i+2}(z_i; \tau_{i+2}) = \mathbb{E}\left[z_i^{L_i(\tau_{i+2})}\right], \tag{14}$$

for $z_i \in \mathbb{C}, i = 1,2,3,4$. Using this expression, it is possible to define the joint PGF for Γ_1, $z_1, z_2 \in \mathbb{C}$:

$$\begin{aligned} &\mathbb{E}\left[z_1^{L_1(\tau_3)} z_2^{L_2(\tau_3)}\right] = \mathbb{E}\left[z_1^{L_1(\tau_3)}\right]\mathbb{E}\left[z_2^{L_2(\tau_3)}\right] \\ &= F_{1,3}(z_1; \tau_3) F_{2,3}(z_2; \tau_3) =: \mathbb{F}_3(z_1, z_2; \tau_3). \end{aligned} \tag{15}$$

Similar expressions are obtained for the rest of the

queues which can be summarized by

$$\begin{aligned}&\mathbb{F}_j(z_1,z_2;\tau_j),\ \text{for } j=3,4 \text{ and}\\&\mathbb{F}_j(z_3,z_4;\tau_j),\ \text{for } j=1,2,\end{aligned}\tag{16}$$

for $z_i\in\mathbb{C}$, $i=1,2,3,4$. Now the joint PGF will be determined for the times that the servers visit each queue in their corresponding system, i.e., $t\in\{\tau_1,\tau_2,\tau_3,\tau_4\}$:

$$\mathbf{F}_j:=\mathbf{F}_j(z_1,z_2,z_3,z_4;\tau_j)=\mathbb{E}\left[\prod_{i=1}^4 z_i^{L_i(\tau_j)}\right]\tag{17}$$

for $z_i\in\mathbb{C}$, $i,j=1,2,3,4$. With the purpose of finding the number of users present in the network when the server ends attending queue Q_1 of systems Γ_1, it is gotten that

$$\begin{aligned}\mathbf{F}_1&=\mathbb{E}\left[z_1^{L_1(\bar\tau_1)}z_2^{L_2(\bar\tau_1)}z_3^{L_3(\bar\tau_1)}z_4^{L_4(\bar\tau_1)}\right]\\&=\mathbb{E}\left[z_2^{L_2(\bar\tau_1)}z_3^{L_3(\bar\tau_1)}z_4^{L_4(\bar\tau_1)}\right]\\&=\mathbb{E}\left[z_2^{L_2(\tau_1)+X_2(\bar\tau_1-\tau_1)+Y_2(\bar\tau_1-\tau_1)}\right.\\&\cdot z_3^{L_3(\tau_1)+X_3(\bar\tau_1-\tau_1)+Y_3(\bar\tau_1-\tau_1)}\\&\left.z_4^{L_4(\tau_1)+X_4(\bar\tau_1-\tau_1)+Y_4(\bar\tau_1-\tau_1)}\right].\end{aligned}\tag{18}$$

This is obtained using equation (7). Now, for $z_1,z_2,z_3,z_4\in\mathbb{C}$,

$$\begin{aligned}\mathbf{F}_1&=\mathbb{E}\left[z_2^{L_2(\tau_1)}z_2^{X_2(\bar\tau_1-\tau_1)}z_2^{Y_2(\bar\tau_1-\tau_1)}z_3^{L_3(\tau_1)}\right.\\&\left.z_3^{X_3(\bar\tau_1-\tau_1)}z_3^{Y_3(\bar\tau_1-\tau_1)}z_4^{L_4(\tau_1)}z_4^{X_4(\bar\tau_1-\tau_1)}z_4^{Y_4(\bar\tau_1-\tau_1)}\right]\\&=\mathbb{E}\left[z_2^{L_2(\tau_1)}\left\{z_3^{L_3(\tau_1)}z_4^{L_4(\tau_1)}\right\}\left\{z_2^{X_2(\bar\tau_1-\tau_1)}\right.\right.\\&\left.z_2^{Y_2(\bar\tau_1-\tau_1)}\right\}\left\{z_3^{X_3(\bar\tau_1-\tau_1)}z_3^{Y_3(\bar\tau_1-\tau_1)}\right\}\\&\left.\left\{z_4^{X_4(\bar\tau_1-\tau_1)}z_4^{Y_4(\bar\tau_1-\tau_1)}\right\}\right]\\&=\mathbb{E}\left[z_2^{L_2(\tau_1)}\left\{z_2^{X_2(\bar\tau_1-\tau_1)}z_2^{Y_2(\bar\tau_1-\tau_1)}\right\}\right.\\&\left.\left\{z_3^{X_3(\bar\tau_1-\tau_1)}z_3^{Y_3(\bar\tau_1-\tau_1)}\right\}\left\{z_4^{X_4(\bar\tau_1-\tau_1)}z_4^{Y_4(\bar\tau_1-\tau_1)}\right\}\right]\\&\mathbb{E}\left[z_3^{L_3(\tau_1)}z_4^{L_4(\tau_1)}\right].\end{aligned}\tag{19}$$

The last equation was obtained applying the fact that the arrivals processes of the queues in each of the systems are assumed to be independent. Hence, it is possible to separate the expectation for the arrival processes at time τ_1, which is the time the server visits Q_1. Recall that $\tilde X_i(t)=X_i(t)+Y_i(t)$ for $i=2,3,4$, then it is obtained for $z_1,z_2,z_3,z_4\in\mathbb{C}$ that

$$\begin{aligned}\mathbf{F}_1&=\mathbb{E}\left[z_2^{L_2(\tau_1)}\left\{z_2^{\tilde X_2(\bar\tau_1-\tau_1)}z_3^{\tilde X_3(\bar\tau_1-\tau_1)}\right.\right.\\&\left.\left.z_4^{\tilde X_4(\bar\tau_1-\tau_1)}\right\}\right]\cdot\mathbb{E}\left[z_3^{L_3(\tau_1)}z_4^{L_4(\tau_1)}\right]=\mathbb{E}\left[z_2^{L_2(\tau_1)}\right.\\&\left.\left\{\tilde P_2(z_2)^{\bar\tau_1-\tau_1}\tilde P_3(z_3)^{\bar\tau_1-\tau_1}\tilde P_4(z_4)^{\bar\tau_1-\tau_1}\right\}\right]\\&\cdot\mathbb{E}\left[z_3^{L_3(\tau_1)}z_4^{L_4(\tau_1)}\right]\\&=\mathbb{E}\left[z_2^{L_2(\tau_1)}\left\{\tilde P_2(z_2)\tilde P_3(z_3)\tilde P_4(z_4)\right\}^{\bar\tau_1-\tau_1}\right]\\&\cdot\mathbb{E}\left[z_3^{L_3(\tau_1)}z_4^{L_4(\tau_1)}\right]=\mathbb{E}\left[z_2^{L_2(\tau_1)}\tilde\theta_1\left(\tilde P_2(z_2)\right.\right.\\&\left.\left.\tilde P_3(z_3)\tilde P_4(z_4)\right)^{L_1(\tau_1)}\right]\cdot\mathbb{E}\left[z_3^{L_3(\tau_1)}z_4^{L_4(\tau_1)}\right]\\&=\mathbf{F}_1\left(\tilde\theta_1\left(\tilde P_2(z_2)\tilde P_3(z_3)\tilde P_4(z_4)\right),z_2\right)\\&\cdot\mathbb{F}_1(z_3,z_4;\tau_1)\\&=:\mathbf{F}_1\left(\tilde\theta_1\left(\tilde P_2(z_2)\tilde P_3(z_3)\tilde P_4(z_4)\right),z_2,z_3,z_4\right).\end{aligned}\tag{20}$$

The last equalities are true because the number of arrivals to Q_4 during the time interval $[\tau_1,\bar\tau_1]$ still have not been attended by the server in Γ_2, then the users cannot transfer to Γ_1 through the queue Q_2. Therefore the number of users switching from Q_4 to Q_2 during the time interval $[\tau_1,\bar\tau_1]$ depends on the policy of transferring between the two systems. The server's switchover times are given by the general equations

$$R_i(z_1,z_2,z_3,z_4)=R_i\left(\tilde P_1(z_1)\tilde P_2(z_2)\tilde P_3(z_3)\tilde P_4(z_4)\right),$$

$z_i\in\mathbb{C}$, $i=1,2,3,4$. Then, to derive and evaluate in $z_i=1$, it is obtained that

$$D_jR_j=r_i\tilde\mu_j,i,j=1,2,3,4.\tag{21}$$

And the second order partial derivatives are given by

$$D_jD_iR_k=R_k^{(2)}\tilde\mu_i\tilde\mu_j+\mathbb{1}_{i=j}r_kP_i^{(2)}+\mathbb{1}_{i\neq j}r_k\tilde\mu_i\tilde\mu_j,\tag{22}$$

for any $i,j,k=1,2,3,4$, where $\mathbb{1}_{i=j}=1$ for $i=j$, and 0 in any other case. (Observe that in the last derivatives the evaluation in $z_i=1$, for $i,k=1,2,3,4$ is omitted, in order to simplify the notation.) Then the joint PGF for Q_1 in Γ_1 is given by

$$\begin{aligned}&\mathbf{F}_1(z_1,z_2,z_3,z_4)=R_2\left(\prod_{i=1}^4\tilde P_i(z_i)\right)\\&\cdot\mathbf{F}_2\left(z_1,\tilde\theta_2\left(\tilde P_1(z_1)\tilde P_3(z_3)\tilde P_4(z_4)\right),z_3,z_4\right),\end{aligned}\tag{23}$$

for $z_i\in\mathbb{C}$, $i=1,2,3,4$. For the rest of the queues similar expressions are gotten by an analogous argument. Now the switchover times from one queue to the other are considered, as well as the number of users present at the time the server leaves the queue to start attending the next one. In analogous way for the rest of the

NCPS it is obtained for $z_i \in \mathbb{C}$, $i = 1,2,3,4$, that

$$\begin{aligned}
&\mathbf{F}_2(z_1,z_2,z_3,z_4) = R_1\left(\prod_{i=1}^4 \tilde{P}_i(z_i)\right)\\
&\cdot\mathbf{F}_1\left(\tilde{\theta}_1\left(\tilde{P}_2(z_2)\tilde{P}_3(z_3)\tilde{P}_4(z_4)\right),z_2,z_3,z_4\right),\\
&\mathbf{F}_3(z_1,z_2,z_3,z_4) = R_4\left(\prod_{i=1}^4 \tilde{P}_i(z_i)\right)\cdot\mathbf{F}_4(z_1,z_2,\\
&z_3,\tilde{\theta}_4\left(\tilde{P}_1(z_1)\tilde{P}_2(z_2)\tilde{P}_3(z_3)\right)\Big),\\
&\mathbf{F}_4(z_1,z_2,z_3,z_4) = R_3\left(\prod_{i=1}^4 \tilde{P}_i(z_i)\right)\cdot\mathbf{F}_3(z_1,z_2,\\
&\tilde{\theta}_3\left(\tilde{P}_1(z_1)\tilde{P}_2(z_2)\tilde{P}_4(z_4)\right),z_4\Big).
\end{aligned} \tag{24}$$

From (16), the following derivatives are obtained:

$$\begin{aligned}
&D_j\mathbb{F}_i(z_1,z_2;\tau_{i+2}) = \mathbb{1}_{j\leq 2}\mathbb{F}^{(1)}_{j,i+2} \text{ and}\\
&D_j\mathbb{F}_i(z_3,z_4;\tau_{i-2}) = \mathbb{1}_{j\geq 3}\mathbb{F}^{(1)}_{j,i-2},
\end{aligned} \tag{25}$$

for $z_i \in \mathbb{C}$, $i = 1,2,3,4$, and the second order derivatives are given by

$$\begin{aligned}
D_jD_i\mathbb{F}_k(z_1,z_2;\tau_{k+2}) &= \mathbb{1}_{k\leq 2}\mathbb{1}_{j\leq 2}\mathbb{1}_{i\leq 2}\Big(\mathbb{1}_{j=i}\mathbb{F}^{(2)}_{i,k+2}\\
&\quad+\mathbb{1}_{j\neq i}\mathbb{F}^{(1)}_{j,k+2}\mathbb{F}^{(1)}_{i,k+2}\Big),\\
D_jD_i\mathbb{F}_k(z_3,z_4;\tau_{k-2}) &= \mathbb{1}_{k\geq 3}\mathbb{1}_{j\geq 3}\mathbb{1}_{i\geq 3}\Big(\mathbb{1}_{j=i}\mathbb{F}^{(2)}_{i,k-2}\\
&\quad+\mathbb{1}_{j\neq i}F^{(1)}_{j,k-2}\mathbb{F}^{(1)}_{i,k-2}\Big),
\end{aligned} \tag{26}$$

for $z_i \in \mathbb{C}$, $i = 1,2,3,4$. The following theorem shows how to find the lengths of the queues of the NCPS at polling instants according to equations (23) and (24):

Theorem 1. *Suppose that $\tilde{\mu} = \tilde{\mu}_1 + \tilde{\mu}_2 < 1$, $\hat{\mu} = \tilde{\mu}_3 + \tilde{\mu}_4 < 1$, then the number of users in the queues conforming the NCPS (24) at polling instants is*

$$\begin{aligned}
&f_j(i) = r_{j+1}\tilde{\mu}_i + \mathbb{1}_{i\neq j+1}f_{j+1}(j+1)\tfrac{\tilde{\mu}_i}{1-\tilde{\mu}_{j+1}}\\
&+\mathbb{1}_{i=j}f_{j+1}(i) + \mathbb{1}_{j=1}\mathbb{1}_{i\geq 3}\mathbb{F}^{(1)}_{i,j+1}\\
&+\mathbb{1}_{j=3}\mathbb{1}_{i\leq 2}\mathbb{F}^{(1)}_{i,j+1}
\end{aligned} \tag{27}$$

for $j = 1,3$ and $i = 1,2,3,4$, and

$$\begin{aligned}
&f_j(i) = r_{j-1}\tilde{\mu}_i\\
&+\mathbb{1}_{i\neq j-1}f_{j-1}(j-1)\tfrac{\tilde{\mu}_i}{1-\tilde{\mu}_{j-1}}\\
&+\mathbb{1}_{i=j}f_{j-1}(i) + \mathbb{1}_{j=2}\mathbb{1}_{i\geq 3}\mathbb{F}^{(1)}_{i,j-1}\\
&+\mathbb{1}_{j=4}\mathbb{1}_{i\leq 2}\mathbb{F}^{(1)}_{i,j-1}
\end{aligned} \tag{28}$$

for $j = 2,4$ and $i = 1,2,3,4$. The solution of the linear system of equations (27) and (28) is given by:

$$\begin{aligned}
&f_i(j) = (\mathbb{1}_{j=i-1} + \mathbb{1}_{j=i+1})\,r_j\tilde{\mu}_j\\
&+\mathbb{1}_{i=j}\left(\mathbb{1}_{i\leq 2}\tfrac{r\tilde{\mu}_i(1-\tilde{\mu}_i)}{1-\tilde{\mu}} + \mathbb{1}_{i\geq 2}\tfrac{\hat{r}\tilde{\mu}_i(1-\tilde{\mu}_i)}{1-\hat{\mu}}\right)\\
&+\mathbb{1}_{i=1}\mathbb{1}_{j\geq 3}\left(\tilde{\mu}_j\left(r_{i+1}+\tfrac{r\tilde{\mu}_{i+1}}{1-\tilde{\mu}}\right)+\mathbb{F}^{(1)}_{j,i+1}\right)\\
&+\mathbb{1}_{i=3}\mathbb{1}_{j\geq 3}\left(\tilde{\mu}_j\left(r_{i+1}+\tfrac{\hat{r}\tilde{\mu}_{i+1}}{1-\hat{\mu}}\right)+\mathbb{F}^{(1)}_{j,i+1}\right)\\
&+\mathbb{1}_{i=2}\mathbb{1}_{j\leq 2}\left(\tilde{\mu}_j\left(r_{i-1}+\tfrac{r\tilde{\mu}_{i-1}}{1-\tilde{\mu}}\right)+\mathbb{F}^{(1)}_{j,i-1}\right)\\
&+\mathbb{1}_{i=4}\mathbb{1}_{j\leq 2}\left(\tilde{\mu}_j\left(r_{i-1}+\tfrac{\hat{r}\tilde{\mu}_{i-1}}{1-\hat{\mu}}\right)+\mathbb{F}^{(1)}_{j,i-1}\right),
\end{aligned}$$

for $i, j = 1,2,3,4$.

Theorem 2. *Suppose $\tilde{\mu},\hat{\mu} < 1$, then from the expressions given in (23) and (24) the second order derivatives for the NCPS are obtained which, in their general form, are*

$$\begin{aligned}
\mathbf{f}_1(i,k) &= D_kD_i(R_2+\mathbf{F}_2+\mathbb{1}_{i\geq 3}\mathbb{F}_4)\\
&\quad+D_iR_2D_k(\mathbf{F}_2+\mathbb{1}_{k\geq 3}\mathbb{F}_4)\\
&\quad+D_iF_2D_k(R_2+\mathbb{1}_{k\geq 3}\mathbb{F}_4)\\
&\quad+\mathbb{1}_{i\geq 3}D_i\mathbb{F}_4D_k(R_2+\mathbf{F}_2),\\
\mathbf{f}_2(i,k) &= D_kD_i(R_1+\mathbf{F}_1+\mathbb{1}_{i\geq 3}\mathbb{F}_3)\\
&\quad+D_iR_1D_k(\mathbf{F}_1+\mathbb{1}_{k\geq 3}\mathbb{F}_3)\\
&\quad+D_i\mathbf{F}_1D_k(R_1+\mathbb{1}_{k\geq 3}\mathbb{F}_3)\\
&\quad+\mathbb{1}_{i\geq 3}D_i\mathbb{F}_3D_k(R_1+\mathbf{F}_1),\\
\mathbf{f}_3(i,k) &= D_kD_i(R_4+\mathbb{1}_{i\leq 2}\mathbb{F}_2+\mathbf{F}_4)\\
&\quad+D_iR_4D_k(\mathbb{1}_{k\leq 2}\mathbb{F}_2+\mathbf{F}_4)\\
&\quad+D_i\mathbf{F}_4D_k(R_4+\mathbb{1}_{k\leq 2}\mathbb{F}_2)\\
&\quad+\mathbb{1}_{i\leq 2}D_i\mathbb{F}_2D_k(R_4+\mathbf{F}_4),\\
\mathbf{f}_4(i,k) &= D_kD_i(R_3+\mathbb{1}_{i\leq 2}\mathbb{F}_1+\mathbf{F}_3)\\
&\quad+D_iR_3D_k(\mathbb{1}_{k\leq 2}\mathbb{F}_1+\mathbf{F}_3)\\
&\quad+D_i\mathbf{F}_3D_k(R_3+\mathbb{1}_{k\leq 2}\mathbb{F}_1)\\
&\quad+\mathbb{1}_{i\leq 2}D_i\mathbb{F}_1D_k(R_3+\mathbf{F}_3),
\end{aligned} \tag{29}$$

for $i,k = 1,2,3,4$. The second order moments are obtained solving the linear systems given by (29).

The proof is given in *Appendix A*.

4 EXPECTED QUEUE LENGTHS AT ANY TIME

Assumption 1. *(i) The arrival processes in the NCPS satisfies $\tilde{\mu},\hat{\mu} < 1$.*

(ii) Each of the queues of the NCPS is an $M/M/1$ system, with $\tilde{\rho}_i := \tilde{\mu}_i/\lambda_i < 1$, for $i = 1,2,3,4$ (observe that in the case considered $\tilde{\rho}_i = \tilde{\mu}_i$, for $i = 1,2,3,4$, given that the service time is assumed to be proportional to the length of the slot).

(iii) The switchover times have a finite first moment.

In this section it is supposed that Assumption 1 holds. Here, the idea given in (Takagi, 1986) is followed, in order to find the expected queue lengths at any time for the NCPS.

Fix $i \in \{1,2,3,4\}$. Let L_i^* be the number of users at queue Q_i at polling instants, then, following Section 3, it is obtained that

$$\begin{aligned} &\mathbb{E}[L_i^*] = f_i(i), \\ &Var[L_i^*] = \mathbf{f}_i(i,i) + \mathbb{E}[L_i^*] - \mathbb{E}[L_i^*]^2. \end{aligned} \tag{30}$$

Consider the cycle time C_i for queue Q_i with duration given by $\tau_i(m+1) - \tau_i(m)$ for $m \geq 1$. The interval between two successive regeneration points will be called regenerative cycle.

In order to guarantee that the cyclic times are a stationary state, it is assumed that each of the polling systems are stable (Boon et al., 2011; Boxma et al., 1992; Cooper et al., 1996; Levy and Sidi, 1990), which ensure the stability of each queue (Fricker and Jaibi, 1994; Vishnevskii and Semenova, 2006), and this implies the stationarity of the cyclic times (Altman et al., 1992). Therefore it is assumed that the cyclic times are stationary as Takagi did (Takagi, 1986).

Let M_i be the number of polling cycles in a regenerative cycle. The duration of the m-th polling cycle in a regeneration cycle will be denoted by $C_i^{(m)}$, for $m = 1,2,\ldots,M_i$. The mean polling cycle time is defined by

$$\mathbb{E}[C_i] = \frac{\sum_{m=1}^{M_i} \mathbb{E}\left[C_i^{(m)}\right]}{\mathbb{E}[M_i]}. \tag{31}$$

For the process $L_i(t)$, $t \geq 0$, their PGF will be denoted by $Q_i(z)$, $z \in \mathbb{C}$, which is also given by the time average of $z^{L_i(t)}$ over the regenerative cycle defined before, so it is obtained that

$$Q_i(z) = \mathbb{E}\left[z^{L_i(t)}\right] = \frac{\mathbb{E}\left[\sum_{m=1}^{M_i} \sum_{t=\tau_i(m)}^{\tau_i(m+1)-1} z^{L_i(t)}\right]}{\mathbb{E}\left[\sum_{m=1}^{M_i} (\tau_i(m+1) - \tau_i(m))\right]}, \tag{32}$$

which can be rewritten in the form

$$Q_i(z) = \frac{1}{\mathbb{E}[C_i]} \cdot \frac{1 - F_i(z)}{P_i(z) - z} \cdot \frac{(1-z)P_i(z)}{1 - P_i(z)}, \tag{33}$$

(see Section 3 in (Takagi, 1986)). The following proposition provides the expected queue lengths for each of the queues in the NCPS at any time.

Theorem 3. *For the queue lengths in the NCPS at any time, with PGF given in (33), the first and second order moments are given by*

$$Q_i^{(1)}(1) = \frac{1}{\tilde{\mu}_i(1-\tilde{\mu}_i)} \frac{\mathbb{E}(L_i^*)^2}{2\mathbb{E}[C_i]} - \sigma_i^2 \frac{\mathbb{E}[L_i^*]}{2\mathbb{E}[C_i]} \cdot \frac{1-2\tilde{\mu}_i}{(1-\tilde{\mu}_i)^2\tilde{\mu}_i^2}, \tag{34}$$

where $\sigma_i^2 = \left(Var\left[\tilde{X}_i(t)\right]\right)^2$, and

$$\begin{aligned} &\mathbb{E}[C_i]\, Q_i^{(2)}(1) = \frac{1}{\tilde{\mu}_i^3(1-\tilde{\mu}_i)^3} \Big\{ -(1-\tilde{\mu}_i)^2 \tilde{\mu}_i^2 O_{1,i}^{(2)}(1) \\ &- \tilde{\mu}_i(1-\tilde{\mu}_i)(1-2\tilde{\mu}_i) O_{1,i}(1) O_{3,i}^{(2)}(1) \\ &- -\tilde{\mu}_i^2(1-\tilde{\mu}_i)^2 O_{1,i}(1) P_i^{(2)}(1) \\ &+ 2\tilde{\mu}_i\left[(1-2\tilde{\mu}_i) O_{1,i}(1) - (1-\tilde{\mu}_i)\right]\left(O_{3,i}^{(1)}(1)\right)^2 \\ &- 2(1-\tilde{\mu}_i)(1-2\tilde{\mu}_i) O_{1,i}(1) O_{3,i}^{(1)}(1) \\ &- -2\tilde{\mu}_i^3(1-\tilde{\mu}_i)^2 O_{1,i}^{(1)}(1) \\ &- 2(1-2\tilde{\mu}_i) O_{3,i}^{(1)}(1) O_{1,i}^{(1)}(1) \\ &- 2\tilde{\mu}_i^2(1-\tilde{\mu}_i)(1-2\tilde{\mu}_i) O_{1,i}(1) O_{1,i}^{(1)}(1) \Big\}, \end{aligned} \tag{35}$$

for $i = 1,2,3,4$.

Proof. Fix $i \in \{1,2,3,4\}$ and $z \in \mathbb{C}$. To remove the singularities in (33) it is necessary to define the following analytic functions:

$$\begin{aligned} &\varphi_i(z) = 1 - F_i(z), \quad \psi_i(z) = z - P_i(z), \\ &\text{and} \qquad\qquad \varsigma_i(z) = 1 - P_i(z), \end{aligned} \tag{36}$$

then

$$\mathbb{E}[C_i]\, Q_i(z) = \frac{(z-1)\varphi_i(z) P_i(z)}{\psi_i(z)\varsigma_i(z)}. \tag{37}$$

For $k \geq 0$, define $a_k = P\{L_i^*(t) = k\}$. It is obtained that

$$\varphi_i(z) = 1 - F_i(z) = 1 - \sum_{k=0}^{+\infty} a_k z^k,$$

therefore

$$\begin{aligned} &\varphi_i^{(1)}(z) = -\textstyle\sum_{k=1}^{+\infty} k a_k z^{k-1}, \text{with} \\ &\varphi_i^{(1)}(1) = -\mathbb{E}[L_i^*(t)], \text{ and} \\ &\varphi_i^{(2)}(z) = -\textstyle\sum_{k=2}^{+\infty} k(k-1) a_k z^{k-2}, \text{ hence} \\ &\varphi_i^{(2)}(1) = \mathbb{E}[L_i^*(L_i^*-1)]. \end{aligned}$$

In the same way it is gotten that

$$\begin{aligned} &\varphi_i^{(3)}(z) = -\textstyle\sum_{k=3}^{+\infty} k(k-1)(k-2) a_k z^{k-3} \text{ and} \\ &\varphi_i^{(3)}(1) = -\mathbb{E}[L_i^*(L_i^*-1)(L_i^*-2)]. \end{aligned}$$

Expanding $\varphi_i(z)$ around $z=1$,

$$\begin{aligned}\varphi_i(z) &= \varphi_i(1)+\frac{\varphi_i^{(1)}(1)}{1!}(z-1)\\ &+ \frac{\varphi_i^{(2)}(1)}{2!}(z-1)^2+\frac{\varphi^{(3)}(1)}{3!}(z-1)^3+\ldots+\\ &= (z-1)\left\{\varphi_i^{(1)}(1)+\frac{\varphi^{(2)}(1)}{2!}(z-1)\right.\\ &\left.+\frac{\varphi_i^{(3)}(1)}{3!}(z-1)^2+\ldots+\right\}\\ &= (z-1)\,O_{1,i}(z)\end{aligned}$$

with $O_{1,i}(z)\neq 0$, given that $O_{1,i}(z)=-\mathbb{E}[L_i^*]$, where

$$\begin{aligned}O_{1,i}(z) = \varphi_i^{(1)}(1)+\tfrac{\varphi_i^{(2)}(1)}{2!}(z-1)\\ +\tfrac{\varphi_i^{(3)}(1)}{3!}(z-1)^2+\ldots+.\end{aligned} \tag{38}$$

Calculating the derivatives of $O_{1,i}(z)$, and evaluating in $z=1$, it is obtained that

$$\begin{aligned}&O_{1,i}(1)=-\mathbb{E}[L_i^*],\\ &O_{1,i}^{(1)}(1)=-\tfrac{1}{2}\mathbb{E}\left[(L_i^*)^2\right]+\tfrac{1}{2}\mathbb{E}[L_i^*]\\ &\text{and}\\ &O_{1,i}^{(2)}(1)=-\tfrac{1}{3}\mathbb{E}\left[(L_i^*)^3\right]+\mathbb{E}\left[(L_i^*)^2\right]-\tfrac{2}{3}\mathbb{E}[L_i^*].\end{aligned} \tag{39}$$

Proceeding in a similar manner for $\psi_i(z)=z-P_i(z)$ and $\varsigma_i(z)=1-P_i(z)$, it is gotten that

$$\mathbb{E}[C_i]\,Q_i(z) = \frac{O_{1,i}(z)\,P_i(z)}{O_{2,i}(z)\,O_{3,i}(z)}. \tag{40}$$

Calculating the derivative with respect to z, and evaluating in $z=1$,

$$\begin{aligned}&\mathbb{E}[C_i]\,Q_i^{(1)}(1)=\tfrac{1}{(1-\tilde{\mu}_i)^2\tilde{\mu}_i^2}\left\{\left(-\tfrac{1}{2}\mathbb{E}\left[(L_i^*)^2\right]\right.\right.\\ &\left.+\tfrac{1}{2}\mathbb{E}[L_i^*]\right)(1-\tilde{\mu}_i)(-\tilde{\mu}_i)(-\mathbb{E}[L_i^*])(1-\tilde{\mu}_i)(-\tilde{\mu}_i)\tilde{\mu}_i\\ &-\left(-\tfrac{1}{2}\mathbb{E}\left[\tilde{X}_i^2(t)\right]+\tfrac{1}{2}\tilde{\mu}_i\right)(-\tilde{\mu}_i)(-\mathbb{E}[L_i^*])\\ &-(1-\tilde{\mu}_i)(-\mathbb{E}[L_i^*])\left(-\tfrac{1}{2}\mathbb{E}\left[\tilde{X}_i^2(t)\right]+\tfrac{1}{2}\tilde{\mu}_i\right)\Big\}\\ &=\tfrac{1}{(1-\tilde{\mu}_i)^2\tilde{\mu}_i^2}\left\{-\tfrac{1}{2}\tilde{\mu}_i^2\mathbb{E}\left[(L_i^*)^2\right]+\tfrac{1}{2}\tilde{\mu}_i\mathbb{E}\left[(L_i^*)^2\right]\right.\\ &+\tfrac{1}{2}\tilde{\mu}_i^2\mathbb{E}[L_i^*]-\tilde{\mu}_i^3\mathbb{E}[L_i^*]\\ &\left.+\tilde{\mu}_i\mathbb{E}[L_i^*]\,\mathbb{E}\left[\tilde{X}_i^2(t)\right]-\tfrac{1}{2}\mathbb{E}[L_i^*]\,\mathbb{E}\left[\tilde{X}_i^2(t)\right]\right\}\\ &=\tfrac{1}{2\tilde{\mu}_i(1-\tilde{\mu}_i)}\mathbb{E}\left[(L_i^*)^2\right]\\ &-\tfrac{\frac{1}{2}-\tilde{\mu}_i}{(1-\tilde{\mu}_i)^2\tilde{\mu}_i^2}\sigma_i^2\mathbb{E}[L_i^*].\end{aligned}$$

It means that

$$\begin{aligned}Q_i^{(1)}(1) = \frac{1}{\tilde{\mu}_i(1-\tilde{\mu}_i)}\frac{\mathbb{E}\left[(L_i^*)^2\right]}{2\mathbb{E}[C_i]}\\ -\sigma_i^2\frac{\mathbb{E}L_i^*}{2\mathbb{E}[C_i]}\cdot\frac{1-2\tilde{\mu}_i}{(1-\tilde{\mu}_i)^2\tilde{\mu}_i^2}.\end{aligned}$$

Deriving again and evaluating in $z=1$, it follows that

$$\begin{aligned}&\mathbb{E}[C_i]\,Q_i^{(2)}(1)=\tfrac{1}{\tilde{\mu}_i^3(1-\tilde{\mu}_i)^3}\left\{-(1-\tilde{\mu}_i)^2\tilde{\mu}_i^2O_{1,i}^{(2)}(1)\right.\\ &-\tilde{\mu}_i(1-\tilde{\mu}_i)(1-2\tilde{\mu}_i)\,O_{1,i}(1)O_{3,i}^{(2)}(1)\\ &--\tilde{\mu}_i^2(1-\tilde{\mu}_i)^2\,O_{1,i}(1)P_i^{(2)}(1)\\ &+2\tilde{\mu}_i\left[(1-2\tilde{\mu}_i)\,O_{1,i}(1)-(1-\tilde{\mu}_i)\right]\left(O_{3,i}^{(1)}(1)\right)^2\\ &-2(1-\tilde{\mu}_i)(1-2\tilde{\mu}_i)\,O_{1,i}(1)O_{3,i}^{(1)}(1)\\ &--2\tilde{\mu}_i^3(1-\tilde{\mu}_i)^2\,O_{1,i}^{(1)}(1)\\ &-2(1-2\tilde{\mu}_i)\,O_{3,i}^{(1)}(1)O_{1,i}^{(1)}(1)\\ &\left.--2\tilde{\mu}_i^2(1-\tilde{\mu}_i)(1-2\tilde{\mu}_i)\,O_{1,i}(1)O_{1,i}^{(1)}(1)\right\},\end{aligned}$$

where $O_{1,i}(1), O_{1,i}^{(1)}(1), O_{3,i}^{(1)}(1), O_{3,i}^{(2)}(1), P_i^{(2)}(1)$ can be obtained using direct operations. □

Remark 1. *To determine the second order moments for the queue lengths, it is necessary to calculate the third derivative of the arrival processes for each of the queues.*

5 CONCLUDING REMARKS

This proposal about polling systems, that could be adressed to polling stations, using the buffer occupancy method allow to find analytical expressions for the first and second moments of the queue lengths at any time $t>0$. The extension of these results to other policies and the continuous case are object of future work.

ACKNOWLEDGEMENTS

Research supported by the UACM/ICyT/SECITI-D.F. through the project PI2014-1

REFERENCES

Altman, E., Konstantopoulos, P., and Liu, Z. (1992). Stability, monotonicity and invariant quantities in general polling systems. *Queueing Systems*, 11(1-2):35–57.

Aoun, M., Beekhuizen, P., and Argyriou, A. (2010). An analytical study of network coding in the presence of real-time messages. In *2010 IEEE International Symposium on Network Coding (NetCod)*, pages 1–6. IEEE.

Beekhuizen, P. (2010). Performance analysis of networks on chips.

Beekhuizen, P., Denteneer, D., and Adan, I. (2008a). Analysis of a tandem network model of a single-router network-on-chip. *Annals of operations research*, 162(1):19–34.

Beekhuizen, P., Denteneer, D., and Resing, J. (2008b). Reduction of a polling network to a single node. *Queueing Systems*, 58(4):303–319.

Beekhuizen, P. and Resing, J. A. C. (2009). Approximation of discrete-time polling systems via structured markov chains. In *Proceedings of the Fourth International ICST Conference on Performance Evaluation Methodologies and Tools*, page 16. ICST (Institute for Computer Sciences, Social-Informatics and Telecommunications Engineering).

Boon, M. A., Van der Mei, R., and Winands, E. M. (2011). Applications of polling systems. *Surveys in Operations Research and Management Science*, 16(2):67–82.

Boxma, O. J., Levy, H., and Yechiali, U. (1992). Cyclic reservation schemes for efficient operation of multiple-queue single-server systems. *Annals of Operations Research*, 35(3):187–208.

Cooper, R. (1970). Queues served in cyclic order: Waiting times. *Bell System Technical Journal*, 49(3):399–413.

Cooper, R. and Murray, G. (1969). Queues served in cyclic order. *Bell System Technical Journal*, 48(3):675–689.

Cooper, R. B., Niu, S.-C., and Srinivasan, M. M. (1996). A decomposition theorem for polling models: The switchover times are effectively additive. *Operations Research*, 44(4):629–633.

Fricker, C. and Jaibi, M. R. (1994). Monotonicity and stability of periodic polling models. *Queueing systems*, 15(1-4):211–238.

Levy, H. and Sidi, M. (1990). Polling systems: applications, modeling, and optimization. *IEEE Transactions on communications*, 38(10):1750–1760.

Takagi, H. (1986). *Analysis of polling models*. Cambridge, MIT Press, New York.

van den Bos, L. and Boon, M. (2013). Networks of polling systems.

Vishnevskii, V. and Semenova, O. (2006). Mathematical methods to study the polling systems. *Automation and Remote Control*, 67(2):173–220.

APPENDIX A: GENERAL CASE CALCULATIONS FOR THE PGF

Recall that (25) and (29) give the first and the second order partial derivatives, respectively. The first moments equations for the expected queue lengths at polling instants are obtained solving the system given in Theorem 1. The second moment for queue Q_1 at polling instants is given by

$$\begin{aligned}\mathbf{f}_1(1,1) &= \left(\frac{\tilde{\mu}_1}{1-\tilde{\mu}_2}\right)^2 \mathbf{f}_2(2,2) + 2\frac{\tilde{\mu}_1}{1-\tilde{\mu}_2}\mathbf{f}_2(2,1)\\ &+ \mathbf{f}_2(1,1) + \tilde{\mu}_1^2\left(R_2^{(2)} + f_2(2)\,\theta_2^{(2)}\right)\\ &+ \tilde{P}_1^{(2)}\left(\frac{f_2(2)}{1-\tilde{\mu}_2} + r_2\right) + 2r_2\tilde{\mu}_2 f_2(1).\end{aligned}$$

Similar argument allows to obtain the following general expressions for Q_1:

$$\begin{aligned}&\mathbf{f}_1(i,j) = \mathbb{1}_{i=1}\mathbf{f}_2(1,1)\\ &+\Big[(1-\mathbb{1}_{i=j=3})\,\mathbb{1}_{i+j\le 6}\,\mathbb{1}_{i\le j}\tfrac{\mu_j}{1-\tilde{\mu}_2}\\ &+(1-\mathbb{1}_{i=j=3})\,\mathbb{1}_{i+j\le 6}\,\mathbb{1}_{i>j}\tfrac{\mu_i}{1-\tilde{\mu}_2}\\ &+\mathbb{1}_{i=1}\tfrac{\mu_i}{1-\tilde{\mu}_2}\Big]\mathbf{f}_2(1,2) + \mathbb{1}_{i,j\neq 2}\left(\tfrac{1}{1-\tilde{\mu}_2}\right)^2\mu_i\mu_j\mathbf{f}_2(2,2)\\ &+\Big[\mathbb{1}_{i,j\neq 2}\tilde{\theta}_2^{(2)}\tilde{\mu}_i\tilde{\mu}_j + \mathbb{1}_{i,j\neq 2}\,\mathbb{1}_{i=j}\tfrac{\tilde{P}_i^{(2)}}{1-\tilde{\mu}_2}\\ &+\mathbb{1}_{i,j\neq 2}\,\mathbb{1}_{i\neq j}\tfrac{\tilde{\mu}_i\tilde{\mu}_j}{1-\tilde{\mu}_2}\Big] f_2(2) + \Big[r_2\tilde{\mu}_i + \mathbb{1}_{i\ge 3}\mathbb{F}_{i,2}^{(1)}\Big] f_2(j)\\ &+\Big[r_2\tilde{\mu}_j + \mathbb{1}_{j\ge 3}\mathbb{F}_{j,2}^{(1)}\Big] f_2(i) + \Big[R_2^{(2)} + \mathbb{1}_{i=j}r_2\Big]\tilde{\mu}_i\mu_j\\ &+\mathbb{1}_{j\ge 3}\mathbb{F}_{j,2}^{(1)}\Big[\mathbb{1}_{j\neq i}\mathbb{F}_{i,2}^{(1)} + r_2\tilde{\mu}_i\Big]\\ &+r_2\Big[\mathbb{1}_{i=j}P_i^{(2)} + \mathbb{1}_{i\ge 3}\mathbb{F}_{i,2}^{(1)}\tilde{\mu}_j\Big] + \mathbb{1}_{i\ge 3}\,\mathbb{1}_{j=i}\mathbb{F}_{i,2}^{(2)}.\end{aligned} \tag{41}$$

In a similar manner, expressions for $\mathbf{f}_2(i,j)$, $\mathbf{f}_3(i,j)$ and $\mathbf{f}_4(i,j)$ are obtained for $i,j = 1,2,3,4$. These expressions give place to a linear system of equations whose some of the solutions are

$$\begin{aligned}&\mathbf{f}_1(1,1) = b_3, \quad \mathbf{f}_2(2,2) = \eta_1,\\ &\mathbf{f}_3(3,3) = \eta_2, \quad \mathbf{f}_4(4,4) = a_{38}\eta_2 + a_{39}K_{29},\end{aligned}$$

where

$$\begin{aligned}&\eta_1 = \tfrac{b_2}{1-b_1}, && \eta_2 = \tfrac{b_5}{1-b_4},\\ &N_1 = a_2K_{12} + a_3K_{11} + K_1, && N_2 = a_{12}K_2 + a_{13}K_5 + K_{15},\\ &b_1 = a_1a_{11}, && b_2 = a_{11}N_1 + N_2,\\ &b_3 = a_1\left(\tfrac{b_2}{1-b_1}\right) + N_1, && N_3 = a_{29}K_{39} + a_{30}K_{38} + K_{28}\\ &N_4 = a_{39}K_{29} + a_{40}K_{30} + K_{40}, && b_4 = a_{28}a_{38},\\ &b_5 = a_{28}N_4 + N_3, && b_6 = a_{38}\left(\tfrac{b_5}{1-b_4}\right) + N_4.\end{aligned}$$

Extended Shortest Path Problem
Generalized Dijkstra-Moore and Bellman-Ford Algorithms

Maher Helaoui
Higher Institute of Business Administration, University of Gafsa, Rades, Tunisia
Maher.Helaoui@gmail.com

Keywords: Combinatorial Optimization, Valuation Structure, Extended Shortest Path Problem, Longest Path Problem, Generalized Dijkstra-Moore Algorithm, Generalized Bellman-Ford Algorithm.

Abstract: The shortest path problem is one of the classic problems in graph theory. The problem is to provide a solution algorithm returning the optimum route, taking into account a valuation function, between two nodes of a graph G. It is known that the classic shortest path solution is proved if the set of valuation is $\mathbb{R}$ or a subset of $\mathbb{R}$ and the combining operator is the classic sum $(+)$. However, many combinatorial problems can be solved by using shortest path solution but use a set of valuation not a subset of $\mathbb{R}$ and/or a combining operator not equal to the classic sum $(+)$. For this reason, relations between particular valuation structure as the semiring and diod structures with graphs and their combinatorial properties have been presented. On the other hand, if the set of valuation is $\mathbb{R}$ or a subset of $\mathbb{R}$ and the combining operator is the classic sum $(+)$, a longest path between two given nodes s and t in a weighted graph G is the same thing as a shortest path in a graph $-G$ derived from G by changing every weight to its negation.
In this paper, in order to give a general model that can be used for any valuation structure we propose to model both the valuations of a graph G and the combining operator by a valuation structure S. We discuss the equivalence between longest path and shortest path problem given a valuation structure S. And we present a generalization of the shortest path algorithms according to the properties of the graph G and the valuation structure S.

1 INTRODUCTION

The shortest path problem is one of the classic problems in graph theory. The problem is to provide a solution algorithm returning the optimum route, taking into account a valuation function, between two nodes of a graph G.
In (Shimbel, 1955; Ford and Lester, 1956; Bellman, 1958; Sedgewick and Wayne, 2011) the classic shortest path solution is proved if

- the set of valuation is $\mathbb{R}$ or a subset of $\mathbb{R}$.
- the combining operator is the classic sum $(+)$

Many combinatorial problems like Fuzzy, Weighted, Probabilistic and Valued Constraint Satisfaction Problem (Schiex et al., 1995; Cooper, 2003; Cooper, 2004; Allouche et al., 2009) use a set of valuation E not subset of $\mathbb{R}$ and a combining operator $\oplus \neq +$ for weighted, fuzzy, probabilistic ... valuations. In (Cooper, 2003), the shortest path algorithm has been used to solve Fuzzy and Valued Constraint Satisfaction Problem.
In (Erickson, 2010), author observes that the classical maximum flow problem (Ford and Fulkerson, 1955; Ford and Fulkerson, 1962) in any directed planar graph G can be reformulated as a parametric shortest path problem in the oriented dual graph G^*. In (Cohen et al., 2004; Helaoui et al., 2013), a submodular decompositions approach has been presented to solve Valued Constraint Satisfaction Problem. This solution use the maximum flow algorithm.
Dijkstra-Moore and Bellman-Ford Algorithms are the most known algorithmic solutions for the shortest path problem.

- Since 1971, the Dijkstra-Moore Algorithm has been used if the set of valuation is $\mathbb{R}^+$ or a subset of $\mathbb{R}^+$ and the combining operator is the classic sum $(+)$.
- The Bellman-Ford Algorithm is the result of (Shimbel, 1955; Ford and Lester, 1956; Bellman, 1958) works. It is used if the set of valuation is $\mathbb{R}$ or a subset of $\mathbb{R}$ and the combining operator is the classic sum $(+)$.

As many combinatorial problems can be solved by using shortest path solution but use a set of valuation

Helaoui, M.
Extended Shortest Path Problem - Generalized Dijkstra-Moore and Bellman-Ford Algorithms.
In *Proceedings of the 6th International Conference on Operations Research and Enterprise Systems (ICORES 2017)*, pages 306-313
ISBN: 978-989-758-218-9

not a subset of $\mathbb{R}$ and/or a combining operator not equal to the classic sum ($+$), then in (Gondran and Minoux, 2008), authors present new models and algorithms discussing relations between particular valuation structure: the semiring and diod structures with graphs and their combinatorial properties.
In (Sedgewick and Wayne, 2011), a longest path between two given nodes s and t in a weighted graph G is the same thing as a shortest path in a graph $-G$ derived from G by changing every weight to its negation. Therefore, if shortest paths can be found in $-G$, then longest paths can also be found in G. This result remains true if we have a valued graph G by a valuation structure S?
In this paper, we provide an answer to this question by discussing equivalence between longest path and shortest path problem given a valuation structure S. We present a generalization of Dijkstra-Moore Algorithm for a graph G with a $S^{\oplus}$ valuation structure. And we present a generalization of Bellman-Ford Algorithm with a more general valuation structure S.
We propose to model both the valuations of a graph G and the combining operator by a valuation structure S, in order to discuss the generalization of the shortest path algorithms according to the properties of the graph G and the valuation structure S:

- The valuation structure of G is $S^{\oplus}$.
- The graph G and the valuation structure S are arbitrary.

The paper is organized as follows: the next Section introduces definitions and notations needed in presenting the generalization of the shortest path algorithms. In Section 3 we study the extended Shortest Path Notion and the equivalence between longest path and shortest path problem. We propose a generalized shortest path algorithms in Section 4. The paper is concluded in Section 5.

2 DEFINITIONS AND NOTATIONS

2.1 A Directed Digraph G

The peculiarity of the shortest path problem requires to distinguish two directions between any two nodes. In this case, the connection between two nodes x and y can be defined by the directed connection between an original node for example x and a destination node y.

Definition 1. *A directed digraph $G = (E_S, E_{\vec{A}})$ is defined by a set of nodes E_S and a set of directed edges $E_{\vec{A}}$, each edge (arc) is the connection between an original node and a destination node.*
If x and y are two nodes:

- *the directed connection from x to y (denoted $\vec{xy}$), if it exists, is a directed connection (arc) of a graph G.*
- *An arc $\vec{xx}$: the directed connection from x to x is known as a loop.*
- *A p-graph is a graph wherein there is never more than p arcs $\vec{xy}$ between any two nodes.*
- *A Monograph is a graph wherein there is never more than 1 arc $\vec{xy}$ between any two nodes and there is never a loop.*

2.2 A Valuation Structure

We assume that E the set of all possible valuations, is a totally ordered set where $\bot$ denotes its minimal element and $\top$ its maximal element. In addition, we will use a monotone binary operator $\oplus$. These elements form a valuation structure defined as follows

Definition 2. *A valuation structure S of a graph G is the triplet $S = (E, \oplus, \preceq)$ such as*

- *E is the set of possible valuations;*
- *$\preceq$ is a total order on E;*
- *$\oplus$ is commutative, associative and monotone.*

We define below a fire and strictly monotone valuation structure.

Definition 3. *A valuation structure S is* fire *if for each pair of valuations $\alpha, \beta \in E$, such as $\alpha \preceq \beta$, there is a maximum difference between β and α denoted $\beta \ominus \alpha$.*
An aggregation operator $\oplus$ is strictly monotonic *if for any α, β, γ in E such as $\alpha \prec \beta$ and $\gamma \neq \top$, we have $\alpha \oplus \gamma \prec \beta \oplus \gamma$.*
A valuation structure S is strictly monotonic *if it has an aggregation operator* strictly monotonic.

In the remainder of this paper, we use only fire and strictly monotone valuation structures.
The fire and strictly monotone valuation structures satisfy the following two Lemmas, that has been proved in (Cooper, 2004), (Lemma 7 and Theorem 38).

Lemma 1. *Let $S = (E, \oplus, \preceq)$ a valuation structure fire and strictly monotone. Then for all $\alpha, \beta, \gamma \in E$ such as $\gamma \preceq \beta$, we have $(\beta \ominus \gamma) \preceq \beta$ and $(\alpha \oplus \gamma) \oplus (\beta \ominus \gamma) = \alpha \oplus \beta$.*

Lemma 2. *Let $S = (E, \oplus, \preceq)$ a valuation structure fire and strictly monotone. Then for all $\alpha, \beta, \gamma \in E$ such as $\gamma \preceq \beta$, we have $(\alpha \oplus \beta) \ominus \gamma = \alpha \oplus (\beta \ominus \gamma)$.*

Using both Lemmas (Lemma 1 and Lemma 2) presented above we can get Lemma 3:

Lemma 3. *Let* $\beta \prec \alpha$ *and* $\gamma \prec \alpha$
$\alpha \ominus \beta \prec \alpha \ominus \gamma$ *if and only if* $\gamma \ominus \alpha \prec \beta \ominus \alpha$.

Proof. ($\Rightarrow$) If we have $\alpha \ominus \beta \prec \alpha \ominus \gamma$
then $\alpha \ominus \beta \oplus (\beta \ominus \alpha \oplus \gamma \ominus \alpha) \prec \alpha \ominus \gamma \oplus (\beta \ominus \alpha \oplus \gamma \ominus \alpha)$
then $\gamma \ominus \alpha \prec \beta \ominus \alpha$
($\Leftarrow$) If we have $\gamma \ominus \alpha \prec \beta \ominus \alpha$
then $\gamma \ominus \alpha \oplus (\alpha \ominus \beta \oplus \alpha \ominus \gamma) \prec \beta \ominus \alpha \oplus (\alpha \ominus \beta \oplus \alpha \ominus \gamma)$
then $\alpha \ominus \beta \prec \alpha \ominus \gamma$. □

We define below a particular valuation structure, widely used in practice, that we will note $S^{\oplus}$

Definition 4. *A valuation structure* $S^{\oplus}$ *of a graph G is the triplet* $S^{\oplus} = (E^{\oplus}, \oplus, \preceq)$ *such as:*

- $E^{\oplus}$ *is the set of possible valuations such as for all* $\alpha, \beta, \lambda \in E^{\oplus}$ *if* $\alpha \preceq \beta$ *then* $\alpha \preceq \beta \oplus \lambda$*;*
- $\preceq$ *is a total order on E;*
- $\oplus$ *is commutative, associative and monotone.*

3 SHORTEST PATH NOTION

3.1 Extended Shortest Path Problem

In the beginning of this paragraph we formally define the shortest path between two nodes *x* and *y* of a graph *G*.
For this way, we start by defining the arc and path valuations.

Definition 5. *Let* $G = (E_S, E_{\vec{A}})$ *a valued directed graph. In each arc* $\vec{xy}$ *we associate a valuation function* $\varphi : E_S \times E_S \rightarrow E$ *such as* $\varphi(x,y)$ *is the valuation of* $\vec{xy}$ *arc. A path between two nodes x and y is denoted* $CH(x,y)$ *from the node x to a node y.*
For each path $CH(x,y)$ *we associate a valuation* $\Phi(CH(x,y))$.

$$\Phi(CH(x,y)) = [\bigoplus_{x_i\vec{x}_j \in CH(x,y)} \varphi(x_i, x_j)]$$

Now we can define the shortest path:

Definition 6. *Let* $G = (E_S, E_{\vec{A}})$ *a valued directed graph. The shortest path between x and y is the path* $\mu(x,y)$ *started from a node x and finished at y such as:*

$$\Phi(\mu(x,y)) = Min_{CH(x,y)}[\Phi(CH(x,y))]$$

3.2 Equivalent Problems of Shortest Path Problem (SPP)

If we have to find the Longest Path, is it possible to use the Shortest Path solution?
Finding the Longest Path is it equivalent to finding the Shortest Path?

Theorem 1. *Given a fire and strictly monotone valuation structure S, finding the Longest Path Problem is equivalent to finding the Shortest Path Problem.*

Proof Theorem 1. ($\Rightarrow$) We start from a shortest path problem. We replace each valuation ($\alpha \ominus \beta$) by the valuation ($\beta \ominus \alpha$) and we prove that a shortest path problem can be transformed in a longest path problem.
Let

$$\Phi(\mu(s,t)) = \min \Phi(CH(s,t))$$
$$\Phi(\mu(s,t)) = (\alpha \ominus \beta_0) \preceq \Phi(CH_1(s,t)) = (\alpha \ominus \beta_1) \preceq \ldots \preceq \Phi(CH_n(s,t)) = (\alpha \ominus \beta_n)$$

If we replace each valuation ($\alpha \ominus \beta$) by the valuation ($\beta \ominus \alpha$)
We get

$$\Phi(\mu(s,t)) = (\beta_0 \ominus \alpha) \succeq \Phi(CH_1(s,t)) = (\beta_1 \ominus \alpha) \succeq \ldots \succeq \Phi(CH_n(s,t)) = (\beta_n \ominus \alpha)$$

then we get

$$\Phi(\mu(s,t)) = \max \Phi(CH(s,t)) = \Phi(\mathcal{L}(s,t))$$

($\Leftarrow$) Now we start from a longest path problem. We replace each valuation ($\alpha \ominus \beta$) by the valuation ($\beta \ominus \alpha$) and we prove that a longest path problem can be transformed in a shortest path problem.
Let

$$\Phi(\mathcal{L}(s,t)) = \max \Phi(CH(s,t))$$
$$\Phi(\mathcal{L}(s,t)) = (\alpha \ominus \beta_0) \succeq \Phi(CH_1(s,t)) = (\alpha \ominus \beta_1) \succeq \ldots \succeq \Phi(CH_n(s,t)) = (\alpha \ominus \beta_n)$$

If we replace each valuation ($\alpha \ominus \beta$) by the valuation ($\beta \ominus \alpha$)
We get by Lemma 3

$$\Phi(\mathcal{L}(s,t)) = (\beta_0 \ominus \alpha) \preceq \Phi(CH_1(s,t)) = (\beta_1 \ominus \alpha) \preceq \ldots \preceq \Phi(CH_n(s,t)) = (\beta_n \ominus \alpha)$$

Then we get

$$\Phi(\mathcal{L}(s,t)) = \min \Phi(CH(s,t)) = \Phi(\mu(s,t))$$

□

Example 1. In February 2017, a large multinational X in Porto wishes to invest the sum of 3.000.000 € in a new project Π. To do this, each year X has d investment choices. One study allowed him to estimate the certainty of acceptable profitability (probabilities) according to the various decisions taken. In order to maximize the certainty of an acceptable overall yield of Π, X wishes to find the longest path in the monograph G_1, such that, $S_1 = (]0,1[, \times, \leq)$.

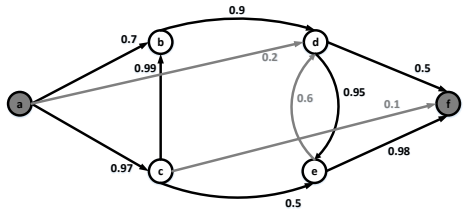

Figure 1: A directed monograph G_1.

By Theorem 1 and in order to maximize the certainty probabilities of an acceptable overall yield of Π, X can find the shortest path in the monograph G_2 minimize the uncertainty probabilities. Such that $S_2 = S_1$. For each valuation α in G_1 we associate a valuation β in G_2 such that $\beta = \ominus \alpha = 1 - \alpha$
$\alpha \oplus \beta = \alpha \times (1-\alpha) \Rightarrow S_1$ **and** S_2 **are different from the semiring or diod structures**.

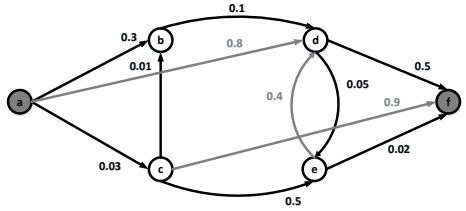

Figure 2: A directed monograph G_2.

3.3 Optimality Notion

The dynamic programming repose on the fundamental principle of optimality:
Given a directed graph G, a sub-path of a shortest path $\mu \in G$ is a shortest path in G_s a sub-graph of G.

Theorem 2. *Let:*

- *A directed graph* $G = (E_S, E_{\vec{A}})$,
- *A valuation function of* G $\varphi : E_S \times E_S \to E$ *with a fire and strictly monotone valuation structure* S,
- *a shortest path* $\mu(x_1,x_k)$ *from* $x_1 \in E_S$ *to* $x_k \in E_S$ $\mu(x_1,x_k) = x_1 \to x_2 \to \ldots \to x_k = x_1 \overset{*}{\to} x_k$,
- *A sub-path* $CH(x_i,x_j)$ *of* $\mu(x_1,x_k)$ *from* x_i *to* x_j: $CH(x_i,x_j) = x_i \to \ldots \to x_j$ *such as* $x_i \overset{*}{\to} x_j$ [1].

Then $CH(x_i,x_j) = \mu(x_i,x_j)$ *is the shortest path from* $x_i \overset{*}{\to} x_j$.

Proof Theorem 2. We proceed by absurd reasoning. Assume that:

1. $\mu(x_1,x_k)$ is a shortest path
2. $\mathrm{CH}(x_i,x_j)$ is a sub path of $\mu(x_1,x_k)$
3. It $\exists$ $\mathrm{CH'}(x_i,x_j)$ of G such as $\Phi(\mathrm{CH'}(x_i,x_j)) \prec \Phi(\mathrm{CH}(x_i,x_j))$.

We proceed to get a contradiction.
Decompose $\mu(x_1,x_k)$ in $\mathrm{CH}(x_1,x_i)$, $\mathrm{CH}(x_i,x_j)$ and $\mathrm{CH}(x_j,x_k)$
then
$\Phi(\mu(x_1,x_k)) = \Phi(\mathrm{CH}(x_1,x_i)) \oplus \Phi(\mathrm{CH}(x_i,x_j)) \oplus \Phi(\mathrm{CH}(x_j,x_k))$.
As it $\exists$ $\mathrm{CH'}(x_i,x_j)$ such as $\Phi(\mathrm{CH'}(x_i,x_j)) \prec \Phi(\mathrm{CH}(x_i,x_j))$ and given that $\oplus$ is strictly monotone
then
$\Phi(\mu(x_1,x_k)) \succ \Phi(\mathrm{CH}(x_1,x_i)) \oplus \Phi(\mathrm{CH'}(x_i,x_j)) \oplus \Phi(\mathrm{CH}(x_j,x_k))$, which is a contradiction by the fact that the path $\mu(x_1,x_k)$ is a shortest path then $\mathrm{CH}(x_i,x_j) = \mu(x_i,x_j)$.

□

4 GENERALIZATION OF DIJKSTRA-MOORE AND BELLMAN-FORD ALGORITHMS

4.1 Common Functions

The generalized Dijkstra-Moore and Bellman-Ford algorithms presented in this paper use

1. Algorithm 1 is an initialization marker algorithm of all nodes of G that we will denote $\textsc{InitMark}(G,s)$;
2. Algorithm 2 is an initialization finding shortest path algorithm that we will denote $\textsc{InitSpp}(G,s)$;

[1]
- x_i is an immediate predecessor or a non immediate of x_j (it exists a path from x_i to x_j).
- x_i is an immediate successor or a non immediate of x_1 or $x_i = x_1$
- x_j is an immediate predecessor or a non immediate of x_k or $x_j = x_k$

3. The updating shortest path Algorithm, denoted UPDATESPP(x_i, x_j, φ).
   Updating the shortest path between two nodes x_i and x_j consists in updating the valuation of one of the arcs $x_i\vec{x}_j$:

   (a) The valuation spv$[x_j]$ of the shortest path until x_j;
   (b) The predecessor of x_j predspp$[x_j]$ in the shortest path until x_j.

Algorithm 1: InitMark(G,s):Mark.

for $(x_i = s \ \ Nbr_{Sommets_G})$ **do**
  Mark$[x_i] \leftarrow 0$;
Mark$[s] \leftarrow 2$;

Algorithm 2: InitSpp(G,s):spv,predspp.

for $(x_i = s \ \ Nbr_{Sommets_G})$ **do**
  spv$[x_i] \leftarrow \top$;
  predspp$[x_i] \leftarrow 0$;
spv$[s] \leftarrow \alpha_0$;

The updating process is based on the Theorem 2 where each sub-path of the shortest path is a shortest path in the sub-graph involving this sub-path.
The UpdateSpp(x_i, x_j, φ) function update the shortest path from one origin node to all other one if a shortest path is detected.

Algorithm 3: UpdateSpp(x_i, x_j, φ):spv,predspp.

if $(spv[x_j] \succ spv[x_i] \oplus \varphi[x_i][x_j])$ **then**
  spv$[x_j] \leftarrow spv[x_i] \oplus \varphi[x_i][x_j]$;
  predspp$[x_j] \leftarrow x_i$;

In the DIJKSTRA-MOORE Algorithm 4, each arc is updated exactly one way. In BELLMAN-FORD Algorithm, each arc can be updated many way.

4.2 Generalization of the Dijkstra-Moore Algorithm

If the arcs valuation, is in $\mathbb{R}$, can model for example

- A distance (kilometers)
- A cost (€)

In this case, the classic Dijkstra-Moore Algorithm can be used.
In this paper, we present a generalization of Dijkstra-Moore Algorithm 4 for a graph G with a $S^{\oplus}$ valuation structure.

Let G a valued directed graph given a valuation structure $S^{\oplus}$. We denote by s the origin node of G and x_i the destination node. For each node x_i of G, the Algorithm 4 associate

- The valuation spv$[x_j]$ for the shortest sub-path until x_i;
- The predecessor of x_i predspp$[x_i]$ in the shortest sub-path until x_i.
- The marker of x_i denoted Mark$[x_i]$ verifying if the distance from s to x_i has been updated.

Principe of the Algorithm:

1. initialization:
   For the node s
   - Mark$[s] \leftarrow 2$
   - predspp$[s] \leftarrow 0$
   - spv$[s] \leftarrow \alpha_0$

   for all other nodes x_i
   - Mark$[x_i] \leftarrow 0$
   - predspp$[x_i] \leftarrow 0$
   - spv$[x_i] \leftarrow \top$
2. Let $X =$ the set of non marked nodes;
   Do
   - **For** each non marked node i successor of y
     - UpdateSpp(y, i, φ)
   - Mark the node y if spv$[y] = \min_{x \in X} pcc[x]$.

   While $X \neq \emptyset$

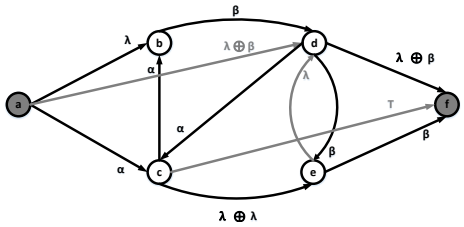

Figure 3: A directed monograph G.

Example 2. Let the directed monograph G presented by Figure 3. And let a valuation structure $S^{\oplus}$ (can be $\neq$ to the semiring or diod structures) such that

- $\{\alpha, \beta, \lambda, \gamma, \top\} \subset E^{\oplus}$
- $\alpha \prec \beta \prec \lambda$
- $\beta = \alpha \oplus \alpha$
- $\lambda = \alpha \oplus \beta$
- if $\gamma \succeq \lambda \oplus \lambda \oplus \lambda \oplus \beta$ then $\gamma = \top$

1. We apply the principle of Generalized Dijkstra algorithm on G: Figure 4
2. We present an algorithmic solution: Algorithm 4.

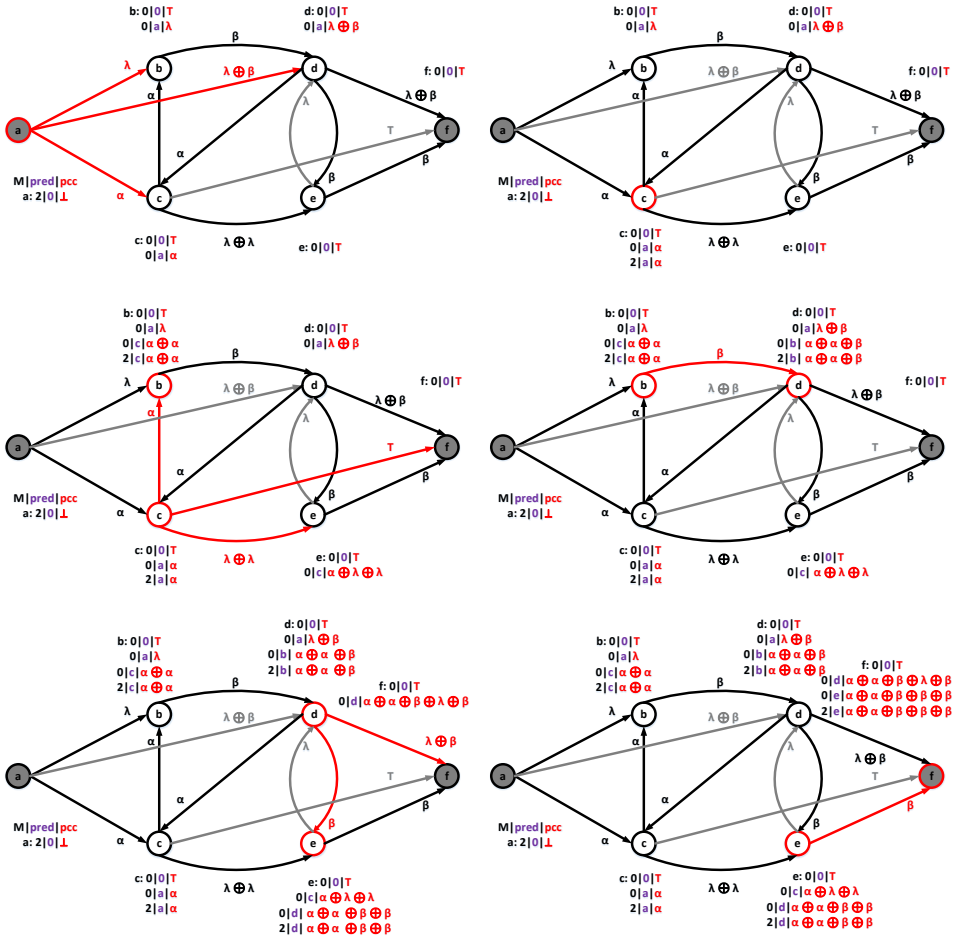

Figure 4: Applying Generalized-Dijkstra-Moore on G.

Algorithm 4: Generalized-Dijkstra-Moore(G,φ,s,t): spv,predspp.

```
InitMark(G,s);
InitSpp(G,s);
recent ← s;
t ← f;
while (Mark[t] = 0) do
    j ← 0;
    while (succ[recent][j]) do
        if (Mark[j] = 0) then
            UpdateSpp(recent, j, φ);
        j ← j+1;
    y ← min(spv);
    Mark[y] ← 2;
    recent ← y;
```

Theorem 3. *Given a directed monograph G with n nodes and a valuation structure $S^{\oplus}$, the shortest path from one started node to all others can be done in $O(n^2)$.*

Proof Theorem 3. *Given a directed monograph G with n nodes and a valuation structure $S^{\oplus}$, and referred to Theorem 2, the shortest path from one started node to all others can be done by applying Algorithm 4 to G. And the Algorithm 4 run in $O(n^2)$.* □

4.3 Generalization of Bellman-Ford Algorithm

Given a fire and strictly monotone valuation structure S we can model as example earnings and bounded costs!

Unfortunately, as nodes may be marked only once, the DIJKSTRA-MOORE algorithm does not guarantee the optimal solution if we consider the valuation structure not a subset of $S^{\oplus}$ (For example the bounded negative arcs). In fact, once the node is marked we cannot change the marking in subsequent iterations.

Fortunately, we can present an algorithm that ensures marking update until the program is not determined:

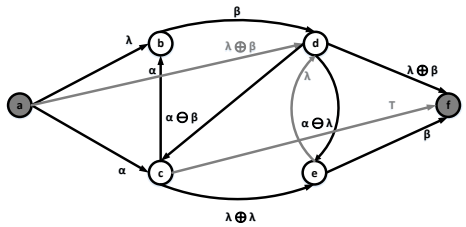

Figure 5: A directed monograph $G^{'}$.

a generalization of the BELLMAN-FORD Algorithm can be used for a fire and strictly monotone valuation structure S.

Theorem 4. *Given a fire and strictly monotone valuation structure S, the final values of the shortest paths are obtained by at most $n-1$ iterations.*

Proof Theorem 4. In the absence of absorbing circuitry, a shortest path from s to all other nodes is an element path, that is to say a path of at most $n-1$ arcs. By consulting the predecessors of all nodes Algorithm 5 must obtain the final values of the shortest paths by at most $n-1$ iterations.

□

Corollary 1. *If after n iterations, the values $spv[i]$ continue to be modified, is that the graph has an absorbent circuitry.*

Based on the results of Theorem 4 and Corollary 1 we can introduce the principle of the BELLMAN-FORD generalization algorithm.

Principle of the BELLMAN-FORD generalization algorithm:

1. InitSpp(G,s)
2. **Do**
   UpdateSpp(i,j,φ)
   While there is an edge to decrease spv[i].

Algorithm 5 presents an algorithmic solution for the generalized BELLMAN-FORD algorithm.

Example 3. Let the directed monograph $G^{'}$ given by Figure 5. And let a valuation structure S (can be $\neq$ to the semiring or diod structures) such that

- $\{\alpha, \beta, \lambda, \gamma, \top\} \subset E$
- $\alpha \prec \beta \prec \lambda$
- $\beta = \alpha \oplus \alpha$
- $\lambda = \alpha \oplus \beta$
- if $\gamma \succeq \lambda \oplus \lambda \oplus \lambda \oplus \beta$ then $\gamma = \top$

1. Present an algorithmic solution: Algorithm 5.

Algorithm 5: Generalized-Bellman-Ford(G,φ,s): spv,predspp.

```
InitSpp(G,s);
k ← 0;
t ← 1;
while (t ou k > N_Sommet_G − 1) do
    t ← 0;
    for (i de 1 N_Sommet_G) do
        j ← 0;
        while (predspp[i][j]) do
            UpdateSpp(j,i,φ);
            if (spv[i] ≻ spv[j] ⊕ φ[j][i]) then
                t ← 1;
            j ← j+1;
    k ← k+1;
```

Theorem 5. *Given a directed monograph G with n nodes and a fire and strictly valuation structure S, the shortest path from one started node to all others can be done in $O(n^3)$.*

Proof Theorem 5. *Given a directed monograph G with n nodes and a fire and strictly valuation structure S, and referred to Theorem 2, Theorem 4 and Corollary 1, the shortest path from one started node to all others can be done by applying Algorithm 5 to G. And the Algorithm 5 run in $O(n^3)$.*

□

5 CONCLUSION

This paper addressed combinatorial problems that can be expressed as shortest path solution but use a set of valuation not a subset of $\mathbb{R}$ and/or a combining operator not equal to the classic sum ($+$).
Firstly, we have modeled the valuations of a graph G by using a general valuation structure S.
Secondly, given a general valuation structure S, we have discussed the equivalence between longest path and shortest path problem.
And finally, we have discussed the generalization of the shortest path algorithms according to the properties of the graph G and the valuation structure S:

1. The valuation structure of G is $S^{\oplus}$.
2. The graph G and the valuation structure S are arbitrary.

REFERENCES

Allouche, D., de Givry, S., Sanchez, M., and Schiex, T. (2009). Tagsnp selection using weighted csp and russian doll search with tree decomposition 1. In *In Proceedings of the WCB09. Lisbon Portugal, 1–8*.

Bellman, R. (1958). On a routing problem. In *Quarterly of Applied Mathematics. 16: 87–90*.

Cohen, D. A., Cooper, M. C., Jeavons, P. G., and Krokhin, A. A. (2004). A maximal tractable class of soft constraint satisfaction. In *Journal of Artificial Intelligence Research 22, 1–22*.

Cooper, M. C. (2003). Reduction operations in fuzzy or valued constraint satisfaction. In *Fuzzy Sets and Systems 134 311–342*.

Cooper, M. C. (2004). Arc consistency for soft constraints. In Artificial Intelligence *154, 199–227*.

Erickson, J. (2010). Maximum flows and parametric shortest paths in planar graphs. In *In Proceedings of the 21st Annual ACM-SIAM Symposium on Discrete Algorithms, 794–804*.

Ford, J. and Lester, R. (1956). Network flow theory. In *RAND Corporation, 923*, Santa Monica, California.

Ford, L. R. and Fulkerson, D. R. (1955). A simple algorithm for finding maximal network flows and an application to the hitchock problem. In *In Rand Report Rand Corporation*, Santa Monica, California.

Ford, L. R. and Fulkerson, D. R. (1962). Flows in networks. In *In Princeton University Press*.

Gondran, M. and Minoux, M. (2008). Graphs, dioids and semirings: New models and algorithms (operations research/computer science interfaces series). In *Springer Publishing Company*.

Helaoui, M., Naanaa, W., and Ayeb, B. (2013). Submodularity-based decomposing for valued csp. In *International Journal on Artificial Intelligence Tools*.

Schiex, T., Fargier, H., and Verfaillie, G. (1995). Valued constraint satisfaction problems: hard and easy problems. In *In Proceedings of the* 14^{th} *IJCAI, 631–637*, Montréal, Canada.

Sedgewick, R. and Wayne, K. D. (2011). Algorithms (4th ed.). In *Addison-Wesley Professional, 661–666*.

Shimbel, A. (1955). Structure in communication nets. In *Proceedings of the Symposium on Information Networks, 199–203*, New York, NY: Polytechnic Press of the Polytechnic Institute of Brooklyn.

Application of the Six Sigma Method for Improving Maintenance Processes – Case Study

Michał Zasadzień
Institute of Production Engineering, Silesian University of Technology, Roosevelta 26, Zabrze, Poland
michal.zasadzien@polsl.pl

Keywords: Maintenance, Six Sigma, Improvement, Breakdown, Process, DMAIC.

Abstract: The article presents an implementation attempt of the DMAIC method used in the Six Sigma concept for the improvement of production processes connected with maintenance. Thanks to the tools included therein (process map, FMEA, SIPOC chart) we were able to define the: problem, i.e. which types of breakdowns cause the most machine stoppage; precise structure of the failure removal process and its needs, owners, resources, client-supplier relationships in particular sub-processes; source causes for overly long stoppages. Learning the process and the causes of malfunctions allowed us to develop improvement procedures aimed at minimising the fault removal times. The procedures developed have been implemented in the company alongside a control plan, which will ensure supervision and their efficient functioning in the future.

1 INTRODUCTION

1.1 Maintenance

Processes connected with maintaining technical resources used in production in good condition are some of the key elements which affect the efficiency of production processes, which directly influences the company's competitiveness on the market (Żurakowski, 2004). Thanks to an efficient machine park, a production company can supply its goods to the customers in required quantity, quality and within the agreed deadlines; it becomes a reliable and trustworthy partner for its clients. A key element to the production process is the availability of machinery and equipment. Availability (operational time) of machines and equipment which take part in the production process is limited by several elements, which can be classified into two main groups: stoppages caused external factors and stoppages caused by internal factors. External factors do not depend on the technical condition of the machinery or the way it is operated. These factors include stoppages caused by e.g. media supply shortages (water, electricity, communication), but also weather conditions which make operation impossible (temperature in the production hall). Internal stoppage factors depend on the way the machines are operated and their technical condition. These include stoppages caused by breakdowns, inspections and renovation works, but it is also the time needed for refitting or calibration of the machines, launching them after a stoppage, introducing improvements, training new employees, etc. An example division is presented in Figure 1.

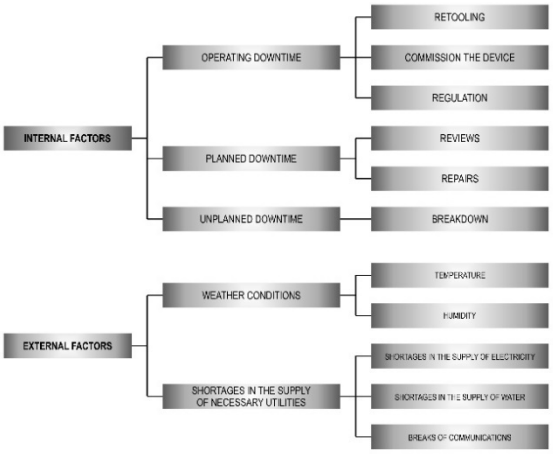

Figure 1: Factors affecting machine unavailability (based on Zasadzień and Midor 2015).

From the availability period we can also distinguish the unused time (the period when the machine is not working despite being operational), which depends on planning, production quantity and

Zasadzień, M.
Application of the Six Sigma Method for Improving Maintenance Processes – Case Study.
In *Proceedings of the 6th International Conference on Operations Research and Enterprise Systems (ICORES 2017)*, pages 314-320
ISBN: 978-989-758-218-9

organisation. It is not considered as either external or internal factor, as the machine is available for work at the time.

The occurrence of a breakdown of a machine involved in the production process can cause delays, endanger its operators or the natural environment; it increases the risk of crossing delivery deadlines or decrease in product quality. The probability of stoppages caused by breakdowns can be minimised by introducing advanced maintenance strategies, which include preventive maintenance based on inspections and preventive renovation, or predictive maintenance, based on monitoring the technical condition (condition based maintenance) (Legutko, 2009). Even the most technically and organisationally advanced preventive measures cannot reduce the probability of a breakdown to an absolute zero.

A breakdown is a sudden and mostly unforeseen occurrence, which is why the process of its removal is very complex; it is necessary to act in a rush and reorganise working schedules. It consists of administrative, organisational and technical activities. Reducing the breakdown removal time, and therefore reducing the downtime of the machine directly affects the efficiency indicators of the production process. It is, therefore, important to skilfully direct the main and auxiliary processes connected with the company's activity in order to efficiently use the working time, materials, machines and equipment (Mikler, 2005). The maintenance department often operates based on no precisely defined schedule and its priorities are set on the fly, usually with not enough human and technical resources available, which is why the skills of managing working time and using it efficiently are especially important here (Midor, Szczęśniak and Zasadzień, 2010; Mączyński and Nahirny, 2012).

Stoppage caused by a breakdown can consist of active and passive time, as presented in Figure 2.

The length of the downtime period caused by a breakdown can be composed of elements whose duration depends on the organisation and management of the maintenance department (administrative delay, waiting for personnel and spare parts), i.e. the so-called support capability, as well as on ease of maintenance, i.e. the ease with which a given machine can be brought back to an operational condition. Ease of maintenance depends primarily on the qualifications and competence of employees, the machine's structure, its technical condition and location. Shortening the downtime caused by a breakdown consists in, for the most part, shortening the passive and/or active time of the breakdown removal process.

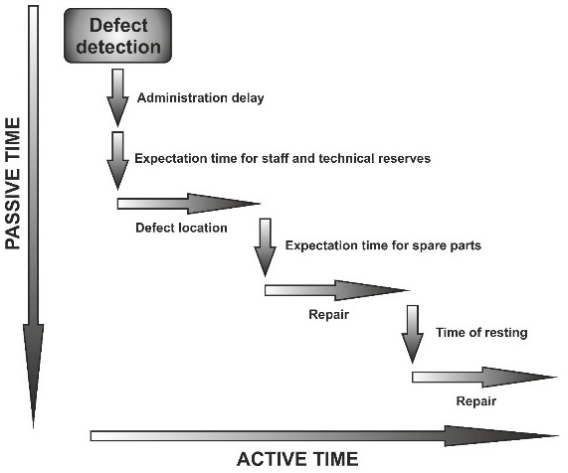

Figure 2: Time in the defect removal process (based on Mikler, 2005).

1.2 DMAIC

Strategies for improving production processes have been described in literature many times (Sahno and Shavtshenko, 2014; Soković et al., 2009). Currently, we have at our disposal such methods and concepts of quality management as: PFMEA, TQM, Six Sigma and others (Tague, 2005; Andrássyová, 2013). Apart from those, many less complex tools, such as the Pareto chart, Ishikawa diagram or 5 WHYs (Midor, 2014) are also used with much success.

One of the elements of streamlining the production process can be the DMAIC (Define - Measure - Analyse - Improve - Control) method, rooted in the automotive industry and successfully utilised in process improvement in accordance with the Six Sigma assumptions (Krzemień and Wolniak, 2007; Wojraszak and Biały, 2013). Six Sigma is a complex and flexible system for achieving, sustaining and maximising business achievements. It is characterised by the understanding of customers' needs and organised use of facts, data and statistical analysis results, and is based on management, streamlining and constantly creating new, ever better solutions with reference to all the processes taking place in the company. Furthermore, it is aimed at minimising the costs of bad quality while simultaneously increasing customer satisfaction (Truscott, 2003)). The method is used to eliminate the causes of defects, losses they incur and any problems related to quality in the aspects of production, services and management. To solve

these problems, the method employs quality tools and statistical techniques (Eckes, 2000).

When implementing the DMAIC method, a number of auxiliary quality improvement tools and methods are used. The improvement cycle using the DMAIC method consists of the following elements (Dreachslin and Lee, 2007; Bargerstock and Richards, 2015):

- Define. In this stage a team is created which will be responsible for the implementation of the method. The defining phase must identify the following elements: determining the problem (description of the problem, time of occurrence), scope of the project (elements of the process the team will work on), aim of the project (a tangible goal to achieve and sustain in the future).
- Measure. During the measurement stage parameters and places of measurement should be defined, i.e. the points of process quality and its costs along with a precise reflection of the actual state. Conducting measurements successfully requires a statistical outlook on the particular production processes and problems related to them. The measurement stage employs methods such as: descriptive statistics, summary charts, the SIPOC method and the process map.
- Analyse. During this stage of the methodology, by analysing the particular parameters of the process, the team will be able to determine the causes of the problem, which will then need to be eliminated or fixed. The results obtained during the measurement stage are used in order to investigate the correlation between causes of defects and process variability sources. In order to identify the causes of process variability, which are a significant factor in defect creation, the PFMEA analysis, the Pareto - Lorenz chart and the Ishikawa diagram are often used.
- Improve. Improvement can otherwise be understood as engagement in the course of the production process, i.e. reduction of the defect rate. It consists in searching for and evaluating potential causes of process variability and investigating their correlations. Learning the multi-factor relations allows for achieving the desired results.
- Control. The control stage takes place after finishing the new process implementation phase. The fundamental goal of Six Sigma is the constant observation of the improvements introduced to maintain a desired level of quality. In this phase of the DMAIC the measurement system and potential verification process are repeated to confirm the improvement of the process. Afterwards, measures are taken to appoint control over the streamlined processes; usually a so-called control plan is created.

As we can infer from the above description, based on the concepts of Six Sigma and Lean, the DMAIC method used in management systems relies on the principle of constant improvement and PDCA formulated by E. Deming (Deming, 2000) and required by the ISO 9001 series standards. A comparison of both concepts has been presented in the literature in many forms (George et al., 2005; Soković et al., 2010) (fig. 3).

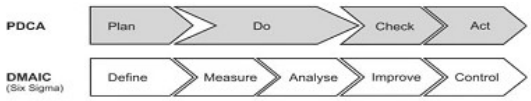

Figure 3: PDCA vs DMAIC.

The DMAIC methodology is used for improving production processes, successfully contributing to the reduction of the number of non-compliant products and reducing production costs. The author of this elaboration decided to introduce this method to processes auxiliary to the production process, i.e. to the maintenance process. The maintenance process, as every other process, has its inputs, outputs, clients, suppliers and can be described using indicators, similar to the production process. The case presented pertains to the breakdown removal process.

2 DMAIC IMPLEMENTATION

2.1 Define

In the company which is the subject of this study the key machines are the extruders producing HDPE (high-density polyethylene) pipes. Due to that fact, a total of 154 breakdowns of these machines were analysed in the period of 32 months. This allowed us to identify those components whose breakdowns caused the longest stoppages, as presented in Table 1.

As can be seen in the above table (Tab. 1), the breakdown that caused the longest downtime was the damaged connector of extruder head heater. In

the examined period of time the downtime due to this failure lasted more than 130 hours (7 breakdowns of this type), and the average time of downtime was 18 hours, therefore, it was decided that the problem should be subjected to analysis. The aim was to reduce the total duration of downtime caused by this failure by reducing the average downtime duration and the number of breakdowns.

Table 1: Extruder component stoppages analysed.

Failure	Average downtime duration [h]	Total downtime duration [h]
Damaged heater supply connector	18.69	130.83
Incorrect caterpillar track haul-off	14.19	103.49
Pipe surface corrugation	10.19	71.31
Leak of oil from transmission gear	9.50	37.99
Crown brush failure	17.80	35.59
Error on controller display	22.83	2.83
No heating	0.98	20.64
Fuse blown	0.48	20.30
Destroyed basket for granulated product	18.60	18.60
No granules haul	1.61	12.88
Failure of ozone exhaust	0.42	7.48
Damaged frequency invertor	7.34	7.34
Leak of mass from the head	1.08	4.32
Leak in heat exchanger	3.81	3.81
No cooling	0.16	2.28
Saw failure	0.22	1.55
Printer failure	0.50	1.00
Clogged head sieve	0.44	0.88
Calibrator failure	0.24	0.72
Vacuum pump	0.21	0.21
Damaged air duct	0.03	0.03
Extractor failure	0.01	0.02
Drive system failure	0.02	0.02

2.2 Measure

Based on the information obtained from the production and maintenance employees, a map for the process of identifying and removing failures of the extruder head heater connector was created. The process map has been presented in Fig. 4.

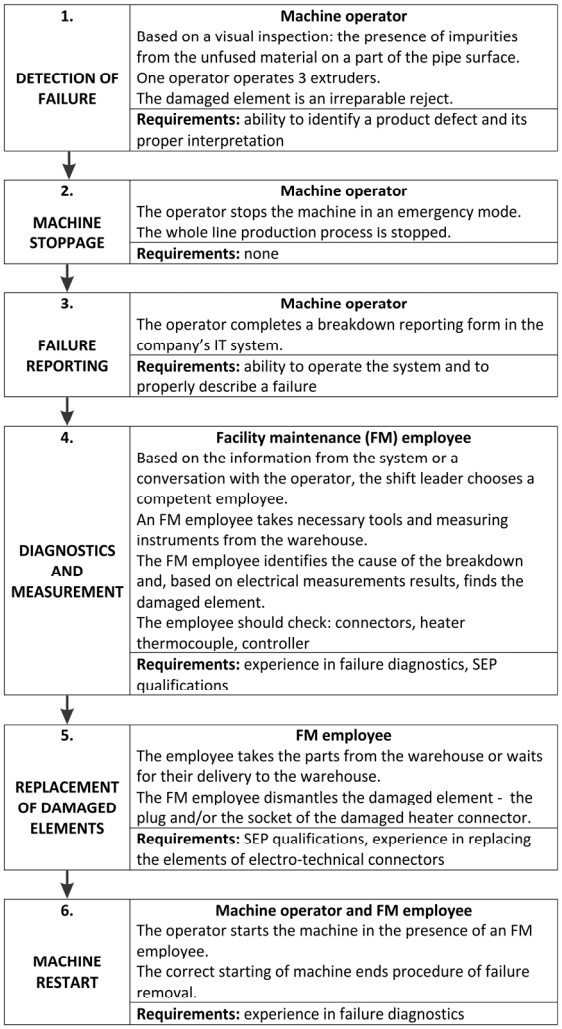

Figure 4: Failure removal process map.

2.3 Analyse

Based on the information collected in the process of identifying all the process steps and creating a process map, a modified PFMEA matrix was developed to identify potential causes and effects of delays during the process of removing a failure of extruder head heater and estimate their importance for the process. For the needs of the case study, a scale from 1 to 4 was adopted, where 1 means a positive situation and 4 – a negative one (Table 2).

Table 2: PFMEA matrix.

Process stage	Problem	Cause	Importance	Effect	Occurrence	Current prevention	Effectiveness of prevention	IOE
1.	Failure detected too late	Connector burnt during work	4	Line stoppage.	3	Observation of the product by the operator	4	48
				Possibility of further defects	1	Observation of the product by the operator	4	16
	Failure occurs after extruder refitting	Connector damaged in the process of refitting	3	Line stoppage	3	None	4	36
3.	Too long time of recording the failure in the system	Insufficient knowledge of the IT system	1	FM is not aware of the failure	3	Training of a newly employed worker	2	6
	FM does not know the failure details	Inaccurate description of failure	3	FM employee does not have the sufficient equipment	4	None	4	48
4.	Incorrect diagnostics	Having identified the cause of the failure, the employee does not control the remaining elements of the system	4	Long duration of failure removal	2	None	4	32
5.	Long waiting time for the parts	Lack of parts in the warehouse	4	Prolonged failure removal	1	None	4	16
		Long searching for parts in the warehouse	3	Prolonged failure removal	2	None	4	24
	Long duration of damaged elements replacement	Waiting for the head temperature to go down	4	Prolonged failure removal	4	None	4	64

The analysis conducted by means of the PFMEA tool revealed which of the analysed causes of the problems was the most important for the process of failure removal. Table 3 contains the analysis synthetic results.

For further works aimed at improving the process, problems whose IOE was at least 40, i.e. three most important items: waiting for the head temperature to go down, connector burnt during work – line stoppage and inaccurate description of the failure were selected.

Table 3: PFMEA analysis results.

Cause	IOE
Waiting for the head temperature to go down	64
Connector burnt during work – line stoppage	48
Inaccurate description of failure	48
Connector damaged in the process of refitting	36
Incorrect diagnostics	32
Long searching for parts in the warehouse	24
Connector burnt during work – possibility of further defects	16
Lack of parts in the warehouse	16
Too long waiting for the failure to be recorded in the system	6

2.4 Improve

At the further stage of analysis, improvement actions for all the important problems were proposed. Their synthetic summary has been given in Table 4.

Table 4: Improvement actions.

Cause	IOE	Improvement actions	Benefits	I	O	E	IOE
Waiting for the head temperature to go down	64	Introducing a system of doubled heads. A spare head is waiting at the quick replacement station.	No need to wait for the head to cool down. Replacement of the head for a cold one enables an immediate failure removal.	4	2	2	16
Connector burnt during work – line stoppage	48	Installing a system of product surface monitoring with software for image analysis.	No need for the operator to observe the pipe surface. Automatic alarm initiation in case of surface defects.	4	2	2	16
Inaccurate description of failure	48	Introducing a uniform base for failure reporting in the IT system and training of machine operators in failure identification.	FM employees receive reliable and precise information enabling their faster preparation for work.	3	1	2	6

The introduced improvement actions allowed a considerable reduction of IOE values for the analysed problems.

An estimation of the costs involved in the improvement actions has revealed that the cheapest solution is improving the process of failure reporting, as the enterprise has a possibility of modifying the IT system. Introducing a spare head at the extruder workstation required constructing and making trolleys for fast head replacements. Since the company manufactures its products on a mass scale, the expensive heads are stored in the company's warehouses. The most costly improvement action is introducing a system for product surface quality monitoring. It has been decided that such a system will be implemented in the places where operators have a hindered access, i.e. where observation of the process is difficult.

2.5 Control

After implementing the actions planned, the values of duration of downtimes due to failures of heaters in extruder heads are monitored on a regular basis and their causes analysed according to the schedule contained in Table 5.

Table 5: Process monitoring.

Element of control	Duration of downtimes due to heater connectors' failures	Elements of downtime duration
Control limit	Downtime duration <10 h	None
Frequency of control	1/half year	1/half year
Control system	Records in IT system	Failure removal reports
Control method	Figures	Charts
Response plan	Meeting with production managers	Meetings with FM shift leaders
Person in charge	FM manager	FM manager

At the last stage of creating a control plan, standardization (Table 6) was taken into consideration, aimed at maintaining the standards which the process of failure removal improvement is based on.

Table 6: Standardization.

Person in charge	Undertaken actions
Quality engineer	Instructions on head replacement using a fast exchange trolley
Quality engineer	Instructions for pipe surface control
Production manager	Operators' training in product surface observation
Quality engineer	Failure reporting instructions
FM manager	Training for operators in failure reporting and diagnostics

Training actions are undertaken in the event new workers are employed and any important changes have been made in the instructions and procedures.

3 CONCLUSIONS

The aim of the undertaken actions has been achieved. The duration of downtimes caused by failures of extruder head heater connectors was reduced. The period of results verification lasted 8 months. During that time there were two such failures and downtime duration decreased from 18 to 9 hours. This process will be further monitored.

DMAIC is a long-term method and despite being very extended and time-consuming, it guarantees proper identification of problems and their effects for the maintenance process. It ensures developing and implementing effective improvement actions and, what is most important, it guarantees that the implemented actions will be continued in the future.

The described case study has proved that it is possible to effectively use quality engineering methods and tools for maintenance process improvement. This allows increasing the availability of machines as well as shortening the duration of downtimes and failure removal.

ACKNOWLEDGEMENTS

This article was prepared within the statutory research titled "Production engineering methods and tools for development of smart specializations", work symbol 13/030/BK_16/0024 performed at Silesia University of Technology, Institute of Production Engineering.

REFERENCES

Andrássyová Z., Žarnovský J., Álló Š., Hrubec J. 2013. *Seven new quality management tools,* Advanced Materials Research. vol. 801, special issue, pp. 25-33.

Bargerstock A.S., Richards S.R. 2015. *Case Study: Application of DMAIC to Academic Assessment in Higher Education Quality Approaches*, Higher Education, vol. 6, no. 2, pp. 31-40.

Deming W.E. 2000. The New Economics for Industry, Government, Education, 2nd edition. MIT Press. Cambridge.

Dreachslin J.L., Lee P.D. 2007. *Applying Six Sigma and DMAIC to Diversity Initiatives*, Journal of Healthcare Management, vol. 52, no. 6, pp. 361-367.

Eckes G. 2000. *The Six Sigma Revolution*, John Wiley & Sons, Inc. New York.

George M., Rowlands D., Price M., Maxey J. 2005. Using DMAIC to improve speed, quality, and cost. In *The Lean Six Sigma Pocket Toolbook: A Quick Reference Guide to Nearly 100 Tools for Improving Process Quality, Speed, and Complexity*, McGraw-Hill, pp. 1-26.

Krzemień E., Wolniak R. 2007. Analysis of process of constant improvement of six sigma. In *Current trends in commodity science. Proceedings of the 9th International Commodity Science Conference (IGWT),* ed. R. Zieliński. Poznan University of Economics Publishing House. Poznan, pp. 227-232.

Legutko S. 2009. *Development trends in machines operation maintenance,* Eksploatacja i Niezawodnosc – Maintenance and Reliability, no. 2, pp. 8-16.

Mączyński W., Nahirny T. 2012. Efektywność służb utrzymania ruchu jako składowa efektywności przedsiębiorstwa. In *Innowacyjność procesów i produktów*, ed. R. Knosala, Oficyna Wydawnicza PTZP. Opole, pp. 203-213.

Midor K. 2014. *An analysis of the causes of product defects using quality management tools*, Management Systems in Production Engineering, no. 4, pp. 162-167.

Midor K., Szczęśniak B., Zasadzień M. 2010. *The identification and analysis of problems within a scope of cooperation between traffic maintenance department and production department.* Scientific Journals Maritime University of Szczecin, vol. 96, no. 24, pp. 48-52.

Mikler J. 2005. *Strategie Utrzymania Ruchu: przegląd i analiza,* Seminar Protech.

Sahno, J., Shevtshenko, E. 2014. Quality improvement methodologies for continuous improvement of production processes and product quality and their evolution. In *Proceedings of 9th International DAAAM Baltic Conference Industrial Engineering,* Tallinn University Of Technology, Tallinn, pp. 181-186.

Soković M., Jovanović J., Krivokapić Z., Vujović A. 2009. *Basic Quality Tools in Continuous Improvement Process*, Strojniški vestnik - Journal of Mechanical Engineering, no 5, pp. 1-4.

Sokovic M., Pavletic D., Kern Pipan K. 2010. *Quality Improvement Methodologies – PDCA Cycle, RADAR Matrix, DMAIC and DFSS*, Journal of Achievements in Materials and Manufacturing Engineering, vol 43, issue 1, pp. 476-483.

Tague N.R. 2005. *The Quality Toolbox* , ASQ Quality Press, Milwaukee, 2nd edition.

Truscott W. 2003. *Six Sigma: Continual Improvement For Businesses,* Butterworth Heinemann. New York.

Wojtaszak M., Biały W. 2013. Measurement system analysis of attribute or continuous data, as a one of the first steps in Lean Six Sigma projects. In *Systems supporting production engineering*, ed. J. Kaźmierczak. PA NOVA. Gliwice, pp. 144-162.

Zasadzień M., Midor K. 2015. Innovative application of quality management tools in a hard coal mine. In *Proceedings of 15th International Multidisciplinary Scientific GeoConference SGEM 2015*, book1, vol. 3, pp. 415-422.

Żurakowski F. 2004. *Funkcjonowanie przedsiębiorstwa. Zarządzanie,* Wydawnictwa Szkolne i Pedagogiczne. Warszawa.

.

Structuring Multicriteria Resource Allocation Models
A Framework to Assist Auditing Organizations

Vivian Vivas[1,2] and Mónica Duarte Oliveira[1]
[1]*Centre for Management Studies of Instituto Superior Técnico (CEG-IST), Universidade de Lisboa, Lisbon, Portugal*
[2]*Department of Planning, Budget and Finance, Comptroller General of the Union, Brasilia, Brazil*
{vivian.vivas, monica.oliveira}@tecnico.ulisboa.pt

Keywords: Audit Planning, Multicriteria Evaluation, Portfolio Decision Analysis, Problem Structuring, Resource Allocation.

Abstract: Multicriteria resource allocation models have been reported in the literature to support decision makers in selecting options/projects/programmes. These models are particularly important in public contexts in which resources are limited and there is an increasing demand for transparency and accountability in spending. Despite the potential of these models to promote an effective use of scarce resources, there is little organized and integrated research on how to structure them. In this paper we propose a framework with techniques and tools to support the structuring of multicriteria resource allocation models, so that these models have a potential to assist organizations in evaluating and selecting audit and control actions; and we provide illustrative examples on to apply these techniques and tools in the context of the Comptroller General of the Union, the Ministry of the Brazilian federal government responsible for helping the Brazilian president regarding the treasury, federal public assets application and the government's transparency policies.

1 INTRODUCTION

Brazil is a large country that has in place governmental programs that reach all its territory, and in which the public spending of federal funds is audited by the Ministry of Transparency, Supervision and Comptroller General of the Union (CGU). Similar to public auditing organizations in other countries, the activities of the CGU integrate actions of corruption prevention, fraud deterrence, public accounting, comptroller, ombudsman activities and increased transparency in management. In a time in which the country is going through a severe economic crisis, CGU has a key role in promoting transparency and accountability in public spending.

Since resources are scarce, CGU public managers must choose the set of projects to be executed with the available budget, considering costs and expected returns. This is a resource allocation situation well recognized in literature and, in this context, the use of multicriteria decision analysis concepts and tools can become useful and necessary.

Several multicriteria models for resource allocation have been reported in literature to support decision-makers in managing portfolios, taking into account of costs, benefits and risks (Liesiö et al., 2007; Phillips and Bana e Costa, 2007; Lourenço et al., 2012; Oliveira et al., 2012). However, there is little indication in the decision sciences and operational research literature on how to structure such type of problems in an integrated and organized manner (Montibeller et al., 2009). Proper structuring is required for building models that can effectively assist decision-makers.

This paper aims to fill this gap by proposing a framework to structure multicriteria resource allocation models (MRAM) in the context of auditing organizations. Specifically, the framework defines procedures and methods that can help to structure MRAM with a potential to improve the internal processes of organizations that have budget constraints and perform audit and inspection actions, such as in the CGU. The remainder of the paper is structured as follows. The next section outlines broadly the multicriteria resource allocation problem and key approaches set out in the literature to address those problems. Then we suggest a set of techniques and tools for the structuring MRAM and provide examples of its application for the auditing context. The paper ends with discussion of some relevant issues and directions for future research.

Vivas, V. and Oliveira, M.
Structuring Multicriteria Resource Allocation Models - A Framework to Assist Auditing Organizations.
In *Proceedings of the 6th International Conference on Operations Research and Enterprise Systems (ICORES 2017)*, pages 321-328
ISBN: 978-989-758-218-9

2 THE (CLASSICAL) RESOURCE ALLOCATION PROBLEM

2.1 General Definition

The multicriteria resource allocation problem is characterized by the selection of attractive projects (portfolio) to be financed under the presence of a limited budget and of other relevant constraints. So, the prioritization and/or selection of options aims at generating portfolios of projects – which entail multiple benefits, costs and uncertainties – that offer the best overall value for a given budget. Clearly, the analyses of portfolios will depend on how the organization's decision-makers values distinct project benefits and risks, as well as on the costs required by those projects and by context constraints. As these benefits are usually multi-dimensional (e.g., losses recovery, strategic fit, social responsibility, safety etc.), this is a multicriteria problem.

The multicriteria resource allocation literature suggests two main modelling approaches that can inform the prioritization and/or the selection of projects and that can be used by the CGU: the **optimization** approach (Bana e Costa and Soares, 2004; Liesiö et al., 2007; Lourenço et al., 2012; Oliveira et al., 2012) and the **prioritization** approach (Bana e Costa et al., 2006; Phillips and Bana e Costa, 2007), which we now briefly describe.

2.2 The OPTIMIZATION Approach

Following Oliveira et al. (2012), the performance x_{ij} of each project j in the benefit criterion i can be measured by a level in the respective descriptor, with partial value $v_i(x_{ij})$. Under an additive structure (which requires the respect for mutual independence conditions), the value of the overall benefit v_j of the project j, with k_i represent the weight assigned to criterion i, can be determined as:

$$v_j(x_{1j}, \dots, x_{nj}) = \sum_{i=1}^{n} k_i . v_i(x_{ij})$$
$$\sum_{i=1}^{n} k_i = 1 \text{ and } k_i > 0 \ \ (i = 1, \dots, n) \quad (1)$$

Considering each project j has $v_j > 0$ and cost c_j, B is the total of available resources, and as $l_j = 1$, if the project j is included in the best portfolio and $zero$ otherwise, we have:

$$maximize: \sum_{j=1}^{m} v_j l_j \quad (2)$$

$$subject\ to: \sum_{j=1}^{m} c_j l_j \leq B,$$
$$l_j \in \{0,1\}, \quad j = 1, \dots, m. \quad (3)$$

The best project portfolio will be found by solving this optimization problem. Additional constraints can be considered.

2.3 The PRIORITIZATION Approach

Following Bana e Costa et al. (2006), the prioritization approach can be applied in six steps, in which the first three steps are similar to the optimization approach but also necessary: 1. List the projects; 2. Use a multicriteria value model, as Equation (1), for instance, to determine the added expected benefit v_j, if the project j is financed; 3. Define the cost c_j of each project, equal to the amount of financial support funding; 4. Calculate the benefit-to-cost ratio ($r_j = v_j / c_j$) of each project; 5. Rank the projects from the highest to the lowest benefit-to-cost ratio; and 6. Go down the list, choosing projects until the available budget is depleted.

A variant of this prioritization approach is found in Phillips and Bana e Costa (2007), that use the Equity, a software for portfolio analysis, which enables a classification of projects within an organizational structure logic. Specifically, the funds can be spent on different levels in various organizational units or functions, called areas. In each of the areas K, the options are evaluated based on criteria of benefits and risks J, resulting in $K \times J$ scales. For a given criteria j is assigned a within criteria weight w_{jk}. The total value of each option i and the benefit-cost ratios are:

$$V_i = c \frac{\sum_j w_j \, . \, w_{jk(i)} . \, v_{ij}}{\sum_j \sum_k w_j \, . \, w_{jk}} \quad (4)$$

$$r_i = \frac{V_i}{C_i} \quad (5)$$

The options are ranked from highest to lowest ratio r_i. The Equity structure can also be used within an optimization approach, although requiring a more sophisticated optimization model.

Several decision support tools assist the implementation of both approaches, being that the case of PROBE - Portfolio Robustness Evaluation (Lourenço et al., 2012), RPM - Robust Portfolio Modelling (Liesiö et al., 2007, 2008; Vilkkumaa et al., 2014) and the resource allocation module of M-MACBETH (Bana e Costa et al., 2012; Hummel et al., 2017).

2.4 Auditing Context

Both the prioritization and optimization modelling approaches can be useful for assisting decision-making processes of auditing organizations, as directly or indirectly shown by distinct studies: Bradbury and Rouse (2002) point out that the audit risk assessment is an essential part of the audit planning process. As the authors explain, numerical risk scores for each audit unit, together with materiality, can be used as the basis for the audit resource allocation. In turn, some studies have presented models to allocate internal auditing time and others auditing resources to projects (Krüger and Hattingh, 2006; Mohamed, 2015), using the optimization approach.

Prior to the use of these models, one needs to structure the multicriteria resource allocation model. I.e., to build such a model it is necessary to get all the information pertaining on models, which means defining the organizational areas, audit units, project options, costs, measurement criteria of benefits, risks, synergies and interdependencies between projects and other necessary factors (Friend and Hickling, 2005; Keeney, 1992; Montibeller et al., 2009), as well as to understand who should participate in model construction and whom the model is expected to assist. Such structuring will show whether an optimization or a prioritization approaches should be used, and whether these approaches need further development (note this is not the focus of this article).

3 STRUCTURING RESOURCE ALLOCATION DECISION MODELS

We herein propose a framework with techniques and tools to help defining and structuring MRAM to assist auditing organizations. Departing from the work presented by Belton and Stewart (2002), the proposed framework, shown in Figure 1, is able to generate background information to build MRAM. Note that applying the propose framework will require the use of technical tools and concepts, as well to involve decision-makers into participatory processes (for instance, to build a multicriteria value model), i.e., the adoption of a socio-technical process (Phillips and Bana e Costa, 2007). In this article, we focus on the techniques, rather than on the social process.

Each stage of the framework must generate relevant information to building the model in a structured way. The choice of which tools to use depends on the context of the problem being addressed, on which tools best fit the organizational culture, and on the user's familiarity with those tools.

Figure 1: Framework to assist the structuring resource allocation models.

3.1 Problem Identification

The first step is to identify the type of decision problem and understand the different perceptions of the actors relevant for the decision. Auditing organizations commonly need to choose the control actions to be performed by audit teams, taking into account the audit risks and available resources. Is this a prioritization problem? Is this a ranking problem? Is this about project selection with budget constraints? Or, moreover, does project selection involve possible conflicts of interest? The identification of the decision problem type is a key factor for MRAM.

In this step we suggest the use of structuring tools for problem definition, such as those cited by Franco and Montibeller (2011): cognitive mapping, dialog mapping, Soft Systems Methodology (SSM), group model building.

As explained by Eden (2004), a cognitive map is a graphical representation of thoughts in a network shape containing nodes and arrows whose direction implies causality. It is a powerful tool to capture different aspects of the problem to be addressed and is helpful to clarify people's ideas and perceptions.

Another tool is Dialog Mapping that seeks to build common understanding for wicked problems, which are ill structured and complex and can lead to different views and solutions depending on different stakeholders' perceptions. A diagram or map is shown in a shared display with use of a conversational grammar called IBIS, Issue Based Information System, that represents the moves in a conversation as questions, ideas (possible answers to the question), and arguments (pros and cons to the ideas) (Conklin, 2006).

Soft systems methodology (SSM) is an approach for dealing with problematical messy situations. Its

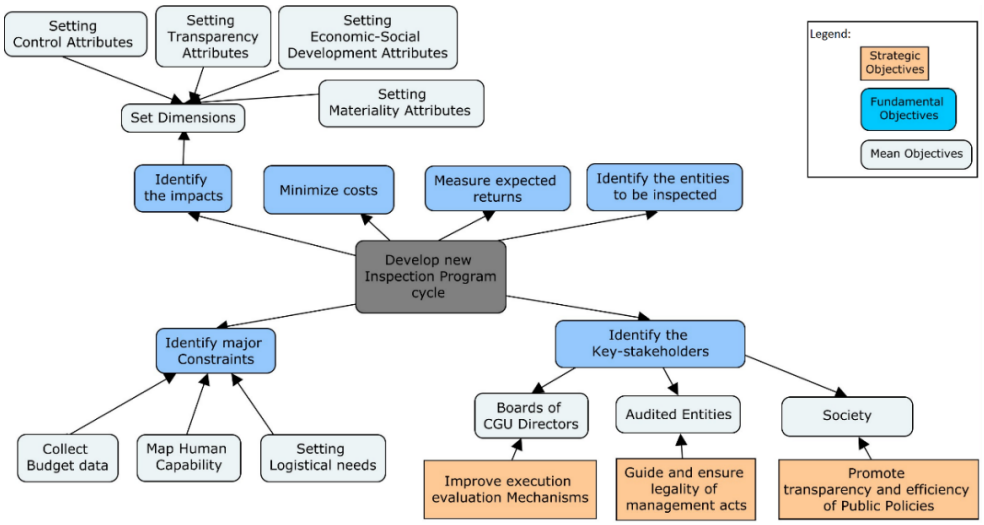

Figure 2: Mapping key concerns for developing an inspection program cycle with a means-ends objectives network.

use is recommended when divergent views on the problem definition exist. It is an action-oriented process of investigation in which users learn their way from finding out about the situation and what can be done to improve it (Checkland and Poulter, 2010).

In turn, a Group Model Building is a data analysis method from a group of decision makers. The dynamic patterns and relationships between key factors discussed by the group are portrayed to talk and analyse, resulting in new insights and possible new strategies or scenarios (Richardson and Andersen, 1995).

In addition, Friend and Hickling (2005) have presented the Strategic Choice Approach (SCA) that is useful to support the creation and definition of the problem in uncertain contexts.

Following Keeney's (1992) guidelines, one can also frame a decision situation by structuring the strategic, fundamental and mean objectives through means-ends relationships. Giving an example on auditing context, CGU performing an inspection program in states and municipalities, in order to assess the expenses incurred by these entities involving federal funds. The scope and entities to be inspected are chosen based on indicators divided into four dimensions: Control, Transparency, Economic and Social Development and Materiality.

Figure 2 illustrates the means-ends network for the CGU problem described. The main objective of an inspection cycle is to define the control actions (projects) that will be performed, within the available resources, which means defining auditing scope, auditees and measure expected returns/impacts. The map highlights key issues of the decision problem, namely the value system organized in a means-ends network. In fact, visual tools are useful to define and clarify the problem may be relevant in this step.

Once the problem is defined, as Franco and Montibeller (2011) well emphasized, it is necessary identify which aspects or particular decisional element of the decision problem will be evaluated in the model to be built. However, before that, we need to identify the key actors involved in the process.

3.2 Stakeholders Identification

The next step seeks to identify the key stakeholders and analyse their power and influence on the decision context. Bryson (2004) presents an array of techniques useful for stakeholders' identification and analysis and which grouped into four categories, which should be used in this step: organizing participation; creating ideas for strategic interventions; building a winning coalition around proposal development, review and adoption; and implementing, monitoring and evaluating strategic interventions. The author highlights five stakeholder identification and analysis techniques to helping organize participation: a process for choosing stakeholder analysis participants; the basic stakeholder analysis technique; power versus interest grids; stakeholder influence diagrams; and the participation planning matrix. He lists six additional techniques to creating ideas for strategic interventions: bases of power and directions of interest diagrams; finding the common good and the structure of a winning argument; tapping individual stakeholder interests to pursue the common good; stakeholder-issue interrelationship diagrams; problem-frame stakeholder maps; and ethical

analysis grids. The author also considers three techniques for proposal development review and adoption: stakeholder support versus opposition grids, stakeholder role plays and policy attractiveness versus stakeholder capability grids. And, finally, presents policy implementation strategy development grid for the last category.

From these techniques, we can highlight grouping the stakeholders in the matrix power/interest, proposed by Mendelow (1981), in which is possible to perceive how communication and relationships between stakeholders can affect the model structure and its implementation. Figure 3, for instance, helps to understand differences in power and influence of key stakeholders in the CGU inspection program.

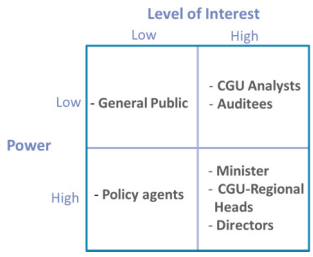

Figure 3: Power-interest matrix applied to an inspection action.

Ferretti (2016) shows that, under the existence of a plurality point of views, one needs to understand these differences, which requires the framework steps that follow.

3.3 Goals and Values Identification

Once the problem and the stakeholders are identified, one needs to have an understanding of the goals and values of the stakeholder(s). We can underline the concept of decision framing presented by Keeney (1992) which points out that values are used for evaluation and should reflect the decision-makers objectives. He highlights that there are two distinct types of objectives, the fundamental objectives and the mean objectives. While the former features an essential reason for the interest in the decision situation, the mean objectives are just a way to achieve them. As the author also emphasizes, structure objectives give the basis for any use of quantitative modelling and the fundamental objectives hierarchy can indicate the set of objectives over which attributes should be defined.

A structuring tool widely used in decision analysis is the value tree, which displays the family of key-concerns in a tree form and offers a useful visual overview of the main objectives in different levels of increasing specification (Bana e Costa, 2001; Bana e Costa et al., 2004). In Figure 4 we present a value tree with the fundamental objectives to be attained with an inspection action. For instance, the "Management Continual Improvement" objective is concerned with the assessment of the inspection program's objective component in terms of efficiency and technical quality as well as the agreement on the entities and the areas to be audited.

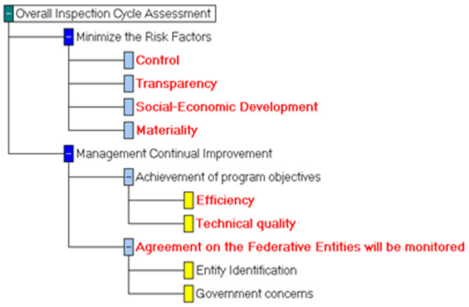

Figure 4: Value tree for an inspection action built with M-MACBETH.

At this stage, it is also important to look for the alternative's costs and identify the measurement criteria of alternative performances (expected benefits). One can make use of the framework for structuring options and areas and criteria presented in Montibeller et al. (2009). The authors propose two approaches to structuring criteria, based on Keeney's concepts: Alternative-focused thinking (AFT), which criteria are defined from the characteristics that distinguish options and Value-focused thinking (VFT), where the evaluation criteria should reflect the organization's values and strategic objectives.

3.4 Alternatives Identification

The identification of decision alternatives, which in auditing context means the identification of audit projects that will be evaluated, is an important step in the structuring process and can be performed through different techniques / tools.

In organizations segregated by pre-defined areas, where the initial set of project options is relatively stable, it can be used the AFT above described, in which, after problem definition, the projects are identified and, then, the values (criteria) to consider in the evaluation are specified. In turn, on the VFT, organizational values and goals are initially set. The options are then created thinking on how to achieve these goals (Keeney, 1992).

Another useful tool presented by Howard (1988) is the strategy-generation table. It shows how a total

strategy can be specified by combination of options under several dimensions, called strategy themes.

In turn, one may apply analysis of interconnected decision areas (AIDA) technique, present in Strategic Choice Approach (Friend and Hickling, 2005), that allows visualization of the compatibilities and incompatibilities of options within a problem focus.

One can still make use of cognitive map to explore/identify decision alternatives (Eden, 2004). Montibeller and Belton (2006) proposed the causal map, which can also be used to identify and agree to a set of potential strategic options. As the authors highlight, a causal map is a network of inter-linked concepts (ideas) which tries to represent the discourse of a person through means-ends structure, whereby decision options are means of achieving the decision-makers' goals.

In the CGU inspection case, since the projects to be evaluated depend on the definition of the federal state to be inspected and the audit scope, we can map the set of options surrounding the inspection program to gain a better understanding of the issues, their interrelations and perceived implications to the model to be built.

3.5 Uncertainties Identification

An analysis of which uncertainties are key for the evaluation of options and for the allocation of resources is required. To exemplify, uncertainties may be related with the budget, with the measurement of options performance and with the importance/weight of objectives.

Vilkkumaa et al. (2014) make a Bayesian modelling of uncertainties, to be considered in the selection of project portfolios. There is still another classification in Strategic Choice Approach to identify the uncertainties relating to the working environment, related to the guiding values and related to the choices in related agendas (Friend and Hickling, 2005). Thus, different uncertainty types may require different analysed with the prioritization and/or optimization modelling approaches.

In the auditing context, as highlighted by Krüger and Hattingh (2006, p.62), we can mention that "*risk is seen as a measure of uncertainty and is linked to the possible loss in an audit area — uncertainty in achievement of business objectives. The possible loss in an audit area will depend on specific characteristics and these characteristics are termed audit risk factors. Examples of well known and frequently used risk factors include complexity of operations, financial implications, recent changes, time since last audit, etc.*" – these issues should be discussed for each context and have naturally an impact on the MRAM to be developed.

In the CGU example, a relevant audit risk factor to be considered in the model may be related to the uncertainty in estimate the project (control actions) values to be included in the inspection program portfolio.

3.6 Constraints Identification

It is also necessary to identify constraints that may be relevant for the allocation of scarce resources to competing projects. For instance, there may be resources/budget restrictions, synergies between projects or interdependencies between projects.

At this stage, in a brainstorm session/focus group, one can use VFT to elicit the main constraints involved in the decision problem by equations (Keeney, 1992). AIDA can also help with Option Bars that bring the incompatibilities that can be translated into equations to be added to the value model used (Friend and Hickling, 2005).

In the CGU case, it is important to consider the following constraints:

Budgetary. Identify financial cost of each control action and prioritize projects within the available budget, so as to be accounted for in equation (3).

Logistical. The distribution of teams available for each control action needs to be accounted for (e.g., equipment, vehicles, and special displacements). Whereas h_{kj} the amount of resources k consumed by the project j and H_k the total available resources k. It has been:

$$\sum_{j=1}^{n} h_{kj} l_j \leq H_k \tag{6}$$

Context. Projects of entities identified as vulnerable should be positively discriminated. Be the corresponding v project to the federal entity identified as vulnerable, one should have:

$$l_v = 1 \tag{7}$$

3.7 Interactions between the Stages

To complete the structuring process, one cannot apply the framework without considering the joint analysis of different framework stages, as these are key to select and/or develop MRAM. Table 1 summarises techniques and tools included in the proposed framework. The diagonal includes techniques and tools previously described, and the remainder cells provide tools that can assist more complex analyses.

Table 1: Selection of techniques and tools that can assist structuring (crossing framework stages).

	Stakeholders	Goals and Values	Alternatives	Uncertainties	Constraints
Stakeholders	Stakeholder Power-interest Grid Stakeholder Visualization Influence Map	Negotiation Analysis Drama Theory	Conflict Dissolution Drama Theory		
Goals and Values	Negotiation Analysis Drama Theory	Value Tree Decision framing Fundamental Objectives Hierarchy	Value Tree Causal Map and MCDA	DSS PROBE RPM	
Alternatives	Conflict Dissolution Drama Theory	Value Tree Causal Map and Multicriteria Decision Analysis (MCDA)	Cognitive Map SCA AFT, VFT Strategy Table		AIDA in SCA RPM
Uncertainties		DSS PROBE RPM		Bayesian modelling SCA Risk Factor Analysis	
Constraints			AIDA in SCA RPM		Brainstorm Focus group VFT AIDA in SCA

For instance, different stakeholders (single, multiple, group) can lead to different goals and values and can generate different sets of alternatives and criteria.

In this situation, it may be useful to apply conflicts dissolution modelling techniques to have an understanding for possible win-win solutions, which are often used for evaluation models but can be adapted to the structuring context. (Bana e Costa et al., 2001; Edwards et al., 2007)

As implications for resource allocation models, we can cite:

- **Multiply stakeholders:** Preparation of a cognitive map to every stakeholder, analysis of common and divergent characteristics. Conducting focus group/brainstorming sessions for the preparation of an aggregated map (Ferretti, 2016). The use of bargain negotiation/drama theory (Edwards et al., 2007; Rosenhead and Mingers, 2001) can be useful.
- **Group of stakeholders**: The necessity for using techniques conflict dissolution in brainstorming session/focus group (Bana e Costa, 2001; Bana e Costa et al., 2001; Salo, 1995).

Regarding uncertainties, it may be related to the objectives and values, since the weights of the criteria might influence the project consequences - in this case robustness analysis and impact measurement can be used.

Thus, the result to be presented will be determined by the whole process and possibly different MRAM may emerge. Therefore, the modelling approaches presented in Section 2 may need to be enhanced and developed for the context.

4 DISCUSSION

This paper combined decision making techniques and tools to support the structuring of multicriteria resource allocation models for the auditing context, in an attempt to aid stakeholders involved in the auditing decisions and which are pressured and charged for transparency and accountability in public spending.

The application of the framework requires thinking about which decision-makers and stakeholders should be directly involved in each framework stage, together with a facilitator/consultant, an analyst, an recorder and/or others necessary roles in the process (Richardson and Andersen, 1995). This is necessary so that decision-makers will have confidence in MRAM results.

For future research, it is relevant: to extend the concepts and techniques to be used in the distinct framework stages; to systematically apply the framework for well-defined decisions at CGU and in other real-world auditing contexts; and, to measure the added value of using the framework.

REFERENCES

Bana e Costa, C.A., 2001. The use of multi-criteria decision analysis to support the search for less conflicting policy options in a multi-actor context: Case study. *Journal of Multi-Criteria Decision Analysis.* 10(2), 111–125.

Bana e Costa, C.A., Antão da Silva, P., Nunes Correia, F., 2004. Multicriteria Evaluation of Flood Control Measures: The Case of Ribeira do Livramento. *Water Resources Management.* 18(3), 263–283.

Bana e Costa, C.A., De Corte, J.-M. and Vansnick, J.-C., 2012. MACBETH. *International Journal of Information Tech. & Decision Making*. 11(2), 359–387.

Bana e Costa, C.A., Fernandes, T.G., Correia, P.V.D., 2006. Prioritisation of public investments in social infrastructures using multicriteria value analysis and decision conferencing: A case study. *International Transactions in Operational Research*. 13(4), 279–297.

Bana e Costa, C.A., Nunes Da Silva, F., Vansnick, J.-C., 2001. Conflict dissolution in the public sector: A case-study. *European Journal of Operational Research*. 130(2), 388–401.

Bana e Costa, C.A., Soares, J.O., 2004. A multicriteria model for portfolio management. *The European Journal of Finance*. 10, 198–211.

Belton, V., Stewart, T., 2002. *Multiple Criteria Decision Analysis: An Integrated Approach*. Kluwer: Dordrecht.

Bradbury, M.E., Rouse, P., 2002. An Application of Data Envelopment Analysis to the Evaluation of Audit Risk. *Abacus*. 38(2), 263–279.

Bryson, J.M., 2004. Stakeholder Identification and Analysis Techniques. *Public Management Review*. 6(1), 21–53.

Checkland, P., Poulter, J., 2010. Soft Systems Methodology. In: Reynolds, M., Holwell, S. (Eds.), *Systems Approaches to Managing Change: A Practical Guide.* Springer-Verlag, London, 191–242.

Conklin, J., 2006. *Dialogue Mapping: Building Shared Understanding of Wicked Problems*. Wiley.

Eden, C., 2004. Analyzing cognitive maps to help structure issues or problems. *European Journal of Operational Research*. 159(3), 673–686.

Edwards, W., Miles Jr., R.F., von Winterfeldt, D., 2007. *Advances in decision analysis: From foundations to applications.* New York: Cambrigde University Press.

Ferretti, V., 2016. From stakeholders analysis to cognitive mapping and Multi-Attribute Value Theory: An integrated approach for policy support. *European Journal of Operational Research*. 253(2), 524–541.

Franco, L.A., Montibeller, G., 2011. Problem Structuring for Multicriteria Decision Analysis Interventions. In: Cochran et al. (Eds.) *Wiley Encyclopedia of Operations Research and Management Science*. Wiley, USA.

Friend, J., Hickling, A., 2005. *Planning Under Pressure: The Strategic Choice Approach*. Third. ed. Elsevier Butterworth-Heinemann.

Howard, R.A., 1988. Decision Analysis: Practice And Promise. *Management Science.* 34(6), 679–695.

Hummel, M.J., Oliveira, M.D., Bana e Costa, C.A., Ijzerman, M.J., 2017. *Supporting the project portfolio selection decision of research and development investments by means of multi-criteria resource allocation modelling*. In: Marsh, K., Goetghebeur, M., Thokala, P., Baltussen, R. (Eds.) *Multi-Criteria Decision Analysis to Support Healthcare Decisions*. Springer.

Keeney, R.L., 1992. *Value-focused thinking: A Path to Creative Decisionmaking*. Harvard University Press.

Krüger, H.A., Hattingh, J.M., 2006. A combined AHP-GP model to allocate internal auditing time to projects. *ORiON*. 22(1), 59–76.

Liesiö, J., Mild, P., Salo, A., 2007. Preference programming for robust portfolio modeling and project selection. *European Journal of Oper Res*. 181(3), 1488–1505.

Liesiö, J., Mild, P., Salo, A., 2008. Robust portfolio modeling with incomplete cost information and project interdependencies. *European Journal of Operational Research*. 190(3), 679–695.

Lourenço, J.C., Morton, A., Bana e Costa, C.A., 2012. PROBE - A multicriteria decision support system for portfolio robustness evaluation. *Decision Support Systems*, 54(1), 534–550.

Mendelow, A.L., 1981. Environmental Scanning - The Impact of the Stakeholder Concept. *International Conference on Information Systems.* 407–417.

Mohamed, A.M., 2015. Operations Research Applications in Audit Planning and Scheduling. *International Journal of Social, Behavioral, Educational, Economic, Business and Industrial Engineering.* 9(6), 2026–2034.

Montibeller, G., Belton, V., 2006. Causal maps and the evaluation of decision options - a review. *Journal of the Operational Research Society*. 57(7), 779–791.

Montibeller, G., Franco, L.A., Lord, E., Iglesias, A., 2009. Structuring resource allocation decisions: A framework for building multi-criteria portfolio models with area-grouped options. *European Journal of Operational Research.* 199(3), 846–856.

Oliveira, M.D., Rodrigues, T.C., Bana e Costa, C.A., Brito de Sá, A., 2012. Prioritizing health care interventions: A multicriteria resource allocation model to inform the choice of community care programmes. In: Tanfani, E., Testi, A. (Eds.), *Advanced Decision Making Methods applied to Health Care*. Springer, 141-154.

Phillips, L.D., Bana e Costa, C.A., 2007. Transparent prioritisation, budgeting and resource allocation with multi-criteria decision analysis and decision conferencing. *Annals of Oper. Research*. 154, 51–68.

Richardson, G.P., Andersen, D.F., 1995. Teamwork in group model building. *System Dynamics Review*. 11(2), 113–137.

Rosenhead, J., Mingers, J.(Eds.), 2001. *Rational analysis for a problematic world revisited: problem structuring methods for complexity, uncertanty and conflict*. Wiley.

Salo, A., 1995. Interactive decision aiding for group decision support. *European Journal of Operational Research*. 84, 134–149.

Vilkkumaa, E., Liesiö, J., Salo, A., 2014. Optimal strategies for selecting project portfolios using uncertain value estimates. *European Journal of Operational Research*. 233(3), 772–783.

On a Traveling Salesman based Bilevel Programming Problem

Pablo Adasme[1], Rafael Andrade[2], Janny Leung[3] and Abdel Lisser[4]
[1]*Departamento de Ingeniería Eléctrica, Universidad de Santiago de Chile, Avenida Ecuador 3519, Santiago, Chile*
[2]*Departamento de Estatística e Matemática Aplicada, Universidade Federal do Ceará, Campus do Pici, BL 910, CEP 60.455-760, Fortaleza, Ceará, Brazil*
[3]*Department of Systems Engineering & Engineering Management, Chinese University of Hong Kong, Shatin, Hong Kong, China*
[4]*Laboratoire de Recherche en Informatique, Université de Paris-Sud 11, Bât. 650 Ada Lovelace, Paris, France*
pablo.adasme@usach.cl, rca@lia.ufc.br, janny@se.cuhk.edu.hk, abdel.lisser@lri.fr

Keywords: Bilevel Programming, Traveling Salesman Problem, Mixed Integer Linear Programming Formulations, Iterative Sub-tour Elimination Constraint Procedure.

Abstract: In this paper, we consider a linear bilevel programming problem where both the leader and the follower maximize their profits subject to budget constraints. Additionally, we impose a Hamiltonian cycle topology constraint in the leader problem. In particular, models of this type can be motivated by telecommunication companies when dealing with traffic network flows from one server to another one within a ring topology framework. We transform the bilevel programming problem into an equivalent single level optimization problem that we further linearize in order to derive mixed integer linear programming (MILP) formulations. This is achieved by replacing the follower problem with the equivalent Karush Kuhn Tucker conditions and with a linearization approach to deal with the complementarity constraints. The topology constraint is handled by the means of two compact formulations and an exponential one from the classic traveling salesman problem. Thus, we compute optimal solutions and upper bounds with linear programs. One of the compact models allows to solve instances with up to 250 nodes to optimality. Finally, we propose an iterative procedure that allows to compute optimal solutions in remarkably less computational effort when compared to the compact models.

1 INTRODUCTION

Bilevel programming is a two level hierarchical optimization framework where the upper level problem is referred to as the leader whilst the lower level problem is referred to as the follower problem. In a bilevel programming problem (BPP), we aim to find an optimal point such that the leader and the follower maximize (or minimize) their respective objective functions subject to linking constraints. Applications concerning BPPs arise in agriculture, economic systems, finance, engineering, banking, transportation, network design, management and planning to name a few. For a more general description of BPP applications and algorithmic approaches to solve these problems see for instance (Dempe, 2003; Floudas and Pardalos, 2001; Migdalas et al., 1997; Thirwani and Arora, 1998; Vicente et al., 1994; Wang et al., 1994).

In this paper, we consider a linear bilevel programming problem (LBPP) where both the leader and the follower maximize their profits subject to budget constraints. Additionally, we impose a Hamiltonian cycle topology constraint in the leader problem. In particular, models of this type can be motivated by telecommunication companies when dealing with traffic network flows from one server to another one within a ring topology framework. As an example, consider the problem of flow traffic management in a backbone wireless token ring network where users connect to any node and pass their messages trough the ring in order to reach another user which is also connected to a node in the ring (Lee et al., 2001; Song and Yang, 1997). In these types of networks, the traffic flows can be significantly large which might require more than one network operator to deal with the flow problem.

We transform the LBPP into an equivalent single level optimization problem that we further linearize in order to derive mixed integer linear programming (MILP) formulations. This is achieved by replacing the follower problem with the equivalent Karush Kuhn Tucker (KKT) conditions and with

Adasme, P., Andrade, R., Leung, J. and Lisser, A.
On a Traveling Salesman based Bilevel Programming Problem.
In *Proceedings of the 6th International Conference on Operations Research and Enterprise Systems (ICORES 2017)*, pages 329-336
ISBN: 978-989-758-218-9

the linearization approach proposed in (Audet et al., 1997) to deal with the complementarity slackness conditions. The topology constraint is handled by the means of two compact polynomial formulations and an exponential one from the classic traveling salesman problem (TSP) (Gavish and Graves, 1978; Letchford et al., 2013; Miller et al., 1960). Thus, we compute optimal solutions and upper bounds with the MILP and linear programming (LP) relaxations, respectively.

Our contribution in this paper is not theoretical, but mainly focussed on computational numerical results on a novel problem in the domain of bilevel programing. As far as we know, LBPPs including Hamiltonian cycle topology constraints have not been considered in the literature so far. We compare numerically the exponential model with the two compact formulations for randomly generated instances. For this purpose, first we solve the exponential model by generating all cycle elimination constraints and then, by using an iterative algorithmic procedure which consists of adding violated cycle elimination constraints within each iteration until no cycle is found in the current solution. Finally, we further propose a relaxed version of the iterative algorithm and compute tight upper bounds as well. Our main numerical result is to show that solving the exponential model with the iterative procedure is by far more convenient than using the compact formulations which are more theoretical based approaches. In fact, we solve to optimality instances with up to 250 nodes so far, in less than 70 seconds in average compared to the higher CPU times required by the compact formulations. It has been proved that BPPs are strongly NP-hard even for the simplest case in which all the involved functions are affine. See for instance (Migdalas et al., 1997; Scholtes, 2004). The reader is referred to the books (Dempe, 2002; Migdalas et al., 1997) for a more general understanding on bilevel programming.

The remaining of the paper is organized as follows. In section 2, first we present and explain the LBPP problem. Then, we discuss three equivalent MILP models while using the exponential and the two compact formulations. Subsequently, in section 3, we present the alternative iterative procedures which allow to obtain optimal solutions and tight upper bounds using the exponential model. Afterwards, in section 4 we compare all the proposed models and the iterative procedures with the optimal solution of the problem. Finally, in section 5 we give the main conclusions of the paper and provide some insight for future research.

2 LINEAR BILEVEL AND MILP MODELS

In this section, we present and explain the LBPP. In particular, we use an exponential number of sub-tour elimination constraints (SECs) to characterize the Hamiltonian cycle condition in the leader problem. Subsequently, we use two additional compact modeling approaches from the traveling salesman problem (Gavish and Graves, 1978; Letchford et al., 2013; Miller et al., 1960) and obtain equivalent MILP models. Let $G(V,E)$ denote a complete graph with set of nodes V and set of directed arcs E. Our LBPP can be formulated as follows

$$\mathrm{BP}_1 : \max_{\{f,g,x\}} \left\{ \sum_{ij\in E} C_{ij} f_{ij} + \sum_{ij\in E} D_{ij} g_{ij} \right\} \quad (1)$$

$$\text{s.t.} \sum_{j:ij\in E} A_{ij} f_{ij} + \sum_{j:ij\in E} B_{ij} g_{ij} \leq c, \forall i \in V \quad (2)$$

$$f_{ij} + g_{ij} \leq M x_{ij}, \forall ij \in E \quad (3)$$

$$\sum_{j:ij\in E} x_{ij} = 1, \forall i \in V \quad (4)$$

$$\sum_{j:ji\in E} x_{ji} = 1, \forall i \in V \quad (5)$$

$$\sum_{ij\in E(S)} x_{ij} \leq |S| - 1, \forall S \subset V \quad (6)$$

$$x_{ij} \in \{0,1\}, f_{ij} \geq 0, \forall ij \in E \quad (7)$$

$$g \in \arg\max_{\{g\}} \left\{ \sum_{ij\in E} H_{ij} g_{ij} + \sum_{ij\in E} P_{ij} f_{ij} \right\} \quad (8)$$

$$\sum_{j:ij\in E} Q_{ij} f_{ij} + \sum_{j:ij\in E} R_{ij} g_{ij} \leq r, \quad \forall i \in V \quad (9)$$

$$g_{ij} \geq 0, \forall ij \in E \quad (10)$$

In BP_1, the input symmetric matrices $\{C,D,A,B,H,P,Q,R\} \in \mathbb{M}_{|V|\times|V|}(\mathbb{R}_+)$ and the scalars $\{c,r\} \in \mathbb{R}_+$, respectively. Constraints (1)-(7) correspond to the leader problem whereas constraints (8)-(10) represent the follower problem. Without loss of generality, we assume that the set V represents servers to visit whereas the set E represents traffic links by which the network flow service should be carried out from one server to another. Thus, the binary decision variable $x_{ij} = 1$ if and only if the leader company decides to use the link (i,j) and $x_{ij} = 0$ otherwise, $\forall ij \in E$. Similarly, the decision variables $f_{ij}, g_{ij} \geq 0$ represent the amount of network flow to transport from i to j for the leader and follower problems, respectively. The objective functions maximize the profits for both the leader and the follower and are given in (1) and (8), respectively. Whereas the constraints (2) and (9) represent the costs structure

associated to each one of them. Constraints (7) and (10) are domain constraints for the decision variables. The constraints (3)-(6) characterize the Hamiltonian cycle condition imposed in the leader problem. In particular, the constraint (3) implies that whenever the variable $x_{ij} = 0$, then the variables f_{ij} and g_{ij} must be equal to zero $\forall ij \in E$. For this purpose, we use a large positive BigM value denoted by M. Constraints (4)-(5) enforce the condition that each node should be connected to two nodes in the circuit. Finally, constraint (6) represents SECs $\forall S \subset V$. Notice that we do not include SECs for $S \equiv V$ in order to allow obtaining feasible solutions, i.e., Hamiltonian cycles.

An equivalent MILP model can be straightforwardly obtained by replacing the follower problem with the equivalent KKT conditions and by using the linearization approach proposed in (Audet et al., 1997) to deal with the complementarity slackness conditions (Audet et al., 1997; Dempe, 2003). This leads to the following equivalent MILP model

$$\text{MIP}_1 : \max_{\{f,g,x,\lambda,\mu,\theta,\nu\}} \left\{ \sum_{ij\in E} C_{ij} f_{ij} + \sum_{ij\in E} D_{ij} g_{ij} \right\}$$

$$\text{s.t.} \sum_{j:ij\in E} A_{ij} f_{ij} + \sum_{j:ij\in E} B_{ij} g_{ij} \leq c, \forall i \in V$$

$$f_{ij} + g_{ij} \leq M x_{ij}, \forall ij \in E$$

$$\sum_{j:ij\in E} x_{ij} = 1, \forall i \in V$$

$$\sum_{j:ji\in E} x_{ji} = 1, \forall i \in V$$

$$\sum_{ij\in E(S)} x_{ij} \leq |S| - 1, \forall S \subset V \quad (11)$$

$$x_{ij} \in \{0,1\}, f_{ij} \geq 0, \forall ij \in E$$

$$H_{ij} - \lambda_i R_{ij} + \mu_{ij} = 0, \forall ij \in E \quad (12)$$

$$\sum_{j:ij\in E} Q_{ij} f_{ij} + \sum_{j:ij\in E} R_{ij} g_{ij} \leq r, \forall i \in V \quad (13)$$

$$r - \sum_{j:ij\in E} Q_{ij} f_{ij} - \sum_{j:ij\in E} R_{ij} g_{ij} + \nu_i L \leq L,$$

$$\forall i \in V \quad (14)$$

$$\lambda_i \leq \nu_i L, \forall i \in V \quad (15)$$

$$\mu_{ij} + \theta_{ij} L \leq L, \forall ij \in E \quad (16)$$

$$g_{ij} \leq \theta_{ij} L, \forall ij \in E \quad (17)$$

$$g_{ij}, \mu_{ij} \geq 0 \forall ij \in E, \lambda_i \geq 0 \forall i \in V \quad (18)$$

$$\nu_i \in \{0,1\} \forall i \in V, \theta_{ij} \in \{0,1\} \forall ij \in E \quad (19)$$

where the constraints (12) are due to the derivatives obtained with the Lagrangian function of the follower problem and with respect to the variables $g_{ij}, \forall ij \in E$. The non-negative variables λ_i, $\forall i \in V$ and μ_{ij}, $\forall ij \in E$ are dual variables for the constraints (9) and (10), respectively. The constraints (13)-(15) enforce the condition that either $\left(r - \sum_{j:ij\in E} Q_{ij} f_{ij} - \sum_{j:ij\in E} R_{ij} g_{ij}\right)$ or λ_i should be equal to zero $\forall i \in V$. This is handled with the binary variable ν_i $\forall i \in V$ and with the large positive value L. Similarly, the constraints (16)-(17) enforce the condition that either μ_{ij} or g_{ij} should be equal to zero for all $ij \in E$. This is handled with the variables $\theta_{ij} \in \{0,1\} \forall ij \in E$. Finally, (18)-(19) are domain constraints for the decision variables.

As it can be observed, the number of SECs in MIP_1 is exponential. To overcome this difficulty, we further consider the following MILP model which uses a well known characterization of the feasible space of the traveling salesman problem (Letchford et al., 2013; Miller et al., 1960)

$$\text{MIP}_2 : \max_{\{f,g,x,u,\lambda,\mu,\theta,\nu\}} \left\{ \sum_{ij\in E} C_{ij} f_{ij} + \sum_{ij\in E} D_{ij} g_{ij} \right\}$$

$$\text{s.t.} \sum_{j:ij\in E} A_{ij} f_{ij} + \sum_{j:ij\in E} B_{ij} g_{ij} \leq c, \forall i \in V$$

$$f_{ij} + g_{ij} \leq M x_{ij}, \forall ij \in E$$

$$\sum_{j:ij\in E} x_{ij} = 1, \forall i \in V$$

$$\sum_{j:ji\in E} x_{ji} = 1, \forall i \in V$$

$$u_1 = 1 \quad (20)$$

$$2 \leq u_i \leq |V|, \forall i \in V, (i \neq 1) \quad (21)$$

$$u_i - u_j + 1 \leq (|V| - 1)(1 - x_{ij}),$$

$$\forall ij \in E, (i \neq 1), (j \neq 1) \quad (22)$$

$$u_j \in \mathbb{Z}_+, \forall j \in V \quad (23)$$

$$x_{ij} \in \{0,1\}, f_{ij} \geq 0, \forall ij \in E$$

$$H_{ij} - \lambda_i R_{ij} + \mu_{ij} = 0, \forall ij \in E$$

$$\sum_{j:ij\in E} Q_{ij} f_{ij} + \sum_{j:ij\in E} R_{ij} g_{ij} \leq r, \forall i \in V$$

$$r - \sum_{j:ij\in E} Q_{ij} f_{ij} - \sum_{j:ij\in E} R_{ij} g_{ij} + \nu_i L \leq L, \forall i \in V$$

$$\lambda_i \leq \nu_i L, \forall i \in V$$

$$\mu_{ij} + \theta_{ij} L \leq L, \forall ij \in E$$

$$g_{ij} \leq \theta_{ij} L, \forall ij \in E$$

$$g_{ij}, \mu_{ij} \geq 0 \forall ij \in E, \lambda_i \geq 0 \forall i \in V$$

$$\nu_i \in \{0,1\} \forall i \in V, \theta_{ij} \in \{0,1\} \forall ij \in E$$

where the constraints (22) ensure that, if the salesman travels from i to j, then the nodes i and j are arranged sequentially. These constraints together with (20)-(21) and (23) ensure that each node is in a unique position. A third formulation can be obtained by using the classic single commodity flow formulation for the TSP (Gavish and Graves, 1978; Letchford et al., 2013). For this purpose, we assume that the salesman carries $|V| - 1$ units of a commodity when he leaves node 1, and delivers 1 unit of this commodity to each node. We can define additional continuous variables

$w_{i,j} \geq 0, \forall ij \in E$ representing the amount of the commodity (if any) routed directly from node i to node j. The new MILP formulation is

$$\text{MIP}_3 : \max_{\{f,g,x,w,\lambda,\mu,\theta,\nu\}} \left\{ \sum_{ij\in E} C_{ij} f_{ij} + \sum_{ij\in E} D_{ij} g_{ij} \right\}$$

$$\text{s.t.} \sum_{j:ij\in E} A_{ij} f_{ij} + \sum_{j:ij\in E} B_{ij} g_{ij} \leq c, \forall i \in V$$

$$f_{ij} + g_{ij} \leq M x_{ij}, \forall ij \in E$$

$$\sum_{j:ij\in E} x_{ij} = 1, \forall i \in V$$

$$\sum_{j:ji\in E} x_{ji} = 1, \forall i \in V$$

$$\sum_{j:ji\in E} w_{ji} - \sum_{j>1:ij\in E} w_{ij} = 1,$$

$$\forall i \in \{2,\ldots,|V|\} \quad (24)$$

$$0 \leq w_{ij} \leq (|V|-1) x_{ij}, \forall ij \in E \quad (25)$$

$$x_{ij}, f_{ij} \geq 0 \forall ij \in E$$

$$H_{ij} - \lambda_i R_{ij} + \mu_{ij} = 0, \forall ij \in E$$

$$\sum_{j:ij\in E} Q_{ij} f_{ij} + \sum_{j:ij\in E} R_{ij} g_{ij} \leq r, \forall i \in V$$

$$r - \sum_{j:ij\in E} Q_{ij} f_{ij} - \sum_{j:ij\in E} R_{ij} g_{ij} + \nu_i L \leq L, \forall i \in V$$

$$\lambda_i \leq \nu_i L, \forall i \in V$$

$$\mu_{ij} + \theta_{ij} L \leq L, \forall ij \in E$$

$$g_{ij} \leq \theta_{ij} L, \forall ij \in E$$

$$g_{ij}, \mu_{ij} \geq 0 \forall ij \in E, \lambda_i \geq 0 \forall i \in V$$

$$\nu_i \in \{0,1\} \forall i \in V, \theta_{ij} \in \{0,1\} \forall ij \in E$$

The constraints (24) ensure that one unit of the commodity is delivered to each node while the bounds in (25) ensure that the commodity can flow only along arcs in the solution. Hereafter, we denote by LP_1, LP_2 and LP_3 the LP relaxations of MIP_1, MIP_2 and MIP_3, respectively.

In the next section, we present an alternative iterative algorithmic procedure that allows to obtain optimal solutions and tight upper bounds for MIP_1.

3 ITERATIVE PROCEDURE FOR GENERATING SECS

The procedure to generate SECs can be easily adapted using Algorithms 4.1 and 4.2 from (Adasme et al., 2015) to MIP_1. The main idea can be described as follows. If we remove constraints (11) from MIP_1 and solve the resulting integer linear programming problem, then the underlying optimal solution induces a graph $\tilde{G}$ that may contain a cycle with at least two nodes. In this case, it can be detected by a depth-first search procedure (Cormen et al., 2009). In this paper, we adapt the procedure 4.1 from (Adasme et al., 2015) to find cycles in directed graphs with at least 2 and up to $|V|-1$ nodes. In particular, if the cardinality of a subset of nodes found with Algorithm 4.1 inducing a cycle equals $|V|$, we do not generate the SEC, otherwise Hamiltonian cycles would be infeasible for the problem.

Algorithm 3.1: Iterative procedure to compute upper bounds for MIP_1.

Data: A problem instance of MIP_1.
Result: An upper bound with solution $(f,g,x_R,\lambda,\mu,\theta,\nu)$ for MIP_1 with objective function value z_b.
Step 0: Set $k=1$;
Let MIP_{1_k} be the problem obtained from MIP_1 by removing the constraints (11) at iteration k;
Solve the MILP relaxation of problem MIP_{1_k} and let $(f^k,g^k,x_R^k,\lambda^k,\mu^k,\theta^k,\nu^k)$ be its optimal solution of value z_k at iteration k;
Let $z_0 = \inf$;
Step 1: **while** $|z_{k-1} - z_k| > \varepsilon$ **do**
  Construct the graph $\tilde{G} = (V,\tilde{E})$ with the rounded solution $(\tilde{f}^k,\tilde{g}^k,\tilde{x}_R^k,\tilde{\lambda}^k,\tilde{\mu}^k,\tilde{\theta}^k,\tilde{\nu}^k)$ obtained from $(f^k,g^k,x_R^k,\lambda^k,\mu^k,\theta^k,\nu^k)$;
  $\mathcal{C} = searchCycles(\tilde{G},V)$;
  foreach *cycle* $\in \mathcal{C}$ **do**
    Add the corresponding constraint (11) to MIP_{1_k};
  Set $k = k+1$;
  Solve the MILP relaxation of problem MIP_{1_k} and let $(f^k,g^k,x_R^k,\lambda^k,\mu^k,\theta^k,\nu^k)$ be its optimal solution of value z_k at iteration k;
return *the solution* $(f^k,g^k,x_R^k,\lambda^k,\mu^k,\theta^k,\nu^k,z_k)$;

Algorithm 4.1 is used iteratively by Algorithm 4.2 in (Adasme et al., 2015) that we adapt to solve MIP_1. The procedures in Algorithms 4.1 and 4.2 can be straightforwardly explained in more detail as follows. First, we remove constraints (11) from MIP_1 and solve the resulting integer optimization problem. Consider the underlying optimal solution graph $\tilde{G} = (V,\tilde{E})$ where V is the set of nodes and $\tilde{E}$ is the set of arcs such that $\tilde{E} \subseteq E$. If $\tilde{G}$ contains a cycle with two or up to $|V|-1$ nodes, then Algorithm 4.1 detects it. A subset of nodes inducing a cycle defines a new constraint (11) which cuts off this cycle from the solution space. Problem MIP_1 is re-optimized taking into account the new added constraints. This iterative process goes on until the underlying current optimal solution of MIP_1 has no more cycles. Since the number of cycles is finite, so is the number of constraints (11) that can be added to MIP_1. Notice that the number of SECs of type (11) that can be added to

MIP_1 is at most $O(2^{|V|})$. Consequently, Algorithm 4.2 adapted to solve MIP_1, converges to the optimal solution of the problem in at most $O(2^{|V|})$ outer iterations. The proof can be directly deduced from Theorem 2 in (Adasme et al., 2015).

The aforementioned procedure can also be used to compute upper bounds for MIP_1. This procedure is depicted in Algorithm 3.1 and is described as follows. First, we remove constraints (11) from MIP_1 and solve the resulting mixed integer linear programming relaxation of MIP_1 obtained while relaxing the variables $0 \leq x_{ij} \leq 1 \ \forall ij \in E$ at step 0. Next, we search cycles in the current rounded solution $0 \leq x_{ij} \leq 1 \ \forall ij \in E$. If $\tilde{G}$ contains a cycle with two or more nodes, then Algorithm 4.1 referred to as "*searchCycles*$(\tilde{G}, V)$" in (Adasme et al., 2015) detects it. A subset of nodes inducing a cycle defines a new constraint (11). The mixed integer programming relaxation of MIP_1 is re-optimized taking into account the new added constraints. This iterative process goes on until the difference between the current optimal objective function value z_k and the previous one z_{k-1} is less than a small positive value ε.

4 PRELIMINARY NUMERICAL RESULTS

In this section, we present preliminary numerical results. A Matlab (R2012a) program is developed using CPLEX 12.6 to solve MIP_1, MIP_2, MIP_3 and their corresponding LP relaxations. The numerical experiments have been carried out on an Intel(R) 64 bits core (TM) with 2.6 GHz and 8 Gigabytes of RAM. CPLEX solver is used with default options. Each entry in matrices $\{C, D, H\}$ and in matrices $\{A, B, R, Q\}$ is randomly and uniformly distributed in the intervals $[0; 10]$ and $[0; 5]$, respectively. The scalar values $c = r = 100$. The BigM values M and L are set to $M = 100$ and $L = 10^{10}$, respectively. We set the parameter $\varepsilon = 10^{-8}$ in Algorithm 3.1. In Table 1, first we solve MIP_1 with up to 15 nodes while generating all cycle elimination constraints. Subsequently, in Table 3, we solve MIP_1 with the iterative procedures presented in section 3. We limit CPLEX to 2 hours of CPU time in order to solve the linear models. The legend in Table 1 is as follows. Column 1 shows the instance number. Column 2 presents the number of nodes. Columns 3-7 and 8-12 present the optimal solution of MIP_1 and MIP_2, the number of branch and bound nodes used by CPLEX, the CPU time in seconds to solve the MILPs and their corresponding LP relaxations together with their CPU time in seconds, respectively. Finally, in columns 13-14, we present gaps we compute as $\left[\frac{LP-Opt}{Opt}\right] * 100$ for MIP_1 and MIP_2, respectively. The legend in Table 2 for MIP_3 is analogous to Table 1. We mention that each row in Tables 1, 2 and 3 corresponds to the same instance.

From Tables 1, 2 and 3, we observe that the optimal objective function values for MIP_1, MIP_2 and MIP_3 are exactly the same. In particular, in Tables 1 and 2, we see that the CPU times are in average significantly lower for MIP_3 than for MIP_2. In particular, when the instance dimensions increase. Regarding the number of branch and bound nodes, we observe that CPLEX requires significantly less nodes for solving MIP_3 than for MIP_2. For MIP_1, the number of nodes equals zero for the instances 1-7. Notice that CPLEX cannot find a feasible solution within 2 hours for the instance #18 using MIP_2. This is somehow reflected by the number of branch and bound nodes which is significantly higher for MIP_2 than for MIP_3. Concerning the LP bounds, the LP relaxations are slightly tighter for MIP_1 than for MIP_2 and MIP_3. Whereas the bounds for LP_2 and LP_3 remain nearly the same. On the opposite, the CPU times for LP_3 are in average larger than for LP_2, in particular for the large size instances. We also see that CPLEX can solve all the instances to optimality using MIP_3 that shows a significantly better performance than the rest of the MILP formulations. Finally, we mention that we cannot solve, with the exponential model, instances with more than 15 nodes due to the large number of sub-tour elimination constraints involved.

In Table 3, the legend is as follows. In column 1, we show the instance number. In columns 2-5, we show the optimal solution obtained with the adapted version of Algorithm 4.2 (Adasme et al., 2015), its CPU time in seconds, the number of cycles found with this algorithm and the number of iterations, respectively. In columns 6-10, we present the upper bounds obtained with Algorithm 3.1, its CPU time in seconds, the number of cycles found with it, the number of iterations, and the optimal solution found with MIP_1 while using all the cycle elimination constraints found with Algorithm 3.1, respectively. For the latter, we do not report the CPU time required by CPLEX. However, we mention that for the largest size instances (e.g. 21-22), these CPU times took less than 20 seconds. The rest of the instances were solved in less than 2 seconds. Finally, in columns 11-12, we provide gaps that we compute by $\left[\frac{Opt_{It}^{R}-Opt_{It}}{Opt_{It}}\right] * 100$ and $\left[\frac{Opt_{It}^{F}-Opt_{It}}{Opt_{It}}\right] * 100$, respectively.

From Table 3, we observe that Algorithm 4.2 can find the optimal solutions for all the instances. In particular, we observe that the large size instances #15-22 are solved in significantly less CPU time compared to

Table 1: Numerical results obtained with MIP_1 and MIP_2.

#	$\|V\|$	MIP_1					MIP_2					Gaps	
		Opt	*B&Bn*	Time (s)	LP	Time (s)	Opt	*B&Bn*	Time (s)	LP	Time (s)	Gap_1 %	Gap_2 %
1	4	945.90	0	0.35	1547.52	0.35	945.90	0	0.36	1547.52	0.41	63.60	63.60
2	6	1223.95	0	0.41	1969.08	0.39	1223.95	0	0.41	1969.08	0.42	60.88	60.88
3	8	1574.80	0	0.37	2990.03	0.42	1574.80	0	0.37	2996.69	0.38	89.87	90.29
4	10	1992.63	0	0.53	5252.53	0.53	1992.63	29	0.34	5368.06	0.40	163.60	169.40
5	12	2781.27	0	1.83	5472.70	1.28	2781.27	6	0.40	5745.17	0.39	96.77	106.57
6	14	3795.17	0	7.13	6476.50	5.45	3795.17	120	0.42	6505.47	0.39	70.65	71.41
7	15	4233.11	0	14.74	6596.09	11.05	4233.11	0	0.39	6723.12	0.34	55.82	58.82
8	20	-	-	-	-	-	5920.61	1886	1.39	10090.09	0.39	-	70.42
9	25	-	-	-	-	-	7979.07	30	0.53	13672.93	0.38	-	71.36
10	30	-	-	-	-	-	11272.16	8	0.50	16961.67	0.41	-	50.47
11	40	-	-	-	-	-	14325.01	0	0.62	25545.21	0.52	-	78.33
12	50	-	-	-	-	-	17772.48	0	0.80	30645.26	0.55	-	72.43
13	60	-	-	-	-	-	23021.58	528	2.63	39462.28	0.86	-	71.41
14	70	-	-	-	-	-	28178.71	54	2.17	47919.83	1.19	-	70.06
15	80	-	-	-	-	-	32776.32	335	3.87	55799.72	1.55	-	70.24
16	90	-	-	-	-	-	35705.34	918	26.15	62552.35	1.90	-	75.19
17	100	-	-	-	-	-	42688.50	44278	452.83	73934.28	2.39	-	73.19
18	120	-	-	-	-	-	*	379412	7200	86563.41	5.50	-	*
19	150	-	-	-	-	-	-	-	-	113013.27	21.22	-	-
20	180	-	-	-	-	-	-	-	-	139047.61	59.52	-	-
21	200	-	-	-	-	-	-	-	-	156705.84	73.85	-	-
22	250	-	-	-	-	-	-	-	-	201738.80	268.30	-	-

-: Instance not solved.
*: No solution found with CPLEX in 2 hours.

Table 2: Numerical results obtained with MIP_3.

#	MIP_3					Gaps
	Opt	*B&Bn*	Time (s)	LP	Time (s)	Gap_3 %
1	945.90	0	0.40	1547.52	0.37	63.60
2	1223.95	0	0.40	1969.08	0.37	60.88
3	1574.80	0	0.37	2996.69	0.39	90.29
4	1992.63	0	0.42	5361.12	0.37	169.05
5	2781.27	9	0.49	5745.17	0.39	106.57
6	3795.17	8	0.49	6485.70	0.42	70.89
7	4233.11	0	0.40	6723.12	0.36	58.82
8	5920.61	10	0.94	10047.35	0.43	69.70
9	7979.07	0	0.54	13618.52	0.41	70.68
10	11272.16	0	0.75	16961.67	0.45	50.47
11	14325.01	0	0.79	25538.77	0.68	78.28
12	17772.48	0	1.17	30645.26	0.64	72.43
13	23021.58	675	10.46	39453.01	1.05	71.37
14	28178.72	8	5.11	47881.09	1.83	69.92
15	32776.31	248	17.79	55799.72	2.93	70.24
16	35705.36	17	15.86	62552.35	2.53	75.19
17	42688.51	621	46.65	73934.28	3.75	73.19
18	50786.93	526	133.94	86493.02	17.00	70.31
19	66770.38	163	123.39	113003.02	58.75	69.24
20	86307.85	4168	2459.89	139046.61	211.01	61.11
21	93444.25	5678	6878.94	156675.69	230.30	67.67
22	122719.37	549	2017.85	201734.01	901.54	64.39

MIP_3. Moreover, the number of cycles and iterations are less or equal than 140 and 11, respectively for all the instances. Notice that the total number of cycles for most of the instances is huge. However, the number of cycles required by Algorithm 4.2 to find the optimal solution is significantly small. In general, we see that Algorithm 3.1 can find tighter bounds when compared to the models LP_2 and LP_3. Regarding the number of cycles required by Algorithm 3.1, we observe that this number is significantly higher compared to Algorithm 4.2. On the opposite, we see that Algorithm 3.1 requires in average less iterations. Fi-

Table 3: Numerical results obtained with the iterative algorithmic procedures.

#	Algorithms 4.1 and 4.2 adapted from (Adasme et al., 2015)				Algorithm 3.1					Gaps	
	Opt_{It}	Time (s)	*#Cycles*	*#Iter*	Opt^R_{It}	Time (s)	*#Cycles*	*#Iter*	Opt^F_{It}	Gap_R %	Gap_F %
1	945.90	0.51	0	1	1443.61	1.09	10	2	945.90	52.62	0
2	1223.95	0.80	3	2	1899.73	0.80	8	1	1239.34	55.21	1.26
3	1574.80	0.76	4	2	2896.01	0.76	12	1	1574.80	83.90	0
4	1992.63	0.80	5	2	4269.07	1.08	32	2	2036.42	114.24	2.20
5	2781.27	1.26	8	3	4447.16	1.20	41	2	2787.50	59.90	0.22
6	3795.17	1.66	9	4	5800.14	1.26	41	2	3995.48	52.83	5.28
7	4233.11	1.25	8	3	5963.58	1.22	45	2	4328.84	40.88	2.26
8	5920.61	2.40	18	6	8952.44	1.23	58	2	6233.36	51.21	5.28
9	7979.07	0.89	12	2	13244.42	1.36	75	2	8441.78	65.99	5.80
10	11272.16	1.34	14	3	15160.96	1.51	97	2	11342.97	34.50	0.63
11	14325.01	1.63	18	3	23008.49	3.05	207	3	14661.88	60.62	2.35
12	17772.48	2.89	27	4	27771.65	2.95	168	2	18442.49	56.26	3.77
13	23021.58	12.30	45	11	36082.31	6.66	312	3	23959.25	56.73	4.07
14	28178.71	7.87	42	6	44084.55	6.28	235	2	29376.14	56.45	4.25
15	32776.31	16.27	55	9	51378.66	20.60	536	4	33437.84	56.76	2.02
16	35705.34	5.95	50	3	56294.82	10.57	323	2	36700.49	57.66	2.79
17	42688.50	27.17	71	10	65957.50	24.66	537	3	44117.89	54.51	3.35
18	50786.93	38.96	83	9	77440.29	25.01	413	2	52118.73	52.48	2.62
19	66770.38	71.56	92	9	101128.60	199.45	1090	4	68005.67	51.46	1.85
20	86307.85	153.10	125	11	127706.66	410.10	1007	3	87895.55	47.97	1.84
21	93444.25	122.41	127	7	141811.63	325.40	706	2	96921.84	51.76	3.72
22	122719.37	122.20	140	4	186448.77	948.96	919	2	126746.65	51.93	3.28

nally, we observe that solving MIP_1 with all the cycle elimination constraints found with Algorithm 3.1 allows to compute tight bounds when compared to the optimal solution of the problem. More precisely, these bounds are computed with gaps which are lower than 6% for most of the instances.

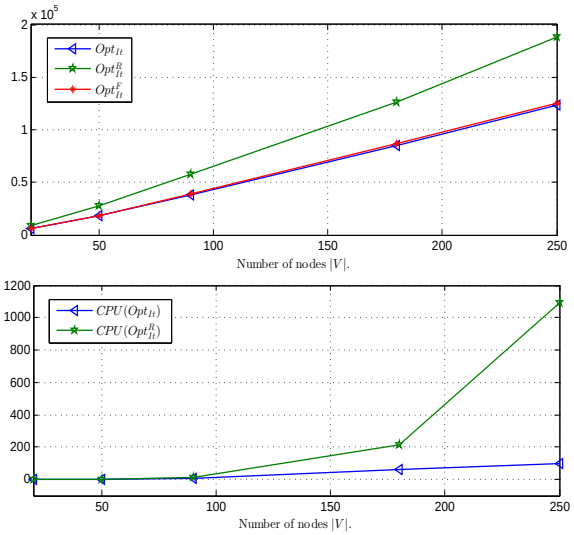

Figure 1: Average optimal solutions, upper bounds and CPU times obtained with the iterative Algorithms 4.2 and 3.1.

In order to give more insight with respect to the performance of Algorithms 4.2 and 3.1 when solving MIP_1. In Figure 1, we present some average numerical results for 20 instances randomly generated with dimensions of $|V| = \{20, 50, 90, 180, 250\}$ nodes, respectively. From Figure 1, we mainly confirm the trends observed in Table 3. We observe that in average obtaining optimal solutions with the iterative Algorithm 4.2 is more effective than computing upper bounds with Algorithm 3.1 in terms of CPU time. This is an interesting result as it confirms that Algorithm 4.2 allows to obtain optimal solutions for the large scale instances more easily. More precisely, in less CPU time than the instances presented in Table 3. Finally, we observe that the upper bounds obtained with Algorithm 3.1 are very tight when solving MIP_1 with all SECs, although they are obtained at a higher CPU time. In Figure 1, we do not plot averages for the number of cycles and iterations as they remain nearly the same as in Table 3 for all the instances. Similarly, we do not plot the average CPU times for Opt^F_{It} since they are slightly larger than those obtained for Opt^R_{It}.

5 CONCLUSIONS

In this paper, we consider a linear bilevel programming problem where both the leader and the follower maximize their profits subject to budget constraints. Additionally, we impose a Hamiltonian cycle topology constraint in the leader problem. In particular, models of this type can be motivated by telecommunication companies when dealing with traffic network flows from one server to another one within a ring topology framework. We transform the bilevel programming problem into an equivalent single level optimization problem and derive mixed integer linear programming (MILP) formulations. The topology constraint is handled by the means of two compact

formulations and an exponential one from the classic traveling salesman problem. Our preliminary numerical results show that one of the compact models allows to solve instances with up to 250 nodes to optimality with CPLEX in less than two hours. Finally, we propose iterative procedures that allow to compute optimal solutions in significantly less computational effort when compared to the compact models. Our main contribution in this paper is not theoretical, but mainly focussed on computational numerical results on a novel problem in the domain of bilevel programing. Our numerical results clearly show that solving the exponential model with the iterative procedure is by far more convenient than using the compact formulations which are more theoretical based approaches. In fact, we solve to optimality instances with up to 250 nodes so far, in less than 70 seconds in average compared to the higher CPU times required by the compact formulations.

As part of future research, we plan to develop further tests in order to confirm the behaviour of the proposed models and algorithms. Finally, we will propose new stochastic models and algorithmic approaches for this type of bilevel programming problems.

ACKNOWLEDGEMENTS

The first author acknowledges the financial support of the USACH/DICYT Project 061513VC_DAS.

REFERENCES

Adasme, P., Andrade, R., Letournel, M., and Lisser, A. (2015). Stochastic maximum weight forest problem. *Networks*, 65:289–305.

Audet, C., Hansen, P., Jaumard, B., and Savard, G. (1997). Links between linear bilevel and mixed 0-1 programming problems. *Journal of Optimization Theory and Applications*, 93:273–300.

Cormen, T. H., Leiserson, C. E., Rivest, R. L., and Stein, C. (2009). *Introduction to algorithms*. MIT Press and McGraw-Hill, Cumberland, RI, USA.

Dempe, S. (2002). *Foundations of bilevel programming. (1st ed.).* Freiberg: Kluwer Academic Publishers.

Dempe, S. (2003). Annotated bibliography on bilevel programming and mathematical programs with equilibrium constraints. *Optimization*, 52:333–359.

Floudas, C. and Pardalos, P. (2001). *Encyclopedia of optimization.* Dordrecht: Kluwer Academic Publishers.

Gavish, B. and Graves, S. C. (1978). The travelling salesman problem and related problems. *Operations Research Centre, Massachusetts Institute of Technology*.

Lee, D., Attias, R., Puri, A., Sengupta, R., Tripakis, S., and Varaiya, P. (2001). A wireless token ring protocol for intelligent transportation systems. In *IEEE Proceedings of: Intelligent Transportation Systems*, pages 1152–1157.

Letchford, A. N., Nasiri, S. D., and Theis, D. O. (2013). Compact formulations of the steiner traveling salesman problem and related problems. *European Journal of Operational Research*, 228:83–92.

Migdalas, A., Pardalos, P., and Varbrand, P. (1997). *Multilevel optimization: Algorithms and Applications.* The Netherlands: Kluwer Academic Publishers.

Miller, C. E., Tucker, A. W., and Zemlin, R. A. (1960). Integer programming formulation of traveling salesman problems. *J. Assoc. Comput. Mach.*, 7:326–329.

Scholtes, S. (2004). Nonconvex structures in nonlinear programming. *Operations Research*, 52:368–383.

Song, J. and Yang, O. (1997). Backbone networks using rotation counters. *IEEE Transactions on Parallel and Distributed Systems*, 8:1288–1298.

Thirwani, D. and Arora, S. (1998). An algorithm for quadratic bilevel programming problem. *International Journal of Management and System*, 14:89–98.

Vicente, L., Savard, G., and Judice, J. (1994). Descent approaches for quadratic bilevel programming. *Journal of Optimization Theory and Applications*, 81:379–399.

Wang, S., Wang, Q., and Rodriguez, R. (1994). Optimality conditions and an algorithm for linear-quadratic bilevel programs. *Optimization*, 31:127–139.

A Single-source Weber Problem with Continuous Piecewise Fixed Cost

Gabriela Iriarte, Pablo Escalona, Alejandro Angulo and Raul Stegmaier
Department of Industrial Engineering, Universidad Técnica Federico Santa María, Valparaíso, Chile
gabriela.iriarte@alumnos.usm.cl, {pablo.escalona, alejandro.angulo, raul.stegmaier}@usm.cl

Keywords: Weber Problem, Fixed Costs, Delaunay Triangulation, Kriging Interpolation.

Abstract: This paper analyzes the location of a distribution center in an urban area using a single-source Weber problem with continuous piecewise fixed cost to find a global optimal location. The fixed cost is characterized by a Kriging interpolation method. To make the fixed cost tractable, we approximate this interpolation with a continuous piecewise function that is convex in each piece, using Delaunay triangulation. We present a decomposition formulation, a decomposition conic formulation and a conic logarithmic disaggregated convex combination model to optimally solve the single-source Weber problem with continuous piecewise fixed cost. Although our continuous approach does not guarantee the global optimal feasible location, it allows us to delimit a zone where we can intensify the search of feasible points. For instances we tested, computational results show that our continuous approach found better locations than the discrete approach in 23.25% of the instances and that the decomposition formulation is the best one, in terms of CPU time.

1 INTRODUCTION

The location of a distribution center (DC) in an urban area, considering the transportation and installation costs, can be treated as an uncapacitated facility location problem (UFLP) or as a Weber problem with fixed cost. It is known that the solution of the UFLP is feasible but not necessarily optimal, due to the use of an incomplete set of possible locations. On the other hand, the Weber problem with fixed cost gives an optimal location probably not feasible.

This paper analyzes the installation of a single DC in an urban area, using the single-source Weber problem with fixed cost to find an optimal location that allows us to delimit a zone around the optimal location previously found, but smaller than the original one. This way, we can focus the search of feasible points, obtaining a more reliable and complete set of possible locations such that, when an UFLP is applied, we find the *optimal feasible location*.

To the best of our knowledge, few papers deal with the inclusion of the fixed costs into the Weber problem. Fixed costs have been considered as a constant cost for all the plane (Brimberg et al., 2004), as zone dependent with a constant cost in a specific convex polygon (Brimberg and Salhi, 2005),(Hosseininezhad et al., 2015), or as a proportion between the fixed cost of two zones and their relative distance, (Luis et al., 2015). To consider that a plane can be partitioned in a finite set of convex polygons, each one with constant fixed costs, is considered a good first approximation to characterize the variating nature of this cost. In this paper we propose that the fixed cost on each convex polygon is a function of its vertices, allowing us to better model the fixed costs in an urban area.

The objective of this paper is to find the best formulation to locate a single DC in an urban area, where the fixed costs depend on the location in a continuous way. The fixed cost function is characterized by a Kriging interpolation method using a set of nodes where the cost is known. To make the formulation tractable, we approximate the interpolation with a continuous piecewise function that is convex in each piece. This is constructed through a convex combination of the vertices of a mesh created with a Delaunay triangulation. The sinlge-source Weber problem with continuous piecewise fixed cost is formulated as an MINLP problem. We take advantage of the problem's structure to propose three solution approaches. The first approach considers a conic reformulation of the single-source Weber problem with continuous piecewise fixed cost using a *logarithmic disaggregated convex combination model*. The second consists of a decomposition method, where we solve a non-linear convex problem for each Delaunay triangle, and using complete enumeration we determine the optimal solution. The last one, consider a conic reformulation for each sub-problem of the sub-

Iriarte, G., Escalona, P., Angulo, A. and Stegmaier, R.
A Single-source Weber Problem with Continuous Piecewise Fixed Cost.
In *Proceedings of the 6th International Conference on Operations Research and Enterprise Systems (ICORES 2017)*, pages 337-344
ISBN: 978-989-758-218-9

sequent decomposition formulation. Each approach was implemented in a series of experiments to compare their performance in CPU time.

The main contributions of this paper are: (*i*) a new way to represent the fixed costs in an urban area and (*ii*) to identify the best solution approach for the single-source Weber problem with continuous piecewise fixed cost.

The paper is organized as follows: Section 2 presents our related work. Section 3 presents a single-source Weber problem with continuous piecewise fixed cost. Section 4 presents three different approaches to solve the problem defined in the previous section. Section 5 presents some experimental results for all the different approaches. Our conclusions and highlights are presented in section 6.

2 RELATED WORK

The continuous location problem for a single-source or single-source Weber problem, described in Weber and Friedrich (1929), has been extensively studied. To find the solution there are different approaches: a one-point iterative method better known as the Weiszfeld algorithm (Weiszfeld and Plastria, 2009), a unified cutting plane method (Plastria, 1987), a dual method (Planchart and Hurter, 1975), a primal-dual algorithm involving mixed norms (Michelot and Lefebvre, 1987), or a primal-dual potential reduction algorithms with the problem formulated in conic form (Xue and Ye, 1997). A comprehensive review of the Weber problem can be found in Drezner et al. (2002).

The multi-source Weber problem, or location-allocation problem, is an NP-hard problem (Megiddo and Supowit, 1984). There are few heuristics that solve it to optimality but they work only in small problems (Cooper, 1972), (Sherali et al., 2002), (Chen et al., 1998). For the heuristic approach to solve the problem to near optimum, there are more publications: Cooper (1964) explored different algorithms with computational experiments. The alternating location-allocation heuristic is used by Cooper (1972). The method used by Bongartz et al. (1994) relaxes the binary constraints on the allocations, and solves both location and allocation simultaneously. An approach based on a nonlinear second-order cone program reformulation is found in Chen et al. (2011). The approach to use the discrete models in solving the continuous location-allocation problems is widely used by Hansen et al. (1998), Brimberg et al. (2014), and others. For this, a survey in the p-median problem with the aim in procedures based on metaheuristics rules (Mladenovic et al., 2007) is useful. For a survey on the multi-source Weber problem there is Brimberg et al. (2000) and Brimberg et al. (2008).

The inclusion of the fixed cost to the Weber problem has little reviews, there are four papers to the best of our knowledge. First it is included as a constant cost for all plane in Brimberg et al. (2004). Later, in Brimberg and Salhi (2005), it was extended to a zone-dependent fixed cost, where zones are non-overlapping convex polygons with a constant fixed cost for each zone. In Hosseininezhad et al. (2015) is developed a metaheuristic Cross Entropy for a continuous location problem, with an fixed cost depending on the zone and on the facility to install. And Luis et al. (2015), proposed a multi-source Weber problem with capacity and zone-dependent fixed cost using the second-order Voronoi regions.

In general, data gathering is expensive in terms of monetary and time-consuming costs (Helbich et al., 2013). Therefore, there is a necessity to estimate the land values in unvisited locations, as geostatistical methods Luo (2004), Cellmer et al. (2014). Here, we use a Kriging method of interpolation (Oliver and Webster, 1990). This method was recommended over other interpolation approaches in Anselin and Le Gallo (2006) and Fernández-Avilés et al. (2012), in an air quality and pollution studies, respectively. The possibilities and limitations of geostatistical methods to approximate the land values are discussed in Cellmer (2014). A comparison between Kriging methods for the real estate market is discussed in Kuntz and Helbich (2014). The Kriging interpolation is used to find the value of land for different cities by Liang and Yi (2012), Hu et al. (2015), Larraz and Poblacin (2013).

In summary, there are few previous works on single-source and multi-source Weber problem that include a second order cone formulation and, to the best of our knowledge, only one paper presents a solution approach. The few papers that include fixed costs make a simplistic representation of them that do not reflect their variations in an urban area. Unlike them, we make a more realistic representation of the fixed costs, considering different possible approaches for the Weber problem with fixed costs.

3 MODEL FORMULATION

3.1 Single-source Weber Problem with Continuous Piecewise Fixed Costs

The generalized single-source Weber problem with fixed costs considers the localization of a single

source with coordinates $(\bar{x},\bar{y}) \in \mathbb{R}^2$. This source must supply a set J of customers with known coordinates, (xc_j, yc_j) for every $j \in J$. Let $f(\bar{x},\bar{y})$ be the fixed cost incurred when the source is installed in $(\bar{x},\bar{y})$. Let w_j be the the expected demand weighted by the transportation ratios, for all $j \in J$. The problem is to determine the optimal location for the single source such that the transportation and the fixed costs are minimized. The generalized single-source Weber problem with fixed costs can be expressed as follows:

$$\min_{(\bar{x},\bar{y})} \quad \sum_{j\in J} w_j \sqrt{(\bar{x}-xc_j)^2+(\bar{y}-yc_j)^2} + f(\bar{x},\bar{y}) \quad (1)$$

$$\text{s.t.} \quad (\bar{x},\bar{y}) \in \mathbb{R}^2 \quad (2)$$

We consider a convenient set I of nodes with known information of their fixed costs, C_i, and their coordinates, (xi_i, yi_i), for every $i \in I$. In our paper, the way to address the fixed costs is by applying a Kriging interpolation method and defining a continuous function for the cost in every point of the convex hull of I. This cost function is not simple and could not be convex. To make the continuous fixed cost function tractable, we are going to approximate the Kriging interpolation with a piecewise function that is convex in each piece. For this, we partition the convex hull of I through a polyhedral mesh and defined the continuous piecewise fixed cost function as the convex combination of the vertices of the mesh. To the best of our knowledge, it is better to use the smallest subset of information nodes possible with empty interior to create the polyhedra, i.e, using Delaunay triangulation.

We applied a Delaunay triangulation over the set I obtaining a set K of triangles; each triangle k-th will be denoted as P_k, with $P_k = \{(x,y) \in \mathbb{R}^2 | (x,y) = \sum_{l=1}^3 \lambda^{k_l}(x_{k_l}, y_{k_l}), \sum_{l=1}^3 \lambda^{k_l} = 1, \forall \lambda^{k_l} : \lambda^{k_l} \geq 0\}$, where (x_{k_1}, y_{k_1}), (x_{k_2}, y_{k_2}) and (x_{k_3}, y_{k_3}) are the vertices of the k-th triangle and $C_{k_1}, C_{k_2}, C_{k_3}$ their fixed cost. We have λ^{k_l} as the convex combination vector for the vertices of the triangle $k \in K$ and $l = 1,2,3$ the vertices of the triangle. The set of all possible locations, $\bigcup_{k\in K} P_k$, can be non-convex if we clean the areas where we can not install, as a lake or a strictly residential area.

Given the above, the facility's location can be expressed as $(\bar{x},\bar{y}) = \sum_{k\in K}\sum_{l=1}^3 \lambda^{k_l}(x_{k_l}, y_{k_l})$ and its fixed cost as a convex combination of the vertices of the triangles's costs, $\sum_{k\in K}\sum_{l=1}^3 \mathbf{C}_{k_l}^T \lambda^{k_l}$. Let Z_k be a binary variable that forces the installation to be in only one triangle, being 1 if it is installed in the k-th triangle and 0 if it is not.

We can formulate the single-source Weber problem with continuous piecewise fixed cost as follows:

Problem $(P0)$*:*

$$\min_{\mathbf{Z},\lambda} \sum_{k\in K} \left(\sum_{l=1}^3 \mathbf{C}_{k_l} \lambda^{k_l} + Z_k \sum_{j\in J} w_j \right.$$

$$\left. \sqrt{(\sum_{k\in K}\sum_{l=1}^3 \lambda^{k_l} x_{k_l} - xc_j)^2 + (\sum_{k\in K}\sum_{l=1}^3 \lambda^{k_l} y_{k_l} - yc_j)^2} \right) \quad (3)$$

$$\text{s.t.} \sum_{l=1}^3 \lambda^{k_l} = Z_k, \qquad \forall k \in K \quad (4)$$

$$\sum_{k\in K} Z_k = 1 \quad (5)$$

$$\lambda^{k_l} \geq 0, \qquad \forall l \in \{1,2,3\}, k \in K \quad (6)$$

$$Z_k \in \{0,1\}, \quad \forall k \in K \quad (7)$$

In what follows, we present different ways to solve the problem $(P0)$.

4 SOLUTION APPROACH

We consider three distinct solution approaches for $(P0)$. For the first approach, we use a monolithic reformulation of $(P0)$. The second approach considers a decomposition of $(P0)$ by fixing the variable $\mathbf{Z}$ and solving the sub-problem generated; we evaluated all the possible values of $\mathbf{Z}$. The last approach considers a conic reformulation of the previous sub-problems.

4.1 Conic Logarithmic Disaggregated Convex Combination Model

Now, we reformulate $(P0)$ in two steps. First, we formulate the problem as a Conic Quadratic Non Linear problem (CQNLP). Afterwards, using the *logarithmic disaggregated convex combination model* (Vielma et al., 2010), we efficiently solve the continuous piecewise fixed cost function.

Next, we formulate the problem $(P0)$ as a CQNLP in order to eliminate the square root terms. First we introduce one set of nonnegative continuous variables, d_j, to represent the square root term in:

$$d_j = \sqrt{(\sum_{l=1}^3 x_{k_l}\lambda^{k_l} - xc_j)^2 + (\sum_{l=1}^3 y_{k_l}\lambda^{k_l} - yc_j)^2}, \forall j \in J \quad (8)$$

$$d_j \geq 0, \forall j \in J \quad (9)$$

For simplicity, we can add two more sets of auxiliary variables, v_j and r_j, leaving (8) as:

$$d_j^2 = z_j^2 + w_j^2, \qquad \forall j \in J \qquad (10)$$

$$v_j = \sum_{l=1}^{3} x_{k_l}\lambda^{k_l} - xc_j, \qquad \forall j \in J \qquad (11)$$

$$r_j = \sum_{l=1}^{3} y_{k_l}\lambda^{k_l} - yc_j, \qquad \forall j \in J \qquad (12)$$

Because the nonnegative variables d_j are introduced in the objective function of $(P0)$ with positive coefficients, and this problem is a minimization problem, the equation can be further relaxed as the following inequalities:

$$d_j^2 \geq v_i^2 + r_i^2, \qquad \forall j \in J \qquad (13)$$

Note that the constraints (9) and (13) define second-order cone constraints. The problem $(P0)$ can be expressed as the following conic problem:
Problem $(CP0)$*:*

$$\min_{\mathbf{Z},\lambda,\mathbf{d},\mathbf{v},\mathbf{r}} \sum_{k\in K}(Z_k \sum_{j\in J} w_j d_j + \sum_{l=1}^{3} \mathbf{C}_{k_l}\lambda^{k_l}) \qquad (14)$$

$$\text{s.t. } (4),(5),(6),(7),(9),(11),(12),(13)$$

The *logarithmic disaggregated convex combination model* consists in replacing the piecewise function $f(\bar{x},\bar{y})$ for its epigraph $epi(f)$ and setting the coordinate $(\bar{x},\bar{y})$ to be contained by one and only one of the domains of f. For a minimization, solving the function f is equivalent to solving $epi(f)$. To construct a model with the least number of binary variables and constraints, we identify each triangle with a binary vector in $\{0,1\}^{\lceil log_2|K|\rceil}$ through an injective function $B : K \to \{0,1\}^{\lceil log_2|K|\rceil}$ and use $\lceil log_2|K|\rceil$ binary variables, $\mathbf{m} \in \{0,1\}^{\lceil log_2|K|\rceil}$, to ensure that the coordinates are in only one triangle. Let Q be $epi(f)$.

Using the *logarithmic disaggregated convex combination model* and a second order cone formulation to reformulate $(P0)$, leaves the following:
Problem $(DlogCP0)$*:*

$$\min_{\lambda,\mathbf{m},\mathbf{d},Q,\mathbf{v},\mathbf{r}} \quad \sum_{j\in J} w_j d_j + Q \qquad (15)$$

$$\text{s.t. } \sum_{k\in K}\sum_{l=1}^{3} \mathbf{C}_{k_l}\lambda^{k_l} \leq Q \qquad (16)$$

$$\sum_{k\in K}\sum_{l=1}^{3} \lambda^{k_l} = 1 \qquad (17)$$

$$\sum_{k\in K^+(B,t)}\sum_{l=1}^{3} \lambda^{k_l} \leq m_t, \qquad \forall t \in T(K) \qquad (18)$$

$$\sum_{k\in K^0(B,t)}\sum_{l=1}^{3} \lambda^{k_l} \leq (1-m_t), \forall t \in T(K) \qquad (19)$$

$$\lambda^{k_l} \geq 0 \qquad \forall l \in 1,2,3, k \in K \qquad (20)$$

$$m_t \in \{0,1\} \qquad \forall t \in T(K) \qquad (21)$$

$$(9),(11),(12),(13)$$

where $B : K \to \{0,1\}^{\lceil log_2|K|\rceil}$ is any injective function, $K^+(B,t) = \{k \in K : B(k)_t = 1\}$, $K^0(B,t) = \{k \in K : B(k)_t = 0\}$ and $T(K) = \{1,\ldots,\lceil log_2|K|\rceil\}$. This problem is a mixed integer conic quadratic nonlinear problem with a linear objective function and can be solved by solvers like GUROBI, CPLEX or MOSEK.

4.2 Decomposition Formulation

From the problem $(P0)$, we can observe that the variables λ and $\mathbf{Z}$ are related in only one constraint. And, fixing the variable $\mathbf{Z}$, the problem is separable in $|K|$ sub-problems where we force the localization of the DC to be in the k-th Delaunay triangle, i.e., forcing $Z_k = 1$ and $Z_{k'} = 0$ for all $k' \in K \setminus k$. Then the k-th sub-problem can be written as:
Sub-Problem $(SP0(k))$*:*

$$\min_{\lambda^k} \quad \sum_{j\in J} w_j \sqrt{(\bar{x}-xc_j)^2 + (\bar{y}-yc_j)^2} + \sum_{l=1}^{3} \mathbf{C}_{k_l}\lambda^{k_l} \qquad (22)$$

$$\text{s.t.} \quad \sum_{l=1}^{3} \lambda^{k_l} = 1 \qquad (23)$$

$$\lambda^{k_l} \geq 0 \quad ,\forall l \in \{1,2,3\} \qquad (24)$$

This sub-problem $(SP0(k))$ is a convex nonlinear problem with linear constraint and can be efficiently solved by MINOS or IPOPT solvers.

Let λ^{k^*} be the optimal solution of the problem $(SP0(k))$; $FO_{(SP0(k))}(\lambda^{k^*})$ be the optimal cost of the objective function in the problem $(SP0(k))$, and let $(\bar{\lambda},\bar{\mathbf{Z}})$ be the optimal solution of the problem $(P0)$. The optimal solution for the $(P0)$ problem is the best solution for all of the sub-problems $(SP0(k))$, i.e. $\bar{\lambda} = \lambda^{k_\dagger}$, where $k_\dagger = \text{argmin}_{k\in K}\{FO_{(SP0(k))}(\lambda^{k^*})\}$. For $\bar{\mathbf{Z}}$, the value of $\bar{Z}_k = 1$ for $k = k_\dagger$ and $\bar{Z}_k = 0$ for every other k.

4.3 Decomposition Conic Formulation

The squared root term in the objective function of problem $(SP0(k))$ can give rise to difficulties in the optimization procedure. Following the logic exposed for the first approach, we reformulate $(SP0(k))$ as a CQNLP, leaving the following conic problem:

Sub-Problem $(SCP0(k))$*:*

$$\min_{\lambda^k,\mathbf{d},\mathbf{v},\mathbf{r}} \quad \sum_{j\in J} w_j d_j + \sum_{l=1}^{3} \mathbf{C}_{k_l}\lambda^{k_l} \tag{25}$$
$$\text{s.t. } (23),(24),(9),(11),(12),(13)$$

The problem $(SCP0(k))$ can be trivially shown to be equivalent to $(SP0(k))$, but it has now conic and nonlinear constraints with a more simple linear objective function. The optimal solution for $(P0)$ is the best solution for all the sub-problems $(SCP0(k))$, equivalently to the decomposition formulation.

The advantage of the CQNLP formulation is that it can be solved directly using standard optimization software packages such as CPLEX, GUROBI or MOSEK.

5 COMPUTATIONAL STUDY

In this section, we present our numerical study and its results. The main objectives of this computational study is to show which solution approach has the best performance in terms of CPU time, and to compare them to an UFLP. To characterize the different approaches, we carried out 400 instances that we denote *test set*. We also corroborate the installation of a single DC in every instance with the UFLP.

All the problems were programmed using AMPL. To solve the decomposition formulation we use the solver MINOS. For $(DlogCP0)$ and the decomposition conic formulation we solve it through CPLEX solver. The Kriging interpolation method and the Delaunay triangulation were made in MATLAB. The *test set* were run on a PC with AMD FX 4,00 GHz processor and 12 GB RAM, and the UFLP were run on a PC with Intel i3 2,10 Ghz and 4 GB RAM.

5.1 Test Set

In order to determine which one has the best performance in CPU time, we generated 100 experiments. In each experiment, we fixed the number of customer nodes and used 4 refinements of the triangulation. Therefore, we have 400 instances. For simplicity, we considered $w_j = 1$, for any $j \in J$.

Each experiment has the same initial set of 100 information nodes, generated randomly. For a better piecewise convex approximation of the continuous fixed cost function, we proposed the following refinement of the mesh. We consider the Delaunay triangulation of the initial set of information nodes as the first refinement, shown in figure 1. The second refinement is generated by creating additional information nodes where their location is at the center of the edge of every triangle and their fixed cost is determined by the Kriging interpolation. Then the Delaunay triangulation is used over the original set I plus the additional information nodes. The third and fourth refinements are applied over the second and third triangulation, respectively. In figure 2 the fourth refinement is shown.

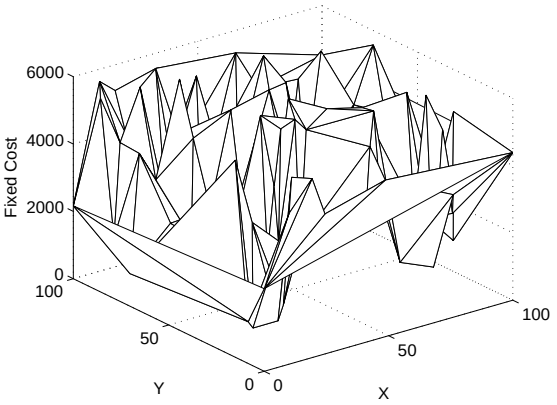

Figure 1: First refinement.

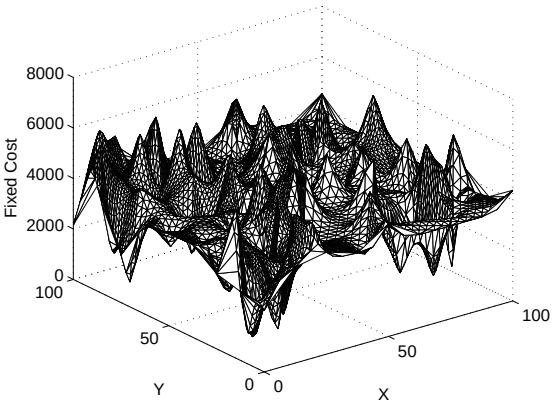

Figure 2: Fourth refinement.

We modified the number of customer nodes from 100 to 1000 customers, i.e., the first 10 experiments have 100 customer nodes, the next 10 experiments have 200 customer nodes, and so on. Each customer location is obtained making random locations, i.e., where $(xc_j, yc_j) \in ([0,100],[0,100])$.

Figure 3 shows the performance profile based on the *performance ratio* of the CPU time for each model (Dolan and Moré, 2002). Considering that t_{pm} is the CPU time for solving the instance p by the model m, we have the *performance ratio*:

$$r_{pm} = \frac{t_{pm}}{\min\{t_{pm} : m \in M\}},$$

where $M = \{DlogCP0,\ min_{k\in K}\{(SP0(k))\},\ min_{k\in K}\{(SCP0(k))\}\}$.

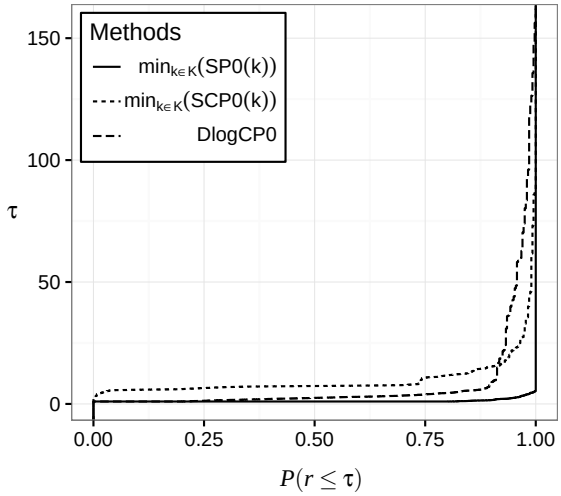

Figure 3: Performance Profile.

We observe in figure 3 that the best model performance is the decomposition formulation, i.e., $min_{k\in K}\{(SP0(k))\}$, because in 80% of the instances has the lowest time, overcome by $(DlogCP0)$, in less than 20% of the instance. The decomposition formulation has the best performance with the greater efficiency, solving all the instances with a $\mathbf{r} \preceq 5$.

There is a pattern in every refinement where $(DlogCP0)$ has the best performance in the instances with a small set of customers nodes, and get outperformed by the decomposition formulation in the rest of the instances. This is shown in table 1, where it shows that the average speedup in the CPU time of the decomposition formulation over $(DlogCP0)$ is greater than $1x$ for all the refinements in the instances with $|J| = 100$. Considering the second and third refinement, $(DlogCP0)$ is better, in average, for the instances with $|J| \leq 200$. For the fourth refinement, $(DlogCP0)$ is better in instances with $|J| \leq 300$ and with an average speedup of over $4x$ when $|J| = 100$.

Table 1: Average Speedup in CPU time of $min_{k\in K}\{(SP0(k))\}$ over $(DlogCP0)$.

	Refinement			
$\|J\|$	First	Second	Third	Fourth
100	1.556x	2.035x	2.808x	4.125x
200	0.574x	1.185x	1.548x	1.944x
300	0.382x	0.865x	0.840x	1.149x
400	0.320x	0.665x	0.697x	0.494x
500	0.258x	0.528x	0.470x	0.308x
600	0.301x	0.530x	0.410x	0.330x
700	0.226x	0.447x	0.416x	0.099x
800	0.214x	0.387x	0.385x	0.036x
900	0.184x	0.373x	0.367x	0.020x
1000	0.172x	0.309x	0.312x	0.012x

We obtain an average speedup of 7.98x and 7.72x for the decomposition formulation over the decomposition conic formulation and $(DlogCP0)$, respectively.

Our numerical results show that the performance from the conic formulations ($(DlogCP0)$ and the decomposition conic formulation) are sensible to the size of the customer set. This is because the conic formulations create $|J|$ cones and $3|J|$ new variables, so the problem grows faster than the number of customers. For this reason, even that $(DlogCP0)$ can better handle a big set of information nodes, this only is seen with a small set of customers.

The performance of the decomposition formulation, shown in figure 3, is the most stable of the performances of the three solution approaches, i.e., with less difference in the extremes values of its *performance ratio*. This indicates that if the decomposition formulation does not have the best performance in an instance, its CPU time is closer to the better one.

The average improvement in the objective function using the different refinements, compared with the first refinement, are: 0.08% for the second, 0.74% for the third, and 1.29% for the fourth refinement.

We can observe in table 1 that in instances with small number of customers is better to use $(DlogCP0)$, considering that can have a speedup over $4x$ against the decomposition formulation, but it is when the CPU times are lower. For example, in all the instances with $|J| = 100$, although we have a better average of CPU time with $(DlogCP0)$, the worst CPU time for the decomposition formulation does not get over 250 seconds. Considering that the decomposition formulation has a more stable performance with the better overall average in CPU time, and because this solves a strategic decision, we recommend to model the single source Weber problem with fixed cost with the decomposition formulation.

5.2 Discrete Model: Uncapacitated Facility Location Problem

The following experiments where made using the instances previously described in the *test set*, considering the set of information nodes without the refinements. We consider the information nodes as the discrete set of possible locations, modelled by an UFLP.

In table 2 are the average and maximum percentage of the improvement in lowering the value of the objective function of the single-source Weber problem with continuous piecewise fixed cost over the UFLP, and the number of cases where this happened.

Table 2 shows, for the fourth refinement an average improvement of 1.42%. From the total of experiments solved with the fourth refinement, the 67% of

Table 2: Percentage of improvement for the continuous model over the UFLP.

	Refinement			
	First	Second	Third	Fourth
Average	0.13%	0.21%	0.86%	1.42%
Max	1.62%	5.80%	16.83%	18.58%
N° Cases	27	8	25	33

the instances have the same result as the UFLP. But in the 33% where they are different, the average improvement is of 4.297%.

The better solutions found in 23.25% of the instances with the single-source Weber problem over the UFLP is because the UFLP only consider the information nodes as possible locations and not always is consider the global optimum in that set. With the inclusion of more information nodes, i.e. closer to reality, the average savings and the number of better cases tend to grow.

We also observed that in all the instances only one facility is installed. This is in accordance to say that, in an urban area, the fixed cost of an extra DC tends to be bigger than the savings in transportation.

6 CONCLUSIONS

This paper analyses the problem of locating a single DC in an urban area considering the fixed and transportation costs using a single-source Weber problem with continuous piecewise fixed cost. The fixed cost is characterized by a Kriging interpolation method. Using a Delaunay triangulation, we make the fixed cost function convex and tractable. We propose and evaluate three solution approaches to optimally solve the single-source Weber problem with continuous piecewise fixed cost: (*i*) decomposition formulation, (*ii*) decomposition conic formulation, and (*iii*) logarithmic disaggregated convex combination model with a conic formulation.

In the instances we tested, in 23.25% of the time, a better solution is found with the single-source Weber problem with continuous piecewise fixed cost than with the UFLP. We observe two possible explanations:(*i*) the set I is complete, and therefore, the solution of the Weber problem is unfeasible, and (*ii*) the set I is incomplete and requires a more thorough search of feasible locations over the urban area, i.e., the UFLP could have found a sub-optimal solution. To ensure a complete set I in an urban area is expensive and almost impossible. It is possible to improve with the continuous approach, the set of feasible locations focusing in a reduced section of the urban area around the optimal location found, where it is more probable to find the *optimal feasible location*, thus reducing the search effort of feasible points. With this, we can apply an UFLP over the new set I.

The computational results show that the best approach for the single-source Weber problem with continuous piecewise fixed cost, in terms of average CPU time, is the decomposition method, with an average speedup of 7.98x and 7.72x over the decomposition conic method and the conic monolithic reformulation, respectively. The first approach has the best performance and can better handle a bigger set of information nodes only with a small number of customers, but this happens in the instances where the difference between the CPU times are smaller.

There are a number of questions and issues left for future research, such as: (*i*) to apply some Weizfield-like algorithm to improve the performance of the decomposition formulation, given that that was the best one, (*ii*) to use the formulation of a stochastic model of the single-source Weber problem with fixed cost using the variance of the Kriging interpolation method, (*iii*) to consider a location-routing problem, and (*iv*) the extension to a multi-source Weber problem with continuous dependent fixed cost considering the best solution approach we obtain.

REFERENCES

Anselin, L. and Le Gallo, J. (2006). Interpolation of air quality measures in hedonic house price models: spatial aspects. *Spatial Economic Analysis*, 1(1):31–52.

Bongartz, I., Calamai, P. H., and Conn, A. R. (1994). A projection method forl p norm location-allocation problems. *Mathematical Programming*, 66(1):283–312.

Brimberg, J., Drezner, Z., Mladenovic, N., and Salhi, S. (2014). A new local search for continuous location problems. *European Journal of Operational Research*, 232(2):256–265.

Brimberg, J., Hansen, P., Mladenovic, N., and Salhi, S. (2008). Survey of solution methods for the continuous location-allocation problem. *International Journal of Operations Research*, 5(1):1–12.

Brimberg, J., Hansen, P., Mladenovic, N., and Taillard, E. D. (2000). Improvements and comparison of heuristics for solving the uncapacitated multisource weber problem. *Operations Research*, 48(3):444–460.

Brimberg, J., Mladenovic, N., and Salhi, S. (2004). The multi-source weber problem with constant opening cost. *Journal of the Operational Research Society*, 55(6):640–646.

Brimberg, J. and Salhi, S. (2005). A continuous location-allocation problem with zone-dependent fixed cost. *Annals of Operations Research*, 136(1):99–115.

Cellmer, R. (2014). The possibilities and limitations of geostatistical methods in real estate market analyses. *Real Estate Management and Valuation*, 22(3):54–62.

Cellmer, R., Belej, M., Zrobek, S., and Šubic-Kovač, M. (2014). Urban land value maps a methodological approach. *Geodetski vestnik*, 58(3):535–551.

Chen, J.-S., Pan, S., and Ko, C.-H. (2011). A continuation approach for the capacitated multi-facility weber problem based on nonlinear socp reformulation. *Journal of Global Optimization*, 50(4):713–728.

Chen, P.-C., Hansen, P., Jaumard, B., and Tuy, H. (1998). Solution of the multisource weber and conditional weber problems by d.-c. programming. *Operations Research*, 46(4):548–562.

Cooper, L. (1964). Heuristic methods fot location-allocation problems. *SIAM Review*, 6(1):37–53.

Cooper, L. (1972). The transportation-location problem. *Operations Research*, 20(1):94–108.

Dolan, E. D. and Moré, J. J. (2002). Benchmarking optimization software with performance profiles. *Mathematical programming*, 91(2):201–213.

Drezner, Z., Klamroth, K., Schöbel, A., and Wesolowsky, G. O. (2002). 1 the weber problem.

Fernández-Avilés, G., Minguez, R., and Montero, J.-M. (2012). Geostatistical air pollution indexes in spatial hedonic models: the case of madrid, spain. *Journal of Real Estate Research*.

Hansen, P., Mladenovic, N., and Taillard, E. (1998). Heuristic solution of the multisource weber problem as a pmedian problem. *Operations Research Letters*, 22(2-3):55–62.

Helbich, M., Jochem, A., Mücke, W., and Höfle, B. (2013). Boosting the predictive accuracy of urban hedonic house price models through airborne laser scanning. *Computers, environment and urban systems*, 39:81–92.

Hosseininezhad, S. J., Salhi, S., and Jabalameli, M. S. (2015). A cross entropy-based heuristic for the capacitated multi-source weber problem with facility fixed cost. *Computers & Industrial Engineering*, 83:151–158.

Hu, S., Tong, L., Frazier, A. E., and Liu, Y. (2015). Urban boundary extraction and sprawl analysis using landsat images: A case study in wuhan, china. *Habitat International*, 47:183–195.

Kuntz, M. and Helbich, M. (2014). Geostatistical mapping of real estate prices: an empirical comparison of kriging and cokriging. *International Journal of Geographical Information Science*, 28(9):1904–1921.

Larraz, B. and Poblacin, J. (2013). An online real estate valuation model for control risk taking: A spatial approach. *Investment Analysts Journal*, 42(78):83–96.

Liang, H. and Yi, W. (2012). Effect of rent spatial distribution to urban business district planning. In *Advanced Materials Research*, volume 374, pages 2001–2008. Trans Tech Publ.

Luis, M., Salhi, S., and Nagy, G. (2015). A constructive method and a guided hybrid grasp for the capacitated multi-source weber problem in the presence of fixed cost. *Journal of Algorithms & Computational Technology*, 9(2):215–232.

Luo, J. (2004). Modeling urban land values in a gis environment. *University of Wisconsin. Milwaukee, USA*.

Megiddo, N. and Supowit, K. (1984). On the complexity of some common geometric location problems. *SIAM Journal on Computing*, 13(1):182–196.

Michelot, C. and Lefebvre, O. (1987). A primal-dual algorithm for the fermat-weber problem involving mixed gauges. *Mathematical Programming*, 39(3):319–335.

Mladenovic, N., Brimberg, J., Hansen, P., and Moreno-Perez, J. A. (2007). The p-median problem: A survey of metaheuristic approaches. *European Journal of Operational Research*, 179(3):927–939.

Oliver, M. A. and Webster, R. (1990). Kriging: a method of interpolation for geographical information systems. *International Journal of Geographical Information System*, 4(3):313–332.

Planchart, A. and Hurter, A. P. J. (1975). An efficient algorithm for the solution of the weber problem with mixed norms. *SIAM Journal on Control*, 13(3):650665.

Plastria, F. (1987). Solving general continuous single facility location problems by cutting planes. *European Journal of Operational Research*, 29(1):98–110.

Sherali, H. D., Al-Loughani, I., and Subramanian, S. (2002). Global optimization procedures for the capacitated euclidean and l_p distance multifacility location-allocation problems. *Operations Research*, 50(3):433–448.

Vielma, J. P., Ahmed, S., and Nemhauser, G. (2010). Mixed-integer models for nonseparable piecewise linear optimization: Unifying framework and extensions. *Operations Research*, 58(2):303–315.

Weber, A. and Friedrich, C. J. (1929). *Alfred Weber's Theory of the Location of Industries*. The University of Chicago Press, Chicago, Illinois.

Weiszfeld, E. and Plastria, F. (2009). On the point for which the sum of the distances to n given points is minimum. *Annals of Operations Research*, 167(1):4–41.

Xue, G. and Ye, Y. (1997). An efficient algorithm for minimizing a sum of euclidean norms with applications. *SIAM Journal on Optimization*, 7(4):1017–1036.

Applying Mathematical Programming to Planning Bin Location in Apple Orchards

Marcela C. González-Araya[1], Carolina A. Urzúa-Bobadilla[2] and Luis G. Acosta Espejo[3]
[1]*Department of Industrial Engineering, Faculty of Engineering, Universidad de Talca, Camino a Los Niches km 1, Curicó, Chile*
[2]*Faculty of Engineering, Universidad de Talca, Camino a Los Niches km 1, Curicó, Chile*
[3]*Departamento de Ingeniería Comercial, Universidad Técnica Federico Santa María, Avenida Santa María 6400, Vitacura, Santiago, Chile*
{mgonzalez, curzua}@utalca.cl, luis.acosta@usm.cl

Keywords: Pome Fruit Harvest, Bin Location, Optimization Models, Mathematical Programming.

Abstract: In Chile, it has been observed that there is downtime during the apple harvest season. This is largely due to the long distances that the workers must cover and the lack of bins in the orchards. Currently, the administrators do not use methods that enable them to estimate the number of bins required or where they should be located. Taking these observations into consideration, this research paper proposes a plan for bin placement in apple orchards by applying a location model with the objective of diminishing distances covered by the harvest personnel. With data from an orchard in the Maule Region of Chile, the number of bins to be used is calculated taking into consideration the particular surface characteristics of the plantation and the apple variety maturity indicators. For the spatial distribution of the bins, the capacitated p-median was used, because better results were obtained with it in terms of reducing travel distance during the harvest and the ease of implementing the solutions.

1 INTRODUCTION

The Chilean apple industry has had a dynamic development which has placed Chile among the five main apple exporters worldwide with 10% of the market participation, equivalent to approximately 760,000 tons exported (Bravo, 2013). Currently, one of the major challenges facing this industry is to increase its leadership which requires better planning and coordination in all stages of the supply chain. However, in the Chilean fruit industry the supply chain activities are mainly based on the experience of its participants.

In the literature, the first authors to use mathematical programming models to support apple orchard management decisions were Willis and Halon (1976). Their research developed a dynamic programming model to determine the optimum mix of apple varieties to be planted over the long term and applied it to an apple orchard in Massachusetts, USA.

Other models developed for planning the fruit industry supply chain were presented by Ortmann et al. (2006), Masini et al. (2007), Masini et al. (2008), Catalá et al. (2013) and Munhoz and Morabito (2014).

In a related line of research, Ahumada and Villalobos (2009) carried out a literature review focused on models based on agricultural harvests for planning supply chain production and distribution of agro foods. Other literature reviews on mathematical programming models to support agricultural supply chain decisions can be found in Weintraub and Romero (2006) and Bjorndal et al. (2012), who dedicated a portion of their research to models in the agricultural area; Higgins, et al. (2010), who discussed the challenges of adopting operations research models in the agricultural value chain; and Shukla and Jharkharia (2013), who classified the models used in the fresh produce supply chain in various ways (country, year, problem context, technique used, among others).

Several mathematical programming models developed in Chile to support harvesting stage decisions have been applied mainly to the forestry industry (Palma and Troncoso, 2001, Troncoso et al., 2002)

González-Araya, M., Urzúa-Bobadilla, C. and Espejo, L.
Applying Mathematical Programming to Planning Bin Location in Apple Orchards.
In *Proceedings of the 6th International Conference on Operations Research and Enterprise Systems (ICORES 2017)*, pages 345-352
ISBN: 978-989-758-218-9

Among the fruit harvest planning in Chile, the well-known research by Ferrer et al. (2008) proposed a mixed integer linear programming model to determine the plan for grape harvesting which would minimize operating costs and maximize grape quality. In later research done by Bohle et al. (2010) they incorporated data uncertainty into the model presented by Ferrer et al.(2008)which was dealt with by robust optimization.

Regarding location model application to agriculture, Lucas and Chhajed (2004) carried out a review of location models based on territorial balance theory and optimal location applied to improving the agricultural supply chain. Found among the research done after that of Lucas and Chhahed (2004), is the work by Rantala (2004) who developed a mixed integer programming model in order to design a production-distribution system in the seed and seedling supply chain for the purpose of evaluating the expansion or closure of facilities (greenhouses and cold storage).In another study, Higgins and Laredo (2006) used two location models to improve the sugar value chain. One of these models is a p-median problem (Hakimi, 1964) which has an additional restriction that limits the largest average distance from the fields to the loading points. The other model is similar to the capacitated clustering problem (Osman and Christofides, 1994) which divides the producing farms into groups and seeks to minimize the sum of the distances from each farm to the center of the group. These models were applied to a sugar producing region in Australia. In a recent study, Srinivasan and Malliga (2013) applied a p-median model to locate collection centers for Jatropha seeds to be used to produce oil for biofuel. The purpose of the model was to minimize distances from the collection centers to the demand points, thus facilitating logistics for the growers.

In a previous study on bin location in apple orchards, González-Araya et al. (2009) proposed improving their distribution by using the capacitated p-median model (Hakimi, 1964, Garey and Johnson, 1979). This study extends the research by González-Araya et al. (2009) by taking into consideration the fruit maturity indicators according to variety, and also including information about the pollinating varieties. These new data permit better adapting to the orchard characteristics, thus obtaining a different bin distribution plan for each variety. In this manner, this research proposes to improve the bin distribution in apple orchards by applying a location model in order to reduce distances covered by the seasonal workers during fruit harvest. The model used is the capacitated *p*-median (Hakimi 1964).

Next, the problem of bin distribution in apple orchards is described. In Section 3 the mathematical formulation of the model and the parameters used are presented. In Section 4 a case study is described for an orchard located in Chile and in Section 5 the main results and discussion thereof are shown. Finally in Section 6 the conclusions and future research are presented.

2 DESCRIPTION OF THE PROBLEM

The pome fruit harvest involves extensive surface areas, and for this reason the orchards are divided into sections. In this manner, each section may have its own particular characteristics, these being: Fruit variety; plantation density (distance between trees in the same row and distance between rows); density (low, medium, high), that refers to the number of trees per hectare; year of plantation; area (hectares per section); type of irrigation; pollinating trees; among others. All these characteristics make it so that each section can be worked in an independent manner (Catalá et al., 2013). Moreover, pome fruit harvest is characteristically seasonal; with the season beginning once the ranges of maturity for each variety have been reached. In Chile, the harvest generally begins in mid-February and ends around mid-April; however, this can vary according to the climatic conditions each year.

The surface area planted with apples in Chile is about 37,297 hectares where the main producing regions are the Maule Region with 22,488 hectares and the O'Higgins Region with 10,011 hectares, uniting 87% of the national apple plantation surface area (Bravo, 2013).The Maule Region is the main apple producer in Chile with 60.3% of the planted surface area nationally, where 18,863 hectares correspond to red apples and 3,625 hectares to green apples (Bravo, 2013).Orchards in this region present an average density of 1,100 trees per hectare for red apples and 933 trees per hectare for green apples, and an average yield of 48.8 and 50.5 tons per hectare, respectively (CIREN and ODEPA, 2013).

The harvest requires seasonal workers, bins in which to put the fruit, harvest equipment (ladders, baskets, among others) and tractors to transport the bins. Coordinating resources during the harvest is a complex process, where the lack of any one of them can slow it down and affect the quality of the fruit.

The apple harvest in Chile is carried out manually to avoid any mechanical damage, given that the

destination markets are very far away (Asia, the United States, Europe and the Middle East). Bins with a capacity of approximately 350 kilograms placed between the rows of trees are used to collect the apples in the orchard. The placement of the bins is done according to the preferences of the tractor driver with little coordination with those responsible for the orchard sectors. On one hand, the drivers know the number of bins that should be distributed in a given section and the harvesters know which rows of apples they should harvest. However, the way in which the bins are distributed results in either a scarcity or an excess of them among the rows. As well, the seasonal workers must frequently relocate the bins as they advance through the harvest sector. This generates down time and a number of extra hours for the tractor driver to collect the bins from the orchard.

3 MATHEMATICAL FORMULATION AND PARAMETER ESTIMATION

In this study the solutions from the capacitated *p*-median model (Hakimi, 1964, Garey and Johnson, 1979) are analyzed, for the purpose of establishing a bin location plan that would reduce travel distance for harvest crews and that the plan would be easy to implement.

3.1 Capacitated *p*-median Problem

In general terms, the problem consists of determining where to locate the bins and assign apples to each bin, minimizing the distance covered by the workers during the harvest. This case can be modeled as a capacitated *p*-median problem (Hakimi, 1964, Garey and Johnson, 1979). Thus, the installations or medians correspond to the bins and the demand areas correspond to the apples to be harvested.

In formulating the capacitated *p*-median model the following nomenclature is considered:

$N = \{1,...,n\}$ the set of possible bin locations within the sector

$M = \{1,...,m\}$ the set of apple trees in the sector

d_{ij} the linear distance between the apple tree i, $i \in M$, and the possible location of the bin j, $j \in N$.

p the number of bins needed in the sector

k the maximum number of apple trees that can be assigned to a bin,

The decision variables of the model are defined in the following manner:

$y_j \in \{0,1\}$, where $y_j = 1$ if a bin is located in position j, $y_j = 0$; if not, $j \in N$.

$x_{ij} \in \{0,1\}$, where $x_{ij} = 1$ if apple tree i is assigned to the bin located in j, $x_{ij} = 0$; if not, $i \in M, j \in N$.

Thus, the formulation of the capacitated *p*-median model is as follows:

$$\text{Minimize} \sum_{i=1}^{m}\sum_{j=1}^{n} d_{ij}x_{ij} \quad (1)$$

s.t.

$$\sum_{j=1}^{n} x_{ij} = 1, \quad i \in M, \quad (2)$$

$$\sum_{i=1}^{m} x_{ij} \le k y_j, \quad j \in N, \quad (3)$$

$$\sum_{j=1}^{n} y_j = p, \quad (4)$$

$$y_j \in \{0,1\}, \ j \in N, \quad (5)$$

$$x_{ij} \in \{0,1\}, \ \forall i \in M, j \in N. \quad (6)$$

The objective function (1) seeks to minimize the sum of the distances covered by the harvesters from each apple tree to each assigned bin. The set of restrictions (2) guarantees that each apple tree be assigned to a single bin, while the set of restrictions (3) assures that a bin located in j can be assigned, at the most, to k apple trees. The restriction (4) establishes that p bins must be located. Finally, restrictions (5) and (6) define the variables that must be binary.

3.2 Estimation of Parameters Used in the Model

The model parameters are calculated in agreement with the description of the problem given in Section 2; those being: distance between an apple tree and the possible bin location points; number of bins to be located in each sector; capacity of each bin (measured in trees), which differs according to apple variety; and plantation characteristics by sector, that is, the number of trees planted and fruit count before harvest.

The potential bin locations are represented as discrete points established midway between apple tree rows and equidistant among the trees. The quantity of potential locations will depend on the

plantation density, the distribution of pollinating trees and quantity of trees per row of surface area.

The distance d_{ij} (in meters) between apple tree i and the potential bin location j is obtained by calculating the Euclidian distance, given that it is a good approximation of the real distance covered by the harvest workers, since, generally there are no obstacles to covering the distance by walking in a straight line.

The parameter p indicates the number of bins to be located in a surface area to receive the gathered apples. Its value is determined with the following formula:

$$p = (PN_S / TA_S) \times (m / C_b) \times P_f \times F_a \quad (7)$$

Where:

PN_S: kg estimated net production for a sector.

TA_S: total trees of the variety to be harvested planted in a sector.

P_f: percentage of fruit on the tree with sufficient maturity for collecting.

C_b: Capacity of the bin selected for the harvest, measured in kg.

m: number of apple trees in the sector.

F_a: adjustment factor.

The adjustment factor permits defining a margin of security in order to avoid running out of bins during the harvest. In this case 1.1 was considered for the F_a. This value was obtained from the average of the variation coefficients in the production of the apple trees, which was 10%.

Once the p parameter has been obtained, the k parameter is calculated. It represents the quantity of trees it is feasible to assign to a bin when harvesting a particular variety so the unit of measurement is trees/bin. The formula is calculated as follows:

$$k = \left\lceil m / p \right\rceil \quad (8)$$

Formula (8) establishes that if the result is a decimal, it is rounded up to the next integer, given that k must be a whole number.

4 CASE STUDY

Data was taken from an orchard in the Maule Region, Chile that has an apple tree plantation of more than 66 hectares. The varieties of trees occupying the most surface area of the orchard were included, these being Royal Gala, Early Red One and Granny Smith. Each section of the orchard corresponds to the area where a specific variety is planted of which the number of hectares may vary. These sections present different types of harvesting; the Royal Gala is harvested by selective picking and the Early Red One and Granny Smith are harvested by strip picking. As is described by Gil (2004), in selective pickings, the sector must be covered at least three times during the season since the fruit does not mature homogeneously. In strip picking, the sectors are covered only once, harvesting all the fruit from the trees.

The instances of the location models were solved using the optimization software, CPLEX 12.0, academic version, for integer linear programming problems.

To generate the parameters of the capacitated p-median model it is necessary to obtain information about the characteristics and production of the sectors, which has to be periodically revised, and also data about the previous and current season. The required information for each sector is as follows: trees planted, surface area (in hectares), location of the pollinating trees, number of pollinating trees per sector and per row, plantation density, year of plantation, number of trees per row and per sector. The required data from the previous season include the kilograms of apples sent to a packing plant, kilograms of apples that did not meet the required quality parameters (discard), and the percentage of apples to be harvested. The necessary data from the current season are the tree load, the weight of the fruit in kilograms, the bin capacity in kilograms, an estimated percentage of apples that will not meet the required quality parameters (discard), and finally, the percentage of apples to be harvested.

In regard to the data from the previous season or that of the current season it is important to mention that both types of data are not used at the same time. One must select which of these information sources to use as input for generating parameters, taking into consideration the rigorousness of data collection in each of the seasons and the seasonal variability of the factors that affect the harvest (climatic conditions, fertilizer application, fruit thinning, fruit count, tree replacement, among others).

Applying the equations described in Section 3.1, the ranges and input parameters of the model for a sector are calculated with the obtained information. The capacity parameters and number of bins used in the model for each variety of apples is shown in Table 1, in which different harvesting methods are observed, and hence, different input parameters.

Table 1: Parameters used in the capacitated p-median location model according to apple variety by sector.

Variety	Harvest Method	Percentage of Harvest (%)	Bin Capacity (trees/bin) (k)	Sector Surface Area (ha.)	N° of bins to be located per sector (p)
Early Red One	Strip picking	100	9	4.5	685
Granny Smith	Strip picking	100	8	4.6	696
Royal Gala	Strip picking	100	7	6.4	848
Royal Gala	Selective pickings	80	8	6.4	680
Royal Gala	Selective pickings	60	10	6.4	508
Royal Gala	Selective pickings	40	14	6.4	336
Royal Gala	Selective pickings	20	28	6.4	181

5 RESULTS AND DISCUSSION

In this section the main bin distribution proposals obtained when applying the capacitated p-median model are presented. The results for the Early Red One and Royal Gala varieties that have the strip picking and selective picking methods, respectively, are described in greater detail.

With the information from the previous harvest season (2010) a plan for collecting according to sector was obtained, indicating the spatial distribution of the bins, and the distance between the bins (metric and practical).The practical distance is understood as the number of trees there should be between individual bins. It turns out that this distance is easier to explain to the tractor drivers who distribute the bins since it is only necessary to indicate the space (number of trees) that should be left between containers.

To estimate the harvest plan and the average distance covered by the seasonal workers in Sector M13 that has the Early Red One variety, the following information is used: 259,321 kg net weight harvested in the 2010 season, 379 kg average bin capacity and the strip picking harvesting method.

After applying the model, it was found that the average distance from the trees to their assigned bin covered by the harvest workers is 2.94 m, approximately. Considering the 119 rows in this sector, 685 bins should be located there in order to collect all of the apples.

Table 2: Bin location plan in the sector with Early Red One at 100% harvest.

Bin Location Plan					
Sector: Early Red One			Harvest method: Strip picking		
Between Rows		Number of bins	Number of apple trees	Metric distance	Practical distance
1	2	11	99	7.9	4
3	4	12	101	7.4	4
5	6	11	99	7.9	4
7	8	12	101	7.4	4
9	10	11	99	7.9	4
11	12	12	101	7.4	4
13	14	11	99	7.9	4
15	16	12	101	7.4	4
17	18	11	99	7.9	4
19	20	12	101	7.4	4

Part of the location plan obtained for harvesting the Early Red One variety which has a 4.5 ha surface area is shown in Table 2. For example, it is indicated on this table that 11 bins (second column) should be located between Rows 1 and 2 at a distance of 7.9 m (fourth column) or a practical distance of 4 trees (fifth column).As a reference, indicated in the third column is the total number of apple trees allotted to the 11 bins for Rows 1 and 2; that is to say, the 11 bins have the capacity to hold the fruit collected from the 99 apple trees between these two rows.

The difference between the metric and practical distance is about 6.2%, equivalent to 0.45m, so it is hoped that the use of the practical distance achieves an improvement similar to that of the metric distance.

In order to propose the bin distribution plan for Sector M4 which has the Royal Gala variety, the following information is used: 320,766 kg net weight harvested in the 2010 season, 386 kg average bin weight and 40% of the orchard production (a 40% selective picking).In this application of the capacitated *p*-median model the proposal described is for a 40% selective picking, which generally corresponds to the initial selective picking of the season. The total surface area of the plantation considered in this case is 6.4 ha.

According to the model results the seasonal workers must walk an average of 8.23 m from the apple trees to their designated bins.

Because of the contour level irrigation system used in the sector with this variety, it presents a different number of trees per row. For this reason, on occasion, locating only one bin between two rows was proposed. This situation is shown in Figure 1, where a bin is located between Rows 7 and 8, placing it at the end of the longest row. In this way this bin embraces a total of 27 apple trees at a distance of approximately 34 m or every 14 trees. Hence, to make the bin location operative, in each row a bin will be placed every 17 m or every 7 trees, which corresponds to the average distance between bins for a 40% selective picking (see Table 3).

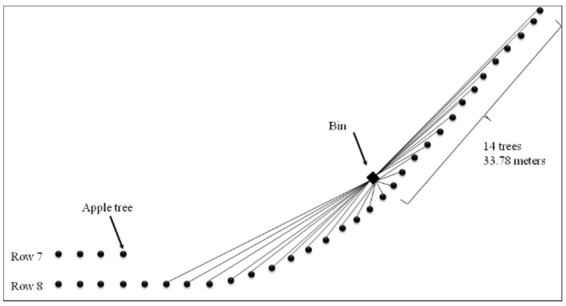

Figure 1: Bin location between rows 7 and 8 in the sector with the Royal Gala variety and the contour irrigation system.

The difference between the estimated metric and practical distances is 3.8%, equivalent to 0.65 m. As with the Early Red One variety, guiding the bin distribution using the practical distance is simpler for the tractor drivers.

For the bin location plans with different percentages of selective picking it was observed that the greater the percentage of selective picking, the lesser the average distance at which bins should be located. Following, Table 4 shows the results for apple varieties with a larger number of hectares planted in the orchard.

Table 3: Bin location plan for the Royal Gala variety at a 40% selective picking harvest.

Bin Location Plan					
Sector: Royal Gala		Harvesting method: 40% selective picking			
Between Rows		N° of bins	N° of Apple trees	Metric distance	Practical Distance
2	3	3	48	19.2	8
3	4	4	48	14.4	6
5	6	3	38	15.0	6
6	7	13	193	18.4	7
7	8	1	16	Locate at the end or beginning of the row	
	11	9	139	19.0	8
11	12	4	52	15.6	6
14	15	13	195	18.6	7
17	18	2	27	15.6	6
18	19	14	214	18.9	8
19	20	1	16	Locate at the end or beginning of the row	

Table 4 indicates how many bins are needed for the complete harvest in a determined sector according to the percentage of mature fruit, the bin location every certain number of rows and the distances between them determined by the number of trees.

It is worth mentioning that according to Gil (2004) it is recommended to do at least three selective pickings during the harvest season for the Royal Gala variety (sector M4), which implies covering the surface area planted with this variety three times. However, during the study season, only selective two pickings were carried out in the orchard for this variety; one 60% selective picking and the remaining 40% was harvested by strip picking. Thus, it is estimated that the location plan proposed for the 60% selective picking reduced the average distance covered by 0.46 m, implying a 5.73% reduction in the average distance covered. Similarly, for the 40% selective picking the average distance covered was reduced by 1.81 m, which means an 18.03% reduction in the average distance covered.

So, when the capacitated p-median model is applied, it is possible to reduce distances covered by the harvest personnel, where the average reduction is approximately 16%. This reduction in distances covered would allow improving the apple harvest productivity.

Table 4: Summary of the results for bin location according to apple variety by sector.

Variety	Sector	Percentage Harvested (%)	N° of bins to be located per Sector (*p*)	N° of rows between which bins are to be located	Average practical distance for locating a bin (number of trees)
Early Red One	M13	100	685	2	4
Granny Smith	M8	100	696	2	4
Royal Gala	M4	100	848	2	3
Royal Gala	M4	80	680	2	4
Royal Gala	M4	60	508	2	5
Royal Gala	M4	40	336	4	7
Royal Gala	M4	20	181	4	14

6 CONCLUSIONS

The capacitated *p*-median model was applied to the sectors of larger size in an orchard located in the Maule Region, Chile, where parameters representing the characteristics of each sector were used. Therefore, the model is flexible in that it adapts to the conditions in a specific surface area, taking into account different input sources. Moreover, it permits the use of various bin capacities, making it adaptable to other types of pome fruit harvest.

In this study a bin location plan was proposed for harvesting the Early Red One, Granny Smith and Royal Gala varieties, which resulted in a reduction in the average distance covered between the apple trees and their specific container of 16.48%, 28.38% and 11.88%, respectively. This reduction in the distances covered would permit an increase in worker productivity and a reduction in harvest operational costs. However, given that there was no study done on harvest times and associated costs, it was not possible to estimate these effects.

The suggested location model can be applied to the harvest of pollinating trees as well, considering these trees represent 11% of the plantation area.

The harvesting process reflects several opportunities for research intended to improve its operation. For example, the system used to determine the fruit load is not based on any statistical procedure to validate its reliability. Therefore, a study could be done based on the particular characteristics of each sector keeping in mind the respective maturity indicators (such as fruit color), and the associated agro climatic variables.

The plantation characteristics of each sector are important parameters to consider for the harvest so maintaining up-to-date information about these parameters is necessary for making good decisions. However, not all the orchards consistently carry out this activity. In the case of the study orchard, the exact distribution of the pollinating trees within a sector is unknown to the administration; they have only an estimated ratio of pollinating trees per sector, which is approximately 11%. According to what was observed for the analyzed varieties, the distribution of the pollinating trees depends on the variety planted in the sector. Also, it should be taken into account that the harvest of these pollinating trees does not occur at the same time as that of the main variety, which involves planning a different harvest in the same sector.

In future research it is recommended to study the operations involved in harvesting the pollinating trees with stationary bins and bin-carrying carts since it could improve the assignment of machinery for the harvest and reduce its cost. This is relevant since, as previously mentioned, the pollinating trees represent approximately 11% of the trees planted in a sector. Thus, for the largest sector in the orchard (sector M4) with 6.4 hectares planted with approximately 5,690 apple trees in all, the 11% pollinating trees corresponds to 626 apple trees which must be harvested. This illustrates the complexity of harvest planning for this sector. Moreover, this difficulty increases considering that during the season several sectors are harvested at the same time.

Finally, other research opportunities arise from the development of simulation models to plan the machinery needed for the harvest and the application of vehicle routing models for the purpose of minimizing distances and fuel costs for the tractors used for collecting and placing the bins in the orchard.

REFERENCES

Ahumada, O., Villalobos., J.R., 2009. Application of planning models in the agri-food supply chain: A review. *Eur. J. Oper. Res*. 195, 1-20.

Bjorndal, T., Herrero, I., Newman, A., Romero, C., Weintraub, A., 2012. Operations research in the natural resource industry. *Int. Trans. Oper. Res*. 19, 39–62.

Bohle, C., Maturana, S., Vera, J., 2010.A robust optimization approach to wine grape harvesting scheduling. *Eur. J. Oper. Res*. 200, 245–252.

Bravo M., J., 2013. *Manzana: una temporada de alto valor de exportaciones*. Publicación de la oficina de estudios y políticas agrarias – ODEPA. Ministerio de Agricultura, Gobierno de Chile, Chile.

Catalá, L.P., Durand, G.A., Blanco, A.M., Bandoni, J.A., 2013. Mathematical model for strategic planning optimization in the pome fruit industry. *Agr. Syst*. 115, 63–71.

CIREN – Centro de Información de Recursos Naturales, ODEPA – Oficina de Estudios y Políticas Agrarias, 2013. *Catastro Frutícola, Principales Resultados, Región del Maule*, Junio 2013, Chile.

Ferrer, J.,MacCawley, A., Maturana, S., Toloza, S., Vera, J., 2008. An optimization approach for scheduling wine grape harvest operations. *Int. J. Prod. Econ*. 112, 985–999.

Garey, M.R., Johnson, D. S. (Eds), 1979. *Computers and intractability: a guide to the theory of NP-completeness*. W.H. Freeman and Co. San Francisco, USA.

Gil S., G. F. (Ed.), 2004. *Fruticultura: Madurez de la fruta y manejo poscosecha: frutas de climas templado y subtropical y uva de vino*, *2*. Ediciones Universidad Católica de Chile, Santiago de Chile, Chile.

González-Araya, M., Acosta-Espejo, L., Ferreira, M., 2009. Una Propuesta de Optimización en el Proceso de Cosecha de Manzanos. In *Anales del XLI Simpósio Brasileiro de Pesquisa Operacional*. Porto Seguro, Brasil.

Hakimi, S.L. 1964. Optimum location of switching centers and the absolute centers and medians of a graph. *Oper. Res*. 12:450–459.

Higgins, A.J., Laredo., L., 2006. Improving harvesting and transport planning within a sugar value chain. *J. Oper. Res. Soc*. 57, 367–376.

Higgins, A.J., Miller, C.J., Archer, A.A., Ton, T., Fletcher, C.S., McAllister, R.R.J., 2010. Challenges of operations research practice in agricultural value chains. *J. Oper. Res. Soc*. 61, 964–973.

Lucas, M.T., Chhajed, D., 2004. Applications of location analysis in agriculture: a survey. *J. Oper. Res. Soc*. 55, 561–578.

Masini, G.L., Blanco, A. M., Petracci, N.C., Bandoni, J.A., 2007. Supply chain tactical optimization in the fruit industry. In: Papageorgiou, L., Georgiadis, M. (Eds.), *Supply Chain Optimization*, Volume 4, Part II. John Wiley & Sons, New York, pp. 121– 172.

Masini, G.L., Blanco, A.M., Petracci, N.C., Bandoni, J.A., 2008. Optimal Operational Planning in the Fruit Industry Supply Chain. In: Ferruh E. (Ed.), *Optimization in Food Engineering*. CRC Press, Taylor and Francis Group, pp. 703–746.

Munhoz, J.R., Morabito, R., 2014. Optimization approaches to support decision making in the production planning of a citrus company: A Brazilian case study. *Comput. Electron. Agric*. 107, 45-57.

Ortmann, F.G., Vuuren, J.H., van Dyk, F.E., 2006. Modeling the South African fruit export infrastructure: a case study. *ORiON*. 22 (1), 35–57.

Osman, I.H., Christofides. N., 1994.Capacitated clustering problems by hybrid simulated annealing and tabu search. *Int. Trans. Oper. Res*. 1, 317–336.

Palma, C., Troncoso, J., 2001. Asignación óptima de equipos en faenas de cosecha forestal. *Revista El Bosque*. 22, 65-73.

Rantala, J., 2004. Optimizing the supply chain strategy of a multi-unit Finnish nursery company. *SilvaFenn*. 38 (2), 203–215.

Shukla, M., Jharkharia, S., 2013.Agri-fresh produce supply chain management: a state-of-the-art literature review. *Int. J. Oper. Prod. Man*. 33 (2), 114–158.

Srinivasan, S.P., Malliga, P., 2013. An Optimal Jatropha Seed Warehouse Location Decision Using Myopic and Exchange Heuristics of P Median. In: Dou R. (Ed.), *Proceedings of 2012 3rd International Asia Conference on Industrial Engineering and Management Innovation (IEMI 2012)*. Springer-Verlag, Berlin Heidelberg.

Troncoso, J., Garrido, R., Ibacache, X., 2002. Modelos de localización de instalaciones: Una aplicación para la producción y logística forestal. *Revista El Bosque*. 23, 57–67.

Weintraub, A., Romero, C., 2006. Operations Research Models and the Management of Agricultural and Forestry Resources: A Review and Comparison. *Interfaces*. 36 (5), 446–457.

Willis, C., Hanlon, W., 1976. Temporal model for long-run orchard decisions. *Can. J. Agr. Econ*. 24 (3), 17–28.

Supporting Harvest Planning Decisions in the Tomato Industry

Eduardo A. Alarcón Gerbier[1], Marcela C. Gonzalez-Araya[2] and Masly M. Rivera Moraga[1]
[1]*Escuela de Ingeniería Industrial, Universidad de Talca, Camino a los Niches km 1, Curicó, Chile*
[2]*Departament of Industrial Engineering, Faculty of Engineering, Universidad de Talca, Camino a los Niches km 1, Curicó, Chile*
ealarcon10@alumnos.utalca.cl, mgonzalez@utalca.cl, mrivera13@alumnos.utalca.cl

Keywords: Scheduling, Logistics, Integer Programming, Tomato Industry, Harvest Planning.

Abstract: Tomato is a raw material that easily deteriorates once harvested and loaded on trucks, losing juice and flesh. Therefore, the reduction of trucks' waiting times in the receiving area of a processing plant can allow reducing tomato waste. In this article, we develop a model that aims to keep a continuous flow of fresh tomato to a paste processing plant and to decrease trucks' waiting times in the plant receiving area. The model is used in a real case of a tomato paste company. The obtained solutions present a better allocation of the harvest shifts, allowing more uniform truck arrivals to the plant during the day. Therefore, trucks waiting times are reduced, decreasing raw material deterioration.

1 INTRODUCTION

The problem of trucks congestion in tomato processing plants is discussed, which causes high trucks' waiting times and deterioration of the transported raw material.

This problem is especially relevant in the competitive tomato industry, where the major world exporters, as USA and China, with 35% and 13% of world production, respectively, exert a strong prices pressure (ODEPA, 2013). In 2012, Chile ranked tenth in the export of tomato paste, with about 100 thousand tons exported per year. On the other hand, the main tomato paste consumers markets are located in Europe, Africa, Asia and Middle East, very far from Chile. Because of this, Chilean companies are constantly seeking to increase their productivity and reduce their production costs.

In the supply chain of tomato paste, the coordination between harvesting, transportation and production stages is necessary because of during a production season the plants work 24 hours. In this sense, a good coordination allows to obtain a continuous fresh tomato supply to the plants during the day, reducing trucks' waiting times and avoiding fresh tomato deterioration. Therefore, the productivity of raw material conversion is increased and so, the production and transportation costs are diminished.

Many researchers have addressed the supply chain planning and coordination of agrifood produce. Ahumada and Villalobos (2009), Díaz-Madroñero et al. (2015) and Soto-Silva et al. (2016) present reviews of optimization models that support decisions in different stages of the supply chain, and for different kind of agricultural products.

Related to harvest planning coordination, in the literature is possible to found a considerable number of articles devoted to the sugarcane industry (Higgins, 2006, López-Milán, and Plà-Aragonés, 2015, Pathumnakul and Nakrachata-Amon, 2015, Lamsal et al., 2015, Lamsal et al., 2016, among others). However, these models are usually specific to each country and industry, because of differing levels and different infrastructures of vertical integration, as specified by Lamsal et al. (2016).

In their work, Higgins (2006) and Lamsal et al. (2015, 2016) present optimization models that aim to reduce trucks' waiting times.

Higgins (2006) presents a mixed integer programming model, which deals with the trucks congestion problem in the sugar mills of Australia. The model seeks to minimize the trucks' queue time and the sum of the mills' idle time. This model has a high complexity, because of it also incorporates the generated queue in each each mill. For this reason, Variable Neighborhood Search (VNS) and Tabu Search algorithms are developed to solve it.

Gerbier, E., Gonzalez-Araya, M. and Moraga, M.
Supporting Harvest Planning Decisions in the Tomato Industry.
In *Proceedings of the 6th International Conference on Operations Research and Enterprise Systems (ICORES 2017)*, pages 353-359
ISBN: 978-989-758-218-9

Lamsal et al. (2015) propose an integer programming model that seeks to coordinate the harvest and transport of sugarcane supply chain in order to reduce trucks waiting times. For achieving this goal, the proposed model maximizes the minimum gap between two successive arrivals in a sugar mill.

Lamsal et al. (2016) propose a model to plan trucks movement between harvest and plants. This model is applicable when there are multiple and independent producers and it is not convenient to store fresh produce in the place of the harvest. The methodology used by these authors is divided in two stages. In the first stage, a model to determine the harvest start times is run. In the second stage, an algorithm for determining the number of trucks to transport raw materials is executed.

In this research is applied a version of the model developed by Lamsal et al. (2016), using data from a Chilean company. The company requires a tool for supporting decision to determine start times of tomato harvesting machines and the number of trucks to assign in each farm, every day. In this way, the company can guarantee a continuous flow of raw materials to the plants and to reduce trucks' waiting times and the tomato deterioration.

Therefore, this paper is structured as follows. In Section 2, the description of transport and harvest problem is presented. In Section 3, the proposed mathematical model for determining daily harvest start times of each tomato farm is explained and, in Section 4, a case study of the tomato paste company is carried out. Finally, in Section 5 the conclusions as further research are presented.

2 HARVEST PLANNING AND TRANSPORT TO A TOMATO PROCESSING PLANT

In agribusiness, companies generally ensure their plants' supplies by purchasing fresh raw materials from different suppliers, located in areas as near as possible to the plants. For this reason, before the harvest season, the companies make contracts to purchase all the yield of the suppliers' farms. This behaviour is also observed in the tomato industry.

In the harvest season, the tomato harvesting machines are outsourced and they move to each farm according to the harvest plan established by the company.

As the tomato harvesting activities, the fresh raw material transport from the harvest sites to the processing plants is also outsourced.

Every day, the selection of tomato farms to be harvested is performed according to the information about tomato ripening in each field and the daily demand of each plant. The trucks allocation to the farms depend on each transport contractor, which has assigned one or more harvesting machines. The contractor is responsible for determining which truck will transport fresh tomato to a plant, based on the number of daily truckload per harvesting machine estimated by the company. In general, it does not exist a decision support system for carrying out this activity.

Each company determines the working hours of tomato harvesting machines, but it is very common that companies have fixed shifts during the day. Most harvesting machines are used during the morning and the afternoon that involves high trucks demand in these periods.

Once a truck arrives to the receiving area of a plant, a download code is assigned to it. Subsequently, it is weighed and recorded at the gathering place, where trucks wait their shift to the next stage. Once the plant requires its fresh raw material, the truck goes to the quality control process, where the percentage of damage is determined based on a sample of 20 kilograms. Finally, the truck is directed to a defined placement area where it proceeds to unload the tomato.

The plants operate 24 hours every day, therefore, they require a continuous flow of raw material and, consequently, a continuous flow of trucks. However, because of work shifts established for the farms are mainly concentrated during the morning and the afternoon, the truck arrivals to the receiving area of the plants are concentrated from the afternoon. This situation causes trucks congestion, so each truck waits in the receiving area on average four hours. This problem involves an increase of transportation costs due to the number of hours spent by trucks in the receiving area and implies a tomato deterioration during waiting time, because of juice and flesh loss.

In Table 1, the effect of waiting times decrease for a constant level of production is shown. It is possible to observe that a decrease in one hour of waiting times, for a same level of production, reduces in 85.4 tons the plant raw material requirements. These data were obtained from a Chilean company that manufactures tomato paste.

Table 1: Effect of waiting times in tomato deterioration.

Decrease in the waiting time (hour)	No. kg tomato per kg tomato paste	No. ton of tomatoes	Daily savings (ton)
0:30	5,42	3.004,6	40,8
1:00	5,34	2.960,0	85,4
1:30	5,25	2.912,5	132,9
2:00	5,16	2.861,7	183,7
2:30	5,06	2.807,8	237,6

In this sense, in order to improve the supply efficiency, the development of a model to plan operations for both, harvest and transport activities, is necessary, aiming to obtain a constant flow of trucks during the day, to decrease the trucks waiting times at the receiving area of plants and so, to reduce raw material deterioration.

3 MODEL FOR HARVEST PLANNING

The following sets are used in the model:
C_i: set of loads at farm i, i ∈ I, j ∈ C_i.
I: set of farms to be harvested.

The parameters considered by the model are the following:
n: number of blocks of time in which the day is divided.
a_k: start time of the block k, for k= 0, 1, …, n. Furthermore $a_0 < a_1 < a_2 \ldots < a_n$, where a_n represents the end time of the delivery window.
h_i: time required to harvest a load at farm i, i ∈ I.
N_k: unloading capacity in the plant for each block k=0, 1, …, n-1.
t_i: travel time between farm i and the plant, i ∈ I.
α: penalization associated with the deviation of the plant's unloading capacity.
lmt: maximum number of farms that can be harvested in shift 3.

The decision variables of the model are the following:
x_{ij}: arrival time at the plant of *i*th farm's *j*th load, i ∈ I y j ∈ C_i.
y_i: time when the harvesting starts at farm I, i ∈ I.
λ_{ij}^k: ∈ R+ and expresses the instant in which the *j*th load of the *i*th farm lies between the time a_k and a_{k+1}, i ∈ I, j ∈ Ci and k= 0, 1, …, n.
b_{ij}^k: ∈ {0,1}, where b_{ij}^k = 1 if the *i*th farm's *j*th load arrives between a_k and a_{k+1}, b_{ij}^k = 0 otherwise.
CS_k: surplus capacity or positive deviation from the plant's unloading capacity, k= 0, 1, …, n-1.
CF_k: slack capacity or negative deviation from the plant's unloading capacity, k= 0, 1, …, n-1.
MX_i: ∈ {0,1}, where MX_i = 1 if the shift 3 is available to be assigned in the farm i, MX_i = 0 otherwise.

The formulation of the proposed model for harvest planning is presented in this section. The indices, parameters and decision variables of the model can be founded in the Appendix.

Mathematical formulation

$$\text{Min } Z = \sum_{k=0}^{n-1} (\alpha * CF_k + (1-\alpha) * CS_k) \quad (1)$$

s.t.

$$x_{ij} = y_i + j * h_i + t_i \quad \forall i \in I, j \in C_i \quad (2)$$

$$x_{ij} = \sum_{k=0}^{n} (\lambda_{ij}^k * a_k) \quad \forall i \in I, j \in C_i \quad (3)$$

$$\sum_{k=0}^{n} \lambda_{ij}^k = 1 \quad \forall i \in I, \quad j \in C_i \quad (4)$$

$$\lambda_{ij}^0 \leq b_{ij}^0 \quad \forall i \in I, \quad j \in C_i \quad (5)$$

$$\lambda_{ij}^k \leq b_{ij}^{k-1} + b_{ij}^k \quad \forall i \in I, j \in C_i, \; k \in 1, \ldots, n \quad (6)$$

$$b_{ij}^n = 0 \quad \forall i \in I, j \in C_i \quad (7)$$

$$\sum_{k=0}^{n} b_{ij}^k = 1 \quad \forall i \in I, j \in C_i \quad (8)$$

$$\sum_{i \in I} \sum_{j \in C_i} b_{ij}^k + CS_k - CF_k = N_k \quad \forall k \in 0, \ldots, n-1 \quad (9)$$

$$b_{ij}^k \in \{0,1\} \quad \forall i \in I, j \in C_i, k \in 0, \ldots, n \quad (10)$$

$$\lambda_{ij}^k \in [0,1] \quad \forall i \in I, j \in C_i, k \in 0, \ldots, n \quad (11)$$

$$CF_k, CS_k \geq 0 \quad \forall k \in 0, \ldots, n-1 \quad (12)$$

$$y_i \geq 0 \quad \forall i \in I \quad (13)$$

$$x_{ij} \geq 0 \quad \forall i \in I, j \in C_i \quad (14)$$

The objective function minimizes positive and negative deviation from the plant's unloading capacity. Depending on the case can be penalized just one of the deviation or more heavily in one direction than the deviation on the other side. For example, to achieve a high utilization of the plant should be penalized the slack capacity (CF_k) and to minimize the downtime of the trucks should be penalized specially the surplus capacity (CS_k).

Constraint (2) states that the arrival time at the plant of *i*th farm's *j*th load depends on the harvest start time in the farm *i*, the harvest rate at that farm and the travel time between the farm and the plant. Constraint (3) – (8) determine the arrival time through a convex combination of the beginning and the end time of each block into which the arrival falls.

Constraint (9) determines the slack or surplus capacity in each block by comparing the quantity of inputs with the unloading capacity.

Finally, the constraints (10) – (14) stablish the nature of the decision variables.

4 CASE STUDY

In this section the model is used in a real case, which is based on data from a tomato paste company.

This company has two production plants, where annually 550,000 tons of fresh tomato are processed. The raw material is purchased from different farmers and it is daily harvested using 40 tomato harvesting machines. These harvesters are mostly subcontracted and assigned to the farms according to the percentage of tomato ready to be harvested in each one (from 90% of ripe tomato). For this assignment is used a manual scheduling.

The company works with three work shifts, which start at 07:00, 13:00 and 17:00 hours; shifts 1, 2 and 3, respectively. In addition, its plants operate 24 hours a day. In order that the model assigns to the harvesting machines these times, the function (15) is established. It is important to mention that 7 hours are subtracted from the schedules with the aim of working with values between 0-24.

$$y_i = \begin{cases} 0{:}00 \\ 6{:}00 \\ 10{:}00 * MX_i \end{cases} \quad \forall i \in I \qquad (15)$$

At the same time, because it is difficult to harvest at night (shift 3), a binary variable (MX_i) and restriction (16) is defined. Thus, the total number of shifts 3 assigned to the harvesters is restricted.

$$\sum_{i \in I} MX_i \leq lmt \quad \forall i \in I \qquad (16)$$

4.1 Dataset

To implement the model are used data of harvest from the season 2016 for one of the plants of the company. This plant is normally supplied for 12 farms.

Table 2 shows the data of the farms that supply the plant.

Table 2: Number of loads, travel time and harvest time from the farms that supply the plant.

Farm	Number of loads	Harvest time (hour)	Travel time (hour)
#1	9	1,1	1,6
#2	6	1,7	0,8
#3	10	1,0	0,3
#4	4	2,5	0,6
#5	3	3,3	1,5
#6	7	1,4	0,6
#7	8	1,3	0,3
#8	6	1,7	0,9
#9	6	1,7	1,1
#10	5	2,0	0,3
#11	9	1,1	0,3
#12	10	1,0	0,8

The case study was performed on an 2,40 GHz Intel Core i3 CPU running the Windows 10 operating system. The computational results associated to the case study are obtained using IBM ILOG CPLEX Optimization Studio version 12.6.

Three scenarios are solved, since the maximum number of work shifts 3 to be allocated is modified. The first run (case 1) uses the same proportion of harvesting machines in each shift that the company assigned on that day for the farms. With this, the goal is to determine the optimal distribution while maintaining the number of harvesting machines working on each shift. In the second run (case 2) is limited to a maximum of 25% of the farms to be harvested on shift 3. This equates to a maximum of three farms. Finally, in the third run (case 3) the amount of farms that can be harvested in shift 3 is not limited.

For all instances, the software takes less than 1 minute. It is noteworthy that, since it is a daily planning, are needed low runtimes software.

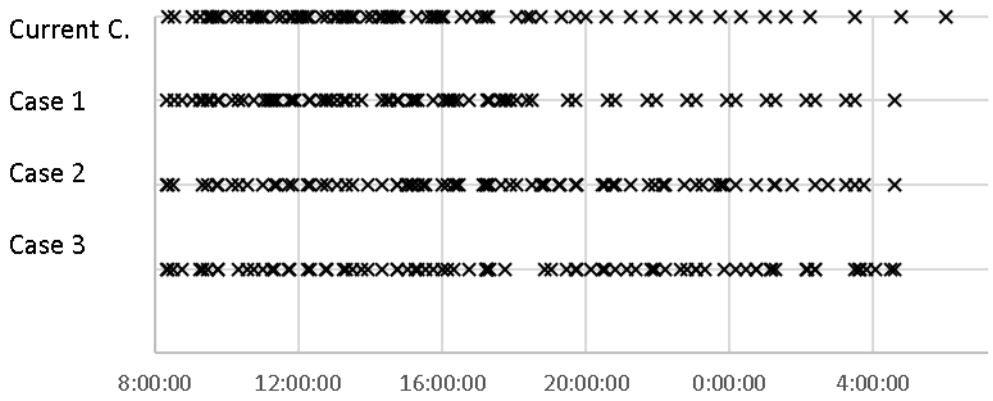

Figure 1: Distribution of arrivals during the day.

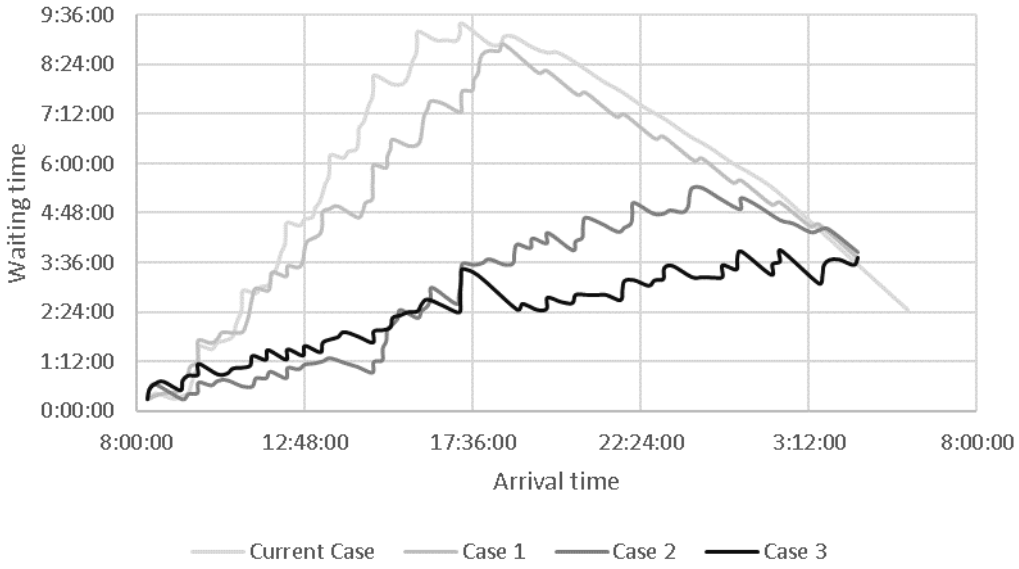

Figure 2: Waiting times per hour for each case.

4.2 Main Results

Table 3 compares the real shifts assigned to the farms with those obtained by the model. It can be seen that in the real distribution of harvesters (real allocation and case 1), the schedule most commonly used is the shift 1. On the other hand, the schedules for unrestricted modelled case (case 3) are spread more evenly between shift 1 and shift 3. This is based on that, a more even distribution of shifts during the day, allows more uniformity in the arrival of trucks and, consequently, of load and raw materials. Regarding the case with restriction (case 2), similar results are obtained to the real distribution (case 1). However, greater use of shift 2 and shift 3 is observed.

Table 3: Results for each case.

Shift	Real allocation and Case 1	Limited allocation in shift 3 (Case 2)	No limited allocation in shift 3 (Case 3)
#1	10	6	5
#2	1	3	1
#3	1	3	6

Figure 1 shows arrivals of trucks to the plant for each case. It can be seen that for the real case the most trucks arrive at the plant during 8:00 and 16:00 hours. For case 1, which considers the same proportion of harvesting machines in each shift that the real allocation, is observed a high arrival rate until about 19:00 hours. The allocation of work shifts, which are obtained for the optimization model for case 2,

generate a more uniform distribution during the day compared to the two previous cases. Finally, arrivals associated to case 3 present a high uniformity.

In order to analyse the impact of the model solutions in improving the planning of harvest shifts, software Arena Simulation, version 14.7 is used to perform this analysis. The simulation allows to calculate waiting times and queues generated on the plants in each case.

Figure 2 shows waiting times of the trucks in plant in relation to its arrival time. The graph shows a significant decrease in waiting times for cases 2 and 3, compared to cases 1. It is important to note that, for example, the trucks arriving at 18:00 hours, based on the allocation of real case and case 1, must wait about 8 hours in the plant for the download process. With respect to cases 2 and 3, waiting times decrease considerably, obtaining a waiting on plant close to 3 hours at 18:00 hours.

Table 4 shows the average and maximum waiting times, as well as the number of trucks in queue for each case.

For case 1 are obtained average waiting times 4:51 hours, which represents a decrease of about 30 minutes compared to the real case. With respect to case 2 and case 3 it is obtained a considerable reduction in waiting times for trucks on plant compared to real case and case 1, yielding an average of 2:53 hours for case 2 and 2:22 hours case 3. With respect to the number of trucks that are in plant for the download process is obtained on average 8.5 trucks for case 2 and 6.9 trucks for case 3.

The implementation of the model in case 3 causes a decrease in waiting times of up to 3 hours compared to the real case. At the same time, the schedules that consider restrictions on the amount of farm that can be harvested in shift 3 (case 2) provide equally better results than manual planning. It is important to emphasize that the scenarios with constraints on shift 3 are more likely to implement in the operations of the company, since working during night hours is more dangerous because of the lack of light and because the night shifts are more difficult to manage and control.

Based on these results, it is possible to conclude that the use of the model allows to obtain a better allocation of the harvest shifts, which allows truck arrivals more uniform during the day and, therefore, shorter waiting times and a decrease in the deterioration of the raw material.

Table 4: Waiting times and trucks queued for each case, according to the simulation.

		Wait time (hour)	**Number of trucks in queue**
Current case	Average	5:22:00	16,2
	Maximum	9:23:12	33
Case 1	Average	4:51:42	13,2
	Maximum	8:54:14	26
Case 2	Average	2:53:35	8,5
	Maximum	5:23:33	18
Case 3	Average	2:22:47	6,9
	Maximum	3:52:55	13

5 CONCLUSIONS

The optimization model was used in a real case of a tomato paste company. In this application, three cases were analyzed. The first case use the same shifts' distribution established by the company (case 1). The second case allows only to allocate a maximum of 25% of the farms in the shift 3 (case 2). Finally, the last case does not limit the allocation of the farms in every shift (case 3).

The use of the model allows obtaining better shift allocation of harvesting machines, which improves the arrival distribution of trucks into the plants. The case 3, that does not limit the number of farms assigned to shift 3, presents the best harvesting machines allocation, which helps to reduce the trucks' waiting times in about three hours. However, this allocation is difficult to implement in any agribusiness company, because it requires that many farms be allocated in the evening or night shift (shift 3). In general, workers do not like be assigned at the last shift. Additionally, night shifts are difficult to manage and control.

For the other hand, the company can implement more easily the obtained solutions for cases 1 and 2. The model solution for case 1 distributes in a better way than the current situation, the farms and harvesting machines allocated in each shift. The solution for case 2, that allows an increase up to 25 percent of farms assigned to shift 3, is more feasible to be implemented by the company and shows a decrease of about 2:30 hours of trucks' waiting time.

According to these results, the impact of solutions implementation in the company could be high. If a decrease of about 2:30 hours of trucks' waiting time takes place, based on the data presented in Table 1, saving of around 237.6 tons of tomato could be obtained. Similarly, the obtained solution in case 1 could allow savings of 40.8 tons per day. In addition,

reducing trucks waiting times in the plant could speed up the tomato supply and help to reduce the number of trucks required for transportation, causing a decrease of transportation costs.

The use of the model for assigning harvest shifts obtain better and faster results than the current allocation method utilized by the company. Moreover, the model execution requires little computational time for obtaining solutions, which is a necessary condition for a daily planning. For implementing the model, a following stage is to develop decision support system, so users could interact easily with the model entering data and parameters, and getting suitable harvest plan reports.

For future extensions of the model, it could be interesting to plan harvest activities for a longer period, as for example a week. This dynamic model could include the reduction of harvesting machines' shift changes that are not considered when a daily plan is executed. Furthermore, this new model extension could also minimize harvesting machines displacement during the period.

REFERENCES

Ahumada, O., & Villalobos, J. R. (2009). Application of planning models in the agrifood supply chain: A review. *European Journal of Operational Research*, 196(1), 1–20.

Díaz-Madroñero, M., Peidro, David & Mula, Josefa (2015). A review of tactical optimization models for integrated production and transport routing planning decisions. *Computer & Industrial Engineering*, 88(10), 518–535.

Higgins, A. (2006). Scheduling of road vehicles in sugarcane transport: A case study at an Australian sugar mill. *European Journal of Operation Research*. 170(3), 987–1000.

Lamsal, K., Jones, P. C. & Thomas, B. W. (2016). Harvest logistics in agricultural systems with multiple, independent producers and no on-farm storage. *Computer & Industrial Engineering*, 91(1), 129–138.

Lamsal, K., Jones, P. C. & Thomas, B. W. (2015). Continuous time scheduling for sugarcane harvest logistics in Louisiana. *Computer & Industrial Engineering*, 54(2), 616–627.

López-Milán, E., Plà-Aragonés, L.M. (2015). Optimization of the supply chain management of sugarcane in Cuba. In *International Series in Operations Research and Management Science*, 224, 107-127.

ODEPA (2016). *La industria de la pasta de tomate* (2016), de Oficina de Estudios y Políticas Agrarias. Avaible from <www.odepa.gob.cl>.

Pathumnakul, S., Nakrachata-Amon, T. (2015). The applications of operations research in harvest planning: A case study of the sugarcane industry in Thailand, *Journal of Japan Industrial Management Association*, 65 (4E), 328-333.

Soto-Silva, W. E., Nadal-Roig, E., González-Araya, M. C., Pla-Aragones, L. M. (2016). Operational research models applied to the fresh fruit supply chain. *European Journal of Operation Research,* 251(2), 245–355.

Designing Charging Infrastructure for a Fleet of Electric Vehicles Operating in Large Urban Areas

Michal Kohání[1], Peter Czimmermann[1], Michal Váňa[1], Matej Cebecauer[2] and Ľuboš Buzna[1,3]
[1]*Department of Mathematical Methods and Operations Research, University of Žilina, Univerzitná 8215/1, SK-01026 Žilina, Slovakia*
[2]*Department of Transport Science, KTH Royal Institute of Technology, Teknikringen 10, SE-100 44 Stockholm, Sweden*
[3]*ERA chair for Intelligent Transport Systems, University of Žilina, Univerzitná 8215/1, SK-01026 Žilina, Slovakia*
{*michal.kohani, peter.czimmermann, lubos.buzna*}*@fri.uniza.sk*, {*michal.vana, matej.cebecauer*}*@gmail.com*

Keywords: Electric Vehicles, Charging Infrastructure, Urban Areas, GPS Traces.

Abstract: Here, we propose a method to design a charging infrastructure for a fleet of electric vehicles such as a fleet of taxicabs, fleet of vans used in the city logistics or a fleet of shared vehicles, operating in large urban areas. Design of a charging infrastructure includes decisions about charging stations location and number of charging points at each station. It is assumed that the fleet is originally composed of vehicles equipped with an internal combustion engine, however, the operator is wishing to replace them with fully electric vehicles. To avoid an interaction with other electric vehicles it is required to design a private network of charging stations that will be specifically adapted to the operation of a fleet. It is often possible to use GPS traces of vehicles characterizing actual travel patterns of individual vehicles. First, to derive a suitable set of candidate locations from GPS data, we propose a practical procedure where the outcomes can be simply controlled by setting few parameter values. Second, we formulate a mathematical model that combines location and scheduling decisions to ensure that requirements of vehicles can be satisfied. We validate the applicability of our approach by applying it to the data characterizing a large taxicab fleet operating in the city of Stockholm. Our results indicate that this approach can be used to estimate the minimal requirements to set up the charging infrastructure.

1 INTRODUCTION

Road transport produces 20% of total carbon dioxide (CO_2) emissions, which is the main greenhouse gas. While these emissions decreased by 3.3% in 2012, they are still 20.5% higher than in 2011 and it could have been even more if there is no economic crises (Europen Commision, 2015). It is therefore expected that in order to reduce CO_2 emission in densely populated urban areas, it will be desired to continue electrification of individual and public transport. However, electrification of transport itself does not ensure the reduction of CO_2 emission, also the the higher penetration of renewable sources of electrical energy is necessary. Advances in battery technologies and continuously decreasing prices of electric vehicles may soon increase the interest in converting large fleets of vehicles serving urban areas into electric, because the expected benefits could be considerable due to high utilization of such vehicles. Thus, high purchase costs of a new electric vehicle can be more easily compensated by lower operational costs. To avoid delays in charging, caused by interaction with other electric vehicles, a choice of a fleet operator can be to build their own charging infrastructure.

The topic of planning charging infrastructure for electric vehicles is rapidly growing in the scientific literature. The attention of researchers has been focusing on creating models that would be able to predict the future expansion of electric vehicles (Sears et al., 2014) as well as models designed to estimate the size of the future demand for charging vehicles (Yi and Bauer, 2014). An approach, where GPS traces of vehicles collected in two Italian cities were used to extract the travel behaviour and to estimate the expected demand for charging vehicles, was used in (Paffumi et al., 2015; Gennaro et al., 2015). Such analysis can provide valuable hints when searching for suitable positions of charging stations. Data driven approach to predict the penetration of EVs in the region of Lisbon and the future refuelling demand was proposed in (Frade et al., 2011).

Optimization algorithms have been often used to address this problem as well. In (Dickerman and Har-

Kohání, M., Czimmermann, P., Váňa, M., Cebecauer, M. and Buzna, Äj.
Designing Charging Infrastructure for a Fleet of Electric Vehicles Operating in Large Urban Areas.
In *Proceedings of the 6th International Conference on Operations Research and Enterprise Systems (ICORES 2017)*, pages 360-368
ISBN: 978-989-758-218-9

rison, 2010) was used a city transportation model to verify various locations of charging stations, which were generated by the genetic algorithm. A bi-level approach was proposed by (Jung et al., 2014). On the upper level is solved the location problem (considering the capacity of charging stations), where the total costs and waiting time are minimized. On the lower level is used simulation approach to evaluate each design. Simulation as a validation tool has been used relatively often (Sweda and Klabjan, 2011). In (Xi et al., 2013) authors developed the simulation-optimization approach, where the area is divided into regions. The OD-matrix for the regions is known and it is used to estimate the EV flows between them. Linear IP model is used to determine the location and size of charging stations subject to limited budget. Simulation model is used to estimate the expected number of vehicles successfully charged at each candidate location. (Dong et al., 2014) proposed an approach that allows for analyzing the impact of public charging infrastructure deployment on increasing electric miles travelled. A genetic algorithm is used to find locations of charging stations and it is evaluated by the activity-based assessment method. Combination of a simulation approach with a genetic algorithm that utilizes GPS traces of vehicles was presented in (Tu et al., 2015).

Several authors considered a location problem leading to a mixed integer programming problem. For example, in (Chen et al., 2013) the demand for charging electric vehicles on public parking lots was estimated, based on a traffic survey conducted in the city of Seattle. The suitable location of charging stations was found by minimising the costs and the optimisation problem was solved by a general purpose optimisation solver. A similar methodology was also used for the city of Lyon (Baouche et al., 2014) and the city of Coimbra (Cavadas et al., 2014). When designing a network of charging stations, capacity constraints are typically included in the model (Lam et al., 2014; Ghamami et al., 2016) and apart from minimising costs, the area covered within the driving distance is maximised (Yi and Bauer, 2014). Methodologically different approach has been presented in (Momtazpour et al., 2012). Here authors considered constraints implied by the daily activity of car users and the capacity of electrical network and the location of charging stations were found by the clustering algorithm. The advantage of this approach is that several types of constraints can be taken into account simultaneously, without significantly affecting the computational complexity of the algorithm.

The special class of models was developed to cover trajectories of vehicles (MirHassani and Ebrazi, 2013; Capar et al., 2013). This approach is applicable in the design of the charging infrastructure along a highway to cover for long distance trips. An elegant way how to locate charging stations along the paths was proposed by (MirHassani and Ebrazi, 2013). The approach is based on adding artificial links to the network graph conecting places that fulfil some reachability rules. The model locates the minimum number of refuelling stations along paths to make the path traversal feasible. The approach (Chung and Kwon, 2015) further extends (MirHassani and Ebrazi, 2013) by considering multi-period case.

As our contribution, we propose an approach that is purely based on an optimization approach where we combine location and scheduling problems and thus we avoid the need to validate the locations and capacity of charging stations by computer simulations. Because the approach is based on historic data it can be used to estimate the minimum design of the system that is sufficient to cope with various scenarios occurring in the past.

The paper is organized as follow: in section 2 we describe the data requirements and the methodology. In section 3, we describe the data used in the case study and we introduce the results of numerical experiments. To conclude, we summarise our main findings in section 4.

2 METHODOLOGY

2.1 Data Requirements

The proposed method to design the network of private charging stations relies on two datasets. The first dataset is expected to contain historical low-frequency GPS data describing the mobility patterns of individual vehicles that belong to the fleet. Data should be collected for several, typical and sufficiently long time periods representing relevant scenarios that should be included in the design of the charging network. To collect low frequency data is much easier in practice as there is no need to use expensive GPS trackers, however, such data are not precise enough to determine the travel distances. Therefore we need the graph model of the road network including data about nodes, edges and their elevation. Using this data we can perform the map matching and estime the travel distances much more precisely by inducing them from the road network.

2.2 Algorithm to Determine a Candidate Set of Charging Station Locations

In this paper, we will explore the case where to recharge an electric vehicle, we use only the time when it is parking for a long enough time. Thus, if possible, we do not wish to affect the current trajectories that are taken by vehicle drivers. The proposed methodology allows then to evaluate what percentage of vehicles could be transformed to electric vehicles without affecting their operation with the minimal requirements on building the charging infrastructure. Therefore, we use the historic GPS data to identify the set of suitable candidate locations for charging stations. Here, we aim to identify locations where the large number of vehicles frequently parks. To do so, we proposed the following two-phase procedure:

- Phase 1: Identify the set of candidate locations for charging stations as locations where many vehicles tend to park for a long enough time.
- Phase 2: Identify the set of vehicles that can be served by selected set of candidate locations.

To determine the set of candidate locations, following parameters are used. As an parking event we identify the time period, when the average speed of a vehicle is below the maximum speed limit V_{max} for at least a time period of T_{min}. To ensure that we select a relevant set of candidate location we require for each candidate to be associated with at least M_{min} parking events taking place in its circular neighbourhood defined by the radius of R_{max}.

In the first phase, we process one-by-one the GPS traces of all vehicles executing the following steps (see Figure 1):

- Step 1: Identify in the GPS trace the traversals that have the average speed below the speed limit V_{max}.
- Step 2: Identify in the GPS trace the maximum connected sequences of traversals longer than the time period T_{min}.
- Step 3: Identify as a candidate location the last node of each connected sequence if there is no other candidate location within the distance R_{max}.

After processing all GPS traces we remove all candidate locations that are associated with less than M_{min} parking events.

The second phase of the procedure evaluates the proposed set of candidate locations and identifies the set of vehicles that could be replaced by the electric vehicles. For each vehicle we evaluate its trajectory and we evaluate whether it could be sufficiently recharged during parking events, to cover the travel distances. Here we consider the unlimited capacity of charging points being locating in each candidate location. We assume that the capacity of each vehicle is K (measured in kilometres), i.e. it corresponds to the reachable driving distance. As a vehicle is driven its state of charge is decreasing by substricting from it the travel distance. Each time unit when the vehicle is charged we increase its state of charge by the value of P. We record the number of vehicles that cannot be served by a given set of candidate locations. In the mathematical model we consider only vehicles that can be recharged, otherwise the proposed mathematical model has no feasible solution.

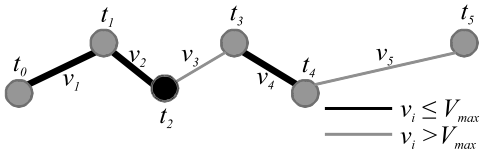

Figure 1: Diagram illustrating the identification of candidate locations. Nodes represent GPS position of the vehicle in time t_i, links are traversals between two GPS positions. Black coloured links represent traversals, where the average speed v_i is below the limit V_{max} and black coloured node represents the candidate location.

2.3 Mathematical Model

We aim to minimize the costs that are required to set up the charging infrastructure. Due to the fact that in our approach we expect to locate charging stations of the same type, we minimize just the number of charging points. Previous studies (Sweda and Klabjan, 2011; Xi et al., 2013; Dong et al., 2014) indicated that an important requirement is to consider queueing behaviour of vehicles while charging. Therefore we formulate a location optimization problem considering the scheduling problem to ensure that there exist a feasible schedule how to recharge vehicles.

We assume that the algorithm introduced in the previous section was used to produce the set of candidate location where it is possible to locate the charging infrastructure I. To schedule the individual charging time slots we split the time into the set of non-overlapping time intervals T. Then for each vehicle we distinguish two possible states (see Figure 2). A vehicle is either parking at the candidate locations and it is available for charging or it is located somewhere else where it cannot be charged.

The maximum number of charging stations is limited to p. We consider that the fleet is composed of the set of vehicles C and each vehicle is equipped by the battery, which when fully charged allows for driving the vehicle for the distance K. From the data we

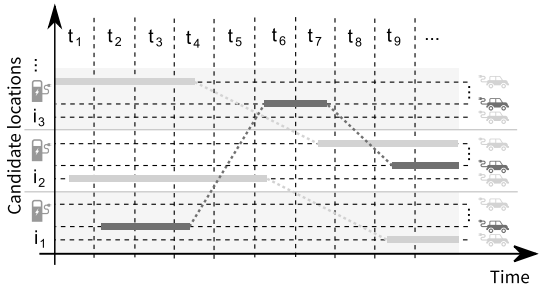

Figure 2: Diagram illustrating the movement of individual vehicles between the candidate locations. Vehicle is either parking at the candidate locations and thus it is available for charging (coloured rectangles) or it is located somewhere where it cannot be charged (coloured dashed lines).

extract for each vehicle $c \in C$ an ordered sequence of parking events R_c and we determine the list N_{cr} of all time intervals $t \in T$ that have an overlap with parking event $r \in R_c$. The fraction of the time interval $t \in T$ the vehicle $c \in C$ is parking we denote as $a_{ct} \in [0,1]$. To simplify the description of the mathematical model we define $B_{itc} \in \{0,1\}$, where $B_{itc} = 1$ if the vehicle $c \in C$ parks at the location $i \in I$ during the time interval $t \in T$ and $B_{itc} = 0$ otherwise. We use the graph of the road network to extract the information about the real travel distances. Vehicle $c \in C$ drives u_{cr} kilometres while driving from the parking event $r-1$ to the parking event r. Each vehicle enters into the model with an fictive parking event $r = 0$ of zero duration and exits with an fictive parking event $r = r_c$ of zero duration. Symbol M denotes the $big-M$ constant. Decisions are described by the set of variables:

- $y_i \in \{0,1\}$ for $i \in I$, where $y_i = 1$ if the charging station is located at the candidate location i and $y_i = 0$ otherwise,
- $s_i \in Z^+$ for $i \in I$, representing the number of charging points allocated to the station $i \in I$,
- $x_{ct} \in \{0,1\}$ for $c \in C, t \in T$, where $x_{ct} = 1$ when vehicle $c \in C$ is being charged during the time interval $t \in T$ and $x_{ct} = 0$ otherwise, and
- $d_{cr} \geq 0$ for $c \in C, r \in R_c \cup \{0\} \cup \{r_c\}$ corresponds to the distance that the vehicle $c \in C$ at the beginning of the parking event $r \in R_c$ is able to drive.

Making use of these notation we formulate the location-scheduling problem that is shown in Figure 3.

In the objective function of the problem (1) we minimize the number of located charging points. Constraint (2) ensures that we do not locate more than p charging stations. This constraints approximates the limitations that are associated with the establishment of a new charging station. Constraints (3) make sure that we can assign charging points only to located charging stations. In each time interval we cannot use more charging points than available as it is specified by the set of constraints (4). We initialize the system by limiting the driving distance to αK, where $\alpha > 0$ is parameter of the model (see constraints (5)). Constraints (6) ensure that battery capacity is not exceeded and constraints (7) ensure contiguity in charging and discharging of batteries.

3 NUMERICAL EXPERIMENTS

3.1 Data

In the case study we consider a fleet of more than 1,500 taxicabs operating in the area of Stockholm district, in Sweden. Each vehicle reported on average every 90 seconds its id, GPS position, time-stamp and information whether it is hired or not. For the case study we selected four weeks (see Figure 4), altogether comprised of 8,989,143 probe data records. These four weeks represent different scenarios: week 1 is a typical spring week with 1542 taxicabs, week 2 represents typical summer week with 1526 taxicabs, week 3 is the Christmas week with 1491 taxicabs and week 4 is a special week, when the major disruption of the public transport occurred due to many failed railway connections, with 1550 taxicabs.

As the reporting frequency of probe data is relatively low, to be able to measure the travel distances more accurately we map-matched the probe data onto the road network using the methodology proposed in (Rahmani and Koutsopoulos, 2013). Thus, we use the road network to estimate the travel distance. In the digital model of the road network each link is attributed a number of parameters, including the length, presence of a traffic signal, road class, speed limit and etc. The graph of road network used in the case study consists of 231,839 links. In Figure 5 we show accumulated number of traversals by taxicabs over all four weeks for all links of the road network. We have no traversals for 97,720 links, where 96% of these are class 5 links. Conversely, the largest frequency of usage we observe on class 1 links connecting the city of Stockholm with the airports and in the city centre.

3.2 Numerical Results

We set the following values of parameters: the driving range of all vehicles $K = 300$ km, the initial fraction of the driving range $\alpha = 0.5$, the charging speed $P =$ 5 km/min., we do not limit the number of charging stations, i.e., $p = |I|$, $V_{max} = 0.1$ m/s and $T_{min} = 15$ min. When constructing the mathematical model we

Model formulation

$$\text{Minimize} \sum_{i \in I} s_i \tag{1}$$

$$\text{subject to} \sum_{i \in I} y_i \leq p \tag{2}$$

$$My_i \geq s_i \qquad \text{for } i \in I \tag{3}$$

$$\sum_{c \in C} B_{itc} x_{ct} \leq s_i \qquad \text{for } i \in I, t \in T \tag{4}$$

$$d_{c0} \leq \alpha K \tag{5}$$

$$d_{cr} + \sum_{t \in N_{c,r}} a_{ct} x_{ct} P \leq K \qquad \text{for } c \in C, r \in R_c \cup \{r_c\} \tag{6}$$

$$d_{cr} \leq d_{c,r-1} - u_{cr} + \sum_{t \in N_{c,r-1}} a_{ct} x_{ct} P \qquad \text{for } c \in C, r \in R_c \cup \{r_c\} \tag{7}$$

Figure 3: Mathematical formulation of the location-scheduling optimization problem.

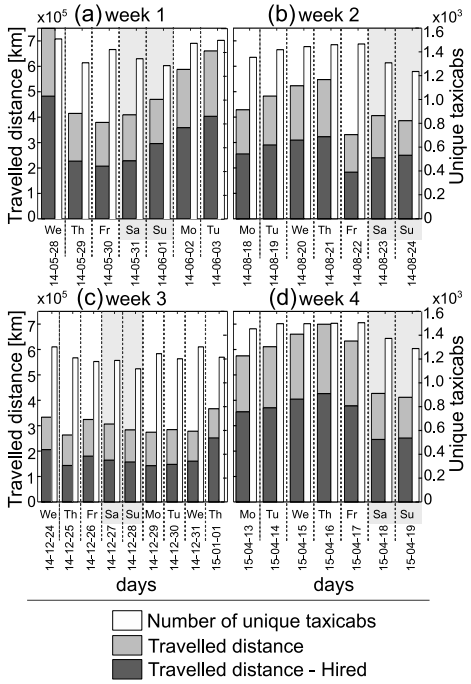

Figure 4: The travel distance, the travel distance when the taxicabs were hired, the number of unique taxicabs and dates of individual weekdays in weeks 1-4 that we selected for the case study.

discretize the time in steps of 15 minutes. Results of experiments are shown in Tables 1 - 4.

Numerical experiments were performed on the computer equipped with CPU Intel (R) Core i7-5500U CPU with two 3 GHz cores and with 8 GB RAM. Mathematical model was solved using IP-solver FICO Xpress IVE 7.3.

Based on the initial experiments we selected the folowing values of input parameters $R_{max} \in \{100, 500, 1000\}$ meters and $M_{min} \in \{100, 150, 800\}$ parking events to cover the broad range of situations. In tables we report the following output values obtained from the algorithm that is used to determine a set of candidate locations : $|I|$ is the cardinality of the set of candidate locations identified in the Phase 1, *Cars* is the number of taxicabs that are determined in the Phase 2 as the vehicles that can be served by the set of candidate locations. Optimization outputs are the following: *Stations* is the number of located charging stations, CP_{total} represents the total number of charging points in all charging stations and CP_{max} is the maximal number of charging points located in one charging station. Column *Time* contains computational time in seconds. We restricted the running time of a single experiment to 30 minutes. If the optimal solution was not found within this time limit, in the column *Gap* we report the relative gap between the upper and lower bounds of the optimal solution. In two cases the solver was not able to find any feasible integer solution within the given time limit what is indicated by the symbols '***' in the particular row of the table.

To verify the proposed approach, we visualised the resulting locations of charging stations for the scenario Week 1 and the parameter values R_{max} = 100 meters and M_{min} = 150 parking events. Results are shown in the Figure 6.

4 EVALUATION OF RESULTS AND CONCLUSIONS

In this contribution we present an initial design of the method to deploy the charging infrastructure for a fleet of electric vehicles operating in large urban areas. The operation of the fleet is described by the GPS traces characterizing the actual travel patterns of

Table 1: Results of numerical experiments for the scenario Week 1.

R_{max}	M_{min}	$Cars$	$\|I\|$	$Stations$	CP_{total}	CP_{max}	$Time[s]$	$Gap[\%]$
100	800	609	3	3	14	9	1.88	0.00
	150	1186	27	27	38	6	1800.00	5.26
	100	1287	44	44	54	6	22.10	0.00
500	800	1102	5	5	20	10	46.05	0.00
	150	1442	46	40	44	5	1800.00	2.27
	100	1475	77	51	54	4	1800.00	4.50
1000	800	1347	7	7	19	6	1800.00	21.05
	150	1499	51	39	42	3	1800.00	4.57
	100	1510	70	51	55	3	1800.00	46.90

Table 2: Results of numerical experiments for the scenario Week 2.

R_{max}	M_{min}	$Cars$	$\|I\|$	$Stations$	CP_{total}	CP_{max}	$Time[s]$	$Gap[\%]$
100	800	785	4	4	17	9	2.828	0.00
	150	1292	30	30	35	4	16.642	0.00
	100	1363	46	44	49	4	27.673	0.00
500	800	1188	5	5	18	7	1800.00	22.22
	150	1477	46	36	38	2	218.37	0.00
	100	1498	73	47	49	2	1800.00	272.97
1000	800	1409	8	8	19	5	1800.00	30.84
	150	1506	50	38	63	3	1800.00	72.03
	100	1513	69	***	***	***	***	***

Table 3: Results of numerical experiments for the scenario Week 3.

R_{max}	M_{min}	$Cars$	$\|I\|$	$Stations$	CP_{total}	CP_{max}	$Time[s]$	$Gap[\%]$
100	800	449	2	2	4	2	0.34	0.00
	150	1019	24	24	27	2	2.84	0.00
	100	1094	36	36	37	2	6.83	0.00
500	800	843	4	4	5	2	6.17	0.00
	150	1324	39	37	39	2	46.86	0.00
	100	1359	57	52	53	2	291.05	0.00
1000	800	1172	6	6	11	2	27.80	0.00
	150	1417	43	38	39	2	547.72	0.00
	100	1445	65	47	48	2	898.37	0.00

Table 4: Results of numerical experiments for the scenario Week 4.

R_{max}	M_{min}	$Cars$	$\|I\|$	$Stations$	CP_{total}	CP_{max}	$Time[s]$	$Gap[\%]$
100	800	631	3	3	17	13	7.66	0.00
	150	1221	33	33	39	7	1800.00	2.56
	100	1325	50	49	53	5	38.21	0.00
500	800	1097	5	5	19	10	1800.00	5.26
	150	1491	50	40	42	3	1800.00	2.38
	100	1515	80	56	58	3	1800.00	16.5
1000	800	1408	9	9	21	6	1800.00	18.67
	150	1525	29	27	39	7	128.50	0.00
	100	1534	74	***	***	***	***	***

individual vehicles. In the first phase we used a practical procedure to derive from data a suitable set of candidate locations for charging stations, where the outcomes can be controlled by setting a few parameter values only. In the next step, vehicles that can be served from the set of candidate locations are selected. In the second phase, we formulated a mathematical model that combines location decisions with

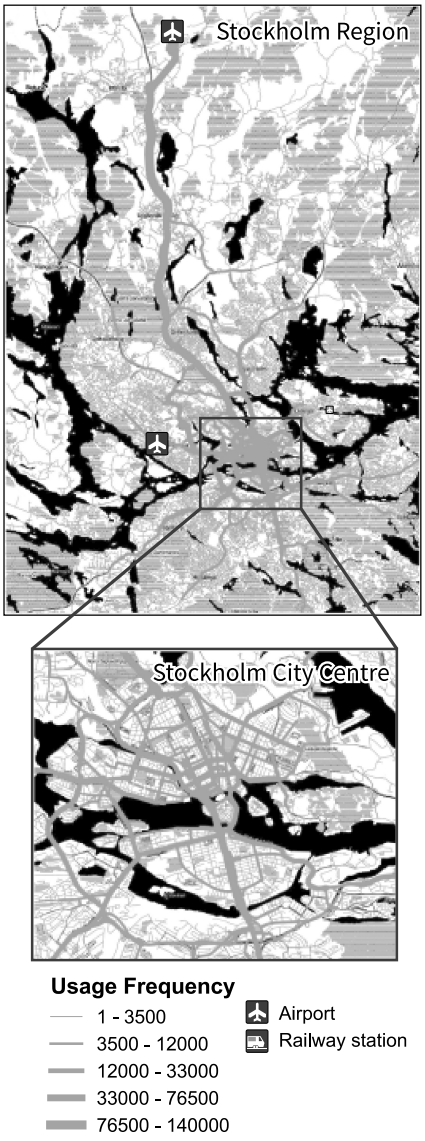

Figure 5: Visualisation of the road network considered in the case study. Thickness of each link indicates the number of traversals by the vehicles belonging to the taxicab fleet.

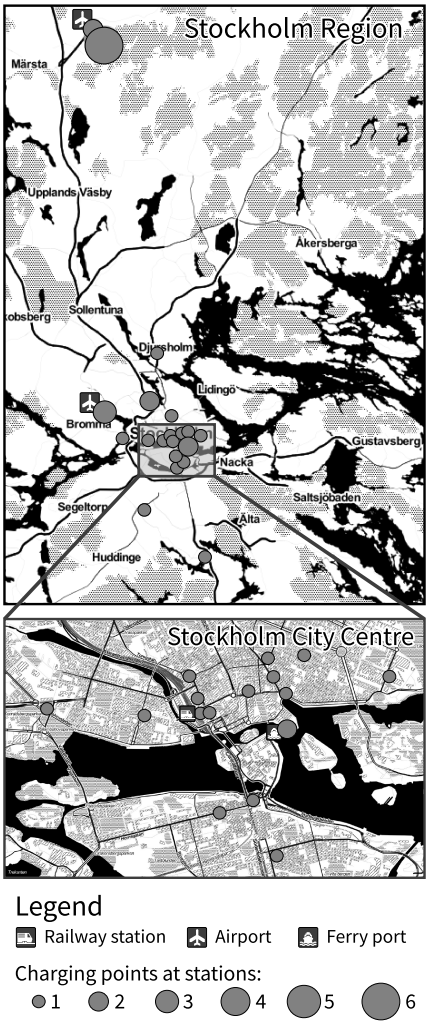

Figure 6: Locations of charging points obtained for the scenario Week 1 and the values of input parameters $R_{max} = 100$ meters and $M_{min} = 150$ parking events.

scheduling decisions to ensure that for a given design there exists a time schedule that allows satisfying requirements of all vehicles selected in the first phase. The limits of the proposed approach were tested by applying it to the real-world data characterizing the driving behaviour of a large taxicab fleet operating in the city of Stockholm. From the numerical experiments we derive the following main conclusions:

- Our results indicate that this approach can be used to estimate the minimal requirements to set up the charging infrastructure. The proposed method is able to handle relatively large instances of problems independently on the scenario. Problems with $R_{max} \in \{100, 500\}$ and $M_{min} \in \{150, 800\}$ are often solved to optimality or with small gap only.
- Charging points are typically located at parking lots in the vicinity of airports, railways stations and other public spaces, which seem to be natural locations for them.
- When comparing the results across selected scenarios we find similar numbers of located stations in weeks 1, 2 and 4 and significantly smaller number of charging points in week 3, which is the most quiet week.
- We did not limit the number of charging stations by setting the value of the parameter p. Hence, the number of charging stations was limited only by the set of candidate locations $|I|$. From the

solutions we can see that if $|I|$ is large enough, the optimization model has the tendency to select the large set of charging stations with only few charging points more frequently than locating only few charging stations with many charging points. Such design can be also favourable for the electricity network as it will not load the network largely at few locations, but the load is spatially more distributed.

- When we set the radius of charging points to $R_{max} = 1000$ meters, the number of charging opportunities gets high and the solved problem, especially during the busy weeks, becomes intractable when solved by a general purpose solver. This result indicates the limits of this methodology.

Although these initial results look promising, further steps are needed to refine the proposed approach. Considering the scheduling problem in the optimization model makes sure that there exists a time schedule to recharge all vehicles. However, this information is derived from the past data and it remains unclear how hard it is to find a feasible schedule in the system operation when the drivers do not have the prior information about the departure from the parking positions. Moreover, we assume that the parameter R_{max} determines the maximum distance the drivers accept to drive from the parking position to the closest charging station. It could be beneficial to consider more complex strategies to determine the charging station the driver decides to use. Another challenge is in combining scenarios in a way that the resulting problem can still be solved for the long enough time period and we obtain as an output the robust design of the charging infrastructure that is suitable for all considered scenarios. To overcome the limits of proposed methodology, it would be beneficial to use heuristic apporoaches to expand the size of solved problems.

ACKNOWLEDGEMENTS

This work was supported by the research grants VEGA 1/0463/16, APVV-15-0179, and it was facilitated by the FP 7 project ERAdiate [621386].

REFERENCES

Baouche, F., Billot, R., Trigui, R., and Faouzi, N. E. E. (2014). Efficient Allocation of Electric Vehicles Charging Stations: Optimization Model and Application to a Dense Urban Network. *IEEE Intelligent Transportation Systems Magazine*, 6(3):33–43.

Capar, I., Kuby, M., Leon, V. J., and Tsai, Y.-J. (2013). An arc cover–path-cover formulation and strategic analysis of alternative-fuel station locations. *European Journal of Operational Research*, 227(1):142–151.

Cavadas, J., Correia, G., and Gouveia, J. (2014). *Electric Vehicles Charging Network Planning*, pages 85–100. Springer International Publishing, Cham.

Chen, T., Kockelman, K., and Khan, M. (2013). Locating Electric Vehicle Charging Stations. *Transportation Research Record: Journal of the Transportation Research Board*, 2385:28–36.

Chung, S. H. and Kwon, C. (2015). Multi-period planning for electric car charging station locations: A case of Korean Expressways. *European Journal of Operational Research*, 242(2):677–687.

Dickerman, L. and Harrison, J. (2010). A New Car, a New Grid. *IEEE Power and Energy Magazine*, 8(2):55–61.

Dong, J., Liu, C., and Lin, Z. (2014). Charging infrastructure planning for promoting battery electric vehicles: An activity-based approach using multiday travel data. *Transportation Research Part C: Emerging Technologies*, 38:44–55.

Europen Commision (2015). Road transport: Reducing CO2 emissions from vehicles. http://ec.europa.eu/clima/policies/transport/vehicles/.

Frade, I., Ribeiro, A., Gonçalves, G., and Antunes, A. (2011). Optimal location of charging stations for electric vehicles in a neighborhood in Lisbon, Portugal. *Transportation research record: journal of the transportation research board*, (2252):91–98.

Gennaro, M. D., Paffumi, E., and Martini, G. (2015). Customer-driven design of the recharge infrastructure and Vehicle-to-Grid in urban areas: A large-scale application for electric vehicles deployment. *Energy*, 82:294–311.

Ghamami, M., Nie, Y. M., and Zockaie, A. (2016). Planning charging infrastructure for plug-in electric vehicles in city centers. *International Journal of Sustainable Transportation*, 10(4):343–353.

Jung, J., Chow, J. Y., Jayakrishnan, R., and Park, J. Y. (2014). Stochastic dynamic itinerary interception refueling location problem with queue delay for electric taxi charging stations. *Transport.Research Part C: Emerging Technologies*, 40:123–142.

Lam, A. Y. S., Leung, Y. W., and Chu, X. (2014). Electric Vehicle Charging Station Placement: Formulation, Complexity, and Solutions. *IEEE Transactions on Smart Grid*, 5(6):2846–2856.

MirHassani, S. A. and Ebrazi, R. (2013). A Flexible Reformulation of the Refueling Station Location Problem. *Transportation Science*, 47(4):617–628.

Momtazpour, M., Butler, P., Hossain, M. S., Bozchalui, M. C., Ramakrishnan, N., and Sharma, R. (2012). Coordinated Clustering Algorithms to Support Charging Infrastructure Design for Electric Vehicles. In *Proceedings of the ACM SIGKDD International Workshop on Urban Computing*, UrbComp '12, pages 126–133, New York, NY, USA. ACM.

Paffumi, E., Gennaro, M. D., Martini, G., and Scholz, H. (2015). Assessment of the potential of electric vehi-

cles and charging strategies to meet urban mobility requirements. *Transportmetrica A: Transport Science*, 11(1):22–60.

Rahmani, M. and Koutsopoulos, H. N. (2013). Path inference from sparse floating car data for urban networks. *Transportation Research Part C: Emerging Technologies*, 30:41–54.

Sears, J., Glitman, K., and Roberts, D. (2014). Forecasting demand of public electric vehicle charging infrastructure. In *Technologies for Sustainability, 2014 IEEE Conference*, pages 250–254.

Sweda, T. and Klabjan, D. (2011). An agent-based decision support system for electric vehicle charging infrastructure deployment. In *2011 IEEE Vehicle Power and Propulsion Conference*, pages 1–5.

Tu, W., Li, Q., Fang, Z., Shaw, S.-l., Zhou, B., and Chang, X. (2015). Optimizing the locations of electric taxi charging stations: A spatial–temporal demand coverage approach. *Transportation Research Part C: Emerging Technologies*, pages –.

Xi, X., Sioshansi, R., and Marano, V. (2013). Simulation–optimization model for location of a public electric vehicle charging infrastructure. *Transportation Research Part D: Transport and Environment*, 22:60–69.

Yi, Z. and Bauer, P. H. (2014). Spatio-Temporal Energy Demand Models for Electric Vehicles. In *2014 IEEE Vehicle Power and Propulsion Conference (VPPC)*, pages 1–6.

A Fuzzy Chance-constraint Programming Model for a Home Health Care Routing Problem with Fuzzy Demand

Yong Shi, Toufik Boudouh, Olivier Grunder
IRTES EA 7274, Université de Bourgogne Franche-Comté, UTBM, Rue Thierry Mieg, 90000 Belfort cedex, France
{*yong.shi, toufik.boudouh, olivier.grunder*}*@utbm.fr*

Keywords: Home Health Care, Fuzzy Chance Constraint Programming, Hybrid Genetic Algorithm, Stochastic Simulation.

Abstract: Home Health Care (HHC) companies are widespread in European countries, and aim to serve patients at home to help them recover from illness and injury in a personal environment. Since transportation costs constitute one of the largest forms of expenditure in the Home Health Care industry, it is of great significance to research the optimization of the Home Health Care logistics. This paper considers the Home Health Care Routing Problem with Fuzzy Demand, which comes from the logistics practice of the home health care company. A fuzzy chance constraint programming model is proposed based on the fuzzy credibility theory, the hybrid genetic algorithm and stochastic simulation method are integrated to solve the proposed model. Firstly the uncertain constraints have been reduced to the deterministic ones, experimental results for the benchmark test problem show the good efficiency of the proposed algorithm. Then the proposed hybrid algorithm has been applied to solve the fuzzy model, the influence of the parameters to the objective function has been discussed. This research will help HHC companies to make appropriate decisions when arranging their vehicle routes.

1 INTRODUCTION

Home health care (HHC) is a growing medical service in France and other developed countries. This service is provided by the Home Health Care companies, which aim to serve the patients at home to help them recover from illness or injury in a personal environment(Liu et al., 2014). Each day, a HHC company carries out various logistics activities including the delivery of drugs or medical instruments from the a pharmacy to patients, and pickup the biological samples from patients' home to the laboratory (Liu et al., 2013). A large number of patients distributed in a town or village, a certain quantity of the drugs needed according to the recovery degree of them. For a HHC company, the transportation cost is one of the most important spendings in the company activities, so it is of great significance to optimize the vehicle routing problem in home health care companies.

According to a survey (Mankowska et al., 2014; Harris, 2015) of the home health care companies, the main operational process of the HHC can be summarized as 3 steps.

(1) The HHC company collects the information from the patients, this information may include: the name, address, sex, type of the illness, symptom and other related information;

(2) The HHC company plan to arrange the visited routes and assign nurses according to the information collected;

(3) The nurses are scheduled to visit the patients. Each nurse is assigned to a planned route, and he/she has to carry out all of the service-related activities for the route. This nurse will drive the vehicle to visit the patients one by one according to the designed route. In case of a lack of drugs, the nurse has to go back to the depot, load more drugs into the vehicle and continue to attend to the remaining patients until all the patients are attended to.

It is easy to find that the home health care routing optimization problem is closely related the Capacitated Vehicle Routing Problem (CVRP) which is one of the most classical combinatorial optimization problems (Eksioglu et al., 2009). CVRP is a basic model in supply chain, and it has been applied into many filed. However, our problem is neither like the classical VRP nor like the Open Vehicle Routing problem (OVRP); all the variations of VRP can be seen in the literature (Pillac et al., 2013; Toth and Vigo, 2014). In the classical VRP, each vehicle needs to return to the depot again, while in the OVRP, each vehicle does not return to the depot after servicing the last customer on

Shi, Y., Boudouh, T. and Grunder, O.
A Fuzzy Chance-constraint Programming Model for a Home Health Care Routing Problem with Fuzzy Demand.
In *Proceedings of the 6th International Conference on Operations Research and Enterprise Systems (ICORES 2017)*, pages 369-376
ISBN: 978-989-758-218-9

a route, but may end at a different location.

Moreover, demand is one of the most important parameters in supply chain optimization. However in previous studies, most researchers have focused on the deterministic demand. While in the real world, it is usually very hard to determine the precise demands of customers and thus they are estimated from historical data. Given this aspect of VRPs, a consideration of stochastic vehicle routing problems (SVRP) and fuzzy vehicle routing problems (FVRP) may be useful (Wen and Iwamura, 2008). In the Vehicle Routing Problem with Stochastic Demand (Bianchi et al., 2006), the demand is a stochastic variable, which is decided by probability distribution parameters, but the parameters are often obtained from the historical data. However sometimes, we could not obtain enough historical data for the new customers or patients. Although stochastic models can cater for a variety of cases, they are not sufficient to describe many other situations, where the probability distribution of customers demands may be unknown or partially known (Wen and Iwamura, 2008). On the contrary, fuzzy language exists everywhere in the health care domain, such as a doctor may inform us "small penicillin", or "you have a little fever ". So, it is very appropriate to describe the non-deterministic demand in HHC domain using fuzzy variables.

This paper contributes to the home health care routing optimization with fuzzy demand in the following aspects: (1) a fuzzy chance constraint programing model is proposed based on the fuzzy credibility theory; (2) hybrid genetic algorithm and stochastic simulation are integrated to solve the proposed model; (3) Some experiments are carried out on the deterministic model to validate the efficiency of the proposed method, and then the heuristic method has been employed to solve the fuzzy model. The rest of this paper is organized as follows: in second section some necessary theory of credibility is introduced, then the home health care problem with fuzzy demand model is constructed, and a hybrid heuristic algorithm is proposed to solve the model, at last some experiments are presented to illustrate the algorithm.

2 SUPPLY CHAIN MODELING

2.1 The Description of Fuzzy Demand Constraints

Liu (Liu et al., 2003) recently developed credibility theory, which can be used to measure the chance of that a fuzzy chance occurs. The law of credibility in the theory of fuzzy sets plays a role similar to that played by the law of probability in measurement theory of the ordinary sets. In this section we will first introduce the credibility theory (Liu et al., 2003), because it is crucial to describe the fuzzy demand.

In the deterministic VRP, it is straightforward to describe the capacity constraints: the total demand of the whole route should not exceed the vehicle capacity. However, in the VRPFD, the capacity constraints become more complex than the deterministic ones for the uncertain demand. Now, we have to consider the relationship between the fuzzy demand and the capacity of the vehicle (Mousavi and Niaki, 2013).

For a vehicle, after serving the j th patient, the remaining capacity is changed and it becomes a fuzzy variable named $\widetilde{Q_j}$, where

$$\begin{aligned}\widetilde{Q_j} &= q-\sum_{i=1}^{j}\widetilde{d_i}\\ &= (q-\sum_{i=1}^{j}d_{3,i}, q-\sum_{i=1}^{j}d_{2,i}, q-\sum_{i=1}^{j}d_{1,i})\\ &= (Q_{1,j}, Q_{2,j}, Q_{3,j})\end{aligned}$$

In the deterministic model, if the remaining capacity of the vehicle is greater than a customer's demand, this vehicle has the chance to serve this customer. However, facing with a fuzzy variable of demand and remaining capacity, how can we make a decision that whether the vehicle should continue visiting the $(j+1)$th patient or go to the lab directly? It should be compared with the demand of the $(j+1)$ th patient, of course, which is also a fuzzy variable. Based the credibility we can derive equation (1) and equation (2) as follows:

$$\begin{aligned}Cr &= Cr\{\tilde{d}_{j+1}\le\tilde{Q}_j\}\\ &= Cr\{(d_{1,j+1}-Q_{3,j}, d_{2,j+1}-Q_{2,k}, d_{3,k+1}-Q_{1,j})\le 0\};\end{aligned} \tag{1}$$

$$Cr = Cr\{\tilde{d}_{j+1}\le\tilde{Q}_j\} = \begin{cases} 0, & d_{1,j+1}\ge Q_{3,j}\\ \frac{Q_{3,j}-d_{1,j+1}}{2(Q_{3,j}-d_{1,j+1}+d_{2,j+1}-Q_{2,j})}, & d_{1,j+1}\le Q_{3,j}, d_{2,j+1}\ge Q_{2,j}\\ \frac{d_{3,j+1}-Q_{1,j}-2(d_{2,j+1}-Q_{2,j})}{2(Q_{2,j}-d_{2,j+1}+d_{3,j+1}-Q_{1,j})}, & d_{2,j+1}\le p_{2,j}, d_{3,j+1}\ge Q_{1,j}\\ 1 & d_{3,j+1}\le Q_{1,j}\end{cases} \tag{2}$$

There is no doubt that if the quantity of remaining drugs is very high, and the demand of the next patient is very low, then the chance of the vehicle of being able to provide the next patient's service becomes greater (Cao and Lai, 2010).

We will describe the preference index by Cr, which denotes the magnitude of our preference to drive the vehicle to the next patient after it has served the current patient according to formulation (2). Note that Cr $\in$[0, 1]. When $Cr = 0$, we declare that the vehicle does not have the capacity to serve the next patient and it should terminate service at the current patient and return to the depot to replenish drugs. When $Cr = 1$, we can be completely sure that the vehicle should serve the next patient. However, in most cases, Cr is neither 0 nor 1, but $Cr \in (0,1)$.

To describe Cr in a convenient way, let us introduce the dispatcher preference index DPI, where $DPI \in [0,1]$. Note that DPI expresses the dispatcher's attitude toward risk. When the dispatcher is not a risk-averse, he/she will choose lower values of parameter DPI, which indicates that the dispatcher prefers to use the vehicle available capacity as much as possible, although there is an increase in the number of cases in which the vehicle arrives at the next customer's home and is not able to carry out planned service due to small available capacity. On the other hand, when the dispatcher is a risk-averse, he will choose greater DPI, this may result in a less complete utilization of vehicle capacity along the planned routes and less additional distance to cover due to failures

2.2 Mathematical Model

In order to describe the supply chain by formulation, we give the assumption as follows.
(1)The vehicles are homogeneous.
(2)Each nurse responds for one route. In the process of delivery, if the remaining drugs is not enough for the patients, she must drive back and fill up the drugs, return to this patient, then she will continue visiting the remaining patients until all the patients she responds are served.
(3)Each vehicle starts from the depot, then visits and attends to patients, and terminates the journey at the laboratory.
(4)we assume that the drugs have their own volume, so the vehicle capacity must be taken into consideration. However, the samples are vials of blood, or temperature record sheets, which could be assumed to be negligible and will not be considered with respect to the capacity of the vehicle.
(5)In the process of delivery, the demand of the drugs is described by fuzzy triangle variable. Only if the nurse arrives the patient's home, can she know the exact quantity of the drugs.

Now, we give the mathematical notations as follows:
V: the set of the vehicles.
N: the set of the all the vertex in the graph, including the depot, patients,and laboratory.
$\tilde{d}_i = (d_{1,i}, d_{2,i}, d_{3,i})$: the fuzzy demand of the patient i;
C: the set of the patients.
$i, j = 0, 1, 2, \ldots, n+1$ is the index of the all the nodes in the graph. Especially 0 stands for the index of the depot, $n+1$ stands for the index of lab, and others are the patients.
$k = 1, 2, \ldots, K$ stands for the index of the vehicle.
q: the capacity of the vehicle.
p: the employee salary for every nurse in this task.
u_i: it is an artificial variable which is used to construct the sub-tour constraint.
f_1: the additional distance caused by failure route.

let us describe the mathematical model with the most common used 3-index method:

$$x_{ijk} = \begin{cases} 1 & \text{if the } k\text{th vehicle traveals from patient } i \text{ to patient } j; \\ 0 & \text{otherwise.} \end{cases}$$

The Home Health Care Routing Problem with Fuzzy Demand (HHCRPFD) model can be mathematically formulated as shown below:

$$\min f = \sum_{i\in V} p \sum_{i\in C} \sum_{j\in N} x_{ijk} + \sum_{k\in V} \sum_{i\in N} \sum_{j\in N} c_{ij} x_{ijk} + f_1 \quad (3)$$

subject to,

$$\sum_{k\in V} \sum_{j\in N} x_{ijk} = 1 \quad \forall i \in C \quad (4)$$

$$\mathrm{Cr}\Big(\sum_{i\in C} \tilde{d}_i \sum_{j\in N} x_{ijk} - q \geq 0\Big) \geq DPI \quad \forall k \in V \quad (5)$$

$$\sum_{j\in N} x_{0jk} = 1, \quad \forall k \in V \quad (6)$$

$$\sum_{i\in N} x_{ihk} - \sum_{j\in N} x_{hjk} = 0, \quad \forall h \in C, \forall k \in V \quad (7)$$

$$\sum_{i\in N} x_{i(n+1)k} = 1, \quad \forall k \in V \quad (8)$$

$$x_{ijk} \in \{0,1\}, \forall i, j \in N, \forall k \in V \quad (9)$$

$$u_i - u_j + q * \sum_{k=1}^{K} x_{ijk} \leq q - d_{1,j}, \forall i, j = 0, 1, \ldots, N+1, i \neq j; \quad (10)$$

The objective function (3) is to minimize the total cost which includes the nurse employee cost, planned transportation cost and the additional cost. The constraints (4) donate that each customer is visited once and only once, and constraints(5) mean that no vehicle is loaded with more than its capacity under the fuzzy credibility theory. The constraints (6) mean each vehicle starts from the depot. Constraints (7)mean that each vehicle visits the patient and then

leaves the patient. Constraints (8) means that the vehicle ends at the laboratory. Constraints (9) make the decision-variable are binary. Constraints (10) are used to eliminate sub-tours.

Our problem is neither like the classical VRP nor like the Open Vehicle Routing problem (OVRP); all the variations of VRP can be seen in the literature (Pillac et al., 2013; Toth and Vigo, 2014). In the classical VRP, each vehicle needs to return to the depot again, while in the OVRP, each vehicle does not return to the depot after servicing the last customer on a route, but may end at a different location.

Remark 1: The mathematical is a typical Fuzzy Chance Constraint Programming(FCCP), which is a new branch in the uncertain programming. What's more, if we assume $d_{1,i} = d_{2,i} = d_{3,i}$, the fuzzy variable become a determinate variable, and the HHCRPFD is reduced to a vehicle routing problem. Considering that VRP has been proved to be the np-hard problem, so there is no wonder that our model is also a np-hard problem with fuzzy chance constraints.

Remark 2: If $d_{1,i} = d_{2,i} = d_{3,i}$, this problem becomes a deterministic model, and in this situation, the additional distance $f_1 = 0$.

3 HYBRID HEURISTIC ALGORITHM

As mentioned above, the proposed model is a NP-hard problem, which is difficult to solve by the exact method when the size of the problem becomes large. Here, we propose a hybrid heuristic algorithm (HHA) by integrating the stochastic simulation method and hybrid genetic algorithm. Generally speaking, in the first stage, we apply the route construction method to generate initial feasible solutions, then hybrid genetic algorithm is employed to improve the initial solution. To accelerate the convergence, elitism selection and local search are employed, while to make the solution escape from the local optima in advance, mutation operators and crossover operators are designed. Considering that our problem is an instance of Fuzzy Chance Constraint Programming (FCCP), Stochastic Simulation method is designed to evaluate the each solution candidate.

The detailed description of the HHA can are described in the rest part of this section.

3.1 Individual Representation

In our research, each individual stands for feasible solution, which is a vehicle routing arrangement. Here we use a List to encode an individual which contains a lot of routes. The process of the encoding and decoding can be seen in Figure 1. The strength of this encode method is that each individual does not need to be decoded and encoded alternately in the optimization process.

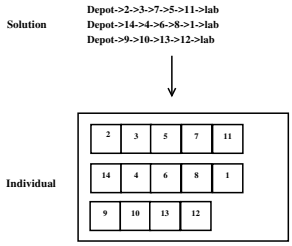

Figure 1: The representation of a individual.

3.2 Initial Population

The initial population are composed by two kinds, most of them are ordinary individuals which are generate randomly, the rest are high-quality ones which are obtained from the classical heuristic algorithm called insertion.

Insertion heuristic are widely used to quickly construct a feasible solution (Toth and Vigo, 2014). In each iteration, a node is selected among all the unvisited nodes, and then insert it in a right position which makes the new route feasible and least cost, while a insertion position couldn't be found, a new route is started. This insertion process repeated until all the nodes are visited. Figure 2 illustrates the insertion of the node k between i and j with the corresponding insertion cost $c_{ik} + c_{kj} - c_{ij}$.

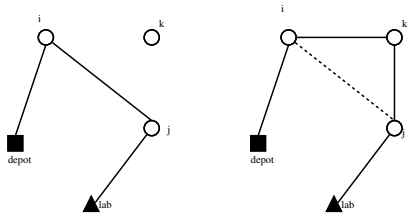

Figure 2: The brief description of the insert method.

3.3 Fitness Evaluation

As mentioned above, the demand of drugs for each patient is a triangular fuzzy number, so it cannot be directly considered as a deterministic one.

Regarding the simulation of the phases of the operation process of the HHC company and related works, we derive an approximate estimate about additional distances (f_1) due to route failures using a stochastic simulation algorithm. We summarize the stochastic simulation (Cao and Lai, 2010) as follows:

Step 1: For each patient, estimate the additional distance by simulating "actual" demand. The "actual" demands were generated by the following process:

(1) randomly generate a real number of x in the interval between the left and right boundaries of the triangular fuzzy number representing demand at the patient, and compute its membership u.

(2) generate a random number a, $a \in [0,1]$;

(3) compare a with u, if $a \leq u$, then "actual" demand at the patient is adopted as being equal to x; in the opposite case, if $a < u$, it is not accepted that demand at the patient equals x. In this case, random numbers x and a are generated again and again until random number x and a are found that satisfy relation $a \leq u$;

(4) check and repeat (1)–(3), and terminate the process when each patient has a simulation "actual" demand quantity.

Step 2: Move along the route designed by credibility theory and accumulate the amounts picked up and calculate the additional distance due to routes failure in terms of the "actual " demand..

Step 3: Repeat Step 1 and Step 2 for M times.

Step 4: Compute the average value of additional distance by M times simulation, and it is regarded as the additional distance f_1.

In the fuzzy demand model, the objective is to minimize the total cost, so the fitness value here we choose to use $f = \frac{1}{AD+PD}$. Specially, if $d_{1,i} = d_{2,i} = d_{3,i}$,this problem becomes a determinate model, and in this situation, the additional distance $f_1 = 0$, the fitness can be described as $f = \frac{1}{PD}$

3.4 Selection

In the evolution process, sometimes the good individuals may lost due to the crossover and mutation, which is not favorable to the convergence of fitness value. To overcome this drawback, we employ the famous elitism strategy in the selection operator.

Here we pick out the top 2% individuals as elite which are retained to the next generation directly without taking part in the crossover, mutation and local search operator.

3.5 Crossover

Crossover provides a chance to enhance the communication between different individuals, and aims to reproduce new offspring. Ombuki proposed a effective crossover operator named Best Cost Route Crossover (BCRC) (Ombuki et al., 2006), the main idea is to select nodes from one sub-route, and find a best position to reinsert them into the other individual one by one. We can call this operator as a global version of BCRC. Although his operator can perform well, it takes a long time to find the best position of whole the potential position. Inspired by his research, we proposed a local version of BCRC. we insert each node to the best position of a randomly selected route of the individual. It is obviously that the local version saves a lot of computing time.

The main steps of the crossover operator an be found in Figure 3.

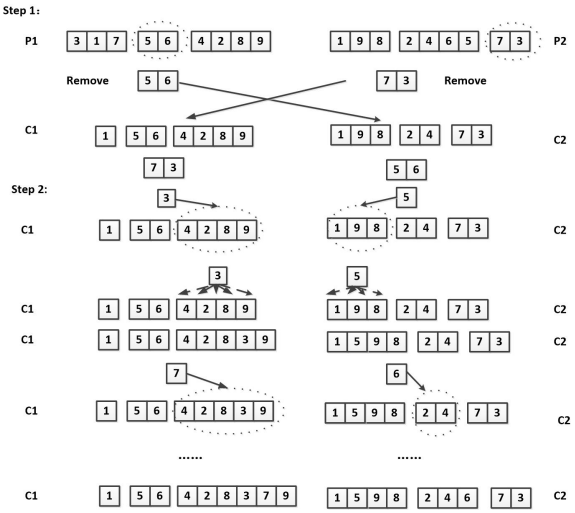

Figure 3: the crossover operator.

Specifically, for two individuals, the crossover is undertaken as follows:

Step 1: For each individual, a route is selected randomly. Before inserting the route into the other individual, the repeating nodes would be removed.

Step 2: The nodes selected from P1 (P2) are inserted in to P2 (P1) one by one. Be attention that, for the insertion of one node, one route is selected randomly. The length of this route is m, and the possible position for insertion is $m+1$, and this node is inserted to the best position. This insertion is undertake until all the selected nodes are inserted to the other individual. while a insertion position could not be found, a new route is started.

3.6 Mutation

Mutation is a divergence operation. It is intended to occasionally break one or more members of a popu-

lation out of a local minimum space and potentially discover a better minimum space. The mutation operator is conducted by bring random, unrelated traits into the present population and increase the variance of the population. According to the characteristic of individuals, two simple mutation operators are introduced in our algorithm.

- inversion: two cut points are generated randomly, and all the nodes between them will be inversed.
- single-point mutation: two nodes are randomly generated, then they are swapped.

3.7 Local Search

In this paper, local search operator is employed to improve the fitness value of the individuals and obtain better solutions. The most commonly-used 2-opt method, or-opt method and their extension (Bräysy and Gendreau, 2005) are used to search the better solution.

Note that the local search operators are quite not the same with the mutation operator in two aspects: (1) the aim of the local search operator is to make an improvement of the solution, while the mutation is just to make the population diversified which aims to avoid the trapping into local optimal in advance. (2) The mutation operator is executed just once in one iteration, while the local search operators are executed many times, until a solution deemed optimal is found or a time bound is elapsed.

4 EXPERIMENTAL RESULTS

Because there was no one does the same work with us, so it can not compare our work with the exist work directly to validate the efficiency of the proposed Hybrid Heuristic Algorithm (HHA). Here, we firstly reduced our problem into the classical CVRP, experimental results are compared with the optimal results. After ensuring the algorithm is effective, we will use it to solve the proposed fuzzy model. Here we need to emphasize that the aim of our research is not to design a new and efficient algorithm to solve the classical CVRP, but just to design an efficient algorithm to solve the fuzzy model.

4.1 Experiments on Determinate Model

The fuzzy model is reduced to CVRP, if we assume the following 3 points: (1) the fuzzy variables reduce to the deterministic ones, namely $d_{i,1} = di, 2 = d_{i,3}, i = 1,2,\ldots,N$; (2) the laboratory is in the same position with the depot. (3) the cost for each nurse is 0. In this situation, the fuzzy chance constraints become the deterministic ones, additional distance become 0.

Note that, when we apply the HHA to solve the deterministic model, for there is no chance constraints, the additional cost is 0. And in the process of fitness evaluation, stochastic simulation doesn't used.

Here we use one of the most famous benchmark instances called A series to test the proposed HHA. The instances and the optimal result can not be downloaded from the website http://neo.lcc.uma.es/vrp/vrp-instances/, and our computing results and the comparison can be found in Table 1.

Note that, in Table 1, NO means the ID of the instance,and the name of instance is composed in 3 parts: for example, the instance named "A-n60-k9", "A" means the instance is from A-series, "n60" means the size of the nodes is 60, and "k9" means that the number of expected used vehicle is 9. As results show, TD means the total distance (also called total cost in some literature), NV means the number of the used vehicles, CT means the computing time, and GAP means the percentage of the error between our result and the optimal result (Juan et al., 2010; MirHassani and Abolghasemi, 2011).

Table 1: Experimental results for the CVRP model.

	HGA			optimal result		GAP
No.	NV	TD	CT(s)	NV	TD	
A-n32-k5	5	787.20	10.54	5	784.00	0.41%
A-n33-k5	5	688.11	10.34	5	661.00	4.10%
A-n33-k6	6	745.80	9.56	6	742.00	0.51%
A-n34-k5	5	794.64	10.39	5	778.00	2.14%
A-n36-k5	5	819.93	11.34	5	799.00	2.62%
A-n37-k5	5	673.50	11.98	5	669.00	0.67%
A-n37-k6	6	961.68	19.77	6	949.00	1.34%
A-n38-k5	5	761.40	21.73	5	730.00	4.30%
A-n38-k5	5	845.00	19.84	5	822.00	2.80%
A-n45-k7	7	1216.56	20.47	7	1146.00	6.16%
A-n60-k9	9	1437.48	17.17	9	1408.00	2.09%
B-n31-k5	5	680.96	10.31	5	672.00	1.33%
B-n41-k6	6	875.31	11.02	6	829.00	5.59%
B-n50-k8	8	1373.56	12.09	8	1313.00	4.61%
B-n63-k10	10	1627.00	55.61	10	1537.00	5.86%
B-n78-k10	10	1305.00	66.50	10	1266.00	3.08%

We can conclude that: (1) the number of used vehicle in our results are quite the same with the expected number; (2) our result is quite close to the optimal solution; (3) our result arrives convergence in a reasonable time even for the big size instance, considering that CVRP is a NP-hard problem. So there is no doubt that the proposed hybrid algorithm have a good performance in solving the CVRP, and we will apply our heuristic algorithm to the fuzzy chance constraint programming in the next subsection.

4.2 Experiments on the Fuzzy Model

In this part, the experiments will be taken on the fuzzy model. Because there is no corresponding benchmark for this problem, we adopted the instance from the exited instance named A-n32-k5, which is a small size instance. The hybrid heuristic algorithm is encoded in Matlab 2015b; in the process of computing the fitness value, the stochastic simulation for every individual is 500 times.

The Value for the Dispatcher's Preference Index (DPI) varied with the interval of 0.1 to 1 with the step of 0.1. The computing results can be seen in Table 2 , Figure 4 and Figure 5.

Table 2: Experimental results for HHCRPFD model.

DPI	NV	TD	PD	AD
0.1	4	969.17	794.25	174.91
0.2	5	968.11	836.88	131.23
0.3	5	998.85	859.09	139.76
0.4	5	973.45	842.37	131.08
0.5	5	967.03	850.38	116.65
0.6	6	936.16	906.71	29.45
0.7	6	946.87	932.58	14.28
0.8	7	1063.27	1063.27	0.00
0.9	8	1163.66	1163.66	0.00
1	8	1203.94	1203.94	0.00

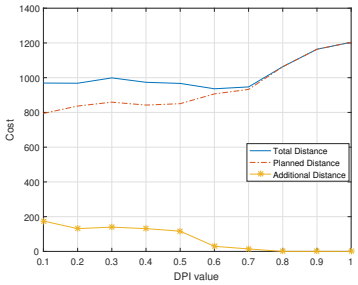

Figure 4: Cost changes for different *DPI* values.

We can find that, as *DPI* rose, the planned distance is increasing. While the additional distance is strictly decreasing as *DPI* value increases from 0 to 0.7. However, when $DPI \in [0.7, 1]$, the additional distance becomes 0, that means there's no failure route. The total distance is increasing, but not in a very strict tendency. We can also find that, with the *DPI* rose, the number of the needed nurses are increasing. It concludes that more used nurses can help to decrease the degree of the failure route.

As a consequence, lower values of parameter *DPI* express our desire to use vehicle capacity the best we can, so less nurses are needed. These values correspond to routes with shorter planned distances. On the other hand, lower values of parameter *DPI* increase the number of cases in which vehicles arrive

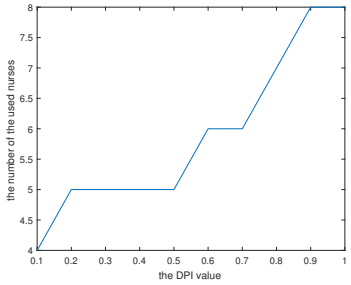

Figure 5: Number of the needed nurses changes for different *DPI* values.

at a customer and are unable to service it, thereby increasing the total additional distance they cover due to the "failure". Higher values of parameter *DPI* are characterized by less utilization of vehicle capacity along the planned routes and less additional distance to cover due to failures, so more nurses are needed. Therefore,when a HHC company makes decision on this scenes (instance), the selected dispatcher preference index should be 0.7 approximate.

5 CONCLUSIONS

Since transportation costs constitute one of the largest forms of expenditure in the Home Health Care industry, it is of great significance to research the optimization of the Home Health Care logistics. Based on a survey of the Home Health Care companies, the basic operational process illustrates that the demand for the required drugs for each patient is nondeterministic when the HHC company makes a decision to arrange the vehicle routing. In this paper, vehicle routing problem with fuzzy demand is considered, and a fuzzy chance constraint is constructed based on the fuzzy credibility theory. Stochastic simulation method and hybrid genetic algorithm are integrated to solve the proposed model.

In order to test the proposed model and algorithm, the fuzzy chance constraints were reduced to the deterministic ones. Hybrid heuristic algorithm were applied to solve the benchmark instances, results show that the proposed hybrid heuristic algorithm perform well. Then the algorithms are applied to the HHCRPFD, the best Dispatcher's Preference Index (DPI) is obtained, and the influence of the parameters to the objective functions are analyzed.

In the future, we will consider some other uncertain information in the routing optimization problem, such as stochastic traveling time, or fuzzy traveling time. Some other heuristic method like Simulated annealing (SA), Tabu search (TS), will also be integrated to solve the related problems.

REFERENCES

Bianchi, L., Birattari, M., Chiarandini, M., Manfrin, M., Mastrolilli, M., Paquete, L., Rossi-Doria, O., and Schiavinotto, T. (2006). Hybrid metaheuristics for the vehicle routing problem with stochastic demands. *Journal of Mathematical Modelling and Algorithms*, 5(1):91–110.

Bräysy, O. and Gendreau, M. (2005). Vehicle routing problem with time windows, part ii: Metaheuristics. *Transportation science*, 39(1):119–139.

Cao, E. and Lai, M. (2010). The open vehicle routing problem with fuzzy demands. *Expert Systems with Applications*, 37(3):2405–2411.

Eksioglu, B., Vural, A. V., and Reisman, A. (2009). The vehicle routing problem: A taxonomic review. *Computers & Industrial Engineering*, 57(4):1472–1483.

Harris, M. D. (2015). *Handbook of home health care administration*. Jones & Bartlett Publishers.

Juan, A. A., Faulin, J., Ruiz, R., Barrios, B., and Caballé, S. (2010). The sr-gcws hybrid algorithm for solving the capacitated vehicle routing problem. *Applied Soft Computing*, 10(1):215–224.

Liu, B., Zhao, R., and Wang, G. (2003). *Uncertain programming with applications*.

Liu, R., Xie, X., Augusto, V., and Rodriguez, C. (2013). Heuristic algorithms for a vehicle routing problem with simultaneous delivery and pickup and time windows in home health care. *European Journal of Operational Research*, 230(3):475–486.

Liu, R., Xie, X., and Garaix, T. (2014). Hybridization of tabu search with feasible and infeasible local searches for periodic home health care logistics. *Omega*, 47:17–32.

Mankowska, D. S., Meisel, F., and Bierwirth, C. (2014). The home health care routing and scheduling problem with interdependent services. *Health care management science*, 17(1):15–30.

MirHassani, S. and Abolghasemi, N. (2011). A particle swarm optimization algorithm for open vehicle routing problem. *Expert Systems with Applications*, 38(9):11547–11551.

Mousavi, S. M. and Niaki, S. T. A. (2013). Capacitated location allocation problem with stochastic location and fuzzy demand: a hybrid algorithm. *Applied Mathematical Modelling*, 37(7):5109–5119.

Ombuki, B., Ross, B. J., and Hanshar, F. (2006). Multi-objective genetic algorithms for vehicle routing problem with time windows. *Applied Intelligence*, 24(1):17–30.

Pillac, V., Gendreau, M., Guéret, C., and Medaglia, A. L. (2013). A review of dynamic vehicle routing problems. *European Journal of Operational Research*, 225(1):1–11.

Toth, P. and Vigo, D. (2014). *Vehicle routing: problems, methods, and applications*, volume 18. Siam.

Wen, M. and Iwamura, K. (2008). Fuzzy facility location-allocation problem under the hurwicz criterion. *European journal of operational research*, 184(2):627–635.

Assessment of Relative Technical Efficiency of Small Mental Health Areas in Bizkaia (Basque Country, Spain)

Nerea Almeda[1], Carlos García-Alonso[2], José Alberto Salinas-Pérez[2], Mencía R. Gutiérrez-Colosía[1] and Luis Salvador-Carulla[3]

[1]*Universidad Loyola Andalucía, Department of Psychology, Seville, Spain*
[2]*Universidad Loyola Andalucía, Department of Quantitative Methods, Seville, Spain*
[3]*University of Sydney, Mental Health Policy Unit, Brain & Mind Research Institute, Sydney, Australia*
{nmalmeda, cgarcia}@uloyola.es

Keywords: Relative Technical Efficiency, Monte-Carlo DEA, Simulation, Data Envelopment Analysis, Expert Knowledge, Decision Support Systems, Operation Research in Health, Small Mental Health Areas.

Abstract: Mental disorders cause an enormous burden to society. Considering the current economic context, an efficient use of scarce inputs, with an appropriate outcome production, is crucial. This situation defines a classical Relative Technical Efficiency (RTE) problem. A well-known methodology to assess RTE is the Data Envelopment Analysis, although it presents some limitations. These may be overcome through a hybrid strategy that integrates Monte-Carlo simulation and artificial intelligence. This study aims to (1) design of a Decision Support System for the assessment of RTE of Small Mental Health Areas based on DEA; and (2) analyse 19 mental health areas of the Bizkaian Healthcare System (Spain) to classify them and to identify potential management improvements. The results have showed higher global RTE in the output-oriented orientation than in the input-oriented one. This suggests that a decision strategy based on improving the input management, within the ranges of the expert-driven model of community healthcare, could be appropriate. A future research line will focus our attention on the validation process through the analysis of micro-management interventions and their potential impacts in the real system.

1 INTRODUCTION

The current high levels of mental disorders prevalence cause an enormous burden to the society and a devastating impact on health and economy (WHO, 2003). The factors involved in the development of these psychopathologies are not only individual features; social, economic and political determinants, such as national policies and community support, have also a relevant influence in the manifestation of the symptomatology (WHO, 2016).Unfortunately, in high-income countries, 35%-50% of people who suffer mental disorders do not receive any treatment; in middle and low-income countries, this percentage increases till 76%-85% (WHO, 2016).

To face this problem, the World Health Organization (WHO) and United Nations (UN) are carrying out specific macro-level strategies. Firstly, the WHO designed a 'Mental Health Action Plan 2013-2020' (WHO, 2013), in which was emphasized the importance of assessing the evidence and developing a deeper research. In addition, this action plan highlighted the provision of health and social care from a community-based perspective. On the other hand, the UN is also supporting the shifting of mental health treatments from hospital to community-based care (United Nations, 1991). The community-based mental health care is focused on caring for individuals with mental illness from institutional environments to the community (Moran & Jacobs, 2013; Shen & Snowden, 2014). This paradigm of intervention presents better outcomes and is more cost-effective than institution-based care (Gutierrez-Recacha, Chisholm, Haro, Salvador-Carulla & Ayuso-Mateos, 2006; WHO, 2005;). According to this model, an increase in outpatient and day care services and a decrease in inpatient services is expected. Therefore, the integration of care and treatment in general hospitals and primary care as well as the collaboration between professionals and informal care providers is fundamental.

In Spain, both the Mental Health Strategy of the Spanish National Health System (Ministerio de

Almeda, N., García-Alonso, C., Salinas-Pérez, J., Gutiérrez-Colosía, M. and Salvador-Carulla, L.
Assessment of Relative Technical Efficiency of Small Mental Health Areas in Bizkaia (Basque Country, Spain).
In *Proceedings of the 6th International Conference on Operations Research and Enterprise Systems (ICORES 2017)*, pages 377-384
ISBN: 978-989-758-218-9

Sanidad, Política e Igualdad, 2011) and the 'Strategy for tackling the challenge of chronic illness in the Basque Country' (Gobierno Vasco, 2011) are now being developed, among others, for handling chronical diseases. The main goals of these strategies and policies are the promotion of mental health, the provision of care, the enhancement of the recovery and the reduction of morbidity and disability.

Regarding economics issues, even though a political responsiveness to burden of mental disorders is consolidated, the amount of resources destined to mental health care depends on the "health" of the economy (Shen & Snowden, 2014). Public mental health services are highly vulnerable to resources constraints in compromising economic situations (Shen & Snowden, 2014). In Spain (2010), according to the Organization for Economic Cooperation and Development (OECD), 9% of the Gross Domestic Product (GPD) was destined to expenditures on health (OECD, 2010). Mental disorders absorbed an expense of 46 billion euros (Parés-Badel el al., 2014). Taking into account the relevance their increasing prevalence and the involved amount of public resources, always scarce, an efficient mental health care system is absolutely crucial in the present economic situation.

Research and empirical evidences are decisive elements for designing suitable mental health policies and, in consequence, improving quality of care. Identification and assessment of potential improvements in the system can be used in designing of new strategies for enhancing efficiency scores of mental health services in real contexts. Policy makers' decisions are usually based on their clinic experience and thus the decisional risk is pretty high taking into account the high uncertainty level: inner and systemic. In the current economic situation, risks could be reduced using Decision Support Systems. These tools can help decision makers to have a better understanding of mental health services performance in a real, dynamic and uncertain context. The lack of previous information and empirical evidence about the potential trade-offs (costs and outcomes) between different policy options, severely affects the selection of the most "suitable" decision in a specific management situation: the "what could or should happen if… problem".

The maintenance of the essential balance between the quality of public mental health services and their financial sustainability is the next challenge. This not necessary means that a mental health system should maximize its outcomes while maintaining the amount of the consumed resources or, sometimes even worst, reducing them. The key question is the optimization of the balance between inputs and outputs in a complex, interrelated and dynamic system under uncertainty. Sherman (1984) introduced Data Envelopment Analysis (DEA) for assessing hospital Relative Technical Efficiency (RTE). Nowadays, there is a growing interest in the evaluation of RTE in health systems (Färe, Grosskopf, Lundström & Roos, 2008; Hollingsworth, 2008; Hollingsworth & Parkin, 2001; Kaya & Cafrı, 2015; Pelone et al., 2012;), but little is known about it in mental health (Torres-Jiménez et al., 2015; Tyler, Ozcan & Wogen, 1995;). Although DEA models have been successfully applied in health, several relevant drawbacks of this analysis have been identified in the literature (Salvador-Carulla et al., 2007; Zhu, 2013): (i) frequently decision makers have difficulties in interpreting DEA results, (ii) DEA models are not appropriate for analysing datasets with low number of decision making units (observations) and high number of inputs (usually resources) and outputs (outcomes of the system), (iii) the management of the inner uncertainty of the real systems is statistically complicated (Monte-Carlo simulation) and very computer demanding and, finally, (iv) real data values (inputs and outputs) have to be interpreted according to expert knowledge for avoiding biased results (this process needs to formalise explicit knowledge in a knowledge-base).

The main goals of the current research are: 1. The design of a Decision Support System for the assessment of RTE of Small Mental Health Areas based on DEA; and 2. The analysis of 19 mental health areas of the Bizkaia (Spain) Healthcare System for identifying potential performance improvements.

2 METHODS

2.1 Inputs, Outputs and Decision-making Units

Original data were collected from "Mental Health Atlas of Bizkaia" (Pereira, Gutiérrez-Colosía & Salinas-Pérez, 2013). In total, the dataset included 52 variables, 39 inputs and 13 outputs, which described the Mental Health Care System in Bizkaia (Spain). This system is structured in 19 Small Health Care Areas that were identified as Decision Making Units (DMU) (19×52 data matrix). The variables were coded into main types of care (Table 1) according to the DESDE-LTC codification system (Salvador-Carulla et al., 2011) and each code was classified based on the Basic-Mental Health Community Care (B-MHCC) paradigm (Salvador-Carulla et al., 2007)

in the following variable groups: service availability, amount of places or beds, amount of professionals and service utilization. Variable values were transformed into rates per 100,000 population. Health planers and policymakers validated the variable (inputs and outputs) set (Table 1).

In order to assess the RTE of the selected areas, 15 scenarios were designed. Each scenario is a set of variables (a meaningful combination of inputs and outputs), which describes a specific type of care or a combination of them selected by experts in mental health care (Table 2). Thus, these scenarios allow to study different perspectives of the management and evolution of the system. By integrating the proposed scenarios, the Decision Support System offers both the RTE for any area in each scenario as well as the global RTE of the system.

Table 1: List of inputs/outputs analyzed for each group of main types of care (DESDE-LTC) and scenario assigned.

Main types of care DESDE-LTC codes in brackets	**Inputs** Scenario number in superscript		**Outputs** Scenario number in superscript
Residential care			
Acute hospital (R0, R1, R2, R3)	MTC[1] Beds[1,7,8,11,12,13,14] Psychiat.[1,9,14] Psychol. & Nurses[1,9] Total staff[4,10]	Beds[15] Total staff[15]	Discharges[1,7,8,9,10,11,12,13,14,15] Length of stay[1,7,8,11,12] Readmissions[1,8,11,13,15]
24h physician cover (R4, R5, R6, R7)	MTC[2] Beds[8,11,14] Psychiat.[2,9] Psychol. & Nurses[9] Total staff[5,10,14]		Bed occupancy[2]
24h support (R8, R11)	MTC[3] Beds[7,13] Psychol.[3] Nurses[3] Total staff	Beds[12,15] Total staff[9,10,15]	Bed occupancy[3]
Non-24h support (R9, R10, R12, R13, R14)	MTC[3] Beds[12]		Bed occupancy[3]
Day care			
Health-related acute (D1)	MTC[4] Places[9]	Places[4,7,11,12,13,14] Psychiat.[4]	Place occupancy[4]
Health related non-acute (D41, D81)	MTC[4] Places[8]	Psychol. & Nurses[4] Total staff[4,9,10]	Place occupancy[4]
Work-related (D2, D3, D6, D7)	MTC[5] Total staff[6]	Places[7,15] Total staff[5,9]	Place occupancy[5]
Other types (D42, D43, D44, D82, D83, D84, D5, D9, D10)	MTC[5] Total staff[6]		Place occupancy[5]
Outpatient care			
Community outpatient (O8, O9, O10)	MTC[6,11,12] Psychiat.[6] Psychol.[6] Nurses[6] Total staff[6,10,14,15]		Prevalence[6,7,8,10,12,13,14,15] Incidence[6,7] Frequency[6,8,11,12,13]

MTC: Main type of care; Psychiat.: psychiatrists; Psychol.: psychologists; Nurses: mental health nurses; Prevalence: treated prevalence; Incidence: treated incidence

Table 2 shows the description of the scenarios where the indictors have been included.

Table 2: Description of the scenarios.

N°	Description of the scenario
1	Residential care, acute hospital, 24 hours physician cover (R0 to R2)
2	Residential care, non-acute, 24 physician cover (R4 to R6)
3	Residential care, non-acute, non-24 hours physician cover (R8 to R14)
4	Day care, health-related (D, D41 and D81)
5	Day care, non-health-related, work-related & other (D2 to D3 and D6 to D7)
6	Outpatient care (O8 to O10)
7	Placement capacity 1, combination of residential, day and outpatient care
8	Placement capacity 2, combination of residential, day and outpatient care
9	Workforce capacity 1, combination of residential, day and outpatient care
10	Workforce capacity 2, combination of residential, day and outpatient care
11	Community mental health 1, combination of residential, day and outpatient care
12	Community mental health 2, combination of residential, day and outpatient care
13	Community mental health 3, combination of residential, day and outpatient care
14	Community mental health 4, combination of residential, day and outpatient care
15	Community mental health 5, combination of residential and outpatient care

Table 1 shows the inputs and outputs included in each scenario

The variables in each scenario were selected by applying two criterions:

1. Methodological: For developing highly discriminating DEA models (Alirezaee, Howland & VandePanne, 1998; Dyson et al., 2001; Staat, 2001; Torres et al., 2015) the number of variables have to be controlled ($2\times(I\times O)\leq DMU$, being I the number of inputs, O the number of outputs and DMU the original number of observations, 19 in this case).

2. Technical: All of the scenarios have to be meaningful for managers and policy makers. According to this principle, results obtained are easy to interpret and facilitate the identification of potential improvements that can be used to design new real interventions and policies.

For better understanding the inner uncertainty of the system, each variable value was transformed in a standard statistical distribution (symmetric triangular T[minimum value, central estimator, maximum value] in this case). Therefore, the original 19×52 data matrix was transformed in a 19×52 statistical distributions matrix. The structure and parameters of these statistical distributions were selected by a panel of experts including managers and policy makers (Torres et al., 2015).

2.2 The Monte Carlo DEA Model and the Decision Support System (DSS)

A hybrid model was used to assess the RTE of the small mental health care areas in Bizkaia. This model integrates classical statistics, mathematical programming and an approximation to artificial intelligence. Regarding classical statistics, Monte-Carlo simulation was used: (1) to incorporate

uncertainty in variable measuring by using statistical distributions rather than the original variable values (i.e. the original value 0.299 was transformed into triangular distribution *T*[0.2691, 0.299, 0.3289] and (2) to artificially multiply the number observations (500 replications of each area and scenario) which makes RTE analysis be more discriminant. In the proposed model, the Monte-Carlo engine allows the simulation of inputs and outputs and offers the statistical distribution of the RTE for each area in each scenario and, by extension, the corresponding one for the global system (Torres-Jiménez et al., 2015).

Once inputs and outputs values were produced by the Monte-Carlo engine, they are mathematically (linear monotone increasing/decreasing functions) interpreted based on expert knowledge formalised in a *IF ... THEN ...* rule-base (knowledge-base), an embryo of a fuzzy inference engine (Torres-Jiménez et al., 2015). The rule design was based on the B-MHCC paradigm (Salvador-Carulla et al., 2007).

Finally, and using the transformed variable values, the operational algebraic model was designed and solved. The BCC-DEA model, variable returns to scale, was selected because there is no evidence of a constant returns to scale rigid behaviour (Salvador-Carulla et al., 2007). Both input and output orientations of the BCC-DEA model were used. Input orientation refers to maintaining a stable level of outputs, while trying to minimize the resources utilized. Output orientation aims to maximize the outcomes for a constant amount of inputs.

In conclusion, for each scenario and BCC-DEA orientation, the Decision Support System analysed 20 times (or repetitions) a 19×25×*V* (being: 19 the number of areas, 25 the number of simulations and *V* the number of variables –inputs and outputs- in the corresponding scenario) datasets. The number of simulations and repetitions was controlled by the Nakayama's error (Torres-Jiménez et al., 2015) that should always be lower than 2.5% over the RTE average.

RTE for each area (19), scenario (15) and orientation (2) has a probabilistic structure that can be statistically studied. By aggregation, the global RTE of the system can also be statistically determined and studied.

3 RESULTS

The results of the analysis showed the statistical RTE assessment of mental health services provision and use in 19 Bizkaia's small areas. 15 different technical

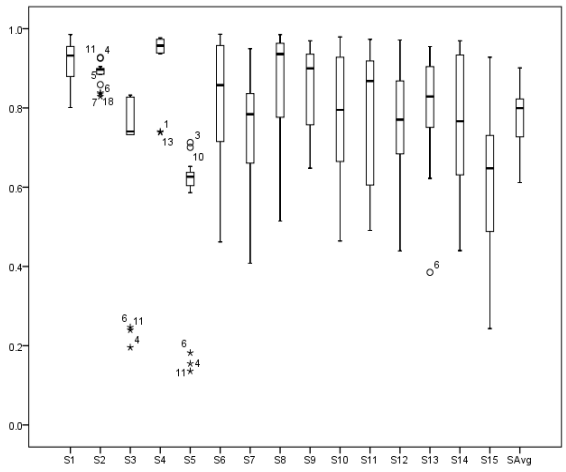

Figure 1: Box-plots of input-oriented relative technical efficiency of mental health areas for each scenario.

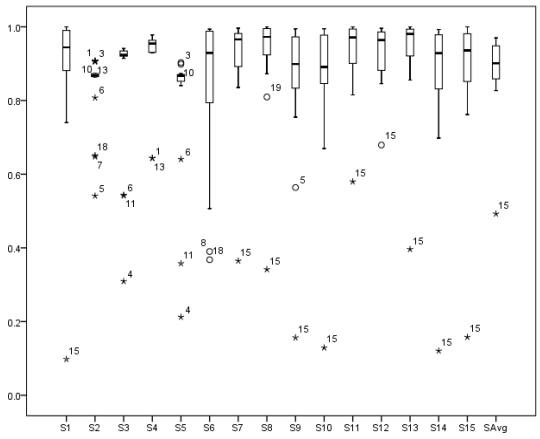

Figure 2: Box-plots of output-oriented relative technical efficiency of mental health areas for each scenario.

perspectives (scenarios) of the RTE problem were taken into account in addition to the two BCC-DEA orientations: input and output. The analysis of the resulting RTE statistical distributions allowed to: (1) rank the areas, and (2) identify and assess potential improvements in key variables by using a benchmarking process (the area that showed the best RTE average and the bigger probability of being efficient is considered the benchmark).

In DEA models, a RTE equal to 1 means that the analysed DMU is efficient (when the sum of the slacks is equal to 0) or weak efficient (when the sum of the slacks is greater than 0). Values lower than 1 show different levels of inefficiency, the lower the value the lower the efficiency. Figures 1 and 2 plot the minimums, maximums, confidence intervals (two-tailed *t*-Student, α=0.95 and 29 freedom degrees), averages and outliers of the resulting ETR

statistical distributions for each scenario (S#) in both the input and output orientations.

The input orientation shows a less number of outliers than the output one. The differences between areas are greater in S1 and S6 to S15 in both orientations, S2 to S5 have a relative homogeneous behaviour.

The mental health areas 4, 6 and 11 appear in three scenarios as outliers in the input-oriented model. On the other hand, areas 6 and 15 are the most recurring as outliers in the output-oriented model. Thus, the area 6 can be considered as a RTE outlier. The area 15 is also an outlier in the most output-oriented scenarios because of several missing data (highly penalised in DEA models) because a private health organization manages this area under contract agreements with the public health system so its information is not integrated.

The most efficient areas reach RTE average values greater than 0.85 in most scenarios and in both orientations. The worst RTE average values are lower than 0.7 in the input orientation a 0.85 in the output one (Figures 3 and 4).

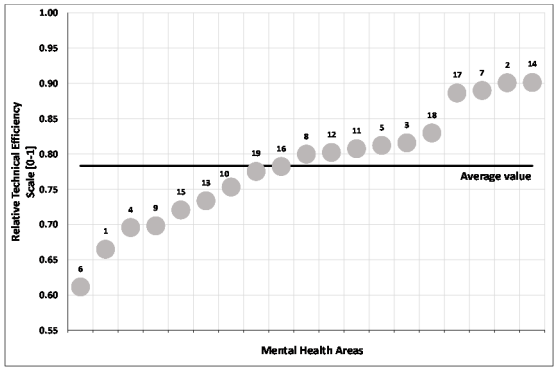

Figure 3: Ranking of mental health areas for the input-oriented model.

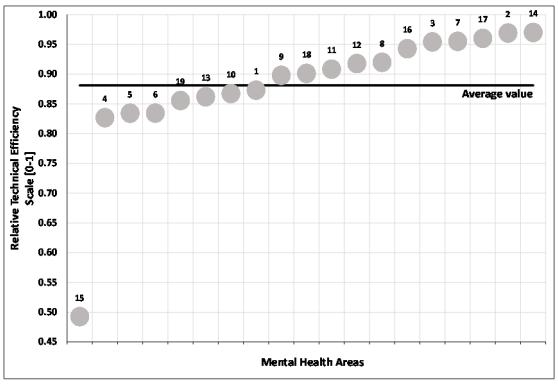

Figure 4. Ranking of mental health areas for the output-oriented model.

The global input-oriented RTE average is 0.78 (Figure 3). Four areas have a RTE average values greater than 0.85, while the lowest value is around 0.6. In the output-oriented model (Figure 4), results are more homogenous and the RTE average is 0.88. There are five areas above 0.95 and an outlier (area 15) close to 0.5 (due to its missing values).

4 DISCUSSION

4.1 The Monte Carlo DEA Model and the Decision Support System (DSS)

The Monte-Carlo DEA model overcomes several limitations of the traditional DEA models. Firstly, the expert-based interpretation of input and output values makes the result interpretation easier for decision makers (Salvador-Carulla et al., 2007; Torres-Jiménez et al., 2015) because it includes the specific interrelations and particular characteristics of mental health systems. For instance, the classical assumption: "a situation which combines a low input consumption with a high outcome production is positive for the system performance" may not be always correct or appropriate in mental health care (Torres-Jiménez et al., 2015). Expert knowledge is formalised in a rule-base by using the B-MHCC paradigm (Salvador-Carulla et al., 2007), which determines an appropriateness degree for each variable value ("non-appropriate" values are penalised in their mathematical transformation).

Secondly, the Monte-Carlo DEA model makes RTE assessment more discriminant by the artificial replication of the observation number. Datasets are generated by the Monte-Carlo engine according to variable values statistical distributions.

Finally, the uncertainty associated to data real values is managed through the transformation of the original variable values into standard statistical distributions. The Monte-Carlo simulation engine explores the variable values spectrum and offers a RTE probabilistic view.

4.2 Strengths of the Study of the Relative Technical Efficiency in Bizkaia

Previous RTE studies have mainly assessed the efficiency of complete systems (Kaya Samut & Cafrı, 2015); specific services, such as nursing homes (Garavaglia, Lettieri, Agasisti & Lopez, 2011; Kleinsorge & Karney, 1992), hospitals (Dash,

Vaishnavi, & Muraleedharan, 2010; Mogha, Yadav & Singh, 2016) or primary care (Cordero et al., 2015; Kirigia et al., 2011). However, they have not allowed to know performance differences within the whole health system. This research has studied different RTE scenarios designed to describe the behaviour of both the partial (i.e. residential care) or mixed (i.e. day and outpatient care jointly) typologies based on the B-MHCC paradigm. Thus, these scenarios incorporate an integrative vision of mental health care, including all the types of care (from a holistic perspective) in which health and social care are highlighted. This fact lets us to understand and assess specific mental health care itineraries that patients should follow in order to increase RTE and quality care. Results include all the RTE statistical distributions as well as the global RTE of the system.

This study has analysed the provision and utilisation of mental health services in a real system through an exhaustive data collection from the Integrated Mental Health Atlas of Bizkaia (Pereira et al., 2013; Salvador-Carulla et al., 2011). The use of a standardized model for mental-health care description and assessment was absolutely essential because the name of the service was not enough for describing its management structure and for making comparisons. The Mental Health Atlas collected information about the availability of specific types of care, placement capacity, availability of workforce and utilization indicators. The Monte-Carlo DEA model integrates the uncertain information with an operational model for assessing RTE and potential managerial improvements.

4.3 Analysis of the Mental Health System RTE in Bizkaia

Efficient mental health areas may be identified as references for benchmarking. The assessed potential improvements can guide management interventions on the provision (inputs) and outcomes (outputs). On one hand, the provision of mental health care in inefficient areas could be adjusted to the values of the efficient ones. On the other, interventions on the service utilization could be direct such as the optimization of facilities, placements and staff; or indirect such as economic incentives, training activities, policy design or good practices promotion.

The global RTE of the system is greater in the output-oriented model than in the input-oriented one. This suggests that a decisional strategy based on optimizing the input amount, within the ranges stablished by the B-MHCC paradigm, may be more adequate for the Mental Health System of Bizkaia.

In the input-oriented analysis and in spite of the existence of outliers, the scenarios where the RTE scores are more homogenous are those that evaluated the residential non-acute care and day hospitals (S2 to S5 and, by extension, S13). This characteristic is the result of the current and careful political planning. Obviously, RTE scores can be improved in each scenario by designing specific policies, especially on the outlier areas.

In the output-oriented analysis (more homogeneous), the most efficient scenarios are S11 and S12 (community mental health 1 and 2) and S4 (health-related day care). According to the results, S2 (non-acute residential and hospital care), S3 (residential care), S5 (non-health-related day care) and s6 (outpatient care) could be main the targets in a decisional environment based on the improvement of the RTE. In this DEA orientation, the area number 15 has a relevant impact on the RTE scores because it was a highly penalised due to the lack of information.

It is highly recommended to increase the day care resources to be equal, at least, to medical ones. This intervention should increase both the RTE and the mental health care quality, in addition to an expected decrease in the economic burden of the system. In this sense, there are empirical evidences that show that community-based care is more cost-effective than institutional-based care (WHO, 2005).

The proposed DSS can assess the impact of an almost infinite number of planning interventions. This process can decrease the intrinsic managerial risk associated to any real management decision. For example, it can evaluate the effects on the system of transferring some professionals from a mental health area, or areas, to other/s: this implies changes in the provision, utilization and outcome variables. This analysis understands that any intervention in a specific geographical area will probably have an impact on the others because of the interrelations between them.

4.4 Limitations

The analysis of RTE in specific mental health areas is relevant and useful but insufficient to evaluate the global situation of mental health care. The pathway of care that should be followed by a specific user has to be designed depending on his clinic status. In Spain, the first point of contact in the health care system is usually located in a primary care service or in a hospital. From these units, the patient can be derived to a secondary care service afterwards. All the mentioned services have been include in this study. Nevertheless, until the patient arrives to this

secondary level, he has followed an itinerary that ought to be studied if RTE scores have to be increased. To avoid an increase in the re-hospitalization number, in the number of stays at the hospitals, in the frequentation, the prevalence or even in the incidence of mental disorders, a most efficient care coordination and an integrative professional practice have to be highlighted (Burns, Goldsmith, & Sen, 2013; Cordero et al., 2015).

In conclusion, it should be necessary to include primary care services in RTE assessment in order to have a complete picture of the mental health system under analysis.

5 CONCLUSIONS

In the decision making processes based on empirical evidence, the intrinsic decisional risk decreases. Therefore, it is fundamental to provide the decision maker as much reliable information as possible to understand the real situation (Gibert, García-Alonso & Salvador-Carulla, 2010).

The Monte-Carlo DEA model has provided high-level and empirical informed-evidence on the RTE based on the provision and utilization of mental health services in small geographical areas of the Bizkaian Health System. Based on the results, it has been possible to identify and analyse potential improvements that can be transformed into decisional interventions to be checked by modifying input or output values (statistical distributions) in the DSS. The obtained results may help decision makers to prioritise them in an uncertain context dominated by economic restrictions.

Future research will be focused on the validation of the DSS analysing real decisional situations with multiple feasible alternatives. Selected micro-management interventions, those that imply a relative small number of variables, based on policymaker interests will be selected to assess potential improvements and risks on the system management prior their implementation, Following this process, the decision making process is supported by empirical evidence. This feature matches with the strategies established in the Mental Health Action Plan 2013-2020 (WHO, 2013).

ACKNOWLEDGEMENTS

This study is part of a bigger Project named “Atlas de Salud Mental de Bizkaia” funded by the “Red de Salud Mental de Bizkaia”. It has been carried out in collaboration with “Osakidetza” and the “Departamento de Sanidad y Consumo del Gobierno Vasco”.

REFERENCES

Alirezaee, M.R., Howland, M. & Van de Panne, C., 1998. Sampling size and efficiency bias in data envelopment analysis. *Journal of Applied Mathematics and Decision Sciences*, 2(1), pp.51-64.

Burns, L.R., Goldsmith, J.C. & Sen, A., 2013. Horizontal and vertical integration of physicians: a tale of two tails. *Advances in health care management*, 15, pp.39–117.

Cordero, J.M. et al., 2016. Technical efficiency assessment of public primary care providers in the Basque Country (Spain), 2010-2013. *Gaceta Sanitaria*, 30(2), pp.104–109. Available at: http://www.scopus.com/inward/record.url?eid=2-s2.0-84959099383&partnerID=40&md5=3043220dd789be1b3dd178769affd73c.

Dash, U., Vaishnavi, S.D. & Muraleedharan, V.R., 2010. Technical Efficiency and Scale Efficiency of District Hospitals: A Case Study. *Journal of Health Management*, 12(3), pp.231–248. Available at: http://www.scopus.com/inward/record.url?eid=2-s2.0-77955896077&partnerID=tZOtx3y1 [Accessed March 14, 2016].

Dyson, R.G. et al., 2001. Pitfalls and protocols in {DEA}. *European Journal of Operational Research*, 132(2), pp.245–259. Available at: http://www.sciencedirect.com/science/article/pii/S0377221700001491.

Färe, R. et al., 2008. Evaluating health care efficiency. *Advances in health economics and health services research*, 18, pp.209–228. Available at: https://www.scopus.com/inward/record.uri?eid=2-s2.0-58849144444&partnerID=40&md5=0156be57de9f254a68436a2db8b6d62f.

Garavaglia, G. et al., 2011. Efficiency and quality of care in nursing homes: An Italian case study. *Health Care Management Science*, 14(1), pp.22–35. Available at: https://www.scopus.com/inward/record.uri?eid=2-s2.0-79551530621&partnerID=40&md5=eddb9c7279a145d0f1c32c9181972ff9.

Gibert, K., Garcia-Alonso, C. & Salvador-Carulla, L., 2010. Integrating clinicians, knowledge and data: expert-based cooperative analysis in healthcare decision support. *Health research policy and systems / BioMed Central*, 8, p.28.

Gobierno Vasco. (2010). Estrategia para afrontar el reto de la cronicidad en Euskadi, Bilbao, Eusko Jaurlaritza-Gobierno Vasco.

Gutierrez-Recacha, P. et al., 2006. Cost-effectiveness of different clinical interventions for reducing the burden

of schizophrenia in Spain. *Acta psychiatrica Scandinavica. Supplementum*, (432), pp.29–38.

Hollingsworth, B., 2008. The measurement of efficiency and productivity of health care delivery. *Health economics*, 17(10), pp.1107–1128.

Hollingsworth, B. & Parkin, D., 2001. The efficiency of the delivery of neonatal care in the UK. *Journal of public health medicine*, 23(1), pp.47–50.

Kaya Samut, P. & Cafrı, R., 2015. Analysis of the Efficiency Determinants of Health Systems in OECD Countries by DEA and Panel Tobit. *Social Indicators Research*. Available at: https://www.scopus.com/inward/record.uri?eid=2-s2.0-84941367202&partnerID=40&md5=77b2c000e68c3d32218b73040f075a46.

Kirigia, J.M. et al., 2011. Technical efficiency of primary health units in Kailahun and Kenema districts of Sierra Leone. *International archives of medicine*, 4, p.15.

Kleinsorge, I.K. & Karney, D.F., 1992. Management of nursing homes using data envelopment analysis. *Socio-economic planning sciences*, 26(1), pp.57–71.

Ministerio de Sanidad, Política e Igualdad (2011). Estrategia en Salud Mental del Sistema Nacional de Salud 2009-2013 [pdf] España. Avaliable at http://www.aepcp.net/arc/SaludMental2009-2013.pdf [Accessed 24 Oct. 2016]

Mogha, S.K., Yadav, S.P. & Singh, S.P., 2015. Slack based measure of efficiencies of public sector hospitals in Uttarakhand (India). *Benchmarking: An International Journal*, 22(7), pp.1229–1246. Available at: http://www.scopus.com/inward/record.url?eid=2-s2.0-84942784709&partnerID=tZOtx3y1 [Accessed March 14, 2016].

Moran, V. & Jacobs, R., 2013. An international comparison of efficiency of inpatient mental health care systems. *Health policy (Amsterdam, Netherlands)*, 112(1-2), pp.88–99. Available at: http://www.scopus.com/inward/record.url?eid=2-s2.0-84885191198&partnerID=tZOtx3y1 [Accessed March 14, 2016].

[OECD] Organisation for Economic Co-operation and Development. (2010). *Health expenditures and financing*. [online] Available at: https://stats.oecd.org/Index.aspx?DataSetCode=SHA [Accessed 20 Oct. 2016]

[OECD] Organisation for Economic Co-operation and Development. (2016). *Mental Health and work*. [online] Available at: https://www.oecd.org/els/emp/mental-health-and-work.htm [Accessed 20 Oct. 2016]

Pares-Badell, O. et al., 2014. Cost of disorders of the brain in Spain. *PloS one*, 9(8), p.e105471.

Pelone, F. et al., 2012. The measurement of relative efficiency of general practice and the implications for policy makers. *Health policy (Amsterdam, Netherlands)*, 107(2-3), pp.258–68. Available at: http://www.scopus.com/inward/record.url?eid=2-s2.0-84865970504&partnerID=tZOtx3y1 [Accessed March 14, 2016].

Pereira, C., Gutiérrez-Colosía, M. and Salinas-Perez, J. (Eds.). (2013). *Mental Health Atlas of Bizkaia.* Bilbao: Osakidetza.

Salvador-Carulla, L., Dimitrov, H., Weber, G., McDaid, D., Venner, B., Šprah, L., ... and Johnson, S. (2011). *DESDE-LTC: Evaluation and Classification of Services for Long Term Care in Europe.* Spain: Psicost and Caixa Catalunya.

Salvador-Carulla, L. et al., 2007. Use of an operational model of community care to assess technical efficiency and benchmarking of small mental health areas in Spain. *The journal of mental health policy and economics*, 10(2), pp.87–100.

Shen, G.C. & Snowden, L.R., 2014. Institutionalization of deinstitutionalization: a cross-national analysis of mental health system reform. *International journal of mental health systems*, 8(1), p.47.

Sherman, H.D., 1984. Hospital efficiency measurement and evaluation. Empirical test of a new technique. *Medical care*, 22(10), pp.922–938.

Staat, M., 2001. The Effect of Sample Size on the Mean Efficiency in DEA: Comment. *Journal of Productivity Analysis*, 15(2), pp.129–137. Available at: http://dx.doi.org/10.1023/A:1007826405826.

Torres-Jiménez, M. et al., 2015. Evaluation of system efficiency using the Monte Carlo DEA: The case of small health areas. *European Journal of Operational Research*, 242(2), pp.525–535. Available at: http://www.scopus.com/inward/record.url?eid=2-s2.0-84920716285&partnerID=tZOtx3y1 [Accessed March 14, 2016].

Tyler, L.H., Ozcan, Y.A. & Wogen, S.E., 1995. Mental health case management and technical efficiency. *Journal of medical systems*, 19(5), pp.413–423.

United Nations. (1991*). The protection of person with mental illness and the improvements of mental health care.* [online] Available at http://www.un.org/documents/ga/res/46/a46r119.htm [Accessed 25 Oct. 2016].

World Health Organization. (2003). *Investing in MENTAL HEALTH* [online] Available at http://www.who.int/mental_health/en/investing_in_mnh_final.pdf [Accessed 25 Oct. 2016].

World Health Organization. (2005). *Mental health policy, plans and programmes. Mental Health Policy and Service Guidance Package.* [online] Available at http://www.who.int/mental_health/policy/services/essentialpackage1v1/en/ [Accessed 25 Oct. 2016].

World Health Organization. (2013). *Mental Health Action Plan 2013 – 2020.* [online] Available at http://www.who.int/mental_health/publications/action_plan/en/ [Accessed 25 Oct. 2016].

World Health Organization. (2016). Mental disorders. [online] Available at http://www.who.int/mediacentre/factsheets/fs396/en/ [Accessed 25 Oct. 2016].

Zhu, J., 2003. Imprecise data envelopment analysis (IDEA): A review and improvement with an application. *European Journal of Operational Research*, 144(3), pp.513–529.

Measuring the Efficiency of the Food Industry in Central and East European Countries by using the Data Envelopment Analysis Approach

Zrinka Lukač and Margareta Gardijan
Faculty of Economics and Business, University of Zagreb, Trg J.F. Kennedyja 6, Zagreb, Croatia
{zlukac, mgardijan}@efzg.hr

Keywords: Efficiency, Competitiveness, Food Industry, Data Envelopment Analysis.

Abstract: The food industry plays an important role in economy of many countries. It is the leading manufacturing industry in EU in terms of turnover, value added and employment. However, it has been facing a decrease in competitiveness lately. In this paper we study the competitiveness of very large companies from the food industry sector in central and east European countries (CEE) by measuring their efficiency within the Data Envelopment Analysis (DEA) approach. The efficiency analysis is conducted by using the BCC model where certain financial ratios are used as its inputs and outputs. The study includes more than 200 very large companies from 13 CEE countries over time period from 2005-2013. The research results have shown that although some countries were more efficient than the others during the entire research period, no patterns in the efficiency of the food industry subsectors could be recognised. On the other hand, DEA approach enabled recognizing sources of inefficiency on a national level.

1 INTRODUCTION

The food industry is a very important component of the economy of many countries and has a unique role in expanding their economic opportunities. Its impact is not limited only to the economic growth but also affects various aspects of the society. Together with agriculture it is the main source of national income for most developing countries. Even in developed countries its role is of utmost importance. For example, the food and drink industry is the first manufacturing industry in the EU, leading in terms of turnover (€1090 billion or 15.6%), value added (€212 billion or 13%) and employment (4.25 billion people in direct employment or 15.2%) (FoodDrink Europe, 2016). Statistical classification of economic activities in the European Community, abbreviated as NACE, classifies food industry as sector C10. Its 9 subsectors are shown in Table 1.

In 2013, the food industry sector in Europe included 264.1 thousand enterprises that employed 13.6% of the total manufacturing workforce in and had a wage-adjusted labour productivity ratio of 157.1% (manufacturing ratio average is 148,0%). Almost 60% of these companies were engaged in activities classified under C.10.7, followed by approximately 15% in C.10.1 and 23.3% in C.10.8 (Eurostat 2013).

Table 1: Classification of food industry sector C10.

C10.1	Production, processing, preserving of meat, meat products
C10.2	Processing and conservation of fish, crustaceans and molluscs
C10.3	Processing and conservation of fruit and vegetables
C10.4	Manufacture of vegetable and animal fats and oils
C10.5	Manufacture of dairy products
C10.6	Manufacture of milling products, starches and starch products
C10.7	Manufacture of bakery products and pastas
C10.8	Manufacture of other foodstuffs
C10.9	Manufacture of products for animal feed

The leading European countries in the food industry are Germany, France, UK and Italy, but certain central and east European (CEE) countries, such as Bulgaria, Romania and Poland, have one of the greatest wage-adjusted labour productivity ratios. However, the EU food and drink industry is facing a decrease in competitiveness lately. Despite

Lukač, Z. and Gardijan, M.
Measuring the Efficiency of the Food Industry in Central and East European Countries by using the Data Envelopment Analysis Approach.
In *Proceedings of the 6th International Conference on Operations Research and Enterprise Systems (ICORES 2017)*, pages 385-392
ISBN: 978-989-758-218-9

that fact, no analysis of the food sector in CEE has been made recently.

In this paper, we study the competitiveness of large companies from food industry sector in 13 CEE countries (Bosnia and Herzegovina, Bulgaria, Croatia, Czech Republic, Hungary, Latvia, Lithuania, Montenegro, Poland, Romania, Serbia, Slovakia and Slovenia). The study includes all very large companies from food sector for which data was provided by AMADEUS database, that is over 200 very large companies during the time period from 2005-2013. We investigated their relative efficiency using the BCC model from the Data Envelopment Analysis (DEA). DEA is a nonparametric method for measuring the relative performance of decision making units (DMU's) and identifying efficient production frontiers in presence of multiple inputs and outputs. The method was developed by Charnes, Cooper and Rhodes (Charnes, Cooper and Rhodes, 1978). In our analysis, DMUs are particular companies, while inputs and outputs of the BCC model are their financial ratios. Based on the efficiency scores of companies, we draw conclusions about the efficiency of the food industry subsectors as well as the efficiency of food industries of particular countries. Also, we were able to identify sources of inefficiency of certain countries, which might assist policy makers in developing strategies which might improve competitiveness of their food industry sectors and thus affect their economic growth.

2 LITERATURE REVIEW

Given the role the food industry plays in the economy of many countries as well as in global economy there are many publications issued by official governmental and non-governmental organizations, such as Food and Agriculture Organization of the United Nations (FAO) or European Commission (EC), that deal with the agribusiness, its role in economic development and its competitiveness. Each year FAO publishes The State of Food and Agriculture report. In its 1997 issue special chapter was devoted to the subject of agro-processing industry and economic development (FAO, 1997). In 2009, FAO has published another document on key factors affecting the development and competitiveness of agro-industries (FAO, 2009).

Given the decrease in the relative competitiveness of EU food and drink industry compared to other world food producers in terms of slower growth in labour productivity and added value, EC is actively taking efforts to come up with the policy measures which would support the competitiveness of that sector. It also publishes studies which assess EU food and drink industry competitive positions. Some of such recent studies on the competitive position of the European food and drink industry commissioned by EC are (Wijnands and Verhoog, 2016) and (European Commission, 2016).

Verschlede et al. (2014) conducted a general study to obtain insight into firm-level competitiveness across all sectors in Europe, including the food industry, by using a semiparametric stochastic metafrontier approach. Many studies have used DEA approach to measure efficiency and competitiveness of the food industry. Charles and Zegarra (2014) have developed a regional competitiveness index by using the methodology based on DEA to measure and rank the competitiveness of all the regions of Peru. Rodmanee and Huang (2013) have used a relational two-stage DEA to evaluate the efficiency of 23 food and beverage companies in Thailand. Shamsudin et al. (2011) used the DEA approach to evaluate the market competitiveness of small and medium enterprises in the food industry in Malaysia. Study conducted by Tektas and Tosun (2010) benchmarks the supply and chain performance of Turkish food and beverage companies by using DEA. The DEA-efficiency and productivity changes in the food industry in India during pre and post liberalisation period were studied by Ali et al. (2009). The former also identifies the causes of inefficiency across various sectors. Kocisova (2015) investigates the relative efficiency of the agricultural sector in the EU using DEA during the period 2007-2011, where decision-making units (DMUs) are agricultural subsectors. The paper by Kocisova (2015) also gives a good literature review of different approaches to measuring efficiency in the agricultural sector in Europe. However, there are no recent studies of the competitiveness of European food industry by using the DEA approach.

3 METHODOLOGY

The mathematical formulation of the basic DEA CCR model (Charnes, Cooper and Rhodes, 1978) is as follows. We observe N decision making units, denoted as DMU_1, DMU_2,…,DMU_N, that use the same n inputs in order to produce the same m outputs. Let x_{ij} be an input i for some DMU_j,

$i \in \{1,\ldots,n\}$ and y_{rj} its output $r, r \in \{1,\ldots,m\}$, $j \in \{1,\ldots,N\}$. Therefore, a particular DMU_j is described by vectors $\mathbf{X} = (x_{1j}, x_{2j},\ldots,x_{nj})$ and $\mathbf{Y} = (y_{1j}, y_{2j},\ldots,y_{mj})$. In order to make the model stable, it is recommended that $N \geq \max\{mn, 3(m+n)\}$. For an arbitrary decision making unit DMU_0=DMU_j, $j \in \{1,\ldots,N\}$, a virtual input $u_1x_{1o} + \ldots + u_nx_{no}$ and a virtual output $v_1y_{1o} + \ldots + v_my_{mo}$ are formed with (initially) unknown weights (v_r) and (u_i). The model can be input or output oriented, depending on whether DMUs' aim is to minimize the inputs for a given level of outputs or vice versa. In the output oriented approach, these weights are determined by solving the following fractional programming model for each DMU_0=DMU_j:

$$\begin{aligned} &\max_{v_1,\ldots,v_m,u_1,\ldots,u_s} \frac{v_1y_{1o} + v_2y_{2o} + \ldots + v_my_{mo}}{u_1x_{1o} + u_2x_{2o} + \ldots + u_nx_{no}}, \\ &\text{subject to} \\ &\frac{u_1y_{1j} + u_2y_{2j} + \ldots + u_my_{mj}}{v_1x_{1j} + v_2x_{2j} + \ldots + v_nx_{nj}} \leq 1,\ j \in \{1,\ldots,N\}, \\ &u_i, v_r \geq \varepsilon > 0, \forall i, r, \end{aligned} \tag{1}$$

where $\varepsilon > 0$ is a non-Archimedean element. Using Charnes-Cooper transformation (Charnes and Cooper, 1962) this fractional programming model can be linearized and also written in its envelopment form (Cooper, Seiford and Zhu, 2011).

Since CCR model assumes constant returns to scale, Banker, Charnes and Cooper (Banker, Charnes and Cooper, 1984) developed a generalised DEA model that assumes variable returns to scale (VRS). Their significant contribution to the DEA was the idea to let each DMU use the set of weights that puts it in the best position regarding the other DMUs (www.deazone.com [10.7.2013]). In output-oriented BCC model, the measure of technical efficiency ϕ is obtained by solving the following linear program for each DMU_0=DMU_j:

$$\begin{aligned} &\max_{\boldsymbol{\lambda},\phi} \phi - e(s^+ + s^-) \\ &\sum_{j=1}^{N} \mathbf{X}_j\lambda_j + s^- = \theta\mathbf{X}_0, \\ &\sum_{j=1}^{n} \mathbf{Y}_j\lambda_j - s^+ \geq \mathbf{Y}_0, \\ &\sum_{j=1}^{N} \lambda_j = 1, \\ &\lambda_j \geq 0\ , (j \in \{1,2,\ldots,N\}), \end{aligned} \tag{2}$$

where s^-, s^+ are vectors of slack variables and θ is the solution of the dual problem. If we denote the optimal solution as (ϕ^*, s^{+*}, s^{-*}), then DMU_0 is efficient iff ϕ=1 and $s^{+*} = s^{-*} = 0$. DMU_0 is weakly efficient iff $\phi^* = 1$ and $s^{+*} \neq 0$ or $s^{-*} \neq 0$ in some alternate optima (Cooper, Seiford and Zhu, 2011).
This study uses BCC model for several reasons. First, it is a relatively simple tool that gives the needed results. Secondly, it allows assuming variable returns to scale, and thirdly, it can handle negative data that is often found in financial analysis (Pastor and Ruiz, 2007).

4 DATA AND RESULTS

The data sample for our study included all the very large food manufacturers in CEE countries for which data were available in AMADEUS database. We considered the time period from 2005-2013. The number of companies varies between 235 in 2005 and 284 in years 2007 and 2008 (table A1 in appendix). There are several reasons why it is interesting to analyse the segment of very large companies. On average, very large companies from this database hold on around 40.2% of total asset and 37,52% of all the capital in food industry of the countries observed during the period of analysis. Also, very large companies have employed 22.28% of the total workforce (on average) within the CEE food industry sector. The data shows that during 2005-2013 the average profit margin (PM) of very large producers in food industry sector was smaller than the PM of large companies. Compared to medium sized companies, the profit margin of very large companies was smaller only in years before 2010. Furthermore, when compared to companies classified as small, they reaped greater profit margin. Data shows that the number of very large food producers has been increasing over the years. The choice of variables used for evaluating the companies was determined by the availability of data. Since the most commonly reported data in AMADEUS dataset are operating revenue, total asset, capital and profit margin, these variables were used to investigate the relative efficiency of the very large food producers in CEE countries. Given the fact that DEA cannot deal with missing values (Smirlis, Maragos and Despotis, 2006), companies with missing data were excluded from the study. This reduced the sample by not more than 5% of the total number of companies in each year. The ratio of profit/loss before tax to total asset (ROA) and profit

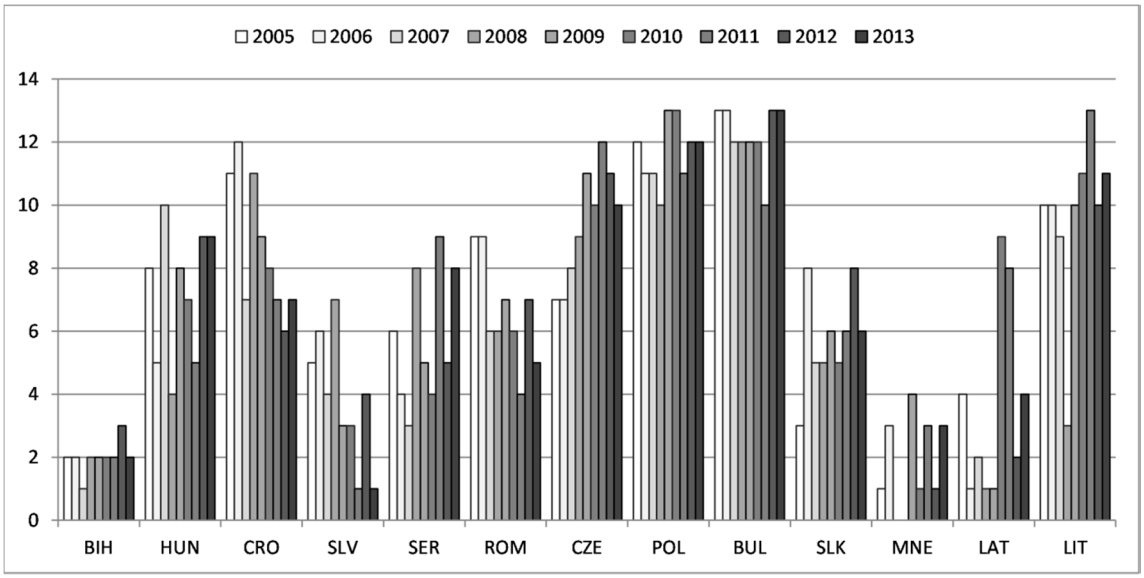

Figure 1: Relative position of countries by years during 2005-2013.

margin were used as indicators of profitability. Since capital and operating revenue are given in absolute terms, we introduce their ratio (capital/operating revenue) as a measure of productivity of capital.

Classification of companies by their subsector is presented in table A2 in the appendix.

DEA demands that there is at least one variable considered as input and one variable considered as output. Since greater values of ROA and profit margin are preferred, these variables were taken as outputs, while the productivity of capital was taken in its inverse form (revenue/capital) and considered as an input of the BCC model. The minimum and maximum values of correlation coefficients among variables for each year during the time period from 2005-2013 are given in Table 2. The correlation coefficients between input and output variables are meaningful and indicate that there are no redundant variables.

Table 2: Minimum and maximum values from the correlation matrix.

	cap/rev	ROA	RM
cap/rev	1		
ROA	-0,22 / -0,08	1	
RM	-0,61 / -0,05	0,6 / 0,73	1

For each year, the rankings of companies were obtained by solving the BCC model. The results showing the most efficient and 5 least efficient companies are reported in tables A3 (years 2005-2009) and A4 (years 2010-2014) in the appendix.

Averaging the efficiency ratios of food companies from a specific country allows ranking of countries by their food industry efficiency. Figure 1 shows the relative positions of countries in time period 2005-2013. It is obvious that Bulgaria, Poland, Czech Republic and Hungary are the leading countries in this sector. Bosnia and Herzegovina is the least efficient country. On the other hand, averaging the rankings within each food industry subsector allows recognising the changes in the relative efficiency over the years. The results illustrated in Figure A1 in the appendix show that subsector C10.7 is strongly at the bottom. Also, C10.9 and C10.2 are in the middle of the range of relative rankings with respect to other sectors for each year of the considered period. However, there are large oscillations of average efficiency ranking within subsectors during 2005-2013.

DEA also allows recognizing the weaknesses of a specific *DMU*. It is given by the percentage difference of *DMU*s inputs and outputs compared to its efficient projection on the efficient frontier. By averaging these percentage differences within a single country, we got indicators of competitive advantages and inefficiency sources, as shown in tables A5, A6 and A7 in the appendix. These results show that, on average, efficient countries have small deviations from their projections in both outputs and input. On the other hand, the inefficient countries have large deviations from projections, again in both outputs and input. Overall, each country has different sources of strengths and weaknesses, as shown by table A5, A6 and A7 in the appendix.. The

results obtained on a company level, as well as on the country level, can be used as guidelines for assisting policy makers in creating policies which might lead to improving efficiency and competitiveness, thus also having positive effects on economic growth.

5 CONCLUSIONS

The food industry plays an important role in the economy of many countries. Developing its competitiveness has positive effects on long-term economic growth. Therefore it is important to assist the policy makers in identifying sources of inefficiency and developing strategies which would improve its competitiveness. In this study we have conducted efficiency analysis of very large companies in the food sector of CEE countries using the DEA approach, namely the BCC model. The results of the BCC model identified Bulgaria, Poland, Czech Republic and Hungary as leader CEE countries in terms of efficiency of very large companies in the food sector in the period of 2005-2013. Bosnia and Herzegovina, Montenegro and Slovakia were relatively inefficient in this dataset. Croatia and Romania showed to be somewhere in the top middle, which is rather surprising since Romanian food industry is considered as more developed. Moreover, the model detects the *ex-post* efficiency/ inefficiency of decision-making units. The results indicate variables where improvements can be made. It also indicates the sources of efficiency which a company/ country should strengthen as its competitive advantage. The findings are company/country specific. However, the analysis does not include any future projections or effects of the uncertainty. Limitations of this study are related to the availability of financial data. It must be noted that small and medium enterprises are poorly covered in AMADEUS database. This restricts the number of companies in the sample, leading to conclusions that cannot be generalized. As for further research, in order to derive the generalized results, the analysis should also include small, medium and large companies within food industry, but that would require using models which allow missing data. Also, it would be interesting to conduct the similar analysis for all European countries.

ACKNOWLEDGEMENTS

This research has been fully supported by Croatian Science Foundation under the project *The role of structural reforms in boosting external competitiveness in European Union countries*.

REFERENCES

Ali, J., Singh, S.P., Ekanem, E., 2009. Efficiency and Productivity Changes in the Indian Food Processing Industry: Determinants and Policy Implications.*International Food and Agribusiness Management*, Vol. 12 (1), pp 43- 66

Banker, R. D., Charnes, A., Cooper, W. W. 1984. Some Models for Estimating Technical and Scale Inefficiencies in Data Envelopment Analysis. *Management Science*, Vol. 30 (9), pp 1078–1092

Charles, V., Zegarra, L.F., 2014. Measuring regional competitiveness through Data Envelopment Analysis: A Peruvian case. *Expert Systems with Applications*, Vol. 41, pp 5371-5381

Charnes, A., Cooper, W.W,. Rhodes, E., 1978. Measuring the efficiency of decision making units, *European Journal of Operations Research*, Vol. 2 (6), pp 429-444

Charnes, A., Cooper, W.W. 1962. Programming with linear fractional functionals. *Naval Research Logistics,* Vol 9 (3-4), September - December 1962, pp 181–186

Cooper, W.W., Seiford, L.M., Zhu, Joe (eds.) 2011. Data Envelopment Analysis: History, Models, and Interpretations, In: *Handbook on Data Envelopment Analysis:International Series in Operations Research & Management Science Springer 2011*, pp. 1-39

European Commission, 2016. *The competitive position of the European food and drink industry, Final report.* Available at: http://edz.bib.uni-mannheim.de /daten/edz-h/gdb/16/EA0416075ENN.pdf

FAO, 1997. *The State of Food and Agriculture 1997* (*SOFA*)*:The Agroprocessing Industry and Economic Development.* Available at: http://www.fao.org/docrep/w5800e/W5800e00.htm

FAO, 2009. *Agro-industries for Development.* Available at: http://www.fao.org/docrep/017/i3125e/i3125e00 .pdf

FoodDrink Europe, 2016. *A Competitive EU Food and Drink Industry for Growth and Jobs: Ambitions for 2025. Priorities and policy recommendations.* Available at: http://www.fooddrinkeurope.eu/uploads/ publications_documents/Competitive_food_industry_ growth_jobs_report.pdf

Kocisova, K., 2015. Application of the DEA on themeasurment of efficiency in the EU countries.*Agricultural Economics – Czech*, Vol. 61 (2), pp 51-62

Pastor, J. T., Ruiz, J. L., 2007. Variables With Negative Values in Dea. In: Modelling Data Irregularities And

Structural Complexities. In *Data Envelopment Analysis, Cook, W., Zhu, J. (eds.)*. Springer, e–book, pp 63–84.

Rodmanee, S., Huang, W., 2013. Efficiency Evaluation of Food and Beverage Companies in Thailand: An Application of Relational Two-Stage Data Envelopment Analysis.*International Journal of Social Science and Humanity*, Vol. 3 (3), pp 202-205

Shamsudin, M.N., Yodfiatfinda, Mohamed, Z.A., Yusop, Z., Radam, A., 2011. Evaluation of market competitiveness of SMEs in the Malaysian Food Processing Industry. *Journal of Agribusiness Marketing*, Vol. 4., pp 1-20

Smirlis, Y. G., Maragos, E. K., Despotis, D. K. 2006. Data Envelopment Analysis with Missing Values: An Interval DEA Approach. *Applied Mathematics and Computation,* Vol. 177 (1), pp 1–10

STATISTICAL OFFICE OF THE EUROPEAN COMMUNITIES. (2016). EUROSTAT: *Manufacturing statistics - NACE Rev. 2.* Available at: http://ec.europa.eu/eurostat/statistics-explained/index.php/Manufacturing_statistics_-_NACE_Rev._2

Tektas, A., Tosun, E.O., 2010. Performance Benchmarking in Turkish Food and Beverage Industry. *Communications of the IBIMA*, Vol. 2010

Verschelde, M., Dumont, M., Rayp, G., Merlevede, B., 2016. Semiparametric stochastic metafrontier efficiency of European manufacturing firms*. Journal of Productivity Analysis*, Vol. 45, No. 1, pp 53-69

Wijnands, J.H.M., Verhoog, D.,2016. *Competitiveness of the EU food industry; Ex-post assessment of trade performance embedded in international economic theory.*Wageningen, LEI Wageningen UR (University & Research centre), LEI Report 2016-018. Available at: http://edepot.wur.nl/369980

APPENDIX

In this section we bring the figure and tables that we have referenced in the text.

Table A1: Number of companies per country per year included in the study.

	2005	**2006**	**2007**	**2008**	**2009**	**2010**	**2011**	**2012**	**2013**
BIH	11	12	15	14	14	12	11	7	8
HUN	11	10	13	13	13	14	15	15	15
CRO	17	17	17	17	17	17	17	17	15
SLV	3	4	4	4	4	4	4	4	4
SER	50	53	54	55	49	48	48	49	43
ROM	40	28	40	42	42	40	43	42	42
CZE	13	11	14	14	16	17	16	17	17
POL	51	65	72	76	86	85	85	84	78
BUL	3	4	5	6	7	6	6	6	7
SLK	6	11	10	11	11	11	11	11	11
MNE	3	3	0	0	6	6	7	6	1
LAT	1	1	1	1	1	1	1	2	2
LIT	7	8	8	8	8	8	8	8	8
	216	227	253	261	274	269	272	268	251

Table A2: Number of companies per activity (by NACE classification) per year included in the study.

	2005	**2006**	**2007**	**2008**	**2009**	**2010**	**2011**	**2012**	**2013**
C10.7	5	5	3	3	5	5	4	4	2
C10.7.1	26	26	28	28	27	29	28	25	24
C10.8.2	16	16	17	18	21	21	20	21	20
C10.8.4	1	1	2	2	2	2	2	2	2
C10.6.1	29	29	31	34	33	32	31	33	29
C10.8.6	3	3	3	3	3	3	3	3	3
C10.5.2	1	1	1	1	1	1	1	1	1
C10.7.3	1	1	2	2	3	3	3	3	3
C10.8.9	3	3	5	6	7	6	9	9	8
C10.9.1	22	22	23	23	24	23	25	23	22
C10.9.2	5	5	5	5	6	6	6	6	6
C10.6.2	6	6	6	7	7	7	7	7	7
C10.8.1	14	14	15	15	18	16	17	17	16
C10.5.1	39	39	47	47	49	49	48	48	47
C10.2	7	7	7	8	9	9	9	8	8
C10.1.1	25	25	29	29	27	26	29	27	26
C10.3.1	2	2	2	2	2	2	2	2	2
C10.1.2	9	9	12	12	12	12	11	12	9
C10.1.3	13	13	15	16	18	17	17	17	16

Table A3: Efficient and 5 least efficient companies, 2005-2009.

2005	2006	2007	2008	2009
ROM124.C10.1.1	POL145.C10.1.3	ROM160.C10.6.2	POL51.C10.8.2	POL94.C10.9.2
CRO143.C10.1.3	SER169.C10.1.1	POL184.C10.1.3	SER120.C10.1.1	POL150.C10.8.2
POL192.C10.9.1	POL191.C10.9.1	POL206.C10.5.1	BUL194.C10.8.6	BUL157.C10.8.6
POL207.C10.8.1		ROM211.C10.1.1	ROM199.C10.1.1	ROM175.C10.5.1
		POL222.C10.9.1	POL228.C10.9.1	ROM177.C10.1.1
		ROM240.C10.1.3		ROM188.C10.1.3
		POL260.C10.3.1		POL239.C10.9.1
…	…	…	…	…
BIH133.C10.1.1	BIH1.C10.7	BIH179.C10.1.1	SER72.C10.6.1	SER78.C10.6.1
MNE161.C10.8.4	ROM154.C10.8.2	SER42.C10.7.1	LAT216.C10.2	BIH6.C10.6.1
SER61.C10.6.1	SER37.C10.8.2	SER74.C10.6.1	SER93.C10.6.2	ROM217.C10.6.1
BIH6.C10.6.1	BIH126.C10.1.1	ROM201.C10.6.1	SLK156.C10.8.1	ROM189.C10.1.3
SER59.C10.6.1	BIH4.C10.6.1	SER193.C10.9.1	ROM205.C10.7.1	BIH77.C10.6.1

Table A4: Efficient and 5 least efficient companies, 2010-2014.

2010	2011	2012	2013
ROM139.C10.1.1	SER55.C10.7.1	ROM127.C10.1.1	HUN8.C10.6.2
POL148.C10.1.1	SER110.C10.8.1	ROM159.C10.1.1	ROM78.C10.8.9
POL180.C10.1.3	ROM135.C10.1.1	ROM198.C10.6.1	ROM116.C10.1.1
BUL193.C10.8.6	MNE197.C10.1.1	SER273.C10.6.1	BUL157.C10.8.1
ROM203.C10.1.1	ROM200.C10.1.1		ROM161.C10.1.1
POL227.C10.1.3	POL233.C10.8.2		POL207.C10.8.2
POL233.C10.8.2	POL238.C10.9.1		SER257.C10.6.1
POL238.C10.9.1			
POL273.C10.1.2			
…	…	…	…
SER86.C10.6.1	POL219.C10.2	CZE 50.C10.7.1	POL24.C10.6.1
BIH1.C10.7	ROM152.C10.1.3	SER68.C10.8.2	HUN44.C10.1.1
SER85.C10.6.1	ROM180.C10.7.1	ROM38.C10.5.1	ROM38.C10.5.1
ROM211.C10.6.1	ROM206.C10.6.1	ROM171.C10.7.1	SER152.C10.9.1
ROM158.C10.1.3	POL226.C10.1.1	POL232.C10.2	ROM37.C10.5.1

Table A5: Average inefficiency of input (%).

	2005	2006	2007	2008	2009	2010	2011	2012	2013	
BIH	-12.47	-93.43	-54.31	-71.16	-71.55	-68.24	-89.83	-69.37	-61.04	-66.30
HUN	0.00	-51.63	0.00	-6.53	-4.20	-3.30	-44.64	0.00	0.00	-13.79
CRO	-4.74	-78.34	-17.33	-29.32	-31.67	-30.31	-62.47	-23.32	-3.32	-34.69
SLV	0.00	-87.01	-1.48	-3.56	-1.79	0.00	-82.84	-1.81	0.00	-22.31
SER	-1.74	-88.61	-26.01	-34.22	-36.78	-33.64	-77.00	-18.06	-14.22	-39.51
ROM	0.00	-59.87	-3.49	-19.73	-15.72	-18.17	-56.67	-11.36	-14.91	-23.13
CZE	0.00	-67.09	0.00	-2.42	-6.37	-6.67	-50.13	-4.07	-3.70	-17.09
POL	0.00	-47.32	-3.23	-13.00	-12.57	-8.13	-37.01	-5.59	-7.65	-15.86
BUL	0.00	-42.88	-6.83	0.00	-13.23	0.00	-45.95	-11.62	-4.18	-15.06
SLK	0.00	-86.68	-20.31	-27.10	-32.90	-31.38	-72.88	-18.95	-20.80	-36.27
MNE	-33.30	-92.81			-61.96	-69.62	-82.42	-74.93	0.00	-69.17
LAT	0.00	-93.18	-13.73	-87.51	-57.19	-32.91	-92.54	-9.04	-16.19	-48.26
LIT	0.00	-75.23	0.00	-5.55	-8.28	-8.30	-66.28	-3.45	-7.47	-20.89
	-4.02	-74.16	-12.23	-25.01	-27.25	-23.90	-66.20	-19.35	-11.81	

Table A6: Average inefficiency of ROA (%).

	2005	2006	2007	2008	2009	2010	2011	2012	2013	
BIH	132.62	202.75	95.25	44.51	180.67	87.99	24.95	27.55	57.74	99.53
HUN	61.85	154.15	64.06	30.88	60.27	54.57	23.12	19.33	45.07	58.53
CRO	75.76	117.78	68.16	23.89	57.40	54.77	21.51	24.26	44.97	55.44
SLV	99.31	178.00	78.30	28.39	67.17	64.45	24.76	25.35	52.31	70.72
SER	130.10	210.06	89.24	36.81	73.81	71.13	19.59	24.73	46.22	81.93
ROM	71.17	149.79	67.95	66.78	187.90	74.18	26.33	21.96	50.27	83.26
CZE	64.00	151.69	68.51	27.62	61.50	50.22	18.84	18.45	36.53	57.60
POL	55.45	98.12	50.72	29.10	56.19	39.77	18.95	18.90	34.95	45.90
BUL	60.21	74.20	53.84	24.77	46.49	38.94	18.16	16.70	27.88	41.66
SLK	150.02	166.41	79.19	41.93	63.50	61.68	21.65	22.11	45.22	75.81
MNE	135.35	184.93			67.16	88.34	22.23	30.35	48.75	88.06
LAT	99.33	250.19	79.78	0.00	75.48	51.94	22.03	28.03	49.93	75.85
LIT	58.88	118.77	68.26	29.79	57.70	44.91	19.59	19.18	36.39	52.14
	91.85	158.22	71.94	32.04	81.17	60.22	21.67	22.84	44.33	

Table A7: Average inefficiency of profit margin (%).

	2005	2006	2007	2008	2009	2010	2011	2012	2013	
BIH	79.26	44.78	281.26	145.80	169.59	87.99	28.68	41.88	85.22	107.16
HUN	27.23	26.89	60.99	29.82	57.04	53.67	24.22	29.04	45.07	39.33
CRO	29.28	19.22	66.83	23.86	55.33	52.77	36.07	37.24	44.97	40.62
SLV	33.85	28.11	78.30	28.39	67.17	64.45	25.54	41.09	52.31	46.58
SER	49.98	33.41	85.23	43.61	72.96	72.64	26.69	53.01	97.32	59.43
ROM	29.35	26.01	72.35	52.22	77.77	88.60	33.93	49.74	53.95	53.77
CZE	26.91	25.99	63.10	26.42	57.31	49.26	20.25	26.69	37.08	37.00
POL	25.25	21.16	50.09	27.23	46.72	38.34	20.23	28.16	34.87	32.45
BUL	23.71	16.48	53.84	24.77	43.70	38.94	18.83	23.00	27.88	30.13
SLK	42.78	24.71	79.19	41.93	63.50	61.68	26.38	33.47	45.22	46.54
MNE	76.80	34.08			67.16	65.20	29.64	299.42	48.75	88.72
LAT	33.45	37.07	79.78	131.69	75.48	51.94	23.11	45.77	49.93	58.69
LIT	27.62	23.84	68.26	29.79	57.70	44.91	21.48	28.79	36.39	37.64
	38.88	27.83	86.60	50.46	70.11	59.26	25.77	56.71	50.69	

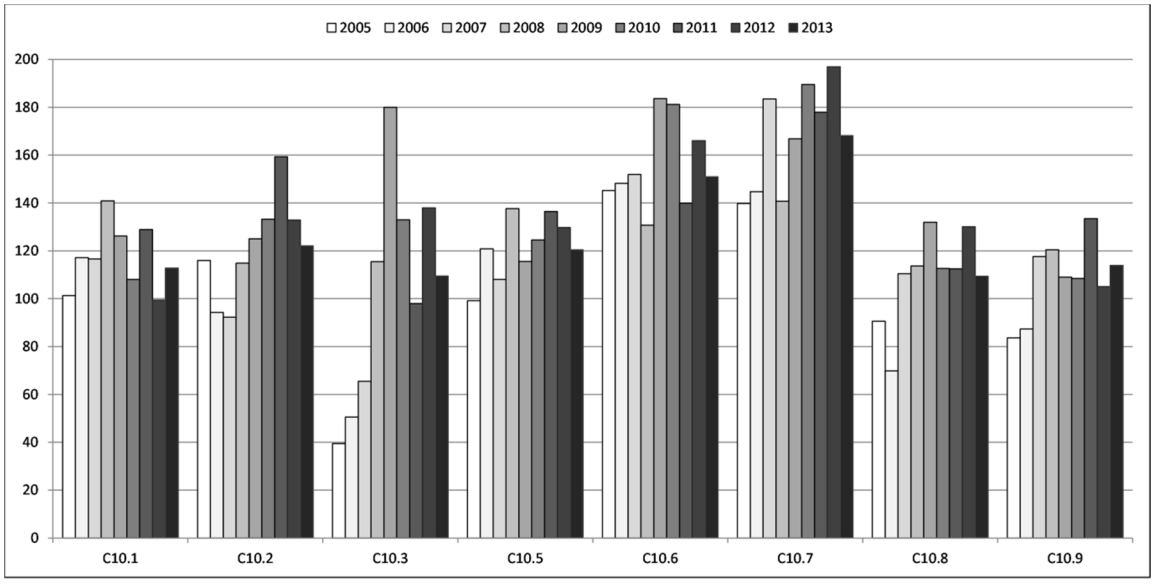

Figure A1: Rankings of food industry subsectors by years.

Survey of Reverse Logistics Practices
The Case of Portugal

Ricardo Simões[1], Carlos Carvalho[2], Ricardo Félix[2] and Amílcar Arantes[3]
[1]*Instituto Superior Técnico, Universidade de Lisboa, Av. Rovisco Pais, Lisboa, 1049-001, Portugal*
[2]*Logistema, Alameda dos Oceanos, 31 1.02.1.1, Lisboa, 1990-207, Portugal*
[3]*CERIS, CESUR, Instituto Superior Técnico, Universidade de Lisboa, Av. Rovisco Pais, Lisboa, 1049-001, Portugal*
ricardo.campino.simoes@tecnico.ulisboa.pt, {ccarvalho, ricardo.felix}@logistema.pt, amilcar.arantes@tecnico.ulisboa.pt

Keywords: Reverse Logistics, Supply Chain Management, Survey.

Abstract: Reverse Logistics (RL) has gained substantial relevance in the field of supply chain management, mainly because RL combines environmental, economic and social factors. Although there are studies on RL practices, none of these studies are related to the Portuguese case. Therefore, a survey was conducted in Portugal to fill this gap. This study was applied to a group of Portuguese companies of four industrial sectors. These four sectors are highly diversified, regarding the way RL is managed. The results demonstrate that companies consider the management of RL important. The most common practice used is the proper disposal of returned products. The companies mainly adopt RL due to the benefits associated with the improvement of customer satisfaction and the reduction in logistics costs. The biggest barrier to the implementation of RL is a lack of strategic planning by the companies on handling returned products. The main reason affecting the performance of RL activities is the lack of quality of the returned product. The study also allowed to estimate the volume of returned products and the costs of RL.

1 INTRODUCTION

Currently, the world faces growing uncertainty on the demand of consumers. Adding to that, the national economic situation represents an aggravating factor for the Portuguese market. Furthermore, the seasonality of the sales and the implementation of various campaigns and promotions throughout the year are also responsible for an increased difficulty in making accurate forecasts for the consumer demand. On other hand, the operations of Reverse Logistics (RL) decisively contribute to the value and competitiveness of enterprises, where margins and profitability are increasingly lower, therefore the challenge is to transform costs in added value to the supply chain management. Hence, it is increasingly important to consider RL essential and stop labelling it as "the forgotten child of the supply chain" (Morrel, 2001).

The poor implementation of RL systems have disastrous effects for businesses and cause high costs in transportation and storage, increase processing times and accumulation of products with no destination, conflicts with customers/suppliers, legal and environmental issues. This lack of planning and implementation of RL systems is a reality in Portugal, making the costs of RL relatively high (Logistica Moderna, 2013). One of the major difficulties for companies is how to effectively and economically collect all the products from the place where they are no longer desired and transfer them to a place where they can be processed, reused or recovered. There are several studies on RL practices, but none contemplates the Portuguese context. This work, "survey of RL practices in Portugal", intends to contribute and fill this gap.

2 LITERATURE REVIEW

In the past, RL was only seen as a cost for the companies, however the perspective on RL is shifting markedly whether by its economic value gained in reusing used products, or by using used components in the manufacture of new products (Savaskan and Van Wassenhove, 2006). With concerns about product returns and proper implementation of RL systems, the academic community has been studying this area and as a result, in recent years, increasingly more scientific articles on this subject have been published (Rubio et al., 2008).

Simões, R., Carvalho, C., Félix, R. and Arantes, A.
Survey of Reverse Logistics Practices - The Case of Portugal.
In *Proceedings of the 6th International Conference on Operations Research and Enterprise Systems (ICORES 2017)*, pages 393-400
ISBN: 978-989-758-218-9

In the early nineties, the first definition of RL emerges. Stock (1992) emphasised the recovery aspects of RL, defining as: "... the term often used to refer to the role of logistics in recycling, waste disposal, and management of hazardous materials; a broader perspective that includes all logistics activities such as recycling, substitution, reuse of materials and disposal of products". Furthermore, Rogers and Tibben-Lembke (1998) summarize RL as the process of moving goods from the final destination to another point in the supply chain, in order to capture unavailable value. More recently, Pokharel and Muha (2009) stated that the focus of RL refers to the waste management, recycling of materials, recovery of components or product recovery. According to the authors RL involves a paradigm shift in terms of product life-cycle. Traditionally the life cycle of a product was between the period of its manufacture and its disposal ("cradle-to-grave"). Currently RL allows a change of the product life cycle, from the period of manufacture to its recovery ("cradle-to-cradle").

Companies have been using more liberal return policies in order to reduce the risk of the final customers and thus increase sales volume (Smith, 2005). In the United States, the estimates are even more significant with the annual costs about $ 100 billion for the manufacturers and retailers corresponding to a reduction in the yield at about 3.8% (Blanchard, 2007), while Greve and Davis (2012) state that the electronics industry is over 14 billion dollars, as well as the rates of returns of the end customers ranging from 5% to 9% of sales for most retailers.

Implementing an effective system generate multiple benefits for businesses, including increased customer satisfaction level, reducing the level of investment in resources, and reduce storage and distribution costs (Andel, 1997). Thus, the integration of RL in supply chains is increasingly used as a strategy to increase profits or to promote sustainability and customer satisfaction (Du and Evans, 2008). That said, Brito and Dekker (2003) identify the main reasons that lead companies to adopt RL operations:

- Economics – RL programs can bring direct gains through lesser use of raw materials, reduction in disposal cost, etc. Companies also have indirect gains due to competition, environmental image, improve customer-supplier relations, etc;
- Legislation - refers to any jurisdiction that indicates that a company should recover all the products produced by them or own responsibility for end-of-life products. With the growing concern for the environment, laws have been emerging in European, that forced companies to develop their RL processes with the introduction of quotas for the recovery, recycling and packaging;
- Corporate citizenship - concerns a set of values and principles that motivate an organization to become involved responsibly in RL activities. This motivation arises from the need to hold a responsible and conscientious stand towards environmental issues.

The activities of a RL network in supply chains may differ, such as, type of products returned, the desired recovery and the logistics network implemented. We can essentially identify 5 groups of recurrent activities in various supply chains with RL (Prahinski and Kocabasoglu 2006; Barker and Zabinsky 2008; Silva et al. 2013). These groups are: acquisition of products, collection of products, inspection and disposal, recovery and distribution and resale.

Ravi and Shankar (2005) studied the main barriers to the implementation of RL operations in the automotive industry. They concluded that there are five main barriers, lack of knowledge of RL, lack of commitment by managers, problems with product quality, lack of strategic planning and financial constraints. However, the lack of knowledge regarding RL practices is the most significant barrier. Therefore, managers should focus on the development of their awareness on the use of RL.

Aberdeen Group (2006) conducted a study on RL based on a survey of 175 companies from various continents. The aim of this study was to analyze the best management practices on RL. From the companies surveyed, 61% mentioned that effective management of RL is very important. The authors also found that companies spend about 9% of sales in costs related with RL.

According to a study by Chan and Chan (2008), successful RL systems may result in greater customer loyalty and reduced operating costs due to the reuse or replacement of products. Their study consisted of a total of 73 companies of the mobile industry in Hong Kong and 34 interviews. This research showed that companies in this sector consider RL important, but compared to other issues RL importance is smaller and this is the biggest barrier to the implementation of RL.

Finally, Ravi and Shankar (2015) developed a study, based on a survey of 105 companies in India, where they investigated RL practices in four sectors of the Indian industry: automotive, paper, food and

electronics. They concluded that the adoption of RL practices is crucial and RL should be integrated at a strategic level and also found that the volume of returned products is a critical factor to RL implementation. Nevertheless, the most important factor to RL implementation is the economic benefit associated.

The main objective of this work is to assess the perception of RL practices in the Portuguese context. In order to achieve this goal, the following research questions (RQ) were addressed: RQ1 - What are the most common RL practices in the Portuguese industry?; RQ2 - What are the main reasons that lead companies to the adoption of RL practices?; RQ3 - What are the main barriers experienced by companies in implementing RL practices?; RQ4 - What are the main reasons affecting RL performance? Accordingly, the work presented herein contributes to expanding the knowledge on RL, in Portugal.

3 RESEARCH METHOD

For this work, a questionnaire survey methodology was used to determine the perception on RL practices in the Portuguese context. The questionnaire was designed to obtain answers to all research questions previously presented. The questions were based on other published works (Andel, 1997; Daugherty, Richey, Genchev, & Chen, 2005; Ravi & Shankar, 2005; Ravi V & Shankar, 2015; Rogers & Tibben-Lembke, 1998; Tibben-Lembke, 2002; Tibben-Lembke & Rogers, 2002), and addresses issues such as the RL practices, reasons to adopt, barriers and performance difficulties. The five point Likert scale was considered appropriate for the evaluation of this type of issues.

The initial questionnaire that resulted from the literature review was validated by a group composed of one teacher, two researchers and two senior consultants specialists in SCM. Later the corrected and improved questionnaire was used in a pilot test envolving five companies. After the pilot, some of the questions were modified to convey their intended meaning and a few other questions were deleted.

In this work, four sectors of Portugal industries dealing with RL operations were selected for this survey: Food Industry (FI), Automotive Industry (AI), ConsumersElectronics (CE) and Manufacturing (Mf) (metallurgical, energy, textile, paper and wood). In the FI, RL has a unique role with regard to food safety. With return policies for food products, companies allow the return of defective or out of date products, preventing infection or intoxication problems. AI is one of the most dynamic and important sectors in Portugal economy. RL is very important, due to the type of returns (defective product, etc.), as well as the reuse of the main components and subsequent resale. In the CE, the kind of product commercialized has short life cycle due to software updates, among others, that originates a high rate of replacement or removal. The very nature of the products makes them obsolete because of the introduction of new equipment and this is the major challenge (Chan and Chan, 2008). Currently, the Mf is losing importance and it is necessary to achieve its revitalization by modernizing their production processes. This is where RL enters since it allows for the reduction of costs and less use of raw materials.These four sectors are highly diversified in nature with respect to how they operate their RL programs.

Most of the companies selected to compose the sample were identified by Logistema, a consultant partner in this study. In total, 225 companies operating in Portugal were identified for the survey. The survey was conducted in May-September 2016. Questionnaires were sent via email to logistics directors and, in some case, to general email addresses, with information about the study, identifying the objectives and scope of the work, and with a link to the questionnaire. Reminders were sent to all the non-respondents. In addition, phone calls were made in order to increase the number of responses to the questionnaire.

4 RESULTS AND DISCUSSION

The analysis was carried out using a statistical software (SPSS) and consisted essentially of ranking the variables based on mean values and frequency distributions. The objective was to test if the mean values of the dependent variables (assumed as normally distributed) differ among the categories. The following procedure was adopted:

- Test the reliability and internal consistency of responses, Cronbach's coefficient (α), for questions on a Likert scale. In this research a Cronbach's $\alpha>0.6$ was considered as acceptable, as it is an exploratory study (Hair et al., 2010);
- The T-test was used to test the "indifferent" value of the overall means, which is the value in the measuring scale that represents a shift in the perception;
- The Levene F homogeneity test was used to verify that the variances of the dependent

variables are similar; If the Levene F statistic has a significance value greater than 0.05 then ANOVA is performed; If the Levene F statistic had a significance value lower than 0.05, which means the variances of the dependent variables are not similar, then the Welch test is used, because is a more robust test for equality of means;

- Finally, when the average values of the dependent variable differ between the categories considered, the post-hoc Tukey test is applied to determine which categories differ.

4.1 Sample

Of a total of 225 questionnaires sent, 43 questionnaires were received (Table 1). This gives an overall response rate of 19.2%. This situation is common in surveys via email and can lead to non-response bias (Kypri et al, 2004; Sax et al, 2003). To test for non-response bias, we compared the sectors distribution of potential respondents (those whom the survey was sent electronically) with the distribution of sectors that effectively answered the questionnaires. Using the $\chi 2$ test, it was determined that there is no statistically significant difference between the sectors, which might indicate a low non-response bias.

Out of 43 usable responses, the food industry accounts for 51.2% of the answers, manufacturing industry and automotive industry accounts for 18.6%, electronic sector 11.6%. In terms of employees, 28 companies had more than 250 employees, 12 in the range of 51-250 and 3 companies had fewer than 50 employees. In relation to the companies' sales volume in the last year, 35% of companies had a turnover between 50 and 250 million euros, 30% had sales of over 500 million euros, 21% between 250-500 million euros, and 14% shows sales lower than 50 million euros. The distribution of firms by the different sectors show that 73.9% of respondents are positioned as producers, 10.9% are positioned as retailers, and 8.7% are wholesalers.

Table 1: Survey respondent distribution.

Industrial Sector	Potential Respondents		Respondents	
	Frequency	%	Frequency	%
Food	94	41.8	22	51.2
Electronics	51	22.7	5	11.6
Automotive	49	21.7	8	18.6
Manufacturing	31	13.8	8	18.6
Total	225	100	43	100

4.2 General Issues

The importance that companies give to RL management is revealed by 33% of the responses, that sees RL with the utmost importance, but for 26% of respondents RL is "indifferent", and only 5% of the companies surveyed claim to RL as "Not Important". With the results we can say that RL in Portugal is important and aligned with previously studies such as the study by the Aberdeen Group (2006), which stated that the majority of companies surveyed (60%) considered that effective management of RL it is extremely important to the overall performance. Also, there is no significant difference between sectors.

RL offers many benefits (Table 2), including: improve logistics efficiency and reduction of logistics cost. With 53.5% of the replies (23 responses each option). The less observed benefits are "Improved employee productivity" with only 2.3% of respondents and "Increase on turnover " with 9.3% of the answers. These results meet expectations of the literature review.

Table 2: Observed benefits.

Benefit	N. of responses
Improve logistics efficiency	23
Reduction of logistics costs	23
Improve relations/satisfaction with partners	22
Improved company image	21
Lower costs resulting from better planning	19
Minimising waste (eco-friendly)	16
Improvement on asset recovery	11
Lower costs in processing of returned products	8
Increase of net sales	4
Improve employee productivity	1

The volume of returned products that are recovered was measured in this work (Table 3). With 26% of companies stated that they recover more than 50% of returned products, this reveals a growing trend of RL practices and awareness of entities to minimize the costs on raw materials. Unfortunately, 30% of the managers could not estimate a value, this shows difficulties for companies to observe the value recovered from returned products.

Table 3: Estimate of the value recovered.

Value (%of the returned product)	Frequency (%)
Not aware	30
More than 50%	26
Less than 5%	21
Between 26% - 50%	14
Between 6% - 25%	9

The respondents were enquired to estimate the costs of RL according to the volume of sales (Table 4). Most companies (about 70%), stated costs lower than 2% of total sales volume. While 19% of respondents indicate that they have no knowledge on this subject and can´t estimate a value, which reveals a lack of visibility of total costs. However, 5% of the companies surveyed say that RL costs are more than 10% of total sales volume. The values obtained in general support the values presented in the literature review. Logistica Moderna (2013) stated that 23% of companies in Portugal had an RL cost of less than 3% of the sales volume, while Greve and Davis (2012) reported values close to 4%. These values are aligned and even exceed the values of previous studies, this allows us to assume that companies have greater knowledge on this topic and have an optimized system that manages the reverse flow, but on the other hand, may show a lack of visibility by managers on the real cost.

Table 4: Costs of reverse logistics.

Costs (% sales volume)	Frequency (%)
Less than 2%	70
Not aware	19
More than 10%	5
Between 2% - 5%	5
Between 5% - 10%	2

The vast majority of respondents already have RL software implemented and operational. On the negative side, investment in new infrastructures specialized in RL management and R&D on new techniques, companies have no plans to invest in the short term.

4.3 Adoption of RL Practices

RL encompasses all the activities in managing and controlling the reverse flow of products from the customer to the manufacturer, for product recovery or proper disposal. Regarding to the frequency which companies execute these practices, the option with the highest score is "Proper disposal of returned products" with 4.05, followed by "Training of employees" with 3.81 points, on other hand the least common practice is "Product collection" with 3.02 points, as can be seen in Table 5. The item "Resale of returned products" was eliminated by the Cronbach's alpha (α). The results show that there is no statistical difference at a significance level of 5% between the most common practices and sectors. However, analyzing the table the most used practice in FI, CE and AI is the "Proper disposal of returned products" while for the Mf sector is the "Training of employees". These results can be explained because not all products can be easily recycled. At this stage, the products are destroyed for lack of knowledge of new value recovery methods and lack of training of employees who send the product for destruction without trying to recapture value from it.

4.4 Reason to Adopt RL

The most important reason for RL adoption perceived by the respondents was to "Improve customer satisfaction", with a score of 4.23, the second most important reason was to "Reduce logistics costs" with 4 points (Table 6). The reason perceived with least importance to companies is the "Lifecycle of products" with a score of 2.86. Most of the implementation factors to RL differ from the score 3 ("indifferent" in a scale of importance), except "Reduce stocks" and "Lifecycles of Product". The results show no significant difference (at the 5% significance level) between the reasons to adopt RL and sectors. By observing the values obtained, is clear that the main reason for companies to implement RL operations is the need to improve customer satisfaction.

4.5 Barriers to RL Adoption

The practice of RL is not free from barriers, so efficient management of these barriers can result in successful RL systems. Table 7 presents the barriers to RL adoption by sector.

The biggest barrier identified by respondents is the "lack of strategic planning related to reverse logistics" with 3.58. The option with the lowest score,

Table 5: Adoption of reverse logistics practices by sector.

Practices	Type of sector (Cronbach's α = 0.62)*				Global	ANOVA	Welch
	FI	CE	AI	Mf		Sig.	Sig.
Proper disposal of returned products	4.00	4.00	4.38	3.88	4.05	0.815	
Training of employees	3.73	3.40	3.88	4.25	3.81	0.313	
Recapturing value from returned products	3.45	3.00	3.75	3.00	3.37	0.511	
Product collection	3.00	3.20	3.50	2.50	3.02		0.184

* Values on a Likert scale of 5 points (1 - Never; 5 – Always).

with 3.02 points, is the "lack of technological systems" which reveals that for companies, technological systems are not the reason for a non-implementation of RL.

Most of the barriers identified differ from the score 3 ("indifferent" in a scale of importance), except "financial constraints" and "lack of technological systems" with significance values less than 5%, as can be observed by T-test. Also, the results show no significant difference at a significance level of 5% between the barriers and the sectors. Is possible to see, that among the sectors studied, CE ranks with a bigger degree of importance in the barriers "lack strategic planning related to reverse logistics" and "lack of training". FI identifies the lack of training of its employees as the biggest barrier. On the other hand, the Mf ranks budget constraints and lack of strategic planning as most significant barriers. As for AI the greatest barriers to RL is lack of training, lack of interest by managers and importance of reverse logistics in relation to other matters"

4.6 Causes Affecting Rl Performance

Measuring the performance of any system is essential to enable improvements in management processes. This is especially important in the management of RL, since it is characterized by high uncertainty in the quality, quantity and timing of the returned products, making the performance measurement a tricky task. The results are shown in Table 8, where we can see that the "uneven returned product" and "difficulty in predicting returns" have the higher scores with 3.88 and 3.83 points, respectively. On the other hand the "marketing difficulty of products used" with 2.81, is identified as a reason that least affects RL. "uneven returned product", "difficulty in predicting returns", "visibility/viability of costs" and "transportation from many sites to one/few places" obtained a different score of 3 ("indifferent"), as can be observed by the T-test.

The results also reveal that there is no statistically significant difference between the reasons and sectors. CE sector, ranks higher on the importance scale for the factor "uneven returned product", but the difference in scores between this sector and the remaining are not significant in order to extrapolate conclusions, but it is important to note this difference.

5 CONCLUSION

This research examines the perceptions of Reverse Logistics (RL) in Portuguese companies through a questionnaire-based survey. The results show that Portuguese companies considered implementing RL

Table 6: Reasons to reverse logistics adoption.

Reasons	Type of sector (Cronbach's α = 0.83)*				Global	T-Student Sig.**	ANOVA Sig.
	FI	CE	AI	Mf			
Improve customer satisfaction	4.23	4.40	4.13	4.25	4.23	0.000	0.947
Reduce logistics costs	4.14	3.80	3.75	4.00	4.00	0.000	0.727
Legal requirements	4.14	4.40	3.75	3.25	3.93	0.000	0.250
Recapturing value of returned products	3.73	4.00	3.50	3.88	3.74	0.000	0.803
Increasing competitiveness	3.73	4.20	3.50	3.50	3.70	0.000	0.598
Reduce stocks	3.32	3.60	3.25	3.38	3.35	0.058	0.962
Lifecycles of Product	3.09	2.40	2.88	2.50	2.86	0.421	0.474

* Values on a Likert scale of 5 points (score of 1 indicates a low importance and 5 a higher one).
** T-Student test for overall means (test value = 3 "indifference").

Table 7: Barriers to RL adoption by sector.

Barrier	Type of sector(Cronbach's α = 0.85)*				Global	T-Student Sig.**	ANOVA Sig.
	FI	CE	AI	Mf			
Lack of strategic planning related to RL	3.50	3.80	3.50	3.75	3.58	0.002	0.926
Lack of training	3.64	3.80	3.63	2.88	3.51	0.002	0.197
Lack of interest by decision makers	3.41	3.60	3.63	3.63	3.51	0.012	0.956
Relations with partners	3.45	3.60	3.50	3.38	3.47	0.012	0.990
Importance of RL in relation to other issues	3.41	3.20	3.63	3.50	3.44	0.007	0.909
Financial constraints	3.05	3.60	3.38	3.75	3.30	0.108	0.501
Lack of technological systems	3.05	2.60	3.50	2.75	3.02	0.898	0.514

* Values on a Likert scale of 5 points (score of 1 indicates a low importance and 5 a higher one), α=0.85
** T-Student test for overall means (test value = 3 "Indifferent")

Table 8: Causes that affect the realization of reverse logistics by sector.

Causes	Type of sector(Cronbach's α = 0.82)*				Global	T-Student	ANOVA
	FI	CE	AI	Mf		Sig.**	Sig.
Uneven returned product	3.86	4.60	3.63	3.75	3.88	0.000	0.323
Difficulty in predicting returns	4.00	4.00	3.25	3.88	3.83	0.000	0.389
Visibility/Viability of costs	3.86	3.80	3.38	3.63	3.72	0.000	0.606
Transportation from many places to one/few places	3.36	3.80	3.25	3.88	3.49	0.002	0.574
Poor inventory management	3.32	3.20	3.25	3.38	3.30	0.079	0.955
Product lifecycle issues	3.32	2.80	2.75	2.75	3.05	0.789	0.364
Lack of clarity in relation to the disposal options	3.36	3.20	2.63	2.38	3.02	0.901	0.161
Difficulties in marketing used products	2.82	3.40	2.38	2.88	2.81	0.263	0.416

* Values on a Likert scale of 5 points (score of 1 indicates a low importance and 5 a higher), α=0.82

** T-Student test for overall means (test value = 3 "Indifferent")

programs in their organization as a strategic-level decision, as RL programs involve significant allocation of capital and resources.

The findings show that organizations with higher volume of returned products tend to develop expertise in operating their RL programs, which is well aligned with the literature. Although, the literature indicates that economic, ecological and legislative are the drivers that initiate RL activities, in the case of the Portuguese companies, the adoption of RL is mainly perceived as associated to economic benefits .

Interestingly, the findings indicated that Portuguese companies have already invested in terms of EDI, RL softwares, new logistic resources, etc., which is a good step in the right direction to adopt RL. These findings are aligned with the literature that consider the technologies for tracking and tracing of products essential for successful RL programs. On the other hand, companies do not have plans to invest in the short term.

The main implications of this work are as follows:

- Managers need to consider integration of collection, inspection and consolidation of used products with forward logistics in RL programs:
- Managers should reinforce the training of their staff on new recovery methods in order to reduce the destruction of returned products without trying to recapture the value associated;
- Enhancing customer satisfaction and reducing logistics costs should be considered key in improving the level of RL adoption;
- The strategic planning of RL should not be neglected by managers;
- Companies should support RL on extended information systems that allow the effective exchange of information between forward flow and reverse flow in the supply chain to ensure good RL management.

For further work/research, it is recommended to repeat this study, but considering a bigger sample size. Also, it would be useful to hold interviews with the entities and their partners in order to understand the motivation factors and the vision that each party provides for the implementation of RL strategies.

The present work has some limitations, mainly the small sample size, which reduces the generalization of the findings. However, it is believed that the work presented expands the knowledge in the RL field by addressing this topic in the Portuguese context thus adding a relevant and empirical study to the literature.

REFERENCES

Aberdeen Group, 2006. *Revisiting Reverse Logistics in the Customer-Centric Service Chain*.

Andel, T, 1997. Reverse logistics: a second chance to profit. *Transportation & Distribution*, vol. *38*, no. 7, pp. 61–66.

Barker, T. J. and Zabinsky, Z. B., 2008. Reverse logistics network design: a conceptual framework for decision making. *International Journal of Sustainable Engineering*, vol. 1, no. 4, pp. 250–260. doi:10.1080/19397030802591196

Blanchard, D., 2007. Supply Chains Also Work In Reverse. *Industry Week,* vol.1, pp. 48-49.

Brito, M. P. de and Dekker, R., 2003. *A Framework for Reverse Logistics*, pp. 29. Rotterdam.

Brito, M. P. de, Dekker, R. and Flapper, S. D. P., 2005. Reverse Logistics: A Review of Case Studies. In B. Fleischmann & A. Klose (Eds.), *Distribution Logistics*, vol. 544, pp. 243–281. Berlin, Heidelberg: Springer Berlin Heidelberg. doi:10.1007/978-3-642-17020-1

Chan, F. T. S. and Chan, H. K., 2008. A survey on reverse logistics system of mobile phone industry in Hong Kong. *Management Decision*, vol. 46, no. 5, pp. 702–708. doi:10.1108/00251740810873464

Daugherty, P. J., Richey, R. G., Genchev, S. E. and Chen, H., 2005. Reverse logistics: Superior performance through focused resource commitments to information technology. *Transportation Research Part E: Logistics*

and Transportation Review, vol. 41, no. 2, pp. 77–92. doi:10.1016/j.tre.2004.04.002

Du, F. and Evans, G. W., 2008. A bi-objective reverse logistics network analysis for post-sale service. *Computers & Operations Research*, vol. 35, no. 8, pp. 2617–2634. doi:10.1016/j.cor.2006.12.020

Greve, C., and Davis, J. (2012). *Recovering lost profits by improving reverse logistics*. *UPS White paper*.

Hair, J. F., Black, W. C., Babin, B. J. and Anderson, R. E., 2010. *Multivariate Data Analysis,* Prentice Hall. New Jersey, 7th edition.

Kypri, K., Stephenson, S. and Langley, J., 2004. Assessment of Nonresponse Bias in an Internet Survey of Alcohol Use. *Alcoholism: Clinical & Experimental Research*, vol. 28, no. 4, pp. 630–634. doi:10.1097/01.ALC.0000121654.99277.26

Logistica Moderna., 2013. Estudo Supply Chain em Portugal, pp. 70–73.

Morrel, A. L., 2001. 'The forgotten child of the supply chain'. *Modern Materials Handling*, vol. *56*, pp. 33–36.

Pokharel, S. and Mutha, A., 2009. Perspectives in reverse logistics: A review. *Resources, Conservation and Recycling*, vol. 53, no. 4, pp. 175–182. doi:10.1016/j.resconrec.2008.11.006

Prahinski, C. and Kocabasoglu, C., 2006. Empirical research opportunities in reverse supply chains. *Omega*, vol. 34, no. 6, pp. 519–532. doi:10.1016/j.omega.2005.01.003

Ravi, V. and Shankar, R., 2005. Analysis of interactions among the barriers of reverse logistics. *Technological Forecasting and Social Change*, vol. 72, no. 8, pp. 1011–1029. doi:10.1016/j.techfore.2004.07.002

Ravi, V. and Shankar, R., 2015. Survey of reverse logistics practices in manufacturing industries: an Indian context. *Benchmarking: An International Journal*, vol. 22, no. 5, pp. 874–899. doi:10.1108/BIJ-06-2013-0066

Rogers, D. and Tibben-Lembke, R. (1998). *Going Backwards : Reverse Logistics Trends and Practices*. Reverse Logistics Executive Council.

Rubio, S., Chamorro, A. and Miranda, F. J., 2008. Characteristics of the research on reverse logistics (1995–2005). *International Journal of Production Research*, vol. 46, no. 4, pp. 1099–1120. doi:10.1080/00207540600943977

Savaskan, R. C. and Van Wassenhove, L. N., 2006. Reverse Channel Design: The Case of Competing Retailers. *Management Science*, vol. 52, no. 1, pp. 1–14. doi:10.1287/mnsc.1050.0454

Sax, L. J., Gilmartin, S. K. and Bryant, A. N., 2003. Assessing Response Rates and Nonresponse Bias in Web and Paper Surveys. *Research in Higher Education*, vol. 44, no. 4, pp. 409–432. doi:10.1023/A:1024232915870

Silva, D. A. L., Santos Renó, G. W., Sevegnani, G., Sevegnani, T. B. and Serra Truzzi, O. M., 2013. Comparison of disposable and returnable packaging: a case study of reverse logistics in Brazil. *Journal of Cleaner Production*, vol. 47, pp. 377–387. doi:10.1016/j.jclepro.2012.07.057

Smith, A., 2005. Reverse logistics programs: gauging their effects on CRM and online behavior. *VINE*, vol. 35, no. 3, pp. 166–181. doi:10.1108/03055720510634216

Tibben-Lembke, R. S., 2002. Life after death: reverse logistics and the product life cycle. *International Journal of Physical Distribution & Logistics Management*, vol. 32, no. 3, pp. 223–244. Retrieved from http://www.emeraldinsight.com/doi/full/10.1108/09600030210426548

Tibben-Lembke, R. S. and Rogers, D. S., 2002. Differences between forward and reverse logistics in a retail environment. *Supply Chain Management: An International Journal*, vol. 7, no. 5, pp. 271–282. doi:10.1108/13598540210447719

Mathematical Modeling Approaches to Solve the Line Balancing Problem

Shady Salama[1], Alyaa Abdelhalim[2] and Amr B. Eltawil[1]
[1]*Industrial Engineering and Systems Management, Egypt-Japan University of Science and Technology (E-JUST), New Borg Elarab City, Alexandria 21934, Egypt*
[2]*Production Engineering Department, Industrial Engineering Division, Alexandria University 21544, Alexandria, Egypt*
{shady.salama, eltawil}@ejust.edu.eg, alyaa.adil@gmail.com

Keywords: Framework, Review, Survey, Assembly Line, Line Balancing, Mathematical Model.

Abstract: The assembly line balancing problem belongs to the class of NP-hard combinatorial optimisation problem. For several decades' line balancing took attention of researchers who are trying to find the solutions for real world applications. Although tremendous works have been done, the gap still exists between the research and the real problems. This paper provides analysis of about 50 papers that used mathematical modeling in solving line balancing problems. Thereafter, a framework is proposed for future work.

1 INTRODUCTION

Assembly lines consist of a number of workstations that are arranged through a material handling equipment where tasks are assigned, and the workpieces are moving from one station to another until the final product is produced. The workstations are equipped with all required machines and skilled operators to perform specific tasks without violating cycle time, which represents the time between two consecutive units produced from the assembly line based on specific production plan. From the first day that Henry Ford introduced assembly line for a mass production in this company, the researchers are seeking for the optimal way to assign all tasks to workstations that is called Assembly Line Balancing Problem (ALBP) without violating assignment constraints (such as precedence constraints). (Dolgui & Battaı 2013). For instance, when we increase the balance of workload among workstations that will lead to increase productivity by removing bottlenecks and reducing idle time. Each task has a particular time to perform called processing time and the workstation time is the sum of all processing times for all assigned tasks. Figure (1): An illustrative example for assembly line balancing problem.
Salveson made the first mathematical model formulation for assembly line balancing problem (Salveson 1955), and from this day the ALBP has become an attractive topic for more research.

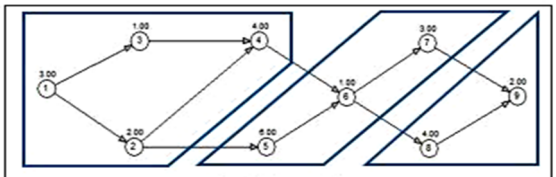

Cycle Time = 10

Tasks	Processing time	Preceding task	workstation
1	3	-	1
2	2	1	
3	1	1	
4	4	2,3	
5	6	2	2
6	1	4,5	
7	3	6	
8	4	6	3
9	2	7,8	

Figure 1: Assembly line balancing problem.

The ALBP is an NP-hard combinatorial optimisation problem (Gutjahr & Nemhauser 1964) and the widely used objective functions are to minimise the number of workstations with fixed cycle time (SALBP-1), minimise the cycle time with fixed number of workstations (SALBP-2) and maximize line efficiency (SALBP-E). The ALBP can be classified based on Industrial environment (Machining, Assembly, Disassembly). Another classification considers the number of product models in the line (Single model, Mixed model, Multi-model). The line layout is also a different theme of classification (Basic straight line, Straight lines with multiple workplaces, U-shaped lines, Lines with the circular transfer, Asymmetric lines). Last but not least the nature of task times (Deterministic – Stochastic)

Salama, S., Abdelhalim, A. and Eltawil, A.
Mathematical Modeling Approaches to Solve the Line Balancing Problem.
In *Proceedings of the 6th International Conference on Operations Research and Enterprise Systems (ICORES 2017)*, pages 401-408
ISBN: 978-989-758-218-9

(Dolgui & Battaı 2013) (Sivasankaran & Shahabudeen 2014a).
In the past, the single-model lines were commonly used for producing large and homogeneous products, so it was a daunting task to provide any customized products. Nowadays, due to the increasing demand and competition for creating customised products, a large number of traditional lines are replaced by mixed-model lines to keep up with current market trends (Vilarinho & Simaria 2002) (Dong et al. 2014). On the other hand, the multi-model lines produce batches of different products that requires setup time to Initialize the machines between different batches. The difference between single model, mixed-model and multi-model are illustrated in figure (2).

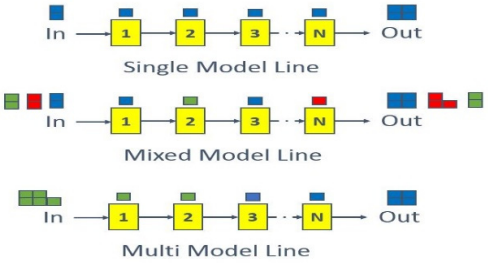

Figure 2: Different line configurations based on a number of models.

Additionally, there are many assumptions used to reduce the level of complexity of the ALBP such as deterministic processing time, fixed cycle time, etc. Consequently, the challenges facing researchers is to reduce these assumptions as possible to simulate the real-life problems. The U-shaped lines have been introduced for the first time by the Japanese Factories where high experience workers were hired to increase variability and quality of products. However, the balancing for U-lines is more complicated compared to traditional lines. Nevertheless, it can provide many advantages such as; less work-in-process, less worker movement, increase line efficiency and increase flexibility in production rate. The straight line and U-shaped line are illustrated in figure (3).

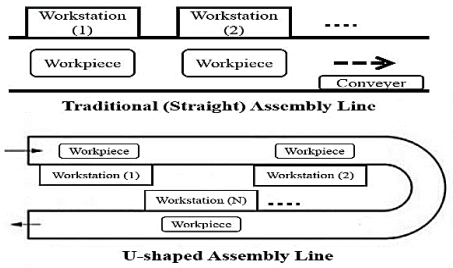

Figure 3: Different line layouts.

The ALBP has been intensively discussed in the literature. As a result, many recent reviews have been published (Boysen et al. 2007), (Battaïa & Dolgui 2013) and (Sivasankaran & Shahabudeen 2014b). In this paper, we focus on analysing published articles that formulated mathematical models to solve different configurations of assembly line balancing problems. Furthermore, a framework with improvements in the model formulations is proposed to tackle ALBP.
The remainder of this paper is organised as follows: The second section presents the classification of assembly line balancing problems as well as reviewing and analysing the articles published in each category. The third section is dedicated to providing further research areas and concludes remarks of this study. The last section explains the proposed framework.

2 REVIEW ON MATHEMATICAL MODELS

This section represents a taxonomy of the mathematical models used in describing a wide range of different assembly lines configurations:

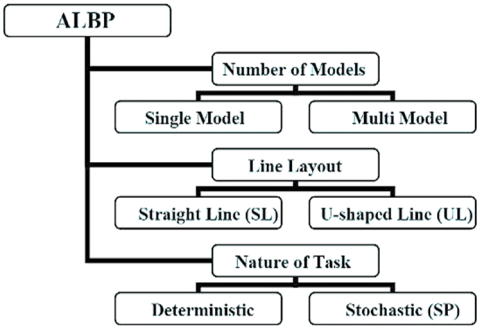

Figure 4: Assembly Lines Configurations.

2.1 Single-Model and Straight Type Assembly Lines with Deterministic Processing Times

The first formulation for SALBP by (Bowman 1960) used linear programming by using two different linear program forms. Also, Some modifications were introduced by (White 1961). Additionally, (Thangavelu & Shetty 1971) developed an improved 0-1 integer programming version of Bowman-White model by simplifying certain steps in (Geoffrion 1967) 0-1 integer programming algorithm. Moreover,

(Patterson & Albracht 1975) formulated an improved 0-1 integer-programming model draws heavily on the work done by (Bowman 1960) taking into consideration to determine feasibility and reduce computational time by reducing the required number of variables. Furthermore, (Talbot & Patterson 1984) presented an integer programming formulation for defining all feasible assignments for each task to a workstation with upper and lower bounds. Thereafter, they solved it by using a modified Balas algorithm (Balas et al. 1965). In (Vitria 2004) the authors analysed different ways for modelling precedence and incompatibility constraints in ALBP to obtain the best modelling formulation and solving procedure. (Pastor & Ferrer 2009) used the two efficient models of (Vitria 2004) for both SALBP-1 and SALBP-2 besides introducing additional constraints based on the upper bound of the number of workstations or the cycle time that belongs to the branch and bound technique. The research carried by (Özcan & Toklu 2009) presented mathematical model used a goal programming and a fuzzy goal programming for a two-sided assembly line to minimise the number of mated workstations at first and then minimise the number of the workstations as a secondary goal. (Esmaeilbeigi et al. 2015) presented the mixed integer programming for maximizing the line efficiency (SALBP-E) as well as providing secondary objectives (SALPB-1, SALBP-2, minimizing smoothness index) for the problem. Their proposed model is considered as the first MILP model for getting an exact solution directly in SALBP-E.

2.2 Single-Model and U-type Assembly Lines with Deterministic Processing Times

(Miltenburg & Wijngaard 1994) proposed the first model for the simple U-line balancing and used a dynamic programming procedure for obtaining the optimal solution. In (Urban 1998) the authors formulated an integer programming model for optimally solving UALBP-1. (Gökçen & Ağpak 2006) introduced the first multi-criteria for decision-making technique for U-shaped lines. They formulated a mathematical model using a goal programming for a UALBP based on the IP model proposed by (Urban 1998). Furthermore, their model was used by (Toklu & özcan 2008) as a base for formulating the first fuzzy goal programming model with multi-objectives aiming at optimising the conflicting goals as well as helping the decision maker to determine goals in the fuzzy environment. (Kara et al. 2009) proposed binary fuzzy goal programming models for each of the traditional and U-shaped assembly lines. They extended the linear programming model of (Urban 1998) in developing their BFGP for balancing U-lines. The improved version of the previous model in (Urban 1998) addressed in the work of (Fattahi et al. 2014), They formulated an integer programming model for UALBP-1 that was able to reduce the binary variables to half by increasing the efficiency of LP relaxation.

2.3 Single-Model and Straight Type Assembly Lines with Stochastic Processing Times

The processing times in deterministic assembly line (AL) are assumed to take constant values. Nonetheless in real life, it takes values based on probability distribution resulting from machine breakdowns, the difference in skills between operators, complex tasks, environment, and so forth. (Moodie 1964) The first research work that addressed the stochastic nature to the ALBP. (Carraway 1989) proposed two dynamic programming approaches for minimising the number of workstations. The task times assumed to be independent and normally distributed. (Ağpak & Gökçen 2007) formulated a chance-constrained 0-1 integer programming model for balancing stochastic traditional assembly line. Additionally, a goal programming has been proposed for increasing the reliability of the assembly line. (Özcan 2010) presented the first study of two-sided assembly lines with variation in task time and formulated a chance-constrained, piecewise-linear and mixed integer programming for solving this problem. In two-sided assembly lines, the workers are assigned in both sides of the production line (left and right) and used in parallel. (Hamta et al. 2013) They formulated a mixed integer non-linear programming model. Their model considered multi-objectives to simultaneously minimise the cycle time, equipment cost and the smoothness index. Finally, they developed a solution method based on the combination of particle swarm optimisation and variable neighbourhood search to solve the problem in reasonable time. (Hazır & Dolgui 2013) proposed robust optimisation models for SALBP-2 considering uncertainty through operations time and they developed an exact decomposition algorithm. They developed two mathematical models in addition to decomposition based algorithm to find the optimal solution for large problems. (Ritt et al. 2016) did not consider the variability in task times rather, they considered it indirectly by representing the variability of the workforce due to absenteeism. They proposed

a two-stage mixed integer models to minimise the cycle time. Furthermore, they presented a local search heuristic procedure based on simulated annealing for solving large instances.

2.4 Single-Model and U-type Assembly Lines with Stochastic Processing Times

The research done by (Nakade et al. 1997) is considered the first work in balancing U-lines taking stochastic nature results from manual work into consideration. They proposed approximate formulation for the upper and lower bound of the expected cycle time. (Guerriero & Miltenburg 2003) They used dynamic programming in balancing U-lines and the recursive algorithm for determining the optimal solution. (Urban & Chiang 2006) formulated a chance constraint programming model for U-line balancing problem, then they used piecewise linear, integer programming for solving the model optimally. The further investigations are to develop an efficient heuristic for solving large problems. (Ağpak & Gökçen 2007) formulated 0-1 integer programming model by using a chance-constrained procedure for balancing stochastic traditional and U-shaped lines. They used the model of (Urban 1998) as the base for their work; also they presented two linear transformations (pure and approximate) to enable the model to solve large problems. Lastly, they introduced goal programming for smoothing the workload among workstations. Most of the researches done in the U-type assembly line problems focused on deterministic processing times comparing to the stochastic time.

2.5 Multi or Mixed Model and Straight Type Assembly Lines with Deterministic Processing Times

(Gökcen & Erel 1998) introduced a binary integer programming model for the Mixed-Model Assembly Line (MMAL). Flexibility ratio has also been presented that is used to compute the computational and storage requirements for solving the problem by measuring the number of possible sequences for the precedence diagram. (Vilarinho & Simaria 2002) developed a mathematical model for balancing mixed-model assembly lines that gives the decision maker the ability to define the limit number of parallel workstations and zoning constraints. (Simaria & Vilarinho 2009) formulated a mathematical model for balancing two-sided mixed-model assembly lines. Moreover, they proposed an ant colony optimisation algorithm for optimally solving the model. (Fattahi & Salehi 2009) developed a mixed-integer linear programming model to minimise the total utility and idle costs. They tried to solve the problem using branch and bound method, but it was very time-consuming so, they used simulated annealing to resolve this issue. (Mosadegh et al. 2012) formulated a mixed-integer linear programming model to provide the exact solution of both balancing and sequencing problems simultaneously for mixed model assembly lines. For solving the problem, they developed a simulated annealing algorithm as well as Taguchi method for calibrating the algorithm parameters. (Kucukkoc & Zhang 2014) proposed a mixed integer programming model to investigate both sequencing and balancing problems simultaneously in mixed model parallel two-sided assembly lines. The objectives of their model were to minimise the number of workstations, reduce the length of production lines and maximise workload smoothness. Furthermore, they presented an agent based ant colony optimisation algorithm for solving the problem. (Zhao et al. 2016) formulated a mathematical model for MMAL focused on the effect of mental workload and the complexity of the operations on balancing the line. They concluded that, the mental workload considered as an essential rule when minimising cycle time also, the mental workload was influenced by the level of experience of the operator.

2.6 Multi or Mixed Model and U-type Assembly Lines with Deterministic Processing Times

(Sparling & Miltenburg 1998) are considered the pioneers in studying MMUL. They presented a model for U-line balancing problem for assigning a set of tasks in a minimum number of workstations. Furthermore, they presented an approximation algorithm to solve large size problems. (Miltenburg 2002) formulated a mixed, zero-one integer, non-linear programming model then used a genetic algorithm for searching for a good solution in a reasonable computational time. (Kara 2008) formulated a non-linear mathematical model to solve balancing and sequencing problem simultaneously for MMUL. The objective of their model was to minimise deviation of workloads among workstations. Due to the complexity so, they proposed simulated annealing algorithm to solve large-scale problems. (Kara & Tekin 2009) proposed a mixed integer linear programming model for optimally balancing mixed-model U-lines. The goal

of their model was to minimise the number of workstations for a given cycle time. (Kazemi et al. 2011) introduced an integer linear programming model. The objective of their presented model was to minimise the number of stations. Furthermore, they developed a two-stage genetic algorithm approach for the large-scale problem. (Rabbani et al. 2012) formulated a multi-objective mixed integer linear programming model for two-sided Als. Finally, they introduced a heuristic based on the genetic algorithm for solving this problem. (Rabbani et al. 2016) formulated a mixed-integer linear programming model for robotic mixed-model assembly lines. The model aimed to minimise the cycle time, robot purchasing and setup costs.

2.7 Multi or Mixed Model and Straight Type Assembly Lines with Stochastic Processing Times

(Paternina-Arboleda & Montoya-Torres 2006) proposed a mathematical model for balancing and sequencing MMAL. The model included multi-objective function aimed to minimise the number of workstations, increase throughput and find the appropriate sequence of models to remove bottlenecks through an assembly line. (Al-e-hashem 2009) formulated a mixed integer robust optimization model to minimize the total costs that include the cost of workstations and duplicated tasks.

2.8 Multi or Mixed Model and U-type Assembly Lines with Stochastic Processing Times

(Agrawal & Tiwari 2008) proposed a model for balancing and sequencing mixed-model U-disassembly lines where the processing times are different depending on the structure of the products and the human factor. The objective function was to minimise the variation of workload and maximise the line efficiency. They solved this problem by using collaborative Ant Colony Optimization, and they tested the results on benchmarks using a design of experiment and analysis of variance to determine which factor is significant in the objective. (Dong et al. 2014) formulated a 0-1 stochastic programming model to solve balancing and sequencing problem simultaneously for MMUL with independently and normally distributed task times. They proposed a simulated annealing algorithm to resolve the issue into both situations (Deterministic and stochastic).

3 DISCUSSIONS AND FUTURE RESEARCH

Although researchers have contributed in various configurations and application of assembly line balancing, the gap still exists between research and real life problems. To the best of our knowledge, only two papers have been published using a mathematical model in each branch of MMAL with stochastic processing times, so the further research may be carried out in developing multi-objective mathematical models including more constraints such as zoning and distance constraints. It is clear that the majority of authors neglected the use of statistical methods in comparing the results to clarify the significant improvement between their proposed methods and previous research in the literature. Also, statistical studies are useful in determining the effect of each variable on the objective function and calibrating algorithm parameters. It is clear that more studies are applied in SLs comparing to U-lines. Thus, further work can be done in a different configuration of U-lines such as two-sided, multi lines, disassembly and rebalancing U-lines. Most of the articles neglect the human factors (skills, experience, learning effect) and working environment that directly affects the operator's performance and productivity. Consequently, it is very crucial to enhance existing mathematical models to consider these aspects in further work. Further work may be directed to consider other objective functions such as maximise the line efficiency, minimising smoothness index and minimise total costs (equipment-duplication-setup). Enhance current meta-heuristics such as simulated annealing algorithm, genetic algorithm, practical swarm optimisation, etc. That will help in solving large instances of ALBP in less computational time and provide better results especially in the case of mixed-models. In MMAL it is important to handle both ALB and ALS problems jointly. Formulate a mathematical model for multi-optimization problems such as the incorporation of line design and balancing problems.

4 THE PROPOSED SOLUTION FRAMEWORK

The objective of the ALBP-2 is to minimise the cycle time as a result of minimising the workload of the bottleneck workstation. Nevertheless, it is also important to consider the second heavily loaded workstation, the third one and so on, to improve the

reliability and the quality of the balance through the line. The proposed solution approach is to modify the model formulated by (Kucukkoc et al. 2015) to include the objective of increasing balance between and within workstations to ensure that all workstations through the line have an equal amount of work also all the workers within the workstations have the same workload. Moreover, the zoning constraints will be added to the model to increase the ability to solve real-life problems with fewer assumptions as possible. The proposed mathematical model will be coded using LINGO optimisation modelling software to solve small-sized problems. The solution from the solver will be utilised as an input to a DES model to test the robustness of solutions when introducing the real-world variability such as stochastic times, breakdowns, etc. Then a comparison will be made between the initial solution and the proposed solution from the model using the performance indicators of the simulation. Finally, statistical analysis will be implemented to evaluate the significant improvement in the assembly line.

5 CONCLUSIONS

The research on ALBP is crucial because it affects the productivity and the competitiveness of the company. This paper surveyed studies of ALBP within the area of mathematical modeling that were published in the eight branches of ALBP. The goal of this analysis was to discover the research gaps in line balancing problems. Furthermore, a proposed framework is introduced to enhance the solution of the MMAL by modifying the objective function and adding more constraints that represent realistic world problems.

ACKNOWLEDGEMENTS

This research project is sponsored by the Mitsubishi Corporation Graduate Scholarship to the Egypt-Japan University of Science and Technology (E-JUST) and support of the Japanese International Cooperation Agency (JICA).

REFERENCES

Ağpak, K. & Gökçen, H., 2007. A chance-constrained approach to stochastic line balancing problem. *European Journal of Operational Research*, 180(3), pp.1098–1115.

Agrawal, S. & Tiwari, M.K., 2008. A collaborative ant colony algorithm to stochastic mixed-model U-shaped disassembly line balancing and sequencing problem. *International Journal of Production Research*, 46(6), pp.1405–1429.

Al-e-hashem, S.M., 2009. Mixed model assembly line balancing problem under uncertainty. *, 2009. CIE 2009.* .... Available at: http://ieeexplore.ieee.org/xpls/abs_all.jsp?arnumber=5223925 [Accessed September 27, 2016].

Balas, E., Glover, F. & Zionts, S., 1965. An Additive Algorithm for Solving Linear Programs with Zero-One Variables Author(s): *Operations Research*, 13(4), pp.517–549.

Battaïa, O. & Dolgui, A., 2013. A taxonomy of line balancing problems and their solutionapproaches. *International Journal of Production Economics*, 142(2), pp.259–277.

Bowman, E.H., 1960. Assembly-Line Balancing by Linear Programming. *Operations Research*, 8(3), pp.385–389.

Boysen, N., Fliedner, M. & Scholl, A., 2007. A classification of assembly line balancing problems. *European Journal of Operational Research*, 183(2), pp.674–693.

Carraway, R.L., 1989. A Dynamic Programming Approach to Stochastic Assembly Line Balancing. *Management Science*, 35(4), pp.459–471. Available at: http://pubsonline.informs.org/doi/abs/10.1287/mnsc.35.4.459 [Accessed September 24, 2016].

Dolgui, A. & Battaı, O., 2013. Int . J . Production Economics A taxonomy of line balancing problems and their solution approaches. , 142, pp.259–277.

Dong, J. et al., 2014. Balancing and sequencing of stochastic mixed-model assembly U-lines to minimise the expectation of work overload time. *International Journal of Production Research*, 52(24), pp.7529–7548. Available at: http://www.tandfonline.com/doi/abs/10.1080/00207543.2014.944280 [Accessed September 28, 2016].

Esmaeilbeigi, R., Naderi, B. & Charkhgard, P., 2015. The type E simple assembly line balancing problem: A mixed integer linear programming formulation. *Computers & Operations Research*, 64, pp.168–177. Available at: http://linkinghub.elsevier.com/retrieve/pii/S0305054815001446.

Fattahi, A. et al., 2014. A novel integer programming formulation with logic cuts for the U-shaped assembly line balancing problem. *International Journal of Production Research*, 52(5), pp.1318–1333. Available at: http://www.tandfonline.com/doi/abs/10.1080/00207543.2013.832489 [Accessed September 21, 2016].

Fattahi, P. & Salehi, M., 2009. Sequencing the mixed-model assembly line to minimize the total utility and idle costs with variable launching interval. *The International Journal of Advanced Manufacturing*. Available at: http://link.springer.com/article/10.1007/s00170-009-2020-0 [Accessed September 25, 2016].

Geoffrion, A.M., 1967. Integer Programming by Implicit Enumeration and Balas' Method. *SIAM Review*, 9(2), pp.178–190. Available at: http://epubs.siam.org/doi/abs/10.1137/1009031 [Accessed October 16, 2016].

Gökçen, H. & Ağpak, K., 2006. A goal programming approach to simple U-line balancing problem. *European Journal of Operational Research*, 171(2), pp.577–585.

Gökcen, H. & Erel, E., 1998. Binary Integer Formulation for Mixed-Model Assembly Line Balancing Problem. *Computers & Industrial Engineering*, 34(2), pp.451–461. Available at: http://www.sciencedirect.com/science/article/pii/S0360835297001423.

Guerriero, F. & Miltenburg, J., 2003. The stochastic U-line balancing problem. *Naval Research Logistics*, 50(1), pp.31–57. Available at: http://doi.wiley.com/10.1002/nav.10043 [Accessed September 22, 2016].

Gutjahr, A.L. & Nemhauser, G.L., 1964. An Algorithm for the Line Balancing Problem. , (August 2015).

Hamta, N. et al., 2013. A hybrid PSO algorithm for a multi-objective assembly line balancing problem with flexible operation times, sequence-dependent setup times and learning effect. *International Journal of Production Economics*, 141(1), pp.99–111.

Hazır, Ö. & Dolgui, A., 2013. Assembly line balancing under uncertainty: Robust optimization models and exact solution method. *Computers & Industrial Engineering*, 65(2), pp.261–267. Available at: http://www.sciencedirect.com/science/article/pii/S0360835213000934.

Kara, Y., 2008. Line balancing and model sequencing to reduce work overload in mixed-model U-line production environments. *Engineering Optimization*, 40(7), pp.669–684. Available at: http://www.tandfonline.com/doi/abs/10.1080/03052150801982509 [Accessed September 26, 2016].

Kara, Y., Paksoy, T. & Chang, C.-T., 2009. Binary fuzzy goal programming approach to single model straight and U-shaped assembly line balancing. *European Journal of Operational Research*, 195(2), pp.335–347.

Kara, Y. & Tekin, M., 2009. A mixed integer linear programming formulation for optimal balancing of mixed-model U-lines. *International Journal of Production Research*, 47(15), pp.4201–4233. Available at: http://www.tandfonline.com/doi/abs/10.1080/00207540801905486 [Accessed September 26, 2016].

Kazemi, S.M. et al., 2011. A novel two-stage genetic algorithm for a mixed-model U-line balancing problem with duplicated tasks. *The International Journal of Advanced Manufacturing Technology*, 55(9–12), pp.1111–1122. Available at: http://link.springer.com/10.1007/s00170-010-3120-6 [Accessed September 26, 2016].

Kucukkoc, I. et al., 2015. A mathematical model and artificial bee colony algorithm for the lexicographic bottleneck mixed-model assembly line balancing problem. *Journal of Intelligent Manufacturing*, pp.1–13. Available at: http://link.springer.com/10.1007/s10845-015-1150-5 [Accessed October 24, 2016].

Kucukkoc, I. & Zhang, D.Z., 2014. Mathematical model and agent based solution approach for the simultaneous balancing and sequencing of mixed-model parallel two-sided assembly lines. *International Journal of Production Economics*, 158, pp.314–333.

Miltenburg, G.J. & Wijngaard, J., 1994. The U-line Line Balancing Problem. *Management Science*, 40(10), pp.1378–1388. Available at: http://pubsonline.informs.org/doi/abs/10.1287/mnsc.40.10.1378 [Accessed September 21, 2016].

Miltenburg, J., 2002. Balancing and Scheduling Mixed-Model U-Shaped Production Lines. *International Journal of Flexible Manufacturing Systems*, 14(2), pp.119–151. Available at: http://link.springer.com/10.1023/A:1014434117888 [Accessed September 26, 2016].

Moodie, C., 1964. A Heuristic Method of Assembly Line Balancing for Assumptions of Constantor Variable Work Element Times. Available at: http://docs.lib.purdue.edu/dissertations/AAI6408691/ [Accessed September 23, 2016].

Mosadegh, H., Zandieh, M. & Ghomi, S.M.T.F., 2012. Simultaneous solving of balancing and sequencing problems with station-dependent assembly times for mixed-model assembly lines. *Applied Soft Computing*, 12(4), pp.1359–1370.

Nakade, K., Ohno, K. & George Shanthikumar, J., 1997. Bounds and approximations for cycle times of a U-shaped production line. *Operations Research Letters*, 21(4), pp.191–200.

Özcan, U., 2010. Balancing stochastic two-sided assembly lines: A chance-constrained, piecewise-linear, mixed integer program and a simulated annealing algorithm. *European Journal of Operational Research*, 205(1), pp.81–97.

Özcan, U. & Toklu, B., 2009. Multiple-criteria decision-making in two-sided assembly line balancing: A goal programming and a fuzzy goal programming models. *Computers and Operations Research*, 36(6), pp.1955–1965.

Pastor, R. & Ferrer, L., 2009. An improved mathematical program to solve the simple assembly line balancing problem. *International Journal of Production Research*, 47(11), pp.2943–2959.

Paternina-Arboleda, C. & Montoya-Torres, J., Mathematical formulation for a mixed-model assembly line balancing problem with stochastic processing times. *laccei.org*. Available at: http://www.laccei.org/LACCEI2006-PuertoRico/Copyright Pending/IT240_PaterninaArboleda.pdf [Accessed September 27, 2016].

Patterson, J.H. & Albracht, J.J., 1975. Technical Note--Assembly-Line Balancing: Zero-One Programming with Fibonacci Search. *Operations Research*, 23(1), pp.166–172.

Rabbani, M., Moghaddam, M. & Manavizadeh, N., 2012. Balancing of mixed-Model two-Sided assembly lines with multiple u-Shaped layout. *International Journal of Advanced Manufacturing Technology*, 59(9–12), pp.1191–1210.

Rabbani, M., Mousavi, Z. & Farrokhi-Asl, H., 2016. Multi-objective metaheuristics for solving a type II robotic mixed-model assembly line balancing problem. *Journal of Industrial and Production Engineering*, 33(7), pp.472–484. Available at: https://www.tandfonline.com/doi/full/10.1080/21681015.2015.1126656 [Accessed September 27, 2016].

Ritt, M., Costa, A.M. & Miralles, C., 2016. The assembly line worker assignment and balancing problem with stochastic worker availability. *International Journal of Production Research*, 54(3), pp.907–922. Available at: http://www.tandfonline.com/doi/full/10.1080/00207543.2015.1108534 [Accessed September 25, 2016].

Salveson, M.E., 1955. The assembly line balancing problem. *Journal of Industrial Engineering*, 6(3), pp.18–25.

Simaria, A.S. & Vilarinho, P.M., 2009. 2-ANTBAL: An ant colony optimisation algorithm for balancing two-sided assembly lines. *Computers & Industrial Engineering*, 56(2), pp.489–506.

Sivasankaran, P. & Shahabudeen, P., 2014a. Literature review of assembly line balancing problems. *The International Journal of Advanced Manufacturing Technology*, 73(9–12), pp.1665–1694. Available at: http://link.springer.com/10.1007/s00170-014-5944-y [Accessed August 20, 2016].

Sivasankaran, P. & Shahabudeen, P., 2014b. Literature review of assembly line balancing problems. *The International Journal of Advanced Manufacturing Technology*, 73(9–12), pp.1665–1694. Available at: http://link.springer.com/10.1007/s00170-014-5944-y [Accessed September 29, 2016].

Sparling, D. & Miltenburg, J., 1998. The mixed-model U-line balancing problem. *International Journal of Production Research*, 36(2), pp.485–501.

Talbot, F.B. & Patterson, J.H., 1984. an Integer Programming Algorithm With Network Cuts for Solving the Assembly Line Balancing Problem. *Management Science*, 30(1), pp.85–99. Available at: http://search.ebscohost.com/login.aspx?direct=true&db=bth&AN=7357463&site=ehost-live&scope=site.

Thangavelu, S.R. & Shetty, C.M., 1971. Assembly Line Balancing by Zero-One Integer Programming. *AIIE Transactions*, 3(1), pp.61–68.

Toklu, B. & özcan, U., 2008. A fuzzy goal programming model for the simple U-line balancing problem with multiple objectives. *Engineering Optimization*, 40(3), pp.191–204. Available at: http://www.tandfonline.com/doi/abs/10.1080/03052150701651642 [Accessed September 21, 2016].

Urban, T.L., 1998. Note. Optimal Balancing of U-Shaped Assembly Lines. *Management Science*, 44(5), pp.738–741. Available at: http://pubsonline.informs.org/doi/abs/10.1287/mnsc.44.5.738 [Accessed September 21, 2016].

Urban, T.L. & Chiang, W.C., 2006. An optimal piecewise-linear program for the U-line balancing problem with stochastic task times. *European Journal of Operational Research*, 168(3), pp.771–782.

Vilarinho, P.M. & Simaria, A.S., 2002. A two-stage heuristic method for balancing mixed-model assembly lines with parallel workstations. *International Journal of Production Research*, 40(6), pp.1405–1420. Available at: http://www.tandfonline.com/doi/abs/10.1080/00207540110116273 [Accessed September 25, 2016].

Vitria, J., 2004. Different ways of modelling and solving precedence and incompatibility constraints in the Assembly Line Balancing Problem. *Recent Advances in Artificial Intelligence Research*. Available at: https://www.google.com/books?hl=en&lr=&id=P7FYs0IvbpoC&oi=fnd&pg=PA359&dq=Pastor,+R.,+Corominas,+A.+and+Lusa,+A.,+2004.+Different+ways+of+modelling+and+solving+precedence+and+incompatibility+constraints+in+the+assembly+line+balancing+problem.+Frontiers+in.

White, W.W., 1961. Comments on a Paper by Bowman. *Operations Research*, 9(August 2015), pp.274–276.

Zhao, X. et al., 2016. A genetic algorithm for the multi-objective optimization of mixed-model assembly line based on the mental workload. *Engineering Applications of Artificial Intelligence*, 47, pp.140–146.

A Stackelberg Game Model between Manufacturer and Wholesaler in a Food Supply Chain

Javiera A. Bustos[1], Sebastián H. Olavarría[1], Víctor M. Albornoz[1],
Sara V. Rodríguez[2] and Manuel Jiménez-Lizárraga[3]
[1]*Departamento de Industrias, Campus Vitacura, UTFSM, Santiago, Chile*
[2]*Facultad de Ing. Mecánica y Eléctrica, UANL, Monterrey, Mexico*
[3]*Facultad de Ciencias Físicas y Matemáticas, UANL, Monterrey, Mexico*
{javiera.bustos, sebastian.olavarria}@alumnos.usm.cl, victor.albornoz@usm.cl, sara.rodriguezsn@uanl.edu.mx, manalejimenez@yahoo.com

Keywords: Stackelberg Game, Food Supply Chain, Bilevel Programming, Pork Supply Chain.

Abstract: This paper describes an application of the Stackerlberg game model for the food supply chain. Specifically, the focus of this work is on the pork industry and considers a production game. Such game includes two players, manufacturer and wholesaler, who both aim to maximize profit. The role of leader is played by the manufacturer, and follower by the wholesaler. Decisions involved in the game are the level of production, quantity to be sold by the leader, and level of purchased products by the follower at each time period. This paper presents a case study, and results show that coordination between these players is seen in cost savings and improved service level.

1 INTRODUCTION

In developing countries, food demand continues growing, given rising incomes and population growth. In the context of countries with a strong and continuous economic development, it is forecasted that protein consumption will rise, along with meat consumption, resulting in an active industry. Meat production will increase by 17% in developing countries and 2% in developed countries from 2014 to 2024. Pork is the most produced and consumed red meat worldwide (FAO, 2016). In this context, several complex problems are faced by chain managers, who need to integrate stakeholder operations in order to coordinate product flow along the chain. One of the most challenging problems is related to planning and scheduling of operations for processing the carcasses (body of the animal gutted and bloodless) into pork and by-products, later to be sold to wholesalers to satisfy required demand. In this framework, the coordination and integration between two agents is critical to improve efficiency and increase supply chain productivity.

Operations Research (OR) is one of the most important disciplines that deal with advanced analytical methods for decision making. OR is applied to a wide range of problems arising in different areas, and their fields of application involve the operations management of the agriculture and food industry. There are several works related to these topics, see (Ahumada and Villalobos, 2009) for a review of agricultural supply chains; see (Bjørndal et al., 2012) for a review of operations research applications in agriculture, fisheries, forestry and mining; see (Higgins et al., 2010) for an application of agricultural value chains using network analysis, agent-based modeling and dynamical systems modeling; (Plà et al., 2014), draw out insights for new opportunities regarding OR for the agricultural industry. Specifically, (Rodríguez et al., 2014) presents a key description of opportunities focused on the pork supply chain.

Furthermore, game theory has been deeply used to analyze the interactions between different agents in the supply chain (Hennet and Arda, 2008). Game theory is a suitable tool to support decision making where there is more than one participant (or player) (Marulanda and Delgado, 2012). The Stackeberg model was originally introduced in the context of static competition games in 1934 by the economist H. von Stackelberg (Von Stackelberg, 1952), with an important impact on economic sciences. Such a problem can be also seen as a bilevel optimization problem (Dempe, 2002). In this model, the leader announces his strategy first. Next, the follower observes the

Bustos, J., Olavarria, S., Albornoz, V., Rodríguez, S. and Jiménez-Lizárraga, M.
A Stackelberg Game Model between Manufacturer and Wholesaler in a Food Supply Chain.
In *Proceedings of the 6th International Conference on Operations Research and Enterprise Systems (ICORES 2017)*, pages 409-415
ISBN: 978-989-758-218-9

leader's actions and reacts to them, so as to maximize profits. Interactions within the food supply chain are captured through a game between a leader and a follower. In this model, here the leader presents advantage, and consequently is who decides first about his operational decisions: location, technology, amount to processing, raw materials, and prices (Yue and You, 2014).

In many decision making processes there is a hierarchical structure among agents and decisions are taken at different levels of the hierarchy. Interactions among participants in the supply chain are captured through a game between a leader with a follower who follows the structure of a Stackelberg game. When we see this model as a two level decision problem, it is called bilevel optimization program. In this case, we have a leader (associated with the top level) and a follower (associated with the lower level). If both the leader's and follower's constraints are linear, it is a bilevel linear programming problem (BLPP) (Migdalas et al., 2013). Here, decisions of a player on one level can affect decision-making behavior on other levels, even though the leader does not completely control the actions of the followers.

A vast majority of research on bilevel programming has centered on the linear version of this problem, alternatively known as the linear Stackelberg game. The BLPP can be written as follows (Bard, 2013):

For $\boldsymbol{x} \in X \subset R^n$, $\boldsymbol{y} \in Y \subset R^m$, $F : X \times Y \to R^1$, and $f : X \times Y \to R^1$.

$$\min_{\mathbf{x} \in X} F(\boldsymbol{x},\boldsymbol{y}) = \boldsymbol{c_1 x} + \boldsymbol{d_1 y} \tag{1}$$

$$\text{s.t } \boldsymbol{A_1 x} + \boldsymbol{B_1 y} \leqq \boldsymbol{b_1} \tag{2}$$

$$\min_{\mathbf{y} \in Y} f(\boldsymbol{x},\boldsymbol{y}) = \boldsymbol{c_2 x} + \boldsymbol{d_2 y} \tag{3}$$

$$\text{s.t } \boldsymbol{A_2 x} + \boldsymbol{B_2 y} \leqq \boldsymbol{b_2} \tag{4}$$

where $\mathbf{c_1}, \mathbf{c_2} \in R^n$, $\mathbf{d_1}, \mathbf{d_2} \in R^m$, $\mathbf{b_1} \in R^p$, $\mathbf{b_2} \in R^q$, $\boldsymbol{A_1} \in R^{p \times n}$, $\boldsymbol{B_1} \in R^{p \times m}$, $\boldsymbol{A_2} \in R^{q \times n}$, $\boldsymbol{B_2} \in R^{q \times m}$. Sets X and Y place additional constraints on the variables, such as upper and lower bounds. In this model, once the Ieader selects an x, the first term in the follower's objective function becomes a constant; and the same is valid for the follower's constraints.

Bard (2013) also presents a necessary condition that $(\boldsymbol{x}^*, \boldsymbol{y}^*)$ solves the linear BLPP (1)-(4) if there exist (row) vectors $\boldsymbol{u}^*$ and $\boldsymbol{v}^*$ such that $(\boldsymbol{x}^*, \boldsymbol{y}^*, \boldsymbol{u}^*, \boldsymbol{v}^*)$ solves:

$$\min \boldsymbol{c_1 x} + \boldsymbol{d_1 y} \tag{5}$$

$$\text{s.t } \boldsymbol{A_1 x} + \boldsymbol{B_1 y} \leqq \boldsymbol{b_1} \tag{6}$$

$$\boldsymbol{u B_2} - \boldsymbol{v} = -\boldsymbol{d_2} \tag{7}$$

$$\boldsymbol{u}(\boldsymbol{b_2} - \boldsymbol{A_2 x} - \boldsymbol{B_2}) + \boldsymbol{v y} = 0 \tag{8}$$

$$\boldsymbol{A_2 x} + \boldsymbol{B_2 y} \leqq \boldsymbol{b_2} \tag{9}$$

$$\boldsymbol{x} \geqq 0,\ \boldsymbol{y} \geqq 0,\ \boldsymbol{u} \geqq 0,\ \boldsymbol{v} \geqq 0 \tag{10}$$

Thus, a new nonlinear constraint (8) is generated, to represent the optimization model for the follower. However, this formulation has played a key role in the development of algorithms. One advantage that it offers is that it allows for a more robust model to be solved without introducing any new computational difficulties. There are several algorithms proposed for solving the linear BLPP since the field caught the attention of researchers in the mid-1970s. Many of these are of academic interest only because they are either impractical to implement or grossly inefficient. The most popular method for solving the linear BLPP is known as the "Kuhn-Tucker" approach and concentrates on (5)-(10). The fundamental idea is to use a branch and bound strategy to deal with the complementary constraint (8). Omitting or relaxing this constraint leaves a standard linear program which is easy to solve. Various methods proposed employ different techniques for assuring that the complementary constraint is ultimately satisfied (Bard, 2013). (Fortuny-Amat and McCarl, 1981), proposed a reformulation of the non-linear constraints; and (Bard and Moore, 1990) developed an algorithm that ensured global optimum with high efficiency.

In what follows, we propose a Stackelberg game between two food supply chain players involved in processing and selling activities. This is carried out assuming that there is a leader-follower relationship among the players. The primary challenge in this model is to support in the coordination and integration of activities and information among two supply chain agents. In Section 2, we detail the proposed Stackelberg game and model to solve this problem. After this, Section 3 presents a case study and provides the obtained results. Finally, in Section 4 main conclusions and future research are presented.

2 MATERIALS AND METHODS

To have a good relationship between agents, coordinate activities and share information , the chain should be aligned, improving efficiency and productivity. This section presents a detailed description of the Stackelberg game between two supply chain agents under the leader and follower scheme; and an optimization problem that models the interaction between the players.

2.1 Games Description

In the meat supply chain, a manufacturer is in charge of processing the raw material, from carcasses to meat products. This player decides based on demand and the yielding rate of each cutting pattern, the level of production and inventory for each product, and hence the number of carcasses required. The processing plant aims to maximize profits through the sale of meat products; and the wholesaler is in charge of distribution and marketing of the products. Meat products are purchased from the manufacturer, and then sold to end customers, with the aim of maximizing level of service.

Interactions between both players in the supply chain are captured through a game with a leader and a follower who follows the structure of Stackelberg game. The problem arises when the optimal quantity produced and sold by the manufacturer is not enough to supply the needs of wholesaler. Thus, the wholesaler imposes a penalty cost on the manufacturer for the unsatisfied demand. This penalty cost can be reduced through coordination and integration of activities, and information exchange between the two supply chain agents. By sharing information about consumer preferences and demand, the manufacturer avoids expired products and cooperates with the wholesaler to maximize their level of service, improving performance of the whole supply chain.

The proposed game considers the manufacturer as the leader and the wholesaler as the follower. Given the characteristics of this Stackelberg game, static and not cooperative, this problem can be modeled by a bilevel linear programming problem.

2.2 Bilevel Linear Programming Model

This model supports and assists in the coordination and integration of two food supply chain agents, under the leader and follower structure given by the Stackelberg game. The main assumptions and considerations for the formulation of this bilevel programming model are based on(Albornoz et al., 2015).

Sets, indexes and variables used in the model are described below:

Sets and Indexes:

T	:	Number of periods of the planning horizon.
J	:	Number of cutting patterns.
$k \in K$	:	Set of sections per carcass.
$j \in J_k$	:	Set of cutting patterns per section k.
$r \in R$	:	Set to represent the different types of carcasses.
$i \in P$	:	Set of Products.

Parameters:

H	:	Carcasses available to process during the whole planning horizon.
α_r	:	Proportion of carcasses of type r .
ψ_{ijr}	:	Yield of product i using cutting pattern j on carcasses of type r .
p_i	:	Selling price per product i .
c_j	:	Operational cost of pattern j .
c_j^e	:	Operational cost of pattern j in overtime.
h	:	Holding cost of product per period for the leader.
f_i	:	Cost for unsatisfied-demand of product i for the leader.
W	:	Warehouse capacity (in kg.) for the leader.
t_j	:	Operation time for cutting pattern j.
T_w	:	Available hours in regular time.
T_w^e	:	Available hours in overtime.
δ	:	Auxiliary parameter for better control the available carcasses .
P	:	Purchase cost of carcasses.
d_{it}	:	Demand of product i at each period t.
G	:	Warehouse capacity (in kg.) for the follower.

Decision Variables:

v_{it}	:	Quantity of product i to be sold in t.
x_{it}	:	Total quantity of product i to have in period t.
s_i	:	Total quantity of excess product i at the end of planning horizon.
H_t	:	Number of carcasses to be processed at each period t.
z_{jt}	:	Number of times to perform the cutting pattern j in period t in normal work hours.
z_{jt}^e	:	Number of times to perform the cutting pattern j in period t, in overtime.
I_{it}	:	Quantity of product i to hold for the leader in t.
u_{it}	:	Unsatisfied-demand of product i in t.
I_{it}^r	:	Quantity of product i to hold for the follower in t.

$$\textbf{max} \sum_{i \in P} \sum_{t=1}^{T} p_i v_{it} - \sum_{t=1}^{T} PH_t - \sum_{t=1}^{T} \sum_{j \in J} \sum_{r \in R} (c_j z_{jrt} + c_j^e z_{jrt}^e)$$

$$-\sum_{i\in P}\sum_{t=1}^{T} hI_{it} - \sum_{i\in P}\sum_{t=1}^{T} f_i u_{it} \quad (11)$$

s.t

$$\alpha_r H_t - \sum_{j\in J_k} (z_{jrt} + z^e_{jrt}) = 0 \; ; t \in T, k \in K, r \in R \quad (12)$$

$$x_{it} - \sum_{r\in R}\sum_{j\in J_k} \psi_{ijr}(z_{jrt} + z^e_{jrt}) = 0 \; ; i \in P, t \in T, k \in K \quad (13)$$

$$\sum_{r\in R}\sum_{j\in J_k} t_j z_{jrt} \leq T_w \; ; t \in T \quad (14)$$

$$\sum_{r\in R}\sum_{j\in J_k} t_j z^e_{jrt} \leq T^e_w \; ; t \in T \quad (15)$$

$$v_{it} - x_{it} - I_{it} + I_{i,t+1} = 0 \; ; i \in P, t = 1, ..., T-1 \quad (16)$$

$$v_{iT} - x_{iT} + s_i - I_{iT} = 0 \; ; i \in P \quad (17)$$

$$\sum_{t=1}^{T} H_t \leq H \quad (18)$$

$$-\sum_{t=1}^{T} H_t \leq -\delta H \quad (19)$$

$$\sum_{i\in P} I_{it} \leq W \; ; t \in T \quad (20)$$

$$v_{it} \geq 0 \; , x_{it} \geq 0 \; , s_i \geq 0 \; , I_{it} \geq 0 \; , H_t \text{ integer}, \; z_{jrt} \text{integer} \; , z^e_{jrt} \text{ integer} \quad (21)$$

$$\textbf{min} \sum_{i\in P}\sum_{t=1}^{T} u_{it} \quad (22)$$

s.t

$$v_{it} + u_{it} + I^r_{it} - I^r_{i,t+1} = d_{it} \; ; i \in P, t = 1, ..., T-1 \quad (23)$$

$$v_{iT} + u_{iT} + I^r_{iT} = d_{iT} \; ; i \in P \quad (24)$$

$$\sum_{i\in P} I^r_{it} \leq G \; ; t \in T \quad (25)$$

$$I^r_{i,T} = 0 \; ; i \in P \quad (26)$$

$$u_{it} \geq 0 \; ; I^r_{it} \geq 0 \quad (27)$$

Where v_{it}, s_i, H_t, z_{jrt}, z^e_{jrt}, I_{it} are decision variables of the leader and u_{it}, I^r_{it} are decision variables of the follower. The manufacturer's objective (16) is to maximize profits. Profits are understood as the difference between total revenues from selling the products and the following costs: inventory, production, purchases of carcasses and unsatisfied-demand penalties. Conversely, the follower (22) is simply trying to maximize his service level.

A feasible solution of the model satisfies a different set of leader's constraints. Constraint (12) ensures a balance between cutting patterns and the number of carcasses to be processed at each time period. Equality is forced because it is not possible to leave unprocessed raw material. Constraint (13) calculates the total kilograms of each product retrieved by all the cutting patterns applied at each time period. Constraint (14) ensures that the labor time does not exceed the viable working hours of regular time. Constraints (15) ensure that the labor time does not exceed the viable working hours during overtime. Constraints (16) and (17) determine the quantity of product to be processed and held considering the excess product. This is the amount that the manufacturer sells when the wholesaler does not purchase all products at the end of the planning horizon (without revenues because it is a sunk cost). Constraints (18) and (19) impose a lower and upper limit according to the animal availability from suppliers and a given percentage δ to allow an extra flexibility in the total number of carcasses to be processed. Constraint (20) ensures that the holding capacity for products is never exceeded. Constraint (21) defines the domain of decision variables.

On the other hand, the set of follower's constraints are the following. Constraints (23) and (24) ensure that the requested level of each product is addressed, allowing the existence of unsatisfied-demand if the manufacturer does not provide enough products to satisfy the demand. Constraint (25) ensures that the capacity for holding products is never exceeded. Constraint (26) satisfies the condition to not holding products at the end of the planning horizon. Constraint (27) defines the domain of decision variables.

In this paper, we solve a linear relaxation of model (11)-(27) using the equivalent reformulation describes in (5)-(10), obtaining a nonlinear optimization problem. To solve this last model, (Fortuny-Amat and McCarl, 1981) propose an equivalent mixed-integer linear program. This formulation adds $(IT + T + I)$ binary variables and $2(IT + T + I)$ new constraints that replace nonlinear constraints of type (8). The resulting model can be solved using a mixed-integer solver only for small size instances. To solve medium and larger instances can be solved by the algorithm proposed by (Bard and Moore, 1990) .

3 RESULTS

In this section, a case study is presented to illustrate the suitability and advantages of the proposed bilevel optimization model. Basic parameters (such as prices, costs and warehouse capacities) were created using market information gathered from different pork producers. Different countries use different cutting patterns for producing meat products according to their

history and gastronomic culture. The case study considers cutting patterns used by a Mexican pork firm that must plan its production over a time horizon. First, pork carcasses were split up into 5 sections, and for each section a set of cutting patterns was assigned. In total, the company operates with 17 cutting patterns, and manages 40 pork products.

The case study represents a batch of fattened pigs arriving every day to the manufacturer to be slaughtered and later processed as carcasses. It is assumed the available amount of carcasses during the whole horizon is fixed and known. The total amount of carcasses available over a time horizon was set at 5000. The yield matrix for a carcass per product, section and cutting pattern was obtained from production lines (in kg). Considering the large amount of products, we selected 15 products with the highest prices, representing 67% of total demand. Labour capacity is considered as 8 hours per day in normal time, and 3 hours per day of overtime. To perform each cutting pattern, a specific amount of labour time is required. The solved instance considered 10 planning periods. In addition, the shelf life was 10 days, not enough to overcome during the planning horizon.

Results in a bilevel linear programming model, for which reformulations are presented, becomes a mixed-integer linear problem with 700 and 300 decision variables for the leader and follower, 2825 constraints and 475 dual variables. The first instance represents the coordination and integration of the two supply chain agents. Moreover, it is also assumed that demand is given, and the available amount of carcasses is fixed and known. Table 1 summarizes the achieved results:

Table 1: Results.

Profit [US$]	3.557.190
Service level	73,7%
Unsatisfied demand [u]	44.522
Carcasses acquired [u]	4.424
Carcasses acquired rate	88%
Excess Product [u]	38.523

Results from the case study showed a net profit of $3.557.190 dollars for the leader a service level of 73,7% for the follower. Under this solution 88% of whole carcasses available in the planning horizon (4.424 carcasses) were used. This demonstrated that the demand was not completely satisfied. It also notes that the manufacturer did not reach its maximum capacity, and the occupancy rate carcasses during the planning horizon was less than 100%, meaning that there was still raw material to be processed.. Table 2 shows the acquisition of carcasses during the planning horizon (10 days):

Table 2: Value of H in each period of time.

Horizon	H_t
1	550
2	516
3	548
4	415
5	555
6	447
7	427
8	506
9	336
10	124

The quantity of carcasses acquired at each period did not show major changes during the planning horizon, except for the last day where the carcasses acquired were to process and sell just for that period, without holding products. The amount of unsatisfied demand had a total of 44.522 products during the planning horizon, and the excess product at the end of the planning horizon is 38.523. The following table shows the detail for each of the products.

Table 3: Unsatisfied demand and excess products.

i	**Unsatisfied demand [u]**	**Excess products [u]**
1	0	0
2	0	0
3	0	4.672
4	4.321	0
5	0	0
6	24.105	1.226
7	6.910	0
8	5.012	0
9	1.297	0
10	0	23.946
11	436	0
12	0	728
13	0	0
14	0	7.950
15	2.380	0

The pattern cuts used resulted in different products. Products in inventory at the end of the planning horizon are excess products, and the manufacturer sells them without revenues because it's a salvage value. This implies that the leader produces to achieve a high follower service level as long as revenues are higher than the production cost of each of product. When the cost exceeds income from sales, the leader will prefer not to produce, and pay a penalty. In this game, the agents related to two levels of the supply chain, and it was observed that decisions have an interdependent relationship. The amount of unsatisfied demand selected by the wholesaler has an effect on

the profit function of the leader Deciding how much to produce has an effect on the quantity of unsatisfied demand by the follower.

In order to see the advantages of the bilevel programming model, these results are compared with the decision making of the leader in Table 4.

Table 4: Comparison of two models.

Models	Bilevel	Leader
Profit [US$]	3.557.190	1.805.780
Service level	73,7%	72,5%
Carcasses acquisition rate	88%	86%
Excess Product [u]	38.523	38.886

A new instance arises when the leader and follower are not coordinated nor integrated. In this case, the leader's model optimizes his operations according to (11) - (21), adding the demand requirement from the wholesaler. Table 4 shows that the leader does not use whole carcasses available. In addition, service level is 72,5% and the production capacity of the plant are not at the maximum. Comparing both models, when the two players are coordinating and integrating information and activities, the profits and service level increases. The carcasses acquisition rate rises because the leader is producing more products so that the unsatisfied demand decreases. In relation to excess product; in the bilevel programming model, the amount at the end of the planning horizon is less than the final quantity in the one-level decision model.

In this case, we show the importance of coordinating and integrating different agents in the supply chain. The leader maximizes profits, and even if the demand is given, profits and service level are lower than when leader and follower are coordinated and integrated. The difference lies mainly in inventory cost; when two players work together, products are held in two warehouses. In this way, costs are shared, unlike when the leader works alone. Coordination and integration is not only for better profits, but also increases service level and productivity.

All instances described in the computational results were implemented and solved using CPLEX 12.6.2.0 as a solver in a Macbook Pro Retine Display, i5-5257U Broadwell and 8Gb RAM with the software optimization package IBM ILOG CPLEX.

4 CONCLUSIONS

This work presents a novel Stackelberg production game between two players in the Pork Industry. The players are manufacturer and wholesaler, representing leader and follower, respectively. This game a coordinates and integrate this link of the supply chain. To represent the game, we propose a linear bilevel programing model, where the leader maximizes profits, and the follower maximizes their service level.

Our model was applied to a case study in the pork industry, concluding that coordinating and integrating both players in the supply chain is a better strategy than previously proposed solutions. In effect, this coordination obtains higher profits and better service level. Furthermore, the reformulations used to solve this bilevel model are useful in this context. They ensure global optimum with computational time required to solve the mixed linear programming problem instances less than 1 minute, proving to be efficient for dimensions resolved in this work.

Game theory in supply chain management proves to be a powerful method that allows modeling games between different players within the food industry. Future research in this area focus on resolution techniques from a bilevel linear mixed-integer programming model as well as the development of a three-level model: supplier, producer and distributor.

ACKNOWLEDGEMENTS

This research was partially supported by DGIIP (Grant USM 28.15.20) and Departamento de Industrias, Universidad Técnica Federico Santa María. Authors also wish to acknowledge to Ibero-American Program for Science and Technology for Development (CYTED 516RT0513).

REFERENCES

Ahumada, O. and Villalobos, J. (2009). Application of planning models in the agri-food supply chain: A review. *European Journal of Operational Research*, 196(1):1–20.

Albornoz, V. M., Gonzalez-Araya, M., Gripe, M. C., Rodriguez, S. V., and Treviño, E. J. (2015). An Optimization Model for Planning Operations in a Meat Packing Plant. *Operation Research and Enterprise Systems. de Werra, D., Parlier G.H., Vitoriano, B. (Eds). Communications in Computer and Information Science*, 577:136–146.

Bard, J. F. (2013). *Practical bilevel optimization: algorithms and applications*, volume 30. Springer Science & Business Media.

Bard, J. F. and Moore, J. T. (1990). A branch and bound algorithm for the bilevel programming problem. *SIAM Journal on Scientific and Statistical Computing*, 11(2):281–292.

Bjørndal, T., Herrero, I., Newman, A., Romero, C., and Weintraub, A. (2012). Operations research in the nat-

ural resource industry. *International Transactions in Operational Research*, 19:39–62.

Dempe, S. (2002). *Foundations of bilevel programming*. Springer Science & Business Media.

FAO (2016). Food and Agriculture Organization of the United Nations. http://faostat3.fao.org/faostat-gateway/go/to/home/E/ [Online; accessed 03-September-2016].

Fortuny-Amat, J. and McCarl, B. (1981). A representation and economic interpretation of a two-level programming problem. *Journal of the operational Research Society*, 32(9):783–792.

Hennet, J.-C. and Arda, Y. (2008). Supply chain coordination: A game-theory approach. *Engineering Applications of Artificial Intelligence*, 21(3):399–405.

Higgins, A., Miller, C., Archer, A., Ton, T., Fletcher, C., and McAllister, R. (2010). Challenges of operations research practice in agricultural value chains. *Journal of the Operational Research Society*, 61(6):964–973.

Marulanda, M. V. and Delgado, J. F. T. (2012). Análisis de teoría de juegos en cadenas de suministros de dos niveles, productor-comprador, bajo esquema vendor managed inventory (vmi). *Iteckne*, 9(1).

Migdalas, A., Pardalos, P. M., and Värbrand, P. (2013). *Multilevel optimization: algorithms and applications*, volume 20. Springer Science & Business Media.

Plà, L., Sandars, D., and Higgins, A. (2014). A perspective on operational research prospects for agriculture. *Journal of the Operational Research Society*, 65:1078–1089.

Rodríguez, S., Plá, L., and Faulín, J. (2014). New opportunities in operations research to improve pork supply chain efficiency. *Annals of Operation Research*, 219:5–23.

Von Stackelberg, H. (1952). *The theory of the market economy*. Oxford University Press.

Yue, D. and You, F. (2014). Game-theoretic modeling and optimization of multi-echelon supply chain design and operation under stackelberg game and market equilibrium. *Computers & Chemical Engineering*, 71:347–361.

Selecting Genetic Operators to Maximise Preference Satisfaction in a Workforce Scheduling and Routing Problem

Haneen Algethami[1], Dario Landa-Silva[1] and Anna Martínez-Gavara[2]
[1]*School of Computer Science, ASAP Research Group, The University of Nottingham, Nottingham, U.K.*
[2]*Estadística y Investigación Operativa, Universidad de Valencia, Valencia, Spain*
{*haneen.algethami, dario.landasilva*}*@nottingham.ac.uk, gavara@uv.es*

Keywords: Genetic Operators, Constraints Satisfaction, Scheduling and Routing Problem, Home Health Care.

Abstract: The Workforce Scheduling and Routing Problem (WSRP) is a combinatorial optimisation problem that involves scheduling and routing of workforce. Tackling this type of problem often requires handling a considerable number of requirements, including customers and workers preferences while minimising both operational costs and travelling distance. This study seeks to determine effective combinations of genetic operators combined with heuristics that help to find good solutions for this constrained combinatorial optimisation problem. In particular, it aims to identify the best set of operators that help to maximise customers and workers preferences satisfaction. This paper advances the understanding of how to effectively employ different operators within two variants of genetic algorithms to tackle WSRPs. To tackle infeasibility, an initialisation heuristic is used to generate a conflict-free initial plan and a repair heuristic is used to ensure the satisfaction of constraints. Experiments are conducted using three sets of real-world Home Health Care (HHC) planning problem instances.

1 INTRODUCTION

The workforce scheduling and routing problem (WSRP) involves scheduling and routing of workforce to visit customers at different locations in order to complete a set of tasks or activities. The problem arises in real-world scenarios, such as home health care, security guard routing and rostering, maintenance personnel scheduling among other worker allocation problems (Castillo-Salazar et al., 2016).

The WRSP is a combination of two combinatorial optimisation problems, personnel scheduling and routing, which are known to be NP-hard problems (Lenstra and Kan, 1981). The scheduling aspect allocates workforce to customers in order to fulfil work demands as well as satisfying their preferences. The routing aspect requires generating routes for workers to visit customers across various locations and within given time windows. Researchers have reported that real-world instances of the WSRP are large and difficult to solve (Mısır et al., 2015; Castillo-Salazar et al., 2016). Hence, there is a need to develop efficient algorithms to solve this type of problem.

Preliminary work evaluated a set of genetic operators within a steady-state genetic algorithm applied to a few instances of a real-world home health care (HHC) problem (Algethami and Landa-Silva, 2015). That work produced evidence that some operators obtain better results than others when used within the steady-state genetic algorithm for WSRP scenarios. The present paper conducts a more comprehensive study in order to achieve a deeper understanding of the behaviour and performance of the various genetic operators when applied to the WSRP.

The aim in this paper is to identify the best combination of genetic operators for each WSRP instance, in order to maximise the satisfaction of customers and workers preference constraints. Twelve genetic operators are considered in different combinations. The two genetic algorithms (GA) applied in this study are a steady state GA and a generational GA.

2 RELATED WORK

The routing component of the WSRP is related to variants of the classical vehicle routing problem (VRP) and in particular to the vehicle routing problem with time windows (VRPTW) (Toth and Vigo, 2014). Many GA applications have been used to tackle VRP including hybrid approaches incorporating heuristic methods and problem-specific operators to avoid pre-

Algethami, H., Landa-Silva, D. and Martínez-Gavara, A.
Selecting Genetic Operators to Maximise Preference Satisfaction in a Workforce Scheduling and Routing Problem.
In *Proceedings of the 6th International Conference on Operations Research and Enterprise Systems (ICORES 2017)*, pages 416-423
ISBN: 978-989-758-218-9

mature convergence of the GA (Prins, 2004; Chang and Chen, 2007). In addition, the study by (Prins, 2004) suggested the best genetic components for an efficient GA to tackle VRP problems. According to that study, order crossover (OX) is the most suitable operator for VRP-like problems.

Genetic algorithms (GAs) have been effective in providing good solutions relatively quickly, particularly when addressing real-world scheduling problems (Kotecha et al., 2004; Aickelin and Dowsland, 2004). It has been argued that this success is a result of the GA's capability to solve different segments of a problem simultaneously (Rothlauf, 2003).

A number of studies have applied GAs to real-world problems where scheduling and routing are combined. Examples include (Cowling et al., 2006; Mutingi and Mbohwa, 2014). In those works, the focus has been on algorithm design in order to obtain good solutions. However, well-known operators and repair heuristics were used to deal with infeasibility issues. Far too little attention has been given to introducing new genetic operators to reduce the overall cost. To date, the impact of selecting compatible operators for tackling WSRP instances has not yet been investigated.

The focus of this paper is not to produce the most competitive genetic algorithm, but to advance the understanding of how different combinations of genetic operators perform when tackling preference constraints in instances of the WSRP. The problem instances used in this study were also tackled in (Laesanklang and Landa-Silva, 2016; Pinheiro et al., 2016). This work seeks to identify effective combinations of genetic operators for tackling preference constraints in WSRP instances to then inform the design of competitive GAs to tackle this difficult problem.

3 PROBLEM DESCRIPTION

A WSRP solution is a daily plan of visits, i.e. a set of workers $W = \{w_1, w_2, \ldots, w_{|W|}\}$ assigned to perform a set of tasks $T = \{t_1, t_2, \ldots, t_{|T|}\}$ for customers at different locations. The assignment of a worker to travel to a customer location in order to perform a task is called a visit. Thus, $x^w_{i,j}$ is a binary decision variable that indicates if a path connects two nodes (visit i and visit j) or not. The assignment $x^w_{i,j} = 1$ means that worker w travels from visit i to visit j, thus w makes both visits. For visit j, if $x^w_{i,j} = 1$ then $y_j \leq r_j - 1$ where r_j is the *number of workers* required for visit j and y_j is an integer decision variable indicating the number of unsatisfied assignments, hence $\sum_{w \in W} \sum_{i \in T} \sum_{j \in T} x^w_{i,j} + y_j = r_j$.

This paper tackles a home health care (HHC) planning problem, in which workers are nurses, doctors, health carers, etc., and customers are patients receiving health care at their home. Several features have been identified as important in solutions to HHC scenarios, such as distance travelled and customers' and workers' requirements and preferences (Mankowska et al., 2014). A good quality plan for an HHC planning problem should have a low operational cost as well as assigning workforce. Thus, a solution requires all tasks to be assigned while satisfying some requirements. That is, assigning tasks according to workers' skills and avoiding time conflicts in respect to workers' time and area availability. A time conflict occurs when a worker is assigned to visits overlapping in time. Additional preferences include workers preferring to work in certain geographical areas, customers requiring workers with special skills or preferring certain workers to perform a task.

Table 1 lists WSRP objectives and constraints considered here. See (Laesanklang and Landa-Silva, 2016) for details of the MIP model of this WSRP. Note that in (Laesanklang and Landa-Silva, 2016), unassigned visits constraint is considered as a soft constraint. However, here this is a hard constraint, hence all visits must be assigned. Additionally, in this paper, time-conflict constraint is introduced, while the study by (Laesanklang and Landa-Silva, 2016) avoided conflicts. The decomposition method divided a problem into sub-problems, then available workers were updated so that no conflicting assignments exists.

A solution S is a set of assignments to workers in order to make visits. The objective function includes the *operational cost* and the *penalty cost*. The operational cost is the accumulated cost $d_{i,j} + p^w_j$, where $d_{i,j}$ is the distance travelled between visit i to visit j and p^w_j is the cost of assigning worker w to visit j, i.e. wages plus journey costs for all workers, as calculated by the service provider in our HHC scenarios.

The penalty cost is the accumulated penalty for the violations on constraints. An assignment can be written as a tuple $x^w_{i,j}, y_j, a^w_j, \psi^w_j, \theta^w_j, \tau^w_j$. Where, a^w_j is the arrival time of a worker w to the location of a visit j. The assignment is also composed of binary decision variables indicating an assignment of worker w to visit j with violations on area availability (ψ^w_j), time availability (θ^w_j) and conflicting assignments (τ^w_j).

The non-satisfaction of preferences is also included in the penalty cost. There are three types of preferences including preferred worker-customer pairing, worker's preferred region and customer's preferred skills. There is a degree of satisfaction for these preferences when assigning a worker w to a task j and

Table 1: Objectives and constraints in the WSRP.

Objectives	Hard constraints	Soft constraints
Minimise the operational cost	Assign all visits	Respect workers area availability
Minimise the penalty cost	Respect visit time (No time-conflicts)	Respect workers time availability
	Respect max working time per week	Assign preferred workers to visits
	Respect min working time per week	Assign preferred workers with a specific skill
	Assign qualified workforce	Assign workers to preferred areas

is given by ρ_j^w which has a value that ranges between $[0,3]$. For each assignment, the satisfaction value for each preference ranges between $[0,1]$, from not satisfied to satisfied. The satisfaction level is reverted to a penalty by subtracting it from the full satisfaction score, which is $3r_j$ for a visit j.

$$f(S) = \lambda_1 \sum_{w\in W}\sum_{i\in T}\sum_{j\in T}(d_{i,j}+p_j^w)x_{i,j}^w + \lambda_2 \sum_{w\in W}\sum_{i\in T}\sum_{j\in T}(3r_j-\rho_j^w)x_{i,j}^w + \lambda_3 \sum_{w\in W}\sum_{j\in T}(\psi_j^w+\theta_j^w) + \lambda_4 \sum_{j\in T} y_j + \lambda_5 \sum_{w\in W}\sum_{j\in T}\tau_j^w \quad (1)$$

The best solution should have: the least *operational cost* and the least *penalty cost*. A weighted sum is proposed to combine the objectives into a single scalar value (Pinheiro et al., 2016; Algethami et al., 2016). The objective function is written as in equation (1), where weights $\lambda_1,\ldots,\lambda_5$ are defined to establish priority between objectives (more about the weights used here later in the paper).

4 ALGORITHMS AND OPERATORS

This paper investigates the behaviour of various genetic operators when tackling instances of the WSRP by analysing their performance within relatively straightforward implementations of two variations of GAs. A simple solution representation allows direct implementation of genetic operators on the genotype (Rothlauf, 2003). Thus, a *direct representation scheme* is used for chromosome encoding. A vector of integers of length equal to the number of visits, $|T|$, represents a one-day plan. Hence, all visits are assigned. Indexes of the chromosome correspond to the set of tasks T, for example the i^{th} gene in the chromosome means the corresponding visit with index $i \in T$. In order to increase the possibility of obtaining a feasible initial plan, indexes in the chromosome are associated to visits in non-decreasing order of visit start time. In this way, index 1 is for the visit with the earliest start time and index $|T|$ is for the visit with the latest start time. For each visit in the vector, a worker w is selected at random from W. A worker w may undertake more than one visit, and some workers may not be utilised as a part of a particular one-day plan.

4.1 Genetic Algorithms (GA)

Two GAs are implemented in this study: a steady-state genetic algorithm (SSGA) and a generational genetic algorithm (GenGA) (Vavak and Fogarty, 1996). Such relatively simple algorithms were selected in order to analyse the emergent behaviour and performance of the operators on a straightforward GA implementation.

Initially, a *time conflict reduction* (TCR) operator is applied to each individual in the initial population in order to reassign visits and reduce the number of time conflicts. After that, the evolutionary process for each GA is executed as follows. For the *SSGA*, there is only one population P of size M during the whole evolutionary process, where parents are selected and the offspring is inserted; thus, no generations required. Two parents i, j are selected by tournament selection from the parent lists L_1 and L_2, each of size $M/2$. To create a parent list, six different individuals are selected at random from P and split into two groups of three; the best individual of one group is added to L_1 and the best individual of the other group is added to L_2. This process is repeated until the two lists of parents are complete. Then, for i, j from $1,\ldots,M/2$, parent i in L_1 and parent j in L_2 are combined through crossover, producing two offspring. The next step is to apply mutation operator. A mutation operator is applied with some probability to the generated offspring. That is, if the mutation is applied to an individual k, the mutated individual k' replaces k, regardless of the objective function value. The recombination plus mutation process is implemented on the two parents; the best two individuals out of the two parents and the two children are added into P so that the population size remains constant.

For the *GenGA* a new population is created at the

start of each generation. The recombination plus mutation process is repeated $M/2$ times until the new population P' is complete. At this point, individuals in P' are sorted in non-decreasing order of their fitness. The best 10% of solutions found are never removed from the population. However, the worst 10% of individuals in P' are replaced by randomly generated individuals to introduce diversity onto the population. After this, the new population replaces the old one, i.e. $P = P'$. Then, the WSR operator (described below) is applied onto infeasible individuals within the population based on hard constraints violations shown in Table 1. Finally, population P' is passed to the next generation.

4.2 Repair Operators

A *time conflict reduction* (TCR) operator works as follows. Each pair of visits, i and j, are compared to identify any time conflicts, i.e. the same worker w being assigned to the two visits at the same time. If there is a time conflict, worker w is replaced in visit j by another worker w', selected from the list of preferred workers for visit j, if that list exists, or selected at random otherwise. Because TCR is applied only once on an individual, by removing one pair of visits at a time, it cannot ensure that all time conflicts are removed, but it does reduce their number.

The *worker suitability repair* (WSR) operator seeks to improve the suitability of workers for each visit, and works as follows. For each visit in an individual, the assigned worker is checked against the skills requirements, maximum hours constraints and time conflicts (i.e. the hard constraints listed in Table 1). If the worker does not satisfy these requirements, the operator aims to find another worker who is feasible for that visit. If no such worker can be found, the operator leaves the original worker in place. Thus, the WSR operator cannot ensure that all visits have a suitable worker, but it does improve the overall assignment with respect to the constraints.

4.3 Genetic Operators

The aim of this study is to select the best configuration of crossover and mutation operators that can tackle the WSRP within the SSGA and GenGA. Twelve operators are implemented, ten well-known operators plus two cost-based operators tailored for the problem tackled here.

Ten well-known operators were chosen after a literature survey of operators applied in WSRP-related problems (Algethami and Landa-Silva, 2015). The operators selected are divided into two groups. One group has five *scheduling operators*: single-point crossover (1PX), uniform crossover (Mitchell, 1998), two-point crossover (2PX) (Hartmann, 1998), half-uniform crossover (HX) (Eshelman, 1991) and random swap mutation (RSM) (Cicirello and Cernera, 2013). The other group has five *routing operators*: order crossover (OX) (Zheng and Wang, 2003), cycle crossover (CX) (Oliver et al., 1987), partially matched crossover (PMX) (Zhu, 2000), inversion mutation (IM) (Eshelman, 1991) and scramble mutation (SM) (Cicirello and Cernera, 2013).

Algorithm 1: Cost-based uniform crossover (CBUX).

Require: parent individuals p_1 and p_2
Ensure: offspring individuals o_1 and o_2
1: $o_1, o_2 \leftarrow$ new empty individual
2: **for** $i \leftarrow 1$ **to** $|T|$ **do**
3: Let w_1^i be worker assigned to visit $i \in p_1$
4: Let w_2^i be worker assigned to visit $i \in p_2$
5: **if** w_1^i and w_2^i are both available for visit i **then**
6: $o_1 \leftarrow o_1 \cup w_1^i$
7: $o_2 \leftarrow o_2 \cup w_2^i$
8: **else**
9: **if** one of w_1^i or w_2^i, called w^i, is available for visit i **then**
10: $o_1 \leftarrow o_1 \cup w^i$
11: $o_2 \leftarrow o_2 \cup w^i$
12: **else**
13: $o_1 \leftarrow o_1 \cup w_2^i$
14: $o_2 \leftarrow o_2 \cup w_1^i$
15: **end if**
16: **end if**
17: **end for**

Two cost-based operators operators have been purposely designed to improve the satisfaction of soft constraints in the WSRP, even at the expense of having a larger total cost in the solution.

One of these operators is a *cost-based uniform crossover (CBUX)* shown in Algorithm 1. Cost-based crossovers have been applied in the literature to produce improved results by restricting mating to the feasible region only (Kotecha et al., 2004). This CBUX operator works as follows. Each position i for the two parents, corresponding to the worker assigned to visit i, is processed one at a time (line 2). The availability, in terms of time and area, of the worker assigned to visit i is examined for each parent. If both parents have an available worker in that position, their gene is copied to the corresponding offspring (lines 5–7). If only one of the parents has an available worker in that position, that gene is copied to both offspring (lines 9–11). If no parent has an available worker in that position, offspring 1 gets the gene from parent 2 and offspring 2 gets the gene from parent 1 (lines 13–14).

Algorithm 2: Cost-based mutation (CBM).

Require: individual k
1: Choose a random mutation point $i \in k$
2: Let w^i be the worker assigned to visit i
3: Let Ω^i be the list of preferred workers for i
4: **if** $w \notin \Omega^i$ **then**
5: Choose a random worker $w' \in \Omega^i$
6: Replace w with w' in k for visit i
7: **end if**

A *cost-based mutation (CBM)* is shown in Algorithm 2. This operator seeks to ensure that workers assigned to visits are among those considered as *preferred workers* for that visit. As part of the input data in the problem instances considered here, a list of preferred workers is given for each visit as defined by the patients. Then, for position i in the individual, CBM tries to assign one of the preferred workers for that visit i, only if the one already assigned is not a preferred worker (lines 4–6).

5 EXPERIMENTS AND RESULTS

Table 2: Parameter settings used in the experiments.

Parameter	Settings
Population size M	100
Crossover operators	1PX, 2PX, UX, HX, PMX, OX, CX, CBUX
Crossover rate P_c	10%, 50%, 100%
Mutation operators	RSM, IM, SM, CBM
Mutation Rate P_m	1%, 10%, 30%
Running time	5 minutes

Experiments were conducted to evaluate the performance of different operators on real-world WSRP scenarios. The GAs described in Section 4 were implemented with different algorithm configurations as stated in Table 2. Values for mutation and crossover rates are taken from previous parameter tuning experiments.

The best suitable combinations of operators, each combination is one crossover operator with one mutation operator, might be later embedded in a more efficient approach. To this end, the experimental study focused on comparing the performance of the various genetic operator combinations aimed at satisfying customers' and workers' preference constraints. Nevertheless, one of the major issues in the random direct representation is allowing infeasible individuals throughout the search process, so that the end result can have individuals with high number of constraint violations. Thus, reducing hard constraint violations, such as skills required, maximum hours requirements and time conflicts, is required to maintain feasibility in WSRP solutions. As explained in Section 4, the WSR mechanism is applied to individuals that present hard constraint violations. WSR implementation occurs in two stages of the GA: after the TCR, and then again after the mutation operator in the optimisation process.

For each GA, 32 mutation-crossover combinations with 9 different rates were applied. Thus 288×2 algorithm configurations and each one was executed 8 times, all seeded with the same initial population. The best cost solution was obtained from each set with the same amount of computation time. The implementation was in Java running on a PC with I7 four-core processor with hyper-threading enabled and 16GB of RAM.

5.1 Problem Instances

Problem instances from three UK real-world HHC scenarios are used as instances of WSRP. The instances data and weights used here (blue setting) are available at https://drive.google.com/open?id=0B2OtHr1VocuSNGVOT2VSYmp6a2M. In this study, three scenarios were used with 7 problem instances each, for a total of 21 instances. Table 3 shows the main features of each problem instance.

Scenario A instances are considered the smallest, while instances in scenario B are larger. Problem instances in scenario C are very different to the instances in the other 6 scenarios in that the number of workers is much larger than the number of visits.

Table 3: Features of the WSRP instances.

Instance	**A1**	**A2**	**A3**	**A4**	**A5**	**A6**	**A7**	**Mean**
Number Visits	31	31	38	28	13	28	13	26
Number Workers	23	22	22	19	19	21	21	21
Number Areas	6	4	5	4	4	8	4	5
Instance	**B1**	**B2**	**B3**	**B4**	**B5**	**B6**	**B7**	**Mean**
Number Visits	36	12	69	30	61	57	61	47
Number Workers	25	25	34	34	32	32	32	31
Number Areas	6	5	7	5	8	8	7	7
Instance	**C1**	**C2**	**C3**	**C4**	**C5**	**C6**	**C7**	**Mean**
Number Visits	177	7	150	32	29	158	6	80
Number Workers	1037	618	1077	979	821	816	349	814
Number Areas	8	4	7	8	6	11	6	7

5.2 Performance of Operators

The first set of experiments was designed to select the best combination of the operators that maximise customer/worker requirements and preferences satisfaction. To do so, all operators listed in Table 2 were examined by statistical analysis to determine their performance. There are four mutation operators (RSM, IM, SM, CBM) and eight crossover operators divided into three different groups: routing crossovers

Table 4: Performance Comparison of Crossover Operators Grouped by Category (Routing, Scheduling, Cost-Based) Under a Mutation Operator.

	Mutation	RSM			SM			IM			CBM		
SSGA	**Crossover**	***OX***	*UX*	*CBUX*	***OX***	*UX*	*CBUX*	***OX***	*UX*	*CBUX*	***OX***	*1PX*	*CBUX*
	Dev.	**0.09%**	1.66%	4.99%	**0.07%**	1.23%	4.90%	**0.04%**	1.47%	4.24%	**0.66%**	1.37%	3.23%
	#Best	**0.71**	0.19	0.00	**0.76**	0.14	0.00	**0.86**	0.05	0.00	**0.48**	0.38	0.05
	Score	**0.90**	0.57	0.57	**0.93**	0.60	0.12	**0.98**	0.50	0.17	**0.76**	0.60	0.29
GenGA	**Crossover**	*PMX*	***UX***	*CBUX*	***PMX***	***IPX***	*CBUX*	*PMX*	***IPX***	*CBUX*	***PMX***	*UX*	*CBUX*
	Dev.	0.87%	**0.70%**	8.98%	2.28%	**1.17%**	9.82%	2.90%	**1.92%**	9.65%	**0.65%**	3.12%	5.19%
	#Best	0.38	**0.38**	0.14	**0.43**	0.38	0.14	0.29	**0.52**	0.19	**0.57**	0.19	0.14
	Score	0.67	**0.74**	0.24	**0.74**	0.69	0.24	0.67	**0.74**	0.31	**0.81**	0.50	0.33

(OX, CX, PMX), scheduling crossovers (1PX, 2PX, UX, HX) and cost-based crossovers (CBUX). Each crossover was combined with one mutation at a time for a total of 32 combinations, however only the best performing crossover operators from each group is presented in Table 4. The GA was executed for 5 minutes using the highest rate values, i.e. $P_c = 100\%$ and $P_m = 30\%$ to ensure that the operators were utilised.

The following three metrics were used to measure the performance of the combinations of operators: **Dev.** average percentage deviation from the best preference value (the three preferences satisfaction value of all the configurations applied). **Best** fraction of instances in a set for which a configuration matches the best preference value. This performance metric is absolute and can be compared across existing results in different tables. **Score** fraction of the instances for which the current method produces better solutions than the other configurations, i.e. 'win'. This score is calculated as $((q \times (p-1)) - r)/(q \times (p-1))$, where p is the number of configurations compared, q is the number of problem instances, and r is the number of instances in which the $p-1$ competing configurations find a better result. Hence, the best score value is 1, when $r = 0$, and the worst score value is 0, when $r = q \times (p-1)$. This is a relative measure of performance. Hence, these values are only meaningful within one table and not across different tables.

The results presented in Table 4 are the performance metrics values that correspond to each of the four mutation operators, including the CBM operator proposed in this study. These values are calculated based on the average preferences satisfaction values for each run. The crossover categories are: the best routing operator, the best scheduling operator and the CBUX operator proposed in this study. Thus, each mutation operator has three comparable crossover operators values, and the best crossover out of the three is highlighted in **bold**. The aim is to identify the best crossovers for each mutation with respect to the preferences value by grouping crossovers based on their category, thus mutation operators are not comparable in this table.

Table 5: Performance Comparison Between the Best Combinations of Operators (Mutation - Crossover).

	Procedur	Dev.	#Best	Score
SSGA	***RSM-OX***	**0.01%**	**0.52**	**0.87**
	SM-OX	0.03%	0.29	0.82
	IM-OX	0.15%	0.00	0.50
	CBM-OX	0.23%	0.10	0.45
GenGA	***RSM-UX***	**0.92%**	**0.57**	**0.84**
	SM-PMX	7.57%	0.05	0.43
	IM-1PX	2.73%	0.24	0.68
	CBM-PMX	18.36%	0.05	0.25

For SSGA, OX provides the best scores, with the highest number of best values and the lowest deviation when combined with all mutation operators. For GenGA, UX provides the best scores for RSM with the highest number of the best values and the lowest deviation. Even though UX is selected as the first competing crossover, PMX obtained the same number of the best values for RSM; the winning crossovers are considered in the next overall comparison. Additionally, 1PX provides the best score value with the highest number of best solutions and lowest on deviations among the compared crossovers for IM, while PMX provides the best score value for both SM and CBM, with the lowest deviation obtained for CBM only.

Table 5 shows a comparison between the chosen combinations of operators (mutation - crossover) from Table 4. The aim is to identify the best combination for each GA by using the same performance measurement matrices explained above. The best combination is highlighted in **bold**.

The results indicate that RSM–UX and RSM–UX obtain the highest score and the smallest deviation value among all methods, with the maximum fractions of the best solutions of 0.87 and 0.84 for SSGA and GenGA respectively. Interestingly, cost-based methods failed to achieve good results in comparison to the generic operators. This result might be due to the search space restrictions that led to infeasible areas. However, when combined with more generic

Table 6: Results of the best $f(S)$ produced by different combinations of operators, crossover probabilities P_c and mutation probabilities P_m.

		SSGA					GenGA				
	Instance	*Procedure*	P_c	P_m	$f(S)$	$Cpt(s)$	*Procedure*	P_c	P_m	$f(S)$	$Cpt(s)$
A	1	*SM-PMX*	0.5	0.3	5.1	176.6	*RSM-PMX*	1	0.3	**3.5**	180.8
	2	*SM-OX*	1	0.3	4.4	184.4	*SM-UX*	1	0.3	**2.8**	190.7
	3	*SM-UX*	1	0.3	6.1	240.8	*SM-1PX*	1	0.3	**3.3**	212.3
	4	*SM-UX*	0.5	0.3	2.3	159.9	*SM-UX*	1	0.3	**1.4**	114.5
	5	*SM-1PX*	1	0.1	3.2	50.7	*SM-HX*	1	0.3	**2.4**	52.4
	6	*SM-2PX*	1	0.1	4.4	198.6	*RSM-HX*	1	0.3	**3.6**	109.0
	7	*SM-2PX*	1	0.1	4.2	32.7	*RSM-HX*	1	0.3	**3.7**	83.2
B	1	*SM-UX*	1	0.3	2.1	239.7	*RSM-PMX*	1	0.3	**1.7**	255.0
	2	*SM-OX*	1	0.1	2.4	50.7	*RSM-HX*	1	0.3	**1.8**	14.7
	3	*RSM-PMX*	0.5	0.3	2.8	292.9	*RSM-PMX*	0.5	0.3	**1.9**	274.1
	4	*SM-2PX*	1	0.3	2.9	75.3	*SM-2PX*	1	0.3	**2.1**	138.0
	5	*RSM-UX*	0.5	0.3	3.8	243.5	*RSM-2PX*	1	0.3	**2**	243.2
	6	*RSM-UX*	1	0.3	2.5	226.1	*RSM-2PX*	0.5	0.3	**1.7**	229.2
	7	*RSM-UX*	0.5	0.3	3.2	231.8	*RSM-1PX*	0.5	0.3	**1.9**	288.2
C	1	*CBM-OX*	1	0.1	**5454.5**	285.0	*CBM-OX*	1	0.3	159418.6	304.8
	2	*SM-HX*	1	0.01	4.8	15.0	*SM-HX*	1	0.3	**3.2**	152.7
	3	*RSM-2PX*	1	0.3	**3270.7**	299.4	*SM-OX*	1	0.3	82582	293.9
	4	*RSM-OX*	1	0.01	22.2	210.0	*IM-HX*	1	0.3	**17.6**	269.8
	5	*SM-PMX*	1	0.1	20.1	172.6	*IM-HX*	1	0.3	**16**	267.3
	6	*CBM-PMX*	1	0.01	**20776.5**	266.6	*CBM-OX*	1	0.01	94335.9	297.8
	7	*SM-UX*	1	0.3	4.9	0.7	*SM-UX*	1	0.3	**4.3**	15.9

operators, in the case of CBM, they generate more diverse individuals that led up to high deviation among all mutations.

5.3 Computational Results for Different Instance Sizes

Table 6 presents the best objective values obtained for all instances. The columns under SSGA and GenGA provide the best values obtained for each GA under the stopping criterion for each combination. All values are averaged and only the best values are presented. The remaining column Cpt shows the computation time where the best value is found in seconds. Two issues were considered to compile this table: the GAs performance on each instance and the best performing combinations/settings under each GA with the minimum computation time.

It appears that GenGA provides better results than SSGA on 85.71% of all instances. The best-performing operators under the methods applied are PMX, UX and HX across all instances when combined with RSM and SM. However, CBM managed to obtain some of the best results, especially for scenario C instances. This indicates that problem domain knowledge needs to be incorporated in operators for more complicated instances. The average computation times for the best solution found for all instances are as follows: SSGA, and GenGA are 173.954 s and 189.88 s respectively. In terms of convergence speed, both SSGAs used here converged earlier to a local minima, with poor results in problem sets A and B. For problem set C, more computation-time provided better results when using GenGA.

Despite the fact that the cost values still need to be improved, this study has helped to understand the performance of various combinations of genetic operators executed with different probability rates and implemented on simple steady-state and generational GAs.

6 CONCLUSION

This paper has investigated the suitability of a set of genetic operators when applied within a steady-state genetic algorithm (SSGA) and a generational genetic algorithm (GenGA) to tackle the workforce scheduling and routing problem (WSRP). Twelve operators were considered in this study including two operators incorporating problem domain knowledge, and ten well-known operators (three mutation operators and

seven crossover operators) from the literature. From the experimental results, existing operators such as RSM and UX perform the best. Future research will look at investigating the performance of the repair operators, parameter setting of the operators and the design of an improved evolutionary approach informed by the better understanding achieved in this paper.

REFERENCES

Aickelin, U. and Dowsland, K. A. (2004). An indirect genetic algorithm for a nurse-scheduling problem. *Computers & Operations Research*, 31(5):761 – 778.

Algethami, H. and Landa-Silva, D. (2015). A study of genetic operators for the workforce scheduling and routing problem. In *11th Metaheuristics International Conference (MIC 2015)*, pages 1–11.

Algethami, H., Pinheiro, R. L., and Landa-Silva, D. (2016). A genetic algorithm for a workforce scheduling and routing problem. In *2016 IEEE Congress on Evolutionary Computation (CEC)*, pages 927–934.

Castillo-Salazar, J. A., Landa-Silva, D., and Qu, R. (2016). Workforce scheduling and routing problems: literature survey and computational study. *Annals of Operations Research*, 239(1):39–67.

Chang, Y. and Chen, L. (2007). Solve the vehicle routing problem with time windows via a genetic algorithm. *Discrete and continuous dynamical systems supplement*, pages 240–249.

Cicirello, V. A. and Cernera, R. (2013). Profiling the distance characteristics of mutation operators for permutation-based genetic algorithms. In Boonthum-Denecke, C. and Youngblood, G. M., editors, *FLAIRS Conference*, Florida. AAAI Press.

Cowling, P., Colledge, N., Dahal, K., and Remde, S. (2006). The trade-off between diversity and quality for multi-objective workforce scheduling. In *Proceedings of the 6th European Conference on Evolutionary Computation in Combinatorial Optimization*, EvoCOP'06, pages 13–24. Springer-Verlag.

Eshelman, L. J. (1991). The CHC adaptive search algorithm : How to have safe search when engaging in nontraditional genetic recombination. *Foundations of Genetic Algorithms*, pages 265–283.

Hartmann, S. (1998). A competitive genetic algorithm for resource-constrained project scheduling. *Naval Research Logistics (NRL)*, 45(7):733–750.

Kotecha, K., Sanghani, G., and Gambhava, N. (2004). Genetic algorithm for airline crew scheduling problem using cost-based uniform crossover. In Manandhar, S., Austin, J., Desai, U. B., Oyanagi, Y., and Talukder, A. K., editors, *AACC*, volume 3285 of *Lecture Notes in Computer Science*, pages 84–91, Kathmandu, Nepal. Springer.

Laesanklang, W. and Landa-Silva, D. (2016). Decomposition techniques with mixed integer programming and heuristics for home healthcare planning. *Annals of Operations Research*, pages 1–35.

Lenstra, J. K. and Kan, A. H. G. (1981). Complexity of vehicle routing and scheduling problems. *Networks*, 11(2):221–227.

Mankowska, D., Meisel, F., and Bierwirth, C. (2014). The home health care routing and scheduling problem with interdependent services. *Health Care Management Science*, 17(1):15–30.

Mısır, M., Smet, P., and Vanden Berghe, G. (2015). An analysis of generalised heuristics for vehicle routing and personnel rostering problems. *Journal of the Operational Research Society*, 66(5):858–870.

Mitchell, M. (1998). *An Introduction to Genetic Algorithms*. The MIT Press, Cambridge, MA, USA.

Mutingi, M. and Mbohwa, C. (2014). Health-care staff scheduling in a fuzzy environment: A fuzzy genetic algorithm approach. In *Conference Proceedings (DFC Quality and Operations Management)*. International Conference on Industrial Engineering and Operations Management.

Oliver, I. M., Smith, D. J., and Holland, J. R. C. (1987). A study of permutation crossover operators on the travelling salesman problem. In *Proceedings of the Second International Conference on Genetic Algorithms and their application*, pages 224–230, Hillsdale, NJ, USA. L. Erlbaum Associates Inc.

Pinheiro, R. L., Landa-Silva, D., and Atkin, J. (2016). A variable neighbourhood search for the workforce scheduling and routing problem. In *Advances in Nature and Biologically Inspired Computing*, pages 247–259. Springer, Pietermaritzburg, South Africa.

Prins, C. (2004). A simple and effective evolutionary algorithm for the vehicle routing problem. *Computers & Operations Research*, 31(12):1985 – 2002.

Rothlauf, F. (2003). Representations for genetic and evolutionary algorithms. *Studies in Fuzziness and Soft Computing*, 104:9–32.

Toth, P. and Vigo, D. (2014). *The vehicle routing problem*, volume 18. Siam.

Vavak, F. and Fogarty, T. C. (1996). Comparison of steady state and generational genetic algorithms for use in nonstationary environments. In *Evolutionary Computation, 1996., Proceedings of IEEE International Conference on*, pages 192–195. IEEE.

Zheng, D.-Z. and Wang, L. (2003). An effective hybrid heuristic for flow shop scheduling. *The International Journal of Advanced Manufacturing Technology*, 21(1):38–44.

Zhu, K. Q. (2000). A new genetic algorithm for VRPTW. In *Proceedings of the International Conference on Artificial Intelligence*. Citeseer.

Multiobjective Optimization using Genetic Programming: Reducing Selection Pressure by Approximate Dominance

Ayman Elkasaby, Akram Salah and Ehab Elfeky
Faculy of Computers and Information, Cairo University, Giza, Cairo, Egypt
ayman.kasaby@gmail.com, {akram.salah, e.elfeky}@fci-cu.edu.eg

Keywords: Genetic Programming, Multiobjective Optimization, Epsilon Dominance, Evolutionary Algorithms.

Abstract: Multi-objective optimization is currently an active area of research, due to the difficulty of obtaining diverse and high-quality solutions quickly. Focusing on the diversity or quality aspect means deterioration of the other, while optimizing both results in impractically long computational times. This gives rise to approximate measures, which relax the constraints and manage to obtain good-enough results in suitable running times. One such measure, epsilon-dominance, relaxes the criteria by which a solution dominates another. Combining this measure with genetic programming, an evolutionary algorithm that is flexible and can solve sophisticated problems, makes it potentially useful in solving difficult optimization problems. Preliminary results on small problems prove the efficacy of the method and suggest its potential on problems with more objectives.

1 INTRODUCTION

Historically, in order to solve optimization problems, classical search methods were traditionally used. In every iteration, a single solution was modified in order to produce better solutions. However, this point-by-point approach was overshadowed by the introduction of evolutionary algorithms(EAs). These algorithms use the concepts of evolution and natural selection in optimization. Using populations of individual solutions, EAs try to capture multiple optimal solutions for problems lacking one global optimal solution.

Some optimization, for example industrial, problems have multiple objectives that need to be optimized in the same time, which poses extra difficulties for algorithms that try to solve these problems. Two main solutions have usually been followed to reduce the complexities:

- Reducing the number of objectives during the search process or a posteriori during the decision making process. This approach tries to identify non-conflicting objectives and discards them.
- Propose a preference relation that induces a finer order on the objective space.

If the aforementioned solutions fail to reduce multi-objective optimization problems' complexity, then the main difficulty facing EAs is incomparable solutions. Incomparable solutions happen in the following case. When one solution optimizes one (or more) objective better than a second solution, but the second solution optimizes another (or more) different objective better than the first one.

If we divide the search space into regions based on how well each solution optimizes each objective, and assuming no bias towards any region, the probability of a solution falling into any of these regions is proportional to the volume of this region divided by the volume of the entire solution set. As the number of objectives increases, the number of regions increases, and the probability that a solution will fall into a region where one solution optimizes all objectives efficiently is reduced significantly.

Problems with a large number of objectives, although apparently similar to problems with less number of objectives, can't be solved efficiently using the same methods used for fewer objectives. They are computationally more intensive, and visualizing their solutions becomes harder as more objectives are added. To avoid these complexities, some approximate measures are used to obtain good-enough results of the problem. Epsilon dominance, notated as ϵ-dominance from now on, is one of these approximate measures (Laumanns, et al., 2002).

In this paper, genetic programming, a flexible and powerful type of evolutionary algorithms (EAs), is used in order to solve optimization problems

Elkasaby, A., Salah, A. and Elfeky, E.
Multiobjective Optimization using Genetic Programming: Reducing Selection Pressure by Approximate Dominance.
In *Proceedings of the 6th International Conference on Operations Research and Enterprise Systems (ICORES 2017)*, pages 424-429
ISBN: 978-989-758-218-9

approximately using ϵ-dominance. We call this method ϵ-GP. Genetic programming, up to our knowledge, has not been used before to solve any optimization problem with an approximate measure. ϵ-GP is compared to regular genetic programming (Koza, 1992) in regards to speed, efficiency, and diversity, and it gives promising results.

The paper is structured as follows. **Section 2** explains related work in the field of evolutionary algorithms. Afterwards, in **Section 3 and 4**, some background information is given about optimization and genetic programming, respectively. An outline and pseudocode of ϵ-GP are given in **Section 5**, while **Section 6** deals with the experimentation and results. Finally, **Section 7** contains a conclusion of the paper and explains future work.

2 RELATED WORK

Evolutionary algorithms have long been successful in solving MOPs. Schaffer (Schaffer, 1985) started the movement of EAs solving MOPs by introducing a vector-evaluated genetic algorithm (VEGA) that finds a set of nondominated solutions.

Afterwards, the first generation of Multi-Objective Optimization Evolutionary Algorithms (MOEAs) started in the early 1990s by using Pareto ranking and fitness sharing. This generation consisted of the multi-objective genetic algorithm (MOGA) (Fonseca & Fleming, 1993), the niched Pareto genetic algorithm (NPGA) (Abido, 2003) which is the first algorithm to use tournament selection, and the nondominated sorting algorithm (NSGA) (Srinivas & Deb, 1994).

The second generation of MOEAs, which emerged in the late 1990s and early 2000s, introduced the concept of elitism (keeping a record of the best-so-far solutions). It includes the strength Pareto evolutionary algorithm (SPEA) (Zitzler & Thiele, 1999) and its improved version(SPEA-2) which adds a fitness assignment technique, a nearest neighbor density estimation, and a preservation truncation method (Zitzler, et al., 2001); the Pareto archived evolution strategy(PAES) (Knowles & Corne, 2000); the Pareto envelope based algorithm(PESA) (Corne, et al., 2000) and its improved version PESA-II (Corne, et al., 2001); and an improved version of NSGA (NSGA-II) which splits the pool of individuals into different fronts according to their dominance and adds a crowding measure to preserve diversity (Deb, et al., 2002).

NSGA-II is one of the most popular algorithms in the literature and is usually considered a benchmark for many new algorithms. This is because it is very quick in obtaining solutions. It also yields very efficient results. Although originally made for problems with smaller number of objectives, NSGA-II has shown to be somewhat successful over the years in solving some problems with more objectives as well.

3 OPTIMIZATION

An optimization problem is a problem where the goal is to find the best solution from all feasible solutions for a specific objective function. However, many of these problems (those that have more than one objective) exist in a setting that cannot be expressed using a single function, as different objectives are usually not measured using the same metrics.

Furthermore, a multi-objective optimization problem is defined as simultaneously optimizing

$$F(x) = min\big(f_1(x), \dots., f_k(x)\big), \quad (1)$$

$$subject\ to\ x \in \bar{X},$$

by changing n decision variables, subject to some constraints that define the universe $\bar{X}$.

In other words, a multi-objective optimization solution optimizes the components of $F(x)$ where x is an n-dimensional decision variable vector $x = (x_1, \dots, x_n)$ from some universe $\bar{X}$. Thus, the problem consists of k objectives reflected in the k objective functions, a number of constraints on the objective functions reflected on the feasible set of decision vectors $\bar{X}$, and n decision variables.

In the case of optimizing multiple objectives, it is usually impossible to find a single solution that optimizes all of the objectives at the same time. This gives rise to the definition of nondominated solutions (also called Pareto-optimal solutions), which are solutions that optimize some objectives but are not worse than other solutions in the rest of the objectives. The Pareto front is the visualization of all these solutions on the search space. Since these solutions are nondominated, no one solution exists that can be said to be better than the other; all of them are presented to the decision maker as a set of solutions called the Pareto optimal set.

Multi-objective optimizers usually have to conform to a few properties; namely, they should present solutions that are close to the Pareto front as possible. They should also present different, diverse solutions to the decision maker that show the

different tradeoffs with respect to each objective. Optimizers also need to present the best few, which means that overwhelming the decision maker by presenting too many solutions is not preferred.

3.1 More Objectives

Optimization problems that have more than 3 objectives are named *many*-objective optimization problems, and problems with 2 or 3 objectives are named *multi*-objective optimization problems. In (Khare, et al., 2003), it was found after testing 3 MOEAs from the 2nd generation of MOEAs (NSGA-II, SPEA2, PESA) that these algorithms showed vulnerability on problems with a larger number of objectives.

The main difficulties with many-objective optimization problems are visualization, how to handle high dimensionality and the exponential number of points needed to represent the Pareto front, the greater proportion of nondominated solutions, and stagnation of search due to larger number of incomparable solutions. Our work tackles the latter two difficulties by changing the definition of dominance to an approximate one, easing the criteria of acceptance of nondominated solutions.

3.2 Dominance

Multi-objective optimization algorithms insisting on both diversity and convergence to the Pareto front face Pareto sets of substantial sizes, need huge computation time, and are forced to present very large solutions to the decision maker. These issues effectively make them useless until further analysis, because speed and presenting few solutions are very important to decision makers.

ϵ-dominance (Laumanns, et al., 2002) tries to fix these problems by quickly searching for solutions that are good enough, diverse, and few in number. It approximates domination in the Pareto set by relaxing the strict definitions of dominance and considering individuals to ϵ-dominate other individuals, whereas previously they would have been nondominated to each other.

In Figure 1, a visual comparison between ϵ-dominance and regular dominance is shown (Laumanns, et al., 2002).

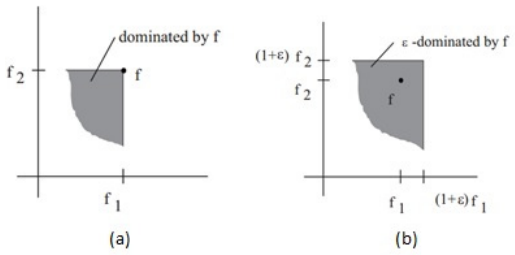

Figure 1: Differences between (a) regular and (b) ϵ -dominance.

4 GENETIC PROGRAMMING

Genetic programming (GP) is one type of evolutionary algorithms. Its main characteristic is that it represents solutions as programs (Koza, 1992). This representation scheme is the main difference between genetic algorithms and genetic programming. Each solution (program) is judged based on its ability to solve the problem, using a mathematical function, the fitness function. Each program, or solution, is represented using a decision tree. GP evolves a population of programs by selecting some candidates that score high on the fitness function and using regular evolutionary variation operators on them (mutation, crossover, and reproduction). New populations are created from these outputs until any specific termination criterion is met.

We use strongly-typed genetic programming (STGP) in this paper, which is one of many enhanced versions of GP. STGP makes GP more flexible, explicitly defining allowed data types beforehand instead of limiting it to only one data type. Genetic programming, and STGP specifically, consists of the following.

1) Representation: individuals are represented as decision trees, but unlike usual GP (Koza, 1992), STGP doesn't limit variables, constants, arguments for functions, and values returned from functions to be of the same data type. We only need to specify the data types beforehand. Additionally, to ensure consistency, the root node of the tree must return a value of the type specified by the problem definition and each nonroot node has to return a value of the type required by its parent node as an argument.

2) Fitness function: scores how well a specific execution matches expected results.

3) Initialization: there are two main methods to initialize a population: *full* and *grow*. Koza (Koza, 1992) recommended using a ramped half-and-half approach, combining the two methods equally.

4) Genetic operators: crossover and mutation.

5) Parameters: maximum tree depth, maximum initial tree depth, max mutation tree depth, population size, and termination criteria.

5 OUR PROPOSED METHOD

Our algorithm, ϵ-GP, has three main characteristics. First, the performance of our algorithm, and of any general ϵ-dominance-based MOEA, depends on the value of ϵ, which is either user defined or computed from the number of solutions required. Bigger ϵ values mean quicker computation of solutions, while smaller values mean solutions that have more quality. Although the value of ϵ doesn't have to be constant for each objective, we make it constant across all objectives in our method for ease of use and for quicker computations.

Second, ϵ-GP comprises two storage locations for solutions:

- An archive that ensures elitism by keeping the best solutions so far and removing solutions iff other better solutions are found. We choose to give this archive a fixed size for several reasons. One is to limit computation time and to protect the decision maker from receiving a big number of nondominated solutions that are incomparable. Finally, due to ϵ-MOEA performing well on all test instances in (Li, et al., 2013), while suffering from archive size instability, we will stabilize and fix the size.
- A population that stores the current generation; this current generation can have worse solutions than a previous generation. This ensures diversity and keeps us from falling into local minima.

Third, crossover is always between a solution from the current generation population and a solution from the archive. This guarantees both elitism and diversity. Offspring from crossover are embedded into the archive if the criteria of acceptance (to dominate another solution) are met. They are automatically inserted into the next generation population as well.

To our knowledge, ϵ-GP is the first algorithm to combine genetic programming with an approximate measure, e.g., ϵ-dominance. ϵ-GP uses its approximation capability to make selection easier between points by reducing competition and tolerating a certain additive factor (ϵ) when calculating dominance. Selection is the most computation-intensive regular task in Many-O algorithms, and this is why ϵ-GP is considered useful.

The initial random generation of the population and archive in our algorithm is done using the ramped half-and-half method discussed earlier. The user inputs in ϵ-GP are the number of runs, the population size (pop_size), the probabilities G_o, Pr, Pc (respectively, probability of a binary or unary genetic operator, probability of reproduction or mutation, and probability of crossover).

The pseudocode of ϵ-GP is as follows:

```
for (i = 0; i < number_of_runs; i++) {
  set gen, score to 0; //generation number
  generate pop[gen], archive randomly;
  while (score <= minimum_threshold && generation < max_generations) {
    evaluate fitness of pop[gen];
    sort individuals in archive and pop; // this is where ϵ-dominance is used
    for (j = 0; j < pop_size; j++) {
      if (random(0,1) >= Go) {
        if (random(0,1) >= Pr) {
          reproduce (copy) individual;
        }
        else {
          mutate individual;
        }
        put individual into pop[gen+1];
      }
      else {
        select two individuals from archive and pop;
        if(random(0,1) >= Pc) {
          crossover the individuals;
        }
        else {
          reproduce both individuals;
        }
        j++;//because we insert 2, not 1, individuals
        put individuals to pop[gen+1];
      }
      if (individuals(s) > archive.worse_result) {
        put individual (s) in archive;
        score = fitness of archive;
      }
```

```
    }
    generation ++;
  }
  set result[i] to score;
}
```

6 EXPERIMENTATION

To measure the performance of our algorithm, it was tested on a basic genetic programming problem: the ant trail problem (Koza, 1992). Two variants of this problem are tested; namely, the Santa Fe Trail problem and the Los Altos Trail problem. The study used the MOEA Framework, version 2.8, available from http://www.moeaframework.org/. Koza's GP (Koza, 1992) was used as a reference for comparison in terms of speed and efficiency. We tested the reference against our algorithm with values of ϵ of 0.1 and 0.01.

We solved each test problem 30 times with different random seeds. In all runs, no more than 500,000 evaluations were allowed to be made. We used a crossover probability rate of 0.9, with a point mutation rate at 0.01. Population size was set to 500.

Since GP is a stochastic algorithm that is affected by the chosen random seed, it was more suitable to make a stochastic comparison instead of a static comparison with the best absolute values. For this purpose, we analyzed the mean, median, and standard deviation of the 30 independent runs.

The Santa Fe problem results are shown in Table 1, with better results highlighted in bold when applicable. The goal is to capture as much pieces of food as possible, with as little moves as possible. We also take into consideration how quickly a run reaches a suitable result.

Table 1: Santa Fe Trail Results.

Variables		Santa Fe Trail				
		Mean	Median	St. Dev.	Worst	Best
Moves	*Koza*	400.533	451	88.1807	494	234
	ϵ = 0.1	**368.067**	**366**	89.7241	**492**	**226**
	ϵ = 0.01	380.733	390	**85.9386**	496	230
Food	*Koza*	80.3	88	10.3629	55	89
	ϵ = 0.1	**81.1**	**89**	11.2322	52	89
	ϵ = 0.01	80.1	86.5	**10.145**	**57**	89
Time	*Koza*	64.5333	64	8.91621	**79**	**45**
	ϵ = 0.1	**58.5**	**56.5**	8.94331	85	46
	ϵ = 0.01	61.7	61	**8.78145**	81	46

The results show that our algorithm, ϵ-GP, has very good performance with regards to all objectives, and runs quickly as well. At both ϵ values of 0.1 and 0.01, ϵ-GP has a better average runtime compared to Koza's GP, and at ϵ of 0.1, the food gathered by ϵ-GP is, on average, more than the food gathered by Koza's GP.

Next, we test the Los Altos problem, a similar but harder problem with a more complex trail to follow to gather the food.

Table 2: Los Altos Trail.

Variables		Los Altos Trail				
		Mean	Median	St. Dev.	Worst	Best
Moves	*Koza*	393.7667	414	80.32635	**497**	221
	ϵ = 0.1	402.1	412	81.66346	499	**132**
	ϵ = 0.01	**389.667**	**375**	**76.2425**	498	250
Food	*Koza*	96.36667	99.5	20.25609	52	116
	ϵ = 0.1	99.43333	104	20.6843	55	**129**
	ϵ = 0.01	**103.933**	**115**	**18.6768**	**65**	**129**
Time	*Koza*	**142.933**	**138**	22.27869	**191**	**107**
	ϵ = 0.1	162.3	159.5	**15.803**	210	139
	ϵ = 0.01	161	150	27.37353	221	129

The obtained results, shown in Table 2, prove that Koza's GP, while quicker than ϵ-GP, trails ϵ-GP in both moves and food. ϵ-GP obtained the best absolute result by eating 129 out of 156 pieces of food, with 392 moves for ϵ value of 0.01 and 410 moves for ϵ value of 0.1. With an ϵ value of 0.01, ϵ-GP was very consistent (low standard deviation) and scored better than the two other sets in both food and moves, although with a slower running time than Koza's GP. Koza's GP was not able to collect more than 116 pieces of food, which was achieved with 335 moves in 2 minutes and 28 seconds. As to the fastest run, it was achieved by Koza's GP, where it collected 52 pieces of food with 493 moves. The lowest number of moves was achieved by ϵ-GP with a value of 0.1, where it took 2 minutes and 37 seconds, collecting 55 pieces of food in the process (the lowest score in all runs).

7 CONCLUSIONS

The previous section shows promising results, as ϵ-GP was shown to simultaneously optimize two objectives, with the algorithm guaranteeing competitive results in all objectives. These results are encouraging for future work as well, as genetic programming, up to our knowledge, has never been used to solve a problem with many (more than 3) objectives using an approximate measure.

Consistency within stochastic algorithms is usually a problem due to the random nature of different runs, but with ϵ-GP with an ϵ value of 0.01,

this is decreased to an acceptable degree. As problems increase in difficulty, the tolerance of a high ϵ value starts to decrease and problems can take longer times to find high-quality solutions and can face a possibility of falling into local minima due to the discarding of many solutions. Therefore, choosing the value of ϵ is very important.

This paper serves as an introduction to further work that will test ϵ-GP on problems with more than 2 objectives. Furthermore, future work includes the following:

- The value of ϵ can be input from the user or dynamically computed. ϵ can also be changed to be variable for each objective.
- A more detailed study with better test-set problems that contain more objectives is needed to prove that ϵ-GP is an efficient many-objective optimizer;

REFERENCES

Abido, M., 2003. A niched Pareto genetic algorithm for multiobjective environmental/economic dispatch. *Electrical Power and Energy Systems,* February, 25(2), pp. 97-105.

Corne, D. W., Jerram, N. R., Knowles, J. D. & Oates, M. J., 2001 . *PESA-II: Region-based Selection in Evolutionary Multiobjective Optimization.* San Francisco, s.n.

Corne, D. W., Knowles, J. D. & Oates, M. J., 2000. *The Pareto Envelope-based Selection Algorithm for Multiobjective Optimization.* Paris, s.n., pp. 839-848.

Deb, K., Pratap, A., Agarwal, S. & Meyarivan, T., 2002. A fast and elitist multiobjective genetic algorithm: NSGA-II. *Evolutionary Computation,* April, 6(2), pp. 182-197.

Fonseca, C. M. & Fleming, P. J., 1993. *Genetic Algorithms for multiobjective optimization: formulation, discussion and generalization.* San Mateo, s.n.

Khare, V., Yao, X. & Deb, K., 2003. *Performance Scaling of Multi-objective Evolutionary Algorithms.* Faro, s.n., pp. 376-390.

Knowles, J. & Corne, D., 2000. Approximating the nondominated front using the Pareto Archived Evolution Strategy. *Evolutionary Computation,* 8(2), pp. 149-172.

Koza, J. R., 1992. *Genetic Programming: On the Programming of Computers by Means of Natural Selection.* 1st ed. London: A Bradford Book.

Laumanns, M., Thiele, L., Deb, K. & Zitzler, E., 2002. Combining Convergence and Diversity in Evolutionary Multiobjective Optimization. *Evolutionary Computation,* September, 10(3), pp. 263-283.

Li, M., Yang2, S., Liu, X. & Shen, R., 2013. *A Comparative Study on Evolutionary Algorithms for Many-Objective Optimization.* Sheffield , s.n., pp. 261-275.

Schaffer, J. D., 1985. *Multiple objective optimization with vector evaluated genetic algorithms.* Pittsburgh, s.n., pp. 93-100.

Srinivas, N. & Deb, K., 1994. Multiobjective optimization using Nondominated sorting in genetic algorithms. *Evolutionary Computation,* September, 2(3), pp. 221-248.

Zitzler, E., Laumanns, M. & Thiele, L., 2001. *SPEA2: Improving the Strength Pareto Evolutionary Algorithm,* Zurich: s.n.

Zitzler, E. & Thiele, L., 1999. Multiobjective Evolutionary Algorithms: A comparative Case study and the Strength Pareto Evolutionary Algorithm. *Evolutionary Computation,* November, 3(4), pp. 257 - 271 .

Optimization and Scheduling of Queueing Systems for Communication Systems: OR Needs and Challenges

Attahiru Sule Alfa[1,2] and B. T. Maharaj[2]
[1]*Department of Electrical and Computer Engineering, University of Manitoba, Winnipeg, MB, Canada*
[2]*Department of Electrical, Electronic and Computer Engineering, University of Pretoria, Pretoria, South Africa*
attahiru.alfa@umanitoba.ca, sunil.maharaj@up.ac.za

Keywords: Optimization, Scheduling, Queueing, Congestion Control, Network Performance, Cognitive Radio Networks, Wireless Sensor Networks, Internet of Things.

Abstract: The modern communication system is growing at an alarming rate with fast growth of new technologies to meet current and future demands. While the development of devices and technologies to improve and meet the expected communication demands keeps growing, the tools for their effective and efficient implementations seem to be lagging behind. On one hand there is a tremendous development and continued advancement of techniques in Operations Research (OR). However it is surprising how the key tools for efficiently optimizing the use of the modern technologies is lagging behind partly because there isn't sufficient cooperation between core OR researchers and communication researchers. In this position paper, using one specific example, we identify the need to develop more efficient and effective OR tools for combined queueing and optimization tools for modern communication systems. OR scientists tend to focus more on either the analysis of communication issues using queueing theory tools or the optimization of resource allocations but the combination of the tools in research have not received as much attention. Our position is that this is one of major areas in the OR field that would benefit communication systems. We briefly touch on other examples also.

1 INTRODUCTION

The demand for communication systems keeps growing on an ongoing basis. Communication industry researchers are continuously working at coming up with new technologies for meeting the demands. In a recent ACG Research report (ACG, 2015) it was pointed out that for an area of 1,200 square kilometer metro area having approximately a population of about 2.5 million people the bandwidth requirement for backhaul at a cell site could be as high as 2.5 Gbps in the year 2018 and about 10 Gbps of Ethernet links and 10 Gbps rings to meet the demand requirements and support the expected growth. Part of these growths in demand have to do with the shifts in customers to data. In the past media and video was less than 10% of the traffic and now it is almost 50% according to the recent Global telecommunications study: navigating the road to 2020 (EYReport, 2015). Bandwidth available is limited however efforts are been made to squeeze more from what is available and also to release some inefficiently utilized radio frequencies for other uses. Hence telecommunication engineers do not only have to ensure that they could provide the capacity for these demand growths but make sure also that the capacity is efficiently well managed.

In trying to provide efficient and effective communication services for the future we need to harness several key tools mostly OR based. Our position is that this has not received the proper attention it deserves from the OR researchers and practitioners. The aim of this paper is to try, with the aid of some examples, to identify the major role that OR researchers can play in planning modern communication systems.

Historically queueing model by itself has been extensively used in analyzing the performance of communication systems. In fact to the extent that when people talk of performance analysis in communication systems they are most likely referring to queueing model analysis of a communication system. Often the model is for a particular protocol. A protocol, in simple terms, is the rule by which a system operates. When the protocol for a system changes, the queueing system that represents it changes and hence the system would need to be re-modelled in order to obtain its performance. Keeping in mind that a communication system designer may have a plethora of

Alfa, A. and Maharaj, B.
Optimization and Scheduling of Queueing Systems for Communication Systems: OR Needs and Challenges.
In *Proceedings of the 6th International Conference on Operations Research and Enterprise Systems (ICORES 2017)*, pages 430-439
ISBN: 978-989-758-218-9

possible protocol designs for a particular system, deciding on the "best" design becomes an exercise of modelling and evaluating the system with each protocol and evaluating it. This could be a nightmare of combinatorial problem. The ideal thing would be to be able to develop a combined queueing and optimization model where the parameters of the queueing system are to be decision variables in the optimization problem and a performance measure of the system is the objective function. This is straightforward enough. However when we look at the literature on this subject the research on the topic lags behind considerably in meeting the challenges of appropriate mathematical modelling of the modern communications needs. That is why we have decided to further bring this to the attention of OR researchers and analysts.

2 COGNITIVE RADIO NETWORKS

Cognitive radio networks (CRN) is one of those technologies that is being pursued as a way to increase capacity for communication. CRN emerged from the observations of some researchers and the FCC (Federal Communications Commission) that some of the licensed frequencies, especially the TV band, are underutilized. As a result CRN is a network in which when the primary user (who has license for a particular channel) is not using it a secondary user may try and access it provided it does not interfere (beyond a tolerable limit) with the primary user. For more details about this technology and associated background see (Mitola and Maguire, 1999) and (Haykin, 2005).

In CRN a secondary user (SU) senses a channel and may access it if it is not in use. We call this access approach the overlay. However if the channel is in use by the primary user (PU) the SU may still access it if the SU can transmit at a power level that will not interfere with the PU. This we call the underlay. The methods for sensing the channels are well documented in the communication literature.

The question here is when a channel can be accessed by SUs how does the system decide on which SU to access which the channel and for how long. This becomes a major queueing and optimization problem which is better addressed by using OR tools. In the next section we show how OR tools can be considered as tools for this and the challenges involved.

In real life there are several channels involved in communication systems. However to make it simple for expositional purposes we consider a single channel model for CRN. Later we discuss how the multiple channel cases are studied.

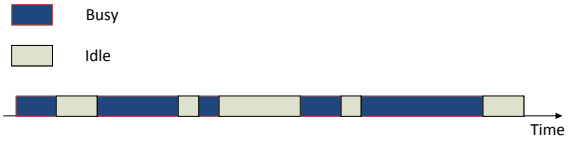

Figure 1: Busy and Idle times (single channel).

Consider a single communication channel used by one or several PUs. For simplicity let us assume that the PUs arrive according to a Bernoulli process with parameter λ_p and the channel can process at geometric distribution with probability μ. Keep in mind that the PUs required processing rate could be $\mu_p < \mu$. This system can be studied as the Geo/Geo/1 queue. Even if the arrival and processing processes are not simple we can still analyze the system using a single server queueing model. We chose to work in discrete time because modern communication systems are digital. Further consider a case on one channel licensed to a PU which is either busy or idle. We can represent it as an alternating stochastic process $\{busy, idle\}$. A simple example of that is an alternating Markov renewal. For the sake of explaining we consider the special case of Markov chain, with two states $\{0,1\}$ where 0 represents busy and 1 represents idle. Let X_n be the state at time n and define $P_{i,j} = Pr\{X_{n+1} = j, X_n = i\}, \forall n$ then we can write the transition matrix of this system as

$$P = \begin{bmatrix} p_{0,0} & p_{0,1} \\ p_{1,0} & p_{1,1} \end{bmatrix}$$

The following diagram (Fig. 1) is a schematic representation of idle and busy periods of this channel.

If we now introduce an SU with arrival probability λ_s, this SU may try and access the channel using the overlay or underlay schemes.

2.1 Overlay Scheme

In the overlay scheme, the SU will only access the channel when it is idle and has to vacate it when the PU returns to the channel, i.e. when it becomes busy again. So in essence an SU sees this channel as a vacation queueing system in which the server (channel) is on vacation when it is busy with the PU. The SU can thus only be served during the queues idle period (when the PU is not occupying it). This is a queueing problem which can be analyzed using standard queueing models. This problem is quite straightforward if all we have is just one SU trying to access the channel. The SU just waits for the time it detects the channel to be idle and then access it. The point in time when

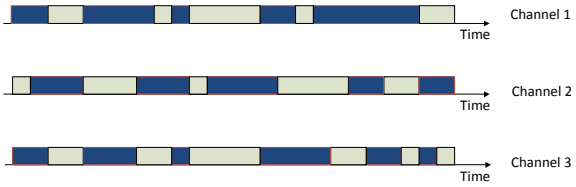

Figure 2: Busy and Idle times (multiple channel).

the channel becomes idle is a point process and the duration of the idle period is stochastic.

The question that arises then is when we have more than one SU waiting to access the channel; how do we allocate the channel to the SUs? What priority schemes do we use? This calls for an optimization tool for scheduling the SUs. Keeping in mind the stochastic nature of the idle and busy periods of the channel a system scheduler has to implement an efficient scheduling procedure. Now if we have multiple channels, which is more realistic, then we are dealing with a system of superposition of several of the channel Markov chains. For simplicity let us assume that the channels are identical with the same Markov chains with representation P, then the resulting Markov chain that represents all the K channels has Markov chain with transition matrix P_K written as

$$P_K = P \otimes P \otimes \cdots \otimes P,$$

where there are K Kronecker products of the matrix P , i.e. $P_K = \bigotimes_{j=1}^{K} P$. A good diagrammatic example of the busy and idle channel behaviours of this can be demonstrated by the case of $K = 3$ in Fig. 2.

In this case we need to keep track of which queue (channel) is idle and which one is busy at all times. Selecting which channel to assign to which SU is a challenging dynamic assignment problem; scheduling when to let a particular SU access a channel is also a challenging OR problem, especially if we assign a group of channels to some SUs ((Jiao et al., 2011; Jiao et al., 2012)).

Finally there are usually some SUs that have high data transmission rate and often are willing to pay for superior service. Such SUs require that more than one channel are assigned to them ((Jiao et al., 2011; Jiao et al., 2012)). How do we develop an optimization to handle this type of problem? For example, consider the case of three identical channels above. If we have say three SUs, and one of them requires two channels while the third channel is shared by the other two, how do we decide which two channels to assign to this special SU? There are three possible ways, all dependent on the stochastic process describing the channels. One just has to imagine what happens when we have $N\,(N >> 1)$ channels and $M\,(M >> 1)$ SUs with the i^{th} SU requiring m_i channels. . Even for the

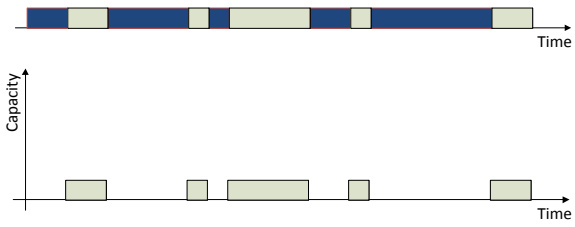

Figure 3: Capacity (single channel).

case when $\sum_i^M m_i \leq N$ it could still be a major combinatorial problem, combining queueing and optimization.

These are some of the issues that arise in the CRN technologies, and which we think can benefit tremendously from the OR communities.

2.2 Underlay Scheme

Dealing with the underlay scheme is about the same as the overlay scheme except that we now have to also allocate a power level to an SU to ensure that it does not interfere with a PU transmission. So the additional question here is what power level should we assign to an SU and to which SU in order to maximize communication capacity?

In addition we may also be in a position to have a hybrid scheme in which some SUs are placed on overlay scheme, some on underlay scheme and some on a combination of both. The question is how do we determine which ones to assign what scheme and how? This is an optimization problem which also has impact of the network performance.

Let us first look at the case of one channel in which an SU wants to consider underlay in addition to overlay, i.e. a hybrid. For the one channel even though we may know the busy and idle period, during the idle period we know that an SU can transmit at its full power (if possible), if it is the only one transmitting. However if it wants to transmit also under the underlay scheme the power level allowed may vary depending on what is the level of power of the PU. We present a schematic diagram of the situation under full capacity below in Fig. 3, i.e. when the channel is idle. For the case of underlay,he available capacity cannot be higher than what is shown in Fig. 3.

If we now consider the case of three channels, superimposed and then capturing the combined capacity we may have a case like the one below in Fig. 4.

How to now assign the channels and power becomes a major queueing, assignment and scheduling problem which is not as straightforward.

In what follows we introduce a small generic resource allocation problem and use that as the basis of our discussions in comparing the papers in the liter-

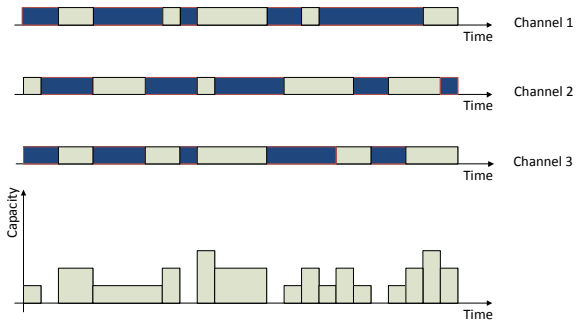

Figure 4: Capacity (multiple channel).

ature. Consider a simple CRN problem in which we have K PU channels. There are M SUs looking for access to the PU channels. Each SU, $s = 1,2,\cdots,M$ has a maximum power source of P^s_{max}. If SU s is allowed to transmit on channel k with power level P^s_k, then its capacity, c^s_k will be given as $c^s_k = \log\left(1+\gamma^s_k P^s_k\right)$, where γ^s_k is the noise level associated with SU s transmitting on channel k. This is essentially a simplified Shannon's capacity formula or a formula derived from it. Whether we are dealing with capacity, throughput or data rate a version of this formula is what we use.

Let $x^s_k = 1$ if channel k is assigned to SU, s and zero, otherwise. Generally the throughput and data rate resulting from this are directly proportional to this capacity. So in essence the total capacity assigned to this SU, s will be

$$z_s = \sum_{k=1}^{K} c^s_k x^s_k.$$

In RA problem our interest would be to maximize the total weighted capacity for all the SUs, with the weight w_s assigned to SU s. Hence the objective function of this generic problem will be

$$\max\ z = \sum_{s=1}^{M} w_s \sum_{k=1}^{K} c^s_k x^s_k. \tag{1}$$

This is a non-linear function in P^s_k and x^s_k.

Next we consider the constraints. The first one is that we want to ensure that at least one channel is assigned to an SU, on the assumption that $M \leq K$. So we need the constraint

$$\sum_{k=1}^{K} x^s_k \geq 1, \quad \forall s = 1,2,\cdots,M, \tag{2}$$

and also a constraint that ensures that we do not assign more than a channel to more than one SU, i.e.

$$\sum_{s=1}^{S} x^s_k \leq 1, \ \forall k = 1,2,\cdots,K. \tag{3}$$

The next constraint is that we cannot allow the total power generated by an SU to exceed its power limit. So we need the constraint that

$$\sum_{k=1}^{K} P^s_k \leq P^s_{max}, \quad \forall s = 1,2,\cdots,M. \tag{4}$$

A key requirement in CRN is that the SU should not interfere with the PU, or at least the interference should not exceed the maximum allowed level. This can be easily captured by requiring that the power reaching the PU should not exceed a particular value $P_{\mathbf{power}}$. So the next constraint is

$$\sum_{s=1}^{S} \sum_{k=1}^{K} P^s_k \gamma^s_k \leq P_{\mathbf{power}}. \tag{5}$$

with the variables allowed to assume any non-negative values.

Given that SUs usually have a minimum requirement for QoS we assume that there is a constraint in this regard also. For example, an SU, s, may require a minimum of σ_s of total capacity after combining a number of sub-channels assigned, so this leads to the constraint

$$\sum_{k=1}^{K} x^s_k c^s_k \geq \sigma_s, \quad \forall s = 1,2,\cdots,M. \tag{6}$$

Finally we have the two critical but common constraints, i.e. that of zero-one on x^s_k and non-negativity on P^s_k, both written as

$$x^s_k \in \{0,1\}. \tag{7}$$

$$P^s_k \geq 0. \tag{8}$$

In summary, Equations (1) to (8) form the resource allocation (RA) problem for this simple example. As one can see, in its simplest form, the objective function in non-linear, and constraint (6) is non-linear. Also one variable, x^s_k is zero-one while P^s_k is a simple non-negative variable. So unless there is a significantly different problem studied, non-linearity and integer variables (zero-one) are unavoidable in the formulations. That is why in general we have a non-linear mixed integer programming problem for RA. The issue now is how it has been handled in the literature. A more detailed discussion of this can be found in (Alfa et al., 2016).

It is however important to point out some aspects of this formulation that could be further improved to reflect an attempt to truly optimize the system as a whole. We know that the resulting capacity available to an SU, after the optimization, determines the delay or latency of packet transmission. So we need to incorporate additional constraints, based on queueing

models, that limit the delay or add a delay cost component to the objective function. These are usually not incorporated in the RA models because of the complexity it would introduce to the problem. This is one major reason why it is important for the communication system researchers and OR analysts/researchers need to collaborate on carrying out major complete model analysis.

SUGGESTED IDEA FOR COLLABORATION:
Telecommunication researchers often resort to the use of simple heuristics to quickly obtain solutions to the type of optimization problems discussed above. The heuristics are usually not rigorously studied before implementation. For example, exploring and understanding how "good" the solutions are is very important especially now that there is a need to "squeeze" as much as possible from the network. Solutions that are not proven to be efficient, for example if the gap between the solution and the bound is large, could be misleading. This is where it is very important for the telecommunication researchers to collaborate more with OR analysts whose interests, capacity and experience are in these aspects. The OR analysts on their own, would probably have more interests in the mathematical analysis of the system and looking for bounds. In the process may assume away some important aspects of the problem which a telecommunication researcher knows is very important for the problem. That is why the two groups need to collaborate and work together in coming up with better solutions. The combined collaborative effort of the two groups would lead to much better solution.

3 WIRELESS SENSOR NETWORKS AND THE INTERNET OF THINGS

The Internet of things (IoT), which is probably more correctly be termed the Internet for Things (IfT) as suggested by Kevin Ashton, the originator of the term IoT (Peter Day's World of Business, 2016 (BBC, 2016)), is seen as one of the technologies that would drive our daily activities and hence very important. To quote the Wikipedia,"IoT is the internet working of physical devices, vehicle, building and other items embedded with electronics, software, sensors, actuators, and networking connectivity that enable these objects to collect and exchange data". It is immediately clear that one of the technologies that would enable the IoT is wireless sensor networks, among many other technologies. A wireless sensor network (WSN) is a self-organizing network that consists of a number of sensor nodes deployed in a certain area. The sensor nodes basically sense and acquire data from the environment, process data for storage, as well as a communicate (transmit) the data to a sink node. It is the communicated data that the IoT system uses to actuate activities in response thereby generating device-to-device activities. With the new 5G technology in discussion it is believed that the IoT will drive most of actions and activities from smart cities to smart grid, to smart health, environmental monitoring, infrastructure management, manufacturing, energy management, city management, home and building automation, transportation, etc. So first we consider the role of OR in sensor networks modelling and analysis.

3.1 Wireless Sensor Networks

There are a number of different applications of sensor networks in areas such as environmental monitoring, industrial control, disaster recovery, and battlefield surveillance. The major constraint in large scale deployment of WSNs is the limited capacity of processing, storage and energy of the wireless sensor nodes. It is important that the buffer capacity is sufficient to avoid data loss, that the processing capacity is high enough to obtain very good latency, especially for time sensitive data for the Internet of Things, and most important is that processing is limited to times when the system can be utilised efficiently, i.e. energy is conserved through the sleep/awake management of the sensors. In order to effectively carry out the design of many aspects of sensor networks, a very good queueing analysis is important. Queueing theory plays a major role than has been emphasized in the literature.

WSN is a collection of several nodes of sensors of all types connected via wireless channels of different capacities with varying channel conditions. The sensor nodes are usually of different capacities and different functionalities. Some of them collect, process and transmit data, and others only carry out a few of the functions. Let us denote by $\mathcal{N}$ a set of sensor nodes where $N = \left|\mathcal{N}\right|$ and $\mathcal{N} = \{N_1, N_2, \cdots N_N\}$. Let $\mathcal{A}$ be the set of channels connecting pairs of sensor nodes. For example, let $A_{i,j}$ be a connection between sensor nodes N_i and N_j, then $\mathcal{A}$ is the set of all those channels. Let $C_{i,j}$ be the capacity associated with channel $A_{i,j}$, and K_i as the buffer capacity and P_i as the processing capacity associated with sensor node i. We can therefore say that a WSN can be

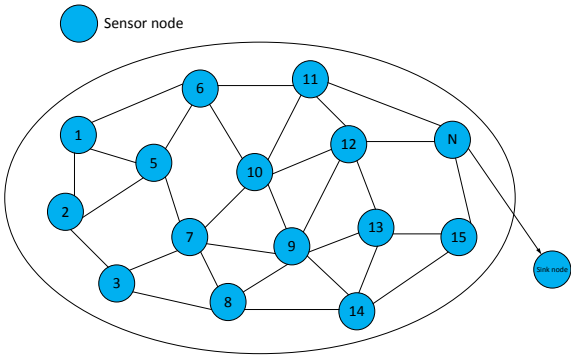

Figure 5: Sensor node distribution.

described by a network $G = \{\mathcal{N}, \mathcal{A}\}$ with attributes $\{(K_i, P_i), (C_{i,j}), i \in \mathcal{N}, (i,j) \in \mathcal{A}\}$. See Fig. 5 as an example.

1) Queueing Aspects of WSN: The first thing one notices about WSN is that it is like a network of queues with each sensor node representing a queueing node. Since data arrival is usually not necessarily Poisson type, and more often kind of correlated, simple single node queues or even simple queueing network models such as the Jackson networks are not appropriate for modelling the WSN. In addition, given that we need to include sleep/awake mode scheduling the model then becomes more complicated. This calls for more sophisticated and more representative queueing models, the types that queueing theoreticians do not seem to have focused on yet. Considering queueing models that assume non-renewal types of arrivals with bursty instances is more appropriate. However then including such processes in a queueing network, which is beyond the Jackson's model, is a challenge which queueing theorists need to tackle.

2) Power Management of WSN: Due to the fact that most sensor nodes are battery operated, i.e. have limited available power source, it is important to efficiently manage them effectively for a long lasting network life. Usually a sleep/awake mode is implemented to achieve this goal; a very good vacation queueing model in which the scheduling of the sleep/awake mode is well controlled. This involves a combined queueing model with optimization techniques. Queueing theory can prove to be an effective tool to analyze and design efficient power allocation schemes to increase the power efficiency of WSNs (see (Kabiri et al., 2014)). Sleep/awake models are based on special kinds of vacation models. When the sensor goes to the sleep mode, that means it is switched off and cannot process data. This is essentially a vacation model. Data arrivals accumulate at the buffer. The node wakes up depending on the time which is based on a policy of how many packets are waiting (N), how long they have been waiting (T) and the total amount of Kilo-bytes of data (D). These models are classified as N-policy, T-policy or D-policy models. Recently there have been combined versions of these models, such as the NT-policy, and there are research activities going on regarding developing ND, and NDT-policies. Sleep/wake-up schemes essentially makes use of duty cycle schemes which are used to wake a node up from an idle state to the busy state by turning on the radio server. This plays an important role in the level of power savings in the context of MAC protocols. The authors in (Kabiri et al., 2014) derived an analytical model utilising a M/G/1 queue to model the sensor node; and by altering the queue parameters, different sleep/wake-up strategies were analysed. Some IEEE 802.11 MAC protocols like the sensor MAC, sparse topology and energy management, or the Berkeley MAC utilize a queued wake-up where a threshold value is used to control the average time of switching on a node and the latency for buffered data packets. Determining the optimal value of the packet queue length of a node after which the node is switched on for transmission, is referred to as the N-policy. For more information see (Jiang et al., 2012).

Let d_i be the sum of the delays to data processing at node N_i and transmission from that node, and if data is generated at node N_i at the rate of λ_i, then we have

$$d_i = d(\lambda_i, P_i, K_i, T_i), \quad \forall i, \tag{9}$$

and ω_i th power consumption at that node, given as

$$\omega_i = \omega(\lambda_i, P_i, K_i, T_i), \quad \forall i. \tag{10}$$

Given the appropriate parameters of the system we can obtain the performance measures, whether we use single node queueing models or queueing network models.

3) Routing Aspects of WSN: Each sensor node needs to send its data (processed or unprocessed) to a sink node where decisions are taken for the whole system, especially for the IoT to be implementable. Apart from the usual link costs associated with networks in computing optimal routing paths for WSN we also need to know the energy level at each node. This aspect has to be incorporated in the routing algorithm keeping in mind that there is a need to preserve energy at nodes with low level of it. Hence routing here considers costs of links and nodes. One other tool that has been incorporated in routing for WSN is selection of cluster head node which is responsible for aggregating data from a group of nodes and then transmitting to the sink node (see Fig.6). This routing aspect for WSN is unique and has not received enough attention from the OR researchers. As the 5G technology is rolled out and the IoT developed to work using

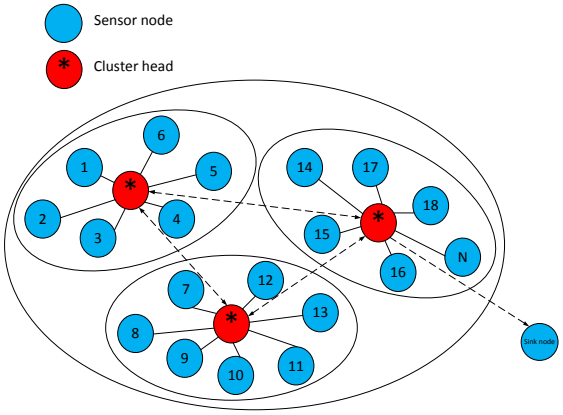

Figure 6: SSensor node distribution with cluster heads.

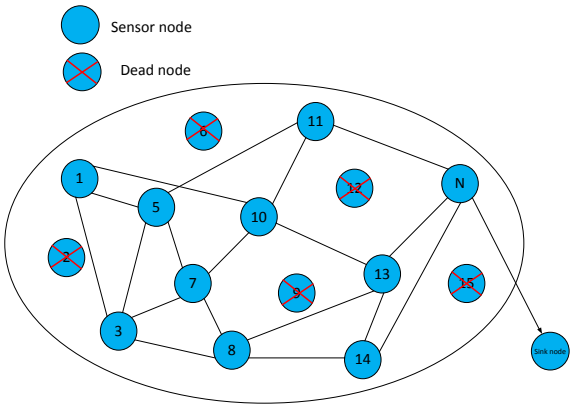

Figure 7: Sensor nodes in a depleting scenario.

that technology we want to maximize the technology to ensure high effectiveness and efficiency. This calls for the use of very effective and well researched OR tools.

4) Reliability of WSN: The reliability of the WSN is key to its effectiveness. It is important that if a sensor node is not in operation due to low power or faulty equipment, that data for the area can still be transmitted. So we need very good reliability model that assesses the impact of dead nodes as shown in Fig. 7.

SUGGESTED IDEA FOR COLLABORATION:
It is important that appropriate queueing models are developed for WSN in order to obtain more accurate estimate of delays at the nodes for the purpose of providing efficient performance. Over-simplified and inappropriate queueing models lead to gross overestimation or underestimation of performance measures leading to poor power management and inefficient routing. It is very common for telecommunication researchers to assume Poisson arrivals, when often the arrival process is far from that; and also ignoring correlations in the arrival process is very common in all the examples discussed in the last few sections. On the other hand, OR analysts tend to be very rigorous by developing general models that are more appropriate sometimes for unrealistic problems. Combining the rigour of OR analysts with the realistic view of the problems by telecommunication researchers would lead to a very appropriate and effective models. A good collaboration between the two professions where more realistic models are developed jointly and the effect of ignoring some aspects of the systems are well understood and accounted for would be the direction to go.

3.2 Sensor Node Placements

The placement of sensor nodes in a WSN is another major factor in the reliability of WSN and its lifetime. First in order for the WSN to be able to cover all areas of interest the selection of the node placements have to be selected strategically. For example, in (Cardei et al., 2005) the optimization problem is to maximize the number of set covers by selecting the optimal sensing range for each sensor in each set cover while ensuring each target is monitored by at least one sensor. This problem is referred to as the Adjustable Range Set Cover (AR-SC) problem and is initially formulated as the following integer linear program: Consider N sensor nodes $s_1,\ldots,s_N$ and M targets $t_1,t_2,\ldots,t_M$. Let the sensor have P sensing ranges $r_1,r_2,\ldots,r_P$ with corresponding energy consumption $e_1,e_2,\ldots,e_P$. If E is the initial sensor energy, and a_{ipj}, a binary coefficient which is 1 if sensor s_i with radius r_p covers the target t_j . Further let K be an upper bound for the number of set covers. Then we have the following decision variables:

Decision Variables:

c_k, boolean variable for $k = 1\ldots K$, 1 if this subset is a set cover
x_{ikp}, boolean variable for $i = 1\ldots N$, $k = 1\ldots K$, $p = 1\ldots P$, 1 if sensor i with range r_p is in cover k

The problem can now be set up as an integer linear program (ILP) as

ILP:

$$maximize \quad \sum_{i=k}^{K} c_k, \tag{11}$$

$$s.t. \quad \sum_{k=1}^{K}\left(\sum_{p=1}^{P} x_{ikp}e_p\right) \leq E \quad \forall i = 1\ldots N, \tag{12}$$

$$\sum_{p=1}^{P} x_{ikp} \leq c_k \quad \forall i = 1 \ldots N,\ k = 1 \ldots K, \tag{13}$$

$$\sum_{i=1}^{N} \left(\sum_{p=1}^{P} x_{ikp} * a_{ipj} \right) \geq c_k \quad \forall k = 1 \ldots K,\ j = 1 \ldots M, \tag{14}$$

$$x_{ikp},\ c_k \in \{0,1\}. \tag{15}$$

In (Cardei et al., 2005) the integer constraint is relaxed to create a linear programming problem which is then used for the proposed LP based heuristic. The LP based heuristic uses the values for each variable obtained from solving the LP. The variables with nonzero values from each cover set are added to the new set in non-increasing order until all of the targets are covered. This was improved further by the authors in (Beynon and Alfa, 2015). If a sensor does not have sufficient energy for the suggested power level or does not cover any new targets it is not added to the set. If no more nonzero variables are left for the current cover and one or more targets remain uncovered then the set is not a cover set. After the maximum number of cover sets have been attempted to be made the solution is the set of all valid cover sets.

SUGGESTED IDEA FOR COLLABORATION:
One may argue that this type of problem has been well studied for years in OR as a class of problem in the family of maximum covering location problem. Yet telecommunication researchers still have unanswered questions about coming up with very good solutions for the maximum network lifetime in wireless sensor networks. Perhaps this is due to some subtleties in the later problem that are probably ignored in the classical OR versions of the problem. In our opinion this calls for more close collaborations between the two groups of researchers to understand the problem better and its associated issues.

3.3 IoT

The IoT is essentially driven by the automatic or "semi-automatic" control system. Data is sent from some form of sensors, e.g. WSN, and based on the data an action is taken as seen appropriate. For example, a sensor network that is monitoring the temperature at a building keeps gathering data and at each point may notice that the temperature is too high and thereby automatically control the system and lowers the temperature. This is one of the most elementary ones. Another simple example could be a case where as soon as a shopper in a grocery store is noticed by a sensor network in the store a message is sent to the shopper's home refrigerator sensors which then sends a message to the shopper's mobile phone to let him/her know they need more milk at home. The communication here is what is called device-to-device. However more important here is the need for a process that determines that the milk has reached low level or expired date etc and request the shopper to purchase some. This is close to an inventory model that is automated. The key difference is that there is a time factor involved. The shopper has to be able to get the message, from its mobile phone, when they are still in the store otherwise it is not very helpful. Hence latency is also a factor.

SUGGESTED IDEA FOR COLLABORATION:
This class of problem is more in the control domain and requires a good collaboration between both OR analysts and telecommunication researchers. It is still an evolving problem which can benefit early from the collaborations.

In the next section we give a brief example of another type of OR challenges for the future communication systems.

4 CONNECTING OPTIMIZATION OF CRN AND QUEUEING OF WSN

Currently WSN is operated on what is called the unlicensed channels. These channels are getting congested and it is being proposed that the licensed channels, which belong to PUs be used for transmitting data in WSN. The sensor nodes are like queueing nodes. Data is stored in the buffer and then transmitted when possible. The transmission will be carried out on licensed channels.

So here is the situation. Considering the PU channels, the SU, in this case the sensor node(s) will be assigned a capacity c_k^s on channel k from the optimization model for CRN in Section III. However, because the assigned capacity and the number of allocated channels are used by the SU to transmit the date the latency depends on this which should actually be incorporated as part of the optimization scheme in the CRN problem. How to capture this feedback is a major challenge. Here we present a possible example method for dealing with it.

Let M be the number of sensor nodes in the WSN, by trying to combine the two aspects then our Eq(1)

in Section III will be

$$\max \; z = \sum_{s=1}^{M} \left[\omega_s \sum_{k=1}^{K} c_k^s x_k^s - f(d_s) - g(\omega_s) \right], \quad (16)$$

where $f(d_s)$ is the cost of delay at sensor node s and $g(\omega_s)$ is the cost of power consumption at node s.

We will also have Eq(9) and Eq(10) as additional constraints for the optimization problem, in addition to stability sets of equations.

SUGGESTED IDEA FOR COLLABORATION:
This will be a new and a bit more complex class of problems. If we decide to include the placement problem with this then the whole model becomes very challenging. The question of how to manage the problem should be of interest to OR analysts who traditionally have the expertise to handle them.

We suggest more close collaborations between OR analysts and Communication network researchers.

5 CONCLUSIONS & THE POSITION

We start by discussing the first example of cognitive radio networks. Given the information about channel capacity, which is usually stochastic, for SUs there are several research results for allocating that resource to the SUs using optimization tools. However, the allocations provide the service capacity to the users and hence a very good queueing model is needed to obtain the performance analysis, which itself will now feed back into the optimization tools. Hence what we need is a combined queueing and optimization model in order to efficiently model these systems.

Next we consider the wireless sensor networks, we see that the optimal placement of the sensor nodes determine network life, its reliability and routing which affects latency. The placements, routing and sleep/awake mode determines the queueing delays at the nodes which need to be included in the optimization component of the placements, etc. Hence for the WSN, combined optimization and queueing models are essential in order to have a well design WSN.

Finally, keeping in mind that an effective operation of IoT depends on accurately gathering information and passing it to the right destination within a very short time it is imperative that a combination of optimization and queueing models are needed for the planning.

In summary OR analysts and communication modelling researchers need to try and work very closely together in order to come up with efficient tools for analyzing modern day communication systems. That is the position that we are taking in this paper.

ACKNOWLEDGEMENT

The authors would like to thank the Advanced Sensor Networks (ASN) South African Research Chairs Initiative (SARChI) for their financial support in making this work possible. Thanks to Babatunde Awoyemi for assisting with drawing the diagrams and to Dr. Haitham AbuGhazaleh for assisting in recovering the Latex file.

REFERENCES

Mitola, J. and Maguire, Jr., G. Q.(1999), Cognitive radio: Making software radio more personal, *IEEE Pers. Communications*, vol. 6, No. 4, Aug. 1999, 13-18.

Haykin, S. (2005), Cognitive radio: Brain-empowered wireless communications, *IEEE Journal of Selected Areas of Communications*, vol. 23, No. 2, Feb. 2005.

Jiao, L. Li, F.Y. and Pla, V. (2012), Modelling and performance analysis of channel assembling in multi-channel cognitive radio networks with spectrum adaptation, *IEEE Trans. Vehicular Technology*, 61 (6), 2686-2697.

Jiao, L. Li, F.Y. and Pla, V. (2011), Dynamic channel aggregation strategies in cognitive radio networks with spectrum adaptation, *IEEE Globecom 2011*, 1-6.

Alfa, A. S., Maharaj, B. T., Lall, S., and Pal, S. (2016), Mixed-Integer programming based techniques for resource allocation in underlay cognitive radio networks: A survey, *Journal of Communications and Networks*, vol. 18, No. 5, October 2016, 744-761.

Peter Day's World of Business, *BBC World Service*, OCTOBER 4, 2016.

Beynon, V. and Alfa, A. S. (2015), An improved algorithm for finding the maximum number of set covers for wireless sensor networks, *Africon, 2015*.

Cardei, M., Wu, J., Lu, M. and Pervaiz, M. O. (2005), Maximum network lifetime in wireless sensor networks with adjustable sensing ranges, *IEEE International Conference on Wireless and Mobile Computing, Networking and Communications*, WiMob 2005 vol. 3, pp. 438-445, 2005.

Kabiri, C., Zepernick, H. and Tran, H. (2014), On Power Consumption of Wireless Sensor Nodes with Min(N,T) Policy in Spectrum Sharing Systems, *Proceedings IEEE Vehicular Technology Conference*, Spring 2014, 1-5.

Jiang, F., Huang, D., Yang, C. and Leu. F. (2012) Lifetime elongation for wireless sensor network using queue-based approaches, *The Journal of Supercomputing*, vol. 59, no. 3, 1312-1335.

Forecasting of Mobile Broadband Bandwidth Requirements, *ACG Research 2015*, www.acgcc.com.

Global telecommunications study: navigating the road to 2020, *2015 report EY Building a better working World*.

Progressive Hedging and Sample Average Approximation for the Two-stage Stochastic Traveling Salesman Problem

Pablo Adasme[1], Janny Leung[2] and Ismael Soto[1]
[1]*Departamento de Ingeniería Eléctrica, Universidad de Santiago de Chile, Avenida Ecuador 3519, Santiago, Chile*
[2]*Shaw College, The Chinese University of Hong Kong (Shenzhen), 2001 Longxiang Blvd., Longgang District, Shenzhen, China*
pablo.adasme@usach.cl, jannyleung@cuhk.edu.cn, ismael.soto@usach.cl

Keywords: Two-stage Stochastic Programming, Traveling Salesman Problem, Progressive Hedging Algorithm, Sample Average Approximation Method.

Abstract: In this paper, we propose an adapted version of the progressive hedging algorithm (PHA) (Rockafellar and Wets, 1991; Lokketangen and Woodruff, 1996; Watson and Woodruff, 2011) for the two-stage stochastic traveling salesman problem (STSP) introduced in (Adasme et al., 2016). Thus, we compute feasible solutions for small, medium and large size instances of the problem. Additionally, we compare the PHA method with the sample average approximation (SAA) method for all the randomly generated instances and compute statistical lower and upper bounds. For this purpose, we use the compact polynomial formulation extended from (Miller et al., 1960) in (Adasme et al., 2016) as it is the one that allows us to solve large size instances of the problem in short CPU time with CPLEX. Our preliminary numerical results show that the results obtained with the PHA algorithm are tight when compared to the optimal solutions of small and medium size instances. Moreover, we obtain significantly better feasible solutions than CPLEX for large size instances with up to 100 nodes and 10 scenarios in significantly low CPU time. Finally, the bounds obtained with SAA method provide an average reference interval for the stochastic problem.

1 INTRODUCTION

Most mathematical programming models in the operations research domain are subject to uncertainties in problem parameters. There are two well known approaches to deal with the uncertainties, the first one is known as robust optimization (RO) while the second one is known as stochastic programming (SP) approach (Bertsimas et al., 2011; Gaivoronski et al., 2011; Shapiro et al., 2009). In this paper, we are devoted to the latter approach. More precisely, we deal with the two-stage stochastic traveling salesman problem (STSP) introduced in (Adasme et al., 2016). We propose an adapted version of the progressive hedging algorithm (PHA) (Rockafellar and Wets, 1991; Lokketangen and Woodruff, 1996; Watson and Woodruff, 2011) and compute feasible solutions for small, medium and large size instances of the STSP. Additionally, we compare numerically the PHA method with the sample average approximation (SAA) method (Ahmed and Shapiro, 2002) for randomly generated instances and compute statistical lower and upper bounds for the problem. For this purpose, we use the compact polynomial formulation extended from (Miller et al., 1960) in (Adasme et al., 2016) as it is the one that allows us to solve large size instances of the problem within a limited CPU time with CPLEX.

Two-stage SP problems similar as the one we consider in this paper are, for instance the knapsack problem (Gaivoronski et al., 2011), the maximum weight matching problem (Escoffier et al., 2010), maximal and minimal spanning tree problems (Flaxman et al., 2006; Escoffier et al., 2010), the stochastic maximum weight forest problem (Adasme et al., 2013; Adasme et al., 2015)), to name a few. For the sake of clarity, the description of the STSP is as follows. We consider the graph $G = (V, E_D \cup E_S)$ to be a non directed complete graph with a set of nodes V and a set of weighted edges $E_D \cup E_S$ where $E_D \cap E_S = \emptyset$. The sets E_D and E_S contain deterministic and uncertain edge weights, respectively. We assume that the edges in the uncertainty set E_S can be represented by a set of $K = \{1, 2, \cdots, |K|\}$ scenarios. The STSP consists of finding $|K|$ Hamiltonian cycles of G, one for each scenario $s \in K$, using the same deterministic edges and

Adasme, P., Leung, J. and Soto, I.
Progressive Hedging and Sample Average Approximation for the Two-stage Stochastic Traveling Salesman Problem.
In *Proceedings of the 6th International Conference on Operations Research and Enterprise Systems (ICORES 2017)*, pages 440-446
ISBN: 978-989-758-218-9

possibly different uncertain edges in each cycle, while minimizing the sum of the deterministic edge weights plus the expected edge weights over all scenarios.

Notice that for $|K| = 1$, the problem reduces to the classical traveling salesman problem. Our preliminary numerical results show that the results obtained with the proposed PHA algorithm are tight when compared to the optimal solutions of small and medium size instances. Additionally, we obtain significantly better feasible solutions than CPLEX for large size instances with up to 100 nodes and 10 scenarios in significantly low CPU time. Finally, the bounds obtained with SAA method provide an average reference interval for the stochastic problem.

Stochastic variants for the traveling salesman problem have been proposed in (Maggioni et al., 2014; Bertazzi and Maggioni, 2014) for instance. The two-stage stochastic problem as presented in this paper can be seen as a particular case of the stochastic capacitated traveling salesmen location problem with recourse (Bertazzi and Maggioni, 2014). As far as we know, PHA and SAA approximation methods for this new variant of the stochastic traveling salesman problem have not been studied so far in the literature.

The remaining of the paper is organized as follows. In Section 2, we present the polynomial two-stage stochastic formulation of the problem. Then, in Section 3, we present PHA and SAA methods. Subsequently, in Section 4 we conduct preliminary numerical results in order to compare all the algorithmic procedures with the optimal solution or best solution found with CPLEX. Finally, in Section 5 we give the main conclusions of the paper.

2 TWO-STAGE STOCHASTIC FORMULATION

In this section, for the sake of clarity we restate the two-stage stochastic formulation adapted from (Miller et al., 1960) in (Adasme et al., 2016) for the traveling salesman problem. For this purpose, let A_D and A_S represent the sets of arcs obtained from E_D and E_S, respectively where an edge (i, j) is replaced by two arcs $(i, j), (j, i)$ of same cost in each corresponding set. This formulation can be written as (Adasme et al., 2016)

$$(STSP_1):$$

$$\min_{\{x,y,u\}} \left\{ \sum_{(i,j)\in A_D} c_{ij}x_{ij} + \sum_{s=1}^{|K|} p_s \sum_{(i,j)\in A_S} \delta^s_{ij} y^s_{ij} \right\} \quad (1)$$

subject to:

$$\sum_{j:(i,j)\in A_D} x_{ij} + \sum_{j:(i,j)\in A_S} y^s_{ij} = 1, \forall i \in V, s \in K \quad (2)$$

$$\sum_{i:(i,j)\in A_D} x_{ij} + \sum_{i:(i,j)\in A_S} y^s_{ij} = 1, \forall j \in V, s \in K \quad (3)$$

$$u^s_1 = 1, \forall s \in K \quad (4)$$

$$2 \leq u^s_i \leq |V|, \forall i \in |V|, (i \neq 1), \forall s \in K \quad (5)$$

$$u^s_i - u^s_j + 1 \leq (|V| - 1)(1 - x_{ij:(i,j)\in A_D} - y^s_{ij:(i,j)\in A_S}), \forall i, j \in V, (i, j \neq 1), s \in K \quad (6)$$

$$x_{ij} \in \{0, 1\}, \forall (i, j) \in A_D, \quad (7)$$

$$y^s_{ij} \in \{0, 1\}, \forall (i, j) \in A_S,\ s \in K \quad (8)$$

$$u^s_i \in \mathbb{R}_+, \forall i \in V, s \in K \quad (9)$$

In $(STSP_1)$, the parameter $p_s, \forall s \in K$ in the objective function (1), represents the probability for scenario $s \in K$ where $\sum_{s\in K} p_s = 1$. Thus, in (1) we minimize the sum of the deterministic edge weights plus the expected cost of the uncertain edge weights obtained over all scenarios. Constraints (2)-(3) force the salesman to arrive at and depart from each node exactly once for each scenario $s \in K$. Next, the constraints (6) ensure that, if the salesman travels from i to j, then the nodes i and j are sequentially ordered for each $s \in K$. These constraints together with (4) and (5) ensure that each node is in a unique position. Finally, (7)-(9) are the domain of the decision variables.

In particular, if the variable $x_{ij} = 1$, it means that the deterministic arc $(i, j) \in A_D$ is selected in each Hamiltonian cycle, $\forall s \in K$, otherwise $x_{ij} = 0$. Similarly, if the variable $y^s_{ij} = 1$, the arc $(i, j) \in A_S$ is selected in the Hamiltonian cycle associated with scenario $s \in K$, and $y^s_{ij} = 0$ otherwise.

3 PROGRESSIVE HEDGING AND SAMPLE AVERAGE APPROXIMATION

In this section, we propose an adapted version of the progressive hedging algorithm (Rockafellar and Wets, 1991; Lokketangen and Woodruff, 1996; Watson and Woodruff, 2011) in order to compute feasible solutions for $(STSP_1)$. Additionally, we present the sample average approximation method that we use to compute statistical lower and upper bounds for the more general case where the two-stage stochastic

objective function is treated as a generic expectation function.

3.1 Progressive Hedging Algorithm

In order to present a PHA procedure, we write for each scenario $s \in K$, the following subproblem obtained from $(STSP_1)$

$$(STSP_1^s):$$

$$\min_{\{x,y,u\}} \left\{ \sum_{(i,j)\in A_D} c_{ij}x_{ij} + \sum_{(i,j)\in A_S} \delta_{ij}^s y_{ij} \right\}$$

subject to:

$$\sum_{j:(i,j)\in A_D} x_{ij} + \sum_{j:(i,j)\in A_S} y_{ij} = 1, \quad \forall i \in V \tag{10}$$

$$\sum_{i:(i,j)\in A_D} x_{ij} + \sum_{i:(i,j)\in A_S} y_{ij} = 1, \quad \forall j \in V \tag{11}$$

$$u_1 = 1 \tag{12}$$

$$2 \le u_i \le |V|, \forall i \in |V|, (i \ne 1) \tag{13}$$

$$u_i - u_j + 1 \le (|V|-1)(1 - x_{ij:(i,j)\in A_D} - y_{ij:(i,j)\in A_S}), \quad \forall i,j \in V, (i,j \ne 1) \tag{14}$$

$$x_{ij} \in \{0,1\}, \forall (i,j) \in A_D, \tag{15}$$

$$y_{ij} \in \{0,1\}, \forall (i,j) \in A_S \tag{16}$$

$$u_i \in \mathbb{R}_+, \forall i \in V \tag{17}$$

Notice that the index "s" is removed from the second stage variables in $(STSP_1^s)$. Thus, $(STSP_1^s)$ has significantly less number of variables than $(STSP_1)$. More precisely, the total number of first and second stage variables is of the order of $O(|A_D| + |A_S|)$ whilst the total number of variables in $(STSP_1)$ is of the order of $O(|A_D| + |A_S||K|)$. Obviously, solving for each scenario $s \in K$ the subproblem $(STSP_1^s)$ is significantly less complex than solving $(STSP_1)$ directly with CPLEX. In this sense, PHA uses a by-scenario decomposition approximation scheme in order to find feasible solutions for the complete problem (Watson and Woodruff, 2011).

The PHA algorithm we adapt for $(STSP_1)$ is depicted in Algorithm 3.1 and it can be explained as follows. First, in step 0 we solve for each $s \in K$, the subproblem $(STSP_1^s)$ with CPLEX and save the first stage solution in x_s^t for the iteration $t = 0$. Next, we compute the average of the obtained first stage solution sets and save this value in $\bar{x}^t$. Finally, for each $s \in K$ we compute the values w_s^t where the parameter $\rho > 0$ represents a penalty factor (Watson and Woodruff, 2011). Subsequently, in step 1 we enter into a while loop with the stopping condition of

Algorithm 3.1: PHA procedure to compute feasible solutions for $STSP_1$.

Data: A problem instance of $(STSP_1)$.
Result: A feasible solution (x,y) for $(STSP_1)$ with objective function value z.

Step 0:
$t = 0$;
foreach $s \in K$ **do**
  $x_s^t := argmin_{\{x,y\}} \{(STSP_1^s)\}$
$\bar{x}^t := \sum_{s\in K} p_s x_s^t$;
foreach $s \in K$ **do**
  $w_s^t := \rho(x_s^t - \bar{x}^t)$
$t = t + 1$;
Step 1:
while $(t < t_{max}$ *and* $x_s^t \ne x_j^t, \forall s,j \in K(j \ne s))$ **do**
  foreach $s \in K$ **do**
    $x_s^t :=$
    $argmin_{\{x,y\}} \left\{ \sum_{(i,j)\in A_D} \left[(c_{ij} + w_{s,ij}^{t-1}) x_{ij} + \frac{\rho}{2} |x_{ij} - \bar{x}_{ij}^{t-1}| \right] + \sum_{(i,j)\in A_S} \delta_{ij}^s y_{ij} \right\}$;
    s.t. (10)-(17)
  $\bar{x}^t := \sum_{s\in K} p_s x_s^t$;
  foreach $s \in K$ **do**
    $w_s^t := w_s^{t-1} + \rho(x_s^t - \bar{x}^t)$
  $t = t + 1$;
Step 2:
if $(t = t_{max})$ **then**
  foreach $i \in K$ **do**
    foreach $s \in K$ **do**
      $y_s := argmin_{\{y\}} \{(STSP_1^s(x_i^t))\}$
    Compute a feasible solution of $(STSP_1)$ with x_i^t and $y_s, \forall s \in K$
  Save the best solution found as (x^t, y^t, z^t);
else
  foreach $s \in K$ **do**
    $y_s := argmin_{\{y\}} \{(STSP_1^s(x_s^t))\}$
  Compute a feasible solution of $(STSP_1)$ with x_s^t and $y_s, \forall s \in K$;
  Save the feasible solution as (x^t, y^t, z^t)
return (x^t, y^t, z^t);

a maximum number of iteration t_{max} while simultaneously checking whether the first stage solution set has converged to a unique solution set. The steps inside the while loop are exactly the same as those in step 0, with the difference that now we solve for each $s \in K$, the subproblem $(STSP_1^s)$ with the objective function $\left\{ \sum_{(i,j)\in A_D} \left[(c_{ij} + w_{s,ij}^{t-1}) x_{ij} + \frac{\rho}{2} |x_{ij} - \bar{x}_{ij}^{t-1}| \right] + \sum_{(i,j)\in A_S} \delta_{ij}^s y_{ij} \right\}$ where the parameters w_s^{t-1} and ρ penalize the difference in the first stage solution sets within each iteration. Notice that this objective function uses absolute terms instead of Euclidean terms as it is performed in (Watson and Woodruff, 2011).

This allows us to formulate the equivalent mixed integer linear program straightforwardly. Finally, in step 2 we check whether the condition of $t = t_{max}$ is satisfied, if so it means we have not found convergence for the first stage variables. In this case, we compute a feasible solution for each set of first stage variables and save the best solution. If $t < t_{max}$, it means we have found a unique set of first stage variables $x = x_s, \forall s \in K$. In this case, we simply obtain a feasible solution for $(STSP_1)$ using this set of variables and save it as best solution found with the algorithm.

3.2 Sample Average Approximation Method

In this subsection, we briefly sketch the SAA method used to compute statistical lower and upper bounds for $(STSP_1)$. It is well known that this method converges to an optimal solution of a continuous two-stage stochastic linear optimization problem provided that the sample size is sufficiently large (Ahmed and Shapiro, 2002). For this purpose, we generate several random samples for the second stage objective function costs.

We compare the SAA method with the numerical results obtained with Algorithm 3.1. We remark that the SAA method allows to obtain only an average reference interval for the stochastic problem. In other words, with SAA method we do not solve exactly the same instances as in the PHA algorithm, since we intend to approximate the expectation function of the second stage objective function rather than solving for a particular set of scenarios. The SAA method is depicted in Algorithm 3.2.

In step zero of SAA method, we generate randomly $|M|$ independent samples $m \in \mathcal{M} = \{1,\ldots,|M|\}$ with scenario sets N_m where $|N_m| = N$. Subsequently, we generate randomly a reference sample set N' with sufficiently large number of scenarios where $|N'| >> N$. Then, in step 1, we solve the referred two-stage stochastic optimization problem for each sample $m \in \mathcal{M}$ where the set K is substituted by N_m. Next in step 2, we compute the average of the optimal objective function values obtained in step 1. The average is saved as a statistical lower bound for $(STSP_1)$ (Ahmed and Shapiro, 2002). Similarly, we solve the referred optimization problem using the fixed first stage solution x_m obtained in step 1 for each $m \in \mathcal{M}$, where the set K is substituted by N'. The latter allows to select the solution x_m with the minimum optimal objective function value as the solution of SAA method. Finally, we generate randomly a first stage solution set $x = x_\xi$ for one sample scenario on the second stage variables and compute the optimal

Algorithm 3.2: SAA procedure for $(STSP_1)$ with expectation second stage objective function.

Data: A problem instance of $(STSP_1)$ with expectation.
Result: Statistical lower and upper bounds for $(STSP_1)$ with expectation.
Step 0:
Generate randomly $|M|$ independent samples $m \in \mathcal{M} = \{1,\ldots,|M|\}$ with scenario sets N_m where $|N_m| = N$;
Select a reference sample N' to be sufficiently large where $|N'| >> N$;
Step 1:
foreach $m \in \mathcal{M}$ **do**
Solve the two-stage stochastic problem

$$\min_{\{x,y,u\}} \quad \left\{ \sum_{(i,j)\in A_D} c_{ij}x_{ij} + |N_m|^{-1} \sum_{s=1}^{|N_m|} \sum_{(i,j)\in A_S} \delta_{ij}^s y_{ij}^s \right\}$$
$$\text{subject to:} (2)-(9)$$

where the set K is replaced by N_m. Save the sample optimal objective function value v_m and the sample optimal solution x_m

Step 2:
Compute the average $\bar{v}_{|M|} = |M|^{-1} \sum_{m=1}^{|M|} v_m$ with the values obtained in the previous step. Save the average as a statistical lower bound for $(STSP_1)$;
foreach $m \in \mathcal{M}$ **do**
Solve the following problem using the first stage solution x_m obtained in step 1

$$\min_{\{x_m,y,u\}} \quad \left\{ \sum_{(i,j)\in A_D} c_{ij}x_m(ij) + |N'|^{-1} \sum_{s=1}^{|N'|} \sum_{(i,j)\in A_S} \delta_{ij}^s y_{ij}^s \right\}$$
$$\text{subject to:} (2)-(9) \text{ for fixed } x = x_m$$

where the set K is replaced by N' ;
Select the solution x_m with the minimum optimal objective function value as the solution of SAA method.
Generate randomly a first stage solution set $x = x_\xi$ with one sample scenario and compute

$$\min_{\{x_\xi,y,u\}} \quad \left\{ \sum_{(i,j)\in A_D} c_{ij}x_\xi(ij) + |N'|^{-1} \sum_{s=1}^{|N'|} \sum_{(i,j)\in A_S} \delta_{ij}^s y_{ij}^s \right\}$$
$$\text{subject to:} (2)-(9) \text{ for fixed } x = x_\xi$$

where the set K is substituted by N' ;
Save the optimal objective function value as a statistical upper bound for $(STSP_1)$;

objective function value of the referred optimization problem as a statistical upper bound for $(STSP_1)$. It is important to note that we compute the SAA solution as well as the lower and upper bounds for $(STSP_1)$ assuming that $(STSP_1)$ has an expectation second stage objective function.

4 PRELIMINARY NUMERICAL RESULTS

In this section, we present preliminary numerical results. A Matlab (R2012a) program is developed using CPLEX 12.6 to solve $(STSP_1)$ and its LP relaxation. The PHA and SAA methods are also implemented in Matlab. The numerical experiments have been carried out on an Intel(R) 64 bits core (TM) with 3.4 Ghz and 8 G of RAM. CPLEX solver is used with default options.

We generate the input data as follows. The edges in E_D and E_S are chosen randomly with 50% of probability. The values of $p_s, \forall s \in K$ are generated randomly from the interval $[0,1]$ such that $\sum_{s\in K} p_s = 1$. Costs are randomly drawn from the interval $[0,50]$ for both the deterministic and uncertain edges. In particular, the cost matrices $c = (c_{ij}), \forall (ij) \in A_D$ and $\delta^s = (\delta^s_{ij}), \forall (ij) \in A_S, s \in K$ are generated as input symmetric matrices.

In Algorithm 3.1, we set the parameter $t_{max} = \{7,12\}$ and save the best run, i.e., the run which allows us to find the best feasible solution. The parameter ρ is calibrated on a fixed value of $\rho = 10$. In Algorithm 3.2, we generate randomly $|M| = 10$ independent samples, each with $|N_m| = 5$ scenarios for the instances 1-10, whilst for the instances 11-12, we generate $|M| = 10$ independent samples each with $|N_m| = 2$ scenarios since the CPU times become highly and rapidly prohibitive in this case. Finally, we generate a reference scenario set with $|N'| = 50$ scenarios.

In Tables 1 and 2, the instances are the same for the first stage costs. In Table 1, the legend is as follows. In column 1, we show the instance number. In columns 2-3, we show the instance dimensions. In columns 4-5 we present the number of deterministic and uncertain edges for each instance, respectively. In columns 6-10, we present the optimal solution of $(STSP_1)$ or the best solution found with CPLEX in two hours of CPU time, CPLEX number of branch and bound nodes, CPU time in seconds, the optimal solution of the linear relaxation of $(STSP_1)$ and its CPU time in seconds, respectively. In columns 11-13, we present the best solution found with Algorithm 3.1, its CPU time in seconds and the number of iterations required to find the feasible solution. Finally, in columns 14-15, we present the gaps that we compute by $\left[\frac{Opt-LP}{Opt}\right] * 100$ and $\left[\frac{B.S.-Opt}{Opt}\right] * 100$, respectively.

In Table 1, we solve small, medium and large size instances ranging from $|V| = 10, |K| = 5$ to $|V| = 100$ nodes and $|K| = 10$ scenarios. From Table 1, first we observe that the number of deterministic and uncertain edges are balanced. Next, we observe that $(STSP_1)$ allows to solve to optimality only the instances 1-11 with up to $|V| = 30$ nodes and $|K| = 5$ scenarios. For the remaining instances, we cannot solve to optimality the problem. However, we obtain feasible solutions for most of them, with the exception of instance # 15. For this instance, we cannot find a feasible solution with CPLEX in two hours of CPU time. For the instance # 11, the problem is solved in 3910.61 seconds whilst the instances 1-10 are solved to optimality in less than 300 seconds. The linear relaxation for the instances 1-10 is solved in less than 1 second, while the LP instances 11-20 can be solved to optimality with CPU times ranging from 1 to 42 seconds. Next, we observe that the gaps for the LP instances go from 10.55 to 54.14. This clearly shows that the LP relaxation is not tight and explain the increase in the number of branch and bound nodes. On the opposite, we observe that the gaps for Algorithm 3.1 are very tight ranging from -66.89% to 11.21%. Negative gaps mean that the feasible solutions obtained with Algorithm 3.1 are significantly better than those obtained with CPLEX in two hours of CPU time. Notice that the CPU times required by Algorithm 3.1 are considerably lower than two hours. This shows the effectiveness of Algorithm 3.1. In particular, when finding feasible solutions for large size instances of the problem. Notice that most of the gap values obtained by Algorithm 3.1 for the instances which are solved to optimality (e.g., instances 1-10) are lower than 9% with the exception of instance # 11. In this case, the gap is 11.21%. Finally, we observe that the number of iterations required by Algorithm 3.1 is either six or eleven.

In Table 2, the legend is as follows. Columns 1-5 show exactly the same information as in Table 1. In columns 6-9, we present statistical lower bounds, the SAA solution, statistical upper bounds and CPU time in seconds found by Algorithm 3.2. Finally, in Columns 10-12 we present gaps that we compute by $\left|\frac{Stat.Lb-Opt}{Opt}\right| * 100$, $\left|\frac{SAALb-Opt}{Opt}\right| * 100$ and $\left|\frac{Stat.Ub-Opt}{Opt}\right| * 100$, respectively where Opt corresponds to the optimal solution or best solution found in Table 1.

In Table 2, we only solve small and medium size instances ranging from $|V| = 10, |K| = 5$ to $|V| = 40$

Table 1: Numerical results for $(STSP_1)$ using 50% of deterministic edges.

#	Inst. Dim.		# of edges		$(STSP_1)$					PHA Algorithm			Gaps	
	$\|V\|$	$\|K\|$	$\|E_D\|$	$\|E_S\|$	Opt	*B&Bn*	Time (s)	LP	Time (s)	*B.S.*	Time (s)	*#Iter*	Gap_1	Gap_2
1	10	5	23	22	125.22	115	0.50	112.02	0.32	126.09	22.53	6	10.55	0.69
2	12	5	42	24	101.95	0	0.43	90.95	0.35	103.28	22.05	6	10.78	1.31
3	14	5	41	50	111.90	1655	3.61	81.18	0.35	112.27	23.60	6	27.46	0.33
4	17	5	61	75	131.46	2009	5.61	111.10	0.33	141.41	23.78	6	15.49	7.57
5	20	5	88	102	148.38	15776	108.27	126.52	0.39	150.61	25.57	6	14.73	1.51
6	10	10	30	15	107.78	7	0.64	84.90	0.34	107.78	63.23	6	21.23	0
7	12	10	26	40	147.72	619	1.78	131.11	0.34	149.05	65.17	6	11.25	0.89
8	14	10	43	48	139.45	275	2.07	122.12	0.39	146.99	86.86	11	12.42	5.41
9	17	10	62	74	133.52	37730	238.27	113.30	0.35	138.81	92.22	11	15.14	3.96
10	20	10	93	97	153.02	21294	229.79	133.57	0.46	166.67	73.30	6	12.71	8.92
11	30	5	199	236	115.63	222400	3910.61	82.80	1.37	128.60	45.02	11	28.40	11.21
12	40	5	401	379	147.27	272361	7200	109.89	1.59	147.10	68.49	11	25.38	-0.12
13	60	5	889	881	194.47	60032	7200	114.96	1.82	174.30	164.17	11	40.88	-10.37
14	80	5	1552	1608	243.86	20885	7200	130.76	3.80	186.13	358.81	6	46.38	-23.67
15	100	5	2516	2434	-	6540	7200	122.02	4.31	177.16	739.57	6	-	-
16	30	10	221	214	148.56	220674	7200	108.33	2.90	155.46	86.57	6	27.08	4.64
17	40	10	368	412	171.46	83242	7200	117.81	1.91	167.69	118.83	6	31.29	-2.20
18	60	10	844	926	244.26	15384	7200	123.38	4.83	169.16	233.10	6	49.49	-30.74
19	80	10	1549	1611	564.93	7703	7200	135.26	15.86	187.07	673.42	6	76.06	-66.89
20	100	10	2545	2405	275.51	1922	7200	126.35	41.51	186.08	3832.77	6	54.14	-32.46

$^-$: No solution found with CPLEX in 2 hours.

nodes and $|K| = 5$ scenarios. We do not solve larger size instances of the problem as in Table 1, since the CPU times become rapidly prohibitive in this case.

From Table 2, we mainly observe that the SAA solution values obtained with Algorithm 3.2 are between the statistical lower and upper bounds for all the instances. We compute an average distance for the lower and upper bounds of 38.74 %, whilst we compute an average distance between the SAA solution and lower bounds of 27.72 %. Similarly, we compute an average distance between the upper bounds and SAA solutions of 11.01 %. We also see that most of the objective function values obtained in Table 1 are near the lower and upper bounds obtained with SAA Algorithm 3.2. Finally, by computing the averages of columns 10-12 in Table 2, we obtain a minimum of 14.32 units for the column # 11. This suggests that the SAA solution values are tighter when compared with the objective function values found in Table 1.

5 CONCLUSIONS

In this paper, we proposed an adapted version of the progressive hedging algorithm (PHA) (Rockafellar and Wets, 1991; Lokketangen and Woodruff, 1996; Watson and Woodruff, 2011) for the two-stage stochastic traveling salesman problem (STSP) introduced in (Adasme et al., 2016). Thus, we computed feasible solutions for small, medium and large size instances of the problem. Additionally, we compared the PHA method with the sample average approximation (SAA) method for all the randomly generated instances and calculated statistical lower and upper bounds for the problem. For this purpose, we used the compact polynomial formulation extended from (Miller et al., 1960) in (Adasme et al., 2016) as it is the one that allows us to solve large size instances of the problem within short CPU time with CPLEX. Our preliminary numerical results showed that the results obtained with the PHA algorithm are tight when compared to the optimal solutions of small and medium size instances. Moreover, we obtained significantly better feasible solutions than CPLEX for large size instances with up to 100 nodes and 10 scenarios in considerably low CPU time. Finally, the bounds obtained with SAA method provide an average reference interval for the stochastic problem.

ACKNOWLEDGEMENTS

The first and third author acknowledge the financial support of the USACH/DICYT Projects 061413SG, 061513VC_DAS and CORFO 14IDL2-29919.

Table 2: Upper and Lower Bounds for the Instances in Table 1 using SAA Algorithm.

#	Inst. Dim.		# of edges		SAA Algorithm				Gap		
	$\|V\|$	$\|K\|$	$\|E_D\|$	$\|E_S\|$	Stat. Lb	SAA Lb	Stat. Ub	Time (s)	Gap_1	Gap_2	Gap_3
1	10	5	23	22	108.88	120.29	143.63	8.85	13.05	3.94	14.70
2	12	5	42	24	114.96	141.19	146.70	9.19	12.77	38.49	43.89
3	14	5	41	50	127.02	131.58	144.24	5.39	24.60	29.07	41.49
4	17	5	61	75	127.89	147.79	162.50	43.85	2.72	12.42	23.61
5	20	5	88	102	135.73	156.73	164.87	60.07	8.52	5.63	11.12
6	10	10	30	15	106.84	117.88	136.77	17.27	0.87	9.37	26.89
7	12	10	26	40	133.05	145.32	146.74	28.52	9.93	1.63	0.67
8	14	10	43	48	104.04	133.21	142.80	24.94	25.39	4.47	2.40
9	17	10	62	74	113.52	146.37	153.21	47.30	14.98	9.63	14.75
10	20	10	93	97	118.20	164.43	174.54	100.27	22.76	7.46	14.07
11	30	5	199	236	93.01	145.12	152.34	186.61	19.57	25.50	31.74
12	40	5	401	379	117.18	183.12	196.86	1748.68	20.43	24.34	33.67

REFERENCES

Adasme, P., Andrade, R., Letournel, M., and Lisser, A. (2013). A polynomial formulation for the stochastic maximum weight forest problem. *ENDM*, 41:29–36.

Adasme, P., Andrade, R., Letournel, M., and Lisser, A. (2015). Stochastic maximum weight forest problem. *Networks*, 65(4):289–305.

Adasme, P., Andrade, R., Leung, J., and Lisser, A. (2016). A two-stage stochastic programming approach for the traveling salesman problem. *ICORES-2016*.

Ahmed, S. and Shapiro, A. (2002). The sample average approximation method for stochastic programs with integer recourse. *Georgia Institute of Technology.*

Bertazzi, L. and Maggioni, F. (2014). Solution approaches for the stochastic capacitated traveling salesmen location problem with recourse. *J Optim Theory Appl*, 166(1):321–342.

Bertsimas, D., Brown, D., and Caramanis, C. (2011). Theory and applications of robust optimization. *SIAM Reviews*, 53:464–501.

Escoffier, B., Gourves, L., Monnot, J., and Spanjaard, O. (2010). Two-stage stochastic matching and spanning tree problems: Polynomial instances and approximation. *Eur J Oper Res*, 205:19–30.

Flaxman, A. D., Frieze, A., and Krivelevich, M. (2006). On the random 2-stage minimum spanning tree. *Random Struct Algor*, 28:24–36.

Gaivoronski, A., Lisser, A., Lopez, R., and Xu, H. (2011). Knapsack problem with probability constraints. *J Global Optim*, 49:397–413.

Lokketangen, A. and Woodruff, D. L. (1996). Progressive hedging and tabu search applied to mixed integer (0-1) multi stage stochastic programming. *Journal of Heuristics*, 2(2):111–128.

Maggioni, F., Perboli, G., and Tadei, R. (2014). The multi-path traveling salesman problem with stochastic travel costs: a city logistics computational study. *Transportation Research Procedia*, 1(3):528–536.

Miller, C. E., Tucker, A. W., and Zemlin, R. A. (1960). Integer programming formulations and travelling salesman problems. *J. Assoc. Comput. Mach.*, 7:326–329.

Rockafellar, R. T. and Wets, R. J. B. (1991). Scenarios and policy aggregation in optimization under uncertainty. *Mathematics and Operations Research*, 16:119–147.

Shapiro, A., Dentcheva, D., and Ruszczynski, A. (2009). Lectures on stochastic programming: Modeling and theory. *MOS-SIAM Series on Optimization, Philadelphia*.

Watson, J. P. and Woodruff, D. L. (2011). Progressive hedging innovations for a class of stochastic mixed-integer resource allocation problems. *Computational Management Science*, 8:355–370.

K-modes and Entropy Cluster Centers Initialization Methods

Doaa S. Ali, Ayman Ghoneim and Mohamed Saleh
Department of Operations Research and Decision Support
Faculty of Computers and Information, Cairo University
5 Dr. Ahmed Zewail Street, Orman, 12613 Giza, Egypt
{d.saleh, a.ghoneim, m.saleh}@fci-cu.edu.eg

Keywords: Multiobjective Data Clustering, Categorical Datasets, K-modes Clustering Algorithm, Entropy.

Abstract: Data clustering is an important unsupervised technique in data mining which aims to extract the natural partitions in a dataset without a priori class information. Unfortunately, every clustering model is very sensitive to the set of randomly initialized centers, since such initial clusters directly influence the formation of final clusters. Thus, determining the initial cluster centers is an important issue in clustering models. Previous work has shown that using multiple clustering validity indices in a multiobjective clustering model (e.g., MODEK-Modes model) yields more accurate results than using a single validity index. In this study, we enhance the performance of MODEK-Modes model by introducing two new initialization methods. The two proposed methods are the K-Modes initialization method and the entropy initialization method. The two proposed methods are tested using ten benchmark real life datasets obtained from the UCI Machine Learning Repository. Experimental results show that the two initialization methods achieve significant improvement in the clustering performance compared to other existing initialization methods.

1 INTRODUCTION

Data clustering extracts the natural partitions in a dataset without a priori class information. It aims to group the dataset observations into clusters where observations within a cluster are more similar to each other than observations in other clusters. Clustering is used as a data processing technique in many different areas, such as artificial intelligence (e.g., Bhagat et al., 2013), medical (e.g., Rahman and Sarma, 2013), pattern recognition (e.g., Pratima and Nimmakant, 2008), and customer analysis (e.g., Alvandi et al., 2012). The most popular clustering algorithms are K-means, K-modes, and K-medoids algorithms. K-means algorithm is efficiently used when processing numerical datasets, where means serve as centers/centroids of the data clusters. In K-means algorithm, observations are grouped into K clusters in which an observation belongs to the cluster with the closest mean (i.e., centroid) (Serapião et al., 2016). When dealing with categorical data (Bai et al., 2013; Kim and Hyunchul, 2008), K-modes (Ammar and Lingras, 2012) and K-medoids (Mukhopadhyay and Maulik, 2007) are used instead of K-means. K-modes algorithm uses a most frequency based method to update modes during the clustering process. While K-medoids algorithm selects a cluster medoid instead of computing the mean of cluster. A medoid is a representative observation in each cluster which has the minimum sum of distances to other observations in the cluster. Evolutionary computation techniques play a vital role in improving the performance of data clustering because of its ability to avoid local optimal solutions. Evolutionary computation techniques are considered global optimization techniques, which use selection and recombination as their primary operators to tackle optimization problems (Kim and Hyunchul, 2008). Data clustering models are very sensitive to the randomly initialized centers used at the beginning of the search process, since such initial centers directly influence the formation of final clusters (Khan and Ahmed, 2013). Furthermore, these random initialized centers may lead to premature convergence to local optimal solutions. To address such concerns, several initialization methods were proposed in the literature. Redmond and Heneghan (2007) propose to initialize cluster centers by first assigning data points to one of the k clusters randomly, and then the centroids of these initial clusters are taken as the

Ali, D., Ghoneim, A. and Saleh, M.
K-modes and Entropy Cluster Centers Initialization Methods.
In *Proceedings of the 6th International Conference on Operations Research and Enterprise Systems (ICORES 2017)*, pages 447-454
ISBN: 978-989-758-218-9

initial cluster centers. Jancey initialization method (Jancey, 1966) aims to allocate each cluster center a synthetic data object generated randomly within the given data space. Ball and Hall's method (Ball and Hall, 1967) takes the center of the entire dataset as the first cluster center, and then picks up the data object which is at least T units away from the existing cluster centers as the next cluster center. Maxmin initialization method (Gonzalez, 1985; Katsavounidis et al., 1994) randomly selects a data object as the first cluster center, and then the data object with the greatest minimum-distance to the existing cluster centers is taken as the next cluster center. This process repeats until k cluster centers are determined. In (Cao et al., 2009), initial centers are determined based on the most frequent values of the attributes, and the average density values. In (Bai et al., 2012), an initialization method based on integrating the distance measure and the density together was introduced. In (Ji et al., 2015), the authors propose a cluster center initialization method for the k-prototypes algorithms based on the neighbor set concept.

Cluster validity indices are used to evaluate the performance of the clustering algorithm (Mukhopadhyay and Maulik, 2007). Some recently studies used the cluster validity indices as objective functions in a multiobjective framework (e.g., Mukhopadhyay and Maulik, 2007; Serapião et al., 2016). Previous work introduced a multiobjective clustering model (MODEK-Modes) based on self-adaptive differential evolution with three cluster validity indices, which are symmetry index, compactness index, and silhouette index (Soliman and Saleh, 2015). The MODEK-Modes model used K-modes algorithm as it deals with categorical data, and it has been implemented using randomly initialized centers. This work aims to enhance data clustering performance through introducing two initialization methods which are the K-Modes (KM) initialization method and the entropy initialization method. These proposed initialization methods are used in conjunction with the MODEK-Modes Model. The two proposed methods are tested using ten benchmark real life datasets obtained from the UCI Machine Learning Repository. To evaluate the performance of the proposed initialization methods, we compared them against four initialization methods from the literature which are the Forgy method (Redmond and Heneghan, 2007), the density method (Bai et al., 2012), the value-attributes (Khan and Ahmed, 2013), and K-Prototype (Ji et al., 2015), in addition to the results of the MODEK-Modes Model with randomly initialized center. The time and space complexity of our proposed methods are analyzed, and the comparison with the other methods confirms the effectiveness of our methods. The rest of the paper is organized as follows. Section 2 introduces preliminary concepts needed in the current work. Section 3 presents the KM initialization method, while Section 4 presents the entropy initialization method. Section 5 shows the experimental results and analysis for the proposed methods in comparison with other initialization methods. Section 6 concludes the work and discusses future work.

2 PRELIMINARY CONCEPTS

This section introduces preliminary concepts needed in our work. We will discuss the K-modes algorithm and the entropy concept followed by a brief overview of the MODEK-Modes model.

2.1 K-modes Algorithm

K-modes algorithm extends the K-means algorithm to cluster categorical data by replacing means of clusters by modes (Bai et al., 2013; Kim and Hyunchul, 2008). K-modes algorithm uses a simple matching distance, or a hamming distance when measuring distances between data observations. Formally, a clustering problem is formulated as an optimization problem as follows:

$$Min_{\mu,Z} \quad F(\mu, Z) = \sum_{i=1}^{n} \sum_{j=1}^{k} \mu_{ij}\, d(z_j, x_i) \qquad 1 \le i \le n, 1 \le j \le k \tag{1}$$

where n is the number of data points, k is the number of data clusters, and μ_{ij} is a membership of i^{th} data observation to cluster j (i.e. μ_{ij} takes binary values in crisp case). $d(z_j, x_i)$ is the matching distance measure between data point x_i and data cluster center z_j. To understand the matching distance measure, let x and y be two data observations in data set D and L be the number of attributes in a data observation. The simple matching distance measure between x and y in D is defined as:

$$d_C(x, y) = \sum_{l=1}^{L} \delta(x_l, y_l) \tag{2}$$

where $\delta(x_l, y_l) = \begin{cases} 0 & if\ x_l = y_l \\ 1 & if\ otherwise \end{cases}$

The center of a cluster is updated using the following equation:

$$z_{jl} = a_{rl} \in DOM(A_l) \ , \quad r \in n_j \tag{3}$$

where z_{jl} represents the new updated value of cluster j in the l^{th} attribute, and a_{rl} is the value of the data observation r which has the most frequent value in the l^{th} attribute for the data observations within cluster j. A_l expresses all the possible values for attribute l, *DOM* is a domain of the attribute, and n_j is the total number of data observations in cluster j. Procedure 1 illustrates the steps of the K-Modes algorithm.

1: *Randomly initialize centers for the k clusters*
2: *Each data point is assigned to the cluster with the nearest center (Eq. 2).*
3: *Update the center of each cluster using (Eq. 3).*
4: *Repeat steps 2 and 3 until the clusters' centers stop changing or other stopping criteria are met.*

Procedure 1: Steps of K-Modes algorithm.

2.2 Entropy Concept

In data clustering, the entropy between each pair of data points helps us visualize the complete dataset. The value of entropy (a value in the range [0, 1]) is low (close to zero) for either very close data points, or very far data points. Here the data points can be easily separated into clusters, thus the uncertainty is low and the entropy is also low. On the other hand, the entropy of high value (close to one) indicates that the data points are separated by a distance close to the average distances of all pairs of data points; i.e., the maximum entropy occurs when the data points are uniformly distributed in the feature space. The entropy depends on the similarity measure. The similarity measure S, in turn, is inversely proportional to the distance; i.e., the similarity measure has a very high value (close to one) for very close data points - which should be located in the same cluster, and a very low value (close to zero) for very far data points should be located in different clusters. As shown in Eq. 4, the entropy between a pair of data points is defined as (Terano et al., 2000):

$$E_{ij} = -S_{ij}\log_2(S_{ij}) - (1 - S_{ij})\log_2(1 - S_{ij}) \tag{4}$$

$$S_{ij} = 0.5 * ({S^d}_{ij} + {S^c}_{ij})$$
$${S^d}_{ij} = \frac{\sum_{d=1}^{D} |x_{id} = x_{jd}|}{D} \tag{5}$$

In this paper, we enhanced the similarity measure via augmenting the traditional distance-based similarity with another term associated with the current clustering of the two data points (Eq. 5). We denote this novel term by the cluster-based similarity measure. Recall that the traditional similarity measure for categorical data is inversely proportional to the Hamming distance; i.e., the distance-based similarity measure between two data points is given as ${S^d}_{ij} = \frac{\sum_{d=1}^{D} |x_{id} = x_{jd}|}{D}$, where i and j be any two data points, D the number of attributes, and $|x_{id} = x_{jd}|$ is 1 if x_{id} equals to x_{jd} and 0 otherwise. In the paper, we define the novel cluster-based similarity measure as follows: ${S^c}_{ij} = 1$ if and only if i and j lie in the same cluster; and 0 otherwise. Finally, the total entropy between all pairs of data points is calculated by the following equation (Terano et al., 2000):

$$E = \sum_{i}^{N}\sum_{j}^{N} E_{ij} \tag{6}$$

2.3 MODEK-Modes Model

MODEK-Modes model is a multiobjective data clustering model based on self-adaptive differential evolution using three cluster validity indices (i.e., objective functions) (Soliman and Saleh, 2015). The three cluster validity indices are symmetry index (to maximize similarity within cluster), compactness index (to maximize dissimilarity between different clusters), and silhouette index (to test a suitability the clustering model to the processed dataset). The MODEK-Modes model starts with initializing a population of random centers, then assigning data points to the initialized centers forming clusters. Next steps are repeated until the total number of iterations is reached. These steps start with updating centers of clusters, reassigning data points to clusters, and evaluating fitness of individuals. The next two steps apply the adapted mutation, crossover, and evaluate the candidates for each parent. The selection operator then creates the new population based on fitness function.

3 K-MODES INITIALIZATION METHOD

This proposed method uses the traditional K-modes algorithm as an initialization method, where the output of K-modes algorithm is considered the input to the MODEK-Modes Model (see Figure 1). The traditional K-modes algorithm has a single objective function which minimizes the total distances

between all data observations and centers of clusters. The traditional K-modes algorithms starts with initializing random centers, and then assign data points to the clusters, then update centers. The k-modes algorithm repeats the last two steps until it converges. These converged centers are considered the initial population for the MODEK-Modes model.

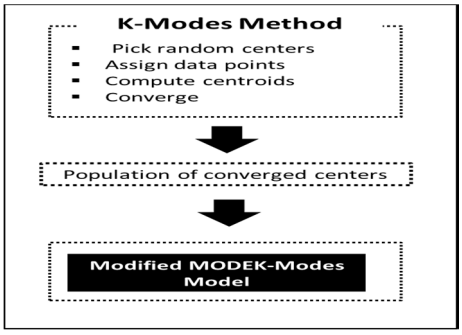

Figure 1: The KM initialization method.

4 ENTROPY INITIALIZATION METHOD

The proposed entropy initialization method consists of two stages (see Figure 3). The first stage is called an entropy stage which produces an accumulated matrix. This accumulated matrix is the input for the second initialization stage. The entropy stage (Procedure 2) operates only once for each dataset under consideration. The entropy stage takes the dataset as an input and outputs an accumulated matrix based on the entropy similarity measure. The entropy stage starts with clustering the data points based on the entropy values. We illustrate an algorithm (inspired by (Li et al., 2004)) to utilize the total entropy in the cluster process. Our contribution is the enhancement of the similarity measure used in this algorithm. The core idea of the algorithm is to try to minimize the total entropy via randomly swapping points between clusters. Recall that the entropy between a pair of data points will be small if either the proposed enhanced similarity measure is low or high. The enhanced similarity measure has a small value only when both the distance-based measure and the cluster-based measure have small values (i.e., large distance and different clusters). The enhanced similarity measure has a large value only when both the distance-based measure and the cluster-based measure have large values (i.e., small distance and same clusters). Thus swapping points between clusters will have significant and meaningful impacts on the total entropy. After clustering the given data points, we need to determine a mode of each cluster by using Eq. 3. The distances between every data point and the k clusters are then calculated to producing a membership matrix (n × K). Elements of the membership matrix will be computed by the following equation:

$$M_{i,j} = \frac{d_{i,j}}{\sum_j d_{i,j}} \quad \forall\, i = 1,..,n \;\&\; \forall\, \mathrm{j} = 1,\ldots,\mathrm{k} \qquad (7)$$

where n is the total number of data points in the used dataset, K is the number of data clusters, $M_{i,j}$ is a membership between data point i and cluster j, and $d_{i,j}$ is the distance between data point i and cluster j.

1. Entropy clustering procedure
   - Input: (data points: X, # of classes: k)
   - Output: cluster assignment;
   - **Begin**
     1. **Initialization:**
        1.1. Put all data points into one cluster
        1.2. Compute Initial Criterion E_0 (Initial total entropy)
     2. **Iteration: Repeat until no more changes in cluster assignment**
        2.1. Randomly pick a point x from a cluster A
        2.2. Randomly pick another cluster B
        2.3. Put x into B
        2.4. Compute the new total entropy E
        2.5. If $E \geq E_0$
             2.5.1. Put x back into A
             2.5.2. $E = E_0$
        2.6. End
        2.7. $E_0 = E$
        2.8. Go to Step 2.1
        2.9. **End**
     3. **Return** the cluster assignment
   - **End**
2. Determine a mode of each cluster using Eq. (3).
3. Measure the distances between each data point and the K clusters by using Eq. (2).
4. Calculate membership values using Eq. (7) to form the membership matrix (n x k), where n: number of data points and k: number of clusters.
5. Building accumulated matrix, where A_{il} be accumulated value between the data point i[th] and cluster l^{th}, and $A_{il} = \sum_{i1=1}^{i-1} M_{i1,l} + M_{i,l}$

Output: the accumulated matrix

Procedure 2: The procedure of the entropy stage.

An accumulated matrix is produced from the computed membership matrix in step 5 (see Procedure 2). This accumulated matrix is the output of the entropy stage and the start of the second initialization stage. Figure 2 presents an example of how to calculate the accumulated matrix.

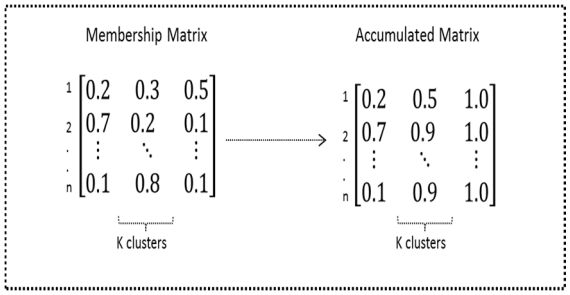

Figure 2: An example of the membership and accumulated matrixes in the proposed entropy initialization method.

The initialization stage mainly depends on the accumulated matrix (Procedure 3).

- For every individual in the population:
- Initialization Stage: (Input: the previous calculated accumulated matrix)
  1. For each data point, i =1,2,…,n.
     - Generate uniform random number U~(0, 1).
     - Assign data point to a cluster (upper bound of U interval) (see the accumulated matrix).
  2. End For
  3. Determine the mode of each cluster (be centroid of this cluster) for categorical data.
- Output: set of the initialized centers of the k clusters.

Procedure 3: Steps of the initialization stage.

This stage is repeated every time we need to generate a new population of centers for the MODEK-modes model. The initialized centers are produced from an initial distribution to the data points based on the accumulated matrix. Let U_1 and U_2 be uniform random numbers for the first and the second data points. According to the accumulated matrix in figure 2, if $U_1 = 0.7$ and $U_2 = 0.3$, then we have to assign the first data point to the third cluster $(0.5 \leq U_1 \leq 1.0)$ and assign the second data point to the first cluster $(0.0 \leq U_2 \leq 0.7)$. This process is repeated for every data point in the dataset. Finally, after distributing all data points, we have to calculate the mode of the cluster by Eq. 3. And hence, the mode of each cluster is considered the initial coordinates for this cluster.

5 EXPERIMENTAL RESULTS

The clustering accuracy of the MODEK-modes model is compared when using the two proposed initialization methods against the Forgy method (Redmond and Heneghan, 2007), the density method (Bai et al., 2012), the value-attributes (Khan and Ahmed, 2013), and K-Prototype (Ji et al., 2015), in addition to the results of the MODEK-Modes Model with randomly initialized centers. The results of 50 independent runs are summarized in Tables 1 and 2. For every dataset, the tables illustrate the mean of the best solution (in 50 runs) and the standard deviation for every initialization method. T-test was performed with confidence level 0.05 to check if the differences between the results are statistically significant or non-significant compared to the second best performing method. As shown in Table 1, the proposed KM initialization method performed better in eight datasets and with significant change compared to other initialization methods. Table 2 illustrates the experimental results for the proposed entropy method, and shows that the proposed entropy method significantly improved the clustering accuracy for seven dataset.

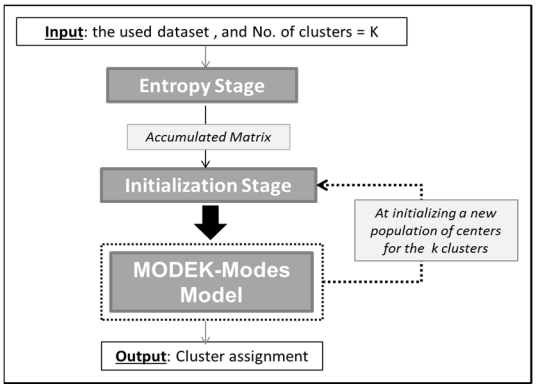

Figure 3: Stages of the entropy initialization method.

Moreover, Table 3 lists the run time of the seven clustering initialization methods on different datasets. From this table, we can see that the KM method needs more time than the random and the Forgy initialization methods. However, the KM method consumes time less than Density, Value-attributes, and K-Prototype initialization methods. On the other hand, the Entropy method needs more time than other methods in comparison except for the K-Prototype initialization method.

6 CONCLUSION AND FUTURE WORK

In the light of the importance of data clustering, the paper aimed to improve the performance of data clustering through addressing and enhancing handling the initialization step, where clustering models start with a set of random initial clusters and are very sensitive to such randomly initialized

Table 1: Mean ± standard deviation of best solution of 50 independent runs and T-test for the KM initialization method and the other compared methods, where "No": refers to non-significant change, and "Yes": refers to significant change.

	KM	Density	Random	Forgy	Value-Attributes	K-Prototype	T-test
Soybean	0.92784921 ± 0.00018	0.8928741 ±0.0000221	0.8961113 ±0.00038	0.885262 ± 0.0071	0.889932 ± 0.0039	0.902728 ± 0.0073	Yes
B. Cancer	0.887345 ± 0.00021	0.86689 ± 0.0027	0.8210432 ±0.00666	0.872992 ± 0.0023	0.878943 ± 0.0011	0.8956345 ±0.0013	No
Spect Heart	0.8198299 ± 0.0010	0.7759342 ±0.0016	0.7782529 ±0.0080	0.7224645 ±0.0031	0.787823 ± 0.0067	0.792651± 0.044	Yes
St. Heart	0.738873 ± 0.0023	0.7493424 ±0.0020	0.6778213 ±0.0018	0.717923 ± 0.0081	0.754592 ± 0.0029	0.7356782 ± 0.0017	Yes
Zoo	0.958879 ± 0.0031	0.9144634 ±0.0017	0.9377262 ±0.0024	0.931978 ± 0.0038	0.933932 ± 0.019	0.928853 ±0.0014	Yes
Liver	0.8845267 ± 0.00041	0.8254823 ± 0.0013	0.8175647 ±0.0280	0.862247 ± 0.0027	0.857934 ± 0.0026	0.845723 ± 0.0011	Yes
HServival	0.6478901 ± 0.0109	0.6106859 ±0.031	0.6014788 ±0.0027	0.6199879 ±0.0037	0. 6204733 ±0.033	0.612411 ± 0.0033	Yes
Dermatology	0.797225 ± 0.0021	0.7406811 ±0.0011	0.710089 ± 0.0031	0.7122794 ±0.0027	0.7588932 ±0.0081	0.764563 ± 0.0055	Yes
L. Cancer	0.696881 ± 0.0020	0.6279032 ±0.0032	0.6015231 ±0.0061	0.6682301 ±0.0170	0.648932 ± 0.0073	0.658932 ± 0.0044	Yes
Computer	0.6790211 ±0.0051	0.6489341 ±0.0037	0.5933928 ±0.0053	0.6378941 ±0.0062	0.6486372 ±0.0016	0.6509342 ±0.023	Yes

Table 2: Mean ± standard deviation of best solution of 50 independent runs and T-test for the entropy initialization method and the other compared methods, where "No" refers to non-significant change, and "Yes" refers to significant change.

	Entropy	Density	Random	Forgy	Value-Attributes	K-Prototype	T-test
Soybean	0.9148790 ± 0.0017	0.8928741 ±0.0000221	0.8961113 ±0.00038	0.885262 ± 0.0071	0.889932 ± 0.0039	0.902728 ± 0.0073	Yes
B. Cancer	0.8482991 ± 0.001	0.86689 ± 0.0027	0.8210432 ± 0.00666	0.872992 ± 0.0023	0.878943 ± 0.0011	0.8956345 ±0.0013	Yes
Spect Heart	0.8256281 ± 0.0011	0.7759342 ±0.0016	0.7782529 ±0.0080	0.7224645 ±0.0031	0.787823 ± 0.0067	0.792651± 0.044	Yes
St. Heart	0.7045282 ± 0.0002	0.7493424 ±0.0020	0.6778213 ± 0.0018	0.717923 ± 0.0081	0.754592 ± 0.0029	0.7356782 ±0.0017	Yes
Zoo	0.957811 ± 0.0031	0.9144634 ±0.0017	0.9377262 ± 0.0024	0.931978 ± 0.0038	0.933932 ± 0.019	0.928853 ± 0.0014	Yes
Liver	0.870003 ± 0.00021	0.8254823 ±0.0013	0.8175647 ± 0.0280	0.862247 ± 0.0027	0.857934 ± 0.0026	0.845723 ± 0.0011	No
HServival	0.6429739 ±0.0011	0.6106859 ±0.031	0.6014788 ±0.0027	0.6199879 ±0.0037	0.6204733± 0.033	0.612411 ± 0.0033	Yes
Dermatology	0.8571158 ± 0.00211	0.7406811 ±0.0011	0.710089 ± 0.0031	0.7122794 ±0.0027	0.7588932 ± 0.0081	0.764563 ± 0.0055	Yes
L. Cancer	0.7287116 ± 0.0003	0.6279032 ±0.0032	0.6015231 ±0.0061	0.6682301 ±0.0170	0.648932 ± 0.0073	0.658932 ± 0.0044	Yes
Computer	0.7963731 ±0.0019	0.6489341 ±0.0037	0.5933928 ±0.0053	0.6378941 ±0.0062	0.6486372 ± 0.0016	0.6509342 ±0.023	Yes

Table 3: The running time of the seven clustering initialization methods on the used datasets.

	Average Running Time (Mintues)						
	KM	*Entropy*	*Density*	*Random*	*Forgy*	*Value-Attributes*	*K-Prototype*
Soybean	2.90	3.11	3.07	2.42	2.37	3.03	3.33
B. Cancer	11.81	12.20	11.89	9.34	9.22	11.84	12.23
Spect Heart	4.82	5.17	4.98	4.23	4.18	4.87	5.21
St. Heart	5.33	5.64	5.37	4.83	4.79	5.32	5.68
Zoo	3.40	3.62	3.43	3.21	3.17	3.41	3.66
Liver	6.91	7.10	6.93	6.67	6.59	6.89	7.24
HServival	6.27	6.68	6.31	5.82	5.66	6.29	6.72
Dermatology	9.62	9.89	9.67	9.32	9.27	9.62	9.95
L. Cancer	3.70	3.87	3.79	3.49	3.23	3.73	3.93
Computer	5.20	5.48	5.37	4.89	4.82	5.33	5.57

centers. Previous work has shown that using multiple clustering validity indices in a multiobjective clustering model (e.g., MODEK-Modes model) yields more accurate results than using a single validity index. Thus, we proposed to enhance the performance of MODEK-Modes model by introducing two new initialization methods. These two proposed methods are K-Modes initialization method and entropy initialization method. The two proposed methods have been tested using ten benchmark real life datasets obtained from the UCI Machine Learning Repository. We applied t-test to check the significance of the results. Based on the experimental results, the two initialization methods achieved a significant improvement in the clustering performance compared to the other initialization methods. The KM method achieved a significant improvement in the clustering performance of 8 datasets, while the entropy method improved the clustering performance in 7 datasets. The time and space complexity of our proposed methods are analyzed, and the comparison with the other methods demonstrates the effectiveness of our methods. For further work, the proposed two initialization methods can be extended to deal with the numerical datasets by replacing k-modes by the k-means algorithm.

REFERENCES

Ammar E. Z., Lingras P., 2012, K-modes clustering using possibilistic membership, IPMU 2012, Part III, CCIS 299, pp. 596–605.

Alvand M., Fazli S., Abdoli F. S., 2012, K-mean clustering method for analysis customer lifetime value with LRFM relationship model in banking services, International Research Journal of Applied and Basic Sciences, 3 (11): pp. 2294-2302.

Bai L., Liang J., Dang Ch., Cao F., 2012, A cluster centers initialization method for clustering categorical data, Expert Systems with Applications, 39, pp. 8022–8029.

Bai L., Lianga J., Dang Ch., Cao F., 2013, A novel fuzzy clustering algorithm with between-cluster information for categorical data, *Fuzzy Sets and Systems (215), pp. 55–73.*

Ball G. H., Hall D. J., 1967, A clustering technique for summarizing multivariate data, Behavioral Science 2 (2) 153–155.

Bhagat P. M., Halgaonkar P. S., Wadhai V. M., 2013, Review of clustering algorithm for categorical data, *International Journal of Engineering and Advanced Technology*, 3 (2).

Cao F., Liang J., Bai L., 2009, A new initialization method for categorical data clustering, Expert Systems with Applications, 36, pp. 10223–10228.

Cao F., Liang J., Li D., Bai L., Dang Ch., 2012, A dissimilarity measure for the k-Modes clustering algorithm, Knowledge-Based Systems 26, pp. 120–127.

Gonzalez T., 1985, Clustering to minimize the maximum intercluster distance, Theoretical Computer Science, 38 (2– 3), pp. 293–306.

Jancey R. C., 1996, Multidimensional group analysis, *Australian Journal of Botany, 14 (1), pp*. 127–130.

Ji J., Pang W., Zheng Y., Wang Z., Ma Zh., Zhang L., 2015, A novel cluster center initialization method for the k-Prototypes algorithms using centrality and distance, *Applied Mathematics and Information Sciences*, No. 6, pp. 2933-2942.

Katsavounidis, C.-C. Kuo J., Zhang Z., 1994, A new initialization technique for generalized Lloyd iteration, IEEE Signal Processing Letters, 1 (10), pp. 144–146.

Khan Sh. S., Ahmed A., 2013, Cluster center initialization algorithm for K-modes clustering, *Expert Systems with Applications*, 40, pp. 7444–7456.

Kim K.K., Hyunchul A., 2008, A recommender system using GA K-means clustering in an online shopping market, *Expert Systems with Applications*, 34, pp. 1200–1209.

Li T., MA S., Ogihara M., 2004, Entropy-based criterion in categorical clustering, The 21rst International Conference on Machine Learning, Banff, Canada.

Mukhopadhyay A., Maulik U., 2007, Multiobjective approach to categorical data clustering, IEEE Congress on Evolutionary Computation, pp. 1296 – 1303.

Pratima D., Nimmakant N. i, 2008, Pattern recognition algorithms for cluster identification problem, Special Issue of *International Journal of Computer Science & Informatics, Vol. II, Issue 1* (2), pp. 2231–5292.

Rahman N., Sarma P., 2013, Analysis of treatment of prostate cancer by using multiple techniques of data mining, International Journal of Advanced Research in Computer Science and Software Engineering 3 (4), pp. 584–589.

Redmond S. J., Heneghan C., 2007, A method for initialising the k-means clustering algorithm using kd-trees, Pattern Recognition Letters, 28(8), pp. 965–973.

Serapião B. S., Corrêa G. S. , Gonçalves F. B. , Carvalho V. O., 2016, Combining K-means and K-harmonic with fish school search slgorithm for data clustering task on graphics processing units, *Applied Soft Computing*, 41, pp. 290–304.

Soliman O. S. , Saleh D. A., 2015, Multi-objective K-modes data clustering algorithm using self-adaptive differential evolution, International Journal of Advanced Research in *Computer Science and Software Engineering,* 5(2), pp. 57-65.

Terano T., Liu H., Chen A. L.P., 2000, Knowledge discovery and data mining. Current Issues and New Applications, *4th Pacific Asia Conference, PAKDD.*

Comparison of Theoretical and Simulation Analysis of Electricity Market for Integrative Evaluation of Renewable Energy Policy

Masaaki Suzuki, Mari Ito and Ryuta Takashima
Department of Industrial Administration, Tokyo University of Science, 2641 Yamazaki, Noda, Chiba, Japan
{*m-suzuki, mariito, takashima*}*@rs.tus.ac.jp*

Keywords: Renewable Energy Policy, FIT, RPS, Social Welfare, Equilibrium Analysis, Multi-agent Simulation.

Abstract: Governments have introduced various policies for promoting renewable energy technologies. In particular, feed-in tariff (FIT) and renewable portfolio standard (RPS) have been introduced in various countries. In this work, multi-agent simulations of electricity markets with FIT/RPS have been conducted for integrative analysis and rational design of renewable energy policies. We analyze the effects of the FIT price and RPS level on social welfare. By comparing the results obtained from the simulation and the equilibrium analysis, we have examined the policies from both bottom-up and top-down viewpoints comprehensively.

1 INTRODUCTION

In recent years, emissions of greenhouse gases such as carbon dioxide and methane have been implicated in the worldwide problem of global warming. One of the solutions being implemented to solve the problem is to increase the adoption of renewable energy (RE) to in turn reduce emissions of greenhouse gases. However, the cost of RE production is high. Governments have introduced various policies for promoting RE technologies. In particular, feed-in tariff (FIT) and renewable portfolio standard (RPS) have been introduced in various countries. FIT is a scheme that requires non-renewable energy (NRE) producers to purchase RE at fixed FIT prices. RPS requires that a certain percentage of NRE producers' electric generation capacity come from RE. RE producers issue and sell renewable energy certificates (REC) to NRE producers in REC markets to comply with the RPS requirement percentage.

There have been few studies discussing whether FIT or RPS is preferable from the aspect of social welfare. (Hibiki and Kurakawa, 2013) explored how FIT and RPS affect social welfare in the case of only one NRE producer and one RE producer in an electricity market by theoretical analysis. Their findings indicated that governments should introduce RPS when marginal damage cost is relatively high. They did not evaluate the effect of the number of NRE and RE producers or market structure. (Siddiqui et al., 2016) studied how RPS requirement percentage and market structure affect social welfare under RPS. They determined the optimal RPS requirement percentage and suggested the importance of considering market structure for setting the optimal RPS requirement percentage to maximize social welfare. (Nishino and Kikkawa, 2013) studied the interdependent effects of multiple energy policies by theoretical analysis and multi-agent simulation. However, they did not discuss the results from the aspect of social welfare.

Our purpose is to clarify how the relationships among policy, market power, and number of producers impact social welfare. In this work, multi-agent simulations of FIT and RPS are conducted for integrative analysis and rational design of renewable energy policies. Multi-agent simulations enable us to evaluate more realistic market and to observe emergent processes of equilibrium states. By comparing the results obtained from the simulation and the equilibrium analysis, we comprehensively examine the policies from both bottom-up and top-down viewpoints.

2 METHODS

For simplicity, in this manuscript, we show the case of only one NRE producer and one RE producer in an electricity market.

2.1 Equilibrium Analysis

The single-level model for determining maximum social welfare is called Central planning (CP). In CP, a

Suzuki, M., Ito, M. and Takashima, R.
Comparison of Theoretical and Simulation Analysis of Electricity Market for Integrative Evaluation of Renewable Energy Policy.
In *Proceedings of the 6th International Conference on Operations Research and Enterprise Systems (ICORES 2017)*, pages 455-459
ISBN: 978-989-758-218-9

central planner decides all power plants' capacity so as to maximize social welfare. Markets with FIT or RPS are analyzed within the bi-level model. At the lower level, NRE and RE producers decide generation capacity to maximize their own profits. At the upper level, policymaker decides the optimal FIT price or RPS requirement percentage to maximize social welfare.

2.1.1 Central Planning

Social welfare SW is defined and maximized as follows:

$$\begin{aligned} SW \equiv\ & A(q_n+q_r)-\frac{1}{2}Z(q_n+q_r)^2 \\ & -C_n(q_n)-C_r(q_r)-D_n(q_n), \end{aligned} \tag{1}$$

$$\begin{aligned} \max_{q_n\geq 0, q_r\geq 0}\ & A(q_n+q_r)-\frac{1}{2}Z(q_n+q_r)^2 \\ & -C_n(q_n)-C_r(q_r)-D_n(q_n) \end{aligned} \tag{2}$$

where electricity price p shows linear inverse demand function (i.e., $p = A - Z(q_n + q_r)$) (in US dollars (USD)), A is the intercept of linear inverse demand function, Z is the slope of linear inverse demand function, q_n is NRE production (in MWh), and q_r is RE production (in MWh). The third, fourth and fifth terms in Eq.(1) are cost functions. Here, $C_n(q_n) = \frac{1}{2}c_n q_n^2$ is the cost function for NRE production, $C_r(q_r) = \frac{1}{2}c_r q_r^2$ is the cost function for RE production, $D_n(q_n) = \frac{1}{2}kq_n^2$ is the damage cost function for NRE production, and $c_n, c_r, k > 0$ are constants (in USD/MWh^2). The optimal solution of CP is obtained by solving Eq.(2) and is as follows:

$$\bar{q}_n = \frac{Ac_r}{c_r(Z+c_n+k)+Z(c_n+k)} \tag{3}$$

$$\bar{q}_r = \frac{A(c_n+k)}{c_r(Z+c_n+k)+Z(c_n+k)} \tag{4}$$

$$\bar{p} = \frac{A\{c_r(Z+c_n+k)+Z(c_n+k)\}-ZA\{(c_n+k)+c_r\}}{c_r(Z+c_n+k)+Z(c_n+k)} \tag{5}$$

$$\bar{\alpha} = \frac{c_n+k}{c_n+k+c_r} \tag{6}$$

where $\bar{q}_n$ and $\bar{q}_r$ are optimal NRE and RE production, respectively, $\bar{p}$ is optimal electricity price, and $\bar{\alpha}$ is optimal proportion of RE.

2.1.2 FIT

At the lower level, we now consider payoff functions for the NRE producer and RE producer:

$$\pi_n = p(q_n+q_r)-C_n(q_n)-p^{FIT}q_r \tag{7}$$

$$\pi_r = p^{FIT}q_r - C_r(q_r) \tag{8}$$

where p^{FIT} is FIT price. When the NRE producer is dominant and behaves *à la* Cournot, optimal solution is as follows:

$$\tilde{q}_n = \frac{Ac_r-2Zp^{FIT}}{c_r(2Z+c_n)} \tag{9}$$

$$\tilde{q}_r = \frac{p^{FIT}}{c_r} \tag{10}$$

$$\tilde{p} = \frac{Ac_r(Z+c_n)-Zc_np^{FIT}}{c_r(2Z+c_n)} \tag{11}$$

$$\tilde{\alpha} = \frac{(2Z+c_n)p^{FIT}}{Ac_r+c_np^{FIT}} \tag{12}$$

At the upper level, we maximize social welfare about p^{FIT}:

$$\begin{aligned} \max_{p^{FIT}}\ & A(\tilde{q}_n+\tilde{q}_r)-\frac{1}{2}Z(\tilde{q}_n+\tilde{q}_r)^2 \\ & -C_n(\tilde{q}_n)-C_r(\tilde{q}_r)-D_n(\tilde{q}_n) \end{aligned} \tag{13}$$

As a result, we obtain the following optimal FIT price $\tilde{p}^{FIT}$:

$$\tilde{p}^{FIT} = \frac{Ac_r(3c_nZ+2Zk+c_n^2)}{4Z^2(k+c_n)+c_n^2Z+c_r(2Z+c_n)^2} \tag{14}$$

2.1.3 RPS

At the lower level, we now consider payoff functions for the NRE producer and RE producer:

$$\pi_n = pq_n - C_n(q_n) - \alpha p^{REC}q_n \tag{15}$$

$$\pi_r = pq_r - C_r(q_r) + (1-\alpha)p^{REC}q_r \tag{16}$$

where p^{REC} is REC price, α is RPS requirement percentage. When the NRE producer is dominant and behaves *à la* Cournot, optimal solution is as follows:

$$q_n^* = \frac{A(1-\alpha)}{(2Z+c_n+c_r)\alpha^2-2(Z+c_n)\alpha+(2Z+c_n)} \tag{17}$$

$$q_r^* = \frac{A\alpha}{(2Z+c_n+c_r)\alpha^2-2(Z+c_n)\alpha+(2Z+c_n)} \tag{18}$$

$$p^* = \frac{A\{(2Z+c_n+c_r)\alpha^2-2(Z+c_n)\alpha+(Z+c_n)\}}{(2Z+c_n+c_r)\alpha^2-2(Z+c_n)\alpha+(2Z+c_n)} \tag{19}$$

$$p^{*\,REC} = \frac{A\{(2Z+c_n+c_r)\alpha-(Z+c_n)\}}{(2Z+c_n+c_r)\alpha^2-2(Z+c_n)\alpha+(2Z+c_n)} \tag{20}$$

At the upper level, we maximize social welfare about α:

$$\begin{aligned} \max_{\alpha}\ & A(q_n^*+q_r^*)-\frac{1}{2}Z(q_n^*+q_r^*)^2 \\ & -C_n(q_n^*)-C_r(q_r^*)-D_n(q_n^*) \end{aligned} \tag{21}$$

We solve the above equation numerically to find the optimal RPS requirement percentage α^*.

2.2 Multi-agent Simulation Analysis

In this work, the deregulated electricity market consists of NRE producer agents, RE producer agents and consumers expressed as the linear inverse demand function, and is modeled as the blind and single-price call auction with reference to (Nishino and Kikkawa, 2013). In this auction, each energy producer agent offers its asking price and production. All orders are aggregated into the market schedules of supply and demand, and their intersection determines a single, market-clearing price for all feasible quantities (Figure 1).

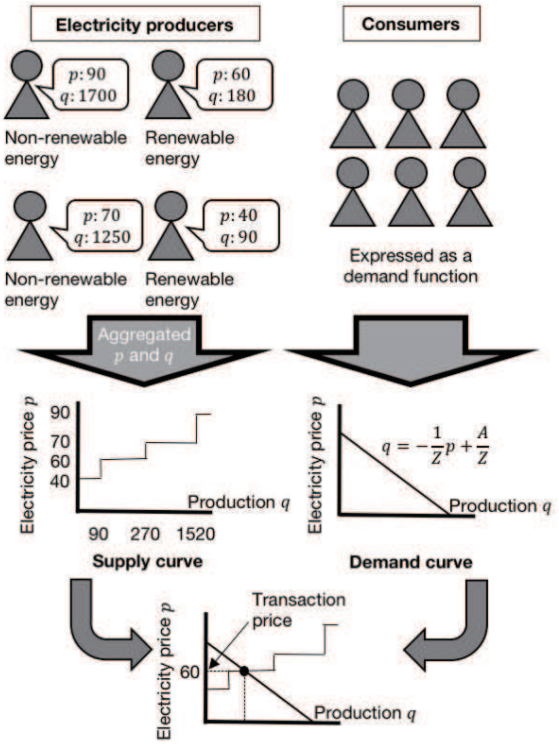

Figure 1: Trading mechanism of multi-agent simulation.

Each agent learns the optimal pricing strategies based on the Q-learning method (Watkins and Dayan, 1992) in order to maximize its profit. The Q-learning procedure used in this work is described below:

1. Decide action based on Q-value by softmax selection with Boltzmann distribution:

$$Prob(a|s) = \frac{\exp\{Q(s,a)/T\}}{\Sigma_{a'}\exp\{Q(s,a')/T\}} \tag{22}$$

where $s = s(p_n^{ask}, p_r^{ask})$ is the state of the market, p_n^{ask} and p_r^{ask} are the asking-price of NRE and RE producer agents respectively, $a \in \{p^{ask}+1, p^{ask} \pm 0, p^{ask}-1\}$ is the action of each producer agent, $Q(s,a)$ is Q-value, $T > 0$ is the "temperature".

2. Calculate the asking-quantity of production of each producer agent as the optimal response for each updated p^{ask}.
3. Decide transaction price and actual quantity of production of each producer agent.
4. Calculate profit of each producer agent and social welfare.
5. Update Q-value of each producer agent using the following equation:

$$\begin{aligned} Q(s_t,a) \leftarrow (1-\beta)Q(s_t,a) \\ +\beta\{r_t/100 + \gamma \max_a Q(s_{t+1},a)\} \end{aligned} \tag{23}$$

where s_t is the state at the t learning step, β is learning rate, $r_t \equiv (\pi_t - \pi_{t-1})$ is the reward of each producer agent at the t learning step, π_t is the profit of each producer agent at the t learning step, and γ is the discount rate.

6. End search if the maximum number of learning steps is reached.

We now consider a electricity market with no renewable energy policy and then obtain the following payoff functions:

$$\pi_n = pq_n - C_n(q_n) \tag{24}$$

$$\pi_r = pq_r - C_r(q_r) \tag{25}$$

Optimal asking-quantity of production q^{ask} for an asking-price p^{ask} is:

$$q_n^{ask} = \frac{p_n^{ask}}{c_n} \tag{26}$$

$$q_r^{ask} = \frac{p_r^{ask}}{c_r} \tag{27}$$

3 RESULTS AND DISCUSSION

We evaluate the effect of the renewable energy policy from the aspect of social welfare. Table 1 shows the evaluation conditions. The parameter values were set by reference to (Hibiki and Kurakawa, 2013) and (Nishino and Kikkawa, 2013).

Figure 2 shows learning history about pricing of each producer agent. Asking-prices of both producer agents converge to specific values. Consequently, transaction price, actual supply quantity of each producer agent and social welfare also converge to specific values (Figure 3 and Figure 4 (top)). Figure 4 (bottom) and Table 2 show comparison of social welfare, energy production, proportion of RE and electricity price between equilibrium analysis and multi-agent simulation. Compared with CP, FIT leads to

Table 1: Evaluation conditions.

	Parameter		Value	Unit
Demand	Intercept of inverse demand function	A	100	USD
	Slope of inverse demand function	Z	0.01	USD/MWh
Cost	Coefficient of NRE production cost	c_n	0.025	USD/MWh^2
	Coefficient of RE production cost	c_r	0.25	USD/MWh^2
	Coefficient of damage cost	k	0.025	USD/MWh^2
Q-learning	Maximum number of learning step	t_{max}	200,000	-
	Temperature	T_t	$50 \times (0.99995)^t$	-
	Learning rate	β	0.5	-
	Discount rate	γ	0.5	-

higher NRE production cost and damage cost while RPS leads to higher RE production cost. We can see that multi-agent simulation (MAS) with no renewable energy policy yields higher producer surplus, lower proportion of RE, higher damage cost, and as a result, social welfare indicates the smallest value.

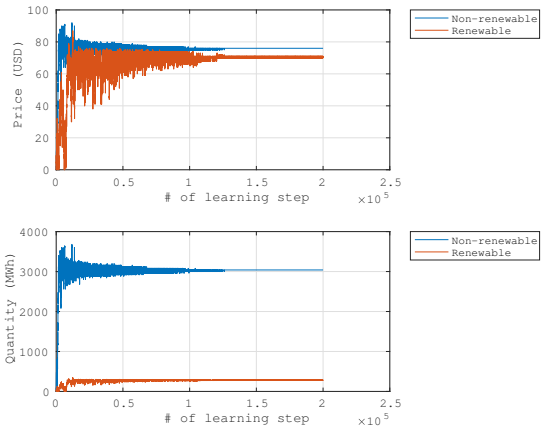

Figure 2: Asking electricity price (top) and quantity (bottom) of each producer agent.

4 CONCLUSIONS

We modeled the deregulated electricity market as the blind and single-price call auction, and constructed multi-agent system in order to clarify how the relationships among renewable energy policy, market power, and number of producers impact social welfare. Under the conditions of this evaluation, RPS achieved superior social welfare value to FIT and MAS (with no renewable energy policy). Additional numerical experiments and assessments of the market dynamics that specifically take into account realistic diversity of agents' characteristics and various uncertainties are important topics for future research.

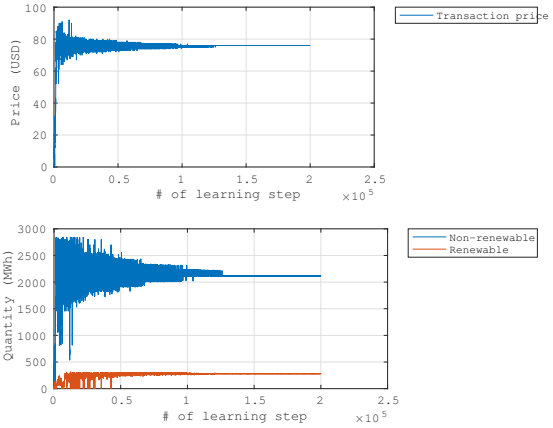

Figure 3: Transaction price (top) and actual supply quantity of each producer agent (bottom).

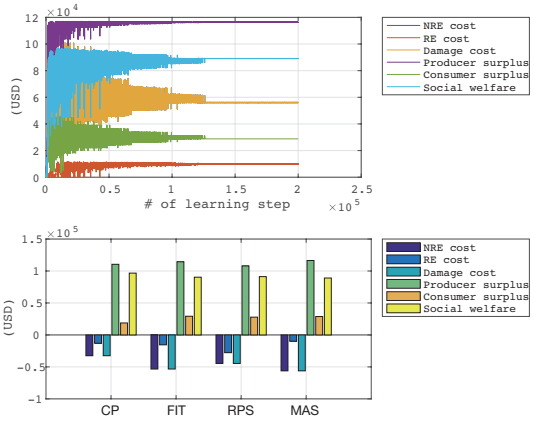

Figure 4: Breakdown of social welfare: (top) Convergence history of multi-agent simulation, (bottom) Comparison between equilibrium analysis and multi-agent simulation.

ACKNOWLEDGEMENTS

This work was supported by JSPS KAKENHI Grant Numbers JP15H02975, JP16H07226.

Table 2: Comparison between equilibrium analysis and multi-agent simulation.

	CP	FIT	RPS	MAS
NRE production cost (USD)	-32,522	-53,354	-44,557	-56,180
RE production cost (USD)	-13,041	-15,488	-27,730	-9,800
Damage cost (USD)	-32,522	-53,354	-44,557	-56,180
Producer surplus (USD)	110,478	114,442	107,941	116,420
Consumer surplus (USD)	18,740	29,234	27,824	28,800
Social welfare (USD)	96,697	90,321	91,208	89,040
NRE production (MWh)	1,613	2,066	1,888	2,120
RE production (MWh)	323	352	471	280
Total production (MWh)	1,936	2,418	2,359	2,400
Proportion of RE (-)	0.17	0.15	0.20	0.12
Electricity price (USD/MWh)	80.6	75.8	76.4	76

REFERENCES

Hibiki, A. and Kurakawa, Y. (2013). Which is a better second best policy, the feed-in tariff scheme or the renewable portfolio standard scheme? *RIETI Discussion Paper*, 13-J-070.

Nishino, N. and Kikkawa, A. (2013). A study about effects on multiple renewable energy policies using multiagent simulation. *IEICE Transactions on Information and Systems*, J96-D(12):2888–2899.

Siddiqui, A., Tanaka, M., and Chen, Y. (2016). Are targets for renewable portfolio standards too low? the impact of market structure on energy policy. *European Journal of Operational Research*, 250(1):328–341.

Watkins, C. and Dayan, P. (1992). Technical note: Q-learning. *Machine Learning*, 8:279–292.

Optimizing Supply Chain Management in Coal Power Generation

Muhamad Iqbal Felani, Ariyana Dwiputra Nugraha and Mujammil Rahmanta
PT PLN (Persero) Research Institute, Duren Tiga Street 102, Jakarta, Indonesia
iqbal.felani@hotmail.com, {ariyana.dp, jammilrahman}@gmail.com

Keywords: Supply Chain Management, Optimization, Simulation, Coal Power Generation.

Abstract: Indonesian government launched Fast Track Program Phase-1 in 2009 to increase national electricity ratio by installing 35 coal power generations with total capacity 10,000 Mega Watt. However only 25 coal power generations had been installed by now, spread all over Indonesia. Coal necessities were supplied by 14 domestic coal mining companies. There are two factors that affect the price of coal i.e : distance and unit price. Distance between supplier and coal power generation would determine the transportation cost while unit price would determine the price of procurement. The aim of this research is to minimize total price of coal by optimizing the distance and unit price (USD/Ton), allocating the coal necessities and scheduling the delivery. The optimization would be simulated using software What'sBest. By this simulation, 24 power plants were suggested to change their existing suppliers, while only one power plant was fitted. This change could reduce USD 27 Million/year for total price of coal.

1 INTRODUCTION

One of the important factor in increasing the national economic development is the availability of low cost energy (Wang, Feng and Tverberg, 2013). Therefore every country tries to minimize the fuel cost in electricity supply. As a development country, Indonesia is in progress to install coal fire power plants with lower cost. The coal power plants spread all over the country, while coal suppliers are concentrated in particular island. The price of coal consists of two factors: transportation cost (USD/nautical mile) and unit price (USD/ton). So the transportation factor will dominate the cost of coal procurement since Indonesia is an archipelago country (PT PLN (Persero) Coal Procurement Division, 2013).

Figure 1: Map of Coal Power Plant and Coal Supplier Spread in Indonesia.

Every power plant requires a specific coal that must be supplied by appropriate supplier. In consequence of this problem, the utility should arrange the best supply chain management to minimize the cost. In case utility could minimize the distance between power plant and appropriate supplier, the cost would be minimal.

There are 25 power plants with specific coal requirement and 14 coal supplier that would be optimized in this paper. The purpose of this paper is to optimize supply chain management by minimizing the distance between power plant and appropriate supplier and ensure that production capacity of supplier could serve the power plant as long as contract duration. Software What'sBest is used to simulate this problem. The results of the simulation are the demand – supply mapping, allocating the coal requirement and scheduling of shipping.

2 METHOD

This paper simulated the coal supply chain management planning according to the real condition. The simulation would be processed by What'sBest software. The first step in this research was data collection. Data used in this simulation;

- Information about coal power plant as a demand, involving the name of Power Plant, the location,

Felani, M., Nugraha, A. and Rahmanta, M.
Optimizing Supply Chain Management in Coal Power Generation.
In *Proceedings of the 6th International Conference on Operations Research and Enterprise Systems (ICORES 2017)*, pages 460-463
ISBN: 978-989-758-218-9

the quantity of coal demand, the quality requirement of power plant, safety stock level, and jetty capacity.

- Information about coal supplier, involving the name of supplier, the quality of coal, unit price (USD/ton), transportation cost (USD/Nautical miles), productivity (ton/year), contract duration and ship capacity.
- Information about ocean condition in Indonesia yearly, involving the height of wave, the velocity and direction of wind (Fig.2).
- Distance and lead time between supplier and demand. The distance is determined by Geographic Information System (GIS) Directorate General of Marine Transportation, The Indonesian Ministry of Transportation. Therefore the distance is not straight line, but following the cruise lane (fig.3).

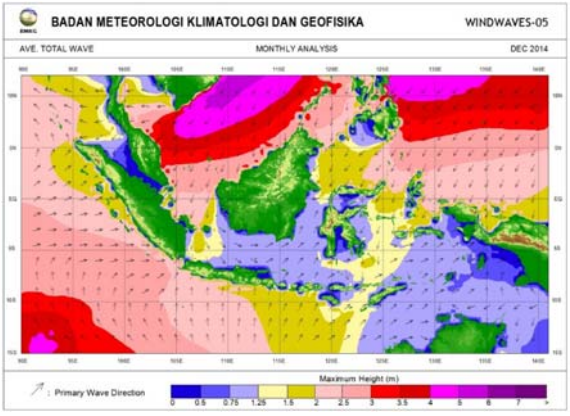

Figure 2: Wind and Wave Ocean Condition in Indonesian.

Based on Fig.2 above, the information is converted in binary number. Number 1 means a high wave that affect the ship velocity, and number 0 means normal condition that not affect the ship velocity.

Figure 3: Wind and Wave Ocean Condition in Indonesian.

The velocity of ship in Fig.2 and the distance between supplier and demand in Fig. 3 results in determining lead time.

All of data above were processed into a database. The next steps were allocating the coal necessity and scheduling. The steps in simulation process could be seen in Fig.4 as follow:

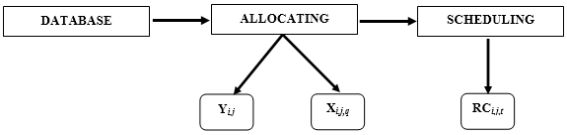

Figure 4: Steps of Simulation Process.

Some decisive variables must be considered when allocating the coal demand. These variables are presented by mathematical equation;

- Supplier i only could send coal q to the power plant j as if coal q has the same specification with power plant requirement. In other word, the caloric value of the coal from supplier must be appropriate with caloric value required by power plant. This decisive variable is *capable or not*, noted by $Y_{i,j}$.
- Coal q ϵ Q was supplied by supplier i ϵ I to power plant j ϵ J. This decisive variable is the amount of each type of coal which is delivered by supplier, noted by $X_{i,j,q}$.

The purpose of this allocation is to minimize total cost (*f*) of coal. There were 2 main components contributing in total cost; procurement cost (f_1) and transportation cost (f_2). Therefore this function can be determined as follows:

$$\text{Minimize } f = f1 + f2 \tag{1}$$

Procurement cost is multiplication between unit price ($P_{i,q}$)of coal *q* to supplier *i* with total amount ($X_{i,j,q}$) of coal *q* that is delivered by supplier *i* to power plant *j*. Therefore the formula of procurement cost (f_1) can be determined by:

$$f_1 = \sum_{i \in I} \sum_{j \in J} \sum_{q \in J} X_{i,j,q} \; P_{i,q} \tag{2}$$

While transportation cost is multiplication between transportation cost ($TC_{i,j}$) from supplier *i* to power plant *j* with total amount (Xi,j,q) of coal *q* that is delivered by supplier *i* to power plant *j* with distance (R_{ij}) from supplier *i* to power plant *j*. Therefore the formula of transportation cost (f_2) can be determined by:

$$F_2 = \sum_{q \in Q} \sum_{i \in I} \sum_{j \in J} X_{i,j,q} \; TC_{i,j} \; R_{i,j} \tag{3}$$

To achieve the optimal function above, then allocation model must comply with these limitation:

1. Maximum amount ($X_{i,j,q}$) of coal *q* that could be procured by power plant *j* is limited by

maximum capacity ($O_{i,q}$) of coal q which is available in supplier i comply with contract document between supplier and utility, this limitation could be formulated as:

$$\sum_{j \in J} X_{i,j,q} \leq O_{i,q} \quad \forall i \in I, j \in J, q \in Q \qquad (4)$$

2. Every power plant has its typical caloric value of coal. Delivery of coal could be processed as if caloric value of coal in supplier comply with power plant's caloric value. The coal which has caloric value beyond the range could be processed. This limitation could be formulated as:

$$Y_{ij} = \begin{cases} Y_{ij} = 1, & \text{if } CV_q \in [CV_{min}, CV_{max}] \\ Y_{ij} = 0, & \text{otherwise} \end{cases} \quad \forall i \in I, j \in J, q \in Q \qquad (5)$$

3. The coal q from supplier must be able to fulfil the demand (D_j) every power plant $_j$. This limitation could be formulated as:

$$\sum_{i \in I} X_{i,j,q} \geq D_{j,q} \quad \forall j \in J, q \in Q \qquad (6)$$

The final step of the simulation is *scheduling*, which time of delivery of coal would be determined. The limitation in scheduling is that power plant j only could receive of coal from supplier i once a day (t). This limitation can be formulated as $RC_{i,j,q,t}$

3 RESULT

The simulation gave a result that from total 25 existing power plant, there are 24 power plants should change their supplier due to cost optimizing. This simulation also gave the optimal amount of coal that should be procured by power plant, it calls optimal allocation. Therefore all of power plants could make a coal procurement plan effectively. The next step is scheduling. All of the limitations of allocating and scheduling are conducted by What'sBest software. The scheduling covers all information about when supplier must deliver their coal to power plant, how much coal that must be delivered to the power plant, when the coal would be received by power plant considering the ocean condition and how much coal that available in power plant inventory as consequence of lead time variance. The example of scheduling table could be seen in Table 1.

From Table 1 above could be seen that power plant "A" would be supplied by supplier "1" as much as 7,500 ton in September 24th (purple cell) and would be received by power plant "A" in September 29th (yellow cell). Safety stock level in power plant "A" in September 24th is 54,080 ton (orange cell). This safety stock level would be maintained in 25 operating days. Lead time is presented as green and blue cell. Green cell is for normal condition (weather) while the blue one is for bad condition (weather).

4 DISCUSSION

Total cost (procurement cost and transportation cost) before simulation and after simulation was compared to evaluate it significance. Transportation cost before simulation was not available due to poor of information. There was no data about the amount of coal that is delivered by supplier to power plant. While total cost after simulation is determined by model. The comparison before and after simulation could be seen in Table 2.

The Table 2 above informed that after simulation procurement cost decreased as much as 24,110,173.53 USD per year. In case it is assumed that amount of coal that is delivered by supplier to power plant before simulation is equal to after simulation, then it definitely results that transportation cost after simulation is less than before simulation. In other word we could say that there is a benefit after simulation.

Table 1: The Example of Scheduling.

Power Plant	Supplier	Total of coal	Ship capacity	Initial Capacity	September						
		Normal*	Bad*		24	25	26	27	28	29	30
A	Level Inventory			51,750	54,080	51,990	57,420	55,350	57,420	58,710	56,640
	1	755,550	7,500	Received	0	0	7500	0	0	7500	0
	Lead Time	5	6	Order	7500				7500		
B	Level Inventory			47,040	48,652	47,771	50,889	49,008	50,889	50,244	48,363
	2	552,151	5,000	Received			5,000	0	0	5,000	0
	Lead Time	16	24	Order			5,000		5,000		
	3	134,632	7,500	Received			0	0	0	0	0
	Lead Time	2	2	Order							

Table 2: The Comparison of Total Cost.

Cost Component	Before Simulation (USD)	After Simulation (USD)	Benefit (USD)
Procurement Cost	897,183,961	873,073,787.5	24,110,173.5
Transportation Cost	Not Available	363,454,502.5	Not Available
Total Cost	**897,183,961 + NA**	**1,236,528,290**	

Last year, Indonesian government launched instalment of power generation program with total capacity 35,000 Mega Watt (MW). This program will be completed in 2019. Majority of them are coal fired power plant. The most critical problem in coal power generation is the reliability of coal supply. It will need a huge demand of coal in 2019. Therefore local coal suppliers need to be mapped. Then scheduling each power generation will be arranged and optimized. The method in this research is being used to solve the problem.

5 CONCLUSIONS

The research proved that the model simulation could optimize total cost of coal demand in power plant. There are 24 of 25 existing power plant that should change their allocating and scheduling planning to increase cost effective. By optimizing supply chain management it could reduce total cost at least 24,110,173.53 USD per year. The method in this research is being used to ensure the reliability of coal supply to support government's program; Instalment of 35,000 MW power generation.

ACKNOWLEDGEMENTS

The author thanks the PT PLN (Persero) Research Institute for the chance and support. The author also thanks to PT PLN (Persero) Head Quarter Division of Coal Procurement for valuable data and direction. Thanks to Indonesian Coal Fire Power Plant for group discussion, data and valuable supports during this research.

REFERENCES

Moore, R., Lopes, J., 1999. Paper templates. In *TEMPLATE'06, 1st International Conference on Template Production*. SCITEPRESS.

Smith, J., 1998. *The book*, The publishing company. London, 2nd edition.

J. Wang, L. Feng, and G. E. Tverberg, 2013. *An analysis of China's coal supply and its impact on China's future economic growth,*. Energy Policy, vol. 57, pp. 542–551,

PT PLN (Persero) Head Quarter Division of Coal Procurement*,2013. Supply and Demand Coal Data*, Jakarta.

Indonesian Agency for Meteorology, Climatology and Geophysics, 2014. *Indonesian Monthly Ocean Condition,* Jakarta..

Indonesian Ministry of Transportation, 2015. *Geography Information System, Jakarta.*

Chat Based Contact Center Modeling
System Modeling, Parameter Estimation and Missing Data Sampling

Per Enqvist[1] and Göran Svensson[1,2]
[1]*Division of Optimization and Systems Theory, Kungliga Tekniska Högskolan, Lindstedtsv 25, Stockholm, Sweden*
[2]*Teleopti WFM, Teleopti AB, Stockholm, Sweden*
{*penqvist, goransv*}*@kth.se*

Keywords: Queueing, Chat, Chat-based Queueing Systems, Parameter Estimation, Gibbs Sampling.

Abstract: A Markovian system model for a contact center chat function is considered and partially validated. A hypothesis test on real chat data shows that it is reasonable to model the arrival process as a Poisson process. The arrival rate can be estimated using Maximum likelihood. The service process is more involved and the estimation of the service rate depends on the number of simultaneous chats handled by an agent. The estimation is made more difficult by the low level of detail in the given data-sets. A missing data approach with Gibbs sampling is used to obtain estimates for the service rates. Finally, we try to capture the generalized behaviour of the service-process and propose to use generalized functions to describe it when little information is available about the system at hand.

1 INTRODUCTION

Contact centers usually offer several types of media to enable customer communication. Chat functionality is one such type of media that in recent years has grown in popularity. This stresses the importance of good modeling and parameter estimations for chat based systems.

In this paper a Markovian chat system model is considered (Enqvist and Svensson, 2017). The chat system is viewed as a queue-based state-space model, akin to traditional queueing systems of inbound telephone call centers, described in detail elsewhere such as in (Koole, 2013; Gans et al., 2003; Aksin et al., 2007). However, chat systems behave slightly different than traditional telephone queues in that an agent can work with several customers simultaneously. We make the assumption that the number of customers an agent is serving effects the service rate with which the service is provided. A queueing based state-space model should capture both how many customers each agent is currently serving and how many customers there are in the system in total, as well as the varying service rates.

The main goals of this paper are to argue that such a queueing-based state-space model is reasonable, to support such a model by use of real world data and to propose methods for estimating the rate parameters for a chat system from real but incomplete data-sets.

The quality and level of detail of the underlying data can severely limit the choice of methods and the uncertainty of estimates. When there exist limitations on available data it may be necessary to rely more on prior information and thus we propose that general parameterized functions are used to lower the variance of the estimates by including empirical information about chat systems general behaviour.

Due to the strong dependence on data we propose a data classification structure that pertains to chat systems. The classification of underlying data would indicate which technique is appropriate. The accuracy and choice of any, realistic, model will be data dependent. For a statistical analysis of a call center see (Brown et al., 2005).

It is natural to divide the problem into two parts, one part for the arrival rate process and one for the service rate process. The former lends itself to standard methods of estimation when the level of detail of the underlying data is good enough. While the latter often leads to complications due to data on aggregated or mean value form, *i.e.*, low level of detail.

We show that it is reasonable to describe the arrival process in terms of a homogeneous Poisson process on 15-minute or 30-minute intervals. We support this position by χ^2-square hypothesis testing at five percent significance level on two data-sets. For more on nonhomogeneous arrival processes we refer to (Green and Kolesar, 1991) and (Whitt, 2007).

Enqvist, P. and Svensson, G.
Chat Based Contact Center Modeling - System Modeling, Parameter Estimation and Missing Data Sampling.
In *Proceedings of the 6th International Conference on Operations Research and Enterprise Systems (ICORES 2017)*, pages 464-469
ISBN: 978-989-758-218-9

When estimating at the service rate process the situation gets more complicated. One possible cause of complications occur if the start and finish times of chat dialogues are not recorded. In our data-sets only the number of initiated chats per agent and interval is available. Since an agent can serve several customers in parallel we make the assumption that the service per customer is a non-increasing function in the number of currently served customers. In (Bekker et al., 2004) the authors explore varying service levels and in (Bekker et al., 2011) adapting service rates are investigated. In computer systems processor sharing is a common phenomena, see (Cohen, 1979). Our model is inspired by both the previous situations, where an agent has capacity to perform simultaneous tasks but at varying rates. A further complication is due to data often only being available on an aggregated level. Thus it is not possible to discern the actual (pointwise) workload distribution for the interval. We suggest a missing data approach, via the expectation maximation algorithm and Gibbs sampling, to handle this problem.

There might also exist general information about the system, such as how likely it is that there are customers waiting in the queue and the arrival rate from a previous estimation. One might also include data from other chat systems and assume that there are similarities. Hence we propose to model service rate per customer as a continuous non-increasing function, depending on the state of the chat system and the specific agent. Such a function can provide answers about the maximum allowed chats in parallel to fullfill some quality of service goal, like maximizing throughput through the system or to support staffing decisions.

In Section 2, data is discussed and the data-sets are presented. In Section 3, the proposed queueing-based state-space model is introduced and parametrized. The parameters to be estimated are also stated. In Section 4, the estimation models for the arrival process is explained and the hypothesis testing is show for specific data-sets. Also the missing data approach for estimation of the service rates is presented.

2 DATA CHARACERISTICS

What can be achieved in terms of reliable estimates, in a contact center environment, is highly dependent on the amount and quality of the available data. Therefore, it makes sense to categorize data in terms of quality. We identify three major aspects that determine the overall quality and three subsets that are important for estimations in queueing systems, namely: 1. Number of data records, 2. The level of detail, 3. Relevant data-sets. The data-sets can be split into general system, agent specific and customer specific data.

The number of data records is an important factor in determining the level of accuracy of estimates. The level of detail determines how easily one can perform estimations. Furthermore, in the context of queueing systems, it is meaningful to differentiate between three types of data-subsets. The first set concerns data on a system level, such as offered load per interval. The second subset pertains to agent specific data, data like agent-id and number of initiated chat dialogues per interval. The third subset of data records contain information on individual customers, such as customer-id, arrival time to the system and waiting time in queue.

In cases where there are few data records, low detail level or when not all three subcategories are available leads to uncertainty in the estimations. This type of uncertainty has to be managed, which motivates why we need methods to provide reliable estimates in the face of poor data quality.

The given data-sets, on which this paper is based, come in two subsets, where the first subset contain general queue data and the second contain agent specific data. Thus customer specific data is missing in all cases. The data deemed useful in the context of this paper is presented, while other data posts not deemed to influence the procedings is supressed.

After discussing the matter with responsible data base administrators it is found that the data is not completely machine generated and thus may contain errors due to human factors. This type of problem requires serious attention but for the purposes of this text it is ignored apart from some pre-processing with respect to outliers and records with low information content.

2.1 General Queue Related Data

In the first type of data subset the important data posts are the ones representing date, intraday intervals and offered load. The data is given per date and per interval, thus we introduce $d \in \mathcal{D} = \{1,\dots,D\}$ indexing the days, $i \in \mathfrak{I} = \{1,\dots,I\}$ indexing the intraday intervals and $w_d \in \{1,\dots,W\}$ index the day of the week, where $W = 7$. Let $N_{d,i} \in \mathbb{N}$ represent the number of arrivals on day d in interval i, *i.e.*, offered load. The notation was inspired by (Gans et al., 2009).

2.2 Agent Specific Data

In the second type of data subset the important data posts are the ones representing date, intraday interval, agent identity, number of initialized chats and aggregated time spent with open chat dialogues. The time spent chatting is the sum of all chat dialogues, thus the total time can be greater than the length of the corresponding interval.

2.3 Customer Specific Data

Many contact centers neglect to record customer specific data, such as arrival time, time waiting, time in service, service provided by agent-id, time of abandonment, etc. When such level of detail exists it is straight forward to estimate service rates and related parameters. The customer specific data-sets are missing for the chat systems investigated in this paper.

2.4 Given Data-Sets

Information of given data-sets. The size is measured as the raw data text file size.

Table 1: Given data-sets.

Data-set	Syst. data	Ag. data	Size
TA: queue	yes	no	5.3 MB
TA: agent	no	yes	49.7 MB
TC: queue1	yes	no	3.5 MB
TC: queue2	yes	no	2.3 MB
TC: agent	no	yes	8.4 MB

Where TA is a large travel agent company and TC is a large telecom company. Syst. data is short for System data and Ag. data is short for Agent data.

3 STATE-SPACE QUEUEING MODEL DESCRIPTION

The queue-based system considered here is approximated by a Markovian state-space model that is described in detail in (Enqvist and Svensson, 2017). The states represent the total number of customers in the system, the number of agents working during that interval and also contains information about the number of customers that each agent is currently serving, possibly up to some maximum number. We refer to (Asmussen, 2003) for queueing theory in general.

State transition rates are determined by new arrivals and completed service sessions. New arrivals are either placed in a common queue or start recieving service from an available agent according to a routing rule.

Completed services depend on the number of agents, the number of customers in parallel that each agent is serving and the corresponding service rates according to a generalized processor sharing model, as in (Cohen, 1979), for each agent.

An example, of a chat queue with one agent and a maximum of three jobs in parallel, is shown in Figure 1. The lower chart shows the jobs as they are seen by the agent. When a new job starts recieving service the number of customers waiting in line, if any, drops by one, as seen in the top figure. The example can be expanded to include more agents which, together with exponential service times and Poisson arrivals, quite naturally gives rise to a Markovian state-space model.

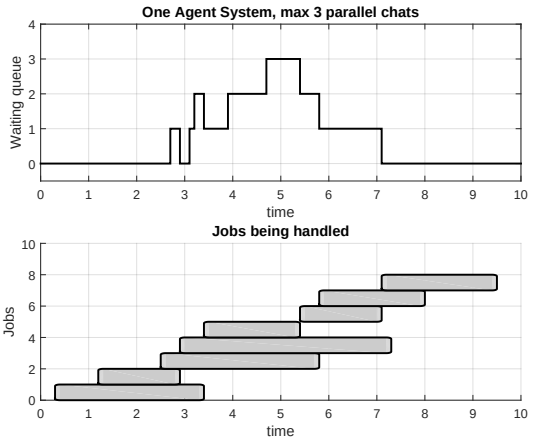

Figure 1: An example of a one agent chat queue. In the upper graph the number of customers currently waiting in queue is depicted. In the lower chart the different jobs are shown, from the time they start recieving service until they leave the system. The maximum number of customers that can be served in parallel, in this example, is three.

3.1 The Arrival Process

New customers enter the system according to an arrival process that is assumed to be Poisson with parameter $\lambda_{w_d,i}$, where w_d correspond to the day of the week and i to the interval. We assume that arrivals are independent and identically distributed. That this is a reasonable assumption is demonstrated in Section 4.1, as part of the model validation process.

Newly arrived customers either have to wait in line or are assigned an agent according to the routing rule. In this paper they are routed to the agent with the least number of customers in service. In the case that there are more than one agent serving the same, least number, of customers then random selection is used.

3.2 The Service Process

The service rates of the agents can be studied per agent, by groups of agents or by assuming all agents perform at the same rate of service. The two former situations require more data and can cause the underlying state-space to grow extremly large, hence in this paper we choose to treat all agents as equivalent. It might also be considered that agents provide the same kind of service during different intraday intervals or it may be assumed that the service rates vary depending on the interval. The latter case requires more data and may be impractical due to the need to solve many versions of the system.

The state of an agent will be taken as the number of currently served customers in parallel, possibly up to some maximum number.

Furthermore, we assume that the service times of the agents are exponentially distributed with rate parameters μ_j, where $j \in \{0,1,\ldots,m\}$ represents the number of currently served customers. These service rates are dependent on the state of the agent and represent the fact that an agent serving several customers simultaneously cannot devote the same type of attention to all of them as to a single customer.

The service times of the agents are assumed to be independent of each other and identically distributed, only depending on the number of customers in parallel. Here we assume that the different customers served by the same agent at the same time are independent.

In Section 4.2, we consider the estimation of the service rates of the agents.

4 PARAMETER ESTIMATION AND MODEL VALIDATION

This section will be divided into two major parts, the first account for the arrival process and the validity of the Poisson assumption and the second part considers the service process and the estimation of the service rates for the agents, subject to varying numbers of chats in parallel.

4.1 The Arrival Process

Data is given on the form of date, 15- or 30-minute interval and offered load, *i.e.*, number of arrivals $N_{d,i}$ per day and interval. We collect all data-points pertaining to each day of the week and intraday interval in a vector, denoted by $\tilde{a}_{w_d,i}$ of length $L_{w_d,i}$.

All the $\{\tilde{a}_{w_d,i}\}$:s are then pre-processed by removing outliers and entire vectors that contain too little information. Let $\{\bar{a}_{w_d,i}\}$ denote the resulting processed set of vectors, now containing only trusted data. Assuming that the arrivals are independent and identically distributed and specifying the likelihood function to be the joint function for all observations in the specified vector $\bar{a}_{w_d,i}$

$$\mathcal{L}(\lambda_{w_d,i};\bar{a}_{w_d,i}) = f(a_1^{w_d,i},\ldots,a_{L_{w_d,i}}^{w_d,i}|\lambda_{w_d,i}). \quad (1)$$

$L_{w_d,i}$ varies from vector to vector depending on the given data-set. Then a maximum likelihood estimation (MLE) of the Poisson parameter can be performed to obtain the corresponding arrival rate per interval and day of the week. The estimation is unbiased and given by the sample mean (Haight, 1967, Ch. 5)

$$\hat{\lambda}_{w_d,i} = \frac{1}{L_{w_d,i}} \sum_{l=1}^{L_{w_d,i}} a_l^{w_d,i}. \quad (2)$$

An example of estimated arrival rates for a chat system of a travel agency are shown in Figure 2. The actual arrival rates have been modified by request from the company, but the general behaviour is captured. It is shown for 30-minute intervals.

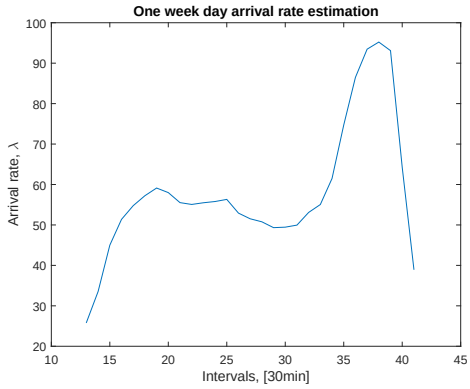

Figure 2: MLE of the arrival rates for one day of the week with half hour intervals. (Rates are modified by request from the company).

A common assumption for many queueing systems is that arrivals can be modeled by a homogeneous Poisson process. To show that this is plausible the data is tested via a Pearson χ^2-test, with test statistic given by

$$\chi^2 = \sum_{i=1}^{n} \frac{(O_i - E_i)^2}{E_i} \quad (3)$$

where n represents the maximum observation value category, O_i the number of observations of type i and E_i the expected number of observations of type i. The

null hypothesis, H_0, is defined to be that data is Poisson distributed with parameter $\hat{\lambda}_{w_d,i}$, and the test is performed at 5% significance level.

Examining the data-sets it is found that the assumed Poisson arrival rate is not rejected for the majority of the intervals and day of the week, results given in Table 2.

Table 2: Example showing the number of non-rejected and rejected H_0-hypothesises for two different pre-processings of the same 15-minute interval data-sets.

Data	Pre-process	Not rejected	Rejected
TA	Low	277	110
TA	High	260	52
TC2	Low	232	210
TC2	High	232	46

The intervals for which the Poisson assumption is rejected are mostly found in the beginning and at the end of the day. When the data is aggregated into half hour intervals the frequency of rejections decrease. In Table 2 it can be seen that the result is dependent on the pre-processing of the data, thus non-automated data processing was needed to obtain the results. Information to this end was supplied by the data-base administrators.

Considering the results we find it reasonable to model the arrivals as a Poisson process for the intents and purposes of this work, for a similar but detailed paper see (Brown et al., 2005)

4.2 The Service Process

The queue and service are modelled as a Markov process, where the service rates of each agent depends on the number of current clients. To decide if this model assumption is reasonable we would like to perform a hypothesis test. However, such a test could be performed in the full information case, where client data is available, but for the given data sets such a test is not easily performed.

To illustrate the difficulties arising from data on an aggregated format we introduce an example case as can be seen in Figure 3, were the cumulative arrivals and the cumulative number of answered chats is shown. Note that only the interval in which arrivals and answered chats occur is known.

Assuming that the model setup is suitable, we concentrate on the problem to estimate the various service intensities of the agents.

For the full data case the intensities can be estimated from information about the state transitions of the system, by using a MLE method. However, the given data-sets lack this level of detail and a direct MLE is not feasible.

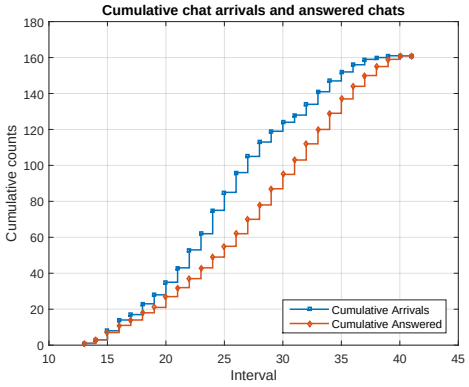

Figure 3: Example showing the cumulative number of arrivals and answered chats for a chat queue where data is aggregated per interval.

One approach is to try to estimate the missing data first and then apply the MLE approach. Consider one agent over a sequence of time windows $i = 1, \cdots, n$ in $\mathfrak{I}$. Let x_i denote the information about block i needed to determine the MLE, and let y_i denote the information about block i that is observable, *i.e.*, the information provided by the considered data set. Assume that θ contains all the unknown intensities μ_j. It would be very difficult, or even impossible, to determine a closed form expression for the probability of observing the provided data given the intensities θ, *i.e.*, for $\Pr_\theta(y_{1:n})$. Here, $y_{1:n}$ denotes the values of y_1 to y_n. Therefore, we propose to apply the expectation maximization (EM) algorithm (Moon, 1996) and (Dempster et al., 1977) to determine the estimate of θ. Starting from an initial guess θ_0 we want to determine

$$Q(\theta;\theta_0) = \mathbb{E}_{\theta_0}\left[\log \Pr_\theta(x_{1:n}, y_{1:n}) | y_{1:n}\right], \qquad (4)$$

for the expectation step of the EM algorithm. To take the expectation under θ_0 it is necessary to have $\Pr_{\theta_0}(x_{1:n}, y_{1:n})$. It can be determined using single site Gibbs sampling (Gelfand and Smith, 1990) where we should make use of the given observable data. Sequentially determine $\Pr_{\theta_0}(x_i | x_{1:i-1}, x_{i+1:n}, y_{1:n})$ for each $i = 1, \cdots, n$. If $y_{1:n}$ contains information about the number of arrivals and working time in the blocks it should be used to determine the probabilities. Thus we need the x_i:s to contain the missing information needed to determine the intensities. Let $x_i = \{d_i, B_1, \ldots, B_{d_i}, T_1, \ldots, T_{\ell_i}\}$, where d_i represents the number of finished chats in interval i, B_j are the inter-departure times, T_j the inter-arrival times and ℓ_i the number of new arrivals in interval i, which is observable. The maximum number of customers in block i is bounded by the number of customers at the beginning of the interval, N_i, and the number of arrivals during the interval ℓ_i. Let $z_i = \{x_{1:i-1}, x_{i+1:n}, y_{1:n}\}$, then the

conditional probabilities

$$\Pr(x_i|z_i) = \sum_{j=1}^{N_i+\ell_i} \Pr(x_1|z_i, d_i = j) \Pr(d_i = j|z_i), \quad (5)$$

can be determined. These correspond to all possible combinations of jumps in an interval.

The final piece is to use that we can observe the total chat time in interval i. This impose a linear equality constraint on the variables in x_i.

In the maximization step of the EM algorithm an updated estimate θ_1 is determined from

$$\theta_1 = \underset{\theta}{\operatorname{argmax}}\, Q(\theta; \theta_0). \quad (6)$$

This process is repeated until sufficient convergence has been achieved.

4.3 Proposed Service Rate Function

In order to reduce the number of parameters to estimate we propose that a parametric function representation of the service rate is used. This function class can be chosen to represent physical properties of the rate parameters. We propose the following function class.

$$f(\tilde{n}) = \begin{cases} 0, & \tilde{n} < 1 \\ \tilde{n}a\left(1 - \frac{1}{1+be^{c(d-\tilde{n})}}\right), & \tilde{n} \geq 1 \end{cases} \quad (7)$$

where $\tilde{n} \in \mathbb{R}$ is the continuous version of the number of customers per agent, and a, b, c and d are nonnegative model parameters. The function captures the desired shape but fitting the parameters from data is not trivial. With this representation we ensure that the service rate per customer is nonincreasing.

5 CONCLUSIONS

We have shown that it is reasonable to model the arrival process as a Poisson process via hypothesis testing. An approach for estimating the service rate parameters from observed data has been proposed.

Implementation and further validation of the model and estimation procedure is currently in process. Other further work would be to use an alternative Bayesian approach.

ACKNOWLEDGEMENTS

This work has been made possible by Teleopti AB, both financially and by providing data. Thanks go to T. Pavlenko, J. Olsson and F. Rios for valuable input.

REFERENCES

Aksin, Z., Armony, M., and Mehrotra, V. (2007). The modern call center a multi disciplinary perspective on operations management research. Production and Operations Management, Vol. 16, Issue 6.

Asmussen, S. (2003). *Applied Probability and Queues*. Springer-Verlag, New York, 2nd edition.

Bekker, R., Borst, S., Boxma, O., and *et al.* (2004). Queues with workload-dependent arrival and service rates.

Bekker, R., Koole, G., Nielsen, B., and *et al.* (2011). Queues with waiting time dependent service.

Brown, L., Gans, N., Mandelbaum, A., Sakov, A., Shen, H., Zeltyn, S., and Zhao, L. (2005). Statistical analysis of a telephone call center. *Journal of the American Statistical Association*, 100(469):36–50.

Cohen, J. W. (1979). The multiple phase service network with generalized processor sharing. *Acta Informatica*, 12(3):245–284.

Dempster, A. P., Laird, N. M., and Rubin, D. B. (1977). Maximum likelihood from incomplete data via the EM algorithm. *Journal of the royal statistical society. Series B (methodological)*, pages 1–38.

Enqvist, P. and Svensson, G. (2017). Chat based queueing systems with varying service rates and simultaneous jobs. To be submitted.

Gans, N., Koole, G., and Mandelbaum, A. (2003). Telephone call centers: Tutorial, review, and research prospects. *Manufacturing & Service Operations Management*, 5(2):79–141.

Gans, N., Shen, H., Zhou, Y.-P., Korolev, K., McCord, A., and Ristock, H. (2009). Parametric stochastic programming models for call-center workforce scheduling. *Technical report*.

Gelfand, A. E. and Smith, A. F. (1990). Sampling-based approaches to calculating marginal densities. *Journal of the American statistical association*, 85(410):398–409.

Green, L. and Kolesar, P. (1991). The pointwise stationary approximation for queues with nonstationary arrivals. Management Science, 1991, Vol.37(1).

Haight, F. (1967). *Handbook of the Poisson distribution*. Publications in operations research. Wiley.

Koole, G. (2013). *Call Center Optimization*. MG Books, Amsterdam, 1st edition.

Moon, T. K. (1996). The expectation-maximization algorithm. *IEEE Signal Proc. Magazine*, 13(6):47–60.

Whitt, W. (2007). What you should know about queueing models to set staffing requirements in service systems. Naval Research Logistics, Volume 54, Issue 5.

Parallel-machine Scheduling with Precedence Constraints and Controllable Job-processing Times

Kailiang Xu[1], Rong Fei[2] and Gang Zheng[1]
[1]*School of Automation and Information Engineering, Xi'an University of Technology, Xi'an, Shaanxi, China*
[2]*School of Computer Science Engineering, Xi'an University of Technology, Xi'an, Shaanxi, China*
{*klxu, annyfei, zhenggang*}*@xaut.edu.cn*

Keywords: Parallel-machine, Precedence Constraint, Controllable Processing Time, Tabu-search.

Abstract: A parallel-machine scheduling problem with tree-formed precedence constraints is studied, where job-processing times can be compressed by allocating extra resource to the jobs. A tabu-search algorithm is developed in this paper, which searches for the near optimal solutions based on the structural characteristics of the problem. Experiment shows the algorithm is capable for providing satisfactory schedules for media and large-sized problems within acceptable computing time.

1 INTRODUCTION

This paper concerns on a parallel-machine scheduling problem with tree-formed precedence constraints, where job-processing times can be compressed by the consumption of extra resources, such as gas, fuel, electricity power, cash and labors. Vickson(Vickson, 1980) was one of the first researchers to consider the scheduling problems with controllable job-processing times. Motivated by his research work, a number of researchers focused their attention on scheduling problems with controllable job-processing times after 1980, and have achieved significant result (for example, Cheng et al.(Cheng et al., 2006), Janiak(Janiak, 1991), Shabtay and Kaspi(Shabtay and Kaspi, 2004; Shabtay and Kaspi, 2006), *etc*.). An excellent survey on this field has been given by Shabtay(Shabtay, 2007). Reader may refer to it for more information.

Alidaee and Ahmadian(Alidaee and Ahmadian, 1993) were the first to consider parallel machine system with controllable job-processing times. They considered two unrelated-machine problems. The first problem has an objective that equals total processing cost plus total flow time, and the second problem has an objective that equals total processing cost plus total weighted earliness and weighted tardiness. Under the assumption that all the jobs have the same linear compression rate, the problem is reduced to a transportation problem and is solved in $O(n^3m + n^2m\log(nm))$ time. Jansen and Mastrolilli(Jansen and Mastrolilli, 2004) successfully applied approximation schemes on several identical machine problems related with maximum completion time and total processing cost, including problem $P_m|lin, C_{\max} \leq K|\sum_{j=1}^{n} v_j u_j$, $P_m|lin, \sum_{j=1}^{n} v_j u_j \leq U|C_{\max}$ and $P_m|lin|C_{\max} + \sum_{j=1}^{n} v_j u_j$. Shabtay and Kaspi(Shabtay and Kaspi, 2006) studied parallel machine scheduling problems under the situation where operations are modeled by non-linear convex resource consumption functions. They showed that the general problem $P_m|conv|C_{\max}$ is $\mathcal{NP}$-hard, and obtained several polynomial time algorithms for special cases. The special case that preemption is allowed is also studied by several researchers. For example, Jansen and Mastrolilli(Jansen and Mastrolilli, 2004) showed that problem $P_m|lin, pmtn, C_{\max} \leq K|\sum_{j=1}^{n} v_j u_j$ can be solved in $O(n)$ time. Nowicki and Zdrzalka(Nowicki, 1995) provided an $O(n\max\{m, \log n\})$ time greedy algorithm to solve the uniform machine problem $Q_m|lin, a_j = 1, pmtn, C_{\max} \leq K|\sum_{j=1}^{n} v_j u_j$ problem.

Parallel machine scheduling with precedence constraints is widely studied in the context of the classical scheduling problems, but is not in literature under the condition that job-processing times are controllable. In this paper, we consider a parallel machine scheduling problem with precedence constraints and controllable job-processing times: Schedule a set of non-preemptive jobs $\mathcal{J} = \{1, 2, \ldots, n\}$ that have tree-formed precedence constraints on m identical machines. Job-processing times p_j are controllable, and can be modeled as the function of a continuously dividable resource u_j via a linear resource consumption

Xu, K., Fei, R. and Zheng, G.
Parallel-machine Scheduling with Precedence Constraints and Controllable Job-processing Times.
In *Proceedings of the 6th International Conference on Operations Research and Enterprise Systems (ICORES 2017)*, pages 470-476
ISBN: 978-989-758-218-9

function,

$$p_j(u_j) = \bar{p}_j - \theta_j u_j \qquad 0 \le a_j \le p_j(u_j) \le b_j \le \bar{p}_j \tag{1}$$

where $\bar{p}_j$ is the non-compressed job-processing time and θ_j is the positive compression rate of job j. The objective is to determine the optimal schedule $\mathcal{S} = \{\sigma_1, \sigma_2, \ldots, \sigma_m, p\}$, where $\sigma_i = \{\sigma_i(1), \sigma_i(2), \ldots, \sigma_i(n_i)\}$ is the optimal job-processing sequence on machine i, and $p = \{p_1, p_2, \ldots, p_n\}$ is the optimal job-processing times, such that the makespan of the jobs ($C_{\max} = \max_{j=1}^{n} C_j$) will not exceed the required deadline K, and the total resource consumption $U = \sum_{j=1}^{n} u_j$ is minimized. Using the three-field problem classification introduced by Graham *et al.*(Graham et al., 1979) and extended by Shabtay and Steiner(Shabtay, 2007), our problem can be denoted as $P_m \,|\, lin, tree, C_{\max} \le K \,|\, \sum_{j=1}^{n} u_j$.

The problem is strongly $\mathcal{NP}$-hard, which can be observed by the fact that it is still strongly $\mathcal{NP}$-hard to find a schedule whose makespan does not exceed deadline K when all the job-processing times are compressed to their lower bound a_j. Unless $\mathcal{P} = \mathcal{NP}$, it is impossible to find the optimal solution within acceptable computing time for large-scaled problems. Therefore, in this paper we designed a tabu-search algorithm to provide optimal or near optimal solutions for large-scaled problems.

Tabu-search(Glover, 1990) is essentially a meta-heuristic method that guides a heuristic local search procedure to explore the solution space beyond local optimality. A large number of successful tabu-search algorithms for scheduling problems can be found in literature (see, e.g., Dell'Amico and Trubian(Dell'Amico and Trubian, 1991), Bilge *et al.*(Bilge, 2004), Venditti *et al.*(Venidtti et al., 2010) and Xu et al.(Xu, 2010)).

2 TABU-SEARCH ALGORITHM

The scheduling algorithm needs to optimize job-processing sequence on the machines, as well as the processing times of the jobs. Suppose a job-processing sequence on the machines is decided, the optimal job-processing times can be calculated by the network flow method (NFM for convenience) introduced by Fulkerson(Fulkerson, 1961). Therefore, the tabu-search algorithm mainly concerns on searching for the optimal or near optimal job-processing sequences on the machines. In the following part of this section, the detail of the tabu-search algorithm will be discussed, which includes the initial solution generation, the neighborhood generation, the tabu mechanism, and the searching procedure.

2.1 The Objective Function

As the algorithm tries to minimize the resource consumption of the jobs, schedules are evaluated by their total resource consumption U. Therefore, the total resource consumption U is selected as the objective function in the tabu-search algorithm.

2.2 The Initial Solution

In this paper, the initial solution is constructed by the LTAP (Largest Total Amount Processing time first) method in the following way:

Algorithm 1: The LTAP method for initial solution generation.

1. Have all the job-processing times compressed to their lower bound a_j;
2. Sort jobs by their total amount of processing time, which is calculated by accumulating the processing time of jobs' successors and their own;
3. Assign jobs in the list to the machines. Each time, assign the first job in the list according to the following rules:
   (a) If there are one or more machines, where the last processed job is one of the direct predecessors of the job to be assigned, then assign it to the latest ready machine among them;
   (b) Otherwise, assign the job to the earliest ready machine.
4. Calculate the optimal processing times of the jobs by NFM.

Since parallel machine scheduling is $\mathcal{NP}$-hard, it shall be noted that the heuristic algorithm cannot guarantee a feasible initial solution when the deadline is very tight. However, as job-processing times are fully compressed, this method is still acceptable in most practical environment.

2.3 Neighborhood Generation

In each iteration, a number of generated neighboring schedules need be evaluated, which is time-consuming since objective values are calculated by solving the optimal resource allocation problem. Therefore, it is necessary to reduce neighboring schedules that need be evaluated. Tabu-search follows a so called "aggressive search" principle, that is, the

best schedule in the neighborhood will always be selected unless it is tabued. Therefore, if an operation leads to a neighboring schedule that is no better than another one, the operation need not be performed. If such dominated schedules can be identified by some simple rules before they are generated and evaluated, much computing time will be saved. In the following part, rules for "promising" neighboring schedules will be discussed based on the structural characteristic of the schedules and operations.

Neighboring schedules are normally generated by insert moves and swap moves. In this paper, insert moves are solely studied in neighborhood generation, which put single jobs to other processing positions either on their current machine or on other machines. As sequence constraint must be obeyed, it is supposed that jobs are always moved to feasible processing positions, such that they will not be processed earlier than their predecessors, or later than successors.

For parallel-machine problems with precedence constraints, critical path method (CPM) calculates the makespan of the jobs(Pinedo, 2012). By this method, jobs are classified as critical jobs and slack jobs. Critical jobs make up critical paths that decide the makespan, while slack jobs have no influence to the makespan. Moreover, it can be observed that $p_j = b_j$ for every slack job j. Therefore, when a slack job is moved to another processing position, the makespan will keep unchanged, if not be increased, which causes the total resource consumption not be reduced. The following lemma states this:

Lemma 1. Suppose job j is a slack job, then inserting job j to any other processing position cannot reduce the total resource consumption.

Therefore, insert moves are performed only on critical jobs.

Apart from this, other structural characteristics of the problem also help to reduce neighboring schedules. As is mentioned, an insert move may put a job to another feasible processing position on its current machine, or put it to another machine. The former operations are named **intra-machine insert moves**, while the latter **inter-machine insert moves**. The two kinds of operations will be discussed in the following.

Intra-machine Insert Moves. Suppose job j is inserted to another processing position on the same machine. If the processing of job j is advanced after insertion, it is inserted forward. Otherwise, it is inserted backward. If job j is processed immediately before job i, it is inserted to the front of job i. If job j is processed immediately after job k, it is inserted to the back of job k (As Fig.1 shows).

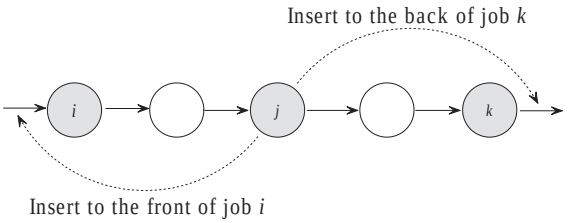

Figure 1: Intra-machine insert moves.

Suppose job i, j, k are processed on different machines, where job i is the direct predecessor and job k the direct successor of job j. In this case, it is said that job j has an emanating constraint to job k, and a sinking constraint from job i. If the precedence constraint $i \rightarrow j$ is part of a critical path, job j has a critical sinking constraint. If $j \rightarrow k$ is part of a critical path, then job j has a critical emanating constraint (As Fig.2 shows).

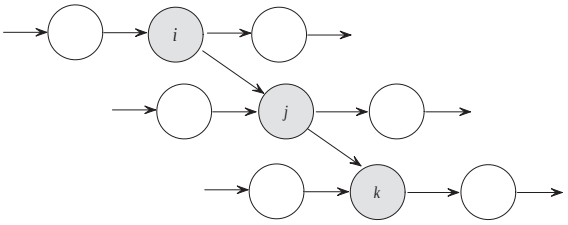

Figure 2: Critical sinking constraint and emanating constraint.

Lemma 2. Suppose job j has a critical emanating constraint in schedule $\mathcal{S}_1$. In the neighboring schedule $\mathcal{S}_2$ generated by inserting job j backward, job j still has a critical emanating constraint.

Lemma 3. Suppose job j has one or more critical sinking constraints in schedule $\mathcal{S}_1$. In the neighboring schedule $\mathcal{S}_2$ generated by inserting job j forward, job j still has one or more critical sinking constraints.

Corollary 1. Suppose job j has no critical sinking constraint in schedule $\mathcal{S}_1$. In the neighboring schedule $\mathcal{S}_2$ generated by inserting job j backward, job j has no critical sinking constraint.

Corollary 2. Suppose job j has no critical emanating constraints in schedule $\mathcal{S}_1$. In the neighboring schedule $\mathcal{S}_2$ generated by inserting job j forward, job j has no critical emanating constraint.

Lemma 4. Suppose there are jobs $j \prec j+1 \prec ... \prec k$ processed on the same machine in schedule $\mathcal{S}_1$, where job j has no critical sinking constraint, and jobs $j+1, ..., k$ have no critical emanating constraint. In this case, the total resource consumption of the neighboring schedule $\mathcal{S}_2$ generated by inserting job j to the back of job k is no less than that of $\mathcal{S}_1$.

Proof. (By contradiction) Assume the resource consumption of schedule $\mathcal{S}_2$ is smaller than that of the schedule $\mathcal{S}_1$, that is, $U_{\mathcal{S}_2} < U_{\mathcal{S}_1}$. Since job j has no critical sinking constraint in $\mathcal{S}_1$, it has no critical sinking constraint in $\mathcal{S}_2$. Similarly, job $j+1,...,k$ also have no critical emanating constraint in $\mathcal{S}_2$. Now construct a new schedule $\mathcal{S}_3$, where all the job-processing times are the same as those in $\mathcal{S}_2$, and job j is moved to its original position in $\mathcal{S}_1$. It can be easily observed that the makespan of $\mathcal{S}_3$ is no larger than K. Now generate a new schedule $\mathcal{S}_4$ by optimizing the job-processing times of $\mathcal{S}_3$. Obviously, there is $U_{\mathcal{S}_4} \leq U_{\mathcal{S}_3}$. However, since schedule $\mathcal{S}_4$ is exactly the same as $\mathcal{S}_1$, it causes a contradiction. The lemma is proved. □

Lemma 5. Suppose there are jobs $i \prec ... \prec j-1 \prec j$ processed on the same machine in schedule $\mathcal{S}_1$, where job j has no critical emanating constraint, and jobs $i,...,j-1$ have no critical sinking constraint. In this case, the total resource consumption of the neighboring schedule $\mathcal{S}_2$ generated by inserting job j to the front of job i is no less than that of $\mathcal{S}_1$.

Suppose there are job j and job k processed on different machines, where job k may or may not be the successor of job j. Because of the precedence constraints, when job j is inserted backward, job k must be processed after job j is completed. In this case, it is said that job j has an emanating constraint path to job k. In the similar way, it can also be defined that job j has a sinking constraint path from job i.

Lemma 6. Suppose there are job $j \prec j+1 \prec ... \prec k$ on the same machine in schedule $\mathcal{S}_1$, where job k has a critical emanating constraint to job l, while other jobs have no critical emanating and sinking constraint. Suppose job j has an emanating constraint path to job l. In this case, the total resource consumption of the neighboring schedule $\mathcal{S}_2$ generated by inserting job j to the back of job k is no less than that of $\mathcal{S}_1$.

Proof. (By contradiction) Assume the resource consumption of schedule $\mathcal{S}_2$ is smaller than that of the schedule $\mathcal{S}_1$, that is, $U_{\mathcal{S}_2} < U_{\mathcal{S}_1}$. Suppose job j has a direct successor job i processed on another machine (As Fig.6 shows). It can be easily seen that job j has a critical emanating constraint to job i, and no critical sinking constraint in schedule $\mathcal{S}_2$. It can also be seen that job $j+1,...,k$ have no critical emanating constraint in schedule $\mathcal{S}_2$. Now construct a new schedule $\mathcal{S}_3$, where all the job-processing times are the same as those in $\mathcal{S}_2$, and job j is moved to its original position in $\mathcal{S}_1$. It can be easily observed that the makespan of $\mathcal{S}_3$ is no larger than K. Now generate a new schedule $\mathcal{S}_4$ by optimizing the job-processing times of $\mathcal{S}_3$. Obviously, there is $U_{\mathcal{S}_4} \leq U_{\mathcal{S}_3}$. However, since schedule $\mathcal{S}_4$ is exactly the same as $\mathcal{S}_1$, it causes a contradiction. The lemma is proved. □

Lemma 7. Suppose there are job $j \prec j+1 \prec ... \prec k$ on the same machine in schedule $\mathcal{S}_1$, where job k has a critical emanating constraint to job l, while other jobs have no critical emanating and sinking constraint. Suppose job j has an emanating constraint path to job l. In this case, the total resource consumption of the neighboring schedule $\mathcal{S}_2$ generated by inserting job j to the back of job k is no less than that of $\mathcal{S}_1$.

Based on the above analysis, a set of rules for intra-machine insert moves are deduced in the following:

1. Job j has no critical emanating and sinking constraint.
   (a) It can be inserted to the back of job k, if job k is the first job with a critical emanating constraint, and job j has no emanating constraint path to the direct successor of job k;
   (b) It can be inserted to the front of job i, if job i is the first job with a critical sinking constraint, and job j has no sinking constraint path from the direct predecessor of job i.
2. Job j only has critical sinking constraint. It can be inserted to the back of the first job k with a critical sinking constraint.
3. Job j only has critical emanating constraint. It can be inserted to the front of the first job i with one or more critical emanating constraints.
4. Job j has critical sinking and emanating constraint. No intra-machine insert move shall be performed with it.

Inter-machine Insert Moves. Suppose there are job i and job j processed adjacently on the same machine, and job i or job j will be inserted to another machine. If job i is the predecessor of job j, the precedence constraint $i \prec j$ still exists after the operation. If not, the constraint will be eliminated. It can be observed, when a job is inserted to other machines, if no such precedence constraint can be eliminated, the resource consumption of the neighboring schedules will certainly not be reduced. Therefore, a job j can be inserted to other machines only if it satisfies one of the following conditions:

1. Job j is processed immediately after job i on the same machine, while job i is not a predecessor of job j;
2. Job j is processed immediately before job k on the same machine, while job k is not the successor of job j.

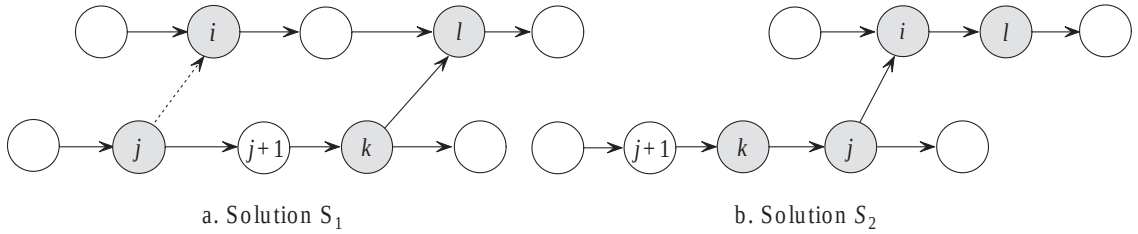

Figure 3: The illustration of lemma 6: (a) Schedule $\mathcal{S}_1$; (b) Schedule $\mathcal{S}_2$.

Otherwise, the operation should not be performed.

When job j is inserted to another machine m, it is first inserted to the earliest feasible processing position, and its optimal resource allocation is calculated. After that, it is inserted to other feasible positions using intra-machine insert moves, until the best processing position is determined, which will be recorded as the neighboring schedule generated by inserting job j to machine m.

2.4 The Tabu Mechanism

Tabu mechanism helps the searching procedure avoid being trapped in the local minimum. Typically, a list of mutations, which the procedure is not allow to make, is kept at any stage of the searching. Every time a mutation is made in the current schedule, the *reversed* mutation is entered at the top of tabu-list, while all other entries are pushed down one position and the bottom entry is deleted. In this paper, the schedule is modified by two kinds of moves, so the tabu-list needs to store them in different ways:

1. Intra-machine insert moves: When a selected schedule is generated by an intra-machine insert move performed on job j, the corresponding tabu-list entry is recorded as (i, j), where i is the job (may possibly be dummy) that is processed immediately before job j before the move is performed. Therefore, any intra-machine insert move that results in job j processed immediately after job i will be tabued.
2. Inter-machine insert moves: Suppose a schedule is generated by inserting job j from machine m to another machine. The tabu-list entry is recorded as (j, m), such that any inter-machine insert move that results in job j processed on machine m will be tabued.

2.5 The Tabu-search Algorithm

Based on the above discussion, the tabu-search algorithm is designed and presented in the following. The algorithm contains two input parameters that need be decided by users, which are:

- **MaxIter**: The algorithm stops when the objective function cannot be further improved after a number of iterations, defined by parameter MaxIter;
- **TabuDepth**: The maximum number of tabu entries that the tabu list contains, which is normally set between 6 and 10.

The tabu-search algorithm is formally stated as follows:

Algorithm 2: The tabu-search algorithm.

1. Have job-processing times compressed to their lower bound a_j, and schedule jobs by LTAP method. If the makespan is no larger than the deadline K, calculate the optimal job-processing times, and let the result be the initial solution.
2. Generate the initial solution by LTAP method. Let IterCounter $= 0$;
3. Improve the initial solution using insert moves:
   1. Generate neighboring schedules for every critical job using insert moves alone;
   2. Select among them the one with the smallest objective function value. If there are more than one such schedules, select one randomly;
   3. If the selected schedule is better than the current schedule, or the operation is not tabued, let the schedule replace the current schedule. Otherwise, remove the schedule from the neighborhood, and repeat Step 2.2;
   4. If the solution is improved, let IterCounter = 0. Otherwise, let IterCounter $=$ IterCounter $+ 1$;
   5. If IterCounter $>$ MaxCntInst, go to Step 3;
   6. If the objective function value of the solutions keeps unchanged over MaxCntObj times, push the objective function value of the selected schedule into the tabu-list. Otherwise, push the reversed operation that leads to the selected schedule into the tabu-list. Go to Step 2.1.
4. Select the best schedule obtained so far as the current schedule. Clear the tabu-list. Let IterCounter $= 0$;

5. Improve the current solution using insert and swap moves:
   1. Generate neighboring schedules for every critical job using insert moves and swap moves. If a schedule that is better than the current schedule is generated, then go to Step 4.2 directly;
   2. Select among them the one with the smallest objective function value. If there are more than one such schedules, select one randomly;
   3. If the selected schedule is better than the current schedule, or the operation is not tabued, let the schedule replace the current schedule. Otherwise, remove the schedule from the neighborhood, and repeat Step 4.2;
   4. If the solution is improved, let IterCounter = 0. Otherwise, let IterCounter = IterCounter + 1;
   5. If IterCounter > MaxCntSwp, go to Step 5;
   6. If the objective function value of the solutions keeps unchanged over MaxCntObj times, push the objective function value of the selected schedule into the tabu-list. Otherwise, push the reversed operation that leads to the selected schedule into the tabu-list. Go to Step 4.1.
6. Select the best schedule obtained so far as the solution, and exit.

3 NUMERICAL EXPERIMENT

A set of numerical experiments were performed in this section. The algorithm is implemented in C++ and is capable for parallel computing. The experiments were carried out on a personal computer with an Intel i7-2600 CPU with 4 cores and 8 independent threads. The algorithm was tested on problem instances generated by following method:

1. The minimum processing time a_j of the jobs are distributed randomly between [10, 50]. The maximum processing time $b_j = a_j + \delta_j$, where δ_j is also distributed between [10, 50];
2. The compression rate θ_j is distributed between [0.5, 1.5];
3. Each job has some predecessors, the number of them is distributed between [0, 5];
4. The maximum depth of the precedence tree is 5.

Because jobs are generated randomly, their number in each problem instance is different. For each instance, jobs are processed on 10 machines first, then on 25 machines. After the initial schedule is determined, a minimum makespan $T_{\min}$ is calculated with all the job-processing times $p_j = a_j$, and a maximum makespan $T_{\max}$ with $p_j = b_j$. The deadline $K = T_{\min} + (T_{\max} - T_{\min}) * \theta$, where θ is random between [0.3, 0.6].

Because no similar study on this problem is known in literature, the experimental result cannot be compared to other algorithms. Therefore, it is analyzed by comparing the scheduling result against the initial solution, which is shown Table 1 by following columns:

- n, m: The number of the jobs and the machines;
- Init, Rst: The resource consumption of the initial solution and that of the scheduling result;
- Imp: The improvement of the scheduling result against the initial solution, calculated as
$$Imp = \frac{Rst}{Init} 100\%$$
- Rst Time: The computing time when the best scheduling result is found;
- Total Time: The total computing time of the scheduling procedure.

The experimental result shows the heuristic initial solutions are significantly improved by the tabu-search algorithm. For most problem instances with job number around 200, the best scheduling results can be obtained normally within 60 minutes. Moreover, as the searching procedure is performed in parallel, the computing time can be easily reduced by using more powerful computers. Therefore, the algorithm is capable for providing satisfactory solutions for media and large-scaled problems within acceptable computing time.

4 SUMMARY

A parallel-machine scheduling problem is considered in this paper, where job-processing times can be compressed by allocating extra resource to the jobs. A tabu-search algorithm is designed to optimize job-processing sequence and processing times, such that the makespan does not exceed deadline K, while the total resource consumption can be minimized. Experiment shows the algorithm is capable for providing satisfactory near optimal solutions for media and large-scaled problems.

ACKNOWLEDGEMENTS

This paper is supported by the National Natural Science Foundation of China (No.61203183), and by CERNET Innovation Project (NGII20161201).

Table 1: Experimental results for problem instances generated with $[a,b] = [10,80]$, MaxPred = 6 and TreeDepth = 8.

n	m = 10					m = 25				
	Init	Rst	Imp	Rst Time	Total Time	Init	Rst	Imp	Rst Time	Total Time
51	1474.4	1314.8	89.2%	00:09:21	00:23:48	1179.8	991.0	83.9%	00:12:24	00:29:17
64	1808.2	1641.8	90.8%	00:11:54	00:35:12	1500.8	1375.5	91.7%	00:09:42	00:27:32
71	2073.4	1730.9	83.4%	00:11:06	00:43:21	1808.2	1616.4	89.4%	00:13:57	00:31:48
78	2152.6	1868.4	86.9%	00:14:13	00:36:04	1956.5	1774.5	90.7%	00:13:42	00:44:40
82	2301.8	1976.5	85.9%	00:13:43	00:42:19	2005.2	1758.6	87.7%	00:10:57	00:26:32
88	2475.6	2153.2	87.0%	00:16:43	00:45:19	2232.3	1959.9	87.8%	00:14:02	00:35:19
93	2481.2	2064.1	83.2%	00:17:23	00:41:14	2132.5	1937.8	90.9%	00:16:44	00:32:47
114	3415.5	3104.7	90.8%	00:20:41	00:53:34	3363.1	2845.1	84.6%	00:15:50	00:38:10
126	3865.7	3486.2	90.2%	00:23:57	00:57:22	3543.4	3029.6	85.5%	00:17:53	00:41:47
130	3644.3	3305.1	90.7%	00:19:31	00:54:22	3513.1	2954.4	84.1%	00:19:26	00:37:53
149	4715.5	3965.4	84.1%	00:19:15	00:58:10	3965.7	3429.7	86.5%	00:17:23	00:36:24
155	4455.8	3697.6	82.9%	00:31:12	01:05:24	4134.7	3596.6	87.0%	00:29:12	00:51:21
166	5158.4	4306.9	83.5%	00:33:52	01:04:13	4814.3	4259.5	88.5%	00:24:26	00:49:31
196	6043.5	5360.1	88.7%	00:42:25	01:23:04	5499.1	4844.6	88.1%	00:37:10	00:57:23
217	6401.7	5472.8	85.5%	00:42:35	01:35:43	5985.0	5081.3	84.9%	00:39:21	01:04:31
233	7024.6	6089.8	86.7%	00:57:51	01:54:53	6712.4	5752.2	85.7%	00:53:54	01:23:19
254	7485.8	6541.9	87.4%	00:55:26	01:56:27	6903.6	5867.6	85.0%	00:48:45	01:21:28

REFERENCES

Graham. R.L., Lawler. E.L., Lenstra. J.K., Rinnooy. A.H.G., 1979. Optimization and approximation in deterministic sequencing and scheduling: a survey. Annals of Discrete Mathematics, 5: 287-326.

Vickson., 1980. Two single machine sequencing problems involving controllable job processing times. AIIE Transactions, 12(3): 258-262.

Cheng. T.C.E, Kovalyov. M.Y., Shakhlevich. N., 2006. Scheduling with controllable release dates and processing times: total completion time minimization. European Journals of Operations Research, 175: 769-781.

Janiak. A., 1991. Single machine scheduling problem with common deadline and resource dependent release dates. European Journal of Operational Research, 53: 317-325.

Shabtay. D., Kaspi. M., 2004. Minimizing the total weighted flow time in a single machine with controllable processing times. Computers and Operations Research, 31(13): 2279-2280.

Shabtay. D., Kaspi. M., 2006. Parallel machine scheduling with a convex resource consumption function. European Journal of Operational Research, 173(1): 92-107.

Shabtay. D., Steiner. G., 2007. A survey of scheduling with controllable processing times. Discrete Applied Mathematics, 155(13): 1643-1666.

Alidaee. B., Ahmadian. A., 1993. Two parallel machine sequencing problems involving controllable job processing times. European Journal of Operations Research, 70: 335-341.

Jansen. K., Mastrolilli. M., 2004. Approximation schemes for parallel machine scheduling problem with controllable processing times. Computers and Operations Research, 31: 1565-1581.

Xu. K.L., Feng. Z.R., Ke. L.J., 2010, A tabu-search algorithm for scheduling jobs with controllable processing times on a single machine to meet due-dates. Computers and Operations Research, 37: 1924-1938.

Glover. F., 1990. Tabu search: a tutorial. Interfaces, 20(4): 665-679.

Dell'Amico. M., Trubian. M., Applying tabu-search to the job shop scheduling problems. Annals of Operations Research, 22: 231-252.

Bilge. U., Kirac. F., Kurtulan. M., Pekgun. P., 2004. A tabu search algorithm for parallel machine total tardiness problem. Computers and Operations Research, 31(3): 397-414.

Venditti. L., Pacciarelli. D., Meloni. C., 2010. A tabu search algorithm for scheduling pharmaceutical packaging operations. European Journal of Operations Research, 202(2): 538-546.

Nowicki., 1995. A bicriterion approach to preemptive scheduling of parallel machines with controllable job processing times. Discrete Appl. Math, 63: 23-256.

Fulkerson. D.R., 1961. A network flow computation for project cost curves. Management Science, 167-178.

Pinedo. M., 2012. *Scheduling: Theory, Algorithms, and Systems*. Springer-Verlag. New York, 4th edition.

Towards Collaborative Optimisation in a Shared-logistics Environment for Pickup and Delivery Operations

Timothy Curtois[1], Wasakorn Laesanklang[1], Dario Landa-Silva[1], Mohammad Mesgarpour[2] and Yi Qu[1]
[1]*ASAP Research Group, School of Computer Science, The University of Nottingham, Nottingham NG8 1BB, U.K.*
[2]*Microlise Ltd, Eastwood, Nottingham, NG16 3AG, U.K.*
{*tim.curtois, wasakorn.laesanklang, dario.landasilva, yi.qu*}*@nottingham.ac.uk,*
mohammad.mesgarpour@microlise.com

Keywords: VRP, PDP, LNS, Horizontal Collaboration, Split-loads.

Abstract: This paper gives an overview of research work in progress within the COSLE (Collaborative Optimisation in a Shared Logistics Environment) project between the University of Nottingham and Microlise Ltd. This is an R&D project that seeks to develop optimisation technology to enable more efficient collaboration in transportation, particularly real-world operational environments involving pickup and delivery problems. The overall aim of the project is to integrate various optimisation techniques into a framework that facilitates collaboration in a shared freight transport logistics environment with the overall goal of reducing empty mileage.

1 INTRODUCTION

This paper provides an overview of the research work being undertaken as part of the COSLE (Collaborative Optimisation in a Shared Logistics Environment) project. This is an R&D project between the University of Nottingham and Microlise Ltd in the UK. The overall objective of the project is to develop optimisation technology to enable more efficient collaboration in transportation. According to a recent report from the Institution of Mechanical Engineers in 2016 (Oldham, 2016), up to 30% of all commercial vehicles on UK roads travel empty, which leads to around 150m wasted road miles, 200,000 additional truck journeys, increased road congestion and about 200,000 tonnes of unnecessary CO_2 emissions. One way to improve this situation is by facilitating collaboration between carriers. The improved cooperation will reduce the total distances that vehicles travel without loads (so called empty miles), increase vehicle utilisation metrics and decrease distribution costs. Already there have been several successful applications of increased cooperation in transportation. (Cruijssen et al., 2007a) modelled a joint route planning problem, used a benchmark case and reported that 30.7% of total distribution costs are saved. (Ergun et al., 2007) proposed a lane covering problem and solved it using heuristics. Results showed that the saving range from about 5.5% to a little over 13%, again using real data. (Frisk et al., 2010) presented a case study of horizontal collaboration in tactical transportation planning between eight forest companies and the results showed up to 14.2% of the transportation cost saved. (Pérez-Bernabeu et al., 2015) discussed horizontal collaboration in road transportation and presented numerical analysis based on a set of well-known benchmarks for the Multidepot Vehicle Routing Problem. The average cost reduction ranges from 5% to 90% depending on the geographical distribution of customers with respect to their transport service providers. It has been proved by researchers that saving of costs and increase of resource utilization can be attained throughout horizontal collaboration (Cruijssen et al., 2007b; Wang and Kopfer, 2014).

The goal of the COSLE project is to develop an innovative service to enable collaboration in a shared freight transport logistics environment to reduce empty freight runs. As part of this, three sub-projects related to scheduling and optimisation have been identified and are currently being undertaken by project team. This position paper provides an overview of these sub-projects and the progress achieved so far. The first sub-project is to develop a methodology to tackle pickup and delivery problems with time windows and other real-world constraints. A metaheuristic approach has been developed and tested on a benchmark data set. This work and a summary of the results is described further in Section 2. The second sub-project is a method to enable opti-

Curtois, T., Laesanklang, W., Landa-Silva, D., Mesgarpour, M. and Qu, Y.
Towards Collaborative Optimisation in a Shared-logistics Environment for Pickup and Delivery Operations.
In *Proceedings of the 6th International Conference on Operations Research and Enterprise Systems (ICORES 2017)*, pages 477-482
ISBN: 978-989-758-218-9

mal load-splitting within routes and schedules. This is presented in Section 3 as well as a review of related research. The third sub-project, discussed in Section 4, is to develop a methodology for assigning new customers within existing routes. The outcomes from these three sub-projects will be integrated into a framework that will aim to enable more efficient collaboration in transportation under real-world operational conditions. The overall approach is to develop an optimisation engine for tackling pickup and delivery routing scenarios in which various transportation operators are willing to collaborate in order to increase the overall utilisation of vehicles by reducing the number of empty runs.

2 A HYBRID METAHEURISTIC FOR PDP

The pickup and delivery problem (PDP) is a widely occurring vehicle routing problem. Similar to other vehicle routing problems it often contains window and capacity constraints. Unlike the general vehicle routing problem however PDP also includes pairing and precedence constraints. The pairing constraint is to ensure that a pickup customer and its associated delivery customer are both serviced by the same vehicle. The precedence constraint does not allow a delivery customer to be visited before its associated pickup customer. The techniques being investigated in this project are for tackling pickup and delivery problems which also contain window and capacity constraints as well as other real world constraints such as driver working time regulations and break requirements. The objective function, similar to other problems, requires the minimisation of the number of vehicles used and the total distance travelled. Other optional objectives allow the minimisation of total driver hours, and a profit maximisation objective for problems in which some customers may be optionally serviced and have an associated completion cost.

Various heuristic and exact methods have been proposed for PDP. Each method has advantages and disadvantages. The exact methods, although extremely effective on smaller instances, appear to still be difficult to apply to the largest instances. Metaheuristics however have been shown to scale much more easily to larger instances although are easily beaten on smaller instances. They can also provide no information on solution optimality or even bounds. However a recent survey (Hall and Partyka, 2016) suggests that most industrial vehicle routing packages are still heavily biased towards using metaheuristics.

Of the exact methods published, many are versions of the column generation and branch and price framework (Dumas et al., 1991; Ropke and Cordeau, 2009; Savelsbergh and Sol, 1998; Venkateshan and Mathur, 2011; Xu et al., 2003) or less commonly, branch and cut (Lu and Dessouky, 2004; Ruland and Rodin, 1997). Examples of metaheuristics include (Bent and Van Hentenryck, 2006; Li and Lim, 2003; Nagata and Kobayashi, 2010; Nanry and Barnes, 2000; Ropke and Pisinger, 2006). Metaheuristics have also been applied to less common variants of PDP (Cherkesly et al., 2015; Kammarti et al., 2004; Masson et al., 2013). Several survey papers are also available (Berbeglia et al., 2007; Parragh et al., 2008; Savelsbergh and Sol, 1995).

The hybrid method that has been developed here combines Local Search, Large Neighbourhood Search (LNS) and Guided Ejection Search (GES). It works in several phases. In the first phase, local search using four different neighbourhood operators is used to create an initial solution. The operators used are:

1. Inserting unassigned customers into routes.
2. Moving a customer from one route to another.
3. Swapping customers between routes.
4. Moving a customer from one route to a second route and simultaneously moving a customer from a second route to a third route.

Even on the largest instances the local search phase is very fast but the solutions produced are nearly always quite sub-optimal. The next phase uses Guided Ejection Search in an attempt to minimise the total number of routes in the solution. The GES implementation is based on (Nagata and Kobayashi, 2010). It works by iteratively, randomly selecting a route, un-assigning all customers in the route and then attempting to re-insert these customers in existing routes. If it is unable to insert a customer it ejects one or more customers from a route to enable it to insert the customer. The ejected customer(s) are then added to the list of customers still to be inserted. After the ejection the solution is perturbed by randomly moving or swapping already assigned customers between routes. This helps to insert un-assigned customers and also prevents infinite loops. This is repeated for a number of iterations or until all customers have been inserted. If all customers are inserted then the process is repeated to try and remove another route. Otherwise the original solution is restored.

After the GES phase, a Large Neighbourhood Search is applied to try and improve the other objectives (total distance for the benchmark instances). The LNS is a simplified version of the adaptive LNS of (Ropke and Pisinger, 2006). One of the simplificati-

Table 1: Summary of Results.

Customers	Instances	New best knowns	Equal best knowns
50	56	0	56
100	60	7	35
200	60	22	19
300	60	33	6
400	60	45	5
500	58	35	4

ons was to remove the adaption procedure which was shown by the authors to have only a small percentage benefit. Our results also confirmed that excellent solutions could still be obtained without the adaption procedure. Another modification was to replace a simulated annealing heuristic with a late acceptance hill climbing heuristic (Burke and Bykov, 2012). The motivation for this was to remove the number of parameters that required setting. The algorithm operates by iteratively un-assigning a small number of customers and then heuristically attempting to re-insert them but in a lower cost configuration. If it is unable to re-insert them in a better way then it restores the original solution and selects a new set of customers for removal and re-insertion. This process is iteratively repeated. The customers for removal are selected randomly or via the Shaw heuristic (Shaw, 1998) which selects customers that are similar in terms of location, time windows and order size. The insertion heuristics are based on the regret assignment heuristic (Ropke and Pisinger, 2006).

After the completion of the LNS phase, if there is time remaining then the best known solution is perturbed by randomly moving or swapping customers between routes. The three phases are then applied again to the perturbed solution. This whole process is repeated until a fixed time limit is reached. At which point the best known solution is returned.

In order to evaluate the efficacy of the algorithm it was applied to the well-known benchmark problem instances of (Li and Lim, 2003)[1]. These instances are divided by size into six groups, ranging from 50 customers up to 500 customers. The results are summarized in Table 1. In Table 1. the column "New best solution" indicates the number of instances that our algorithm was able to find a new best known solution. The column "equal best knowns" indicates the number of instances on which the algorithm was able to equal the current best known solution for that instance.

[1]Available at http://www.sintef.no/projectweb/top/pdptw/li-lim-benchmark/

3 LOAD SPLITTING

Often job loads can be partially collected and delivered multiple times provided they are completed in entirety within the given time windows. This option allows the possibility of split loads to be used operationally.

The obvious case is when a requested demand exceeds vehicle capacity. Demands in this case must be split before the optimisation process. The research question in this case is how to split the requested demands so that the split loads aid the optimisation process. Some of the papers in the literature saw this case as a part of pre-processing in optimisation problem.

The other case is to gain additional savings in the operational plan. The literature shows split loads can reduce operational costs (Andersson et al., 2011; Nowak et al., 2009). The benefits of split loads were subject to problem characteristics such as load size, stopping cost, and frequency of loads having common pickup and delivery locations.

The transportation problem with split loads arose in the generic vehicle routing problem (VRP) in (Dror and Trudeau, 1989). The idea was to relax the VRP so that a customer can be visited more than once. A k-split interchange is also proposed as a heuristic procedure to split a demand into multiple loads. The solution after the split procedure was expected to have cost reduction from the generic problem.

(Dror and Trudeau, 1989) used a heuristic process to tackle a split load problem in two stages: construct a solution to the generic VRP; and apply k-split interchange and improvement routine to get a solution to the split load problem. The k-split interchange was also used as a move in a tabu search algorithm for the split delivery vehicle routing problem by (Archetti et al., 2006). They describe k-split interchange in two main procedures:

1. Remove a demand i from all routes where it is visited; and
2. Find a route subset R where the summation of remaining capacity is larger than the demand i so that the demand i is split into every route in the route subset R.

The route subset R should have the least insertion cost.

A randomised granular tabu search heuristic was used to solve the split delivery vehicle routing problem by (Berbotto et al., 2014). The method builds a granular neighbourhood to reduce the computational time required to explore solution neighbourhood.

Pickup and delivery with split loads was tackled by a heuristic where two route segments of different routes can visit the same pickup and delivery demand

by (Nowak et al., 2008). The demand can be carried by two vehicles.

A requirement of split delivery in simultaneous pickup and delivery arose in automobile industries in (Tang et al., 2009). At the supplier location, a truck must deliver empty bins to the pickup locations in order to pick up the full bins. In the same way, at the manufacturer, the truck must deliver full bins and pick up empty bins. Bins are cycled between the manufacturer and the suppliers.

Coordination split delivery can also benefit retailers in maintaining stock levels (Li et al., 2011). This approach can reduce retailer inventory costs while the transportation cost remains the same. A similar application can apply to the natural disaster relief distribution problem (Wang et al., 2014). The goal of this case was to distribute sufficient aid to the disaster areas. A disaster area can be visited multiple times. A full review on split delivery transportation problems can also be found in (Archetti and Speranza, 2012).

The closest application to the split pickup and delivery in the collaborative logistics environment considered here is the pickup and delivery problem with split load proposed by (Nowak et al., 2008). Therefore, we adopt their split load creation procedure and apply it to the large neighbourhood search method. The same procedure can also be used to split demand that exceeds vehicle capacity. The split load creation procedure works similarly to the k-split interchange procedure. The procedure is as follows:

1. Find a segment i to split;
2. Find a segment j the load should move to;
3. Split the load in the segment i where the first split load is equal to the excess capacity of segment j, and the second split load is the remainder;
4. Move the split load to segment j and the remainder load is kept in the segment i;
5. Perform the search heuristic.

The proposed approach in this sub-project is to implement move operators within LNS in order to handle split loads. This includes the delete split operator, exchange split operator, etc. These operators were applied to VRP (Berbotto et al., 2014). The delete split operator removes a set of split loads to become a full demand load.

The exchange split operator swaps the load splitting position in a selected route. In VRP, the idea was to swap the position to split a load while maintaining vehicle capacity. Suppose we have a load i and a load j where load i is split into two smaller loads and load j and one of the split loads of i are assigned to a vehicle. This operator relocates the split position from load i to load j which results in the vehicle taking the full load i and a partial load j. For our PDP, the operator starts from selecting an interval where a vehicle has split loads in their fill. The exchange split operator will:

1. Delete the split of a demand; and
2. Apply a split to one of the other demands.

The demands that the exchange split operator can select must be the fill in the selected interval only. The operator keeps the visit order of the selected route but may change the order of the routes that operate on the split demands.

This splitting heuristic and move operators will be integrated into the hybrid metaheuristic for PDP outlined in Section 2 and applied to large real-world instances. The benefits of providing splitting options will then be analysed. Optionally, the splitting heuristic can be adapted to increase vehicle empty space available for taking advantage of new collaborative opportunities. In the same way, the heuristic can split the collaborative jobs so that they can be inserted into the existing routes.

4 CUSTOMER INSERTION INTO EXISTING ROUTES

Another requirement in collaborative transport operations is to be able to insert new customers into existing routing plans. It might be that the ordering of the customers in the routes of the existing solution cannot be changed but their arrival times could be adjusted provided that their window constraints are still respected. Existing customers must also remain within their current routes. Hence, the hybrid LNS+GES algorithm outlined in Section 2 cannot simply be applied to a new instance which includes the new customers. Instead, a separate mechanism is being developed to insert the new customers.

To the best of our knowledge this problem has little or no previously published research articles. Modified but similar versions of the problem do sometimes appear as sub-problems in methodologies for vehicle routing problems though. For example, related problems are solved using branch and bound and constraint programming algorithms in (Bent and Van Hentenryck, 2006; Shaw, 1998). In (Ropke and Pisinger, 2006) also use a heuristic method to solve a version of the sub-problem for pickup and delivery with time window problems.

For the insertion problem considered here two separate objectives for two different scenarios are proposed:

1. Maximise the number of customers inserted.
2. Maximise profit. In this scenario customers are assigned values (revenue) and a cost is calculated based on total solution distance and/or total driver hours.

The insertion problem can be formulated as an integer programming problem and solved using a mathematical programming solver. We will also be investigating and comparing heuristic methods and alternative exact methods to establish the computation time/efficiency trade-off for the different approaches. For example, the hybrid LNS+GES algorithm already contains an existing insertion algorithm in the form of the regret heuristic. Greedy insertion heuristics are also feasible options. Other insertion algorithms that we will be developing and testing are the branch and bound approaches in (Shaw, 1998) and (Bent and Van Hentenryck, 2006).

To analyse the algorithms a testing framework has been created to allow us to efficiently repeat and reproduce the results. The test instances were created by taking existing instances, removing sets of customers and solving the reduced instances using the LNS+GES algorithm. The original instance is then used with this initial solution to form a new insertion instance. This procedure is repeated with different parameter settings to generate a large set of test instances to apply the algorithms to.

Another motivation for developing and analysing several insertion methods is to investigate whether a more efficient and effective method can be developed for the LNS algorithm. If so then it is possible that the LNS algorithm can be further improved by incorporating the new insertion algorithm.

ACKNOWLEDGEMENTS

We thank Innovate UK for funding the COSLE project (grant 102037).

REFERENCES

Andersson, H., Christiansen, M., and Fagerholt, K. (2011). The maritime pickup and delivery problem with time windows and split loads. *INFOR: Information Systems and Operational Research*, 49(2):79–91.

Archetti, C. and Speranza, M. G. (2012). Vehicle routing problems with split deliveries. *International transactions in operational research*, 19(1-2):3–22.

Archetti, C., Speranza, M. G., and Hertz, A. (2006). A tabu search algorithm for the split delivery vehicle routing problem. *Transportation Science*, 40(1):64–73.

Bent, R. and Van Hentenryck, P. (2006). A two-stage hybrid algorithm for pickup and delivery vehicle routing problems with time windows. *Computers & Operations Research*, 33(4):875–893.

Berbeglia, G., Cordeau, J.-F., Gribkovskaia, I., and Laporte, G. (2007). Static pickup and delivery problems: a classification scheme and survey. *TOP*, 15(1):1–31.

Berbotto, L., García, S., and Nogales, F. J. (2014). A randomized granular tabu search heuristic for the split delivery vehicle routing problem. *Annals of Operations Research*, 222(1):153–173.

Burke, E. K. and Bykov, Y. (2012). The late acceptance hill-climbing heuristic. *University of Stirling, Tech. Rep*.

Cherkesly, M., Desaulniers, G., and Laporte, G. (2015). A population-based metaheuristic for the pickup and delivery problem with time windows and lifo loading. *Computers & Operations Research*, 62:23–35.

Cruijssen, F., Bräysy, O., Dullaert, W., Fleuren, H., and Salomon, M. (2007a). Joint route planning under varying market conditions. *International Journal of Physical Distribution & Logistics Management*, 37(4):287–304.

Cruijssen, F., Dullaert, W., and Fleuren, H. (2007b). Horizontal cooperation in transport and logistics: a literature review. *Transportation journal*, pages 22–39.

Dror, M. and Trudeau, P. (1989). Savings by split delivery routing. *Transportation Science*, 23(2):141–145.

Dumas, Y., Desrosiers, J., and Soumis, F. (1991). The pickup and delivery problem with time windows. *European Journal of Operational Research*, 54(1):7–22.

Ergun, O., Kuyzu, G., and Savelsbergh, M. (2007). Reducing truckload transportation costs through collaboration. *Transportation Science*, 41(2):206–221.

Frisk, M., Göthe-Lundgren, M., Jörnsten, K., and Rönnqvist, M. (2010). Cost allocation in collaborative forest transportation. *European Journal of Operational Research*, 205(2):448–458.

Hall, R. and Partyka, J. (2016). Vehicle routing software survey: Higher expectations drive transformation. *ORMS-Today*, 43(1).

Kammarti, R., Hammadi, S., Borne, P., and Ksouri, M. (2004). A new hybrid evolutionary approach for the pickup and delivery problem with time windows. In *Systems, Man and Cybernetics, 2004 IEEE International Conference on*, volume 2, pages 1498–1503. IEEE.

Li, H. and Lim, A. (2003). A metaheuristic for the pickup and delivery problem with time windows. *International Journal on Artificial Intelligence Tools*, 12(02):173–186.

Li, J., Chu, F., and Chen, H. (2011). Coordination of split deliveries in one-warehouse multi-retailer distribution systems. *Computers & Industrial Engineering*, 60(2):291–301.

Lu, Q. and Dessouky, M. (2004). An exact algorithm for the multiple vehicle pickup and delivery problem. *Transportation Science*, 38(4):503–514.

Masson, R., Lehuédé, F., and Péton, O. (2013). An adaptive large neighborhood search for the pickup and de-

livery problem with transfers. *Transportation Science*, 47(3):344–355.

Nagata, Y. and Kobayashi, S. (2010). Guided ejection search for the pickup and delivery problem with time windows. In *European Conference on Evolutionary Computation in Combinatorial Optimization*, pages 202–213. Springer.

Nanry, W. P. and Barnes, J. W. (2000). Solving the pickup and delivery problem with time windows using reactive tabu search. *Transportation Research Part B: Methodological*, 34(2):107–121.

Nowak, M., Ergun, O., and White, C. C. (2009). An empirical study on the benefit of split loads with the pickup and delivery problem. *European Journal of Operational Research*, 198(3):734–740.

Nowak, M., Ergun, Ö., and White III, C. C. (2008). Pickup and delivery with split loads. *Transportation Science*, 42(1):32–43.

Oldham, P. (2016). UK Freight: in for the long haul. *Institution of Mechanical Engineers*.

Parragh, S. N., Doerner, K. F., and Hartl, R. F. (2008). A survey on pickup and delivery problems. *Journal für Betriebswirtschaft*, 58(1):21–51.

Pérez-Bernabeu, E., Juan, A. A., Faulin, J., and Barrios, B. B. (2015). Horizontal cooperation in road transportation: a case illustrating savings in distances and greenhouse gas emissions. *International Transactions in Operational Research*, 22(3):585–606.

Ropke, S. and Cordeau, J.-F. (2009). Branch and cut and price for the pickup and delivery problem with time windows. *Transportation Science*, 43(3):267–286.

Ropke, S. and Pisinger, D. (2006). An adaptive large neighborhood search heuristic for the pickup and delivery problem with time windows. *Transportation science*, 40(4):455–472.

Ruland, K. and Rodin, E. (1997). The pickup and delivery problem: Faces and branch-and-cut algorithm. *Computers & mathematics with applications*, 33(12):1–13.

Savelsbergh, M. and Sol, M. (1998). Drive: Dynamic routing of independent vehicles. *Operations Research*, 46(4):474–490.

Savelsbergh, M. W. and Sol, M. (1995). The general pickup and delivery problem. *Transportation science*, 29(1):17–29.

Shaw, P. (1998). Using constraint programming and local search methods to solve vehicle routing problems. In *International Conference on Principles and Practice of Constraint Programming*, pages 417–431. Springer.

Tang, G., Ning, A., Wang, K., and Qi, X. (2009). A practical split vehicle routing problem with simultaneous pickup and delivery. In *Industrial Engineering and Engineering Management, 2009. IE&EM'09. 16th International Conference on*, pages 26–30. IEEE.

Venkateshan, P. and Mathur, K. (2011). An efficient column-generation-based algorithm for solving a pickup-and-delivery problem. *Computers & Operations Research*, 38(12):1647–1655.

Wang, H., Du, L., and Ma, S. (2014). Multi-objective open location-routing model with split delivery for optimized relief distribution in post-earthquake. *Transportation Research Part E: Logistics and Transportation Review*, 69:160–179.

Wang, X. and Kopfer, H. (2014). Collaborative transportation planning of less-than-truckload freight. *OR spectrum*, 36(2):357–380.

Xu, H., Chen, Z.-L., Rajagopal, S., and Arunapuram, S. (2003). Solving a practical pickup and delivery problem. *Transportation science*, 37(3):347–364.

Integrated Production and Imperfect Preventive Maintenance Planning
An Effective MILP-based Relax-and-Fix/Fix-and-Optimize Method

Phuoc Le Tam[1], El-Houssaine Aghezzaf[1], Abdelhakim Khatab[2] and Chi Hieu Le[3]
[1]*Department of Industrial Systems Engineering and Product Design, Faculty of Engineering, Ghent University, Technologiepark 903, B-9052 Zwijnaarde, Belgium*
[2]*Industrial Engineering and Production Laboratory, National School of Engineering, Metz, France*
[3]*Faculty of Engineering and Science, University of Greenwich, Kent, U.K.*
{*phuoc.letam, elhoussaine.aghezzaf*}*@ugent.be, khatab@enim.fr, c.h.le@gre.ac.uk*

Keywords: Production Planning, Imperfect Preventive Maintenance, Optimization, Integrated Strategies.

Abstract: This paper investigates the integrated production and imperfect preventive maintenance planning problem. The main objective is to determine an optimal combined production and maintenance strategy that concurrently minimizes production as well as maintenance costs during a given finite planning horizon. To enhance the quality of the solution and improve the computational time, we reconsider the reformulation of the problem proposed in (Aghezzaf et al., 2016) and then solved it with an effective MILP-based Relax-and-Fix/Fix-and-Optimize method (RFFO). The results of this Relax-and-Fix/Fix-and-Optimize technique were also compared to those obtained by a Dantzig-Wolfe Decomposition (DWD) technique applied to this same reformulation of the problem. The results of this analysis show that the RFFO technique provides quite good solutions to the test problems with a noticeable improvement in computational time. DWD on the other hand exhibits a good improvement in terms of computational times, however, the quality of the solution still requires some more improvements.

1 INTRODUCTION

Even though managed by two different departments in some factories, the production planning and maintenance planning are two closely interrelated functions. In the major modern factories effort is done to also carry these two planning functions in an integrated manner. Researchers have also proposed strategies and developed models to integrate the production and maintenance planning decisions both at the tactical as well as at the operational levels. Various mathematical models focusing on coordinating production and maintenance plans are proposed in (Lin et al., 1992; Gurevich et al., 1996; Agogino et al., 1997; Ben-Daya and Rahim, 2000; El-Amin et al., 2000; Kiyoshi et al., 2002; Chattopadhyay, 2004; Martorell et al., 2005; Aghezzaf et al., 2007; Dahal and Chakpitak, 2007; El-Ferik, 2008; Fitouhi and Nourelfath, 2012; Wang, 2013). A wide variety of solution techniques and algorithms including the whole spectrum of heuristic techniques, dynamic programming, tabu-search multi-objective optimization, expert systems and many other hybrid techniques are also proposed, see for example (Lin et al., 1992; Gurevich et al., 1996; Agogino et al., 1997; Ben-Daya and Rahim, 2000; Kiyoshi et al., 2002; Chattopadhyay, 2004; Martorell et al., 2005; Dahal and Chakpitak, 2007). Integrated production and imperfect preventive maintenance planning models were also proposed, see for example (Chung and Krajewski, 1984; Ben-Daya and Rahim, 2000; Sana and Chaudhuri, 2010; Fitouhi and Nourelfath, 2012; Aghezzaf et al., 2016). Imperfect preventive maintenance, when performed, brings the manufacturing system to an operating state that is between as bad as old and as good as new. The resulting mathematical models are naturally non-linear and involve many binary variables. In (Aghezzaf et al., 2016), the authors proposed a reformulation for the natural integrated production and imperfect preventive maintenance planning problem. The resulting optimization model is a mixed-integer linear programming problem which is solved using a MILP-based approximation method. The current paper proposes to adopt a Relax-and-Fix/Fix-and-Optimize approach and analyse its results.

This Relax-and-Fix/Fix-and-Optimize approach results in quite good solutions. However, it still requires a large amount of the computational time for medium and large scale instances of the problem. To deal with these large scale instances, some heuris-

Tam, P., Aghezzaf, E-H., Khatab, A. and Le, C.
Integrated Production and Imperfect Preventive Maintenance Planning - An Effective MILP-based Relax-and-Fix/Fix-and-Optimize Method.
In *Proceedings of the 6th International Conference on Operations Research and Enterprise Systems (ICORES 2017)*, pages 483-490
ISBN: 978-989-758-218-9

tics based on the Dantzig-Wolfe decomposition techniques and a new version of the Relax-and-Fix/Fix-and-Optimize method are investigated and developed. The main goal is to obtain good quality solutions within a reasonable amount of the computational time frame.

The remainder of this paper is organized as follows. In section 2, a slightly modified version of the mathematical model, for integrated production planning and imperfect preventive maintenance planning, propose in (Aghezzaf et al., 2016) is presented. In section 3, the developed Relax-and-Fix/Fix-and-Optimize techniques (RFFO) is introduced and presented in details. Section 4 presents the Dantzig-Wolfe (DWD) decomposition to solve the reformulated production and maintenance planning model. Computational results of a set of benchmark cases are presented and discussed in Section 5. Finally, Section 6 summarizes the main findings of this research work and discusses some possible research directions.

2 THE INTEGRATED PRODUCTION AND IMPERFECT PREVENTIVE MAINTENANCE MODEL

In this section, the mathematical optimization model for integrated production and imperfect preventive maintenance problem described in (Aghezzaf et al., 2016) is briefly summarized. Then, the reformulation proposed by the authors for this production and imperfect preventive maintenance problem is shown and used as the underlying optimization model for the detailed subsequent discussion.

2.1 A Mathematical Optimization Model for the Integrated Production and Imperfect Preventive Maintenance Problem (IPImPMP)

In the IPImPMP problems, it is assumed that the systemś operating state is stochastically predictable, in terms of its operating age, and that it can accordingly be preventively maintained during preplanned periods. The preventive maintenance is assumed to be imperfect, so that after each maintenance action the manufacturing system is at an operating state that is between as bad as old and as good as new.

Along the same lines as in (Aghezzaf et al., 2016), we consider a planning horizon $H = \{1, ...T\}$ of T periods, each having a duration τ, and a set of products $j \in P = \{1, ...N\}$ to be planned during this horizon. Let d_{jt} be the demand for item j in period t, f_{jt} be the fixed cost of producing item j in period t, p_{jt} be the variable cost of producing item j in period t, and h_{jt} be the variable holding cost of item j in period t. The production system has a known maximum constant production capacity κ_{max} (given in time units) and the processing time of each unit of item j is given by ρ_j. The system can be maintained preventively or correctively when a failure occurs. The cost of carrying out a k^{th} preventive maintenance action is denoted by C^k_{PM} and the cost of performing a corrective maintenance action on the system when a failure occurred, right after k^{th} preventive maintenance, is denoted by C^k_{CM}. Finally, let δ^k_{PM} be the expected time required for the k^{th} preventive maintenance action, and δ^k_{CM} the expected time required to perform a corrective maintenance action on the system when a failure occurred, right after k^{th} preventive maintenance.

The variables of the model are: Q_{jt} the quantity of item j produced during period t; I_{jt} the inventory of item j at the end of period t; x_{jt} a binary variable set to 1 if item j is produced during period t and 0 otherwise; y_t a binary decision variable set to 1 if the machine is setup to production during period t and 0 otherwise; and finally z^k_{st} a binary variable set to 1 if the last preventive maintenance of the system before the time period t is the k_{th} one and has taken place during the time period s and 0 otherwise. By convention we assume that the manufacturing system is preventively maintained in the beginning of period 1, that is $z^1_{11} = 1$ for $k \leq s \leq t$. The optimization model for the Integrated Production and Imperfect Preventive Maintenance Planning Problem (IPImPMP) is given by:

Minimize

$$Z^{IP}_{ImPMP} = \sum_{t=1}^{T}\sum_{j=1}^{N}(f_{jt}x_{jt} + p_{jt}Q_{jt} + h_{jt}I_{jt}) + \sum_{t=1}^{T}\sum_{k=1}^{t} C^k_{PM} z^k_{tt} + \sum_{t=1}^{T}\sum_{s=1}^{t}\sum_{k=1}^{s} C^k_{st}(\mathbf{y}) y_t z^k_{st}$$

subject to:

$$Q_{jt} + \begin{cases} I_{j,t-1} & if\ t > 1 \\ 0, & if\ t = 1 \end{cases} - I_{jt} = d_{jt}, \quad \forall j \in P, \forall t \in H \tag{1}$$

$$Q_{jt} - \kappa_{max} x_{jt} \leq 0, \quad \forall j \in P, \forall t \in H \tag{2}$$

$$x_{jt} - y_t \leq 0, \quad \forall j \in P, \forall t \in H \tag{3}$$

$$\sum_{j=1}^{N} \rho_j Q_{jt} + \sum_{k=1}^{t} \delta_{PM}^k z_{tt}^k + \sum_{s=1}^{t}\sum_{k=1}^{s} \kappa_{st}^k(\mathbf{y}) y_t z_{st}^k \leq \kappa_{max}, \forall t \in H \quad (4)$$

$$\sum_{s=1}^{t}\sum_{k=1}^{s} z_{st}^k = 1, \quad \forall t \in H \quad (5)$$

$$z_{st}^k - z_{s,t+1}^k \geq 0, \quad \forall k,s,t \in H, k \leq s \leq t \leq T-1 \quad (6)$$

$$z_{tt}^k - \sum_{s=k-1}^{t-1} z_{s,t-1}^{k-1} \leq 0, \quad \forall t,k\backslash\{1\} \in H, 1 < k \leq t \quad (7)$$

$$\sum_{t=2}^{T}\sum_{s=2}^{t} z_{st}^1 = 0 \quad \forall s,t \geq 2 \in H, s \leq t \quad (8)$$

$$\sum_{k=1}^{t} z_{tt}^k \leq y_t, \quad \forall t \in H \quad (9)$$

$$Q_{jt}, I_{jt} \geq 0, \quad x_{jt}, y_t, z_{st}^k \in \{0,1\} \quad \forall j \in P, s,t \in H, k \leq s \leq t$$

Constraints (1) are the flow conservation constraints. They guarantee that the available inventory augmented with the quantity produced in period t is sufficient to satisfy the demand d_{jt} of item j in that period. The remainder is stocked for the subsequent periods. Constraints (2) make sure that, when the production of an item is scheduled in certain period, the system is setup accordingly to produce that item in that period. These constraints force also disbursement of the fixed costs. Constraints (3) indicate whether the system is operating or not in each period, in which it is setup to produce some products. Constraints (4) are the capacity restrictions which are defined for each period $t \in H$. They guarantee that the quantity which is produced in a period t does not exceed the available capacity of the system, given its status in terms of the expected capacity loss during that period. Constraints (5) determine the periods during which the preventive maintenance activities take place. In order to assure the consistency, constraints (6) are established to guarantee that if the last preventive maintenance action, before a time period $t+1$, takes place in a period $s < t$ and it is the k^{th} one, then this preventive maintenance action must also be the k^{th} and the last one before a period t. Again, in order to keep the consistency, constraints (7) assure that the k^{th} preventive maintenance takes place in some period $t \geq k$, only if the $(k-1)^{th}$ preventive maintenance took place in some period before t. Constraints (8) assures that the system is always maintained for the first time in the first period. Constraints (9) ensure that the k^{th} preventive maintenance takes place only once and when the system is setup to production.

As in (Aghezzaf et al., 2016), the function $\kappa_{ts}^k(y)$ and $C_{ts}^k(y)$ are the expected production capacity loss and expected maintenance cost during the time period t when the k^{th} and the last preventive maintenance action before time period t has taken place in the time period s, with $k \leq s \leq t$. These parameters depend on the system's setup vector $\mathbf{y}$ and are given by

$$\kappa_{st}^k(y) = \begin{cases} \delta_{CM}^k \int_0^\tau \beta^k r_0\left(u + \alpha^k \left[\sum_{t'=1}^{s-1} y_{t'}\right]\tau\right) du \\ \qquad \text{if } t = s, k \leq s, \\ \delta_{CM}^k \int_0^\tau \beta^k r_0\left(u + \alpha^k \left[\sum_{t'=1}^{s-1} y_{t'}\right]\tau + \left[\sum_{t'=s}^{t-1} y_{t'}\right]\tau\right) du \\ \qquad \text{if } s \leq t \leq T. \end{cases} \quad (10)$$

$$C_{st}^k(y) = \begin{cases} C_{CM}^k \int_0^\tau \beta^k r_0\left(u + \alpha^k \left[\sum_{t'=1}^{s-1} y_{t'}\right]\tau\right) du \\ \qquad \text{if } t = s, k \leq s, \\ C_{CM}^k \int_0^\tau \beta^k r_0\left(u + \alpha^k \left[\sum_{t'=1}^{s-1} y_{t'}\right]\tau + \left[\sum_{t'=s}^{t-1} y_{t'}\right]\tau\right) du \\ \qquad \text{if } s \leq t \leq T. \end{cases} \quad (11)$$

We adopt a hybrid failure rate model which was defined in (Aghezzaf et al., 2016). If after k^{th} preventive maintenance the failure rate function remains below some threshold function, $r_{k_{max}}(t)$, the system can again be preventively maintained. However, if it reaches or exceeds this threshold level, it is overhauled and will be returned to an "as-good-as-new" state. We considers a lifetime of a whole system is randomly distributed and for which the corresponding initial hazard rate function is given by the function $r_0(t)$. If the k^{th} preventive maintenance takes place $T_k\tau$ units of time after an overhaul, that is in the beginning of period T_k having fixed length τ, the hazard rate function $r_k(t)$ of the system is then defined as:

$$r_k(t) = \beta_k r_0(t + \alpha_k T_{AOT}^k), \quad t \in [0, (T_{k+1} - T_k)\tau], \forall k, 1 \leq k \leq k_{max} \quad (12)$$

where T_{AOT}^k is the actual operating time of the system since the beginning of the planning horizon until the beginning of period T_k, the period during which the k^{th} preventive maintenance is taking place. The parameters α_k and β_k stand, respectively, for the age reduction coefficient and the hazard rate increasing coefficient (adjustment factor) such that $0 \leq \alpha_1 \leq \alpha_2 \leq \ldots \leq \alpha_{kmax} \leq 1$ and $1 \leq \beta_1 \leq \beta_2 \leq \ldots \leq \beta_{kmax}$.

2.2 Reformulation of the Problem (Re_IPImPMP)

The natural formulation of problem (IPImPMP) is nonlinear. It can be reformulated and modeled as a mixed-integer linear program as is shown in (Aghezzaf et al., 2016). We propose a slight variation of the mathematical reformulation proposed in (Aghezzaf et al., 2016) by adding the variables $v^k_{st}(p,q)$, with $p \le s \le t, k \le s$ and $q \le t-s+1$, to be a binary variable assuming value 1 if the system is setup to production with p time during the horizon $1,...,s-1$ and q time during the period s,..,t, and the k^{th} maintenance takes place in period s and, $w^k_{st}(p,q)$, with $p \le s \le t, k \le s$ and $q \le t-s+1$, to be a binary variable assuming value 1 if the system is setup for production p time during the horizon $1,...,s-1$ and q time during the period $s,..,t$ and the k^{th} maintenance takes place in period s and the system must be produced at period t.

$$(Re\_IPImPMP): Minimize \quad Z^{Re\_IP}_{ImPMP} = \sum_{t=1}^{T}\sum_{j=1}^{N}\left(f_{jt}x_{jt}+p_{jt}Q_{jt}+h_{jt}I_{jt}\right)+\sum_{t=1}^{T}\sum_{k=1}^{t}C^k_{PM}z^k_{tt} + \sum_{t=1}^{T}\sum_{s=1}^{t}\sum_{k=1}^{s}\sum_{p=0}^{s-1}\sum_{q=0}^{t-s}C^k_{st}(p,q)v^k_{st}(p,q)$$

subject to :

Eq. (1) - (3) and (5) - (9)

$$\sum_{j=1}^{N}\rho_j Q_{jt}+\sum_{k=1}^{t}\delta^k_{PM}z^k_{tt} + \sum_{s=1}^{t}\sum_{k=1}^{s}\sum_{p=0}^{s-1}\sum_{q=0}^{t-s}c^k_{st}(p,q)v^k_{st}(p,q) \le \kappa_{max}, \forall t \in H \tag{13}$$

$$\sum_{p=0}^{s-1}\sum_{q=0}^{t-s}p.u_{st}(p,q)-\begin{cases}\sum_{s'=1}^{s-1}y_{s'}, & if\ s>1\\ 0, & if\ s=1\end{cases} \le 0, \quad \forall t,s \in H, 1 \le s \le t \tag{14}$$

$$\sum_{p=0}^{s-1}\sum_{q=0}^{t-s}q.u_{st}(p,q)-\begin{cases}\sum_{s'=s}^{t-1}y_{s'}, & if\ t>1\\ 0, & if\ t=1\end{cases} \le 0, \quad \forall t,s \in H, 1 \le s \le t \tag{15}$$

$$\sum_{p=0}^{s-1}\sum_{q=0}^{t-s}u_{st}(p,q)=1, \quad \forall t,s \in H, 1 \le s \le t \tag{16}$$

$$z^k_{st}+u_{st}(p,q)-v^k_{st}(p,q) \le 1, \quad \forall k,s,t,p,q \in H, p \le s-1, q \le t-s \tag{17}$$

$$y_t+v^k_{st}(p,q)-w^k_{st}(p,q) \le 1, \quad \forall k,s,t,p,q \in H, p \le s-1, q \le t-s \tag{18}$$

$$Q_{jt}, I_{jt} \ge 0, \quad x_{jt}, y_t, z^k_{st}, u_{st}\{p,q\}, v^k_{st}\{p,q\}, w^k_{st}\{p,q\} \in \{0,1\} \quad \forall j \in P, s,t \in H, k \le s \le t, p \le s-1, q \le t-s$$

where $u_{st}(p,q)$, with $p \le s \le t$ and $0 \le q \le t-s+1$, to be a binary variable assuming value 1 if the system is setup to production p times during the horizon 1,..., s-1 and q times during the periods s,..., t-1.

Constraints (1) - (3) and (5) - (9) are the same as before. Constraints (13) are revisited from (4). However constraints (14), (15), (16) determine the values of the variables u and v. The constraints (17) relate the variables z with u and v, meaning that if the k^{th} and last preventive maintenance before t takes places in period $s \le t$ and if the system is setup to production p times during the horizon $\{1,...,s-1\}$ and q times during the periods $\{s,...t-1\}$ then $v^k_{st}(p,q)$ =1. The constraints (18) relate the variables v with y and w, meaning that if both the k^{th} and last preventive maintenance before t takes places in period $s \le t$ and if the system is setup to production p times during the horizon $\{1,...,s-1\}$ and q times during the periods $\{s,...t-1\}$ and the system must be produced at period t then $w^k_{st}(p,q)$ =1.

Here again, as reported in (Aghezzaf et al., 2016), we let $C^k_{st}(p,q)$ and $\kappa^k_{st}(p,q)$ be respectively the expected maintenance cost and expected loss in production capacity of the system during period t, when the last preventive maintenance action before time period t has taken place in the beginning of period s, $s \le t$. These parameters are given by:

$$C^k_{st}(p,q)=\begin{cases}C^k_{CM}\int_0^{\tau}\beta_k r_0(u+\alpha_k p\tau)du\\ \quad if\ t=s,\\ C^k_{CM}\int_0^{\tau}\beta_k r_0(u+\alpha_k p\tau+q\tau)du\\ \quad if\ s \le t \le T.\end{cases} \tag{19}$$

and

$$\kappa^k_{st}(p,q)=\begin{cases}\delta^k_{CM}\int_0^{\tau}\beta_k r_0(u+\alpha_k p\tau)du\\ \quad if\ t=s,\\ \delta^k_{CM}\int_0^{\tau}\beta_k r_0(u+\alpha_k p\tau+q\tau)du\\ \quad if\ s \le t \le T.\end{cases} \tag{20}$$

3 RELAX-AND-FIX WITH FIX-AND-OPTIMIZE HEURISTIC (RFFO) TO SOLVE THE Re_IPImPMP MODEL

The Relax-and-Fix (RF) heuristic solves MIP problem by sequentially resolving sub-problems in which some variable are fixed and others are relaxed. To

solve production planning problems, for example, the planning horizon is partitioned and the setup variables are fixed backward or forward. Fix-and-Optimize is an improvement heuristic also based on decompositions of the original problem into multiple sub-problems with smaller number of binary variables. The RFFO method is a framework designed to combine the Relax-and-fix (RF) and fix-and-optimize (FO) heuristics. In (Toledo et al., 2015), the authors propose an approach in which most binary variables are fixed or relaxed and only few of them are forced to be integer and are optimized. They named this small set of integer variables a "window" and suggested three window type strategies: row-wise, in which the window moves along rows; column-wise, in which the window moves along columns; and value-wise, in which the window selects the variables with relaxed values closest to 0.5. As in (Toledo et al., 2015), For both heuristics applied to the Re_IPImPMP model, we consider a matrix Y where each of its entries is the binary varaible y_t. The inputs of the RF are the set of binary variables ($sol.y$), the number of binary variables (*windowSize*) to be chosen, the selection criteria to choose variables (*windowType*), the overlap rate of binary variables to be re-optimized (*overlap*) and the execution time limit (*timeLimit*). Initially, all binary variables in the RF solution ($sol.y$) are relaxed, and a window is defined as a set that includes a fixed amount of (*windowSize*) variables. Then, those variables which are inside the window are enforced to be integer in the set y_{MIP}, while the others are kept in y_{LP}. We solve the problem to get the results of MIP. Next, a new set of variables (*window*) is defined by a subset of fixed integers (y_{fixed}), sets of optimized integer (y_{LP}) and relaxed variables (y_{MIP}). The *window* moves forward by the *step* parameter at each iteration on which each $step = round(|overlap * windowSize|)$, $overlap \in [0,1]$. All variables that leave the window are fixed in the next iteration, and the same number of relaxed variables are enforced to be integer. The algorithm proceed in this way until all variables are fixed. After the RF phase is complete, FO tries to improve this initial solution until the time limit has been reached. If the improvement achieved by a FO solution is not satisfactory, the window size is increased. The MIP subproblems become larger as an attempt to find better solutions.
The pseudo-code of the method can be provided to interested researchers upon request.

4 SINGLE DANTZIG-WOLFE BY PRODUCT DECOMPOSITION WITH FIX AND OPTIMIZE TO SOLVE THE MINLP IPImPMP MODEL

Dantzig-Wolfe decomposition (DWD) method is used in (Pimentel et al., 2010) to solve the multi-item capacitated lot sizing problem with setup times. The authors applied the standard DantzigWolfe decomposition (DWD) in three different ways. In the first the subproblems are defined by items (PIDWD), in the second they are defined by periods (PJDWD) and a third decomposition in which the subproblems of both types are integrated in the same model (MDWD). The three approaches were tested on the IPImPMP model defined in Section 2.1. Based on the results, the suitable approach seems to be the production decomposition which is then selected for the comparison of the results. We consider the capacity constraints 4, linking constraints the the variables associated with different products as the master problem for this decomposition.

4.1 Master Problem

The master problem includes the collections of production plans of each items and the maintenance planning. The decision variables are ϑ_j^m, corresponding to the items production plans m generated by the subproblems for products j, and z_{st}^k are the variables corresponding to the maintenance plan developed at the master problem level. The linear programming relaxation of the master problem of the production decomposition is given below:
(MPJ-PPM) : Minimize $Z_{IPImPPM}^{MPJ} =$

$$\sum_{j=1}^{N}\sum_{m=1}^{Mj}\left[\sum_{t=1}^{T}(f_{jt}\bar{x}_{jt}^m + p_{jt}\bar{Q}_{jt}^m + h_{jt}\bar{I}_{jt}^m)\right]\vartheta_j^m + \sum_{t=1}^{T}\sum_{k=1}^{t}C_{PM}^k z_{tt}^k + \sum_{t=1}^{T}\sum_{s=1}^{t}\sum_{k=1}^{s}c_{st}^k(\bar{y}).\bar{y}_t z_{st}^k$$

subject to:

$$\sum_{j=1}^{N}\sum_{m=1}^{Mj}\rho_j\bar{Q}_{jt}^m\vartheta_j^m + \sum_{t=1}^{T}\sum_{k=1}^{t}\delta_{PM}^k z_{tt}^k + \sum_{s=1}^{t}\sum_{k=1}^{s}\kappa_{st}^k(\bar{y})z_{st}^k \leq \kappa_{max}, \forall t \in H(\mu_t) \quad (21)$$

$$\sum_{m=1}^{Mj}\vartheta_j^m = 1, \qquad \forall j \in N(\pi_j) \quad (22)$$

$$\sum_{m=1}^{Mj} \bar{x}_{jt}^{m} \vartheta_{j}^{m} <= \bar{y}_{t}, \quad \forall j \in N; t \in H \quad (\eta_{jt}) \tag{23}$$

$$\vartheta_{j}^{m} \geq 0, \qquad \forall j \in N \tag{24}$$

$$z_{st}^{k} \geq 0, \qquad \forall j \in N; t, s \in H \tag{25}$$

and Eq. (5) - (9)

where $\bar{y}_t = max_{j,m}\left\{\bar{x}_{jt}^{m}\right\}$ and the objective function minimizes the overall production and maintenance costs. The set of constraints (21) are capacity constraint. These constraints impose that the combination of the chosen production plans satisfies the available capacity in each period based on the maintenance plans. Constraints (22) are the convexity constraints. The mixing of the chosen production plans is forced by constraints (23) to satisfy the production setup requirements. Constraints (24) and (25) force the decision variables to take nonnegative values.

Of course at the end of the process, the problem is solved again but then with the variables ϑ_j^m and z_{st}^k satisfying the following conditions:

$$\vartheta_{j}^{m}, z_{st}^{k} \in \{0,1\} \forall j \in N, s, t \in H, k \leq s \leq t, m \in Mj$$

To recover solution of problem IPImPMP, in terms of the original variables, we can obtain the value of (Q_{jt}, x_{jt}) from a solution of master problem (MPJ_PPM) as follows:

$$Q_{jt} = \sum_{m=1}^{Mj} \bar{Q}_{jt}^{m} \vartheta_{j}^{m}, \qquad \forall j \in N, \quad \forall t \in T \tag{26}$$

$$x_{jt} = \sum_{m=1}^{Mj} \bar{x}_{jt}^{m} \vartheta_{j}^{m}, \qquad \forall j \in N, \quad \forall t \in T \tag{27}$$

4.1.1 Subproblem

Assuming that μ_t is the vector of dual variables associated with the constraints (21), indexed by t, the π_j the vector of dual variables associated with the set of convexity constraints (22) and the η_{jt} is a dual associated variables with constraints (23). Each subproblem is one of following types:

$$Z_{IPImPMP}^{SPJ} = \sum_{t=1}^{T} (f_{jt} x_{jt} + p_{jt} Q_{jt} + h_{jt} I_{jt}) - \sum_{t=1}^{T} \rho_j Q_{jt} \pi_j - \mu_t - \sum_{t=1}^{T} \eta_{jt} x_{jt}, \forall j \in N$$

or

$$Z_{IPImPMP}^{SPJ} = \sum_{t=1}^{T} [(f_{jt} - \eta_{jt}) x_{jt} + p_{jt} Q_{jt} + h_{jt} I_{jt}] - \sum_{t=1}^{T} \rho_j Q_{jt} \pi_j - \mu_t, \forall j \in N$$

subject to:

Eq. (1) - (2)

$$Q_{jt}, I_{jt} \geq 0, \quad x_{jt}, y_t \in \{0,1\}$$

$$\forall j \in N, s, t \in H, k \leq s \leq t, p \leq s-1, q \leq t-s$$

variables :$Q_{jt}, I_{jt} \geq 0, \quad x_{jt}$

parameters: $d_{jt}, \mu_t, \pi_j, \eta_{jt}$

The pseudo-code of the proposed DWD approach can be provided to interested researchers upon request.

5 RESULTS AND DISCUSSIONS

In order to evaluate the effectiveness of the Re_IPImPMP model and the developed algorithms, the following paragraphs present the results of the computational experiments on some test instances, available in the literature. In particular, a collection of test instances from the LOTSIZELIB (Trigeiro, 1989) is used to evaluate the performance of the model (Re_IPImPMP) and developed algorithm. Of course, the instances from the LOTSIZELIB were extended and adapted to the integrate maintenance optimization aspect as done in (Aghezzaf et al., 2016).

5.1 The Test Instances

The algorithms presented above are coded in AMPL using the callable CPLEX 12.6 library to solve the MILP problems. The computation tests were carried out on an Intel(R) Core(TM) i7-3770 CPU @ 3.40 GHz, 3401 MHz, 4 Core(s), 8 Logical with 32 GB RAM. under windows 7. CPU times are given in seconds. For the maintenance part, we assumed that the machine is subject to the random failures according to a Gamma distribution Γ(m=2, ν=2) with a shape parameter m = 2 and a rate parameter ν = 2 as in (Aghezzaf et al., 2016). We also assume imperfect preventive maintenance with $\alpha_k = k/(3k+7)$ and $\beta_k = (12k+1)/(11k+1)$ for all k.

Table 1: Initial value of *WindowSize* and *Overlap* chosen in RFFO Algorithm.

Instances	*WindowSize*	*Overlap %*
A2007	5	60
tr6_15	8	60
tr6_30	12	60
tr12_15	8	60
tr12_30	12	60
tr24_15	8	60
tr24_30	12	60
set1ch	8	60

Table 2: A Summary of the experimental results for comparision between the Re_IPImPMP and RFFO Heuristic algorithm.

Instances	Re_PPImPMP	CPU Time (sec)	RFFO	CPU Time(sec)	GAP %
A2007	815.435	1.05	815.435	51.25	0.00
tr6_15	337,355.000	4,339.16	337,355.000	210.59	0.00
tr6_30	675,607.000	2,103,730.00	676,080.000	642,130.00	0.07
tr12_15	1,245,920.000	2,710.00	1,252,120.000	520.00	0.50
tr12_30	4,387,470.000	2,088,910.00	4,387,470.000	1,126,980.00	0.00
tr24_15	2,502,640.000	2,920.00	2,502,640.000	245.89	0.00
tr24_30	8,272,760.000	2,031,020.00	8,272,760.000	752,230.00	0.00
set1ch	107,532.000	130.00	107,532.000	244.69	0.00

Table 3: A summary of the experimental results of the DWD applied algorithm.

Instance	Value DWD	CPU Time (sec)	GAP %
A2007	875.520	1.95	7.37
tr6_15	337,787.000	1.65	0.13
tr6_30	859,051.000	1.29	27.15
tr12_15	2,159,410.000	1.05	73.32
tr12_30	8,917,970.000	3.59	103.26
tr24_15	4,829,470.000	1.01	92.98
tr24_30	16,945,000.000	3.76	104.83
set1ch	172,504.000	1.72	60.42

In this study, to evaluate the effect of *windowSize* and *overlap* for the RFFO heuristic method, we tested all the *windowSize* parameters from 1 to the last period of the planning horizon, and increasing *overlap* by $step$ from 1 to *WindowSide* for instances $A20007$ and $tr6\_15$ to get initial value of the problem as shown in table 1.

5.2 Analysis and Discussions about the Experiments

Table 2 summarizes the results of the experiments which were carried out to compare the Re_IPImPMP (Aghezzaf et al., 2016) and the RFFO heuristic method. The first column of the table identifies the solved instances. The second column reports the optimal value of each instance which was obtained from the Re_IPImPMP model and the third column reports the resulted CPU running time. The fourth column describes the value of each instance which was obtained by the proposed RFFO heuristic algorithm and the fifth column presents the obtained CPU running time. The last column shows the GAP between the RFFO heuristic value and the Re_IPImPMP value. When comparing the results of the proposed RFFO with the results of the Re_IPImPMP model, it is clear that the proposed RFFO algorithm has the same optimal value with a considerable saving of the CPU (solve) time; it is faster from 4 to 10 times for the cases of the medium and/or large scale problems. However, in the small scale problems (A2007 and set1ch instances) was increasing large CPU time by the inner loop algorithm.

Table 3 summarizes the results of the computational experiments carried out for the DWD decomposition method. The first column of the table identifies the instances solved. The second column presents the value of each instance which was obtained via the proposed DWD decomposition algorithm; and the third column reports the CPU (solve) time. The last column describes the GAP between the DWD decomposition value and the Re_IPImPMP value by

$$GAP\% = \frac{(valueDWD - valueRe\_IPImPMP)}{valueRe\_IPImPMP} * 100.$$

As shown in Table 3, the proposed DWD provides solutions which are not so far from the optimal Re_IPImPMP value, with the less CPU time and memory which is used to reach the optimality for the same instance. However, the GAP, which is defined as the ratio of the difference between the value of the DWD algorithm and the value of the Re_IPImPMP model, showing it is just suitable for small and medium scale instances.

6 CONCLUSIONS

In this paper, we investigated the optimization model of an integrated production planning and imperfect preventive maintenance. The natural optimization

model for this problem is as a nonlinear mixed integer problem. We slightly modified the reformulation (Re_IPImPMP) the problem proposed in (Aghezzaf et al., 2016) that solves the problem as a linear mixed integer program. There are a few major limitations for this reformulated model, including the time consuming as well as the increased number of variables and constraints for the large and medium-sized problems. We applied the Relax-and-Fix/Fix-and-Optimize heuristics and the Dantzig-Wolfe Decomposition (DWD) methods to select the suitable strategies to solve the proposed optimization models. The developed algorithm are tested and compared for CPU time and gap. The results from the numerical examples and computational experiments showed that the developed algorithm for solving the Re_IPImPMP problem has a very good solution quality with reduced computational time. Further studies are currently investigated to improve the DWD method in order to obtain better quality solutions and increase computational time savings, especially for large scale, block structured, and linear programming problems of integrated production planning and imperfect preventive maintenances.

ACKNOWLEDGMENTS

We would like to express our sincere appreciation to the reviewers for their helpful comments. These helped improve the quality of this research work.

REFERENCES

Aghezzaf, E., Khatab, A., and Tam, P. L. (2016). Optimizing production and imperfect preventive maintenance planning's integration in failure-prone manufacturing systems. *Reliability Engineering & System Safety*, 145:190–198.

Aghezzaf, E. H., Jamali, M. A., and Ait-Kadi, D. (2007). An integrated production and preventive maintenance planning model. *European Journal of Operational Research*, 181(2):679–685.

Agogino, A. M., Chao, S. Y., and Lee, Z. (1997). Development of decision strategies for scheduling outages of power plants. *Final Report*, 1998:1997–2004.

Ben-Daya, M. and Rahim, M. A. (2000). Effect of maintenance on the economic design of x-control chart. *European Journal of Operational Research*, 120:131–143.

Chattopadhyay, D. (2004). Life-cycle maintenance management of generating units in a competitive environment. *Power Systems, IEEE Transactions on*, 19(2):1181–1189.

Chung, C.-H. and Krajewski, L. J. (1984). Planning horizons for master production scheduling. *Journal of Operations Management*, 4(4):389–406.

Dahal, K. P. and Chakpitak, N. (2007). Generator maintenance scheduling in power systems using metaheuristic-based hybrid approaches. *Electric Power Systems Research*, 77(7):771–779.

El-Amin, I., Duffuaa, S., and Abbas, M. (2000). A tabu search algorithm for maintenance scheduling of generating units. *Electric Power Systems Research*, 54(2):91–99.

El-Ferik, S. (2008). Economic production lot-sizing for an unreliable machine under imperfect age-based maintenance policy. *European Journal of Operational Research*, 186(1):150–163.

Fitouhi, M.-C. and Nourelfath, M. (2012). Integrating noncyclical preventive maintenance scheduling and production planning for a single machine. *International Journal of Production Economics*, 136(2):344–351.

Gurevich, V., Frant, S., and Bianu, A. (1996). Generating units maintenance scheduling optimizing production cost and reliability. *Power systems computation conference*, 2:9–9.

Kiyoshi, S., Shigeo, S., Hideaki, I., and Fumiyuki, H. (2002). Advanced technologies of preventive maintenance for thermal power plants. *Hitachi Hyoron*, 84(2):6–6.

Lin, C. E., Huang, C. J., Huang, C. L., Liang, C. C., and Lee, S. Y. (1992). An expert system for generator maintenance scheduling using operation index. *Power Systems, IEEE Transactions on*, 7(3):1141–1148.

Martorell, S., Villanueva, J. F., Carlos, S., Nebot, Y., Snchez, A., Pitarch, J. L., and Serradell, V. (2005). Rams+c informed decision-making with application to multi-objective optimization of technical specifications and maintenance using genetic algorithms. *Reliability Engineering & System Safety*, 87(1):65–75.

Pimentel, C. M. O., Alvelos, F. P. e., and Valrio de Carvalho, J. M. (2010). Comparing dantzig-wolfe decompositions and branch-and-price algorithms for the multi-item capacitated lot sizing problem. *Optimization Methods & Software*, 25(2):299–319.

Sana, S. S. and Chaudhuri, K. (2010). An emq model in an imperfect production process. *International Journal of Systems Science*, 41(6):635–646.

Toledo, C. F. M., da Silva Arantes, M., Hossomi, M. Y. B., Frana, P. M., and Akartunal, K. (2015). A relax-and-fix with fix-and-optimize heuristic applied to multi-level lot-sizing problems. *Journal of Heuristics*, 21(5):687–717.

Trigeiro, W. W. (1989). A simple heuristic for lot sizing with setup times. *Decision Sciences*, 20(2):294–303.

Wang, S. (2013). Integrated model of production planning and imperfect preventive maintenance policy for single machine system. *International Journal of Operational Research*, 18(2):140–140.

Optimal Combination Rebate Warranty Policy with Second-hand Products

Sriram Bhakthavachalam[1], Claver Diallo[1], Uday Venkatadri[1] and Abdelhakim Khatab[2]
[1]*Department of Industrial Engineering, Dalhousie University, 5269 Morris Street, Halifax, Canada*
[2]*Laboratory of Industrial Engineering, Production and Maintenance (LGIPM), Lorraine University, National School of Engineering, Metz, France*
{*sriram.bhakthavatchalam, claver.diallo, uday.venkatadri*}*@dal.ca, abdelhakim.khatab@univ-lorraine.fr*

Keywords: Second-hand Products, Warranty Policy, Consumer Perspective, Remaining Useful Life.

Abstract: With the increased awareness for sustainability, many engineered products are being recovered and reconditioned for secondary useful lives. These second-hand products can serve as replacement products to honour warranty pledges. This paper presents two mathematical models to determine the optimal combination rebate warranty policy when refurbished products are used for replacements from both the manufacturer and consumer point of views. Several numerical experiments are conducted to derive useful managerial knowledge.

1 INTRODUCTION

A warranty is a contractual agreement offered by the manufacturer at the point of sale of a product (Blischke, 1995), (Blischke, 1993). The use of warranties is universal and serves numerous purposes. It helps the buyers to rectify all the failures occurring within the warranty period at lower or no cost. Whereas, for manufacturers, it acts as a promotional tool to increase sales and revenue (Blischke, 1995). American manufacturers spend over 25 billion dollars to service warranty claims which is about 2% of their annual revenue from sales (Chukova and Shafiee, 2013; Shafiee and Chukova, 2013). In the 2009 General Motors annual report, the company had a total revenue of $104.2 billion and the future warranty cost on sold cars estimated to be $2.7 billion, about 2.6% of the revenue (Shafiee and Chukova, 2013). When buying a product, the consumer usually faces the difficult task of deciding between buying the warranty or not. And when the decision is made to get the warranty, choosing between different characteristics and warranty policies is another daunting task. When the warranty period is optional, the consumer has to decide if the warranty is worth the additional cost based a very limited knowledge of the product. This is becoming more and more important, since there is a growing trend among the manufacturers to offer extended term warranties. These involve additional costs, and the terms can vary considerably (Blischke, 1995; Blischke, 1993; Yun et al., 2008). Blischke & Murthy gave the example of a warranty or extended warranty that might cover both labor and parts initially and only cover parts later in the warranty period. The consumer has to decide, often at the time of purchase and based on very limited information, whether to opt for an extended warranty or not and to determine the best extended terms for his situation when there are multiple options (Blischke, 1995), (Blischke, 1993). The everyday consumer is not capable of conducting a mathematical analysis before making a choice because the consumer neither has the expertise for such an analysis nor the bargaining power to obtain relevant data from the manufacturer. However, consumer bureaus and regulatory agencies can carry out such analyses and inform the consuming public. Any model developed from the consumer's point of view in this chapter is then assumed to have been done for a consumer agency on behalf of all consumers and with data obtained by the agency from the manufacturers or from established and recognized independent reviewing bodies such as the Consumer Reports magazine.

There are many different types of warranty policies designed to cover the needs of manufacturers, dealers and consumers. A policy which is based on one factor (usually age) alone is said to be one-dimensional, on the other hand a two dimensional warranty is limited by two factors, usually age and a measure of usage of the product. One-dimensional policies are selected for products which are known to last for a fixed time period. This is common in the

Bhakthavatchalam, S., Diallo, C., Venkatadri, U. and Khatab, A.
Optimal Combination RebateWarranty Policy with Second-hand Products.
In *Proceedings of the 6th International Conference on Operations Research and Enterprise Systems (ICORES 2017)*, pages 491-498
ISBN: 978-989-758-218-9

marketplace for products such as cell-phones, computers, and projectors. Two-dimensional warranties apply to products that display wear and tear, degradation with usage. Automobiles, aircraft and heavy-duty machinery are examples of products with 2-D warranty policies. It is common to see car advertisements stating coverage of 60 months, 120 000 kilometres which ever occurs first.

Some basic warranty types are the Free replacement (FRW), Pro-rata (PRW), and Rebate warranty.

1. **Free replacement warranty (FRW)**: The manufacturer agrees to repair/replace a failed item during the warranty period at no charge to the customer. Example: small household appliances, electronics.
2. **Pro-rata warranty (PRW)**: The customer covers a proportion of the repair cost prorated to the age of the item at failure. Example: Tires.
3. **Rebate warranty**: The seller agrees to refund some proportion of the sale price to the buyer, if the product fails during the warranty period. The refund amount may be a linear or non-linear function of the failure time. Example: Money back Guarantee for electronic components such as hard drives, computer screens, and storage devices.

A basic taxonomy of warranty policies is presented by (Blischke, 1993; Blischke, 1995). An integrated warranty-maintenance taxonomy based on three categories ,i.e. product type, warranty policy, and maintenance strategy, is proposed in (Shafiee and Chukova, 2013).

Hybrid (combination) warranties are designed to utilize the desirable characteristics of the pure warranties and downplay some of their drawbacks (Blischke, 1993; Blischke, 1995). The combination warranty gives the buyer full protection against full liability for later failures, where the buyer has received nearly the full amount of service that was guaranteed under the warranty. It has a significant promotional value to the seller while at the same time providing adequate control over costs for both buyer and seller. An example for hybrid warranty is seen in the FRW/PRW policy offered on Firestone tires. During the first 2 years of service, the tire is replaced free of charge. Beyond year 2, the replacement price is pro-rated based on years of service from the original purchase date. Some advantages of combination warranties are improved protection towards the product, customer satisfaction, higher ownership lifetime for the buyers and higher sales volume to increase profit to manufacturers.

Combination warranty is a good type of warranty for second-hand products (SHPs) as its offers a good protection to both manufacturers and consumers (Chari, 2015). Two main problems faced by the consumers acquiring SHPs are their uncertainty and durability (Shafiee and Chukova, 2013) due to the lack of past usage and maintenance history. In order to reduce the risk and impact of product malfunctioning, dealers offer generous warranty policies. A review of warranty models currently available in the literature for SHPs show that there are very few of them and all deal with the manufacturers perspective (Shafiee and Chukova, 2013; Chari et al., 2016b; Su and Wang, 2016; Diallo et al., 2016). The goal of this article is to address this shortcoming by proposing a warranty policy and develop mathematical models from both the manufacturer and consumer perspectives.

2 OPTIMAL COMBINATION WARRANTY MODELS USING SHPS

For most warranty policies, failed products are repaired or replaced with new components or products. In the context of remanufacturing, second-hand products may be available and can therefore be re-used as replacements when consumers return failed products (Yeh et al., 2005; Yeh et al., 2011; Chari et al., 2016a). In doing so, the manufacturers can lower their costs and consumers can extend their ownership of the products. However, due to the lower reliability of SHP, it is crucial to determine the optimal parameters of the warranty policy to be offered to avoid higher costs to the manufacturer and less than anticipated performance/ownership time for the consumer. In this article, we will develop two mathematical models for a combination rebate warranty policy using SHPs as replacement products.

2.1 Proposed Warranty Policy

Under the proposed warranty policy, a brand new product is sold with a total warranty coverage period of length w. Under this policy, the seller will replace a defective product with:

- A new product if the failure occurs before w_1 (Phase 0);
- A refurbished product of high quality if the failure occurs between w_1 and w_2 (Phase 1);
- A refurbished product of normal quality if the failure occurs between w_2 and w_3 (Phase 2).

It should be noted that $w = w_1 + w_2 + w_3$. The proposed warranty policy is depicted in Figure 1. New products have age $\tau_0 = 0$. Refurbished or second-hand products of high quality have age τ_1 that is greater than 0. Refurbished or second-hand products of normal quality have age τ_2 that is greater than τ_1. Therefore, we have: $0 < \tau_1 < \tau_2$.

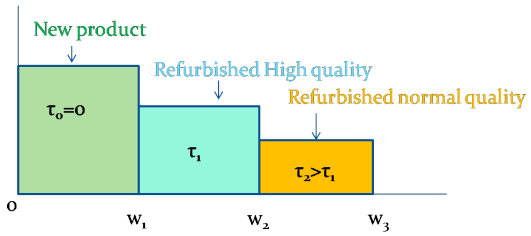

Figure 1: Proposed Warranty Policy.

The policy offered here is Non Renewing Free Replacement Warranty policy (NRFRW). The following notation is used.

2.1.1 Parameters

C_i: Cost of replacement product in phase i
C_0: Unit cost for a new product
C_u: Warranty cost
a: Price coefficient
b_i: Warranty coefficient
d_0: Market demand amplitude factor
ε, η: Age coefficients for the acquisition cost of reconditioned components
β: Slope parameter of the Weibull distribution
θ: Scale parameter of Weibull distribution
λ: Inverse of the Scale parameter ($\lambda = 1/\theta$)
m: Number of warranty periods

2.1.2 Functions

$f(t)$: lifetime prob. density function (pdf)
$F(t)$: Cumulative distribution (cdf)
π: Expected unit profit
$\mathcal{P}(p, w_i, \tau_i)$: Total expected profit for the Seller
$D(p, w_i)$: Total demand
EOT: Expected ownership time
$MTTF_0$: Expected lifetime of the original new product
$MTTF_1$: Expected lifetime for high quality SHPs
$MTTF_2$: Expected lifetime for low quality SHPs
$EOCR_1$: EOT per cost ratio of the product when warranty is purchased
$EOCR_2$: EOT per cost ratio of the product without warranty

2.1.3 Decision Variables

p: Unit sale price of the new product
w_i: Warranty periods
τ_i: Age of the SHP products offered as replacements in phase i

In the following section, two mathematical models will be developed for the maximization of the manufacturer's expected profit and the maximization of the consumer's ownership time.

2.2 Model 1: Maximization of Manufacturer's Expected Profit

If the product fails within w_1, a full refund of C_0 is given to the customer to buy a new product. When it fails between w_1 and w_2 a refund of C_1 is returned to the customer that is sufficient to buy a high reliability SHP. When the product fails between w_2 and w_3, a lump sum C_2 is given back to the consumer which is sufficient to buy a normal quality SHP. Warranty is not extended when the system fails.

$C(\tau_i)$, the unit cost of a replacement product with age τ_i, is given by Equation (1) where C_0 is the base price and ε, η are positive parameters (Chari, 2015). Parameter ε represents the discount rate offered on used products, and parameter η models the increase in cost due to aging.

$$C(\tau_i) = C_0 \times (1 + \tau_i)^{(-\varepsilon)} + \tau_i^{\eta} \tag{1}$$

A new product will therefore cost

$$C(\tau_0 = 0) = C(0) = C_0 \tag{2}$$

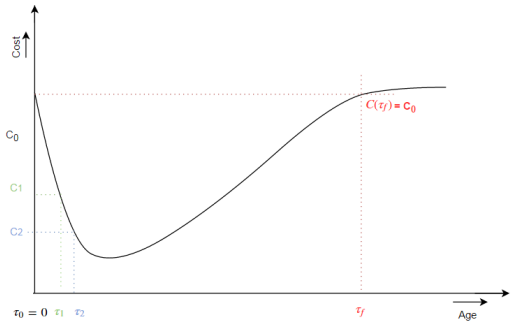

Figure 2: Cost as a function of age.

The profile of $C(\tau_i)$ is depicted in Figure 2. The cost of replacement products initially decrease with age (refurbished cost less) but reaches a minimum then increases with age to account for technical and practical difficulties encountered when trying to disassemble and recondition very old products

(availability of parts, obsolescence, corrosion, etc.). Beyond this point $C(\tau_f) = C_0$, customers should buy a new product rather than a second-hand product because the cost of a new product is less than SHP.

$$C(\tau_1) = C_1 = C_0 \times (1+\tau_1)^{(-\varepsilon)} + \tau_1^{\eta} \quad (3)$$

$$C(\tau_2) = C_2 = C_0 \times (1+\tau_2)^{(-\varepsilon)} + \tau_2^{\eta} \quad (4)$$

The probability that a product will fail between w_{i-1} and w_i for $i = 1,...,m$ is given by:

$$[F(w_i) - F(w_{i-1})] \quad (5)$$

where $w_0 = 0$.

The total expected warranty cost (C_u) is given by the weighted average of the replacement costs in each phase i given in Equation (7) shown below.

$$C_u = \sum_{i=1}^{m} C(\tau_i) \times [\text{Prob. failure in phase } i] \quad (6)$$

$$C_u = C_0 \left[\sum_{i=1}^{m} \left[(1+\tau_{i-1})^{-\varepsilon} + \frac{\tau_{i-1}^{\eta}}{C_0} \right] [F(w_i) - F(w_{i-1})] \right] \quad (7)$$

Failure Distribution:

The Weibull distribution is used as the product failure distribution. The lifetime cumulative distribution function of the product is then given by

$$F(x) = 1 - \exp^{-(\frac{x}{\theta})^{\beta}}, \qquad 0 \leq x \quad (8)$$

Demand Function:

The market demand function $D(p, w_i)$ for the product is modelled to take into account consumers' preferences for lower prices and longer warranty coverage. $D(p, w_i)$ is modelled as a displaced log-linear function of w_i and p as in (Glickman and Berger, 1976; Chari et al., 2016b).

$$D(p, w_i) = d_0 p^{-a} \Pi_{i-1}^{m} (d_1 + w_i)^{b_i} \quad (9)$$

Parameter a is the rate of decrease of the sales volume with the increasing price of the product. Parameters b_i are the rate of increase of the sales volume with the increasing of the warranty lengths w_i. The factor d_0 is the demand amplitude and d_1 is the warranty displacement constant.

Total Expected Profit:

The total expected profit (TEP) $\mathcal{P}$ is the product of the expected unit profit with the demand as in Equation (10). The expected unit profit is obtained in Equation (11) by subtracting the cost of the original product C_0 and the expected warranty cost C_u from the sale price p of each unit sold.

$$\mathcal{P} = \pi \cdot D(p, w_i) \quad (10)$$

$$\mathcal{P} = (p - C_0 - C_u) \cdot D(p, w_i) \quad (11)$$

2.2.1 Numerical Results

For illustration purposes and without loss of generality, an example with only two decision variables is considered by setting τ_2 as a proportion of τ_1 using: $\tau_2 = k \cdot \tau_1$. For the arbitrarily chosen parameter values given below, we solve for the solution (p, τ_1) which maximizes the manufacturers' total expected profit: $w_1 = 0.5; w_2 = 1; w_3 = 2 : m = 3, \theta = 1.5, \beta = 1.5; C_0 = 15; d_0 = 100,000; a = 2.6; b_1 = 1.9, b_2 = 1.5, b_3 = 1.1; \varepsilon = 3.3; \eta = 0.7; \lambda = 1/\theta; k = 1.5$. Figure 3 shows a 3D-plot of the total expected profit $\mathcal{P}$ as a function of purchase price p and age τ_1. There is a clear optimal solution at $p^* = \$30.68$, $\tau_1^* = 1.43$ and $\mathcal{P}^* = \$3,287$.

Several numerical experiments have been conducted to analyze the behavior of the model when key parameters change. The first experiment consisted in varying the values of k, a parameter that dictates how old the replacement products are in phase 2 in comparison with the replacement products used in phase 1 according to the formula: $\tau_2 = k \cdot \tau_1$. The results obtained are plotted in Figures 4 to 6.

In Figure 4, $\mathcal{P}$ increases until the value of k reaches 1 and after that point, $\mathcal{P}$ decreases. For $k = 1$, the replacement products in phase 1 and 2 are the same. This represents the best case scenario as profit is maximum and price is the lowest. For $k < 1$, phase 2 replacement products are younger than phase 1 products, which is bad because components failing in phase 1 are replaced with older parts and the larger proportion of failures occurring in phase 2 are covered with newer products which are more expensive. This explains why the slope when $k < 1$ is steeper than the slope when $k > 1$. Figure 5 shows that price p behaves in an exact opposition to the behavior of $\mathcal{P}$. For values near and around $k = 1$, it is the cheapest to honour the warranty, so the manufacturer can afford to reduce the price of the product and therefore increase demand, which in return boosts profit.

Figure 6 depicts the relationship between the optimal value τ_1^* and τ_2^*. For smaller values of τ_1^* the model uses larger values of τ_2^* to keep warranty costs under control. When the values of τ_1^* start to increase $(1 < \tau_1^* < 3)$, the model restricts the values of τ_2^* between values of 3 and 1.5 to keep warranty costs low by decreasing the probability of failure in phase 2. For values of $\tau_1^* > 3$ the values of τ_2^* tend to stabilize around 1 and 1.5 for the same reasons as before.

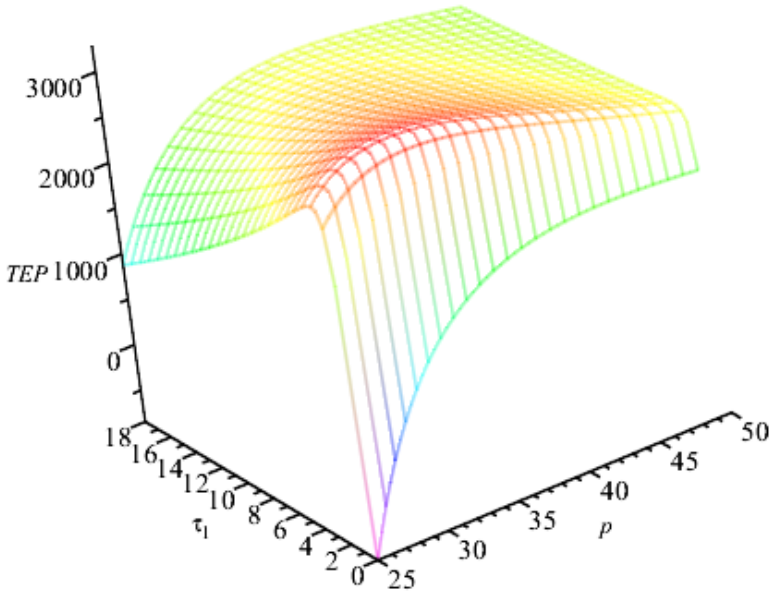

Figure 3: Total expected profit as a function of purchase price p and age τ_1.

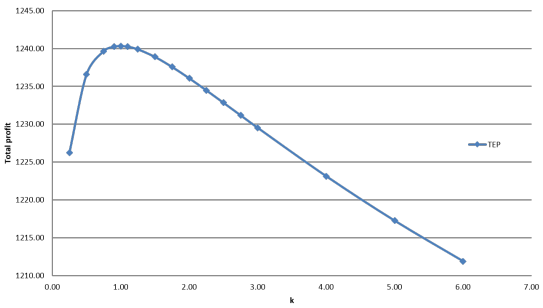

Figure 4: Seller expected profit as a function of k.

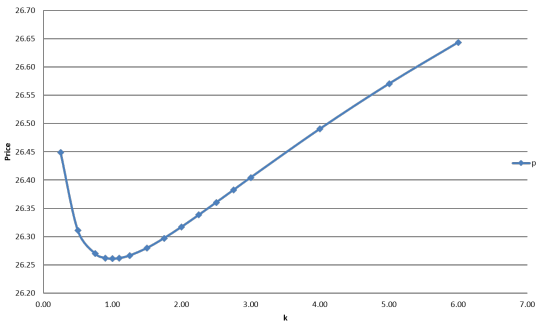

Figure 5: Optimal price as a function of k.

Another set of numerical experiments was conducted by varying β, the shape parameter of the Weibull distribution. The results are plotted on Figure 7. In general, the figure shows an increasing trend and a plateau after $\beta = 4$. Increasing the shape parameter β

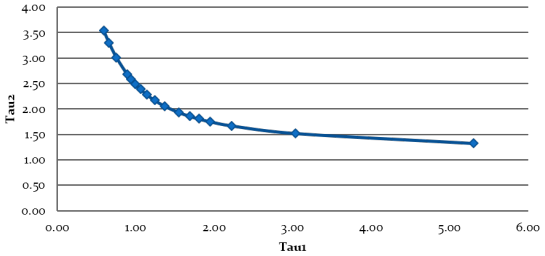

Figure 6: τ_1 vs τ_2 for varying values of k.

newpage
increases reliability of the product so that the warranty cost reduces. There is very little return on investment to improve reliability of the products beyond $\beta = 4$. Figure 8 shows that with improving reliability (increasing β), the warranty costs reduce and therefore the model can afford to reduce the unit price which increases profits. For the same reliability reasons, when β increases, the model can afford to use newer parts which causes τ_1^* to decrease as depicted in Figure 9.

2.3 Model 2: Maximization of Customers' Expected Ownership Time

In the previous model, the focus was on the manufacturers' interests. In this subsection, a model developed from the consumer's perspective will be presented. The warranty policy introduced in sub-section

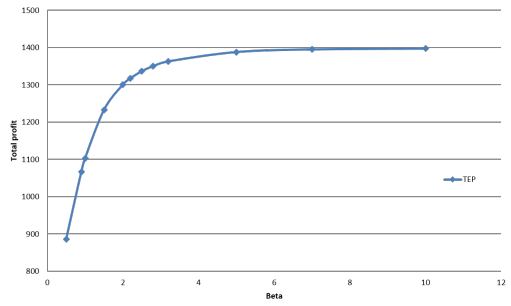

Figure 7: Seller's expected profit as β varies.

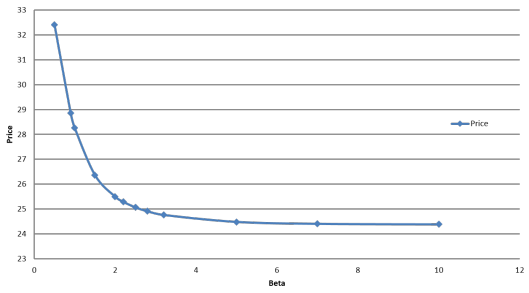

Figure 8: Selling price for varying β.

2.2 is still under consideration here.
At time of purchase, the consumer has two choices:

- Option 1: Buy the original product without warranty at a fraction ρ $(0 \leq \rho \leq 1)$ of the price p set by the manufacturer and determined using model 1 presented above; or
- Option 2: Buy the original product with warranty at price p.

The goal of model 2 is to formulate the Expected Ownership Time per Cost Ratio ($EOCR_i$) for both options ($i = 1,2$) and compare their behaviour through the analysis of their difference Δ:

$$\Delta = EOCR_2 - EOCR_1. \tag{12}$$

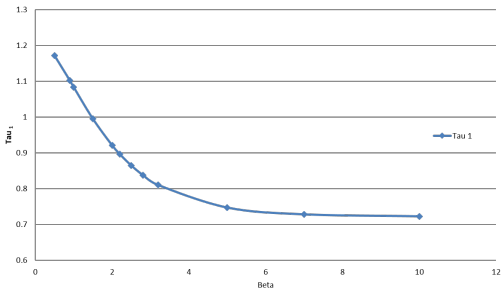

Figure 9: Profile of the optimal τ_1 as β varies.

Option 1: without warranty

$$EOCR_1 = \frac{EOT_1}{\rho \cdot p}$$

$$EOCR_1 = \frac{MTTF_0}{\rho \cdot p}$$

where $MTTF_0$ is the expected lifetime of the original product

$$EOT_1 = MTTF_0 = \theta \cdot \Gamma\left[1 + \left(\frac{1}{\beta}\right)\right].$$

$\Gamma(.)$ is the gamma function. Therefore,

$$EOCR_1 = \frac{\theta \cdot \Gamma\left[1 + \left(\frac{1}{\beta}\right)\right]}{\rho \cdot p}. \tag{13}$$

Option 2: with warranty

$$EOCR_2 = \frac{EOT_2}{p} \tag{14}$$

A consumer enjoys his original new product from purchase time up to the instant of the first failure which has expected duration $MTTF_0$. At failure, the consumer gets a replacement product that will have an expected remaining lifetime of length $RMTTF_i$ if the failure occurred in phase i. The original product fails in phase i with probability $[F(w_i) - F(w_{i-1})]$. Therefore, the expected ownership time for option 2 is given by

$$EOT_2 = MTTF_0 + \sum_{i=1}^{m} RMTTF_{i-1}[F(w_1) - F(w_{i-1})] \tag{15}$$

where

$$RMTTF_i = \frac{1}{1 - F(\tau_i)} \int_{\tau_i}^{\infty} [1 - F(x)].dx \quad \forall i \in 1,2. \tag{16}$$

By definition, $RMTTF_0 = MTTF_0$. Combining Equations (14) and (15), gives the expression for $EOCR_2$:

$$EOCR_2 = \frac{MTTF_0 + \sum_{i=1}^{m} RMTTF_{i-1}[F(w_1) - F(w_{i-1})]}{p} \tag{17}$$

Finally, Equations (12) becomes:

$$\Delta = \frac{1}{p}\left[MTTF_0 + \sum_{i=1}^{m} RMTTF_{i-1}\left[F(w_1) - F(w_{i-1})\right] - \frac{\theta}{\rho} \cdot \Gamma\left[1 + \left(\frac{1}{\beta}\right)\right]\right] \tag{18}$$

The obtained mathematical model is solved for various scenarios in order to derive decision making policies for the consumer organizations.

2.3.1 Numerical Results

Experiment #1: Change in w_1 and varying β

The first set of experiments is designed to analyze the recommendations made by the model for 4 warranty policies when β changes. The 4 warranty policies differ in their value of w_1. The values of w_2 and w_3 are the same for all policies. Table 1 presents the results obtained.

Table 1: Values of Δ for various w_1 and varying β.

β	$w_1 = .5$ $w_2 = 2$ $w_3 = 3$	$w_1 = .75$ $w_2 = 2$ $w_3 = 3$	$w_1 = 1$ $w_2 = 2$ $w_3 = 3$	$w_1 = 2$ $w_2 = 2$ $w_3 = 3$
0.5	0.06	0.05	0.04	0.03
0.9	0.02	0.02	0.02	0.02
1.0	0.02	0.02	0.02	0.02
1.5	0.01	0.01	0.01	0.02
2.0	0.01	0.01	0.01	0.01
3.0	0.00	0.01	0.01	0.02
4.0	0.00	0.00	0.01	0.02
5.0	0.00	0.00	0.01	0.02
6.0	-0.01	0.00	0.01	0.02

The results are also plotted on Figure 10 from where two clear zones can be defined. The zone delimited by the red dotted outline depicts the area where products can be bought without warranty. Products falling in the zone above the red zone need to be purchased along with one of the 4 warranty policies offered. The following other observations can be made:

- The general profile of each plot of Δ as a function of β shows a fast decrease for low values of β and a stabilization for higher values. Δ is higher for $\beta << 1$ because early failures make the purchase of warranty more valuable. Δ stabilizes when increasing β because of the resulting increase in reliability which decreases the likelihood of failure and therefore the purchase of warranty does not add significant value to the consumer.
- Different warranty policies have different slopes of the same profile.
- A clear crossover point can be noticed on Figure 10. Policies with shorter Phase 0 (shorter w_1) that are preferred before the crossover point perform poorly after the crossover point when the products have higher reliability. Conversely, policies with longer Phase 0 (longer w_1) perform better after the crossover point. In other words, a policy that is good for newly designed products do worse with seasoned or proven products with good reliability.
- Warranty policies with longer w_1 coverage are less sensitive to increase in β values. It can be seen on Figure 10 that the 4th policy has the smallest amplitude over the complete range of β.

Experiment #2: Change in ρ and varying β

Here, numerical results are generated for two values of ρ (0.95 and 0.85) to analyze the impact of the selling price over the decision to purchase the warranty or not. The results obtained are in Table 2.

Table 2: Values of Δ for varying β.

$w_1 = .75$	$w_2 = 2$	$w_3 = 3$
β	ρ=0.95	ρ=0.85
0.5	0.06	0.05
0.9	0.03	0.02
1.0	0.02	0.02
1.5	0.02	0.01
3.0	0.01	0.01
4.0	0.01	0.00
6.0	0.00	0.00

As in the previous experiment, Δ shows a decreasing trend with increasing β. The higher the price without warranty (or the lower the warranty cost over premium ratio) the higher the return or incentive to buy the warranty.

3 CONCLUSIONS

This paper presented two mathematical models to determine the optimal combination rebate warranty policy when refurbished products are used for replacements from both the manufacturer and consumer point of views. One model was developed from the manufacturers' point of view to maximize the total expected profit and the second model dealt with the maximization of the consumer's expected ownership time. Numerical experiments showed that appropriate optimal decisions can be reached in the reuse of second-hand products in honouring warranty. Both the manufacturer and consumer groups can use these models to improve profitability levels and increase ownership durations.
The authors are currently investigating a joint analysis that considers both the seller and buyers' perspectives by formulating a multi-objective model to integrate key factors such as brand loyalty and incentives. Case studies from an appliance remanufacturer will be conducted to validate the theoretical results obtained. A

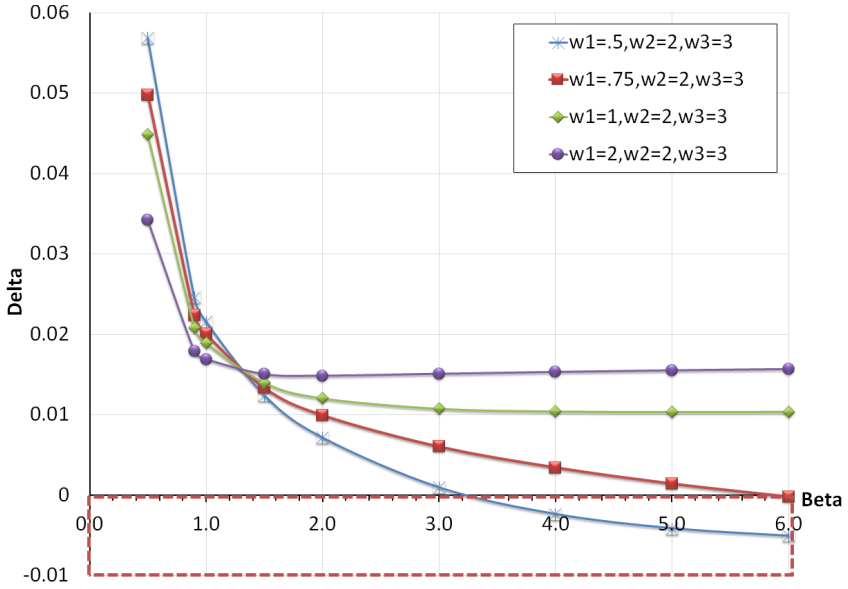

Figure 10: Profile of Δ for varying β.

variability analysis on a reduced set of selected solutions (with high expected values) will also be performed to test the robustness of the solutions. Future extensions of this study can also cover new warranty models suited for remanufactured products such as pro-rata and hybrid pro-rata policies, and integration of reconditioned products of different quality levels.

REFERENCES

Blischke, W. (1993). *Warranty cost analysis*. CRC Press.

Blischke, W. (1995). *Product warranty handbook*. CRC Press.

Chari, N. (2015). *Thematic Development of Recovery, Remanufacturing, and Support Models for Sustainable Supply Chains*. PhD thesis, Dalhousie University, Halifax.

Chari, N., Diallo, C., Venkatadri, U., and Aït-Kadi, D. (2016a). Production planning in the presence of remanufactured spare components: an application in the airline industry. *The International Journal of Advanced Manufacturing Technology*, pages 1–12.

Chari, N., Diallo, C., Venkatadri, U., and Khatab, A. (2016b). Modeling and analysis of a warranty policy using new and reconditioned parts. *Applied Stochastic Models in Business and Industry*, 32:539–553.

Chukova, S. and Shafiee, M. (2013). One-dimensional warranty cost analysis for second-hand items: an overview. *International Journal of Quality & Reliability Management*, 30(3):239–255.

Diallo, C., Venkatadri, U., Khatab, A., and Bhakthavatchalam, S. (2016). State of the art review of quality, reliability and maintenance issues in closed-loop supply chains with remanufacturing. *In Press, International Journal of Production Research*, 0(0):1–20.

Glickman, T. S. and Berger, P. D. (1976). Optimal price and protection period decisions for a product under warranty. *Management Science*, 22(12):1381–1390.

Shafiee, M. and Chukova, S. (2013). Maintenance models in warranty: A literature review. *European Journal of Operations Research*, 229(3):561–572.

Su, C. and Wang, X. (2016). Optimal upgrade policy for used products sold with two-dimensional warranty. *Quality and Reliability Engineering International*.

Yeh, R. H., Chen, G.-C., and Chen, M.-Y. (2005). Optimal age-replacement policy for nonrepairable products under renewing free-replacement warranty. *IEEE Transactions on Reliability*, 54(1):92–97.

Yeh, R. H., Lo, H.-C., and Yu, R.-Y. (2011). A study of maintenance policies for second-hand products. *Computers & Industrial Engineering*, 60(3):438–444.

Yun, W. Y., Murthy, D. N. P., and Jack, N. (2008). Warranty servicing with imperfect repair. *International Journal of Production Economics*, 111(1):159–169.

AUTHOR INDEX

Proceedings of ICORES 2017

6th International Conference on Operations Research and Enterprise Systems

http://www.icores.org

LOGISTICS PARTNER

EVENT MANAGEMENT SYSTEM

IN COOPERATION WITH

PROCEEDINGS WILL BE SUBMITTED FOR INDEXATION BY

ISBN: 978-989-758-218-9